Volume 23, Number 1

January-February, 1961

COLLOID JOURNAL

(KOLLOIDNYI ZHURNAL)

A publication of the Academy of Sciences of the USSR

IN ENGLISH TRANSLATION

Year and issue of first translation:
Vol. 14 No. 1 Jan.-Feb. 1952

545-158
8

Annual subscription *$80.00*
Single issue *20.00*

Copyright © 1961
CONSULTANTS BUREAU ENTERPRISES, INC.
227 West 17th Street, New York, N. Y.

Editorial Board
(KOLLOIDNYI ZHURNAL)

P. N. Antipov-Karataev, B. V. Deryagin, B. A. Dogadkin
(Acting Editor), A. V. Dumanskii (Editor-in-Chief),
V. A. Kargin, S. M. Lipatov, P. A. Rebinder,
I. P. Serdobolskii (Secretary),
M. P. Volarovich

A complete copy of any paper in this issue may be purchased from the publisher for $7.50

Note: The sale of photostatic copies of any portion of this copyright translation is expressly prohibited by the copyright owners.

Printed in the United States of America

COLLOID JOURNAL

Volume 23, Number 1 January-February, 1961

CONTENTS

	PAGE	RUSS. PAGE
Adsorption of Ammonia Vapor on Carbon Black. A. A. Voskresenskii	1	3
Thermomechanical Properties of Plasticized Ethylcellulose. D. I. Gal'perin, V. V. Moshev, and V. G. Stepanova	5	8
Quick and Thixotropic Properties of Disperse Sedimentary Rocks. I. M. Gor'kova	9	12
Extrusion of a Viscoplastic Dispersed Phase Between Sliding Plane-Parallel Walls. A. M. Gutkin	16	20
Electrification and Rheological Properties of Nonaqueous Plastic Dispersed Systems. Yu. F. Deinega, A. V. Dumanskii, and G. V. Vinogradov	21	25
Volumetric Determination of Colloidal Solubility (Solubilization). P. A. Demchenko	26	31
Solubilization of Aromatic Hydrocarbons in Hydrosols of Saturated Fatty Acid Soaps. P. A. Demchenko	30	36
Effect of Surface Forces on Phase Equilibria of Polymolecular Layers and on Contact Angle. B. V. Deryagin and L. M. Shcherbakov	33	40
Diffusiophoresis in Electrolyte Solutions and Its Role in the Mechanism of Film Formation from Rubber Latexes by the Method of Ionic Deposition. B. V. Deryagin, S. S. Dukhin, and A. A. Korotkova	44	53
The Reversion of Electrolyte Adsorption by Ferri- and Aluminosilicate Mixed Gels. O. I. Dmitrenko and A. A. Ryabinina	50	59
Effect of Compression of Carbon Black on the Adsorption Isotherm of n-Hexane. A. A. Isirikyan and A. V. Kiselev	56	67
A Spectrophotometric Study of the Adsorption of Methylene Blue by Highly Dispersed Aluminosilicates. L. I. Kul'chitskii	63	76
Capillary-Retained Liquid in Disperse Systems of Contacting Particles. L. V. Radushkevich and V. A. Kolganov	71	86
Study of Latex Foams. D. M. Sandomirskii and A. A. Korotkova	78	95
Molecular Adsorption of Certain Aromatic Acids on Ion-Exchange Resins. O. R. Skorokhod and L. M. Sergeeva	83	100
Relation Between Dynamic Stability of Droplets and Critical Vapor Supersaturation during Condensation. V. P. Skripov	88	106
The Sorption of Binary Solutions by Butadiene-Nitrile Copolymers. G. L. Starobinets and V. F. Tikavyi	93	112
Methods of Investigating the Frictional Properties of Polymers under Strong Unidirectional Compression. B. V. Deryagin and Yu. P. Toporov	99	118
LETTERS TO THE EDITOR		
Kinetics of the Growth of Contraction Stresses in Systems Undergoing Drying. M. S. Ostrikov, N. D. Vitkevich, and O. D. Svirskaya	103	122
Normal Stresses in Polyisobutylene Solution as Derived from Elastic Deformation and Tangential Force Data. A. A. Trapeznikov	105	125

ADSORPTION OF AMMONIA VAPOR ON CARBON BLACK

A. A. Voskresenskii

Moscow Institute of Chemical Machine Construction, Department of General Chemistry
Translated from Kolloidnyi Zhurnal, Vol. 23, No. 1, pp. 3-7, January-February, 1961
Original article submitted December 19, 1959

The study of the surface properties of carbon black by the gas-adsorption method presents a very definite interest in connection with the importance that carbon black has taken on as a filler in the manufacture of resins, plastics, lacquers, etc. Worthy of special attention is the adsorption of the vapors of polar substances such as water, methyl alcohol, and ammonia. In this connection, a study of the adsorption of ammonia vapor on carbonacious adsorbers was undertaken at temperatures near the boiling point.

References [1,2] have shown the effect of surface oxides on the adsorption of ammonia, in which the ammonia behaves similarly to water and methyl alcohol. The adsorption isotherms of ammonia on oxidized carbon black, at low relative pressures, lie somewhat below the desorption isotherms, which can be explained by the slow establishment of an adsorption equilibrium on the oxidized carbon surface. Our measurements were made for the purpose of explaining the nature of the nonequilibrium adsorption of ammonia in the presence of surface oxides. A channel black, spheron 6, was used as adsorbent. Constant temperature of the adsorbent was assured by a cryostat [3]. Temperature fluctuations did not exceed $\pm 0.1°$, which means that the vapor pressure of ammonia deviated from the mean value of 620 mm by $\pm 0.8\%$. The measurements were carried out at $-36.3°$, by the volume method.

Channel blacks are known to be characterized by an abundance of stable surface oxides. In order not to change the composition of the surface oxides, the vacuum treatment of the surface layer of spheron 6 carbon black was carried out at room temperature, without heating. On the adsorption branch of the isotherm, taken over the course of several days, with interruptions in the operation of the cryostat (Fig. 1), the curved segments correspond with series of measurements made at constant cryostat temperature ($-36.3°$), while the breaks correspond with two periods of warming the cryostat up to room temperature. The first series of measurements, represented on the curve by four points, was carried out over an 8-hr period, at constant cryostat temperature. The next series of measurements was preceded by shutting down the cryostat, and warming the adsorbent up to 20-25°. On again cooling the cryostat to $-36.3°$, it was found that, during the 24-hr period at room temperature , a considerable absorption of ammonia vapor had taken place, in view of which the pressure in the system was reduced twice. The next cryostat warmup was preceded by a series of measurements up as far as $p/p_s = 0.3$. At the warmup, a sharp increase in the sorption rate was again observed. During the time at room temperature, although a partial desorption took place, the absorption of ammonia was more intense. The experiment described indicates the considerable role played by activated adsorption of ammonia in the presence of surface oxides. The temperature dependence of the absorption rate speaks for a substantial activation energy.

It presented some interest to investigate the nonporous carbon surface, freed of oxides. At the time the samples in question were prepared, contact with air could not be prevented, but we felt that, at room temperature, there would not be any noticeable formation of stable surface oxides on the reduced carbon adsorbents Actually, as was shown in [4], storing reduced activated charcoal for four months did not produce any change in the water-adsorption isotherm. In addition to removing the surface oxides by baking, special attention should be given to Tesner's [5] special method of charcoal preparation, based on the property which benzene has, of decomposing quantitatively at 780-790° on the surface of charcoal, according to the reaction $C_6H_6 = 6H + 3H_2$. This technique

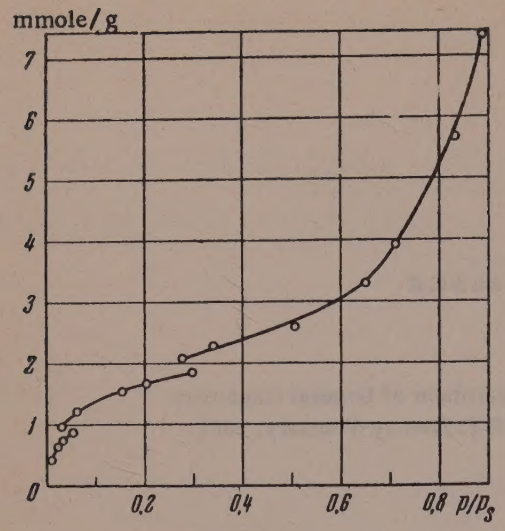


Fig. 1. Adsorption of NH_3 (mmole/gm) on Spheron 6 channel black.

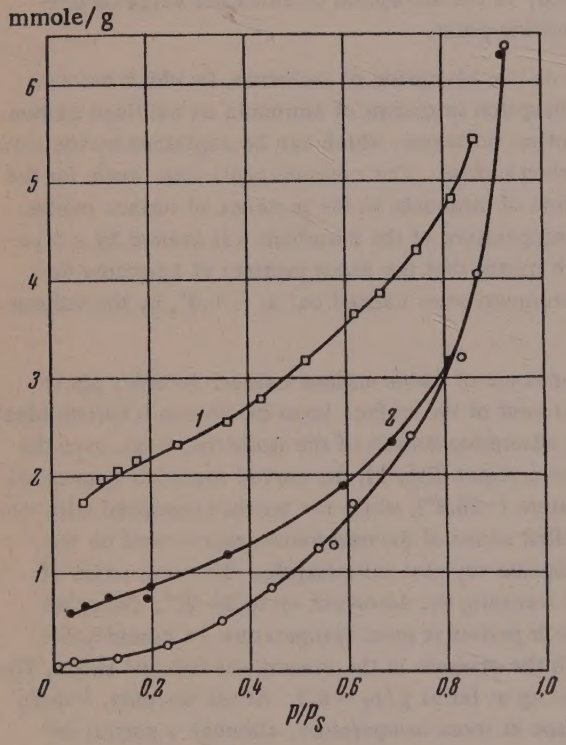


Fig. 2. Adsorption of NH_3 on anthracine black: 1) desorption on the original black; 2) adsorption and desorption on treated black with surface-layer increase of 8.7%.

has the effect of covering the charcoal surface with several molecular carbon layers, after which the charcoal surface is reliably isolated from the influence of surface oxides.

Figures 2 and 3a give a comparison between the ammonia adsorption on the original anthracine black, and the same charcoal subjected to Tesner's technique. The original German anthracine black had specific surface 110 m^2/gm. A water suspension of the charcoal gave a clearly acid reaction (pH 3.6), which indicated a considerable content of acid surface oxides, capable of ion exchange. Since, on oxidized blacks of the channel type, the adsorption branch of the isotherm shows a shift with time (Fig. 1), and does not coincide with the desorption branch, we took only the desorption branch for comparison (Figs. 2 and 3a). Preparing the anthracine black by the method selected gave an increase in surface layer of 8.7%. This technique, it turned out, resulted in a reduction of the specific surface to 84 m^2/gm. Also, it produced a marked change in the character of the ammonia adsorption. The isotherm began to resemble the one obtained formerly [2] for channel black, baked at 1000°, but, in our case, the hysteresis was more noticeable. Reference [6] deals with the study of similar hysteresis in the adsorption of ammonia on acetylene black. In our case, as a result of the reaction $C_6H_6 = 6C + 3H_2$, the specific surface of the charcoal falls, the pores fill up, and the surface of carbon-black particles becomes covered with a nonporous carbon layer. The appearance of hysteresis on such a surface is especially interesting. The explanation of the hysteresis by the penetration of ammonia molecules into the micropores [2,4] appears somewhat artificial here, since the magnitude of the hysteresis amounts to more than half of the monolayer (Fig. 2).

More extensive treatment of the original anthracine black up to 60% increase led to caking of the layer into a coarse-grained mass. The specific surface of the carbon black was reduced to 42 m^2/gm, and appreciable hysteresis appeared in the adsorption isotherm, Fig. 3a. Part of the product prepared with 60% increase in surface layer was subjected to heat-treatment in a reducing atmosphere at 1250° for 3 hr. Baking did not remove the hysteresis, and the form of the adsorption isotherm did not change (Fig. 3c). Since the preparation was not subjected to any special pulverization or mixing, the lack of coincidence between the adsorption isotherms for baked and unbaked samples (Figs. 3a,c) is perfectly natural.

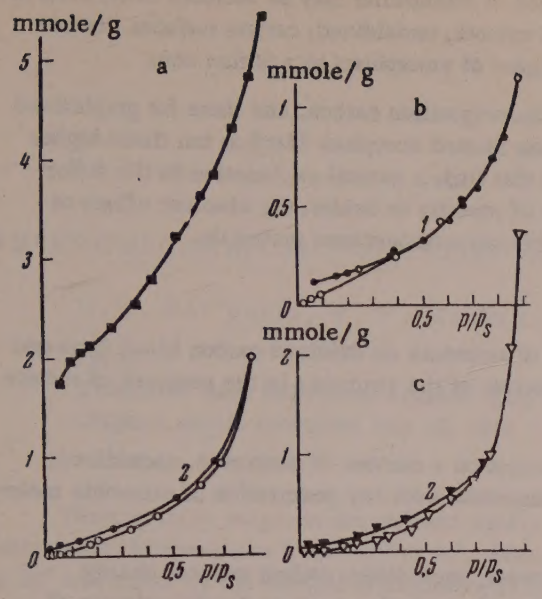


Fig. 3. Adsorption of NH_3 on anthracine black (a) and (c), and on stove black (b): 1) original carbon black; 2) treated black with surface layer increase of 60%; c) the same, followed by baking at 1250°.

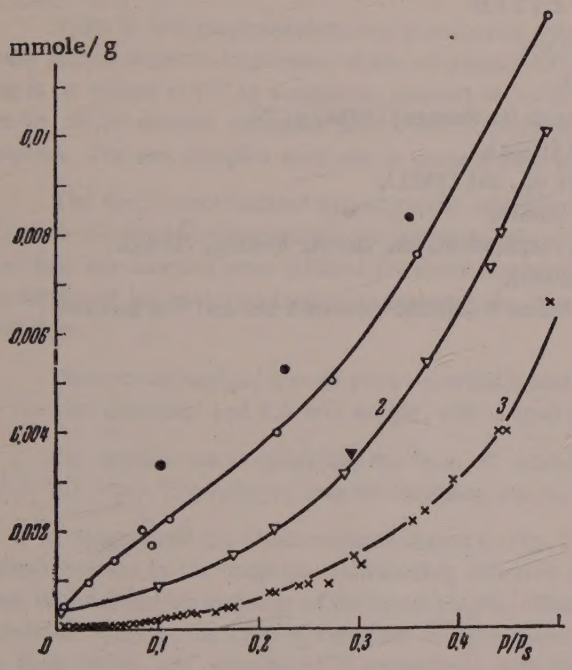


Fig. 4. Adsorption of NH_3 on the following surfaces: 1) acetylene black, covered with decomposition carbon; 2) the original acetylene black; 3) Spheron-6 black, baked at 1700°.

As a nonporous carbon adsorbent, free of surface oxides, we chose stove black, subjected to a preliminary baking at 1250°. The hydrogen index of the suspension, prepared from the stove black, was above 7. The results of an elementary analysis of this black [7] indicated an insignificant surface-oxide content. Measurements (Fig. 3b) showed that, for baked stove black, the elevation of the desorption branch above the adsorption was likewise quite insignificant.

In the cases studied, where hysteresis was observed, any influence of surface oxides on the adsorption was completely excluded. The rapid establishment of equilibrium on the adsorption, as well as the desorption branch of the isotherm, showed the absence of activated adsorption. The carbon surfaces could be considered relatively smooth and nonporous, but the character of the adsorption interaction with ammonia is different, and this shows up, in part, in the hysteresis value (Figs. 2 and 3a).

The change in the adsorption affinity toward ammonia on a nonporous, unoxidized carbon surface was verified by us on the following blacks: channel black, and black graphitized at 1700°, acetylene black untreated, and acetylene black treated by the method described.

The German acetylene black P-1250 was treated with benzene in such a way that the original surface was covered by at least a single monolayer of carbon. The absolute adsorption isotherms of ammonia on the original and the treated acetylene black are compared (Fig. 4) with the isotherm for graphitized black [8]. As may be seen from Fig. 4, as a result of the treatment, the specific surface of the acetylene black, determined by the "BET"* from the low-temperature adsorption of ammonia, was reduced from 72 to 59 m^2/gm, and the adsorption isotherm of the treated black showed noticeable hysteresis. On the original and graphitized blacks, the desorption at $p/p_s < 0.3$ was not measured. The desorption points at $p/p_s > 0.3$ fitted satisfactorily on the adsorption branch. In [6], it was shown that hysteresis is insignificant in the adsorption of ammonia on graphitized black.

Comparing the curves (Fig. 4), it is interesting to note the increase in the absolute value of the adsorption of ammonia on decomposition carbon, as compared with the original acetylene black. This increase in adsorption may be compared with the increase in catalytic activity, described by Tesner [9] for an analogous case: the reaction $C_6H_6 = 6C + 3H_2$ goes more rapidly on the decomposition carbon than on the surface of the original acetylene black. Tesner's conclusion as to the qualitative change in the surface, when decomposition carbon is formed upon it, is supported by the comparison of the absolute values of the ammonia adsorption. The temperature of formation of the

* Brunauer, Emmett, and Teller.

decomposition carbon is relatively low (800°). Thus, a lower degree of orientation may be ascribed to it, even in comparison with the original acetylene black. Apparently, on the smooth, unoxidized, carbon surfaces, the absolute ammonia absorption increases on transition from a lesser degree of amorphism to a higher one.

The divergence between the absolute adsorption values for decomposition carbon, and those for graphitized black, are still considerable. Thus, at $p/p_s = 0.1$, the adsorption on treated acetylene black is ten times higher than the adsorption on graphitized black. Also, a divergence like this finds a natural explanation in the difference in degree of orientation of the carbon. Thus, in the absence of porosity or oxides, the absolute values of the ammonia adsorption can be used as a method of comparing different carbonaceous materials.

SUMMARY

1. The rate of establishment of the adsorption equilibrium of ammonia on oxidized carbon black increases markedly with temperature. The role of the chemosorptive interaction of the ammonia in the presence of surface oxides is quite considerable.

2. Adsorption hysteresis was observed at small relative pressures on a number of nonporous, unoxidized, carbon adsorbents. The hysteresis mechanism is apparently not connected with any penetration of ammonia molecules into micropores.

3. The absolute values of the ammonia adsorption on nonporous, unoxidized, carbon surfaces change sharply on going from one carbon modification to another, and can serve to make an approximate estimate of the degree of amorphism of the carbon.

We wish to express our gratitude to P. A. Tesner and N. N. Lezhnev for valuable advice and aid in performing the experiments.

LITERATURE CITED

1. R. B. Anderson and P. H. Emett, J. Phys. Chem. 56, 756 (1952).
2. R. A. Beebe and R. M. Dell, J. Phys. Chem. 59, 754 (1955).
3. K. V. Chmutov, Technique of Physical Chemical Experiments [in Russian] (1954) p. 72.
4. H. L. McDermott and I. C. Arnell, J. Phys. Chem. 58, 492 (1954).
5. P. A. Tesner and I. S. Rafal'kee, Doklady Akad. Nauk SSSR 80, 401 (1951).
6. I. M. Holmes and R. A. Beebe, Canad. J. Chem. 35, 1542 (1957).
7. V. V. Kel'tsev and P. A. Tesner, Carbon Black Properties, Preparation, and Use [in Russian] (1952).
8. A. A. Voskresenskii, Doklady Akad. Nauk SSSR 119, 724 (1958).
9. P. A. Tesner and I. S. Rafal'kee, Transactions of the All-Union Scientific-Research Natural Gas Institute, Reprocessing and Transport of Gas (1953) p. 3.

THERMOMECHANICAL PROPERTIES OF PLASTICIZED ETHYLCELLULOSE

D. I. Gal'perin, V. V. Moshev, and V. G. Stepanova

Perm'

Translated from Kolloidnyi Zhurnal, Vol. 23, No. 1, pp. 8-11, January-February, 1961
Original article submitted July 10, 1959

Thermoplastic polymers are utilized widely in practical applications as structural and fabricating materials at temperatures from −30° to 40°. Manufactured articles from similar thermoplastics are usually formed at 90° and higher by the method of extrusion; in this connection it is of interest to study the temperature dependence of the viscoelastic properties of such materials at temperatures of their processing and use.

For clarifying some of the regularities of the physicomechanical behavior of similar substances, an investigation was carried out on ethylcellulose plasticized with 25% dibutyl phthalate. Such a material represents a semirigid plastic which has sufficient thermal stability in the chemical sense, and is convenient for investigation in regard to its mechanical qualities.

Type K-100 ethylcellulose was plasticized with dibutyl phthalate by introducing the latter into a continuously stirred aqueous suspension of the ethylcellulose, subsequently centrifuging the mass from the water and working it on rollers at 80° to a moisture content of 0.6%. The weight composition of the dried mass: 73% ethylcellulose, 25.5% dibutyl phthalate (DBP), and 1.5% vaseline oil (introduced to reduce adhesion of the mass to the rollers). The test samples were cut or pressed from the rolled sheets.

The thermomechanical investigations of the samples were carried out in a Kargin dynamometric balance [1], in a tensile and compression test apparatus described by Lazurkin [2,3], and in a capillary type plastometer. The first two devices were utilized for determining the glass and flow temperatures, and also the forced elastic properties of the material in the glassy state; the plastometer was used to investigate the fluidity of the ethylcellulose.

Thermomechanical curves were recorded according to the method of Kargin over 2-min periods on disks of 7.5 mm diameter and 5.5 mm height, with a load of 0.45 kg/cm^2. The heating rate was 0.25° per minute.

The tensile test samples had the form of small bars with effective length 16 mm and cross section 2.7 × 2.7 mm. The relative rate of extension was $5.3 \cdot 10^{-5}$ sec^{-1}.

A diagram of the plastometer is shown in Fig. 1. The basic feature of the apparatus is the presence of lateral grooves in the bushings, eliminating adhesive sliding. Losses of pressure with flow at a given volume rate were determined on bushings of different length. This permits the elimination of entrance losses of pressure, which are large in the case of extrusion of rigid plastics. The treatment of the experimental data and plotting of the flow curves was conducted in accordance with the general theoretical representations on the operation of capillary type plastometers [4]. The experiments in the plastometer were carried out at various rates of shear, from $3.1 \cdot 10^{-1}$ to $6.4 \cdot 10^{-4}$ sec^{-1}. The temperature of the experiments was varied from 60° to 140°.

From the thermomechanical curve (Fig. 2) obtained on the Kargin dynamometric balance, it follows that the glass temperature (T_g) of the plastic under investigation is about 67°, and the flow temperature (T_f) is above 140°; higher temperatures were not investigated in view of possible destruction of the material.

In Fig. 3 there is shown the temperature dependence of the limit forced elasticity σ_e, obtained by the method of Lazurkin [2,3]. The glass temperature is recorded as the point of intersection of the extrapolated curve

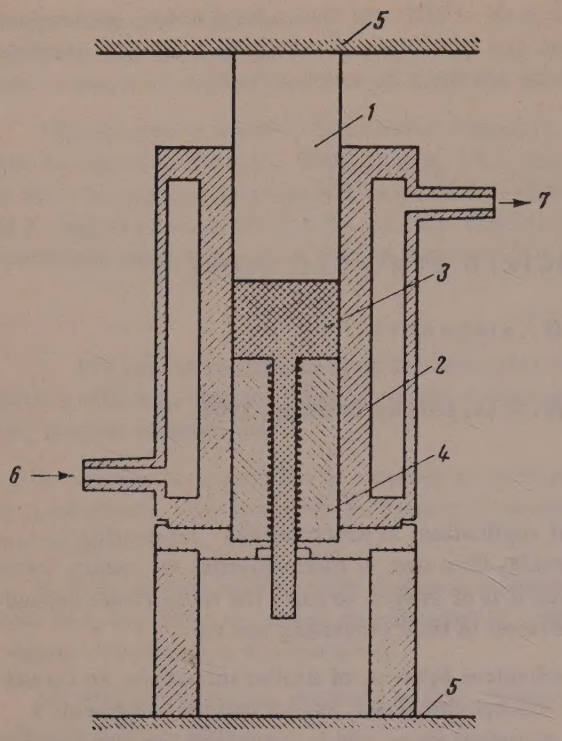


Fig. 1. Diagram of capillary type plastometer: 1) plunger; 2) cylinder; 3) ethylcellulose mass; 4) removable bushing; 5) plate of mechanical press; 6) and 7) inlet and outlet of thermostating liquid.

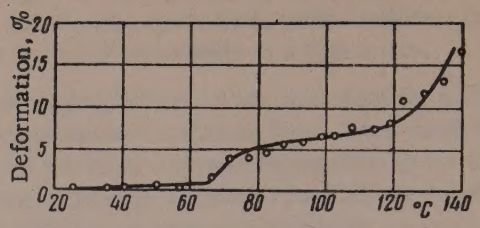


Fig. 2. Thermomechanical curve of ethylcellulose plastic.

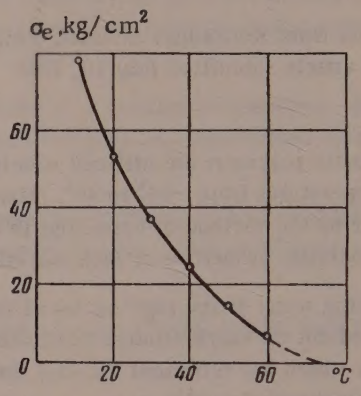


Fig. 3. Temperature dependence of limit of forced elastic deformation σ_e at deformation rate $v = 5.3 \cdot 10^{-5}$ sec^{-1}.

with the temperature axis ($\sigma_e \to 0$), and is equal to approximately 72°, which is close to the corresponding value determined on the dynamometric balance.

The results obtained show that the polymeric system under consideration, with the time schedule selected for its investigation, exists in the glassy state below 70°; in the interval from 70° to 140° or higher, it is a highly elastic material; and at still higher temperatures it passes over to the state of fluidity. The curve $\sigma_e = f(T)$ (Fig. 3) has a character that is typical for cellulosic plastics [3,5].

The results of the rheological investigation of the ethylcellulose are shown in Fig. 4 in the form of flow curves (relationship between shearing stress τ and the corresponding rate of shear $\dot{\gamma}$). From Fig. 4 it follows that the system under consideration is characterized over the entire range of temperatures (from 60° to 140°) by a sharply expressed nonlinear relationship between rate of shear and stress. On logarithmic coordinates (Fig. 5), the resulting rheological characteristics are linearized, which permits writing the relationship between stress and rate of shear in the form of the well-known empirical formula used widely in application to polymeric substances:

$$\dot{\gamma} = k\tau^n,$$

where $\dot{\gamma}$ is the rate of shear (sec^{-1}), τ is the shearing stress (kg/cm^2), and $\underline{k}$ and $\underline{n}$ are empirical constants for the given temperature. The variation of $\underline{k}$ and $\underline{n}$ within the range of temperatures investigated is shown in the table.

T°,C	60	70	80	90	100	120	140
n	4,8	4,4	4,3	4,2	4,1	4,0	3,5
k	$2,8 \cdot 10^{-8}$	$4,8 \cdot 10^{-6}$	$1,8 \cdot 10^{-3}$	$1,3 \cdot 10^{-2}$	$2,6 \cdot 10^{-1}$	4,8	17,8

The value of $\underline{n}$ is a convenient index of the nonlinearity of the system properties. For normal Newtonian liquids, in which the rate of shear is directly proportional to the shearing stress, n = 1. The greater is $\underline{n}$, the greater is the deviation of the liquid properties from the Newtonian flow law. In the case under consideration, the value of $\underline{n}$ averages 4.0, regularly decreasing from 4.8 at 60° to 3.5 at 140°.

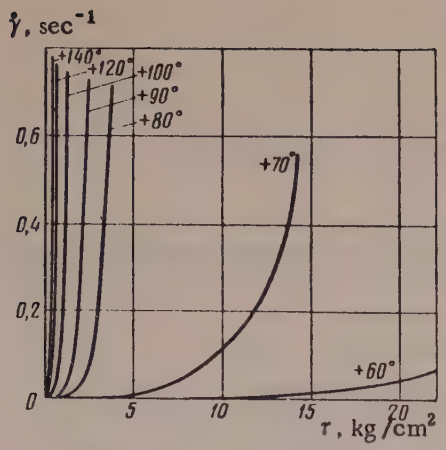


Fig. 4. Flow curves of ethylcellulose plastic at various temperatures.

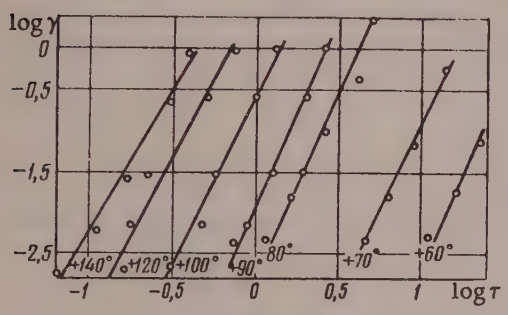


Fig. 5. Flow curves of ethylcellulose plastic on logarithmic coordinates.

The cited data show that, at shearing stress from 0.1 to 25 kg/cm^2, the ethylcellulose plastic is able to flow irreversibly at a temperature considerably below the flow temperature, and even below the glass temperature. In a similar manner, in the polymer under consideration, greater stresses cause high elastic deformations below the glass temperature (phenomenon of forced elasticity).

In deformation under higher stresses, the relaxation times and the corresponding values of micro- and macroviscosity are decreased markedly, owing to the reduction of the activation energy barrier. For forced elastic deformation below T_g, this concept has been expressed by Aleksandrov [6], and Lazurkin [3], and for flow by Eyring [7], Frenkel' [8], Gurevich [9], and others.

The usual methods of determining glass and flow temperatures give a representation of the temperature points of transition only for certain standard conditions, which are characterized by very low loads or the complete absence of load (for example, in dilatometric measurements). Therefore, the transition temperatures should not be regarded as absolute limits dividing the different possible types of deformation of the material, not only because of the necessity of accounting for the time schedule of determining these characteristics, but also because the physical significance of these transition temperatures assumes that the relaxation period is influenced only by temperature and not by external forces. The latter are either absent or are insignificantly small.

It is noteworthy that the flow curves of the plastic show pronounced nonlinearity (large values of $\underline{n}$) even at high temperatures which approach the region of the viscous-fluid state (140°). Probably the polymers acquire the properties of Newtonian liquids only at sufficiently high temperatures, which lie several tens of degrees above the flow temperature determined by the usual methods.

It is also interesting to note that the nonlinearity of the plastic properties (value of $\underline{n}$) not only shows little change with temperature within the range tested, but remains almost constant within the larger interval of rate of shear from 0.3 to $5 \cdot 10^{-4}$ sec^{-1}, even though it could have been expected that, at low rates, a tendency would be manifested for $\underline{n}$ to decrease to unity. This situation evidently denotes the fact that transition to Newtonian flow character is determined not by low rates of shear, but depends on the magnitude of the shearing stress, and is manifested only at very low values of the shearing stress, calculated in fractions of a gram per square centimeter, which is realized only in low-viscosity liquids.

SUMMARY

1. A study has been conducted on the thermomechanical properties and fluidity of ethylcellulose plasticized with dibutyl phthalate, at temperatures from 10° to 140°. The glass and flow temperatures have been determined.

2. At shearing stress from 0.1 to 25 kg/cm^2 the ethylcellulose is capable of irreversible flow at a temperature considerably below the flow temperature, and even below the glass temperature.

LITERATURE CITED

1. V. A. Kargin and T. I. Sogolova, Zhur. Fiz. Khim. 23, 530 (1949).
2. Yu. S. Lazurkin and R. L. Fogel'son, Zhur. Tekh. Fiz. 21, 267 (1951).
3. Yu. S. Lazurkin, Doctoral Dissertation [in Russian] (Institute of Physical Problems, AN SSSR, 1954).
4. M. Reiner, Deformation and Flow (1949)
5. M. Wadano, Kolloid. Zhur. 92, 362 (1940); 93, 103 (1940).
6. N. P. Aleksandrov, Transactions of the First and Second Conferences on High Molecular Weight Compounds [in Russian] (AN SSSR Press, 1945) p. 49.
7. R. Ewell and H. Eyring, J. Chem. Phys. 5, 726 (1937).
8. Ya. I. Frenkel', Kinetic Theory of Liquids [in Russian] (AN SSSR Press, 1945).
9. G. I. Gurevich, Zhur. Tekh. Fiz. 17, 1941 (1947).

QUICK AND THIXOTROPIC PROPERTIES OF DISPERSE SEDIMENTARY ROCKS

I. M. Gor'kova

Moscow Laboratory of Hydrogeology Problems, Academy of Sciences of the USSR
Translated from Kolloidnyi Zhurnal, Vol. 23, No. 1, pp. 12-19, January-February, 1961
Original article submitted December 24, 1959

In engineering geology practice there are known fine-sandy and pulverized rocks, in particular fine-grained sands with admixture of colloidal particles and organic material (true quicksands) which lose stability suddenly and swell catastrophically upon shock [1]. There are also encountered "quick-clays" which, with moisture above the liquid limit, display a sharp reduction of solidity upon mechanical action [2], and which cause great damage by sudden swelling.

For a scientifically based quantitative evaluation of the quick and thixotropic properties of sedimentary rocks, which properties are of prime importance for engineering geology, certain rheological investigations were carried out on a number of sedimentary rocks in the light of modern concepts of physicochemical mechanism [3].

The following rocks were studied:

Quaternary alluvial-estuary sandy-colloidal rocks (true quicksands) of the Salekhard district, from a depth down to 60 m, with structure broken down in sampling. The dispersion structures of these rocks are of the stabilization type. Their peculiarities are occasioned by a combination of the dilatant properties of the fine-sandy and pulverized constituents (contained in the rock in quantity up to 90% by weight), with the low viscosity of the mass of finely dispersed hydromica (sericite), firmly stabilized by organic material [4].

Deep-water contemporary silts (oozes) of the Black Sea, from a depth down to 60 cm from the sea bottom, sampled by means of piston tubes, with partially broken-down structure. They are highly disperse (particles <1 micron up to 57%), highly porous (up to 90%), and watered (W = 200-300%; W/W_f = 1.9-2.2) sediments, with coagulation structures plasticized by adsorbed and free organic compounds and all types of colloidal admixtures. The fine fractions of these silts are represented by hydrophilic mixed-layer hydromicas (sericites) and kaolinite [5].

Marinte quaternary (Khvalynsk) clays of the Trans-Volga, from a depth down to 10 m, very highly disperse (particles < 1 micron are contained up to 86%), containing absorbed sodium and a considerable quantity of electrolytes (up to 2.5%). The fine fractions of these clays are represented by hydromicas (sericites). Their natural porosity is equal to 41-53%; water content varies from 22 to 42% (W/W_f = 0.4-0.64); monoliths are taken as samples, with a natural syneretically hardened coagulation structure [6].

Marine Jurassic hydromica–kaolinite clays of Baios, Oboyan district, KMA, from a depth of about 480 m, representing compact, syneretically dehydrated coagulation structures; they have low porosity (31-37%) and low natural water content, about 18-21% (W/W_f = 0.4). The content of particles <1 micron in these clays reaches 50-60%. The samples are taken in the form of monoliths with the natural structure [7].

Turon-Kon'yaksk writing chalk of marine deposits of the upper Cretaceous period, district of Voronezh Oblast', from a depth of 10 m. The great bulk of the rock (up to 99%) consists of $CaCO_3$, represented by 60% finely disperse (<5 microns) uncemented (loose) calcite, and by shell fragments. The porosity of the chalk varies from 44 to 55%, the natural water content from 23 to 32% (W/W_f = 0.9-1.4). In the natural deposit the chalk represents syneretically hardened coagulation structures (approaching condensation structures in their properties). Upon breakdown of the natural structure, the chalk acquires some dilatant properties, being decomposed into microaggregates with dimensions of 50 to 5 microns.

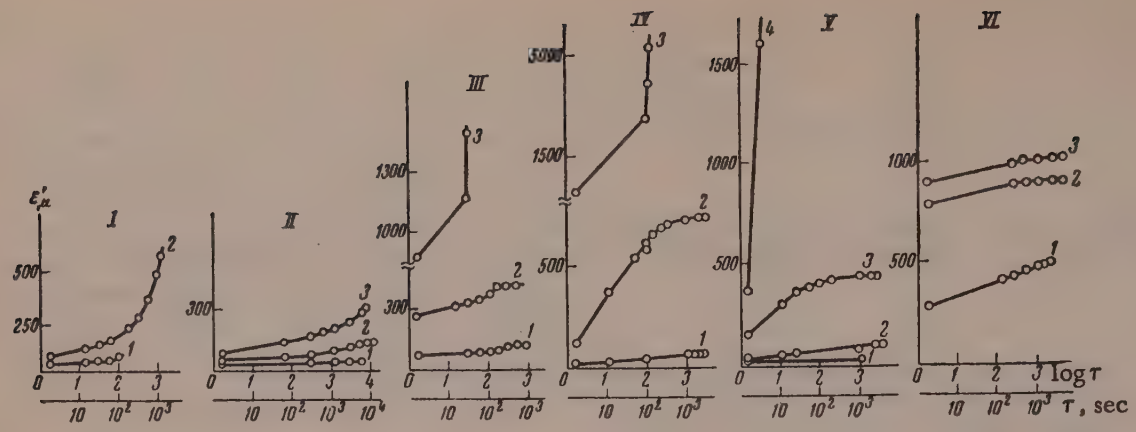


Fig. 1. Kinetics of the development of deformation with different constant shearing stresses: I) sandy-colloidal rocks of Salekhard with W = 24% (after vibration); value of P, dynes/cm^2: 1) $2.6 \cdot 10^3$; 2) $3.2 \cdot 10^3$. II) Contemporary silts of the Black Sea from 50-cm depth, W = 100% ($W/W_f = 1.8$); value of P, dynes/cm^2: 1) $9.8 \cdot 10^2$; 2) $2 \cdot 10^3$; 3) $3.3 \cdot 10^3$. III) Sandy-colloidal rocks of Salekhard, with W = 29%; value of P, dynes/cm^2: 1) $7 \cdot 10^2$; 2) $2.9 \cdot 10^3$; 3) $6.4 \cdot 10^3$. IV) Khvalynsk clay from 7-m depth, with W = 84% ($W/W_f = 1.4$); value of P, dynes/cm^2: 1) $6.5 \cdot 10^3$; 2) $1.3 \cdot 10^4$; 3) $2 \cdot 10^4$. V) Jurassic clay from 500-m depth, with W = 39% ($W/W_f = 0.8$); value of P, dynes/cm^2: 1) 10^4; 2) $2 \cdot 10^4$; 3) $3.9 \cdot 10^4$; 4) $6.5 \cdot 10^4$. VI) Jurassic clay: 1) with W = 28% ($W/W_f = 0.5$), P = $= 1.8 \cdot 10^5$ dynes/cm^2; Jurassic clay with natural structure (2) and (3) with W = 20% ($W/W_f = 0.4$); P = $9.8 \cdot 10^5$ and $1.2 \cdot 10^6$ dynes/cm^2.

Santonian marls of marine deposits of the upper Cretaceous period, district of Voronezh Oblast', from a depth of 10 m. They contain up to 86% of particles <5 microns, and represent compact coagulation structures with a large quantity of active filler in the form of finely disperse calcium carbonate. The natural water content of the marl varies from 21 to 23% ($W/W_f = 0.6$). Clay minerals are represented by montmorillonite.

The rheological and structural-mechanical properties of these rocks were studied by two methods: 1) by the method of obtaining families of curves of the kinetics of development of deformation with different constant shearing stresses, in the apparatus of Tolstoi and Maslov. This method makes it possible to characterize the behavior of disperse rocks with natural or dispersion structure over a wide range of water content, at low shearing stresses in the region of $P_{k-1} - P_r^*$, corresponding to a minimum degree of structural breakdown (Fig. 1).

2) By the method of obtaining complete rheological curves and curves of the dependence of effective viscosity on the working shearing stress, by means of the viscosimeter of Volarovich. This method permits evaluating the behavior of dispersion structures of rocks, with moisture content near the liquid limit, over the entire range of stresses $P_{k-1} - P_m$ and, in particular, at the highest degree of their breakdown (Fig. 2).

The first method made it possible to distinguish three groups of rocks:

1. Liquid-form rocks with stabilization and plasticized structures (for example, sandy-colloidal rocks, silts), which have practically no conventional yield point P_{k-1}, and which exhibit residual deformation at extremely low shearing stresses (0.1-1 g/cm^2) (Fig. 1, I and II). With an increase of shearing stress, there is observed a decrease of the value of the conventional instantaneous modulus of elasticity of the rocks, E_1, by 1.5 to 3 times, which attests to the breakdown of their structure in the process of investigation. Precipitous breakdown of structure sets in at stresses from 1 to 6 g/cm^2. Continuous prolonged submersion of the cone in the study of these rocks confirms their liquid condition.*

* Under water, the sandy-colloidal rocks, the silts, and the liquid clay pastes behave like friable structured systems, maintaining perpendicular walls, forming vertical fissures, and easily cut by a blade into thin layers.

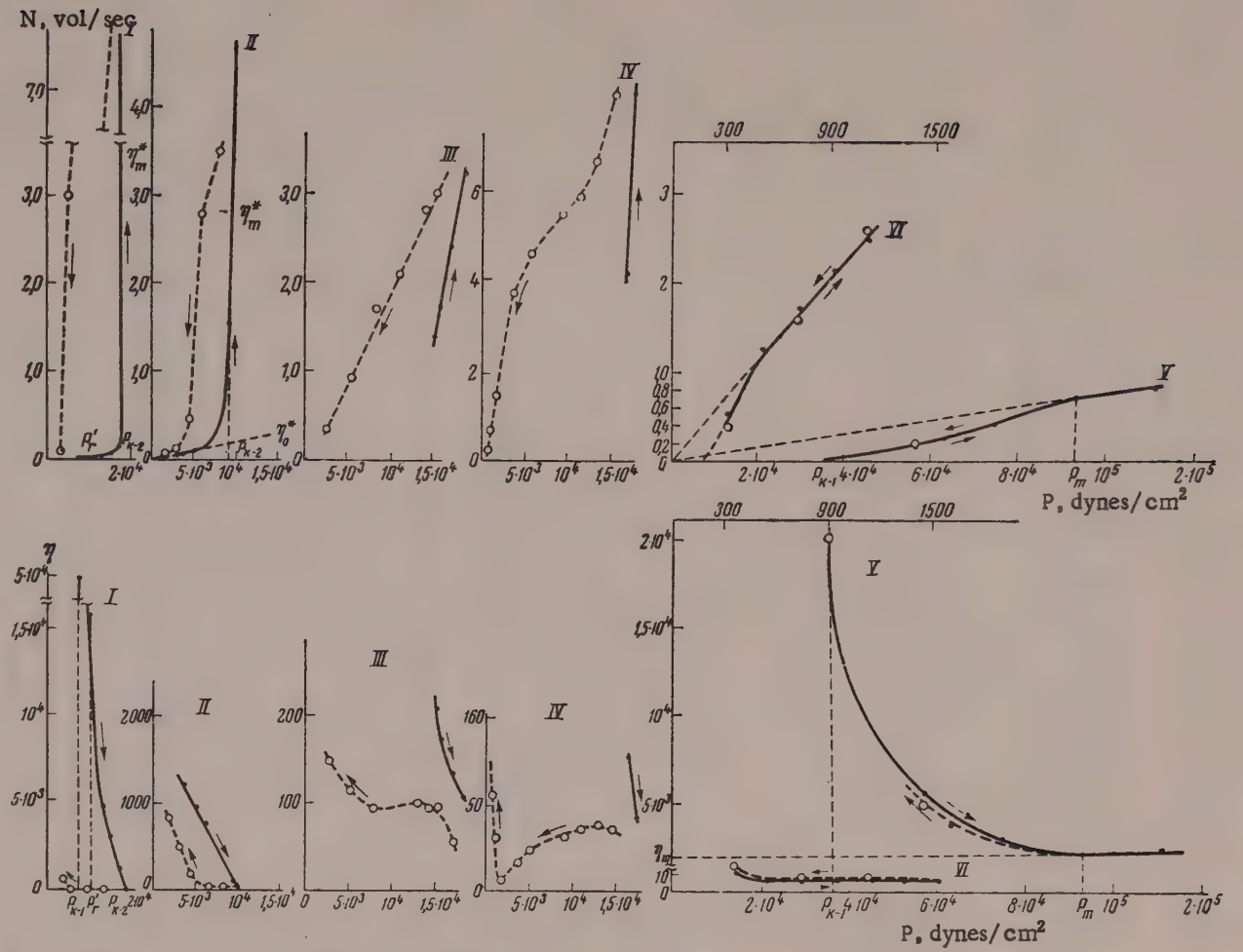


Fig. 2. Rheological curves and curves of the dependence of effective viscosity on working shearing stress (open points – reverse branch): I) Khvalynsk clay from 7.75-m depth, W = 66.5% (W/W_f = 1.12); II) Black Sea silts from 50-cm depth, W = 100% (W/W_f = 1.8); III) writing chalk of Voronezh Oblast' from 4-m depth, W = 29% (W/W_f = 1.09); IV) sandy-colloidal rocks of Salekhard from 54-m depth, W = 26.9%; VI) the same from 56-m depth, W = 58.3%; V) Jurassic clay of KMA from 450-m depth, W = 39.3% (W/W_f = 0.93).

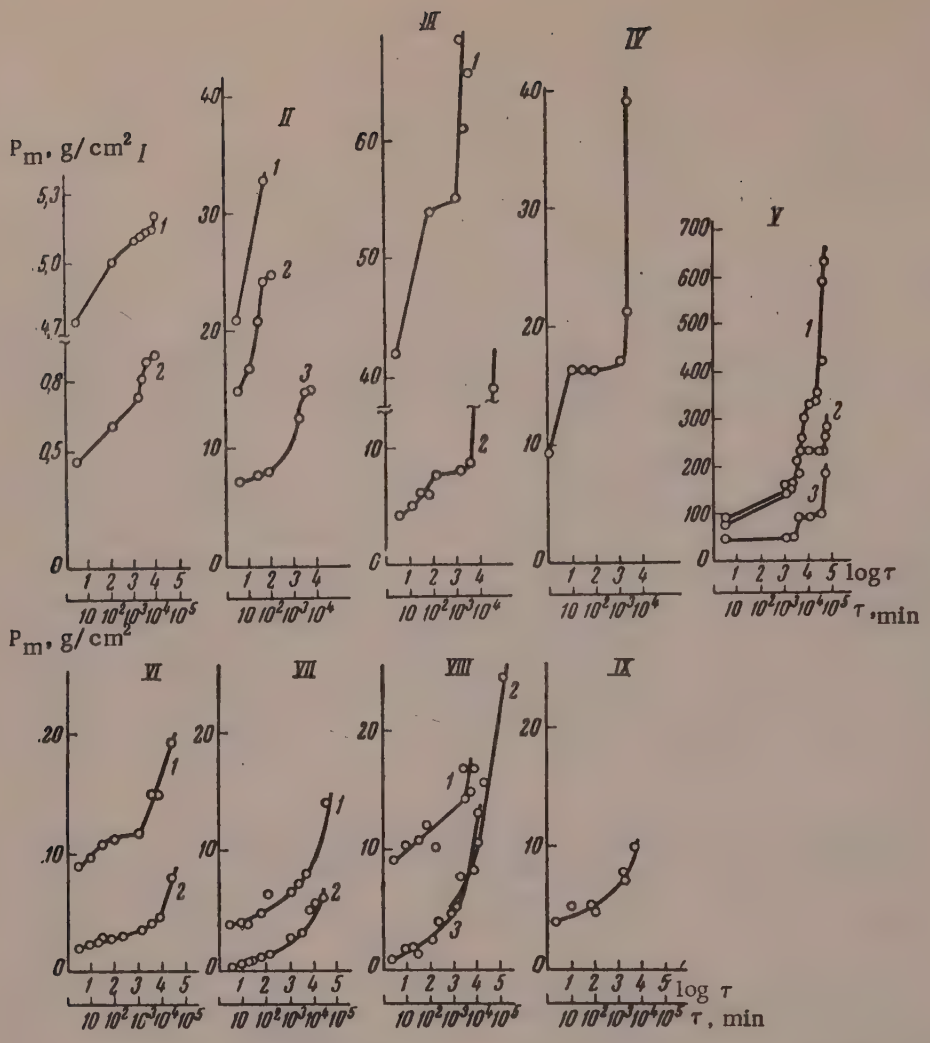


Fig. 3. Kinetics of thixotropic hardening. I) Suspension of Oglanlinsk betonite (according to the data of [9]): 1) 30%; 2) 20%. II) Khvalynsk clay: 1) W = 81-80%; 2) W = 98-95%; 3) W = 130-123%. III) Jurassic clay: 1) W = 54-47%; 2) W = 92-73%. IV) Santonian marl, W = 42%. V) Silts of the Black Sea: 1) from 218-cm depth, W = 41-37%; 2) from 230-cm depth, W = 54-51%; 3) from 60-cm depth, W = 152-117%. VI) Jurassic clayey soil, KMA district: 1) W = 45-42%; 2) W = 60-50%; VII) Jurassic sandy-colloidal rocks: 1) KMA district from 101-m depth, W = 38.6-34.2%; 2) Moscow district, from 60-m depth, W = 44-35%. VIII) Quaternary sandy-colloidal rocks, Salekhard district: 1) from 49-m depth, W = 27.7%; 2) from 52-m depth, W = = 28.5%; 3) from 61-m depth, W = 27.9%. IX) Upper Cretaceous writing chalk, W = = 32%. Kinetics of hardening were determined by: I) torsion apparatus; II), III), VI), VII) Veiler – Rebinder blade; IV), V), VIII), IX) conical Rebinder plastometer.

2. Rocks with loose coagulation structures (clay pastes) with a water content near the liquid limit (W/W_f = = 0.8-1.4), displaying a sharp breakdown of structure with an increase of the constant shearing stress. The value of E_1 is thereby reduced by 26 to 257 times, being changed the most sharply in the case of the Khvalynsk clays (Fig. 1, IV, V).

The rocks of the first and second groups are characterized by considerable hardening under the influence of constant shearing stresses, causing a rapid attenuation of plastic flow and an increase of the value of E_1 by 2-20 times, manifested after momentary unloading of the samples. In the coagulation structures of the silts and clays, a similar hardening is caused by the formation of more stable bonds between the molecules of the organic

material and the oriented clay particles in the process of deformation. In stabilization structures it is caused by the random accumulation of pulverized and sandy particles in the planes of shear (dilatancy) with an increase of the friction between them.

3. Semisolid (Jurassic) clays with compact structures with $W/W_f = 0.5\text{-}0.4$, distinguished by a capacity for slow plastic flow of the creep type, with the greatest stable viscosity (practically without breakdown of structure) in the interval of stresses $P_{k-1} - P_r^*$. The conventional yield point of these rocks is increased to 200-600 g/cm^2, and precipitous breakdown of structure appears at 400-2000 g/cm^2 (Fig. 1, VI).

Thus, in the region of low stresses ($P_{k-1} - P_r^*$) far from the breakdown stresses, there is an entirely clear demonstration of the characteristic features of the behavior of rocks in deformation, depending on their structure and the character of the structural bonds.

The viscosimetric investigations make it possible to distinguish two types of rocks in accordance with their behavior upon complete destructurization: 1) rocks distinguished by a small drop of viscosity for the least and most broken-down structures $\eta_0/\eta_m = 4\text{-}23$; 2) rocks which sharply liquefy within a narrow range of stresses, and are distinguished by a large drop of viscosity on breakdown of their loose structure, $\eta_0/\eta_m = 10^2\text{-}10^6$.

The first type includes sandy-colloidal rocks with water content above 27-30% (and also other disperse rocks in the fluid state), which practically do not have any P_{k-1}, and which flow with breakdown of structure with the lowest stable viscosity (about 10 poises)(Fig. 2, VI). The flow of similar layers of true quicksands on slopes often causes a settling or collapsing of the superincumbent strata. Other representatives of rocks of this type are the Jurassic clays of KMA from a depth of occurrence of about 500 m. In contrast with the liquid-form rocks, they possess marked limits P_{k-1} and P_m, but flow as very viscous liquids with the lowest constant viscosity equal to 500-2000 poises with $W/W_f = 0.8$ (Fig. 2, V). Similar rocks are prone to the formation of slides:flows and slide extrusion on the base of the slopes.

Sandy-colloidal rocks with water content of 27-20% or lower, writing chalk, Khvalynsk clays, and silts with water content near the liquid limit belong to the second type of rocks. Dilatant fine-sandy, pulverized, and pseudopulverized rocks (sandy-colloidal rocks and writing chalk), which are hardened and loosened in the process of shear, resist the rheological measurements up to attaining the final deformation, when there occurs a brittle collapse of the contacts between the coarsely dispersed particles or aggregates, and instantaneous release for flow of the finely dispersed mass, including sandy and pulverized particles (η_m = 10-20 poises) (Fig. 2, III, IV).

A similar sudden collapse of the slopes of true quicksands is the cause of many accidents in sinking shafts and mine excavations. Since they are firmly stabilized, they remain in the fluid state for long periods. Writing chalk is liquified in well drilling, with opening of the rock excavations. Slides,cave-ins, or total collapse often may result.

Finely dispersed high-porosity silts (having practically no P_{k-1}) and Khvalynsk clays are sharply liquefied at stresses above the dynamic yield point P_{k-2}, reaching η_m which, at this water content, is equal to 10-40 poises, owing to the low concentration of the suspension formed upon liberating the water of the pores (Fig. 2, I, II). Therefore, the silt stratum studied abounds in all types of submerged slides, heaves, and dislocations. The Khvalynsk clays,when wetted on the slopes of canals, give sharply pronounced slip phenomena.

Rocks of the second type (Fig. 2, I-IV), in which there is observed a sharp drop of viscosity of several orders of magnitude, owing to breakdown of structure on deformation, are deservedly termed "quick" in the international literature, i.e., suddenly liquefied.

With transition of the rocks to the plastic state, with an increase of density and a decrease of hydration, the degree of breakdown of their structure under the influence of stress is reduced, and the capacity for sharp liquefaction is gradually lost. The magnitude of the ratio η_0/η_m at $W/W_f = 0.8$, decreases to 30-100, and the viscosity η_m increases to 300-600 poises or higher. The value of E_1 is decreased not more than 4-6 times on increasing the shearing stress. For Jurassic and Khvalynsk clays: P_{k-1} = 10-14 g/cm^2, P_r^* = 35-40 g/cm^2; P_m = = 80-90 g/cm^2, $E_1 = 10^6$ dynes/cm^2; $E_2 = 10^5$ dynes/cm^2.

With a decrease of relative water content ($W/W_f < 0.5$), the clays acquire a capacity for flow of the creep type, owing to rapid recovery of structure in the process of flow. Hence, the same rocks in different stages of formation, and under different conditions of occurrence, may differ sharply in their rheological behavior. The

nature of the diagenetic and epigenetic processes of petrogenesis also results in a gradual change of the properties of sedimentary rocks from liquid- to solid-form, from quick to capable of creep.

The investigations of the change of effective viscosity with a decrease of the working shearing stress showed that, in quick rocks, the broken-down structure is recovered only below the conventional yield point, the value of which is usually reduced in connection with the increase of mobility of the system. The higher the ratio η_0/η_m, the greater is the observed hysteresis loop in the recovered viscosity.

In rocks which are capable of flow with the greatest constant viscosity of the creep type, and with the lowest constant viscosity of the broken-down structure, the structure is recovered at once to the extent of reduction of the working stress.

Investigations [8] have shown that, upon intensive vibration, all clayey rocks, even semidry Cambrian clays, are liquefied, liberating water, but are immediately solidified when the action ceases. Hence, all uncemented (loose) disperse rocks which have residual hydration layers in the sites of contacts of the particles are thixotropic and can momentarily occur in the liquefied, flowing state. Practical significance is attached to the intensity of the action required for reducing the rocks to the fluid state, the value of viscosity of their completely broken-down structures, and the possible duration of their residence in the liquefied state.

An investigation of thixotropic hardening of dispersion structures of rocks was conducted by means of measuring the increase of the ultimate shearing stresses with respect to time, in apparatus of the Veiler – Rebinder type, and by the conical plastometer of Rebinder (Fig. 3).

The bentonite suspensions [9], the Khvalynsk and Jurassic clays, the marls, and the silts over a wide range of concentrations have identical character of the kinetics of structure formation after destructurizing by thorough mixing, fully conforming to the classical concepts of colloid chemistry (Fig. 3, I-V). The greater the dispersity and concentration of particles of the solid phase, the greater the rate of thixotropic hardening.

After a few days, a marked hardening sets in (for the rocks investigated), simultaneously with a certain loss of water, evidently in consequence of syneretic processes.

The preliminary destructurizing of the sandy-colloidal rocks and the chalk was carried out not by mixing, as in the case of the clays, since it contributes to their intense hardening, but by vibration, which causes breakdown of the structural bonds, and contraction of the rocks. The subsequent thixotropic hardening of these rocks, which are distinguished by a low concentration of structure-forming , highly disperse particles, is explained by the spontaneous tightening of the packing of the pulverized and fine-sandy particles, and by slow syneresis, as a result of which dense, low-water structures develop, and separation of water occurs (Fig. 3, VII-IX). In proportion to the caking of the particles, the bonds between them are gradually strengthened; however, this process takes place more slowly than in highly disperse rocks, notwithstanding the considerably higher concentration of the solid phase.

The clayey soils have an intermediate character of the kinetics of hardening (Fig. 3, VI).

In evaluating the thixotropic (structure-forming) ability of rocks according to the final hardness of the statically developed structures, the rocks which were studied are placed in the following order: 1) fluid but not quick, instantaneously but little-hardened types (liquid true quicksands); 2) highly quick, but with slow and weak thixotropic hardening, types (true quicksands, chalk); 3) highly quick and strongly thixotropically hardened types (Khvalynsk and other clays at the liquid limit); 4) nonquick, instantly thixotropically hardened types (Jurassic and other clays at the limit of expansion).

SUMMARY

1. Rheological investigations of a number of sedimentary rocks over a wide range of stresses which covers the regions of practically no breakdown and complete breakdown of structures, has made it possible to show the nature of creep, quickness, fluidity, and percolation in thixotropic and dilatant rocks. The rheological properties of the rocks should be taken as a basis for their classification for the purpose of engineering geology.

2. The quickness of the rocks is caused by the presence in them of unstable loose structures, and is explained by the high fluidity ($1/\eta$) attained with complete destructurization, and the liberation of the immobilized water. The quickness of the rocks is most pronounced at a water content near to or above the liquid limit, and is

determined by the following quantitative characteristics: yield points (P_{k-1}; P_{k-2}) and ultimate strengths (P'_r; P_m); ratio of viscosities of the least and most broken-down structures η_0/η_m; viscosity of the most broken-down structure η_0; ability to recover the broken-down structure and the rate of this process.

3. Highly disperse plastic rocks (silts, clays), quick and thixotropically recovered broken-down structures in time at water content near the liquid limit possess a capacity for pronounced flow of the creep type, owing to the instantaneous thixotropic hardening at water content below the limit of adherence. The capacity for thixotropic structure formation in them is manifested over a wide range of concentrations, owing to the pronounced interparticle adhesion.

4. Fine-sandy and pulverized rocks (sandy loams, loesses, chalk, and others) are distinguished by dilatant properties. They are hardened and loosened upon deformation, swell markedly in a state of complete water saturation upon reaching maximum deformation, and display considerable contraction of the broken-down structures at rest, causing a different type of settling and sag (for example, in loesses). Similar rocks are little and slowly hardened with time, notwithstanding the high concentration of the solid phase, owing to the weakly marked interparticle or interaggregate adhesion.

LITERATURE CITED

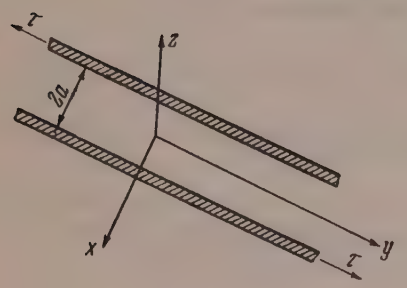
1. A. F. Lebedev, Volgostroi No. 3 (1935); N. N. Maslov, Conditions of Stability of Inclines and Slopes in Water Power Construction (Gosénergoizdat, 1955); Coll. Trans. LITI No. 18 (1954).
2. E. Ackermann, Geologishe Rundschau 36, (Dec., 1948); L. Bjerrum, Geotechnique 4, No. 2 (1954); P. Holmsen, Geotechnique 3, No. 5 (1954); G. Th. Rosenquist, Geotechnique 3, No. 5 (1954); 5, No. 6 (1956).
3. G. V. Vinogradov and K. I. Klimov, Doklady Akad. Nauk SSSR 57, 911 (1947); Zhur. Tekh. Fiz. 18, 355 (1948); M. P. Volarovich and N. I. Malinin, Kolloid. Zhur. 20, 3, 311 (1958); M. P. Volarovich and D. M. Tolstoi, Zhur. Fiz. Khim. 4, 6, 815 (1934); N. V. Mikhailov and P. A. Rebinder, Kolloid. Zhur. 17, 107 (1955); P. A. Rebinder, Transactions of Conference on Engineering Geological Properties of Rocks and Methods of Their Study (Izd. AN SSSR, 1956) Vol. 1, p. 31; E. A. Segalova and P. A. Rebinder, Kolloid. Zhur. 10, 223 (1948); N. N. Serb-Serbina and P. A. Rebinder, Collected Proceedings of the International Conference on Clays, in Brussels [Russian translation] (AN SSSR, Moscow, 1958) p. 115; N. V. Tyabin and G. V. Vinogradov, Abstracts of Proceedings of the Fourth All-Union Conference on Colloid Chemistry (Izd. AN SSSR, 1958).
4. I. M. Gor'kova, Transactions of Conference on Engineering Geological Properties of Rocks and Methods of Their Study (AN SSSR Press, 1956) Vol. 1, p. 98.
5. I. M. Gor'kova, N. A. Dushkina, and K. N. Ryabicheva, Collection: To the Knowledge of Diagenesis (Izd. AN SSSR, 1959).
6. V. A. Priklonskii, I. M. Gor'kova, N. A. Oknina, et al., Trudy Lab. Gidrogeologich. Problem Akad. Nauk SSSR 13 (1956).
7. I. M. Gor'kova and K. N. Ryabicheva, Trudy Lab. Gidrogeologich. Problem Akad. Nauk SSSR 22 (1959).
8. B. M. Gumenskii, Kolloid. Zhur. 16, 421 (1954); Vibrodrilling of Clay Soils [in Russian] (Leningrad, 1954).
9. L. A. Abduragimova, P. A. Rebinder, and N. N. Serb-Serbina, Kolloid. Zhur. 17, 184 (1955).

EXTRUSION OF A VISCOPLASTIC DISPERSED PHASE BETWEEN SLIDING PLANE-PARALLEL WALLS

A. M. Gutkin

Moscow Energy Institute, Department of Physics
Translated from Kolloidnyi Zhurnal, Vol. 23, No. 1, pp. 20-24, January-February, 1961
Original article submitted December 19, 1959

To investigate abnormally viscous and viscoplastic dispersed phases under the conditions of a complex state of stress, it is of interest to analyze very simple cases of such a state. An example is when displacement takes place in a body in two mutually perpendicular directions. This problem was considered by Vinogradov, Pavlov, and Mamakov [1]. They obtained a considerable amount of experimental data on the flow of homogeneous lubricants, extruded through a narrow gap between two coaxial cylinders, one of which is rotated. Since these authors did not aim at specific rheological equations of state, they limited themselves to a qualitative discussion of the results. But quantitative conclusions from experiments on a complex state of stress can only be drawn by taking as a basis a specific model of a body.



We will consider the problem of the flow of a Shvedov–Bingham viscoplastic medium in a planar gap under the effect of a pressure acting in one direction, and a tangential stress acting in a perpendicular direction. We will set the axis (see figure) perpendicular to the walls. Let the tangential stress τ act along the y axis, and a decreasing pressure p act in the direction of the z axis. From considerations of symmetry and boundary conditions, it follows that $v_x = 0$ and v_y and v_z depend only on x.

Hence, the intensity of the shear rate h is equal to [2]:

$$h = \sqrt{\left(\frac{dv_y}{dx}\right)^2 + \left(\frac{dv_z}{dx}\right)^2}. \qquad (1)$$

The components of the stress tensor are expressed as

$$p_{xx} = p_{yy} = p_{zz} = -p;\ p_{xy} = \left(\mu + \frac{\theta}{h}\right)\frac{dv_y}{dx};\ p_{xz} = \left(\mu + \frac{\theta}{h}\right)\frac{dv_z}{dx};\ p_{yz} = 0, \qquad (2)$$

where θ is the ultimate shear stress.

For the given case, the equilibrium equations have the form

$$\frac{dp_{xz}}{dx} = \frac{dp}{dz};\quad \frac{dp_{xy}}{dx} = 0. \qquad (3)$$

Integration of Eq. (3) gives

$$p_{xz} = \frac{dp}{dz}x + C;\ p_{xy} = \text{const} = \tau. \qquad (4)$$

Since the stress components p_{xz} on the right- and left-hand boundaries of the gap can differ only in sign, the constant C in the first equation of (4) must be assumed to be zero.

Hence, from Eqs. (2) and (4), we have

$$\frac{p_{zx}}{p_{yx}} = \frac{\frac{dv_z}{dx}}{\frac{dv_y}{dx}} = \frac{x}{\tau}\frac{dp}{dz}, \tag{5}$$

and the intensity of the shear rate is

$$h = \left|\frac{dv_y}{dx}\right| \sqrt{1 + \frac{x^2}{\tau^2}\left(\frac{dp}{dz}\right)^2}. \tag{6}$$

Substituting Eq. (6) in Eq. (2), and employing Eq. (4), we obtain

$$\frac{dv_y}{dx} = \frac{\tau}{\mu} - \frac{\theta \frac{dv_y}{dx}}{\mu\left|\frac{dv_y}{dx}\right| \sqrt{1 + \frac{x^2}{\tau^2}\left(\frac{dp}{dz}\right)^2}}; \tag{7}$$

$$\frac{dv_z}{dx} = \frac{x}{\mu}\frac{dp}{dz} - \frac{\theta \frac{dp}{dz} x \frac{dv_y}{dx}}{\mu\tau\left|\frac{dv_y}{dx}\right| \sqrt{1 + \frac{x^2}{\tau^2}\left|\frac{dp}{dz}\right|^2}}. \tag{8}$$

Before integrating Eqs. (7) and (8), it is necessary to establish the coordinates of the elastic zone, because Eqs. (7) and (8) hold true only in the zone of flow, i.e., where

$$T \geqslant \theta, \tag{9}$$

where $T = \sqrt{p_{xy}^2 + p_{xz}^2}$ is the intensity of the tangential stresses. If, instead of p_{xy} and p_{xz} we substitute their expressions, Eq. (9) assumes the form:

$$\sqrt{\tau^2 + x^2\left(\frac{dp}{dz}\right)^2} \geqslant \theta. \tag{10}$$

From (10) it follows that the elastic zone occupies an area

$$-x_1 \leqslant x \leqslant x_1,$$

where

$$x_1 = \frac{\sqrt{\theta^2 - \tau^2}}{\left|\frac{dp}{dz}\right|}. \tag{11}$$

From Eq. (11) it follows that, if the tangential stress $p_{xy} = \tau \geq \theta$, the elastic zone disappears, and viscous stresses occur in the whole gap.

At the boundaries of the elastic zone, dv_y/dx and dv_z/dx must become zero.

From Eq. (7) it follows that, throughout the whole region of flow,

$$\frac{dv_y}{dx} > 0.$$

Hence, Eqs. (7) and (8) can be rewritten in the form

$$\frac{dv_y}{dx} = \frac{\tau}{\mu} - \frac{\theta}{\mu\sqrt{1 + \frac{x^2}{\tau^2}\left(\frac{dp}{dz}\right)^2}}; \tag{12}$$

$$\frac{dv_z}{dx} = \frac{x}{\mu}\frac{dp}{dz} - \frac{\theta\frac{dp}{dz}x}{\mu\tau\sqrt{1+\frac{x^2}{\tau^2}\left(\frac{dp}{dz}\right)^2}} \tag{13}$$

Integrating Eq. (13), and taking into account that $v_z = 0$ when $x = \pm a$, we obtain

$$v_z = \frac{1}{2\mu}\frac{dp}{dz}(x^2 - a^2) - \frac{\frac{dp}{dz}\theta\tau}{\mu\left(\frac{dp}{dz}\right)^2}\left(\sqrt{1+\frac{x^2}{\tau^2}\left(\frac{dp}{dz}\right)^2} - \sqrt{1+\frac{a^2}{\tau^2}\left(\frac{dp}{dz}\right)^2}\right). \tag{14}$$

The value of the flow through a unit length of the capillary is

$$Q = 2\left(v_{z_0}x_1 + \int_{x_1}^{a} v_z dx\right) = -\frac{2}{3\mu}\frac{dp}{dz}(a^3 - x_1^3) - \frac{\theta}{\mu}\left(a\sqrt{a^2+\frac{\tau^2}{\left|\frac{dp}{dz}\right|^2}} - \frac{x_1\theta}{\left|\frac{dp}{dz}\right|}\right) +$$

$$+ \frac{\theta\tau^2}{\mu\left|\frac{dp}{dz}\right|^2}\ln\frac{a\left|\frac{dp}{dz}\right| + \sqrt{\tau^2 + a^2\left|\frac{dp}{dz}\right|^2}}{\theta + \sqrt{\theta^2 - \tau^2}}. \tag{15}$$

With $\tau = 0$, the equation for Q is converted to the previously obtained Eq. (3).

Equation (15) is only correct with $\tau \leq \theta$. If $\tau \geq \theta$, the width of the zone is zero, and the flow through a unit length of the capillary is expressed by the equation

$$Q = -\frac{2a^3}{3\mu}\frac{dp}{dz} - \frac{\theta a}{\mu}\sqrt{a^2+\frac{\tau^2}{\left|\frac{dp}{dz}\right|^2}} + \frac{\theta\tau^2}{\mu\left(\frac{dp}{dz}\right)^2}\ln\frac{a\left|\frac{dp}{dz}\right| + \sqrt{\tau^2 + a^2\left|\frac{dp}{dz}\right|^2}}{\tau} \tag{16}$$

The velocity v_y is obtained from Eq. (12) if it is assumed that the left-hand plate of the capillary is stationary, i.e., $v_y = 0$, with $x = -a$, it is found that

$$v_y = \frac{\tau(x+a)}{\mu} - \frac{\theta\tau}{\mu\left|\frac{dp}{dz}\right|}\ln\frac{\left|\frac{dp}{dz}\right|x + \sqrt{\tau^2 + x^2\left(\frac{dp}{dz}\right)^2}}{-\left|\frac{dp}{dz}\right|a + \sqrt{\tau^2 + a^2\left(\frac{dp}{dz}\right)^2}} \tag{17}$$

with $-a \leq x \leq -x_1$ and

$$v_y = \frac{\tau(a - 2x_1 + x)}{\mu} -$$

$$- \frac{\theta\tau}{\mu\left|\frac{dp}{dz}\right|}\ln\frac{\left(-x_1\left|\frac{dp}{dz}\right| + \sqrt{\tau^2 + x_1^2\left(\frac{dp}{dz}\right)^2}\right)\left(x\left|\frac{dp}{dz}\right| + \sqrt{\tau^2 + x^2\left(\frac{dp}{dz}\right)^2}\right)}{\left(x_1\left|\frac{dp}{dz}\right| + \sqrt{\tau^2 + x_1^2\left(\frac{dp}{dz}\right)^2}\right)\left(-a\left|\frac{dp}{dz}\right| + \sqrt{\tau^2 + a^2\left|\frac{dp}{dz}\right|^2}\right)} \tag{18}$$

with $x_1 \leq x \leq a$.

The velocity of the right-hand plate at the fixed values of dp/dz and τ is

$$v_y = \frac{2\tau(a - x_1)}{\mu} - \frac{2\theta\tau}{\mu\left|\frac{dp}{dz}\right|}\ln\frac{\left(a\left|\frac{dp}{dz}\right| + \sqrt{\tau^2 + a^2\left(\frac{dp}{dz}\right)^2}\right)\left(-x_1\left|\frac{dp}{dz}\right| + \sqrt{\tau^2 + x_1\left|\frac{dp}{dz}\right|^2}\right)}{\tau^2} \tag{19}$$

In the absence of an elastic zone, i.e., when $\tau \geq \theta$, the velocity of the right-hand plate is obtained from Eq. (19) if it is assumed that $x_1 = 0$

$$v_y = \frac{2\tau a}{\mu} - \frac{2\theta\tau}{\mu\left|\frac{dp}{dz}\right|} \ln \frac{a\left|\frac{dp}{dz}\right| + \sqrt{\tau^2 + a^2\left(\frac{dp}{dz}\right)^2}}{\tau}. \tag{20}$$

It is seen, therefore, that, in contrast to a truly viscous liquid, for a viscoplastic dispersed phase both tensor components of the rate of flow depend on the value of each of the two stresses causing flow. The principle of superposition is not observed, because a viscoplastic medium is essentially a particular case of a nonlinear viscous medium. It is assumed that, as a result of a quantitative examination of the results of observations based on equations obtained in the present work, experiments on two-way shear with viscoplastic dispersed phases would also help to resolve the problem as to what extent in actual dispersed systems closely resembling viscoplastic bodies, the rheological properties are independent of the history of the load.

In conclusion, it may be noted that the equations obtained in this work are also tenable for the case of the extrusion of a dispersed system in a narrow gap between two coaxial cylinders, one of which is rotated. An exception occurs only when the tangential stress τ on any one of the cylinders differs little from the ultimate shear stress θ, and the pressure gradient is also low, i.e., if the conditions

$$\frac{|\theta - \tau|}{\theta} \ll 1, \quad \frac{a\left|\frac{dp}{dz}\right|}{\theta} \ll 1.$$

are simultaneously satisfied. In this case, the inequality of the tangential stresses on the surface of the inner and outer cylinders becomes substantial.

In the whole of the remaining region of tangential stresses, the flow θ through a narrow gap between two cylinders with radii R_1 and R_2 and height L is readily obtained from Eqs. (15) and (16). For this purpose, it is necessary to multiply θ in Eqs. (15) and (16) by $\pi(R_1 + R_2)$, and instead of the values $\underline{a}$, τ, dp/dz, and x_1, substitute:

$$a = \frac{R_2 - R_1}{2}, \tag{21}$$

$$\tau = \frac{M}{\pi(R_1 + R_2)L}, \tag{22}$$

$$x_1 = \frac{\sqrt{\theta^2 - \tau^2}}{\left|\frac{dp}{dz}\right|}, \text{ with } \tau < \theta \tag{23}$$

and

$$x_1 = 0, \text{ with } \tau > \theta.$$

The angular velocity of the inner cylinder can be obtained from Eqs. (19) and (20), by dividing $\underline{v}$ in them by $R = \frac{1}{2}(R_1 + R_2)$, and substituting by means of Eqs. (21)-(23).

SUMMARY

1. A solution is given for the problem of the flow of a viscoplastic phase in a planar gap under conditions where the tangential stress is perpendicular to the pressure.

2. The equations obtained are extended to cover the case of the extrusion of a viscoplastic phase through a gap between coaxial cylinders, one of which is rotated.

The author would like to express his gratitude to Professor M. P. Volarovich for his advice during this work, and also to Professor G. V. Vinogradov, who pointed out to him the importance of examining this problem.

LITERATURE CITED

1. G. V. Vinogradov, A. A. Mamakov, and V. P. Pavlov, Doklady Akad. Nauk SSSR 127, 362 (1959).
2. A. M. Gutkin, Proceedings of the Second All-Union Conference on Friction and Wear in Machines [in Russian] (1947) Vol. 1, p. 31.
3. M. P. Volarovich and A. M. Gutkin, Zhur. Tekh. Fiz. 16, 321 (1946).

ELECTRIFICATION AND RHEOLOGICAL PROPERTIES OF NONAQUEOUS PLASTIC DISPERSED SYSTEMS

Yu. F. Deinega, A. V. Dumanskii, and G. V. Vinogradov

Institute of General and Inorganic Chemistry,
Academy of Sciences of the UkrSSR, Kiev
Translated from Kolloidnyi Zhurnal, Vol. 23, No. 1, pp. 25-30, January-February, 1961
Original article submitted June 20, 1960

A number of effects associated with the behavior of nonaqueous plastic dispersed systems of the type of homogeneous lubricants in electrical fields were described in [1,2]. It was found that there is a considerable variation in the dielectric permeability (ϵ) under the effect of the orientation of the particles of the dispersed phase in the current of particles, the formation of stabilized charged electrical structures when it is cut off, and also substantial variations of the tangent of the loss angle ($\mathrm{tg}\,\delta$), as a result of deformation and reduced efficiency of the lubricants. All these factors taken together make a more extensive joint investigation of electrical and rheological phenomena in nonaqueous dispersed systems a matter of vital importance. It was found [3] that a jet of lithium lubricant flowing from a capillary has a negative charge. The presence of a negative potential on a lithium lubricant, when it undergoes deformation, was also noted in [1]. This effect was attributed to electrokinetic phenomena, and is associated with the displacement of particles of the dispersed phase with respect to the dispersion medium, and also with the possibility of transfer of the dispersion medium in a radial direction in an apparatus with concentric cylinders. This assumption essentially requires confirmation of the presence of an electric double layer at the surface of particles of the dispersed phase. In a case where there is actually a potential jump at the boundary between the dispersed phase and the dispersion medium, a phase displacement in the electrical field may be expected. There have evidently been no attempts as yet to investigate nonaqueous dispersed systems of lubricants from this viewpoint. As follows from the discussion with respect to [1], the explanation of the occurrence of the electrical charging effect was therefore unconvincing.

Electrical charging phenomena during the flow of lubricants may take place in a far more complicated manner than is described in [1], where the appearance of only a negative potential in an Li lubricant is indicated. Our examination of a sodium lubricant showed [2,4] that at low rates of deformation is acquires a positive potential. A change-over to high rates of deformation leads to the appearance of a negative potential. A simultaneous investigation of the dielectric and rheological properties of plastic lubricants convinced us [2] that a potential jump does actually exist at the interfacial boundary in lubricants.

In the present work, it was necessary to show the presence of a charge on the particles of the dispersed phase of lubricants by direct methods, and investigate the process of electrical charging of lubricants during their deformation.

The presence of a potential jump at the boundary between a dispersed phase and the dispersion medium is most simply detected in experiments with an apparatus of the Perrin osmometer type. The role of a porous diaphragm was played by a 5-mm thick layer of lubricant, located in a glass ring with ground end surfaces. The ring was fastened by means of rubber gaskets between the two elbows of the apparatus, in which the electrodes were sealed. The apparatus was filled with MVP petroleum oil of low viscosity. A potential of 2.5 kv was applied to the electrodes, the distance between which was 10 mm. The movement of the oil through the layer of lubricant (forming a pseudogel) during the application of the potential was observed in a capillary, graduated in 0.001 ml.

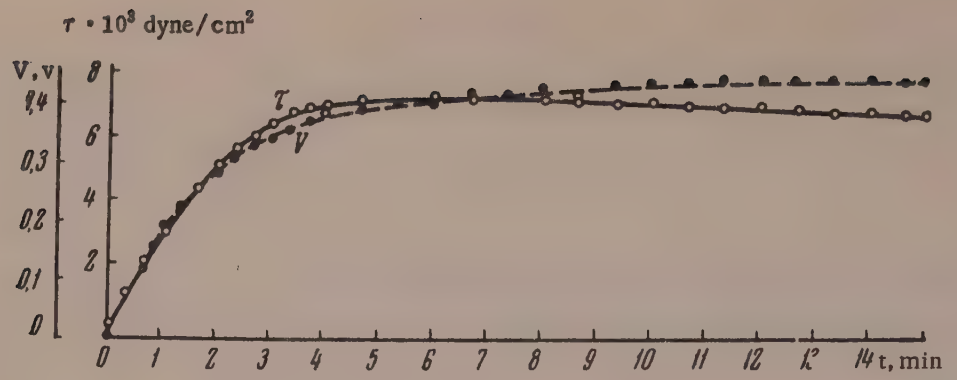


Fig. 1. Variation in time with gradual increase of the shear stresses (τ) and the electric charge potential (V) in the case of a sodium lubricant with a nonoriented structure.

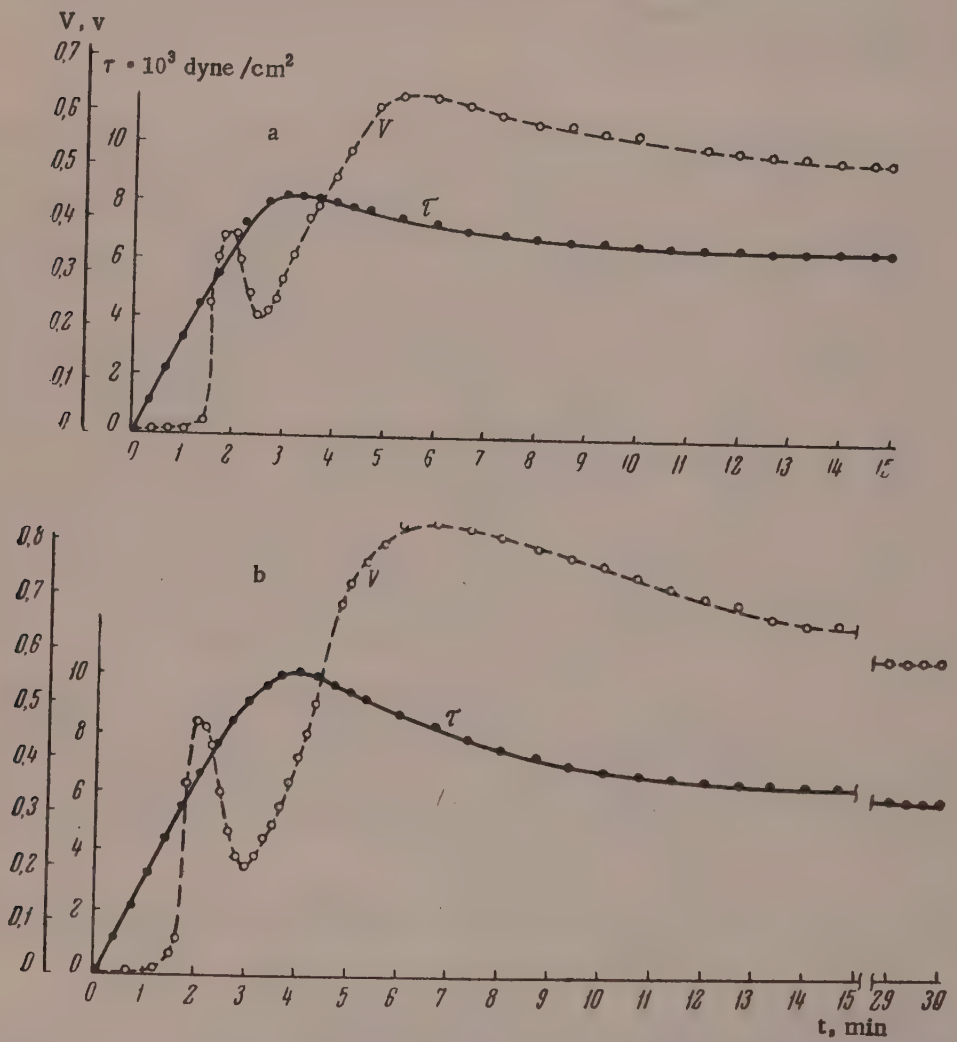


Fig. 2. Variation in time with gradual increase of the shear stresses (τ) and electrical charge potential (V) in the case of a sodium lubricant with an oriented stabilized structure: a) current stabilized structure and its subsequent deformation as a result of rotation of the rotor to one side; b) the same, with slow rotation of the rotor in the reverse direction.

The investigation of the electric charging of dispersed systems was carried out in a rotary plastoviscometer, in which the inner and outer cylinders are the linings of a condenser [5]. The radial gap formed by the two concentric surfaces of the electrodes was 0.25 mm. The radius of the inner cylinder-rotor was 6.25 mm. The apparatus was filled with the material to be tested by rotating the rotor at 0.96 rev/min by means of a charging mechanism, screwed into the lower part of the body. The torque produced in the concentric gap as a result of the deformation of the material was measured by a torsion dynamometer connected to the body of the apparatus by a fine metal wire. In the present investigation, a dynamometer with a modulus of 30 G • cm • radian^{-1} was used.

The potential was measured in an apparatus consisting of a GV-2a constant-voltage amplifier with an input resistance of 10^{11} ohms and a KO-2 cathode-ray oscillograph. The screen of the tube was calibrated by means of an amplifier in volts per millimeter. The measurement accuracy of the potential in the 0-0.5 v range was ± 6 mv, and about ± 15 mv from 0.5 to 1 v. The inner cylinder of the condenser was connected to the amplifier by means of a slide contact, while the outer cylinder was earthed via the metal wire connecting it to the dynamometer.

Plastic lubricants were used as the objects of investigation: sodium (Constalin), calcium (Solidol), and lithium (Tsiatim-201) lubricants. The most convenient object for the investigation was a sodium lubricant obtained by thickening spindle oil with 20.6% of sodium soaps of castoric acids. Particular attention had to be paid that the sodium lubricant used had a dispersed phase consisting of microcrystallites, forming fairly large lumps of disintegrated homogeneous pseudogel. This was a relatively coarsely dispersed system in which the wall effect (P effect) occurs in a marked form. During the investigation of electroosmosis, and in the experiments on the investigation of the electrification of a sodium lubricant during its deformation, it was found that the moisture content has a marked influence on the value of the effects. In lubricants which have been in long contact with steam, electroosmosis takes place more intensely, and the phenomenon of electrification could not be studied quantitatively, due to the marked increase in their conductivity. Thus, to standardize the moisture content, the sodium lubricant was always kept at 80° for 4 hr.

Tests of lubricants in a Perrin osmometer, carried out by A. M. Vovnenko, showed that, when the field is imposed, transfer of the dispersion system to the cathode is readily detected. In the case of reversal of electrode polarity, movement of the oil in the opposite direction took place. The maximum effect, assessed by the electroosmotic rate of transfer of the liquid, was found for the sodium lubricant (about 0.2 ml/hr), the minimum effect was found in the case of the calcium lubricant (about 0.1 ml/hr); there was a slight effect in the case of the lithium lubricant.

Electroosmotic phenomena depend, to a very marked extent, on the moisture content of the system. It was found that movement of the dispersion medium in the electric field is not observed in the case of a sodium lubricant kept in a fine layer at 120° for 4 hr. After this system had been kept in air for a long time, the electroosmosis effect reappeared.

The experiments on electroosmosis indicate the presence of a potential jump at the boundary between the dispersed phase and the dispersion medium. Moisture content plays the decisive role in the formation of electric double layers in soap-hydrocarbon systems.

The investigation of the electrification of plastic lubricants showed a considerable difference in their electrical properties. No electrical charging effect was detected during the investigation of Solidol. This is evidently due to the appreciable conductivity of the lubricant (10^{-10} ohm^{-1} • cm^{-1} in direct current). In the case of lithium lubricant, which has a very low conductivity, electrification was so marked that the apparatus we employed did not allow this phenomenon to be investigated in detail.

As already mentioned, the most suitable system for the investigation of electrical charging was sodium lubricant. The possibility of obtaining stabilized flow structures by rapidly stopping the current [2,6] opens up a method of carrying out experiments with anisotropic forms of a lubricant. This, in turn, makes it possible to establish the character of the influence of different rates of deformation (D) and shear stresses (τ) on such forms, which also includes cases of the disorientation and reorientation of structural elements. Moreover, the use of the method of current-stabilized structures opens up the possibility of changing the structure of the layer adjacent to the wall. It is known [7] that, at high deformation rates, the individuality of the layer adjacent to the wall decreases, it becomes diffuse, and its properties approach those of the general system. The conditions of the

deformation of systems with a stable oriented structure of a rapid current must, therefore, be essentially different from those which occur in the case of systems which have not been first subjected to the effect of high rates of deformation.

For this reason, experiments were carried out with fresh quantities of sodium lubricant (Fig. 1) and sodium lubricants (Fig. 2) with an anisotropic structure of rapid (D = 312 sec^{-1}) stabilized currents. Stable-oriented structures were obtained by rapid braking of the rotor, rotating at a fixed speed. In these experiments, the shear stresses and the potential at the rotor with gradual loading of the system were recorded, the latter being obtained by rotating the rotor at a speed of 0.96 rev/min.

The regular curve $\tau(t)$, with a weakly expressed maximum, given in Fig. 1, shows that system has a considerable P effect, which screens the brittleness of its general structural envelope [8]. As mentioned above, at a high deformation rate the wall layer is not so markedly separate, and its properties approximate to the physical properties of the lubricant. This is shown during deformation of the stabilized rapid-current structures. In such a case, the process of gradual loading is accompanied by the appearance of a more or less clearly expressed maximum on the $\tau(t)$ curve shown in Fig. 2. When rapid and slow rotation of the rotor take place in different directions during the process of formation of the stabilized rapid-current structures and during the deformation of the stabilized structure, the maximum on the $\tau(t)$ curve is expressed still more clearly, and is located higher (Fig. 2b). This is due to the effect of reorientation of the particles, and is known from [2,9,10].

On the curves of the relation between the potential and the duration of rotation of the rotor, small variations in the potential are observed initially. It may be assumed that the deformation character of a system in which the leading role is played by elastic deformations corresponds to this. The development of flow in the layer adjacent to the wall is accompanied by a marked increase in the positive potential of the rotor. As was shown in [7,8], the wall effect is expressed most markedly when passing through the breaking point (τ_{us}). It was subsequently established [11], that the P effect is first shown before passing through the breaking point, i.e., $\tau < \tau_{us}$. Thus, enrichment of the layer adjacent to the wall with dispersion medium increases with an increase in the shear stresses, reaches a maximum at τ values close to the breaking point τ_{us}, and then gradually decreases with the development of viscous flow of the system. The layers adjacent to the wall, enriched with liquid hydrocarbon, are thin, and very high-velocity gradients may occur in them. It may be assumed that, under these conditions, static electricity will appear and, consequently, there will be a considerable positive charge on the rotor.

From Figs. 2a and 2b it is evident that during deformation of the stabilized rapid current the structure of the system changes, which is accompanied by a marked fall, and then by a further increase, in the positive potential of the rotor. These phenomena are developed at shear stresses close to the breaking point, which is recorded by the maximum on the $\tau(t)$ curves.

During the process of gradual loading, disorientation, and reorientation of the particles takes place at loads approaching the breaking point in the diffuse layer adjacent to the wall. Rotation of the particles of the dispersed phase in the current leads to an increase in the number of their collisions with the rotor. As is shown by experiments on electroosmosis, since soap crystallites in the sodium lubricant have a negative charge, an increase in their contact with the rotor reduces its positive potential.

The second maximum on the V(t) curves is displaced to the right of the breaking point. This is evidently due to the fact that the maximum of the positive potential is determined both by the state of the layer adjacent to the wall and its velocity gradients. After the system has passed through the breaking point, the relative influence of the wall effect is reduced, but, as a result of the reverse movement of the body of the apparatus, the velocity gradient in the wall layer (experiments with a soft dynamometer) increases. The positive potential may therefore increase up to a specific value. The subsequent reduction in the potential is due to a reduction in the velocity gradient in the wall layer and its gradual disintegration.

The potential on the threshold of stabilized conditions is considerably higher for oriented systems than for nonoriented. This is explained by the fact that the zone of flow at a velocity gradient of 2.42 sec^{-1} — as was shown by dielectric measurements [2, Fig. 4] in a sodium lubricant with a marked wall effect — is not distributed over the whole layer of deformed lubricant. A highly oriented structure, having a lower conductivity in a radial direction than a structure which is not oriented in the direction of the current, i.e., perpendicularly to the electric field, is preserved in the layers distant from the rotor. As a result, in the case of highly oriented structures, the rate of flow of the charges, and equalization of the potential between the electrodes, is less, which leads to the formation of a higher potential.

The phenomena examined here show that the electrical properties of plastic lubricants may be sensitive,to a high degree,to variations in structure, particularly of the wall layer, during flow. A composite investigation of the electrical and rheological properties of plastic dispersed systems thus opens up new possibilities for a more fundamental investigation of these complex systems.

SUMMARY

1. The electroosmotic effect in plastic soap lubricants is shown most profoundly in sodium lubricants, and least of all in calcium lubricants. The dispersed phase in these systems has a negative charge. In soap-hydrocarbon systems there is an electric double layer at the interfacial boundary. In wetted systems with a hydrophylic soap (sodium lubricant), this layer evidently has a diffuse character.

2. During the process of gradual loading at low velocity of a sodium lubricant, freshly introduced into a plastoviscometer, there is a continuous increase in the positive potential of the rotor to a steady value. This is due to the flow in the layer adjacent to the wall.

3. By means of the method of stabilized rapid-current structures, a pronounced change in the potential can be observed during the deformation of preliminarily oriented (anisotropic) systems under conditions of change-over from elastic deformations to steady flow via the breaking point.

4. Depending on the character of its anisotropy, the difference in potential changes during the deformation of a sodium lubricant is due to the characteristics of the formation of the layer adjacent to the wall.

LITERATURE CITED

1. A. Bondi and C. Penther, J. Phys. Chem. 57, 72 (1953).
2. Yu. F. Deinega, A. V. Dumanskii, G. V. Vinogradov, and V. P. Pavlov, Kolloid. Zhur. 22, 16 (1960).
3. V. V. Sinitsyn, Viscous Properties and Wall Slip of Plastic Lubricants, Thesis [in Russian] (Petroleum Institute, AN SSSR, Moscow, 1954).
4. M. F. Deinega and A. V. Dumanskii, Doklady Akad. Nauk SSSR 798 (1960).
5. Yu. F. Deinega, V. P. Pavlov, and G. V. Vinogradov, Zavod. Lab. 26, 353 (1960).
6. G. V. Vinogradov, Proceedings of the Conference on Colloid Chemistry [in Russian] (AN UkrSSR, Kiev, 1952) p. 249 .
7. V.V.Sinitsyn and G. V. Vinogradov, Kolloid. Zhur. 17, 255 (1955).
8. G. V. Vinogradov, V. G. Lebedev, and V. A. Protd'yakonov, Kolloid. Zhur. 18, 633 (1956).
9. G. V. Vinogradov and V. P. Pavlov, Izvest. Akad. Nauk SSSR, Otd. Tekh. n., Mekh. i Mashinostroenie No. 2, 134 (1959).
10. Yu. F. Deinega, Doklady Akad. Nauk SSSR 655 (1960).
11. V. P. Pavlov, G. V. Vinogradov, V. V. Sinitsyn, and Yu. F. Deinega, Reports to the Third World Congress on Rheology [in Russian] (1958).

VOLUMETRIC DETERMINATION OF COLLOIDAL SOLUBILITY (SOLUBILIZATION)

P. A. Demchenko

Institute of General and Inorganic Chemistry, Academy of Sciences of the UkrSSR, Kiev
Translated from Kolloidnyi Zhurnal, Vol. 23, No. 1, pp. 31-35, January-February, 1961
Original article submitted October 26, 1959

In the production of synthetic detergents, synthetic fatty acids, naphthenic acids, and petroleum sulfonic acids from individual fractions of petroleum, colloidal systems are formed: detergent–hydrocarbon (oil)–water, and surfactant–polar liquid–hydrocarbon–water, in which water-insoluble hydrocarbons and polar materials are bound in micelles by the mechanism of colloidal solubility (solubilization), forming transparent, thermodynamically stable systems with a colloidal degree of dispersion [1,2]. The same types of systems are formed in the emulsion polymerization of monomers in the production of synthetic plastics and rubbers [3,4]. In connection with solving the problem of replacing edible fats by synthetic products for industrial use and in connection with an increase of the production of emulsion-polymerized plastics and synthetic rubbers, the quantitative determination of the solubilization of hydrocarbons, monomers, and polar materials in solutions of detergents and emulsifiers is acquiring great practical significance.

TABLE 1

Solubilization of Styrene, Toluene, and n-Heptane in 0.1 M Solutions of Potassium Soaps of Saturated Fatty Acids and in 0.3 M Solutions of Sodium Soaps of Naphthenic Acids (Temperature 60°)

Soaps	Mol. wt. of soap	Solubilization, moles per mole of soap		
		styrene	toluene	n-heptane
Potassium laurate	238	0.38	0.50	0.08
Potassium myristate	266	0.77	1.04	0.29
Potassium palmitate	294	1.43	1.64	0.53
Sodium naphthenate	244	0.19	0.28	0.13
The same	334	1.5	2.1	0.48

As yet, no direct and convenient laboratory methods have been developed for determining the solubilizing capacity of detergents and emulsifiers of differing nature and molecular weight [2,3]; this lack is holding back the progress of work on establishing the connection between structure and properties which are of practical importance [5,6].

For investigating the solubilizing capacity of surface-active detergent solutions by a volumetric method, we constructed and tested out several devices of differing design. The devices described below proved to be the most convenient for laboratory practice and for series determinations of the solubilization of hydrocarbons and polar materials with specific gravity below and above unity.

Apparatus for Determining Solubilization of Hydrocarbons and Polar Materials with Specific Gravity Below Unity

For investigating the solubilization of hydrocarbons and polar materials in aqueous detergent solutions, a glass apparatus (Fig. 1) was used. The apparatus consists of bulbs 1 and 3 connected by a graduated tube 2. The bulb 1 is spherical, drawn out to a cone in the upper part. On the bulb 3 there is sealed along the axis of the apparatus a 5-8 mm diameter tube 4 with a well-ground stopcock 5.

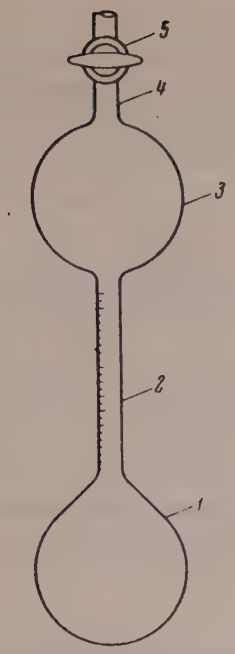


Fig. 1. Apparatus for determining solubilization of hydrocarbons and polar materials with specific gravity below unity: 1) lower bulb; 2) graduated tube; 3) upper bulb; 4) tube; 5) stopcock.

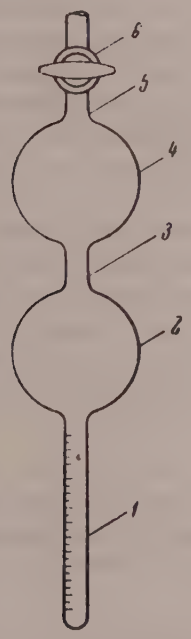


Fig. 2. Apparatus for determining solubilization of water in hydrocarbon solutions of surfactants and solubilization of liquids with specific gravity above unity in aqueous detergent solutions: 1) graduated tube; 2) lower bulb; 3) tube; 4) upper bulb; 5) tube; 6) stopcock.

The prepared solution of the solubilizing agent (soap or detergent) is poured hot through the tube 4 into the lower bulb, up to the zero mark on the measuring tube 2, by means of a funnel with drawn-out stem (not shown in Fig. 1). The capacity of the lower bulb, depending on the solubilizing capacity and concentration of the detergent being investigated and the desired accuracy of measurement, may be from 30 to 500 ml, but it is convenient to operate and to carry out the calculations when the capacity of the lower bulb (to the mark) is 100 ml. After filling the apparatus with a determined quantity of the solubilizer solution, a measured quantity of the solubilizate (hydrocarbon, monomer, or polar liquid) is introduced through the same funnel, up to a given mark on the measuring tube 2. After filling, the stopcock 5 is closed, the apparatus is placed in a thermostat (water bath), and the kinetics of the process are observed on the basis of volume change (in the graduated tube) of the liquid being solubilized. To accelerate attainment of the final value of solubilization, the components are mixed by alternately pouring from the lower part of the apparatus to the upper, with simultaneous shaking. For the best mixing, it is necessary that the capacity of the upper bulb should be 20-30% greater than the capacity of the lower bulb. The upper bulb is also a receiver of the pressure generated in the apparatus by temperature changes during experiment. If the quantity of solubilizate which is added is less than that necessary for reaching the saturation limit, then mixing the components results in an unstable, rapidly broken emulsion. With an excess of the solubilizate, more stable emulsions are formed, requiring about ten hours for separation into layers. If the vertically mounted apparatus is held in the thermostat at a temperature slightly below the boiling point of one of the components of the system, the emulsion is broken more rapidly, and clear limits are defined for the phase boundaries between the solution of surface-active solubilizer and the excess solubilizate. Breaking the emulsion in the measuring tube of the apparatus is also accelerated by heating it to the boiling point of the solubilizate. The solubilization is considered complete if no change of volume of the solubilizate is observed in the tube on subsequent mixing and settling in the apparatus. The volume changes were determined, taking into account the temperature, specific gravity, and solubility of the solubilizate in water, and the results were expressed in percent or in moles per mole of anhydrous soap-form material occurring in the test solution. The apparatus proved to be convenient for investigating the solubilization of hydrocarbons and polar materials with specific gravity less than unity.

Experimental data on the solubilizing capacity of solutions of several detergents are given in Table 1.

As is evident from Table 1, an increase of molecular weight of the saturated fatty-acid potassium soaps and of the sodium naphthenates results in an increase of the solubilizing capacity of their solutions.

TABLE 2

Solubilization of Water in Hydrocarbon Solutions of Lecithin, at 25°

Solvent	Lecithin content in solution, g	Water solubilized by solution	
		g	g/g lecithin
Benzene	0.4	0.13	0.320
	6.0	1.97	0.330
Toluene	2.0	0.65	0.32
	5.0	1.64	0.33
Xylene	3.0	0.68	0.33
	5.0	1.58	0.32

TABLE 3

Solubilization of Chlorinated Hydrocarbons in 0.1 N Aqueous Solutions of Sodium Soaps of Saturated Fatty Acids, at 60°

Soaps	Solubilization, moles/mole soap		
	chloroform	dichloroethane	carbon tetrachloride
Sodium palmitate	1.77	1.31	1.45
Sodium myristate	1.22	0.75	0.85
Sodium laurate	0.44	0.36	0.40

The naphthenic acid soaps possess a high solubilizing capacity for styrene, which permits their recommendation as possible emulsifiers for emulsion polymerization.

Apparatus for Determining Solubilization of Water and of Liquids with Specific Gravity Above Unity

For studying the solubilization of water in hydrocarbon solutions of surfactants and the solubilization of halogenated hydrocarbons and other materials with specific gravity above unity, we used the glass apparatus depicted in Fig. 2. The apparatus consists of bulbs 2 and 4 connected by a tube 3. A graduated tube 1 is sealed to bulb 2; a tube 5 with stopcock 6 is sealed to bulb 4. Depending on the solubilizing capacity of the surfactant, and the concentration of the solutions being studied, the capacity of the graduated tube is taken from 2 to 10 ml, and the capacity of the bulb 2 from 50 to 500 ml. In carrying out experiments, the upper bulb is not submerged in the thermostat liquid; it serves as a receiver of the pressure arising in the closed apparatus on increase of temperature during the investigation. A determined quantity of the test liquid is placed in the graduated tube 1 through the tube 5, by means of a funnel with a drawn-out stem. Then the apparatus if filled to two-thirds the capacity of bulb 2 with a surfactant solution of known concentration, the specific gravity of which must be lower than that of the solubilizate placed in tube 1. The apparatus, thus prepared for experiment, is closed by the stopcock 6 to prevent evaporation of the components; then it is placed in a thermostat (water bath), and the kinetics of the process of solubilization of the test liquid in the graduated tube 1 are observed on the basis of volume change. As indicated above, the limit of solubilization is considered as having been reached when absorption of the solubilizate by the solubilizer solution practically ceases. The decrease of the quantity of liquid in the graduated tube 1 is determined, allowing for the specific gravity and mutual solubility of the components, and the results are expressed in grams per gram, or in moles per mole, of the anhydrous solubilizer contained in the solution. This apparatus was applied in determining the solubilization of water in hydrocarbon solutions of lecithin (Table 2) and of chlorinated hydrocarbons in 0.1 N aqueous solutions of sodium soaps of saturated fatty acids (Table 3).

The quantity of solubilized water in benzene, toluene, and xylene solutions of lecithin is nearly equal, and constitutes from 31 to 33%, calculated on dry lecithin (Table 2). The absorption of water by a hydrocarbon solution of lecithin increases proportionally with an increase of lecithin concentration. The solubilization limit is characterized by the cessation of absorption of water from the solution, and the appearance of a slight cloud of hydrated lecithin, which does not disappear with time.

The solubilization of chlorinated hydrocarbons in solutions of sodium soaps of saturated fatty acids increases with an increase of the length of the soap's hydrocarbon chain.

The solubilization of water in micellar hydrocarbon solutions of lecithin, and the solubilization of chlorinated hydrocarbons in aqueous solutions of saturated fatty-acid soaps, takes place by a similar colloidal mechanism [7], by which insoluble materials are solubilized in the bulk of the solution by the surfactant micelles. If the surfactant solutions are transparent at room temperature, and the test liquid is nonvolatile, its consumption by solubilization can be determined by titration. The kinetics of the process, and the limiting value of solubilization of water in hydrocarbon solutions of surfactants, can also be determined by a more complex method by means of the Fisher reagent [8].

In comparative ability to dissolve in micellar soap solutions, the test hydrocarbons are arranged in the following decreasing order: chloroform > toluene > carbon tetrachloride > styrene > dichloroethane > n-heptane.

The devices described above are being used successfully for studying the solubilizing capacity of various detergents over a wide range of temperatures and concentrations. The reproducibility of the measurements is 2-3%.

SUMMARY

1. A method has been developed for the volumetric determination of the solubilization of water in hydrocarbon solutions of surfactants, and the solubilization of hydrocarbons and polar liquids in aqueous detergent solutions, with specific gravity of the solubilizate greater and less than that of the solubilizer solution.

2. With an increase of molecular weight of sodium naphthenates and saturated fatty acid soaps, the solubilizing capacity of their solutions (with respect to styrene, toluene, heptane, and chlorinated hydrocarbons) increases sharply.

3. The solubilization of water in hydrocarbon solutions of lecithin does not depend on the dispersion medium, and varies proportionally to the lecithin concentration in the solution.

LITERATURE CITED

1. Z. N. Markina, K. A. Pospelova, and P. A. Rebinder, Transactions of the Third All-Union Conference on Colloid Chemistry [in Russian] (AN SSSR Press, Moscow, 1956) p. 410; K. A. Pospelova and P. A. Rebinder, Acta Phys. Chem. USSR 16, 71 (1942).
2. J. W. McBain and Z. McBain, J. Am. Chem. Soc. 58, 2610 (1936); J. W. McBain, Advances Coll. Sci. 1, 99 (1942); L. McBain and E. Hutchinson, Solubilization and Related Phenomena (New York, 1955).
3. A. I. Yurzhenko, Zhur. Obshchei Khim. 16, 1171 (1946); A. I. Yurzhenko and N. V. Tsvetkov, Doklady Akad. Nauk SSSR 90, 421 (1953).
4. P. M. Khomikovskii, Uspekhi Khim. 27, 1025 (1958).
5. P. A. Demchenko, A. V. Dumanskii, and L. G. Demchenko, Kolloid. Zhur. 14, 164 (1952).
6. P. A. Demchenko, Ukrain. Khim. Zhur. 25, 624 (1958).
7. K. A. Pospelova, Kolloid. Zhur. 11, 187 (1949).
8. D. Mitchell and D. Smith, Aquametry [Russian translation] (IL, 1952).

SOLUBILIZATION OF AROMATIC HYDROCARBONS IN HYDROSOLS OF SATURATED FATTY ACID SOAPS

P. A. Demchenko

Institute of General and Inorganic Chemistry, Academy of Sciences of the UkrSSR, Kiev
Translated from Kolloidnyi Zhurnal, Vol. 23, No. 1, pp. 36-39, January-February, 1961
Original article submitted September 3, 1959

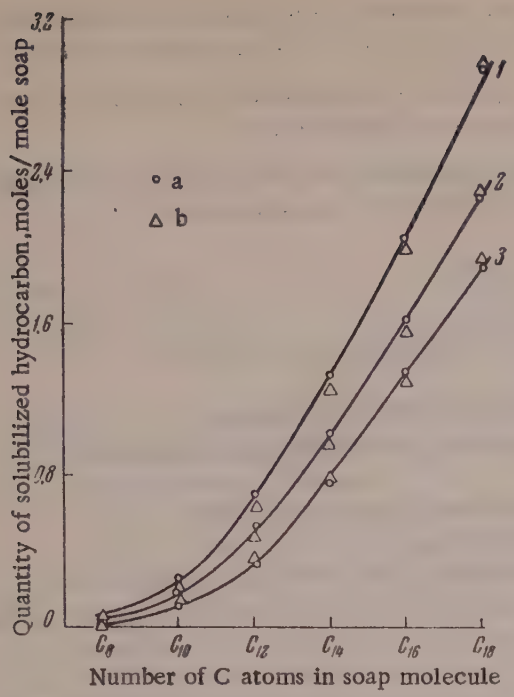
The bulk properties of solutions of soaps and synthetic detergents have not been studied adequately [1-5], which is retarding the development of their production technology and their efficient application in everyday use and in various branches of industry. Solubilization, and the critical concentration for micelle formation have been utilized recently for characterizing the effectiveness of detergents, and for determining the hydrophilic-oleophilic balance in evaluating known surfactants and in the synthesis of new surfactants [6]. However, many factors affecting these processes still have not been studied, and there has been no adequate explanation of the mechanism of solubilization and desolubilization of hydrocarbons and polar materials in solutions of surfactants with differing structure and differing length of the hydrocarbon portion of the surfactant molecules [2-7].

In the present work, a study has been conducted on the solubilization of aromatic hydrocarbons in 0.1 N aqueous solutions of sodium soaps of saturated fatty acids with hydrocarbon chain length from C_8 to C_{18}.

Aqueous solutions of sodium soaps form bulk crystallization structures at a temperature near the melting point of the corresponding fatty acid. Reproducible results are obtained by investigation of the solubilization of hydrocarbons in homogeneous solutions. Taking these factors into consideration, the experiments were carried out at a temperature near 60°. At this temperature, the 0.1 N solutions of soaps from sodium caprylate to stearate remained transparent and uniform. The samples of pure soaps used in studying the solubilizing capacity of their solutions were prepared by a method described in [5,6].

The saturation equilibrium quantity of the aromatic hydrocarbons passing into the micellar soap solutions was determined in a closed apparatus on the basis of volume decrease, and was calculated with allowance for the specific gravity and water solubility of the hydrocarbons at the test temperature. It was found that the rate of solubilization depends on the contact area of the hydrocarbon with the detergent solution, the length and structure of the hydrocarbon portion of the fatty acid, the concentration of the solution, and the test temperature. The saturation equilibrium value of hydrocarbon solubilization is determined mainly by the concentration, molecular weight, and structure of the detergent. At a temperature near 60° the solubilization of aromatic hydrocarbons in the soap solutions investigated was practically complete in 3-5 hours. At the end of the solubilization process, an emulsion layer is often formed on both sides of the soap solution – hydrocarbon interface; this hinders the accurate fixation of the final results of the experiment. By local heating of the interface in the measuring tube to a temperature near the boiling point of one of the components, the emulsion is broken more rapidly than by the usual settling; this permits a more accurate determination of the test results. The relative error of the experiments is about 2%.

As is evident from the figure, the solubilization of aromatic hydrocarbons in 0.1 N soap solutions decreases sharply from stearate to laurate, an almost linear relationship being observed between decrease of solubilization and shortening of the soap radical. A flatter curve is shown for the change of the solubilization effect on going from sodium laurate to sodium caprylate. Practically no solubilization is observed for lower (below seven-carbon) homologous saturated fatty acid sodium soaps. We have termed this length of the soap radical as "critical" [8].



Solubilization of benzene (1), toluene (2), and xylene (3) in 0.1 N solutions of sodium soaps of saturated fatty acids: a) experimental data; b) data calculated according to formula.

An excess length of the hydrocarbon chain of a soap above the critical value gives rise to an increase of solubilization. This effect can be explained by the increase of oleophilicity of the soaps [5], which is accompanied by an increase of the capacity of the centers of the micelles for taking up hydrocarbons. On the basis of the indicated properties, a formula is proposed which permits calculating the solubilization of a hydrocarbon in a solution of a soap homolog, depending on the effective length of its hydrocarbon radical

$$L = K(n - 7)^2,$$

where L is the solubilization (moles of hydrocarbon per mole of soap), n is the number of carbon atoms in the soap radical (stearate 18, palmitate 16, myristate 14, etc.), and K is a coefficient characterizing the structure and properties of the hydrocarbon (solubilizate) and the concentration of the soap solution.

At the indicated concentration for benzene, toluene, and xylene, K equals, respectively, 0.025, 0.019, and 0.016. Solubilization values calculated by this formula for aromatic hydrocarbons in solutions of saturated fatty acid soaps agree well with the experimental data (figure).

It is interesting to note that the sodium salts of saturated fatty acids containing less than 7-8 carbon atoms do not form micellar colloidal solutions or systems of the type of lubricating greases.

It is still more difficult to explain solubilized systems than the normal detergent solutions, since our knowledge of the intermolecular forces involved in this process is still inadequate. In order to be a solubilizer, the surfactant molecules must have a hydrophilic-oleophilic balance displaced in the direction of oleophilic forces, with a relationship providing association of the molecules by connecting the hydrocarbon radicals in micelles with a developed oleophilic center. The micelles should be regarded as isolated phases with well-ordered structure, but the micellar solutions as two-phase thermodynamically stable systems. Solubilization in detergent solutions apparently takes place in consequence of a uniform distribution of the hydrocarbon between the micellar and aqueous part of the system. The experimentally observed limit of solubilization indicates the fact that the detergent micelles possess a fixed capacity, in consequence of which excess hydrocarbon separates in the form of a discrete phase.

The solubilization effect depends on the length and structure of the hydrocarbon radicals of the detergent molecules, the degree of their association, the degree of order of the micelle structure, and the properties of the solubilizate. An increase of the length of the hydrocarbon molecule results in a decrease of its capacity for being solubilized in surface-active detergent solutions. The aromatic hydrocarbons which were investigated are arranged in the following order of capacity for being solubilized in solutions of saturated fatty acid soaps: benzene > toluene > xylene.

Electrolytes and surface-active additives increase the degree of order of the structure of micellar solutions and their solubilizing capacity and detergency. A separate communication will be devoted to these questions.

The solubilization phenomenon can be used as an objective method of determining the micellar structure of detergent solutions, quantitative characterization of their oleophilicity, and their practical value.

SUMMARY

1. With a decrease of molecular weight from sodium stearate to sodium laurate, the solubilization of benzene, toluene, and xylene in 0.1 N aqueous soap solutions decreases almost linearly. For lower molecular weight

homologs – from sodium laurate to sodium caprylate – the effect of solubilization is expressed more feebly. For solutions of soaps with less than seven carbon atoms, practically no solubilization of hydrocarbons is observed.

2. A formula has been proposed for calculating the solubilization of hydrocarbons in solutions of saturated fatty acid soaps on the basis of the effective length of the hydrocarbon radical of the soap.

3. The solubilization effect can be utilized as a method for determining the oleophilicity of soaps, their hydrophilic-oleophilic balance, micellar structure, and the practical value of detergent solutions.

LITERATURE CITED

1. N. Veikhkherts and N. Pleteneva, Kolloid. Zhur. 2, 133 (1936).
2. M. E. L. McBain and E. Hutchinson, Solubilization and Related Phenomena (New York, 1955).
3. H. B. Klevens, Chem. Rev. 47, 1 (1950).
4. P. A. Rebinder, Izvest. Akad. Nauk SSSR, Otdel. Khim. Nauk 1284 (1957); Z. N. Markina, K. A. Pospelova, and P. A. Rebinder, Transactions of the Third All-Union Conference on Colloid Chemistry [in Russian] (AN SSSR Press, Moscow, 1956) p. 410.
5. P. A. Demchenko, A. V. Dumanskii, and L. G. Demchenko, Kolloid. Zhur. 14, 164 (1952).
6. P. A. Demchenko, Masloboino-zhirovaya Promysh. No. 7, 36 (1959).
7. P. A. Demchenko, Reports, Proceedings, and Communications of the Eighth Mendeleev Conference on General and Applied Chemistry, Colloid Chemistry Section [in Russian] (AN SSSR Press, 1959) No. 5, p. 111.
8. P. A. Demchenko, Ukrain. Khim. Zhur. 24, 746 (1958).

EFFECT OF SURFACE FORCES ON PHASE EQUILIBRIA OF POLYMOLECULAR LAYERS AND ON CONTACT ANGLE

B. V. Deryagin and L. M. Shcherbakov

Institute of Physical Chemistry, Academy of Sciences of the USSR, Moscow;
Tula Mechanical Institute
Translated from Kolloidnyi Zhurnal, Vol. 23, No. 1, pp. 40-52, January-February, 1961
Original article submitted January 11, 1959

The question of the effect of surface forces on the properties of thin liquid layers has an important theoretical and practical significance for problems of flotation and wetting, capillary permeation, and capillary condensation, equilibrium and movement of moisture in soils and earths, stability of lyophobic colloids, and a number of other problems in the study of surface phenomena and colloids. The existence of thermodynamically equilibrated polymolecular layers covering the surface of a solid body was demonstrated for the first time by direct experiments of one of the authors [1,2]. In [3-5] an analysis was made of the effect of the excess free energy of the layer on its individual properties. In [6] a general outline was given of the thermodynamics of a thin liquid layer without solid substrate. The more complex case of layers occurring on the surface of a solid body is examined in the present communication.

Conditions of Thermodynamic Equilibrium of a Polymolecular Adsorbed Layer

Let us represent a system occurring under a given pressure P, consisting of an adsorbed layer (index ') on a uniform plane surface of the adsorbent, and vapor ("); for the variable part of its thermodynamic potential we have

$$\Phi = \mu'_{\infty}(P, T)\, N' + \mu''_{\infty}(P, T)\, N'' + \omega A. \qquad (1)$$

Here μ_{∞} is the value of chemical potential (referred to one particle) corresponding to a phase of infinite thickness; $N^{(i)}$ is the number of particles in the ith phase; A is the area of the layer; ω is the specific excess free energy of the layer caused by the action of surface forces. The quantity ω is considered as a function of adsorption $\Gamma = N'/A$, and temperature T, this function being assumed as normalized, such that, for the initial value, there is taken the value $\omega_0 = \sigma_{solid}$ (σ_{solid} is the specific free surface energy of the surface of the adsorbent). Minimizing Φ with P, T, A, $N' + N'' = \text{const}$, we find the condition of equilibrium of the layer with its vapor

$$\mu'_{\infty}(P, T) + \frac{\partial \omega}{\partial \Gamma} = \mu''_{\infty}(P, T). \qquad (2)$$

Generalizing the concept of chemical potential, we can designate the value

$$\partial \Phi / \partial N' = \mu'_{\infty}(P, T) + \frac{\partial \omega}{\partial \Gamma} = \mu'(\Gamma)$$

as the chemical potential of the layer.* Then condition (2) reduces simply to equality of the chemical potentials of the layer and the vapor. Let us note, in addition, that, in contrast with the bulk phase, the chemical potential for the layer is made up of two values: the "bulk" part $\mu'_{\infty}(P,T)$ and an additional term $\partial \omega / \partial \Gamma$, dependent on the "thickness" of the layer Γ.

* An analogous generalization is introduced, for example, in considering systems occurring in a gravitational force field; see also [7].

The conditions of equilibrium (2) can be represented graphically by means of a curve μ, P (Fig. 1). In this figure, the solid curves correspond to the chemical potentials of infinitely extended phases.* The point of intersection of these curves determines the saturated vapor pressure P_s. The curve of chemical potential of the layer (broken curve in Fig. 1) is obtained by shifting the curve μ'_∞ upward or downward, depending on the sign of the derivative $\frac{\partial \omega}{\partial \Gamma}$. From Fig. 1 it is evident that with $\frac{\partial \omega}{\partial \Gamma} < 0$ (Curve 1), the equilibrium vapor pressure of the layer $P < P_s$; with $\frac{\partial \omega}{\partial \Gamma} > 0$, we have $P > P_s$ (Curve 2).

For finding the equilibrium vapor pressure of the layer, we transform the condition of adsorption equilibrium. For a condensed layer, we may write, with sufficient rigor,

$$\mu'_\infty(P, T) = \mu'_\infty(P_s + \Delta P, T) \approx \mu'_\infty(P_s, T) + \frac{\partial \mu'_\infty}{\partial P}(P - P_s),$$

where $\frac{\partial \mu'_\infty}{\partial P} = v'$, the volume required in the layer for one particle. Replacing here $\mu'_\infty(P_s, T)$ by $\mu''_\infty(P_s, T)$, and substituting the result into condition (2), we obtain

$$\mu''_\infty(P_s T) + v'(P - P_s) + \frac{\partial \omega}{\partial \Gamma} = \mu''_\infty(P, T).$$

Hence, taking the approximation of an ideal gas for the chemical potential of the vapor

$$\mu''_\infty(P, T) = \mu^*(T) + kT \ln P^{**}$$

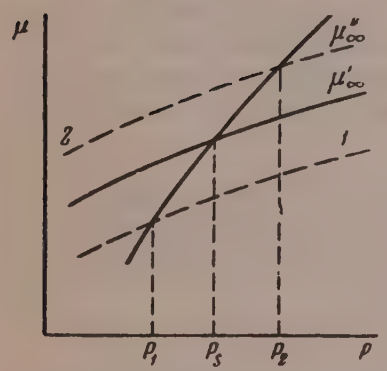


Fig. 1. For deriving the condition of equilibrium of wetting films.

and taking into account that $v'P_s \ll v''P_s \approx kT$, we find, for the equilibrium vapor pressure of the adsorbed layer,

$$kT \ln P/P_s = \frac{\partial \omega}{\partial \Gamma}. \qquad (3)$$

As follows from the derivation itself, the resulting equation of the adsorption isotherm is equally applicable to the cases of both mono- and polymolecular adsorption. In the latter case, the thickness of the adsorbed layer $h = v'\Gamma$; the derivative $\frac{\partial \omega}{\partial \Gamma} = v' \frac{\partial \omega}{\partial h}$; and Eq. (3) changes into an equation derived previously [3,5,6]:

$$RT \ln P/P_s = v_m \cdot \frac{\partial \omega}{\partial h}$$

(here v_m is the molar volume, and $\frac{\partial \omega}{\partial h}$ is the disjoining pressure of the layer*** taken with reverse sign).

Equation (2) is a necessary but still insufficient condition of equilibrium. From the general thermodynamic criterion of stability of equilibrium $\delta^2 \Phi > 0$ it is not difficult to obtain the condition of stability (in the sense of metastability) of a polymolecular layer $\frac{\partial^2 \omega}{\partial \Gamma^2} > 0$,**** from which it follows that the regions of values of Γ corresponding to metastable states coincide with the regions of concavity of the curve $\omega = \omega(\Gamma)$.

---

*Since $v'' \gg v'$ (v is the volume required in the given phase for a single particle), then the slope coefficient of the curve μ''_∞ will be significantly greater than that of the curve μ'_∞.

**Here and later, k is the Boltzmann constant.

***The disjoining pressure of the layer [4] is $p(\Gamma) = P_s - P'$, where P' is the phase pressure in the layer.

****For thin liquid layers, an equivalent condition was established [8] on the basis of the concept of disjoining pressure of the layer.

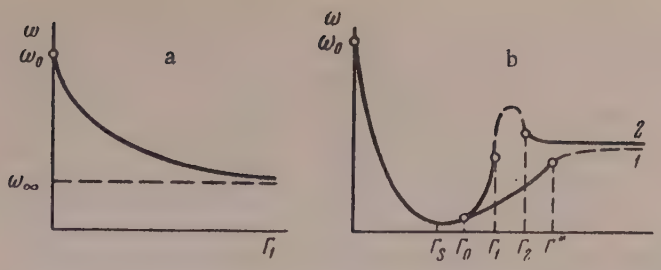


Fig. 2. Relationship between specific excess free energy of layer ω and the magnitude of adsorption Γ for the cases of nonpolar (a) and polar (b) liquids: 1) oriented single-phase α-modification of film (boundary phase); 2) two-phase β-modification of film (layer of normal liquid underlain by oriented "sublayer").

Nature of the Relationship Between the Excess Free Energy of a Layer and Its Thickness

The considerations which have been presented make it possible to visualize the relationship between ω and Γ. It was established experimentally [2] that, for nonpolar liquids, as the vapors approach saturation, the adsorption tends toward infinity, which corresponds to a continuous transition from an adsorbed layer to a macroscopic liquid phase. In the light of what has been stated, this signifies that, for nonpolar liquids, the relationship between ω and Γ is represented by a monotonically decreasing curve, approaching asymptotically the limiting value $\omega_\infty = \sigma_{\text{solid-liquid}} + \sigma_\infty$ (Fig. 2a), this curve in its entire range corresponding to stable (in the sense of metastability) states of the layer.

For polar liquids, according to experimental data [2], upon reaching saturation the adsorbed layer has a finite thickness. There is even some supersaturation possible at a finite thickness of the layer, as was witnessed by the appearance in isolated experiments of embryonic droplets of liquid, having the form of lenses, on the surface of the adsorbed layer.

A number of experimental data on "thick" films (see, for example, [1,2,9]) indicate that, for polar liquids, a specific oriented structure appears in the liquid layers adjacent to the surface of a solid body, under the action of surface forces. At the same time, the region of modified structure is separated from the remaining volume of the liquid by a sharp line of demarcation, which permits speaking of a specific boundary phase, different from the normal bulk phase. The thickness h_c of the boundary phase for a number of individual liquids amounts to 10^{-6} to 10^{-5} cm. If a liquid film on the surface of a solid body has a thickness less than h_c, then it wholly represents the boundary phase, i.e., it will be single-phase. When $h > h_c$, then it is not obligatory that the two-layer, and hence also two-phase, state of the film (oriented sublayer and "normal" liquid above) be uniquely stable, nor even that it be the more stable. As will be shown below, for small excesses of h over h_c the single-phase state likewise will be stable (although it may also be metastable), at which time the entire layer will exist in the state of a boundary phase oriented under the influence of the solid "sublayer." With an increase of the difference $(h - h_c)$, lability may set the limit for this state. Thus, in a certain region of thicknesses, for one and the same thickness (or adsorption Γ) there may correspond two equilibrium states of the layer, in effect two polymorphic modifications: a single-phase α-modification and a two-phase β-modification. This permits speaking of polymorphism (in its own way) of polymolecular adsorbed films of polar liquids.

Depending on the distance to which the oriented structure is propagated in the liquid, two possible cases may be distinguished. When this distance is finite, polymorphism itself is possible only for layers of certain intermediate thicknesses. This also will be the case of the appearance of boundary phases. If the same oriented structure can be extended to infinity, then the difference between the polymorphic modifications of the layers α and β is also retained for infinitely extended (infinitely thick) phases. This means that here the question is now one of anisotropic modification of the bulk liquid phase. Up to this time, the sole class of substances for which this case has been established is that of liquid crystals.

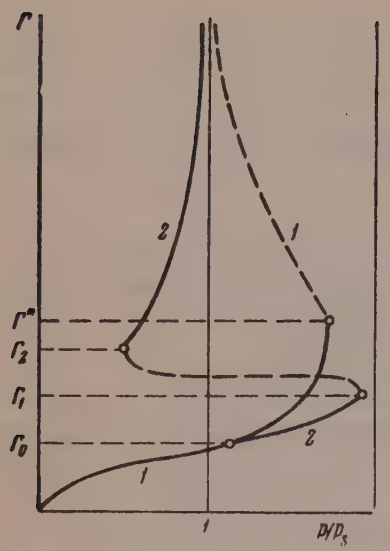


Fig. 3. Adsorption isotherms of two types.

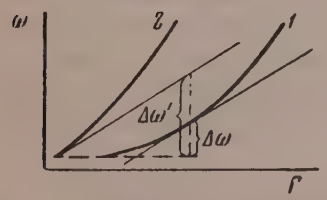


Fig. 4. Analysis of relative stability of α- and β-modifications of film: 1) single-phase α-modification of film; 2) two-phase β-modification of film.

Turning to a discussion of the case in which the oriented structure is propagated from the solid wall into boundary layers of finite thickness, let us note that one may speak of the possibility of polymorphism of films only with adsorptions $\Gamma > \Gamma_0$, where Γ_0 corresponds to the minimum thickness h_c of the "sublayer" underlying two-phase films of arbitrary thicknesses. As $\Gamma \to \infty$ in the case under consideration, only the two-phase β-modification can exist. However, in the region of finite thicknesses there exists, as shown by experiment [2], such an interval of "thicknesses" $\Gamma_0 < \Gamma < \Gamma^*$, in which the single-phase α-modification of the polymolecular films is the more stable, i.e., $\mu^\alpha(\Gamma) < \mu^\beta(\Gamma)$. Since $\mu^\alpha_\infty = \mu^\beta_\infty$, then, in agreement with Eq. (2), the difference in the thermodynamic properties of the α- and β-modifications is explained by the difference of their excess free energies. Supported by the considerations, and bringing in the experimental facts [2], it is possible to draw a number of inferences concerning the path of the curves $\omega^\alpha = \omega^\alpha(\Gamma)$ and $\omega^\beta = \omega^\beta(\Gamma)$.

Since the two-phase β-modification can exist only at thicknesses $\Gamma > \Gamma_0$, then the first section of the curve $\omega = \omega(\Gamma)$ in the case of polar liquids, will pertain to the single-phase α-modification (boundary phase). At the initial point, the indicated curve (Fig. 2b) touches the ordinate axis,* which follows directly from the condition $P \to 0$ as $\Gamma \to 0$. With an increase of Γ, the curve in Fig. 2b at first decreases, reaching a minimum at the "point of saturation," $\Gamma = \Gamma_s$,** after which it goes upward. Certain observations force us to assume that the lower limit of the region of possible polymorphism of the films will be located at the point of saturation, i.e., $\Gamma_0 \geq \Gamma_s$.***

Since, in the region of the "supersaturated" state of the β-modification ($\Gamma_s < \Gamma < \Gamma^*$) the embryonic drops of liquid forming on the oriented "sublayer" (boundary phase) form a finite contact angle with this sublayer, then the curve $\omega^\alpha = \omega^\alpha(\Gamma)$ (Curve 1, Fig. 2b) in this region, at least in a certain section, will be located below its maximum branch.**** From the experimental data it also follows that, at slight supersaturations, the oriented single-phase α-modification will be, for the present, more stable than the two-layer, two-phase β-modification. This implies that, near the point $\Gamma = \Gamma_0$, the curve $\omega^\beta = \omega^\beta(\Gamma)$ (Curve 2, Fig. 2b) breaks upward more abruptly than the curve $\omega^\alpha = \omega^\alpha(\Gamma)$ (Curve 1, Fig. 2b). The single-phase α-modification can be realized in experiment only for Γ lower than a certain Γ^*,***** whereas the normal β-modification under corresponding conditions may have a greater thickness, it following from experiments on wetting films [1] that, in the region of greater thicknesses, the β-modification is stable, i.e., $\frac{\partial^2 \omega^\beta}{\partial \Gamma^2} > 0$. This signifies that at large Γ Curve 1 must correspond to labile states, and Curve 2 to metastable states. Summarizing what has been stated, one may represent schematically the paths of Curves 1 and 2 (Fig. 2b). Proceeding from these curves, it is possible to represent graphically, by means of Eq. (3), the nature of the dependence of thickness of the α- and β-modifications of the film on the given vapor pressure (Fig. 3) (or on the disjoining pressure).

---

*The same as the curve in Fig. 2a, in the case of nonpolar liquids.

**The question is one of saturation with respect to the β-modification.

***This is evidenced, in particular, by the experimentally observed sharpness of the boundary between a layer and an embryonic drop appearing on it, which is possible only in the case of a phase difference between the drop and the underlying "sublayer."

****The necessity of satisfying the condition $\omega(\Gamma_s) < \omega_\infty$ in incomplete wetting is shown below (see also [10]).

*****Otherwise we will have no longer a boundary phase, but simply a layer of an anisotropic phase differing from the original (for more detail, see p. 37).

Summing up, we note that the most important of the results obtained is the inference of polymorphism of the film of a polar substance in the interval $\Gamma_0 < \Gamma < \Gamma^*$ (Fig. 2b). In this interval, two different states correspond to each value of film thickness: the single-phase α-state with wholly oriented structure, and the two-phase β-state, corresponding to a film of normal liquid underlain by an oriented "sublayer" (boundary phase). Practically, in view of the presence in Curve 2 of a labile section, the region of polymorphism of the films is somewhat contracted, depending on the location of the final points $\Gamma = \Gamma_1$ and $\Gamma = \Gamma_2$ (Fig. 2b). If the points Γ_1 and Γ_0 do not coincide, then the first interval of thicknesses in which polymorphism is possible corresponds to $\Gamma_0 < \Gamma < \Gamma_1$. The second interval of thicknesses $\Gamma_2 < \Gamma < \Gamma^*$ occurs in that case in which the point Γ_2 is located to the left of Γ^*.

The form obtained for the relationship $\omega^\beta = \omega^\beta(\Gamma)$ for the two-phase β-modification of the film (Curve 2, Fig. 2b) agrees on the whole with the analogous curves presented in the work of Frumkin [10]. In our analysis for this case, there is effected only an increase of accuracy, in connection with the concept of an oriented sublayer.* The form of Curve 1, Fig. 2b for the wholly oriented α-modification has been established for the first time.

In the region $\Gamma_0 < \Gamma < \Gamma^*$ in which polymorphism is possible, every value of Γ will correspond to two physical states of the film, with differing values of the equilibrium vapor pressure. This conclusion obtained experimental verification in the work of Everett [11]. If the vapor pressure P is fixed (or the chemical potential of the vapor), then in the region of polymorphism for each value of P lying in the interval $P(\Gamma_0) < P < P(\Gamma^*)$ (Fig. 3) there correspond two equilibrium "thicknesses" of the layer: Γ_α (for the single-phase modification) and Γ_β (for the usual two-phase).** In addition, it is not difficult to show that at a given P in the indicated region the single-phase α-modification will be the more stable, for which it is sufficient to calculate the difference
Utilizing condition (2), we have, for the thermodynamic potential of the film – vapor systems:

$$\Phi_\alpha = \mu_\infty \Gamma_\alpha A + \mu(N - \Gamma_\alpha A) + \omega^\alpha A = \mu N - \frac{\partial \omega^\alpha}{\partial \Gamma} \Gamma_\alpha A + \omega^\alpha A,$$

$$\Phi_\beta = \mu_\infty \Gamma_\beta A + \mu(N - \Gamma_\beta A) + \omega^\beta A = \mu N - \frac{\partial \omega^\beta}{\partial \Gamma} \Gamma_\beta A + \omega^\beta A$$

(N is the total number of particles in the system), from which, taking into account the condition $\frac{\partial \omega^\alpha}{\partial \Gamma} = \frac{\partial \omega^\beta}{\partial \Gamma}$, (which follows from the equality of the vapor pressures), we obtain

$$\frac{\Delta \Phi}{A} = -\Delta\omega + \frac{\partial \omega^\beta}{\partial \Gamma} \Delta\Gamma,$$

where $\Delta\omega = \omega^\alpha - \omega^\beta$ and $\Delta\Gamma = \Gamma_\alpha - \Gamma_\beta$ are essentially positive in the region of polymorphism, i.e., with $P(\Gamma_0) < P < P(\Gamma^*)$. From Fig. 4 it is evident that, in this region, $\Delta\omega < \Delta\omega' = \frac{\partial \omega^\beta}{\partial \Gamma} \Delta\Gamma$ from which it follows that, in the indicated region, $\Delta\Phi > 0$. Consequently, at supersaturations corresponding to the region of polymorphism, $P(\Gamma_0) < P < P(\Gamma^*)$, the single-phase α-modification is the more stable, which also causes its preferential realization in experiment (in the indicated region of supersaturations).***

Effect of Layer Thickness on Its Thermodynamic Characteristics

To the thermodynamic characteristics of a layer one may relate, in particular, its disjoining pressure $p(\Gamma)$, vapor pressure P, transition temperature T, and heat of transition λ.

The disjoining pressure of the layer is determined by the relationship****

$$p(\Gamma) = -\frac{1}{v} \frac{\partial \omega}{\partial \Gamma} \qquad (4)$$

* Taking this circumstance into account leads, in particular, to a change of the value of ω_∞, since the film proves to be in direct contact not with the surface of the solid body, but with the sublayer.

** A similar situation may also occur with other values of P, for example, those corresponding to the initial section $0 < \Gamma < \Gamma_s$, and the right-hand branch $\Gamma_2 < \Gamma < \infty$ of Curve 2 (Fig. 2b). But, in this case, polymorphism no longer occurs, since each value of Γ corresponds here to one definite value of P.

*** With specific precautionary measures it is probably possible, in this region, to realize also the β-modification, but it will be unstable.

**** Formula (4) may be obtained most simply from the equilibrium (2) (for example, see [6]).

(v is the volume required in the layer for one particle). Utilizing the information on the path of the curve $\omega^{\alpha} = \bar{\omega}^{\alpha}(\Gamma)$ (Curve 1, Fig. 2b), we find that, with an increase of Γ, the disjoining pressure of the single-phase modification of the layer decreases, the "thickness" $\Gamma = \Gamma_s$ being a unique point of inversion corresponding to the transition from positive (with $\Gamma < \Gamma_s$) to negative (with $\Gamma > \Gamma_s$) values of the disjoining pressure.

The dependence of vapor pressure on layer thickness Γ is given by Eq. (3). From this equation it follows that, for the single-phase modification of the film, the equilibrium vapor pressure is increased with an increase of Γ, passing from unsaturation (with $\Gamma < \Gamma_s$) to a certain supersaturation (with $\Gamma > \Gamma_s$). The maximum possible value of supersaturation* conforms to the thickness $\Gamma = \Gamma^*$ corresponding to the point of discontinuity in Curve 1, Fig. 2b; this is determined by the relationship

$$kT \ln (P/P_s)_{\max} = \left(\frac{\partial \omega^{\alpha}}{\partial \Gamma}\right)_{\Gamma = \Gamma^*}.$$

The temperature of transition can be defined as the temperature at which both phases, existing under a given pressure (or, more accurately, pressures), coexist in equilibrium with each other. In our case, this will be the equilibrium temperature of the layer at which the pressure of its saturated vapor assumes the given value. For an infinitely small reversible isobaric change of state, Eq. (2) gives

$$\frac{\partial \mu'_{\infty}}{\partial T} dT + d\left(\frac{\partial \omega}{\partial \Gamma}\right) = \frac{\partial \mu''_{\infty}}{\partial T} dT$$

or

$$-\eta'_{\infty} dT + d\left(\frac{\partial \omega}{\partial \Gamma}\right) = -\eta''_{\infty} dT,$$

where η'_{∞} and η''_{∞} are the specific entropies (calculated for a single particle) of the infinitely extended liquid and vapor. Taking into account that $\eta''_{\infty} - \eta'_{\infty} = \lambda_{\infty}/T$ (λ_{∞} is the heat of vaporization of the "bulk" liquid calculated for a single particle), we then obtain

$$-d\left(\frac{\partial \omega}{\partial \Gamma}\right) = \lambda_{\infty} \frac{dT}{T}.$$

Hence, neglecting in the first approximation the temperature dependence of λ_{∞}, and integrating within limits from $\Gamma = \infty$ to $\Gamma = \Gamma$, we find for the dependence of transition temperature on "thickness" of the layer Γ

$$\ln \frac{T}{T_{\infty}} = -\frac{1}{\lambda_{\infty}} \frac{\partial \omega}{\partial \Gamma}. \qquad (5)$$

Here T_{∞} is the transition temperature for the "bulk" liquid.**

From Eq. (5) it follows that, for the single-phase modification with $\Gamma < \Gamma_s$, the transition temperature is higher than for the "bulk" liquid ($T > T_{\infty}$); with $\Gamma = \Gamma_s$, $T = T_{\infty}$; and with $\Gamma > \Gamma_s$, $T < T_{\infty}$.

In order to analyze the effect of layer thickness on heat of vaporization,*** we take advantage of the relationship $H = \mu - T\frac{\partial \mu}{\partial T}$,**** connecting the specific enthalpy of the phase H (referred to one particle) with its chemical potential. In our case,

---

*In practice, this supersaturation apparently is not attained since, before reaching this supersaturation, there begins the energetically more favorable process of dropwise condensation on the surface of the layer, about which see, for example, [2].

**With moderate values of $\partial\omega/\partial\Gamma$, this equation is converted into that derived previously [6]:

$$\frac{\Delta T}{T_{\infty}} = -\frac{1}{\lambda_{\infty}} \frac{\partial \omega}{\partial \Gamma}.$$

***See also [6].

****See, for example, [12].

$$H'' = \mu''_\infty - T\frac{\partial \mu''_\infty}{\partial T} = H''_\infty,$$

$$H' = \left(\mu'_\infty - T\frac{\partial \mu'_\infty}{\partial T}\right) + \frac{\partial \omega}{\partial \Gamma} - T\frac{\partial}{\partial T}\left(\frac{\partial \omega}{\partial \Gamma}\right) = H'_\infty + \frac{\partial \omega}{\partial \Gamma} -$$

$$- T\frac{\partial}{\partial T}\left(\frac{\partial \omega}{\partial \Gamma}\right) = H'_\infty + \frac{\partial}{\partial \Gamma}\left(\omega - T\frac{\partial \omega}{\partial T}\right)$$

(the index ∞ denotes values of specific enthalpy corresponding to infinitely extended phases); subtracting the second equality from the first, we find for the specific heat of vaporization of the layer (calculated for one particle)

$$\lambda = \Delta H = (H''_\infty - H'_\infty) - \frac{\partial}{\partial \Gamma}\left(\omega - T\frac{\partial \omega}{\partial T}\right) = \lambda_\infty - \frac{\partial}{\partial \Gamma}\left(\omega - T\frac{\partial \omega}{\partial T}\right)$$

Without particular disadvantage for generality of the results, one can represent the function $\omega(\Gamma)$ in the form $\omega(\Gamma) = \omega_\infty \varphi(\Gamma)$, where $\varphi(\Gamma)$ is a function solely of adsorption Γ, then:

$$\omega - T\frac{\partial \omega}{\partial T} = \left(\omega_\infty - T\frac{\partial \omega_\infty}{\partial T}\right)\varphi(\Gamma) = \varepsilon_\infty \varphi(\Gamma) = \frac{\varepsilon_\infty}{\omega_\infty}\cdot\omega(\Gamma)$$

(here ϵ_∞ is the specific excess total energy of a layer of infinite thickness), whence, for a change of the heat of vaporization of the layer caused by a change of its "thickness" Γ, we obtain

$$\Delta\lambda = \lambda - \lambda_\infty = -\frac{\varepsilon_\infty}{\omega_\infty}\cdot\frac{\partial \omega}{\partial \Gamma}. \qquad (6)$$

Utilizing the considerations presented earlier as to the path of the curve $\omega^\alpha = \omega^\alpha(\Gamma)$, we find from Eq. (6) that, for the single-phase modification of the layer, the heat of vaporization of the layer decreases with an increase of Γ. Thereby, with $\Gamma < \Gamma_s$, the heat of vaporization of the layer will be greater than for the "bulk" liquid; with $\Gamma = \Gamma_s$, the heats of vaporization coincide; and with $\Gamma > \Gamma_s$, the heat of vaporization of the layer will be less than λ_∞. The maximum reduction of the heat of vaporization, corresponding to the point of discontinuity $\Gamma = \Gamma^*$ on Curve 1, Fig. 2b, will be equal to:

$$\Delta\lambda_{max} = -\frac{\varepsilon_\infty}{\omega_\infty}\cdot\left(\frac{\partial \omega^\alpha}{\partial \Gamma}\right)_{\Gamma\ \Gamma^*}.$$

A comparison of the relationships obtained shows that changes of the various thermodynamic characteristics of the layer with a change of its thickness are expressed in terms of one and the same derivative $\partial\omega/\partial\Gamma$, and hence also in terms of its disjoining pressure $p(\Gamma) = -\frac{1}{v}\frac{\partial \omega}{\partial \Gamma}$. This implies that the indicated changes are not specific for any one property, but have a general character. In exactly the same way, the considerations presented above, as to the nature of the change of thermodynamic properties of the single-phase modifications of the layers with a change of their thickness, also are of a general character.

The derived relationships (4), (5), and (6) are also equally applicable to the two-phase, two-layer modification of films. If it is considered that such films are sufficiently stable only for the right-hand decreasing branch of Curve 2, Fig. 2b, corresponding to "unsaturated" thick (wetting) films,* then this case will be analogous to the case of films of nonpolar liquids.

Boundary Phases and the Contact Angle of Small Drops

The special role of polymolecular liquid layers in incomplete wetting was noted as long ago as by Frumkin [10], who indicates that a finite contact angle of the drop is formed not with the solid-body surface itself, but with the overlying polymolecular liquid layer. In the light of what was stated above, this is possible only for polar liquids, since only for them is achieved, at least in a certain section (Fig. 2b), the condition necessary for

*In the region of film polymorphism the β-modification is less stable than the α-modification.

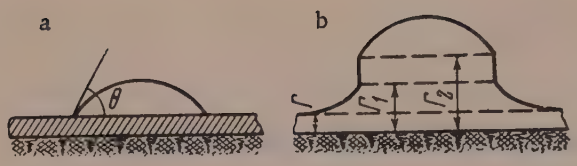


Fig. 5. Micropicture of perimeter of wetting: a) case of single-phase film (boundary phase); b) case of two-layer, two-phase film (film of normal liquid, underlain by oriented "sublayer").

incomplete wetting: $\omega(\Gamma) < \omega_{\infty}$.* Thereby, the perimeter of wetting will exist as a clearly manifested over-all boundary of division of the three phases only in that case in which the polymolecular layer represents the oriented single-phase α-modification (boundary phase), differing from the liquid forming the drop (Fig. 5a). If we have the normal two-phase film, then the perimeter of wetting (as such) will be, strictly speaking, absent (since here the transition from the layer to the drop no longer corresponds to a phase transition). Nevertheless, as was shown by Frumkin [10], owing to the presence in Curve 2, Fig. 2b of a region of disruption of stability (labile interval of thicknesses), the coexistence of a drop with the layer seems to be in some degree possible. The probable configuration of the drop and the layer, in this case, is pictured in Fig. 5b.** Considering, however, that, with thicknesses $\Gamma_s < \Gamma < \Gamma^*$ the two-phase film is less stable than the single-phase, it is difficult to expect realization of this case in experiment.

Thus, incomplete wetting must be the most clearly manifested with the presence of a boundary phase on the surface of the wetted body, i.e., an oriented polymolecular (but single-phase) layer. From experiments on measurement of viscosity of liquids by a blowoff method [9], it follows that an oriented boundary phase also is retained in that case when it comes into contact with the "bulk" liquid. Taking this into consideration, we will assume, in examining the equilibrium of the drop with the boundary phase, that the latter serves directly as that "sublayer" on which the drop rests.

It is evident that a drop for which $P > P_s$ can exist in equilibrium with the boundary phase only at thicknesses of the boundary phase in the interval $\Gamma_s < \Gamma < \Gamma^*$ (Curve 1, Fig. 2b). For a concave meniscus, equilibrium is possible on the initial part of the section ($\Gamma < \Gamma_s$) of Curve 1. In the derivation of the equation determining the equilibrium value of contact angle, it is necessary to take into account the possibility of mass exchange between the drop (or meniscus) and the layer. Therefore, as a basis of the analysis, there should be adopted not the principle of Gibbs – Curie (usually utilized in such cases), but general conditions of thermodynamic equilibrium, for example, the condition of a minimum thermodynamic potential of the entire system.

For the thermodynamic potential of a system consisting of a drop ('), oriented boundary phase ($^{\alpha}$), and vapor (''), we have

$$\Phi = \mu'_{\infty}(P, T)\, g + \sigma_{\infty} S + \mu^{\alpha}_{\infty}(P, T)\, \Gamma A + \omega^{\alpha}(A - Q) + \omega^{\alpha}_{1} Q + \mu''(P, T)\, N'', \qquad (7)$$

here g is the number of particles in the drop; σ_{∞} is the specific free surface energy, and S is the area of the free surface of the drop; ω^{α} is the specific excess free energy; $(A - Q)$ is the area of the free portion of the oriented boundary phase, ω^{α}_1 and Q are the corresponding energy and area for the portion of the boundary phase in contact with the drop; the remaining symbols are the same as previously. In the case of small drops, it is also necessary to take into account Type II capillary effects [5].

According to the general theory of Type II capillary effects [13], with sufficiently small dimensions of the object the deviations from an additive distribution of free energy (or of other potentials) through the phases can no longer be expressed (as is usually assumed) by means of the single term $\sigma_{\infty}S$, proportional to the area of the surface of demarcation of the phases, but require the addition of new terms related to the dimensions of the object. Correspondingly, it is necessary to introduce into expression (7) an additional term $f(a)$, where $a = KV'/S$, a linear parameter characterizing the dimensions of the drop***; V' is the total volume of the drop. The excess

* According to Frumkin [10]: $\cos\theta = [\omega(\Gamma) - \sigma_{solid}]/\sigma_{\infty}$, whence, for incomplete wetting ($\cos\theta < 1$) we have: $\omega(\Gamma) < \sigma_{\infty} + \sigma_{solid} = \omega_{\infty}$. Accounting for the presence of the oriented "sublayer," or the entire boundary phase, leads to replacement of σ_{solid} by ω^{α}_1 (see below); the final result remains the same.

** The vertical portion of the surface corresponds here to the transition from one metastable region of thicknesses of the film to another.

*** K is a proportionality coefficient; regarding its selection, see below.

free energy $f(a)$ refers to the drop as a whole; however, with a view to retaining the usual form of the analysis, it may be referred formally to unit free surface of the drop, and may be combined with the term $\sigma_\infty S$. Then, introducing the designation $\sigma_\infty + f(a)/S = \sigma(a)$, it is possible to rewrite expression (7) in the form

$$\Phi = \mu_\infty(P, T)\, g + \sigma(a)\, S + \mu_\infty(P, T)\, \Gamma A + \omega^\alpha (A - Q) + \omega_1^\alpha Q + \mu''(P, T)\, N''. \tag{8}$$

In this expression, $\sigma(a)$ may be regarded formally as the specific free surface energy of the free surface of the drop, but then it is necessary to consider it dependent on the dimensions of the drop, i.e., on the linear parameter a.

Taking advantage of the evident equalities

$$V' = v'g; \quad S = (v'g)^{2/3}\xi \tag{9}$$

(ξ is a form factor), we have, for the linear parameter,

$$a = K(v')^{1/3}\frac{g^{1/3}}{\xi}. \tag{10}$$

This makes it possible to differentiate the isothermal change of excess free energy of the drop $\delta(\sigma S)_{T=\text{const}}$ into components which are determined separately by the change of the number of particles, and the change of the form of the drop. Taking into consideration that $\delta\sigma_{T\ \text{const}} = \frac{\partial\sigma}{\partial a}\delta a$, and taking into account the equalities (9) and (10), we obtain

$$\delta(\sigma S)_{T\ \text{const}} = \sigma\delta S + S\delta\sigma = -\frac{K}{3}v'\left(\frac{2\sigma}{a} + \frac{\partial\sigma}{\partial a}\right)\delta g + \left(\sigma + a\frac{\partial\sigma}{\partial a}\right)(v'g)^{2/3}\delta\xi = -\frac{K}{3}v'\left(\frac{2\sigma}{a} + \frac{\partial\sigma}{\partial a}\right)\delta g + \left(\sigma - a\frac{\partial\sigma}{\partial a}\right)\delta S_{g\ \text{const}}. \tag{11}$$

Here the second term contains the change of area of the free surface of the drop with constant number of particles or, which is the same, with constant volume of the drop.

The conditions of equilibrium of the system in question are determined from the minimum of Φ with the additional conditions T, P, N, A = const. Utilizing the Lagrange method of undetermined multipliers, it is possible to reduce this problem to finding the minimum of the expression $\Psi = \Phi + \nu N$, where $N = g + \Gamma A + N''$. Varying Ψ with regard for condition (11), and equating $\delta\Psi$ to zero, we obtain a series of equations determining (together with the additional conditions T, P, A = const), the equilibrium of the system

$$\left.\begin{aligned} &\mu_\infty(P, T) + \frac{\partial\omega^\alpha}{\partial\Gamma} = \mu_\infty(P, T) + \frac{\partial\omega_1^\alpha}{\partial\Gamma} = \mu_\infty(P, T) + \\ &+ \frac{K}{3}v'\left(\frac{2\sigma}{a} + \frac{\partial\sigma}{\partial a}\right) = \mu''(P, T) \\ &\left(\sigma - a\frac{\partial\sigma}{\partial a}\right)\delta S + (\omega_1^\alpha - \omega^\alpha)\,\delta Q = 0; \quad \delta V' = 0. \end{aligned}\right| \tag{12}$$

The first group of these equations represents, as is not difficult to see,** the known condition of equality of all parts of the equilibrium system. The equality which follows from this, $\frac{\partial\omega_1^\alpha}{\partial\Gamma} = \frac{\partial\omega^\alpha}{\partial\Gamma}$ must be satisfied within the entire interval of stability of the boundary phase $0 < \Gamma < \Gamma^*$, from which it follows

$$\omega_1^\alpha(\Gamma) - \omega^\alpha(\Gamma) = \text{const} = \omega_1^\alpha(\Gamma_s) - \omega^\alpha(\Gamma_s) = \Delta\omega_s.$$

---

* Taking into account that $\mu_\infty^* = \mu_\infty$, we designate them henceforth simply as μ_∞.

** For the layer the chemical potential is equal to $\mu(\Gamma) = \mu_\infty + \partial\omega/\partial\Gamma$. In analogous manner, as will be shown below, the expression $\mu_\infty + \frac{K}{3}v'\left(\frac{2\sigma}{a} + \frac{\partial\sigma}{\partial a}\right) = \mu_\infty + v'\left(\frac{2\sigma}{r} + \frac{\partial\sigma}{\partial r}\right) = \mu(r)$ represents the chemical potential of the drop.

The second group, which can be reduced to the single equation $\left(\sigma - a\frac{\partial\sigma}{\partial a}\right)\delta S + \Delta\omega_s\delta Q + \tau\delta V' = 0$ (τ is the Lagrange multiplier), affords the possibility of finding the boundary conditions. Let $z = z(x,y)$ – the equation of the free surface of the drop; then

$$S = \iint \sqrt{1 + p^2 + q^2}\,dx\,dy; \quad Q = \iint dx\,dy; \quad V' = \iint z\,dx\,dy,$$

where the flat base of the drop serves as the region of integration.* This permits rewriting the latter equation in the form

$$\delta\iint\left[\left(\sigma - a\frac{\partial\sigma}{\partial a}\right)\sqrt{1 + p^2 + q^2} + \Delta\omega_s + \tau z\right]dx\,dy = 0. \qquad (13)$$

The solution of this variation problem reduces to the solution of the Euler equation $\frac{\partial\psi}{\partial z} - \frac{\partial}{\partial x}\frac{\partial\psi}{\partial p} - \frac{\partial}{\partial y}\frac{\partial\psi}{\partial q} = 0$ [Ψ is the subintegral expression in Eq. (13)], it being necessary that, for points of the perimeter of wetting, the solution which is found must satisfy the boundary conditions

$$\psi_п - \left(\frac{\partial\psi}{\partial p}\right)_п p_п - \left(\frac{\partial\psi}{\partial q}\right)_п q_п = 0; \quad z_п = 0.$$

Substitution of the value of Ψ into the Euler equation after simple transformations leads to the relationship

$$2C = \frac{\sigma}{\sigma - a\,\partial\sigma/\partial a} = \text{const},$$

indicating that also for small drops the average curvature 2C of the equilibrium free surface of the drop (or meniscus) in the absence of a gravitational field is identical at all points. This facilitates the selection of the linear parameter a, making it possible to choose a proportionality coefficient K in expression (10), such that $(3/K)a = r$ ($r = 1/C$, the average radius of curvature). Then, the chemical potential of the drop, which figures in the conditions (12), assumes the more customary form

$$\mu_\infty(P,T) + \frac{K}{3}v'\left(\frac{2\sigma}{a} + \frac{\partial\sigma}{\partial a}\right) = \mu_\infty(P,T) + v'\left(\frac{2\sigma}{r} + \frac{\partial\sigma}{\partial r}\right) = \mu(r),$$

and the multiplier $\sigma - a\frac{\partial\sigma}{\partial a}$, which enters into the expression for Ψ, is converted to $\sigma - r\frac{\partial\sigma}{\partial r}$.

In analogous manner, substituting the value of Ψ into the boundary conditions, we obtain, with regard for the observations made on the selection of the parameter a,

$$\left(\frac{1}{\sqrt{1 + p^2 + q^2}}\right)_п = \frac{-\Delta\omega_s}{\sigma - r\,\partial\sigma/\partial r}.$$

But $1/\sqrt{1 + p^2 + q^2}$ is the cosine of the angle which the normal to the surface of the meniscus forms with the z axis. For points of the perimeter of wetting, this angle is equal to the contact angle θ, i.e., the angle at which the surface of the meniscus meets the surface of the oriented boundary phase. Consequently,

$$\cos\theta = \frac{\omega^\alpha(\Gamma_s) - \omega_1^\alpha(\Gamma_s)}{\sigma - r\,\partial\sigma/\partial r} = \frac{\omega^\alpha(\Gamma_s) - \omega_1^\alpha(\Gamma_s)}{\sigma_\infty}\cdot\frac{\sigma_\infty}{\sigma - r\,\partial\sigma/\partial r}$$

or

$$\cos\theta = \cos\theta_\infty\frac{\sigma_\infty}{\sigma - r\,\partial\sigma/\partial r}, \qquad (14)$$

where θ_∞ signifies the contact angle for a drop of very large dimensions.

*Here p and q are the symbols adopted in the analysis for the partial derivatives $\partial z/\partial x$ and $\partial z/\partial y$.

The formula obtained coincides with that found previously for the case of a monomolecular adsorbed layer [14].

According to literature data [15], for liquid–gas surfaces of demarcation, the derivative $\frac{\partial \sigma}{\partial r} > 0$. Consequently, with a decrease of the radius of the drop, $\cos\theta$ must increase, and the contact angle itself must decrease.

We note, in conclusion, that, in the equation of the contact angle, there enter not the surface tensions (or specific free surface energies) of the solid body, as is sometimes assumed, but the corresponding magnitudes characterizing the oriented boundary phase. This makes illusory any attempts to determine the magnitude of surface tension of a solid body by experiments on wetting.

SUMMARY

1. The conditions of thermodynamic equilibrium of an adsorption or wetting layer have been established. From an analysis of experimental data, carried out on the basis of these conditions, a deduction has been made on the possibility of polymorphism of films of polar liquids in a definite interval of thicknesses. Within the indicated interval, for each value of thickness of the film, there correspond two phase states: a single-phase state with entirely anisotropic (oriented) structure (boundary phase), and a state corresponding to a film of the normal isotropic liquid, underlain by an anisotropic (oriented) "sublayer." There has been shown the greater stability of the single-phase layers (boundary phases) in the region of bivalency.

2. An analysis has been made of the nature of the dependence of the excess free energy of the layer on its thickness.

3. An investigation has been made of the influence of the thickness of the layer on its thermodynamic characteristics: disjoining pressure, vapor pressure, transition temperature, and heat of transition.

4. There has been clarified the role of single-phase layers (boundary phases) in the formation of finite contact angles on the surface of a solid body. The dependence of the magnitude of contact angle on the drop dimensions has been established.

LITERATURE CITED

1. B. Deryagin and E. Obukhov, Kolloid. Zhur. 1, 385 (1935); B. Deryagin and M. Kusakov, Izvest. Akad. Nauk SSSR, Ser. Khim. No. 5, 741 (1936); No. 5, 1119 (1937).
2. B. V. Deryagin and Z. M. Zorin, Zhur. Fiz. Khim. 29, 1755 (1955).
3. B. V. Deryagin, Zhur. Fiz. Khim. 14, 157 (1940); Doklady Akad. Nauk SSSR 113, 842 (1957).
4. B. V. Deryagin, Kolloid. Zhur. 17, 207 (1955).
5. L. M. Shcherbakov, Dissertation: Phase Equilibria in Systems with Evolved Surfaces of Phase Demarcation [in Russian] (Moscow, 1950); L. M. Shcherbakov, Trudy Tul'sk. Mekh. Inst. 7, 117 (1955); 8, 173 (1958).
6. L. M. Shcherbakov, Kolloid. Zhur. 22, 111 (1960).
7. O. M. Poltorak, Zhur. Fiz. Khim. 34, 3 (1960).
8. B. Deryagin, M. Kusakov, and L. Lebedeva, Doklady Akad. Nauk SSSR 23, 670 (1939).
9. B. V. Deryagin and V. V. Karasev, Doklady Akad. Nauk SSSR 101, 289 (1955).
10. A. N. Frumkin, Zhur. Fiz. Khim. 12, 337 (1938); A. N. Frumkin and A. Gorodetskaya, Zhur. Fiz. Khim. 12, 511 (1938).
11. D. H. Everett, Proceedings of the Second International Congress on Surface Activity (London, 1957) p. 224.
12. E. A. Guggenheim, Modern Thermodynamics [in Russian] (Moscow-Leningrad, 1941) p. 44.
13. L. M. Shcherbakov, "General theory of Type II capillary effects," Collection: Transactions of Jubilee Conference on Surface Forces (Institute of Physical Chemistry, AN SSSR) (in press).
14. L. M. Shcherbakov and P. P. Ryazantsev, Zhur. Fiz. Khim. 34, No. 9, 2120 (1960).
15. R. C. Tolman, J. Chem. Phys. 17, 333 (1949); F. P. Buff, J. Chem. Phys. 19, 1591 (1951); 23, 419 (1955); L. M. Shcherbakov, Kolloid. Zhur. 14, 379 (1952).

DIFFUSIOPHORESIS IN ELECTROLYTE SOLUTIONS AND ITS ROLE IN THE MECHANISM OF FILM FORMATION FROM RUBBER LATEXES BY THE METHOD OF IONIC DEPOSITION

B. V. Deryagin, S. S. Dukhin, and A. A. Korotkova

Institute of Physical Chemistry, Academy of Sciences of the USSR, Moscow.
Translated from Kolloidnyi Zhurnal, Vol. 23, No. 1, pp. 53-58, January-February, 1961
Original article submitted July 12, 1960

The deposition of films of rubber latexes on forms by a layer of electrolyte applied to its surface is usually explained by gelation of the latex under the action of ions diffusing deeply into the latex from the surface. This explanation, however, does not clarify an essential point: the significant increase of latex concentration near the surface of the form during the process. The sources of the forces capable of transporting particles of the latex in a direction toward the form may be gradients of electrical and chemical potentials accompanying diffusion (into the depth of the solution) of ions of the electrolyte applied to the form.

A formula for diffusiophoresis in a nonelectrolyte solution [1], derived by means of a simple generalization, is transformed, in the case of electrolytes, to the following form:*

$$v^D = \frac{z^- \xi^+ + z^+ \xi^-}{\eta} c \operatorname{grad} \mu \approx \frac{z^- \xi^+ + z^+ \xi^-}{\eta} RT \operatorname{grad} c, \qquad (1)$$

where η is the viscosity, c is the so-called molar concentration of the electrolyte $c^+/z^- = c^-/z^+$; μ is the chemical potential; R is the universal gas constant; T is the absolute temperature; z^+ and z^- are the electrovalences of the ions; $\xi^+ = \frac{1}{c_0^+}\int_0^\infty \gamma^+ h dh$; $\xi^- = \frac{1}{c^-}\int_0^\infty \gamma^- h dh$ **; $\gamma^\pm$ is the excess cation or anion concentration (compared to the bulk concentration) in the double layer at a distance h from the shear surface; c^+ and c^- are the concentrations of cations and anions in the bulk of the solution.

*In this formula there is omitted the multiplier $^2/_3$ which was erroneously introduced (following Hueckel) into formula (20) of [1], which was indicated to us in his time by A. N. Frumkin.

**Utilizing the Gouy–Chapman theory of the electrical double layer, it is possible to express ξ^+ and ξ^- separately through ζ:

$$\xi^\pm = \frac{\varepsilon}{8\pi\kappa' I}\int_\Phi^\zeta \frac{[-\exp(\mp z^\pm e\psi/kT) - 1]\int_\psi^\zeta \{c_0^+[1-\exp(-z^+e\psi'/kT)] + c_0^-[1-\exp(z^-e\psi'/kT)]\}^{-1/2} d\psi'}{\{c_0^+[1-\exp(-z^+e\psi/kT)] + c_0^-[1-\exp(z^-e\psi/kT)]\}^{1/2}} d\psi.$$

Integration is carried out successfully for $z^+ = z^- = z$

$$\xi^\pm = \frac{\varepsilon kT}{2\pi F c_0 z^2 e}\{\ln[1 + \exp(\mp ze\zeta/2kT)] - \ln 2\}. \qquad (2)$$

Utilizing the result of [2], one can find the electrical field E, connected with the concentration field by the relationship

$$\vec{E} = \frac{RT}{F} \frac{(D^+ - D^-)}{(z^+D^+ + z^-D^-)} \frac{\operatorname{grad} c}{c}, \tag{3}$$

where F is the Faraday number; D^+ and D^- are the coefficients of diffusion of positive and negative ions.

If it is taken into account that the ζ-potential is equal to $\frac{4\pi}{\varepsilon} Fcz^+z^- (\xi^+ - \xi^-)$, where ϵ is the dielectric constant, for the rate of electrophoresis [3], utilizing Eq. (3), we obtain

$$\vec{v}_E = \frac{Fcz^+z^- (\xi^+ - \xi^-)}{\eta} \vec{E}(x, t) = \frac{(\xi^+ - \xi^-) z^+z^- (D^+ - D^-) RT}{\eta (z^+D^+ + z^-D^-)} \operatorname{grad} c. \tag{4}$$

Adding Eqs. (1) and (4) by terms, we obtain the resultant rate of diffusiophoresis of the latex particles

$$\vec{v} = \vec{v}_E + \vec{v}_D = \frac{RT}{\eta} D_{eff} \left(\frac{z^-\xi^+}{D^+} + \frac{z^+\xi^-}{D^-} \right) \operatorname{grad} c, \tag{5}$$

where $D_{eff} = \frac{D^+D^- (z^+ + z^-)}{z^+D^+ + z^-D^-}$.

In Eq. (5), $\vec{v}$ is found to be expressed through D_{eff}, and is two-membered, differing from the ζ-potential by the presence of coefficients, depending on D^+ and D^-. This is connected with the fact that diffusion is primary in the effect under consideration (not the electrical field, which has a secondary derivation). Therefore, diffusiophoresis should be termed a phenomenon characterized on the whole by the velocity of the particles $\vec{v}$. As follows from the theory of the double layer, the total $z^-\xi^+ + z^+\xi^-$ is always positive, even though one of its terms is negative. Therefore, $\vec{v}$ will more often be directed toward the surface of the form, and in the opposite direction only with a proper value of the ratio D^+/D^-, differing substantially from unity. Since the ζ-potential of the latex globules is usually negative and, consequently, $\xi^+ > 0$, $\xi^- < 0$, then, for $CaCl_2$, which is often utilized in industrial ionic deposition, and for which $D^+ < D^-$, $\vec{v}$, in accordance with Eq. (4), is known to be directed toward the form.

An accurate description of the process for high concentrations of latex (say 30%) conforming to industrial conditions involves great difficulties. Therefore, let us examine the precipitation of a latex with such concentrations that the adjacent particles do not show a significant influence on the field of diffusion around a given particle and on its movement. Let us note further that the thickness of the latex layer from which precipitation occurs is, as a rule, several orders of magnitude less than the dimensions of the form, in connection with which one can be limited to consideration of a plane problem of diffusion.

In order to find the distribution of an electrolyte diffusing into a semispace from a plane layer of the fixing agent of thickness h, let us examine the equivalent problem of nonstationary diffusion of an electrolyte into an

---

With a sufficiently low value of ζ-potential (practically, at $\zeta < 25$ mv), the exponents in the subintegral expressions are expanded in a series, and integration also proves to be possible:

$$\xi^{\pm} = \mp \frac{\varepsilon\zeta}{4\pi Fc_0 z^+ (z^+ + z^-)}. \tag{2a}$$

It is also possible to evaluate $\xi^{\pm}$ for large absolute values of the ζ-potential:

$$\text{if} \quad \zeta \gg 25 \text{ mv, then } |\xi^+| \ll |\xi^-|, \ \xi^- \simeq \zeta \frac{\varepsilon}{4\pi Fcz^+z^-}, \tag{2b}$$

$$\text{if} \quad \zeta \ll -25 \text{ mv, then } |\xi^-| \ll |\xi^+|, \ \xi^+ \simeq \zeta \frac{\varepsilon}{4\pi Fcz^+z^-}. \tag{2c}$$

unlimited space from a layer of thickness 2h. The functions c'(x,t) and c(x,t), where x is the distance from the plane of symmetry, coinciding with the central plane in the layer of fixing agent, and t is the time from the start of the process, which characterize the nonstationary fields of diffusion of ions within the fixing agent ($|x| < |h|$) and beyond it ($|x| > |h|$), satisfy, in addition to the equations

$$\frac{\partial c'}{\partial t} = D'_{eff}\frac{\partial^2 c'}{\partial x^2}, \quad \frac{\partial c}{\partial t} = D_{eff}\frac{\partial^2 c}{\partial x^2},$$

(where D'_{eff} is the diffusion coefficient of the electrolyte in the fixing agent, which may be considered as a capillary-porous medium), also the initial and boundary conditions*

$$c'(x, t)|_{t=0} = c_0, \; c(x, t)_{t=0} = c_1, \tag{6}$$

$$c'(x, t)|_{x=\pm h} = c(x, t)_{x=\pm h}, \; D'_{eff}\frac{\partial c'}{\partial x}(x, t)|_{x=\pm h} = D_{eff}\frac{\partial c}{\partial x}(x, t)|_{x=\pm h}. \tag{7}$$

Utilizing the solution of an analogous heat problem on the cooling of a plate, we obtain

$$c(x, t) = c_0 + (c_1 - c_0)\frac{(D'_{eff}/D_{eff})^{1/2}}{1 + (D'_{eff}/D_{eff})^{1/2}}\left[erfc\frac{x-h}{2(D_{eff}t)^{1/2}} - \right.$$
$$\left. -(1-\varkappa)\sum_{n=1}^{\infty}(-\varkappa)^{n+1}erfc\frac{x-h+2nh(D'_{eff}/D_{eff})^{1/2}}{2(D_{eff}t)^{1/2}}\right], \tag{8}$$

where

$$\varkappa = \frac{1-(D'_{eff}/D_{eff})^{1/2}}{1+(D'_{eff}/D_{eff})^{1/2}}.$$

A particle located at time t at a distance x from the surface of the form can be considered as existing in a quasi-homogeneous field with intensity equal to E(x,t), and a quasi-homogeneous field of chemical potential $\partial\mu/\partial x$ corresponding to a field of concentration gradient $\partial c/\partial x$. Taking this into consideration, we can utilize Eq. (5) for calculating the rate of diffusiophoresis, where, for c(x,t) we substitute Eq. (8).

$$v(x, t) = \frac{dx}{dt} = -\frac{A}{2\sqrt{D_{eff}t}}\left[e^{-\frac{(x-h)^2}{4D_{eff}t}} - \right.$$
$$\left. -(1+\varkappa)\sum_{n=1}^{\infty}(\varkappa)^{n+1}e^{-\frac{[x-h+2nh(D'_{eff}/D_{eff})^{1/2}]^2}{4D_{eff}t}}\right], \tag{9}$$

where

$$A = \frac{2(c_0-c_1)RT(D'_{eff}D_{eff})^{1/2}D_{eff}}{\sqrt{\pi}\eta[1+(D'_{eff}/D_{eff})^{1/2}]}\left(\frac{z^-\xi^+}{D^+} + \frac{z^+\xi^-}{D^-}\right); \tag{10}$$

A depends on c, through ξ^+ and ξ^-.

Let us calculate the time at which a particle, located at the moment t = 0 at a distance x_0, reaches the surface of ionic deposition. Being limited to the case of relatively thin films, the time of formation of which satisfies the condition

$$t_0 \ll h^2/D'_{eff}, \tag{11}$$

it is possible, in the first part of Eq. (9), to consider only the first item. Let us write Eq. (9) in dimensionless quantities, taking into account the condition (11):

* In order not to complicate the analysis by calculation of an extraneous electrolyte, we will consider that there is previously established in the latex a given concentration of the electrolyte introduced into the fixing agent, and that other ions are absent.

$$\frac{dy}{d\tau} = -ke^{-y^2/\tau}\frac{1}{\sqrt{\tau}}, \tag{12}$$

where $y = \frac{x-h}{x_0-h}$, $\tau = \frac{4D_{eff}t}{(x_0-h)^2}$,

$$k = \frac{A}{4D_{eff}} = \frac{(c_0-c_1)\,RT\,(D'_{eff}/D_{eff})^{1/2}}{2\sqrt{\pi}\,\eta\,[1+(D'_{eff}/D_{eff})^{1/2}]}\left(\frac{z^-\xi^+}{D^+}+\frac{z^+\xi^-}{D^-}\right), \tag{12a}$$

whereupon the initial condition will be

$$y|_{\tau=0} = 1. \tag{13}$$

Multiplying both parts of Eq. (12) by 2y, we transform it to the form

$$\frac{dy^2}{d\tau} = -f(z), \tag{14}$$

where

$$z = y^2/\tau,\ f(z) = 2ke^{-z}\sqrt{z}, \tag{15}$$

in which it should be remembered that k(c), being a function of $\underline{c}$, depends on $\underline{z}$, tending at $z \to 0$ to a value $k_0 = k(c_0)$. From Eq. (14) we obtain

$$-\frac{dz}{d\ln\tau} = f(z)+z, \tag{16}$$

whence

$$d\ln\tau = \frac{-dz}{f(z)+z},\quad d\ln y^2 \equiv d\ln\tau + d\ln z = \frac{f(z)\,dz}{z\,(f(z)+z)}. \tag{17}$$

For determining the total time of movement τ_∞ corresponding to a change of $\underline{y}$ from 1 to 0 (at $\tau \to \infty$) and a change of $\underline{z}$ from ∞ to 0, we break up τ_∞ into two stages: τ_1, corresponding to the limits of change from $z = \infty$ to $z_1 = 1$, and τ_2, from $z_1 = 1$ to $z = 0$; thereby,

$$\tau_\infty = \tau_1 + \tau_2.$$

Integrating Eq. (17) in the first stage, we obtain

$$\ln y_1^2 = \ln(z_1\tau_1) = \ln\tau_1 - \int_1^\infty \frac{f(z)\,dz}{z\,(z+f(z))}. \tag{18}$$

The direct integration of Eq. (16) in the first interval is impossible, as it leads to diverging integrals.

For determining τ_2, we integrate Eq. (16) within the limits z = 1, 0, obtaining

$$\ln\left(\frac{\tau_1+\tau_2}{\tau_1}\right) = \int_0^1 \frac{dz}{z+f(z)}. \tag{19}$$

From Eqs. (18) and (19) we find

$$\ln\tau_\infty \equiv \ln(\tau_1+\tau_2) = \int_0^1 \frac{dz}{f(z)+z} - \int_1^\infty \frac{f(z)\,dz}{z\,(f(z)+z)}. \tag{20}$$

If the condition*

$$f(1) \ll 1 \tag{21}$$

is fulfilled, then the first integral in the right-hand part of Eq. (20) can be calculated approximately, since the only significant values of $f(z)$ are those near $z = 0$, when $f(z) \approx 2k_0\sqrt{z}$, it being found equal to $\ln(2k_0)^{-2}$. The second integral in Eq. (20) may be neglected in comparison with the first,** so that, in this case,

$$\tau_\infty = 4D_{eff}t_\infty/(x_0 - h)^2 = (4k_0^2)^{-1},$$

whence, for total time of movement, we obtain

$$t_\infty = (x_0 - h)^2/16D_{eff}k_0^2. \tag{22}$$

Having noted that, at time t_∞, globules located to the left of the plane x_0 reach the surface of the form, it can be concluded that the precipitation of the globules from a layer of latex of thickness x_0 is accomplished at time t_∞, whence follows a simple formula for surface density $\Gamma(t)$ (g/cm^2) of the precipitated layer of latex as a function of time*** (we omit the index ∞ for t)

$$\Gamma(t) = \rho_0(x_0(t) - h) = \rho_0 4k_0(D_{eff}t)^{1/2} =$$
$$= \frac{2\rho_0 RT}{\eta}\left(\frac{z^-\xi^+}{D^+} + \frac{z^+\xi^-}{D^-}\right)(c_0 - c_1)\frac{(D'_{eff}t)^{1/2}}{(\pi)^{1/2}[1 + (D'_{eff}/D_{eff})^{1/2}]}, \tag{23}$$

where c_1 is the initial concentration of the latex (g/cm^2). A time dependence similar to that described by Eq. (23) was observed experimentally [4], the observed values having an order of magnitude close to the theoretical.****

In conclusion, let us express by means of Eqs. (2) and (2b) the rate of ionic deposition $\Gamma(t)$ directly through the ζ-potential in those cases for which this proves to be possible:

$$\Gamma(t) = \frac{\rho_0\xi(c_0 - c_1)(kT)^2(D'_{eff}t)^{1/2}}{\pi^{3/2}\eta c_0 z^2 e^2[1 + (D'_{eff}/D_{eff})^{1/2}]}\left\{\frac{\ln[1 + \exp(-ze\zeta/2kT)]/2}{D^+} + \right.$$
$$\left. + \frac{\ln[1 + \exp(ze\zeta/2kT)]/2}{D^-}\right\}, \quad (z^+ = z^- = z)$$

$$\Gamma(t) = \frac{\rho_0\xi\zeta kT(c_0 - c_1)(D^+ - D^-)(D'_{eff}t)^{1/2}}{2\pi^{3/2}\eta e c_0(z^+ + z^-)D^+D^-[1 + D'_{eff}/D_{eff})^{1/2}]}, \quad (|\zeta| < 25 \text{ mv})$$

---

* The condition (21) is equivalent to the condition $k \gg 1$, which is fulfilled with great accuracy.

** This signifies that, on the whole, the particle moves in an environment of concentrations close to c_0. From Eq. (18) it follows simultaneously that the route which is practicable beyond the first stage (i.e., beyond time equal to τ_1) also can be neglected. This justifies disregarding the dependence of k on c.

*** A comparison of Eq. (22) and condition (11) permits the conclusion that Eq. (23) may be applied for describing the kinetics of formation of thin film, the thickness of which is much less than the thickness of the layer of fixing agent h. Let us note further that a description of the formation of thicker films is complicated by gravitational convection of the latex, developed according to the measure of change of its specific gravity (in the layer bordering on the fixing agent) in the process of diffusion.

**** Equations (1) and (3), which were utilized above, were derived for the case where the lines of flow of diffusion and the lines of force of the electrical field in effect bypass the globule. Meanwhile, part of the current of diffusion is directed toward the surface of the globule, and goes to the formation of an adsorbed layer, which continuously undergoes change, since the bulk concentration in the vicinity of the particle is changed continuously. However, we saw that, in ionic deposition, the principal stage of movement of the latex particles is completed in an environment of concentration close to c_0; therefore, no large changes of adsorption of ions on the surface of the globules can occur in the course of the principal time of their migration to the form.

$$\Gamma(t) = \frac{\varepsilon\rho_0 kT\,(c_0 - c_1)\,\zeta\,(D'_{eff}t)^{1/2}}{2\pi^{3/2}\eta e c_0 z^- D^- [1 + (D'_{eff}/D_{eff})^{1/2}]}, \quad (\zeta \gg 25\ \text{mv})$$

$$\Gamma(t) = \frac{\varepsilon\rho_0 kT\,(c_0 - c_1)\,\zeta\,(D'_{eff}t)^{1/2}}{2\pi^{3/2}\eta e c_1 z^+ D^+ [1 + (D'_{eff}/D_{eff})^{1/2}]}, \quad (-\zeta \gg 25\ \text{mv}).$$

SUMMARY

1. A formula of diffusiophoresis in a nonelectrolyte solution, being generalized for the case of an electrolyte, permits calculation of the rate of diffusiophoresis as a function of ζ-potential.

2. A demonstration has been given of the role of diffusiophoresis in the kinetics of gel formation from rubber latexes by the method of ionic deposition.

3. A computation has been made of the precipitation of latex particles on the surface of a form by the method of ionic deposition, and on this basis a formula has been obtained for the surface density of the deposited gel as a function of time; this formula is found to be in satisfactory order-of-magnitude agreement with experiment.

LITERATURE CITED

1. B. V. Deryagin, G. P. Sidorenkov, E. A. Zubashchenko, and E. V. Kiseleva, Kolloid. Zhur. 9, 335 (1947).
2. S. S. Dukhin and B. V. Deryagin, Kolloid. Zhur. 21, 37 (1959).
3. B. V. Deryagin and S. S. Dukhin, Doklady Akad. Nauk SSSR 129, 1328 (1959).
4. D. M. Sandomirskii and V. A. Chernaya, Trudy Nauch. Issledovatel. Inst. Rezinovoi Promysh. No. 1 (1954).

THE REVERSION OF ELECTROLYTE ADSORPTION BY FERRI- AND ALUMINOSILICATE MIXED GELS

O. I. Dmitrenko and A. A. Ryabinina

Moscow Oceanology Institute, Academy of Sciences of the USSR
Translated from Kolloidnyi Zhurnal, Vol. 23, No. 1, pp. 59-66, January-February, 1961
Original article submitted October 29, 1959

In earlier work we observed the phenomenon of a decrease in the adsorptive capacity of finely dispersed (colloidal) precipitates on the removal of contaminating electrolytes during purification of the precipitates by electrodialysis. A decrease in the adsorptive capacity of ferri- and aluminosilicate mixed gels has been observed in the study of the exchange–adsorption properties by a potentiometric method at different degrees of purification [1], in the construction of acid-base titration curves [2], and in direct analytical determinations of the magnitude of the exchange absorption capacity before and after electrodialysis [3]. Data characterizing the order of change in the magnitude of the exchange capacities during electrodialysis processes are given in Table 1.

TABLE 1

Change in the Magnitude of the Absorptive Capacity of Mixed Gels During Purification by Electrodialysis (According to O. I. Dmitrenko and M. M. Kolesnikov)

Purification of gel	Exchange capacity according to Bobko – Askinazi, mg-equiv per 100 g of dry substance	
	$Al_2O_3 \cdot 2SiO_2$	$Al_2O_3 \cdot SiO_2$ + Na humate
Dialysis	53.20	25.42
Electrodialysis	25.17	22.18

By using extremely rigorous purification conditions, Shishniashvili and Kargin [4] prepared pure uncharged aluminosilicate sols whose stability was attributed to their hydrophilic properties. The authors of the work cited concluded that the aluminosilicate gels are not electrolytes, since the position of the isoelectric point is independent of the composition of these adsorbents in their reaction with acids and alkalies. It was further shown that the pH of the solution increases in the potentiometric titration of mixed gels with K_2SO_4 or KH_2PO_4, indicating hydrolytic adsorption of the acid. In these cases, the potential-determining ions are the hydrogen ions producing a positive charge on the particles [5,6].

Thus, in the reaction of electrodialyzed gels with neutral salt solutions, acid was adsorbed, and the pH of the solution increased as a result of hydrolysis of the salts. If the pH was kept constant during prolonged washing of the gel with the salt solution, the quantity of acid sorbed by the gel became very high. From this it follows that the adsorptive capacity of electrodialyzed gels can be varied as desired. In this connection, it has become necessary to establish whether the effect of increase in the adsorptive capacity also takes place when some readily hydrolyzed compound such as $CuCl_2$ is present in the liquid phase of previously highly purified systems. If ferri- and aluminosilicates subjected to rigorous purification by electrodialysis are, in fact, no longer electrolytes, then an increase in their adsorptive capacities will be observed in the presence of electrolytes, under any conditions. The present study was devoted to an examination of this question.

In the study of the reaction of solutions of hydrolyzed salts and ashless activated charcoal, it was established [7] that exchange absorption of anions takes place with the liberation of hydroxide ions into the solution according to the scheme: $\equiv C - OH + Cl \rightarrow \equiv C - Cl + OH$; where $\equiv C - OH$ and $\equiv C - Cl$ are surface compounds of the carbon. In dilute solutions, the adsorption of chloride increased, and the pH of the solution changed. If the OH^- concentration was controlled, the magnitude of the Cl^- adsorption increased, and the adsorption process

TABLE 2

The Change in pH (Glass Electrode) During the Prolonged Interaction of Dialyzed and Electrodialyzed Mixed SiO_2 and R_2O_3 Gels with Cupric Chloride Solutions (According to O. I. Dmitrenko and A. A. Ryabinina)

Gels	pH
Electrodialyzed gels and $CuCl_2$ solution	
$4Fe_2O_3 \cdot SiO_2$	3.56
$Fe_2O_3 \cdot 2SiO_2$	3.45
$Al_2O_3 \cdot 2SiO_2$	3.56
$Al_2O_3 \cdot 2SiO_3$	3.58
Dialyzed gels and $CuCl_2$ solution	
$4Fe_2O_3 \cdot SiO_2$	3.43
$2Fe_2O_3 \cdot SiO_2$	3.45
$Fe_2O_3 \cdot 2SiO_2$	3.42
$Al_2O_3 \cdot 2SiO_2$	3.46
Control (H_2O and 1 N $CuCl_2$)	3.56

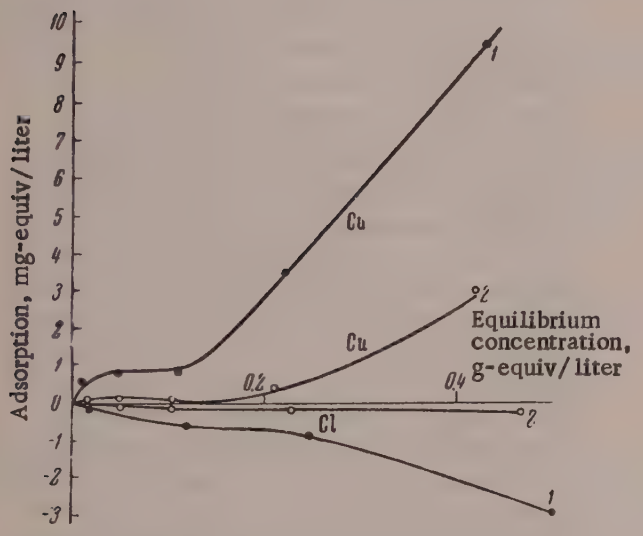


Fig. 1. Nonequivalent absorption of Cu^{2+} and Cl^- during the prolonged interaction of dialyzed (1) and electrodialyzed (2) $Al_2O_3 \cdot 2SiO_2$ gels with $CuCl_2$ solution.

proved to be completely reversible. The influence of the salt cations was revealed as a decrease in the effective concentration of the anions, i.e., it was related to the electrostatic interionic interaction. In the opinion of the authors of [7], the magnitude of the adsorption of anions from solutions of hydrolyzing salts should be much greater than that from solutions of nonhydrolyzing salts and acids. They considered the formation of structural elements in the solutions to be of great importance. Thus, the reaction of hydrolyzed salts with ashless activated charcoal was defined as a surface-chemical reaction involving exchange between the anions of the electrolyte and the hydroxide groups of the carbon surface with simultaneous binding of the cations of the solution in the form of hydroxides or almost undissociated aquocomplexes. In the study of the adsorption of silver salts by coagulated sols of ferric, aluminum, and silicon hydroxides [8], the phenomenon of apparent molecular adsorption of silver sulphate on adsorbents contaminated with chloride ions was observed. The silver cations were removed from solution in the form of hydroxides, or as a precipitate of silver chloride, and, in this connection, it was suggested that the Ag^+ and SO_4^{2-} are fixed by different regions of the surface of the micelle, and do not enter the crystal lattice of the colloid.

In [9,10] a study was made, by the single-specimen method [12], of the exchange adsorption of divalent cations (including copper cations) by bentonite and kaolin clays, natrolite, red-brown clays, and soils in aqueous and aqueous-alcohol media. The work was carried out extremely thoroughly, since constant ionic strength of the solutions was observed. In both cases, the absorption of copper ions was of the irreversible and chemisorptive type, and involved the adsorption of basic and complex copper salts (for example, diethanolcopper chloride $CuCl_2 \cdot 2C_2H_5OH$). These compounds were formed in the solutions as a result of hydrolysis of the copper salts.

In the present work, the materials studied were ferri- and aluminosilicate mixed gels with different $SiO_2 \cdot R_2O_3$ ratios, prepared by Mattson's method [11]; some specimens were purified from electrolyte impurities by electrodialysis, and others were not. The reagent chosen was cupric chloride ($CuCl_2 \cdot 2H_2O$).

The experiments were carried out as follows: 50 ml of 0.05 N $CuCl_2$ solution was added to 75 ml of suspension. After periodic shaking for three days in a closed vessel, 50 ml was removed (specimen 1) and 20 ml of 0.25 N $CuCl_2$ and 30 ml of H_2O were added. After 3 days, as in the first case, 50 ml was removed (specimen 2), and 40 ml of 0.25 N $CuCl_2$ and 10 ml of H_2O were added. The standing and shaking were repeated, and 50 ml was removed (specimen 3). A further 20 ml of 1 N $CuCl_2$ and 30 ml of H_2O were then added. After 3 days with periodic shaking, 50 ml was removed (specimen 4) and 40 ml of 1 N $CuCl_2$ and 10 ml of H_2O were added. After 3 days with periodic shaking, the last specimen, 5 (50 ml), was removed. This gave a series of successive extractions with the same suspension and increasing $CuCl_2$ concentrations.

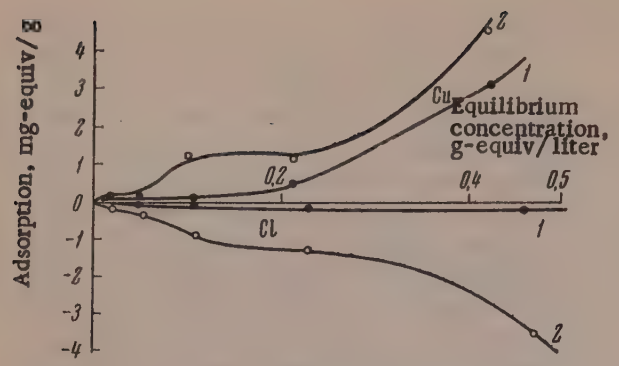


Fig. 2. Comparison of the magnitudes of the nonequivalent absorption of Cu^{2+} and Cl^- by an electrodialyzed aluminosilicate of composition $Al_2O_3 \cdot 2SiO_2$ during prolonged interaction with $CuCl_2$ solution: 1) experiment with gel; 2) experiment with powder.

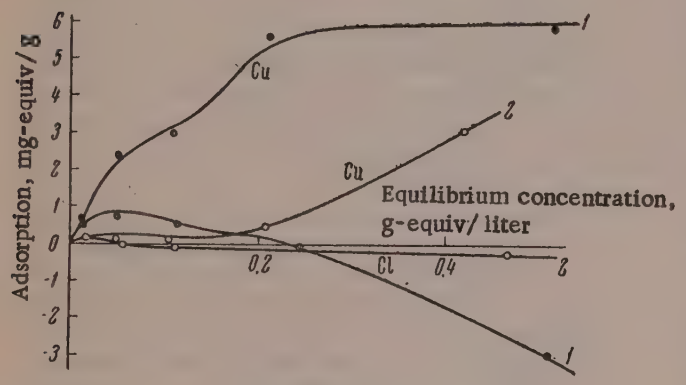


Fig. 3. Nonequivalent absorption of Cu^{2+} and Cl^- by electrodialyzed aluminosilicates of composition $Al_2O_3 \cdot 2SiO_2$: 1), 2) precipitates at different stages of purification.

TABLE 3

pH Measurements During the Prolonged Interaction of Electrodialyzed Mixed $Al_2O_3 \cdot SiO_2$ Gel with Cupric Chloride Solutions

$CuCl_2$ solutions, N	Components of solution, ml			pH of solution, (glass electrode)
	$CuCl_2$	H_2O	$Al_2O_3 \cdot SiO_2$ suspension	
0,25	20	105	—	4,96
0,25	40	85	—	4,62
1	20	105	—	4,28
0,25	20	30	75	4,82
0,25	40	10	75	4,42
1	20	30	75	4,06

The experimental procedure was the same as that described in [12].

The copper was determined iodometrically by G. Bruhn's method, and the chloride was determined potentiometrically by titration with 0.025 N $AgNO_3$ and a silver electrode from the position of the point of inflection on the titration curve.

Control experiments were carried out under conditions identical to those in the adsorption experiments, but with water in the place of the test suspensions.

In the experiments with electrodialyzed aluminosilicates (Fig. 1) the adsorption of copper cations, throughout the whole length of the curves, was found to be positive, while that of the chloride ions was found to be negative. Thus, these adsorbents adsorbed predominantly the weakly dissociated hydrolysis product, i.e., $Cu(OH)_2$, or possibly some other basic copper compound. The reaction of the equilibrium $CuCl_2$ solutions did not become acidic to any significant extent, since they exhibit buffer properties (Table 2).

During the adsorption of $Cu(OH)_2$, the aluminosilicates acquired a negative charge, and the ability to show negative sorption of chloride ions. Similar considerations are encountered in [13].

The phenomenon of negative adsorption of chloride was observed in all the experiments with mixed aluminosilicate gels (Figs. 1-3), and in all the experiments with ferrisilicate gels (Figs. 4, 5). The maximum values of the absorption of copper cations (mg-equiv/1 g of gel) were 3.07 for the electrodialyzed $Al_2O_3 \cdot 2SiO_2$ gel, and 9.63 for the dialyzed gel, at an equilibrium concentration of about 0.4 g-equiv/liter (Fig. 1). For electrodialyzed powder at the same equilibrium concentration the magnitude of the observed adsorption was slightly higher than for pure $Al_2O_3 \cdot 2SiO_2$ gel, and was equal to 4.98 (Fig. 2).

The phenomenon of reversion of electrolyte adsorption is extremely clearly defined (for Cu^{2+} and Cl^-) in the experiments with dialyzed and electrodialyzed ferrisilicates (Figs. 4a, 4b, and 5). Positive adsorption of cations and anions took place at comparatively low equilibrium concentrations up to 0.3 g-equiv/liter. In the range of high equilibrium concentrations, negative adsorption of both these components of the solution took place, the magnitude of the adsorption of Cl^- being negative with respect to the magnitude of the adsorption of Cu^{2+}. This phenomenon of adsorption reversion, the theory of which has been given by Semenchenko

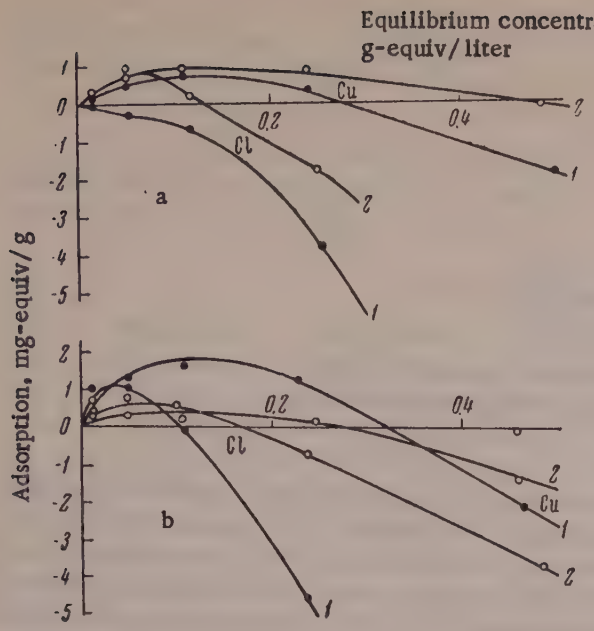


Fig. 4. Nonequivalent absorption of Cu^{2+} and Cl^- during prolonged interaction of dialyzed (1) and electrodialyzed (2) gels with $CuCl_2$ solution: a) $Fe_2O_3 \cdot 2SiO_2$; b) $Fe_2O_3 \cdot SiO_2$.

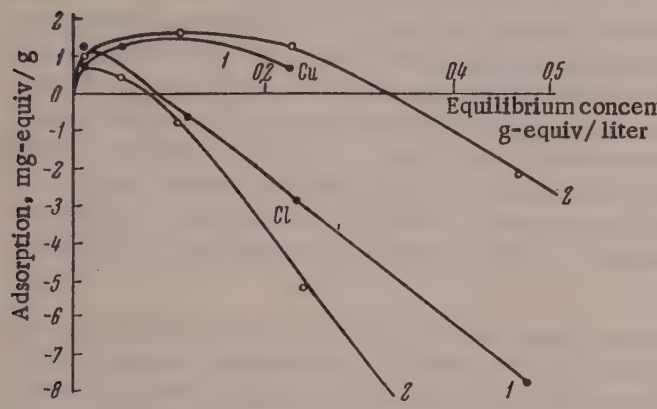


Fig. 5. Nonequivalent absorption of Cu^{2+} and Cl^- by dialyzed gels, $2Fe_2O_3 \cdot SiO_2$ (1) and $4Fe_2O_3 \cdot SiO_2$ (2) during prolonged interaction with $CuCl_2$ solution.

[14], can be attributed to specific interactions between adsorbent and solvent. Up to a definite moment in dilute solutions, positive adsorption of cations and anions takes place, and in this range the two adsorption branches approach closer to one another with increase in the degree of purity of the adsorbent. When the concentration of the products of the splitting of the electrolyte in the solid phase increases, the adsorption of solvent, i.e., water molecules, begins to predominate; the adsorption of the dissolved substances ($CuCl_2$) changes sign simultaneously, since the forces of repulsion between the molecules of electrolyte and the surface of the adsorbent begin to predominate, as a result of the production of a potential barrier. On top of this process there is usually superimposed the specific process of chemisorption of the least dissociated compounds from solution, i.e., chemisorption of either basic or complex salts, and also possibly of large copper cations, depending on the pH. At low concentrations the $Cu(OH)_2$ possibly does not exist in the solid phase but, nevertheless, since it is irreversibly bound to the surface of the mixed gels, equilibrium in the solution is shifted towards its formation. For the dialyzed mixed gel $Fe_2O_3 \cdot 2SiO_2$ (Fig. 4a) the maximum positive absorption of copper cations amounted to 0.64 mg-equiv/1 g of gel, and the maximum negative absorption to 1.92 mg-equiv/1 g of gel, at equilibrium $CuCl_2$ concentrations of 0.12 and 0.5 g-equiv/liter, respectively. The values of the negative adsorption of chloride at almost the same equilibrium $CuCl_2$ concentrations were 0.65 and 10.96 mg-equiv/1 g of gel. In the case of the electrodialyzed mixed $Fe_2O_3 \cdot 2SiO_2$ gel the reversal of the sign of adsorption was observed for copper at an equilibrium $CuCl_2$ concentration of 0.5 g-equiv/liter, and for chloride at an equilibrium $CuCl_2$ concentration of 0.25 g-equiv/liter, or slightly less. These values were observed with slight fluctuations for all experiments with ferrisilicate gels at all SiO_2:Fe_2O_3 ratios.

Thus, the radical change in the conditions of interaction of electrodialyzed highly dispersed precipitates, and increase in the duration of the interaction of the precipitates with cupric chloride solutions, has made it possible to observe those retarded reactions between the precipitates and solvent molecules which normally remain outside the field of view of workers studying the exchange reactions of adsorbents with electrolyte solutions under static conditions.

In order to verify that this is, in fact, the case, we carried out a series of static experiments with electrodialyzed mixed $Al_2O_3 \cdot 2SiO_2$ gels. $CuCl_2$ solutions of increasing concentration and a definite quantity of water were poured into Jena glass vessels. Volumes of suspensions equal to the control volumes of water were placed in a parallel series of vessels, and exactly the same quantities of cupric chloride solutions of the same concentrations

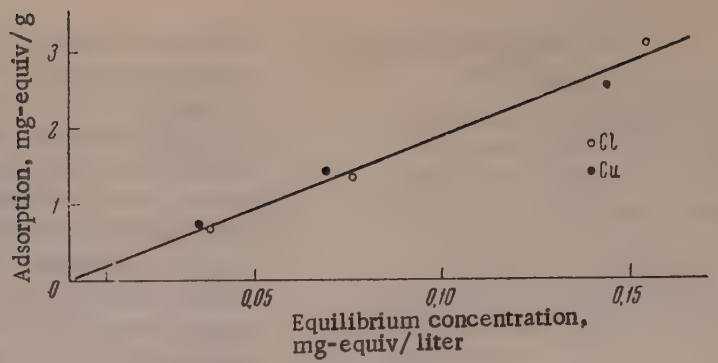


Fig. 6. The adsorption of cupric chloride by electrodialyzed aluminosilicate of composition $Al_2O_3 \cdot 2SiO_2$ under static conditions.

as in the control experiments were added. The vessels were shaken for 2 hr, and then left for 24 hr. After 24 hr, specimens of the transparent supernatant solution were removed. The magnitude of the adsorption of copper and chloride was calculated from the difference between the control and equilibrium solutions, and was recalculated for 1 g of dry gel. Figure 6 shows that these data coincide within the limits of experimental error, i.e., an electrodialyzed precipitate of this type absorbs electrolytes in the form of molecules or ionic associates. The maximum value of the adsorption of both ions did not exceed 3 mg-equiv/g at an equilibrium concentration of 150 mg-equiv/liter. The measured values of the pH of the control and equilibrium solutions are given in Table 3.

Comparison of the values of the pH in the control and adsorption experiments carried out with a short period of interaction between the electrodialyzed gel and the $CuCl_2$ solution shows that, in this case, no pH shift appears to take place. A very interesting feature is that when the values of the pH obtained in experiments with prolonged and brief interaction between adsorbents and cupric chloride solutions are compared, we observe an increase in the acidity of the solutions in the first series of experiments; this increase takes place as a result of the adsorption of basic copper compounds after prolonged interaction between the adsorbents and the cupric chloride solutions. The values of the pH of the equilibrium solution do not differ significantly from the values of the pH of an aged $CuCl_2$ solution, i.e., exchange separation of hydroxide ions does not take place. These results confirm completely the conclusions reached in [9,10], that the absorption of basic copper salts is irreversible; the results may also be compared with those of [4-6], in which the study of the phenomenon of adsorption of neutral salts in pure systems showed hydrolytic splitting of the neutral salts, and sorption of the acid formed, as a result of which the equilibrium solutions became alkaline.

In our experiments on the study of the phenomenon of adsorption of hydrolyzed salts in pure systems, we observed sorption of the least dissociated basic components, as a result of which the equilibrium solutions became slightly more acidic. In both cases, the production of adsorptive capacity is due to molecular absorption of the least dissociated component of the solution. The reaction of the equilibrium solutions may be shifted toward the alkaline or acid range, depending on whether this component is acidic or basic.

From the results of the present work, it follows that the phenomenon of reversion of adsorption may be extremely marked: this explains the data obtained by those authors who have studied adsorption effects in contaminated systems.

It will subsequently be necessary to study processes associated with molecular absorption of solvent, and their influence on the adsorption of dissolved substances.

SUMMARY

1. On prolonged interaction between hydrolyzed salts ($CuCl_2$) and electrodialyzed mixed gels containing SiO_2 and Fe_2O_3 or Al_2O_3, adsorption of basic copper compounds, and increase in the acidity of the equilibrium solutions are observed.

2. The accumulation of alkaline products of hydrolysis in the solid phase of the adsorbents changes the nature of the adsorption distribution of molecules of dissolved substance and solvent, leading to the predominant absorption of solvent molecules, and reversion of adsorption of the dissolved substances.

3. Radical change in the conditions of the interaction of electrodialyzed highly dispersed precipitates with solutions of a hydrolyzed salt makes it possible to observe retarded reactions between the adsorbents and molecules of solvent; these reactions cannot be studied under static conditions during the brief interaction between the adsorbents and the solutions.

4. A solution to the problem of the production of exchange–adsorption properties on electrodialyzed and dialyzed precipitates can be found only by taking account of the magnitude of the adsorption of the third component of the solution, namely water molecules.

LITERATURE CITED

1. O. I. Dmitrenko, V. A. Kargin, and A. A. Ryabinina, Kolloid. Zhur. 13, No. 1, 3 (1951).
2. O. I. Dmitrenko, Collection of Works on Physical Chemistry [in Russian] (AN SSSR Press, 1947) pp. 376 and 388.
3. O. I. Dmitrenko and M. M. Kolesnikov, Kolloid. Zhur. 8, No. 5, 319 (1946).
4. M. E. Shishniashvili and V. A. Kargin, Kolloid. Zhur. 8, Nos. 1-2, 101 (1946).
5. Z. Ya. Berestneva and V. A. Kargin, Zhur. Fiz. Khim. 10, 8, 35 (1936).
6. M. E. Shishniashvili, V. A. Kargin, and A. A. Bachnadze, Soobshch. Akad. Nauk Gruzinskoi SSR 1, 25 (1943).
7. L. Lepin' and G. Strakhova, Zhur. Fiz. Khim. 13, 216 (1939); 20, 743 (1946).
8. V. N. Krestinskaya and Z. V. Khakimov, Zhur. Obshch. Khim. 14, 70, 129 (1944).
9. I. N. Antipov-Karataev and G. M. Kader, Kolloid. Zhur. 9, 81, 162 (1947).
10. I. N. Antipov-Karataev, G. M. Kader, and V. N. Filippova, Kolloid. Zhur. 10, No. 2, 73 (1948).
11. S. Mattson, Soil Sci. 30, 6, 459 (1930).
12. L. Lepin' and G. Strachova, Z. Phys. Chem. 176, 44 (1936).
13. F. Kayser and I. M. Bloch, Compt. rend. 226, 251 (1948).
14. V. K. Semenchenko, Kolloid. Zhur. 11, 2 (1949).

EFFECT OF COMPRESSION OF CARBON BLACK ON THE ADSORPTION ISOTHERM OF n-HEXANE

A. A. Isirikyan and A. V. Kiselev

Lomonosov Moscow State University, Faculty of Chemistry, Adsorption Laboratory
Translated from Kolloidnyi Zhurnal, Vol. 23, No. 1, pp. 67-75, January-February, 1961
Original article submitted October 12, 1959

Powders, made up of nonporous particles, particularly carbon blacks, are used in different technological processes, for example as polymer fillers and lubricant thickeners in the varnish and polygraphic industries. Their important characteristics are their dispersion and the chemical composition of their surfaces, and data about these characteristics are obtained mainly from adsorption studies. However, complications arise due to agglomeration of the particles, and some forcing together of the powders. Such agglomerates, or compressed briquets, appear to be porous bodies with a more or less rigid structure, and their adsorption properties can be considerably different from those of the original powders.

This work was carried out in order to explain the nature of the heterogeneity arising during compression of the black and its effect on the adsorption properties of the black – the adsorption isotherm and heat of adsorption of a hydrocarbon vapor. Experimental and theoretical studies of vapor adsorption isotherms on compressed powders, and their corresponding models have already been published [1-10], but they only deal with the variation of the form of the adsorption isotherms for compressed powders at high relative pressures of the adsorbate vapor p/p_s, i.e., in the region of capillary condensation; information about the porosity of the compressed powders can only be gained from the increase in sorption of the hysteresis loops which emerge. In the pure adsorption region, i.e., the low p/p_s region, investigations showed [6,7] that the isotherms and heats of adsorption are unchanged after compression of a loose powder consisting of sufficiently coarse particles of a thermal black. However, a nongraphitized black with an extremely nonhomogeneous surface was used for these studies, and the effect of the increased number of contacts of the particles was masked. The latter should always result in an increase in the heterogeneity of the surface and, therefore, to some slight change in the form of the adsorption isotherm and heat of adsorption, not only in the capillary condensation region of high p/p_s, but also in the region of preferential monolayer formation. Therefore, in the case of compression of graphitized blacks with extremely homogeneous surfaces, one would expect a strengthening of adsorbate–adsorbent interactions at low coverages, and at coverages corresponding to completion of a monolayer, not such a clear display of adsorbate–adsorbate interactions, and a less clear transition from preferential adsorption in the first layer to preferential adsorption in the second. This latter effect should

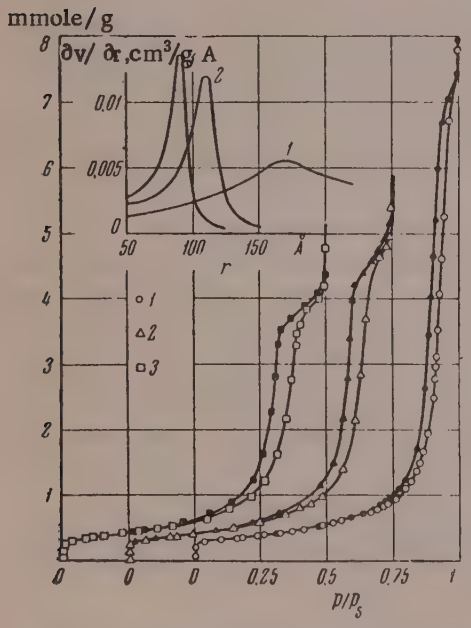


Fig. 1. Adsorption isotherms of n-hexane vapor on original sample of Spheron-6, 2800° (1) and on samples compressed at 4 ton/cm² (2) and 10 ton/cm² (3). Inset – corresponding pore-size distribution curves (according to radius). (In all diagrams the black points represent desorption.)

TABLE 1

Structural Characteristics of the Original Black Spheron-6, 2800° (Sample C-0), and Samples Compressed at 4 ton/cm^2 (Sample C-4) and 10 ton/cm^2 (Sample C-10)

Black sample	Specific surface area (BET) s, m^2/g	Pore volume v_s, cm^3/g	Average number of contacts of particles, n	Most probable diameter of necks of pores d, A
C-0	89.8	0.98	3.8*	340
C-4	96.6	0.70	4.7	220
C-10	98.4	0.56	5.3	180

* At $n < 4$, capillary condensation hysteresis can be due to superposition of multilayer adsorption [10].

TABLE 2

Standard Differential Thermodynamic Characteristics of n-Hexane Adsorption on Spheron-6, Which Has Been Subjected to Different Thermal and Mechanical Treatments

Calcination temp. of Spheron-6, °C	Compression pressure, ton/cm^2	heat of adsorption Q_a^0, kcal/mole	Standard differential values energy of adsorption, kcal/mole		entropy of adsorption, ΔS_a^0, e.u.	Heat of adsorption at zero coverage Q_0, kcal/mole
			net, ΔU_a^0	free, $\Delta\mu_a^0$		
1700 [12]	–	12.10	−4.50	−3.65	−2.90	11.8
2800	–	12.35	−4.75	−3.70	−3.58	11.6
2800	4	12.40	−4.80	−3.68	−3.82	11.9
2800	10	12.40	−4.80	−3.65	−3.92	12.2

also mask the development of adsorbate – adsorbate interaction which, in this region of coverage for a homogeneous surface, results in a maximum on the differential heat of adsorption curve [11,12].

One would therefore expect that, after compression, the form of the heat-of-adsorption curve in the adsorption region should change in the opposite direction to its change during graphitization of the blacks [11,12], when the surface becomes more homogeneous. In the high p/p_s region, one would expect maxima to appear on the heat-of-adsorption curves, corresponding to completion of capillary condensation in the pores, formed during the compression – the spaces between the original particles. These maxima appear clearly in the case of completely porous adsorbents [13-16].

A sample of the channel black Spheron-6* (used previously [17]), calcined in a helium atmosphere at 2800°, was selected as an adsorbent. This sample was subjected to compression in a mechanical press under pressures of 4 and 10 ton/cm^2. The adsorption isotherms and differential heats of adsorption of n-hexane vapor were studied on both the compressed samples so obtained, and on the original sample. The adsorption-calorimetric apparatus, and some of the constants of the n-hexane used have already been given [13].

Structural Characteristics of the Samples

The adsorption isotherms obtained are given in Figs. 1 and 2. It can be seen from Fig. 1 that the original sample of black already possesses a porous structure, and has a limiting sorption volume V_s. The adsorption–desorption isotherm has a narrow hysteresis loop. However, compression leads to a clear decrease in V_s, and broadening and displacement of the hysteresis loop to lower p/p_s values. Pore-size distribution curves (with respect to radius), obtained from the desorption branches of the isotherms, are shown in Fig. 1, and indicate

* The channel black calcined at 2800° was not ideal for our purpose, since it already possesses some porosity as a result of preliminary granulation and possible partial sintering of the particles. However, the large specific surface area (about 90 m^2/g) is necessary for reliable measurements (especially of heats), both in the region of monolayer adsorption and particularly in the region of completion of capillary condensation.

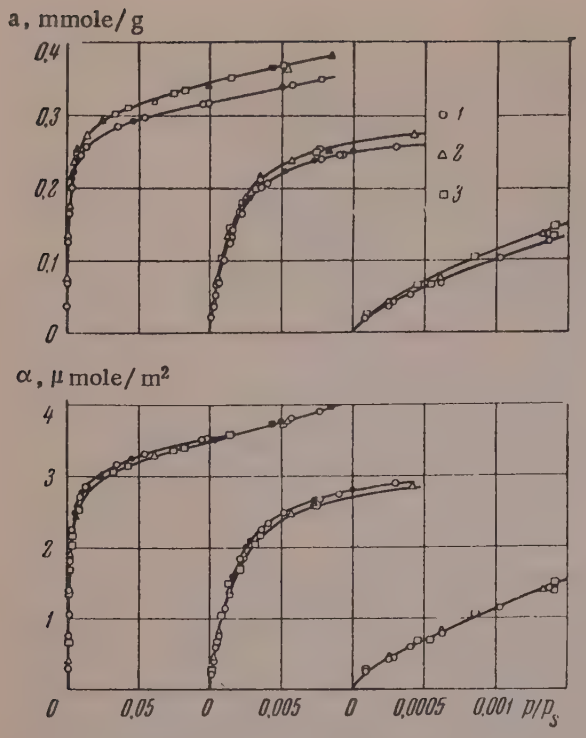


Fig. 2. Initial regions of the adsorption isotherms of n-hexane on the carbon black sample (1) and on samples compressed at 4 ton/cm^2 (2) and 10 ton per cm^2 (3) (lower diagram – corresponding absolute adsorption isotherms).

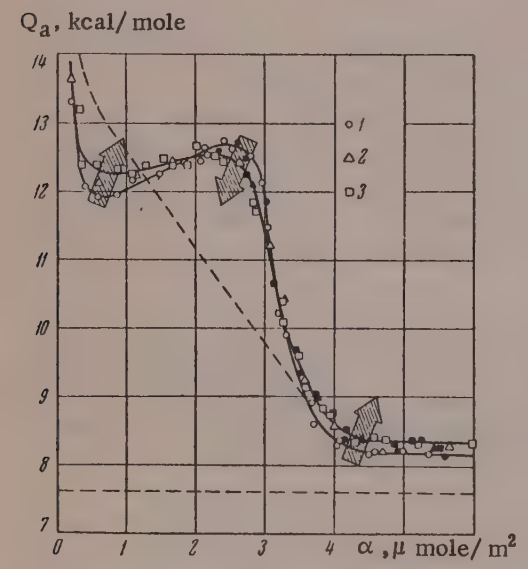


Fig. 3. Differential heats of adsorption of n-hexane on the original black sample (1) and on samples, compressed at 4 ton/cm^2 (2) and 10 ton/cm^2 (3), and, similarly, on the thermal black P-33 [6] (here and in subsequent diagrams the horizontal dotted lines represent the heat of condensation of n-hexane).

contraction of the pores. These facts are not unexpected [1-10], and we will not, therefore, dwell on them at length here. Table 1 contains just a few of the structural characteristics of the samples, determined from these isotherms.

The first column of the table contains values for the specific surface areas, determined by the BET method from the adsorption isotherms of n-hexane. The surface area of a n-hexane molecule in a completed monolayer w_m, is taken to be 51.5 sq. A [12]. The specific surface area of the original sample, determined by the BET method from low-temperature nitrogen gas adsorption (w_m = = 16.2 sq. A) was 89 m^2/g [17], which is in good agreement with the value determined from the n-hexane adsorption isotherm. As can be seen from Table 1, the specific surface area of the black increases on compression. This could be brought about both by rupture of little chains of the black at points where the particles are joined, and by strengthening of the adsorption potential at the points of the newly formed contacts of the particles (the coordination number n increases on compression). During the formal use of the BET method, this would lead to an increase in the monolayer capacity a_1 and s. It is difficult to determine the comparative roles of these effects in increasing the surface of the compressed samples of black, and this requires further study.

The determined sorption volume V_s (total pore volume) is strongly decreased after comparatively weak compression (4 ton/cm^2), and only alters slightly on further compression of 10 ton/cm^2. A similar characteristic is the increase in the coordination number n (Table 1). The maximum effective diameters of the pore necks [4,9,10] d (Table 1), were obtained from the distribution curves in Fig. 1.

Region of Preferential Monolayer Formation

The absolute adsorption isotherms obtained, and the heat-of-adsorption curves in the region of monolayer formation, and the transition to multilayer formation, are shown in Fig. 2 (lower diagram), and Fig. 3. Table 2 contains the standard differential thermodynamic characteristics of n-hexane adsorption, corresponding to formation of half-complete monolayer $\theta = 0.5$, on Spheron-6, calcined at 1700° in a stream of hydrogen [12], and on our samples of black. The standard values of the heats, net energy, free energy, and entropy of adsorption for our three samples are seen to be about the same.

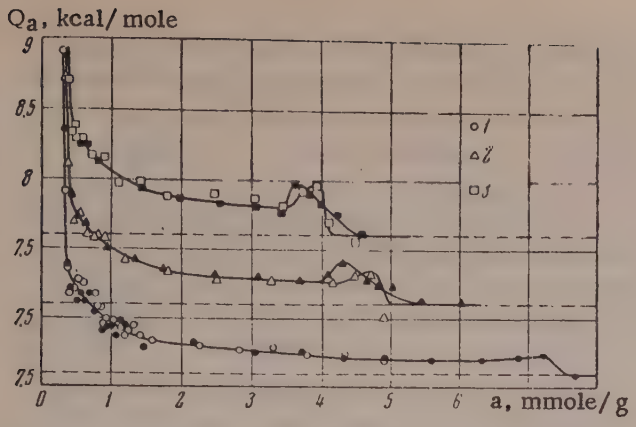


Fig. 4. Differential heats of capillary condensation of n-hexane of the original black sample (1) and on samples, compressed at 4 ton/cm^2 (2) and 10 ton/cm^2 (3).

This is clearly shown up for the standard heats of adsorption in Fig. 3, where the differential heat-of-adsorption curves cross near the formation of half-complete monolayer (α_θ =0.5= 1.61 μmole /m^2).

Comparison of the uncompressed samples of Spheron-6, subjected to thermal treatment at 1700 and 2800°, shows, from Table 2, that, at 1700° graphitization of a channel black only occurs to a small degree, since the energy of adsorption of n-hexane increases by 0.25 kcal/ mole on further heating of the black to 2800° and, in addition, the entropy of adsorption decreases by 0.68 entropy units (e.u.). Although small in value, these changes indicate the continuation of the process of ordering of the crystal structure in the bulk phase of the adsorbent, and development of surface homogeneity.

It was of interest to compare the values for the heats of adsorption at $\theta = 0$ with data on theoretical calculations of the energy of adsorption. These heats were found by extrapolating the approximately linear section of the differential heat-of-adsorption curve (in the region of half-complete monolayer) to its intersection with the ordinate axis at $\theta = 0$ [12]. The values of Q_0 (Table 2) obtained in this way showed that graphitization at the higher temperature led to some lowering of the heat of adsorption at zero coverage, but compression, by increasing the heterogeneity of the surface, led to an increase in Q_0. Thus, the most reliable values of Q_0 are obtained by extrapolation of the heat-of-adsorption curves, measured on uncompressed blacks with the most homogeneous surface. Our previous measurements on a thermal black, graphitized at 3000°, gave Q_a^0 = = 12.55 and Q_0 = 11.4 kcal/ mole, i.e., the standard adsorption energy of n-hexane is higher on a thermal black, graphitized at 3000°, than on Spheron-6, calcined at 2800°, and the heat of adsorption at $\theta = 0$ is correspondingly lower. However, this difference is still very small.

A detailed investigation of adsorption over the whole of the monolayer region showed (Fig. 2) that the adsorption isotherms of n-hexane went higher on compressed samples than on the original sample. In the lower part of Fig. 2, the absolute adsorption isotherms are shown, in which the amounts of vapor adsorbed have been reduced to unit surface of sample. In the initial region, the adsorption on the compressed samples and on the original is practically the same. However, the increase in energy of adsorption for the compressed samples was shown up quite clearly on the differential heat-of-adsorption curves (Fig. 3). The increase in heat of adsorption, and practical constancy of the adsorption isotherm, i.e., the change in free energy, are evidently associated with a decrease in adsorption entropy in the initial region of the isotherm. This can be explained as due to the retarding action of the adsorbed molecules in the narrow necks around the points of contact between the particles of black, drawn together as a result of compression. In the region of monolayer completion we succeeded in showing up a slight decrease in the adsorption compared to the adsorption on the original uncompressed black sample. The variation in the differential heat of adsorption in this region is in accordance with the variation in adsorption, i.e., the heat of adsorption is somewhat lower on compressed samples than on the original. This indicates that there arise, on the surface of the compressed samples of black, obstacles to the free development of adsorbate – adsorbate interactions. Also, the decrease in the heat of adsorption in this region is brought about by a less clear transition from preferential adsorption in the first layer to preferential adsorption in the second, since regular filling up of the layers does not occur in the narrow necks near the points of contact of the particles.

In the region of multilayer adsorption and the beginning of capillary condensation, the adsorption isotherms and heats of adsorption for the compressed blacks are higher than for the original sample (Figs. 1, 3, and 4). This is explained as being due to the narrowing of the spaces between the black particles, as a result of which the dispersion potential increases in these places, and conditions are created favoring more intensive multilayered adsorption and capillary condensation.

In Fig. 3, the differential heat-of-adsorption curve of n-hexane on the black P-33, which was only heated at 1000° [6], is given for comparison. At such a temperature the geometrical heterogeneity, i.e., the surface

TABLE 3

Integral Thermodynamic Characteristics of n-Hexane Adsorption on Carbon Blacks

Sample of black	A_l, erg/cm^2	Q_l, erg/cm^2	Δs_l, erg per deg·cm^2	ΔS_m, cal per deg·mole
Spheron 6 1700°	82	123	—0,14	—2,5
C-0	80,8	120±3	—0,13	—3,5
C-4	80,3	119±2	—0,13	—3,6
C-10	79,4	119±2	—0,14	—3,7

TABLE 4

Surface Areas of Adsorption Films, Calculated from the Work of Adsorption s'_A and Heat of Adsorption s'_Q for the Two Lower Limits of Integration of the Curves of Work and Heat of Adsorption $a_1 = 0.4$ and $a_2 = 0.6$ mmole/g

Sample of black	According to BET, m^2/g	s'_A, m^2/g		s'_Q, m^2/g		
		a_1	a_2	a_1	a_2	average
C-0	89,8	124	101	88	82	85
C-4	96,6	132	107	97	86	91
C-10	98,4	133	106	98	87	92

roughness of the particles, has not disappeared [11], and this is the main reason for the sudden decrease in the heat of adsorption in the region of monolayer formation. Considerable geometrical heterogeneity of the adsorbent surface can strongly hinder the development of normal interaction among the adsorbed molecules; if attractive forces predominate, the differential heat-of-adsorption curve can be changed from a wavelike form with a large maximum, for a completely homogeneous surface, to a continuous decrease over the whole adsorption region.

The arrows in Fig. 3 indicate how the course of the differential heat-of-adsorption curves change in direction on a nonporous homogeneous black during its compression. Thus, compression of a homogeneous black leads to the formation of a porous graphitic body with a geometrically heterogeneous surface. The adsorption properties of the black also change, so that, at low surface coverages, the adsorption energy increases, in the region of monolayer completion it decreases, and during the transition to multilayered adsorption and capillary condensation it increases again.

Work, Heat, and Entropy of Wetting

Turning to an examination of capillary condensation at high p/p_s, we should point out that, in this region, calorimetric measurements for adsorption can be quite accurately and reliably found from desorption measurements. At vapor pressures approaching saturation, it is difficult, on the one hand, to prevent completely partial condensation of the vapor at the entrance to the calorimeter, which leads to lowered values of the heats of capillary condensation and, on the other hand, in trying to eliminate this source of error, it is difficult to avoid superheating the vapor in relation to the calorimeter temperature, which leads to increased values. Therefore, our future calculations of heats of adsorption and wetting are based on results of desorption measurements, since they are free from the sources of error indicated. Since, on all the samples of black, the heats of capillary condensation are very near to the heat of condensation in the normal liquid L (at most they are only 0.1-0.2 kcal/mole larger), a knowledge of the accurate value of the latter was of importance. In order to do this, we made measurements of L under conditions analogous to those under which the adsorption-calorimetric experiments were carried out. Taking the constant average value of L obtained for a series of measurements, we were able to calculate the integral values of heat and entropy of adsorption sufficiently accurately.*

This was accomplished as in our preceeding work [13] by graphical integration of the experimental graphs of the differential work and net heat of adsorption ($Q_a - L$) in the adsorption range $a = 0$ to saturation $a = a_s$. Values were obtained for the works of wetting ΔA and heats of wetting, and Q_l, and hence the entropy of wetting Δs_l also. These values, and similarly that of the average molar change in entropy during adsorption of a monolayer ΔS_m, are given in Table 3.

The values of the work, heat, and entropy of wetting obtained for our samples are in good agreement with those calculated earlier for a sample of Spheron-6, calcined at 1700° [12]. The value of Q_l is similarly very near to the heat of wetting of graphite by n-hexane (118 erg/cm^2 [18]), measured directly in a calorimeter.

*Due to very small dead-space corrections, and by having large measured values of Δa in these experiments, we were able to improve the accuracy of the measurements of differential heats of desorption in the region of capillary condensation, and the heat of evaporation of the liquid to ±0.01 kcal/mole.

Increase of the calcination temperature of the black from 1700 to 2800° affects the change in entropy during adsorption of a monolayer, and also the heat of monolayer adsorption. The integral values of heat, work, and entropy of wetting are practically insensitive to variation in the degree of surface heterogeneity.

Integration of the experimental curves of differential work and net heat of adsorption between the adsorption limits a_h, corresponding to the beginning of hysteresis, and saturation a_s, gave values for the surface areas of the adsorption films s', which, for our homogeneous porous samples, should not differ much from the specific surfaces of the adsorbent frames s [13]. Some difficulty in determining where hysteresis begins, due to some swelling of the black skeleton, which is not altogether rigid (the hysteresis loop for compressed samples begins to develop at $p/p_s = 0.1$), forced us to calculate over the range of adsorption values from 0.4 to 0.6 mmole/g, inside which pure capillary condensation hysteresis probably begins. The corresponding results are shown in Table 4, together with the specific surface areas of the solid skeletons s, determined by the BET method.

The surface areas of the films, calculated from the work of adsorption, are 20 to 30% higher than those obtained from the heat of adsorption. A similar relation between s'_A and s'_Q was also obtained in the case of adsorption of hydrocarbons on a widely pored silica gel [13]. This difference is possibly linked with the characteristic temperature dependence of the surface tension, and total surface energy of the liquid adsorbate. It can be seen from Table 4 that the variation in the values of s'_Q due to selection of a_h value in the limits 0.4 to 0.6 mmole/g is smaller, than the corresponding variation in s'_A. Therefore, the results from thermal measurements are more reliable.

Maximum Heats of Capillary Condensation

This work was aimed at artificially reproducing the maximum heat of capillary condensation at sorption completion. We had only previously investigated such maxima in the case of ready-made porous adsorbents of silica gel [13-16], and active charcoal [6]. We had linked this effect with the action of capillary forces and, more precisely, with the sudden increase in the hydrostatic pressure in the capillary condensate during adsorption, and with its still more sudden decrease during desorption [13-16]. It was shown earlier [16], that sorption completion on a nonporous quartz powder was not accompanied by a maximum on the heat-of-adsorption curve; it was of great interest to bring about its appearance by just modifying the nonporous powder geometrically, not altering the form or chemical composition of its particle surface. We were also able to do this in the case of the compressed samples of the black, graphitized at 2800°. In fact, in this case, because of the indeterminacy of hysteresis completion at high p/p_s (see Fig. 1), such a sudden maximum was not obtained, as in the case of adsorption of hydrocarbons on a widely pored silica gel [13], but the expected maxima appeared quite clearly on all the compressed samples of black (Fig. 4). If, on the original sample, the differential heats of capillary condensation approaching adsorption saturation hardly passed through a maximum and differed from the heat of condensation of the normal liquid by 0.1 kcal/mole at most, on the compressed samples clear maxima developed for both the heats of adsorption and desorption, which were from 0.3 to 0.4 kcal/mole higher than the heat of condensation. Thus, it can be considered as definitely proved, that these maxima are linked only with the geometrical structure of the adsorbent, and appear at the completion stage of capillary condensation, when a sufficiently homogeneous porosity exists.

SUMMARY

1. The adsorption isotherms and differential heats of adsorption of n-hexane have been measured on samples of the channel black Spheron-6, heated at 2800°, and compressed into briquets of varying porosity.

2. The compression of the black leads firstly to an increase in the surface heterogeneity, which is manifested as an increase in the heats of adsorption at low surface coverages, and a decrease in the maximum adsorption heats in the region of monolayer completion; and, secondly, as a general increase in the differential heat of capillary condensation, with the appearance of distinct peaks, when sorption is complete.

3. The work, heat, and entropy of wetting of the carbon black by n-hexane were determined by integrating the differential work curves and the curves for the net heat of adsorption, the results being in good agreement with published data.

LITERATURE CITED

1. P. C. Carman and F. A. Raal, Proc. Roy. Soc. A209, 59 (1951).
2. N. N. Avgul', O. M. D higit, and A. V. Kiselev, Doklady Akad. Nauk SSSR 86, 95 (1952).
3. J. Higuti and H. Utsugi, J. Chem. Phys. 20, 1180 (1952).
4. A. V. Kiselev, Doklady Akad. Nauk SSSR 98, 431 (1954).
5. V. M. Lukyanovich, L. V. Radushkevich, and D. G. Kadaner, Doklady Akad. Nauk SSSR 87, 1001 (1952).
6. N. N. Avgul', G. I. Berezin, A. V. Kiselev, I. A. Lygina, and G. G. Muttik, Zhur. Fiz. Khim. 31, 1111 (1957).
7. A. V. Kiselev (editor): Methods of Structural Investigation of Highly Dispersed and Porous Materials (Izd. AN SSSR, 1958) p. 47.
8. L. V. Radushkevich, Collection: Methods of Structural Investigation of Highly Dispersed and Porous Materials (Izd. AN SSSR, 1958) p. 60.
9. A. P. Karnaukhov, Collection: Methods of Structural Investigation of Highly Dispersed and Porous Materials (Izd. AN SSSR, 1958) p. 71.
10. A. P. Karnaukhov and A. V. Kiselev, Zhur. Fiz. Khim. 31, 2635 (1957).
11. R. A. Beebe and D. M. Young, J. Phys. Chem. 58, 95 (1954).
12. N. N. Avgul', G. I. Berezin, A. V. Kiselev, and I. A. Lygina, Zhur. Fiz. Khim. 30, 2106 (1956); Izd. Akad. Nauk SSSR, Otd. Khim. Nauk 1304 (1956); 1021 (1957).
13. A. A. Isirikiyan and A. V. Kiselev, Doklady Akad. Nauk SSSR 110, 1009 (1956); Zhur. Fiz. Khim. 31, 2127 (1957); 32, 679 (1958).
14. A. V. Kiselev, Proceedings of the Second International Congress on Surface Activity (London, 1957) Vol. 2, p. 189; A. A. Isirikyan and A. V. Kiselev, Proceedings of the Second International Congress on Surface Activity (London, 1957) Vol. 2, p. 222.
15. A. A. Isirikyan, Collection: Methods of Structural Investigation of Highly Dispersed and Porous Materials (Izd. AN SSSR, 1958) p. 85.
16. A. A. Isirikyan and A. V. Kiselev, Doklady Akad. Nauk SSSR 119, 731 (1958).
17. N. N. Avgul', G. I. Berezin, A. V. Kiselev, and A. Ya. Korolev, Kolloid. Zhur. 20, 298 (1958).
18. F. E. Bartell and R. M. Suggit, J. Phys. Chem. 58, 36 (1954).

A SPECTROPHOTOMETRIC STUDY OF THE ADSORPTION OF METHYLENE BLUE BY HIGHLY DISPERSED ALUMINOSILICATES

L. I. Kul'chitskii

Hydrogeology and Engineering Geology Scientific Research Institute,
Physical Methods of Study Laboratory
Translated from Kolloidnyi Zhurnal, Vol. 23, No. 1, pp. 76-85, January-February, 1961
Original article submitted October 23, 1959

Much work has been done on the adsorption of organic substances by clay minerals and aluminosilicate catalysts. The most complete studies, up to the present, have been carried out on the reactions of organic substances with synthetic silicates (silica gels) and, in the case of clay minerals, with minerals of the montmorillonite group.

It has been shown [1-4] that complex-formation takes place on the surface of silica gels and alumina–silica gels as a result of the formation of hydrogen bonds with the adsorbents via the OH-groups of the adsorbents. The absorption spectra in the visible range of the spectrum for organic substances adsorbed on aluminosilicates has been little studied: the most interesting works in this field are [5-7].

On the basis of work in the field of heterogeneous catalysis, the late N. E. Vedeneeva put forward the hypothesis of "doublet adsorption" of basic dyes on clay minerals. The present work is a continuation of Vedeneeva's work; we have used modern spectrophotometric apparatus, and have paid particular attention to one of the most significant problems in adsorption – the problem of surface chemical compounds.

In order to obtain continuous spectral absorption curves for the light reflected from the dyed surfaces of highly dispersed minerals in the form of an aqueous suspension or colored powder, we used an SF-2M recording spectrophotometer. We measured the reflection of light compared with that from an undyed specimen [$(I/I_0)100\%$] (the use of a logarithmic scale in the study of these compounds gives less satisfactory results). For convenience in comparing the results of the spectrophotometric studies with Vedeneev's results, i.e., in order to obtain the light-absorption maxima, the spectral curve was subsequently constructed from the values of $\frac{I_0 - I}{I_0}\ 100\%$.

The sorptive capacity with respect to the dyestuff methylene blue (MB) for all the adsorbents studied was first determined by the previously developed method [8] on which [9] was based. The adsorbents were dyed with increasing quantities of MB, equal to: 0.1, 0.5, 1, 5, 10, 30, 50, 70, and 100% of the sorptive capacity (E). The spectral curves were assessed quantitatively from the ratio of the light-absorption maxima.

The phenomenon of the adsorption of organic basic dyes by natural aluminosilicates has been insufficiently studied. Some workers have classified these reactions as chemisorption [10], others as irreversible physical adsorption, assuming that the nature of this phenomenon is similar to the phenomenon of ion exchange [11]. Here we regard this phenomenon as the formation of surface chemical compounds.

The concept of surface compounds and surface reactions was first clearly formulated by Shilov [10], although the idea of surface compounds had been anticipated by Faraday. It has been shown [13] that the range of surface chemical reactions is intermediate between molecular or physical adsorption and chemisorption. As in the case of physical adsorption, surface chemical reactions do not lead to the formation of new substances but, nevertheless, as in the case of chemisorption, the result of these reactions is that the surface atoms of the solid, and the

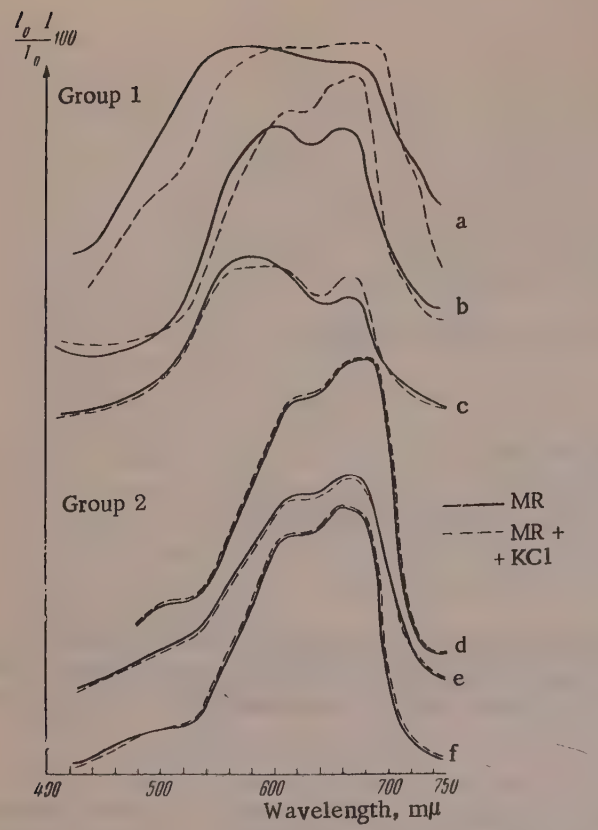


Fig. 1. Spectral curves for MB on various minerals (fraction <1 μ from clay minerals of group 1): MB 0.5% of E: a) askangel; b) hydromica No. 32; c) Prosyanaya kaolin; d) sepiolite; e) silica gel; f) talc.

molecules of the surrounding medium undergo a chemical change with the formation of a genuine chemical bond. The atoms of the solid which have taken part in the surface chemical reaction do not break the bonds with the other atoms making up the three-dimensional lattice of the solid. The surface compounds are thus stoichiometrically indefinite compounds. Nevertheless, as a result of the presence of the chemical bond, the surface compounds exhibit the chemical properties of ordinary bulk compounds—acids, bases, and salts. The surface compounds are formed at measurable rates, depending on the temperature.

Chemisorption, unlike surface chemical reactions, is an absorption process taking place as a result of a chemical reaction which gradually spreads through the whole bulk of the solid. In this process, both the molecules of the surrounding medium and the atoms or molecules of the solid undergo a chemical change to produce a new substance in the form of a new phase (for example, the absorption of carbon dioxide by calcium oxide).

X-ray structural studies of MB [14] have confirmed the ionic model of the structure of the dye, and have established that the nearest atom in the complex ion to the halide is the sulfur atom on which the main charge of the cation is localized.

The nonuniformity of a clay mineral with respect to mineralogical composition, and the crystallochemical and crystallographic character of its surface, is revealed as a difference in the adsorption energies of the active centers of the adsorbent. It may therefore be assumed that the surface chemical reactions between the clay minerals and the MB will lead to the formation of several types of surface saltlike compounds on the edges, corners, and faults on the crystals and on their different faces. The formation of surface compounds on the faces will be possible only in those cases where the faces are active with respect to the surrounding dye molecules. In aluminosilicates with a layer structure, the basal faces having the maximum development will be active with respect to the basic dye if they carry a negative charge on the faces made up of layers of silicon – oxygen tetrahedra, or have, in the surface layer, hydroxide groups with a tendency to form hydrogen bonds with the electrophilic groups of the dye. A negative charge is present on the basal faces of clay minerals whose crystal lattices show isomorphous replacement of metal atoms (montmorillonite, hydromica, chlorite, etc.). The active surface groups in these minerals are oxygen atoms. Certain minerals with a layer structure, such as talc and pyrophyllite, do not have active faces, since their structures show no isomorphous replacement of this kind, and there are no surface hydroxide groups on the faces. In minerals of the kaolinite group, basal faces formed by the surface hydroxide groups of the hydrargillite layer can be active with respect to the dye MB. The basal faces formed by the oxygen atoms of the silicon – oxygen tetrahedra cannot, however, be active to any significant extent, since isomorphous replacement of metal atoms is not a characteristic feature of these minerals. Reaction between the dye and clay minerals should lead to changes in the molecule of the organic compound, which decrease or increase the constant (i.e., independent of the action of light) displacement of π-electrons in the system of conjugated double bonds of the dye. This, in turn, should be accompanied by a displacement of the absorption toward the short-wave (hypsochromic effect), or long-wave (bathochromic effect) regions of the spectrum. It is known that the production of a chemical bond between the surface layer of atoms of adsorbent and a dye should be accompanied by a bathochromic effect [15]. The formation of different associates of dye and water, however, is accompanied by a hypsochromic effect [16,17].

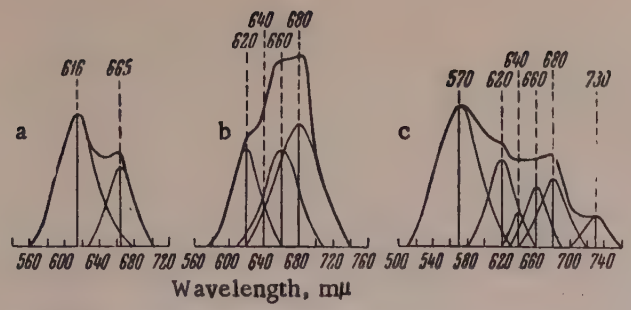


Fig. 2. Spectral light-absorption curves for MB in aqueous solution and adsorbed on highly dispersed aluminosilicates in aqueous medium: a) aqueous MB solution (<0.02% at 20°); b) minerals of group 2; c) minerals of group 1.

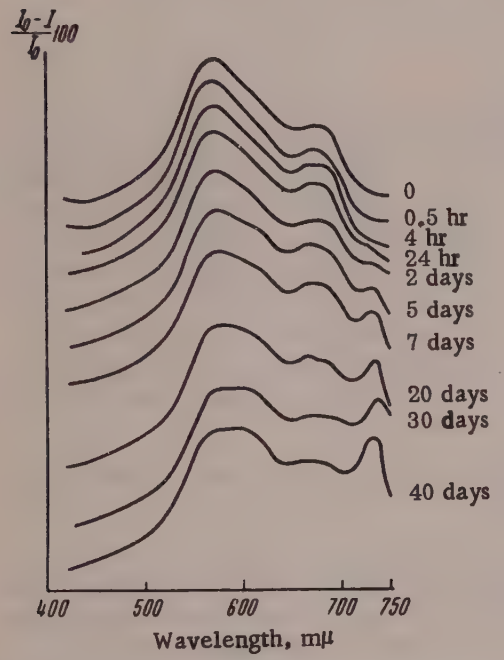


Fig. 3. Change in the spectral light-absorption curve for MB on montmorillonite (fraction <1 μ Oglanly bentonite) with time.

An aqueous solution of MB absorbs light in the visible range of the spectrum with absorption maxima at 600 and 656.6 mμ [15]. The first absorption region is characteristic of the dimers of the dye, and the second is characteristic of the monomeric molecules [5, 15]. The ratio of the intensities of the light-absorption maxima depends on the temperature and concentration of the solution.

As a result of the spectrophotometric study of colored suspensions of various highly dispersed silicate minerals, and of certain organic substances, we obtained a number of spectral absorption curves which can be divided qualitatively (like the minerals themselves with respect to the dye) into two groups (Figs. 1 and 2):

1. Spectral curves characterizing MB on minerals with a layer structure and active basal groups: these curves have light-absorption maxima at 570, 620, 640, 660, 680, and 730 mμ (minerals of group 1).

2. Spectral curves characterizing MB on minerals with a layer structure and inactive faces (talc, pyrophyllite), minerals with a chain structure (sepiolite), and amorphous substances: these curves have the same light-absorption maxima, except those at 570 and 730 mμ (minerals of group 2).

Change with time in the surface compounds formed by MB with highly dispersed aluminosilicates in aqueous suspensions at different temperatures. Aqueous suspensions of minerals of group 2, colored with MB, show no significant color changes on prolonged storage (30-40 days) in the dark, or when boiled for several hours. Aqueous suspensions of minerals of group 1 colored by MB show a color change on storage in the dark, or when the suspension is heated. The changes taking place when the temperature of the suspension is increased are the same as those observed with time, but are much more rapid. Figure 3 gives a number of spectral light-absorption curves for a colored aqueous suspension of montmorillonite, obtained by spectrophotometric study over a period of time at 20°. Analogous spectral curves were obtained for suspensions of hydromica and kaolinite. Figure 3 shows that the absorption maximum at 730 mμ gradually appears and increases with time, while the intensity of the maximum at 570 mμ shows a relative decrease. The relative magnitude of the other maxima remains almost unchanged.

In order to examine the influence of temperature on the color change shown by colored suspensions of minerals of group 1 (montmorillonite, hydromica, kaolinite), these minerals were kept for successive periods of 20 min at 20, 40, 60, 80, and 100°, and then boiled for 2 hr. Figure 4 shows that the color changes taking place, when suspensions colored with MB are heated, are analogous to the changes taking place with time. In order to produce the changes observed when a colored suspension is boiled for 2 min, however, it is necessary to store the same suspensions at 20° for one month.

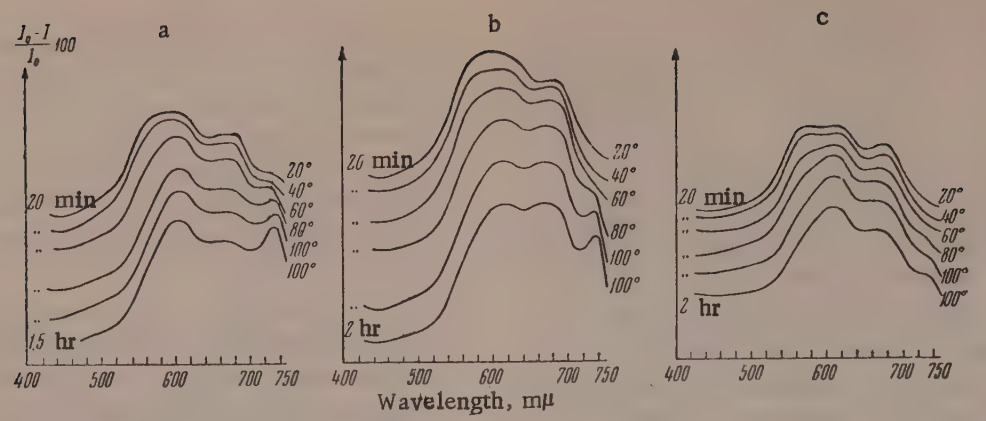


Fig. 4. Changes in the spectral light-absorption curves for MB on: a) montmorillonite (fraction < 1μ Oglanly Bentonite); b) hydromica (fraction < 1μ Pokrovnyi loam No. 32); c) kaolinite (fraction < 1μ Kyshtym kaolin); (changes taking place when colored aqueous suspensions were heated).

Change in the surface compounds formed by MB with highly dispersed aluminosilicates during the dehydration and hydration of colored specimens. No significant color changes take place when colored aqueous suspensions of minerals of group 2 are dried. When colored aqueous suspensions of minerals of group 1 are dried, however, color changes take place leading to a sharp decrease in the intensities of the light-absorption maxima at 570 and 730 mμ. Their relative values depend on the magnitude of the hygroscopic moisture content of the colored mineral powder. With the gradual hydration of the colored mineral powder, which takes place when the relative humidity of the air is increased, a gradual relative increase in the maxima at 570 and 730 mμ is observed. As a result of these studies, it was established that the value of I_{570}/I_{680} is linearly dependent on the moisture content of the colored clay specimen [for Oglanly bentonite colored with MB, up to 0.5% of E, for example, this relationship was of the form: $I_{570}/I_{680} = 0.075W + 0.555$, where W is the moisture content (%) of the colored specimen].

No change in color was observed when colored powdered minerals of groups 1 and 2 were moistened with nonpolar organic liquids.

The action of K^+, Rb^+, Cs^+, and NH_4^+ ions on aqueous suspensions of aluminosilicates colored with MB. N. E. Vedeneeva noted that K^+, Rb^+, Cs^+, and NH_4^+, when introduced into a colored aqueous suspension of certain clay minerals (chiefly those of the montmorillonite group), produce a definite color effect which results in an increase in the intensity of the long-wave light absorption, and a decrease in the intensity of the short-wave absorption. From the concept of doublet adsorption of MB, Vedeneeva considered that this type of dye adsorption is unstable only for montmorillonite minerals, and that the action of ions with small generalized moment (that is, according to Semenchenko, large ions with small charge) involves the creation of unfavorable conditions for the production of the pseudomonocrystalline flakes of montmorillonite, on which this type of adsorption is possible. On the larger flakes, with higher degrees of crystallinity, of kaolinite, doublet adsorption is always possible [7]. The results of our studies do not confirm this. According to our observations, the efficiency of the action of K^+ decreases with increase in the degree of saturation by the dye of all minerals of group 1, since this evidently decreases the number of exchange positions available to the K^+. For minerals of group 2, no color effects resulting from the action of K^+ were observed. With saturation of different clay minerals with dye (> 10% of E), spectrophotometric analysis detected no color changes when K^+, Rb^+, Cs^+, and NH_4^+ were added. Although the nature of the above phenomenon is extremely complex, examination of the results of spectrophotometric analysis shows clearly that the addition of potassium ions to a colored suspension leads to a relative decrease in the intensity of the light-absorption maxima at 570 and 730 mμ on the spectral-absorption curves, i.e., the same effect as that observed on dehydration of a colored specimen. It is known that when clay minerals with a layer structure are saturated with K^+, Rb^+, Cs^+, and NH_4^+, these ions are arranged chiefly on the basal faces. The cations adsorbed by clay minerals influence the nature of their hydration. According to Samoilov's studies [18], all the above cations exhibit "negative" hydration, i.e., they intensify the translational movement of the water molecules nearest to the ion. It is known, for example, that potassium-substituted clays exhibit marked minimum hydrophilic

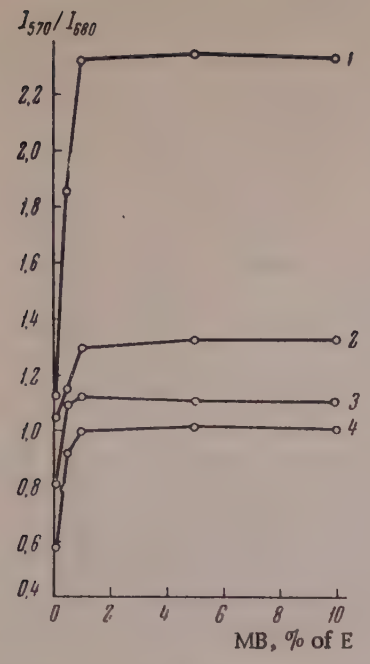


Fig. 5. The influence of the quantity of MB on the color of aqueous suspensions of minerals of group 1: 1) Mama muscovite; 2) Glukhov kaolin; 3) gumbrin; 4) Oglanly bentonite.

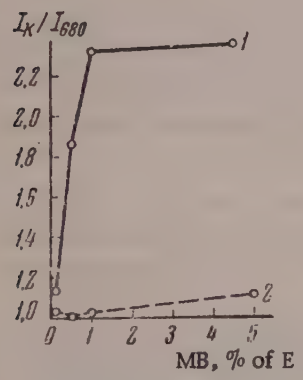


Fig. 6. The influence of increase in the degree of dispersion of muscovite on the value of I_{570}/I_{680} with change in the dose of MB: 1) muscovite ground in an eccentric mortar for 10 min; 2) muscovite ground to a state amorphous with respect to x rays.

properties [19,20]. Spectrophotometric studies of the dehydration of colored minerals of group 1 leads to the suggestion that the color effects resulting from the introduction of K^+, Rb^+, Cs^+, or NH_4^+ to an aqueous suspension of clay minerals colored with MB are associated with a change in the nature of the hydration of basal faces of the crystals of these minerals, and possibly with dehydration of surface organomineral saltlike compounds formed during the process of MB adsorption.

The influence of the magnitude of the dye dose on the results of coloring aqueous suspensions of aluminosilicates. The color of aqueous suspensions of highly dispersed aluminosilicates colored with MB depends to a considerable extent on the quantity of dye taking part in the reaction with the minerals. The effect of the quantity of dye used is particularly marked for minerals of group 1, which includes the majority of clay minerals. This can be attributed to two main factors: 1) the nonuniformity of the active centers of the mineral adsorbents with respect to adsorption energy; 2) physical conditions leading to the superposition of a large number of broad light-absorption bands [4-6] within the spectral range 550-750 mμ.

At the present time it is assumed that, for clay minerals, the adsorption potential of the active centers arranged on the edges, corners, and faults of the crystals is greater than the adsorption potential of the active centers on the faces of the crystals. Figure 5 shows that, at small doses of MB, the intensity of light absorption is greater in the long-wave region of the spectrum (the ratio I_{570}/I_{680} has minimum values), which characterizes surface compounds of the dye with active centers on the edges, corners, and faults of the crystals. Aqueous clay suspensions in this case have a greenish color, which becomes pale blue, then dark blue, with increase in the dye dose. Further increase in the dye dose leads to an increase in the absorption maximum in the short-wave region of the spectrum (570 mμ), which characterizes surface compounds of the dye with active basal faces of the clay minerals; the color of the suspension becomes violet. According to our data, the surface of the edges and angles of aluminosilicate crystals with a layer structure amounts to about 1% of their total surface. The greater part of the surface is made up, however, of the basal faces of the minerals.

The change in color of minerals of group 2 with change in the magnitude of the dye dose is less marked, and is due chiefly to the second of the factors given above.

The influence of change in the degree of dispersion and aggregation of the minerals on the results of coloring their aqueous suspensions. According to the spectrophotometric analysis data, change in the degree of dispersion and aggregation of minerals of group 2 has no effect on the results of the adsorption of MB in aqueous suspensions, and leads merely to a change in the sorptive capacity of the sorbents.

In the adsorption of MB on highly dispersed minerals of group 1, obtained by mechanical grinding of their more coarsely crystalline forms, there is an increase in the relative quantity of surface compounds in the sites of bond rupture on the deformed crystals. Spectrophotometrically, this is shown by predominant absorption in the long-wave region of the spectrum (620, 640, 660, and 680 mμ). With increase in the degree of dispersion, the

Influence of the State of Aggregation of the Particles in Aqueous Suspensions of Clay Minerals on the Nature of their Coloring by the Dye MB

Method of preparing suspension	I_{570}/I_{680}			
	gumbrin	Oglanly betonite	Na^+ montmorillonite*	Glukhov kaolin
Dry powder shaken with water for 10 min	1.49	1.09	1.15	1.42
The same, with boiling for 3 min	1.69	2.05	1.43	1.62

*Fraction <1μ of Oglanly bentonite saturated with Na^+.

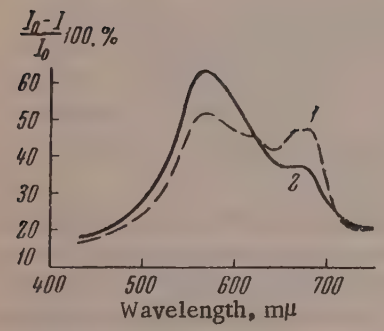


Fig. 7. The influence of the state of aggregation of Oglanly bentonite in aqueous suspension on the nature of the coloring by MB: 1) suspension prepared by shaking bentonite powder with water for 10 min; 2) the same, with additional boiling of the suspension for 3 min.

sorptive capacity of muscovite changes from 7.8 to 12.5 mg-equiv per 100 g. Figure 6, constructed from the spectrophotometric results, shows the change in the ratio of the intensities of light absorption at 570 and 680 mμ. For the surface compounds of MB with muscovite amorphous with respect to x rays, there is a relative displacement of the absorption of light into the long-wave region of the spectrum.

In the majority of cases, the aggregates of layer minerals consist of compact superimposed fine plates of primary particles. When the aggregates of particles are broken up in aqueous suspension by various methods (boiling, ultrasonic vibration, etc.), there is an increase in the number of crystalline plates, leading to a relative increase in the total surface of the basal faces. This leads to the formation of a relatively large number of surface compounds of the dye with the active basal faces. The table shows the ratio of the intensities of the light-absorption maxima at 570 and 680 mμ for clays with different degrees of aggregation in aqueous suspension.

The table shows that the changes in the color of the suspensions are extremely marked. When the aggregates of adsorbent particles are broken up, there is a relative increase in the intensity of the short-wave (570 mμ) light-absorption maximum on the spectral curve for the adsorbed dye (Fig. 7).

The presence of films of $Fe(OH)_3$ on the surface of clay minerals leads to an increase in the stability to water of the microaggregates of clay. In this case, the clay suspensions, even at relatively high dye doses, have a greenish-blue color, and the intensity of the maximum at 570 mμ on the spectral curves remains less than the intensity of the long-wave maxima. An example of this is provided by the spectral curve for MB on hydromica No. 32 (Fig. 1), containing 10% of free $Fe(OH)_3$.

Spectrophotometric characteristics of MB adsorbed on certain amorphous silicates and organic substances. The amorphous silicate adsorbent used was finely porous silica gel, and the organic adsorbent used was starch. The sorptive capacities of silica gel and starch with respect to MB in the presence of excess of the dye are 17 and 5 mg-equiv/100 g, respectively. The results of a spectrophotometric analysis of aqueous suspensions of these adsorbents colored with MB showed that the nature of the light absorption in the visible region of the spectrum by the surface compounds formed by the dye with amorphous silicates and starch is similar to that for the surface compounds of minerals which we have classified in group 2. Figure 1 gives the spectral light-absorption curve for MB adsorbed on silica gel. Analogous curves were obtained for MB on starch. None of these curves show absorption maxima at 570 and 730 mμ.

Hypothesis regarding the nature of the adsorption of the basic organic dye MB on highly dispersed aluminosilicates. The interaction of MB with highly dispersed aluminosilicates in aqueous medium leads to the formation of surface saltlike compounds of two types. On the surface of the active basal faces of minerals with a layer structure, saltlike hydrated compounds characterized by absorption of light in the short-wave region of the spectrum with a maximum at 570 mμ are formed. The observed hypsochromic effect compared with aqueous MB solution does not contradict the report [17] that the association of MB with water produces a hypsochromic effect. The reaction involved in the formation of these surface hydrated compounds takes place at a measurable velocity which is dependent on the temperature. The increase in the strength of the chemical bond between the dye and adsorbent, which takes place over a period of time, is characterized spectrophotometrically by a bathochromic effect. At the same time, there is a relative decrease in the intensity of the maximum at 570 mμ, and an increase in the intensity of the maximum at 730 mμ. Increase in the temperature of the colored suspension leads to a marked increase in the rate of this process. Drying of the colored suspension leads to reversible dehydration of the surface hydrated saltlike compounds. Spectrophotometrically, the dehydration of these compounds is characterized by the decrease and complete disappearance (drying at 100°) of the absorption maxima at 570 and 730 mμ. In this process, saltlike surface compounds with no water in their structure are evidently formed. The color effect produced by potassium ions introduced into a suspension colored with MB, and hence into the exchange complex of the minerals, is analogous, according to the spectrophotometric data, to the partial dehydration of the surface hydrated MB compounds, i.e., there is a decrease in the intensities of the absorption maxima at 570 and 730 mμ. The intensity of this color effect decreases with the decrease in the number of sites available to potassium ions on the adsorbent surface when the dye dose is increased. This explanation of the nature of the color effect produced by potassium ions does not contradict published studies on the specific character of the adsorption of these ions by clay minerals or their properties with respect to water molecules [18-20].

Methylene blue forms a second type of surface chemical compound in aqueous suspensions of aluminosilicates with a layer structure at the sites of bond rupture at the edges, corners, and faults of the crystals, on minerals with a nonlayer structure (chain structure, etc.), and on amorphous adsorbents. Spectrophotometrically, this type of compound is characterized by absorption of light in the visible region of the spectrum with maxima at 620, 640, 660, and 680 mμ. This type of compound is stable over a period of time, and is unchanged by increase in the temperature of the colored suspensions. Thus, minerals of the silicate class can be subdivided into two groups according to the nature of the surface compounds formed with MB. All aluminosilicates having a layer structure with active basal faces are put in one group.

The above hypothesis regarding the nature of the adsorption of MB by clay minerals provides a better explanation of our factual material than the "doublet adsorption" hypothesis of N. E. Vedeneeva, but further studies are necessary.

SUMMARY

1. Data obtained from spectrophotometric analysis in the visible region of the spectrum of aqueous suspensions of aluminosilicates colored with methylene blue (MB) make it possible to distinguish two groups of organomineral compounds formed during the adsorption of the dye. Group 1 consists of compounds formed on the active basal faces of minerals with a layer structure (clay minerals): group 2 consists of compounds of the dye with adsorbents at the sites of bond rupture on the edges, corners, and faults of the crystals, and also on certain amorphous and organic adsorbents.

2. The nature of the adsorption of MB on highly dispersed aluminosilicates is that of a surface chemical reaction, as a result of which organomineral surface compounds of saltlike character are formed: the compounds formed in aqueous medium on the active basal faces of clay minerals with a layer structure have specific properties. These compounds have been arbitrarily referred to as surface organomineral hydrated compounds.

LITERATURE CITED

1. M. M. Dubinin, Collected Papers from the Conference on Adsorption [in Russian] (Moscow University Press, 1957) p. 180.
2. A. V. Kiselev, Collected Papers from the Conference on Adsorption [in Russian] (Moscow University Press, 1957) p. 90.

3. A. N. Terenin, Collected Papers from the Conference on Adsorption [in Russian] (Moscow University Press, 1957) pp. 206, 271.
4. N. D. Sokolov, Collected Papers from the Conference on Adsorption [in Russian] (Moscow University Press, 1957).
5. T. P. Kravets, A. L. Pes'kina, and Z. V. Zhidkova, Izvest. Akad. Nauk SSSR, Ser. Fiz. 14, No. 4, 99 (1950).
6. N. E. Vedeneeva, Problems of the Mineralogy of Sedimentary Deposits [in Russian] (L'vov University Press, 1956).
7. N. E. Vedeneeva and M. F. Vikulova, A Method for Studying Clay Minerals with the Aid of Dyes (Spectrophotometric Analysis) [in Russian] (L'vov University Press, 1956).
8. L. U. Kul'chitskii, Byull. Nauchno-Tekhn. Inform. Ministerstva Geologii i Okhrany Nedr. Gosgeoltekhizdat No. 7 (24), 60 (1959).
9. R. H. S. Robertson and R. M. Ward, J. Pharm. Pharmacol. 3, 27 (1951).
10. Hundeshagen, N. Jahrbuch für Min. Beil. 28 (1909).
11. S. B. Hendricks, J. Phys. Chem. 45, 65 (1941).
12. N. Schilow, Koll. Z. 52, No. 1, 107 (1930).
13. L. K. Lepin', Uspekhi Khim. 9, 5 (1940).
14. G. S. Zhdanov, Z. V. Zvonkova, and L. G. Vorontsova, Kristallografiya 1, No. 1 (1956).
15. A. N. Terenin, The Photochemistry of Dyes and Related Organic Compounds [in Russian] (AN SSSR Press,1947).
16. L. A. Lyzina and A. T. Vartanyan, Optika i Spektroskopiya 6, No. 2 (1959).
17. G. N. Lewis, O. Goldshmid et al., J. Am. Chem. Soc. 65, 1151 (1943).
18. O. Ya. Samoilov, The Structure of Aqueous Electrolyte Solutions and the Hydration of Ions [in Russian] (AN SSSR Press, 1957).
19. F. D. Ovcharenko, N. G. Kirichenko, D. N. Kovalenko, and A. I. Rastrenenko, Ukrainian Bentonites [in Russian] (AN UkrSSR Press, 1958).
20. A. I. Rastrenenko, Collection: Ukrainian Bentonite Clays [in Russian] (AN UkrSSR Press, 1959).

CAPILLARY-RETAINED LIQUID IN DISPERSE SYSTEMS OF CONTACTING PARTICLES

L. V. Radushkevich and V. A. Kolganov

Institute of Physical Chemistry, Academy of Sciences of the USSR, Moscow
Translated from Kolloidnyi Zhurnal, Vol. 23, No. 1, pp. 86-94, January-February, 1961
Original article submitted October 30, 1960

Many disperse systems consist of hard contacting particles, in the spaces between which, as well as near the places where they make contact, a certain amount of liquid may be retained by capillary forces. Capillary-retained liquid remains in quicksand, after water or petroleum has filtered through it, in sorbents consisting of contacting particles of colloidal dimensions (carbon black, silica gel), and in various granular foodstuffs, as a result of capillary condensation of vapor, if they are stored in an atmosphere where such vapor occurs. In general, the quantity of retained liquid in such systems changes with time, from diffusion and heat-exchange processes, but equilibrium states between liquid and vapor are also possible in these systems, which are reflected in the form of the corresponding sorption isotherm. For the equilibrium states, it often becomes necessary to estimate by calculation the quantity of capillary-retained liquid at a given temperature, and assigned vapor pressure. A number of attempts have been made in this direction, but the majority of them gave unreliable results since, on the one hand, the geometric properties of the system were simplified excessively and, on the other hand, primitive, thermodynamically unfounded calculations were made for the liquid volumes near the points of contact [1]. In our investigations, one of the authors [2-4] derived the form of the liquid meniscus from thermodynamic considerations, leading to the result that, at equilibrium, the curvature of the liquid surface should be constant at all points, from which parameters were calculated for the corresponding equilibrium configuration. It was shown that the simplified calculations made previously lead, as a rule, to highly elevated values for the retained volumes [3]. Kruyer [5] presented a simplified method of calculation [5], leading to values close to our accurate values, good for different contact angles, but applicable to only one special case of contact.

In the present paper, we have calculated the volume of capillary retained liquid for elementary systems, consisting of two particles. The calculation assumes filling to saturation, where the equilibrium vapor pressure corresponds with the pressure of saturated vapor over a plane surface ($p/p_s = 1$). In the following, it is assumed that the particles do not swell in the liquid, and that the contact angle is zero. The effect of gravitational forces could be neglected, because of the smallness of the liquid volumes.

Corresponding with the possible situations that can be met within disperse systems, we shall consider the following types of two-particle systems:

1. Spherical particles of a single radius, in point contact with one another.

2. Spherical particles of a single radius, at some distance from one another, without contact (a case encountered in systems consisting of a large number of contacting particles).

3. Two spherical particles of a single radius, coalesced.

4. Spherical particles of different radii, in contact at a single point.

5. Particles of irregular shape in point contact with one another.

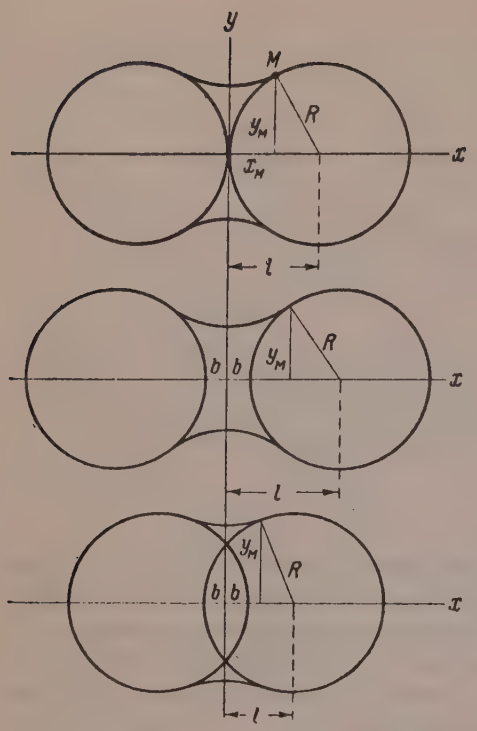


Fig. 1.

System 4 was investigated earlier [4]; therefore, we limited ourselves to comparing the results with the new data. For simplifying the problem, and convenience in calculations, the first three cases were considered together. System 5 should be treated specially, as it requires an additional assumption as to the form of the particles. The purpose of the calculations was to compare the volumes of capillary retained liquid at $p/p_s = 1$, for all the cases considered. If the system is filled to saturation, the liquid layer formed should give a surface of zero curvature at equilibrium, thus, obviously, the concave liquid meniscus should be a catenary, and from the axial symmetry of the system, the surface of the liquid will be a catenoid of revolution. The problem consisted in finding the parameters of the catenoid, and determining its volume.

Particles of regular shape, having the same dimensions. (Systems 1, 2, and 3). First of all, a parameter was introduced to represent the separation between the particles. Figure 1 is a schematic representation of all three systems, differing in the value of the parameter b, the distance of the nearest axial point on each particle from the vertical axis of symmetry. Introducing the distance l of the center of the particle from the origin of coordinates (i.e., the y axis), and using the dimensionless parameter $q = l/R$, we have:

for system 1: $l = R$; $q = 1$;

for system 2: $l = R + b$; $q = 1 + b/R$ $(q > 1)$;

for system 3: $l = R - b$; $q = 1 - b/R$ $(q < 1)$.

In the (x,y) plane, the problem consists in finding the coordinates x_M and y_M of the point of tangency of the circumference with the catenary. Combining all three cases into one, we have the equations of the circumference and the catenary:

$$y^2 + (qR - x)^2 = R^2; \quad y = a \operatorname{ch} x/a.$$

We now introduce the dimensionless transformation $z = x/a$, and the dimensionless parameter of the catenary $z_0 = R/a$. Then, from the two equations, the value of y_M for the common point of the two curves can be found, giving:

$$\operatorname{ch}^2 z + (qz_0 - z)^2 = z_0^2, \tag{1}$$

where $z = x_M/a$. The condition for tangency at the point of contact of the two curves, corresponding with zero contact angle, is:

$$\operatorname{sh} x/a = \frac{qR - x}{a \cdot \operatorname{ch} x/a}$$

or

$$\operatorname{sh} z = \frac{qz_0 - z}{\operatorname{ch} z} \tag{2}$$

from which

$$z_0 = 1/q\,(z + \operatorname{sh} z \operatorname{ch} z). \tag{3}$$

Substituting the value of z_0 in relation (1), we obtain, after solving the quadratic equation for $z > 0$:

$$z = q \operatorname{ch}^2 z - \operatorname{sh} z \operatorname{ch} z. \tag{4}$$

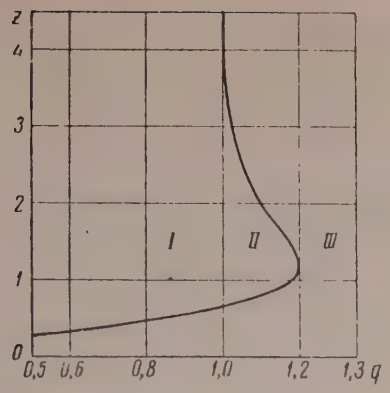


Fig. 2.

For q = 1, this equation takes on the same form that was derived in [4]. Assigning different values to q, the corresponding values of z may be found by graphical solution of Eq. (4). But there is another more rational method, which reveals some of the features of the problem. From Eq. (4) we find:

$$q = z(1 - \mathrm{th}^2 z) + \mathrm{th}\, z. \tag{5}$$

Obviously, it is simpler to assign values to z, and then calculate the corresponding values of q from Eq. (5), as needed to find the volume of the liquid phase. Further, combining Eqs. (3) and (4) gives the relation:

$$z_0 = \mathrm{ch}^2 z, \tag{6}$$

which is also needed to find the volume.

Examination of Eq. (5) shows that the curve $q = f(z)$ passes through the origin, has a maximum at $z = z_K = q_K$, and an asymptote parallel to the z axis, where, as $z \to \infty$, q = 1. Hence, it follows that the curve of z against q has the form shown schematically in Fig. 2. In region I (Fig. 2), where q < 1, the function is single-valued, i.e., for tangent spheres or coalesced particles, there is only one stable catenoid. In region II, for distances between spheres from $q \geq 1$ to some critical value q_K, there are two values of z and, consequently, for nontangent spheres two different stable values of the liquid volume are possible, the larger volume corresponding with the smaller value of z. Finally, when the distance between the spheres exceeds the critical value q_K (region III), no stable liquid volume can be formed, and the problem loses significance. We come to the same conclusions if we consider the roots of the transcendental equation (4). At the critical separation between spheres, the following relation holds:

$$z_K = q_K, \tag{7}$$

corresponding with the maximum in the function $q = f(z)$. Substituting this value of q_K into Eq. (5), we find

$$z_K = \mathrm{cth}\, z_K. \tag{8}$$

Hence, it is easily determined from tables that

$$z_K = q_K = 1.200. \tag{9}$$

If the spheres are separated a distance greater than that corresponding with q_K, no stable volume of retained liquid can exist between them. It is easily shown that, for the critical catenoid, $a \approx 0.305R$ and $H \approx 1.132R$, where H is the altitude of the catenoid. Thus, for the configurations considered, the liquid volumes are to be found within the range of values $0 \leq q \leq q_K$.

The volumes of the liquid phase are calculated in the way described in [2-4]. However, in the calculations, it is more convenient to use only powers of the hyperbolic tangent, since the other functions can be eliminated from the equations.

For all three cases we have:

$$V_L = V_K - 2v, \tag{10}$$

where V_L is the volume of the retained liquid phase; V_K is the volume of the catenoid; and v is the volume of either the spherical segment (v_c), for systems 1 and 2, or the spherical lamina (v_{cl}) for system 3. The relative volume of the liquid phase in a system of two solid particles is equal to $U = V_L/V_T$, if V_T is twice the volume of the particle. The volume of the catenoid is given by the formula $V_K = \frac{1}{2}\pi a^3(\sinh 2z + z)$ which, with the help of the preceding formula, is easily rearranged into the simpler form:

$$V_K = \pi R^3 q\, (\mathrm{ch}\, z)^{-4}. \tag{11}$$

Here z is a function of q as given by Eq. (4); therefore, in general, Eq. (11) should be written in the form $V_K = F(R, q)$. Consequently, to calculate V_K from Eq. (11), Eq. (4) or (5) has to be used also, although the parameter q can be eliminated, giving V_K as a function of z and R.

Relative Volume of Retained Liquid as a Function of Particle Separation

z	q	U, %	z	q	U, %	z	q	U, %
0,1	0,198	0,102	0,65	1,009	5,356	1,20	1,200	2,22
0,2	0,389	0,712	0,7	1,048	5,654	1,40	1,188	1,18
0,3	0,568	1,827	0,8	1,111	5,508	1,6	1,162	0,54
0,4	0,722	3,271	0,9	1,154	4,799	1,8	1,133	0,15
0,5	0,855	4,406	1,0	1,181	3,891	5,0	1,001	0,00
0,6	0,964	5,070	1,10	1,195	2,998	∞	1,000	0,00

From Eq. (11) we have:

$$V_K = \pi R^3 q (1 - \mathrm{th}^2 z)^2. \tag{12}$$

The volumes v_c and v_{cl} are calculated from the usual formulas which, after simple rearrangements, take the form:

$$\left.\begin{aligned} v &= {}^1/_3 \pi R^3 (\mathrm{th}^3 z - 3\mathrm{th}\, z + 2), \text{ for } q \geq 1 \\ v &= {}^1/_3 \pi R^3 (\mathrm{th}^3 z - 3\,\mathrm{th}\, z + 3q - q^3), \text{ for } q < 1 \end{aligned}\right\} \tag{13}$$

Finally, from Eqs. (10), (12), and (13), we find:

$$\left.\begin{aligned} V_L &= \pi R^3 [\Phi - ({}^1/_3 - q)], \text{ for } q \geq 1 \\ V_L &= \pi R^3 [\Phi - q(1 - {}^2/_3 q^2)], \text{ for } q < 1 \end{aligned}\right\} \tag{14}$$

where, for brevity, we have written:

$$\Phi = q\,\mathrm{th}^4 z - {}^2/_3 \mathrm{th}^3 z - 2q\,\mathrm{th}^2 z + 2\,\mathrm{th}\, z.$$

The relative volumes of the liquid phase for all three cases are:

$$\left.\begin{aligned} U &= {}^3/_8 [\Phi - ({}^4/_3 - q)], \text{ for } q \geq 1 \\ U &= {}^3/_2 [\Phi - q(1 - {}^2/_3 q^2)] : [4 - (1-q)^2 (2+q)], \text{ for } q < 1 \end{aligned}\right\} \tag{15}$$

The calculation consists of simultaneous application of Eqs. (5) and (15), in which it is more convenient to assign the value z, and then, after finding q, to calculate U. The results of the calculation are given in the table.

Contacting spherical particles of different dimensions. The calculation for a pair of contacting spherical particles of different radii R_1 and R_2 ($R_1 < R_2$) is given in our earlier paper [4]. The volume of the liquid phase in this case is given by the relation:

$$V_L = {}^1/_3 \pi R_1^3 U_{12},$$

where U_{12} is a function of the ratio of the radii $\lambda = R_2/R_1$, the values of which, for different λ and $p/p_s = 1$, were tabulated and given in the reference quoted. The relative volume is given by:

$$\omega_{12} = V_L [{}^1/_3 \pi (R_1^3 + R_2^3)]^{-1} = {}^1/_4 U_{12} (1 + \lambda^3)^{-1}. \tag{16}$$

The change in relative volume as a function of ω_{11}, for equal radii of the spheres ($\lambda = 1$), is given by the relation:

$$\varkappa = \omega_{12}/\omega_{11} = 2(1 + \lambda^3)^{-1} U_{12}/U_{11}.$$

The change in the ratio with change in λ is given in Fig. 3, from which it can be seen that the relative volume of the liquid phase decreases monotonically with increasing difference in the dimensions of the spheres, although the volume of the liquid itself increases with increasing λ. The maximum relative volume of liquid is found at $\lambda = 1$, i.e., in the case where the spheres have the same dimensions.

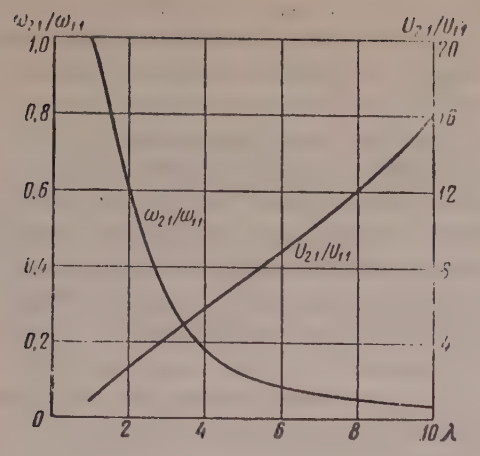


Fig. 3.

Contacting particles of irregular shape. For systems of contacting particles of irregular shape, there is no possibility of making a rigorous estimate of the volume of retained liquid near the point of contact. If we limit the discussion to particles of not very complicated shape, a sufficiently good estimate can be obtained from the data obtained above for spherical particles. Obviously, a generally complicated shape of the individual particle has no direct influence on the small volume of capillary retained liquid in the immediate vicinity of the point of contact. Thus, if two amorphous particles have small spherical bumps on the surface, and this is where the particles touch, the volume calculation will not differ from the one given above for ideal spherical particles. The degree of unevenness of the surface, or "height of projection" limits this result to some extent. Using the calculations given above for two spherical particles to determine the position of the edge of the meniscus on the surface of the sphere shows that the height of the segment is equal to $x_M = 0.436R$. Therefore, if the radius of curvature R of the irregularity on the irregularly shaped particle constitutes a fraction R/A of the radius A of the whole particle, then h/A = 0.436. If h/A is less than this value, the filling process will be more complicated than we have described. For example, if the radius of curvature of the irregularity is R = 0.1A, then h/A = 0.0436. Consequently, in this case, the height of the irregularity should be not less than about 4% of the radius of the particle. These considerations show that we have the possibility in hand of describing capillary retention of a liquid by a wide variety of particles of irregular shape.

No difficulty is presented in isolating a few portions of the surface of an amorphous particle, which can be considered to be segments of a sphere. Thus, the contact between particles of irregular shape can always be reduced to a contact between their spherical portions. To get some idea of the dimensions of irregular particles, it is helpful to use the concept of the weight radius A, defined as the radius of a sphere of the same mass as the irregular particle itself. Thus, we have $m = \frac{4}{3}\pi A^3 \rho$, where m is the mass of the particle, and ρ is the density. The case $R \gg A$ is rarely encountered on the surface of irregularly shaped particles because, otherwise, they would, on the average, be of dimensions greater than R, which doesn't make sense. The problem under consideration corresponds closely with the case $R < A$, i.e., to "rough" particles of more or less generally rounded shape. The effect of the condensation of vapor in depressions near the irregularities can also be estimated, but their role is not great, and we neglect them completely.

For q = 1, the volume of the liquid phase for spherical particles, as given by the preceding formulas, is equal to

$$V_L = \pi R^3 (\Phi - 1/3).$$

The relative volume of liquid in a system of irregular particles, in contact at identical spherical surfaces of radius R, is equal to:

$$U = 3/8 (R/A)^3 (\Phi - 1/3). \quad (17)$$

Compared with the relative volume U_0, for a pair of ideally smooth particles, we have:

$$U/U_0 \sim (R/A)^3. \quad (18)$$

Hence, it follows that, for $R < A$, the relative volume of liquid in a system of two identical rough particles, with the same mean degree of roughness, is much less than for ideally smooth, identical spherical particles. Formula (18) is approximate but, obviously, various sorts of corrections produce no essential change in the results. It can be shown that the state of affairs remains the same if the roughnesses are different. For this, it is sufficient to look at system 4, modifying the results to take account of the roughness of the particles.

The present calculation of several varieties of the simpler disperse systems shows that the value of the relative volume of capillary retained liquid is, in general, not large. This volume reaches its highest value for

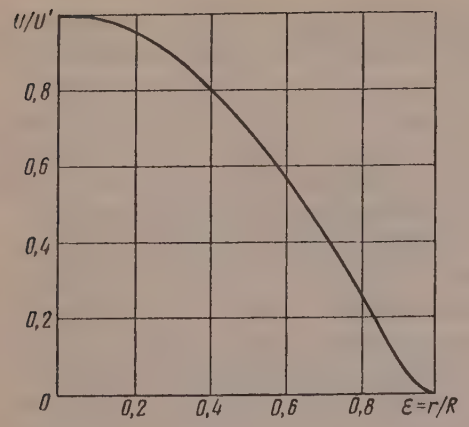


Fig. 4.

ideally smooth identical spherical particles, slightly separated from one another ($q \approx 1.05$). It has practically the same value, if the particles are simply in contact at one point. With distributions of this sort, the relative volume amounts to about 5.5%, which is close to the maximum. In all other cases, the effect should be even smaller, if we accept the assumptions that were made in the calculations. For coalesced particles, the volume decreases markedly with increasing contact area, while for sufficiently separated spheres it disappears completely, if the distance q becomes greater than 1.2. In the case of contact between a pair of spherical particles of different radii, the relative volume of liquid is small, and decreases with increasing particle radii. Finally, for rough particles, the effect becomes very insignificant, and decreases sharply with decrease in the ratio R/A, i.e., with increasing degree of roughness.

In practice, in many systems having globular structure, one can expect contact in the form of ideal spheres of nearly the same radius, so that the quantity of capillary retained liquid can be near its maximum value. Using the above data, it is easily shown that the absence of ideal point contact does not materially change the resulting value of the volume of retained liquid in any real system. Actually, if the results are used for coalesced particles, and if, for a better estimate, we introduce the radius r of the contact circumference, then U may be expressed as a function of the parameter $\epsilon = (1 - q^2)^{\frac{1}{2}} = r/R$. Obviously, ϵ varies from $\epsilon = 0$ (point contact) to $\epsilon = 1$ (a single sphere in the range $q = 0$). This gives a curve, shown in Fig. 4, representing the dependence of U on ϵ. The form of this curve is such that, at $\epsilon \approx 0.1$, the value of U is only slightly different from the value U', for ideal point contact between spheres. For sufficiently large spheres (~1000 A), the contact area may be considered vanishingly small, if its radius is near 100 A, i.e., a realistically admissible value for contact between solid bodies. Now the whole process proceeds as for ideal point contact, the result being even more accurate for spheres of macroscopic dimensions. Thus, the imperfect contact of real spherical particles decreases the quantity of capillary retained liquid by a very insignificant amount.

The case of separated particles is often encountered in real systems since, along with the contacts, there are always spaces, formed by close, but not touching, neighboring particles. These spaces, generally speaking, may be completely filled with capillary retained liquid [6]. However, the above calculations have shown that, if two particles are closely approximated, an equilibrium "hanging" column of liquid is formed between them, if the remaining particles are sufficiently far away. The existence of a maximum critical distance, with the parameter $q_K \sim 1.2$, at which the effect is still possible, may be explained from purely geometric considerations, since, with complete wetting, it is impossible to form a liquid column between particles, at a separation greater than q_K, in such a way that it can be tangent to the surface of the particle over the whole contact boundary. A suspended liquid column cannot be formed with cubical packing for, in this case, $q = 1.41$, i.e., greater than q_K. It is absent in hexagonal packing, too. It is easily shown that it is possible in systems where the elementary rhombohedron has inferior angles in the range between 60° and 73°40'.

The double value for the retained liquid volume, which we found at $q > 1$, is not lacking in physical content. It is possible that either of the volumes for the given q is formed, depending upon the path by which the equilibrium state of the system is approached. It is not impossible that the considerable fluctuations in the sorption values, which are observed in all sorption measurements in the region very close to $p/p_s = 1$, are a result of the existence of double values for the relative liquid volumes in the spaces between the particles. Further, it should be kept in mind that one of the volumes is often so small that the column is easily broken up from chance external causes, and only the large liquid volume turns out to be really stable. The calculation in the region $p/p_s < 1$, for closely approximated particles, is of fundamental interest, since the possibility of the existence of double-valued solutions in this region may provide the explanation of the well-known phenomenon of hysteresis in capillary condensation.

We have looked into the simplest cases of capillary retained liquid in disperse systems of two particles. Also, it is not difficult to consider various arrangements of these simpler cases, but this will reflect only slightly

on the results already obtained for the values of the retained volumes. More fundamental results are obtained on going over to systems of a large number of contacting particles, since, in these systems, account must be taken of the packing of the particles, as well as the possibility of fusion of the menisces and flooding of the interstitial spaces. The two-particle model taken for calculation corresponds most closely with the loose packing of a large number of particles where, even for $p/p_s = 1$, separately distributed liquid meniscuses are possible, and complete flooding of the interstices is absent. However, in real systems, the packing can never be ordered and, in practice, it is unknown. Therefore, the results obtained can serve, in all types of packing, as a criterion for the existence of separate meniscuses, without fusion between them. If, in such systems, the relative volumes, determined by experiment, exceed the values found, this is evidence for the predominance of such effects as meniscus fusion, and liquid flooding of the spaces between the particles. For systems of sufficiently large particles (radii > 1 μ), the volume contribution of the adsorbed film is vanishingly small at $p/p_s = 1$, and it can always be neglected.

SUMMARY

1. In simpler elements of disperse systems, at relative vapor pressure $p/p_s = 1$, the equilibrium volume of capillary retained liquid does not exceed 5.5-5.6% of the volume of the solid phase. It reaches its maximum value for slightly displaced spherical particles of identical radius. When the particles are in contact, the relative liquid volume is very close to the maximum.

2. For spherical particles of different radii in contact, for coalesced particles, and particles with a rough surface, the relative volume, as a rule, is substantially less than 5.5-5.6%.

3. In disperse systems consisting of a large number of particles of different forms and dimensions, the relative volume of capillary retained liquid at $p/p_s = 1$ cannot exceed the indicated maximum value at equilibrium as long as the liquid meniscuses remain separated. Higher values of the relative liquid volume indicate the presence of such effects as meniscus fusion, liquid flooding of the spaces between the particles, or absence of equilibrium in the system.

LITERATURE CITED

1. J. Higuti and H. Utsugi, Sci. Reports of the Tohoku University, Ser. I, 36, No. 1, 27 (1952); P. C. Carman, J. Phys. Chem. 57, 56 (1953); R. M. Barrer, N. McKenzie, and J. S. S. Reay, J. Colloid Sci. 11, 479 (1956).
2. L. V. Radushkevich, Izd. AN SSSR, Otdel. Khim. Nauk No. 6, 10 (1952).
3. L. V. Radushkevich, Izd. AN SSSR, Otdel. Khim. Nauk No. 3, 285 (1958).
4. L. V. Radushkevich, Izd. AN SSSR, Otdel. Khim. Nauk No. 4, 403 (1958).
5. S. Kruyer, Trans. Faraday Soc. 54, No. 11, 175 (1958).
6. A. P. Karnaukhov and A. V. Kiselev, Z. Fiz. Khim. 31, 2635 (1957).

STUDY OF LATEX FOAMS

D. M. Sandomirskii and A. A. Korotkova

Scientific Research Institute of Rubber and Latex Manufactures
Translated from Kolloidnyi Zhurnal, Vol. 23, No. 1, pp. 95-99, January-February, 1961
Original article submitted July 8, 1959

The production of sponge rubber from latex is based on the foaming of a latex mix, carried out by mechanical means, followed by gelling of the foam and vulcanization of the gel [1,2].

Despite the wide practical application of latex foams, the study of their properties as colloidal systems, and the influence exerted on them by the various parameters of the original latex, has received little attention.

The present communication gives the result of an investigation of the influence of some characteristics of synthetic latexes (concentration, surface tension, viscosity) on the foaming ratio, dispersion, and stability of mechanically produced foams.

Foaming of the latex was carried out in an 0.75 liter flask by means of a propellor agitator under constant conditions (2000 rpm, foaming time 15 min, temperature 20-22°C), ensuring reproducibility of the properties of the foam.

The foaming ratio K (ratio of volume of the foam to the volume of liquid phase contained in it) was determined by weighing a definite volume of foam, and was calculated from the equation

$$K = V_f/V_f = V_l\gamma_f/g_l,$$

where V_f is the volume of the foam (ml), V_l is the volume of the latex (ml), γ_l is the specific gravity of the latex (g/cm^3), and g_f is the weight of the foam (g). For determining the degree of dispersion, the foam was placed between two object glasses (gap 0.05 mm), and photographed together with an eyepiece micrometer scale at a magnification of eight times. The diameters of the bubbles (cylinders) obtained in the photograph were converted to the corresponding diameters of the original spherical bubbles. The mean diameter of the bubbles was calculated from the formula

$$d_m = \sum d_i n_i / \sum n_i$$

and distribution curves were plotted.

Stability of the foam was observed in a period of 30 min in a special funnel having a sealed lower end, a definite volume of foam being placed in the wide portion. The time to commencement of drainage of the foam into the narrow, calibrated part of the funnel (τ), the rate of its drainage (v_1), and the rate of separation of the latex (v_2) were determined.

The structural-mechanical properties of the foam were investigated by the grooved-plate method [3], using the apparatus shown in Fig. 1.

The plate 1 (2 × 3 cm) with horizontal cuts, was suspended from a thread 6 passing over a pulley 7. The foam was poured into a vessel 2, which had plane-parallel sides and was mounted on a movable table 3. In carrying out an experiment, the plate 1 was immersed in the foam by steady raising of the table 3, and was balanced by the weights 8. The hinged platform was then released, and the plate was withdrawn from the foam under constant load, i.e., the weights in the scale 9.

TABLE 1

Dependence of the Properties of Foam on the Concentration of Latex Nairit L-4*

Concentration of latex, %	K	τ, min	v_1, ml/min	v_2, ml/min
50	9,2	4,0	1,25	0,06
40	8,0	2,25	1,70	0,25
30	10,0	1,5	1,25	0,40
20	7,9	1,5	1,5	0,6
10	7,0	1,25	2,0	0,8

*The initial 50% latex was diluted with distilled water.

TABLE 2

Dependence of the Properties of Foam on the Surface Tension of Latex SKS-50H

Nekal, %	σ, dyne per cm	η, centipoise	K	τ, min	v_1, ml per min	v_2, ml per min
0	45,4	4,7	1,7	1,5	2,2	1,0
1	40,4	4,4	3,0	2,6	1,5	0,55
2	37,6	4,3	3,3	2,5	1,75	0,44
3	33,7	4,4	3,8	2,5	1,75	0,44

After a predetermined interval of time, the displacement of the plate was measured on the microscale 4 by means of the microscope 5.

Table 1 shows the dependence of the foam properties on the concentration of latex L-4.

With dilution of the latex, the foaming ratio is reduced, and the stability of the foam falls. Reduction in the foaming ratio has less influence, however, than the dilution of the foam on the reduction in stability of the foam (τ and v_2). This may be gathered from Fig. 2.

Table 2 shows the influence of surface tension (σ) on the properties of foam of divinylstyrene latex SKS-50H, into which, after dialysis, nekal was introduced in amounts of 1.2 and 3% of dry latex substance.

A reduction in the surface tension of the latex to 40 dyne/cm results in an increase in the foaming ratio and in the stability of the foam. Further reduction in surface tension has no influence on either of these properties. A similar relationship was found in the case of the latex Nairit L-4.

Table 3 shows the influence of the viscosity of the latex Nairit L-4 on the properties of the foam. The viscosity of the latex was increased on the addition of ammonium caseinate to the latex.

TABLE 3

Dependence of Foam Properties on the Viscosity of 47% Nairit L-4 Latex

Ammonium caseinate, %	σ, $\frac{\text{dyne}}{\text{cm}}$	η, centipoise	K	τ, min	v_1 $\frac{\text{ml}}{\text{min}}$	v_2 $\frac{\text{ml}}{\text{min}}$	d_m, cm
0	36,0	7,4	8,5	2,9	2,5	0,44	0,019
0,5	36,8	12,4	7,2	10,7	0,5	0,08	0,017
1,0	36,8	31,0	6,2	22,0	0,14	0,05	0,016
1,25	36,8	59,0	5,0	63,0	0,02	0	0,015

The viscosity of the latex was also increased by the addition to the latex of a 1% gelatin solution in amounts of from 0.1 to 0.5%, reckoned on the dry latex substance. The viscosity of the latex also has a considerable influence on the dispersion. Figure 3 shows curves of bubble diameter distribution of foams, made from latexes of different viscosities. With increase in viscosity, the maximum becomes less pronounced, and is shifted toward smaller bubble diameters, i.e., a foam made from a more viscous latex is less uniform, but more disperse.

The curves in Fig. 4 show the deformation kinetics of a foam made from the latex Nairit L-4, thickened with ammonium caseinate to a viscosity of 59 centipoise. The foaming ratio of the initial foam was $K = 5$, stability $\tau = 35$ min. The measurements were made for a shearing stress $P_s = 49$ dyne/cm^2 (the limit shearing stress for such a foam is $P_s = 65$-75 dyne/cm^2).

The curves of Fig. 4 show that, up to 45 min after production, the foam represents a plastic system, it becomes gradually more fluid, the rate of deformation and permanent deformation increasing.

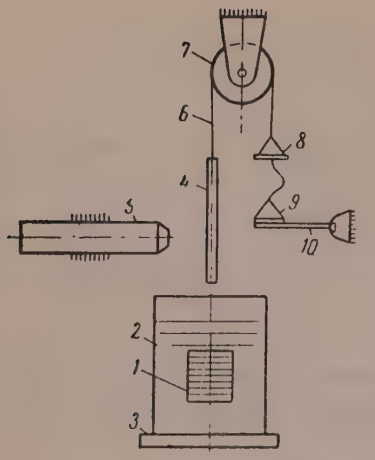


Fig. 1. Apparatus for studying the structural-mechanical properties of foam.

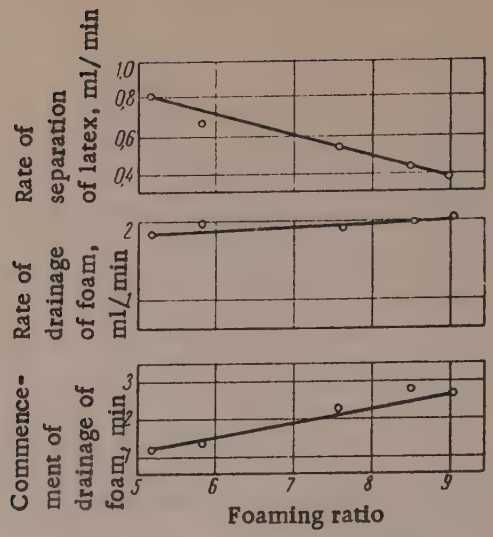


Fig. 2. Dependence of the properties of a 47% latex foam on its foaming ratio.

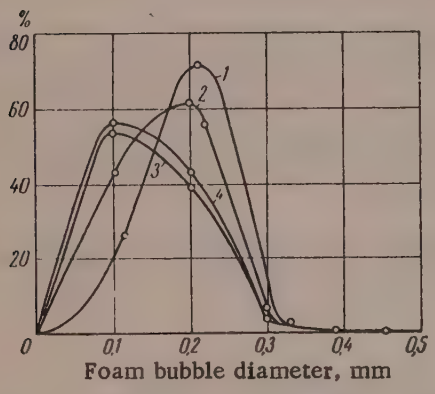


Fig. 3. Bubble diameter distribution curves for foams made from latexes of different viscosities (centipoise): 1) 7.3; 2) 12.8; 3,4) 59.

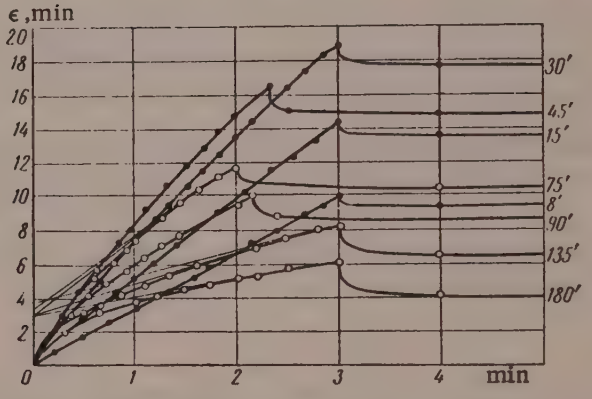


Fig. 4. Kinetic deformation curves of foam made from latex having a viscosity of 59 centipoise.

Subsequently (after 75-180 min), a section corresponding to elastic deformation becomes increasingly more distinct on the curves, and a reduction in residual deformation is observed, i.e., the foam assumes properties characteristic of structured systems. The variation in the structural-mechanical properties of the foam can be seen clearly in Fig. 5 from the minimum of limit viscosity calculated from the experimental curves of Fig. 4 in accordance with the equation

$$\eta = \frac{P - P_k}{d\varepsilon / d\tau},$$

where P is the applied stress (dyne/cm^2), P_k is the elastic limit (in view of its low value for latex foam, P_k was ignored in the calculations), and $d\epsilon/d\tau$ is the rate of relative deformation [4].

Figure 6 shows that a similar relationship is found for foams made from latex of lower viscosity.

Mechanically produced latex foams differ from pneumatic foams [2], principally in their much lower foaming ratio [K]. For pneumatic foams, K is 70-100, while for mechanical foams it is usually 3-10. The foaming ratio determines a number of properties of the foam, including the mechanism of its destruction. In typical foams of high-foaming ratio, consisting of structured systems, destruction sets in as the result of the rupture of the thin

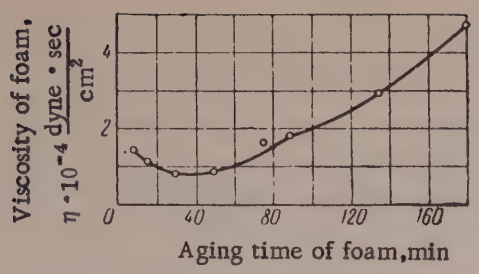


Fig. 5. Dependence of limit viscosity of a foam on its aging time. η_{lat} = 59 centipoise.

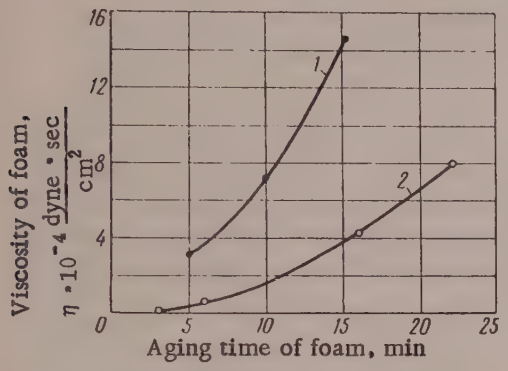


Fig. 6. Dependence of limit viscosity of a foam on its aging time. η_{lat} = 7.4 (2) and 12.8 (1) centipoise.

films. The stability of such foams is determined mainly by the strength of the films. In latex foams of low-foaming ratio, the laminas of dispersion medium between the air bubbles are large, and it may be assumed that these laminas retain their liquid properties to a considerable extent. Such foams may be regarded as dilute emulsions, and their destruction takes place by separation of the disperse phase and the dispersion medium. The rate of this process, i.e., the speed of movement of the particles of the disperse phase, ought to obey Stokes law. It follows from this that the stability of foams of low-foaming ratio ought to depend on the degree of dispersion of the foams, i.e., the diameter of the bubbles, the difference in the densities of air, and the foamed liquid, and the viscosity of the latter. The results we have obtained show that such a relationship can evidently occur only in foams of very low concentration ($K \leq 1$). With increase in the foaming ratio, movement of the bubbles in the foam becomes difficult, and latex separation diminishes (Fig. 2).

Table 3 shows that the viscosity of the latex has the greatest influence on the resistance of the foam to latex separation, this influence being greater than that required by Stokes' law. It is possible that this is due to the fact that latex has a structural viscosity. The reduction in the mean size of the foam bubbles with increase in viscosity of the latex is also indirect evidence of its influence on the resistance of the foam to separation. In addition, there is no doubt that an increase in viscosity of the latex leads to an increase in the strength of the films of the foam, and increases its resistance to destruction. The destruction of air bubbles on the surface of the foam has not been observed in practice. Thus, the viscosity of the latex is a decisive factor in the stability of a latex foam of low-foaming ratio.

The surface tension of the latex has no appreciable influence on the stability of the foam, provided it is low enough (<40 dyne /cm).

The three criteria of the stability of foam: τ, v_1, and v_2, vary correlatively with variation in the properties of the latex, the separation of the latex from the foam commencing simultaneously with the draining of the latter. This is in agreement with the results of a study of the structural-mechanical properties of the foam in its aging process. At first, there is a reduction in viscosity of the foam, which may be due to the establishment of equilibrium in the system after the removal of the mechanical field of force produced by the high-speed agitator. Then, after passing through a minimum, the viscosity increases. Minimum viscosity of the foam corresponds, according to time, to τ. Since the separation of the latex occurs simultaneously, the foaming ratio is increased, in consequence of which the foam acquires elastic properties.

In the practical production of sponge rubber from latexes, it is important for separation of the latex from the foam to commence a definite time after its production. It follows from the foregoing that the value of τ may be used for assessing this property.

SUMMARY

1. A study has been made of the dependence of the properties of latex foams of low-foaming ratio (dispersion, stability, structural-mechanical properties) on the concentration, viscosity, and surface tension of the latex.

2. The criterion of the stability of latex foams of low-foaming ratio is τ, the time to the commencement of latex separation from the foam. The fundamental factor in the determination of the stability τ is the viscosity of the latex. As the viscosity of the latex increases, its stability also increases.

3. In the aging process, latex foams of low-foaming ratio pass from the viscous-flowing to the structured state. The viscosity of the foams passes through a minimum.

LITERATURE CITED

1. R. Noble, Latex in Industry (New York, 1953).
2. D. M. Sandomirskii and A. Korotkova, Kolloid. Zhur. 21, 679 (1959).
3. S. Ya. Veiler and P. A. Rebinder, Doklady Akad. Nauk SSSR 49, 354 (1945).
4. E. E. Segalova and P. A. Rebinder, Kolloid. Zhur. 10, 223 (1948); E. E. Segalova, P. A. Rebinder and L. N. Setryukhina, Kolloid. Zhur. 13, 461 (1951).

MOLECULAR ADSORPTION OF CERTAIN AROMATIC ACIDS ON ION EXCHANGE RESINS

O. R. Skorokhod and L. M. Sergeeva

V. I. Lenin Belorussian University, Minsk

Translated from Kolloidnyi Zhurnal, Vol. 23, No. 1, pp. 100-105, January-February, 1961
Original article submitted September 8, 1959

The chromatographic separation of various kinds of compounds, particularly organic acids, frequently makes it possible to solve problems which could not have been solved by ordinary chemical methods. A rational utilization of the method requires that one know the adsorption characteristics of various adsorbents with regard to the individual compounds. The largest amount of quantitative data has been accumulated for the adsorption of organic acids on activated charcoal. It has recently been discovered [1] that certain ion-exchange resins will selectively adsorb certain organic acids from solution. However, as has already been pointed out [2], relatively little work has been done on the molecular adsorption of weak organic acids on ion-exchange resins. The accumulation of experimental data dealing with these properties is of certain theoretical value, and can also be of some use in the design of several technological processes.

TABLE 1

Exchange Capacity of Ion Exchange Resins

Ion-exchange resin	Exchange capacity,	
	with NaCl	with NaOH
Sulfonated coal	0.75	3.28
KU-1	1.63	4.40
KU-2	3.84	4.08

We are going to present in this paper the results of an investigation concerning the molecular adsorption of four aromatic acids on several ion-exchange resins made in the USSR. The following adsorbers were examined: cation exchange resins KU-1 in the H- and NH_4-forms, and KU-2 in the H-form; sulfonated coal in the H-, NH_4-, Ca-, and Fe-forms; and the anion exchange resin ÉDÉ-10 in the Cl- and OH-forms. The treatment of the cation-exchange resin and anion-exchange resin with an 0.2 N solution of HCl in a chromatographic column converted them into the H- and Cl-forms, respectively; similarly, treatment of the cation-exchange resin with 0.2 N NH_4Cl, 0.2 N $CaCl_2$, and 0.2 N $FeCl_3$, converted it, respectively, into the NH_4, Ca, and Fe forms. Once the resins were converted into the desired forms, they were thoroughly washed with twice-distilled water, and dried at room temperature to a constant weight. We worked with 0.25-0.50 mm fractions.

The recorded characteristics of these ion-exchange resins are presented in Table 1.

The determination of exchange capacities has been described by Vainshedt [3].

As is well known [4], the ion-exchange resins listed above are all polyfunctional acids, which is also confirmed by the fact that the exchange capacity varies with pH.

After placing 100 mg of the ion-exchange resin in a glass beaker, we added to it 20 ml of an aqueous solution (of known concentration) of the acid under investigation. Equilibrium was achieved by shaking the mixture for 2 hrs and allowing it to stand for 20 hrs. The equilibrated solution was analyzed acidimetrically. The amount of material adsorbed was then computed from the formula

$$A = \frac{(c_0 - c)V}{m}, \text{ mmole/g},$$

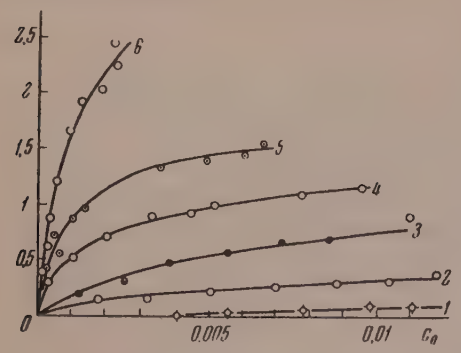


Fig. 1. Adsorption isotherms of salicylic and anthranilic acids on ion-exchange resins in the H form: 1) salicylic acid on KU-2; 2) the same on KU-1; 3) the same on sulfonated coal; 4) anthranilic acid on sulfonated coal; 5) the same on KU-1; 6) the same on KU-2.

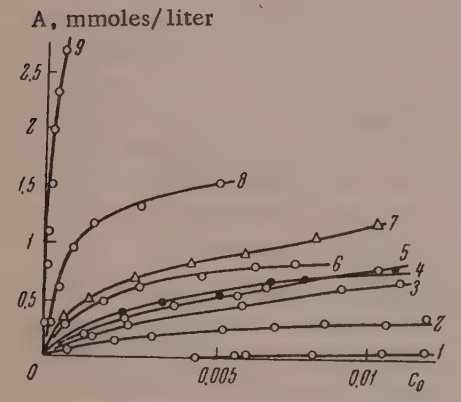


Fig. 2. Adsorption isotherms of salicylic acid on ion-exchange resins in various forms: 1) KU-2 in the H form; 2) KU-1 in the H form; 3) sulfonated coal in the Fe form; 4) KU-1 in the NH_4 form; 5) sulfonated coal in the Ca form; 6) sulfonated coal in the H form; 7) sulfonated coal in the NH_4 form; 8) ÉDÉ-10 in the Cl form; 9) ÉDÉ-10 in the OH form.

where V is the volume of solution (ml), C_0 is the initial acid concentration, c is the equilibrium acid concentration, and m is the amount of ion-exchange resin (g).

We investigated the adsorption of benzoic, salicylic, o-aminobenzoic, and p-aminobenzoic acids on the resins enumerated above. The resulting adsorption isotherms had the usual shape: the amount of adsorption increased with acid concentration. Similar adsorption isotherms were obtained for these acids on activated charcoal [5]. In many cases, even at the concentrations studied by us, limiting adsorption could be attained. In Fig. 1 we have reproduced the adsorption isotherms of salicylic and anthranilic acids on sulfonated coal, KU-1, and KU-2 resins, all in the H form. Benzoic and p-aminobenzoic acids yield similar curves, except that the isotherm of the latter lies somewhat above that for the anthranilic acid. We would like to point out that, in certain cases, particularly with the sulfonated coal and the KU-1 resin in the H and NH_4 forms, the adsorption isotherms of benzoic acid rise smoothly at low equilibrium concentrations, but above a concentration of about 0.007 moles/liter the curve suddenly undergoes a sharp rise.

One can safely assume that the observed adsorption of our acids on the enumerated ion-exchange resins involves a simple intermolecular interaction (van der Waals adsorption). The following experimental results tend to confirm this assumption. In the case of salicylic acid, the equilibrated solution was analyzed by two independent methods: by titration with barium hydroxide to a phenolpthalein endpoint and photocolorimetrically, by determining the optical density of ferric salicylate. Both methods yielded identical results, indicating that the ion-exchange resins adsorbed equivalent quantities of both the H^+ and the salicylate ion; or, in other words, the entire salicylic acid molecule is adsorbed. In addition to this, if ionic exchange were taking place, then an equivalent amount of metal ions would have to be released by a cation-exchange resin (in the Me form) into the equilibrated solution. Attempts to detect the NH_4^+ ion in an equilibrated solution in contact with the cation exchange resins in the NH_4 form were unsuccessful (KOH and $K_2[HgI_4]$ were used); likewise, no Ca^{++} could be detected {by means of $(NH_4)_2C_2O_4$, $K_4[Fe(CN)_6]$} in the case of sulfonated coal in the Ca form or Fe^{+++} in the case of sulfonated coal in the Fe form [$K_4Fe(CN)_6$, salicylic acid, and KCNS were used].

The specific surface, and the exchange capacity (which is a measure of the number of active groups), increases in the order: sulfonated coal < KU-1 < KU-2. The adsorption of o- and p-aminobenzoic acids increases in the same order. On the other hand, the adsorption of salicylic and benzoic acids increases in a reverse order. The observed behavior of ion-exchange resins apparently depends on the relationship between the reactive groups of the resin and the individual acids. The basic nature of the amino group in the aminobenzoic acids promotes the adsorption of these acids on ion-exchange resins containing a large number of strongly acidic groups (in our case, KU-2, which has an exchange capacity of 3.84 in a neutral medium, while the sulfonated coal has a capacity of only 0.75). In such cases, there is presumably extensive hydrogen bonding between the ion-exchange resin and the nitrogen of the amino acid.

The data clearly indicate that the KU-2 ion-exchange resin is more suitable for extracting amino acids than is the sulfonated coal. When the labile hydrogen on the ion-exchange resin is replaced by a metal ion, the

TABLE 2

Selectivity Coefficient of Anthranilic Acid on Various Ion-Exchange Resins

Ion-exchange resin	Resin conc., moles/liter	
	0.004	0.002
	selectivity coefficient	
KU-2 in H form	78.2	–
NH_4 form of sulfonated coal	19.7	9.0
Ca form of the same	3.2	3.1
H form of the same	2.7	1.7
Fe form of the same	1.7	0.5

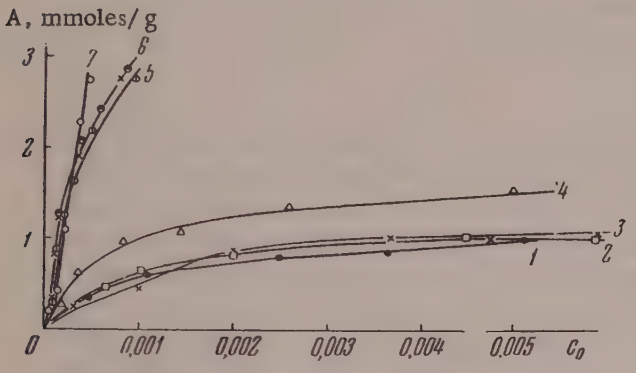


Fig. 3. Adsorption isotherms of aromatic acids on an ÉDÉ-10 anion-exchange resin: 1) benzoic acid on ÉDÉ-10 in the Cl form; 2) p- and o-aminobenzoic acid on ÉDÉ-10 in the Cl form; 3) salicylic acid on ÉDÉ-10 in the Cl form; 4) benzoic acid; 5) anthranilic acid; 6) p-aminobenzoic acid; 7) salicylic acid. Nos. 4-7 were on ÉDÉ-10 in the OH form.

adsorption of aromatic acids becomes quite different. This can be readily seen by comparing the adsorption isotherms of salicylic acid on ion-exchange resins in various metal forms (Fig. 2). When the adsorption isotherms of salicylic acid on sulfonated coal and on KU-1 in the H form are compared with the corresponding curves obtained on the same exchangers in the NH_4 form, it is perfectly obvious that salicylic acid is adsorbed much better on the NH_4 forms. Benzoic acid behaved likewise. However, the form of the ion-exchange resin (H or NH_4) has very little effect on the adsorption of aminobenzoic acids.

If we analyze the adsorption on various Me forms of ion-exchange resins to see how the cation charge influences the adsorption, we can see that the adsorption of salicylic acid on various forms of sulfonated coal increases in the order: Fe form < < Ca form < NH_4 form; hence, the molecule adsorption decreases with increasing charge of the cation.

The adsorption isotherms of our acids on the ÉDÉ-10 anion-exchange resin in the Cl and the OH form are presented in Fig. 3. The figure shows that the acids are adsorbed much better on the ÉDÉ-10 resin than they are on either of the two cation-exchange resins. At the same time, the OH form of the EDÉ-10 resin is a better adsorber than the Cl form. This may possibly be due to an acid–base interaction between the OH group of the resin and the carboxyl groups on the acids.

An examination of our adsorption isotherms reveals that the adsorption in the investigated systems is highly selective, since various acids exhibit varying degrees of adsorption on any one of the investigated ion-exchange resins. Hence, it may be possible to use these ion-exchange resins for separating mixtures of such acids.

We decided to try and separate a mixture of salicylic and anthranilic acids chromatographically by using one of the above-discussed ion-exchange resins. In order to choose the best adsorbent, we have to know the selectivity of various ion-exchange resins with respect to these acids. To get an idea of how selective is the adsorption on various resins, we investigated the relative distribution of salicylic and anthranilic acids between the adsorbent and the mixture after equilibrium is established (under static conditions). In Fig. 4 we have reproduced the distribution curves for anthranilic acid; we have plotted the mole fraction of the acid in the equilibrium solution (N_s) against the mole fraction of the same acid in the adsorber (N_a). As a rule, the adsorption phase becomes enriched in the more readily adsorbed component, which, on cation-exchange resins, is the anthranilic acid and salicylic acid on anion-exchange resins. Only in the case of sulfonated coal in the H form in the concentration range 0.0005-0.001 moles/g, and sulfonated coal in the NH_4 form at concentrations from 0.0003-0.0005 moles/g is the adsorption of salicylic acid favored by the exchanger, but at high anthranilic acid concentrations the cation-exchange resins will, of course, contain predominantly the latter.

We would like to point out that, on any particular ion-exchange resin, the selectivity is not the same for various Me forms; in the case of sulfonated coal, the selective adsorption of anthranilic acid increases in the order: Fe form < Ca form < NH_4 form. Hence, the adsorption of anthranilic acid is most favorable when the sulfonated coal is in the NH_4 form. This is even more apparent when the selectivity coefficients (K_s) are compared (Table 2).

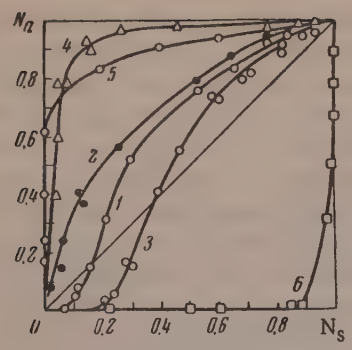


Fig. 4. Anthranilic acid distribution between a mixture with salicylic acid and the following ion-exchange resins: 1) sulfonated coal in the H form; 2) sulfonated coal in the Ca form; 3) sulfonated coal in the Fe form; 4) KU-2 in the H form; 5) sulfonated coal in the NH_4 form; 6) ÉDÉ-10 in the Cl form.

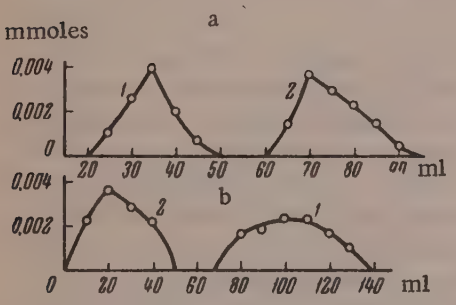


Fig. 5. Elution curves from a KU-2 ion exchange resin in the H form: 1) salicylic acid; 2) anthranilic acid.

The selectivity coefficient of anthranilic acid on the NH_4 form of sulfonated coal is almost 7.3 times as large as K_s on the H form of sulfonated coal. Figure 4 and Table 2 illustrate very clearly how the selectivity depends on the nature of the adsorber. If we compare the H forms of sulfonated coal and of KU-2, we can see that the K_s is almost 29 times greater on the latter. Of all the investigated resins, KU-2 yields the most divergent set of adsorption isotherms for the anthranilic and salicylic acids (individually determined); hence, the adsorption isotherms of pure acids also indicate that selective adsorption of the two acids should be most favorable on the KU-2 resin.

The adsorption data obtained under static conditions clearly indicate that, of the investigated ion-exchange resins, KU-2 in the H form should be most suitable for the separation of a mixture of anthranilic and salicylic acids. And we therefore selected this cation-exchange resin in our attempt to separate the two components of a real mixture of salicylic and anthranilic acids.

The separation was achieved by means of elution chromatography in a colum 35 cm long and 0.7 cm wide. The column was filled with 1.5-2 g of preswelled ion-exchange resin and a mixture of anthranilic and salicylic acids of known composition was introduced. Distilled water, aqueous solutions of dioxane, and aqueous sodium chloride solutions were used as eluents. The elution rate was 5-6 drops per minute. From our experimental results we constructed elution curves by plotting the amount of eluted acid against the volume of solution passed through the column. In Fig. 5a we have reproduced the elution curve for a mixture of anthranilic and salicylic acids adsorbed on the KU-2 cation-exchange resin in the H form. The figure clearly illustrates that salicylic acid can be eluted quantitatively with distilled water while anthranilic acid can be likewise eluted with 10% aqueous dioxane. The same mixture can be separated successfully on the ÉDÉ-10 anion-exchange resin in the Cl form (Fig. 5b). Though the distribution curve for the two acids (Fig. 4, Curve 6) does indicate good selectivity, in our case the selective adsorption of salicylic acid was so good that the distribution curve for the anthranilic acid lies well below the equilibrium distribution curve. Hence, one would expect the anthranilic acid to be eluted first from the anion-exchange resin, since it is less strongly bonded to the resin than is salicylic acid. And, indeed, elution with 5% aqueous dioxane recovers only the anthranilic acid, while salicylic acid has to be eluted with 0.2 N aqueous sodium chloride.

In this manner, we have been able to achieve a complete separation of a mixture of salicylic and anthranilic acids by means of a KU-2 cation-exchange resin and an ÉDÉ-10 anion-exchange resin; the feasibility of such a separation was predicted from a study of the adsorption isotherms of individual acids and from distribution curves obtained under equilibrium conditions in such mixtures. Elution chromatography in a column under flow conditions permits a complete separation of two aromatic acids from a mixture.

SUMMARY

1. The adsorption isotherms of benzoic, salicylic, o-aminobenzoic, and p-aminobenzoic acids on KU-1, KU-2, and sulfonated coal cation-exchange resins, and on an ÉDÉ-10 anion-exchange resin, have been recorded. The effect of the resin species on selective adsorption was investigated. The ÉDÉ-10 anion-exchange resin adsorbs aromatic acids much better than the cation-exchange resins do. The adsorptivity of aminobenzoic acids increases in the order: sulfonated coal < KU-1 < KU-2 < ÉDÉ-10. The effects of various Me forms on selective adsorption were examined.

2. A mixture of salicylic and anthranilic acids was separated into the component acids by means of elution chromatography on a KU-2 cation-exchange resin and an EDE-10 anion-exchange resin.

LITERATURE CITED

1. C. W. Davies and G. G. Thomas, J. Chem. Soc. 2624 (1951).
2. S. L. Bafna and K. P. Gowindan, Industr. and Engng. Chem. 48, No. 2, 310 (1956).
3. A. A. Vainshedt, A. A. Vasil'ev, and O. I. Okhrimenko, Ion Exchange Materials in Theory and Practice [in Russian] (Izd. AN SSSR, Moscow, 1955) p. 110.
4. K. M. Saldadze and Z. G. Demonterik, Studies in the Field of Ion Exchange Chromatography [in Russian] (Izd. AN SSSR, Moscow, 1957) p. 106.
5. O. R. Skorokhod, N. F. Ermolenko, and N. I. Lukomskaya, Ucheb. Zap. Belorus. Universiteta im. V. I. Lenin No. 42, Ser. Khim. (1958) p. 159.

RELATION BETWEEN DYNAMIC STABILITY OF DROPLETS AND CRITICAL VAPOR SUPERSATURATION DURING CONDENSATION

V. P. Skripov

S. M. Kirov Ural Polytechnic Institute, Sverdlovsk
Translated from Kolloidnyi Zhurnal, Vol. 23, No. 1, pp. 106-111, January-February, 1961
Original article submitted July 9, 1959

1. Considering a liquid droplet in a liquid or gaseous phase different from itself, the question arises as to the stability of the droplet. In the framework of phenomenological thermodynamics, this question is resolved by varying a suitable potential, such as the free energy, and examining the limiting conditions. For a drop of pure liquid of radius r, surrounded by saturated vapor, the condition is given by Thomson's formula:

$$\frac{p_r}{p_\infty} = \exp\left[\frac{2\sigma V_L}{rRT}\right], \quad (1)$$

where p_∞ is the pressure of saturated vapor at temperature T over the plane boundary of the region; p_r is the equilibrium pressure over the spherical drop of radius r; σ is the surface tension; V_L is the molar volume of the liquid; and R is the universal gas constant. Thomson's formula is derived for the case that the equation of state of an ideal gas is applicable to the vapor. For small values of supersaturation, instead of Eq. (1), we can use the equivalent relation from [1],

$$\frac{p_r}{p_\infty} = 1 + \frac{2\sigma}{\left(\frac{V_n}{V_L} - 1\right) p_\infty r}, \quad (2)$$

which is free from the above assumption. In Eqs. (1) and (2), the dependence of the surface tension on the curvature of the surface is not taken into account. The equilibrium, determined by the formulas given, is unstable, since it corresponds, not with a minimum, but with a maximum of the thermodynamic potential. This is brought about by the contribution of the surface energy of the system, which plays the role of an energy barrier in the initial stage of the phase transition.

There is another essential side of the question of the stability of the drop, namely, its stability toward disturbances from thermal motion, i.e., its dynamic stability. If the surface energy of the drop σS is comparable with the mean energy of thermal motion kT, then the value of the thermal disturbances will be sufficient for spontaneous dispersion of the drop by fission. Volmer [2] has used the spontaneous dispersion condition ($\sigma S \approx kT$) to explain the properties of lyophilic colloids. However, up to the present time, the question of the role of the dynamic stability of the disperse phase has not been sufficiently developed. More fruitful results have been obtained in nuclear physics (with the aid of the liquid-drop model of the nucleus) than in molecular physics, which has to do with ordinary drops of ordinary liquids.

The dynamic stability of the droplet does not always turn out to be the essential feature of the phenomenon. In a number of cases, the determining value is given by the law of the stationary distribution of droplets according to dimensions, but not by their mean lifetime. However, the stability of the disperse formations can have a marked influence on the kinetic properties of the system (viscosity, heat, and electrical conductivity), and it can determine the initial stage of phase transformation in the absence of ready made centers of the new phase. The spontaneously formed seed is capable of life only in case it is not destroyed by thermal motion the moment it appears, and during the lifetime of the initial state it succeeds in growing enough to increase its stability

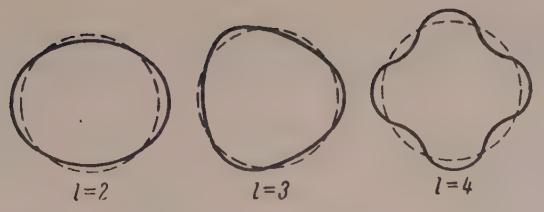


Fig. 1.

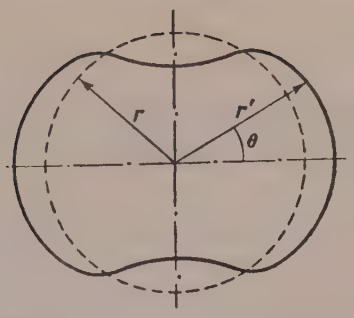


Fig. 2.

appreciably. We are trying to develop this point of view with supersaturated vapor, and we want to show that the idea of a connection between the stability of seed droplets and critical supersaturation leads to the well-known Volmer – Farkash formula for the critical supersaturation value.

2. A liquid droplet can be considered as a Brownian particle, and to each degree of freedom of its motion the mean energy $\frac{1}{2}kT$ can be assigned for the translational and rotational energy, and kT for the vibrational energy. The stability of the drop is determined largely by its internal vibrational degrees of freedom. These vibrations, to a first approximation, correspond with the capillary vibrations of an uncompressed liquid. They are accompanied by a periodic increase in drop energy, as a result of increasing the surface. Under favorable circumstances (small r and σ), the mean amplitude of the vibrations reaches such a large value that the drop decomposes, for example, into two drops of smaller dimensions. If this happens, the drops formed in the decomposition will be all the more unstable, and the process of atomization proceeds apace.

The problem of the capillary vibrations of a spherical drop of uncompressed liquid has been solved for small vibrations [3,4]. With axial symmetry, the spectrum of characteristic frequencies is given by the expression:

$$\nu^2 = \frac{\sigma}{(2\pi)^2 \rho r^3} l(l-1)(l+2), \tag{3}$$

where ρ is the density of the liquid, l is a positive integer, determining the type of vibration, and the degeneracy is $q = 2l + 1$. The case $l = 0$ corresponds with a radial vibration, $l = 1$ corresponds with a displacement of the drop as a whole. The characteristic deformations for $l = 2$, $l = 3$, and $l = 4$ are illustrated in Fig. 1. The minimum characteristic frequency of vibration of the drop is equal to:

$$\nu = \frac{1}{2\pi}\sqrt{\frac{8\sigma}{\rho r^3}}. \tag{4}$$

We shall now formulate the problem of the dynamic stability* of a drop of radius r, relative to its decomposition into two identical daughter drops. We introduce the transformation $\xi = r - r'$, where $r' = r'(\theta)$ is the modulus of the radius vector of the deformed drop in the plane of principal section (Fig. 2). For symmetric deformations, the function may be expanded in a series of Legendre polynomials $P_l(\cos\theta)$:

$$\xi = r - r' = -\alpha_2 P_2(\cos\theta) - \alpha_3 P(\cos\theta) - \alpha_4 P(\cos\theta) - \ldots, \tag{5}$$

where the α_l are deformation parameters which play the role of normal coordinates in the case of small vibrations. The drop deformation given by Eq. (5) represents, for every moment of time, a superposition of the disturbances produced by the set of independent vibrations. The drop disintegration, which we are interested in, begins with a narrow necking down in the middle of the drop [$r'(\pi/2) \approx 0$], and is determined by the mean value of the variable ξ for $\theta = \pi/2$. At this value of the angle, after the fashion of Legendre polynomials, all the odd terms in Eq. (5) go to zero, leaving the sum:

* The term "dynamic stability" does not reflect the source of the disturbance, in relation to which the degree of stability of the drop is being determined. From this point of view, preference should be given to the term "Brownian stability," i.e., the stability toward Brownian thermal motion.

$$\xi = -\frac{1}{2}\alpha_2 - \frac{3}{8}\alpha_4 + \frac{5}{16}\alpha_6 - \ldots$$

$$\ldots, -(-1)^{l/2}\frac{1\cdot 3\cdot 5\cdots(l-1)}{2\cdot 4\cdot 6\cdots l}\alpha_l.$$

The capillary vibrations of the drop, which we are considering, are essentially a form of thermal motion. Therefore, for a set of given conditions (δ, r, T) the mean value of the deformation $\xi(\theta = \pi/2)$ has the perfectly definite value

$$\bar{\xi} = \sum_{(l)} -(-1)^{l/2}\frac{1\cdot 3\cdot 5\cdots(l-1)}{2\cdot 4\cdot 6\cdots l}\bar{\alpha}_l, \tag{6}$$

depending upon the mean values of the parameters α_l. In turn, $\bar{\alpha}_l$ may be found with the help of the equipartition of energy theorem for degrees of freedom. Designate by $\Delta_l S = f(\alpha_l, r)$ the increase in surface of the drop, produced by the vibrations of order l. This gives the following equations:

$$\sigma\overline{\Delta_l S} = kT, \quad l = 2, 4, 6, \ldots \tag{7}$$

Solving for $\bar{\alpha}_l$, and substituting the values in Eq. (6), we get

$$\bar{\xi} = F(T, \sigma, r). \tag{8}$$

Splitting in two of the drop, for given T and σ, occurs at a value of $r = r^*$, for which $\bar{\xi} \approx r^*$. After substituting $r = r^*$ and $\bar{\xi} = r^*$ in Eq. (8), we have:

$$r^* = F(T, \sigma, r^*),$$

from which

$$r^* = \Phi(T, \sigma). \tag{9}$$

At $r \approx r^*$, the drop is dynamically unstable, and should decompose rapidly. The difficulty in carrying out the calculations according to the above scheme resides in the fact that the vibrations that interest us are not small. If, however, the theory of small vibrations is used as a rough approximation, direct calculations lead to the following dependence of the critical radius on the temperature and surface tension:

$$r^* = A\sqrt{T/\sigma}, \tag{10}$$

where A is a dimensional coefficient which is the sum of the finite, alternating, numerically decreasing series.

Equation (10) may be derived from simpler considerations [5]. We introduce formally the number of effective vibrational degrees of freedom n, which essentially determine the stability of the drop to division into two parts. Using the law of the equipartition of energy among degrees of freedom, we express the mean energy of the vibrations in the form nkT. When the mean vibrational energy becomes comparable with the increase in surface energy for fission of the drop, the probability of such a fission rises sharply. The limit of dynamic stability is fixed by the equation:

$$\sigma\Delta S(r^*) = nkT, \tag{11}$$

where $\Delta S(r^*) = 0.26\,S(r^*) = 0.26 \cdot 4\pi r^{*2}$ is the increase of surface on formation of two identical drops of the same density from the original drop. From Eq. (11) we find:

$$r^* = 0{,}65 \cdot 10^{-8}\sqrt{n} \cdot \sqrt{T/\sigma},$$

i.e., we come back to Eq. (1), where $A = 0.65\sqrt{n \cdot 10^{-8}}\ (\text{erg/deg})^{\frac{1}{2}}$.

The mean lifetime of the drop τ, inversely proportional to the decomposition probability, may be evaluated from the period τ_0 of the fundamental vibrations of the drop, and the value of the fission-energy barrier $E = \sigma\Delta S = 0.26\sigma S$; thus:

$$\tau = \text{const} \cdot \tau_0 \exp(E/kT). \tag{12}$$

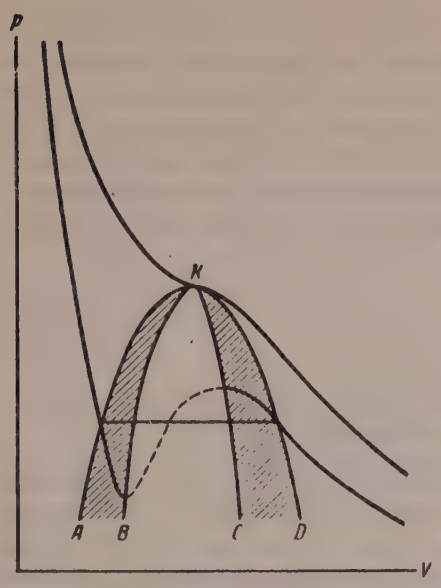


Fig. 3.

The drops of critical radii for different liquids, or for one liquid at different temperatures, have different lifetimes, but from Eqs. (11) and (12), they all have the same ratio of $\tau/\tau_0 = \text{const} \cdot \exp(n)$, i.e., approximately the same mean number of vibrations from the moment of appearance of the drop to the moment of disintegration.

3. We shall now consider the question of the free condensation of a vapor, from the point of view of the stability of small drops. It is known from experiment that, in the absence in the system of artificial centers of formation of the liquid phase, condensation of a vapor may be brought about by adiabatic expansion, or by isothermal compression up to the point where a definite critical supersaturation $S^* = p^*/p_\infty$ is reached, which depends upon the temperature and nature of the liquid. In this case, the condensation starts on spontaneously formed droplets of some radius r^*. The values S^* and r^* are connected through Eq. (1) or (2). If there is no criterion for finding r^* explicitly, then the dependence of the critical supersaturation on the temperature is not sufficiently determined.* We shall start with the requirement of dynamic stability of the seed drops. This is equivalent to the assertion that the critical supersaturation of the vapor is determined by the ability of the seeds to maintain their existence in the face of the Brownian motion, account being taken of the internal vibrational degrees of freedom. The droplets with radii $r < r^*$ have too small a lifetime to become condensation centers. On the other hand, the probability of spontaneous appearance of droplets decreases rapidly with increasing r. Therefore, the condensation proceeds, basically, on drops which are near the critical dimension $r^* = A\sqrt{T/\sigma}$. Substituting this value of r^* in the preceding formula, we have:

$$S^* = \frac{p^*}{p_\infty} = \exp\left[BV_L\left(\frac{\sigma}{T}\right)^{3/2}\right], \qquad (13)$$

where $B = 2/RA$ is a constant, independent of the nature of the liquid. Equation (13) agrees with the expression for the critical supersaturation found by Farkash, on the basis of Volmer's ideas [7]. Farkash considered the kinetics of the evaporation and condensation process on the surface of a seed drop, taking account of its formation probability. The value of the critical radius was found from the condition $Z(r^*) = 1$, where $Z(r)$ is the number of seed drops of radius r formed per cm^3 per second. The coefficient B was a complicated function of many parameters. Without great error, it can be considered as a constant. The value of B was determined [8] from observations on the critical supersaturation of water vapor at $T = 264°K$, giving $B = 0.56\ (\text{deg/erg})^{3/2}\,\text{mole}$. Volmer and Flood [8] have shown that Eq. (13) is a good representation of the temperature dependence of the critical supersaturation of water, and that it gives correct values for six out of seven substances investigated.

Let us take the value of B from [8], and find the constant A along with the effective number of vibrational degrees of freedom of the drop n. This gives $A = 0.43 \cdot 10^{-7}\ (\text{erg/deg})^{\frac{1}{2}}$, and $n = 44$. We notice that each type of vibration is represented by several degrees of freedom.

Farkash and a number of other authors are investigating the development of the seed along the lines of a sequence of elementary condensation and evaporation events. This scheme reflects only one mechanism of the process, and is in need of amplification. For drops which are near the limit of dynamic stability, we have to take account of the possibility of spontaneous fission of a collective sort.

Supersaturation in the free condensation of a vapor not only insures the conditions for the growth of seed droplets, it favors the actual formation of the latter. Macroscopically, this shows up in the increase in compressibility of a vapor in the metastable-state region. This behavior of the compressibility is illustrated graphically by

*In this connection, an interesting thermodynamic criterion has been proposed by Shcherbakov [6]. This author considered the dependence of the surface tension of a drop on its radius, as well as the effect of the same factor on the saturation vapor pressure and the energy of formation of a seed. For a drop of critical dimensions, this energy is considered to be equal to zero.

the p – V diagram of a real gas, shown in Fig. 3. The region in which isothermic supersaturation is possible is bounded by the branches of the binodal (KD) and the spinodal (KC); K is the critical point for the liquid-vapor equilibrium. On the points of the spinodal (KC) $(\partial p/\partial V)_T = 0$; consequently, the compressibility approaches infinity. The curve of the pressures $p^* = p^*(T)$ for critical supersaturation lies inside the region CKD, near the spinodal (KC). On approaching the critical temperature, the value of $S^* = p^*/p_\infty$ decreases, with a limiting value of unity. This variation of S^* is reflected by Eq. (13), but it ceases to hold when the density of the liquid becomes comparable to the density of the vapor. In this case, the supersaturation condition should be found from Eq. (2), taking into account Eq. (10),

$$\frac{p^*}{p_\infty} = 1 + \frac{2\sigma^{3/2}}{A\left(\frac{V_{II}}{V_L} - 1\right)pT^{1/2}}. \qquad (14)$$

As $T \to T_K$, the second term on the right-hand side approaches zero, since the surface tension decreases much more rapidly than the difference between the specific volumes of vapor and liquid.

The critical radius of the seed drops increases with increasing temperature. From Eq. (10) this is connected fundamentally with the reduction in surface tension which is, in itself, a measure of the difference in molecular interaction in the coexisting phases. If $T \to T_K$, $r^* \to \infty$. This result means physically that, near the critical point, even the comparatively large seed droplets become unstable toward thermal fluctuation disturbances. The details of surface phenomena during phase transitions in the vicinity of the critical point have been investigated by Semenchenko [9].

SUMMARY

1. The question of the dynamic stability of small drops is considered from the standpoint of the deformations produced by the thermal motion of the system. Use is made of the approximate theory of the capillary vibrations of a spherical drop of incompressible liquid, and the equipartition of energy theorem for degrees of freedom. The expression obtained for the critical radius of the drop is: $r^* = A\ T/\sigma$.

2. Applying the dynamic stability criterion to the seed droplets in the supersaturated vapor leads to the well-known Volmer – Farkash critical supersaturation formula. This result is no accidental coincidence. It arises from the fact that the energy of formation of a seed, $W = \frac{1}{3}\sigma S$, derived by Gibbs, and used by Volmer, contains the same physical quantities which determine the dynamic stability of the drop.

LITERATURE CITED

1. Ya. I. Frenkel', Kinetic Theory of Liquids [in Russian] (AN SSSR Press, 1945).
2. M. Volmer, Z. Phys. Chem. 125, 151 (1927).
3. John William Strutt (Lord Rayleigh), Theory of Sound [Russian translation] (State Press for Technical and Theoretical Literature, Moscow, 1955) Vol. 2.
4. L. D. Landau and E. M. Lifshits, Mechanics of Continuous Media [in Russian] (State Press for Technical and Theoretical Literature, Moscow, 1953).
5. V. P. Skripov, Dissertation [in Russian] (Moscow Government University, 1953).
6. L. M. Shcherbakov, Kolloid. Zhur. 20, 759 (1958).
7. M. Volmer and A. Weber, Z. Phys. Chem. 119, 277 (1926).
8. M. Volmer and H. Flood, Z. Phys. Chem. 170, 273 (1934).
9. V. K. Semenchenko, Collection: Application of Supersonics to the Study of Matter [in Russian] (Izd. MOPI, 1956) No. 3.

THE SORPTION OF BINARY SOLUTIONS BY BUTADIENE-NITRILE COPOLYMERS

G. L. Starobinets and V. F. Tikavyi

V. I. Lenin Belorussian University, Chemical Faculty, Minsk
Translated from Kolloidnyi Zhurnal, Vol. 23, No. 1, pp. 112-117, January-February, 1961
Original article submitted July 1, 1959

Rubberlike high molecular weight polymers and copolymers are now acquiring widespread application as highly selective extracting agents and chromatographic sorbents [1]. They make possible, for example, extension of the method of distributive chromatography to such important materials as mixtures of hydrocarbons [2]. The intelligent application of rubberlike polymers to the solution of these problems demands a study of the sorptive properties of the materials.

One of the authors has undertaken a detailed study of the sorption of binary solutions, mainly of the type solvent–polar nonsolvent, by resins based on natural and butadiene rubbers [3]. The sorption potential of a component of the solution has been determined from the difference between the chemical potentials of this component in the polymer phase and in the solution phase, so that its value depends both on the nature of the solution and on that of the polymer. But, since the values of the specific cohesion energies of natural and butadiene rubbers lie close together [4], the most important effect in [3] was that of the thermodynamic properties of the solution on the sorption potentials of its components.

The question has so far not been examined of the effect of the nature of the polymer on the selective sorption of solutions. Now, however, the phenomenon of copolymerization opens up wide possibilities for the synthesis of polymers with predetermined values of the sorption potentials for the components of mixtures. It follows that the application of copolymers as extracting agents and chromatographic sorbents holds out considerable promise.

The object of the present work is the study of the sorptive properties of butadiene–nitrile copolymers.

The sorption properties of butadiene–nitrile copolymers containing 18, 26, and 40% of acrylonitrile have been investigated:

	Resin composition (parts by weight)
SKN	100
Sulfur	2
Stearic acid	1.5
Captax	1.5
Zinc oxide	5

Vulcanization was performed at 143° under a pressure of 3 atm, and for a period of 40 minutes.

Mixtures of two types were used as the binary systems: 1) a solvent* – polar nonsolvent system, the specific

*From now on the term "solvent" will be used for the component whose specific cohesion energy lies close to the specific cohesion energy of the polymer, while the term "nonsolvent" will be taken to apply to the component whose specific cohesion energy is significantly higher or lower than the specific cohesion energy of the polymer.

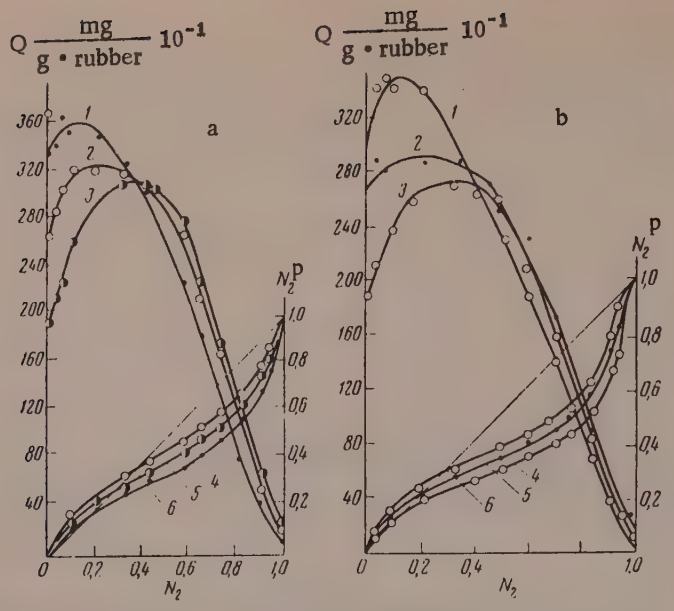


Fig. 1. Sorption of a benzene–methanol solution by butadiene–nitrile copolymers at a) 25° and b) 50°: 1), 2), and 3) curves for total sorption on SKN-18, SKN-26, and SKN-40; 4), 5), and 6) equilibrium curves for SKN-18, SKN-26, and SKN-40.

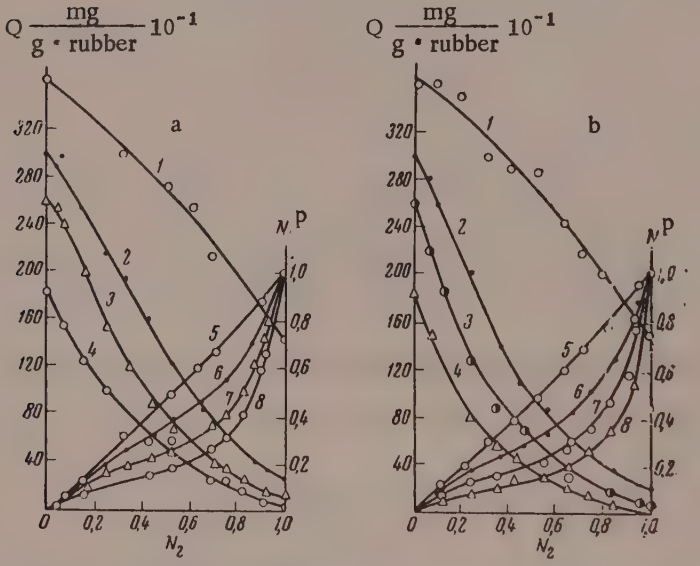


Fig. 2. Sorption of: a) benzene–hexane solutions, and b) benzene–nonane solutions by butadiene–nitrile copolymers and SKB: 1), 2), 3), and 4) curves for total sorption by SKB, SKN-18, SKN-26, and SKN-40; 5), 6), 7), and 8) equilibrium curves for SKB; SKN-18, SKN-26, and SKN-40.

Distribution Coefficient of Solvent (K_1) and Nonsolvent (K_2) Between Polymer and Solution

Nitrile content in copolymer, %	K_1	K_2	ψ_1, cal/mole	ψ_2, cal/mole	K_1	K_2	ψ_1, cal/mole	ψ_2, cal/mole
	Benzene-methanol $t = 25°$				Benzene-methanol $t = 50°$			
0	17,5	1,1	1705	57	10,0	1,3	1487	170
18	6,7	1,2	1133	108	5,0	1,4	1033	218
26	4,0	1,4	826	200	3,0	1,5	710	262
40	18,0	1,7	654	315	2,2	2,0	508	447
	Benzene-hexane $t = 25°$				Benzene-nonane $t = 25°$			
0	1,16	0,9	88	— 63	1,16	0,88	88	— 77
18	2,64	0,82	579	—117	2,80	0,72	613	—195
26	3,58	0,65	760	—258	5,2	0,59	982	—314
40	5,26	0,54	989	—368	6,7	0,42	1133	—855

cohesion energy of which was larger than with the polymer; and 2) a solvent – nonpolar nonsolvent system, the specific cohesion energy of which was less than with the polymer.* Systems of the first type include mixtures of aromatic hydrocarbons and aliphatic alcohols, while those of the second type include mixtures of aromatic hydrocarbons and aliphatic hydrocarbons.

The methods used for extracting the samples, for studying the general sorption isotherms and the partial sorption isotherms of the components, and for the interferometric analysis of the composition of the solution in the polymer phase during the investigation of the sorption of solutions of the solvent–polar nonsolvent type, has already been described [5]. Analysis of the composition of the solvent– polar nonsolvent binary system was performed by means of a refractometer of type IRF-23.

The experimental data obtained are shown for typical systems in Figs. 1-3, in the form of curves for the mole fraction of nonsolvent in the polymer phase (N_2^P), and mole fraction of nonsolvent in the equilibrium binary solution (N_2)** ; also, in the form of curves for the total sorption ($Q - N_2$) and curves for the partial sorption of the nonsolvent ($Q_2 - N_2$). The experiments were carried out in a water thermostat provided with a propeller stirrer and a contact thermometer. Temperature variation did not exceed ± 0.5°.

The initial slopes of the equilibrium curves were used to calculate the distribution coefficients of the components between the polymer phase and the solution phase:

$$K_1 = \left(\frac{dN_1^P}{dN_1}\right)_{N_1 \to 0}; \quad K_2 = \left(\frac{dN_2^P}{dN_2}\right)_{N_2 \to 0}.$$

The sorption potentials of the components were also calculated (in calories per mole):

$$\psi_1 = RT \ln K_1; \quad \psi_2 = RT \ln K_2.$$

The solvent–polar nonsolvent system. We shall consider as an example the data obtained for the benzene–methanol system at 25° and 50°.

It can be seen from Fig. 1a that increase in the nitrile content of the polymer brings about a reduction in the asymmetry of the equilibrium curve, which then approximates to a diagonal of the $N_2^P - N_2$ square, which corresponds to the case of equal distribution of the components between the polymer and solution phases. It follows that, with increase in the polarity (and so the cohesion energy) of the polymer, the selectiveness of the sorption of the solvent from the solvent–polar nonsolvent system is diminished.

* The values of the square roots of the specific cohesion energy ("solubility parameters") are: Buna rubber N, 9.5; benzene, 9.2; methyl alcohol, 14.5; hexane, 7.2 [6].

** These curves will, from this point, be called equilibrium curves.

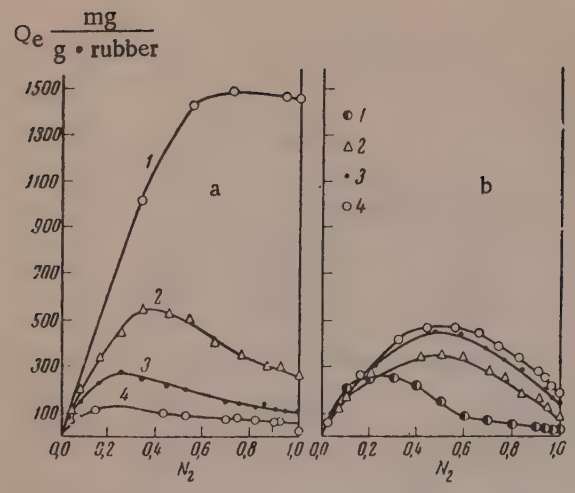


Fig. 3. Sorption isotherms for: a) hexane, and b) methane on butadiene–nitrile copolymers and SKB: 1), 2), 3), and 4) SKB, SKN-18, SKN-26, and SKN-40.

The selective sorption of the solvent, and the sharp asymmetry of the equilibrium curve, is explained by the supposition that the sorption potential of the solvent is appreciably greater than the sorption potential of the nonsolvent. The sorption of the nonsolvent is due to the interaction of its molecules with the polar groups (nitrile groups, double bonds, etc.) of the polymer. This interaction is apparently of a dipole–dipole nature, and cannot attain to high values. As far as the solvent is concerned, the loss of free energy in transition to the polymer from its infinitely dilute solution in the nonsolvent takes place owing to the abrupt increase in the configurational arrangement of the system. Consequently, the distribution coefficient of the solvent, and its sorption potential, depend on the elasticity of the polymer chains, while the latter diminishes in moving from butadiene rubber to a copolymer containing 40% nitrile (see table).

The distribution coefficient of the nonsolvent and the free energy of transfer to the polymer from the solution at infinite dilution in the solvent increase with increase in the nitrile group concentration in the copolymer. It can be seen from Fig. 1 that the analogy with the Konovalov Law and the Vrevskii Rule is well followed by the nitrile copolymers. The points of intersection of the equilibrium curves with the diagonal of the $N_2^P - N_2$ square (i.e., the points at which the composition of the solution in the polymer phase is the same as that of the equilibrium solution) correspond to maxima on the total sorption isotherms. Increase in temperature causes the maximum on the sorption isotherm to be shifted in the direction of the nonsolvent, i.e., in the direction of the component which possesses the higher value of the heat of evaporation. The reasons governing the existence of maxima on the sorption isotherms for the nonsolvent have been given in an earlier paper [3].

The solvent–nonpolar nonsolvent system. Figure 2 shows a clear expression of selective sorption of benzene from a system of the type solvent–aliphatic nonsolvent. A nitrile copolymer may therefore be used for the separation of a mixture of aromatic and aliphatic hydrocarbons. It is seen from Fig. 2, for example, that a resin based on SKN-40 contains 30 mole% of hexane and 70 mole% benzene when in equilibrium with a solution containing 75 mole% hexane and 25 mole% benzene. Thus, even at the first stage of the extraction, the polymer phase is greatly enriched in benzene. A multistage repetition of the process would produce complete separation of the components.

There is nothing unexpected in the fact itself, that selective sorption of one of the components of a system of the type aromatic hydrocarbon – aliphatic hydrocarbon can be performed, since a necessary condition of selective sorption from a binary solution is that its behavior should deviate from the law of ideal solutions [6]. Such a deviation does occur in the case under consideration, since the mixing of the components causes the destruction of the structure of the tightly packed, rod-shaped molecules of the aliphatic hydrocarbon, and the tightly packed benzene rings, and leads to the formation of a mixed structure. What was unexpected, however, was the converse result, that, when this takes place in the system benzene–aliphatic alcohols, the sorption potential of the benzene increases with increase in the concentration of nitrile groups in the copolymer (see table).

In order to elucidate the problem as to why the sorption potential of the solvent in systems of this type increases with increase in the potential barrier for the rotation of the chain lengths, we consider the systems polymer–polar nonsolvent, and polymer–nonpolar nonsolvent. Figure 3 gives the sorption isotherms for nonsolvents of both types by nitrile copolymers. The values of the sorption when $N_2 = 1$ correspond to the solubility of the individual nonsolvents in the polymers.

Figure 3 shows that, in the polymer–polar nonsolvent system the sorption of the nonsolvent increases with increase in the concentration of the nitrile groups, while in the polymer–nonpolar nonsolvent system the reverse condition is found.

Thus, in nitrile copolymer – aliphatic hydrocarbon systems, there is a clear tendency toward separation into two phases, which increases with increase in the concentration of nitrile groups in the copolymer. In the acetonitrile–methanol system [7], and, therefore, also in the nitrile copolymers which are capable of swelling in alcohols, positive deviation from ideal behavior is also found. In systems containing polar nonsolvents (Fig. 3), the tendency toward phase separation increases as we move from SKN-40 to butadiene rubber, while,in systems with nonpolar nonsolvent, the tendency to separate into two phases diminishes as we move from SKN-40 to the butadiene rubber. We must also note that the system with the greatest tendency to separate into two phases possesses the largest excess heat of formation, using the Scatchard terminology [8], and the least degree of thermodynamic irreversibility.

In the presence of solvent of the system, a polymer capable of swelling in the nonsolvent may increase its thermodynamic irreversibility through increase in the number of configurations between the chain lengths of the polymer and the molecules of the solvent. This tendency is most strongly expressed in the system with the greatest deviation from ideal behavior. In the case of the nonpolar nonsolvent, the system most capable of increase in thermodynamic irreversibility is the system made up of nonsolvent and the vulcanizate based on SKN-40; while, in the case of a polar nonsolvent, such a system is that made up of nonsolvent and the vulcanisate based on butadiene rubber (see table and Fig. 3). There is thus a direct contrast between the order of sorption potentials in systems in which polar and nonpolar nonsolvents participate.

Increase in the molecular weight of the nonsolvent is accompanied by increase in the tendency of the binary system to resolve itself into two phases, on the one hand, and increase in positive deviation from ideal behavior of the polymer–nonsolvent system on the other. These factors promote an increase in the tendency to a greater degree of thermodynamic irreversibility of the system, which is attained through a more intensive transfer of the solvent from the binary solution to the polymer phase. This, in its turn, leads to an increase in the sorption potential of benzene in line with the increase in the molecular weight of the nonpolar nonsolvent, as can be seen from Fig. 2 for the system polymer–benzene–nonane.

SUMMARY

1. The sorption of binary systems of the solvent–polar nonsolvent (benzene–aliphatic alcohols) type, and of the solvent–nonpolar nonsolvent (aromatic hydrocarbons–aliphatic hydrocarbons) type, has been studied on vulcanized butadiene–nitrile rubbers, containing 18, 26, and 40% acrylonitrile, respectively. The equilibrium curves between the polymers and the binary solutions have been considered, as well as the isotherms for total and partial sorption of the components of the solvent and nonsolvent. The distribution coefficients of the components between the polymer and solution phases have been determined, and the sorption potentials of the components have been calculated.

2. In all the systems studied, the solvent undergoes selective sorption. In systems containing polar nonsolvent, the sorption potential is diminished with increase in the concentration of nitrile groups in the polymer, while in those containing nonpolar nonsolvent the sorption potential of the solvent increases with increase in the concentration of nitrile groups in the polymer.

This difference is due to the fact that, in the binary systems consisting of polymer and polar nonsolvent, the thermodynamic irreversibility is increased with increase in the nitrile group concentration, while in the binary systems consisting of polymer and nonpolar nonsolvent, the opposite relationship occurs.

3. The nitrile copolymers act as sorbents for the separation of mixtures of aromatic and aliphatic compounds. Increase in the molecular weight of the aliphatic hydrocarbon increases the effectiveness of the separation.

LITERATURE CITED

1. E. E. Morris and P. T. Wagner, Industr. and Engng. Chem. 49, 445, (1957); I. C. Hwa, F. E. Meitzner, and C. H. McBurney, Industr. and Engng. Chem. 49, 1829 (1957).
2. V. Carelli, A. Lignori, and A. Hell, Nature 176, 4471, 70 (1955); G. L. Starobinets and E. V. Pobarkov, Zhur. Anal. Khim. 15, 405 (1960).
3. G. L. Starobinets, Zhur. Fiz. Khim. 30, 1626 (1956).

4. M. Magat, J. Chim. Phys. 46, 352 (1949).
5. G. L. Starobinets and V. S. Komarov, Doklady Akad. Nauk SSSR 86, 771 (1952); Kolloid. Zhur. 15, 60 (1953).
6. G. L. Starobinets, Uspekhi Khim. 25, 1502 (1956).
7. E. L. Zhukova, Optika i Spektroskopiya 5, 270 (1958).
8. G. Scatchard and C. Raymond, J. Am. Chem. Soc. 60, 1278 (1938).

METHODS OF INVESTIGATING THE FRICTIONAL PROPERTIES OF POLYMERS UNDER STRONG UNIDIRECTIONAL COMPRESSION

B. V. Deryagin and Yu. P. Toporov

Institute of Physical Chemistry, Academy of Sciences of the USSR, Moscow
Translated from Kolloidnyi Zhurnal, Vol. 23, No. 1, pp. 118-121, January-February, 1961
Original article submitted January 19, 1960

The ever-more extensive use of polymeric materials in contemporary mechanical engineering evokes an urgent need of developing new methods for the investigation of their mechanical and, in particular, frictional properties. For practice it is very important to know the frictional properties of polymers under strong compression, since it is known that, under working conditions, pieces made from polymer materials (for instance, from rubber) more often are exposed to deformation by compression than by extension. Investigation of polymers under high compression stresses certainly is of scientific-theoretical importance for ascertaining the physical nature of friction.

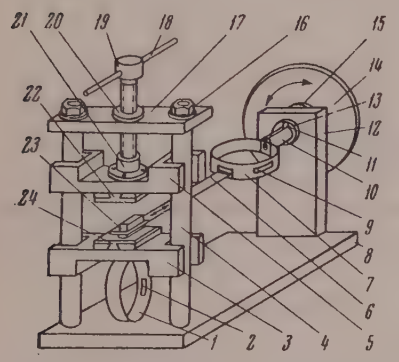


Fig. 1. Diagram of the apparatus for measuring friction: 1) dynamometer ring; 2) strain gauge; 3) support; 4) guide bar; 5) plunger; 6) shaft; 7) dynamometer ring; 8) base; 9) strain gauge; 10) guide screw; 11) wedge; 12) pillar; 13) bearing; 14) disk; 15) nut of guide screw; 16) nut; 17) sheet; 18) spike; 19) bolt; 20) collar; 21) bearing; 22) upper clamped sample; 23) movable sample; 24) lower clamped sample.

In spite of this, the frictional properties of polymers under strong unidirectional compression have been investigated quite insufficiently. The fact that there are no simple methods enabling the study of the frictional properties of materials under strong compression is one of the reasons for the said state of affairs. Generally, heavy and expensive equipment, in the form of presses or explosion engines, is used for such investigations.

In the present paper simple methods, which enable the study of the frictional properties of materials under strong unidirectional compression by means of simple equipment, are proposed.

An apparatus for studying the friction of materials is shown diagrammatically in Fig. 1. The apparatus consists of two hand-operated screw presses mounted on one base. The first upright press enables the application of normal stresses on the contacting samples to be studied in friction, and the second with its axis perpendicular to the first screw allows the displacement of one of the contacting samples with respect to the other.

Possible arrangements of testing with the apparatus are shown in Fig. 2. When the arrangement A is used, the movable sample 2 in the form of a slab from the polymer for which the friction has to be studied is pressed between two polymer slabs 1 and 3 clamped in a horizontal plane. This arrangement can be used in tests where all polymer slabs (the two clamped and the movable one) have been prepared from the same material. This arrangement can be used for investigating both dry and boundary layer friction of polymers, and also for studying the behavior of polymer boundary layers on the surface of a solid body. In the latter case, it is convenient to use flat caliber gauges as slabs.

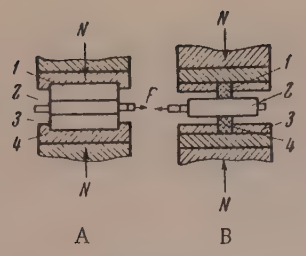


Fig. 2. Arrangements of testing: A) when using metallic caliber gauges; 1) and 3) are the upper and lower clamped sample, respectively; 2) movable sample; 4) holder. B) For testing polymers: 1) and 4) are the upper and lower rods tested; 2) movable sample; 3) holder.

Arrangement B can be used for tests at still higher pressures. In this case, the clamped slabs 1 and 3 (arr. A) have holes into which rods 1 and 4, made from the material to be tested, are inserted. Here, the surface of the protruding rod is pressed against the surface of the movable slab 2. Because, in this arrangement, the contact area is decreased, higher specific compression loads can be realized.

The stress on the contact is exerted by the plunger 5, which can be moved on a vertical plane along the guiding bar 4 by means of the screw 19 when turned by the hand-operated spike 18.

In order to measure the normal forces in the contact, the support 3, to which the lower clamped slab 24 is fastened, and which moves freely along the guide bar 4, rests on the hardened-steel dynamometer ring 1. When the contact is stressed, the ring is deformed proportionally to the force applied. After the contact has been set under stress by a normal force N, a horizontal force is applied to the movable sample 23 by means of a special shaft 6, which is connected to the screw 10 via the dynamometer ring 7.

The shaft 6, which is provided with a key groove, is displaced horizontally by turning manually or by a motor and driving belt, with the nut 15 clamped to the pillar 12.

The magnitude of the horizontal force is also derived from the deformation of the dynamometer ring 7; the maximum value of this force at the start of sliding is equal to the friction force F, which originates from both sliding surfaces of the movable sample.

In order to measure the normal and the tangential forces by means of the dynamometer rings, wire strain gauges have been glued on the outer and inner surface in one and the same section of the rings: each pair of gauges is connected to a bridge system, the balanced arms of which are similar strain gauges glued on special compensated springs, which are bent by a micrometer screw. The measurements are carried out in an unbalanced bridge. As measuring apparatus, a POB14 oscillograph with a type GBIII galvanometer is used, which is sufficiently sensitive for work without a tensimetric amplifier. The friction coefficient (μ) was calculated from the relation

$$\mu = F/2N.$$

The setup described allows the measurement, in a simple way, of the static and even the kinetic friction at small velocities and specific compression loads up to 100 kilogram per cm^2 (when arrangement B is used, up to 1000 kilogram per cm^2).

A second method of testing polymers, in which use is made of the tapering of a cone mounted in a conical hole, also enables one to obtain, in a very simple way, the contact area of samples investigated in friction specific compression loads up to 1000 kilogram per cm^2.

The apparatus is shown diagrammatically in Fig. 3, and V. P. Lazarev took part in developing it. The device consists of the removable metallic conical plug 8, which is fastened to the vertical bar 2, and is inserted into the hole in the massive thick-walled socket 9; the latter, made from acrylate glass, has been fixed rigidly to the base plate. Plug and socket have the same tapering.

The sample to be tested 10 is put on the tapered part of the plug; it has the form of a ring, and has been stamped by a punching press, or cut on a lathe from a sheet of the material. When it has been put on, the bar with the plug is inserted into the socket and is loaded by a vertical force. Meanwhile, the axial position of the plug in the socket is fixed by means of the teflon bearing 11, in which the lower part of the bar is adjusted. Axial pressure on the plug is exerted by weights on the lever 4, and it is transmitted to the bar via the spherical support 3. The axial load N produces a compression of the tested ring between the surfaces of plug and socket; the specific compression stress p is found from the angle α of the cone, the thickness a, and the radius r, by using the relation

$$p = \frac{N}{2\pi r a \sin \alpha}.$$

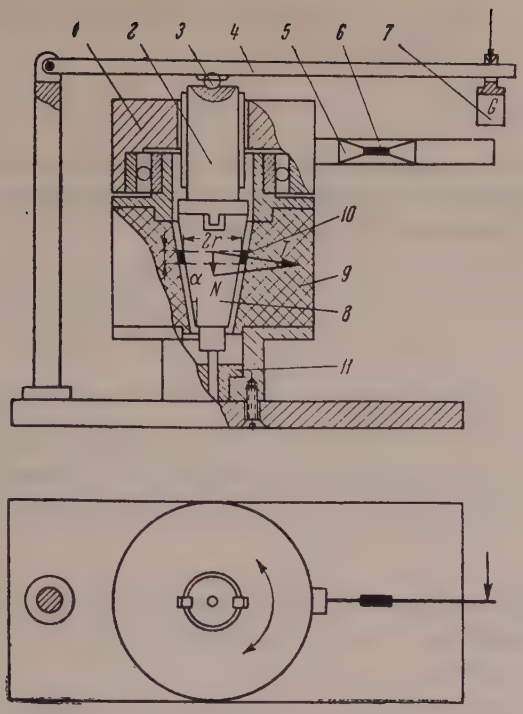


Fig. 3. Diagram of the conical device for testing the friction of polymers.

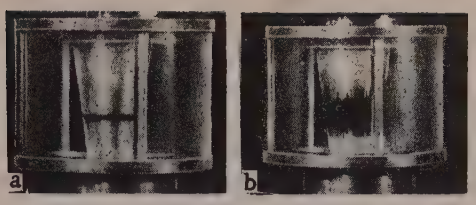


Fig. 4. Photograph of a sample in the device before (a) and after (b) a test.

By visual observation through the socket wall, α and r are measured by means of a cathetometer with an accuracy of 0.1 mm. For this purpose, the inner and outer surface of the socket sides have been polished.

Since the possibilities for the deformation of the ring-shaped material are restricted, one may obtain very high specific compression stresses attaining even hundreds of kilograms per square centimeter for rubberlike materials. It is difficult to realize such compression stresses at the contact with high-elastic materials with other methods.

The frictional properties were studied by rotating the loaded plug inside the socket. This was done by means of the special detachable head 1 mounted on a ball bearing coaxially with the socket. Wedges of the bar, which can slide freely in the head around its axis, fit in grooves inside the hole in the head. At the same time, the head also serves for an additional fixation of the axial position of the plug in the socket. The head and, consequently also, the plug, are turned by means of the crank 5 at the end of which presses a slider, which is moved along a guide by means of a nut and a guide screw; the latter is turned by an electric motor (the gearing is not shown in Fig. 3). The crank 5 is a sturdy flat steel spring which, when the head is turned, is bent proportionally to the applied torsional moment.

The deformation of the crank is recorded by means of wire strain gauges mounted on it; the gauges are connected to a bridge system with usual tensimetric apparatus. By using the latter, the moment required for turning the plug can be measured, since it is equal to the sum of the shear moment M_n in the bearings and the spherical support, which is easily taken into account, and the moment required to overcome the friction forces originating in the contact between the tested ring and the plug surface. The friction coefficient is found from the formula

$$\mu = \frac{(M - M_n)\sin\alpha}{Nr}.$$

When the device described was used, it appeared that, during the testing, the degree of deformation in the sample increases gradually by turning the plug. The latter finds its explanation in the changed conditions of deformation, which result from the application of an additional shear force at the turning of the plug.

The increased degree of deformation leads ultimately to disintegration of the sample. The character and the degree of the ultimate deformation at the moment of breakdown depends upon the properties of the material. In Fig. 4, photographs taken before and after a test with a sample of common packing rubber pressed between the plug and the socket at one and the same axial force are given.

The noted feature of polymeric material behavior at friction tests in the described device may be used to evaluate comparatively some mechanical properties of polymeric materials. For instance, by comparing the times during which the plug, at a given load, must be turned to give complete disintegration of the various samples, one may evaluate the relative stability against crushing and wear under the simultaneous action of normal and tangential stresses.

Although this method has a provisory character, in the opinion of the authors, nevertheless, it may find application, thanks to its simplicity, in studying the properties of rubberlike polymers.

SUMMARY

Methods which enable the testing, by means of simple apparatus, of the frictional properties of polymers at friction under strong unidirectional compression were studied. The methods described may be used for comparatively evaluating some mechanical properties of high-molecular polymeric materials.

KINETICS OF THE GROWTH OF CONTRACTION STRESSES IN SYSTEMS UNDERGOING DRYING

M. S. Ostrikov, N. D. Vitkevich, and O. D. Svirskaya

Rostov University

Translated from Kolloidnyi Zhurnal, Vol. 23, No. 1, pp. 122-124, January-February, 1961
Original letter submitted August 10, 1960

The magnitude of the free surface energy in a great deal determines the processes which take place in heterogeneous disperse systems [1]. It has a very substantial influence, too, on the mechanical action of the capillary contraction forces (F_σ), which are investigated in the present paper. At the drying of various disperse materials,* the change of these forces with time proceeds always along an S-shaped curve [2,3]. However, while retaining this general character (Fig. 1), the dependency of F_σ upon the time of drying τ may vary considerably in the separate stages of the process, and this finds expression in the shape of the corresponding curve regions. For instance, the initial period τ_A (region OA) may vary in the range between a few minutes and 40 or more hours. The position of the inflection point M, the value of $F_{\sigma\,max}$, and the angle γ are changed. In this, particularities of the drying method used, the structure of the substance, its physicochemical properties, and the liquid to be removed find their reflection.

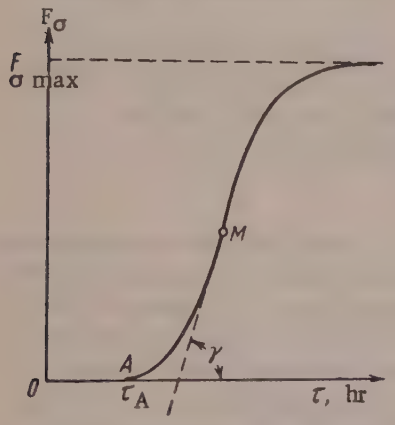


Fig. 1. A typical curve showing how the contraction stress depends upon the time of drying a high-molecular or high-disperse material. τ_A – Induction period required for the formation of a surface layer with a compact structure.

For some substances the initial region of the $F_\sigma(\tau)$ curve (the region where it is concave to the ordinate axis) is developed very weakly. Such steeply rising curves without inflection point (at the start) may be described in first approximation as a part of a hyperbola

$$F_\sigma = F_{\sigma\,max}\left[1 - \frac{1}{(\tau+1)^n}\right]. \qquad (1)$$

Here $F_{\sigma\,max}$ and n are constants characteristic for the system studied. In the general case, this relation is an exponential one. For typical S-shaped curves, where the initial concave (to the ordinate axis) region has been developed quite clearly, the following empirical relation, which embraces all stages in the growth of the capillary contraction forces from the start to the end of the drying process, is proposed:

$$F_\sigma = F_{\sigma\,max}\, e^{-q/\tau^n}, \qquad (2)$$

where $F_{\sigma\,max}$ and n are coefficients which reflect the type of material and the drying regime.

A comparison with the experimental data has shown that Eq. (2) quite satisfactorily describes the growth of contraction stresses at the drying of systems with various compositions and structures. This is confirmed by the results shown in Figs. 2 and 3. The values of the constants for the materials investigated are given in the table.

*Viscose filament, gelatin, paper, acetylcellulose, nitrocellulose, starch, bentonites, cement, wood pulp, and so on.

Materials	F_σ max	q	n	τ_A, hr
Acetylcellulose film	11.5	0.70	3	0.67
Nitrocellulose film	6.5	0.15	4	0.28
Viscose filaments (800 × 14 monofilaments)	6.6	1.10	3	0.78
Writing paper	6.7	0.14	2	0.08

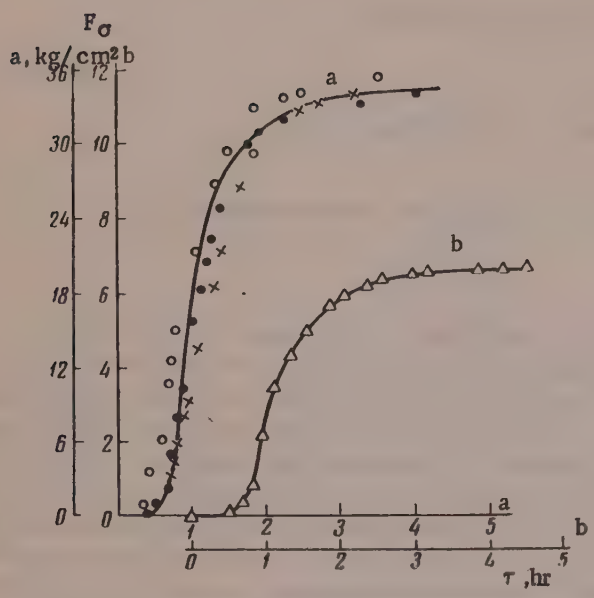


Fig. 2. Comparison of the F_σ values calculated from formula (3) (drawn curves) with experimental data (points) for three samples of acetylcellulose films (a) and a viscose filament (b).

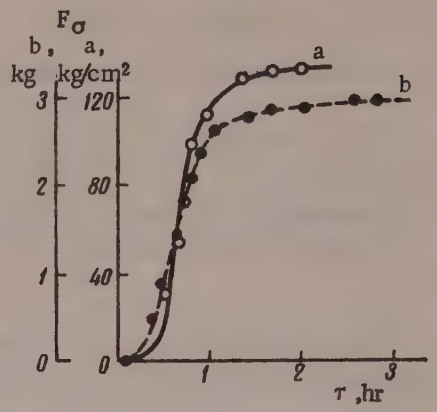


Fig. 3. Comparison of data calculated from formula (2) (curves) with experimental results (points) for nitrocellulose (a) and paper (b) films.

By comparing the various experimental data, it can be seen that the induction period τ_A is shortened, when the rigidity and the density of the initial structure is raised, the drying rate is increased, or the thickness of the sample to be dried is decreased. At the very end of the induction period τ_A the liquid content of the sample studied is lowered to 40-70% (on the dry substance). Further on, the period of rapidly accelerated growth of contraction stresses starts. The growth rate of F_σ attains a maximum at the point of inflection. The last stage completes the attainment of $F_{\sigma\ max}$. The interaction between the adjacent particles or macromolecules of the solid body, which up to here had been brought about via the liquid layer along chains of orientated polar or polarized molecules, now becomes direct (cohesive) and has its maximum. Further prolongation of the drying often results in a lowered stress, because, in the elastoplastic structures, relaxation processes take place and partly since, after the removal of the liquid, the capillary contraction forces have been cut off from the set of forces which create the contraction stress.

The comparison of all discussed experimental data with the proposed relation (2) indicates that the said relation describes quite satisfactorily the growth of contraction stresses during the drying of systems with different physicochemical and structural mechanical properties. The quantitative differences and the qualitative particularities of the systems are reflected by a change in the numerical values of the constants ($F_{\sigma\ max}$, q, n).

The authors express their sincere thanks to Academician P. A. Rebinder for very valuable suggestions.

LITERATURE CITED

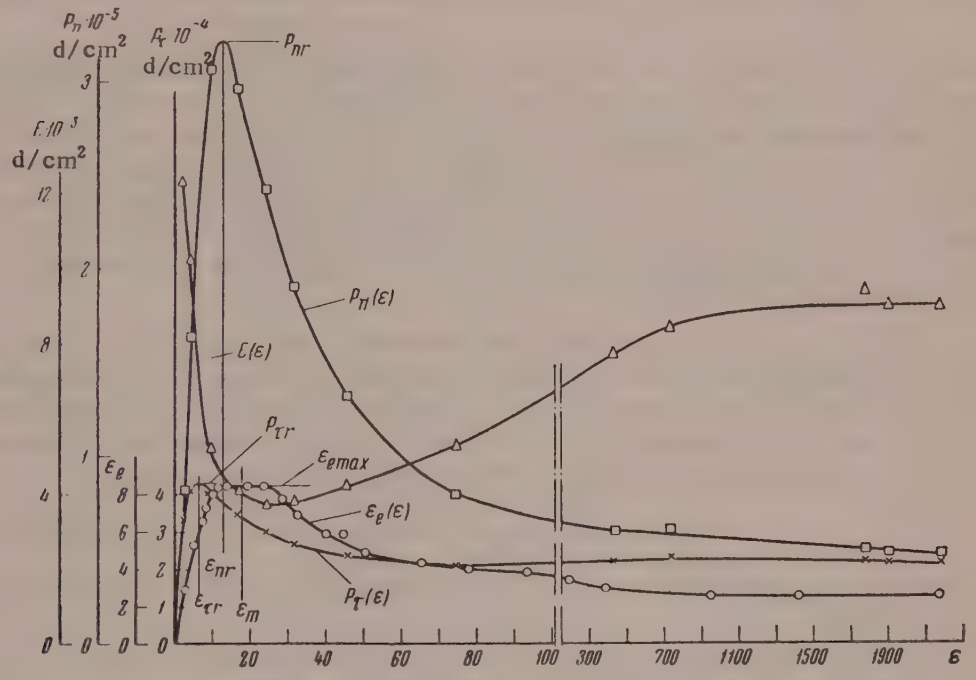
1. P. A. Rebinder, Kolloid. Zhur. 20, 527 (1959).
2. M. S. Ostrikov, G. D. Dibrov, and E. P. Danilova, Doklady Akad. Nauk SSSR 118, 751 (1958).
3. M. S. Ostrikov and E. P. Danilova, Uchenye Zapiski Rostov Univ. 10, No. 10, 37 (1959).

NORMAL STRESSES IN POLYISOBUTYLENE SOLUTION AS DERIVED FROM ELASTIC DEFORMATION AND TANGENTIAL FORCE DATA

A. A. Trapeznikov

Institute of Physical Chemistry, Academy of Sciences of the USSR, Moscow
Translated from Kolloidnyi Zhurnal, Vol. 23, No. 1, pp. 125-127, January-February, 1961
Original letter submitted December 25, 1960

When aluminum naphtenate gel was studied, it was established experimentally [1] that the normal stresses, which, for flowing colloid systems have been recorded for the first time by Weissenberg [2], go through a maximum P_{nr}, if the deformation ϵ is increased continuously. It has been found that P_{nr} occurs at a deformation $\epsilon = \epsilon_{nr}$ which, by about two times, exceeds the deformation $\epsilon_{\tau r}$ at which the maximum $P_{\tau r}$ of the tangential stress (P_τ) is situated.



Experimental $P_\tau(\epsilon)$ and $\epsilon_e(\epsilon)$ curves and calculated $P_n(\epsilon)$ and $E = P_\tau/\epsilon_e = f(\epsilon)$ curves for a 20% solution of polyisobutylene in orthoxylene at $\dot{\epsilon} = 294$ sec^{-1}.

In [3-5], especially dealing with the normal stresses, measurements of P_n and P_τ were used to calculate the elastic deformation ϵ_e (and the shear modulus E) which, as a rule, are not measured experimentally. In these studies, P_n and P_τ were only measured in the stationary flow, without taking into account the initial deformation stage. The following relation was used for the calculation of ϵ_e:

$$P_n = P_\tau \varepsilon_e = E\varepsilon_e^2.$$

In our studies, regardless of the investigation of the normal stresses, long ago we had paid special attention to measuring directly the elastic deformation ϵ_e which, at high deformation rates $\dot{\epsilon} = \text{const}$, is characteristic for the deformability of the network structure and the chain length [6].

In order to obtain data on the relation between $\epsilon_e(\epsilon)$ and $P_\tau(\epsilon)$ at the transition from the state at rest

($\epsilon = 0$) to the stationary flow ($\epsilon \to \infty$) we have studied solutions of polyisobutylene in orthoxylene by means of an elastorelaxometer [6], which had been adapted for measuring ϵ_e at high ϵ (up to 2000). From the measured ϵ_e and $P_\tau(\epsilon)$ values, and using the above-mentioned relation, we have calculated the normal stresses $P_n(\epsilon)$ during the entire extension from $\epsilon = 0$ to $\epsilon \to \infty$, which embraces the transition to the stationary flow via the breakdown of the "solid" body.

As can be seen in the figure, the $\epsilon_e(\epsilon)$ and the $P_\tau(\epsilon)$ curves go through a maximum at $\epsilon = \epsilon_m$ and $\epsilon = \epsilon_{\tau r}$, respectively, and the position of the latter does not coincide. Moreover, it is particularly interesting that $\epsilon_{e\,max} > \epsilon_{\tau r}$, that is, the highest reversible deformation is found to be greater than the deformation at breakdown. This particularity is explained by the action of the network structure [7]. Correspondingly, the maximum P_{nr} occurs at $\epsilon = \epsilon_{nr}$ between the previous maxima, that is, $\epsilon_{\tau r} < \epsilon_{nr} < \epsilon_m$. The fact that the maxima ϵ_m and $\epsilon_{\tau r}$ do not coincide may be one of the reasons for the previously found [1] relation $\epsilon_{nr} \approx 2\epsilon_{\tau r}$.

From the curves in the figure, it follows that the calculated P_n is particularly high in the initial and transitional stages of the deformation, which embrace the region of structure breakdown, i.e., where both P_τ and ϵ_e have their greatest values. Therefore, $(P_{nr})_{\dot{\epsilon}}$ may be considered as a new system characteristic which, however, is based on ϵ_e and P_τ.

Further, it has to be verified experimentally that the P_n values we have obtained are right. This is of interest for checking the relation in general, as well as for verifying that it may be applied in the region of structure breakdown.

From the $E = P_\tau / \epsilon_e = f(\epsilon)$ curve in the figure, and similar curves for other sharply differing ϵ, it follows that E is not a constant. For the stationary stage (index s), E_s increases at raised $\dot{\epsilon}$, because ϵ_{es} is lowered as a result of intensified disintegration of the structure, whereas $\epsilon_{e\,max}$ continues to increase at raised $\dot{\epsilon}$. This confirms the previous assumptions [8] that ϵ_{es} may go through a maximum, when $\dot{\epsilon}$ is raised. In connection with this, the over-all E in the relation giving P_n gets the meaning of some effective "structural" modulus, and not that of the modulus of a Hook's body. The considerable separation between the $P_\tau(\epsilon)$ and $\epsilon_e(\epsilon)$ curves in the figure beyond the maximum $P_{\tau r}$ does not exclude the possibility that the directions of the stress and the deformation ellipsoids are different in this range of ϵ.

So it follows that there may be no complete agreement between the experimental data and the relation given above. By comparing P_n/P_τ [1] and ϵ_e [9], data on naphtenate gels with similar compositions and structures, the relation was checked approximately, and it was found that P_n/P_τ in the region of the maxima P_{nr_1} and $P_{\tau r_1}$ lies in the range 30-50, whereas ϵ_e = 30-35. Consequently, in first approximation, the relation may also be valid in the breakdown region; however, this is not necessarily true for all systems.

LITERATURE CITED

1. A. A. Trapeznikov, A. S. Morozov, and G. G. Petrzhik, Doklady Akad. Nauk SSSR 133, 637 (1960); Kolloid. Zhur. 22, 761 (1960).
2. K. Weissenberg, Proceedings of the First International Congress on Rheology (Holland, 1948) Vol. 1, p. 29.
3. N. Pilpel', Trans. Faraday Soc. 50, 1389 (1954); 51, 1307 (1955).
4. A. Jobbing and I. E. Roberts, Rheology Theory and Applications (1958) Vol. 2, p. 503; J. Polymer Sci. 36, 421, 433 (1959).
5. W. Philippoff, Trans. Soc. Rheol. 1, 95, 109 (1959); J. Appl. Phys. 27, 984 (1956); 28, 1118 (1957).
6. A. A. Trapeznikov, Vestnik Akad. Nauk SSSR No. 6, 70 (1960).
7. A. A. Trapeznikov, Kolloid. Zhur. 20, 476 (1958).
8. A. A. Trapeznikov and T. G. Shalopalkina, Doklady Akad. Nauk SSSR 111, 350 (1956).
9. T. G. Shalopalkina and A. A. Trapeznikov, Kolloid. Zhur. 22, 735 (1960).

SIGNIFICANCE OF ABBREVIATIONS MOST FREQUENTLY ENCOUNTERED IN SOVIET PERIODICALS

FIAN	Phys. Inst. Acad. Sci. USSR.
GDI	Water Power Inst.
GITI	State Sci.-Tech. Press
GITTL	State Tech. and Theor. Lit. Press
GONTI	State United Sci.-Tech. Press
Gosenergoizdat	State Power Press
Goskhimizdat	State Chem. Press
GOST	All-Union State Standard
GTTI	State Tech. and Theor. Lit. Press
IL	Foreign Lit. Press
ISN (Izd. Sov. Nauk)	Soviet Science Press
Izd. AN SSSR	Acad. Sci. USSR Press
Izd. MGU	Moscow State Univ. Press
LEIIZhT	Leningrad Power Inst. of Railroad Engineering
LET	Leningrad Elec. Engr. School
LETI	Leningrad Electrotechnical Inst.
LETIIZhT	Leningrad Electrical Engineering Research Inst. of Railroad Engr.
Mashgiz	State Sci.-Tech. Press for Machine Construction Lit.
MEP	Ministry of Electrical Industry
MES	Ministry of Electrical Power Plants
MESEP	Ministry of Electrical Power Plants and the Electrical Industry
MGU	Moscow State Univ.
MKhTI	Moscow Inst. Chem. Tech.
MOPI	Moscow Regional Pedagogical Inst.
MSP	Ministry of Industrial Construction
NII ZVUKSZAPIOI	Scientific Research Inst. of Sound Recording
NIKFI	Sci. Inst. of Modern Motion Picture Photography
ONTI	United Sci.-Tech. Press
OTI	Division of Technical Information
OTN	Div. Tech. Sci.
Stroiizdat	Construction Press
TOE	Association of Power Engineers
TsKTI	Central Research Inst. for Boilers and Turbines
TsNIEL	Central Scientific Research Elec. Engr. Lab.
TsNIEL-MES	Central Scientific Research Elec. Engr. Lab.—Ministry of Electric Power Plants
TsVTI	Central Office of Economic Information
UF	Ural Branch
VIESKh	All-Union Inst. of Rural Elec. Power Stations
VNIIM	All-Union Scientific Research Inst. of Metrology
VNIIZhDT	All-Union Scientific Research Inst. of Railroad Engineering
VTI	All-Union Thermotech. Inst.
VZEI	All-Union Power Correspondence Inst.

Note: Abbreviations not on this list and not explained in the translation have been transliterated, no further information about their significance being available to us. — Publisher.

CONTRIBUTION TO THE INVESTIGATION OF PROCESSES OF CRYSTALLIZATION STRUCTURE FORMATION IN AQUEOUS SUSPENSIONS OF TRICALCIUM ALUMINATE IN THE PRESENCE OF ELECTROLYTES

E. P. Andreeva and E. E. Segalova

Department of Colloid Chemistry, Moscow University
Translated from Kolloidnyi Zhurnal, Vol. 23, No. 2, pp. 129-133,
March-April, 1961
Original article submitted April 1, 1960

We investigated in previous work [1] processes of structure formation and chemical interactions which take place in suspensions of tricalcium aluminate and its hexahydrate after tempering with calcium chloride solutions. The results of previous investigations showed that the effect of calcium chloride on structure formation is due to the fact that calcium hydrochloroaluminate is formed, and that the latter on crystallization from the solution is capable of giving rise to a hardening structure. However, the suspensions which have been studied cannot duplicate the behavior of cement in the initial stages of its interaction with water or calcium chloride solutions, primarily because they do not contain the gypsum which is usually added to cement clinker during its milling. From this standpoint, the work done in this instance was concerned with structure formation and chemical interactions in suspensions of tricalcium aluminate (C_3A) and tricalcium aluminate hexahydrate ($C_3A \cdot aq$) to which gypsum had been added. These solutions were tempered with calcium chloride solutions having concentrations within the extensive range of 0.5-6 N.

The processes of structure formation were characterized by the kinetics of the increase of plastic strength [1]. The quantity of chemically combined gypsum was determined by using methods developed by Gudovich [2] and that of chemically combined calcium by methods described in reference [1]. The samples were kept in the presence of moisture.

Table 1 lists the results of analyses which indicate the kinetics of the interaction of C_3A and $C_3A \cdot aq$ with electrolytes that have been introduced while Table 2 gives data pertinent to the kinetics of structure formation in the suspensions investigated.

It can be seen from the data in Table 1 that in the suspensions investigated calcium chloride was bound together with gypsum, which indicates that there was simultaneous formation of calcium hydrochloroaluminate and calcium sulfatoaluminate. It was shown in paper [3] that on tempering of C_3A with solutions containing both SO_4^{2-} and Cl^- ion binding of SO_4^{2-} with the formation of hydrosulfatoaluminate takes place first and formation of calcium hydrochloroaluminate begins only after all of the gypsum has entered into combination. This is in complete accordance with the fact that the sulfatoaluminate has a considerably lower solubility than the hydrochloroaluminate [3,4]. However, in the concentrated suspensions investigated by us the gypsum was in the solid phase, whereas the calcium chloride was introduced together with the water of tempering. Under the circumstances the quantity of SO_4^{2-} that entered into solution was restricted by the rate of dissolution of gypsum. In the case when the gypsum dissolves more slowly than the aluminate, there must be formation of hydrochloroaluminate together with that of sulfatoaluminate. The quantity of hydrochloroaluminate that forms depends on the over-all velocity of the solution of gypsum, i.e. the initial quantity of gypsum which is present and its specific surface. We found that when the quantity of gypsum introduced into the suspension had been increased by a factor of 2 ($n = 6$) at the same specific surface of the gypsum, there was in a suspension of essentially the same composition as suspension 1 (cf. Table 1) binding of 17% of the C_3A with the formation of hydrochloroaluminate within 5 min, as compared with the binding of 26% of C_3A at a lower content of gypsum ($n = 3$).

It can be seen from Table 1 that the quantity of chemically bound gypsum increased continuously in time, while that of chemically bound calcium chloride first reached a maximum and then dropped in value. This can be

TABLE 1

Kinetics of the Chemical Binding of $CaCl_2$ and $CaSO_4$ in C_3A and $C_3A \cdot aq$ Suspensions; t = 20°

Time elapsed since completion of tempering	Quantity of chemically bound salt					
	$CaSO_4$		$CaSO_4$		$CaCl_2$	
	g/g C_3A	bound C_3A, %	g/g C_3A	bound C_3A, %	g/g C_3A	bound C_3A, %
	tempering with water		tempering with a 3N $CaCl_2$ solution			
Suspension 1: 5% C_3A + 10% $CaSO_4 \cdot 2H_2O$ ($n = 3$)* + 85% SiO_2** + 35 ml 3N solution $CaCl_2$ на 100 g of dry mixture						
5 min	—	—	0,907	60,0	0,108	26,4
10 »	—	—	0,930	61,5	—	—
30 »	—	—	0,983	65,0	0,091	22,2
1 days	—	—	1,361	90,0	0,026	6,50
30 »	—	—	1,380	91,8	0,020	5,00
Suspension 2: 7% $C_3A \cdot aq$ + 10% $CaSO_4 \cdot 2H_2O$ ($n = 3$) + 83% SiO_2 + 29 ml H_2O or of a 3N solution $CaCl_2$ per 100 g of dry mixture						
0 min	0,043	2,90	0,043	2,9	0,053	13,1
1 hr	0,074	4,9	0,189	12,5	—	—
3 »	0,240	15,8	1,112	73,4	0,107	26,2
5 »	0,010	66,8	1,280	84,7	—	—
1 day	1,410	93,3	1,404	92,4	0,030	7,3

* n) gypsum content in the suspension in moles per 1 mole of C_3A.

** SiO_2) ground quartz sand with a $S_{sp} = 0.32$ m^2/g.

*** bound C_3A in %) quantity of C_3A in percent of the initial that has entered into reaction with the salt in question under formation of the complex salts $3CaO \cdot Al_2O_3 \cdot 3CaSO_4 \cdot aq$ or $3CaO \cdot Al_2O_3 \cdot CaCl_2 \cdot aq$.

explained only by conversion of the more soluble calcium hydrochloroaluminate into the less soluble hydrosulfatoaluminate. Experiments especially conducted for this purpose showed that in suspensions which contained hydrochloroaluminate prepared beforehand and $CaSO_4 \cdot 2H_2O$, and had then been tempered with a 3N $CaCl_2$ solution, there was within 4 days conversion into sulfatoaluminate of 33% of the initial amount of hydrochloroaluminate, and within 10 days conversion of 84% of the initial amount of that salt. The conversion of the hydrochloroaluminate into the hydrosulfatoaluminate as a result of its reaction with gypsum was accompanied both in water and in calcium chloride solutions of different concentrations by the formation of structures due to the hardening of hydrosulfatoaluminate (cf. Table 2, suspension 1).

Thus, in the suspensions investigated, which contained C_3A or $C_3A \cdot aq$ in addition to gypsum at a concentration corresponding to an "n" equal to or greater than 3, the end product of the reaction was calcium hydrosulfatoaluminate, which in the process of crystallization gave rise to a hardening structure.

Formation of hydrosulfatoaluminate takes place at a greatly increased velocity in calcium chloride solutions. This can be seen by comparing the kinetics of the binding of gypsum in $C_3A \cdot aq$ suspensions tempered with water with those in suspensions tempered with a 3N solution of $CaCl_2$ (cf. Table 1, suspension 2). The same relationships was observed in the case of suspensions containing C_3A. Thus, according to data reported by Tu Yu-ju [5] for suspensions containing a mixture of tricalcium aluminate and gypsum (n = 3), 19% of the initial quantity of C_3A was transformed into sulfatoaluminate within approximately 30 min after tempering with water and 75% within 24 hr after tempering. On the other hand, when the same suspensions were tempered with a 3N solution of $CaCl_2$, the quantities of C_3A transformed within the periods of time indicated amounted to 60 and 90%, respectively.

The increase in strength brought about by the crystallization of hydrosulfatoaluminate and consequent structure formation was also found to proceed at a markedly faster rate in the case of suspensions containing calcium chloride (cf. Table 2, suspensions 2 and 3).

The final strength of hydrosulfatoaluminate structures that formed in the presence of calcium chloride proved to be invariably lower than in the case of suspensions which had been tempered with water. After reaching a maximum value, the strength of the structure began to decrease. When the suspensions contained hydroaluminate, this decrease was accompanied by a very strong expansion of the structure. The decrease in strength continued even

TABLE 2

Kinetics of Structure Formation in C_3A and $C_3A \cdot aq$ Suspensions Containing Electrolytes. Duration of Stirring During Tempering 30 sec, t = 20°

Time elapsed since the completion of tempering	Content of $CaCl_2$ in the water, g-eq/l					
	0	0,5	1,5	3,0	4,5	6
	plastic strength (P_m) in kg/cm²					
Suspension 1: 20% of $C_3A \cdot 10H_2O$ + 20% of $CaSO_4 \cdot 2H_2O$ + 60% of SiO_2 + 30 ml of H_2O or of a $CaCl_2$ solution per 100 g of dry mixture						
1 min	0,20	0,20	—	0,16	0,16	0,16
10 »	1,0	0,30	—	0,20	0,20	0,20
1 hr	23,0	20,2	—	17,2	13,3	0,3
1 day	41,3	18,6	—	8,0	5,6	13,3
15 »	27,0	14,6	—	7,4	1,4	7,4
3 months	21,3	7,2	—	6,6	0,8	6,6
Suspension 2: 5% of C_3A + 10% of $CaSO_4 \cdot 2H_2O$ (n* = 3) + 85% of SiO_2 + 35 ml of H_2O or of a $CaCl_2$ solution per 100 g of dry mixture						
1 min	0,20	0,20	0,20	1,5	4,2	4,5
10 »	2,4	1,3	13,3	6,4	13,3	21,6
30 »	9,8	6,9	20,7	13,3	27,0	53,7
1 hr	18,6	11,4	32,9	32,5	32,9	53,7
6 hr	23,6	22,8	35,5	32,5	27,0	41,2
1 day	41,1	41,1	32,5	28,6	25,5	35,5
3 »	105	73	27,0	27,0	24,2	35,5
10 »	105	73	19,6	10,6	11,4	15,9
30 »	105	73	17,8	9,3	10,0	10,6
Suspension 3: 7% of $C_3A.aq$ + 10% of $CaSO_4 \cdot 2H_2O$ (n=3) + 83% of SiO_2 + 29 ml of H_2O or of a $CaCl_2$ solution per 100 g of dry mixture						
1 min	0,08	0,10	0,20	0,20	—	0,20
1 hr	2,0	3,2	2,9	6,1	—	2,5
5 »	105	73,0	41,4	53,5	—	24,0
1 day	164	105	73,5	53,5	—	41,0
5 »	164	105	73,5	53,5	—	41,0
10 »	164	105	42,0	28,0	—	20,0
30 »	164	105	8,0	6,0	—	5,0
Suspension 4: 5% of C_3A + 5% of $CaSO_4 \cdot 2H_2O$ (n=1.5) + 90% of SiO_2 + 35 ml of H_2O or of a $CaCl_2$ solution per 100 g of dry mixture						
1 min	0,32	0,18	0,20	1,6	2,4	2,9
10 »	0,35	1,0	0,40	5,90	6,6	20,7
30 »	27,0	15,9	8,00	13,2	10,6	41,1
1 hr	41,1	73,1	13,2	17,2	21,8	41,1
6 »	73,0	105	16,7	21,1	19,3	53,7
1 day	73,0	105	21,2	20,0	20,0	53,7
5 »	73,0	105	53,7	16,0	10,6	21,8
10 »	73,0	105	73,2	13,2	8,00	11,4
30 »	73,0	105	73,2	9,8	6,4	8,2

* n) gypsum content in the suspension in moles per 1 mole of C_2A.

TABLE 3

Kinetics of Chemical Interaction in Suspensions Containing 5% of C_3A + 5% of $CaSO_4 \cdot 2H_2O$ (n = 1.5) + 35 ml of a $CaCl_2$ solution; t = 20°

Time elapsed since the completion of tempering	Concentration of calcium chloride in water, g-eq/l							
	0,5				1,5			
	quantity of chemically combined salt							
	$CaSO_4$		$CaCl_2$		$CaSO_4$		$CaCl_2$	
	g/g C_3A	bound C_3A in %	g/g C_3A	bound C_3A in %	g/g C_3A	bound C_3A, %	g/g C_3A	bound C_3A, %
30 min	—	—	0,010	2,4	—	—	—	—
6 hr	0,637	42,2	0,021	5,1	0,690	45,6	—	
10 days	0,732	48,4	0,188	45,8	0,731	48,5	0,190	46,2

after completion of the chemical interaction in the suspension. The reduction of strength and the expansion of the structure which occur during the process of the crystallization of the hydrosulfatoaluminate can be explained by the inner strains which accompany any process of structure formation due to crystallization [6]. The decrease in strength after the crystallization of the hydrosulfatoaluminate has been practically completed is due to the great hygroscopicity of the suspensions under investigation: absorption of moisture by them leads to plastification of the coagulation bonds which are present in the suspension and which have formed as a result of the destruction of crystallization structures under the effect of inner strains.

Table 3 represents the kinetics of the chemical interaction and Table 2 (suspension 4) the kinetics of structure formation in the case of aqueous suspensions of C_3A which contain calcium chloride and gypsum in quantities insufficient to bring about complete combination of all of the C_3A in the form of hydrosulfatoaluminate (n = 1.5).

In this case one half of the aluminate combines under formation of hydrosulfatoaluminate and the other half under formation of calcium hydrochloroaluminate, with the result that the crystallization structures of both substances appear in the suspensions.

When tempering of the suspensions is carried out with calcium chloride solutions having concentration equal to or greater than 1.5 N, inner strains become pronounced which bring about reduction of the strength of the structure and the suspensions become hygroscopic as a result of the presence of calcium chloride in them.

Special experiments have shown that lowering of the temperature to minus 10° does not produce any marked change in the nature of the processes of structure formation taking place in C_3A and $C_3A \cdot aq$ suspensions which contain gypsum and have been tempered with calcium chloride solutions.

SUMMARY

1. An investigation has been carried out of the kinetics of structure formation and chemical interaction in suspensions containing C_3A or $C_3A \cdot aq$ and also gypsum in a quantity sufficient to bring about combination of all of the aluminate in the form of hydrosulfatoaluminate (i.e., at n = 3), when the suspensions have been tempered with calcium chloride solutions of different concentrations in the range of 0.5-6 N.

2. It was found that calcium hydrosulfatoaluminate constitutes the end product of chemical interaction in the suspensions investigated. It was also found that in addition to calcium hydrosulfatoaluminate, calcium hydrochloroaluminate may form as an intermediate product. As a result of further interaction with gypsum, the latter salt is converted into calcium hydrosulfatoaluminate.

3. It was established that formation of calcium hydrosulfatoaluminate and the process of structure formation by its crystallization are sharply accelerated in the presence of calcium chloride and are accompanied by the generation of inner strains which bring about expansion and lowering of the strength of structures.

4. When C_3A suspensions containing gypsum in quantities insufficient for complete conversion of all of the aluminate into hydrosulfatoaluminate had been tempered with calcium chloride solutions, both calcium hydrosulfatoaluminate and calcium hydrochloroaluminate formed, crystallizing with the formation of hardening structures.

5. Lowering of the temperature (down to minus 10°) had no effect either on the nature of the chemical interaction or the course of processes of structure formation in C_3A and $C_3A \cdot aq$ suspensions which contained gypsum and had been tempered with calcium chloride solutions.

LITERATURE CITED

1. E. P. Andreeva, E. E. Segalova, and E. E. Volynets, Doklady Akad. Nauk SSSR 123, No. 6, 1052 (1958); E. P. Andreeva and E. E. Segalova, Kolloid. Zhur. 22, No. 4, 385 (1960).
2. L. A. Gudovich, Tsement 3, 16 (1950).
3. T. V. Rubetskaya, Dissertation: Conditions of the Formation of Calcium Sulfatoaluminate and the Effect of Chlorides on Its Existence [in Russian] (Moscow, 1958).
4. F. F. Jones, Proceedings of the Symposium on the Chemistry of Cements (Stockholm, 1938), p. 231.
5. Tu Yu-ju, Dissertation: Investigation of Processes of Crystallization Structure Formation by Calcium Hydrosulfatoaluminates [in Russian] (Moscow, 1958).
6. E. E. Segalova and P. A. Rebinder, Stroitel'nye Materialy, No. 1, 21 (1960).

THE EFFECT OF FREEZING ON THE PROPERTIES OF METAL HYDROXIDE COAGULATES

PART 2. EFFECT OF ELECTROLYTES ON CHANGES OF THE VOLUME OF FERRIC HYDROXIDE COAGULATE AS A RESULT OF FREEZING

V. V. Vol'khin and V. L. Zolotavin

S. M. Kirov Ural Polytechnic Institute, Sverdlovsk
Translated from Kolloidnyi Zhurnal, Vol. 23, No. 2, pp. 134-139,
March-April, 1961
Original article submitted July 17, 1959

In a previous communication the effects of the conditions of freezing and thawing on some properties of coagulates of ferric hydroxide from which electrolytes had been removed by washing were considered [1]. In the work reported at present we investigated the effects of freezing on volume changes of ferric hydroxide coagulates in the presence of electrolytes of different concentrations.

Very few data on the subject have been published and a single point of view for considering the mechanism of the processes involved is absent. For instance, some authors [2] have demonstrated that the coagulation of sols which takes place on freezing and the conversion of metal hydroxide coagulates into a more compact precipitate occur as a consequence of the increased concentration of electrolytes that is due to the separation of pure ice. In other words, it is assumed that electrolytes play a positive role in connection with the effect exerted by freezing on sols and also on coagulates.

Other investigators [3] noted that hydroxide coagulates from which the electrolytes have been washed out and sols which have been subjected to dialysis are less resistant to the effect of freezing, from which it follows that the effect of freezing is reduced in the presence of electrolytes.

In considering the effect exerted by electrolytes in connection with the freezing of sols and gels, Buzagh [4] selected a group of electrolytes which facilitate the formation of sols and investigated the role played by them in freezing in sufficient detail. Nevertheless, general relationships pertaining to the phenomena in question have not yet been established.

We used in all experiments samples of ferric hydroxides prepared by a method described earlier [1], employing in every case 25 ml of ferric hydroxide (approx. 225 mg of Fe_2O_3), which corresponded to 17.5 ml of precipitate after the latter had settled to a fixed level. The electrolytes were introduced separately into each sample one hour before freezing and thoroughly stirred in. The method of freezing has also been described earlier.

After the ferric hydroxide had been frozen in air at minus 10° for 4 hr and thawing had been carried out in the presence of low concentration of electrolytes ($5 \cdot 10^{-3}$M), the observed reduction of the volume of the precipitate was the same as in the case of a coagulate that had been washed. As the concentration of electrolytes was increased, their effect on the process of freezing became greater to a marked extent (cf. Fig. 1). It was found that at minus 10° some electrolytes reduced the effect of freezing more strongly than others.

The two groups of electrolytes differ from each other in that the temperature of the formation of cryohydrates is lower than the experimental temperature for representatives of the first group and higher for those of the second group.

The temperatures of the formation of cryohydrates of some salts and the composition of these cryohydrates are listed in the table.

To check the correctness of the conclusion that has been made the experiments were repeated at minus 4° (cf. Fig. 2, a). Under these conditions sodium sulfate, sodium carbonate, and potassium nitrate formed cryohydrates, as in

Temperatures of the Formation of Cryohydrates and Their Composition

Electrolyte	Temperature of formation of the cryohydrate, °C	Composition of cryohydrate	Literature reference
$Ba(NO_3)_2$	—0,55	$Ba(NO_3)_2$ + ice	[5]
Na_2SO_4	—1,2	$Na_2SO_4 \cdot 10H_2O$ + ice	[6]
KNO_3	—2,88*: —2,6	KNO_3 + ice	[7,8,9]
Na_2CO_3	—2,05	$Na_2CO_3 \cdot 10H_2O$ + ice	[6]
KH_2PO_4	—2,6	K_2HPO_4 + ice	[8,9]
Na_2CrO_4	—5,0	$Na_2CrO_4 \cdot 10H_2O$ + ice	[10]
K_2HPO_4	—13,5	$K_2HPO_4 \cdot 6H_2O$ + ice	[11]
$(NH_4)_2SO_4$	—18,4	$(NH_4)_2SO_4$ + ice	[12]
$NaNO_3$	—18,5	$NaNO_3$ + ice	[10,7]
NaCl	—21,3	$NaCl \cdot 2H_2O$ + ice	[6]
$Al(NO_3)_3$	—27	$Al(NO_3)_3 \cdot 9H_2O$ + ice	[13]
$Ca(NO_3)_2$	—28	$Ca(NO_3)_2 \cdot 4H_2O$ + ice	[5]
HCl	—70,5**	$HCl \cdot 3H_2O$ + ice	[14]
NH_4OH	—101,3	$NH_3 \cdot H_2O$ + ice	[15]

* According to reference [7].

** This solution has a tendency towards deep supercooling.

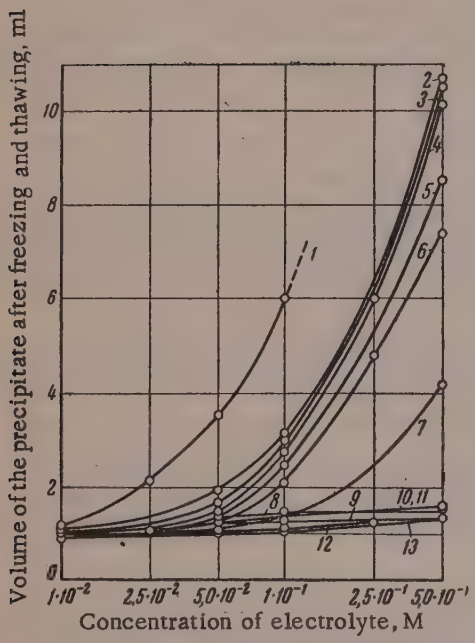


Fig. 1. Dependence of the volume of the precipitate on the concentration of electrolytes in the initial coagulate: 1) $Al(NO_3)_3$; 2) $Ca(NO_3)_2$; 3) K_2HPO_4; 4) $(NH_4)_2SO_4$; 5) NaCl; 6) $NaNO_3$; 7) NH_4OH; 8) Na_2SO_4; 9) Na_2CrO_4; 10) Na_2CO_3; 11) KH_2PO_4; 12) $Ba(NO_3)_2$; 13) KNO_3.

the preceding experiments, and exerted, as before, only a relatively small effect on the volume of the precipitates after freezing and thawing. Sodium chromate does not yet form a cryohydrate at minus 4°, so that an increase in the concentration of this electrolyte resulted in a strong increase of the volume of the precipitate, i.e. its effect was similar to that exerted under the conditions of the preceding experiments by electrolytes which do not form cryohydrates at minus 10°.

Thus, the same electrolyte present in a coagulate may, depending on the temperature of the formation of a cryohydrate by it and the temperature of freezing, exert different effects on the volume of the precipitate after thawing. If the temperature of the formation of the cryohydrate is lower than the temperature of freezing, the effect of freezing is considerably reduced by the presence of the electrolyte in question. If this temperature is higher than that of freezing, a considerable reduction of the volume of the precipitate takes place subsequently to freezing and thawing, even when the content of the electrolyte is high.

In other words, the electrolyte does not prevent reduction of the volume of the precipitate as a result of freezing and thawing only in cases when the temperature of the formation of a cryohydrate by it is higher than the temperature of freezing, i.e. only under the condition that it does not interfere with solidification of the liquid phase of the coagulate.

It follows from this that in the general case the effect of freezing on the volume of the coagulate must be greater when the solidification of the liquid phase in the coagulate is more complete.

To elucidate the effect of the velocity of freezing on the volume of the precipitate, experiments were carried out in an air-filled chamber at the temperature of dry ice (from minus 70 to minus 78°), so that the intensity of heat transfer was increased considerably. Notwithstanding the fact that under the conditions in question all electrolytes investigated formed cryohydrates and the hydroxide samples and the samples of hydroxide were frozen through completely, the volume of the precipitate increased markedly with increased concentrations of the electrolytes (Fig. 2, b). This reduction of the effect of freezing on the hydroxide took place by reason of the fact that because of the supercooling produced by the intensive outflow of heat in the case under consideration the rate of the formation of nuclei

of crystallization became significantly greater than the rate of crystal growth, so that the crystals were of a small size; if the size of the crystals is so small that they become commensurate with the cells of the coagulate, destruction of these cells must take place to a lesser extent.

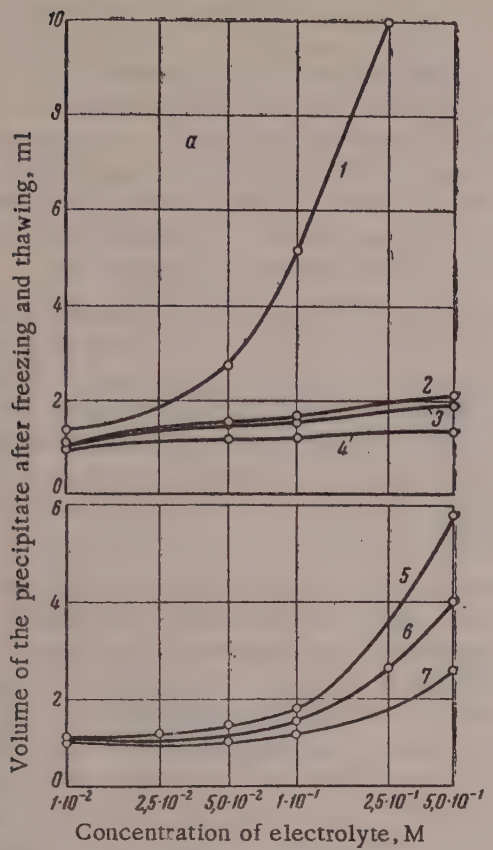


Fig. 2. Dependence of the volume of the precipitate on the concentration of electrolytes in the initial coagulate; freezing in air at minus 4° (a) and minus 70° (b): 1) Na_2CrO_4; 2) Na_2CO_3; 3) KNO_3; 4) Na_2SO_4; 5) $Ca(NO_3)_2$; 6) $(NH_4)_2SO_4$; 7) $NaNO_3$.

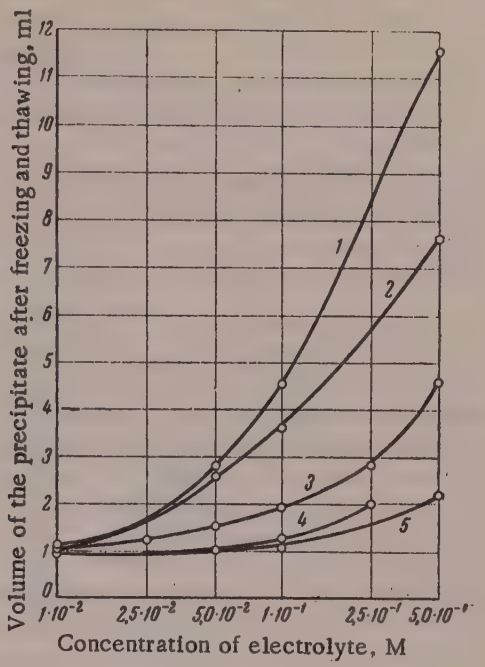


Fig. 3. Dependence of the volume of the precipitate on the concentration of electrolytes in the initial coagulate: 1) $Ca(NO_3)_2$; 2) $(NH_4)_2SO_4$; 3) $NaNO_3$; 4) $Ba(NO_3)_2$; 5) KNO_3.

When samples of ferric hydroxide were subjected to freezing in the presence of electrolytes in acetone (at minus 78°), i.e. in a medium where the rate of heat transfer is greater than in an air chamber, the effect of freezing was reduced to a still greater extent (cf. Fig. 3), which is understandable, because the crystals of ice and cryohydrate must be particularly small in this case. One may note that a similar phenomenon was observed when living tissues were frozen [16]. The latter are destroyed when frozen slowly and are preserved to a much greater extent when their freezing is carried out in an acetone bath at minus 78°.

In the experiments conducted at minus 10° (in air) and at minus 78° (in acetone) it was observed that the nitrates of sodium and barium exerted the least effect on the volume of the precipitate as compared with the other electrolytes investigated.

Buzagh [4], in investigating the effect of sol-forming electrolytes in the freezing of metal hydroxides, found that beginning with definite concentrations the peptizing action of these electrolytes increased considerably. We repeated his experiments on ferric hydroxide and hydrochloric acid and also investigated the effect of aluminum and thorium nitrates. It was established that peptization of ferric hydroxide begins immediately after thawing and proceeds independently of the fact whether or not the electrolyte present in the coagulate forms a cryohydrate at the temperature in question; thus, in the presence of aluminum nitrate noticeable peptization as a result of freezing began at a concentration of the electrolyte amounting to approximately $5 \cdot 10^{-3}$M and increased at higher concentrations. It was found that thorium nitrate is capable of peptizing completely the ferric hydroxide when present in a concentration of $5 \cdot 10^{-5}$– $10 \cdot 10^{-5}$M and hydrochloric acid of producing the same effect when present in a concentration of approximately $1.5 \cdot 10^{-2}$M. The effect in question was observed immediately after thawing of the sample.

Mechanism of freezing of ferric hydroxide coagulate in the presence of electrolytes. On the basis of the investigation which has been carried out, the mechanism of the process of freezing of a ferric hydroxide coagulate in the presence of electrolytes can be imagined as follows. First, crystallization of ice begins at the walls of the vessel when a temperature has been reached which corresponds to the beginning of freezing of a solution having the concentration in question. Because water does not form solid solutions, the concentration of the electrolyte and that of the hydroxide particle become greater as more ice forms. The boundary of propagation of ice into the depth of the hydroxide does not constitute a flat surface [7], so that the hydroxide becomes gradually interpenetrated by dendrites and needles of ice. The particles of hydroxide located between crystals are gradually compressed because of the growth of the latter and the intermicellar liquid which is squeezed out of these particles is frozen out in its turn. The principal force which brings about compression is presumably the expansion of water during its solidification. In this manner, the electrolyte and particles of hydroxide accumulate in the interlaminar space between ice crystals. Whether or not complete solidification of the solution will take place in the interlaminar space depends on the interrelationship between the temperature of freezing and that of the formation of a cryohydrate by the electrolyte.

In the case that the temperature of freezing is lower than the temperature of formation of the cryohydrate, the electrolyte solution, on reaching a definite concentration, solidifies in the interstices between the ice crystals, forming a eutectic. In connection with this, independently of the initial concentration of the electrolyte, there is thorough freezing through of the coagulate, with the result that its volume after thawing is considerably reduced. In the case when the temperature of freezing is higher than that of the formation of the cryohydrate, the electrolyte accumulates in the interstices between the ice crystals at a concentration at which its solution will no longer be frozen out at the given temperature. Further compression of the hydroxide particles ceases and the volume of the precipitate will be the greater the higher the initial concentration of the electrolyte has been.

However, solidification of the intermicellar liquid does not always result in a disturbance of the structure of the coagulate. If good heat transfer during the formation of the eutectic is ensured, the particles of cryohydrate become so small that their dimensions are of the same order as those of the elementary coagulate cells; under the circumstances, the latter will be preserved to a predominant extent after freezing. Furthermore, compression of the coagulate in the interstices between crystals and disturbance of its spatial structure merely create conditions under which large, compact particles of hydroxide may form; whether or not they will actually form depends on the characteristics of the hydroxide and specifically the surface charge of its particles. Multivalent cations and hydrochloric acid, which even under ordinary conditions are capable of increasing the surface charge of ferric hydroxide particles, concentrate on freezing in consequence of the separation of pure ice and acquire a still greater capacity for peptizing the coagulate. Mechanical disturbances in the spatial structure of the coagulate which are produced by the growing ice crystals most likely contribute to peptization.

Thus, as far as the reduction of the volume of metal hydroxides due to the action of freezing is concerned, electrolytes present in the metal hydroxides, generally speaking, exert a negative effect, because they may prevent complete freezing out of the liquid phase of the coagulate. However, in the freezing of sols concentration of coagulating electrolytes may bring about coagulation before complete freezing of the sample has taken place. But even in this case the final volume of the precipitate after thawing will depend on the completeness with which the freezing out of the liquid phase has taken place.

One must furthermore keep in mind that the degree of freezing of the coagulate will depend not only on the electrolytes which are present in the solution, but also on the hydrophilic capacity of the precipitate itself. The greater the quantity of bound water that is contained in the particles of the precipitate, the smaller will be the extent of solidification of the liquid phase in the precipitate and the lower the degree of compression of its particles. It is to be expected that with increased hydrophilic capacity of the precipitates the effect of freezing on their volume will be reduced.

SUMMARY

1. It was established that the reduction of the volume of ferric hydroxide as a result of freezing and thawing of this hydroxide depends on the temperature at which the liquid phase of the precipitate has been frozen out. If in the presence of an electrolyte the temperature of freezing is lower than the temperature of the formation of a cryohydrate by the electrolyte, the effect of freezing on the volume of the precipitate is practically independent of the quantity of electrolyte that is present; if the temperature of freezing is higher than that of the formation of a cryohydrate, the effect of freezing is greatly reduced as the concentration of the electrolyte increases.

2. Rapid freezing of the coagulate at a low temperature has a relatively small effect as far as interference with the structure of the coagulate is concerned and the precipitate retains a sizable volume after thawing.

3. Freezing increases the peptizing action of sol-forming electrolytes and thus expedites the transfer of the coagulate into the sol.

LITERATURE CITED

1. V. L. Zolotavin, V. V. Vol'khin, and V. V. Rezvushkin, Kolloidnyi Zhur. 22, 305 (1960).
2. E. I. Kvyat, Zhur. Fiz. Khim. 12, 634, 660 (1938).
3. N. N. Lyubavin, Zhur. Russ. Fiz.-Khim. Obshch. 21, 397 (1889); A. Lottermoser, Z. Phys. Chem. 60, 462, 1907; A. Lottermoser and F. Langenscheidt, Koll.-Z. 58, 336, 1932; A. Lottermoser and Q. Schmole, Koll.-Z. 89, 328, 1939.
4. A. Buzagh, Koll.-Z. 146, 133, 1956; A. Buzagh, and S. Rohrsetzer, Acta chim. Acad. Sci. hung. 10, 427, 1957.
5. A. Sieverts, and W. Petzold, Z. anorgan. und allgem. Chem. 212, 233, 1933.
6. S. V. Makarov and V. P. Blidin, Izv. Akad. Nauk SSSR, Ser. Khim. Nauk, No. 4, 865 (1938).
7. F. Jahr, A. Brechein, M. Blanke, and R. Kubens, Z. anorgan. und allgem. Chem. 270, 240, 1952.
8. P. F. Bochkarev and A. G. Bergman, Izv. Akad. Nauk. SSSR, Ser. Khim. Nauk,No. 3, 379 (1940).
9. A. G. Bergman and P. F. Bochkarev, Izv. Akad. Nauk SSSR, Ser. Khim. Nauk, No. 1, 237 (1938).
10. M. I. Ravich, Izv. Akad. Nauk SSSR, Ser. Khim. Nauk,No. 3, 233 (1943).
11. M. I. Ravich, Izv. Akad. Nauk SSSR, Ser. Khim. Nauk,No. 1, 137 (1938).
12. V. A. Sokolov, Izv. Akad. Nauk SSSR, Ser. Khim. Nauk No. 1, 123 (1938).
13. Q. Malguori, Atii Accad. Lincei 5, 892, 1927, quoted acc. to [6]; Chem. Abstrs. 21, 3842, 1927.
14. A. G. Kogan and V. I. Nikolaev, Izv. Akad. Nauk SSSR, Ser. Khim. Nauk No. 4, 823 (1937).
15. K. E. Mironov, Zhur. Obshchei Khim. 25, 1081 (1955).
16. H. T. Meryman, Proc. Roy. Soc. B 147, No. 929, 434, 1957.
17. B. J. Lyet, Proc. Roy. Soc. B 147, No. 929, 434, 1957.

All abbreviations of periodicals in the above bibliography are letter-by-letter transliterations of the abbreviations as given in the original Russian journal. *Some or all of this periodical literature may well be available in English translation.* A complete list of the cover-to-cover English translations appears at the back of this issue.

SPECTRAL INVESTIGATION OF CATION EXCHANGE ON CARBOXYMETHYLCELLULOSE

S. S. Gusev, M. A. Katibnikov and I. N. Ermolenko

Institute of Physics, Academy of Sciences, Belorussian SSR, Minsk
Translated from Kolloidnyi Zhurnal, Vol. 23, No. 2, pp. 140-144,
March-April, 1961
Original article submitted January 19, 1960

Carboxymethylcellulose and water-soluble salts of alkali metals of carboxymethylcellulose are of practical interest because the presence of carboxyl groups endows them with ion-exchange properties. The high viscosity of the solutions and the insolubility of the heavy-metal salts open up extensive possibilities for the use of carboxymethylcellulose in a number of branches of the paper, petroleum and textile industries and, in particular, in medicine[1-5]. However, ion-exchange reactions with participation of carboxymethylcellulose have been inadequately studied.

Several investigations have been carried out in which the effect of metal impurities on the physicochemical characteristics of carboxymethylcellulose was determined [1-3, 6,7]. From the analytical data of the infrared absorption spectra of carboxymethylcelluloses in the 1400-2000 cm^{-1} region for a number of exchange systems it was possible to establish the exchange equilibrium proportion of cations in the polymer phase, and on this basis to calculate the apparent equilibrium constants and activity coefficients as a function of the pH and the ion concentration [8].

Sorption by carboxylated celluloses consists mainly in ion exchange of carboxyl groups with metal cations [4, 9-11], the course of this reaction depending on the pH, the concentration and the nature of the cations [12,13]. The case of the sorption of iron cations from dilute solutions is particularly important and interesting because it is the most widespread in practice [14-16]. An investigation by means of infrared spectroscopy of the sorption of iron by celluloses oxidized by periodate and chlorite [17] led to the assumption that the sorption of cations by these products from dilute solutions takes place via reaction with carboxyls, the most important factor determining the sorption of cations by this means being the equilibrium pH of solutions.

Together with an investigation of the thermodynamics of the process, infrared spectroscopy can give additional information on the kinetics and mechanism of ion exchange. It is known that in the majority of cases the kinetics of sorption on different acid cationites is determined by diffusion [18]. But this is sometimes not the case for carboxylic cationites [19]. It was therefore important to assess the role of diffusion in sorption on cellulose carboxylic cationites, which would make it possible to select the most favorable conditions for their use. H-Fe exchange on fibrous preparations of oxidized celluloses was investigated in [17].

In the present work, exchange on more densely packed preparations in the form of films was investigated. In addition, exchange on cationite in salt form by the system Na-Fe was investigated, the mechanism of this being of independent interest.

For the spectral investigation we used a previously developed [8] method for obtaining thin films of Na-carboxymethylcellulose (degree of esterification 78%) from aqueous solutions.

A specific amount of a 1% solution of Na-carboxymethylcellulose was poured onto a horizontal glass surface. After they had been dried slowly under high moisture conditions the even films which formed were removed from the base and treated with 0.1 N ferric chloride solutions. The pH of the equilibrium solutions was determined by means of an LP-5 pH-meter with a glass electrode. The treated films were washed with ethyl alcohol, dried at room temperature and used for the spectral investigation. The films obtained were insoluble in water and were stronger than films of the initial Na-carboxymethylcellulose. This is explained among other reasons by the character of the sorption of polyvalent cations in contrast to monovalent cations. When polyvalent cations combine with carboxyl groups each cation can react with more than one group [20-22]. The latter leads to the formation of a space lattice and therefore to an increase in the packing density.

The film thickness, determined by means of an IZV-1 device (for measuring thickness), was 8-15 μ. The ultraviolet absorption spectra were obtained in an IKS-11 spectrophotometer with recording of the spectrum on a self-recording potentiometer and in an IKS-14 spectrophotometer with NaCl prisms in the 1300-2000 cm^{-1} region. The optical density D was converted to unit thickness of the film d (in centimeters).

The total value of the sorption of iron cations was assessed qualitatively from the absorption spectra in the ultraviolet region [23]. Processing of films of Na-carboxymethylcellulose by $FeCl_3$ solutions with different pH leads to a marked increase of absorption in the 300-400 mμ region (Fig. 1).

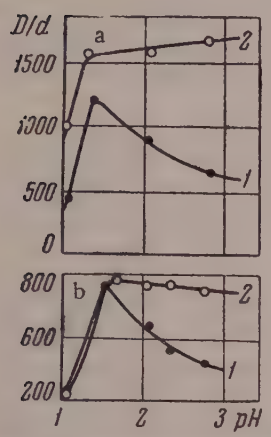


Fig. 1. The relationship between the absorption of films of Na-carboxymethylcellulose treated with $FeCl_3$ solutions for 15 min (I) and 180 min (2): a) in the ultraviolet region at 350 mμ; b) in the infrared region at 1580 cm^{-1}.

The contact time of the film with the $FeCl_3$ solution was selected on the basis of preliminary experiments in such a way that it corresponded to the commencement of the sorption process (15 min) and the end (180 min), close to equilibrium sorption. In the latter case, for less acidic solutions sorption is close to the limiting value, in contrast to more acidic solutions, where there is partial transfer of the polymer into the solution.

Similar results were obtained during an investigation by physicochemical methods of hydrogen-deuterium exchange for carboxylic cationites [24]. A decrease in pH causes a reduction in sorption, and the rate of exchange is greater in acid media than in neutral media. To determine the mechanism of the reaction of cations with an ion exchanger, infrared spectra of these products were investigated. The position of the maximum of the absorption band, corresponding to antisymmetric vibration of the carboxylate group, depends on the character of the cation of the salt formed [13]. This makes it possible to determine in sorption products both the content of undissociated carboxyls and also the Na- and Fe-carboxylate groups separately. The stretching vibration $\rangle C=O$ of the free carboxyl groups occurs at 1730 cm^{-1}. As a result of salt formation a metal-carboxylate group is formed. Antisymmetric vibration of the $\rangle COO^-$ ion occurs in the 1550-1640 cm^{-1} region, depending on the mass of the substituting cation [12,13,25,26].

Figure 2 gives the absorption spectra of the investigated films in the 1500-1800 cm^{-1} region. When Na-carboxymethylcellulose is treated with a solution of ferric chloride, and Na^+ in carboxylate groups is replaced by Fe^{3+} in carboxylate there is a reduction absorption at 1610 cm^{-1} and an increase at 1580 cm^{-1}. At the same time there is an increase of absorption in the region of free C=O at 1730 cm^{-1}, which indicates an accumulation of free carboxyl groups. This effect is observed for both acidic and less acidic solutions, but in the early stages of sorption. The general character of the sorption of iron (Fig. 1, a and b) is determined by its sorption with participation of carboxyl groups.

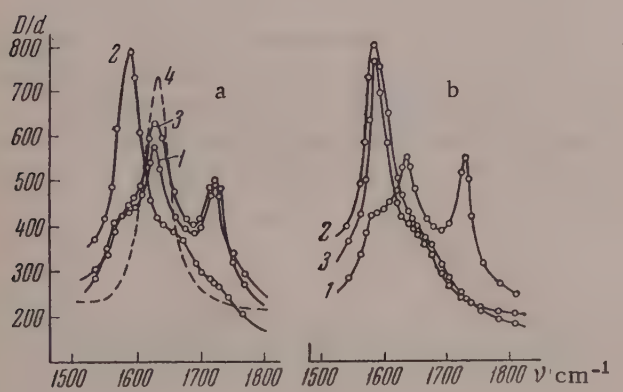


Fig. 2. Infrared absorption spectra of films of Na-carboxymethylcellulose treated with $FeCl_3$ for 15 min (a) and 180 min (b): 1) pH 1; 2) pH 1.3; 3) pH 2.8; 4) initial Na-carboxymethylcellulose.

It may be assumed that the reduction in the rate of ion exchange with an increase in pH is due to the following factors:

1. With a change in pH the state of the solution changes, influencing the ratio of the content of simple and complex ions (which in the present case includes Cl^-, OH^- and H^+ ions as well as Fe^{3+}).

2. At low pH the reaction does not extend into the bulk of the solution and sorption is localized in the surface layer, in contrast to sorption from solutions with a high pH. The kinetics of this process are determined mainly by a rapid surface reaction.

3. A reduction in the diffusion rate after saturation of the outer layers of the film, in which the packing den-

sity increases as a result of cross linking by the polyvalent iron cation. A similar effect is observed for many heterogeneous reactions.

The latter factor evidently plays an essential role in the observed reduction of the rate of ion exchange. Although our experimental data do not contradict the assumption of the localization of the reaction in the surface layer for more acid solutions, the low value of equilibrium sorption at these pH's for insoluble preparations of fibrous celluloses makes it possible to assume that in the present case the observed effect is not related only to localization of the reaction at the surface.

A very interesting sorption phenomenon is the desorption of Na^+ without corresponding absorption of Fe^{3+}, observed at the commencement of the reaction, as shown by Fig. 2. Sorption from a solution with pH 2.8 takes place initially with an increase in the total content of free carboxyls; it then decreases again. In the case of sorption from a solution with pH 1.1, the content of free carboxyls in the sample increases continuously with the sorption time up to the equilibrium state corresponding to the acidity of this solution.

These variations may be expalined by the fact that, in contrast to the slow diffusion of Fe^{3+}, the diffusion of acid into the volume of the polymer takes place rapidly and causes desorption of Na. The subsequent sorption of Fe^{3+}, slowly undergoing diffusion and sorption from a more acid medium than Na^+, leads again to a reduction in the strength of the C=O bond in the absorption spectrum.

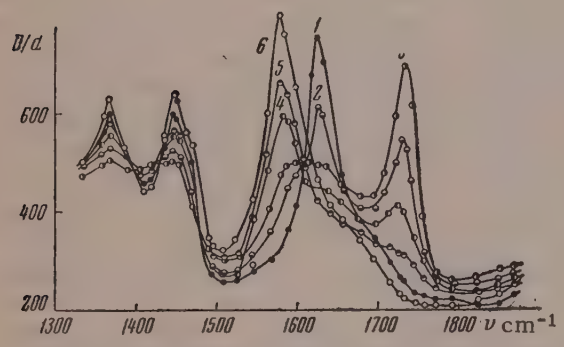


Fig. 3. Infrared absorption spectra of Na-carboxymethylcellulose treated with buffer solutions of $FeCl_3$ for 180 min: 1) initial Na-carboxymethylcellulose; 2) pH 1.2; 3) pH 1.4; 4) pH 1.8; 5) pH 1.9; 6) pH 2.8.

The relation between the strengths of the absorption bands of carboxyl, Na- and Fe-carboxylate groups and the acidity of the solutions was determined in a wide range of pH, using buffer solutions (HCl + NaCl buffer). The results of the experiment are given in Figs. 3 and 4. The partial transfer of the polymer into the solution, which takes place simultaneously with iron exchange, prevents investigation in solutions of higher acidity. Moreover, in the latter, equilibrium is not reached during the 180 minutes of the experiment. On this basis, the considerable strength of the absorption band of COONa groups in the undissolved residue of the film treated with more acid solutions, and the reduction in the strength of this band with an increase in pH (curve 1, Fig. 4), are explained by the variation in the rate of dissolution of the polymer. At low pH, dissolution takes place far more rapidly than ion exchange, and the residue contains a greater amount of combined Na. This process is accompanied by COONa → COOH ion exchange (curve 2, Fig. 4). The marked fall of curve 2 after the maximum corresponds to the combination of COOH groups with iron cations

cel. − O − CH_2 − COOH → cel. − O − CH_2 − $COOFe_{(1/3)}$

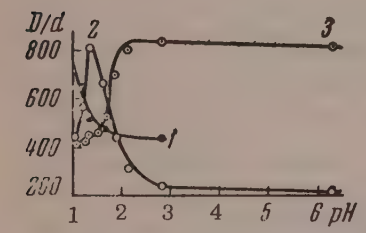


Fig. 4. Variation of the absorption intensity at 1610 cm^{-1} (1), 1730 cm^{-1} (2) and 1580 cm^{-1} (3) in relation to the pH of the solutions. Sorption time 160 min.

Thus, Na → Fe ion exchange in carboxymethylcellulose films takes place according to the system: Na → H → Fe, the essential role in the kinetics of this process being played by diffusion. The use of fibrous carboxyl ion exchangers with a highly developed surface, for which the role of diffusion into the volume is not as important, would obviously make it possible to accelerate the process of ion exchange.

SUMMARY

1. Like the sorption of iron via reaction with carboxyl groups, the over-all sorption of iron by Na-carboxymethylcellulose films takes place more slowly at high pH.

2. In the early stages of sorption from solutions a considerable increase in the strength of absorption bands of COOH groups is observed in the infrared spectra; this strength then decreases with a corresponding increase in the strength of the band of the Fe-carboxylate groups. In the given case, exchange includes two stages

cel. − O − CH_2 − COONa → cel. − O − CH_2 − COOH → cel. − O − CH_2 − $COOFe)_{(1/3)}$

In the case of films, there is a significant time lag between these stages as a result of the slower diffusion of Fe^{3+} compared with H^+ in the layer of the product.

The authors wish to express their thanks to A. N. Sevchenko and B. I. Stepanov for their valuable advice, and to N. A. Borisevich for his help in carrying out the experiment.

LITERATURE CITED

1. G. A. Petropavlovskii and G. G. Vasil'eva, Zhur. prikladnoi khim. 30, 1932 (1957).
2. E. Wurz, Oster. Chem. Ztg. 59, 41, 1958.
3. O. Wurz and E. Wurz, Techn. Rundschau 12, 259, 1957.
4. R. Rummerer, Chem. Textilfasern, Filme und Folien., 1953, p. 723.
5. K. F. Zhigach, M. Z. Finkel'shtein and E. M. Mogilevskii, Khim. nauka i prom. 2, 1, 76 (1957).
6. S. Sansel, Analyt. Chem. 20, 142, 1948.
7. N. Asandei, C. H. Vasilin, and C. Simionesku, Stadii si ceretari stiiut. Acad. RPR, Fil Jasi. Chem. 8, No. 1, 201, 1957.
8. H. Sobue and Y. Tabata, J. Polymer. Sci. 20, 567, 1956.
9. E. Ott, Cellulose a. Cellulose Derivatives, N.Y., 1954.
10. V. I. Ivanov and I. Ya. Lenshina, Izvestiya Akad. Nauk SSSR, otd. khim. n. 1956, 4, 506.
11. E. Husemann and O. H. Weber, J. prakt. Chem. 159, 339, 1942.
12. I. I. Ermolenko and R. G. Zhbankov, Kolloidn. zhur. 20, 429 (1958).
13. I. I. Ermolenko and R. G. Zhbankov, Zhur. fiz. khimii 33, 6 (1959).
14. W. A. Bell and I. M. Gibson, Nature 180, 1065, 1957.
15. E. D. Kaverzneva, Doklady Akad. Nauk SSSR, 3, 481 (1951).
16. V. I. Ivanov, E. D. Kaverzneva and Z. P. Kuznetsova, Izvestiya Akad. Nauk SSSR, otd. khim. n. 1953, 2, 374.
17. I. N. Ermolenko and R. G. Zhbankov. Doklady Akad. Nauk Belorrusian SSR 3, 5 (1959).
18. M. M. Senyavin, "Ion exchange;its use", abs. symp., 84 (1959).
19. D. Conway, I. Green, D. Reichenbery, Trans. Farad. Soc. 50, 511, 1954.
20. A. M. Sookne and M. Hurris, J. Res. Nat. Bur. Stand. 26, 205, 1947.
21. O. G. Efremova and I. K. Kosyreva, Nauchn. ezhegodn. Saratovsk. un-ta, 552 (1954).
22. S. I. Orlov and S. A. Glikman, Nauchn. ezhegodn. Saratovsk. un-ta, 446 (1956).
23. I. Abraham and I. Hegedus, Z. Anorg. Chem. 244, 98, 1940.
24. Fodorne, Ganyi. Maghar. kem. folgóirat. 64, 417, 1958.
25. I. Schorz, and E. Kienzl, Monatsh. Chem. 88, 1017, 1957.
26. L. Robert, and I. Favre, Microchim. acta. No. 2-3, 517, 1955.

All abbreviations of periodicals in the above bibliography are letter-by-letter transliterations of the abbreviations as given in the original Russian journal. *Some or all of this periodical literature may well be available in English translation.* A complete list of the cover-to-cover English translations appears at the back of this issue.

THE AGING OF ANION EXCHANGERS

A. T. Davydov and G. M. Lisovina

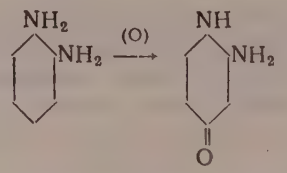
Khar'kov University, Department of General Chemistry
Translated from Kolloidnyi Zhurnal, Vol. 23, No. 2, pp. 145-149.
March-April, 1961
Article submitted January 22, 1960

The change in the physical and chemical properties of ion exchangers which results in the partial or the complete loss of their sorption capacity has been called aging. The aging of anion exchangers originates from an unfortunate choice of the operating conditions or from mechanical destruction of the sorbent granules [1]. Frequent sharp rises and lowerings in the temperature of the solutions treated have a great influence on the wear characteristic of resins [2]. The presence of hydroxyl ions in the resin has a noticeable repercussion in the gradual lowering of the sorption capacity, when the exchangers are stored [3]. Varying flow rates during filtration, arbitrary dimensions and shape of the filters, frequent sharp changes in the pH values of the solutions treated and other factors [4] contribute also to the aging of anion exchangers.

Solutions of the various oxidizing agents are the most aggressive media in which aging takes place. It has been shown [5,6] that, after treatment with such oxidizers as $KMnO_4$, HNO_3, chlorine water or oxygen dissolved in water, the sorption capacity of the anion exchangers studied had decreased noticeably. Simultaneously with the loss of basic properties, by oxidation the anion exchangers acquire acidic functions and this gives them an amphoteric character. The latter indicates that not only the number of functional groups is lowered and the sorption capacity is diminished but that also more thorough processes take place inside the resin (condensation reactions).

When the causes of anion exchanger aging were studied, it was pointed out [6,7] that during the use of the exchangers there are sorbed products, insoluble in water and containing the hydrogen cation, which can be exchanged for other cations. Moreover, the ability of anion exchangers to exchange cations is explained by a slow diffusion of the sodium hydroxide molecules which have been sorbed during the regeneration of the sorbent and by the oxidation of the exchanger by the oxygen of the air dissolved in the solutions treated. The known schemes of exchange reactions on an aged anion exchanger point out which ion exchange mechanism is possible, but do not disclose the chemical nature of the aging process.

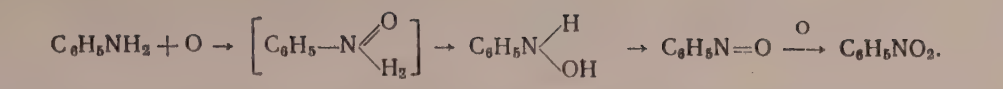
By the oxidation of amines, according to existing schemes [8], there is formed a series of unstable intermediary products, which by further oxidation are converted into azobenzene, hydrazobenzene, azoxybenzene, paraquinone and even into quinones and quinone imines. The composition of the thus-formed colored products is insufficiently clear. According to these ideas, aminoresins when oxidized may give compounds of the quinone imine type



(1)

The obtained oxidation product of the amines—quinone imine— obviously will have an amphoteric character, since it contains a primary amino group with basic properties and an imino group, which is able to display an acidic character. For instance, in sulfathiazole the hydrogen atom in the imino group adjacent to the SO_2-group can be replaced quantitatively by metals. An acidic character of the imino group is found in pyrrole, carbazole, diphenylamine and others. Consequently, in all those cases where the hydrogen atom of the imino group is influenced by negative groups or suitably located double bonds, this group acquires an acidic character. In the quinone imine mentioned above the acidic properties of the imino group originate from the influence of the system of conjugated double bonds.

It is known that aromatic amines and other amino derivatives when deprived of impurities are good antioxidants, but lose their antioxidation ability, when they are mixed with other components [9]. In our case the oxidation of amines even may not lead to an end product containing hydrogen, but may give a nitro group or a free radical [10]



(2)

We attempted to study the causes of the fundamental changes in the anion exchanger structure and the influence of aging upon the exchange capacity and the kinetic properties of the sorbents.

The anion exchangers MFD, MN, MMG(1), N, MD, AN-9F, ÉDÉ-10, which were selected for their various degrees of basicity and time of preparation, were examined experimentally. The said exchangers were saturated with chlorine ions and, after that, their sorption capacity was determined by taking the nitrate ion as the displacing anion. The oxidation of the anion exchangers saturated with the nitrate ion was carried out in 1 N solutions of $KMnO_4$ and H_2O_2 in an acid or a basic medium at 70° during three hours. In the first case the reaction between the anion exchanger in the nitrate form and the oxidizer took place in a 0.2 N H_2SO_4 solution and in the second case in a 0.2 N NaOH medium, but now the exchanger was used in its hydroxyl form. After the oxidation the sorbents were saturated with chlorine ions from a $CaCl_2$ solution and then again their sorption capacity was determined from the amount of chlorine and Ca ions desorbed by a KNO_3 solution.

The influence which aging of the resins has upon their kinetic properties was investigated on the anion exchanger ÉDÉ-10 in various sizes, saturated with chlorine ions, that is, for granule sizes 3-2 mm and 0.5-0.25 mm. Before and after oxidation the exchange of the chlorine ions with anions of various natures and sizes (OH^-, SO_4^{2-} and $C_6H_5SO_3^{2-}$) was followed as a function of time.

TABLE 1

The Influence of Oxidation upon the Sorption Capacity of Anion Exchangers

Anion exchanger brand	Sorption capacity after oxidation. mg-eq 100 g	Sorption capacity after oxidation (mg-eq/100 g)				Amount of Ca^{2+} desorbed				
		in alkaline medium		in acidic medium		in alkaline medium		in acidic medium		before oxidation of the anion exchanger
		$KMnO_4$	H_2O_2	$KMnO_4$	H_2O_2	$KMnO_4$	H_2O_2	$KMnO_4$	H_2O_2	
MN	146,3	80,5	58,6	—	148,0	6,6	2,0	—	1,6	—
MFD	15,0	2,6	0,0	4,8	15,1	13,6	10,2	6,4	2,4	—
MMG(1)	307,5	167,2	85,9	193,0	261,5	7,8	2,6	5,5	2,2	—
N	156,9	111,0	75,3	102,5	158,0	3,8	4,1	3,9	2,6	2,6
MD	106,8	35,6	0,0	71,1	87,9	1,7	2,8	2,5	2,6	—
AN-9F	279,8	121,6	0,0	113,9	217,9	1,8	3,5	6,8	2,7	—
EDE-10	473,0	75,0	—	—	—	3,7	—	—	—	2,7

As is evident from Table1, all exchanger samples investigated are oxidized the most intensively by hydrogen peroxide in the alkaline medium. The sorption capacity decreased by 2-3 and 5 times, but the exchangers MFD, MD and AN-9F had completely lost their ability to sorb. The low value of the sorption capacity of the unoxidized exchanger MFD (15 mg-eq/100 g sorbent) draws the attention. The anion exchanger MFD was synthesized in our laboratory in 1945 and had a sorption capacity of 140 mg-eq/100 g sorbent. After it had been operated during 20-30 regeneration cycles, this exchanger was stored in the laboratory in a plain glass jar during 15 years. The fact that the sorption capacity of the anion exchanger MFD has decreased by about ten times shows that there are not only external changes in the sorbent surface resulting from a slow oxidation, but also more complex processes occur, which take place inside the resin granules.

The anion exchangers MMG(1) and N were found to have the greatest stability both in the alkaline and the acidic medium. In the acidic medium the weakly basic exchangers MFD, MN and AN-9F did not lose much of their sorption capacity. Simultaneously with the ageing of the anion exchangers, which is manifested by a sharp drop in the sorption capacity, it was found that amphoteric properties, that is, acidic functionalities make their appearance. All exchangers, when oxidized in the alkaline or acidic medium sorbed the Ca-ion and exchanged it with other cations from the solution. The highest value for this exchange was attained in the anion exchangers: MFD, MN and MMG (1).

Attempts to restore the completely lost sorption capacity of the anion exchangers MFD, MD and AN-9F by treatment with such a strong reducing agent as $(NH_4)_2SO_3$ did only give negative results. A lowering of the amphoteric properties was only found for the exchanger brand MFD.

TABLE 2

The Influence of Oxidation upon the Desorption Kinetics of Anions

Time, hr	Sorption capacity of the exchanger, mg-eq/100 g											
	before oxidation		after oxidation		before oxidation		after oxidation		before oxidation		after oxidation	
	1*	2**	1*	2**	1*	2**	1*	2**	1*	2**	1*	2**
	EDE-10Cl + NaOH				EDE-10Cl + Na_2SO_4				EDE-10Cl + $NaC_6H_5SO_3$			
0,25	372	—	55,6	—	—	—	54,2	46,3	186	—	—	53,5
0,50	386	—	58,7	—	343	340	55,9	51,2	262	273	—	54,3
0,75	395	398	58,8	—	349	340	55,9	51,2	—	274	—	54,3
1	400	400	58,8	—	349	340	55,9	51,2	270	278	—	—
1,5	410	402	—	—	350	341	—	51,2	—	279	—	—
2	415	403	—	—	351	341	—	51,2	282	279	—	54,3
2,5	420	406	58,6	—	351	341	55,9	—	282	279	—	—
3	427	406	—	—	351	—	—	51,2	282	279	—	—
4	427	406	58,8	—	351	341	55,9	—	—	—	—	54,3
4,5	427	406	—	—	351	—	—	51,2	—	279	—	—
6	427	406	58,5	—	351	341	55,9	51,2	282	279	—	54,3
24	427	406	58,8	—	351	341	55,9	51,3	282	279	—	54,3
96	427	406	—	—	—	—	—	51,3	—	—	—	—

* 1) granule size 2-3 mm; ** 2) granule size 0.25-0.5 mm.

From the data given in Table 2 it is evident that an increased dispersion of the anion exchangers has hardly any influence on the sorption capacity, whereas such an influence has been found for sorbents of mineral origin. In all cases considered in this paper, the anion exchangers with granule size 3-2 mm certainly had a higher sorption capacity than the same exchanger with granule size 0.5-0.25 mm had, but these differences are small. The same results were also found for the anion exchangers which had been oxidized. On aged and oxidized anion exchangers, independent of the nature of the anions exchanged and the granule size, the sorption equilibria is established considerably faster than is the case before oxidation (0.5 and 1.5-2 hours, respectively). Obviously, in an aged ion exchanger the number of ionogenic groups has decreased and for this reason aged exchangers are more accessible for exchange. The amount of chlorine ions exchanged with the other anions at a constant concentration of the latter varies and is found to be 427, 351, 181 mg-eq/100 g sorbent. As regards aged anion exchangers, there such variations in the sorption capacity were not observed but the existing variations were small (58.8; 51.2; 54.3).

In order to confirm the situation explained above and to verify whether the amines age to quinone imines or to compounds, aqueous and alkaline extracts from the aged anion exchangers were tested for the presence of quinones by means of the usual reaction with KI. Quinones were detected in almost all exchangers studied, the following ones excepted: ÉDÉ-10, which does not contain phenol rings and the brands MFD and MD, which contain metaphenylenediamine. The nitro group, which we tried to determine by the reaction of Konovalova [11], in no case could be detected. It must be supposed that during oxidation the anion exchangers are mainly converted into quinone imines and other similar reaction products.

The degree of swelling hardly changes during aging, that is, the changes taking place during aging of anion exchangers mainly occur on their surface and do not result in the destruction of the resins.

SUMMARY

1. When samples of the anion exchangers MFD, MN, MMG(1), N, MD, AN-9F and ÉDÉ-10 were oxidized by hydrogen peroxide in an alkaline medium, their sorption capacities were found to have decreased sharply. MMG(1) and N appeared to be the most stable of the anion exchanger brands studied, but in an acidic medium this was the case for the weakly basic exchangers MFD, MN and AN-9F.

2. As a result of aging nearly all anion exchangers studied acquire the ability to exchange cations and this is most clearly manifested at the oxidation of weakly basic exchangers.

3. After the oxidation of an aged resin the sorption equilibrium was established 3-4 times faster than was found on the same anion exchanger before the oxidation.

4. It has been proposed that the aging mechanism and the appearance of amphoteric properties of anion exchangers as a result of their oxidation is confirmed by the presence of quinones and quinone imines having an imino group with an acidic character, as is found in all aged resins, except MFD, MD and ÉDÉ-10.

5. Attempts to revive the lost sorption capacity of aged anion exchangers by treating them with such a strong reducing agent as $(NH_4)_2SO_3$ only led to negative results.

6. To protect anion exchangers against untimely aging it is necessary to choose such operation conditions that the influence of oxidizers (especially in alkaline media) is excluded as far as is possible and to avoid frequent changes in the pH of the solutions treated.

LITERATURE CITED

1. F. G. Prokhorov and N. P. Lapotyshkina, Izvest. VTI, No. 4, 7 (1953); V. P. Meleshko, O. V. Chervinskaya, M. N. Romanov and D. P. Izmailova, Zhur. Priklad. Khim. 30, 5, 808 (1957).
2. N. G. Polyanskii, Izvest. Vyssh. Shkoly, Khim. i Khim. Tekhn. No. 1, 164 (1958); Wear of High-Polymers [in Russian] (State Technical Press, 1957), p. 108.
3. A. B. Davankov and V. M. Laufer, Studies in Ion Exchange Chromatography [in Russian] (Acad. Sci. USSR Press, 1957), p. 129; R. M. Wheaton and W. C. Bauman, Industr. and Engng. Chem. 43, No. 5, 1088, 1951.
4. E. B. Trostyanskaya and A. S. Tevlina, Studies in Ion Exchange Chromatography [in Russian] (Acad. Sci. USSR Press, 1957), p. 117.
5. K. M. Saldadze and Z. G. Demonterin, Studies in Ion Exchange Chromatography [in Russian] (Acad. Sci. USSR Press, 1957), p. 106.
6. F. G. Prokhorov, Theory and Practice of the Use of Ion Exchanging Materials [in Russian] (Acad. Sci. USSR Press, 1955), p. 59.
7. F. G. Prokhorov, A. M. Prokhorova and K. Ya. Yankovskii, Teploénergetika, No. 3, 3 (1954).
8. L. F. Fieser and M. Fieser, Organic Chemistry [Russian translation] (Moscow, IL, 1949), p. 536.
9. N. I. Chernozhukov and S. É. Krein, Oxidizability of Mineral Oils [in Russian] (State Fuel Technics Press, 1946), p. 107; K. P. Medvedev, Dissertation [in Russian] (Khar'kov, 1948), p. 48.
10. R. P. Goldschmidt, Ber. 53, 28, 1920.
11. M. I. Konovalov, Ber. 28, 1851, 1895.

All abbreviations of periodicals in the above bibliography are letter-by-letter transliterations of the abbreviations as given in the original Russian journal. *Some or all of this periodical literature may well be available in English translation.* A complete list of the cover-to-cover English translations appears at the back of this issue.

THE PREPARATION AND PROPERTIES OF AQUEOUS DISPERSIONS OF VULCANIZED SYNTHETIC AND NATURAL RUBBERS

B. A. Dogadkin, G. N. Zachesova and I. A. Shokhin

Scientific and Research Institute of the Tire Industry, Moscow

Translated from Kolloidnyi Zhurnal, Vol. 23, No. 2, pp. 150-156,
March-April, 1961
Original article submitted October 26, 1960

Aqueous dispersions of polymers are of great interest, in that they represent complicated and peculiar colloidal systems with a very wide field for practical application. The dispersion process for rubber and crude synthetic rubber mixtures has been studied in the works of Dogadkin [1]. The process for obtaining dispersions of vulcanized synthetics has not been sufficiently studied up to now, in spite of its fundamental importance, which is due to the possibility which this would open up for widespread and effective application of shock-absorbing synthetic rubber materials.

As early as the 1930's, Dogadkin, Koshelev and Tartakovskii [2] suggested a method for regenerating synthetics based upon dispersing them in an aqueous medium. For a variety of reasons, however, this method did not receive wide industrial application*.

As the result of recent investigations [3], the procedure necessary for the dispersion of synthetic rubbers in an aqueous medium has been materially simplified, and a continuous method has been developed which produces very fine and stable dispersions. The regenerate obtained from an aqueous dispersion of vulcanizates of divinylstyrene rubber by means of electrolytic coagulation is of high quality and, in the vulcanized state, approximates the quality of the original rubber obtained from caoutchouc. The aqueous resin dispersion ("resin latex") may be capable of application in road surfaces, and also for the preparation of sponge rubber articles, for impregnation of fibrous materials, etc.

The investigations have mainly been performed on resins of the protector type, impregnated with highly dispersed active carbon, prepared under laboratory conditions from divinylstyrene rubber SKS-430ARM. These resins are most difficult to destroy, and their regeneration by any method is always most complicated. The effect of the type of polymer present in the initial resin on the course of its dispersion has been studied on protector resins from cis-polyisoprene (SKI), natural (NK) and also sodium butadiene (SKB) rubbers.

Aqueous dispersions of the vulcanizates were prepared by the method worked out by Dogadkin and Pevzner [4]. The essence of the method consists in introducing into the hydrocarbon medium (rubber, plastic mass or vulcanizate) an olephilic emulsifier which is insoluble in water (fatty acids, resin acids, etc.), of a nature easily dispersed in the hydrocarbon medium. Subsequently, with continuous stirring, an aqueous solution of a saponifying agent (alkali) is introduced gradually. In the initial stages this is distributed in the hydrocarbon medium as the disperse phase. When the necessary quantity of water and emulsifying agent, according to the Bancroft equation, has been introduced, phase reversal occurs, producing an aqueous dispersion of the hydrocarbon. This sequence of operations, as many experiments have shown, leads to the formation of a highly dispersed system with only slight loss of mechanical energy. The theoretical basis of the process is presented in [1].

In our case the ground resin containing the emulsifier and an activation substance was treated for 8-10 minutes on laboratory grinding rollers with clearance of 0.3-0.5 mm. The roller temperature was varied according to the nature of the emulsifier. It is known that the stabilizing power of an emulsifier is most effective when the emulsifier particles have the optimum degree of micelle formation, which depends on the temperature. Increase in temperature may cause the emulsifier to give a true, rather than a colloidal solution. In particular, salts of oleic acid have optimum stabilizing power at room temperature, and the resin acids at 50-60°.

* In the factory "Red Triangle" this method was used in 1938 to plan the production of a regenerator from pressings. Production was discontinued in 1941 on account of the war.

TABLE 1

Dimensions of Particles in an Aqueous Dispersion of a Protector Resin from SKS-30ARM, Obtained by the Use of Emulsifiers in the Form of Acids

Emulified	Quantity of emulsified, g/100 g resin	Mean particle radius, microns
Resin	10	0.241
Oleic Acid	10	0.514
Naphthalene β-Sulfonic acid	5	2.045
β-Dinaphthylmethanesulfonic acid	5	3.14
The same	10	4.41

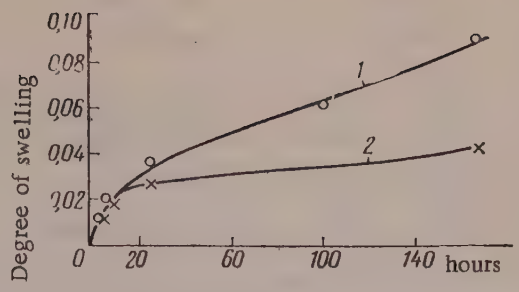


Fig. 1. Kinetics of swelling of a resin sheet containing resin at 20° during a period of 170 hours: 1) in distilled water; 2) in 5% aqueous sodium acetate.

After the formation on the rollers of a relatively dense sheet an aqueous alkali solution was gradually added to the resin. The alkali concentration in different experiments varied from 2 to 10% and the time taken in adding the solution was varied accordingly. In the first stage absorption of the alkaline solution was accompanied by the dispersion of the water within the resin, which was in consequence softened. This fact permitted of gradual widening of the roller spacing, and increase in the rate of alkaline addition. After sufficient of the alkaline solution has been added for the complete saponification of the emulsifier in the resin, and its conversion into a water-soluble form, phase reversal takes place, forming a dispersion of the resin in water in the form of a pasty mass. This mass was removed from the rollers and diluted with water to give a dispersion of predetermined concentration. The time which elapses before phase reversal takes place depends on the concentration of the alkali and the conditions under which it is added [1]. At this point the resin has absorbed 7-8% of water.

The aqueous dispersion is evaluated according to the size of its particles. Relatively coarse dispersions were studied by a sedimentation method by means of a Figurovskii balance [5]. For finer dispersions electron-microscopic* and photoelectrocolorimetric methods were used [6].

In the course of dispersing the vulcanized resin was submitted to the influence of a number of physico-chemical and mechanico-chemical factors. Mechanical factors played a twofold role. On the one hand, mechanical treatment produces a direct plasticizing effect on the resin, due to the mechanical rupture of the molecular chains and cross-links of the vulcanizate structure; and, on the other hand, it facilitates the entry of the aqueous alkali into the resin: that is, it facilitates the subsequent splitting up of the vulcanizate under the peptizing influence of the emulsifiers. The fact of the acceleration of resin swelling in aqueous alkali may be established by the observation that 30 minutes treatment on the rollers causes a resin containing emulsifier to absorb 7-9% of moisture independent of the nature of the emulsifier used and of the temperature of the rollers. At the same time the swelling of the resin through diffusion of the alkali is very slight and proceeds at a low rate (Fig. 1).

TABLE 2

Dispersion of Protector Resin from SKS-30ARM Using Various Saponifying Agents

Saponifying agent	NaOH	KOH	KOH	NH_4OH	NH_4OH
Concentration of saponifying agent %	5	5	7	5	10
Mean particle radius %	0,24	0,22	0,20	Not dispersed	

The basic physico-chemical factors effecting the duration of the resin-dispersion process are: the nature of the emulsifier, and the concentration and conditions of addition of the alkaline solution.

* Electron microphotography was performed by S. A. Simanovskii.

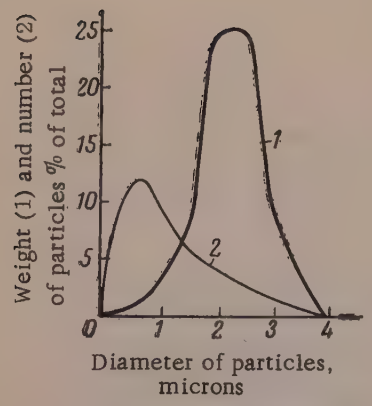


Fig. 2. Weight (1) and numerical (2) distribution of particles of a dispersion obtained from resin (from electron microscope data).

The most important mechanico-chemical factors are: distance between the rollers, friction, energy consumption, and effect of chemical plasticizing agents.

Nature of emulsifier. The emulsifiers used were: oleic acid, rosin, naphthalene-β-sulfonic acid, β-dinaphthylmethanesulfonic acid, and the sodium soaps of long chain acids. Preliminary experiments showed that the optimum quantity of emulsifier was 5-10% of the resin weight.

Table 1, Fig. 2 and Fig. 3 show that the best results were obtained using rosin. The dispersion obtained with this stabilizer was subsequently used for various practical purposes.

The use of ready-made soaps as emulsifiers led to the formation of coarsely dispersed systems (Fig. 4) with a tendency to aggregation on slight dilution. It is thus seen that a necessary condition for procuring fine and stable dispersions is the saponification of the emulsifier in situ in the course of dispersion. This principle lies at the basis of the method for obtaining dispersions used by Dogadkin [4].

Nature of saponifying agent. To elucidate the effect of different saponi-

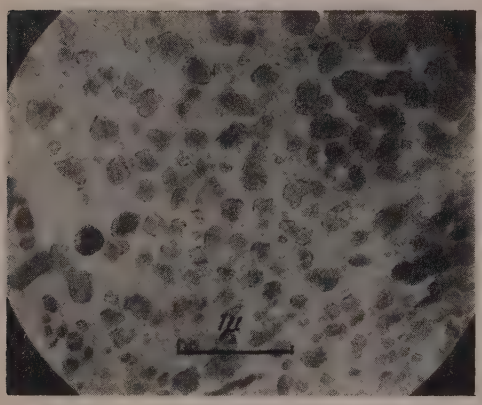


Fig. 3. Electron microphotograph of a dispersion obtained using rosin.

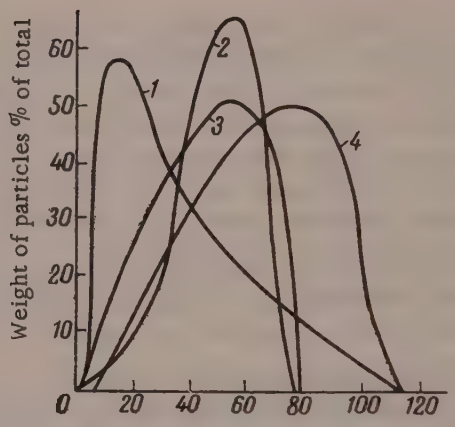


Fig. 4. Curves for the weight distribution of particles in dispersions obtained using various emulsifiers in the form of soaps (from sedimentation analysis data): 1) leucanol; 2) hexal; 3) sodium naphthalenesulfonate; 4) rosin soap.

fying agents on the properties of the dispersions, aqueous solutions of sodium, potassium and ammonium hydroxides and of borax were used, dispersion being carried out on a resin containing rosin (Table 2). From Table 2 it is seen that the dispersions obtained from the caustic alkalis are closely alike in their characteristics. Using ammonia to achieve dispersion on rollers, however, it was not possible to reach the phase-reversal point because of the volatility of the ammonia.

Phase-reversal was also unobtainable with borax. It appeared from experiment, however, that borax might be used to replace two thirds of the alkali requirement, giving a dispersion with particle radius of 0.59 micron.

Concentration of alkali solution. Increase in alkali concentration led to a reduction in the time required to disperse the resin , and in the quantity of solution needed for phase-reversal. Change also occurred in the dispersivity of the particles, as the data on the next page show.

Conditions of addition of alkali solution. Particle sizes depends considerably on conditions of addition of alkali

Concentration of aqueous alkali, %	2	5	10
Dispersion time minutes	90	50	35
Quantity of alkali solution required for phase reversal g/100 g resin	67–83	33	25
Mean particle radius, microns	.0.249	0.241	0.555

to the resin-emulsifier mixture. Rapid addition of alkali (Fig. 5, Curve 2) forms a dispersion with relatively coarse resin particles. In this case the alkaline solution is poorly distributed through the resin and saponification of the emulsifier occurs on the surface of large aggregates separated from the main bulk of the resin. Too slow addition of the alkali may produce an equilibrium between the quantity of water introduced in the solution and that evaporated from the system.

The alkaline solution should be added at such a rate as will produce deep-seated penetration and even distribution in the resin. Saponification then occurs in thin films of the aqueous phase, which constitute the "spumoid" structure of the system* [7]. When this structure is destroyed at the time of phase-reversal, a fine dispersion of the resin in water is obtained (Fig. 5, curve 1).

If the aqueous dispersion is to be sufficiently stable, its pH should not be less than 11.5-12.0. Lower values of the pH lead, on storage and dilution, to local coagulation of the dispersion.

Spacing between rollers. Treatment of a vulcanized resin on rollers spaced at 1.5 mm and more produces a non-uniform, coarsely dispersed system not suitable for practical application. When the spacing is reduced to 0.3-1.2 mm, the dispersion proceeds smoothly. The mean particle size of the dispersion obtained depends on the spacing between the rollers: the smaller this is, the greater is the dispersivity of the particles (see below).

Spacing between rollers, mm	0.3	0.5	0.8	1.2
Mean particle radius in dispersion, microns	0.241	0.539	0.601	0.785

Consumption of electrical energy in the process. It is seen from Fig. 6 that the consumption of electricity in the plasticizing of the resin remains practically at the same level throughout the process. During the dispersing process, the energy consumption begins to fall at the commencement of alkali addition, and drops rapidly in time with the absorption of alkali by the resin. When phase reversal occurs, the electrical energy consumption approximates to a value like that of the free running rollers. The over-all energy consumption during the dispersion of the resin is some 30% less than that in ordinary plasticization under similar conditions.

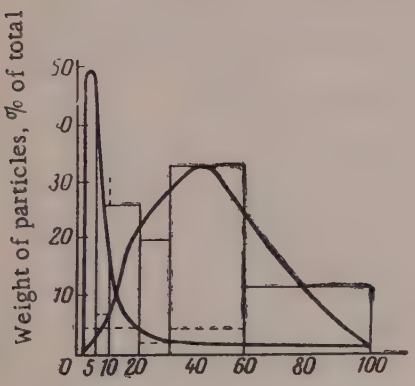


Fig. 5. Curves for the weight distribution of particles in aqueous dispersions of a vulcanized resin obtained by dispersion by means of 2% sodium hydroxide, with various times of alkali addition: 1) 90 min; 2) 30 min.

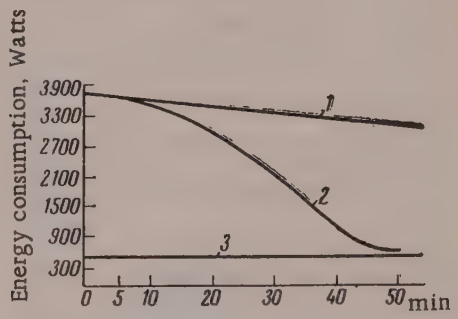


Fig. 6. Consumption of electrical energy on laboratory rollers: 1) in plasticizing the mixture; 2) during the dispersing process; 3) free running.

Effect of activators on the plasticization. Increase in the plasticity, or reduction in the viscosity of the system being treated, facilitates the dispersion of the resin in an aqueous medium. It was therefore a matter of interest to investigate the effect of renacite-2 (a preparation containing 42.5% trichlorothiophenol), which has the property of facilitating the mechanical plasticization of the resin, on the rate of its dispersion and

*As in the Russian original.

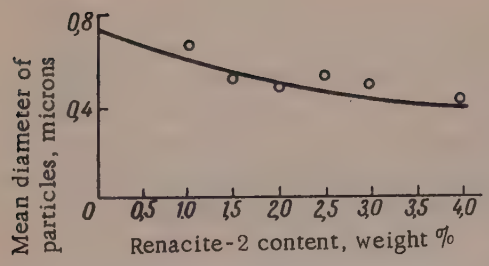


Fig. 7. Effect of renacite-2 on the particle dimensions of dispersion produced.

on the quality of the dispersion obtained. Experiment showed, however, that the use of renacite-2 did not reduce the dispersion time, and subsequent work was devoted to elucidating its effect on the properties of the resulting dispersion. For the plasticizing of a mixture of 100 parts by weight of crushed resin with 10 parts by weight of rosin there was added from 1 to 4 parts by weight of renacite-2.

It can be seen from Fig. 7 that the plasticization activator makes possible the production of finer dispersions. The reason for this may well be that the renacite, being an acceptor of the free radicals formed by the mechanical disruption of the vulcanized resin, hinders their recombination and so enhances the dispersivity of the polymeric system.

Dispersion of resins containing various polymers. In order to elucidate the effect of polymer type in the initial resin on the duration of the dispersing process in an aqueous medium, and on the properties of the dispersion obtained, we prepared protector vulcanizates based on natural and synthetic polyisoprene and sodium butadiene rubbers.

For the first group of experiments, vulcanizates were prepared from formulas and under conditions corresponding to those obtaining in the preparation of protector resins in industry. The vulcanizates were distinguished not only as to polymer type, but also in over-all composition, conditions of vulcanization, etc.

For the second group of experiments, vulcanizates of the protector type were prepared according to a single formula, and were only distinguished by the type of polymer. For these resins, such a vulcanization time was selected as would give vulcanizates having the same space lattice consistency.

It can be seen from Table 3 that, in the dispersing of industrial protector resins of synthetic rubbers, finer dispersions were obtained than from resins based on natural rubber. In dispersing resins from natural rubber the greatest energy consumption is required for the formation of unit specific surface of the dispersion particles. As we move over to resins

TABLE 3

Dispersion of Vulcanizates from Various Rubbers

Polymer type	NK		SKI		SKS-30ARM		SKB	
Group of experiments	1	2	1	2	1	2	1	2
Number of micelles per unit vol x 10^{-9}, ml^{-1}	4,63	4,68	3,99	4,86	1,65	4,01	2,39	4,28
Molecular weight of chain section in vulcanizate	6000	6000	6850	6450	17 200	7050	11 550	6500
Mean particle radius in dispersion microns	0,428	0,388	0,279	0,362	0,241	0,306	0,270	0,328
Specific surface of particles in dispersion m^2/g	6,16	7,46	8,90	7,45	10,82	8,7	9,86	8,31
Energy consumption in formation of unit specific surface of dispersion phase x 10^{-4}, kwt. hr/$/m^2g^{-1}$	10,9	—	6,5	—	5,44	—	5,90	—

of unified composition with equal lattice consistency (two groups of experiments), however, no essential difference between the sizes of particles of dispersions of vulcanized resins depend, not only on the polymer type, but also on the consistency of the vulcanized lattice of the initial resin. An inverse relationship was observed between the consistency of the vulcanized lattice and the mean particle radius. It has to be said, however, that the properties of aqueous dispersions of vulcanized resins, using this term in the broad sense, are not only characterized by particle sizes. It has been shown, for example, that in the electrolytic coagulation of the aqueous dispersions in the second group of experiments, regenerates are obtained of widely different qualities in moving from one polymer to another. A relationship has been found between the properties of the dispersions and those of the regenerates prepared by the dispersion method, which will be the subject of a subsequent communication.

SUMMARY

1. Dispersion on rollers, by introducing an emulsifier which dissolves in it into the resin, followed by the conversion of this into a water soluble condition by saponification, makes it possible to produce finer dispersions that can be obtained by introducing aqueous soap solutions into the resin.

2. Of the emulsifiers tested, rosin, saponified by aqueous caustic alkali, gave the highest dispersivity of the resin.

3. The time of dispersion and the properties of the dispersions depend on the concentration of the saponifying solution and its rate of addition to the resin mixture. In general, increase in concentration and rate of addition of saponifying solution give more rapid production of dispersion, but a reduction in its dispersivity.

4. The use of a plasticizing agent (renacite-2), capable of interaction with the free radicals formed from the vulcanizate by mechanical and thermooxidative disruption, leads to a reduction in the mean size of the particles in the aqueous dispersion of the resin.

5. Increase in vulcanization (consistency of the spatial lattice) increases the energy consumption in dispersion and diminishes the dispersivity of the aqueous dispersion.

6. The total energy consumption in the dispersion of the vulcanizate on rollers amounts to ca. 2/3 of that used in the plasticization of the polymer.

7. The degree of dispersion of the resin depends on the spacing of the rollers. The less this is, the greater is the degree of dispersion of the aqueous dispersion.

LITERATURE CITED

1. B. A. Dogadkin, Kolloidn. Zhurn., 1, 5, 499 (1935).
2. B. A. Dogadkin, F. F. Koshelev and I. A. Tartakovskii, Avt. Svid., No. 46356 of March 31 (1936); Zhurn. Rezin. Prom. No. 8-9, 941 (1936); Kauchuk i Rezina 5, 73 (1937).
3. B. A. Dogadkin, G. N. Zachesova and I. A. Shokhin, Avt. Svid., No. 127382; Biol. Izobr., no. 7 (1960).
4. B. A. Dogadkin and D. M. Pevzner, Avt. Svid., No. 29973, of April 30, (1933).
5. N. A. Figurovskii, Sedimentation Analysis [in Russian] (Izd. Akad. Nauk SSSR, Moscow and Leningrad, 1948).
6. K. A. Pechkovskaya, P. N. Orlovskii and S. A. Simanovaskaya, Kauchuk i Rezina, 3, 28 (1957).
7. B. A. Dogadkin and Ts. M. Gel'fer, Zhurn. Rezin. Prom., No. 5, 547 (1936).

All abbreviations of periodicals in the above bibliography are letter-by-letter transliterations of the abbreviations as given in the original Russian journal. *Some or all of this periodical literature may well be available in English translation.* A complete list of the cover-to-cover English translations appears at the back of this issue.

INFRARED SPECTRA AND THERMODYNAMIC PROPERTIES OF WATER ADSORBED ON A HYDRATED SILICA SURFACE

A. V. Kiselev and V. I. Lygin

Adsorption Laboratory, Chemical Faculty, The M. V. Lomonosov Moscow State University

Translated from Kolloidnyi Zhurnal, Vol. 23, No. 2 pp. 157-162, March-April, 1961

Original article submitted January 20, 1960

In connection with the problem of calculating adsorption equilibrium from the properties of adsorbent and adsorbate only [1-2], and calculations of adsorption energy [1-15], great interest attaches to the statistical method for calculating free energy or entropy of adsorption [2,5,12,16-21]. It is not possible to carry out precise calculations of the entropy change for the system adsorbent-adsorbate owing to deficiencies in our knowledge of the properties of the adsorption complex and the force field of the adsorbent. Adsorption entropies are usually calculated [17-21] for arbitrary chosen models of the adsorption complex, based on approximate values of the vibration frequencies, moments of inertia, and symmetry groups of the adsorbed molecules. In consequence, except in the simplest cases, comparison of the calculated and experimental results for the adsorption entropy cannot provide a clear confirmation of the correctness of our assumptions as to the state of the adsorbed material.

In order to progress further in the study of the state of adsorbed molecules by the methods of statistical thermodynamics, it is necessary to make an independent investigation by the method of infrared spectroscopy. In principle, this method makes it possible to establish a model for the adsorption complex [22,23] and the nature of the symmetry change for the molecule in the adsorbent field [22,24]. However, there are considerable experimental difficulties associated with spectral investigation of the state of adsorbed molecules. So far only a few cases have been studied, and those far from completely; the work has not been directed to obtaining the vibration and rotation frequencies of adsorbed molecules relative to the adsorbent surface, which are required to calculate the thermodynamic characteristics of the adsorbed materials. The only relevant work is that of Kington [25], who used spectral data to explain the very high experimental values for the thermal capacity of water adsorbed in the channels of a zeolite-type porous crystal.

Great interest attaches to a study of the thermodynamic properties of water adsorbed on a hydrated silica surface. In the present paper we set out to establish a model of the adsorption complex for water adsorbed on a hydrated silica surface, based on the results of spectral investigation and appraisal of the adsorption entropy. It is clear that a long investigation would be required to solve this and similar problems. In this first paper we have used our previous data on the structure of the hydroxyl coating on silica [26] and the valency and deformation vibration frequencies of the hydroxyl groups of adsorbed water [27].

The spectra of adsorbed water molecules. The motion of water molecules in the adsorbed state can be separated into internal vibrations of the component atoms relative to each other and motion of the water molecule as a whole relative to the silica surface. The water molecule shows C type symmetry and has three normal vibrations of its atoms relative to each other [28]; symmetrical valency vibration ν_1 deformation vibration ν_2 and antisymmetrical valency vibration ν_3. The vibrations ν_2 and ν_3 are associated with a change in dipole moment, and are active in the infrared absorption spectrum. The vibration ν_1 is associated with a change in polarizability, and is therefore only active in the Raman spectrum. The vibration frequencies of the water molecule are shown in Table 1.

When the surface is approximately covered with a water monolayer, the ν_3 absorption band shifts to 3670 cm^{-1} [27-29] and the ν_2 band to 1620 cm^{-1} [27]. The absorption bands for water in the capillary condensed state do not differ in position from those for liquid water (Table 1). It has been previously noted, by McDonald [32] and by the authors [27], that there are changes in the ν_2 and ν_3 bands as the result of hydrogen bond formation between surface hydroxyl groups of the silica and oxygen atoms of the adsorbed water molecules. The corresponding adsorption complexes have a different structure, but a comparison of the adsorption data with determinations of hydroxyl group contents of the silica surface at different degrees of dehydration makes it possible to distinguish at least two states, shown diagrammatically in Fig. 1 [33-36].

TABLE 1

Vibration Frequencies of the Water Molecule

Vibration type	Water vapor*	Adsorbed water**		Liquid water*
		monolayer	capillary condensate	
Symmetrical, ν_1	3651	—	—	3200****
Deformation, ν_2	1595	1620	1640	1640
Antisymmetrical, ν_3	3755	3670	3450	3450
Hydrogen bond, ν	—	—	—	175***
$\nu_L + \nu_2$ (ν_L is the libration frequency)	—	—	—	2200****

*[28]; **[27-29];*** [30]; **** [31].

The vibration frequency of the center of gravity of an adsorbed water molecule about its equilibrium position, according to the schemes shown in Fig. 1 a and 1 b, is determined by the strength of the hydrogen bond between the surface hydroxyl group and the oxygen atom of the adsorbed water molecule, and lies in the far infra-red region of the spectrum. Water has an absorption band for such vibrations at about 175 cm^{-1} [30]. It is natural to suppose that localization of water molecules at surface hydroxyl groups, by means of hydrogen bonds according to scheme 1 a, should make possible free rotation of a molecule about the axis AA. However, rotation about this axis should be prevented in the case of adsorption according to Fig. 1 b. With filling of successive layers the adsorbed water molecules in the first layer become joined by hydrogen bonds to molecules in the second layer, and so, according to Bernal [37], as is obviously the case with liquid water, they can only take part in twisting vibrations (librations) with a frequency ν_L in the region 450-780 cm^{-1} [31]. Observation of the ν_L bands of adsorbed water molecules is very difficult, since the silicon oxygen tetrahedra have intense absorption bands in this region. [27]. It is therefore necessary to investigate the combination band $\nu_L + \nu_2$, which is in the region of 2200 cm^{-1} in the case of liquid water [31].

The entropy of water in the adsorbed state. The change in frequency of the internal vibrations of adsorbed water molecules is small (Table 1), so that the effect of adsorbent field on the internal vibrations can be neglected in determining the entropy of an adsorbed substance. The entropy corresponding to oscillating movements of a molecule is usually a considerable proportion of the total entropy. Adsorption of water molecules on a hydrated silica surface with hydrogen bond formation [27,29] and the high differential heat of adsorption [38] are evidence that there is fairly tenacious localization of the adsorbed molecules on the silica surface. The considerable decrease in entropy on adsorption, found experimentally, indicates that there is no oscillating movement of water molecules along the hydrated surface. In [19] this decrease in entropy is estimated to be 34.3 entropy units.

It is therefore important to calculate the entropies of rotation and vibration of water molecules relative to the silica surface, and also to calculate the combination entropy associated with localization of water molecules on surface hydroxyl groups.

Rotation entropy. In calculating the rotation entropy it is very important to be able to establish whether there can be changes in the symmetry and moment of inertia of a molecule in the adsorbed state. Evidence of the change in symmetry of a molecule, as the result of deformation in the force field of the adsorbent [22, 24], would be provided by the appearance of an absorption band in the infrared spectrum, which in the normal state is only active in the Raman spectrum. However, a decision on these lines is not possible in the case of adsorbed water, since,as shown in Table 1, the symmetrical vibration ν_1 is masked by the absorption band ν_2.

It should be noted, however, that deformation of the skeleton of an adsorbed water molecule is evidently not very great, since there are only relatively small shifts in the adsorption bands ν_2 and ν_3 (Table 1), and the deformation can only result in some change in the angle between the OH groups, which should not,in itself, lead to any change in the symmetry of the molecule. For the same reason, there should be no marked change in the moment of inertia of the water molecule. We can therefore make an approximate estimate of the rotation entropy of water (S_{rot}), adsorbed according to the scheme of Fig. 1a, using a model with free rotation about the axis AA, by means of the equation [20]:

$$S_{rot} = R\left[\ln\frac{1}{\pi\sigma}\left(\frac{8\pi^3 IkT}{h^2}\right)^{1/2} + \frac{1}{2}\right], \quad (1)$$

and substituting in this the symmetry number of the free water molecule ($\sigma = 2$) and the moment of inertia in the equilibrium state ($I = 1.920 \times 10^{-40}$ g/cm^2) [28]. The entropy for this rotation at 300°K is about 1 entropy unit. In the case of adsorption according to the scheme of Fig. 1b, the water molecule is localized more firmly, and can evidently only take part in rotatory vibrations (librations) about the axis AA. The entropy corresponding to such vibrations, assuming that the maximum angle of rotation from the equilibrium position $\leq \pi/6 \sim 1/2$, is less than the entropy for free rotation [17].

Vibration entropy. The entropy of adsorbed water molecules corresponding to vibrations normal to the surface can be calculated from the equation [20]:

$$S_{vib} = R\left[\frac{h\nu}{kT}(e^{h\nu/kT} - 1)^{-1} - \ln(1 - e^{h\nu/kT})\right]. \quad (2)$$

The vibration entropy of water molecules adsorbed according to the scheme of Fig. 1a can be derived by substituting in equation (2) the vibration frequency ($\nu = 175$ cm^{-1}) for the hydrogen bond O–H. . .O of a liquid water molecule [30], and amounts to 2.5 entropy units.

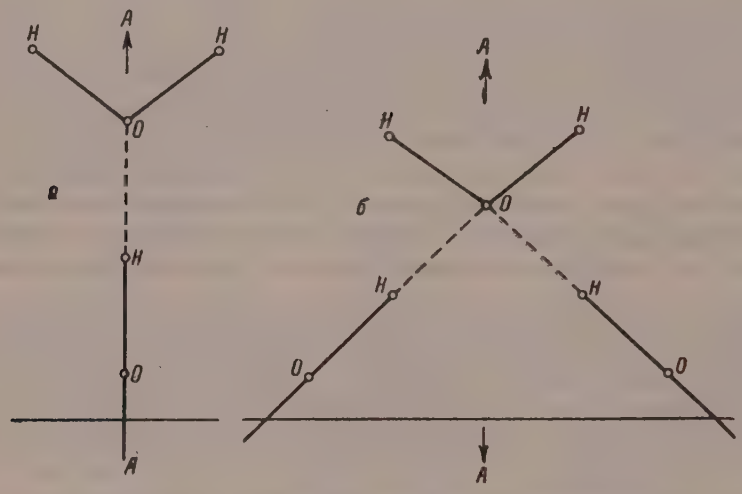


Fig. 1. Adsorption complex diagrams for water adsorption on a hydrated silica surface: a) bond with one OH group, b) bonds with two OH groups.

Assuming that, in the case of Fig. 1b type adsorption, the water molecule is more firmly localized and has a higher vibration frequency estimated at 300 cm^{-1}, the value obtained for the vibration entropy is less than 1 entropy unit.

Combination entropy. The combination entropy is associated with the number of possible methods of distributing adsorbed molecules per adsorption center of the surface, and can be evaluated from equation [20]:

$$S = R[x\ln x - (x-1)\ln(x-1)], \quad (3)$$

where x is the number of adsorption centers per adsorbed molecule. The concentration of hydroxyl groups on a saturated hydrated surface is close to 12μ M/m^2. When 3.2μ M/m^2 of water is adsorbed on such a surface to occupy about half a monolayer [34], the combination entropy is about 4 entropy units for adsorption as shown in Fig. 1a, and about 2.5 entropy units for adsorption as in Fig. 1b.

The calculated value for the entropy of water vapor at 1 atm pressure and 298.1°K is 45.1 entropy units [39], and the experimental value is 44.2 entropy units [40]. The decrease in entropy, when half a monolayer of adsorbed

water molecules is formed on a silica surface, was found to be 34.3 entropy units [19], but this result was not very precise. The difference between these two values gives the entropy for adsorbed water molecules as about 11 entropy units. The lack of agreement with the calculated entropy (Table 2) may be due to our neglect of vibrational movements of water molecules along the adsorbent surface and to the effect of nonuniform distribution of hydroxyl groups on the silica. There is at present no available information on the vibration frequencies of water molecules along the surface. The assumption made in [19], that the vibrations of water in a three dimensional oscillator are isotropic, appears to be unrealistic.

TABLE 2

Estimated Results for the Entropy of Water in the Adsorbed State on a Hydrated Silica Surface

Form of adsorption complex	Entropy of adsorbed molecules, entropy units			
	Rotation	Vibration	Combination	Total
Water molecule forming hydrogen bond with one surface hydroxyl group	1	2.5	4	7.5
Water molecule forming hydrogen bonds with two surface hydroxyl groups	1	1	2.5	4.5

The above estimate for the entropy is only very approximate. The choice of model was based only on mean adsorption characteristics [34]. The choice of vibration frequency was based on spectral data obtained only in the fundamental region of the spectrum, which gives information mainly only on the internal vibrations of atoms in the molecules. The necessary more detailed information on the structure of a sufficiently heterogeneous hydrated silica surface is not available for calculating the possible configuration entropy. Finally, this heterogeneity is not limited to the schemes shown in Fig. 1a and b. In order to improve the precision, it would be necessary to make detailed investigations of the structures of surface and adsorption complexes by chemical, isotopic exchange, adsorption (equilibrium), calorimetric (adsorption heat and thermal capacity), and spectral methods. The first subject for study should be the vibration and rotation spectra of the molecules as a whole with respect to the adsorbent surface, in the far infrared region. This should make it possible to select a more precise model, and to obtain the vibration frequencies of the molecules in the adsorption complexes should, in turn, serve as a basis for calculating the height of the potential barrier for adsorbents with an ordered surface structure, since it is possible to derive theoretically the form of the potential barrier in this case, and hence to calculate precisely the hindered molecular rotation. It would also be of considerable interest, in this case, to obtain experimentally precise values for the adsorption entropy and other thermodynamic properties. The greatest interest would attach to a study of the thermal capacities of normal and heavy water in the adsorbed state. From this, independently of the spectral method, it should be possible to determine the terms for rotational movement of the molecules, since the difference in thermal capacity in the two cases should be determined by the change in rotation, as the result of a doubling of the moment of inertia with very little alteration in total mass, on changing from H_2O to D_2O.

Analysis of the fine structure of adsorption bands of adsorbed substances in the fundamental spectral region should also be valuable as a means for determining the form of the molecular rotation, to be used in calculating the rotation entropy.

SUMMARY

1. Consideration has been given to a method of calculating the entropy of water adsorbed on a hydrated silica surface, based on some adsorption complex models and the vibration frequencies of the molecules in the complexes, as shown by their infrared spectra.

2. The total entropy estimated in this way, the sum of terms for vibration, rotation, and combination, is about 4 to 7 entropy units, which does not differ greatly from the experimental value. Experimental and theoretical approaches are discussed for the development of a more precise statistical thermodynamic treatment of adsorption complexes.

LITERATURE CITED

1. A. V. Kiselev, Vestnik Akad. Nauk SSSR, 10, 43 (1957); N. N. Avgul', G. I. Berezin, A. A. Isirikyan, A. V. Kiselev, I. A. Lygina, and D. P. Poshkus, Izvest. Akad. Nauk SSSR, Otdel. Khim. Nauk, 1314 (1957).
2. A. V. Kiselev and D. P. Poshkus, Doklady Akad. Nauk SSSR, 132, 876 (1960).
3. R. M. Barrer, Proc. Roy. Soc., A161, 476, 1937.
4. W. J. G. Orr, Proc. Roy. Soc., A173, 349, 1939.
5. T. L. Hill, J. Chem. Phys. 16, 181, 1948.
6. T. Hayakava, Bull. Chem. Soc., Japan 30, 236, 1957.
7. A. V. Kiselev and D. P. Poshkus, Zhur. Fiz. Khim., 32, 2824 (1958).
8. E. L. Pace, J. Chem. Phys. 27, 1339, 1957.
9. A. D. Crowell, J. Chem. Phys. 22, 1897, 1954.
10. A. V. Kiselev and D. P. Poshkus, Doklady Akad. Nauk SSSR, 120, 834 (1958).
11. N. N. Avgul', A. V. Kiselev, I. A. Lygina, and D. P. Poshkus, Izvest. Akad. Nauk SSSR, Otdel. Khim. Nauk, 1196 (1959).
12. B. B. Fisher and W. G. McMillan, J. Chem. Phys. 28, 562, 1958.
13. R. A. Pierotti and D. Halsey, J. Phys. Chem. 63, 680, 1959.
14. D. P. Poshkus and A. V. Kiselev, Zhur. Fiz. Khim., 34, 2640, 2646 (1960).
15. A. Yu. Babkin and A. V. Kiselev, Doklady Akad. Nauk SSSR, 129, 357 (1959).
16. T. L. Hill, J. Phys. Chem. 63, 456, 1959.
17. G. Damköler, and R. Edse Z. Phys. Chem. 53, 117, 1943.
18. R. M. Barrer, Trans. Faraday Soc. 40, 374, 1944.
19. A. G. Foster, J. Chem. Soc. 1945, 360.
20. C. Kemball, Proc. Roy. Soc. A187, 73, 1946; Collection, Catalytic Problems and Methods of Investigation [Russian translation] (IL, 1955), p. 256.
21. R. M. Barrer, "The Structure and Properties of Porous Materials", London, 1958, p. 6.
22. N. Sheppard and D. J. C. Yates, Proc. Roy. Soc. A238, 69, 1956.
23. R. P. Eischens, and W. A. Pliskin, Advances in Catalysis, 10, 1, 1958.
24. G. Katagounis, and O. Peter, Z. Electrochem. 61, 827, 1957.
25. C. L. Kington, Cb. "The Structure and Properties of Porous Materials", London, 1958, p. 274; G. J. C. Frohnsdoriff, and G. L. Kington, Proc. Roy. Soc. A247, 469, 1958.
26. V. I. Lygin, Vestnik Mosk. Inst., No. 1, 223 (1958); A. V. Kiselev and V. I. Lygin, Kolloid. Zhur., 21, 581 (1959).
27. A. V. Kiselev and V. I. Lygin, Kolloid. Zhur., 22, 403 (1960).
28. G. Herzberg, Vibration and Rotation Spectra of Polyatomic Molecules [Russian transltation] (IL, 1949), p. 304.
29. V. A. Nikitin, A. N. Sidorov, and A. V. Karyakin, Zhur. Fiz. Khim., 30, 117 (1956).
30. E. F. Gross and V. I. Val'kov, Doklady Akad. Nauk SSSR, 67, 619 (1949).
31. P. Giguere, and K. B. Harvey, Canad. J. Chem. 34, 798, 1956.
32. R. McDonald, J. Amer. Chem. Soc. 79, 850, 1958.
33. A. V. Kiselev, Collection, Surface Chemical Compounds and their Role in Adsorption Phenomena [in Russian] (Moscow State University, 1957), p. 90, 199.
34. L. D. Belyakova, O. M. Dzhigit, and A. V. Kiselev, Zhur. Fiz. Khim., 31, 1577 (1958).
35. A. V. Kiselev, Collection, The Structure and Properties of Porous Materials (London, 1958), p. 195.
36. S. P. Zhdanov, Zhur. Fiz. Khim., 32, 699 (1958).
37. D. Bernal, Uspekhi Fiz. Nauk, 14, 586 (1934).
38. A. V. Kiselev, K. G. Krasil'nikov, N. L. Pokrovskii, N. N. Avgul', O. M. Dzhigit, and K. D. Shcherbakova, Zhur. Fiz. Khim., 26, 1986 (1952).
39. W. F. Giague, and J. W. Stout, J. Amer. Chem. Soc. 58, 1144, 1936.
40. A. R. Gordon, J. Chem. Phys. 2, 65, 1934.

APPROXIMATE EXPRESSION FOR THE WAVE-LIKE ADSORPTION ISOTHERMS OF NITROGEN ON GRAPHITIZED CARBON BLACK, TAKING INTO ACCOUNT ADSORBATE-ADSORBATE INTERACTIONS IN THE FIRST AND THE SECOND LAYER

A. V. Kiselev and E. V. Khrapova

Moscow University, Chemistry Department, Adsorption Laboratory
Translated from Kolloidnyi Zhurnal, Vol. 23, No. 2, pp. 163-169,
March-April, 1961
Original article submitted October 7, 1959

In the papers [1-2] it has been shown that at the adsorption of some vapors, in particular nitrogen vapor, on graphitized carbon blacks, which have a nearly homogeneous surface, adsorbate-adsorbate interaction manifests itself clearly. For this reason the adsorption isotherm of nitrogen in the regions where mainly the first layer is filled has a complicated wave shape starting concavely.

In the papers [3,4] it has been found that the adsorption isotherms of nitrogen and argon on graphitized carbon black are concave at the start. It is quite impossible to describe such isotherms by the equations of Langmuir and BET. An examination of the simplest isotherm equations which take into account adsorbate-adsorbate interaction has pointed out [2] that many experimental adsorption isotherms (concave at the start and passing through two or more inflection points) in the region where mainly the first layer is filled are fully described by an approximate isotherm equation for monomolecular localized adsorption [5].

$$h = \frac{\theta}{K'_1 (1-\theta)(1+K_n\theta)}, \qquad (1)$$

or, when linearized

$$\frac{\theta}{h(1-\theta)} = k'_1 + K'_1 K_n \theta, \qquad (1')$$

where h represents the relative vapor; θ the total degree of surface coverage; K'_1 the equilibrium constant for adsorbate-adsorbent interaction; K_n the equilibrium constant for adsorbate-adsorbate interaction. In the region of transition to adsorption mainly in the second layer they are described by the corresponding approximate equation for the multimolecular adsorption isotherm [6,5]

$$h = \frac{\theta(1-h)^2}{K'_1 [1-\theta(1-h)][1+K_n\theta(1-h)]} \qquad (2)$$

or, when linearized

$$\frac{\theta(1-h)^2}{h[1-\theta(1-h)]} = K'_1 + K'_1 K_n \theta(1-h). \qquad (2')$$

As has been shown in the paper [2], these approximate equations describe the experimental nitrogen adsorption isotherm obtained in the studies [3,4,7] in the region where mainly the first layer is filled and that where filling of the second layer starts. It was of interest to examine whether the experimental isotherm is described by a similar equation at higher coverages too.

In the papers [8,9] it has been proved that in the region of multimolecular adsorption the step-like adsorption isotherm of krypton on thermally graphitized carbon blacks at temperatures below the critical temperature of a two-dimensional layer may be described by the equation given in the paper [8]

$$\ln (p/p_s)_n = -E_1/n^3 kT + (E_g/kT)(1-g), \qquad (3)$$

where n represents the number of the step; E_1, E_g and g are constants (E_1 is the heat of adsorption in the first layer; E_g the energy of lateral adsorbate-adsorbate interaction; g a factor taking into account the mutual arrangement of the molecules in a horizontal layer). In the papers [8,9] the values $E_g/kT = 7.9$ and $1-g = 0.09$ were found by matching

the experimental krypton isotherm. For these values of the constants, equation (3) gives the p/p_s value corresponding to a given step in the isotherm n = 1;2;3,etc. The adsorption isotherms measured above the critical temperature of the adsorbed layer do not satisfy equation (3), since they have a wave-like and not a step-like shape, that is, they can only be expressed by a continuous function. There exist attempts to describe [7,10] the wave-like adsorption isotherm of argon on graphitized carbon black and that of krypton on iron crystals obtained from sintered magnetite by means of Halsey's equation [11]

$$\theta = \exp\{\Delta E_0/\Delta E_m\} \sum_{n=1}^{\infty} [(p/p_s)^{RT/\Delta E_m}]^{n^3} \qquad (4)$$

or by means of a similar equation which takes into account the inhomogeneity of the surface [12]

$$\theta = \sum_{n=1}^{\infty} \exp\{n\,\Delta E_B/\Delta E_m\}\,[(p/p_s)^{RT/\Delta E_m}]^{n^4}, \qquad (5)$$

where θ represents the total degree of surface coverage; n the number of layers; ΔE_0, ΔE_m and ΔE_B are constants. The authors of the papers [7, 10] remark that neither equation (4) nor (5) reproduce the experimental isotherms, although both predict a step-like character of the isotherm at the successive filling of the adsorbed layers.

As regards experimental investigations of nitrogen adsorption on graphitized carbon blacks, the most careful experiments have been done with the thermally graphitized carbon black P-33, which has an almost homogeneous surface [3,4], and the adsorption was studied at surface coverages from very small values to $\theta \approx 0.8$-0.9, and in the paper [7] from $\theta \approx 1$ to $\theta \approx 4$.* It was of interest to study nitrogen adsorption in a broad range of θ values on one and the same sample of carbon black with as homogeneous a surface as possible and to describe, even approximately, their wave-like shape both in the region of monomolecular and in that of multimolecular coverages.

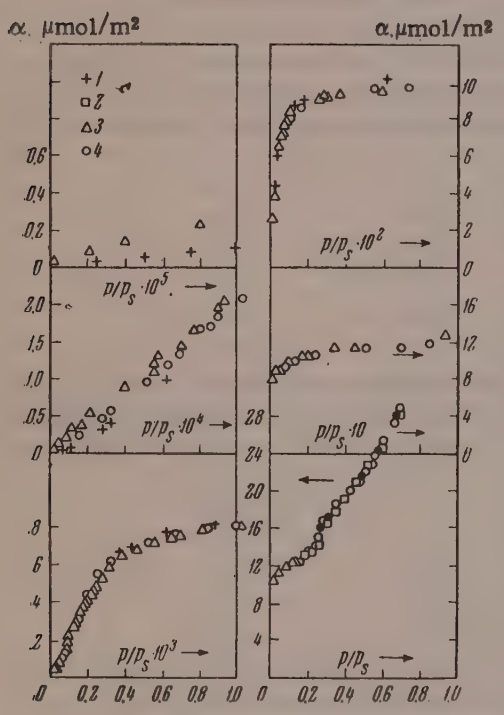


Fig. 1. Absolute nitrogen adsorption isotherms at -195° on samples of carbon black graphitized at about 3000°. 1) and 2) data for the carbon black P-33 from the papers [3,4] and [7], respectively; 3) and 4) our data for the carbon blacks T-1 and T-2. Here and further filled points represent desorption.

By means of the arrangement described in the paper [15] we have measured the nitrogen isotherm at -195° on two samples of 3000 and 3200° respectively.

As is evident from Fig. 1, in accordance with the data of the papers [3,4], the nitrogen adsorption isotherms on thermally graphitized carbon blacks are concave at the start and, therefore, they are not fully described by the BET equation. In this case the following way to determine the specific surface area has a more logical foundation. Since the samples of carbon black graphitized at 3000° have an almost homogeneous surface, as was proved by measuring the differential heats of adsorption as a function of the degree of coverage [2,16], the isotherm of multimolecular adsorption in the general case is approximately given by equation (2). In the special case of strong adsorbate-adsorbent interactions and relatively weak adsorbate-adsorbate interactions (small K_n) equation (2) approaches the BET equation. Therefore, in the latter case the BET method may be used to find the monolayer capacity α_m and the specific surface area s (for instance, for the strong adsorption of benzene on graphitized carbon black). Since for benzene we know the area occupied by a flat-lying molecule in a compact monolayer, namely, $\omega_m = 40$ Å^2 [17], which corresponds to an absolute monolayer capacity $\alpha_m = 1/\omega_m = 4.15$ μmole/m^2 or 2.50 molecules per 100 Å^2, s may be determined. When s is known, one may further find the value of ω_m for other vapors for which α_m may be estimated. However, since at the adsorption of nitrogen on graphite the adsorbate-adsorbent interaction energy greatly surpasses that of the adsorbate-adsorbate interaction, the BET equation describes this isotherm over a quite broad range of θ (from 0.6 to 1.3) corresponding to the transition from adsorption mainly in the first to that mainly in the second layer. By applying the BET equation to this part of the isotherm we have determined the monolayer capacity for nitrogen (α_m) and taking $\omega_{mN_2} = 16.2$ Å^2 ** we obtained the following values

* More recent data from [13] are not discussed in our present paper; they are treated in [14].

** This value of ω_m, which is generally used as a standard, corresponds to an absolute monolayer capacity for nitrogen $\alpha_m = 10.2_5$ μ mole/m^2 or 6.1_7 molecule per 100 Å^2.

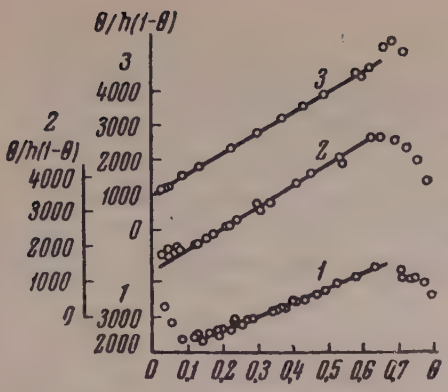


Fig. 2. Nitrogen adsorption isotherms at -195° on graphitized carbon blacks T-1 (1), T-2 (2) and P-33 (3) plotted according to equation (1').

for the specific surface areas: carbon black T-1, $\underline{s} = 28.1$ m^2/g, black T-2, $\underline{s} = 6.9$ m^2/g. These values were found to be nearly equal to the specific surface areas as determined for these same carbon blacks from the benzene adsorption isotherms [14].

The absolute (that is, referred to unit surface area) nitrogen isotherms on these carbon blacks calculated by means of these $\underline{s}$ values, as can be seen in Fig. 1, nearly coincide with the absolute adsorption isotherm on the carbon black P-33 (2700°), which we obtained in [2] from the data of [4] and [7]. As has been remarked above, this isotherm is concave at low coverages. The convex initial part of the nitrogen isotherm on less homogeneous carbon black samples [1] is connected with the higher heat of adsorption found, when the most active parts of the surface are filled up; this is indicated by measurements of the adsorption heat on carbon black samples treated at various temperatures [16].

It should be remarked that the samples of thermally graphitized carbon black T-1, T-2 and P-33 have somewhat different degrees of homogeneity. The lowest absolute magnitude of adsorption in the initial region of the isotherm was found for P-33. When the surface of carbon black is smoothed, the relative importance of the adsorbate-adsorbent interactions diminishes and that of adsorbate-adsorbate interactions grows. Correspondingly, the values of the constants K'_1 and K_n in equation (1), which approximately take into account these interactions, change too. The constants K'_1 and K_n, as determined from the plots of the linear formula (1') shown in Fig. 2, are given in Table 1.

A semiempirical expression for the wave-like isotherm. Equation (4) and the approximate expressions (1) and (2) for monomolecular and multimolecular adsorption, respectively, were applied to the absolute adsorption isotherms (Fig. 1) obtained experimentally and this was done by taking $\theta = \alpha/10.2_5$ (when α is expressed in μmole/m^2). The adsorption isotherm calculated from equation (4) with the values $\exp(-\Delta E_0/\Delta E_m) = 0.16$ and $\Delta E_m/RT = 4$ [18] is shown

TABLE 1

Values of the Constants K'_1 and K_n in Equation (1) for Nitrogen Adsorption on Thermally Graphitized Carbon Blacks.

Carbon black sample	T-1	T-2	P-33 [4]	Carbon black sample	T-1	T-2	P-33 [4]
K'_1	1650	1250	1000	K_n	2,6	4,9	6,0

in Fig. 3 by the drawn curve. As is evident from Fig. 3, equation (4) does not describe accurately the nitrogen adsorption isotherm as it did not do in the cases of argon adsorption at -195° on a graphitized carbon black [7] and krypton adsorption on iron crystals at -183° [10]. The substitution of 20 other sets of $\exp(-\Delta E_0/\Delta E_m)$ and $\Delta E_m/RT$ values gave no better results. In the monolayer region at $\theta < 1$ neither equation (4) nor (5) describes these isotherms.

It has been shown [2] that, in the case of nitrogen and argon adsorption on graphitized carbon blacks, the entire monomolecular region may be described by equation (2), when the constants K'_1 and K_n of equation (1) are determined from a plot of (1') in the region of monomolecular coverages and the K'_1 and K_n values found thus are substituted in equation (2). Since the shape of the nitrogen and argon isotherms in their course changes from concave to convex and each isotherm passes at least three times through a point of inflection (Fig. 1), not only the first but any wave in the isotherm consisting of a concave and a convex part should be described by taking account of the adsorbate-adsorbate interaction, for instance by using the corresponding number of multimolecular adsorption equations of the type (2). This may be done, if it is assumed that filling of the first layer with nitrogen molecules has practically been completed in the first wave of the isotherm so that the second wave may be considered to result from multimolecular nitrogen adsorption on top of an already filled first layer*.

* This assumption is confirmed by the fact that "point B" lies at a very small value $p/p_s = 0.05$ and the value of the monolayer capacity α_m as found from this point practically coincides with our value $\alpha_m = 10.2_5$ μmole/m^2.

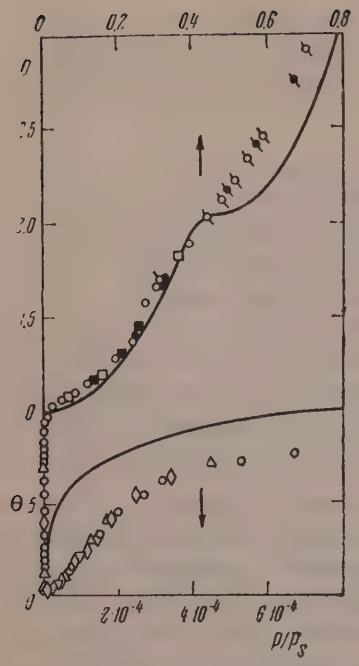


Fig. 3. The application of Halsey's equation (4) to the adsorption isotherm of nitrogen at -195° on the thermally graphitized carbon black T-2. The points represent experiments; the curve was calculated from equation (4) by using $\exp(-\Delta E_0/\Delta E_m) = 0.16$ and $\Delta E_m/RT = 4$. The various series of measurements are denoted by different signs.

When this assumption is used, the degree of coverage in the second layer may be determined in the form $\theta'' = (\alpha - \alpha_m)/\alpha_m$ where $\alpha_m = 10.2_5$ μmole/m^2. For one of our carbon black samples studied, the application of equation (2) to describe the nitrogen adsorption in the first wave* with $\theta' = \alpha/\alpha_m$ is shown in Fig. 4a, and that for the second wave with $\theta'' = (\alpha - \alpha_m)/\alpha_m$ in Fig. 4b. It is evident that these parts of the isotherm are described by one and the same equation (2) where, of course, the interaction constants for the first wave, $K'_{1(1)}$ and $K_{n(1)}$, differ from those, $K'_{1(2)}$, $K_{n(2)}$, for the second wave.

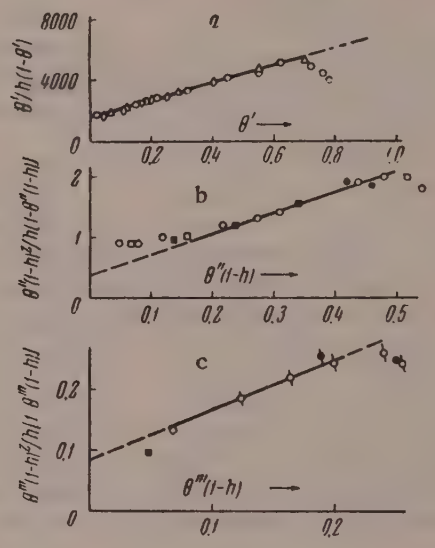


Fig. 4. Linearization of the first (a), second (b) and third (c) wave in the adsorption on the graphitized carbon black T-2 in the coordinates of equations (1) and (2) with θ', θ'', and θ''' (Table 2).

As an example of the application of the method described we will take the adsorption isotherm of nitrogen on the carbon black T-2, which is shown in Fig. 5 by the drawn curve. The first wave of the isotherm was calculated with $\theta' = \alpha/\alpha_m$ by means of the constants $K'_{1(1)}$ and $K_{n(1)}$ determined from Fig. 4a. As can be seen in Figs. 4a and 4b, the nitrogen adsorption isotherm calculated by means of equation (2) with constant $K'_{1(1)}$ and $K_{n(1)}$ deviates from the experimental points beyond $\theta' = \alpha/\alpha_m = 1.28$ ($p/p_s = 0.15$). Beyond this θ value, instead of θ', $\theta'' = (\alpha - \alpha_m)/\alpha_m$ was substituted in equation (2) and the constants $K'_{1(2)}$ and $K_{n(2)}$ found graphically from Fig. 4b were used.

In this way, the isotherm shown in Fig. 5 was calculated and constructed from $p/p_s = 10^{-5}$, $\theta = 0.02$ to $p/p_s = 0.15$, $\theta = 1.28$ and from $p/p_s = 0.15$, $\theta = 1.28$ to $p/p_s = 0.35$, $\theta = 1.75$. In the rest of the paper we denote the value $\alpha = 18.0$ μmole/m^2 corresponding to $p/p_s = 0.35$ by α_2. In further calculations $\theta''' = (\alpha - \alpha_2)/\alpha$ and a third set of constants, $K'_{1(3)}$ and $K_{n(3)}$ was calculated from Fig. 4c. By substituting these values in equation (2) we have calculated the next part of the adsorption isotherm (Fig. 5). Thus, as is evident from Fig. 5, the experimental adsorption isotherm of nitrogen may be described beginning with $p/p_s = 0.54$, $\theta = 2.3$. This was done by means of only one equation (2), but with the three sets of constants K'_1 and K_n given in Table 2.

* The first wave in the adsorption isotherm of nitrogen on carbon black at -195° occurs at such small p/p_s ($< 10^{-4}$) values that in this region p/p_s equation (2) does not differ from the simpler equation (1); therefore, the latter was used to construct the plot in Fig. 4a, and to calculate the constants $K'_{1(1)}$ and $K_{n(1)}$.

TABLE 2

Values of the Constants in the Multimolecular Adsorption Equation (2), as Are Used For Describing the Nitrogen Adsorption Isotherm on the Thermally Graphitized Carbon Black T-2

Part of the isotherm Fig. 4	θ values	Range of			Approximated values	
		p/p_s	α, μ mole/ /m²	θ	K'_1	K_n
a	$\theta' = \frac{\alpha}{\alpha_m} = \frac{\alpha}{10{,}25}$	10^{-5}—0,15	0,205—10,3	0,02—1,28	1250	4,9
б	$\theta'' = \frac{\alpha - \alpha_n}{\alpha_m} = \frac{\alpha - 10{,}25}{10{,}25}$	0,15—0,35	10,3—18,0	1,28—1,75	0,33	10,7
в	$\theta''' = \frac{\alpha - \alpha_2}{\alpha_m} = \frac{\alpha - 18{,}0}{10{,}25}$	0,35—0,54	18,0—23,6	1,75—2,3	0,07	12,8

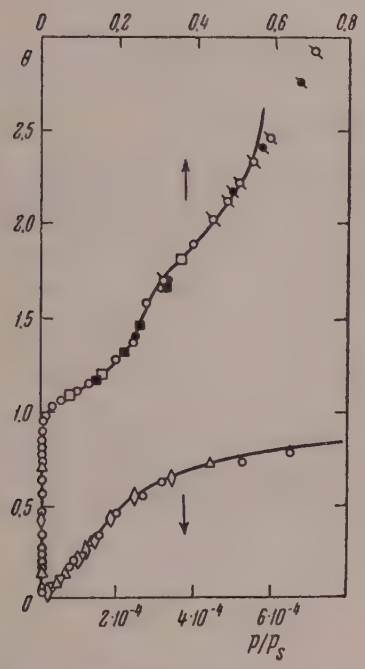


Fig. 5. Comparison of the isotherm (curve) calculated by means of equations (1) and (2) with the experimental points of nitrogen adsorption on the graphitized carbon black sample T-2; $\alpha_m = 10.2_5$ and $\alpha_2 = 18.0$ μ mole/m². The various series of measurements are denoted by different signs.

The constant α_2 is smaller than $2\alpha_m$. Obviously, this, firstly, is connected with the fact that the transition from mainly filling the second layer to mainly filling the third layer is less sharp than the transition from filling the first layer to filling the second layer. Secondly, it may even be connected with a less dense packing of the nitrogen molecules in the second layer when compared with the first layer, just as has been noticed for argon in the paper [3]. The value $\alpha_2 - \alpha = 7.8$ μ mole/m² or 4.7 N_2 molecules per 100 A² corresponds to $\omega_m = 16.2$ A² corresponds to the most densest packing of spheres with a diameter D = 4.33 A, in a plane, then primitive square packing corresponds to an area $D^2 = 18.8$ A² and this is close to the value $\omega_{m(2)} = 21._3$ A².

Thus, it is evident from Fig. 5 that by means of the multimolecular adsorption equation (2) not only the first but also second wave of the nitrogen adsorption isotherm on the homogeneous surface of a graphitized carbon black may be described. In this it is assumed that up to the α value, corresponding to the second point of inflection in the isotherm at its transition from a convex to a concave shape (from the first to the second wave), the nitrogen molecules are adsorbed almost exclusively in the first layer, but beyond this point mainly in the second and further layers. In an analogous way even the third wave of this isotherm may be partly described.

This method of describing the successive waves of the adsorption isotherm by one equation with different constants is, of course, only semiempirical. A more general description requires the use of statistical mechanics and the solution of the entire problem by taking into account the interaction potential of any molecule not only with all force centers of the adsorbent [19] but also with all adsorbate molecules present in the adsorbed layer.

SUMMARY

1. The adsorption isotherms of nitrogen at -195° on two carbon black samples graphitized thermally at 3000 and 3200° and having the specific surface areas 28.1 and 6.9 m²/g, respectively, start with a concave part. The absolute nitrogen isotherms on all thermally graphitized carbon black samples which have been studied previously and in this paper nearly coincide and trace a wave-like curve starting with a concave part and having at least three points of inflection.

2. The first, the second and part of the third wave in the adsorption isotherm of nitrogen on a thermally graphitized carbon black which has a nearly homogeneous surface may be described by means of one and the same equation in which a different set of constants is used for each wave. This equation approximately takes into account the adsorbate-adsorbate interactions in the corresponding adsorbed layers.

LITERATURE CITED

1. A. B. Kiselev and E. B. Khrapova, Kolloid. Zhur. 19, 572 (1957).
2. A. V. Kiselev, N. V. Kovaleva, V. A. Sinitsyn and E. V. Khrapova, Kolloid. Zhur. 20, 444 (1958).
3. S. Ross and W. Winkler, J. Colloid. Sci. 10, 319, 1955.
4. S. Ross and W. W. Pultz, J. Colloid. Sci. 13, 397, 1958.
5. A. V. Kiselev, Doklady Akad. Nauk SSSR, 117, 6 (1957); Kolloid. Zhur. 20, 338 (1958).
6. A. V. Kiselev and D. P. Poshkus, Izvest. Akad. Nauk SSSR Otdel. Khim. Nauk, 520 (1958).
7. M. H. Polley, W. D. Schaeffer, and W. R. Smith, J. Phys. Chem. 57, 469, 1953.
8. J. H. Singleton and G. D. Halsey, J. Phys. Chem. 58, 1011, 1954.
9. H. Clark, J. Phys. Chem. 59, 1068, 1955.
10. R. A. Haul, and E. R. Swart, Z. Elektrochem. 61, 380, 1957.
11. G. D. Halsey, J. Chem. Phys. 16, 931 (1948).
12. G. D. Halsey, J. Amer. Chem. Soc. 74, 1082, 1952.
13. R. A. Beebe and J. M. Holmes, J. Phys. Chem. 61, 1684, 1957.
14. A. A. Isirikyan and A. V. Kiselev, Zhur. Fiz. Khim. (in the Press).
15. A. V. Kiselev and E. V. Khrapova, Izvest. Akad. Nauk SSSR Otdel. Khim. Nauk, 390 (1958).
16. R. A. Beebe, and D. M. Joung, J. Phys. Chem. 58, 95, 1954.
17. N. N. Avgul', G. I. Berezin, A. V. Kiselev and A. Ya. Korolev, Kolloid. Zhur. 20, 298 (1958).
18. G. D. Halsey, J. Amer. Chem. Soc. 73, 2693, 1951.
19. N. N. Avgul', A. A. Isirikyan, A. V. Kiselev, I. A. Lygina and D. P. Poshkus, Izvest. Akad. Nauk SSSR, Otdel. Khim. Nauk, 1314 (1957); N. N. Avgul', A. V. Kiselev, I. A. Lygina and D. P. Poshkus, Izvest. Akad. Nauk SSSR Otdel. Khim. Nauk, 1196 (1959).

All abbreviations of periodicals in the above bibliography are letter-by-letter transliterations of the abbreviations as given in the original Russian journal. *Some or all of this periodical literature may well be available in English translation.* A complete list of the cover-to-cover English translations appears at the back of this issue.

STABILIZATION OF ALUMINUM SOLS IN BENZENE BY SURFACE-ACTIVE SUBSTANCES

M. A. Lunina and M. F. Kolosova

D. I. Mendeleev Moscow Institute of Chemical Technology, Department of Colloid Chemistry

Translated from Kolloidnyi Zhurnal, Vol. 23, No. 2, pp. 170-172, March-April, 1961
Original article submitted January 25, 1960

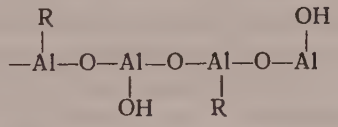
Metal sols in nonaqueous nonpolar media are usually very unstable with respect to aggregation, and in the absence of a stabilizer they last for a few hours. In addition, the concentration of the dispersed material is not large (not more than 1%). The introduction of stabilizers such as high molecular weight compounds or soaps increases the stability of metal organosols [1,2].

The addition of surface-active substances to the dispersion medium sharply reduces the adhesion of the dispersed metal particles and favors their breakup [3]; however, only highly disperse suspensions, not metal sols, are formed thereby.

Studies of the conditions of stabilization of metal organosols [1,4] have shown that optimum stabilization of metal sols is attained by the joint addition of two types of stabilizers: 1) "hydrophobizing" ("carbophilizing") surface-active substances, which are fixed chemically on adsorption on the oxide-filmed surfaces of the metal particles, and 2) high molecular weight compounds, which form a loose three-dimensional structure in the entire volume of the sol and include the colloidal metal particles as units of the lattice.

From this point of view there is great interest in nonionogenic semicolloidal substances, namely soaps, which are dispersed in nonaqueous media with the formation of oleogels.

The powdered Al soaps studied in detail in [5], which are aluminum salts of organic acids (fatty and naphthenic), have the ability to swell and dissolve in hydrocarbon media, forming colloidal systems of a different degree of viscosity. The primary particles of the soap have an elongated form (but probably not very large dimensions), owing to polymerization through the oxygen atoms, of the type



There are also other data [6] on the ability of semicolloidal substances to form micellar systems in nonaqueous media.

The present investigation was directed toward the preparation of Al sols in benzene with the greatest possible stability, utilizing Al soap as a stabilizer. The Al soap, being well dispersed in benzene, possesses surface-active properties; therefore, it should be well sorbed on the surfaces of the solid particles of dispersed Al.

The Al soap, in the form of an aluminum naphthenate powder, was first dispersed in the benzene in a known concentration. In the resulting solution, at intervals of 2-3 days, Al powder was electrodispersed between aluminum electrodes (30 min at room temperature) in a unit which has been described previously [7]. The concentrations of all the resulting sols were determined by a gravimetric method.

As is evident from Fig. 1, an increase of the Al soap concentration results in an increase of the weight concentration of the sol which is obtained. Increasing the soap concentration to more than 1% introduced difficulty, since the viscosity of the medium became very substantial and dispersion of the metal ceased.

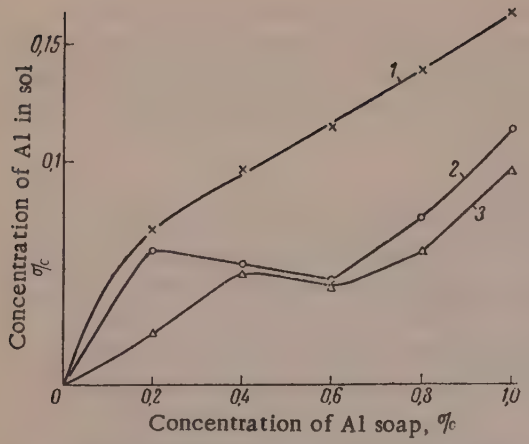


Fig. 1. Effect of aluminum soap concentration on dispersion of Al in benzene ($t = 20°$; $\tau = 30$ min): 1) Freshly prepared system; 2) after 96 hr; 3) after 720 hr.

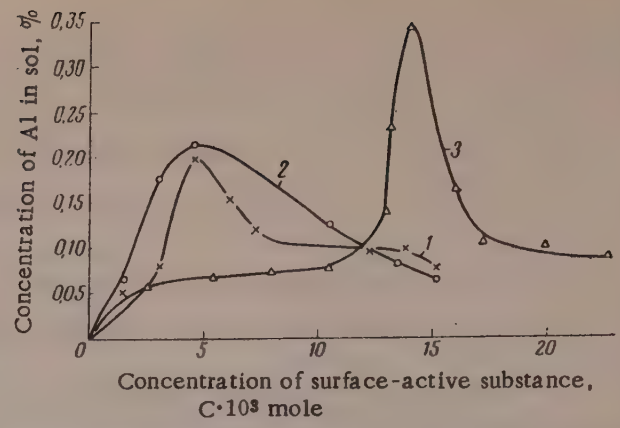


Fig. 2. Combined effect of surface-active substances and Al soap on dispersion of aluminum in benzene ($t = 20°$; $\tau = 30$ min): 1) Oleic acid; 2) stearic acid; 3) octanol.

From Fig. 1 (Curves 2 and 3) it is evident that on storage the concentration of the resulting sols is decreased, especially for sols of high concentrations. In testing the joint action of two stabilizers, Al soap and fatty acid or alcohol, we considered that upon sorption of the Al soap on the surface of a solid particle certain portions of the particle remain free, and on these portions there can be additional sorption of molecules of the surface-active substance.

The addition of surface-active substances to benzene before dispersing the Al (with constant concentration of Al soap, 0.6%) is accompanied by an increase of the resulting sol concentration up to a definite maximum, depending on the nature of the substance added. Further addition of the surface-active substance leads to a reduction of the sol concentration (Fig. 2).

Judging by the data obtained, the stabilizing action of the Al soap with reference to the dispersed Al increases in proportion to the soap concentration. It may be assumed that the surface-active molecules (or micelles) of the Al soap are sorbed on the surface of the dispersed Al particles, forming a molecular (micellar) adsorption layer. This adsorption layer apparently is the source of stability of the resulting system.

With an increase of soap concentration the diffusion coefficient of the particles of the Al sol is reduced in proportion to the viscosity increase, and thereby the probability of their collision and adherence is decreased, which favors stability of the resulting sols.

This circumstance—the increase of sol stability observed on introducing fatty surface-active substances together with the Al soap—compels us to assume additional sorption of the molecules of the surface-active substances on those portions of the solid Al particles which remained unoccupied after sorption of the molecules (micelles) of soap. It is possible that at the same time there is even some displacement of the soap molecules (micelles) by molecules of the surface-active substance, which is pointed out by the dropoff in all the curves of Fig. 2. At the same time the possibility of chemical interaction is not ruled out, i.e., chemical interaction between the molecules of the surface-active substance and individual portions of the surface of the solid Al particles, for example, in the case of stearic acid.

SUMMARY

1. Stable sols of aluminum in benzene, stabilized by a soap (Al naphthenate) have been obtained.

2. The stability and concentration of the aluminum sols increases as the added Al soap concentration is increased.

3. The concentration of the Al sol is decreased with storage.

4. The combined presence of Al soap and a nonionogenic and surface-active substance favors the dispersion of Al, within a definite zone of concentrations of the surface-active substances.

LITERATURE CITED

1. É. M. Natanson, Kolloid. Zhur. 20, 556 (1958).
2. M. A. Nikolaeva, Candidate's Dissertation (Moscow, 1942).
3. V. I. Likhtman, P. A. Rebinder, and G. V. Karpenko, Influence of a Surface-Active Medium on the Deformation of Metals (Acad. Sci. USSR Press, Moscow–Leningrad, 1954).
4. É. M. Natanson and N. I. Kozachek, Kolloid. Zhur. 18, 724 (1956); 19, 698 (1957).
5. G. V. Belugina and A. A. Trapeznikov, Kolloid. Zhur. 20, 3 (1958); A. A. Trapeznikov, Collection: New Methods of Physicochemical Investigation of Surface Phenomena (1950), Vol. 1, p. 20; A. A. Trapeznikov and E. M. Shlosberg, Collection: New Methods of Physicochemical Investigation of Surface Phenomena (1950), Vol. 1, p. 39; A. A. Trapeznikov and V. A. Fedotova, Doklady Akad. Nauk SSSR 81, 1101 (1951); 82, 87 (1952); 95, 595 (1954).
6. M. B. Mathews and E. J. Hirschhevn, Coll. Sci. 8, 86, 1953; J. G. Honig and C. R. Singletevry, Phys. Chem. 58, 201, 1954.
7. M. A. Lunina, Nauch. Doklady Vysshei Shkoly 2, 275 (1958); M. A. Nikolaeva and E. M. Preis, Kolloid. Zhur. 8, 409 (1946).

All abbreviations of periodicals in the above bibliography are letter-by-letter transliterations of the abbreviations as given in the original Russian journal. *Some or all of this periodical literature may well be available in English translation.* A complete list of the cover-to-cover English translations appears at the back of this issue.

ON THE THEORY OF CAPILLARY OSMOSIS

M. M. Milekhina

Institute of Physical Chemistry, Academy of Sciences, USSR
Translated from Kolloidnyi Zhurnal, Vol. 23, No. 2, pp. 173-176,
March-April, 1961
Original article submitted January 3, 1960

The work of a number of investigators [1] has shown that polymolecular layers of a liquid at an interface with a solid body have thermodynamic properties which are different from their volume properties. In particular, in the layer next to the wall, one observes a change in the concentration of a dissolved substance, which, according to some authors, leads to the formation of an "un-dissolving volume". If a concentration gradient is formed along the solid wall, this causes not only a diffusion current of the dissolved substance, but slip of the liquid in the adjacent layer [2], which owes its existence to the properties of the polymolecular liquid layers. This slip must be taken account of in calculations on the diffusion of solutions through porous diaphragms. The formulas for the velocity of the kinetic slip of the liquid in the layer adjacent to the wall were derived by Deryagin [2], using the auxiliary force field method.

The present paper gives a thermodynamic derivation of these formulas, at the same time taking account of convective diffusion, and deriving expressions for the simultaneous kinetic and diffusion currents of the material.

To find the pressure drop caused by the slip, consider the thermodynamic potential identity:

$$d\Phi = -SdT + Vdp + \sum_i \mu_i dN_i, \tag{1}$$

where S is the entropy; T is the absolute temperature: V is the volume; p is the pressure; μ_i is the chemical potential of a particle of the i-th sort; and N_i is the number of particles of the i-th sort.

Using the relationship

$$\Phi = \sum N_i \mu_i,$$

we obtain from Eq. (1)

$$\sum_i N_i d\mu_i = -SdT + Vdp.$$

For isothermal processed $dT = 0$, therefore

$$dp = \frac{1}{V} \sum_i N_i d\mu_i.$$

Having defined the concentration as $C_i = N_i/V$, we have, at equilibrium

$$dp = \sum_i c_i d\mu_i. \tag{2}$$

We shall apply the above relation to the flow of a liquid through a capillary under the influence of a concentration drop between the ends. In this case, the system as a whole will not be in a state of thermodynamic equilibrium. We shall assume, however, that equilibrium will be established in small parts of the system, having dimensions of the order of the diameter of the capillary, that is, in particular, that the layer adjacent to the wall can be formulated under the influence of surface forces. If external forces are present, the equilibrium condition is, as we know

$$\mu_i + U_i = \text{const}, \tag{3}$$

where U_i is the potential energy of a particle of the i-th sort in the external force field. Assume that $U = U_i(h)$, where

h is the distance from the wall of the capillary, that is, we assume that U_i is independent of z coordinate along the axis of the capillary. This assumption is correct for dilute solutions. It is natural to expect that we will get results correct to order of magnitude using this last relation even for concentrated solutions. We shall find the derivative $\partial p/\partial z$ on the basis of the above assumption. From Eq. 2, we have, for a mixture of two substances

$$\frac{\partial p}{\partial z} = c_1 \frac{\partial \mu_1}{\partial z} + c_2 \frac{\partial \mu_2}{\partial z}. \tag{4}$$

In particular, for $h \to \infty$, we have

$$\frac{\partial p^0}{\partial z} = c_1^0 \frac{\partial \mu_1^0}{\partial z} + c_2^0 \frac{\partial \mu_2^0}{\partial z}, \tag{5}$$

where, with index 0, we designate the thermodynamic quantities at $h \to \infty$.

According to Eq. 3, at constant z

$$\mu_i + U_i(h) = \text{const} = \mu_i^0(z),$$

therefore

$$\frac{\partial \mu_i}{\partial z} = \frac{\partial \mu_i^0}{\partial z}.$$

Subtracting Eq. (5) from Eq. (4) we get

$$\frac{\partial p}{\partial z} - \frac{\partial p^0}{\partial z} = (c_1 - c_1^0)\frac{\partial \mu_i^0}{\partial z} + (c_2 - c_2^0)\frac{\partial \mu_2^0}{\partial z}. \tag{6}$$

That is, at those points where $c_i \neq c_i^0$, there appear the additional pressure gradients $\frac{\partial p}{\partial z} - \frac{\partial p^0}{\partial z}$, caused by the slip of the layer of liquid adjacent to the wall.

Hydrodynamic considerations of the flow of liquid through a capillary lead to the idea that the radius of action of the forces near the wall is small compared with the radius of the capillary, and the movement of the liquid in the capillary can be considered as the motion of a liquid among a plane wall. To find the velocity of kinetic slip of the liquid, we shall use the Navier-Stokes equation, and the equation of continuity.

$$\frac{\partial \vec{v}}{\partial t} + (\vec{v}\nabla)\vec{v} = -\frac{1}{\rho}\operatorname{grad}(p - p_0) + \frac{1}{\rho}(\nabla\eta\nabla)\vec{v} + \frac{1}{\rho}\vec{F}(h), \tag{7}$$

$$\frac{\partial \rho}{\partial t} + \operatorname{div}\rho\vec{v} = 0, \tag{8}$$

where $\vec{v}$ is the velocity, t is the time, ρ is the density, η is the coefficient of viscosity, and F(h) is the force acting in the layer adjacent to the wall per unit of volume of the liquid.

We are looking for a solution of the form $v_h = 0$. Further, we consider the flow to be stationary, and the liquid to be incompressible. From the continuity equation (8), we obtain

$$\frac{\partial v_z}{\partial z} = 0, \text{ т. е. } v_z = v_z(h),$$

where the z component of the Navier-Stokes equation takes the form

$$\frac{\partial (p - p^0)}{\partial z} = \frac{\partial}{\partial h}\left(\eta \frac{\partial v_z}{\partial h}\right).$$

The solution of the last equation, from Ref. [2], is

$$\underset{h\to\infty}{v(h)} = u = -\sum_i \frac{c_i^0}{\eta}\frac{\partial \mu_i}{\partial z}\xi_i,$$

where

$$\xi_i \approx \int_0^\infty \frac{c_i - c_i^0}{c_i^0} h dh,$$

i.e., a quantity having the dimensions cm^2, the square root of which characterizes the erosion of the adsorbed layer.

Examining the processes in systems formed of solutions of different concentration, separated by porous diaphragms, one has to take account of both the kinetic slip and the diffusion at the same time. To allow for diffusion, it is very convenient, in our derivation, to define the concentration (c) as the ratio of the mass of one of the components of the mixture to the whole mass of liquid in a given volume element. The transfer of dissolved material in the liquid occurs in two ways: by indirect convection transfer when the liquid moves, and by direct diffusion. The total current of dissolved material is equal to

$$\vec{j} = \rho c \vec{u} + \vec{i}, \tag{10}$$

where $\vec{i}$ is the diffusion current, from Ref. [10] equal to

$$\vec{i} = -\rho D \left(\nabla c + \frac{k_T}{T} \nabla T + \frac{k_p}{p} \nabla p \right).$$

Here D, k_T, and k_p are the coefficients of diffusion, thermodiffusion, and barodiffusion. Neglecting the barodiffusion, which need be considered only with large pressure gradients, and setting T = constant, we obtain

$$\vec{j} = \rho c \vec{u} - \rho D \nabla c. \tag{11}$$

In the stationary case, the current of dissolved substance along the axis of the capillary must be constant, consequently

$$j_z = \rho c u_z - \rho D \frac{\partial c}{\partial z} = \text{const}.$$

Integrating this relation, we obtain

$$c = K e^{\frac{u_z}{D} z} + \frac{j_z}{\rho u_z},$$

where K is the integration constant. For simplicity we drop the subscript z. From the conditions $c = c_a$ at $z = 0$, and $c = c_b$ at $z = l$ we find

$$K = \frac{\Delta c}{1 - e^{\frac{u}{D} l}}$$

and

$$j = \rho u \frac{c_a e^{\frac{u}{D} l} - c_b}{e^{\frac{u}{D} l} - 1}. \tag{12}$$

$\Delta c = c_a - c_b$. For the special case in which macroscopic transfer plays a small role in comparison with diffusion, that is, when $\frac{u}{D} l \ll 1$, we have

$$j = \rho D \frac{\Delta c}{l} + \frac{1}{2} \rho u (c_a + c_b). \tag{13}$$

In the other limiting case, when $(u/D) l \to \infty$, we obtain (for $u > 0$)

$$j = \rho u c_a.$$

Thus the difference between the thermodynamic properties of the liquid layer adjacent to the wall and the properties of the liquid in the rest of the volume lead (for the case $[u/D]\, 1 \ll 1$) to an additional current of dissolved substance, equal to $\frac{1}{2} \rho u (c_a + c_b)$. Measuring the total current experimentally, and subtracting out the diffusion current, found from supplemental experiments, we determine ξ and, consequently, the quantity which determines the thickness of the layer adjacent to the wall.

In the other limiting case of $[u/D]\, 1 \to \infty$, in view of the absence of any diffusion current, even in second order approximation, there is no need to carry out supplemental experiments to measure it. The velocity of kinetic slip u, and, consequently, ξ is determined from direct measurement of the velocity of transfer of the dissolved substance.

SUMMARY

If the thermodynamic properties of the liquid in the layer adjacent to the wall are different from the volume properties, then the presence of a concentration gradient at the ends of the capillary gives rise to a corresponding pressure gradient at the ends, which leads to motion of the liquid in the capillary. The result is the appearance of additional (over and above the diffusional) transfer of material through the capillary.

I wish to express my gratitude to B. V. Deryagin for his valuable comments, and for his direction of the work.

LITERATURE CITED

1. B. V. Deryagin and V. V. Karasev, Doklady Akad. Nauk SSSR, 101, 289 (1955); B. V. Deryagin, V. V. Karasev, N. N. Zakhavaeva and V. P. Lazarev JETP 27, 1077 (1957); V. V. Karasev and B. V. Deryagin, Kolloidn. Zh. 15, 365 (1953); É. M. Zorin, Dissertation [in Russian], Moscow (1952); B. V. Deryagin, Doklady Akad. Nauk SSSR 129, No. 6 (1959).
2. B. Deryagin, G. Sidorenkov, E. Zubashchenko, and E. Kiseleva, Kolloidn. Zh. 9, 335 (1947).
3. L. Landau and E. Lifshits, Mechanics of Complex Media [in Russian] Moscow, Izd. Tekhn.-teor. lit. (1954).

All abbreviations of periodicals in the above bibliography are letter-by-letter transliterations of the abbreviations as given in the original Russian journal. *Some or all of this periodical literature may well be available in English translation.* A complete list of the cover-to-cover English translations appears at the back of this issue.

ELECTRON MICROSCOPE INVESTIGATION OF COLLOID PARTICLE FORMATION OF WHITE FILLERS IN LATEXES

A. R. Narinskaya, A. P. Pisarenko, and B. V. Shtarkh

Scientific Research Institute for Film Materials and Artificial Leather, Moscow
Translated from Kolloidnyi Zhurnal, Vol. 23, No. 2, pp. 177-179,
March–April, 1961
Original article submitted February 8, 1960

It is a known fact that the degree of dispersion of fillers is one of the factors that determines their activity. The problem of the effect of the dispersion of fillers on the properties of vulcanizates consisting of synthetic and natural rubbers has been studied repeatedly [1-3], but for synthetic latexes, as they are used in the artificial leather industry, the question has been studied very little. The synthetic latexes, which are widely used in the artificial leather industry as coatings for fabrics, are complicated mixtures, the majority of which include white fillers in their composition. However, the low degree of dispersion which is found in natural white fillers (chalk, kaolin, etc.), and their tendency to form aggregates, renders the production of high stability white coatings difficult.

Recently, in addition to natural chalk, synthetic calcium carbonate called precipitated chalk, has been widely used as a filler. The calcium carbonate is made from calcium chloride, or calcium hydroxide, by precipitation with sodium carbonate or carbonic acid. The size of the precipitated chalk particles, as well as its activity, depends upon the way in which it is produced. The mean particle dimensions of the precipitated carbonates varies from 0.1 to 3 mμ. Increased activity is observed with precipitated chalk having particle dimensions from 0.1 to 1.0 mμ [1].

In the present work, we have carried out an electron microscope study of the formation of precipitated chalk from calcium hydroxide and sodium carbonate.

In our observations, we used calcium carbonate prepared both in the presence of surface-active material, and in its absence, as well as the systems: SKS-30 latex and chalk, prepared by precipitation in the latex. The preparations were examined with an ÉM-3 electron microscope. The photomicrographs were enlarged 7500 times. As may be seen from the electron microscope pictures, a sufficiently large excess of slaked lime and soda led to the formation of monolithic large rhombic crystals of calcium carbonate (Fig. 1a), having dimensions of ~2 μ or aggregates of such crystals (Fig. 1b). It should be noted that in the present case smaller crystals are also formed, or seedlings of such (Fig. 1c, and d).

A completely different picture takes the screen, if the calcium carbonate is formed from slaked lime and soda, but in the presence of small quantities of the surface-active substance OP-10. The crystal seedlings have a predominantly rounded shape (Fig. 1e), and are 0.1- 0.12μ in diameter, with a pronounced tendency to form strings of chain like structures (Fig. 1f). These formations are characterized by a very loose structure. However, as a result of the crowding of the system, more monolithic aggregates are formed at the same time (Fig. 1g, and h).

The photographs of precipitated chalk, prepared in the presence of OP-10, but made after the removal of the surface-active material (Fig. 1i), show agglomerations, formed, not of large rhombic crystals, as is the case when the calcium carbonate is prepared without any surface active material (Fig. 1a and 1b), but formed of loose particles, quite distinctly observable when the preparations are examined visually under the microscope (Fig. 1j).

Thus, the use of surface active agents in the preparation of the chalk leads to the formation of fillers having a looser structure.

Agglomerations of crystals of various shapes (Fig. 2a), which increase in size with time (Fig. 2b), were formed when calcium chloride and sodium bicarbonate were taken as the reactants. It should be pointed out that the formation of calcium carbonate crystals could be observed with the electron microscope only in case the sodium bicarbonate and calcium chloride concentration in the solution was greater than 0.1 mole/liter.

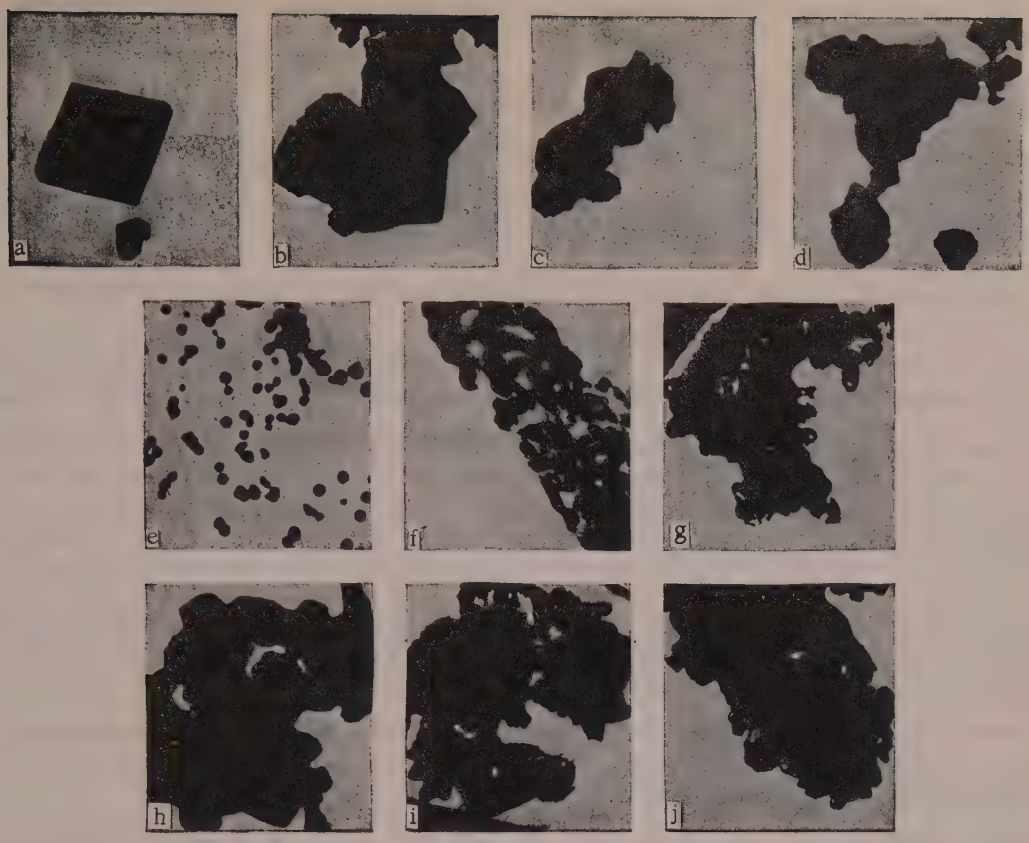


Fig. 1. Calcium carbonate prepared from slaked lime and soda in water: a,b,c,d) without surface active substances, e,f,g,h) in the presence of OP-10, immediately after reaction, i,j) in the presence of OP-10, after washing out and 6 hours standing.

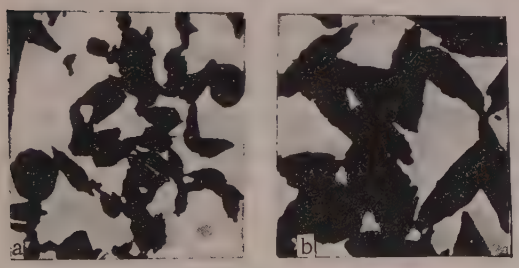


Fig. 2. Calcium carbonate prepared from calcium chloride and sodium bicarbonate without surface active substances. a) prepared immediately after reaction, b) after 6 hours standing.

The chalk, prepared in the latex, ought to be characterized by a high degree of dispersion, and a more uniform distribution throughout the mass of the latex, than the chalk prepared in water, and then added to the latex in dispersed form, since it forms on the globules as colloid particles, increasing the size of the molecular systems in the process, which is what the filler has got to do if it is going to strengthen the latex film [4].

Technique of preparing chalk in the latex. To an SKS latex, constantly stirred, a 40% solution of crystalline sodium carbonate was added, and then a 50% suspension of hydrated calcium oxide 0.5–1% OP–10 (surface active agent) according to the quantity of chalk to be formed. The dispersion of hydrated calcium oxide was added in small portions at intervals of 2–3 minutes, with constant stirring. After the necessary amount of hydrated calcium oxide has been added, the stirring is continued for 5 minutes more. The quantity of soda and hydrated calcium oxide added was varied according to the amount of filler required in the latex, but in all cases the reactants were taken in stoichiometric proportions.

The latex mixtures so prepared were stabilized by 1–2 days storage. The most stable mixtures were those having 10 parts by weight of filler to 100 parts by weight of latex polymer. A chalk content above this amount caused rapid settling. Apparently, in this case, there is some additional agglomeration of the filler particles, forming a compact structure. The same thing is observed on raising the temperature of the latex, or of the suspension of hydrated calcium oxide.

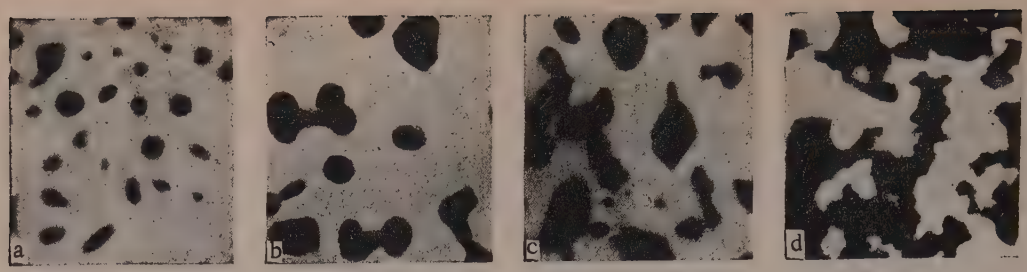


Fig. 3. Calcium carbonate prepared from slaked lime and soda in the latex a) control (SKS-30 latex); b,c,d) precipitated chalk in the latex.

Combustion of a latex film containing one part of chalk by weight showed 0.42% Ca (calculated 0.40%). Results just as close to the calculated value were found for latex films containing 5 and 10 parts by weight of chalk.

When the chalk is formed in the latex (Fig. 3), a sharp increase in the size of the globules is distinctly visible, which can be explained by the precipitation of chalk on the surface of the globules as well as on the seedlings, the moment it is formed. This view is supported by the fact that the globules of the original SKS-30 latex (Fig. 3a) retain their globular shape even though they increase in dimensions from 0.50— 0.5μ to 0.5 - 0.6μ while the chalk is being formed (Fig. 3b).

At the same time, separate globules (Fig. 3c, d) may be observed in the mass of the chalk, which is formed as a loose precipitate. In the photomicrographs, large particles (Fig. 3d) are clearly visible, which, probably, have appeared as a result of fusion of globules in the chalk deposit.

These observations suggest that the latex medium provides favorable conditions for the formation of fillers in a highly disperse, active form. This view is supported by the increase in strength of the latex vulcanizates from 12 to 50 kg/cm^2, when the films contain chalk formed in the latex.

The increased activity of white fillers, prepared in the presence of surface active agents, is observed not only with chalk and colloidal silica [5], but also with aluminate type fillers. Photomicrographs of fillers, prepared by the reaction between aluminum sulfate and sodium carbonate in the presence of OP-10 (Fig. 4a, b) show that the aluminate filler consists of particles having a high degree of dispersivity. The particles, just as in the initial stages of the formation of chalk or white lamp-black [5], are inclined to form net-like structures. The presence of a highly developed surface is the basis for ascribing the aluminates formed in this way to the category of high-activity fillers, adding them to the latex and separating them out along with the rubber made it possible to produce high-strength, filled butadienenitrile rubbers, considerably exceeding in strength rubbers of the same sort, which had been strengthened by adding the same quantity of aluminate filler at the rolls [6].

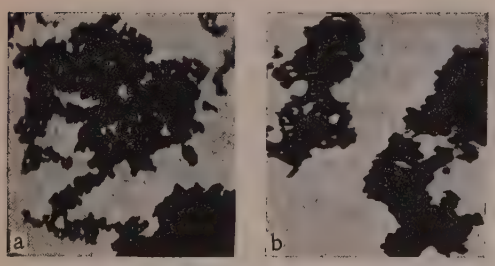


Fig. 4. Aluminate type filler prepared in the presence of a surface active agent.

SUMMARY

1. An electron microscope study has been made of the formation of high-dispersion white fillers of carbonate and aluminate type.

2. Surface active agents favor the preparation of filler particles in a highly dispersed state.

3. It has been found possible to strengthen latex films by the latex films by the formation of highly dispersed chalk in the latex.

LITERATURE CITED

1. V. H. Vodra, Rubber Age 4, 71, 507, 1952.
2. P. Delfosse, Rubber and Plast. Age 38, 257; 259, 1957.
3. G. Hoffmann, Plaste und Kautschuk 4, 471, 1957.
4. B. A. Dogadkin, L. G. Senatorskaya, V. I. Guseva, A. V. Suslyakov, and P. I. Zakharchenko, Kolloidn. zh. 18, 528 (1956).
5. B. V. Shtarkh, A. P. Pisarenko, Scientific Papers of the All-Union Scientific Research Institute for Film Materials and Artificial Leather, Collection 11 [in Russian] (1960).
6. V. A. Shvetsov, A. P. Pisarenko, B. V. Shtarkh, and A. S. Novikov, Kolloidn. zh. 22, 743 (1960).

THE ADHESION OF DOUGH TO THE SURFACE OF A SOLID

B. A. Nikolaev and R. P. Glukhova

Scientific Research Institute for the Baking Industry, Moscow

Translated from Kolloidnyi Zhurnal, Vol. 23, No. 2, pp. 180-185, March-April, 1961

Original article submitted February 25, 1960

Dough (45-50% moisture) adheres well to solid surfaces revealing a cohesion character of tearing. The ability of dough to adhere (stickiness) is directly determined by the moisture content in it and is in a reverse relationship with the characteristics of the hydrophilic nature and quality of the flours. The optimum value of the stickiness helps some of the mechanical treatment and too much stickiness hinders transportation, division of the dough into parts and other operations. The stickiness of the dough is reduced by pouring flour or starch onto its surface or drying it with warm dry air. The stickiness of dough is best studied in connection with its mechanical properties, such as elasticity, resilience and viscosity, affecting the force of adhesion.

Despite numerous investigations the theory of adhesion has still not been sufficiently developed [1]. For dough ionically conducting an electric current, the adhesion was considered as the action of intermolecular forces in connection with the value of contact surface and layer thickness which changed with time. Since fairly high viscosity and resilience of the dough prevent the attainment of instantaneous, complete contact with the surface, the force of adhesion should depend directly on the time and stress of contact. Since the actual area of contact can be many times greater than the measured area [2] an arbitrary value was taken for the latter. The characteristics of the adhesion forces in the form of pressure or work of tearing are in reverse relationships to the thickness of adhesive layer. Consequently, in these cases it is essential to achieve a minimum and constant thickness of the layer. This latter depends on the degree of smoothness of the surfaces between which the adhesive is situated and the mechanical characteristics of its volume (shear modulus, viscosity). For dough of normal moisture content, placed between ground metal surfaces under a load of 0.1 kg/cm^2 the layer thickness was 0.2–0.3 mm. However, as shown by experiment, the layer thickness of dough between two plates, initially equal to 0.25 mm, was gradually reduced; after 5 min of contact it was reduced by ~15%. The greatest change in the layer thickness of dough (~10%) was observed in the first minute of contacting due to the dough surface being smoothed out. The adhesion forces of the dough were measured from the tearing pressure (P_o, g/cm^2 or d/cm^2), equal in value and opposite in sign to the tearing stress (P_k).

The measuring instrument was a double arm weighing mechanism; to one arm, suspended on a connecting link, was a disk of certain area (usually 10 cm^2) with a smooth lower surface balanced by the other arm of the mechanism, fitted with a scale from which the suspended tearing load was established. The smooth surface of the disc was covered with a thin layer of dough and applied to the smooth surface of the fixed plate (the base of the instrument). Iron and teflon contacting surfaces were tested. To even out the thickness of the dough layer and provide contact, before the test the disc was loaded with a constant load for a fixed time, setting up a known contacting stress (P_k). The center of the disc coincided with the vertical connecting link. The disc coated with dough was torn instantaneously (except in special experiments) by freeing the stopping device of the balance beam. The tearing stress (P_s) was found by multiplying the weight of the load by the coefficient of the scale (the ratio of the arms of the beam during tearing), and dividing by the disc area. An advantage of this method was the possibility of controlling the adhesion forces over wide limits by changing the discs, the load and changing its position. The measurements were carried out in a thermostat at 30°. The shear modulus and viscosity of the dough were measured on an instrument with plane-parallel clearance on an inclined plane at a gradient rate of ~0.03 sec^{-1} [3].

Studies were made of specimens of ordinary fermenting and nonfermenting doughs obtained from commercial wheat flour and artificial dough obtained from dehydrated material by the method of sublimating wheat proteins of flour gluten and wheat starch. Not less than three determinations were made in each experiment.

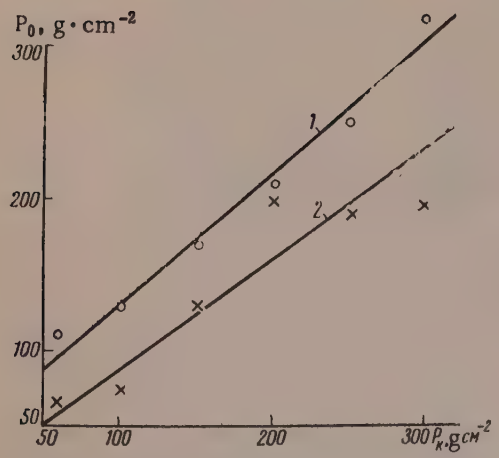


Fig. 1. Dependence of the tearing pressure P_o on the contacting stress P_k: 1) nonfermenting dough; 2) fermenting dough.

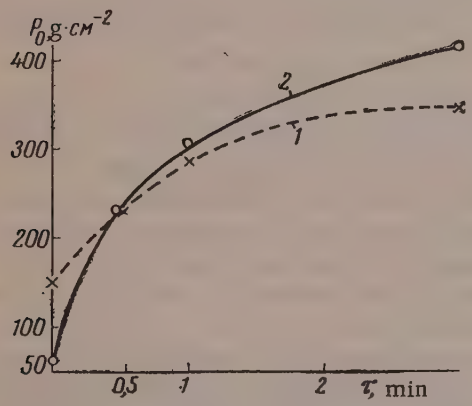


Fig. 2. Dependence of the tearing pressure P_o on the time of contacting of the nonfermenting doughs with a surface of iron (1) and teflon (2).

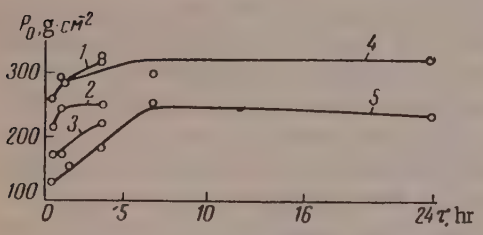


Fig. 3. Dependence of the tearing pressure P_o on the duration of contacting of nonfermenting dough with an iron surface of discs of area: 1,4) 5 cm^2; 2,5) 10 cm^2; 3) 20 cm^2.

On this basis it might have been expected that the tearing pressure of the dough (P_0) would depend directly on the contacting pressure (P_k) and its time of action. It can be seen from Fig. 1 that the dependence of P_o on P_k for nonfermenting (without yeast and salt) and fermenting dough of first grade wheat flour with 44% moisture after 1 min of contacting was close to linear. For later tests on wheat dough it was assumed that $P_k = 100$ g/cm^2.

It can be seen from Fig. 2 that the tearing pressure of the dough (P_0) from a disc of area 10 cm^2, regardless of the material of the surfaces, increases the most rapidly in the first minutes of contacting (~10%). This corresponds to a nonlinear character of decrease in layer thickness of the dough and presumably to the development of the contact surface during contacting. A decisive factor in this phenomenon is apparently the development of highly resilient elastic shear deformation, usually occurring in the wheat dough (with a speed gradient of 0.03 sec^{-1}) within 1 min. In later experiments the time of contacting was taken equal to 1 min.

The working parts of the machines and transport mechanisms in the food industry are coated with teflon or treated with a silicone liquid to reduce the adhesion of raw materials and semifinished products. As can be seen from Fig. 2, teflon should only be used for short contacting.

The state of the contacting surface (its degree of smoothness) is very important for adhesion: it affects the size and accessibility of the actual contacting surface and the final thickness of the dough layer depends on it. Iron surfaces coated with films of a silicone liquid (GKZh-94) showed less (by ~10%) tearing pressure of the dough compared with untreated surfaces. After 1 min contacting the tearing pressure of the dough from surfaces of plexiglas and textolite hardly differs from that obtained for iron surfaces.

As can be seen from Fig. 3, the tearing pressure of the dough increases considerably with reduction in the area of the disc. It may be supposed that with the same treatment of the surfaces with small area discs thinner layers of dough may be obtained, adhering more strongly to the contacting surfaces.

The stickiness of the dough increases during the first 6 hours after preparation (curves 4 and 5, Fig. 3). Consequently the adhesion of the dough depends on its "age" and the function of distribution of the molecular weight of the polymers and also the presence in it of natural structure plasticizers (water-soluble proteins, amino acids, dextrins, sugars, etc.).

With increase in the moisture content in the dough the tearing pressure increases and the shear modulus, viscosity and thickness of the layer decrease (Table 1). The ratio of the tearing pressures to the trebled shear modulus ($P_o/3E$), characterizing the ratio of the adhesion forces to the cohesion forces, also increases and with 44% moisture in the dough becomes greater than unity. In agreement with this the character of tearing becomes cohesion. Changing the dough moisture content by 2% on both sides of the mean value (44%) did not show a sufficiently uniform change in the tearing pressure whereas the moduli and viscosity were reduced with increase in the moisture content. Consequently, this method of measuring the dough stickiness is less sensitive than the measurement of moduli and viscosity.

TABLE 1

Dependence of the Tearing Pressure on the Dough Moisture Content

Moisture %		32	44	60
Tearing pressure	$(P_0)\times10^{-5}$, d·см$^{-2}$	0,71	2,28	2,65
Shear modulus	$(E)\times10^{-4}$, d см$^{-2}$	22,6	2,2	0,073
Viscosity, poises		$1,1\cdot10^{7}$	$3,7\cdot10^{5}$	$2,8\cdot10^{4}$
$P_0/3E$		0,11	3,4	120,5
Layer thickness, mm		0,8	0,3	0,2
Character of tearing		Adhesion	Cohesion	

It is very important to study the dependence of tearing pressure on the time of action of the stress, starting from the moment of loading the weighing mechanism to the moment of tearing. This dependence should be inverse since the development at the surface of defects and weak spots depends directly on the time of action of the tearing stresses.

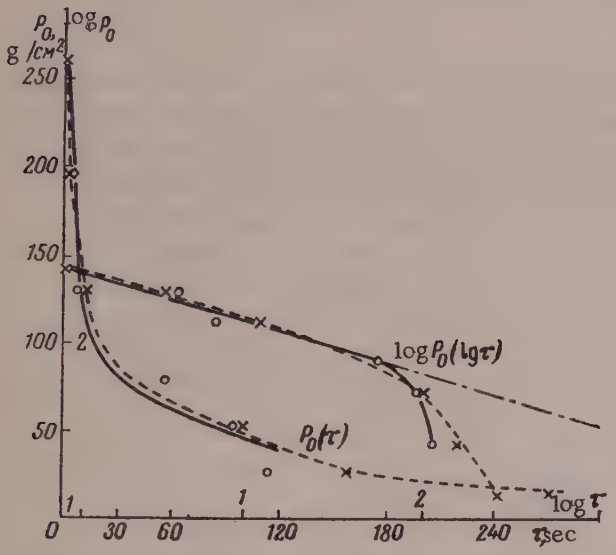


Fig. 4. Dependence of the tearing pressure P_0 on the time of action of the stress (τ).

It can be seen on Fig. 4 that the initial section of the P_0 (τ) curves has a logarithmic character. In connection with this it would be presumably advisable to use designs of adhesiometers with gradual loading of the springs or other weighing instrument. The instantaneous tearing method is the more correct.

It can be seen from Fig. 5 that two dough specimens (without heating and kept for $2\frac{1}{2}$ hr) have the same character for the dependence of tearing pressure on the dough temperature. As the dough is kept its stickiness increases (Figs. 3 and 5). The obtained results are explained by the change in viscosity and shear moduli of the dough determined by the elasto-resilient deformation. It can be seen from Fig. 6 that the moduli and viscosity of the dough kept for 30 min were much greater than for dough kept for 3 hr. After 3 hr the dough had less layer thickness, made better contact and was stickier than after 30 min. With increase in temperature the viscosity of dough decreased and the shear moduli, starting with 20°, increased. This difference in the temperature dependence of viscosity and moduli of the dough is shown graphically by the continuous reduction in their ratio, characterizing the relaxation of internal stresses under conditions of constant deformations. The reduction in stickiness of the dough with increase in temperature from 10 to 40° (Fig. 6) is due to the increase in shear modulus of the dough or reduction in its elasto-resilient properties, presumably due to the greater swelling of the polymers (proteins, starch). Consequently, the resilient properties of the dough in this range of temperatures has an effect on its stickiness.

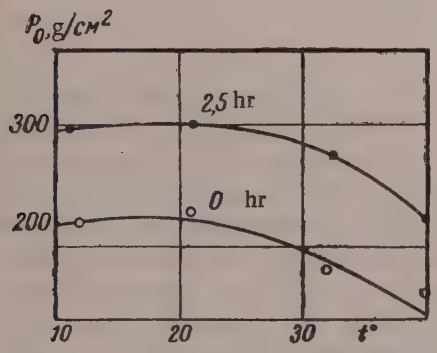


Fig. 5. Dependence of the tearing pressure P_0 on the dough temperature (t).

Table 2 gives data on the value of the tearing pressure for hydrated basic elements of the complex structure of dough.

It can be seen from Table 2 that for hydrated first grade starch the tearing pressure is greater than for wheat dough of approximately the same moisture content Figs. 1,2). Second grade starch, containing much protein and cellulose, had high moisture content and low tearing pressure. The shear modulus and viscosity of a paste of second grade starch was much higher than for a first grade starch [4]. It may well be that the small value of the tearing pressure of a given structure is due to the presence of these mentioned impurities and the high indices of the mechanical characteristics of the volume (moduli, viscosity).

TABLE 2

The Tearing Pressure (P_o) of Basic Elements of the Chemical Composition and Structure of Dough

Name of structure and its composition (by weight)	Moisture, %	Thickness of the layer, mm	Tearing pressure $g.cm^{-2}$	Character of tearing
Hydrated first grade starch	44.7	0.28	380	Cohesion
Hydrated second grade starch	69.6	0.25	185	The same
Hydrated proteins of cellulose	64.7	0.55	170	Adhesion
A hydrated mixture of first grade starch and cellulose proteins—68:12	43.5	0.54	295	Cohesion
The same and 5 parts of glucose	43.6	0.50	320	The same
Hydrated mixture of first grade starch and cellulose proteins and tvin-80, 68:12:0.25	44.0	0.52	285	" "
A hydrated mixture of first grade starch and cellulose proteins and washed bran, 68:12:20	50.1	0.61	170	Adhesion

Hydrated proteins of cellulose have high elasticity and resilience [4] which prevents them being obtained in the form of thin layers. A large amount of adsorbed and immobilized cellulose when it is exposed to moisture presumably hinders contact with the solid surface. The proteins of cellulose therefore have a low tearing pressure and adhesion character. When these proteins are dried by vigorously forcing out the moisture and mixing the structure their high stickiness is revealed.

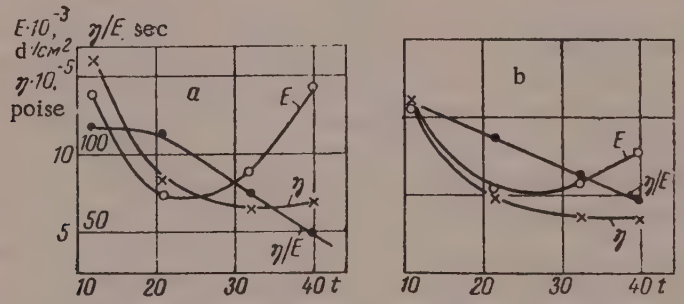


Fig. 6. Dependence of the elastic-resilient-viscosity characteristics of dough E, η, η / E on the temperature (t) when kept for 30 min (a) and 3 hr (b).

A hydrated mixture of first grade starch and proteins of cellulose in a ratio corresponding approximately to their content in the dough had a tearing pressure close to that of the natural structure of dough from first grade wheat flour. After the introducing ~5% glucose into this mixture the tearing pressure and stickiness of the structure were somewhat increased. The introduction of 0.25% of a surface active compound tvin-80 (the polyethylene glycol ester of the monooleate of anhydrosorbitols) hardly changed the value of the tearing pressure of the mixture. Bran or cellulose obtained from it, on being added to dough, strongly increases its viscosity and reduces the resilient properties [4]. These facts can presumably explain the considerable increase in moisture of a mixture of starch, proteins of cellulose and bran, the increase in thickness of the layer, low pressure and also adhesion character of tearing of this structure (Table 2). The pressure and character of tearing of dough depend on the chemical composition of the flour. Under the tested conditions the stickiness of the dough depends mainly on the content of starch in it. In the normal state under free soaking, cellulose proteins have low stickiness. However, in additional tests on wheat dough made from a grain with the proteins damaged by chinch bugs the tearing pressure was 20-25% greater than for a dough from normal grains (200-250 g/cm^2). Dough from second grade wheat flour (containing ~10% bran) had an adhesion character of tearing and a tearing pressure of 140-150 g/cm^2.

* Transliteration of the Russian Original.

The tearing pressure of bread crumbs from wheat flour was ~2 orders less than the tearing pressure of dough. This phenomenon can be explained by the fact that during fermentation and heating of the dough a porous structure of the crumb is formed, devoid of flow and having moduli of elasticity about a hundred times greater than for the dough.

SUMMARY

1. The adhesion of dough to a solid surface, measured by the tearing pressure, is considered as being due to the action of intermolecular forces and the contact conditions (thickness of the dough layer, development of true surface of contact), depending on the chemical composition, structure and mechanical properties of its volume.

2. The dependence is shown of the tearing pressure of fermenting and nonfermenting dough on the stress during contacting before the test, duration of contacting of nonfermenting dough to surfaces of iron and teflon, the size of the area of the contacting surface, the keeping time of the dough, its moisture, time of action of the stress during tearing of the surface and the dough temperature.

3. Data are given on the tearing pressure for the basic elements of the dough structure (starch, proteins) and artificial "dough".

LITERATURE CITED

1. B. V. Deryagin and N. A. Krotova, Adhesion (Acad. Sci. USSR Press, 1949); S. S. Voyutskii, A. I. Shapovalova and A. P. Pisarenko, Doklady Akad. Nauk SSSR 105, 5 (1955); Adhesion (Glues, Cements, Solders). Collection, edited by N. Debroin and R. Guvnick [Russian translation] (Foreign Literature Press, 1954); Collection: "Symposium on Adhesion and Adhesives" New York, Wiley (1954).
2. A. Ya. Drinberg, E. S. Gurevich and A. V. Tikhomirov, The Technology of Nonmetallic Coatings [in Russian] (State Chemistry Press, 1957), p. 57.
3. B. A. Nikolaev and L. S. Beganskaya, Transactions of the Third All-Union Conference on Colloid Chemistry [in Russian] (Acad. Sci. USSR Press, 1956), p. 209.
4. B. A. Nikolaev and I. A. Samarina, Zh. Khlebopekarnaya i Konditerskaya Prom-st', 8, 4 (1958).

All abbreviations of periodicals in the above bibliography are letter-by-letter transliterations of the abbreviations as given in the original Russian journal. *Some or all of this periodical literature may well be available in English translation.* A complete list of the cover-to-cover English translations appears at the back of this issue.

ADSORPTION ISOTHERMS OF IONOGENIC SEMICOLLOIDAL SURFACE ACTIVE SUBSTANCES

N. S. Razumikhina and E. M. Aleksandrova

D. I. Mendeleev Moscow Institute of Chemistry and Technology,
Department of Colloidal Chemistry
Translated from Kolloidnyi Zhurnal, Vol. 23, No. 2, pp. 186-189,
March-April, 1961
Original article submitted November 12, 1959

The practical importance of synthetic ionogenic surface-active substances (SAS) is well known. In many production processes the decisive role is played by adsorption of SAS on solid sorbents. The theory of such adsorption has still not been developed. The adsorption isotherms of SAS on solid sorbents have also been little investigated.

During an investigation of the sorption of polystyrene latexes [1] adsorption isotherms of two cation-active stabilizers were obtained: stabilizer A (VA-a representative of the quaternary salts of aminomethylated polyglycol esters of alkyl phenols) and octadecylhydroxymethylpyridine chloride (OOPC). The adsorption isotherms of these SAS on filter paper in the region of low concentrations have been previously described [2].

In the present work, adsorption isotherms of VA and OOPC on filter paper and cotton gauze were obtained in a wider range of concentrations. The equilibrium concentrations of the stabilizers were determined by the Kryukova method [3]. Equilibrium was established after approximately one day and all the equilibrium concentrations were therefore determined after 2 days. The critical concentrations of micelle formation and the physicochemical properties of VA and OOPC are given in [4].

As may be seen in Fig. 1, the adsorption isotherms of VA and OOPC stabilizers on filter paper and cotton gauze have a complex character; in the region of low concentrations they have a normal appearance. With an increase in the concentration of the stabilizers, kinks appear on the isotherms. With a further increase in concentration, a clearly expressed maximum is observed on the isotherms.

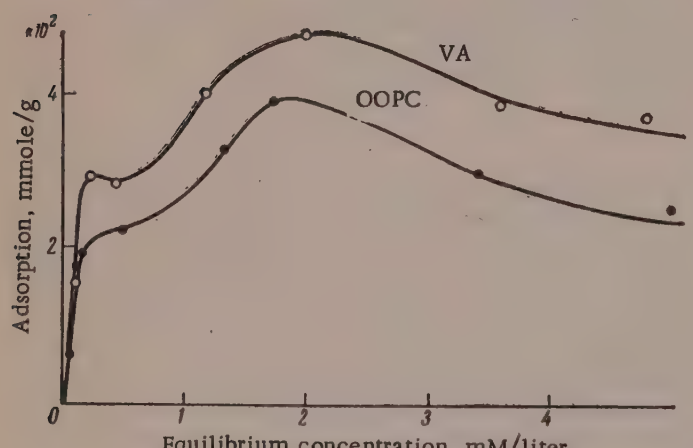


Fig. 1. Adsorption isotherms of OOPC on filter paper and VA on cotton gauze.

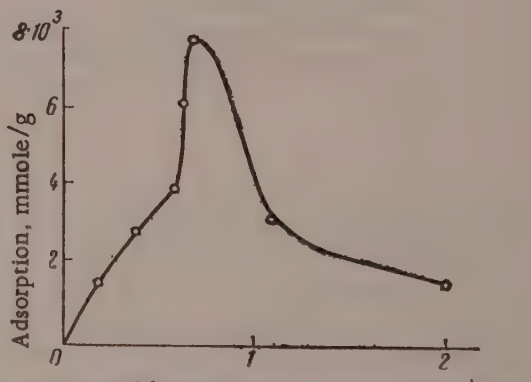


Fig. 2. Adsorption isotherm of VA on ground glass.

In all probability, kinks on the isotherms, in the form of small minima, are possible in other cases. However, it is very difficult to detect these minima because they are observed in a very narrow region of concentrations.

The adsorption isotherm of VA on a non-porous hydrophilic sorbent, ground glass (Fig. 2), has the same appearance as on porous sorbents (Fig. 1). Therefore it cannot be assumed that the fleeting semicolloidal character of the stabilizers is due to the appearance of micelles which cannot penetrate the pores of the sorbent.

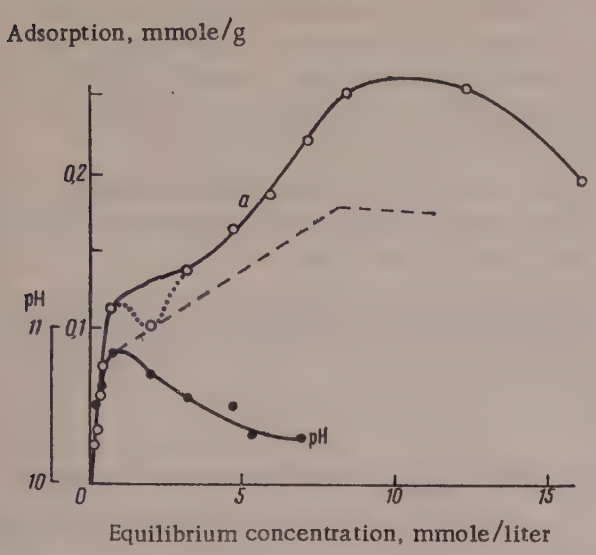


Fig. 3. Adsorption isotherm of NB wetting agent on activated charcoal.

Isotherms of similar pattern to those in Figs. 1 and 2 were found by the authors in the case of the adsorption of an anion-active stabilizer, sodium N-dibutylnaphthalene sulfonate (NB wetting agent), on filter paper, overcharged with a cation-active substance, sapamine. NB wetting agent was not adsorbed from an aqueous solution by filter paper with a negatively charged surface at the boundary with the water. Adsorption of NB wetting agent was only observed when the paper surface was overcharged. Equilibrium concentrations of NB wetting agent were characterized by a surface tension at the solution-air boundary, measured by a modified method of raising a liquid in an inclined glass capillary with a suspended drop [5].

The adsorption isotherm of NB wetting agent on a heteropolar absorbent—activated wood charcoal with a high ash content and a large specific surface (Fig. 3) - is also similar to those described above.

The adsorption of all the SAS investigated by us is not completed by the formation of a monomolecular layer. The adsorption of NB wetting agent on charcoal has a hydrolytic character. Anions of NB wetting agent are adsorbed on the surface of the charcoal, and OH ions pass into solution. From Fig. 3 it is seen that with an increase in the adsorption of NB wetting agent the pH of the solutions increases and reaches a maximum at the concentration at which a kink is observed on the adsorption isotherm (completion of the monomolecular layer). With a further increase in concentration (second step on the isotherm) the increase of adsorption takes place without appreciable changes in the pH of the solution. If adsorption took place subsequently directly on the surface of the charcoal, the pH of the solutions would continue to increase (dotted line in Fig. 3).

Adsorption isotherms of SAS which do not have a semicolloidal character - sodium caprylate and sodium enanthate - on activated wood charcoal have a similar appearance to the isotherms (Figs. 1 and 2); this also indicates the polymolecular character of the process, although there is little probability of the formation of micelles in a solution of these salts.

From the above data it may be concluded that the character of the adsorption isotherms of ionogenic SAS, which are strong organic electrolytes and have a diphilic structure, is not due to the semicolloidal state but to the ionic structure. The diphilic character leads to a specific orientation of the ions on the surface of the sorbent. In the case of polar sorbents, electrostatic forces predominate and the ions of the stabilizers are oriented by the ionogenic part to the sorbent. This orientation of the ions is completed by the saturation of the monomolecular layer (on the isotherms of Figs. 1 and 2 this was expressed by the first step) and leads to an increase in the energy barrier between the sorbent and the polar medium. Therefore, with an increase in the stabilizer concentration in the solution, further adsorption takes place with the formation of a second layer and orientation of the ions by the non-polar part to the sorbent occurs. This leads to the appearance of a second step on the isotherm. It is probably not accidental that on all our isotherms the height of the second step is twice that of the first step.

Such orientation of SAS (for example, soaps) is employed in industry for obtaining water-repellent or water-retaining surfaces, for example, during the flotation of various ores or the clarification of drinking water and effluent [6].

The explanation of the appearance of a second step on the isotherm by the possibility of the adsorption of micelles near the critical concentration points of micelle-formation does not correspond satisfactorily to certain experimental data. Thus, according to the literature, the critical concentration of micelle-formation (CCM) for NB wetting agent is observed at 1.26 mmole/liter. In the case of the adsorption of NB wetting agent on paper, the marked rise of the isotherm coincides with CCM. But for the adsorption of the wetting agent on charcoal, which has a large specific surface, this rise is observed at a concentration much greater than CCM.

It must be noted that the asociation of the ions into micelles near the CCM nevertheless influence the process of adsorption and the appearance of a maximum on the isotherms. The position of the maximum on the isotherms depends on the value of CCM.

As in the case of solutions of NB wetting agent, the surface tension (σ)-concentration (c) isotherms for solutions of VA and OOPC have an ordinary appearance, characteristic of surface-active substances [4]. In the region of concentrations at which a reduction in adsorption (a fall on the isotherms) on solid sorbents is observed, a regular, very slight reduction insurface tension is observed on the σ-c curves. An increase of σ in this region of concentrations is not observed.

The determination of the causes of the appearance of a maximum on the adsorption isotherms requires further exact experiments. The diphilic semicolloidal character of surface-active ionogenic stabilizers leads to a number of anomalies of both the surface and all the colloidal-chemical properties of their solutions.

Isotherms of this type were described in [7,8]. The anomalous character of the isotherms for the adsorption of sodium dodecyl sulfate on charcoal may be explained by bimolecular adsorption on the polar parts of the sorbent and adsorption of micelles [8].

SUMMARY

1. The adsorption isotherms of ionogenic surface-active substances (SAS) on solid sorbents were obtained.

2. With an increase in the concentration of SAS, an increase in sorption is observed, the isotherms pass through a maximum but with a further increase in concentration the sorption of SAS decreases in all cases.

3. The course of the isotherms reflects the formation of bimolecular layers from ions of surface-active substances, the first layer being oriented by the polar group to the sorbent, the second layer being oriented towards the water.

LITERATURE CITED

1. N. S. Razumikhina, Candidate's Thesis [in Russian] (Moscow, 1959).
2. E. M. Aleksandrova and N. S. Razumikhina, Kolloidnyi Zhur. 19, 2 (1957).
3. E. M. Aleksandrova and L. S. Kryukova, Nauchn. Doklady vysshei shkoly, seriya khim. 3 (1958).
4. Yu. Kertes-Mureshan, Candidate's Thesis [in Russian] (Moscow, 1954); Doklady Akad. Nauk SSSR 103, 269 (1955).
5. V. N. Tsvetkov, Candidate's Thesis [in Russian] (Moscow, 1958).
6. P. A. Rebinder, Physical Chemistry of Flotation Processes [in Russian] (Metallurgy Press, 1933).
7. M. L. Corrin and E. L. Lind, J. Coll. Sci. 4, 485, 1949; R. D. Vold and A. K. Phansalkar, Rec. Trav. Chim. 74, No. 1, 1955.
8. R. D. Vold and N. H. Sivaramakrishnan, J. Phys. Chem., 62, No. 8, 1958.

All abbreviations of periodicals in the above bibliography are letter-by-letter transliterations of the abbreviations as given in the original Russian journal. *Some or all of this periodical literature may well be available in English translation.* A complete list of the cover-to-cover English translations appears at the back of this issue.

THE INFLUENCE OF POLYPHOSPHATES ON CLAY SUSPENSIONS

V. P. Rudi and A. M. Mandel'eil'

Physical Chemistry Faculty, Chernovtsy University
Translated from Kolloidnyi Zhurnal, Vol. 23, No. 2, pp. 190-193,
March-April, 1961
Original article submitted January 12, 1960

Sodium pyrophosphate and hexametaphosphate are used in boring oil wells in the USSR. In other countries other polyphosphates are used [1]. The action of polyphosphates on clay suspensions has been studied by a number of authors. Some state that sodium pyrophosphate converts the clay suspension to a state of aggregate stability [2-3]. In the opinion of others, the pyrophosphate in this case is adsorbed on the clay particles, increasing their hydration [4]. Sodium tetraphosphate also influences the viscosity of the suspension [5]. Polyphosphates are able to peptize suspensions of many sparingly soluble inorganic compounds [6]. The adsorption of sodium pyrophosphate and tripolyphosphate on particles of montmorillonite clay has been proved [7].

We have studied the action of sodium tetrapolyphosphate, tripolyphosphate, hexametaphosphate, hydrogen pyrophosphate and orthophosphate on the properties of suspensions of clay from the Dolina quarry, Stanislav Oblast, with the following chemical composition (%):

H_2O	3.9	FeO	0.36
SiO_2	60.6	CaO	5.4
Al_2O_3	8.6	MgO	2.3
Fe_2O_3	4.4	Loss on ignition	13.5

In the preparation of the suspension, the clay was first finely ground and passed through a sieve with mesh diameter 0.25 mm. Sodium hexametaphosphate was prepared from monosodium phosphate [8], sodium hydrogen pyrophosphate was prepared by the well-known method [9], the tetrapolyphosphate was prepared by the method of Campbell and Schenker [10], and the sodium tripolyphosphate was prepared from the trimetaphosphate [11].

The properties of the clay suspensions were determined by the methods generally used in the oil industry [12]. The specific gravity of the suspensions was kept constant (d = 1.3). The concentration of phosphates was varied from 0.25 to 3.0% of the volume of the clay suspension.

All the polyphosphates studied decrease the viscosity, static yield value, and water emission of the clay suspensions; sodium orthophosphate has a smaller effect on these properties (Fig. 1).

In order to examine the action of the polyphosphates, the clay suspensions were filtered, washed to remove excess reagent, and dried at 105°. The clay specimens prepared in this way were used to determine the magnitude of the ζ-potential on a Gortikov apparatus [13] and the concentration of divalent ions (magnesium and calcium) before and after treatment of the clay with phosphates by Gedroits' method [14]. The magnitude of the ζ-potential of the clays increased during the treatment with phosphates, the increase being fairly high for treatment with sodium tetrapolyphosphate, hexametaphosphate, and tripolyphosphate, and only slight for treatment with sodium orthophosphate (Fig. 2).

The increase in the value of the ζ-potential of the clay particles during the treatment with polyphosphates can be related both to the process of ion exchange between the phosphate and the clay, involving replacement of calcium and magnesium ions by sodium in the exchange complex and also to the adsorption of phosphate anions on the clay. In both cases the aggregate stability of the clay particles is increased, leading to a decrease in the water emission of the clay suspension.

Fig. 2,b,shows that in the case of treatment of the clay with sodium hexametaphosphate, hydrogen pyrophosphate, tripolyphosphate, and tetrapolyphosphate, the quantity of divalent calcium and magnesium ions in the exchange complex of the clay decreases regularly and to a much greater extent than during treatment with sodium orthophosphate. This indicates that ion exchange is taking place.

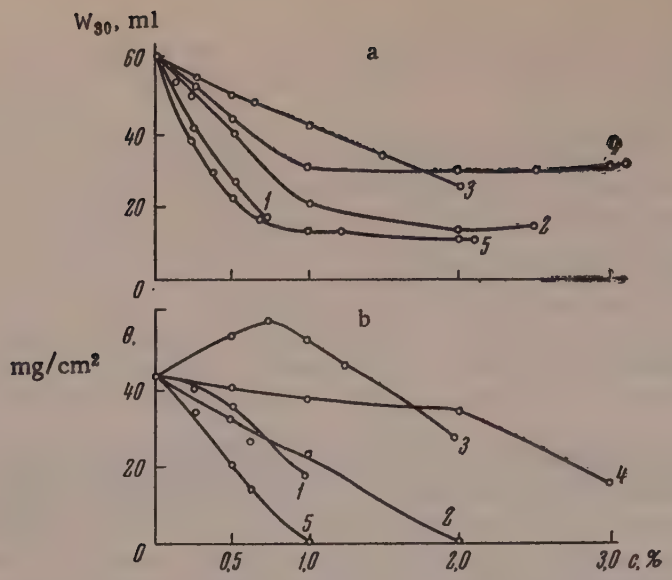


Fig. 1. Dependence of the water emission of the clay suspension (a) and static yield value (b) on the concentration of phosphates; 1) hexametaphosphate; 2) tetrapolyphosphate; 3) orthophosphate; 4) hydrogen pyrophosphate; 5) tripolyphosphate (sodium salts).

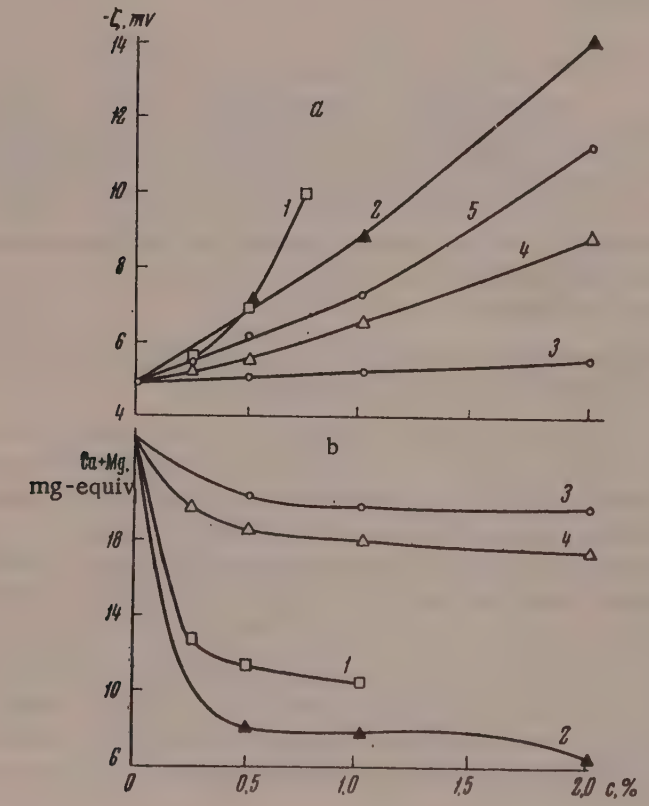


Fig. 2. Change in the electrokinetic potential of the clay during treatment with phosphates (a) and the change in the concentration of calcium and magnesium ions in the exchange complex of the clay with change in the concentration of phosphates (b): 1) hexametaphosphate; 2) tetrapolyphosphate; 3) orthophosphate; 4) hydrogen pyrophosphate (sodium salts).

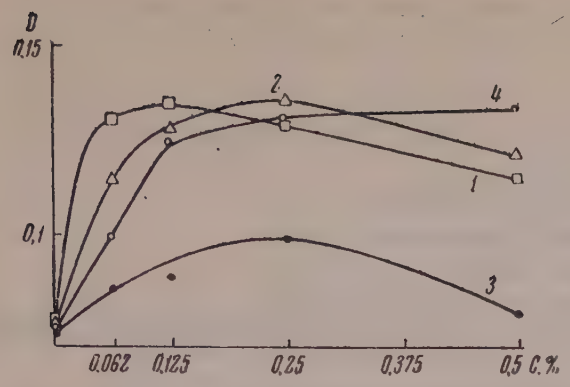


Fig. 3. Optical density of clay suspensions (c = 0.04%) at different phosphate concentrations: 1) hexametaphosphate; 2) tetrapolyphosphate; 3) orthophosphate; 4) tripolyphosphate (sodium salts).

The assumption that the aggregate stability of the clays increases during treatment with phosphates was confirmed by measuring the optical density of suspensions with different concentrations of phosphates [15]. In all cases (Fig. 3) the optical density of the clay suspension increased with the addition of phosphates, the increase being least in the case of sodium orthophosphate. These data agree with the data given above, i.e., the increase in the aggregate stability associated with the increase in the negative value of the ζ-potential of the clay particles leads to a decrease in the water emission of the clay suspension and to an increase in its mobility.

A marked disadvantage of the sodium hexametaphosphate used in boring oil wells is its high hydrolyzability at increased temperature. This is encountered under deep boring conditions.

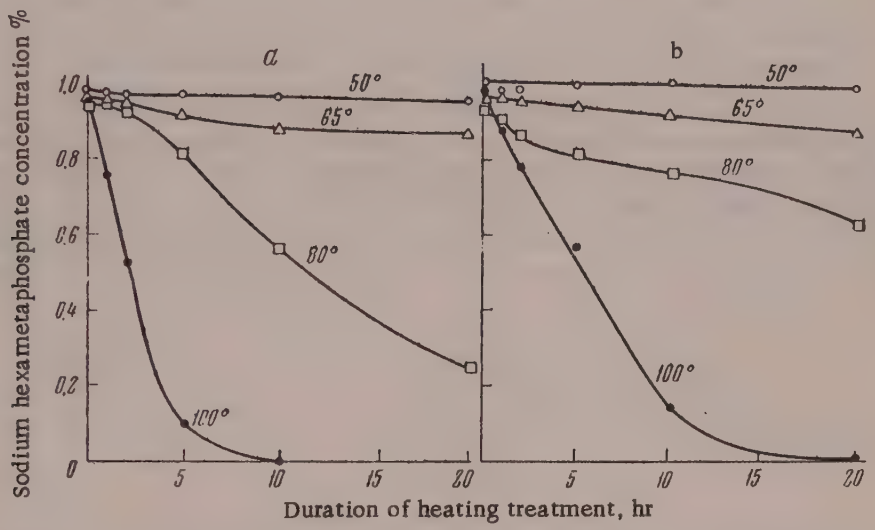


Fig. 4. Change in concentration of sodium hexametaphosphate with duration of heating treatment at different temperatures: a) neutral solution; b) alkaline solution at pH 9.6.

To supplement the available literature data on the hydrolyzability of sodium hexametaphosphate [16,8], we studied the change in concentration of sodium hexametaphosphate in a clay suspension with time for heating at different temperatures. The sodium hexametaphosphate concentration was determined gravimetrically as barium hexametaphosphate (Fig. 4, a). The degree of hydrolysis of sodium hexametaphosphate is reduced in alkaline solution at pH 9.5-10.5 (Fig. 4, b).

SUMMARY

1. The water emission, viscosity, and static yield value of clay suspensions decreases when polyphosphates are added.

2. The value of the negative ζ-potential of the clay increases on treatment with polyphosphates.

3. Polyphosphates increase the aggregate stability of the clay particles.

LITERATURE CITED

1. Principles of the Control of Boring Solutions [Russian translation edited by Shatsov] (Gostoptekhizdat, 1957).

2. P. A. Rebinder, K. F. Zhigach, and P. A. Shreiner, Neftyanaya Promyshlennost', No. 5, 1954 (1940).
3. L. V. Lyutin, The Stabilization of Mineral Suspensions [in Russian] (Moscow–Leningrad, 1947).
4. V. L. Kvarikashvili, Kolloid. Zhur., 16, 442 (1954).
5. C. F. Bennet, Oil Gas J. 1, 39, 1940.
6. I. L. Gofman, Khim. Nauka i Prom., 2, 705 (1957).
7. W. Engelhardt and A. Smolinsky, Kolloid.-z. 151, No. 1, 1957.
8. A. V. Pamfilov and N. M. Dombrovskii, Zhur. Obshch. Khim., 23, 1249 (1953).
9. N. G. Klyuchnikov, Textbook of Inorganic Synthesis [in Russian] (Goskhimizdat, 1953).
10. J. A. Campbell and C. Schenker, J. Amer. Chem. Soc. 67, 767, 1945.
11. A. V. Pamfilov and N. M. Dombrovskii, Uch. Zap. Chernovitskogo Univ., 20, 36 (1956).
12. V. S. Varanov, Clay Suspensions for Boring Oil Wells under Difficult Conditions [in Russian] (Gostopizdat, 1955).
13. V. N. Gortikov, Kolloid. Zhur., 1, 233 (1935).
14. K. K. Gedroits, The Chemical Analysis of Soils [in Russian] (Sel'khoizdat, 1955), Vol. 2.
15. L. I. Edel'man and D. S. Sominskii, Kolloid. Zhur., 21, 126 (1959).
16. R. N. Bell, Industr. and Engng. Chem. 39, 136, 1947.

All abbreviations of periodicals in the above bibliography are letter-by-letter transliterations of the abbreviations as given in the original Russian journal. *Some or all of this periodical literature may well be available in English translation.* A complete list of the cover-to-cover English translations appears at the back of this issue.

THE INFLUENCE OF TEMPERATURE ON THE PROCESSES OF CRYSTALLIZATION STRUCTURE-FORMATION IN TRICALCIUM ALUMINATE SUSPENSIONS

E. E. Segalova, E. S. Solov'eva, and P. A. Rebinder

Colloid Chemistry Faculty, M. V. Lomonosov Moscow State University

Translated from Kolloidnyi Zhurnal, Vol. 23, No. 2, pp. 194-199, March-April, 1961
Original article submitted November 19, 1960

The study of the processes involved in the hardening of tricalcium aluminate (C_3A) at different temperatures is of particular interest since it makes it possible to study the influence of temperature on the strength of the crystallization structure produced during the hydration process, and also to examine the influence of phase changes on the process of crystallization structure-formation, since increase in temperature leads to a sharp acceleration of the conversion of hexagonal tricalcium hydroaluminate to the cubic form.

The study of the processes of structure-formation of C_3A at different temperatures was carried out with suspensions containing a large quantity of an inert filler—finely-ground quartz sand—in addition to the binding agent (C_3A) [1]. With increase in temperature, the rate of increase in the strength of the C_3A suspension increases sharply and the decrease in strength after the maximum value has been reached is also accelerated (Fig. 1). The curve showing the relationship between the final strength of the structure and the temperature has a clearly-defined maximum (Fig. 2).

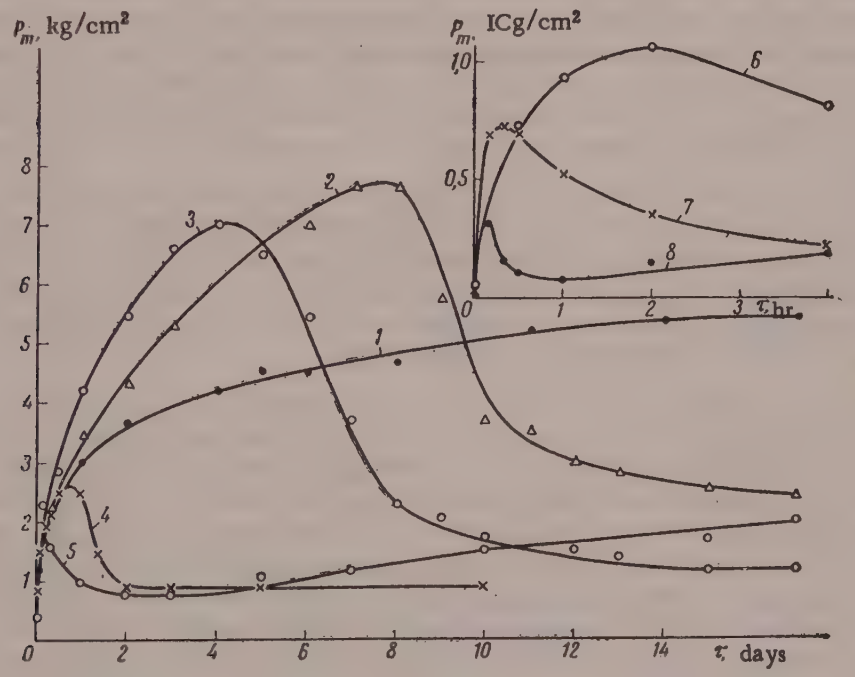


Fig. 1. The kinetics of crystallization structure-formation in C_3A suspensions (s_1 = 4000 cm²/g) at different temperatures: 1) 5°; 2) 15°; 3) 20°; 4) 25°; 5) 30°; 6) 40°; 7) 50°; 8) 65°. Composition of suspension 5% C_3A, 95% finely-ground sand; W/S 0.50.

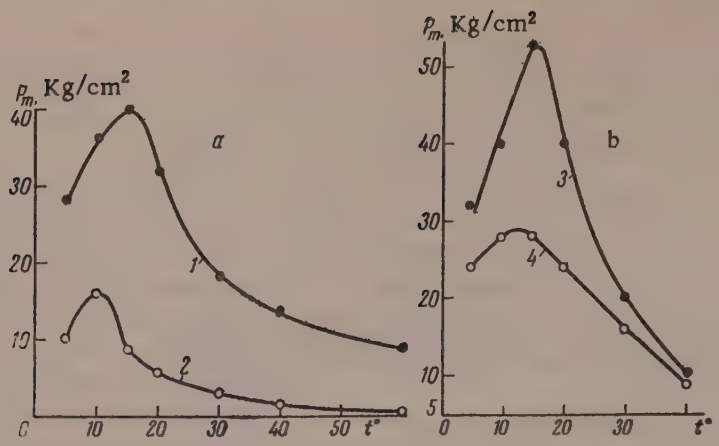


Fig. 2. Dependence of the strength of the crystallization structure of hexagonal hydroaluminate on the temperature at different values of W/S (a) and different values of the degree of dispersion of the original binding agent C_3A (b): 1) W/S 0.30, $s_1 = 4000$ cm²/g; 2) W/S 0.40, $s_1 = 4000$ cm²/g; 3) W/S 0.30, $s_1 = 520$ cm²/g; 4) W/S 0.30, $s_1 = 5250$ cm²/g. Composition of original suspension: 5% C_3A, 95% finely-ground sand.

The curve showing the relationship between the strength of the crystallization structure of the hexagonal hydroaluminate and the degree of dispersion of the original C_3A also passes through a maximum [2]. The decrease in strength with increase in the degree of dispersion of the original binding agent above the optimum value is due to the decrease in the size of the crystallites forming the hardened structure. The same decrease in size of the hydroaluminate crystals, leading to a decrease in the strength, takes place with increase in temperature, since this leads to a sharp increase in the rate of dissolution of the C_3A and, as a result of the increase in the solubility of the original binding agent, there is an increase albeit slight, in the supersaturation produced in the liquid phase of the hardening suspension [3]. The decrease in the strength of the structure with increase in the temperature takes place more rapidly for a low degree of dispersion of the original binding agent (Fig. 2,b) since in this case the increase in the rate of dissolution produced by increase in temperature becomes of greater importance.

In those cases where the process of structure-formation takes place above room temperature, the usual decrease in strength which could be attributed to dissolution of crystallization contacts in thermodynamic nonequilibrium [4] is followed by a second increase in strength (Fig. 1). More detailed study has shown that the secondary increase in strength starts earlier, the higher the temperature at which the process of structure-formation takes place, and leads to the production, in the suspension, of a new hardened structure whose strength in may cases is greater than the strength of the initial structure produced by the hexagonal calcium hydroaluminate.

Fig. 3 gives the results of the observations on the process of structure-formation in C_3A suspensions over a prolonged period of time. The results show that in C_3A suspensions, after the spontaneous breakdown of the initially-formed crystallization structure, a secondary structure is formed, whose strength decreases sharply with increase in the temperature at which it is formed. These phenomena are attributed to the metastable nature of hexagonal tricalcium hydroaluminate, which forms the initial crystallization structure, and to its conversion to the stable form—the cubic hydroaluminate. The crystallization structure of the hexagonal hydroaluminate, as a result of its greater solubility (0.67 g $3CaO \cdot Al_2O_3$ per liter), become supersaturated with respect to the cubic hydrosilicate, whose solubility is much lower (~0.28 g/liter calculated as $3CaO \cdot Al_2O_3$) [5]. This supersaturation is sufficient to produce in the system a new crystallization structure formed by the cubic hydroaluminate. In this case the hexagonal hydroaluminate acts as the original binding agent maintaining the supersaturation necessary for hardening. In the process of the recrystallization of the hexagonal hydroaluminate, the first stage is the dissolution of the crystallization contacts in its structure, leading to a very sharp decrease in its strength. Gradually, the crystals forming the crystallization structure also dissolve, and finally, only the cubic hydroaluminate remains in the structure. These theories have been confirmed by thermographic studies. For these experiments the C_3A suspension, hardened initially at room temperature, was left until the structure formed in it had reached its maximum value and was then placed in a thermostat at 30 or 65° to accelerate the re-

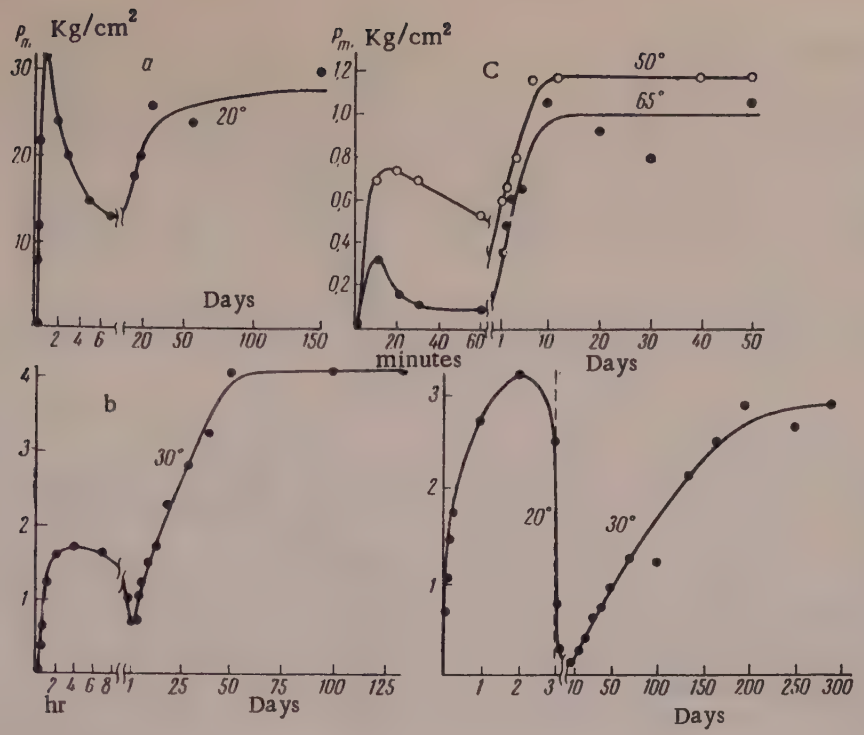


Fig. 3. Kinetics of crystallization structure-formation in C_3A suspensions (s_1 = = 4000 cm²/g): a) W/S 0.37; b) W/S 0.50; c) W/S 0.50; d) W/S 70—for the first three days the suspension was stored at 20° and subsequently at 30°. Composition of the suspensions: a, b, and c) 5% C_3A, 95% finely-ground sand; d) 15% C_3A, 85% finely-ground sand.

crystallization processes taking place within it. Figure 3, shows that when the C_3A suspension is placed in the thermostat, the increase in temperature leads to a very sharp acceleration of the decrease in strength, after which a new hardened structure appears in the suspension.

Kinetics of Structure-Formation in Suspensions Containing 20% C_3A

Time from start of experiment	Plastic strength, kg/cm²	
	B/T = 0.7	B/T = 0.5
Hardened at 20°		
1 min	0.001	0.005
1 hr	1.3	3.7
4 "	2.3	—
6 "	2.3—1*	16
1 day	1.2—2*	26
2 days	—	30—1*
Suspensions placed in thermostat at a temperature of 65°		
1 hr	—	6.0
4 "	0.08—3*	2.5
1 day	0.29	5.0—2*
2 days	0.61—4*	16—3*
9 "	2.0—5*	28—4*
21 "	2.3	28

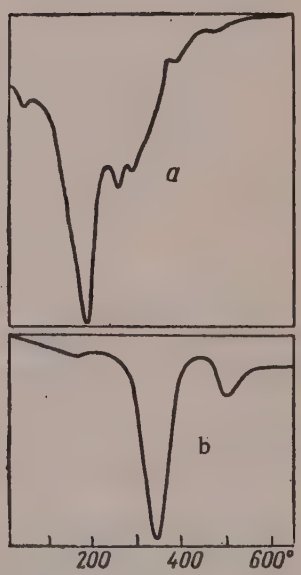


Fig. 4. Thermograms for hexagonal (a) and cubic (b) tricalcium hydroaluminate.

* Sample number for thermographic studies (Fig. 5).

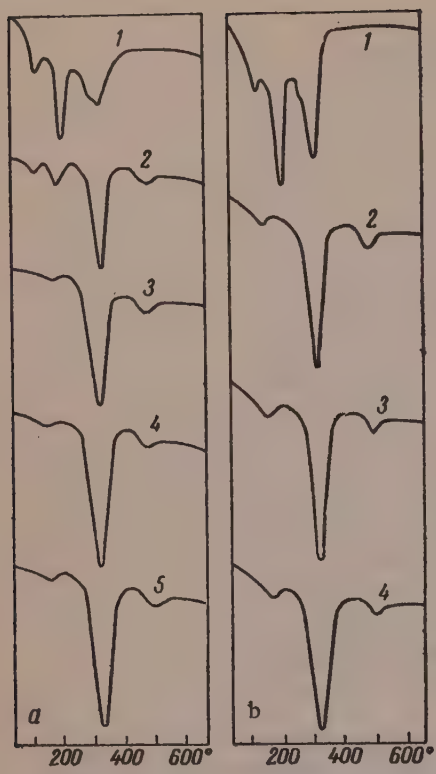


Fig. 5. Thermograms for specimens taken from a hardening suspension containing 20% C_3A ($s_1 = 4000$ cm^2/g), 80% finely-ground sand: a) W/S = 0.70; b) W/S = 0.50. The figures over the thermograms correspond to the specimen numbers in the Table.

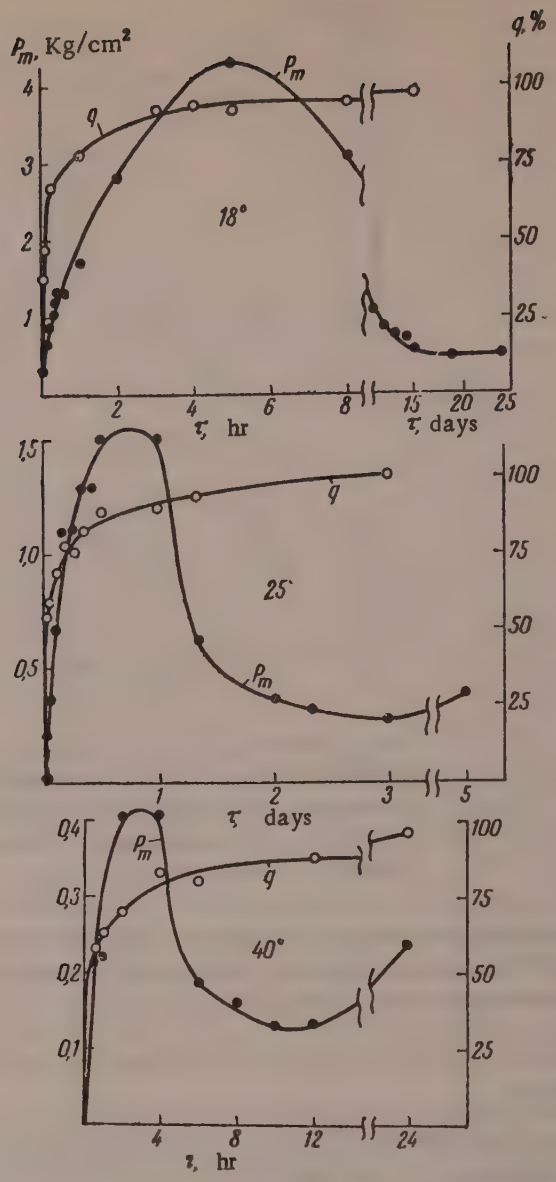


Fig. 6. Kinetics of crystallization structure-formation (Pm) and hydration (q) in suspensions containing 5% C_3A (s_1 = = 4000 cm^2/g), 95% finely-ground sand, W/S = 0.60.

The table gives the kinetics of structure-formation in the C_3A suspensions used for the thermographic studies, and Figs. 4 and 5 give the thermograms for specially-prepared hexagonal and cubic calcium hydroaluminate, together with the thermograms for specimens taken from the C_3A suspensions at different stages of the formation of the hardened structure.

The hexagonal hydroaluminate was prepared as described by Thorwaldson [6], by hydrating C_3A at reduced temperature (3-5°) and the cubic form was obtained by prolonged hydration of C_3A at 65°.

Even when the C_3A is hydrated under very low temperature conditions, the thermogram (Fig. 4,a) is obtained only 24 hours after preparation of the suspension; even on the second day the thermogram shows, in addition to the peak characteristic of hexagonal hydroaluminate, a peak corresponding to the cubic form, although only very little cubic hydroaluminate can have formed in the suspension in this time, since the conversion of the hexagonal hydroaluminate to the stable form at this temperature is very slow.

The results given in Figs. 4 and 5 and in the table show that the final hardened structure in the C_3A suspensions studied is made up of the cubic form of tricalcium hydroaluminate, since the thermograms for the last specimens

coincide completely with the thermogram for the cubic hydroaluminate (Fig. 4,b) The thermograms for the first specimens show the presence of the hexagonal hydroaluminate. The peak on the thermogram, belonging to the cubic hydroaluminate, appears even before the strength of the primary structure of hexagonal hydroaluminate starts to decrease. This inidcates that the cubic hydroaluminate is accumulating in the system even while the strength of the structure is still produced by the hexagonal hydroaluminate. As a result of the acceleration of the conversion of the hexagonal hydroaluminate to the cubic form, the breakdown of the crystallization structure of the hexagonal hydroaluminate with increase in temperature begins before the hydration is complete.

Figure 6 shows the results of a number of parallel measurements of the kinetics of structure-formation (Pm) and hydration (q) in suspensions of C_3A hardened at different temperatures. The calculation was carried out from the formula:

$$q = \frac{W_\tau}{W_m} \cdot 100\%,$$

where $W\tau$ is the quantity of chemically-combined water at time τ and Wm is the quantity of chemically-combined water at the end of the hydration of the C_3A.

With increase in temperature, the completion of hydration and the attainment of maximum strength by the crystallization structure of the hexagonal hydroaluminate show an increasing divergence with time. At 18-20° these two processes are complete at practically the same time; at 25° the hydration is only 85-90% complete when the strength of the structure has reached its maximum; and at 38° the hydration is only 75% complete at this stage. These suspensions (Fig. 6) were prepared under conditions in which the internal stresses produced in the hardening process cannot significantly influence the kinetics of structure-formation (low concentration of binding agent and high W/S ratio). Under these conditions the decrease in strength taking place during hydration is due not to internal stresses, as is the case during the hardening of binding agents which form a stable hydrate immediately on hydration, but to the conversion of the metastable compound which crystallizes initially—the hexagonal hydroaluminate—to the stable cubic hydroaluminate.

SUMMARY

1. Two crystallization hardened structures are produced successively in suspensions of tricalcium aluminate (C_3A): the first is produced as a result of crystallization of metastable hexagonal tricalcium hydroaluminate from a supersaturated solution formed by dissolution of the anhydrous aluminate, and the second is produced as a result of the subsequent recrystallization of this hydrate to form the stable cubic hydroaluminate. In this case the supersaturation is due to the higher solubility of the unstable hexagonal hydroaluminate compared with the stable cubic form.

2. The graph showing the relationship between the strength of the crystallization structure of the hexagonal hydroaluminate and temperature passes through a maximum. The decrease in strength with increase in temperature is related to a decrease in the particle size of the hydroaluminate crystallites forming the hardened structure, together with acceleration of the conversion of the hexagonal hydroaluminate to the cubic form, which accelerates the process of spontaneous breakdown of its crystallization structure and as a result causes the strength of the hardened structure of the hexagonal hydroaluminate to start to decrease with increase in temperature even before the hydration of the C_3A is complete.

LITERATURE CITED

1. E. S. Solov'eva and E. E. Segalova, Kolloid. Zhur., 20, No. 5, 621 (1958).
2. E. E. Segalova and P. A. Rebinder, Stroitelnye Materialy, No. 1, 21 (1960); E. S. Solov'eva and E. E. Segalova, Kolloid. Zhur., 23, No. 2, (1961).
3. E. E. Segalova and E. S. Solov'eva, Doklady Akad. Nauk SSSR, 117, No. 5, 841 (1957); E. S. Solov'eva and E. E. Segalova, Kolloid. Zhur., 23, 3 (1961).
4. E. E. Segalova, V. N. Izmailova, and P. A. Rebinder, Kolloid. Zhur., 20, No. 5, 601 (1958).
5. R. Peppler and Z. Wells, J. Res. Nat. Bur. Standards 52, No. 2, 75, 1954; Translated into Russian in the Collection of Translations by the Promstroiizdat; Tsement, No. 4, 36 (1956).
6. G. M. Harris, W. G. Schneider, and T. Thorwaldson, Canad. J. Res. 21B, No. 4, 65, 1943.

THE RELATIONSHIP BETWEEN THE STRENGTH OF A CRYSTALLIZATION STRUCTURE AND THE DEGREE OF DISPERSION OF THE ORIGINAL BINDING AGENT IN TRICALCIUM ALUMINATE SUSPENSIONS

E. S. Solov'eva and E. E. Segalova*

Colloid Chemistry Faculty, Moscow University
Translated from Kolloidnyi Zhurnal, Vol. 23, No. 2, pp. 200-203,
March-April, 1961
Original article submitted September 27, 1956

The study of the processes of crystallization structure-formation in suspensions of gypsum hemihydrate and calcium oxide has shown that the relationship between the final strength of the hardened structure and the degree of dispersion of the original binding agent passes through a maximum. The decrease in strength in either direction from the maximum value is produced by different factors: decrease in the degree of dispersion leads to a deterioration of the conditions for the formation of crystallization contacts and increases the internal stresses accompanying the hardening process; marked increase in the degree of dispersion of the original binding agent leads to an excessive decrease in the size of the crystallites of the new formations of which the hardened structure is composed, leading to a decrease in its strength [1].

Study of the processes of structure-formation in suspensions of tricalcium aluminate (C_3A) with different initial degrees of dispersion leads to analogous results.

The table and Fig. 1 show that increase in the degree of dispersion of the original binding agent leads to a sharp increase in the rate of the process of structure-formation, and the strength of the crystallization structure of the hexagonal hydroaluminate [2] has a maximum value at an initial degree of dispersion $s_1 = 1000$ cm^2/g for the tricalcium aluminate.

Kinetics of Structure-Formation in Suspensions of Tricalcium Aluminate with Different Initial Degrees of Dispersion (s_1). Composition of suspension: 5% $3CaO \cdot Al_2O_3$, 95% finely-ground quartz sand; W/S = 0.28.

Time from start of experiment	Relative specific surface of C_3A (s_1) m^2/g							
	450	520	1400	1820	2320	3250	4000	5250
	plastic strength (Pm), kg/cm^2							
1 min	0,018	0,018	0,018	0,018	0,020	0,040	0,050	0,19
1 hr	0,42	1,5	2,7	5,2	5,2	2,9	13	16
4 »	1,7	4,2	8	16	20	26	22	22
7 »	5,8	11	12	18	30	32	24	24
1 days	24	32	35	40	44	34	26	16
3 »	46	55	58	50	40	34	24	10
6 »	46	54	58	32	34	34	18	11
10 »	46	55	58	20	34	32	16	8

* In the article by E. E. Segalova, E. Stoklosa and Z. N. Markina [Kolloid. Zhur., 22, No. 4, 464 (1960)], the values given for the specific surface of the original gypsum in the text and figure captions should be reduced by a factor of 10.

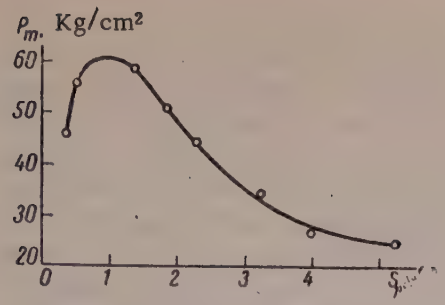


Fig. 1. Relationship between the strength of the crystallization structure (Pm) and the degree of dispersion of the original tricalcium aluminate ($s_1 \times 10^{-3}$ cm²/g). Composition of suspension: 5% C_3A, 95% finely-ground quartz sand; W/S = 0.28.

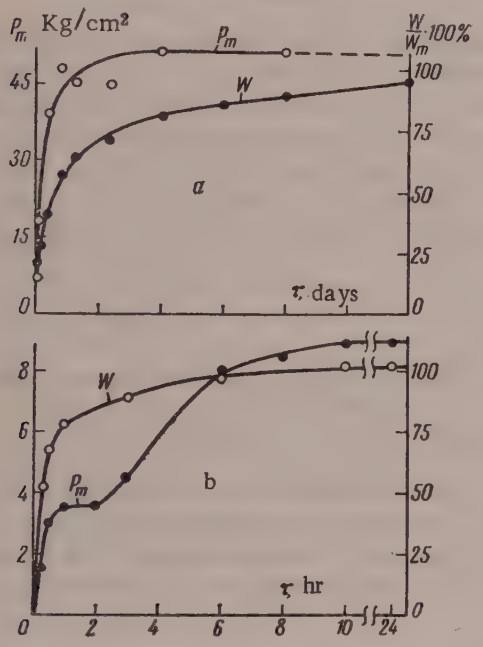


Fig. 2. Kinetics of crystallization structure-formation (Pm) and hydration (W) in suspensions containing 5% C_3A, 95% finely-ground quartz sand; t = 18-20°. Relative specific surface of the original material: a) s_1 = 1820 cm²/g, W/S = 0.30; b) s_1 = 4000 cm²/g; W/S = = 0.37.

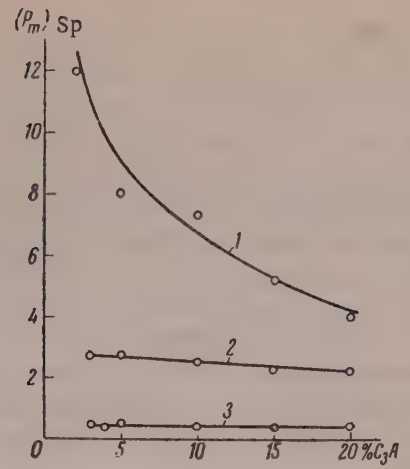


Fig. 3. Relationship between the relative specific strength of the crystallization structure and the concentration of C_3A in the mixture: 1) W/S = 0.28; 2) W/S = 0.37; 3) W/S = 0.70; s_1 = 4000 cm²/g.

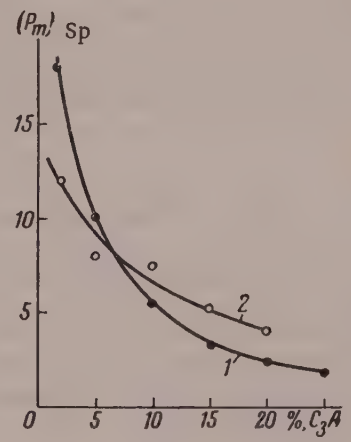


Fig. 4. Relationship between the relative specific strength of the crystallization structure and the concentration of C_3A in the mixture: W/S = 0.28; 1) s_1 = 5250 cm²/g; 2) s_1 = 4000 cm²/g.

In the case of C_3A the falling branch of the curve on the Pm(s_1) curve (Fig. 1) is extremely clearly defined. This is due to the fact that in the hydration of C_3A, packets of hydroaluminate [3] are formed on its surface, retarding the dissolution of the original binding agent and, as a result, leading to an increase in the particle size of the final hydroaluminate crystallites. With increase in the degree of dispersion of the C_3A the retarding effect of the packets is decreased, leading to an even greater decrease in the size of the hydroaluminate crystals from which the hardened structure is composed and to a sharp decrease in its strength.

In earlier works devoted to the study of the process of structure-formation in C_3A suspensions, it was shown that the increase in strength of these suspensions and the hydration of the C_3A are complete almost simultaneously [4]. More detailed study of this question with C_3A specimens with different initial degrees of dispersion showed that in fairly concentrated suspensions the above is true only when the degree of dispersion of the C_3A is high. For a low degree of

dispersion of the original aluminate and a water: solid (W/S) ratio equal to 0.3, as shown in Fig. 2, the increase in the plastic strength is complete long before the hydration process is complete (the kinetics of hydration were calculated from the results of determinations of the chemically-combined water by the usual procedure [2]). This divergence in the times taken for these two processes, as shown for the case of gypsum hemihydrate [5] and calcium oxide [1], is produced by internal stresses accompanying the process of crystallization structure-formation and leading to partial breakdown of the resultant hardened structure along its weakest regions. Since the internal stresses, other conditions being equal, are greater, the lower, the degree of dispersion of the original binding agent, the divergence in the times taken to complete the hydration and for the structure to attain its maximum strength is most marked in suspensions with a low degree of dispersion of the original binding agent. When the degree of dispersion of the original binding agent is high, this divergence is less marked, but in this case, as a result of the marked decrease in the size of the crystallization structure framework and the decrease in strength, sharp breaks are observed on the curve giving the kinetics of structure-formation (Fig. 2): these breaks are produced by breakdown of the structure under the influence of the internal stresses. The kinetics of structure-formation in suspensions of highly-dispersed calcium oxide [1] are analogous.

The existence of the internal stresses is shown in a decrease in the relative specific strength, i.e.,the strength per g of binding agent, with increase in the concentration of binding agent in the given mixture.

Figure 3 shows that the relative specific strength, calculated by dividing the plastic strength of the crystallization structure of the hexagonal hydroaluminate by the percentage concentration of C_3A in the mixture with the filler decreases more sharply, the lower the value of W/S, since decrease in W/S leads to an increase in the internal stresses produced in the process of crystallization structure-formation. Comparison of the relationship between the specific strength and the concentration of binding agent in the mixture for a given value of W/S and different initial degrees of dispersion of binding agent (Fig. 4) shows that the decrease in the specific strength takes place much more sharply in suspensions of aluminate with a low degree of dispersion; this also indicates an increase in the internal stresses with decrease in the degree of dispersion of the original binding agent.

SUMMARY

1. In the suspensions of tricalcium aluminate (C_3A) which were studied, the maximum strength of the hardened structure is observed for an initial degree of dispersion of the C_3A equal to approximately 1.0 m^2/g. With increase in the relative dispersion of the C_3A to 5.2 m^2/g the strength of the crystallization structure decreases sharply.

2. The process of hardening of the C_3A is accompanied by the production of internal stresses, as is shown by a divergence in the times taken to complete hydration and for the hardened structure to attain its maximum strength, and also by a decrease in the relative strength with increase in the concentration of binding agent in the mixture with the filler. The internal stresses are more marked, the lower the degree of the original binding agent and the lower the water: solid ratio.

LITERATURE CITED

1. E. E. Segalova and V. N. Izmailova, Kolloid. Zhur., 20, No. 5, 601 (1958); E. E. Segalova, S. I. Kontorovich, and P. A. Rebinder, Kolloid. Zhur., 22, No. 1, 74 (1960); Z. N. Markina, E. E. Segalova, and E. Stoklosa, and P. A. Rebinder, Stroitel'nye Materialy, No. 1, 21 (1960).
2. E. S. Solov'eva and E. E. Segalova, Kolloid. Zhur., 20, No. 5, 620 (1958).
3. E. E. Segalova, E. S. Solov'eva, and P. A. Rebinder, Doklady Akad. Nauk SSSR, 117, No. 5, 841 (1957).
4. E. E. Segalova, E. S. Solov'eva, and P. A. Rebinder, Doklady Akad. Nauk SSSR, 113, No. 1, 134 (1957).
5. E. A. Amelina, E. E. Segalova, and P. A. Rebinder, Doklady Akad. Nauk SSSR, 131, No. 5, 1123 (1960).

AN ELECTROCHEMICAL STUDY OF BENTONITE SUSPENSIONS

5. THE ELECTROKINETIC POTENTIALS OF ELECTRODIALYZED ASCANGEL AS A FUNCTION OF THE DEGREE OF NEUTRALIZATION BY HYDROXIDES OF THE ALKALI METALS

E. T. Uskova

Kiev Technological Institute for the Food Industry
Translated from Kolloidnyi Zhurnal, Vol. 23, No. 2, pp. 204-208,
March-April, 1961
Original article submitted January 12, 1960

In a previous paper [1] we studied the reaction of electrodialyzed ascangel with different alkalis and showed the effect of properties of the ions (for example the polarizability) on their adsorption by the surface of the bentonite particles. It would be interesting to check the effect of these properties of ions on the electrokinetic potential of bentonite particles—one of the most important characteristics of the surface state. In a previous study of the electrokinetic potential of bentonite mainly its dependence on the value of the ion charge was investigated. The importance of other properties of the ions forming the outside covering of the double electrical layer was not studied.

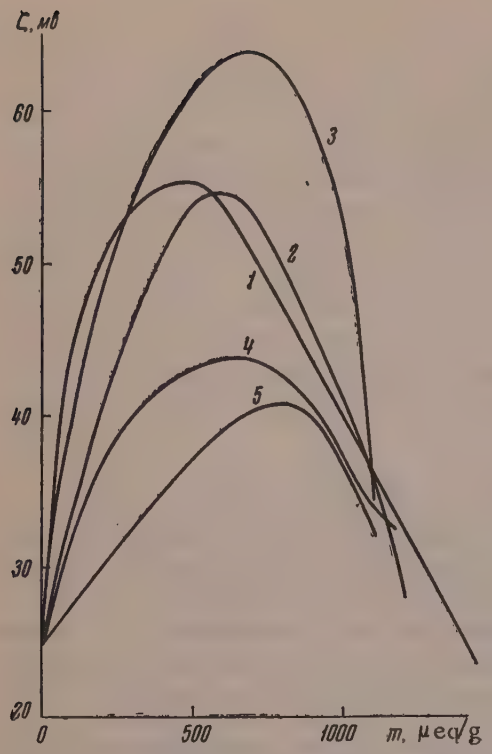
The present work studies the change in electrokinetic potential at a different degree of neutralization of electrodialyzed ascangel by different alkalis—the hydroxide of lithium, sodium, potassium, rubidium and cesium. The ions of these metals have the same charge but differ in their dimensions and coefficients of polarizability. In the neutralization of ascangel by these alkalis there is mainly replacement of aluminum ions situated in the electrodialyzed bentonite at the places of exchange by alkali metal ions. Therefore, each specimen of bentonite suspension had exchange ions of aluminum and an alkali metal in different relationships.

The electrodialyzed ascangel was prepared according to the previously described method [2]. The obtained suspension was used to prepare specimens in which the electrodialyzed bentonite was neutralized to different extents by the hydroxides of lithium, sodium, potassium, rubidium and cesium. For this purpose the initial 0.5% suspension of ascangel was poured in 25 ml quantities into bottles with pyrex glass stoppers. To the suspension additions were made of different volumes of 0.05 N alkali solutions and sufficient distilled water so that the total volume of the suspension was 40 ml. Measurements were then made of the ζ-potential of the obtained specimens by the electrophoresis method [2].

The value of the electrokinetic potential was calculated from the Smolukhovskii formula since, according to Kreut and Overbeck [3], this equation can be used for coarsely dispersed colloids and suspensions without allowing for the surface conductivity and the effect of relaxation. As shown in our previous work, electrodialyzed bentonite reacts with alkali in time [4], the rate of reaction depending on the nature of the alkali cation [1]. Furthermore, it was found that with increase in the time of reaction the difference in the action of alkalis of different metals becomes less apparent. In this connection measurements of electrokinetic potential were made 15 days after the adhesion of the corresponding alkali metal hydroxides to the electrodialyzed ascangel.

The figure shows curves for the change in the ζ-potential of electrodialyzed ascangel as a function of the amount of added base. As can be seen from the figure, all curves have a maximum. Therefore, in the neutralization of electrodialyzed ascangel by alkalis at first there is an increase in the ζ-potential; at a certain degree of neutralization the ζ-potential takes on a maximum value, after which it reduces.

A potentiometric study of the reaction of electrodialyzed bentonite with alkali metal hydroxide showed that on the 14th day complete neutralization of the suspension does not occur, i.e., a certain part of the aluminum ions remains unsubstituted by alkali metal ions. From the data of potentiometric titration it follows that during this time the following have reacted: LiOH—920 μequiv/g; NaOH—860 μequiv/g; for KOH—830 μequiv/g; RbOH—890 μequiv/g; CsOH—900 μequiv/g, whereas the capacity of the cation exchange of the investigated bentonite is 1000 μequiv/g. In our experiment it was therefore not possible to obtain specimens of bentonite for which all the exchange places were occu-



ζ -Potential of electrodialyzed ascangel as a function of the degree of neutralization: 1) LiOH; 2) NaOH; 3) KOH; 4) RbOH; 5) CsOH.

pied only by ions of any one alkali metal. Consequently, our data cannot be used to compare values of the electrokinetic potential of Li-, Na-, K-, Rb- and Cs-bentonite.

An analysis of these curves, however, does not give an indication of the effect of some properties of the ions on the electrokinetic potential of the studied suspensions.

Experience showed that when a trivalent aluminum ion in the outer shell of the double electrical layer of electrodialyzed bentonite is replaced by monovalent alkali metal ions there is no continuous increase in the electrokinetic potential, as would be expected on the basis of existing ideas on the structure of the double layer. The largest values of the electrokinetic potential are observed not with the greatest content of alkali metal ions in the external layer but with a certain relationship between the Al-ions and ions of the alkali metals. In the region of the above amounts of alkalis reacting with electrodialyzed ascangel there is very little change in the electrical conductivity [1].

Earlier we observed a similar phenomenon where in the exchange complex of sodium montmorillonite additions were made of different amounts of calcium and magnesium ions [5]. From this it follows that the presence in the double electrical layer in a certain relationship of two different ions—polyvalent and monovalent is apparently more favorable with respect to increase in the ζ -potential than the presence of only monovalent weakly attracted ions. When explaining this phenomenon allowance should be made not only for the reaction of ions of the outer shell with the oppositely charged surface of the particle but also the effects of ions of the outer shell on one another. In this case processes occurring in the outer shell of the double electrical layer during the replacement of Al-ions by alkali metal ions can be represented in the following way.

Electrodialyzed bentonite contains mainly aluminum ions as the exchange ions. Due to the strong electrostatic attraction to the surface of the particles these ions are mainly situated in the absorption layer of the outer shell, which determines the low values of the ζ -potential. In the case of electrodialyzed ascangel these values are not so small but this can be explained by the presence in them, apart from aluminum ions, of a certain number of hydrogen ions [4].

In the neutralization of electrodialyzed ascangel by alkalis there is first the replacement of H-ions by ions of the corresponding metals; however, this process occurs instantaneously and in addition forms a comparatively small and constant fraction and we will not consider it here. We are interested in the substitution of aluminum ions by alkali metal ions.

In the reaction of electrodialyzed ascangel with alialis at first there is replacement of aluminum ions in the diffuse layer of the outer shell. The introduced monovalent ions are more weakly attracted to the surface, are more subjected to thermal scatter due to which there is an increase in the thickness of the diffusion layer. After this there is substitution of the aluminum ions in the adsorption layer of the outer shell. The monovalent alkali metal ions which take their place are now not in the absorption layer but in the diffuse layer. In the first place this is due to the fact that the alkali metal ions, owing to their small charge, are more weakly attracted to the surface and in the second place to the fact that the more highly charged aluminum ions strongly repel monovalent ions, preventing their entry into the absorption layer. This causes a considerable increase in the thickness of the diffusion part of the double layer and, consequently, an increase in the ζ -potential.

This increase in the ζ -potential will occur until the aluminum ions are so few that they cannot prevent the entry of alkali metal ions into the absorption layer and also affect the thickness of the diffuse layer by electrostatic repulsion. As a result of this, the monovalent alkali metal ions will begin to be located in the absorption layer of the outer shell, the thickness of the diffuse layer will decrease, leading to a reduction in the value of the ζ -potential. Therefore, in the case of replacement of trivalent aluminum ions by monovalent alkali metal ions at a certain content of aluminum ions we observe a reduction in the ζ -potential rather than an increase.

Therefore, the presence of aluminum ions in the double electrical layer together with monovalent ions can have a double action on the value of the ζ -potential. On the one hand the aluminum ions, having a greater charge, are strongly electrostatically attracted to the oppositely chared surface, which causes a reduction in the ζ -potential. This action is especially clearly shown with large amounts of Al-ions in the double layer (more than 50%). On the other hand the aluminum ions react electrostatically on the monovalent ions and increase the diffuseness of the outer shell, which causes an increase in the ζ -potential. If the double layer contains 50% aluminum ions then the prevailing tendency is for a reduction in the ζ -potential and if there is 25-50% then the tendency to an increase in the ζ -potential predominates. With a content of aluminum ions <20% their presence is not very noticeable and the values of the ζ -potential are mainly determined by the alkali metal ions. The result is that the maximum values of the ζ -potential are observed not with total replacement of all exchange ions by alkali metal ions but with a certain relationship between the number of Al ions and alkali metal ions.

From the curves shown in the figure it can be seen that the position of the maximum is displaced from lithium to cesium toward higher quantities of the added base. This displacement of the maximum is obviously determined by the properties of the alkali metal ions.

The table gives concentrations of bases at the maximum on the curves and the maximum values of the ζ -potential as a function of the ion dimensions and their polarizability. On the basis of the above it can be assumed that the maximum will correspond to smaller amounts of the neutralizing alkali the more readily its ions enter into the adsorption layer of the outer shell together with the aluminum ions. The capacity for entry of alkali metal ions into the adsorption layer containing aluminum ions decreases from lithium to cesium. The ion dimensions are obviously taking part here, the smaller the ion the more readily will it penetrate to the surface of the particle.

The Effect of Nature of the Ions on the Maximum Values of the ζ -Potential in the Neutralization of Electrodialyzed Bentonite by Different Bases

Cations	Size of non-hydrated ions, A	Coefficient of polarizability	Amount of MeOH at the maximum μeq/g	ζ -Potential
Lithium	0,68	0,029	450	55
Sodium	0,98	0,187	600	57
Potassium	1,33	0,888	650	64
Rubidium	1,48	1,49	700	44
Cesium	1,65	2,57	800	41

As well as the difference in the position of the maximum there is also a difference in the maximum values of the ζ -potential (table). The value of the ζ -potential at the maximum point increases from lithium to potassium, and then decreases from potassium to cesium. This dependence of the ζ -potential on the nature of the cation is observed not only at the maximum points but also at all sections of the curves shown except for those sections where there was an excess of alkali in the suspension (after the neutralization point).

This phenomenon can be explained by the opposite effect of two properties of the ions—dimensions and polarizability. An increase in dimensions of the ions leads to an increase in thickness of the diffuse part of the outer shell and hence to an increase in the ζ -potential. The values of the ζ -potential should therefore increase from lithium to cesium. However, strongly polarizing ions are drawn closer to the surface of the particle due to their possible deformation. The increase in the coefficients of polarizability from lithium to cesium should therefore affect the values of the ζ -potential, causing it to decrease.

These two factors, acting oppositely on the thickness of the double electrical layer, also cause the ζ -potential to increase from lithium to potassium (the effect of the ion size predominates) and from potassium to cesium it decreases (the effect of polarizability predominates).

SUMMARY

1. The change in ζ -potential of electrodialyzed ascangel has been studied as a function of the degree of neutralization by alkali metal hydroxides. The values of the ζ -potential pass through a maximum. An explanation is suggested for this phenomenon based on the features of reaction of ions in the outer shell of the double electrical layer.

2. The value of the ζ-potential is affected by the size and polarizability of the ions in the external shell.

LITERATURE CITED

1. I. A. Uskov and E. T. Uskova, Kolloid. Zhur. 21, 231 (1959).
2. I. A. Uskov and E. T. Uskova, Kolloid. Zhur. 19, 361 (1957).
3. G. R. Kreut, The Science of Colloids [Russian translation] (Foreign Literature Press, 1955) p. 291.
4. I. A. Uskov and E. T. Uskova, Kolloid. Zhur. 20, 487 (1958).
5. E. T. Uskova, Kolloid. Zhur. 20, 102 (1958).

All abbreviations of periodicals in the above bibliography are letter-by-letter transliterations of the abbreviations as given in the original Russian journal. *Some or all of this periodical literature may well be available in English translation.* A complete list of the cover-to-cover English translations appears at the back of this issue.

INVESTIGATION OF STRUCTURE FORMATION IN AQUEOUS SOLUTIONS OF HUMIC SUBSTANCES

Chiang-lung, N. N. Serb-Serbina, L. E. Kuznetsova and V. S. Zhurina

Institute of Physical Chemistry Academy of Sciences USSR, Dispersed Systems Section, Moscow
Translated from Kolloidnyi Zhurnal, Vol. 23, No. 2, pp. 209-214, March-April, 1961
Original article submitted April 26, 1960

The humic substances present in soils and certain types of ground determine to a considerable extent their characteristics as natural dispersion media, evidently by assisting three-dimensional structure formation, whereas in the form of hydrophilic alkaline humates (water-soluble) humic substances are powerful stabilizers and peptizers.

The humates extracted from brown coal and peat are widely used in various branches of industry as additives for improving the structural-mechanical and technological properties of concentrated mineral suspensions, particularly suspensions of clays in the ceramic industry, in flushing (clay) solutions used in deep-borehole drilling, in the technology of constructional materials and for improving land.

However, the mechanism of the action of humates on the structure and rheological properties of aqueous dispersions of clays has hitherto been inadequately investigated. No investigation has been made of structure formation in aqueous solutions (dispersions) of the humates themselves, which always takes place in a dispersion medium of any mineral suspensions in which humic substances are present as impurities. Such investigations were the object of the present work. The following article gives the results of an investigation of the effect of humates on the formation and properties of coagulation structures in aqueous suspensions of clays in the presence of electrolytes.

These investigation should help to establish a scientific basis for the use of humates in various branches of industry and explain their role in soil structures. Investigations of structure formation in solutions of humic substances themselves and their salts are of independent scientific interest because these dispersions are characteristic examples of spontaneously formed semicolloidal systems at the boundary of true solution of high-molecular compounds with two-phase colloidal systems of intermediate type (between lyophilic and lyophobic dispersions).

Humic substances are compounds with condensed aromatic nuclei, differing from each other by the degree of condensation, the character and ratio of the heterocyclic groups with side chains and functional groups of different type [1]. In the region of application of humic substances, examined by the authors, carboxyl groups are of particular importance.

Humic substances were obtained by treating brown coal with a solution of NaOH (1 liter of 0.5 N NaOH per 100 g of brown coal). The excess alkali in the extract (after the insoluble part of the brown coal in it had been separated by standing, followed by centrifuging) was removed by means of KU-2 cationite in N-form or by precipitating the humic acids with a 2% solution of HCl and transferring the fresh, moist precipitates (washed until a negative reaction for Cl^- in the filtrate was obtained) to an NaOH solution of different concentration.

The structural-mechanical and rheological properties of solutions of Na humates were measured in instruments based on the principle of net shear [2]:

1. In a Shvedov apparatus with two coaxial corrugated cylinders with a gap of 2 mm, a set of torsion dynamometer (steel wires) and a reducing gear, giving a variation in the strain rate in the 10 sec^{-2}-10 sec^{-1} range.

2. In a Weiler-Rebinder elasticity gauge with a tangentially displaced corrugated plate in the center of a closed vessel, with corrugated walls and a gap of 2 mm between the shear planes.

3. In apparatus of the capillary type, i.e., Ostwald or Ubellohde viscometer.

The viscosity (η) of aqueous solutions of Na humates in relation to their concentration (c) was measured in a Shvedov apparatus (for high η) and in capillary viscometers (for low η) in the case of a disturbed structure. From Fig. 1 it is evident that in the range of low humate concentrations (the humate concentration is calculated on the N-form throughout) the viscosity of their solutions is close to that of water and increases linearly with the concentration. With an increase in the concentration of Na humates, gelatination with thixotropic strengthening in time and a marked increase in the effective viscosity of the solutions are observed. The region of humate concentration corresponding to this rise in viscosity depends on the pH of the solutions: at pH 8 the linear nature of the relation $\eta = t(c)$ is retained in a considerably wider range of concentrations than at pH 11.

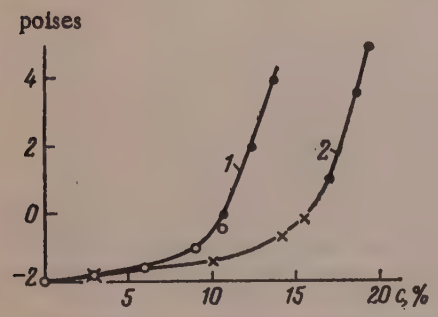


Fig. 1. Viscosity (η) of aqueous solutions of Na humates in relation to the concentration (c) and pH: 1) pH 11; 2) pH 8.

The relations established between the viscosity of disturbed structures and the solution concentration are due to the fact that, being soluble salts of humic acids, Na humates are high-molecular systems of the semicolloidal type, the properties of which depend on the pH of the solutions and the degree of substitution of exchange cations by Na^+

The exchange capacity of the humic acids investigated (with respect to the amount of Ca^{2+} corresponding to complete substitution of the exchange capacity of the acid according to Lein [3]) was 362-mg-equiv/100g. To obtain a 14.5% solution of humates with pH 7.17 it was necessary to substitute only 50% of the total capacity of Na^+. At pH 9.07 the exchange complex contained ~ 350 mg-equiv Na^+, but since the exchange capacity of humates increases with an increase in the pH of their solutions [4], at these pH values a certain amount of H^+ is still retained in the exchange complex. At comparatively low pH (7-8) a considerable part of the humic substances is evidently present as symmetrically constructed micelles, with a hydrophilic outer envelope and macromolecules globulized by hydrogen bonds. For this reason the viscosity in such solutions is increased comparatively little, while, according to our measurements (Fig. 2), the surface tension at the aqueous solution-air (vapor) boundary is slightly reduced (close to the value for water).

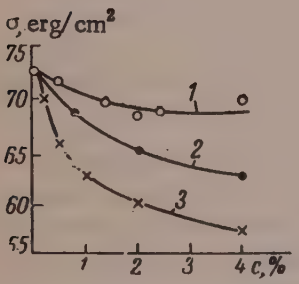


Fig. 2. Relation between the surface tension (σ) of solutions of sodium humates and the concentration (c) and pH at the air-water boundary: 1) pH 8.4; 2) pH 11.5; 3) pH > 13.

At increased pH, with transfer to the strongly alkaline region the micelles are peptized and deglobulization of the macromolecules take place, evidently with a certain reduction in the mean molecular weight; this leads to a marked increase in the surface activity (a reduction in the surface tension) as a result of an increase in the capacity of the less symmetric macromolecules to be oriented on the surface of the water, with the formation of an adsorption layer (Fig. 2). At the same time (Fig. 1), in concentrated solutions the viscosity of the solution also increases with an increase in the pH, as a result of the development of a coagulation structure, i.e., gelatination.

Measurements of the equivalent electrical conductivity of solutions (λ) of humates in relation to their concentration at different pH, indicating their polyelectrolytic character, confirm that an increase in pH assists the solubility and peptization of the micelles (Fig. 3). Thus, the $\lambda - \sqrt{c}$ curves show that with an increase in pH the conductivity of solutions of humates increases, at ~ 10% (0.3 g-equiv/liter) there is a kink, corresponding to the critical concentration of micelle-formation [5]. At pH 7, this kink is not observed on the curve, at pH > 11 the kink is masked by the excess alkalinity of the solution.

On the basis of the data obtained, solutions of Na humates may be considered as hydrophilic semicolloidal systems, the properties of which depend on the degree of replacement of H^+ of the exchange capacity of humic acids by Na^+

The addition of electrolytes with polyvalent cations ($CaCl_2$, $FeCl_3$) to solutions of humates causes a reduction in solubility. Fairly complete substitution of the exchange capacity leads to precipitation of the humates. Depending on the degree of substitution of the exchange capacity, concentrated solutions of humates pass from the liquid state

with different strength values and strength character. Fig. 4 gives the results of the measurement of the unit limiting shear stress (P_m) of thixotropically strengthened systems in relation to the amount of electrolyte introduced. As may be seen from Fig. 4, electrolytes with polyvalent cations cause structure formation with a markedly expressed strength maximum in solutions of humates.

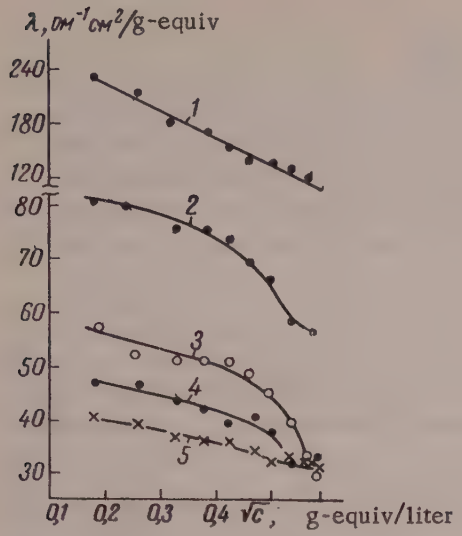


Fig. 3. Relation between the equivalent electroconductivity (λ, ohm^{-1}, cm^{-2}) of solutions of humates and the concentrations (c) and pH at 18°; 1) pH 11.5; 2) pH 10.0; 3) pH 9.5; 4) pH 7.7; 5) pH 7.0.

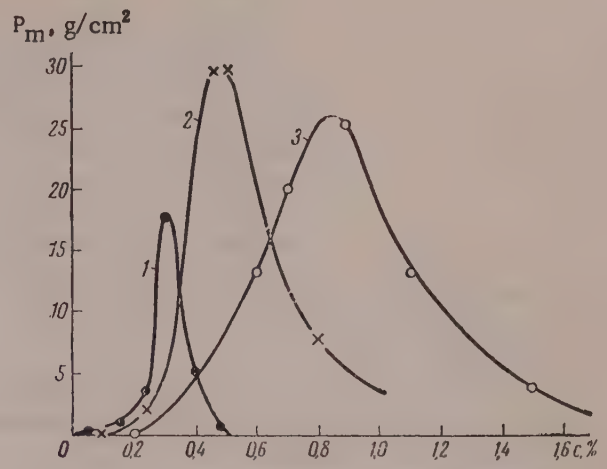


Fig. 4. Structure formation (P_m) in a solution of humates in relation to the amount of electrolyte (c) added: 1) 9.3% solution of Na humates (initial solution pH 7), with HCl; 2) 14.3% solution of Na humates with $FeCl_3$; 3) ditto with $CaCl_2$.

Investigations of structure formation in solutions of humates with respect to time, showed that the structurized systems have different characters in relation to to the degree of substitution of the exchange capacity in humates by different cations. In solutions of humates with a small addition of electrolyte, corresponding to an increase in strength on the P-c curve (where c is the concentration of electrolyte), structures of the coagulation type with ideal thixotropic strengthening are formed, i.e.,complete restoration of the structure to a constant value for the same residence time under quiescent conditions is observed. In a case where the amount of electrolyte added is correlated with a fall in strength, although thixotropic strengthening of the structure in time is observed a regular fall in P_m and P_s (P_s is the residual strength of an incompletely disturbed structure under the experimental conditions) is found after each re-mixing (Fig. 5). The measurements were carried out in solutions of humates with pH 8.7 before the addition of the electrolyte.

These investigations show that under conditions where the colloidal particles of humates retain the mosaic character of the structure of the surface layer with predominance of hydrophilic areas they lead to the formation of a gel-like thixotropic structure of ordinary coagulational character. In this case the structurized solutions of humates are not water-resistant, and the colloidal particles of humates are peptized with further addition of water.

When the amount of $CaCl_2$ added can cause replacement within the exchange complex by Ca^{2+} to the extent of more than half the total capacity on the surface of the colloidal particles of humates formed, areas which cause coagulation of a compact character predominate. Being separate structural elements of low dispersion, such compact aggregates of particles form a structural skeleton with a relatively reduced strength. With repeated mixing the strength of this skeleton is reduced as a result of the fact that during the mixing of the paste the diffusion process of more uniform distribution of Ca^{2+} in the system is accelerated; this brings the system to an equilibrium state with constant value of P_m and P_s.

In this case the initial period of stirring shows that mixing of the freshly prepared systems causes an increase in the strength of the structural skeleton, which may be explained by an increase in the number of contacts between the molecules of humates in the aqueous paste at the newly formed hydrophobic areas of their surface, which at this

stage of the chemical process are insufficiently large, leaving the surface of the humate molecules still relatively hydrophilic. After an equilibrium state has been established in the system the humate aggregates are not peptized with further addition of water, and they become water-resistant.

Thus, the investigations of the reaction of humic acids from brown coal and humates in a wide range of their concentration in water with electrolytes, the cations of which take part in exchange with the cations of the exchange capacity of humic acids, show that, depending on saturation by different cations, solutions of humates are: 1) hydrophilic highly dispersed semicolloidal systems, spontaneously dispersed by water to macromolecules; 2) colloidal solutions with micelles of mosaic character, on the surface of which, in addition to hydrophilic areas, there are relatively large hydrophobic areas which cause aggregation and the formation of strong skeleton structures, or 3) systems in which hydrophobic areas predominate on the surface of the molecules, as a result of which the humates become insoluble in water and are not peptized by the latter.

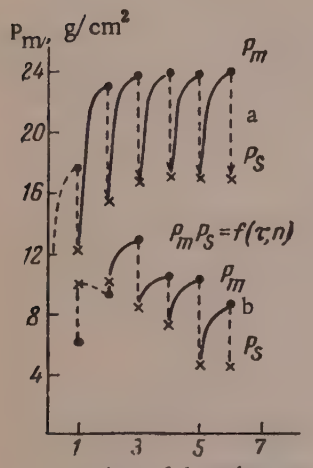


Fig. 5. Variation of the strength of the structure (P_m) during periodic mixing of a 14.6% solution of Na humate in $CaCl_2$ solutions: a) 0.6%; b) 1.2%.

SUMMARY

1. Aqueous dispersions of humates vary in properties from strongly hydrophilic systems to the formation of a compact aggregated precipitate of hydrophobic character.

2. In alkaline solutions, with replacement of H^+ in the exchange capacity of humic acids by Na^+ hydrophilic highly dispersed semicolloidal systems are formed, which are spontaneously dispersed by the water of the medium. Like the viscosity of true solutions, at low concentrations the viscosity of such solutions is close to water and increases linearly up to a certain humate concentration. The region of transition of true viscosity of humate solutions to structural viscosity (gelatination) depends on the pH of the solution: at low pH the region of the linear areas is greater.

3. Solutions of humates, on the surface of which, relatively large hydrophobic areas appear (together with hydrophilic areas) with weakened reaction with water, acquire the capacity for structure formation. The formation of highly dispersed colloidal particles with a mosaic structure of the surface layer assists the creation of strong structures in these systems, but the latter are not water-resistant and may be peptized with further addition of the dispersion medium.

4. With formation of aqueous dispersions of humates, on the surface of the molecules of which, hydrophobic areas predominate, the humates become insoluble and non-peptizing with further addition of the dispersion medium.

LITERATURE CITED

1. T. A. Kikharenko, Tr. In-ta goryuchikh iskopaemykh, Akad. Nauk SSSR 5, 11 (1955).
2. L. V. Chumakova-Ivanova and P. A. Rebinder, Advances in the Chemistry and Technology of Polymers [in Russian] Symp. 2, 1957, p. 146.
3. Z. Ya. Lein, Tr. Pochvennogo in-ta im. V. V. Dokuchaeva 23, 68 (1940).
4. I. V. Vol'f, Candidate's Thesis [in Russian] (Leningrad, 1953).
5. J. W. McBain, Coll. Sci. Boston, USA, 1950; Z. N. Markina and P. A. Rebinder, Doklady Akad. Nauk SSSR 109, 156 (1956); A. B. Taubman and S. A. Nikitina, Doklady Akad. Nauk SSSR 135, 1179 (1960).

All abbreviations of periodicals in the above bibliography are letter-by-letter transliterations of the abbreviations as given in the original Russian journal. *Some or all of this periodical literature may well be available in English translation.* A complete list of the cover-to-cover English translations appears at the back of this issue.

THE SURFACE TENSION OF A SOLID AT THE INTERFACE WITH ITS OWN MELT

L. M. Shcherbakov

Tula Mechanical Institute

Translated from Kolloidnyi Zhurnal, Vol. 23, No. 2, pp. 215-220,
March-April, 1961
Original article submitted December 7, 1959

Recently proposed methods [1-2] of calculating the surface tension σ_s* of a solid make it possible to determine the function at the crystal—vacuum and the crystal—saturated vapor interface. However, in several cases (as for example in studying crystallization from a molten solution) it is very important to know as well the surface tension σ_{sl} of a crystal at the interface with its own melt. A literature search failed to reveal any important theoretical work on the subject, except that the surface tensions apparently do not exceed several units [4]. A method has been worked out [5,6] for the determination of σ_{sl} from the plot of the number of crystallization centers versus temperature. Using this method we calculated σ_{sl} for sulfur, bismuth, tin, lead, sodium, and potassium (at temperatures close to those at which crystallization is observed).

The lack of satisfactory theoretical data regarding the magnitude of the surface tension of a solid at the interface with its own melt have prompted us to attempt a thermodynamic calculation of σ_{sl}. The results are presented below.

At first let us make certain that we clearly understand what is meant by the term surface tension (partial free energy of the surface) of a crystal. Strictly speaking, each face of a crystal has its own surface tension σ_i; according to Wulff's theorem [7] the σ_i values of various faces of an equilibrium crystal are related to each other as shown below,

$$\sigma_1 : \sigma_2 : \sigma_3 : \ldots = l_1 : l_2 : l_3 : \ldots$$

where l_i is known as the Wulff distance for the i-th face of a crystal. In thermodynamic calculations it is permissible to use a value average over all the faces,

$$\sigma = \frac{\sum \sigma_i S_i}{\sum S_i} = \frac{\sum \sigma_i S_i}{S}, \tag{1}$$

which we will call from now on the surface tension (partial free energy of the surface) of a crystal.**

Let us examine now a one-component equilibrium system consisting of a crystal grain (denoted by a single prime) and the surrounding medium*** (denoted by a double prime). Taking into account the fact that according to Wulff's theorem equilibrium species are homothetic we can denote the degree of dispersion in a system by the number of particles g contained in a crystal grain. For a crystal with a surface area (s) and volume (v) we get

$$V = v_0 g; \; S = (v_0 g)^{2/3} \xi, \tag{2}$$

* We are using this commonly accepted term to denote the partial surface free energy.

** Let us note that most of the commonly used experimental methods for the determination of the surface tension of solids do not yield the surface tension of individual faces but an average value which corresponds to our σ.

*** Vapor or melt.

where ζ is the form factor, and v_0 is the volume per unit particle in an infinite crystal phase.* The free energy of this system can be represented in the form

$$\Phi = \mu_0'(P, T)\, g + \mu_0''(P, T)(N - g) + \sigma S \tag{3}$$

where μ'_0 and μ''_0 are the respective chemical potentials of an infinite crystal phase and of the medium (reduced to the pressure of the medium and given per unit particle) and N is the total number of particles in the system.

When g is small second order capillary effects have to be taken into account. According to the general theory of second order capillary effects [8], when dealing with very small particles we can not represent the deviations from an additive free energy distribution by means of only the term σS, which is proportional to the interface area, but have to add additional terms dependent on the dimensions of the particle (in our case g). Moreover the additional "excess" energy is not confined exclusively to the surface layer but refers to the bulk of the grain, so that the theory can be extended also to particles so small as to make a clear distinction between surface and bulk properties practically impossible. Such second order effects were first detected by Deryagin and co-workers [9] in experiments dealing with the wedge pressure of thin films. They found that thin liquid films ($h < 10^{-4}$ cm) exhibit a stationary excess phase pressure (over the "normal" hydrostatic pressure), which has been named the wedge pressure. This anomalous behavior of thin liquid films has been attributed by Deryagin [9] to "excess" free energy in the film.

In accordance with the theory of second order capillary effects instead of using Equation (3) we should represent the free energy of a system consisting of a small crystal grain and a surrounding medium by the equation

$$\Phi = \mu_0'(P, T)\, g + \mu_0''(P, T)(N - g) + \psi(g), \tag{4}$$

where ψ (g) is the "excess" free energy in the particles composing the grain over that found in the particles of the surrounding medium. The function ψ (g) can be conveniently represented in the form

$$\psi(g) = \sigma v_0^{2/3} g^{2/3} \varphi(x), \tag{5}$$

where $\varphi(x)$ is a function of the dimensionless parameter $x = (g/g_0)^{1/3} = r/r_0$;** g_0 is the minimum number of particles capable of forming the crystal grain***. Into the function $\varphi(x)$ we can introduce two boundary conditions.

$$\lim_{x \to 1} \varphi(x) = 0; \quad \lim_{x \to \infty} \varphi(x) = \xi, \tag{6}$$

which stem from the fact that when $g \to g_0$ the phases become undistinguishable, while for $g \gg g_0$ the function ψ (g) is simply transformed into $\sigma S = \sigma v_0^{2/3} g^{2/3} \xi$.

From the requirement that Φ be minimum without overlooking Equation (5) and keeping P, T, N = const.) we get the conditions for equilibrium between a small crystal grain and the surround medium (vapor or melt),

$$\mu_0'(P, T) + \frac{1}{3} \frac{\sigma v_0^{2/3}}{g_0^{1/3}} \left[\frac{2\varphi(x)}{x} + \frac{\partial \varphi}{\partial x} \right] = \mu_0''(P, T).$$

Simplifying the notation as shown below,

$$\alpha = \frac{1}{3} \frac{\sigma v_0^{2/3}}{g_0^{1/3}}; \quad \theta = \frac{2\varphi}{x} + \frac{\partial \varphi}{\partial x}, \tag{7}$$

we can rewrite the equilibrium equation in the form

$$\mu_0'(P, T) + \alpha\theta = \mu_0''(P, T), \tag{8}$$

where α is constant; θ is a function of the dimensionless parameter $x = (g/g_0)^{1/3} = r/r_0$, which represents the degree of dispersion of the system.****

---

* For a one-component system such v corresponds to a Gibbs interface located so as to make the surface compressibility of mass zero.

** r is the affective radius of the grain.

*** g_0 can not be any smaller than the number of molecules in a unit cell of the crystal.

**** Let us note that in Equation (8) the free energies of both phases are reduced to the pressure P of the medium; if, however, each free energy should be reduced to the pressure of its own phase we sould simply have $\mu'(P,T) = \mu''(P,T)$, where $p' \neq p''$.

We will now use Equation (8) to study the effects of crystal grain dimensions (i.e., the number of particles in it) on the phase transition temperature. The latter can be defined as the temperature at which both phases remain in equilibrium with each other at a given pressure (or more precisely pressures*). In our case this will correspond to the equilibrium temperature of the medium at which its pressure acquires a given value. For an infinitesimally small reversible isobaric change of state Equation (8) yields

$$\frac{\partial \mu_0^{'}}{\partial T} dT + \alpha d\theta = \frac{\partial \mu_0^{''}}{\partial T} dT \quad \text{or} \quad -\eta_0 dT + \alpha d\theta = -\eta_0^{''} dT,$$

where $\eta_0^{(i)}$ is the partial molar entropy of the i-th phase (per particle). Assuming that $\eta_0^{''} - \eta_0^{'} = L^0/T$ (L^0 is the enthalpy per unit particle) we get the equation

$$-\alpha d\theta = L^0 \frac{dT}{T}$$

If we integrate this Equation, assuming that in the first approximation α and L_0 are temperature independent, we get an equation for the transition temperature as a function of the crystal grain dimensions (number of particles in the grain),

$$\ln T/T_0 = -\frac{\alpha}{L^0}\theta = -\frac{\alpha}{L^0}\left(\frac{2\varphi}{x} + \frac{\partial \varphi}{\partial x}\right). \tag{9}$$

where T_0 is the transition temperature for an infinite crystal phase.

When dealing with moderately small crystals (linear dimensions > 10^{-4} cm) we can neglect the second order capillary effects and take $\partial \varphi / \partial x \approx 0$ and $\varphi(x) \approx \zeta$. As a result if we substitute the original values of α, θ, and x in Equation (9) and simplify the resulting expression we will get

$$\ln T/T_0 = -2\sigma v_0 \frac{f}{r},$$

where r is the effective radius of the crystal grain; f is the so-called asphericity factor [2] which indicates by what amount the grain surface area exceeds the area of an equivalent (in volume) sphere.

This last relationship has previously been derived by several workers [2, 10] for systems containing a gaseous dispersed medium. We have just shown, however, that it can also be extended to systems containing a liquid dispersion medium, i.e., such systems as the one containing crystal grains in a melt.

Using the general Equation (9) we get the equation

$$\ln \frac{T}{T_0} = -\frac{\alpha_{12}}{L_{12}^0}\theta = -\frac{\alpha_{12}}{q_0}\theta \tag{10}$$

for the temperature at which crystals come out of the melt and a similar equation

$$\ln \frac{T}{T_0} = -\frac{\alpha_{13}}{L_{13}^0}\theta = -\frac{\alpha_{13}}{\rho_0}\theta. \tag{11}$$

for the temperature at which crystals form in the vapor phase. The subscripts 1,2, and 3 refer to the crystal, liquid, and vapor phases respectively; q_0 and ρ_0 are the heats of fusion and sublimation respectively (per unit particle); the subscript 0 denotes a solid (bulk) piece of material. The function θ and parameter g_0 contained in the α_{12} and α_{13} terms will, each have the same value in the crystals formed in the melt as in those deposited from the vapor phase.

Equations (10) and (11) give the phase transition temperature at a given pressure P of the medium surrounding the crystal. If we treat the two Equations simultaneously and substitute for P and T_0 the values of P_t and T_t corresponding to the triple point of a one-component bulk** three-phase system we get a system of equations

$$\left.\begin{aligned} \ln \frac{T}{T_t} &= -\frac{\alpha_{12}}{q_0}\theta \\ \ln \frac{T}{T_t} &= -\frac{\alpha_{13}}{\rho_0}\theta' \end{aligned}\right\} \tag{12}$$

* In a dispersed system the various phases will not generally have the same pressure.

** Consisting of continuous (undispersed) phase only.

defining the triple point of a one-component system with one dispersed and two-continuous phases. The dispersed phase is represented in this case by two crystal grains the degrees of dispersion of which are given by the dimensionless parameters x and x' or the corresponding dimensionless functions θ and θ'.

The ordinary one-component three-phase system composed of bulk phases is invariant and has only a single isolated triple point (point at which the three phases are in equilibrium). But the three-phase system examined by us, which contains a dispersed phase consisting of two grains, will be univariant* (have one degree of freedom) and will consequently have a whole line of triple points. If we should, however, impose on the dispersed phase the condition that the dispersion be uniform so that $\theta = \theta'$, then the system will again become invariant and have a single isolated triple point. Taking $\theta = \theta'$ in the system of Equations (12) we find that at this point

$$\alpha_{12}/q_0 = \alpha_{13}/\rho_0, \tag{13}$$

substituting for α_{12} and α_{13} the original terms and simplifying the resulting equation we get the surface tension of a crystal at the interface with its own melt,

$$\sigma_{sl} = \sigma_s \frac{q_0}{\rho_0} \tag{14}$$

where σ_s is the surface tension of the crystal at the interface with its own vapor q_0 and ρ_0 are the heats of fusion and sublimation respectively of the bulk (undispersed) phase.

Using this last Equation we can compute the surface tension of the solid at the interface with its own melt from readily obtainable thermodynamic data for the corresponding bulk material. Though we can only calculate σ_{sl} for the temperature at the triple point of the dispersed system, one can safely assume that as in the case of liquids σ_{sl} does not change much with temperature.

Surface Tension of Solids at the Interface with Their Own Melts

Compound	Calculated Temp.°C	Heat of fusion	Heat of sublimation	σ_s erg/cm²	σ_{sl}, erg/cm² from eq. (14)	σ_{sl}, erg/cm² lit. data
Sulfur	119	37	496	74	5,5	3,84 [5]
Bismuth	270	43	717	386	23,1	20 [6]
Ice	0	334	2494	80	10,9	—
Cadmium	321	46	933	715	33,5	—
Tin	232	58	2375	567	13,1	17 [6]
Benzene (crystalline)	6	127	394	45	14,5	21,7 [12]
Sodium chloride	804	517	3599	158	22,7	—

As an example we will tabulate the σ_{sl} values calculated from Equation (14). The values of σ_s needed in our calculations were taken from [2] and [14]. For comparison we have also included the values obtained by plotting the number of crystallization centers versus temperature [5,6] and the σ_{sl} for benzene [12].

SUMMARY

1. We have examined the effect of crystal dimensions on the phase transition temperature in a system containing a dispersed crystalline phase.

2. From a study of the triple points of a three-phase system containing a dispersed crystalline phase we derived an equation in which the surface tension of a crystal at the interface with its own melt is given as a function of the surface tension of the same crystal at the interface with its vapor and the heats of fusion and sublimation of the bulk compound.

In concluding we would like to thank Corresponding Member Acad. Sci. USSR B. V. Deryagin for a valuable discussion.

* This is obvious from the simple fact that the system of Equations (12) involves three variable: T, θ, and θ', which are connected by two equations.

LITERATURE CITED

1. M. Born, O. Stern, Sitzungsber. d preuss Acad. 33, 901, 1919; Ya. I. Frenkel', Electrical Theory of Solids [in Russian] (Moscow, 1924); A. E. Glauberman, Zhur. Fiz. Khim. 23, 115, 124 (1949).
2. P. E'. Strebeiko, Dissertation: The Effects of Fragmentation on the Phase Transition Temperature [in Russian] (1939); L. M. Shcherbakov, Izvest. Vysshykh. Uch. Zaved., Fizika, 4, 77 (1959).
3. S. N. Zadumkin, Doklady Akad. Nauk SSSR, 112, 453 (1957); Izvest. Vysshykh Uch. Zaved., Fizika, 2, 151 (1958).
4. Ya. I. Frenkel', Kinetic Theory of Liquids [in Russian] (Moscow—Leningrad, 1945).
5. F. K. Gorskii, Zhur. Eksper. i Teoret. Fiz. 18, 24 (1948).
6. V. I. Danilov, ibid, 19, 235 (1949); V. I. Danilov and A. G. Pomogaibo, Doklady Akad. Nauk SSSR, 68, 843, (1949).
7. G. W. Wulff, Selected Papers on Crystal Physics and Crystallography [Russian translation] (Moscow—Leningrad, 1952).
8. L. M. Shcherbakov, Trudy Tulskogo Mekhanicheskogo Instituta, 7, 117, (1955); 8, 173 (1958); The General Theory of Second Order Capillary Effects, Coll. Trans. Anniversary Confer. on Surface Forces [in Russian] (izd AN SSSR), in print.
9. B. V. Deryagin and E. Obukhov, Kolloid. Zhur. 1, 385 (1935); B. V. Deryagin and M. M. Kusakov, Izvest. Akad. Nauk SSSR, Ser. Khim. 5, 741 (1936); 6, 1119 (1937); B. V. Deryagin and Z. M. Zorin, Zhur. Fiz. Khim. 29, 1755 (1935); B. V. Deryagin, Kolloid. Zhur. 17, 207 (1955).
10. V. K. Semenchenko, Zhur. Fiz. Khim. 19, 298 (1945).
11. Handbook of Physical, Chemical and Engineering Functions (edited by L. K. Martens), [in Russian], vol. 1,2,5,7, 10, Moscow, 1929-30; G. M. Bartenev, Zhur. Tekh. Fiz. 17, 1325 (1947); A. Granovskaya and A. Lyubimov, Zhur. Fiz. Khim. 22, 103, 527 (1948); N. A. Pokrovskii and N. D. Galanina, ibid, 23, 324 (1949).
12. A. Skapski, R. Billups, and D. Casavant, J. Chem. Phys. 31, 1431, 1959.

All abbreviations of periodicals in the above bibliography are letter-by-letter transliterations of the abbreviations as given in the original Russian journal. *Some or all of this periodical literature may well be available in English translation.* A complete list of the cover-to-cover English translations appears at the back of this issue.

THE HEATS OF VAPORIZATION OF SMALL DROPS

L. M. Shcherbakov and V. I. Rykov

Tula Mechanical Institute and Kishnev University
Translated from Kolloidnyi Zhurnal, Vol. 23, No. 2, pp. 221-227,
March-April, 1961
Original article submitted December 28, 1959

It is well known fact that the saturated vapor pressure, dew point, and other thermodynamic properties of small drops are quite different from the regular tabulated bulk properties. Sreznevskii [1] had derived a formula,

$$\Delta\lambda = a^2(1 - \alpha T)\frac{1}{r}, \tag{1}$$

which could be used to calculate the decrease in the heat of vaporization of small drops. In this formula $a^2 = 2\sigma/\delta$ is known as the capillary constant, α is its temperature coefficient, and r is the radius of the drop. Later similar expressions were derived by Helmholtz [2] and Houllevigue [3]. Though the inverse relationship between $\Delta\lambda$ and r shown in this formula does represent moderately well the relationship between λ and r the proportionality constant should be different.

As a matter of fact the heat of vaporization depends basically on the change in the internal energy of a system taking place when a molecule undergoes a transition from the liquid into the vapor phase. Consequently the decrease in the heat of vaporization caused by the dispersion of the liquid should be expressed in terms of the total and not just the free surface energy. We would like to point out that Equation (1) was not derived rigorously enough in the past [1-3].

We will now present a rigorous thermodynamic derivation of the relationship between the heat of vaporization and drop dimensions.

Let us first examine the necessary conditions for a thermodynamic equilibrium between a small drop (prime) and its saturated vapor (double prime). The free energy of the system is

$$F = F' + F'' + 4\pi r^2\sigma,$$

where the partial surface free energy σ is treated as a function of temperature (T) and drop radius (r). Differentiating to get the minimum F with the additional requirement that the system be mechanically insulated (isothermal) we get the conditions for a thermodynamic equilibrium between a drop and its own saturated vapor [4]:

$$\mu'(P', T) = \mu''(P'', T); \quad P' - P'' = \frac{2\sigma}{r} + \frac{\partial\sigma}{\partial r}, \tag{2}$$

where $\mu^{(i)}$ is the chemical potential of the i-th phase. Differentiating with respect to r and remembering that $\partial\mu/\partial P = v$, the molar volume of the examined phase, we get the following equation for the change in the saturated vapor pressure:

$$\frac{\partial P''}{\partial r} = \frac{v'}{v'' - v'}\frac{\partial}{\partial r}\left(\frac{2\sigma}{r} + \frac{\partial\sigma}{\partial r}\right) \cong \frac{v'}{v''}\frac{\partial}{\partial r}\left(\frac{2\sigma}{r} + \frac{\partial\sigma}{\partial r}\right).$$

For an ideal gas we can use the approximation $v'' = RT/P''$. If we now integrate from $r = \infty$ to $r = r$ we get an equation for the saturated vapor pressure of a drop [5],

$$P'' = P_\infty \exp\left[\frac{v'}{RT}\left(\frac{2\sigma}{r} + \frac{\partial\sigma}{\partial r}\right)\right].$$

where P_∞ is the saturated vapor pressure over a flat liquid surface.

Similarly we can get an equation to express the change in the hydrostatic (phase) pressure inside the drop as a function of the change in drop dimensions.

$$\frac{\partial p'}{\partial r} = \frac{v''}{v'' - v'} \frac{\partial}{\partial r}\left(\frac{2\sigma}{r} + \frac{\partial \sigma}{\partial r}\right) \cong \frac{\partial}{\partial r}\left(\frac{2\sigma}{r} + \frac{\partial \sigma}{\partial r}\right).$$

If we now integrate from r = ∞ to r = r we will get the improved Laplace equation for phase pressure [4],

$$P' = P_\infty + \frac{2\sigma}{r} + \frac{\partial \sigma}{\partial r}. \tag{3}$$

Let us now examine a transition from an equilibrium state represented by parameters T and r to another infinitesimally close to equilibrium state represented by T + dT and r + dr. Using the conditions given in Eq. (2) we get the expression shown below for such a transition,

$$d\mu' = d\mu''; \; dP' - dP'' = d\left(\frac{2\sigma}{r} + \frac{\partial \sigma}{\partial r}\right). \tag{4}$$

But a change in chemical potential satisfies the equation

$$d\mu = v dP - \eta dT$$

where v is the molar volume and η the molar entropy of the given phase. Using this relationship we can rewrite the first of the two expressions (4) in the form

$$v' dP' - \eta' dT = v'' dP'' - \eta'' dT.$$

If we now take $\eta'' - \eta' = \lambda / T$ (where λ is the molar heat of vaporization of the drop) then instead of Eq. (4) we will get another system of Equations [4],

$$v'' dP'' - v' dP' = \frac{\lambda}{T} dT; \; dP' - dP'' = d\left(\frac{2\sigma}{r} + \frac{\partial \sigma}{\partial r}\right), \tag{5}$$

which are analogous to the well known Clausius - Clapeyron equation.

Thus in a system with an extended interface where the phases are under different pressures instead of the usual Clausius-Clapeyron equation

$$(v'' - v')\frac{dP_\infty}{dT} = \frac{\lambda_\infty}{T},$$

we should use the system of equations (5). The inadequacy of Sreznevskii's equation [1] can be therefore attributed to the fact that he derived it from the normal Clausius-Clapeyron equation.

Let us now calculate the heat of vaporization of a drop. In calculating thermal effects it is most convenient to use enthalpies: H = U + PV. Whenever a system includes the surface phase it is necessary to introduce the surface enthalpy H_s, which is defined by the equation $H_s = \epsilon S - \sigma S$* [6].

We will assume that the amount of saturated vapor is so large that the evaporation of one drop has no significant effect on the pressure. The enthalpy change which accompanies the evaporation of one drop will be

$$\Delta H = H'' - (H' + H_s).$$

Differentiating with respect to the evaporated mass (in moles) we get the following expression for the molar heat of vaporization of a drop:

$$\lambda = h'' - h' - \frac{\partial H_s}{\partial m}, \tag{6}$$

where $h^{(i)}$ is the molar enthalpy of the i-th (bulk) phase.

By definition

$$h' = u' + P'v'; \quad h'' = u'' + P''v''.$$

* In contrast to the bulk phase where the work of expansion is taken positive, in the surface phase the work required to diminish the surface area is taken as positive (ϵ is the total specific surface energy of the drop).

But for the liquid phase $v' \approx v'_\infty$ and in addition from Equation (3) we get

$$P' = P_\infty + \frac{2\sigma}{r} + \frac{\partial\sigma}{\partial r}.$$

For the vapor phase our approximations yield $P''v'' = P_\infty v''_\infty$. We can now rewrite the preceding expressions in the form

$$h' = u' + \left(P_\infty + \frac{2\sigma}{r} + \frac{\partial\sigma}{\partial r}\right) v'_\infty = u' + P_\infty v_\infty + v'_\infty \left(P_\infty + \frac{2\sigma}{r} + \frac{\partial\sigma}{\partial r}\right) =$$

$$= h'_\infty + v'_\infty \left(\frac{2\sigma}{r} + \frac{\partial\sigma}{\partial r}\right),$$

$$h'' = u'' + P_\infty v''_\infty = h''_\infty.$$

In addition we get

$$\frac{\partial H_s}{\partial m} = \frac{\partial H_s}{\partial V'}\frac{\partial V'}{\partial m} = v'' \left[\frac{\partial(\varepsilon S)}{\partial V'} - \frac{\partial(\sigma S)}{\partial V'}\right] = v'_\infty \left[\left(\frac{2\varepsilon}{r} + \frac{\partial\varepsilon}{\partial r}\right) - \left(\frac{2\sigma}{r} + \frac{\partial\sigma}{\partial r}\right)\right]$$

Substituting the respective expressions for h', h'', and $\partial H_s/\partial m$ into Equation (6) we obtain

$$\lambda = (h''_\infty - h'_\infty) - v'_\infty \left(\frac{2\varepsilon}{r} + \frac{\partial\varepsilon}{\partial r}\right) = \lambda_\infty - v'_\infty \left(\frac{2\varepsilon}{r} + \frac{\partial\varepsilon}{\partial r}\right).$$

If we now express the molar volume of the liquid v'_∞ in terms of its density δ and molecular weight M we get an equation for the decrease in the molar heat of vaporization of a drop caused by the increase in surface.

$$\Delta\lambda = -\frac{M}{\delta}\left(\frac{2\varepsilon}{r} + \frac{\partial\varepsilon}{\partial r}\right). \tag{7}$$

Considering that the terms on the right hand side of the equation are intrinsically positive we conclude that $\Delta\lambda < 0$, or in other words that the dispersion of any liquid will decrease its heat of vaporization.

According to Frenkel' [7] the association of molecules into various complex aggregates precedes the formation of even the smallest nuclei of liquid drops in a supersaturated vapor. We can use the surface energy as a criterion for distinguishing liquid drops from associated complexes. According to the literature data [8] the specific surface energy of a drop ϵ should decline with decreasing drop radius r. Hence the minimum radius r_0 at which ϵ becomes zero can be taken as the dividing line between associated complexes ($r > r_0$).*

With these facts in mind we can write a general expression for ϵ as a function of r,

$$\varepsilon = \varepsilon_\infty \cdot \varphi(r/r_0) = \varepsilon_\infty \cdot \varphi(x). \tag{8}$$

In this Equation ϵ_∞ is the tabulated value of the specific total surface energy of the bulk liquid, while $\varphi(x)$ is a certain function which we will only describe by giving for it two obvious boundary conditions: $\lim \varphi(x) = 1$ and $\lim \varphi(x) = 0$. Substituting this function into Eq. (7) we will get

$$\Delta\lambda = -\frac{M}{\delta}\frac{\varepsilon_\infty}{r_0}\left(\frac{2\varphi}{x} + \varphi'\right). \tag{9}$$

If we now change from the radius r_0 for the minimum drop size to one for a drop containing g_0 particles in accordance with the relationship

$$\frac{4}{3}\pi r_0^3 = \frac{v'_\infty}{N_A} g_0 = \left(\frac{M}{\delta} \Big/ N_A\right) g_0$$

where N_A is the Avogadro's number, we will get the formula shown below for the decrease in the heat of vaporization of small drops,

* With reference to these criteria we would like to say a few words about the frequently voiced objections (see [9]) concerning the use of concepts such as interface and surface tension in describing particles as small as drop nuclei. Of course, when $r \sim r_0$ the usual definition of these properties, which involves a clearly defined physical boundary between the liquid and the vapor (i.e., a finite intermediate layer), becomes meaningless. It would be more appropriate in such a case to use concepts such as those used in the liquid drop model of atomic nucleii [10].

$$\Delta\lambda = -\left(\frac{4\pi N_A}{2}\right)^{1/3}\left(\frac{M}{8}\right)^{2/3}\frac{\varepsilon_\infty}{g_0^{1/3}}\left(\frac{2\varphi}{x}+\varphi'\right). \tag{10}$$

We will now examine some possible applications of the derived equations. In cases of maximum dispersion ($r = r_0$, or $x = 1$) the heat of vaporization will simply be equal to the association energy (per mole): $\lim_{x\to 1}\lambda = E_{ass}$, where the latter one can be taken as equal to $RT_{crit.}$ [11]. Hence in the limiting case Equation (10) will be reduced to

$$\lim_{x\to 1}\Delta\lambda = RT_{crit} - \lambda_\infty = -\left(\frac{4\pi N_A}{3}\right)^{1/3}\left(\frac{M}{\delta}\right)^{2/3}\frac{\varepsilon_\infty}{g_0^{1/3}}\varphi'(1).$$

But according to the theory of corresponding states [11] the ratio $\lambda_\infty/RT_{crit.}$ remains constant for all chemically similar compounds. We can therefore presume that g_0 will also remain the same in compounds with similar chemical properties*.

In that case the last expression will yield the simple relationship

$$\lambda_\infty/\varepsilon_\infty\,(v'_\infty)^{2/3} \cong \text{const} = B. \tag{11}$$

The results presented in Table 1** show that our assumptions yield satisfactory results for a variety of liquids. It seems that this Equation holds as well for the liquid as it does for the solid phase of any one compound in the vicinity of its melting point.*** So that if we write this Equation for both the liquid and the solid phases we will get the relationship shown below,

$$\frac{\varepsilon_{s,\infty}}{\varepsilon_{l,\infty}} = \left(\frac{\delta_s}{\delta_l}\right)^{2/3}\frac{\rho_\infty}{\lambda_\infty} \tag{12}$$

where ρ is the molar heat of sublimation for bulk compound and ϵ_{s_∞} is the specific total surface energy of a microscopic crystal averaged over all the faces as shown below,

$$\varepsilon_{T,\infty} = \Sigma\,\varepsilon_i S_i/\Sigma S_i.$$

Equation (12), which is analogous to the one derived by Strebeiko [13], represents an improved version of the formula proposed some time ago by one of the authors of this paper [14] for calculating the surface energy of solids. In Table 2 we have listed the specific total surface energies of some solids (at the interface with their vapors) calculated by using Equation (12). All the data required for our calculations were obtained from [12,14].

TABLE 1

Values of the B Constant Calculated from Equation (11)

Liquid	Temp. OC	$v^{2}/_{3}$ cm²/mole	ϵ_∞ erg/cm²	λ_∞ cal/mole	$B\times 10^{-7}$
n-Hexane	20	25,74	47,7	7580	0,26
n-Octane	20	29,78	51,1	9970	0,27
Benzene	20	19,91	68,2	8145	0,25
Chloroform	20	18,60	67,4	8500	0,28
Carbon tetrachloride	20	21,04	62,6	8186	0,26
Acetic acid	20	15,08	57,0	5040	0,25

* The validity of this assumption was confirmed by direct calculations by Martynov and Deryagin.

** In compiling this table use was made of data given in [12].

*** Equation (10) was derived in such a way that it as well as other equations derived from it should be equally applicable to a crystal grain. The assumption that g_0 should be the same for liquids and solids appears to us quite obvious and needs no futher comment.

We will now use the improved Laplace equation for the molecular pressure in a drop [4]*,

$$K = K_\infty - \left(\frac{2\epsilon}{r} + \frac{\partial \epsilon}{\partial r}\right). \tag{13}$$

Substituting into this Equation the expression given for ϵ in Eq. (8) we get

$$K = K_\infty - \frac{\epsilon_\infty}{r_0}\left[\frac{2\varphi(x)}{x} + \varphi'(x)\right]$$

where K_∞ is the molecular pressure for bulk liquid with a flat interface.

If r is quite small the molecular pressure in the drop will be much smaller than K_∞. Hence in evaluating K we can use the Van der Waals approximation, $K \cong E_{ass}/v' \cong E_{acc}/v'_\infty$. If we again consider the limiting case of dispersion the last equation will yield

$$\lim_{x\to 1} K = \frac{E_{ass}}{v'_\infty} = K_\infty - \frac{\epsilon_\infty}{r_0}\varphi'(1).$$

On the other hand for the same limiting case Equation (9) yields (assuming $\frac{M}{\delta} = v'_\infty$)

$$\lim_{x\to 1} \Delta\lambda = E_{ass} - \lambda_\infty = -v'_\infty \frac{\epsilon_\infty}{r_0}\varphi'(1).$$

Combining the last two expressions we get Stefan's law [15],

$$K_\infty = \frac{\lambda_\infty}{v'_\infty}, \tag{14}$$

where λ_∞ is the molar heat of vaporization; v'_∞ is the molar volume; K_∞ is the molecular pressure in a large amount of liquid.

TABLE 2

The Specific Total Surface Energy of Solids Calculated from Equation (12)

Compound	Temp °C	Density g/cm³		Specific heat, Joules/g		ϵ_∞ for the melt $\frac{erg}{cm^2}$	ϵ_∞ erg/cm²
		$\delta_т$	$\delta_ж$	ρ_∞	λ_∞		
Sodium chloride	804	1,907	1,541	3599	3082	166	224
Potassium chloride	772	1,784	1,524	3000	2690	156	201
Ice	0	0,917	0,999	2494	2160	114	125
Sulfur	119	1,940	1,805	496	459	85	97
Bismuth	270	9,68	10,00	717	674	417	434
Cadmium	321	8,64	8,02	983	937	670	739
Tin	232	7,19	6,97	2375	2317	576	603

SUMMARY

1. We have provided a thermodynamic derivation of the formula for the decrease in the heat of vaporization of small drops. We have also established that the decrease depends not on the free but the total surface energy.

* This equation can most readily be derived from Equation (3) by using the thermodynamic identity $K = T\frac{\partial P'}{\partial T} - P'$, and assuming that $\sigma - T\frac{\partial \sigma}{\partial T} = \epsilon$.

2. Using the derived formulas we computed the surface energies of several solids.

3. We have also substantiated the well known Stefan's law connecting molecular pressure in liquids with the heat of vaporization.

We would like to express our gratitude to Corresponding Member Acad. Sci. USSR B. V. Deryagin for some valuable discussion.

LITERATURE CITED

1. B. Sreznevskii, Zhur. Russ. Fiz. Khim. Obshchestva, Chast'Fiz., 15, 39 (1883).
2. R. Helmholtz, Ann. phys. 27, 508, (1886).
3. M. L. Houllevigue, J. phys. theor. et appliq. 3, 159 (1896).
4. L. M. Shcherbakov, Uch. Zap. Kishnevskogo Universiteta 5, 117 (1952); Kolloid. Zhur. 20, 502 (1958).
5. L. M. Shcherbakov, Trudy Tulskogo Mekhanicheskogo Instituta 7, 117 (1955); Kolloid. Zhur. 20, 759 (1958).
6. Guggenheim, Modern Thermodynamics [Russian translation] (Moscow-Leningrad, 1941), p. 149.
7. Ya. I. Frenkel', Zhur. Eksper. Teoret. Fiz. 9, 199, 952 (1939).
8. R. C. Tolman, J. Chem. Phys. 17, 333 (1949); J. G. Kirkwood and F. P. Buff, ibid. 17, 558 (1949); L. M. Shcherbakov Kolloid. Zhur. 14, 379 (1952); F. P. Buff, J. Chem. Phys. 19, 1591 (1951), 23 419 (1955).
9. S. V. Gorbachev and A. V. Shlykov, Zhur. Fiz. Khim. 29, 1777 (1955).
10. Ya. I. Frenkel', Zhur. Eksper. Teoret. Fiz. 9, 641 (1939).
11. M. P. Vukalovich and I. I. Novikov, The Equation of State for Real Gases [in Russian] (Moscow-Leningrad, 1948), p. 191.
12. Handbook of Physical, Chemical, and Engineering Functions (edited by L. K. Martens) [in Russian], Vol. 1,2,5, 7,10, Moscow, 1929-1930; Physicochemical Properties of Pure Hydrocarbons, Nos. 1-5 [in Russian] (Gostekhizdat, 1952-1954); Thermophysical Properties of Materials (Handbook) [in Russian] (Gosenergoizdat, 1956).
13. P. É. Strebeiko, Dissertation: The Effects of Fragmentation of Phase Transition Temperatures [in Russian] (IONKh, Acad. Sci. USSR, 1939).
14. L. M. Shcherbakov, Izvest. Vysshykh. Uch. Zaved, Fizika, 4, 77 (1959).
15. J. Stefan, Ann. Phys. 29, 655 (1886).

All abbreviations of periodicals in the above bibliography are letter-by-letter transliterations of the abbreviations as given in the original Russian journal. *Some or all of this periodical literature may well be available in English translation.* A complete list of the cover-to-cover English translations appears at the back of this issue.

PORE SIZE DISTRIBUTION IN CEMENT ROCKS

L. I. Edel'man, D. S. Sominskii, and N. V. Kopchikova

The Scientific Research Institute for New Structural Materials, Moscow
Translated from Kolloidnyi Zhurnal, Vol. 23, No. 2, pp. 228-233,
March-April, 1961
Original article submitted January 22, 1960

In connection with the problem of obtaining long-lived and frost-resisting structural materials, it is interesting to study the microstructure of structural rock, with particular reference to the character of its porosity. It is not sufficient to consider only the total porosity or even separate groups of pores. The published work on the pore size distribution in hardened cement solutions and concretes is unsystematic [1,2]. We have, therefore, investigated the differential porosity, which is a function of the distribution of pore volume according to pore size, in cement rock, and have studied the effects of hardening conditions on the structure formation process.

For this purpose we used the mercury porometry method [3-5], by which means it was possible to find the pore distribution as a function of pore size over a wide enough range. A high pressure mercury porometer [4] was used for the pore radius range 0.006 to 5 microns, and we developed a low pressure dilatometer for use with pore radii of 5 to 300 μ.

In order to calculate the effective pore radii, the surface tension of mercury was taken as $\sigma = 471.6$ erg/cm^2, and the wetting angle of mercury at the sample surface as $\theta = 145°$ [4]. Hence, the equation for calculating the limiting pore radius, namely $r = 2\sigma \cos\theta/p$, took the form:

$$r = \frac{78740}{p}, \text{ Å},$$

where p is the pressure (in atmospheres) on the mercury in the porometer bomb.

The materials investigated were cement work samples, stored at atmospheric humidity, without filler. Two sets of samples were prepared, based on the bibro-ground, alite, medium aluminate clinker with 4% of gypsum. In the first set of samples, the specific surface (s) of the cement was 0.22, 0.4, and 0.6 m^2/g (by the Cozen-Karman method), and the samples were prepared from materials of the same consistency; the water cement ration (W/C) was altered from 0.27 to 0.30. In the second set of samples, the W/C was varied (0.28, 0.5, 0.7) to preserve the same specific surface of the cement (0.4 m^2/g). The differential porosity was investigated after various hardening times. The total porosity was determined from measurements of the bulk density and true specific gravity.

Fig. 1 shows the effect of W/C on the pore size distribution for cement samples after 28 days storage, and Fig. 2 shows the dispersions obtained from measurements with the high pressure porometer. In these, and in the other figures, the pore radius is plotted on a logarithmic scale. The curves of Fig. 1 are shown in the integrated form; the pore volume (V, cm^3) is expressed as a percentage of the sample volume. The full curve for sample 2 (W/C = 0.5) was obtained using the high and low pressure porometers. For samples 1 and 3, the parts of the curves for $r > 5\ \mu$ were calculated from the difference between the total porosity and the pore volume for the range 0.006 to 5 μ. Fig. 2 shows differential distribution curves, calculated from the integral curves as $\Delta V/\Delta \log r$, over the radius range 0.006 to 5 μ.

The results show that the pore radii, for a cement rock one month after preparation from a clinker of normal mineralogical composition, were mainly < 1 μ. According to measurements with the low pressure porometer, the upper limit of pore radius was in the region 300 to 400 μ. With a normal thickness cement mix more than half the pores had a radius of < 0.1 μ, and the total pore volume for the radius range 0.006 to 1 μ was 80 to 90% of the total porosity, whereas in a highly disperse cement there were hardly any pores with radius > 1μ. In the case of high water to cement ratios (0.5 to 0.7), the low pressure porometer showed that the cement rock contained 20 to 45% of pores with $r > 1\ \mu$.

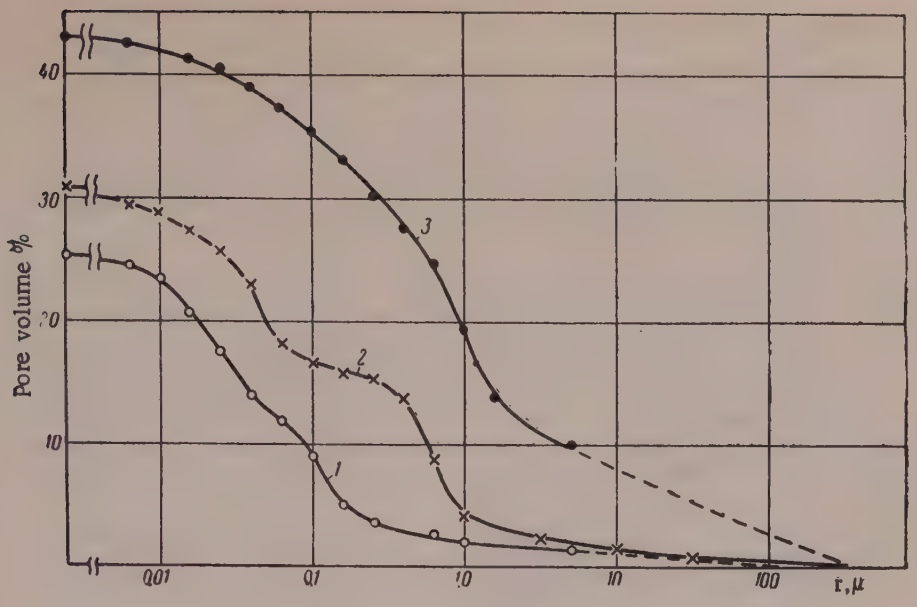


Fig. 1. The effect of water-cement ratio on the pore size distribution of cement rock (s_{sp} = 0.4 m^2/g): 1) W/C = 0.28, 2) W/C = 0.5, 3) W/C = 0.7.

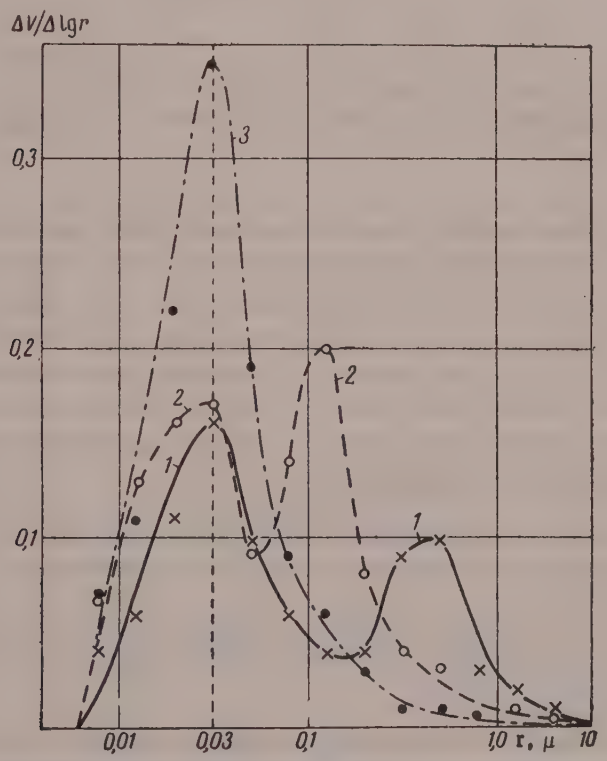


Fig. 2. Differential distribution curves for pore volume as a function of pore size: s_{sp} = 1) 0.22 m^2/g, 2) 0.4 m^2/g, 3) 0.6 m^2/g. The hardening time was 28 days.

With an increase in hardening time there was a shift in the pore volume distribution curve towards smaller dimensions as the result of a decrease in the volume and size of the coarse pores. Thus, for a cement sample with an initial s = 0.4 m^2/g, there were no pores with r > 1 μ after a years hardening. There was also a decrease in the total porosity of this cement rock (Fig. 3).

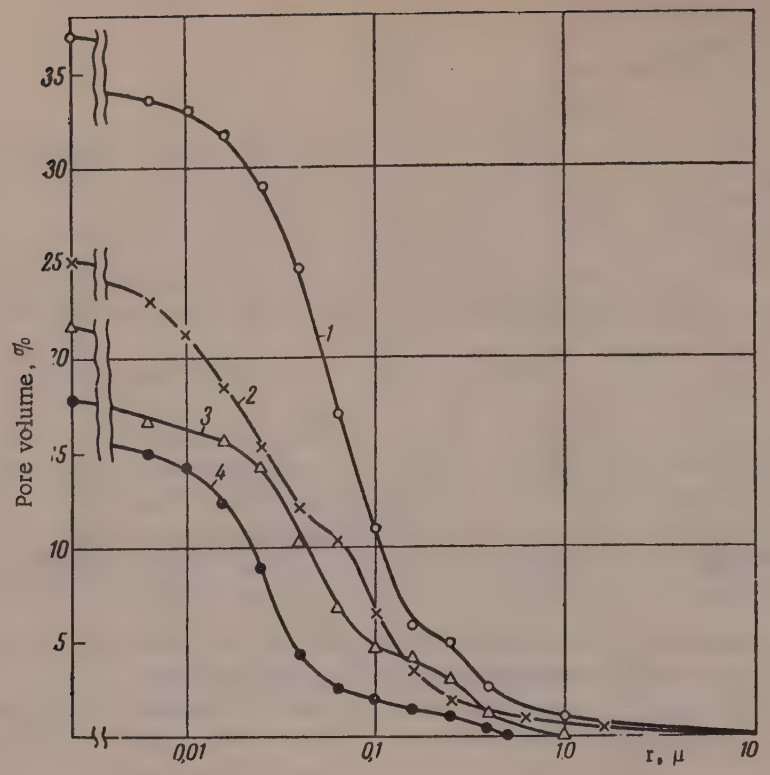


Fig. 3. Variation in the pore size distribution of cement rock with hardening time: 1) 1 day, 2) 28 days, 3) 5 months, 4) 1 year. s_{sp} = = 0.4 m^2/g, W/C = 0.28

A characteristic feature of cement rock in general is the existence of two preponderating sizes; this is shown by two steeply sloping regions of the integral curves and the corresponding maxima of the differential curves.

With a W/C value corresponding to a normal thickness cement mix, independent of the cement dispersion, there was one large group of pores in the pore radius ragion less than 0.05 μ, with a maximum between 0.025 and 0.030 μ (Fig. 2), and the absolute value of the maximum increased with increasing specific surface of the cement. The second maximum shifted in the direction of coarser pores when the clinker was of lower dispersion.

With samples hardened for a moderate period (28 days), a stepwise increase in W/C led to regular shifts in the distribution curve maxima in the direction of larger pores (Fig. 1).

The pores of radius less than 0.05 μ remained predominant during the hardening process of cement rock. When samples with different initial dispersions of the cement were stored for a year at normal humidity, there was a decrease in the differences between the absolute values of the maxima in the fine pore region, as compared with the results after a month (Fig. 4). The second maximum (in the coarse pore region of 0.1 to 1 μ) either greatly decreased (curve 1 of Fig. 4) or vanished altogether (curve 2 of Fig. 4). However, the clear relation between the distribution of these pores and the dispersion of the cement was retained.

The above experimental data enabled us to make suggestions as to the nature of both the pore groups found in cement rock. The fine pore group of radius below 0.05μ, characterized by a maximum in the distribution curve in the region of 0.025 to 0.03 μ, clearly corresponded to pores in the crystalline structure between the adhering newly formed crystals [6], and the dimensions of these pores were determined by the formation conditions of this structure. A confirmation tion of this suggestion was the practical independence of the position of this maximum on the dispersion of the cement and the simultaneous marked increase in its absolute value (for one month samples) on changing to a highly disperse cement, explained by the more intense hydration of the cement (Fig. 2). In low W/C samples, the same pore group was retained when the hardening period was lengthened, but differences in the absolute value of the maximum, associated with changes in the dispersion of the clinker, decreased after a year's storage (Fig. 4), following convergence to the same value for the degree of hydration.

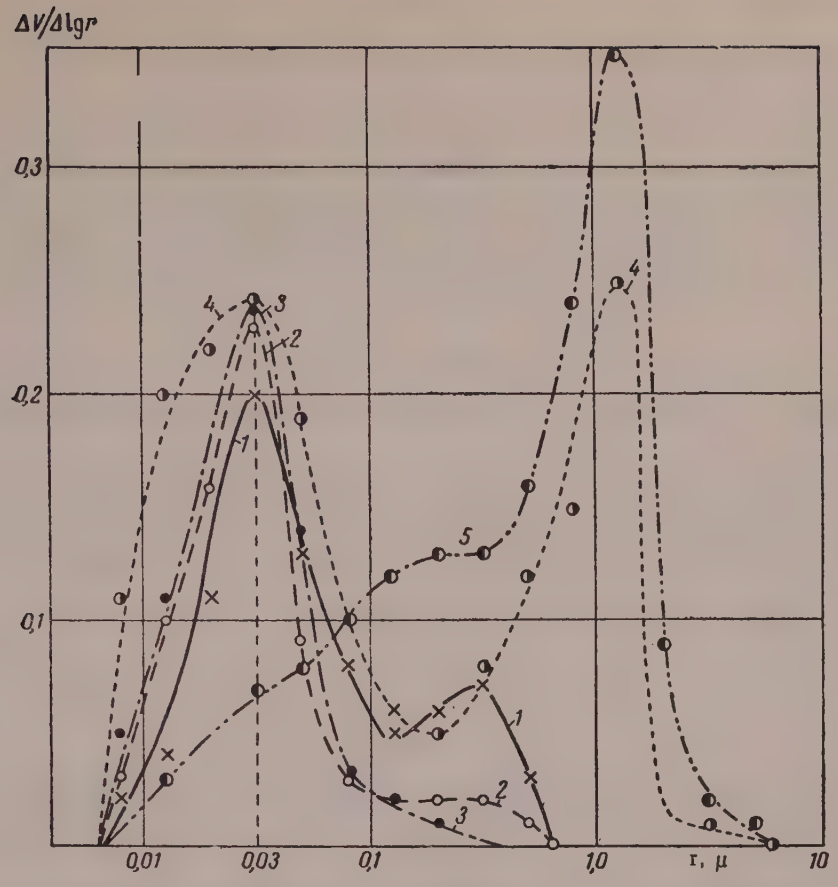


Fig. 4. Relation between the pore distribution of a cement rock, the dispersion of the cement, and the water-cement ratio, for a hardening time of 1 year: 1) $s_{sp} = 0.22$ m^2/g, W/C = 0.27; 2) $s_{sp} = 0.4$ m^2/g, W/C = 0.28; 3) $s_{sp} = 0.6$ m^2/g, W/C = 0.305; 4) $s_{sp} = 0.4$ m^2/g, W/C = 0.7; 5) the same after 28 days hardening.

Increase in W/C led to a considerable increase in pore dimensions of the newly formed crystal structure for short and medium hardening times (displacement of this maximum in the direction of larger pore size in curve 2, and disappearance of the maximum in curve 3 of Fig. 1). With prolonged hardening there was agglomeration of the newly formed crystals, and the pore distribution curve altered considerably for the samples with a high W/C: After 1 year a maximum appeared in the 0.02 to 0.03 μ region, and the volume of pores with radius greater than 1 μ markedly decreased. A characteristic example was the sample with W/C = 0.7 (curves 4 and 5 of Fig. 4).

The second maximum of the distribution curves, corresponding to the pore radius region 0.1 to 1μ, could evidently be attributed to capillary pores between the remaining unhydrated clinker granules and the newly formed material. Sand granules obviously play a part in cement-sand mixes. The position and value of this maximum were essentially determined by the granulometric composition of the initial clinker, the amount of water used, and the hardening time of the rock. The less the dispersion of the cement and the greater the W/C, the greater was the pore radius corresponding to this maximum in the distribution curves. The dimensions and total volume of the capillary pores decreased with increasing hardening time of the cement rock, and this, as noted above, led to a disappearance of the 0.1 to 1 μ maximum in the case of low W/C samples.

We also investigated the effects of a plasticizing additive, namely sulfite-alcohol slops (0.25% by weight to cement with $s_{sp} = 0.37$ m^2/g), on the differential porosity of cement rock after different hardening times. It was found that, after short hardening times (the first few days after mixing), the slops somewhat increased the total porosity and produced some shift in the distribution curve towards large pore size. However, after 28 days the slops ensured a denser structure and shifted the maximum of the differential curve in the direction of smaller pore size.

SUMMARY

The open pore size distribution of cement rock has been investigated by the mercury porometer method, over the pore radius range 0.006 to 300 μ.

The differential pore size distribution curves were, in general, characterized by two maxima. The first maximum, in the pore size range 0.025 to 0.030 μ, evidently corresponded to pores in the crystalline structure between the adhering newly formed crystals; its absolute value time. The second maximum, at a pore radius between 0.1 and 1μ, was attributed to capillary pores in the cement rock. Its position and value were essentially determined by the hardening conditions, the granulometric composition of the original cement, the water-cement ratio, and the hardening time.

LITERATURE CITED

1. V. V. Stol'nikov and E. V. Lavrinovich, Izvest. Vses. Nauchno-Issledovat. Inst. Gidrotekhniki, No. 47, 208 (1952).
2. P. P. Stupachenko, Izvest. Vyssh. Uchebn. Zaved., Ser. Stroitel'stvo i Arkh., No. 3, 30 (1958).
3. H. L. Ritter, and L. C. Drake, Industr. and Engn. Chem. (Anal. Ed.) 17, 782(1945) 41, 780 (1949).
4. T. G. Plachenov, Zhur. Priklad. Khim., 28, 245 (1955).
5. V. V. Khodot and Yu. S. Premysler, Doklady Akad. Nauk SSSR, 105, No. 3, (1955).
6. E. E. Segalova and V. N. Izmailova, Kolloid. Zhur., 20, 601 (1958).

All abbreviations of periodicals in the above bibliography are letter-by-letter transliterations of the abbreviations as given in the original Russian journal. *Some or all of this periodical literature may well be available in English translation.* A complete list of the cover-to-cover English translations appears at the back of this issue.

A FLOW ULTRAMICROSCOPE WITH AUTOMATIC AEROSOL PARTICLE COUNTING

B. V. Deryagin, V. V. Churakov, and G. Ya. Vlasenko

Laboratory for Surface Phenomena, Institute of Physical Chemistry, Academy of Sciences, USSR

Translated from Kolloidnyi Zhurnal, Vol. 23, No. 2, pp. 234-237, March-April, 1961
Original article submitted April 28, 1960

Flow ultramicroscopes of the VDK type [1] are used to an ever increasing extent in measuring the amount of dust in the air in factory rooms and for controlling the degree of purification of industrial gas waste that is performed by means of various filtering devices.

The principle of flow ultramicroscopy consists in the fact that the particles which follow one another in an aerosol flow scatter the light when passing through the illuminated zone; this light, in the form of separate flashes, can be observed visually or recorded by means of a photocell [2]. Visual counting of the number of aerosol particles in the microscope field of view limits the possibility of enlarging the scope of applicability of this instrument, for instance, for remote measurements, apart from the fact that prolonged visual counting is tiring for the observer's eyes. All this prompted us to develop an automatic variant of the flow ultramicroscope by using photoelectric transducers [3]. In this, the position of the light source that creates the illuminated zone with respect to the direction in which the particles move is of primary importance.

At the present time, two basic arrangements are used for counting aerosol particles in flow; these arrangements differ from each other by the direction of particle flow with respect to the photoelectric transducer or microscope (Fig. 1).

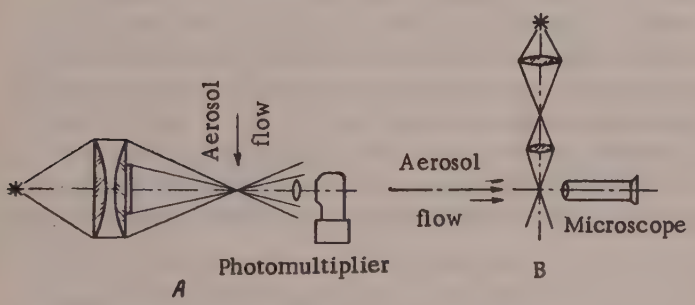


Fig. 1. Arrangements for aerosol particle counting.

The arrangement A, which was first used by Gucker and O'Konski [4] and later, in a somewhat modified form, by Mikirov [5] and Laktionov [6], makes it possible to use the maximum amount of the light scattered by an aerosol particle. However, a considerable disadvantage of arrangement A is the fact that, in order to secure single "flashes" from particles flying through the illuminated zone in the microscope field of view, it is necessary to provide a very thin aerosol flow and to dilute the flow in the case of high aerosol concentrations. Therefore, the devices based on this arrangement do not permit the measurement of high aerosol count concentrations (if the number of particles per unit volume is greater than 10^5 particles per 1 cm^3) without dilution.

The arrangement B, which is used in the VDK flow ultramicroscope, is universal in this respect, since it makes it possible to investigate any aerosol count concentration. According to the arrangement B, the aerosol flow, moving toward the objective, intersects with the light cone under a 90° angle. Due to this, a dark field is created in the system, which facilitates the recording of "flashes" of light scattered on individual particles. Single "flashes" are secured in the microscope field of view by means of interchangeable diaphragms, by means of which the diameter of the microscope field of view can be varied within a wide range. This makes it possible to investigate aerosols with count concentrations attaining 10^7 particles/cm^3 and over. Therefore, we used the arrangement B for the automatic flow ultramicroscope.

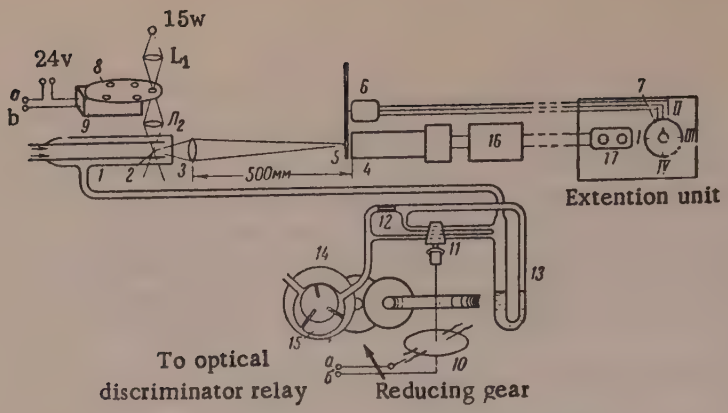


Fig. 2. Automatic flow ultramicroscope layout.

The aerosol flow, which is drawn into bulb 1 (Fig. 2), intersects the illuminated zone 2 in its motion. The light that is scattered by aerosol particles is focused by means of objective 3 (magnification: 12) on the cathode of of an FÉU-19 photomultiplier, 4, which is located at a distance of 500 mm from the objective. A revolving diaphragm, 5, is installed in front of the photomultiplier cathode; the diaphragm has five openings whose diameters are 0.5, 1.5, 7.5, 20, and 30 mm, which are chosen in dependence on the aerosol count concentration*.

Simple lenses with a large aperture ratio are used for the condenser and the objective, while a 75-w K-21 lamp for 10 v serves as the light source.

An optical discriminator, 8, which is mounted in the illuminator, serves for dispersion analysis. The discriminator is made in the shape of a disk with 5 openings, where filters made of neutral grey glass of different density are inserted. The discriminator is fixed on the axle of an SChZ telephone relay, 9. When the relay is actuated, the discriminator turns through an arc amounting to $^1/_{10}$ of its circumference. Thus, the relay must be actuated twice if one opening is to be replaced by another. The relay actuation occurs at the closing of the contacts on disk 10, when a double valve, 11, which has openings in the stem whose diameters are equal to 1 mm and which is mounted on the same axle, closes or opens. Valve 11 is driven by a (15-20)-w electric motor, 14, through a reducing gear. An air pump, 15, which reduces the pressure to 20 to 30 mm Hg below atmospheric pressure, is mounted on the other end of the electric motor shaft. When valve 11 is in the position shown in Fig. 2, the bulb is directly connected to the pump, and aerosol is intensively drawn through. When valve 11 is closed, the pump is connected to the bulb through capillary 12 and a U-shaped tube, 13, which is permanently filled with a liquid. The necessary aerosol flow velocity is at this moment established in the bulb. The change in the liquid volume in one of the elbows of tube 13 is equal to the aerosol volume that has passed through the bulb during measurement. The required aerosol flow velocity in the bulb (2-6 cm/min) is set by selecting a suitable diameter for capillary 12 when the device is constructed. The amount of liquid 13 that is introduced between capillary 12 and the bulb makes it possible not only continuously to control the amount of aerosol passing through the bulb, but also to prevent the capillary from becoming contaminated with aerosol particles.

Due to the low aerosol flow velocity, large particles may settle in the bulb some time after the beginning of measurements. In order to eliminate this, it is necessary to blow through the bulb with a strong blast of the aerosol under investigation over periods of 5-10 sec every 20-25 sec during measurements. This is secured by the periodical opening of valve 11. A single measurement (i.e., the blowing through of the bulb and the particle count) last approximately 30 sec. Therefore, the gear ratio of the electric motor to valve 11 transmission was chosen in such a manner that the valve rotating speed did not exceed 1 rpm.

The voltage pulse obtained at the photomultiplier output is fed to a pulse amplifier, 16, to the output of which an SB-1M mechanical counter, 17, is connected**.

* For the remote control of the diaphragm, the latter can be fixed on the shaft of a controllable BD-404A selsyn, 6, which is coupled with the controlling selsyn 7 (Fig. 2).

** If remote control of the device is required, the selsyn by means of which the openings in the revolving diaphragm are selected and the SB-1M mechanical counter are mounted together in a separate extension unit, which can be located at a certain distance from the device (Fig. 2).

The circuit of the three-stage pulse amplifier is shown in Fig. 3. Since the current intensity at the output of tube L_3 is independent of the magnitude of the voltage pulse that is fed from the photomultiplier to the input of tube L_1, an electronic pulse accumulator with a self-recorder can be connected to the circuit instead of the mechanical counter. In order to eliminate the effect of various inductions caused by the ac current network, which influence the operating stability of the device's electronic section, the photomultiplier is fed by GB-300 batteries, and the amplifier anode and heating circuits are fed by a stabilized rectifier.

The over-all count concentration of the aerosol contained in the bulb is measured first; in this, the light beam in the illuminator passes through the optical discriminator opening without the filter, and the diameter of the revolving diaphragm opening is chosen in such a manner that the mechanical counter actuation frequency does not exceed 50 pulses/sec. After the bulb is blown through with the aerosol under investigation, the disk 8 of the optical discriminator (Fig. 2) is rotated so that, instead of the blank opening, the opening with the optical filter is in position. In this, the illuminated zone brightness in the bulb decreases, and we determine the count concentration of only those particles whose flash brightness is sufficient for their registration by the photomultiplier. The optical filters are then successively interchanged after first blowing through the bulb each time, and the last of these filters will reduce the illuminated zone brightness to such an extent that only the "flashes" of the largest particles contained in the aerosol under investigation will be counted.

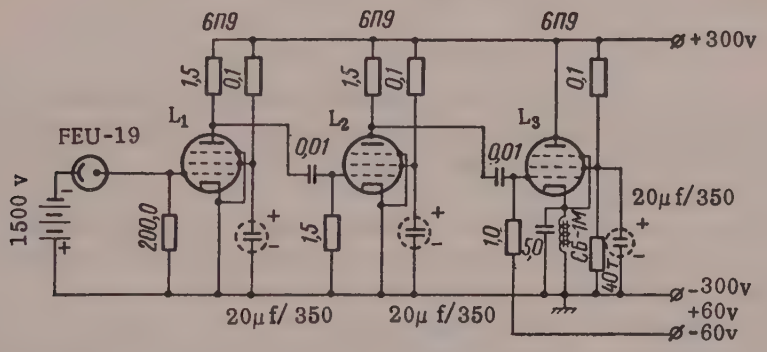


Fig. 3. Pulse amplifier circuit.

If, during the measurement process, the aerosol count concentration does not change by more than two orders of magnitude, the work can be performed without changing the diaphragm opening diameter. Thus, one investigation cycle, which consists in measuring the count concentration of the aerosol and in dividing it into five fractions, is performed. Since the time required for counting the number of particles and for blowing through the bulb amounts to 30 sec, approximately 2.5 min are necessary for the entire cycle of fractional composition determination. In order to average the obtained results, three to five measurement cycles can be performed (if the aerosol is stable in time). Thus, the time necessary for performing a complete series of aerosol investigation consisting of three to five cycles will be 7 to 12 min.

Device	Count concentration of oil fog particles per 1 cm^3				
Automatic	$5,3 \cdot 10^3$	$5,4 \cdot 10^4$	$1,7 \cdot 10^5$	$5,9 \cdot 10^6$	$1,2 \cdot 10^7$
VDK	$5,5 \cdot 10^3$	$5,5 \cdot 10^4$	$1,3 \cdot 10^5$	$6,0 \cdot 10^6$	$1,3 \cdot 10^7$

The aerosol concentration is calculated by using the equation

$$N = na/V,$$

where N is the number of particles (per 1 cm^3), n is the number of particles counted by the mechanical counter, V is the aerosol volume that passed through the bulb (cm^3), and a is a constant for each revolving diaphragm opening for the given optical system [1 and 2].

The table provides a comparison of count concentrations which were obtained by means of the automatic device prototype and a VDK flow ultramicroscope. Oil fog, obtained by the condensation method, was used as the aerosol.

Since the optical discriminator was not mounted in the illuminator of the automatic device prototype. No comparative data on fractional composition determination by means of the VDK ultramicroscope are given.

SUMMARY

1. We have developed the prototype of a device based on a VDK ultramicroscope for the automatic counting of aerosol particles.

2. This device makes it possible to measure aerosol count concentrations from 10 to 10^7 particles per 1 cm^3 without dilution.

3. The device can be used for recording particles with diameters from 10^{-5} to $\sim 20 \times 10^{-4}$ cm.

4. Seven to twelve minutes are required for measuring the aerosol count concentration and for dividing the aerosol into five fractions with respect to size.

5. The device can be provided with remote control.

LITERATURE CITED

1. B. V. Deryagin and G. Ya. Vlasenko, Author's Certificate No. 86851 (1944); Doklady Akad. Nauk SSSR, 63, 155 (1948); "New ideas in the field of aerosol studies", Collection of articles [in Russian] (AN SSSR Press, 1948), Ed. by B. V. Deryagin; Kolloidnyi Zhurnal, 12, 249 (1950); Priroda, 11 (1953); "Silicosis prevention", Collection of articles [in Russian] (1955).
2. B. V. Deryagin and G. Ya. Vlasenko, Author's Certificate No. 39547-1V (1949), Section 1.
3. G. Ya. Vlasenko, B. V. Deryagin, V. V. Churakov, et al., Collection of Reports submitted to the Fifth Interdepartmental Conference [in Russian] (Gidrometeoizdat, 1957), p. 185.
4. F. T. Gucker and C. T. O'Konski, J. Amer. Chem. Soc. 69, 2422, 1947.
5. A. E. Mikirov, Collection of Reports Submitted to the Fifth Interdepartmental Conference [in Russian] (Gidrometeoizdat, 1957), p. 197.
6. A. G. Laktionov, Collection of Reports Submitted to the Fifth Interdepartmental Conference [in Russian] (Gidrometeoizdat, 1957), p. 200.

All abbreviations of periodicals in the above bibliography are letter-by-letter transliterations of the abbreviations as given in the original Russian journal. *Some or all of this periodical literature may well be available in English translation.* A complete list of the cover-to-cover English translations appears at the back of this issue.



IN MEMORY OF SERGEI MIKHAILOVICH LIPATOV

Sergei Mikhailovich Lipatov died January 8, 1961. He was an outstanding scholar and communist who gave all his talent, all his knowledge and powers to the development of science in his native land.

Lipatov was a foremost specialist in the field of colloidal chemistry and the physical chemistry of polymers; he was one of the first in the Soviet Union to work on the investigation of high-molecular compounds, and founded his own scientific school in that area.

He did not tread beaten paths in science; he was an advanced, progressive scholar. The scientific foresight, great talent and erudition of this scholar enabled him to choose the right direction in science and solve important scientific problems. In his fundamental investigations light was thrown on the phenomena of the solvation, swelling and dissolution of polymers, the properties of solutions of polymers, and the phenomena of gelation and syneresis. The principles of the thermochemistry of polymers were laid down by the works of Lipatov; he wrote the only monograph in the Soviet Union on "The physicochemical principles of dyeing" (1929). He was the first in the Soviet Union to write a monograph on the physical chemistry of polymers, in which he emphasized the individuality of polymers and the need for a special approach to the study of these systems ("High-molecular compounds", 1934; "Problems in the study of high polymers", 1941; "High-molecular compounds", 1943).

Lipatov was an eminent organizer; he did a great deal of work in founding laboratories of high-molecular compounds in a number of Institutes of the Union. In particular, he founded the first laboratory of synthetic fibers in the Soviet Union, at the Karpov Scientific-Research Institute, on the basis of which the All-Union Scientific-Research Institute of Synthetic Fibers was afterwards organized.

He was an active participant in a number of scientific conferences on colloidal chemistry, discussions of basic problems of colloidal chemistry and the physical chemistry of polymers. He was a member of the editorial staff of COL from the day it was founded and over a period of many years, and for a number of years was a member of the scientific-technical council of the Ministry of the Food Industry. He carried out great organizational work in the Academy of Sciences of the Belorussian SSR as an Academician and vice-president of that body.

He was a talented teacher, a brilliant lecturer. He devoted thirty years of his working activity to the university. Being an excellent specialist in method, he founded a number of new lecture courses at the University and was the first in the Soviet Union to give a course in high-molecular compounds and the physical chemistry of dyeing.

Lipatov was a thoroughly educated man who imparted his knowledge to youth unstintingly, and youth knew and loved him. He was a man of profound principles in the scientific problems of the Soviet Union. A sympathetic, considerate, unassuming man, he earned the great respect and love of all who knew him closely, worked with him and studied with him. In recent years he was very ill but still did a great deal of work and writing. His premature death prevented him from bringing many of his creative projects to completion.

The image of S. M. Lipatov, a charming man, an eminent scholar, a social worker and a talented teacher, will long remain in the memory of his friends, students and readers.

V. A. Dogadkin, V. A. Kargin,

S. I. Meerson and Z. A. Rogovin

SIGNIFICANCE OF ABBREVIATIONS MOST FREQUENTLY ENCOUNTERED IN SOVIET PERIODICALS

FIAN	Phys. Inst. Acad. Sci. USSR.
GDI	Water Power Inst.
GITI	State Sci.-Tech. Press
GITTL	State Tech. and Theor. Lit. Press
GONTI	State United Sci.-Tech. Press
Gosenergoizdat	State Power Press
Goskhimizdat	State Chem. Press
GOST	All-Union State Standard
GTTI	State Tech. and Theor. Lit. Press
IL	Foreign Lit. Press
ISN (Izd. Sov. Nauk)	Soviet Science Press
Izd. AN SSSR	Acad. Sci. USSR Press
Izd. MGU	Moscow State Univ. Press
LEIIZhT	Leningrad Power Inst. of Railroad Engineering
LET	Leningrad Elec. Engr. School
LETI	Leningrad Electrotechnical Inst.
LETIIZhT	Leningrad Electrical Engineering Research Inst. of Railroad Engr.
Mashgiz	State Sci.-Tech. Press for Machine Construction Lit.
MEP	Ministry of Electrical Industry
MES	Ministry of Electrical Power Plants
MESEP	Ministry of Electrical Power Plants and the Electrical Industry
MGU	Moscow State Univ.
MKhTI	Moscow Inst. Chem. Tech.
MOPI	Moscow Regional Pedagogical Inst.
MSP	Ministry of Industrial Construction
NII ZVUKSZAPIOI	Scientific Research Inst. of Sound Recording
NIKFI	Sci. Inst. of Modern Motion Picture Photography
ONTI	United Sci.-Tech. Press
OTI	Division of Technical Information
OTN	Div. Tech. Sci.
Stroiizdat	Construction Press
TOE	Association of Power Engineers
TsKTI	Central Research Inst. for Boilers and Turbines
TsNIEL	Central Scientific Research Elec. Engr. Lab.
TsNIEL-MES	Central Scientific Research Elec. Engr. Lab.—Ministry of Electric Power Plants
TsVTI	Central Office of Economic Information
UF	Ural Branch
VIESKh	All-Union Inst. of Rural Elec. Power Stations
VNIIM	All-Union Scientific Research Inst. of Metrology
VNIIZhDT	All-Union Scientific Research Inst. of Railroad Engineering
VTI	All-Union Thermotech. Inst.
VZEI	All-Union Power Correspondence Inst.

Note: Abbreviations not on this list and not explained in the translation have been transliterated, no further information about their significance being available to us. — Publisher.

Soviet Journals Available in Cover-to-Cover Translation

ABBREVIATION	RUSSIAN TITLE	TITLE OF TRANSLATION	PUBLISHER	TRANSLATION BEGAN Vol.	Issue	Year
AÉ	Atomnaya énergiya	Soviet Journal of Atomic Energy	Consultants Bureau	1	1	1956
Akust. zh.	Akusticheskii zhurnal	Soviet Physics – Acoustics	American Institute of Physics	1	1	1955
	Antibiotiki	Antibiotics	Consultants Bureau	4	1	1959
Astr(on). zh(urn).	Astronomicheskii zhurnal	Soviet Astronomy–AJ	American Institute of Physics	34	1	1957
Avto(mat). svarka	Avtomaticheskaya svarka	Automatic Welding	British Welding Research Association (London)		1	1959
	Avtomatika i Telemekhanika	Automation and Remote Control	Instrument Society of America	27	1	1956
	Biofizika	Biophysics	National Institutes of Health*		1	1957
	Biokhimiya	Biochemistry	Consultants Bureau	21	1	1956
Byull. éksp(erim). biol. i med.	Byulleten' éksperimental'noi biologii i meditsiny	Bulletin of Experimental Biology and Medicine	Consultants Bureau	41	1	1959
DAN (SSSR) / Dokl(ady) AN SSSR	Doklady Akademii Nauk SSSR	The translation of this journal is published in sections, as follows:				
		Life Sciences: Doklady Biochemistry Section	American Institute of Biological Sciences	106	1	1956
		Life Sciences: Doklady Biological Sciences Sections (Includes: Anatomy, biophysics, cytology, ecology, embryology, endocrinology, evolutionary morphology, genetics, histology, hydrobiology microbiology, morphology, parasitology, physiology, zoology sections)	American Institute of Biological Sciences	112	1	1957
		Life Sciences: Doklady Botanical Sciences Sections (Includes: Botany, phytopathology, plant anatomy, plant ecology, plant embryology, plant physiology, plant morphology sections)	American Institute of Biological Sciences	112	1	1957
		Chemical Sciences: Proceedings of the Academy of Sciences of the USSR, Section: Chemical Technology	Consultants Bureau	106	1	1956
		Chemical Sciences: Proceedings of the Academy of Sciences of the USSR, Section: Chemistry	Consultants Bureau	106	1	1956
		Chemical Sciences: Proceedings of the Academy of Sciences of the USSR, Section: Physical Chemistry	Consultants Bureau	112	1	1957
		Earth Sciences: Doklady Earth Sciences Sections (Includes: Geochemistry, geology, geophysics, hydrogeology, mineralogy, paleontology, petrography, permafrost sections)	American Geological Institute	124	1	1959
		Earth Sciences: Proceedings of the Academy of Sciences of the USSR, Section: Geochemistry	Consultants Bureau	106-123	1 6	1957-1958
		Earth Sciences: Proceedings of the Academy of Sciences of the USSR, Sections: Geology	Consultants Bureau	106-123	1 6	1957-1958
		Mathematics: Doklady Soviet Mathematics	The American Mathematics Society	131	1	1961
		Physics: Soviet Physics–Doklady (Includes: Aerodynamics, astronomy, crystallography, cybernetics and control theory, electrical engineering, energetics, fluid mechanics, heat engineering, hydraulics, mathematical physics, mechanics, physics, technical physics, theory of elasticity sections)	American Institute of Physics	106	1	1956
		Physics: Proceedings of the Academy of Sciences of the USSR, Applied Physics Sections (does not include mathematical physics or physics sections)	Consultants Bureau	106-117	1	1956-1957
Derevoobrabat. prom-st'.	Derevoobrabatyvayushchaya promyshlennost'	Wood Processing Industry	Timber Development Association (London)		9	1959
	Élecktrosvyaz	Telecommunications	Massachusetts Institute of Technology*		1	1957
Éntom(ol). oboz(renie)	Éntomologicheskoe obozrenie	Entomological Review	American Institute of Biological Sciences	38	1	1959
Farmakol. (i) toksikol(ogiya)	Farmakologiya i toksikologiya	Pharmacology and Toxicology	Consultants Bureau	20	1	1957
FMM	Fizika metallov i metallovedenie	Physics of Metals and Metallography	Acta Metallurgica*	5	1	1957
Fiziol. zhurn. SSSR (im. Sechenova)	Fiziologicheskii zhurnal im. I. M. Sechenova	Sechenov Physiological Journal USSR	National Institutes of Health*		1	1957
Fiziol(ogiya) rast.	Fiziologiya rastenii	Plant Physiology	American Institute of Biological Sciences	4	1	1957
	Geokhimiya	Geochemistry	The Geochemical Society		1	1958
FTT	Fizika tverdogo tela	Soviet Physics–Solid State	American Institute of Physics	1	1	1959
Izmerit. tekh(nika)	Izmeritel'naya tekhnika	Measurement Techniques	Instrument Society of America		1	1959
Izv. AN SSSR, O(td). Kh(im). N(auk)	Izvestiya Akademii Nauk SSSR: Otdelenie khimicheskikh nauk	Bulletin of the Academy of Sciences of the USSR: Division of Chemical Sciences	Consultants Bureau		1	1952

ADSORPTION ISOTHERMS AND HEATS OF ADSORPTION OF PROPYLENE ON SILICA GEL

A. G. Bezus, V. P. Dreving and A. L. Klyachko-Gurvich

Chemistry Department, M. V. Lomonosov, Moscow University
Translated from Kolloidnyi Zhurnal, Vol. 23, No. 3, pp. 241-247, May-June, 1961
Original article submitted March 29, 1960

Previous work done in our laboratory was devoted to the investigation of the adsorption and the determination of the heat of adsorption of n-alkanes from n-pentane to n-octane [1-7] and of benzene [1,4,6,7] on silica gel. It seemed important that the study be extended to smaller hydrocarbons, particularly the unsaturated ones, the adsorption of which should depend on the degree of hydration of the silica gel surface. The present work represents the first stage of this study.

The investigation of the adsorption of the lower hydrocarbons presents certain difficulties due to the high vapor pressure of these compounds at ordinary temperatures. In order to obtain complete adsorption isotherms one has to either use equipment capable of withstanding high pressures or work at very low temperatures [8]. The chemical literature contains very little data on the adsorption of lower hydrocarbons [9-12].

The adsorption isotherms of propane and propylene on pure and palladium-coated silica gels have been determined for the temperature range from -25 to +35°; on both adsorbents propylene had a higher heat of adsorption than did propane. The adsorption of many other hydrocarbons on silica gel has also been investigated [14]. The heat of adsorption of propylene on silica gel at 0°C has been measured calorimetrically [15], but at this temperature a pressure of 1 atm corresponds to a partial pressure of propylene of approximately 0.1, which means that the adsorbate had not even formed a unimolecular layer (this we will prove below).

Lower hydrocarbons had also been used for the determination of pore dimensions in adsorbents [9,16].

Frequently it is impossible to correlate the results reported by various workers due to the fact that various types of silica gel were used and no attempt was made to standardize the structural characteristics of the investigated adsorbents. In few instances the study of hydrocarbon adsorption was accompanied by a determination of the adsorbent structure using low-temperature adsorption isotherms of nitrogen [9, 10,17]. The work published so far fails to provide even a crude estimate of the interaction energy between lower hydrocarbons and the silica gel surface during the formation of a unimolecular layer. We have therefore selected (same as before [1-3, 5,7]) a silica gel with fairly homogeneous large pores (KSK-2) in order to eliminate any effects of pore-constriction on the shape of the purely adsorptional portion of the isotherms. After determining the adsorption isotherms of propylene on this silica gel at -35, -45, and -55°C and constructing the corresponding isosters we determined the differential heat and entropy of adsorption of propylene.

The adsorption apparatus (Fig. 1) consisted of two identical measuring sections which were mirror images of each other (only the left side is described). The section inclosed within the dashed rectangle was thermostated. Glass tube 1 containing a weighted sample of the adsorbent was lowered into the cool shell of a cryostat [18]; the temperature in the cryostat was maintained constant to within ±0.3°. The investigated vapor was stored in cylinder 7 whence it was passed into bulb 5, where vapor samples were prepared for successive introduction into glass tube 1. A U-shaped mercury manometer 4, a McLead gauge 2, and a bulb 3 which could be filled with mercury from a reservoir at the bottom were all connected to bulb 5. When the mercury level is lowered the volume of bulb 3 is added to that of the preparatory section of bulb 5. The volume of the preparatory section and the volume of the extra space in the glass tube containing the adsorbent were calibrated with helium, which was stored in cylinder 9.

In order to keep grease away from the working part of the apparatus the stopcocks surrounding it were replaced by magnetic values, 6a and 6b [19]. Mercury was kept out of the glass tube by means of a trap 11 filled with strips of gold foil. The mercury level in the U-shaped manometers were regulated by means of a siphon 13. The vacuum jacket 12 provided thermal insulation for portions of the capillary tube outside the thermostat.

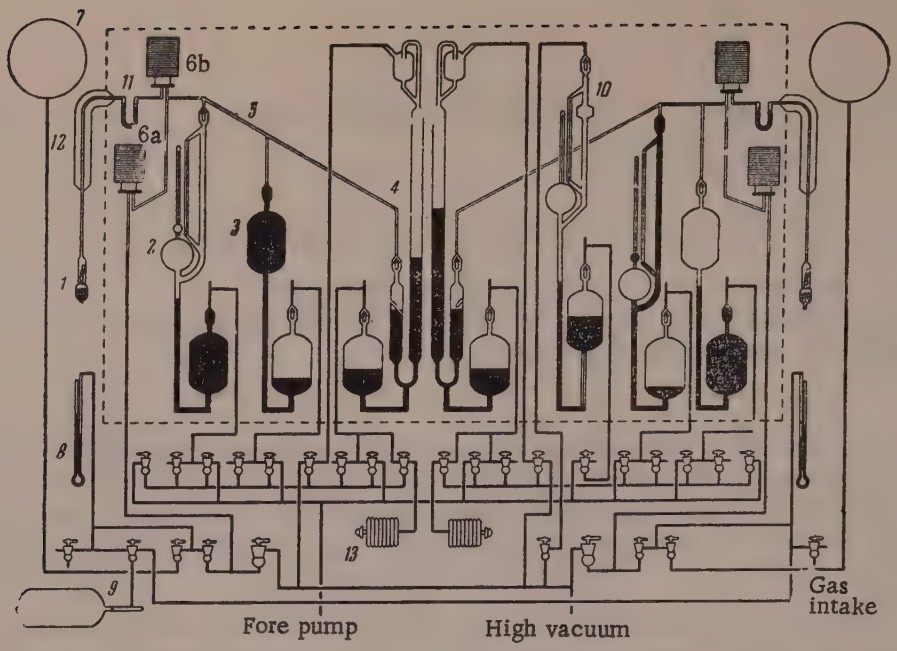


Fig. 1. Adsorption apparatus.

Propylene was prepared by the catalytic dehydration of isopropyl alcohol (b.p. 81-82° at 740 mm; $n_D^{20} = 1.3780$; $d_4^{20} = 0.7895$) over aluminum oxide. The olefins constituted 98% of the hydrocarbon mixtures. The propylene was further purified by passage through a -40° trap, in which less volatile impurities were retained, and condensation in a liquid nitrogen trap, from which more volatile components were removed by pumping at high vacuum.

Propane was synthesized, and it was purified by fractional condensation in the same way as propylene.

Adsorbent. The silica gel used in our work had a specific surface of 330 m^2/g (the surface was determined by the BET method from the adsorption isotherm of nitrogen); the median pore diameter (at the mouth) was 105A; the total pore volume was 0.93 cm^3 [20]. Weighed samples of silica gel were degassed by pumping at 200° and the true weight of samples at the start of the experiment was determined from the weight loss of a control sample.

We determined the adsorption isotherms of propylene on silica gel at -35, -45, and -55° up to a relative pressure of $p/p_s = 0.5$ and an approximate adsorption isotherm of propane at -45° (Figs. 2 and 3).

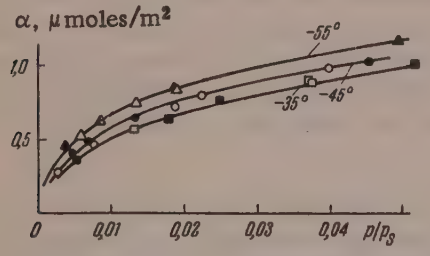


Fig. 2. Adsorption isotherms of propylene on silica gel (here and in the future the solid markings represent desorption).

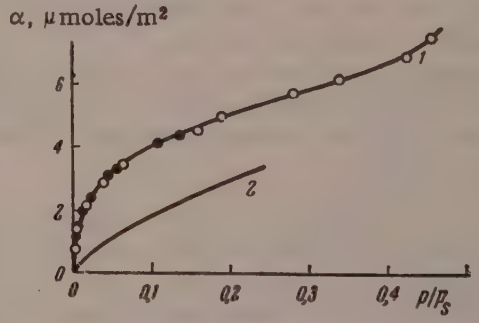


Fig. 3. The adsorption isotherms of propylene (1) and propane (2) on silica gel at -45°C.

The lower the temperature the sharper the initial rise on the adsorption isotherms of propylene. The adsorption isotherm of propane lies much lower than that of propylene, since the silica gel surface containing polar OH-groups interacts much more strongly with unsaturated propylene molecules. For the same reason benzene is more strongly adsorbed on silica gel than is hexane [2].

In the range of relative pressures from 0.01 to 0.23-0.35 the adsorption isotherms of propylene on silica gel (Fig. 2) yield nice straight lines when plotted in BET coordinates (Fig. 4). The slight dip in the initial portion of the isotherms plotted in BET units indicates that the first few aliquots of propylene interact very strongly with the adsorbent as they become adsorbed on the most active portions of the inhomogeneous surface of silica gel.

We have tabulated in the Table the constants C of the BET equation, which represent the amount of adsorbed material in a complete unimolecular layer (a_m), and the area occupied by each adsorbed molecule (ω_m); in addition we have also included the area per propylene molecule calculated from bond lengths and Van der Waals atomic radii.

The Values of C, a_m, and ω_m Determined From the BET Equation and ω_m Calculated From Van der Waals Radii for the Adsorption of Propylene on Silica Gel

Temperature, °C	−35	−45	−55
The BET constant, C	39	46	65
Size of the unimolecular layer a_m in mmoles/g	1.42	1.41	1.41
ω_m calculated from BET, A^2	38.5	39.0	39.0
ω_m calculated from Van der Waals Radii, A^2	27	27	27

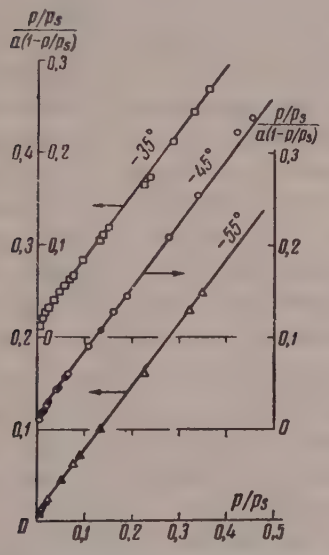


Fig. 4. The adsorption isotherms of propylene on silica gel in BET coordinates.

The constant C in the BET equation increases at lower temperatues since it represents the equilibrium between the adsorbent and adsorbate. The contour area of a propylene molecule calculated from Van der Waals radii [21] is $27A^2$. Since it is not easy to define precisely the shape of an adsorbed molecule the adsorber area per propylene molecule can not be less than $30A^2$ even under conditions of closest packing. The ω_m determined from the BET equation is $39A^2$. The difference may be attributed to the fact that the BET approximation does not hold too well on an inhomogeneous surface such as that of our silica gel. Also if we compare this area with the area per hydroxyl group on the silica gel surface ($\sim 13A^2$ on KSK-2 [22]) it is apparent that a propylene molecule requires more room than that occupied by two hydroxyls. The BET value of $\omega_x = 39A^2$ is three times as large as $\omega_m = 13A^2$. This would suggest that at the given content of structural water a propylene molecule bonded to one hydroxyl can screen two other hydroxyls. Hence the packing of propylene molecules may be related to the structure of the hydroxyl layer on the silica gel surface. In addition ω_m may also depend on the mobility of adsorbate molecules on the adsorber surface.

Using the experimentally determined isotherms we constructed the corresponding isosters from which the differential heats of adsorption of propylene on silica gel were computed. In Fig. 5 we have plotted these differential heats of adsorption as a function of surface coverage θ. As one would expect from the chemical and geometrical surface inhomogeneity the heat of adsorption of propylene on silica gel declines steadily as the area of the unimolecular layer increases. When $\theta = 1$ the curve exhibits no sharp break as in the case of hydrocarbon adsorption on graphitized carbon black [23], which has a highly homogeneous surface. In our case the curve continues to decline smoothly approaching the condensation heat. This indicates two things: first, that the surface of silica gel is not homogeneous; second, that the formation of the first layer is accompanied by a simultaneous deposition of another layer.

The standard (at $\theta = 0.5$) heat of adsorption of propylene on silica gel is 7.4 kcal/mole (Fig. 5). We have also calculated the approximate heat of adsorption of propane by using an additive formula derived for the adsorption of hydrocarbons on coarsely porous silica gels (the heat of adsorption of normal hydrocarbons was found to be a linear function of the number of carbon atoms in the chain [5]),

$$Q_a^0 = 1{,}0 + 1{,}3n. \qquad (1)$$

For propane the formula yields $Q_a^0 = 5.0$ kcal/mole. Hence the standard differential heat of adsorption of propylene on the hydrated surface of silica gel exceeds that of propane by about 2.5 kcal/mole.

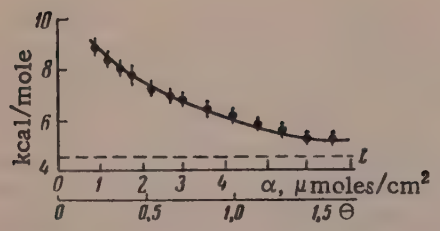


Fig. 5. The differential heat of adsorption of propylene on silica gel as a function of surface coverage θ; L is the heat of condensation (the vertical lines through the dots represent probable errors in the calculated isotherms).

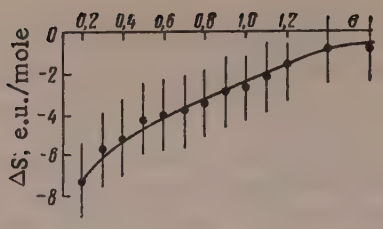


Fig. 6. The differential entropy of adsorption of propylene as a function of surface coverage (the zero line represents the entropy of liquid propylene. The vertical lines represent probable errors in calculations).

To see how much the cohesive forces in adsorbed propylene differ from the intermolecular bonding in liquid propylene we studied the change in the differential entropy of adsorption (ΔS) as a function of θ as one proceeds from the liquid to the adsorbed state (Fig. 6). As in the case of benzene on silica gel [8] the entire entropy curve lies below the zero line indicating that intermolecular attraction in the first layer of adsorbed propylene is stronger than it is in the liquid state, but as more material is adsorbed the state of the adsorbed material approaches that of pure liquid.

The difference between the standard heats of adsorption of propylene and propane on silica gel (the former being greater by about 2.4 kcal/mole) can be attributed primarily to the possibility of an interaction between the π-electrons of the double bond in propylene and the hydroxyls on the silica gel surface. Complex molecular orbital calculations are required to get the total energy of such an interaction [24]. However, one can get an approximate value for the coulombic component of this interaction by evaluating the interaction of the hydroxyl dipole with the quadrupoles formed by the π-electrons in the double bond and the residual charge on the two carbons flanking the double bond. Since the actual electron density distribution in not known, as a rough approximation we will assume. (see [6]) that the maximum π-electron charge density is at 0.81A from the carbon atoms, and we will disregard the overlap between π-electron clouds. The energy of this coulombic interaction can be determined approximately by using a scheme (Fig. 7) similar to that used before [6] for estimating the same interaction between hydroxyls and benzene, except that in the case of benzene π-π overlap was taken into account. We have computed the interaction energy between the two quadrupoles on the propylene and the hydroxyl dipole on the surface for two possible orientations of the double bond relative to the hydroxyl group: A) the OH-group is located right below one of the carbon atoms, B) it is located below the midpoint between the two carbon atoms forming the double bond.

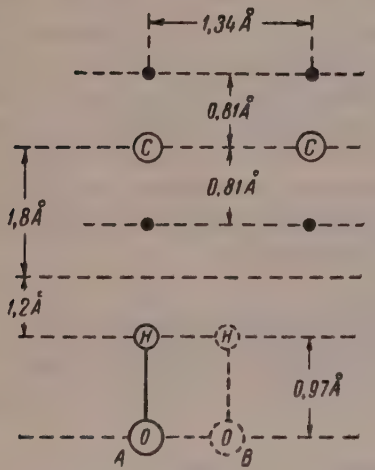


Fig. 7. A schematic diagram showing the relative positions of the olefinic C=C-group and the OH-group on the silica gel surface. A) One carbon above the hydroxyl; B) the midpoint between the carbon atoms lies above the hydroxyl group.

The hydroxyl dipole moment was taken as 1.6D [6]; the Van der Waals width of the propylene molecule at the center of the double bond is 3.6A [25]. The distance between the carbon atom and the hydroxyl hydrogen in position (A) is taken as the sum of half the Van der Waals width of the propylene molecule and the Van der Waals radius of hydrogen, 1.2A [6]. The O—H bond in SiOH is 0.97A long [18]. The C—C bond in propylene is 1.34A [24]. The distance from the line joining the two carbons to the center of gravity of the π-electron charge cloud is taken to be 0.81A [6]. We calculated the energy for interactions involving all the quadrupole charges and the O—H dipole charges using the equation

$$E = \int_{\infty}^{r_0} f\, dr, \qquad (2)$$

where r_0 is the equilibrium distance between the interacting charges e_1 and e_2, and $f = e_1 e_2 / r^2$. The evaluated integrals were added up. As we had already mentioned before, exchange between the π-electrons of the two carbons in C=C was neglected entirely.

Position (A) yielded 2.45 kcal/mole, while position (B) yielded 2.3 kcal/mole, or in other words there was very little difference between the two positions. Both of these values, however, are very close to the difference between the standard heats of adsorption of propylene and propane on silica gel (2.4 kcal/mole). One should not attach too much significance to this close agreement, since the true interaction between propylene and the hydroxyls on the silica gel surface is much more complex. Nevertheless the fact that the calculated interaction energy is very close to the difference between the adsorption heats of propane and propylene would support our contention that the difference is indeed due to an additional (in addition to the Van der Waals interaction) interaction between the π-electrons of the propylene and dipoles on the surface, which accounts for the stronger adsorption of propylene.

SUMMARY

1. We have determined the adsorption isotherms of propylene on coarsely porous silica gel at -35, -45, and -55°C.

2. From the isosters constructed from the adsorption isotherms we computed the differential heats of adsorption of propylene on coarsely porous silica gel at surface coverages close to the unimolecular layer. The curve of differential heat of adsorption versus surface coverage indicates that the surface is very inhomogeneous.

3. The plot of the change in differential entropy of adsorption of propylene determined from the experimental isotherms and from the calculated differential adsorption heats shows that the molecules in the first adsorbed layer of propylene are more strongly bound than in the pure liquid state. As the first and subsequent layers fill up the entropy of adsorbed propylene approaches that of liquid propylene.

4. Determination of the coulombic interaction between an isolated hydroxyl dipole and the isolated quadrupoles of the double bond yielded an energy close to the experimentally determined difference between the heats of adsorption of propylene and propane on silica gel. This provides new evidence for the interaction between hydroxyls on the surface and the π-electrons of a double bond whenever unsaturated hydrocarbons are adsorbed on hydrated surfaces.

The authors wish to express their gratitutde to A. V. Kiselev for his continuous interest in this work, for the numerous suggestions, and for the discussion of results.

LITERATURE CITED

1. A. V. Kiselev, Uspekhi Khim. 25, 705 (1956).
2. A. V. Kiselev and A. A. Isirikyan, Doklady Akad. Nauk SSSR 115, 343 (1957); Zhur. Fiz. Khim. 31, 2127 (1957).
3. A. A. Isirikyan and A. V. Kiselev, Zhur. Fiz. Khim. 32, 679 (1958).
4. A. V. Kiselev, Vestnik Akad. Nauk SSSR No. 10, 43 (1957).
5. A. V. Kiselev, A. A. Isirikyan and B. A. Frolov, Zhur. Fiz. Khim. 33, 389 (1959).
6. A. V. Kiselev and D. P. Poshkus, Doklady Akad. Nauk SSSR 120, 835 (1958).
7. L. D. Belyakova and A. V. Kiselev, Coll. Preparation, Structure, and Properties of Adsorbents [in Russian], Trans. Scientific Technical Conference, 1957, (Goskhimizdat, 1959), p. 130; Doklady Akad. Nauk SSSR 119, 298 (1958).
8. A. V. Kiselev, F. Z. Sabirov, I. L. Étinger, and M. F. Yanovskaya, Doklady Akad. Nauk SSSR 111, 129 (1956).
9. W. T. Granquist, F. R. Metch and C. H. Edwards, Industr. and Engng. Chem. 46, 358 (1954).
10. W. T. Granquist, and R. C. Amero, J. Amer. Chem. Soc. 70, 3265 (1948).
11. H. D. Schreiber, R. Mac-Intosh, Canad. J. Chem. 33, 259 (1955).
12. H. D. Schreiber and R. Mac-Intosh, ibid, 32, 842, (1954).
13. L. N. Reyerson and R. M. Cines, J. Phys. Chem. 46, 1060 (1942).
14. W. K. Lewis, E. R. Gilliland, B. Chertow and W. H. Hoffman, J. Amer. Chem. Soc. 72, 1153, 1950; W. K. Lewis, E. R. Gilliland, B. Chertow, and W. Milliken ibid, p. 1158; W. K. Lewis, E. R. Gilliland, W. Chertow and D. Baries, ibid, p. 1160; W. K. Lewis, E. R. Gilliland, B. Chertow, and W. P. Cadogan, Industr. and Engng. Chem. 42, 1312, 1326 (1950); L. N. Reyerson, and L. E. Swearingen, J. Phys. Chem. 31, 88 (1927); W. Kälberer, and C. Schuster, Z. Phys. Chem. A—141, 270 (1929).
15. W. R. Smith and R. A. Beebe, Industr. and Engng. Chem. 41, 1431 (1949).
16. R. N. Barrer and D. A. Ibbitson, Trans. Faraday Soc. 40, 195, 263 (1944); N. V. Kel'tsev, and A. L. Khalif, Trudy Vsesoyuz. Neftyanogo Nauchno Isledovatelnogo Instituta, 5, 208 (1954).
17. P. H. Emmett and T. W. De-Witt, J. Amer. Chem. Soc. 65, 1253 (1943); R. T. Davies, T. W. De-Witt, ibid. 70, 1135 (1948).
18. G. G. Muttik, Zavodskaya Laboratoriya 17, 1403 (1951).

19. A. V. Kiselev and G. G. Muttik, Kolloid. Zhur. 19, 562 (1957).
20. L. D. Belyakova, O. M. Dzhigit, and A. V. Kiselev, Zhur. Fiz. Khim. 31, 1577 (1957).
21. A. I. Kitaigorodskii, Organic Crystallography [in Russian] Izd AN SSSR (1955); Pauling, The Nature of the Chemical Bond [Russian translation], Goskhimizadat (Moscow - Leningrad, 1947).
22. L. D. Belyakova, Dissertation: Physical and Chemical Adsorption of Various Compounds on Silica Gels with Different Degrees of Surface Hydration [in Russian] (Moscow, 1959).
23. N. N. Avgul', G. I. Berezin, A. V. Kiselev, and I. A. Lygina, Izvest. Akad. Nauk SSSR, Otdel Khim. Nauk, 1957, No. 9, 1021.
24. A. V. Kiselev, Ya. Koutetskii, and I. Chizhek, Doklady Akad. Nauk SSSR, 137, 638 (1961).
25. M. V. Vol'kenshtein, The Structure and Physical Properties of Molecules [in Russian] (Izd AN SSSR, 1958), pp. 127, 129.

All abbreviations of periodicals in the above bibliography are letter-by-letter transliterations of the abbreviations as given in the original Russian journal. *Some or all of this periodical literature may well be available in English translation.* A complete list of the cover-to-cover English translations appears at the back of this issue.

EFFECT OF VAPOR-PHASE FORMING AGENTS ON POROUS STRUCTURE AND SORPTIVE PROPERTIES OF THE SURFACE OF SILICA GELS

Z. Z. Vysotskii, L. F. Divnich, and M. V. Polyakov

L. V. Pisarzhevskii Institute of Physical Chemistry, Academy of Sciences, UkrSSR

Translated from Kolloidnyi Zhurnal Vol. 23, No. 3, pp. 248-254, May-June, 1961
Original article submitted June 29, 1959

A review [1] has been made of work devoted to the problem of specific adsorption. Recently, new results have been obtained which indicate the possibility of preparing stereoselective adsorbents, formed in the presence of organic bases of the pyridine series [2] or of living microorganisms [3]. Results were obtained in [4] which gave evidence that when silicic acid xerogels are formed by dehydration in an atmosphere of vapors of organic forming agents, the final porous structure of the xerogel is influenced by the chemical nature of the forming agent. In the present communication new experimental data are presented, permitting a closer approach to an explanation of the mechanism of the formation of micro-relief [micro-topography] and the sorptive properties of the surface of xerogels.

Method of Investigation. Toluene vapor sorption isotherms were measured at 20° in a vacuum unit with a quartz spring balance on samples of silica gels [4] formed in vapors of benzene, toluene, o-xylene, dioxane, isopropanol, and methanol, and on the corresponding control samples. Also, benzene vapor sorption isotherms were taken on the methanol, dioxane, and isopropanol gels. As in previous work [4], evacuation of the samples were taken immediately after measuring the benzene vapor sorption isotherms. The magnitudes (S) of the specific surface areas of the samples studied were calculated from the benzene adsorption isotherms by the BET method (the area occupied per benzene molecule was taken equal to $32A^2$).

The most probable pore radii of the silica gels were determined on the basis of the desorption branches of the toluene sorption isotherms.

On the benzene, toluene, and xylene gels kept both in the a desiccator in an atmosphere of forming-agent vapors and in air in test tubes, isotherms were taken for methyl orange adsorption from a 5% (aqueous) acetic acid solution. The methyl orange concentrations were measured on an SF-5 spectrophotometer. The conditions of the adsorption experiments were analogous to those used in [5,6]. The methyl orange adsorption kinetics were also measured on the toluene and control silica gels.

The relative position of the toluene vapor adsorption isotherms on the benzene, toluene, and xylene gels (Fig. 1) is the same as in the case of benzene sorption isotherms on these same samples [4]. At low p/p_s the isotherm of the benzene sample [the benzene-formed silica gel] lies below the other curves, but in the region corresponding to capillary condensation it rises far above the other two curves. The desorption branch in the case of the benzene sample corresponds to a higher p/p_s, which indicates that the pore radius for this sample is larger than for the toluene and xylene gels (table).

Figure 2 shows the adsorption isotherms for vapors of benzene (from [4]) and toluene on the same samples of benzene gel, plotted on the same scale. The initial adsorption isotherm of the toluene vapors was obtained immediately after outgassing the sample which had been used previously to measure the adsorption of benzene. From Fig. 2 it follows that at low p/p_s the repeat toluene adsorption isotherm lies above the benzene adsorption isotherm. At the same time, the initial curve for toluene is located much lower than either of these isotherms.

The relative position of the sorption isotherms of vapors of toluene (initial and repeat) and benzene on the dioxane, isopropanol, methanol, and control gels is the same as for the benzene sample in Fig. 2.

The adsorption isotherms of methyl orange on the gels formed in vapors of benzene, toluene, and o-xylene are shown in Fig. 3. The adsorption values are referred to 1 m^2 surface of each sample. Curves of the kinetics of adsorption of methyl orange are presented in Fig. 4 for the toluene and control samples.

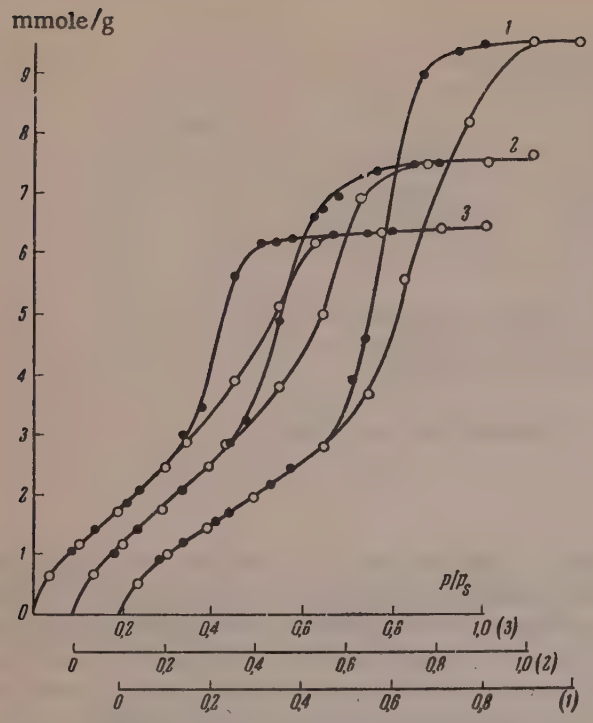


Fig. 1. Toluene vapor sorption isotherms at 20° on benzene (1), toluene (2), and o-xylene (3) gels (here and henceforth, the solid points represent desorption).

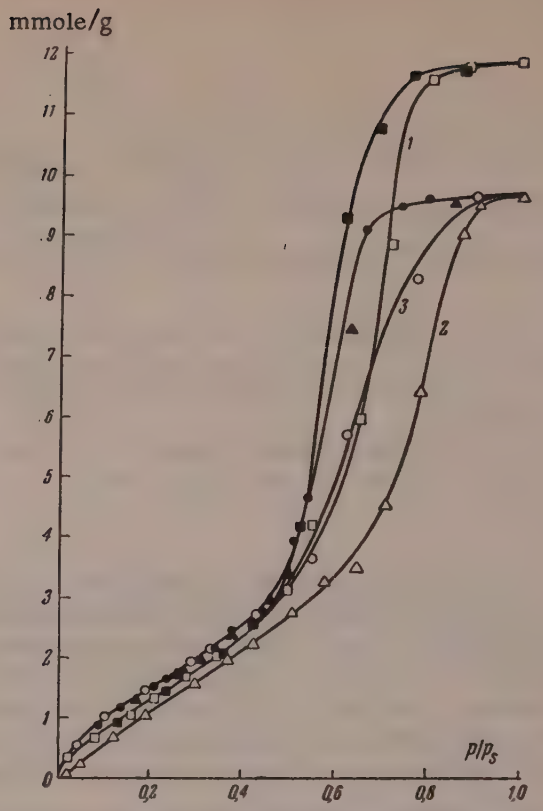


Fig. 2. Sorption isotherms of vapors of benzene (1) and toluene (2-initial, 3-repeat) on benzene gel.

Structural-Sorptive Characteristics of Gels Investigated

Gel	Saturated sorption volume based on adsorption isotherm cm^3/g		Radius of predominant pores, based on desorption isotherm, A		Specific surface area based on benzene adsorption isotherms by the BET method m^2/g
	benzene	toluene	benzene	toluene	
Benzene	1.04	1.03	40	46	340
Toluene	0.83	0.82	30	30	445
o-Xylene	0.70	0.71	25	27	445
Dioxane	0.69	0.69	20	18	685
Isopropanol	0.80	0.80	28	29	540
Methanol	0.70	0.69	18	18	680
Control (dehydrated in air)	0.24	0.24	10	10	—

Figure 5 shows sorption isotherms of benzene vapors on the methanol, dioxane, and isopropanol silica gels. A comparison of the isotherms and the data of the table shows that the porous structure of the methanol and dioxane gels are almost identical, but the isopropanol sample is larger-pored and has a smaller specific surface area.

The results cited (table and Figs. 1-2) confirm the information obtained previously on the porous structure of the gels studied and the conclusions as to the regular changes of the porous structure of the gels with the use of a homologous series of forming agents. These results also allow us at once to draw certain preliminary conclusions on the influence of the forming agents on the structure of the surface of the gels formed. In this connection, special attention should be directed to: 1) the coincidence of the initial adsorption and desorption branches of the benzene vapor sorption isotherm in the region of low p/p_s for all samples, and the noncoincidence of the corresponding branches of the isotherms in the case of toluene adsorption; 2) the increased adsorption of toluene in comparison with benzene on the reversible s section of the isotherm with a variation of p/p_s from 0 to 0.5; 3) the significant change of specific surface of the gels formed in relation to the chemical nature of the forming agent used; 4) the isotherms and kinetics of adsorption of methyl orange.

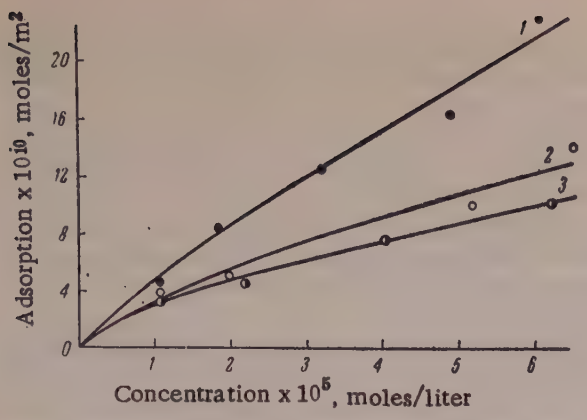


Fig. 3. Adsorption isotherms of methyl orange on benzene (1), toluene (2), and o-xylene (3) gels, kept in an atmosphere of vapors of the forming agents.

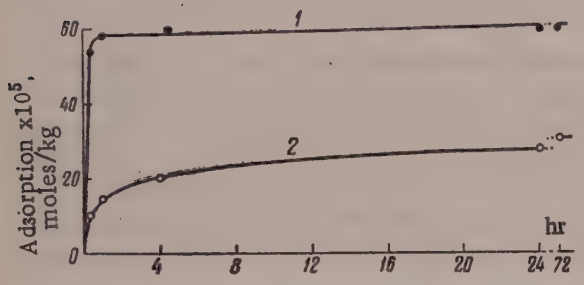


Fig. 4. Kinetics of adsorption of methyl orange on toluene (1) and control (2) gels. Dye concentration $4.5 \cdot 10^{-5}$ mole/liter.

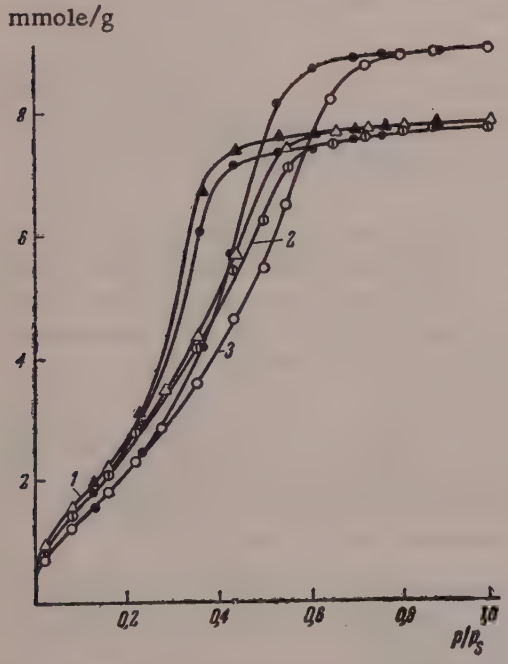


Fig. 5. Sorption isotherms of benzene vapors at 20° on methanol (1), dioxane (2), and isopropanol (3) gels.

The first of these facts can be explained if we adopt a previously advanced hypothesis [4] on the change of the relative position of labile surface groups, for example, hydroxyls, under the influence of the orienting action of the adsorbate molecules which will be the greater for more polar adsorbate molecules [7-9]. In our case one can expect that the nonpolar molecules of benzene will interact with the surface hydroxyls of silica gel more weakly than the polar molecules of toluene. It is possible that this is also the precise explanation for the coincidence of the adsorption and desorption branches of the isotherm on a gel not flushed with benzene vapors.

In the measurement of the adsorption of toluene (Fig. 2), which was conducted following the measurement of a benzene adsorption isotherm, the initial desorption branch of the isotherm goes far above the initial adsorption curve in the entire interval of p/p_s. The repeat adsorption branch at low p/p_s falls exactly on the first desorption curve, but in the region of capillary condensation a reproducible hysteresis loop is observed. Usually a noncoincidence of the adsorption and desorption branches of the initial isotherm is explained by insufficient sample outgassing.

We are not inclined to attach such a great significance to the slightest traces of nonevacuated foreign matter, and consider it possible to explain the results we obtained by the stronger adsorptive interaction of the polar molecules of toluene (compared to benzene) with the surface hydroxyls of the silica gel, and by reorientation of the hydroxyls. It is possible that the basic process here is a decrease of the number of hydrogen bonds between neighboring surface hydroxyls, releasing hydroxyls for subsequent participation in the adsorption of molecules from the vapor phase. Such a reorientation of the gel surface is hampered by the marked rigidity of the surface structure of a xerogel. This apparently explains also the low values of adsorption in the first experiment. With an increasing coverage of the gel by toluene, and especially after toluene condensation in the silica gel pores, the "release" and change of the relative position of the surface hydroxyls should be facilitated. By the moment of filling the entire sorption space by toluene, such reorientation of the gel surface is completed, and the desorption branch at low p/p_s will represent the equilibrium which is also observed on toluene adsorption isotherms. The irreversibility which was observed [10] in the region of monolayer formation in the adsorption of triethylamine on silica gels possibly is also explained by the proposed mechanism of reorientation of the surface layer of adsorbent under the influence of the adsorbate.

The increased adsorption of toluene in comparison with benzene in the region of mono- and polymolecular adsorption (Fig. 2) also can be explained by the stronger interaction of the the adsorbate and adsorbent in the case of toluene adsorption, in comparison with the nonpolar benzene.

The substantial influence of the nature of the vapor-phase forming agent on the S of the gel which is formed (table)

can be explained by the influence of the chemical interaction between the molecules of the forming agent and the surface groups of the hydrogel elementary particles, as it affects the structure of the xerogel surface and its porous structure.

From the table it is evident that the lowest specific surface area (S) corresponds to the gel formed in an atmosphere of the nonpolar benzene, which is less water-soluble than the other forming agents and apparently is weaker than the other forming agents in interacting with the particles of the silicic acid in the hydrogel. In the case of polar molecules of toluene, o-xylene, and isopropanol, S increases. Methanol and dioxane, which are closer to water in their properties than are the other forming agents, form gels with maximum S.

The magnitude of S is directly connected with the dimensions of the elementary particles making up the skeleton of the xerogel. Hence it follows that in our case the weak interaction of the benzene with the silicic acid particles in the hydrogel leads to a certain enlargement of these particles. The more strongly the molecules of other forming agents are bonded with the silicic acid particles, the less these particles will be aggregated in the process of curing the gels and forming their structure, and the greater the S which will be shown by the corresponding xerogels. Thus, the forming agents in question, interacting chemically with the silicic acid particles, apparently exert first of all a direct influence on the size of the elementary particles forming the framework of the gel. However, the influence of the forming agent on the porous structure of the xerogel is not limited only to this, since the forming agent in the later stages of the forming, being in the pores of the gel in the condensed state, also exerts a direct influence on the magnitude of the capillary forces (through the wettability of the skeleton, radius of the "pores" of the gel, etc.).

In connection with the above discussion, there is certain interest in the work of [5], in which by the use of extremely active forming-dyeing agents of the methyl orange series specific silica gels were obtained having S $\approx$ 1000 m^2/g. If the results cited on the significant influence of the nature of the forming agent on S are taken into account, then the magnitude of S found in [5], which seems amazing at first glance, acquires a more real basis. Furthermore, if in subsequent investigations it is confirmed that the more active forming agents, imparting marked specific properties to the gel surface, always lead to an increase of S, than it is probable that the ability of a forming agent to increase the surface of the gel may be taken as a criterion of its activity.

In contrast to the sorption of vapors, the adsorption of a dye from an aqueous acetic acid solution takes place in a monolayer, so that the structural features of gel surfaces are manifested more readily. Therefore, in our opinion, the most important result giving evidence in favor of the concept of a differing structure of the surface of xerogels formed in an atmosphere of different vapors is the differing and (in addition) regular position of the adsorption isotherms (related to 1 m^2 of surface) of methyl orange on these samples.

The adsorption isotherm of methyl orange on the benzene gel is located above that for the toluene gel, and the adsorption on the xylene gel is lowest over the entire interval of dye concentrations. In the case of storage of the samples (formed in vapors of these aromatic hydrocarbons) in open test tubes at room temperature for 6-12 months, the methyl orange adsorption isotherms on these gels retain their relative positions, and adsorption of the dye per unit of surface decreases in the order benzene→toluene→xylene.

In analyzing the results on methyl orange adsorption account should be taken of the possible effect of differing accessibility of the internal surface of various gels for the relatively large molecules of methyl orange. The kinetic measurements (Fig. 4) showed that the process of adsorption on the toluene gel with a pore radius of 30 A is practically completed in 20-30 min, and only in the case of the control gel, with pore radius below 10 A, is there observed a lag in the penetration of the molecules being adsorbed into the pores of the gel. Hence it follows that the internal surface of the formed gels is accessible for the methyl orange molecules.

On the basis of the stated results, it is possible to draw the conclusion that forming agents of differing chemical nature, used for preparing gels with a given porous structue and texture of the surface, apparently influence simultaneously the magnitude of the elementary particles making up the skeleton of the gel, the chemical nature and relief [topography] of the surface of these particles, and the distribution of pore sizes (radii) of the xerogel.

It is necessary to consider also the influence of the nature of the intermicellar liquid of gels on the magnitude of the capillary forces binding the skeleton of the gel on its drying, since vapor-phase forming agents in the later stages of forming exist in the pores of the gel in the capillary-condensed state.

It was shown [4] that the magnitudes of the surface tension of the forming agents—benzene, toluene, and o-xylene—do not have any connection with the variation of structure of the silica gels which are formed, on transition from

benzene to xylene. From the results of the present work it follows that the methanol and dioxane samples (Fig. 5), in spite of the differing surface tension (methanol 22.5, dioxane 33.7 dynes/cm), have almost identical porous structure, since the benzene vapor adsorption isotherms on these gels almost coincide. At the same time, the structure of the methanol and isopropanol gels is substantially different, even though the surface tension for isopropanol and methanol is almost identical (~21 dynes/cm).

These experimental facts give evidence that is is impossible to find a simple relationship between any one physical property of the forming agent (or intermicellar liquid) and the final structure of the silica gel, if the chemical properties of the forming agent are not considered. In particular, the statement as to the decisive influence of surface tension of the intermicellar liquid upon the magnitude of capillary forces [11,12] is at variance with the experimental facts. Indirect proofs of the incorrectness of this statement were found previously [13-15], and more direct proofs have been obtained herein and in preceding work [4].

SUMMARY

1. By means of sorption isotherms of benzene and toluene vapors and the adsorption of methyl orange from solution, a study has been made of the porous structure and adsorptive properties of the surface of silica gels prepared by dehydrating silicic acid hydrogels in an atmosphere of vapors of organic substances—forming agents.

2. The chemical nature of the forming agents exerts a decisive influence on the structural-sorptive characteristics of the gels which are formed. For forming agents with differing structure (benzene, toluene, o-xylene) a gradual regular change of structure of the silica gels is observed.

3. A mechanism has been suggested for the action of forming agents, influencing simultaneously the porous structure of the gels and the amount and structure of the surface of their elementary particles, it is surmised that the basic cause of this influence is chemical interaction of the forming agent with the gel.

4. The experimental data which are cited do not confirm the point of view as to the decisive influence of surface tension of the intermicellar liquid on the formation of porous structure of silica gels.

LITERATURE CITED

1. M. V. Polyakov and Z. Z. Vysotskii, Collection: Preparation, Structure, and Properties of Sorbents (State Press for Chemical Literature, Leningrad, 1959), p. 94.
2. A. Waksmundzki, Roczn. chem. 32, 323 (1958).
3. V. V. Patrikeev, A. A. Balandin, E. I. Klabunovskii, Yu. S. Mordashev, and G. I. Maksimova, Doklady Akad. Nauk SSSR, 132, 850 (1960).
4. Z. Z. Vysotskii and M. V. Polyakov, Doklady Akad. Nauk SSSR 129, 831 (1959).
5. R. G. Haldeman and P. H. Emmett, J. Phys. Chem. 59, 103 (1955).
6. F. H. Dickey, J. Phys. Chem. 59, 695 (1955).
7. D. J. C. Yates, Proc. Roy. Soc. A 224, No. 1159, 526 (1954).
8. D. J. C. Yates, J. Phys. Chem. 59, 1980 (1955).
9. D. J. C. Yates, J. Phys. Chem. 60, 543 (1956).
10. A. V. Kiselev and V. V. Kulichenko, Doklady Akad. Nauk SSSR 93, 101 (1953).
11. V. S. Veselovskii and I. A. Selyaev, Zhur. Fiz. Khim. 6, 1171 (1935).
12. I. E. Neimark, Uspekhi Khim. 25, 748 (1956).
13. Z. Z. Vysotskii and V. V. Shalya, Kolloid. Zhur. 20, 29 (1958).
14. Z. Z. Vysotskii and V. V. Shalya, Zhur. Priklad. Khim. 32, 35 (1959).
15. Z. Z. Vysotskii and V. V. Shalya, Collection: Preparation, Structure, and Properties of Sorbents (State Press for Chemical Literature, Leningrad, 1959), p. 125.

All abbreviations of periodicals in the above bibliography are letter-by-letter transliterations of the abbreviations as given in the original Russian journal. *Some or all of this periodical literature may well be available in English translation.* A complete list of the cover-to-cover English translations appears at the back of this issue.

THE POSSIBILITY OF PREPARING ULTRAPOROUS SILICA GELS WITH INTRAPARTICLE POROSITY

Z. Z. Vysotskii and M. V. Polyakov

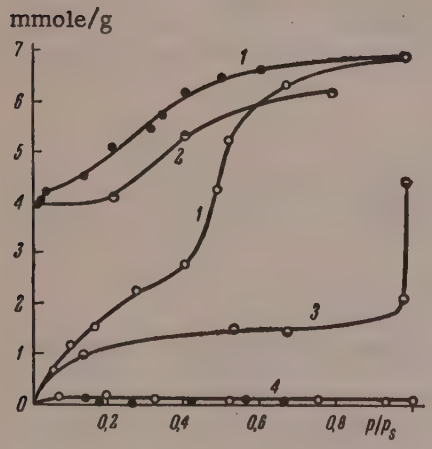
L. V. Pisarzhevskii Institute of Physical Chemistry, Academy of Sciences, UkrSSR

Translated from Kolloidnyi Zhurnal Vol. 23, No. 3, pp. 255-256, May-June, 1961
Original article submitted May 24, 1960

The usual industrial and laboratory methods of preparing silica gels include dehydration of silicic acid hydrogels either at comparatively high temperatures, at which they may lose the features of structure of the primary particles of the initial hydrogels, or at fairly low temperatures, where the water of the hydrogel freezes and there also occurs disarrangement of the structure of the hydrogel, although from a different cause.

In the course of investigating the influence of vapor pressure of water over the hydrogel, temperature, and rate of drying on the structure of silica gels, we developed a method of intensive dehydration of silicic acid hydrogels under mild conditions which apparently preserve the fine features of structure of the hydrogels.

The salt-free silicic acid hydrogel, obtained by mixing sodium silicate and sulfuric acid solutions and washing the gel free of salt, was dried in a desiccator by means of previously calcined P_2O_5, $CaCl_2$, alumina gel, silica gel, or concentrated H_2SO_4. For maximum reduction of vapor pressure of water, the hydrogel was placed in a Petri dish and covered with a screen (glass cloth, gauze). The Petri dish with the hydrogel was set in an inverted position in the center of a desiccator filled with grains of the desiccant. For dehydrating with H_2SO_4, an inverted procelain dish with the hydrogel (retained by glass cloth) was suspended as close as possible to the surface of the acid. For the purpose of the "freezing" the process of aging the hydrogel, the desiccator was placed in a refrigerator at a temperature of about 0°. Under these conditions the hydrogels in the course of 10-15 days lost 98-99 % of the water removable by six-hour heating in an oven at 180°. After dehydration, the gels were held in a vacuum oven at 80-100° for 4-6 hr.



Vapor sorption isotherms at 20° on Sample S-211: 1) Initial adsorption and desorption of water; 2) second adsorption of water; 3) adsorption of water after repeated steaming of samples at 200°; 4) methanol sorption isotherm.

Sample	Static activity, %	
	C_6H_6	H_2O
S -209	4,2	17,8
S -210	1,5	21,5
S -211	3,3	16,4
S -212	2,2	16,6

Some of the silica gels prepared by this method absorb benzene from air very poorly, but adsorb comparatively large quantities of water (table). In vacuum at all values of p/p_s they adsorb methanol vapors to a very small extent, but reversibly. However, the water vapor adsorption isotherm for these gels breaks sharply upward at $p/p_s = 0.45$ and has a very wide hysteresis loop (figure).

Such unusual sorption properties of silica gels prepared by relatively rapid removal of the dispersion medium of the hydrogel at reduced temperatures, where

thermal aging of the gel is clearly retarded (condensation of polysilicic acids, with the formation of intraparticle and interparticle siloxane bonds, is retarded) allows the assumption that in the present case we possibly have obtained ultraporous xerogels, retaining the intraparticle porosity of the initial hydrogels. An additional possibility which is not excluded is that the sorption properties of such silica gels are caused by a change of the chemical nature of their surface in the process of preparation.

SUMMARY

1. By a method of low-temperature dehydration of a silicic acid hydrogel and subsequent evacuation and heating in vacuum, silica gels have been prepared which adsorb benzene and methanol poorly and adsorb water in considerably greater quantities.

2. It is suggested that the sorption properties of these gels may be explained by retention of the intraparticle porosity of the hydrogels and a change of the chemical nature of the surface of the silica gels.

ELECTROKINETIC PHENOMENA IN HYDROCARBON SYSTEMS WITH A HYDROPHILIC DISPERSE PHASE

Yu. F. Deinega, G. V. Vinogradov, and A. M. Vovnenko

Institute of General and Inorganic Chemistry, Academy of Sciences, UkrSSR, Kiev
Translated from Kolloidnyi Zhumal Vol. 23, No. 3, pp. 257-261, May-June, 1961
Original article submitted September 15, 1960

A number of phenomena in such nonaqueous systems as soap greases make it possible to assume the presence of an electrical double layer on the surface of the disperse-phase particles. These phenomena include the significant dependence of dielectric permeability (ϵ) on rate of deformation [1,2], the strong dispersion of ϵ in the low frequency range (a phenomenon which we discovered recently) the change of potential on the plates of a capacitor-viscosimeter with the flow of plastic greases [1-3], and the effect of a high-voltage electric field on the deformability of greases. It had been suggested [2] that the appearance of a potential with flow of a lithium grease was caused by electrokinetic phenomena; however, prior to our studies there had been no attempts at the direct investigation of these phenomena in similar systems.

The study of electrokinetic phenomena in nonaqueous disperse systems has been begun comparatively recently [4]. Such investigations are important because the electrical properties of disperse systems are connected with electrokinetic phenomena, but in addition are extremely important for explaining the mechanism of structure formation. Up to now this has not received due attention.

The objective of the present work is a demonstration of the existence of electrokinetic phenomena and phase transport in a constant high-voltage electrical field in nonaqueous disperse systems with a hydrophilic disperse phase.

For investigating the electrokinetic phenomena, the simplest Perren-type osmometer was used. This device consists of two Γ-shaped glass tubes with sealed-in electrodes, between which an 11-mm I. D. glass ring is clamped by means of rubber gaskets. The distance between the electrodes is equal to 10 mm. The end surfaces of the ring and the tubes are ground. One of the arms of the apparatus is fitted with a stopcock and a capillary with 0.001-ml graduations.

The role of a porous diaphragm was played by a 5-mm thick layer of the grease located in the glass ring. After clamping the ring (containing the grease), the apparatus was filled with mineral oil and held for one day. Movement of the liquid upon imposing potential was observed by the movement of the oil meniscus in the horizontally mounted capillary. The source of high-voltage direct current was a unit consisting of a laboratory autotransformer, a high-voltage transformer, and a full-wave rectifier of the alternating current, 2Ts2S tubes.

The objects of investigation were plastic greases: sodium (Konstalin), calcium (Solidol), and lithium (Tsiatim 201), prepared by thickening mineral oils with (respectively) sodium soaps of castor oil acids (20.6%), hydrated calcium soaps of cottonseed oil acids (17.5%), and technical lithium stearate (10%).

Typical soap greases within the entire range of their normal use temperatures are pseudogels, having a three-dimensional structure framework formed by micro- and submicrofibers of the soaps. This framework is a loose spatial structure which contains many times its own weight and volume of the dispersion medium. These characteristics of the structure of greases permit their use as a porous diaphragm for studying the phenomena of electroosmosis. The medium used for filling the osmometer was MVP low-viscosity white instrument oil. A test of the oil according to GOST-1547-42 showed the presence of water in the oil.

Upon applying a voltage up to 5 kv there was observed movement of the oil through the layer of grease toward the negative pole. On reversing the polarity, oil migration in the opposite direction occurred. Experiments were carried out on greases which had been in open containers at room temperature for a long period of time. The rate of electroosmotic transport of the dispersion medium was determined first in one direction and then in the other by reversing polarity. Thus, the average value of the rate of electroosmotic transport was found. The results of the investigation are presented in the table.

Electroosmotic Effect in Greases

Grease	Voltage, kv				
	1	2	3	4	5
	Electroosmotic effect*				
Konstalin	0,02 / 0,01	0,04 / 0,04	0,17 / 0,11	0,18 / 0,23	0,18 / 0,39
Solidol	0,02 / 0,08	0,03 / 0,28	0,04 / 0,44	0,05 / 0,56	0,08 / 0,85

* The numerator of the fraction is the average rate of electroosmotic transport (ml/hr); the denominator is the current intensity (μa).

The electroosmotic effect is the most pronounced for the sodium grease, less pronounced for the calcium grease, and practically absent for the lithium grease. With an increase of voltage, the rate of migration of the oil is increased, especially in the case of the sodium grease. However, the volume of oil which passes through per unit of current was decreased with an increase of voltage. It is possible that this is connected with polarization of the electrodes.

Along with the electroosmosis, upon imposing the field there is observed a gradual formation of a highly porous soap deposit at the anode. The breaking loose of particles of the disperse phase from the membrane, their movement toward the positive electrode, and their deposition on this electrode indicates the presence of a negative charge on the disperse-phase particles. Prolonged contacting of the oil with the grease leads to destruction of the membrane.

An investigation by electron microscopy of the particles which were precipitated at the anode showed that large crystallites of the soaps are transported to the anode (Fig. 1).



Fig. 1. Electron microphotographs of disperse phase of sodium grease: a) Initial sample; b), c) deposits taken from the anode. Magnification 5000 x.

A reversal of polarity changes the direction of movement of the disperse-phase particles. This leads to a marked decrease of the deposit at the cathode and the deposition of the disperse phase at the anode in a considerably smaller quantity.

The greater the moisture content of the grease, the more strongly the electrokinetic phenomena are manifested. Electroosmosis is practically absent in Konstalin which has been held 4 hr at 120°. It appears again after prolonged residence of the grease in air. The phenomenon of current hysteresis, recorded on increasing and subsequently decreasing the voltage, evidently is also connected with a change of moisture content. This may be explained by the fact that passage of the oil through the grease with an increase of voltage results in a more rapid increase of the moisture in the oil up to the equilibrium state. In repeated experiments the current hysteresis is decreased sharply and disappears.

The above-described electrokinetic phenomena in greases confirm qualitatively the existence of an electrical double layer on the boundary of the disperse phase and the dispersion medium. The water which is present in hydrocarbon systems with a hydrophilic disperse phase plays a decisive role in the formation of the diffusion double layer. The presence of the electrical double layer on the phase boundary in plastic greases can play an important role in the process of structure formation. In investigating the interaction of the particles in such systems one must take into account their electrostatic interaction, which previously had not been considered. A change of the structure of the electrical double layer (for example, by adjusting moisture content), which sharply affects the electrical properties of greases, does not influence their mechanical properties. Investigations in this direction present considerable interest.

The electroosmotic effect in greases affords the opportunity of replacing the disperison medium without destroying the structure of the system. As is well known, on cooling a soap–hydrocarbon melt the structure of the pseudogel formed at low temperatures may depend essentially on the nature of the solvent [5]. Therefore, the electroosmotic method of replacing the medium may prove to be very effective for investigating the influence of the solvent on the properties of plastic disperse systems.

The formation of solid flow structures upon rapid interruption of the flow ofgreases [1,6] makes it possible to obtain membranes with differently oriented structure. The possibility of flow of the dispersion medium relative to the polar solid phase under the action of sufficiently high potential differences can lead to separation of the liquid from systems of such a type in the form of a free phase. This was displayed in the following experiment (Fig. 2). On the surface of one of the disc electrodes there was placed a 2-mm layer of the sodium grease, separated from the upper electrode by a 2-mm air space. The discs were under a 5-kv voltage difference. If the upper electrode is negative, within a few minutes jets of oil break loose from the grease, joining the grease layer with the negative electrode. Eventually the air space is completely filled with oil and the deoiled grease is shrunk. The drops of oil formed in the space can drift along the surface of the grease and coalesce with each other.

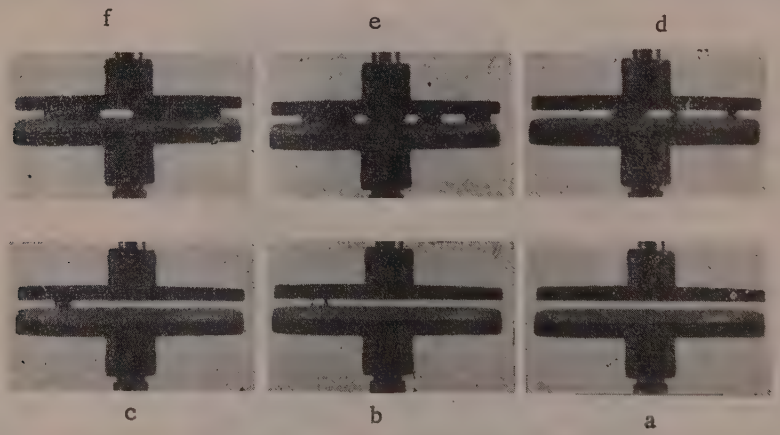


Fig. 2. Kinetics of separation of dispersion medium from Konstalin in an electric field: a) 0 min; b) after 5 min; c) after 15 min; d) after 30 min; e) after 60 min; f) after 120 min.

Here two phenomena are observed simultaneously: first, the electroosmotic transport of the oil toward the negative electrode and accumulation of the oil at the grease–air boundary, second, the upheaval of the oil through the air space to the electrode, owing to redistribution of the electric field in the nonhomogeneous (three-layer) dielectric, which was described at one time in [7]. With an increase of potential the rate of separation of the dispersion medium from the grease is increased. The liquid can be recovered in quantities commensurate with those ob-

tained by mechanical pressing. Upon subsequent reversal of polarity there is observed absorption of the oil and swelling of the system at the sites of the drops on its surface. If a positive potential is applied to the upper electrode and a negative potential to the bottom electrode at the start of the experiment, no separation of free dispersion medium takes place, since the oil concentrates the layer of grease contacting the lower electrode.

The extraction of the dispersion medium in strong electric fields is possible only from greases which had shown a marked electroosmotic effect (Konstalin, Solidol). The greater the rate of electroosmotic transport, the more intensive is the separation of the liquid from the pseudogel. On the surface of the lithium grease, for which electroosmosis is manifested very weakly, no drop formation was observed in the high-voltage field. As a result of preliminary drying of the Konstalin, the separation of the dispersion medium on applying an electric field is decreased sharply, as is electroosmosis. Increasing the moisture content of the grease reestablishes these effects. Thus, the extraction of the dispersion medium from greases in electric fields is connected closely with the presence of a potential drop at the boundary between the disperse phase and the dispersion medium.

Electrokinetic phenomena in plastic greases make it possible to explain a number of peculiarities of their electrification during flow and the effect of strong electric fields on the deformability of greases.

SUMMARY

1. A method has been proposed for investigating electroosmosis in plastic disperse systems of the lubricating grease type, utilizing the grease itself as the membrane separating the cathode and anode.

2. In moist greases with a hydrophilic disperse phase, electroosmosis and electrophoresis are observed under the action of a high-voltage electric field. In electrophoresis, large crystallites of the soap are transported, as was demonstrated by investigating them by electron microscopy. The dispersion medium for the greases investigated was charged positively, and the disperse phase negatively.

3. The strong influence of moisture on the intensity of electroosmosis in plastic greases has been established. The presence of water in sodium greases, for which the disperse phase is distinguished by considerable hydrophilicity, plays a decisive role in the formation of electrical double layers.

4. When sodium and calcium greases are placed in a high-voltage field between the positively charged plate of a condenser and the air space, a considerable quantity of the dispersion medium is separated from the grease, and a reversible shrinkage of the structural framework of the soap—oil gel occurs. This effect includes electroosmotic transport of the liquid to the free surface of the grease and the formation of drops in the air space of the condenser.

LITERATURE CITED

1. Yu. F. Deinega, A. V. Dumanskii, G. V. Vinogradov, and V. P. Pavlov, Kolloid. Zhur. 22, 16 (1960).
2. A. Bondi and C. Penther, J. Phys. Chem. 57, 72 (1953).
3. Yu. F. Deinega, A. V. Dumanskii, and G. V. Vinogradov, Kolloid. Zhur. 23, 25 (1961).
4. B. Bernelin, Rev. Inst. Franc. Petrole 14, 1295 (1959); I. Bryant and B. Bernelin, 14, 1295 (1959), p. 1767.
5. G. V. Vinogradov, Uspekhi Khim. 20, 533 (1951).
6. G. V. Vinogradov, Transactions of All-Union Conference on Colloid Chemistry (UkrSSR Acad. Sci. Press, Kiev, 1951), p. 248.
7. A. Gemant, Elektrotechn. Z. 34, 1225 (1929).

All abbreviations of periodicals in the above bibliography are letter-by-letter transliterations of the abbreviations as given in the original Russian journal. *Some or all of this periodical literature may well be available in English translation.* A complete list of the cover-to-cover English translations appears at the back of this issue.

KINETICS OF EVAPORATION OF LIQUID DROPS COVERED BY AN INSOLUBLE FILM OF A FOREIGN SUBSTANCE

B. V. Deryagin, S. P. Bakanov and Yu. S. Kurgin

Laboratory of Surface Phenomena, Institute of Physical Chemistry, Academy of Sciences USSR

Translated from Kolloidnyi Zhurnal Vol. 23, No. 3, pp. 262-271, May-June, 1961
Original article submitted June 1, 1960

Rideal [1] observed experimentally that films of surface-active substances strongly retard the evaporation of water. Having assumed that a monolayer on a water surface offers a certain resistance to evaporation of the water, Langmuir [2] called this phenomenon the diffusional resistance of the monolayer and, by analogy with Ohm's law, defined it by the equation:

$$\text{Rate} = \frac{\text{moving force}}{\text{resistance}}$$

Langmuir considered that the resistance to evaporation consists of two resistances, including the following: ω_a the resistance of the air layer, and ω_f, the resistance of the surface itself, including the resistance of the monolayer.

Two experiments—evaporation of water through a film and evaporation of water without the film—permit calculating the film resistance ω_f as the difference between the total resistances in the two experiments. Considering evaporation into a vacuum, for which $\omega_a = 0$, Langmuir obtained a relationship between the resistance of a monolayer ω_f and the condensation coefficient α

$$\omega_f = 6.8 \cdot 10^{-5}/\alpha, \text{ sec/cm}. \quad (1)$$

The condensation coefficient α indicates that of all the molecules of vapor impinging on the liquid surface (here, water) covered by the film, a part α of the molecules passes into the liquid phase, and the remaining part $(1 - \alpha)$ of the molecules rebounds into the vapor.

For the case of evaporation of water through a monolayer, Langmuir described by one value of ω_f two different phenomena: diffusion of the water molecules into the monolayer and evaporation from the surface of the monolayer. For the case of evaporation from a pure water surface, Formula (1) becomes the relationship between the resistance of the "adhesion" of the molecules of water to the pure water surface and the condensation coefficient of water ($\alpha = 0.034$). From results of measurement of resistances to water evaporation of monolayers of fatty acids having from 16 to 23 carbon atoms in the molecule, and also of monolayers of oleic and stearic acids and cetyl alcohol, Langmuir deduced that monolayers have an exclusively retarding influence on the rate of water evaporation.

Bradley [3] considered the retardation of the evaporation of 1-micron water droplets by insoluble monolayers as evaporation with a negligibly small value $\alpha \sim 10^{-6}$. Let us note that such values of α are obtained from Formula (1) by substituting in place of ω_f the numerical values of the monolayer resistances from the experiments of Langmuir. Bradley's results showed that the rate of evaporation of such monolayer-covered droplets at $t = 20°$ and $P = 1$ atms is reduced almost 30,000 times in comparison with the rate of evaporation of water droplets of the same dimension without the monolayer.

However, depending on the nature of the film material, some films increase the rate of evaporation of water; this was observed in two different experiments.

1. Izmailova, Prokhorov, and Deryagin [4], measuring the critical supersaturation for NaCl condensation nuclei and the critical supersaturation for the same condensation nuclei covered with adsorbed layers of various surface-active substances, came to the conclusion that a monolayer of formaldehyde brought to the surface of an aqueous drop reduces α in comparison with α_{H_2O}, whereas monolayers of acetone or isoamyl alcohol increase α and under specific conditions can increase the rate of evaporation of the drops.

2. Tovbin and Savinova [5], investigating the kinetics of the nonstationary evaporation of water through adsorbed layers, showed that at a very short time of contact between the water jet and the air, when the role of vapor diffusion in the air is negligible, the rate of evaporation of water covered with a monolayer of octyl or isoamyl alcohol

exceeds the rate of evaporation of water without the monolayer.

In order to explain not only the retarding but also the accelerating influence of films on the rate of evaporation of liquids, depending on the nature of the films, a theory has been developed as set forth below.

Problem of the Quasistationary Evaporation of a Liquid Drop Covered with an Insoluble Film of a Foreign Substance. Let us examine the quasistationary evaporation of a liquid drop of radius a, covered with a macroscopic insoluble liquid film of a foreign substance of thickness δ, motionless with respect to an infinite homogeneous air medium. Let us define the rate of evaporation of the drop as the change of mass of the drop in unit time, dM/dt. The liquid of the drop is dissolved in the film, and it is assumed that it forms a dilute solution in the film. Let us assume also that the substance of the film is nonvolatile. Within the film there occurs stationary diffusion of the liquid molecules, which is described by the Laplace equation

$$\Delta c_1 = 0, \quad a < r + \delta, \tag{2}$$

where c_1 is the number of liquid molecules in 1 cm^3 of the film; let us call it the solution concentration of the drop liquid in the film. In the following discussion, all concentrations are taken in this same sense. Molecules of the liquid are evaporated from the film surface into the air; this latter circumstance is considered according to the Fuks theory [6] of a two-stage process of evaporation. Through the region directly adjacent to the film surface, of a thickness Δ (in the order of the mean free path of the molecules of the vapor in air), the vapor is transported by molecular flow; then, beginning with the surface of a sphere with radius $a + \delta + \Delta$, it diffuses in the air.

Bradley evaluated the magnitude of Δ:

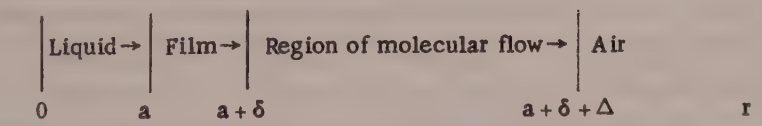
$$\Delta = \frac{8D}{3\pi v}\sqrt{\frac{m_1}{m_1 + m_2}} = \sqrt{\frac{m_1 + m_2}{m_1}}\lambda_2 ,$$

where

$$v = \sqrt{\frac{kT}{2\pi m_2}} = \frac{\bar{v}}{4};$$

D is the diffusion coefficient of the vapor in the air; m_1 is the mass of the air molecule; m_2 is the mass of the vapor molecule; $\bar{v}$ is the mean speed of the vapor molecules; λ_2 is the mean free path of the vapor molecules in air.

The process scheme may be represented thus:



The stationary diffusion of vapor molecules in the air is described by the equation

$$\Delta c_2 = 0, \quad r > a + \delta + \Delta, \tag{2a}$$

where c_2 is the concentration of vapor in the air.

Since our problem possesses spherical symmetry, the solutions of Eqs. (2) and (2a) in this case are

$$c_1 = \frac{A_1}{r} + B_1, \quad a < r < a + \delta,$$
$$c_2 = \frac{A_2}{r} + B_2, \quad r > a + \delta + \Delta. \tag{3}$$

For determining the constants, let us indicate the boundary conditions. It is evident that at the boundary r = a the solution of the liquid in the film exists in equilibrium with the liquid of the drop, and at this boundary the concentration of the liquid-in-film solution c_1 is equal to the concentration of a saturated solution of the liqud in the film, c_p

$$c_1 \big|_{r=a} = c_p. \tag{4}$$

It is evident that at the boundary $r = a + \delta$ there is equilibrium between the liquid-in-film solution and the vapor above the solution, the concentration of which is designated as c_0'. In accordance with Henry's law, the vapor pressure

over the solution P_0' is proportional to the concentration of the solution

$$P_0' = kc_1|_{r=a+\delta},$$

where k is some constant.

Theoretically applying Henry's law to the vapor with pressure P_0 over the saturated liquid-in-film solution with concentration c_p, we obtain $P_0 = kc_p$ with the same proportionality constant k. It is evident that the pressure P_0 is the saturated vapor pressure at the temperature of the drop.

Assuming that the vapor obeys the ideal gas laws, i.e., $P = RTc$, where c is the concentration of vapor in the air, let us write these Henry's-law expressions as

$$c_0' = \bar{k}\ c_1|_{r=a+\delta}, \quad c_0 = \bar{k}c_p$$

and, having divided one by the other, we obtain

$$c_1|_{r=a+\delta} = \frac{c_p}{c_0} c_0', \tag{5}$$

where c_0 is the concentration of saturated vapor at the temperature of the drop, c_0' is the concentration of the vapor over the liquid-in-film solution at the boundary $r = a + \delta$.

The conditions of applicability of Henry's law—diluteness of the solution, nonvolatility of the solvent, and absence of specific chemical interaction between liquid and film—in the present case are fulfilled. Let us note that condition (5) may be obtained by another method, equating at the boundary $r = a + \delta$ the chemical potentials of the liquid dissolved in the film and of the vapor over the solution.

Again let us return to the equilibrium between the liquid-in-film solution and the vapor above the solution at the boundary $r = a + \delta$. The number of molecules of liquid leaving the surface of the film is equal to the number of molecules of vapor depositing on this surface (within the same time interval) and "adhering" to it. The rate of evaporation of a solution of the liquid from 1 cm^2 surface of the film into the vapor (in equilibrium with the solution) is equal to $\alpha(\bar{v}/4)\, mc_0'$, where m is the mass of the vapor molecule. The coefficient of "adhesion" α indicates that out of all the molecules of vapor impinging on the surface of the film, a portion α of the molecules passes into the film, and the remaining part $(1 - \alpha)$ of the molecules rebounds into the vapor. If the equilibrium vapor pressure is not too large, the number of molecules of liquid leaving the surface of the film is independent of whether or not there is vapor in the surrounding space, such that the written expression defines the rate of evaporation into a vacuum.

In the given problem the evaporation takes place not into a vacuum, but into vapor with concentration $c_2|_{a+\delta+\Delta}$; thereby, together with the process of liquid evaporation there occurs the reverse process of condensation of $\alpha \frac{\bar{v}}{4} mc_2|_{r=a+\delta+\Delta}$ on 1 cm^2 of film surface. The resulting molecular flow of vapor is equal to

$$\alpha \frac{\bar{v}}{4}(c_0' - c_2)|_{r=a+\delta+\Delta}.$$

The equality of the diffusional flow of dissolved liquid in the film and the molecular flow of vapor at the boundary $r = a + \delta$ gives the boundary condition

$$-D_1 \frac{dc_1}{dr}\bigg|_{r=a+\delta} = \alpha \frac{\bar{v}}{4}(c_0' - c_2)\bigg|_{r=a+\delta+\Delta}, \tag{6}$$

where D_1 is the diffusion coefficient of the liquid molecules in the film.

The equality of the molecular flow of vapor and the diffusional flow of vapor at the boundary $r = a + \delta + \Delta$ gives the boundary condition

$$4\pi(a+\delta)^2 \alpha \frac{\bar{v}}{4}(c_0' - c_2)|_{r=a+\delta+\Delta} = 4\pi(a+\delta+\Delta)^2 \left(-D_2 \frac{dc_2}{dr}\bigg|_{r=a+\delta+\Delta}\right), \tag{7}$$

where D_2 is the diffusion coefficient of the vapor in air.

Finally, let us set the concentration of vapor in the air at infinite withdrawal [distance] from the drop

$$c_2\big|_{r=\infty} = c_\infty. \tag{8}$$

From the five boundary conditions (4)-(8) there are determined the four constants A_1, A_2, B_1, B_2, and the concentration c_0'.

The rate of evaporation, as the change of drop mass in unit time, is evidently equal to the product of the mass of the vapor molecule and the number of vapor molecules passing per unit time through the surface of a sphere of radius $r = a + \delta + \Delta$, starting from which the molecules of vapor diffuse into the air

$$-\frac{dM}{dt} = m\,4\pi(a+\delta+\Delta)^2\left(-D_2\frac{dc_2}{dr}\bigg|_{r=a+\delta+\Delta}\right).$$

Having substituted into this formula the value of c_2 from Eq. (3), where A_2 and B_2 are determined from the system of equations (4)-(8), we obtain a formula for the rate of quasistationary evaporation of a drop covered by a thick film of thickness δ

$$-\frac{dM}{dt} = \frac{4\pi a D_2 (c_0 - c_\infty)_m}{\dfrac{D_2}{\alpha\dfrac{\bar{v}}{4}}\dfrac{a}{(a+\delta)^2} + \dfrac{a}{a+\delta+\Delta} + \dfrac{D_2}{D_1}\dfrac{c_0}{c_p}\dfrac{\delta}{a+\delta}}. \tag{9}$$

Let us note that without the film, i.e., with $\delta = 0$, Formula (9) coincides with the Fuks formula for the evaporation rate of pure liquid drops

$$-\frac{dM}{dt} = \frac{4\pi a D_2 (c_0 - c_\infty)_m}{\dfrac{D_2}{\alpha\dfrac{\bar{v}}{4}a} + \dfrac{a}{a+\Delta}}$$

Evaporation of a drop cannot be a stationary process, since the radius of the drop and hence also the evaporation rate are continually decreasing. In quasistationary evaporation, by definition, at each given moment of time the diffusion is described by the equations of stationary diffusion (2) and (2a) with the boundary conditions (4)-(8), and hence the rate of evaporation at any given moment is given by Formula (9).

Let us assume that the corresponding formula for the rate of evaporation of a drop through a monolayer can be obtained from Formula (9) with the over-all transition from a film of thickness δ to a monolayer (i.e., $\delta \ll a$). Thus, we obtain an expression for the rate of quasistationary evaporation from 1 cm^2 of a liquid drop surface covered by a monolayer

$$-\frac{dM}{dt} = \frac{m(c_0 - c_\infty)}{\dfrac{c_0}{c_p}\dfrac{\delta}{D_1} + \dfrac{1}{\alpha\dfrac{\bar{v}}{4}} + \dfrac{1}{D_2}\dfrac{a^2}{a+\Delta}}. \tag{10}$$

The items of the denominator in expression (10) can be treated as partial resistances to evaporation: $1/D_2\,(a^2/\alpha + \Delta)$ is the partial resistance caused by diffusion of the vapor in the air; $c_0/c_p\,(\delta/D_1)$ is the partial diffusional resistance of the monolayer, which is increased with a decrease of the solubility of the liquid in the film; $1\,[\alpha(v/r)]$ is the partial resistance caused by the "adhesion" of the molecules of the liquid to the film.

Two phenomenological parameters figure in the development of our theory: α and $1/c_p\,(\delta/D_1)$, which depend on the nature of the monolayer. The theoretical result which is obtained disagrees with the hypotheses of Langmuir and Bradley, (which lead to an exclusively retarding influence of monolayers on the rate of evaporation of liquid drops) and agrees qualitatively with the aforementioned experiments, from which it follows that some monolayers can increase α in comparison with α_{H_2O} and under specific conditions increase the rate of evaporation of water. The above-developed theory gives the criterion for an accelerating action of monolayers on the rate of evaporation of liquid drops

$$\frac{c_0}{c_p}\frac{\delta}{D_1}+\frac{1}{\alpha\frac{\bar{v}}{4}}<\frac{1}{\alpha_{H_2O}\frac{\bar{v}}{4}}. \qquad (11)$$

Carrying out an optical analogy, let us note that describing the influence of the monolayer on evaporation by two parameters is equivalent to attributing to the monolayer certain coefficients of absorption and reflection for molecules of the liquid. If the absorption and reflection coefficients for the monolayer and the reflection coefficient for water satisfy condition (11), then the rate of evaporation is increased; if the reverse inequality is satisfied, the evaporation rate is decreased.

As a result of an analogous solution of the stationary problem for evaporation from a plane surface of liquid, covered by a monolayer, a formula is obtained for the rate of evaporation I_0 from 1 cm^2 of surface

$$I_0=\frac{m(c_0-c_L)}{\frac{L-\Delta}{D_2}+\frac{1}{\alpha\frac{\bar{v}}{4}}+\frac{c_0}{c_p}\frac{\delta}{D_1}}, \qquad (12)$$

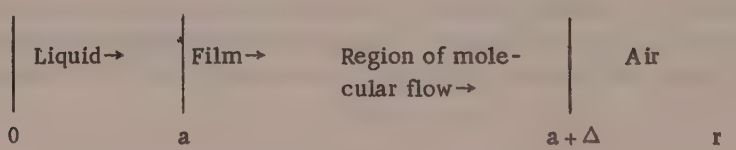
where c_L is the concentration of vapor in the air at a distance L from the surface of the liquid. This formula has an identical form for the case of a macroscopic film of thickness δ on the liquid and for the case of a monolayer. In addition, for sufficiently great thicknesses of the diffusional layer of air, Formula (12) is changed to the formula

$$I_0=m(c_0-c_L)\frac{D_2}{L-\Delta},$$

i.e., the rate of stationary evaporation from 1 cm^2 of a plane film-covered liquid surface for great thicknesses of the diffusional layer of air is independent of the nature of the film, which agrees with the well-known proposition of physical kinetics to the effect that if several processes take place simultaneously in a system, the resulting rate is determined by the rate of the slowest process.

Problem of the Nonstationary Evaporation of a Liquid Drop Covered by an Insoluble Monolayer of a Foreign Substance. Let us examine the nonstationary evaporation of a liquid drop of radius a, covered by an insoluble monolayer of a foreign substance with thickness δ ($\delta \ll a$).

The scheme of the process will have the form:



Let us consider that the nonstationary state occurs because of the nonequilibrium initial condition on introduction of the drop into the air medium with a constant vapor concentration in the air c_∞ which differs from the equilibrium concentration, the density of the vapor being much less than the density of the liquid, i.e., $mc_\infty \ll \gamma$ where γ is the liquid density. As was indicated above, the change of mass of the drop in unit time is equal to the diffusional flow of vapor molecules through the surface of a sphere of radius $r = a + \Delta$

$$J=-\frac{dM}{dt}=m4\pi(a+\Delta)^2\left(-D_2\frac{dc}{dr}\Big|_{r=a+\Delta}\right). \qquad (13)$$

From expression (13), utilizing the expression for drop mass $M = 4/3\pi a^3\gamma$, we obtain the rate of movement of the boundary

$$\frac{da}{dt}=\frac{mc_\infty}{\gamma}D_2\left(\frac{a+\Delta}{a}\right)^2\frac{1}{c_\infty}\frac{\partial c}{\partial r}\Big|_{r=a+\Delta}$$

Hence it is evident that with $mc_\infty/\gamma \gg 1$* the Peclet number is low, and the phase boundary may be considered as immobile [7].

*As in Russian. Should probably read $\ll 1$.

Since the thickness of the monolayer is much less than the drop radius, i.e., $\delta \ll a$, the influence of the monolayer can reduce to a change of the equilibrium vapor concentration c_0' at the boundary $r = a$, in comparison with the saturated vapor concentration c_0 in the case of evaporation of a pure liquid. Since equilibrium is established rapidly in the monolayer, in a time in the order of

$$T \sim \frac{\delta^2}{D_1} \sim 10^{-11} \text{ sec},$$

it is possible to consider nonequilibration only in the gas and to obtain the concentration of vapor in equilibrium with the liquid-in-film solution by solving the corresponding quasistationary problem, i.e., to determine c_0' from the system of equations (4)-(8).

$$c_0' = \frac{\frac{c_\infty}{c_p}\frac{\delta}{D_1} + \frac{1}{\alpha\frac{\bar{v}}{4}} + \frac{1}{D_2}\frac{a^2}{a+\Delta}}{\frac{c_0}{c_p}\frac{\delta}{D_1} + \frac{1}{\alpha\frac{\bar{v}}{4}} + \frac{1}{D_2}\frac{a^2}{a+\Delta}} c_0. \tag{14}$$

Nonstationary diffusion of the vapor in the air is described by the equation

$$D_2 \Delta c = \frac{\partial c}{\partial t}, \quad r > a + \Delta, \quad t > 0, \tag{15}$$

where c is the concentration of vapor in the air.

Let us obtain the limiting condition from the equality of the molecular flow of vapor with the diffusional flow of vapor in the air at the boundary $r = a + \Delta$

$$4\pi a^2 \alpha \frac{\bar{v}}{4}(c_0' - c|_{r=a+\Delta}) = 4\pi (a+\Delta)^2 \left(-D_2 \frac{\partial c}{\partial r}\Big|_{r=a+\Delta}\right). \tag{16}$$

Let us set the initial condition

$$c(r, 0) = c_\infty, \quad r > a + \Delta. \tag{17}$$

We solve Eq. (15) with conditions (16) and (17) and with the value of c_0' from Eq. (14). From Eq. (13) we obtain an expression for the rate of nonstationary evaporation of a drop covered by a monolayer

$$J = J_0 f(t),$$

$$f(t) = (1+\nu)\sqrt{\frac{D_2 t}{\pi}} \frac{a+\Delta}{(a+\Delta)^2 + (1+\nu) D_2 t} e^{-\frac{(a+\Delta)^2}{4D_2 t}} +$$

$$+ \frac{1+\nu}{2} \frac{(a+\Delta)^4 + (\nu+2)(a+\Delta)^2 D_2 t + 2(1+\nu) D_2^2 t^2}{[(a+\Delta)^2 + (1+\nu) D_2 t]^2} \left[1 - \operatorname{erf}\left(-\frac{a+\Delta}{2\sqrt{D_2 t}}\right)\right] -$$

$$- \frac{D_2 t}{2}(1+\nu) \frac{(a+\Delta)^2 + 2(1+\nu) D_2 t}{[(a+\Delta)^2 + (1+\nu) D_2 t]^2} e^{1+\nu+\left(\frac{1+\nu}{a+\Delta}\right)^2 D_2 t} \left[1 -\right.$$

$$\left. - \operatorname{erf}\left(\frac{a+\Delta+2\frac{1+\nu}{a+\Delta} D_2 t}{2\sqrt{D_2 t}}\right)\right], \tag{18}$$

where

$$\nu = \frac{\alpha\frac{\bar{v}}{4}}{D_2}\frac{a^2}{a+\Delta}; \quad J_0 = \frac{4\pi a^2 (c_0 - c_\infty)_m}{\frac{c_0}{c_p}\frac{\delta}{D_1} + \frac{1}{\alpha\frac{\bar{v}}{4}} + \frac{1}{D_2}\frac{a^2}{a+\Delta}},$$ the rate of quasistationary evaporation of the drop.

Analyzing expression (18), let us note that $f(t) \to 1$ with $t \gg (a+\Delta)^2/D_2$. At times which satisfy this inequality, the rate of evaporation is equal to the rate of quasistationary evaporation, $J = J_0$. Hence, the initial nonequilibrium is "resolved," and the quasistationary condition of evaporation is established for the time $T \sim (a+\Delta)^2/D_2$, which could be expected from elementary physical considerations, since diffusion begins at the boundary $r = a + \Delta$. For the evaporation of drops in air at atmospheric pressure, $\Delta \sim 10^{-4}$ cm and $T_{min} \sim 10^{-8}$ sec; for large drops $a \gg \Delta$ and $T_{min} \sim a^2/D_2$. For evaporation into a medium under subatmospheric pressure, Δ increases, and the time of "resolution" of the initial nonequilibrium may be increased at the exprense of Δ.

From the expression (18) let us obtain the rate of evaporation of the drop at the initial moment

$$J|_{t=0} = J_0\left(1 + \frac{\alpha \frac{\bar{v}}{4}}{D_2} \frac{a^2}{a+\Delta}\right).$$

As a result of an analogous solution of the nonstationary problem for the evaporation from a plane surface of a liquid covered with a monolayer, we obtain a formula for the rate of evaporation from 1 cm^2 of surface

$$I = I_0\left[1 - \left(1 + \alpha \frac{\bar{v}}{4} \frac{L-\Delta}{D_2}\right) \sum_{n=1}^{\infty} b_n \sin \mu_n (L-\Delta) e^{-\mu_n^2 D_2 t}\right], \tag{19}$$

where I_0, the rate of stationary evaporation from 1 cm^2 of surface, is given by Formula (12);

$$b_n = \frac{2\sqrt{1 + \left(\frac{D_2}{\alpha \frac{\bar{v}}{4}}\right)^2 \mu_n^2}}{\mu_n \left[L - \Delta + \left(\frac{D_2}{\alpha \frac{\bar{v}}{4}}\right) \mu_n^2 \left(L - \Delta - \frac{1}{\mu_n}\right)\right]},$$

μ_n represents positive roots of the transcendental equation

$$\operatorname{tg} \mu_n (L-\Delta) = -D_2/\alpha \frac{\bar{v}}{4} \mu_n.$$

Analyzing Eq. (19), we find that for $t \gg (L-\Delta)^2/\gamma_1^2(\alpha)D_2$ the rate of evaporation is equal to the rate of stationary evaporation I_0; i.e., that the time of "resolving" of the initial nonequilibrium $T \sim (L-\Delta)^2/\gamma_1^2(\alpha)D_2$, where $(L-\Delta)$, is the thickness of the air layer through which the vapor molecules diffuse; γ_1 is the first positive root of the equation

$$\operatorname{tg} \gamma_n = -\frac{D_2}{\alpha \frac{\bar{v}}{4}(L-\Delta)} \gamma_n.$$

Solving this equation, we obtain:

$$\text{with} \quad \frac{D_2}{\alpha \frac{\bar{v}}{4}(L-\Delta)} \gg 1, \quad \gamma_1 \approx \frac{\pi}{2},$$

$$\text{with} \quad \frac{D_2}{\alpha \frac{\bar{v}}{4}(L-\Delta)} \ll 1, \quad \gamma_1 \approx \pi.$$

Thus, with small α, $\gamma_1 \approx \pi/2$, with large α, $\gamma_1 \approx \pi$. We find that the time of establishing the stationary condition of evaporation is a function of α and is approximately 4 times greater in the case of small α than in the case of large α.

From expression (19) we obtain the rate of evaporation from 1 cm^2 of a plane surface of the liquid at the initial moment

$$I\Big|_{t=0} = I_0\left(1 + \alpha\frac{\bar{v}}{4}\frac{L-\Delta}{D_2}\right) \qquad (20)$$

This expression agrees qualitatively with the results of the experiments of Tovbin and Savinova [5]. If the presence of a monolayer on the water leads to an excess of α over $\alpha_{H_2O} = 0.034$, then the rate of evaporation of the water through the monolayer at the initial moment of time is higher than the rate of evaporation of pure water.

Based on an experimentally determined rate of stationary evaporation from 1 cm^2 of a plane surface of the liquid [expression (12)] and the corresponding rate of nonstationary evaporation in the initial period of instability ("nonstationariness") [expression (20)] it is possible to determine the parameters of the theory developed here, α and $1/c_p(\delta/D_1)$, for each given monolayer.

SUMMARY

1. Formulas have been obtained for the rate of quasistationary evaporation of a liquid drop covered with an insoluble liquid film of a foreign substance, motionless with respect to an infinite homogeneous air medium, and for the rate of stationary evaporation from 1 cm^2 of a film-covered liquid plane surface.

2. An expression has been obtained for the rate of quasistationary evaporation of a liquid drop covered by a monolayer, in which there figure two phenomenological parameters which depend on the nature of the monolayer. This theoretical result disagrees with the hypotheses of Langmuir and Bradley (which lead to an exclusively retarding influence of monolayers on the rate of evaporation of liquid drops) and agrees qualitatively with certain experiments relative to the acceleration of liquid evaporation by monolayers of isoamyl alcohol and acetone. Depending on its nature, a monolayer may both retard and accelerate the evaporation of liquids.

3. A formula has been obtained for the rate of nonstationary (owing to initial nonequilibrium) evaporation of a liquid drop covered by a monolayer. An expression has been adduced for the time in which the initial nonequilibrium is "resolved" and a quasistationary condition of evaporation is established.

A formula has been obtained for the rate of evaporation of a drop covered by a monolayer, at the initial moment, which agrees qualitatively with experiments on the kinetics of the nonstationary evaporation of liquids through monolayers.

4. It is possible in principle to determine both of the phenomenological parameters of the theory by a combination of experiments on determining the rate of stationary evaporation from 1 cm^2 plane surface of the monolayer-covered liquid and the corresponding rate of nonstationary evaporation in the initial period of instability ("nonstationariness").

LITERATURE CITED

1. Adam, Physics and Chemistry of Surfaces.
2. G. Langmuir and V. Schaefer, J. Franklin Inst. 235, 119 (1943).
3. R. Bradley, J. Colloid Sci. 10, 571 (1955).
4. G. I. Izmailova, P. S. Prokhorov, and B. V. Deryagin, Kolloid. Zhur. 19, 556 (1957).
5. M. V. Tovbin and E. V. Savinova, Zhur. Fiz. Khim. 31, 2717, (1957).
6. N.A. Fuks, Evaporation and Growth of Drops in a Gaseous Medium (USSR Acad. Sci. Press, 1958), p. 95.
7. L. Frisch and E. C. Collins, J. Chem. Phys. 21, 2158 (1953).

All abbreviations of periodicals in the above bibliography are letter-by-letter transliterations of the abbreviations as given in the original Russian journal. *Some or all of this periodical literature may well be available in English translation.* A complete list of the cover-to-cover English translations appears at the back of this issue.

INFLUENCE OF RESINS, NAPHTHENIC ACIDS, AND WATER ON THE ELECTRICAL PROPERTIES OF TRANSFORMER OIL CONTAINING SODIUM SOAPS

Ch. M. Dzhuvarly and L. A. Mukharskaya

Power Engineering Institute, Academy of Sciences, AzerbSSR, Baku

Translated from Kolloidnyi Zhurnal Vol. 23, No. 3, pp. 272-275, May-June, 1961
Original article submitted April 14, 1960

The electrical conductivity of fresh transformer oils is caused by the cataphoretic conductivity of the sodium naphthenates which are formed in the oils in their preparation by acid–alkali treatment [1]. However, the oils also contain a greater or lesser amount of resinous substances, naphthenic acids, and water. Therefore, it is of interest to study the influence of these substances on the electrical properties of the soap-containing transformer oils.

For investigating the influence of resinous substances on the electrical properties of transformer oils, samples were prepared by three methods:

1. A transformer oil distillate after treatment with aqueous sodium hydroxide solution to neutral reaction was settled and dried without washing: Thereby the naphthenic acids contained in the distillate were neutralized and converted to sodium soaps. The alkali-treated distillate contains (along with the soaps) the resinous substances which were present in the original distillate and which were unchanged by the sodium hydroxide treatment.

2. A transformer oil distillate without any pretreatment was dried in a thermostat, after which 0.1% sodium soaps was added.

3. Resinous substances and sodium soaps which were separated from a transformer oil distillate were introduced simultaneously into a fresh portion of the oil, having an adequately low electrical conductivity.

Influence of Resinous Substances on the Electrical Properties of Soap-Containing Transformer Oils

Sample	Temp. °C	tan δ, %	$\gamma_s \cdot 10^{-12}$, $ohm^{-1} cm^{-1}$	ε
Transformer distillate	20	0,5	0,31	2,23
	70	5,6	3,37	2,17
Transformer distillate alkali-treated without washing	20	0,5	0,31	2,23
	70	5,6	3,37	2,17
Transformer distillate plus 0.1% sodium naphthenates	20	0,5	0,31	2,23
	70	5,6	3,37	2,17
Standard transformer oil	20	0,07	0,04	2,23
	70	0,6	0,36	2,17
Standard transformer oil plus 2.5% resins	20	0,5	0,31	2,23
	70	5,4	3,36	2,17
Standard transformer oil + 2.5% resins + 0.1% Na naphthenate	20	0,5	0,31	2,23
	70	5,4	3,36	2,17
Standard transformer oil + 0.1% Na naphthenates	20	4,6	2,84	2,23
	70	34	20,5	2,17
Standard transformer oil + 0.1% Na naphthenates + 0.5% naphthenic acids	20	0,3	0,18	2,23
	70	3,8	2,28	2,17

The oil samples obtained as described above were filtered and dried, after which the following electrical characteristics were determined: dielectric loss-angle tangent (tan δ), specific volume electrical conductivity γ_s, and dielectric permeability ϵ.

The results of themeasurements are found to be identical for the samples prepared by the different methods. Thus, the soaps in the presence of the resinous substances do not manifest their characteristic electrical properties (it is known that the introduction of 0.1% sodium soap into a transformer oil increases tan δ up to 34% at 70°). The resins passivate the action of the soaps, which should be explained by their adsorptive interaction with the soap particles. The resins, enveloping the soap micelles, create protective shells which reduce their electrophoretic mobility in an electrical field.

Naphthenic acids also show an analogous effect; being adsorbed on the colloidal soap particles, they reduce the electrical conductivity of the soap-containing transformer oil.

The dependence of the electrical characteristics of the indicated systems upon the content of naphthenic acids and resins is shown in the table.

Mollinger [2] investigated the change of tan δ of oils with time, depending on their water content; however, the cause was not found. Therefore, we conducted the measurement of tan δ against time for various insufficiently washed commercial transformer oils, characterized by high values of tan δ. The oils were investigated in the dry state, after humidifying, and after adding sodium naphthenates. The dielectric loss-angle tangent was determined at 20° and a frequency of 50 cps.

The results showed that only the humidified oils showed a change of tan δ with time. A change of tan δ is caused by a very small quantity of hygroscopic water (not detectable by "crackling" or by the Dean and Stark method). Consequently, the moisture content of the oils can be characterized by the magnitude of tan δ.

For investigating the influence of moisture content of the oil on the time dependence of tan δ, a transformer oil with added sodium naphthenates, having an initial value tan δ = 4.6%, was held in a humidity cabinet for various periods. The resulting samples had differing moisture contents and correspondingly different values of tan δ: 7, 10, and 16%.

Measurements in an electrical field showed that tan δ of a dry oil containing sodium soaps is unchanged with time. The same oil after humidifying gives an increase of tan δ with time; the greater the moisture content of the oil, the sharper is this increase. With an increase of moisture of the oil, the time necessary to establish tan δ increases.

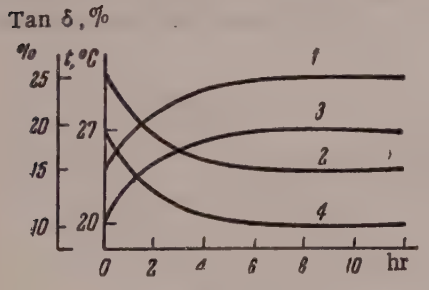


Fig. 1.

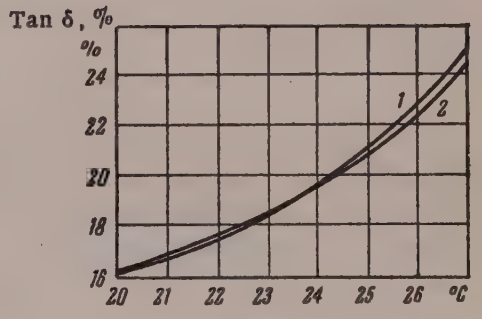


Fig. 2.

Figure 1 shows the time dependence of tan δ for a strongly humidified sample, with an initial value of tan δ = 16%, under stress (Curve 1) and after removal of the stress (Curve 2).

Putting the current on an oscillograph according to the method proposed by Gemant [3] did not reveal distortions of the sinusoidal form of the current curve; neither was there detected any change of the chemical characteristics of the oils in question. The increase of tan δ proved to be directly connected with the change of temperature of the oil. The dry oils, which are characterized by a time-constant value of tan δ in an electrical field, also showed a constant temperature. For the humidified oils the increase of tan δ with time was accompanied by an increase of the oil temperature; the initial state was restored on removal of the stress.

Curve 3 in Fig. 1 shows the increase of temperature of a humidified sample of oil containing sodium soaps, in relation to time under stress, and Curve 4 shows the lowering of its temperature on removal of the stress.

The parallel course of Curves 1 and 3 and of 2 and 4 permits the assumption that a change of tan δ with time is caused by the increase of oil temperature. As a check, from Curves 1 and 3 (Fig. 1) the relationship of tan δ and temperature was plotted (Curve 1, Fig. 2); this curve coincided with the temperature dependence of tan δ obtained for the same oil on heating (Curve 2, Fig. 2).

The heating of humidified oils in an electrical field is connected with the polar character of the water molecules. On adding water to a soap-containing transformer oil, the water is absorbed by the polar part of the soap micelles which are colloidally dissolved in the oil. The exterior portion of the micelles which is exposed to the external phase of the system (oil) consists of the nonpolar hydrocarbon chains of the soap molecules. The interior portion of the micellar structure consists of the polar groups of the soap, which are hydrated by water [4,5]. Water which penetrates into the micelle increases considerably the degree of dissociation of the soap molecules into anions (RCOO) and cations (Na), leading to a change of the mechanism of electrical conductivity of the oils. Humidification adds ionic electrical conductivity caused by the soap ions to the cataphoretic conductivity which is characteristic of the dry oils.

Thus, humidified oils are characterized by the presence of two electrical conductivities: cataphoretic and ionic. The predominance of one or the other electrical conductivity depends on the moisture content of the oils, soap concentration, temperature, and other factors. The formation of hydrated shells in itself exerts an influence on the behavior of humidified oils in an electrical field. Besides the increase of the number of dissociated particles and their mobility, the increase of tan δ is connected also with an increase of the surface of the colloidal particles and dissociated ions by the formation of the hydrated shells.

SUMMARY

1. The addition of resinous substances of naphthenic acids to a transformer oil containing sodium soaps reduces the electrical conductivity of this system, which is explained by the adsorptive interaction of the resins and naphthenic acids with the colloidal soap particles.

2. The addition of water to a sodium soap-containing transformer oil leads to a change of the character of electrical conductivity of the oils. To the cataphoretic electrical conductivity which is characteristic of the soap-containing transformer oil, there is added ionic electrical conductance.

3. The presence of water in a soap-containing transformer oil leads to an increase of the electrical conductivity with time, which is explained by the increase of the degree of dissociation of the soap molecules in the presence of water, and also by their hydration.

LITERATURE CITED

1. Ch. M. Dzhuvarly and L. A. Mukharskaya, Khim. i Tekhnol. Topliva 5, 59 (1956).
2. U. Möllinger, Archiv Für Elektrotechnik 18, No. 5, 450(1927).
3. A. Gemant, Archiv Für Elektrotechnik 23, No. 6, 683,(1930).
4. P. A. Rebinder, Kolloid. Zhur. 8, 3, 157 (1946).
5. K. A. Pospelova, Kolloid. Zhur. 11, 3, 187 (1949).

All abbreviations of periodicals in the above bibliography are letter-by-letter transliterations of the abbreviations as given in the original Russian journal. *Some or all of this periodical literature may well be available in English translation.* A complete list of the cover-to-cover English translations appears at the back of this issue.

THE EFFECT OF FREEZING ON THE PROPERTIES OF METAL HYDROXIDE COAGULATES

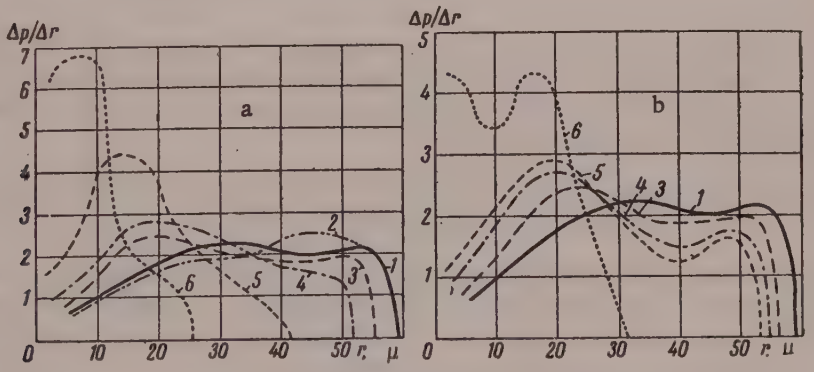
3. THE EFFECT OF ELECTROLYTES ON THE CHANGE IN PARTICLE SIZE OF IRON HYDROXIDE AND ON THE RATE OF FILTRATION

V. L. Zolotavin and V. V. Vol'khin

S. M. Kirov Urals Polytechnical Institute, Sverdlovsk
Translated from Kolloidnyi Zhurnal, Vol. 23, No. 3, pp. 276-280, May-June, 1961
Original article submitted July 17, 1959

There are almost no data in the literature on the problem of the influence of electrolytes present in metal hydroxide coagulates on the particle size of the precipitates after freezing and thawing, and on the rate of filtration of liquids through these precipitates. We have examined the influence of electrolytes, during freezing, on the volume of iron hydroxide and have put forward suggestions regarding the mechanism of this process [1]. In the present work we have made an attempt to establish possible regular features of the influence of electrolytes, during freezing, on the change in the particle size and rate of filtration for the precipitates obtained and also to confirm the suggestions previously put forward regarding the mechanism of the effect of freezing on the coagulates.

The influence of electrolytes on the particle size of an iron hydroxide precipitate after freezing. The conditions of preparation of the iron hydroxide coagulate have been described earlier [2]. The electrolytes were added separately to each specimen of iron hydroxide one hour before freezing. The particle size was determined by gravimetric sedimentation analysis by Figurovskii's method. The results of the experiments are given in the form of differential distribution curves. The Figure shows the influence of sodium and potassium nitrates on the particle size of the hydroxide precipitate at electrolyte concentrations in the coagulate of 2.5×10^{-3} to 5×10^{-1} M. The freezing process was carried out in an air thermostat at -10°.



Change in the particle size of iron hydroxide with change in the concentration of potassium nitrate (a) and sodium nitrate (b) in the original coagulate: 1) without added electrolyte; 2) 3×10^{-3} M; 3) 1×10^{-2} M; 4) 5×10^{-2} M; 5) 1×10^{-1} M; 6) 5×10^{-1} M electrolyte.

The results of the experiments show that the presence of small quantities of electrolytes during freezing leads to an increase in the particle size compared with that of the precipitate obtained from washed hydroxide, but increase in the electrolyte concentration above 10^{-2} M leads to an increase in the degree of dispersion of the precipitate. The influence of an electrolyte on the increase in the degree of dispersion and on the change in volume of the precipitate [1] depends on the ratio of the freezing temperature and the temperature of cryohydrate formation. The Figure shows that when the electrolyte forms a cryohydrate, the particle size decreases rapidly with increase in the electrolyte

concentration in the coagulate. If however the electrolyte does not form a cryohydrate at the given temperature or above, an appreciable decrease in the particle size is observed only at electrolyte concentrations greater than 1×10^{-1} M.

An analogous picture is observed for the other electrolytes studied. Thus is the case of sodium sulfate, carbonate and chromate, which form cryohydrates at -10°, the changes in the degree of dispersion of the precipitate with increase in the concentrations are the same as in the case of potassium nitrate. Sodium chloride, ammonium sulfate, and calcium nitrate, which do not form cryohydrates at the temperature of the experiment, influence the particle size in the same way as sodium nitrate. Change in the ratio of the freezing temperature and the temperature of cryohydrate formation by the electrolyte leads to a change in its influence on the particle size. The reason for the fact that a given electrolyte influences the particle size in different ways, depending on the ratio of these temperature, lies in the difference in the nature of the freezing of its solutions.

We have previously noted [1] that complete freezing of a coagulate in the presence of considerable quantities of electrolytes takes place only when the electrolytes form a cryohydrate at the temperature of the experiment or above. In the process, the layers between the ice crystals, in which the particles of hydroxide and electrolyte are concentrated, freeze in the form of a eutectic of the salt and ice. Microscope studies have shown that the eutectic freezes fairly rapidly to form a uniform mass of very fine crystals [3]. The hydroxide particles, however, are dispersed throughout the whole volume of the eutectic and are obtained in finely-dispersed form after thawing. It is natural that with increase in the electrolyte concentration in the original coagulate the volume of coagulate will be greater and the concentration of hydroxide in it lower, so that the particle size of the precipitate will show a corresponding decrease.

If the electrolyte present in the coagulate forms a cryohydrate at a temperature below the experimental temperature, complete freezing of the liquid does not take place if the electrolyte concentration is sufficiently high. The particles of hydroxide in the layers between the ice crystals, in contrast to the previous case, undergo no further change and after thawing they retain to some extent the dimensions and shape of these layers. In this case also there is a relationship between the particle size and the initial electrolyte concentration in the coagulate. The determining factor in this process is the stability of the particles of the precipitate obtained. In the presence of large quantities of electrolyte, compression of the hydroxide in the layers takes place to a lesser extent, and the condition leading to aggregation of the particles becomes less marked. In accordance with this, the hydroxide particles obtained are less stable and break down on thawing to form a precipitate similar to that formed by a coagulate which has not been frozen. This becomes particularly noticeable at electrolyte concentrations in the original coagulate of approximately 5×10^{-1} M and above.

Since at lower concentrations freezing produces the force necessary for aggregation, the particles retain their dimensions more effectively after thawing and change with change in the electrolyte concentration to a lesser extent than in the previous case (Figure). Electrolytes can also have some influence on the particle size as a result of their effect on the shape and dimensions of the ice crystals [4].

All the data obtained on the influence of electrolytes on the particle size of the precipitate confirm the previously-proposed mechanism [1] for the effect of freezing on metal hydroxide coagulates.

The influence of electrolytes on the rate of filtration. In the determination of the rate of filtration, specimens of the coagulate were filtered at -10° and thawed in air at room temperature. The rate of filtration of distilled water through the precipitate was measured not more than 8 hours after thawing. The method of measuring the rate of filtration and the treatment of the experimental results were the same as those described in our earliest work [2]. The data obtained are given in the Table.

The electrolytes can be divided roughly into three groups according to the nature of their effect on the rate of filtration at a given temperature of preparation of the precipitate.

The first group consists of electrolytes which form cryohydrates at the freezing temperature or above [KNO_3, Na_2SO_4, $Ba(NO_3)_2$ for -10°] and which decrease the rate of filtration compared with that for the precipitate obtained from iron hydroxide washed free from electrolytes. This decrease takes place in accordance with the decrease in the particle size accompanying increase in the electrolyte concentration in the original coagulate.

The second group consists of electrolytes which do not form cryohydrates under the experimental conditions and which do not contain polyvalent cations [$NaNO_3$, $(NH_4)_2SO_4$, NH_4OH for -10°]. With increase in the concentration of these electrolytes, the rate of filtration again decreases, but to a slightly lesser extent than in the previous cases, and

The Influence of Electrolytes in the Coagulate on the Rate of Filtration Through an Iron Hydroxide Precipitate

Electrolyte	S_0, cm·min^{-1}	$K\cdot10^{-5}$, cm^{-1}	S_0^*, cm·min^{-1}	$K^{**}\cdot10^{-5}$, cm^{-1}	S_0, cm·min^{-1}	$K\cdot10^{-5}$, cm^{-1}	S_0, cm·min^{-1}	$K\cdot10^{-5}$, cm^{-1}	S_0, cm·min^{-1}	$K\cdot10^{-5}$, cm^{-1}	S_0, cm·min^{-1}	$K\cdot10^{-5}$, cm^{-1}	S_0, cm·min^{-1}	$K\cdot10^{-5}$, cm^{-1}
	Electrolyte concentration M													
	$1\cdot10^{-3}$		$2{,}5\cdot10^{-3}$		$5\cdot10^{-2}$		$1\cdot10^{-2}$		$5\cdot10^{-2}$		$1\cdot10^{-1}$		$5\cdot10^{-1}$	
KNO_3	14,8	153	14,5	150	13,7	143	11,6	135	5,2	105	2,9	110	3,1	135
Na_2SO_4	14,4	148	14,2	149	12,3	133	9,8	115	3,8	106	1,0	120	1,5	200
$Ba(NO_3)_2$	18,2	190	19,0	180	17,6	162	12,9	140	3,8	140	1,3	500	—	—
$NaNO_3$	14,6	139	13,5	130	11,5	110	10,0	120	7,0	115	4,8	120	<1	620
$(NH_4)_2SO_4$	14,1	110	13,3	99	11,0	92	10,2	85	7,6	80	5,3	115	<1	650
NH_4OH	13,5	95	13,4	80	14,2	81	14,8	78	13,7	75	12,6	125	1,5	500
	Electrolyte concentration, M													
	$5\cdot10^{-5}$		$1\cdot10^{-4}$		$2{,}5\cdot10^{-4}$		$5\cdot10^{-4}$		$1\cdot10^{-3}$		$2{,}5\cdot10^{-3}$		$1\cdot10^{-2}$	
$Ca(NO_3)_2$	32,2	34	30,3	28	30,1	43	27,5	39	29,3	45	24,6	57	12,4	150
$Al(NO_3)_2$	35,3	37	37,2	41	35,6	38	29,4	42	25,6	58	19,3	61	0,9	365
$Th(NO_3)_4$	51,7	45	—	—	40,7	47	—	—	11,4	40	<1	—	—	—
HCl	33,4	33	—	—	32,3	45	23,2	49	24,7	53	10,1	118	—	—

* S_0 — rate of filtration at start of process

** K — filtration constant

this is particularly noticeable for a change in concentration from 0.05 to 0.5 M. Increase in the concentration of these electrolytes above 0.5 M, as expected from the corresponding determination of the particle size of the precipitate, leads to a sharp decrease in the rate of filtration.

The third group consists of electrolytes which again do not form cryohydrates under the conditions of the experiment, but which contain polyvalent cations or are capable of exhibiting a peptizing action (Table) and are able, when added in small quantities to a coagulate before freezing, to increase the rate of filtration through the precipitate by a factor of 3-4. This action is probably related to their ability to increase the surface charge of the particles during freezing. When the electrolyte concentration in the original coagulate reaches a value at which considerable peptization of the resultant precipitate takes place during freezing, the rate of filtration through the precipitate decreases sharply. The high rates of filtration through precipitates frozen in the presence of small quantities of iron and aluminium sulfates or ferric chloride have already been reported [5].

Thus the nature of the change in the rate of filtration through a precipitate with increase in the electrolyte concentration in the original coagulate is to a great extent determined by the ratio of the freezing temperature and the temperature of formation of a cryohydrate by the electrolyte, since the degree of dispersion of the precipitate after freezing and thawing depends on this ratio. Exceptions are electrolytes capable of peptizing the precipitate. This influence of electrolytes on the particle size and rate of filtration is in complete agreement with the proposed mechanism of the effect of freezing on the coagulate.

SUMMARY

1. The effect of freezing on the particle size and rate of filtration for an iron hydroxide coagulate in the presence of different concentrations of electrolytes has been studied.

2. Increase in the concentration of electrolytes which form cryohydrates above the temperature of freezing decreases considerably the particle size of the precipitate and hence the rate of filtration through the precipitate. Electrolytes which form cryohydrates below the temperature of freezing have a less marked effect when present in the coagulate in concentrations less than approximately 0.5 M, and decrease sharply the rate of filtration and increase the degree of dispersion of the precipitate at higher concentrations.

3. Polyvalent cations and electrolytes which are able, at definite concentrations, to peptize the coagulate during freezing, produce a further increase in the rate of filtration through the iron hydroxide precipitate by a factor of 3-4 when present in small quantities before freezing.

LITERATURE CITED

1. V. V. Vol'khin and V. L. Zolotavin, Kolloid. Zhur. 23, 2 (1961).
2. V. L. Zolotavin, V. V. Vol'khin, and V. V. Ruzvushkin, Kolloid. Zhur. 22, 305 (1960).
3. B. J. Luyet, Proc. Roy. Soc. B147, No. 929, 434 (1957).
4. Jun Arakawa, and Keiji Higuchi, Low. Temp. Sci. (Japan), N 12A, 73 (1954). Chem. Abstrs 2, 827e (1955).
5. A. S. Clements, R. J. Stephenson and C. J. Regan; J. and Proc. Inst. Sewage Purif. 318 (1950). Chem. Abstrs 4017 (1953).

All abbreviations of periodicals in the above bibliography are letter-by-letter transliterations of the abbreviations as given in the original Russian journal. *Some or all of this periodical literature may well be available in English translation.* A complete list of the cover-to-cover English translations appears at the back of this issue.

EFFECT OF GRAPHITIZATION AND INTERGRANULAR CAPILLARY CONDENSATION IN CARBON BLACK ON THE ISOTHERM AND DIFFERENTIAL HEAT OF n-HEXANE ADSORPTION

A. A. Isirikyan and A. V. Kiselev

M. V. Lomonosov Moscow University, Chemical Department
Translated from Kolloidnyi Zhurnal, Vol. 23, No. 3, pp. 281-289, May-June, 1961
Original article submitted January 30, 1960

Nowadays the adsorptive properties of industrial carbon black samples are studied extensively. This is provoked, in particular, by the need to improve the quality of the carbon blacks which are used as fillers in various media [1,2].

The chemical and adsorptive properties of carbon black can be changed by modifying its surface chemically [3,4] and also by modifying crystallochemically at high temperatures [5-9]. Thermal treatment, particularly in the case of thermal blacks [5,10-12] results in a surface which is homogeneous to a considerable extent and is composed mainly of the basal faces of graphite. Therefore, such carbon blacks are an excellent object on which to base theoretical studies on adsorption energy [7,13-17] and adsorption equilibria where adsorbate-adsorbate interactions are taken into account [10, 17-19].

A very clear characteristic for both the inhomogeneity of the surface and for adsorbate-adsorbate interactions is obtained by studying the differential heats of adsorption. An investigation of the effect which thermal treatment at 1000, 1500, 2000 and 2700° has upon the shape of the differential heat curves for argon adsorption at -195° has shown [6] that, when the temperature of treating the channel black Spheron-6 is raised to 2000° or higher (which corresponds to a complete removal of chemical surface compounds and to growth and orientation of the crystallites), the initial region where the adsorption heats fall sharply at increasing coverage, which drop is connected with the inhomogeneity of the surface, practically disappears. When the heats of krypton adsorption on the thermal carbon black P-33 treated at 2700° were measured [11] such a region could no longer be found.

By investigating the heats of SO_2, CO_2 and NH_3 adsorption on graphitized thermal carbon blacks [12] it has been shown that in the case of CO_2 a very weak degree of inhomogeneity becomes apparent in raised adsorption heats in the initial regions of coverages for the sample Sterling FT, 2700°, with a surface area 12.5m^2/g, similarly for the carbon black P-33, but is not found for the sample Sterling MT, 3100°, which has a smaller surface area, viz., 6.3 m^2/g. For the latter sample in the case of NH_3 adsorption a somewhat raised heat of adsorption is still found in the very beginning.

It is of great interest to investigate the adsorption heats of hydrocarbons [7,8,14,20-22] and their derivatives [23] on graphitized carbon blacks with a surface as homogeneous as possible. Here it is of great importance to know the reasons for the residual inhomogeneity of the surface; these may be: 1) imperfect emergence of the basal faces of the graphite crystallites on the surface, 2) the presence of contacts between the crystallites on the surface of the carbon black granules and possibly a slight protrusion of prismatic faces; 3) the presence of contacts between the carbon black granules in the powder. In the paper [22] we discussed the third cause of inhomogeneity.

In the present study we investigated the effect which thermal treatment of channel and thermal blacks has upon the heat of n-hexane adsorption. Here it has been studied and taken into account how the powered granules are compressed by the liquid menisci between the granules, which compression occurs during the sorption process itself as a result of capillary condensation in the free spaces between the granules [24].

We used carbon black Spheron-6 heated in a helium atmosphere at 2800° [4,22] and the highly disperse thermal black T-1 heated during 45 min at 3000° [19]. The specific surface areas of these carbon blacks were determined by the BET method from nitrogen and n-hexane adsorption. The measurements with n-hexane were done in the study [25] where the apparatus and the experimental procedure were also described. When working with the thermal black, which has a small surface area, we were obliged to take a greater amount; because of this the carbon black was filled in a

calorimetric case without copper discs [25], but this gave only a small increase in the main calorimetric period. All experiments were done at a temperature of about 20°.

The isotherm of n-hexane adsorption on the carbon black T-1, 3000°, is shown in Fig. 1. The first series of measurements carried out up to the relative vapor pressure $p/p_s = 1$ showed that the loosely filled sample had a free sorption volume $v_s = 0.8$ cm³/g and gave a rather broad hysteresis loop in the region of high p/p_s. At small p/p_s values, up to $p/p_s = 0.05$, a small hysteresis loop was found too. After evacuating the sample at 350° and repeating the experiments, the isotherm at $p/p_s > 0.05$ did not coincide with the first one, whereas v_s had decreased to 0.5 cm³/g, the hysteresis loop had narrowed and upon desorbing from $p/p_s = 1$, hysteresis disappeared at $p/p_s = 0.4$.

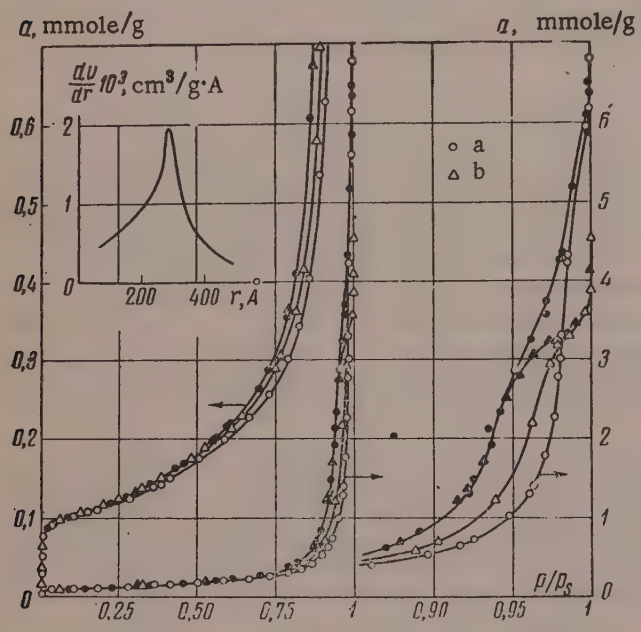


Fig. 1. Adsorption isotherm of n-hexane on the carbon black T-1, which had been heated at 3000°: a) first series, b) second series of measurements; inset above, distribution of the pore volume plotted versus the corresponding radius. Here and elsewhere filled points denote desorption.

In Fig. 2 the differential heats of n-hexane adsorption are plotted. The degrees of coverage of the carbon black T-1, 3000° (the curve with experimental points). The initial heat of adsorption is high, but at 10-15% surface coverage it rapidly decreases to 11.7 kcal/mole and drops again sharply to a value surpassing only slightly the heat of condensation L (the dashed line in Fig. 2). Measuring the heats of multimolecular adsorption was here still more difficult than was the case for Spheron-6, 2800° [22].

The general shape of the adsorption isotherm. Compression of carbon black by capillary condensation. During the first complete adsorption-desorption cycle (Fig. 1) the pore structure changed sharply. In this cycle the sample consisting of separate granules is compressed by capillary forces [24] and this process is not complicated by particle growth and coalescence, as occur in the formation of xerogels by drying hydrogels. The capillary compression results mainly from the hydrostatic pressure [24,26] ΔP

$$\Delta P = \frac{\Delta\mu}{v_m} \approx \frac{RT \ln p/p_s}{v_m} = \frac{4\sigma}{d} \approx 12(\text{atm}), \quad (1)$$

where $\Delta\mu$ is the change in the chemical potential of the adsorbate; v_m the molar volume of the liquid; σ the surface tension; d the effective pore diameter at the maximum of the distribution curve in Fig. 1.

The samller the size of the carbon black granules and the higher the σ of the wetting liquid, the stronger the compression of the sample. Such a sorptive compression occurs during wet agglomeration because the carbon black paste shrinks considerably when dried. Because the adsorbent in the first measuring cycle was compressed by the capillary condensation, we also got a hysteresis loop, which reached further into the region of small p/p_s (in comparison with the loop of the first adsorption). When the series of measurements was repeated, we did not find hysteresis in the region of small p/p_s, since the sample had already been partly compressed. A sample compressed in the first adsorption-desorption cycle continues to keep its porosity and gives a reproducible hysteresis loop of capillary condensation. The phenomenon of sorptive compression, which raises the number of contacts between the particles, results, of course in some additional inhomogeneity [22]. However, in the case of thermal carbon blacks with coarse particles the effect of this inhomogeneity on the initial part of the isotherm and the adsorption heat is small. Some structural characteristics of the carbon blacks are given in Table 1.

Effect of a thermal treatment of carbon blacks upon the adsorption isotherm of n-hexane. The adsorption isotherms of n-hexane on the carbon black Spheron-6 outgassed at 900° [7], heated in hydrogen at 1700° [7] or in helium at 2800° [22] and also those on the carbon black T-1 heated at 3000° are compared in Fig. 3. The sample T-1, 3000° for which the initial, sharply convex part of the isotherm is the smallest, has the most homogeneous surface. Further on, the isotherm of hexane adsorption on the carbon black T-1, 3000°, corresponds to mainly monomolecular adsorption on the relatively homogeneous part of the surface. Here at first the isotherm is even slightly concave, which,

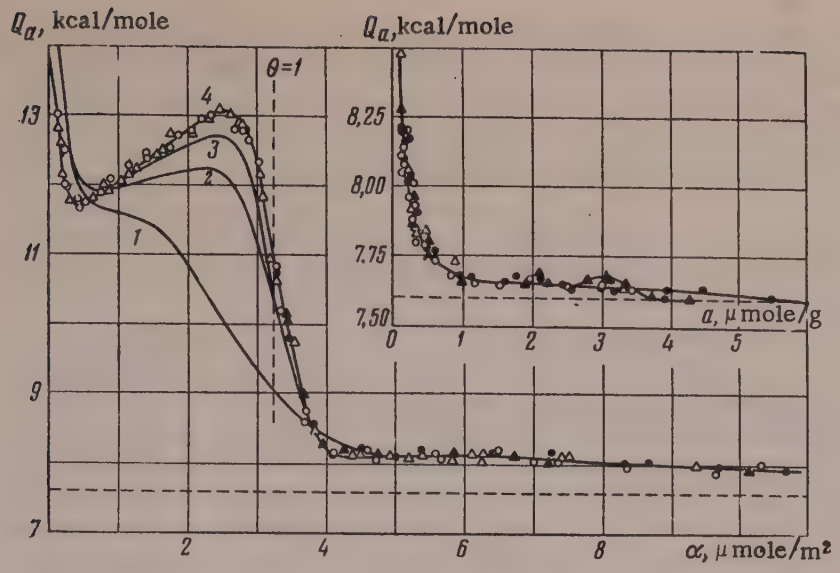


Fig. 2. Differential heats of n-hexane adsorption on the carbon blacks: 1) Spheron-6, 900°; 2) Spheron-6, 1700°; 3) Spheron-6, 2800°; 4) T-1, 3000°. Above to the right: heat of multimolecular adsorption and capillary condensation of n-hexane on the carbon black T-1, 3000°. The dashed horisontal line represents the heat of condensation L.

TABLE 1. Structural Characteristics of the Graphitized Carbon Blacks and Their n-Hexane Adsorption Isotherms

Carbon black	Specific surface area S_{N_2}, m^2/g	Pore volume v_s, cm^3/g	Pore diameter, d	Mean number of particle contacts, n	BET constant, C	Film area m^2/g	
						s'_A	s'_Q
Spheron-6, 2000°	90	1.0	340	38	650	108	85
T-1, 3000°	29.1	0.8→0.5	600	4.3→5.5	950	35	30

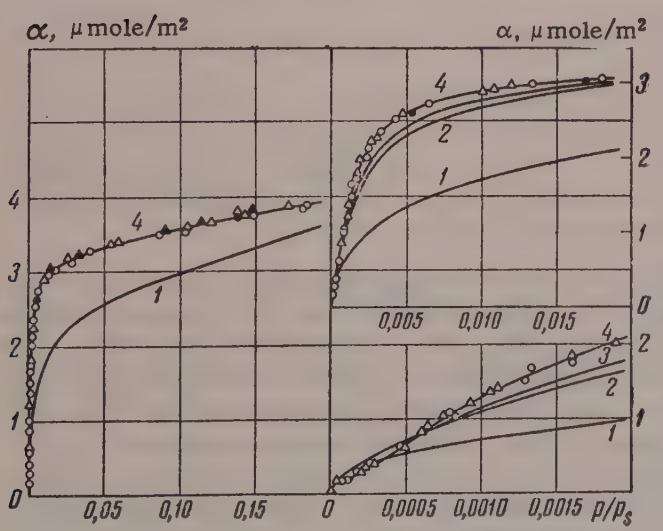


Fig. 3. Isotherms of n-hexane adsorption on the carbon blacks: 1) Spheron-6, 900°; 2) Spheron-6, 1700°; 3) Spheron-6, 2800°; 4) T-1, 3000°.

obviously, is connected with the mutual attraction between the adsorbed molecules on the homogeneous part of the surface. The n-hexane adsorption isotherm on the carbon black T-1, 3000°, in the p/p_s range from 0.002 to 0.25 is satisfactorily described by the BET equation and this is connected with the fact that the mutual interaction between the adsorbed molecules is only a relatively small contribution to the total adsorption energy [18,19,27]. When the temperature of the heating is increased and one goes from channel carbon blacks to thermal ones, the constant C of the BET equation rises (table 1).

Differential heat and entropy of adsorption. In agreement with the adsorption heats measured for argon [6], the thermal treatment of the channel carbon black Spheron-6 at a temperature of ~900° resulted in a sharp change in the character of the relation between the differential heat of n-hexane adsorption and the degree of coverage θ in the region where mainly a monolayer is filled; that is, it changes from a continuously falling curve for the sample treated at 900° to a curve with a sharp rise for the sample

treated at 1700° [7] and to a still more steeply rising curve for the sample treated at 2800° [22]. For carbon black T-1, 3000°, the region of the initial drop in adsorption heat on the remaining inhomogeneous part of the surface has contracted very clearly and the rise of the adsorption heat in the region where the first layer is filled is very steep. It should be emphasized that even in this case, in a contracted θ region, we still got an initial drop of the adsorption heat, that is, the sample had some residual inhomogeneity (Fig. 2).

TABLE 2. Differential Heats of n-Hexane Adsorption on Graphitized Carbon Blacks at Various Degrees of Monolayer Coverage and Integral Molar Values of the Heat, Free Energy and Entropy of Monolayer Adsorption

Carbon black	Differential values kcal/mole				Intermolar values θ to 0 and 1		
	Standard Q_a^0 (θ = 0.5)	Initial Q_a^0 a (θ = 0)	Minimum Q_a, min	Maximum Q_a, max	Q_m, kcal/mole	A_m, kcal/mole	ΔS_m, cal/degree·mole
Spheron-6, 900°	11.3	12.0	–	–	–	–	–
Spheron-6, 1700°	12.10	11.8	11.9	12.2	–	–	−2.6
Spheron-6, 2800°	12.35	11.6	11.9	12.7	12.0	3.77	−3.5
T-1, 3000°	12.55	11.4	11.7	13.1	12.43	3.85	−3.4

The standard (at θ = 0.5) values of the differential heat of adsorption Q_a^0 are given in Table 2. When the temperature of graphitizing Spheron-6 is raised from 900 to 1700°, Q_a^0 rises steeply, but when this temperature is raised from 1700 to 2800°, the rise is considerably smaller.

For the carbon black T-1, 3000°, obviously, Q_a^0 is very close to the limit value for adsorption on the basal face of a perfect graphite crystal. When the temperature of graphitizing is raised, the inhomogeneity of the surface decreases, but it does not disappear completely. For the carbon black T-1, 3000°, the region where mainly the inhomogeneous part of the surface is filled still extends to θ = 0.1-0.15. This inhomogeneity has been related to the junctions of the basal crystal faces in the carbon black granules [19, 28]. When thermal blacks are heated at 3000°, the size L_a of the basal faces in the separate crystallites is about 150 A [11]. The amount of n-hexane adsorbed on the perimeter of the junctions between these faces is about 0.2 μmole/m² or θ = 0.1 in the case of the sample T-1, 3000°, that is, it is nearly as much as the amount consumed in covering mainly the inhomogeneous part of the surface. About the same amount of n-hexane may be adsorbed around the contacts between the various carbon black granules where crystallites of adjacent granules touch.

In the case of n-hexane adsorption on the carbon black T-1, 3000° Q_a increases approximately linearly with θ, in the range θ = 0.1-0.8

$$Q_a = 11{,}4 + 2{,}3\ \theta,\ \text{kcal/mole}. \qquad (2)$$

Extrapolating the linear relation of the adsorption heat for the carbon blacks Spheron-6, 1700°, Spheron-6, 2800° and T-1, 3000° to θ = 0 gives little differing $Q_{a(\theta=0)}$ values (Table 2). For this reason in the range of small coverages the rise in adsorption heat at increasing n-hexane coverages (in contrast with the adsorption heats of alcohols [23]) cannot be great. For the initial adsorption heat of isolated hexane molecules on an ideal basal plane of graphite one may take $Q_{a(\theta=0)} = 11.5 \pm 0.3$ kcal/mole, which is close to the value found previously [7].

The plots of the differential adsorption entropies of n-hexane. θ for the graphitized carbon blacks (Fig. 4) enables us to elucidate the effect which the increasing homogeneity of the carbon surface at raised heating temperatures has upon the adsorption properties. For the samples heated at lower temperatures the region of strong adsorption with restricted molecular mobility at small coverages is broader (the dashed parts of the curves). Owing to the less sharp transition between monomolecular and multimolecular adsorption, for these samples the restriction of mobility caused by adsorbate-adsorbate interactions is found only in the form of a small minimum in the curve for the adsorption entropy. Graphitization at higher temperatures partially eliminates the formation of immobile complexes at small θ and more clearly reveals the restrictions by adsorbate-adsorbate interactions when θ = 1 is approached (the minimum in the adsorption entropy curve is lowered to -8 eu). After a monolayer has been filled the curves for all samples practically coalesce. The path of the dashed curve, which connects the minima in the entropy curves, also indicates that the surface properties of thermal carbon blacks heated at 3000° are nearly equal to those in the limit of the homogeneous surface of the graphite basal face. In the paper [29] it has been noted that the limit of complete graphitiza-

tion is reached in the vicinity of 3200°. For the perfectly homogeneous graphite surface the differential adsorption entropy at small coverages is higher than the entropy of the adsorbate in the normal liquid state.

The linear relation, visible in Fig. 4, between ΔS_a and θ in a broad range of monolayer coverages ($\sim\theta$ from 0.1 to 0.8) on the sample T-1, 3000°, which has the most homogeneous surface, is probably characteristic for the relation between the differential adsorption of strongly adsorbed substances and the coverages of homogeneous surfaces in similar cases. This may simplify future calculations of adsorption equilibria. In the said range the adsorption entropy on the carbon black T-1, 3000°, is given by

$$\Delta S_a = 4{,}0 - 15{,}5\ \theta,\ \text{eu} \qquad (3)$$

The region of multimolecular adsorption and capillary condensation. After the sharp drop in adsorption heat near the complete filling of a monolayer, further (multimolecular) adsorption is accompanied by very small values of the net heat of adsorption Q_a-L. Moreover, already beyond $\theta \approx 1.5$ capillary condensation of hexane at the contacts between the carbon black granules sets in, so that the heat of capillary condensation is superimposed on the heat of multimolecular adsorption. Obviously, the net heat of multimolecular adsorption is very small at $\theta > 2$ and the heat effect, here, is mainly connected with capillary condensation. Near the completion of the second and the third layer we were unable to detect noticeable maxima, whereas they were found in the case of argon [6] and n-octane [30] adsorption on the carbon black Spheron-6 treated at 2700° [6] or 1700° [30].

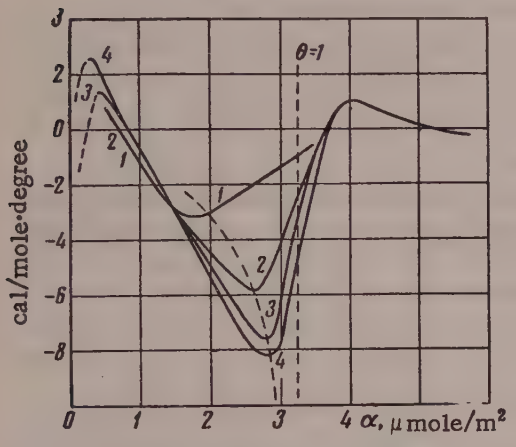


Fig. 4. Differential adsorption entropies of n-hexane on the carbon blacks: 1) Spheron-6, 900°; 2) Spheron-6, 1700°; 3) Spheron-6, 2800°; 4) T-1, 3000°.

Above in Fig. 2 the complete curve for the differential heat of multimolecular adsorption and capillary condensation is shown. The first series of measurements gave a Q_a falling monotonously down to L at saturation. However, in the second series, after the first one the carbon black has been compressed by capillary condensation at the end of the sorption process. Such maxima, which are connected with changes in the meniscus curvature of the sorbed liquid in the pore mouths, have been investigated by us in deatil for vapor adsorption on silicagels [26, 31] and mechanically compressed samples of carbon black [22].

A calculation of the integral net heat and free energy of adsorption from $\theta = 1.5$ to saturation enabled us to determine, just as was done in the paper [22], values for the surface area of the adsorbed films formed at $\theta \approx 1.5$: s'_A (via the integral free energy of capillary condensation); these values are given in Table 1. In this case the accuracy of the determination is low, because it is difficult to estimate where capillary condensation starts, this condensation occurs near to $p/p_s = 1$ where the free energy change by the simultaneously proceeding multimolecular adsorption can no longer be neglected [22] and also, because in this region Q_a-L is very small [22]. The total integral heat and free energy of adsorption, which are equal to the heat and free energy of wetting, amounted to 123 and 84 erg/cm^2, respectively. These values are close to those calculated in the paper [7] (123 and 82 erg/cm^2) and, as concerns the heat of wetting, also to the directly measured value (118 erg/cm^2 [32]).

SUMMARY

1. We have measured (up to saturation) the isotherm and the differential heat of n-hexane vapor adsorption on a thermal carbon black (T-1) heated at 3000° and having a specific surface area of 29.1 m^2/g.

2. It was revealed that capillary condensation compresses the carbon black during the first adsorption-desorption cyclus.

3. The isotherms and the differential heats of n-hexane adsorption on the channel carbon black Spheron-6 heated at 900, 1700 or 2800° and those on the thermal carbon black heated at 3000° have been compared. The carbon black surface is homogenized intensively up to 1700° and the process becomes slower, when the heating temperature is raised further. The surface of the carbon black sample heated at 3000° still has a small residual inhomogeneity, which becomes apparent in the sharp drop in adsorption heat found when the first 10% of the surface is covered.

4. In the range of 10 to 80% monolayer coverage the adsorption heat and entropy change approximately linearly with the degree of coverage.

5. We have determined the standard differential and integral values of the heat, free energy and entropy of adsorption, the adsorption heat at zero coverage of "the basal face of graphite" and the heat and free energy of wetting.

LITERATURE CITED

1. M. H. Polley, D. W. Schaeffer and W. R. Smith, Canad. J. Chem. 33, 314 (1955);W. D. Schaeffer and W. R. Smith, Industr. and Engng Chem. 47, 1286 (1955).
2. V. V. Kel'tsev and P. A. Tessner, Carbon Black: Its Properties, Production and Use [in Russian] (Moscow-Leningrad, 1952).
3. R. N. Smith, D. Lesnini and J. Mooi, J. Phys. Chem. 61, 81 (1957).
4. A. V. Kiselev, N. V. Kovaleva, A. Ya. Korolev and K. D. Shcherbakova, Doklady Akad. Nauk SSSR 124, 617 (1959); V. I. Lygin, N. V. Kovaleva, N. N. Kavtaradze and A. V. Kiselev, Kolloid. Zhur. 22, 334 (1960).
5. M. H. Polley, W. D. Schaeffer and W. R. Smith, J. Phys. Chem. 57, 469 (1953).
6. R. A. Beebe, and D. M. Young, J. Phys. Chem. 58, 93 (1954).
7. N. N. Avgul', G. I. Berezin, A. V. Kiselev and I. A. Lygina, Zhur. Fiz. Khim. 30, 2106 (1956).
8. N. N. Avgul', G. I. Berezin, A. V. Kiselev and A. Ya. Korolev, Kolloid. Zhur. 20, 298 (1958).
9. A. V. Kiselev and N. V. Kovaleva, Izvest. Akad. Nauk SSSR, Otdel. Khim. Nauk, 989 (1959).
10. S. Ross, and W. Winkler, J. Colloid Sci. 10, 319, 330 (1955); S. Ross and W. Pultz, J. Colloid Sci. 13, 397 (1958).
11. C. H. Amberg, W. B. Spencer and R. A. Beebe, Canad. J. Chem. 33, 305 (1955).
12. R. A. Beebe and R. M. Dell, J. Phys. Chem. 59, 746 (1955);W. B. Spencer, C. H. Amberg and R. A. Beebe, J. Phys. Chem. 62, 719 (1958).
13. R. M. Barrer, Proc. Roy. Soc. A161, 476 (1937).
14. N. N. Avgul', A. A. Isirikyan, A. V. Kiselev, I. A. Lygina and D. P. Poshkus, Izvest. Akad. Nauk SSSR, Otdel. Khim. Nauk, 1314 (1957); N. N. Avgul', A. V. Kiselev, I. A. Lygina and D. P. Poshkus, Izvest. Akad. Nauk SSSR, Otdel. Khim. Nauk, 1196 (1959).
15. A. D. Crowell and D. M. Young, Trans. Faraday Soc. 49, 1080 (1953).
16. A. D. Crowell, J. Chem. Phys. 22, 1897 (1954).
17. E. L. Pace, J. Chem. Phys. 27, 1339 (1957).
18. A. V. Kiselev, Kolloid. Zhur. 20, 338 (1958); A. V. Kiselev, N. V. Kovaleva, V. A. Sinitsyn and E. V. Khrapova, Kolloid, Zhur. 20, 444 (1958).
19. A. V. Kiselev and E. V. Khrapova, Kolloid. Zhur. 23, 163 (1961).
20. R. A. Beebe, M. H. Polley, W. R. Smith and C. B. Wendell, J. Amer. Chem. Soc. 69, 2294 (1947).
21. J. W. Ross and R. J. Good, J. Phys. Chem. 60, 1167 (1956).
22. A. A. Isirikyan and A. V. Kiselev, Kolloid. Zhur. 23, 67 (1961).
23. N. N. Avgul', G. I. Berezin, A. V. Kiselev and I. A. Lygina, Izvest. Akad. Nauk SSSR, Otdel. Khim. Nauk SSSR No. 2 (1961).
24. A. A. Isirikyan, Zhur. Fiz. Khim. 34, 1652 (1960).
25. A. A. Isirikyan and A. V. Kiselev, Zhur. Fiz. Khim. 31, 2127 (1957).
26. A. V. Kiselev, Proc. of the Second International Congress on Surface Activity, Vol. 2 (London, 1957), p.189.
27. A. A. Isirikyan and A. V. Kiselev, Zhur. Fiz. Khim. 34, 2817 (1960).
28. W. R. Smith and M. H. Polley, J. Phys. Chem. 60, 689 (1956).
29. J. Biscoe, and B. E. Warren, J. Appl. Phys. 13, 364 (1942).
30. N. N. Avgul', G. I. Berezin, A. V. Kiselev and I. A. Lygina, Izvest. Akad. Nauk SSSR, Otdel. Khim. Nauk 1021 (1957).
31. A. A. Isirikyan and A. V. Kiselev, Doklady Akad. Nauk SSSR 110, 1009 (1956); Zhur. Fiz. Khim. 32, 639 (1958); A. A. Isirikyan, Collection: "Methods of Investigating the Structure of Highly Disperse and Porous Solids" [in Russian] (Acad. Sci. USSR Press, 1958), p. 85.
32. F. E. Bartell, and R. M. Suggit, J. Phys. Chem. 58, 36 (1954).

SPECIFIC FEATURES IN THE STABILIZATION OF BITUMINOUS AND TAR EMULSIONS FOR USE ON ROADS

L. Ya. Kremnev and L. A. Borodina

The All-Union Scientific Research Institute for Roads, Leningrad Branch
Translated from Kolloidnyi Zhurnal Vol. 23, No. 3, pp. 290-294, May-June, 1961
Original article submitted February 29, 1960

Special features have been observed in the formation of bituminous and tar emulsions which are not characteristic of two immiscible liquids of low Newtonian viscosity. In considering the emulsification process we start with the bitumen or tar as a thixotropic structurized liquid at a definite temperature. A hard grade of bitumen is in a semiplastic state resembling a solid at ordinary temperature, and changes to a highly structurized liquid above 40° [1]. With further rise in temperature, the high effective (structural) viscosity of the bitumen falls considerably, as the result of break down of the three-dimensional structure due to the kinetic energy of thermal motion, and the bitumen behaves as a Newtonian liquid above 140°.

In accordance with these conceptions of P. A. Rebinder, it was found [1] that bitumens, in the structurized liquid state, showed the enormous true viscosity of the practically unbroken structure at low velocity gradients, and the lowest true viscosity of the limiting broken down structure under flow conditions corresponding to a high velocity gradient.

Bitumens and tars can only be emulsified, either at high or low viscosity gradients, when in the state of a structurized liquid, and this fact also determines the choice of method of mechanical dispersion. Circulating homogenizers of the Gurrel type cannot be used for obtaining highly concentrated emulsions of high dispersion, with concentrations by volume of disperse phase considerably exceeding that corresponding to dense packing of uniform spheres, since the high velocity gradients break down the thin protective films which separate the deformable droplets of a highly concentrated emulsion. On the other hand, the possibilities of obtaining and using highly concentrated emulsions are of particular interest for road construction.

Highly Concentrated Emulsions. Hard grade bitumens and tars are in the state of structurized liquids at relatively low temperatures (above 40°), so they can be emulsified with the aid of paddle stirrers. It is recommended that a slow stirring rate should be used (up to 100 rpm) in order to avoid breaking down the protective film between the droplets with highly concentrated emulsions.

If a hard grade of bitumen is preheated to 60-90° and added gradually to an aqueous solution of emulsifier at the same temperature, then the effect of stirring is to give a highly concentrated or saturated emulsion of the oil in water (O/W) type, which can readily be diluted with water to any desired concentration. The table shows the production, by means of a paddle stirrer, of a saturated emulsion of bitumen grade BN-II, , using the cationic emulsifier VA-20 i.e. methylethyl(2,5-dioctylphenoxyeicosaethyleneoxidomethyl)ammonium benzenesulphonate.

Emulsification was carried out in seven stages; there was an increase in the bitumen concentration of the emulsion at every stage up to the saturated direct emulsion at the sixth stage, containing 94.6% of bitumen. Further increase in concentration caused a change from a direct to an inverse emulsion (phase inversion), i.e., to a dilute water in oil system.

Fig. 1 shows emulsification curves for bitumen grade BN-II over wide concentration ranges of the cationic emulsifier VA-20 and the anionic emulsifier ssr (sulfite-spirit residue). Direct saturated emulsions were not formed at low emulsifier concentrations. The direct emulsions formed with high emulsifier concentrations were highly disperse; Fig. 2 shows that the maximum on the differential drop size distribution curves corresponded to about 1μ, which corresponded with the results of kinetic analysis of the emulsification process [2].

Some Special Features of theEmulsification of Bitumens and Tars. When assessing the final results of emulsification, we must not only consider the thixotropic structurized liquid state of the bitumen (or tar), but must also take into account the presence in these of oleophilic surfactant substances which can form reverse emulsions of the W/O type.

Direct O/W type emulsions will, therfore, only be formed after the tendency has been overcome for these oleophilic emulsifiers to emulsify water. There is an antagonistic interaction here between the hydrophilic emulsifier in the aqueous phase and the oleophilic emulsifiers in the system. It has been shown that equivalent quantities of these antagonistic emulsifiers neutralize each other [3], and do not take part in the emulsification process. Only the excess of hydrophilic or hydrophobic emulsifier can take part in emulsification. Fig. 3 shows isotherms for the emulsification of bitumen grade B-5, at normal temperature, under these conditions.

Production of Saturated Emulsion from Bitumen Grade BN-II, with Bitumen Temperature 85°, Emulsification Temperature 60°, Emulsifier Concentration 50% w/w, Weight of Aqueous Emulsifier Solution 20 g

Emulsification stage	1	2	3	4	5	6	7
Weight of bitumen in emulsion, g	40	100	162	212	276	352	364
Emulsion concentration, % w/w	66.6	83.4	89,0	91.4	93,2	94.6	5.5
Emulsion type	O/W	O/W	O/W	O/W	O/W	O/W	W/O

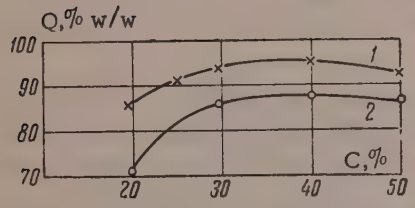


Fig. 1. Bitumen BN-II concentrations (Q,% w/w) in saturated emulsions as a function of the emulsifier concentration (C, % w/w) in the aqueous solution: 1) VA-20, 2) ser.

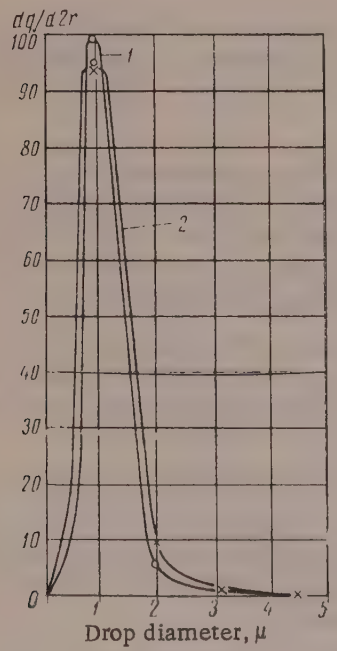


Fig. 2. Differential curves for drop size distribution in saturated emulsions with 50% aqueous solutions of: 1) VA-20, 2) ser.

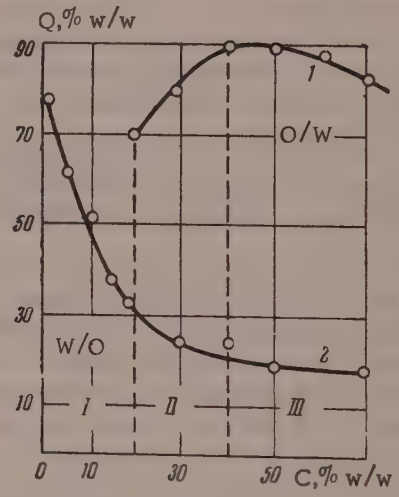


Fig. 3. Limiting concentrations of disperse phase (Q, % w/w) as a function of the emulsifier concentration (C, % w/w). 1) Direct emulsions; 2) inverse emulsions.

It follows, from Fig. 3, that bitumen can form direct and inverse emulsions with one and the same hydrophilic emulsifier. Gradual introduction of aqueous emulsifier solution gives rise to a reverse emulsion of the W/O type. Stirring of the same aqueous emulsifier solution and addition of bitumen eventually gives rise to a direct saturated emulsion of the O/W type. There are three separate ranges of emulsifier concentration with different effects on the emulsification process. Only inverse emulsions can be obtained in range I (Fig. 3), and their concentration decreases with increasing emulsifier concentration (pure water gives a 78.8% emulsion). In this range of relatively low emulsifier concentration, all the added hydrophilic emulsifier and a corresponding quantity of oleophilic emulsifier from the bitumen are neutralized, and this leads to a reduction in the concentration of the disperse phase. This neutralization and exclusion from the emulsification process of all the hydrophilic emulsifier makes it impossible to obtain direct emulsions in range I.

In range II (medium emulsifier concentration) there is a small decrease in the disperse phase concentration in inverse emulsions (curve 2), which may be due to a change in the structural-mechanical properties of the bitumen under the influence of the hydrophilic emulsifier. Direct emulsions can also exist in this range; these are coarse at first, and more disperse later.

In range III, depending on the conditions as discussed above, emulsions of both types can be stabilized with equal success. There is here sufficient excess of hydrophilic emulsifier over the antagonistic oleophilic emulsifier to stabilize direct emulsions (the slight decrease in disperse phase concentration with increasing emulsifier concentration, shown by the curve, can be attributed to an increase in droplet dispersion in the saturated emulsions). As in range II, inverse emulsions are completely stabilized at these hydrophilic emulsifier concentrations by the three-dimensional mechanically strong structure of the bitumen, which includes droplets of aqueous phase. In spite of the high hydrophilic emulsifier concentration, the aqueous phase is invariably in a dispersed state in accordance with Rebinder's ideas [4], and the structural mechanical barrier ensures that the system shall be highly stable.

Repeated Phase Inversion. Inversion of a concentrated direct O/W type emulsion into an inverse W/O type emulsion usually occurs when there is a change in emulsifier properties, as by the conversion of a hydrophilic alkaline soap to an oleophilic alkaline earth soap, or by salting out of the soap from the aqueous solution with a neutral electrolyte. Experimental data on this matter is mainly concerned with two immiscible liquids of low viscosity [5]. Highly concentrated emulsions break down under these conditions, when phase inversion is attempted.

As seen above, thixotropic structurized liquids, such as bitumens and tars, form either direct or inverse emulsions depending on the emulsification conditions. This makes it possible to obtain repeated phase inversion.

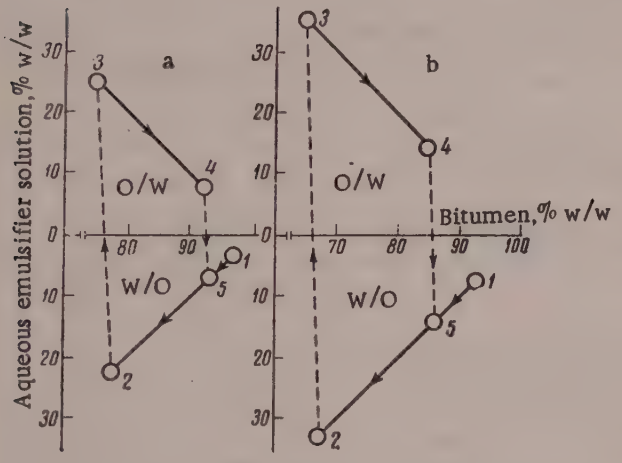


Fig. 4. Cycle of repeated phase inversion in emulsions. a) With VA-20, b) with ssr. The numbers show the successive stages of the emulsion and of its inversion in the cycle. The continuous lines show stable emulsion states, and the dotted lines show phase inversion.

A W/O type emulsion is always formed in the first stages of stirring a liquid structurized bitumen with an aqueous solution of hydrophilic emulsifier; the aqueous phase droplets in this can be stabilized by oleophilic surfactant present in the bitumen or by the mechanically strong bitumen structure. Such an inverse emulsion, like the original bitumen, is a connected structural system, i.e., a three-dimensional lattice filled with liquid aqueous droplets. The maximum concentration of an inverse emulsion depends on the emulsifier content in the aqueous phase, but is usually considerably less than corresponds to the limiting packing density of uniform droplets (Curve 2 of Fig. 3).

In the process of stirring with excess of aqueous emulsifier solution, the W/O type emulsion inverts, and the resulting direct emulsion easily reaches its limiting concentration as successive fresh portions of bitumen are dispersed in it. In turn, the resulting saturated O/W type emulsion again inverts to a W/O type emulsion when stirred with a slight excess of nonemulsified bitumen. This completes one cycle of phase inversion, which can be repeated several times, i.e., there can be repeated phase inversions according to the scheme $(W/O \rightleftarrows O/W)_n$; the restriction is the dimensions of the vessel in which emulsification is carried out.

Fig. 4 shows the results of emulsification and phase inversion obtained at normal temperature which bitumen grade B-5 and aqueous solutions of anionic and cationic hydrophilic emulsifiers. We carried out 4-5 cycles of inversion without difficulty.

The mechanisms for phase inversion are different with direct and inverse emulsions. In the case of saturated direct emulsions, the bitumen droplets, in the shape of deformed pentagonal dodecahedra, are separated by a thin film of aqueous emulsifier solution, which prevents them from coalescing. According to our data, obtained from complete differential curves for drop size distribution, the smallest (critical) thickness for the protective film in direct bitumen emulsions is of the order 10^{-6} cm. The continuous three-dimensional lattice of thin protective water films is not very strong [6], so that the saturated emulsion can be broken down by mechanical action and it is suffi-

cient to stir it with a small excess of nonemulsified bitumen (Table, stage 7). When the lattice is broken down, the individual aqueous films take on the form of spherical droplets under the influence of surface tension molecular forces. These aqueous droplets are enclosed in the new continuous three-dimensional lattice formed by coalescence of the unprotected bitumen droplets. In this way the direct emulsion is converted into an inverse emulsion, whose high stability can be explained by a structural-mechanical barrier. The concentration of this inverse emulsion can be increased to a known value by stirring with additional water or with aqueous emulsifier solution.

W/O type emulsions are gel-like systems of bitumen with entrained water droplets; they disperse in excess of aqueous emulsifier solution under favorable conditions, and are inverted from W/O to O/W type emulsions.

The above special features, including a capacity for repeated phase inversion, are inherent in bitumens and tars of various grades.

SUMMARY

1. Depending on the emulsification conditions, road bitumens and tars can be obtained as direct or inverse emulsions when added to an aqueous hydrophilic emulsifier medium.

2. The oleophilic surfactants existing in the organic binding materials interact antagonistically with the hydrophilic emulsifier in the aqueous solution. This antagonistic action effectively neutralises the action of equivalent quantities of both types of emulsifier, and theresulting emulsifying action is due to the excess of hydrophilic or oleophilic emulsifier.

3. It has been shown that it is possible to produce repeated phase inversion with road emulsions.

4. A main factor in the stability of road emulsions is the structural-mechanical barrier, as described by Rebinder.

5. High concentration and saturated direct bitumen emulsions have been obtained and investigated, using both anionic and cationic emulsifiers.

LITERATURE CITED

1. N. V. Mikhailov, and S. Ya. Shalyt, Kolloid. Zhur. 18, 609 (1956).
2. L. Ya. Kremnev and A. A. Ravdel', Kolloid. Zhur. 16, 17 (1954).
3. L. Ya. Kremnev, Kolloid. Zhur. 20, 546 (1958).
4. P. A. Rebinder, Kolloid. Zhur. 20, 527 (1958).
5. V. Clayton, Emulsions [Russian translation] (Edited N. A. Rebinder, IL, M., 1950).
6. L. Ya. Kremnev and S. A. Soskin, Kollidn. Zhur. 11, 24 (1949).

All abbreviations of periodicals in the above bibliography are letter-by-letter transliterations of the abbreviations as given in the original Russian journal. *Some or all of this periodical literature may well be available in English translation.* A complete list of the cover-to-cover English translations appears at the back of this issue.

THE POROUS STRUCTURE OF ELECTROPHORETIC DEPOSITS

I. S. Lavrov

Lensovet Leningrad Technological Institute
Translated from Kolloidnyi Zhurnal, Vol. 23, No. 3, pp. 295-298, May-June, 1961
Original article submitted February 10, 1960

The heat-resistant electrically-insulating coatings on the heating filaments of radio valves and other current-carrying apparatus, and the carbonate coatings on the cores of oxide cathodes, are readily obtained by the electrophoretic precipitation of suspensions. The quality of these coatings is estimated from the uniformity of the covering and its density, which determines the mechanical strength of the coating and also, in many cases, the chief operating characteristic (emission, electrically-insulating properties, etc.). It is usually impossible to establish a direct relationship between the mechanical strength and density of coatings.

In practice, the density of coatings formed from particles of the triple carbonate [(BaSrCa) $(CO_3)_3$] with dimensions from 1 to 10 μ varies from 2.0 to 3.0 g/cm^3, i.e., the volume of the pores amounts to 25-50% of the total volume of the coatings. The points of contact of the particles characterize the mechanical strength of the coating. Determination of the number of points of contact in a coating is difficult, but the porous structure of coatings can easily be determined [1,2]. A knowledge of the porous structure of the coatings enables us to calculate the exposed surface of the crystal framework.

Study of the porous structure of electrophoretic deposits enables us to approach closer to the essential features of the mechanism of formation of a coating, which is a complex coagulation process. The aim of the present study was to find the factors influencing the porous structure in the process of formation of an electrophoretic coating.

By varying the conditions for the electrophoretic precipitation of suspensions of the triple carbonate in methanol–acetone medium, it is possible to obtain deposits with densities from 0.7 to 3.0 g/cm^3, with a total pore volume in the precipitate of 0.710 to 0.150 cm^3/g.

Two valve rectifiers fitted with a time relay were included in the electrical circuit of the apparatus used for precipitating the suspensions. One of the rectifiers was stabilized with respect to voltage and the other with respect to current. The precipitation bath consisted of a glass beaker with coaxial nickel electrodes; the distance between the electrodes was 30 mm. The determination of the porous structure of the deposit was carried out by forcing mercury into the pores of the coating at a pressure of up to 800 kg/cm^3, by means of a PA-2 porimeter [3].

It was first of all of interest to examine the influence of the shape and size of the particles on the porous structure of the deposits. The deposits were formed from three suspensions of the triple carbonate in methanol–acetone medium (1:3). The first suspension was prepared by mixing highly-dispersed carbonate powder, synthesized in aqueous methanol, with the methanol–acetone mixture. The carbonate crystals are shaped like sheafs. The second suspension was prepared by grinding coarse crystals of the carbonate in a ball mill in the presence of the dispersion medium. After the grinding process, the carbonate particles had approximately the same dimensions as those in the first suspension, but their shape was almost cylindrical. The disperse phase of the third suspension consisted of the coarser fraction of the carbonate, separated from the finely–ground powder.

The composition of the carbonate powders used is given by differential distribution curves (Fig. 1).

The porosity of the coatings of thickness 40-50 μ, obtained by precipitation of the suspensions, varies for different suspensions. The pore volume of the coating obtained from the first suspension amounts to 0.679 cm^3/g, whereas the pore volume of the coatings from the second and third suspensions is much smaller and equal to 0.156 and 0.258 cm^3/g respectively. The branched shape of the carbonate crystals of the first suspension (Curve 1, Fig. 2) prevents the particles from forming a compact arrangement and the coating has pores with an average radius of the order of 2000 A; it has a high mechanical strength, however. The most compact coating was that obtained from the comparatively rounded particles of the polydisperse second suspension (Curve 2, Fig. 2). This coating has pores of

the order of 800 A. The large pores in the deposit are evidently filled with fine particles of carbonate; the coating is extremely strong. The large particles of the coarse fraction form a coarsely-porous coating with pores of the order of 5-8 thousand A (Curve 3, Fig. 2). These pores lead to a slight increase in the surface of the crystal framework, but also produce a sharp decrease in its mechanical strength.

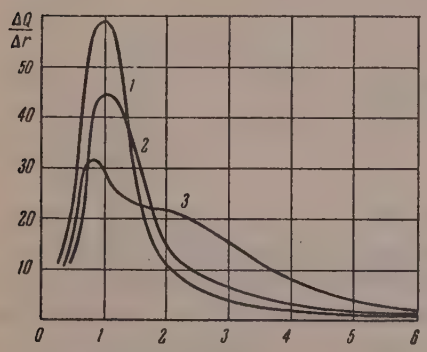


Fig. 1. Differential distribution curves for the particles in the first (1), second (2), and third (3) suspensions.

Coarsely-porous coatings of low strength are also obtained from the second suspension if the electrophoretic precipitation is carried out at high voltages. Curve 4 (Fig. 2) characterizes the porosity of a coating obtained at a voltage of 1500 v/cm. During the deposition process, considerable structure-formation takes place in the volume between the electrodes and this is accompanied not only by formation of a coating on the electrode but also by the formation of a voluminous friable deposit at the foot of the bath.

Change in the voltage at the electrodes in the bath in the range up to 100 v/cm (Curves 5,6, and 7, Fig. 2) leads to a significant change in the total pore volume and in the nature of the porosity of the deposit. Increase in the voltage increases the volume of the large pores and coatings obtained at a voltage of 100 v/cm have low strength. The formation of the deposit at the electrode during the precipitation of the particles at constant voltage is always accompanied by a sharp fall in the current. If it is assumed that the current compresses the deposit, we should expect an increase in the density of the deposit with increase in the voltage, but this is not observed in practice. Curves 8,9, and 10 give the pore distribution diagrams for deposits obtained at current strength; comparison of these curves with those obtained for deposits obtained at stabilized voltages indicates that change in the current also influences the nature of the porosity, but in this case the deposits are stronger and the nature of the porosity is more reproducible. The formation of a coating on the electrode under stabilized current conditions takes place with an increase in the voltage at the electrodes in the bath, so that it may be concluded that the choice of precipitation conditions (constant voltage or constant current) is closely related to a change in the resistance of the layer of coating being formed. To obtain carbonate coatings with reproducible porosities, constant current conditions are to be preferred.

The aggregate stability of carbonate suspensions changes sharply with change in the composition of the dispersion medium. The coatings from unstable suspensions are friable and coarsely-porous.

When methanol is added to an acetone medium, there is an increase in the stability of the suspensions and the coatings becom finely-porous. When an alcoholic solution of cerium nitrate is added to a suspension in methanol, the aggregate stability of the carbonates is broken down, so that the electrophoretic deposit becomes coarsely-porous, as in the case of the unstable suspensions in a dispersion medium of acetone.

SUMMARY

1. A study has been made of the porous structure of electrophoretic deposits obtained from carbonate suspensions. The size and shape of the particles of the disperse phase of the suspensions has been shown to influence the nature of the porosity of the deposits.

2. Breakdown of the aggregate stability of the suspensions with change in the composition of the dispersion medium and conditions of electrophoretic precipitation leads to an increase in the pore size and the deposits become friable and weak.

3. An electrical field produces a decrease in the aggregate stability of the suspensions. The porosity of deposits formed during precipitation under constant-current conditions is more reproducible.

LITERATURE CITED

1. I. S. Lavrov, Fourth All-Union Conference on Colloid Chemistry [in Russian] (Acad. Sci USSR and Acad. Sci. Gruz. SSR Press, Tbilisi, 1958), p. 57.
2. I. S. Lavrov, Elektronika, No. 6, 124 (1960).
3. T. G. Plachenov, Mercury Porimeters [in Russian] (Leningrad, 1957).

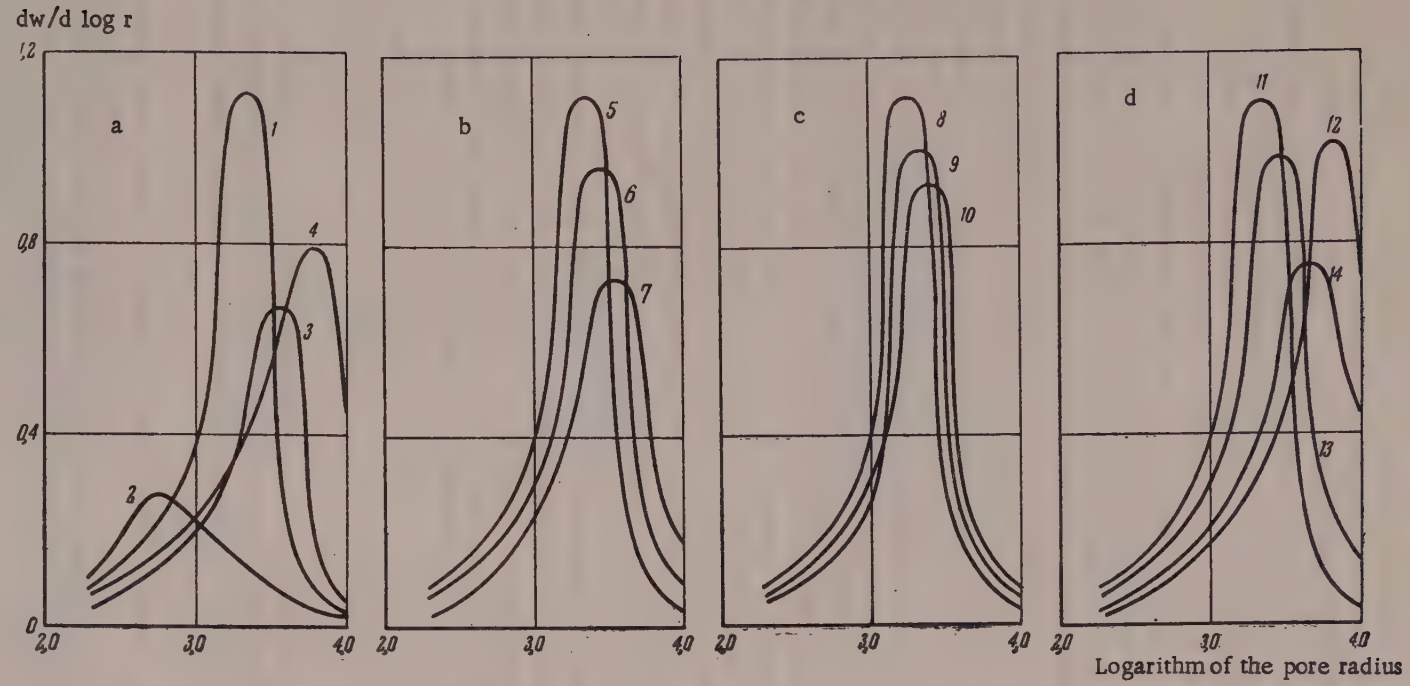


Fig. 2. Differential distribution curve for the pore radii in electrophoretic deposits from the following suspensions: 1,2,3) from the first, second, and third, at a voltage of 20 v/cm; 4) from the second suspension at 1500 v/cm; 5,6,7) from suspensions with a methanol medium, nonground carbonate, at voltages of 15,25, and 50 v/cm; 8,9,10) from the same suspension at currents of 2,7, and 15 ma; 11) from a suspension in methanol medium; 12) from a suspension in acetone medium; 13) from a suspension in methanol–acetone medium (1:3); 14) from a suspension in methanol medium enriched with cerium nitrate.

AN INFRARED SPECTROSCOPIC STUDY OF ISOTOPIC EXCHANGE WITH THE SURFACE HYDROXYL GROUPS OF CHEMICALLY MODIFIED SILICAS

V. I. Lygin and A. V. Kiselev

Adsorption Laboratoy, Chemical Faculty, M. V. Lomonosov Moscow University
Translated from Kolloidnyi Zhurnal, Vol. 23, No. 3, pp. 299 303, May-June, 1961
Original article submitted April 28, 1960

The surface chemical compounds of adsorbents and fillers determine their adsorptive properties and their interaction with various media, particularly when the latter are highly polymerized. The adsorptive properties of silicas with respect to substances whose molecules have high dipole or quadrupole moments depends to a marked extent on the degree of hydration of their surfaces [1]. For example, the adsorption of vapors is greatly decreased by increasing the degree of replacement of surface hydroxide groups by trimethylsilyl groups [2]. When a surface is chemically modified by surface chemical reactions, it is often impossible to bring about complete replacement of the surface hydroxide groups by organic radicals [3]. As a result, the adsorptive interaction is often determined by the over-all effect of the different chemical groups of the surface on the molecules of the substance being adsorbed. It then becomes necessary to examine the extent to which these different surface groups take part in the adsorptive interaction. An adsorption experiment does not always give this information, since adsorptive interactions may be nonadditive. In the study of adsorption processes on complex surfaces, it is very convenient to use a spectral method of examination [4], since the changes observed, on adsorption, in the spectrum of the surface chemical compounds and the adsorbed molecules should give a direct indication of whether the various chemical groups are taking part in the adsorptive interaction. Of particular interest in this connection is a special study of the residual hydroxide groups left on the surface after the introduction of trimethylsilyl groups by reaction with trimethylchlorosilane [2,3]. As a result of the large size of the $-Si(CH_3)_3$ group, the spaces between these groups and possibly to some extent the spaces underneath them should contain hydroxide groups which are to varying degrees accessible to different molecules being adsorbed on the modified surface. The accessibility of these residual hydroxide groups on the surface is most easily estimated from the exchange of the surface OH groups with OD groups during the adsorption of D_2O, since it has already been shown in a number of works [5,6] that the OH groups on the surface of hydrated silicas readily exchange with OD groups in the reaction with D_2O vapor. In the present work we have studied the deuteration of the surface hydroxide groups of aerosils with chemically modified (by the introduction of trimethylsilyl groups) surfaces.

The present work is a continuation of our series of works on the spectral study of the hydroxide covering on silicas [6], the oxygen groups of specially oxidized carbons [7], and the interaction between surface hydroxide groups and molecules undergoing adsorption [8, 9].

Procedure and materials studied. The materials chosen for study were specimens of an aerosil with partly hydrated surface, the same aerosil modified with liquid trimethylchlorosilane, and the aerosil modified with trimethylchlorosilane vapor after preliminary hydration of its surface. The adsorptive properties of these specimens were studied in earlier works [2,3].

Powdered aerosil specimens have a marked scattering effect on infrared radiation. In our previous works [6,7], the scattering of the radiation was reduced by preparing specimens from powder particles with dimensions less than the wavelength of the radiation used. During the preparation of a layer of powder from these particles on a transparent support, however, the particles form aggregates with dimensions greater than the wavelength of the radiation used, as a result of which the transmittance in the range of the hydroxide group valence vibrations (3750 cm^{-1}) was only 30% in the best cases. In the present work the scattering of the infrared radiation was reduced by compressing the powder to form a disc of 2.5 mm diameter. When compressed under a pressure of 20 kg/mm^2, the original aerosil forms pale blue discs which have a fairly high mechanical strength, are completely transparent, and slightly opalescent. The cohesion of the particles of the modified aerosil, as a result of the decrease in the adsorption field and hence in the

adhesion [2], is much lower. Mechanically strong but less transparent discs can thus be obtained only by compressing the powder under a pressure of 70 kg/mm^2. The weight of aerosil in the discs in all cases was ~ 15 mg/cm^2.

The vacuum thermal treatment, deuteration, and recording of the spectra were carried out in the vacuum cell previously described [8,10]. The spectra were recorded on an IKS-12 spectrometer with LiF prism. The spectral width of the slit was 8 cm^{-1} in the 3700 cm^{-1} range and 4 cm^{-1} in the 2600 cm^{-1} range.

Results and discussion. Figure 1 (Curve 1) gives the absorption spectrum of the compressed aerosil treated in vacuum at 10^{-4} mm Hg and 200° for 6 hours. In the range of the valence vibrations of the aerosil OH groups, the spectrum shows a sharp band at 3750 cm^{-1} produced by the "free" hydroxyl groups of the surface [4,6]. The broad band superimposed on the 3750 cm^{-1} band towards the region of longer wavelengths can be attributed to hydroxide groups which are situated close together and interact with one another [6]. The passage of D_2O vapor into the cell at a pressure corresponding to the formation of an aqueous monolayer on the surface and subsequent evacuation of the specimen lead to a decrease in the absorption in the range of the OH group valence vibrations (3750 cm^{-1}) and to the appearance of absorption in the OD group range (2760 cm^{-1}). The replacement of the surface OH groups by OD groups is practically complete, and subsequent evacuation and passage of fresh D_2O vapor do not lead to any significant change in the shape of the spectrum. The absorption band of the OD groups (Curve 2) has the same shape as the original absorption band of the surface OH groups (Curve 1). The sharp band at 2760 cm^{-1} can thus be attributed to absorption by the "free" surface OD groups and the broad band superimposed on this narrow band towards longer wavelengths at 2650 cm^{-1} can be attributed to surface OD groups which are joined to one another by a weak hydrogen bond. The spectrum (Curve 2) shows however that a small broad band remains in the range of absorption of the surface OH groups at ~3650 cm^{-1}, and this band does not disappear on repeated evacuation and passage of D_2O vapor. The difficulty of replacing the OH hydroxide groups responsible for this absorption by OD groups, the blurring of this absorption band, and its displacement towards longer wavelengths relative to the absorption band of the free hydroxide groups at 3750 cm^{-1} suggest that this absorption band probably corresponds to interacting hydroxide groups blocked at the point of contact between adjacent particles of the aerosil framework. McDonald [5] has observed directly the dependence of the absorption in this range on the pressure used to compress the aerosil.

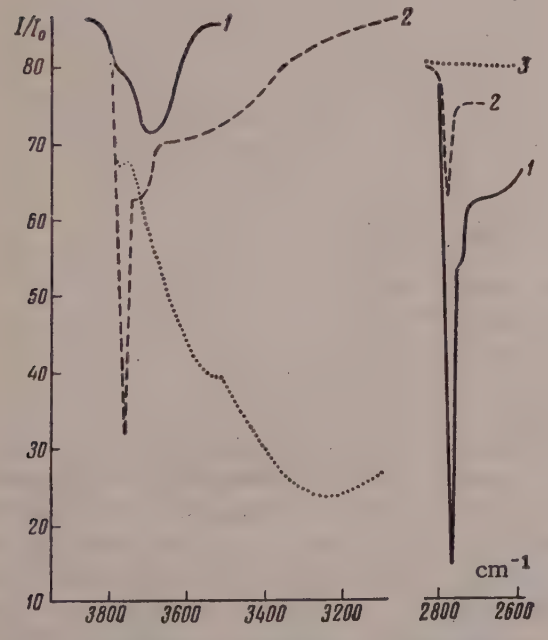


Fig. 1. The infrared spectrum of a compressed aerosil at 200° before the reaction (1) and after the reaction (2) between the surface OH groups and D_2O vapor. Treated in vacuo at 200°.

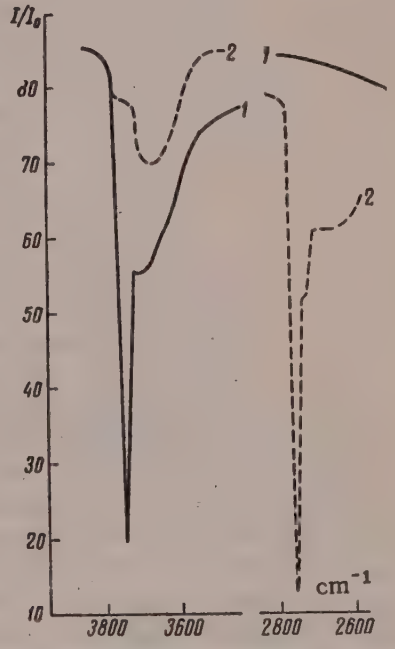


Fig. 2. The infrared spectrum of an aerosil containing OD groups on the surface, after treatment in vacuo at 200° (1), the spectrum of the same aerosil after reaction between the surface OD groups and C_2H_5OH vapor (2), and after the adsorption of a monolayer of C_2H_5OH molecules (3).

The OD groups formed during deuteration of the surface of the silicas are able to undergo the reverse exchange with H_2O vapor to produce surface OH groups again [5]. The replacement of the surface OD groups by OH groups takes place equally readily in the reaction with alcohol molecules. Figure 2 (Curve 1) gives the spectrum of an aerosil with a deuterated surface. The passage of small quantities of C_2H_5OH vapor into the cell leads to the appearance and gradual increase in intensity of the 3750 cm^{-1} band (Curve 2) and a simultaneous decrease in the intensity of the 2760 cm^{-1} band in the range of absorption of the OD surface groups. At a C_2H_5OH vapor pressure corresponding approximately to the formation of a monolayer, the 2760 cm^{-1} band disappears completely (Curve 3). Simultaneously the spectrum shows a marked decrease in the absorption band of the free OH hydroxide groups at 3750 cm^{-1} and the appearance of absorption in the 3200 cm^{-1} range as a result of the adsorption of alcohol molecules by formation of a hydrogen bond between the surface OH groups and the C_2H_5OH molecules being adsorbed.

The spectrum of an aerosil in which some of the hydroxide groups have been replaced by trimethylsilyl groups (Fig. 3, Curve 1) shows a broad absorption band at 3650 cm^{-1} corresponding to the hydroxide groups remaining on the surface. In this spectrum the absorption band at 3750 cm^{-1} corresponding to the free hydroxide groups on the surface is absent. The blurring of the band and its displacement towards longer wavelengths relative to the absorption band at 3750 cm^{-1} indicate excitation of the hydroxide groups remaining on the surface after the reaction with $ClSi(CH_3)_3$. This excitation apparently does not result from the formation of a hydrogen bond between the hydroxide groups of neighboring particles of the modified aerosil, as in the case of the compressed specimen of the original aerosil, since the external hydrophobic covering of the particles prevents the formation of a hydrogen bond between the residual hydroxide groups. The residual hydroxide groups are apparently excited by the $-Si(CH_3)_3$ groups chemically combined with the surface, since these groups, as a result of their large size [2], lie partly above the residual hydroxide groups and restrict their valence vibrations.

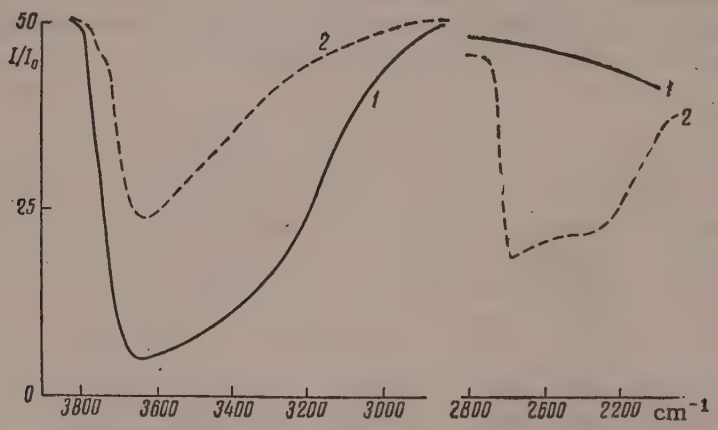


Fig. 3. The infrared spectrum of an aerosil modified to the extent of 60% with trimethylchlorosilane (1) and after reaction with D_2O vapor (2). The specimen was treated in vacuo at 200° before the spectrum was recorded.

Since the methyl groups present in the $-Si(CH_3)_3$ group cover only ~ 60% of the surface, some of the residual hydroxide groups are still accessible to the water molecules being adsorbed. In fact, the passage of D_2O vapor leads to a decrease in the 3650 cm^{-1} band and to the appearance of an equally broad band corresponding to the vibrations of the OD group. Repeated passage of D_2O vapor and prolonged storage of the specimen in D_2O vapor do not lead to any significant change in the spectrum (Curve 2), indicating that some of the hydroxide groups of the modified specimens are completely inaccessible*. The screening effect of the surface layer of trimethylsilyl groups is even more marked in the case of an aerosil specimen whose surface is covered by trimethylsilyl groups to the extent of 93% (Fig. 4, Curve 1). The passage of D_2O vapor into a cell containing this specimen leads to replacement of only an insignificant fraction of the OH groups by OD groups.

* The same phenomenon was previously observed by Nikitin, Sidorov, and Karyakin [5] in the reaction between D_2O and a specimen of porous glass methylated in methanol vapor.

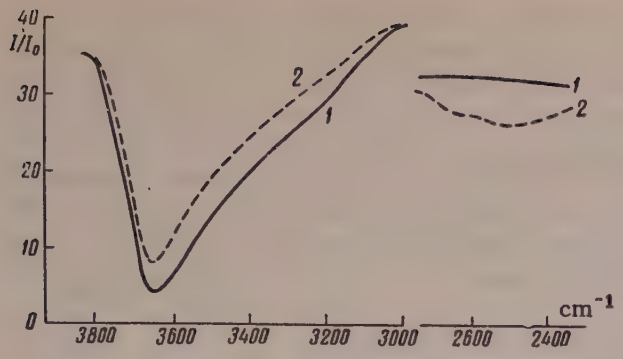


Fig. 4. The infrared spectrum of an aerosil modified to the extent of ~90% by trimethylchlorosilane (1), and after reaction with D_2O vapor (2). The specimen was treated in vacuo at 200° before the spectrum was recorded.

SUMMARY

1. In the reaction between D_2O vapor and a compressed aerosil specimen, the OH groups of the aerosil surface are readily replaced by OD groups, with the exception of those groups which are blocked at the points of contact of the individual particles.

2. The trimethylsilyl groups on modified aerosil specimens replace a large number of the surface hydroxide groups excite the hydroxide groups remaining on the surface, and interfere in the reaction between some of these groups and D_2O molecules.

LITERATURE CITED

1. L. D. Belyakova, O. M. Dzhigit, and A. V. Kiselev, Zhur. Fiz. Khim. 31, 1577 (1957); A. A. Isirikyan and A. V. Kiselev, Doklady Akad. Nauk SSSR 115, 393 (1957); A. V. Kiselev and E. V. Khrapova, Kolloid. Zhur. 19, 572 (1957); L. D. Belyakova and A. V. Kiselev, Doklady Akad. Nauk SSSR 119, 298 (1958); Zhur. Fiz. Khim. 33, 1534 (1959).
2. I. Yu. Babkin, V. S Vasil'eva, I. V. Drogaleva, A. V. Kiselev, A. Ya. Korolev, and K. D. Shcherbakova, Dokl. Akad. Nauk SSSR 129, 131 (1959); I. Yu. Babkin and A. V. Kiselev, Dokl. Akad. Nauk SSSR 129, 357 (1959); I. Yu. Babkin, A. V. Kiselev, and A. Ya. Korolev, Doklady Akad. Nauk SSSR 136, 373 (1961).
3. A. V. Kiselev, A. Ya. Korolev, R. S. Petrova, and K. D. Shcherbakova, Kolloid. Zhur. 22, 671 (1960).
4. A. N. Terenin, Collection "Surface Chemical Compounds and Their Role in Adsorption Phenomena" [in Russian] (Moscow University Press, 1957), p. 206.
5. G. C. Pimentel, C. W. Garland and G. Jura, J. Amer Chem. Soc. 75, 803 (1953);V. A. Nikitin, A. N. Sidorov, and A. V. Karyakin, Zhur. Fiz. Khim. 30, 117 (1956); R. S. McDonald, J. Phys. Chem. 62, 1168 (1958).
6. A. V. Kiselev and V. I. Lygin, Proc.of the Second Intern. Congr. on Surface Activity, v. 2, (London, 1957). p. 204; V. I. Lygin, Vestnik Moskovskogo Universiteta 1, 223 (1958); A. V. Kiselev and V. I. Lygin, Kolloid. Zhur. 21, 581 (1959).
7. V. I. Lygin, N. V. Kovaleva, N. N. Kavtaradze, and A. V. Kiselev, Kolloid. Zhur. 22, 334 (1960).
8. A. V. Kiselev and V. I. Lygin, Kolloid. Zhur. 22, 403 (1960).
9. A. V. Kiselev and V. I. Lygin, Kolloid. Zhur. 23, 157 (1961).
10. N. N. Kavtaradze and V. I. Lygin, Zhur. Fiz. Khim. 34, 462 (1960).

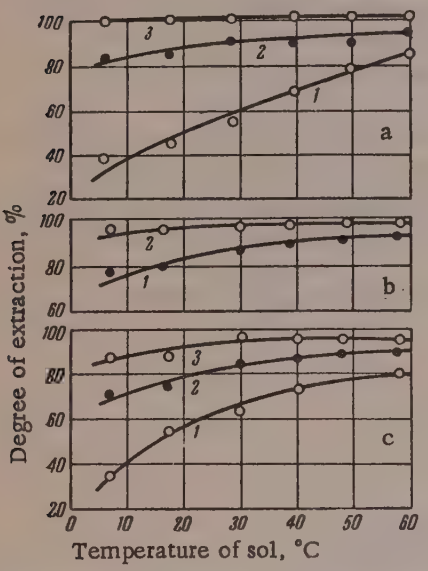
All abbreviations of periodicals in the above bibliography are letter-by-letter transliterations of the abbreviations as given in the original Russian journal. *Some or all of this periodical literature may well be available in English translation.* A complete list of the cover-to-cover English translations appears at the back of this issue.

THE EFFECT OF TEMPERATURE ON THE KINETICS OF EXTRACTION OF MIXED COLLOIDAL HEAVY-METAL FERROCYANIDES WITH A GELATIN FOAM

L. D. Skrylev and S. G. Mokrushin

S. M. Kirov Urals Polytechnical Institute, Sverdlovsk
Translated from Kollodnyi Zhurnal, Vol. 23, No. 3, pp. 304-305, May-June, 1961
Original article submitted February 1, 1960

Temperature is one of the chief factors influencing the process of foam formation. The stability of a foam usually decreases with increase in temperature [1]. In some cases, however, increase in temperature leads to a considerable increase in the stability of a foam [2]. For every sol there exists an optimum temperature for the foam extraction of the disperse phase [3,4].



Influence of temperature on the kinetics of the extraction of mixed colloidal ferrocyanides of copper (a), cobalt (b), and iron (c) with gelatin foam. Duration of foam-formation process in minutes: 1) 3; 2) 6; 3) 12.

In the present work we studied the influence of temperature on the kinetics of extraction of mixed colloidal heavy metal ferrocyanides from their hydrosols with gelatin foam. The materials studied were hydrosols of the mixed ferrocyanides of copper, cobalt, and iron, obtained by the reaction of $K_4[Fe(CN)_6]$ with $CuSO_4$, and $FeCl_3$. The reagents were added in quantities calculated to give 100 mg/g of solid phase of composition $K_2Cu_3[Fe(CN)_6]_2$, $K_4Co_{10}[Fe(CN)_6]_6$ and $KFe[Fe(CN)_6]$ [5], with a 50% excess of potassium ferrocyanide, which acted as peptizing agent [6]. All the solutions necessary for the preparation of the hydrosols were prepared from distilled water and chemically pure reagents. The hydrosols were prepared 24 hours before the start of the experiments. A 1% gelating solution was used as foaming agent.

The test sol (100 ml) was heated to the required temperature, the foaming agent (1 ml of 1% aqueous gelatin solution) was added, and the mixture was poured into a vertical glass tube 1 m high and 30 mm in diameter. The foot of the tube consisted of a fine porous plate. The foam was produced by blowing air, dispersed by the porous plate, through the sol. The rate of passage of air was 600 cm^3/min. The tube was kept in a thermostat.

The degree of extraction of the colloids was determined colorimetrically by means of a photoelectric colorimeter. The results of the studies which we carried out are given in the Figure.

The Figure shows that the degree of extraction of the colloids increases with increase in the temperature of the sol. The influence of temperature decreases with increase in the duration of the foam-formation process (6 and 12 min).

Further mention must be made of the influence of temperature on the process of foam-formation. Special experiments [3] have shown that the height of the column of foam formed when air is blown through a 0.01% aqueous gelatin solution containing no solid foam stabilizers decreases with increase in temperature. When air is blown through a sol of mixed heavy metal ferrocyanides containing gelatin, increase in temperature led not to a deterioration but to an improvement in the process of foam-formation. The most voluminous, fine-celled and moist foam was obtained in the first few minutes of the process of foam-formation at a sol temperature of 50-60°; the driest and least voluminous foam was obtained at a sol temperature of 6-7°.

The formation of a voluminous fine-celled foam with increase in the temperature of the test sols and the resultant increase in the degree of extraction of the colloid appears to be due to thermal breakdown of the aggregates of the gelatin [7], which leads to an increase in the partial concentration of gelatin in the sol, and to the specific properties of the surface-active gelatin–ferrocyanide complex, which lead to the formation of a particularly stable surface film which does not break down even at increased temperature. In addition, increase in temperature leads to a decrease in the surface tension at the hydrosol–air interphase boundary, and this in turn leads to a decrease in the free surface energy of the system and thus increases the stability of the foam. Increase in temperature increases the mobility of the gelatin–ferrocyanide complex, leading to a higher rate of attainment of adsorption equilibrium at the liquid–gas interphase boundary. This should finally increase the rate of extraction of the disperse phase.

SUMMARY

1. The degree of extraction of mixed colloidal ferrocyanides of copper, cobalt and iron by a gelatin foam increases with increase in the temperature from 10 to 60°.

2. The increase in the degree of extraction of the colloids, observed in these experiments, may be attributed to the thermal breakdown of the aggregates of gelatin and the specific properties of the surface-active gelatin–ferrocyanide complex.

LITERATURE CITED

1. I. I. Bikerman, Foams: Theory and Industrial Applications Reinhold Corporation, N. Y., (1953), p. 91.
2. G. O. Erchikovskii, The Formation of a Flotation Foam [in Russian] (GONTI, 1939), p. 166.
3. R. V. Shveikina and S. G. Mokrushin, Zhur. Prikl. Khim. 31, 1109 (1958).
4. F. Schutz, Trans. Faraday Soc. 42, 437 (1946).
5. I. V. Tananaev, Izvest. Akad. Nauk SSSR Otd. Khim. Nauk, No. 12, 1421 (1957).
6. I. V. Tananaev and M. I. Levina, Zhur. Anal. Khim. 3, 31 (1948).
7. S. M. Lipatov, Colloid Teaching [in Russian] (Moscow, 1933), p. 184.

All abbreviations of periodicals in the above bibliography are letter-by-letter transliterations of the abbreviations as given in the original Russian journal. *Some or all of this periodical literature may well be available in English translation.* A complete list of the cover-to-cover English translations appears at the back of this issue.

A STUDY OF THE KINETICS OF SUPERSATURATION IN AQUEOUS SUSPENSIONS OF TRICALCIUM ALUMINATE AND THE DETERMINATION OF ITS METASTABLE SOLUBILITY

E. S. Solov'eva and E. E. Segalova

Chemical Faculty, M. V. Lomonsov Moscow University
Translated from Kolloidnyi Zhurnal, Vol. 23, No. 3, pp. 306-314, May-June, 1961
Original article submitted November 1, 1960

The study of the processes of hydration and crystallization structure-formation during the hardening of mineral binding agents has revealed the important part played by the magnitude and the kinetics of the change in the supersaturation in the liquid phase of the suspension undergoing hardening [1,2]. The formation of supersaturated solutions during the hardening of mineral binding agents was noted very early, but it was usually assumed that the magnitude of the supersaturation was fortuitous and determined entirely by the experimental conditions [3,4]. The indefinite nature of the magnitude of the supersaturation during hardening is in good agreement with the theory of binding agent hydration in the solid phase. At the present time it may be taken as firmly established [1,2] that in the hardening of mineral binding agents, a decisive part is played by processes associated with the dissolution of the original binding agent and the crystallization of new formations from the resultant supersaturated solution; this view was held by Le Chatelier. This theory of the hydration process assumes the existence of a constant maximum supersaturation corresponding to the metastable solubility of the original binding agent. For gypsum hemihydrate this solubility has been known for long [5], and it has also been detected for other single-mineral binding agents such as tricalcium and monocalcium aluminates, and calcium oxide [6].

This article gives the results of a determination of the solubility and the kinetics of supersaturation in aqueous suspensions of tricalcium aluminate $3CaO \cdot Al_2O_3$ (C_3A) at 20 and 40°.

Tricalcium aluminate was prepared by four-fold ignition of chemically pure calcium oxide and aluminum oxide at 1380° [7]. The synthetic mineral contained 61.98% CaO and 37.53% Al_2O_3; the losses on ignition amounted to 0.02%. The arbitrary specific surface (s_1) of the finely-ground C_3A, determined by the air-permeability method on a Tovarov apparatus, was equal to 4000 cm^2/g.

The study was carried out with suspensions containing from 0.1 to 4.0% of the solid phase. As a result of the high rate of dissolution of anhydrous C_3A, small lumps of nonhydrated material covered with compact coatings of hydrate microcrystallites are formed when the material is added to water [8]. To prevent this phenomenon, the weighed specimen of C_3A was ground beforehand for 1-1.5 minutes with a small quantity of water, after which the resultant concentrated suspension was added to the necessary volume of water.

The kinetics of supersaturation in the C_3A suspensions was measured by a conductometric method [6,9] at the optimum rate of stirring of the suspension, equal to 400 rpm, since special experiments showed that increase in the rate of stirring beyond 300 rpm has no influence on the electrical conductivity kinetics. The temperature in the thermostat was maintained constant throughout the experiment to within ± 0.3°. All the measurements were carried out in an atmosphere of nitrogen to prevent carbonation of the suspensions.

Figure 1 gives typical curves showing the change in the electrical conductivity in tricalcium aluminate suspensions at 20 and 40°. For comparison, the changes in the electrical conductivity for the dissolution of tricalcium hydroaluminate at the same temperatures are also shown (Curves 2 and 4, Fig. 1). Figure 1 shows that in a C_3A suspension the electrical conductivity reaches its maximum value comparatively rapidly and then starts to decrease to a level corresponding to a solution saturated with respect to the hydrate. Increase in temperature leads to a sharp increase in the rate of dissolution of the C_3A and also in the rate of crystallization of the new formations: at 20° the maximum electrical conductivity level is reached in 4 hours, and at 40°, in spite of the lower concentration of the suspension, it is reached in 5 minutes. The decrease in the supersaturation also takes place much more rapidly. To determine

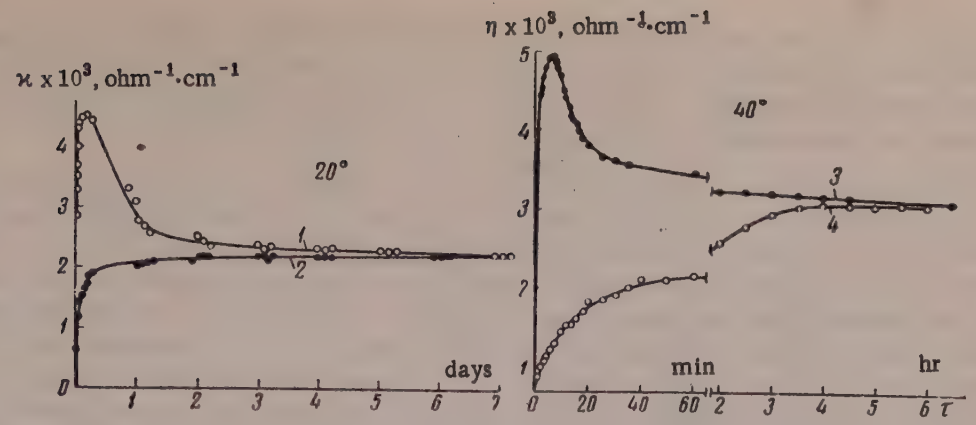


Fig. 1. Kinetics of the change in the specific conductance of the suspensions in 150 ml of water at 20 and 40°: 1) 3 g C_3A; 2) 1 g C_3A.aq; 3) 2 g C_3A; 4) 2 g C_3A.aq.

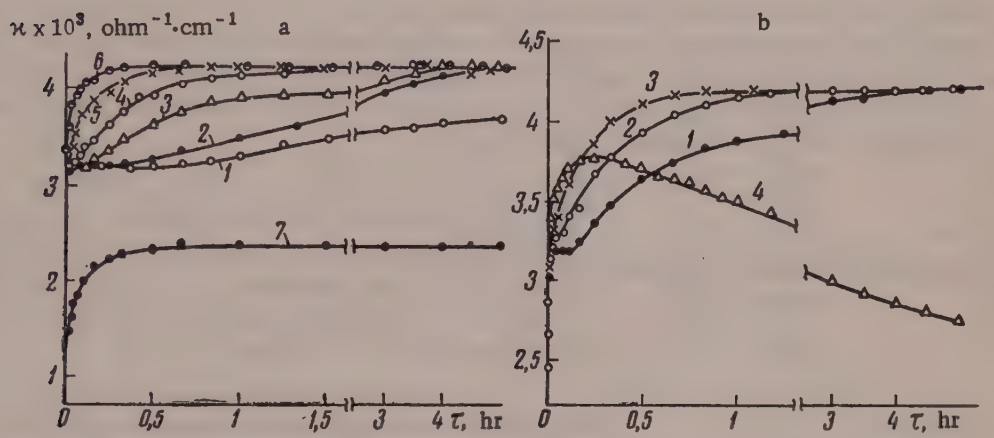


Fig. 2. Kinetics of the change in the specific conductance at 20° in the suspensions: a) containing in 150 ml of water: 1) 0.5 g; 2) 1.0 g; 3) 1.5 g; 4) 2.0 g; 5) 4.0 g; and 6) 6.0 g C_3A; 7) 4.0 g C_3A.aq; b) containing in 150 ml of water 1.5 g C_3A and the following quantities of hydroaluminate: 1) 0 g; 2) 0.5 g; 3) 2.0 g; 4) 6.0 g.

the metastable solubility of C_3A it was necessary to find the highest value of the electrical conductivity independent of the weight of the C_3A specimen and to determine the concentration of the liquid phase of the suspension, corresponding to this value.

Figure 2, a shows that a constant electrical conductivity level corresponding to the metastable solubility of C_3A is established at 20° in all C_3A suspensions in which the concentration is sufficiently high. The electrical conductivity kinetic curves can be divided into two sections which are most clearly-defined at low concentrations of the suspension. At first the electrical conductivity increases very rapidly but at $\varkappa = 3.2 \times 10^{-3}$ ohm^{-1}.cm^{-1} there is an inflection with a slightly sloping section, whih is more clearly-defined the lower the disperse solid phase content of the suspension. After this inflection the electrical conductivity increases much more slowly than at first. The point of inflection on the curve corresponds to the appearance of the new formations—very fine hydroaluminate crystallites—throughout the whole volume of the suspension, and this is readily detected from the marked turbidity produced in the suspension.

These kinetics can be explained as follows. Nuclei of the new phase—hydroaluminate microcrystallites—start to form in C_3A suspensions at supersaturations far below the maximum determined by the metastable solubility of the C_3A. These microcrystallites are deposited on the surface of the original C_3A particles, cover them with an effective protective film, and retard their further dissolution. The retardation of the increase in the electrical conductivity is related both to this retardation of the dissolution and also to the fact that part of the material passing into solution appears in the form of hydroaluminate without increasing the concentration of the solution.

The suggestion that effective protective coverings are formed on the surface of the C_3A particles is confirmed by a study of the electrical conductivity kinetics in C_3A suspensions containing small quantities of a surface–active agent–Ca lignosulfonates in the form of sulfite–alcohol wastes (s.a.w.) —or ready-made crystallization centers in the form of tricalcium hydroaluminate crystallites.

Figure 2,b shows that in the presence of hydroaluminate the increase in the electrical conductivity is much more rapid, i.e., the C_3A concentration in the liquid phase of the suspension increases more rapidly. Since the rate of dissolution of the C_3A cannot increase in the presence of hydroaluminate and the increase in the electrical conductivity should have been retarded as a result of the increase in the rate of crystallization of the hydroaluminate on the ready–made centers, the increase in the rate of saturation of the solution can only be due to the fact that in the presence of hydroaluminate a coating of hydroaluminate crystallites is not formed to block the surface of the original C_3A particles, so that no retardation of the C_3A dissolution takes place. The greater the quantity of hydroaluminate added to the C_3A suspension, the lower the probability of formation of hydroaluminate nuclei on the surface of the original C_3A particles and the greater the rates of C_3A dissolution and hydrate crystallization, so that when a large quantity of hydroaluminate is added, the upper electrical conductivity level is not reached (Fig. 2,b, Curve 4).

Figure 3 shows that small quantities of added surface–active agent (s.a.w.) which are completely adsorbed by the C_3A particles [10] do not change the maximum electrical conductivity level but have a marked influence on the kinetics of the process: the initial rate of the dissolution of the C_3A before the appearance of the nuclei of the new phase is much lower in the presence of 0.5% s.a.w. In the presence of s.a.w., however, as in the presence of hydroaluminate, there is no inflection on the curve showing the increase in the electrical conductivity, and the maximum electrical conductivity value is reached much more rapidly.

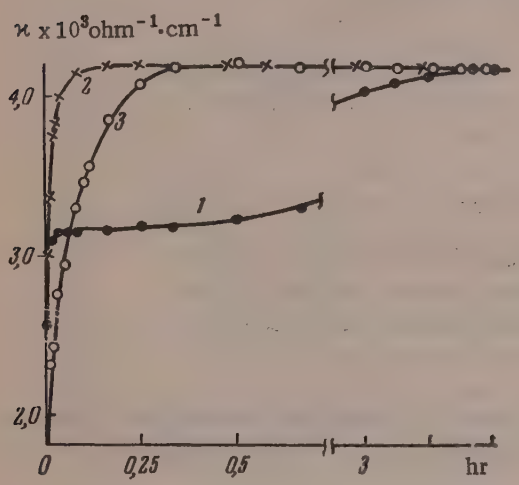


Fig. 3. Kinetics of the change in the specific conductance at 20° in a suspension containing 1 g of C_3A in 150 ml of water or s.a.w. solution: 1) water; 2) 0.05% s.a.w. solution; 3) 0.5% s.a.w. solution.

When large quantities of s.a.w. are present, its retarding influence on the initial rate of dissolution of the C_3A is much more marked, but in this case, as a result of the presence of s.a.w. in the liquid phase of the suspension, there is a change in the electrical conductivity value and the results of the measurements are not comparable with earlier data.

These results can be explained only by the fact that, although the adsorption of s.a.w. on the surface of the C_3A particles leads to a certain retardation of its dissolution, the predominating effect is the prevention of the formation of protective hydroaluminate coatings on the surface of the original particles. As a result, the rate of saturation of the solution is greatly increased in the presence of small quantities of s.a.w.

In order to determine the magnitude of the metastable solubility of C_3A it was necessary to separate the liquid phase of the suspension and to determine its CaO and Al_2O_3 contents.

An attempt to filter or centrifuge off the C_3A suspension after the maximum supersaturation had been reached did not give satisfactory results. The hydroaluminate crystals which are formed are so small that almost no sedimentation takes place in an ordinary centrifuge and on filtration the pores of the filter become blocked; the liquid filters so slowly that any supersaturation has time to decrease to zero.

It is known [10] that in the presence of small quantities of s.a.w., larger hydroaluminate crystals are formed, and as can be seen from Fig. 3 the maximum electrical conductivity level in tricalcium aluminate suspensions remains unchanged. The s.a.w. is very rapidly and completely adsorbed from the liquid phase of the suspension without influencing the magnitude of the electrical conductivity, which in this case also is determined entirely by the solubility of the tricalcium aluminate. This made it possible to measure the solubility of C_3A using suspensions containing small quantities of s.a.w. (0.03-0.1% s.a.w. in solution). In order to find the time necessary for the greatest supersaturation to be established in the suspension, we first made measurements of the electrical conductivity. After the electrical conductivity had reached the constant level determined by the solubility of the tricalcium aluminate, a specimen was removed from the suspension and filtered on a No. 2 Schotte filter. The suspension obtained in the

TABLE 1. Determination of the Metastable Solubility of $3CaO \cdot Al_2O_3$

Quantity of $3CaO \cdot Al_2O_3$, g per 150 ml of solution	Conc. of s.a.w. in solution %	CaO, g/liter*	Al_2O_3 g/liter*	$3CaO \cdot Al_2O_3$, g/liter	CaO/Al_2O_3 (mole ratio)
		at 20°			
1,5	0,03	0,873	0,539	1,412	2,96
1,5	0,03	0,912	0,544	1,456	3,05
1,5	0,05	0,907	0,575	1,482	2,86
1,5	0,05	0,876	0,527	1,403	3,04
1,5	0,05	0,930	0,538	1,468	3,15
1,5	0,05	0,906	0,572	1,478	2,90
1,5	0,1	0,920	0,546	1,466	3,06
1,5	0,1	0,896	0,542	1,438	2,97
1,5	0,1	0,892	0,545	1,437	2,98
Average . . .		0,901	0,547	1,448	3,00
		at 40°			
1	0,05	0,927	0,628	1,555	2,70
1	0,07	0,940	0,602	1,542	2,84
1	0,07	0,963	0,683	1,646	2,56
2	0,10	1,116	0,694	1,810	2,94
2	0,10	0,929	0,629	1,558	2,70
2	0,10	0,941	0,662	1,603	2,59
2	0,10	0,960	0,692	1,652	2,53
2	0,10	0,922	0,619	1,541	2,72
3	0,10	0,993	0,671	1,664	2,68
2	0,25	1,018	0,620	1,638	2,99
2	0,50	1,082	0,624	1,706	3,17
3	0,50	1,080	0,638	1,718	3,08
Average . . .		1,026	0,632	1,658	2,95

*Average value from two determinations

TABLE 2. The Solubility of Hexagonal Tricalcium Hydroaluminate

Solid phase of the suspension	Conc. of the suspension, g/150 ml of solution	Conc. in solution, g/liter		Solubility of $3CaO \cdot Al_2O_3$ g/liter	CaO/Al_2O_3 mole ratio
		CaO	Al_2O_3		
at 20°, measurements carried out 10-15 days after preparation of the suspension					
$3CaO \cdot Al_2O_3$	2,0	0,425	0,336	0,661	3,28
$3CaO \cdot Al_2O_3 \cdot aq$	1,4	0,412	0,260	0,672	2,89
"	2,0	0,418	0,250	0,698	3,05
"	2,2	0,421	0,276	0,687	2,72
at 40°, measurements carried out 10 days after preparation of the suspension					
$3CaO \cdot Al_2O_3$	2	0,427	0,330	0,757	2,36
"	2	0,437	0,241	0,678*	3,31
"	3	0,452	0,236	0,688	3,49
$3CaO \cdot Al_2O_3 \cdot aq$	3	0,439	0,230	0,669	3,48

*1 month after preparation of the suspension.

presence of small quantities of s.a.w. filtered very readily; the filtrate was initially completely transparent and then rapidly became turbid as a result of the production of hydroaluminate microcrystallites. The CaO and Al_2O_3 contents of the filtrate were determined gravimetrically: the Al_2O_3 was precipitated with ammonia and the CaO with ammonium oxalate.

The results of the analysis of a suspension of the optimum composition are given in Table 1.

It has thus been possible to determine for the first time the magnitude of the metastable solubility of tricalcium aluminate. At 20° the value is 1.448 g $3CaO \cdot Al_2O_3$ per liter of solution, which corresponds to concentrations of 0.901 g CaO and 0.547 g Al_2O_3 per liter of solution.

The solubility of hexagonal tricalcium hydroaluminate (Table 2), determined by the same method by hydration of tricalcium aluminate and by dissolution of previously-prepared hydroaluminate has an average value of 0.679 g/ /liter at 20° (calculated as $3CaO \cdot Al_2O_3$), which shows good agreement with the literature data [11,12].

Table 2 shows that the maximum supersaturation which can be reached in C_3A suspensions at 20° is approximately 1.448/0.679 = 2.13.

The kinetics of supersaturation in C_3A suspensions at 40° was measured by the method used at 20°. Figure 4,a shows that in this case the electrical conductivity does not remain constant with change in the concentration of the suspension, but after reaching a maximum value of the electrical conductivity is higher, the greater the concentration of the suspension. At 40° no inflection is observed on the curve even at low concentrations of the suspension. This change in the electrical conductivity is related to the marked acceleration of the processes of C_3A dissolution and hydroaluminate crystallization, brought about by the increase in the temperature. In order to attain a constant electrical conductivity level corresponding to the solubility of C_3A at 40°, it would be necessary to retard these processes, particularly the process of crystallization of the new formations. For this purpose we added s.a.w., which is adsorbed on the original C_3A particles and also on the crystallites of the new formations being produced, leading to their stabilization and retardation of their growth [10,13]. Figure 4,b shows that when $3CaO \cdot Al_2O_3$ is dissolved in water, the resultant supersaturation begins to decrease rapidly and the maximum value of the specific conductance observed in this case is low. In the presence of very small quantities (0.01%) of s.a.w. in the solution, the supersaturation which can be observed in the suspension becomes very much greater but decreases very rapidly (Curve 2, Fig. 4,b). In the presence of 0.05-0.5% s.a.w., the maximum supersaturation attained in this suspension has the same value and is independent of further increase in the quantity of s.a.w. In the case where 1.0% s.a.w. is present in the solution, apparently as a result of a marked decrease in the rate of dissolution of the tricalcium aluminate, the increase in the electrical conductivity takes place very slowly and a value of the specific conductance close to the maximum value is attained only after 2 hours. These results show that the most convenient solutions for study are those containg 0.05-0.5% s.a.w.

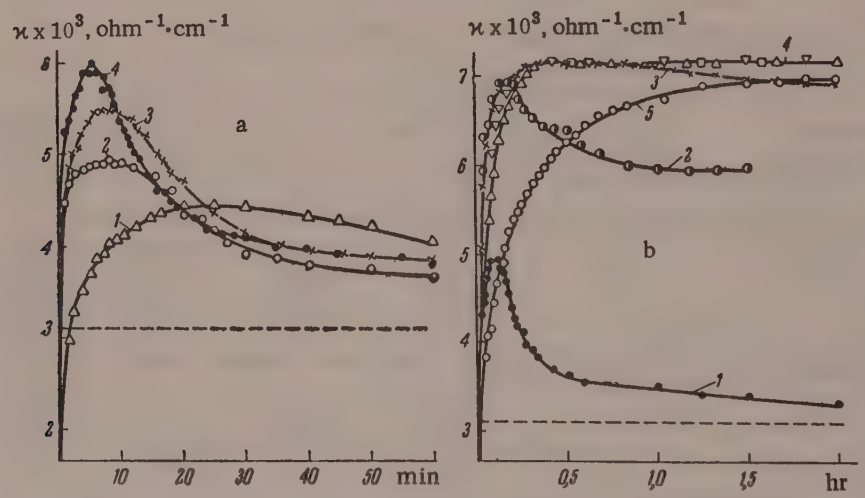


Fig. 4. Kinetics of the change in the specific conductance at 40° in the suspensions: a) containing in 150 ml of water: 1) 0.25 g; 2) 1.0 g; 3) 3.0 g; 4) 5.0 g C_3A; b) containing 2 g C_3A in 150 ml of water or s.a.w. solution: 1) water; 2) 0.01%; 3) 0.2%; 4) 0.05, 0.1, and 0.5%; 5) 1.0% s.a.w. solutions (the broken line denotes the level corresponding to a solution saturated with respect to the hydroaluminate).

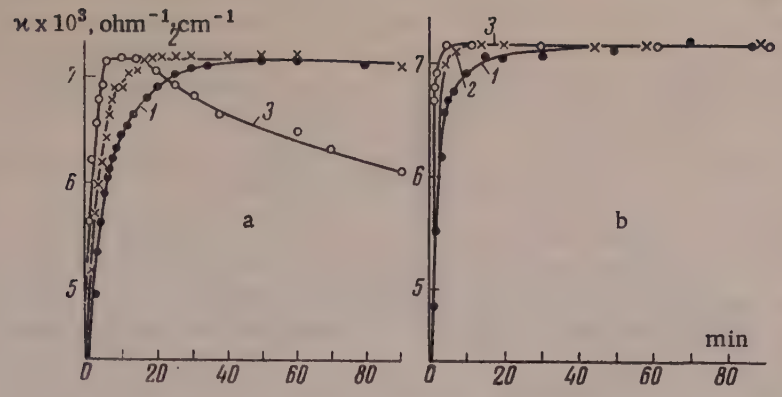


Fig. 5. Kinetics of the change in specific conductance at 40° in suspensions of C_3A in 0.05% (a) and 0.3% (b) solutions of s.a.w. Quantity of C_3A in 150 ml of solution: 1) 1 g; 2) 2 g; 3) 3 g.

Figure 5 shows that in the presence of 0.05 and 0.3% s.a.w. in the solution at 40°, a constant electrical conductivity level, independent of the concentration of the suspension, is reached in the C_3A suspensions. In order to determine the composition of the liquid phase of the suspension, corresponding to this electrical conductivity value, we filtered the suspension rapidly through a hot funnel. The CaO and Al_2O_3 contents of the filtrate were determined in the usual way (Table 1).

Table 1 shows that the deviation of the individual measurements from the average value is greater at 40° than at 20°. It is often found, moreover, that $CaO:Al_2O_3 \gg 3$, apparently as a result of an increase in carbonization. The average value of the solubility of $3CaO \cdot Al_2O_3$ at 40°, calculated from three determinations in which $CaO:Al_2O_3 > 2.70$, amounts to 1.658 g $3CaO \cdot Al_2O_3$ per liter of solution, which corresponds to concentrations of 1.026 g CaO and 0.632 g Al_2O_3 per liter of solution. At the same time $CaO:Al_2O_3 = 2.95$.

The solubility of hexagonal tricalcium hydroaluminate at 40° was determined by hydration of $3CaO \cdot Al_2O_3$ at 40° and by dissolution of previously-prepared hydroaluminate at this temperature (Table 2).

The very poor reproducibility of experiments on the determination of the solubility of calcium hydroaluminate has often been noted in the literature. This is particularly true for hexagonal tricalcium hydroaluminate [3,12], since this compound is metastable and is converted by recrystallization via solution to the more stable form—the cubic hydroaluminate—which has a lower solubility. In hydroaluminate solutions obtained by hydration of $3CaO \cdot Al_2O_3$, therefore, supersaturation is readily observed and on prolonged storage of the solution the concentration in it may decrease as a result of the conversion of the hexagonal form of the hydroaluminate to the cubic form. The repoducibility of the results obtained in the determination of the solubility of hydroaluminate at 40° is even better than that at 20° but in this case, as can be seen from Table 1, $CaO:Al_2O_3 > 3$ (in the first experiment this ratio is lower, as a result of the obviously high Al_2O_3 content). The increased value of $CaO:Al_2O_3$ at 40° indicates that at this temperature the incongruent solubility of hexagonal tricalcium hydroaluminate is having an effect.

The experiments which have been carried out show that the solubility of $3CaO \cdot Al_2O_3$ and its hydrate at 40° increases only slightly and the acceleration of the hydration, which is observed at 40°, is due chiefly not to a change in the magnitude of the supersaturation produced in the suspension, but to the very marked acceleration of the dissolution of the original C_3A and the crystallization of the new formation—the hydrate.

SUMMARY

1. The magnitude and kinetics of supersaturation in dilute aqueous suspensions of tricalcium aluminate have been measured at 20° and 40°.

2. In aqueous suspensions of tricalcium aluminate, there is established a constant supersaturation level which is independent of the concentration of the suspension and is determined by the metastable solubility of the original anhydrous aluminate. Tricalcium aluminate dissolves congruently and its solubility at 20° is 1.448 g $3CaO \cdot Al_2O_3$ per liter, which corresponds to a CaO concentration of 0.901 g/liter and an Al_2O_3 concentration of 0.547 g/liter. The solubility of hexagonal tricalcium hydroaluminate at 20° is 0.679 g/liter, calculated as $3CaO \cdot Al_2O_3$.

3. Increase in the temperature to 40° leads to a sharp increase in the rate of the hydration process, which is due chiefly to an increase in the rate of dissolution of the C_3A and in the rate of crystallization of the hydrate. The solubility of C_3A at 40° is only slightly increased and is equal to 1.658 g $3CaO \cdot Al_2O_3$ per liter, which corresponds to a CaO concentration in the solution of 1.026 g/liter and an Al_2O_3 concentration of 0.632 g/liter. The solubility of the hexagonal hydroaluminate at 40° is 0.698 g/liter, calculated as $3CaO \cdot Al_2O_3$.

LITERATURE CITED

1. E. E. Segalova and P. A. Rebinder, Stroitel'nye Materialy, No. 1, 21 (1960).
2. V. B. Ratinov, Ya. L. Zabezhinskii, and T. I. Rozenberg, Collected Works of the Reinforced Concrete Scientific Research Institute, No. 1 [in Russian] (Promstroiizdat, Moscow, 1957).
3. R. H. Bogue, The Chemistry of Portland Cement, N.Y., 1952; M. J. Brocard, Ann. Inst. Techn, des Batiments et des Travaux publ, No. 12 (1948).
4. A. M. Kuznetsov and A. I. Sosnina, Izvest. Estestvenno-nauchn. Inst. pri Permskom Univ. im. Gor'kogo, 14, No. 1, 107 (1957).
5. K. Kelley, D. Southard and K. Andersen, The Thermodynamic Properties of Gypsum [Russian translation by S. S. Pechuro, BTI Ministerstvo Prom. Stroit. Materialov RSFSR] (Moscow, 1949).
6. E. E. Segalova, E. S. Solov'eva, and P. A. Rebinder, Doklady Akad. Nauk SSSR 117, No. 5, 841 (1957); E. E. Segalova, S. I. Kontorovich, and P. A. Rebinder, Doklady Akad. Nauk SSSR 123, No. 3, 509 (1958); E. E. Segalova, Z. D. Tulovskaya, and E. A. Amelina, Doklady Akad. Nauk SSSR 124, No. 4, 876 (1959).
7. Yu. M. Butt and E. I. Onishchik, Collected Scientific Works on Glass [in Russian] (Promstroiizdat, Moscow, 1950).
8. L. S. Wells, J. Res. Nat. Bur. Stand. 1, 951 (1928).
9. E. E. Segalova, V. N. Izmailova, and P. A. Rebinder, Doklady Akad. Nauk SSSR 114, No. 3, 594 (1957).
10. E. E. Segalova, E. S. Solov'eva, and P. A. Rebinder, Doklady Akad. Nauk SSSR, 113, No. 1, 134 (1957).
11. V. M. Moskvin and T. V. Rubetskaya, Collection, Concretes and Binding Agents [in Russian] (Gosizdat po Stroit. i Arkhitekt., Moscow, 1955).
12. R. Nacken and R. Mosebach, Z. anorgan. und allgem. Chem. 225, 299 (1935); R. Nacken, Zement 34, 565 (1936).
13. S. I. Kontorovich, E. E. Segalova, and P. A. Rebinder, Doklady Akad. Nauk SSSR 129, No. 4, 847 (1959).

All abbreviations of periodicals in the above bibliography are letter-by-letter transliterations of the abbreviations as given in the original Russian journal. *Some or all of this periodical literature may well be available in English translation.* A complete list of the cover-to-cover English translations appears at the back of this issue.

THE AGGREGATION STATES OF HIGH-MOLECULAR COMPOUNDS

VIII. EFFECT OF TEMPERATURE ON RAMIE CELLULOSE FIBER AND HYDROCELLULOSE FILM

R. I. Fel'dman

N. K. Krupskaya Moscow Regional Pedagogic Institute
Translated from Kolloidnyi Zhurnal, Vol. 23, No. 3, pp. 315-321, May-June, 1961
Original article submitted March 8, 1960

The linear dilatometry method [1-4] can be used to study the behavior of various high-molecular compounds and their transitions from one state to another under the influence of temperature. Investigations of this type are interesting not only from the theoretical point of view, but they also possess practical interest, since they make it possible to follow the change in the properties of materials during heating and cooling. This information is necessary in designing the operational technique of the technological processes and for establishing the temperature range in which articles with a given set of properties can be utilized.

The results of the temperature-dilatometric measurements [3] using natural ramie cellulose fibers and hydrocellulose films as representatives of high-molecular systems, into the composition of which, depending on external conditions, a variable amount of water enters, are described in the present paper. In such systems it is possible to consider the water as a plasticizing component. Removal of the water from the system by heating leads to the situation that up to a certain temperature the material becomes stiffer [1]. In cellulose specimens an increase in the stiffness can be explained by the fact that the hydroxyl groups liberated in the removal of the water react with each other, despite an increase in the heat motion of the kinetic units of the system as the result of increasing the temperature. Observation of the changes in the linear dimensions of cellulose was made in the temperature range corresponding approximately to the temperature conditions of its utilization and technological processing. It is interesting to compare the behavior of cellulose under changing temperature conditions with that of other hydrophilic high-molecular compounds of both natural [1] and synthetic [2] origin.

Although a study of cellulose and its derivatives has attracted the attention of many investigators for a long time, still the question as to the phase condition of these products remains one of discussion at the present time. Discussion is still being held on whether the amorphous or microcrystalline state is the equilibrium condition for cellulose and its derivatives [5-15]. There is no argument about the fact that in natural cellulose fibers (ramie, cotton, etc.) long-chained molecules with a molecular weight of several millions, formed by biosynthesis, are arranged mainly parallel to the fiber axis. The high degree of orientation of the long-chained molecules, accomplished during growth, is supported by the results of x-ray and electronographic studies, made by various investigators.

Intermolecular reaction between the chains, composed of repeating units of cellobriose radicals, is accomplished mainly via hydrogen bonds, the presence of which was shown in studying the absorption spectra in the infrared region [7]. According to these data, nearly all of the hydroxyl groups in ramie cellulose, cotton and mercerized cellulose fibers and hydrocellulose films are involved in the hydrogen bond. The distribution of the hydrogen bonds based on the energy values is different for the different specimens studied. In mercerized cellulose and hydrocellulose the amount of hydrogen bonds with a smaller energy is greater than in ramie cellulose and cotton fibers [7]. Starting from the values of the heats of wetting with water, it was calculated that natural cellulose contains 27% free and 63% bound hydroxyl groups, while in hydrocellulose the amounts are 55% and 45%, respectively [9].

It is possible to assume that a change in the properties of natural regenerated cellulose when the temperature and moisture content of the surrounding medium are changed is to a large degree determined by the destruction and reduction of the hydrogen bonds between the long-chained molecules. The existing information on the smaller values of the density, stiffness and orderliness of the chains in regenerated products when compared with the natural should probably be associated for the most part with the quantitative and qualitative characteristics of the hydrogen bond, directly depending on the coordination of the links of the molecular chains.

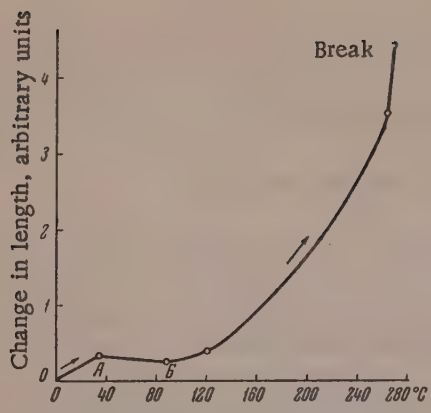


Fig. 1. Dependence of the length of ramie cellulose fiber on the temperature.

Ramie cellulose fivers. Fibers with a cross-section area of 0.9×10^{-5} to 1.3×10^{-5} sq cm and a length of 5 to 7 cm were tested under loads ranging from 150 to 600 g/sq mm. It should be mentioned that the testing of fine fibers and threads by the method adopted by us, at relatively small loads, cannot be accomplished in practice, and consequently mounting the ramie fiber in the operating part of the dynamometer, employed by us as a dilatometer [3], is only possible at P = 150 g/sq mm and higher, depending on the diameter of the fiber. As an example, we have shown in Fig. 1 the dependence of the fiber length on the temperature, obtained when the specimen was heated to the destruction (break) temperature, equal to 266°, at P = 239 g/sq mm. The same as for other high-molecular compounds [1], the break temperature of the ramie cellulose fiber can to some degree be regarded as the starting point of flow under the influence of two simultaneously operating factors: mechanical action (loading) and increase in the intensity of the heat motion. The fiber length from the start to finish of testing (Fig. 1) increases by about 1.0%; the change in the length from 36° (point A) to 87° (point B) is equal to 0.01%. The coefficient of linear expansion α (cm/degree·cm), calculated along the linear portion of the curve, extending up to 36°, is equal to 1.67×10^{-5}. The temperature region, in which the fiber contracts when heated, is smaller the greater the load. When the load is decreased both the linear expansion coefficients and the temperature of the start of specimen contraction, after elongation in the heating process, decrease.

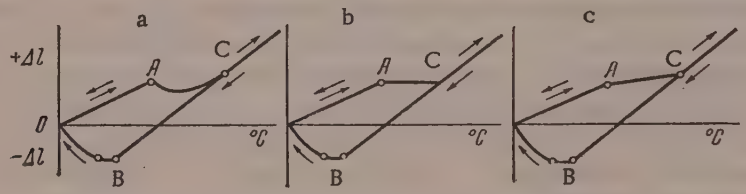


Fig. 2. Diagrams of the dependence of the length of ramie cellulose fiber on the temperature during heating and cooling.

The data at our disposal made it possible to show by extrapolation that for unloaded specimens (P = 0) the temperature region of contraction should range from ~ 25 to ~ 100° and the coefficient of linear expansion—up to the temperature of starting change in the shape of the dilatometric curve—should equal approximately 1.25×10^{-5}. Fiber contraction under the influence of temperature should cease when P ≈ 700 g/sq mm. The shrinkage value for ramie cellulose fiber when heated is smaller than for the other specimens studied earlier [1,2]. In comparable temperature intervals the shrinkage of silk fibroin fibers is equal to 0.76% (P = 434 g/sq mm); nylon filaments = 1.75% (P = 178 g/sq mm); polycaprolactam filaments = 3.5% (P = 371 g/sq mm), while for ramie cellulose fibers the shrinkage under the adopted test conditions did not exceed 0.015%. The same thing is observed when the hysteresis loops on the curves (Fig. 2) are compared with the analogous data for silk fibroin, polycaprolactam, nylon, etc. [1-4]. The observations made on the changes in fibers after mechanical and thermal action, which reflects on the length, cross-section area and density of the specimens, prove to be interesting. Thus, in ramie cellulose fibers, rapidly cooled to 20°, after break at 266°, the cross-section area decreases by 45-50%, and then for a period of 30 days it increases, but does not reach the original values; the irreversible changes equal 20-25%.

To determine the temperature limits of possible reversibility of the linear dimensions, the starting temperatures of the hysteresis loops on the dilatometric curves and the effect of the maximum heating temperature on the position of the cooling curve relative to the heating curve, we ran a series of tests under various conditions. In particular, to establish the effect of prior heat treatment, the fiber was subjected to repeated heating and cooling (multicyclic tests). The dilatometric measurements were made with a variable sequence of the heating and cooling operations and up to different final temperatures. The specimens, like in all of the other experiments, were placed under a load, the value of which must always be taken into account in the utilization and fabrication of articles made from cellulose and other fibers. From the experimental material it is possible to conclude that when ramie cellulose fiber is heated at

150–180°, under a load up to 560 g/sq mm, the changes in the length are reversible. The results of the observations are depicted as diagrams in Fig. 2. The hysteresis loops during cooling begin (point C) from ~80 to ~110°, depending on the test conditions and previous history of the fibers. The cooling curve in the region of the hysteresis loop lies below the heating curve. The presence of hysteresis should most probably be regarded as being due to the loss of moisture by the fibers (the initial amount of moisture in the fibers was approximately 6%). Under isothermal conditions, with time and during cooling in the temperature interval from ~40 to ~25°, the length of ramie cellulose fibers, after normal contraction, begins to increase and is restored to the original value. The same is also observed for polyamides of synthetic and natural origin [1,2], which, in our opinion, is associated with the lability of a certain portion of the hydrogen bonds. During heating and cooling, hysteresis is practically absent in the interval where the length is linearly dependent on the temperature (up to point A, Figs. 1 and 2). The lines, showing the changes in the length as a function of temperature lying above the start of hysteresis (point C, Fig. 2) should be regarded as belonging to practically dehydrated cellulose.

The magnitude of fiber shrinkage decreases not only with increase in the applied load, but also after prior heat treatment, which was also observed for other high-molecular compounds [1-3] and testifies to the residual compression of the material. Depending on the value of the load, length of the heat treatment and the temperature at which it was done, fiber shrinkage is replaced by either a constant length (Fig. 2,b)or an increase in it, but with a smaller linear expansion coefficient (Fig. 2,c). For example, if the fiber is first heated up to 150° at the rate adopted in our tests (1° in 3-5 min), then the shrinkage, previously established for the not heat treated fibers at P = 560 g/sq mm, is replaced by elongation.

The position of the transition points on the dilatometric curve depends on the applied load, the previous history of the specimen, and the kinetics of the process of temperature action. When the heating rate is increased the points shift toward higher temperatures, while when the cooling rate is increased they shift toward lower temperatures. The dependence of the position of the transition points on the enumerated factors was described by us earlier [1-3] for other high-molecular compounds and is a general rule. The start of fiber elongation when cooling from point B (Fig. 2) is stabilized under the influence of heat treatment and is realized around 40°, which, probably, is associated with the nature and properties of the hydrogen bond [16].

The linear expansion coefficients, calculated for temperatures above 100°, characterize the behavior of practically dry ramie cellulose; their value is approximately twice as great as for specimens containing moisture.

The dialatometric curves for the heating and cooling of the specimen from ~86 to 150–180° practically coincide. The good reproducibility of the linear dimensions of ramie cellulose fiber under the adopted test conditions results from retaining a relatively complete orientation of the long-chain molecules. This is evidenced by a comparison with other materials and the small dependence of the linear expansion coefficient on the load and the magnitude of the shrinkage. Consequently, change in the linear dimensions of ramie cellulose fibers when heated to 150–180° depends mainly on normal thermal expansion and loss of moisture with a practically fixed structure; this differentiates them from other artificially oriented, predominantly synthetic polymers, like poly(vinyl chloride), polystyrene, poly (methyl methacrylate), etc. [3], where residual changes in the structure are observed under the same conditions. The closeness of the transition points, established from the disturbance of the monotonic shape of the temperature-dilatometric curves, for the ramie cellulose fibers with the transition points for protein specimens and synthetic polyamides [1,2] deserves attention. The transition points, taking into consideration their shift due to the above indicated factors, are found to lie in the range 30 to 50°, 90 to 120°, and above 200°. It is possible that this similarity is the result of the presence of bound water in these systems and a common type of structure with a preponderance of hydrogen bonding, as a form of intermolecular reaction characteristic for them.

Hydrocellulose (regenerated cellulose) film. Hydrocellulose specimens as strips with an average width of 0.84 cm, an average thickness of 60 microns and a length of 10 to 15 cm were cut from film that had been dried in the stretched state (moisture content ≈ 11%). Such a method of drying assured a set orderliness of the chains in the hydrocellulose films, although there was a certain shift of the glucose units when compared with their position in natural cellulose [12]. The load during the dilatometric measurements did not exceed 20 g/sq mm. The temperature was varied at the rate of 1° per 3-5 min. If the measurements were made with a markedly reduced rate of temperature change, then the corresponding sections on the curves expressing the dependence of the length on the temperature were depicted by dotted lines.

In Fig. 3, for example, two cycles of heating and cooling, at P = 18.2 g/sq mm, are given for a hydrocellulose strip, cut from the film in the direction of the orientation: first cycle (22° → 180° → 22°), and second cycle–12 hr

after the first (22° → 170° 22°). The linear expansion coefficients are: in the first cycle, $\alpha_{180-116} = 4.07 \times 10^{-5}$ and $\alpha_{116-34} = 2.89 \times 10^{-5}$, and in the second cycle, $\alpha_{170-98} = 3.49 \times 10^{-5}$ and $\alpha_{98-36} = 2.72 \times 10^{-5}$.

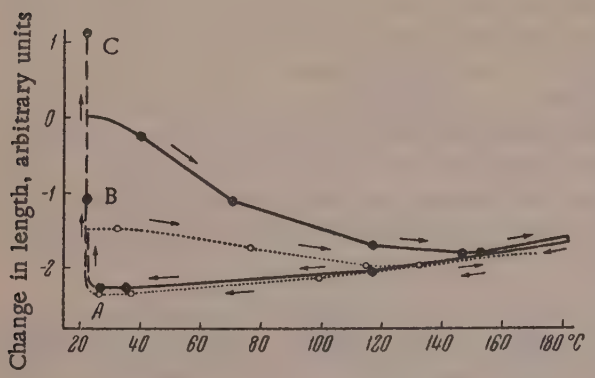


Fig. 3. Dependence of the length of hydrocellulose film on the temperature.

The shrinkage during heating in the first cycle (up to 146°) was equal to approximately 1.5%, and in the second cycle (from 32 to 116°) it was equal to 0.4%. After the temperature action, made in the first cycle and then allowing the specimen to relax for 12 hr at 22°, the length of the specimen at the start of the second cycle was 1.25% less than the original. The maximum reduction in the length from the start of testing to the minimum point A (Fig. 3) on the cooling curve at 27° is equal to 1.9%, while from the start of the second cycle it is equal to 0.65%. After the second cycle of heating and cooling, a practically constant length (point B) of the specimen is established in 6 days, exceeding the length measured at the start of the second cycle by 0.3% and smaller than the initial length by 1.0%. If such specimens (from point B) are placed in supplementally moistened air with a relative moisture constant close to 100% [1], then in a matter of approximately 3 hr their length is restored to the original. Under these conditions the original length is not the equilibrium length. Specimens kept for 68 days in supplementally moistened air, become longer by 1.0% due to moisture absorption (point C, Fig. 3). The results, obtained in a cyclic carrying out of the processes, must be evaluated taking into consideration the shape and size of the specimens, their moisture content, their previous history, the rates of heating and cooling, and the magnitude of the load. However, despite the great complexity of the obtained pictures, it is still possible by comparing with other analogous examples to disclose some characteristic and quite reproducible material properties of the investigated specimens. The described properties have certain common features for a group of polymers of different nature and are specific for the given specimens. In particular, the values of the expansion coefficients, shrinkage, and areas of the hysteresis loops testify to the fact that like influences produce greater changes in hydrocellulose films than in ramie cellulose fibers. The performed experiments also indicate that the structure of hydrocellulose films is relatively stable toward the action of temperature up to 150–180°.

SUMMARY

1. The behavior of ramie cellulose fibers, characterized by a thermal linear expansion, testifies to the presence in them of a relatively strongly fixed structure, not undergoing irreversible changes up to 150–180°.

2. Hydrocellulose films give indications of having a more open structure than ramie cellulose fibers, which affects both the shrinkage and the size of the hysteresis loops. The original dimensions are restored to the films after heat treatment to 150–180°, which is evidence that the hydrocellulose structure also fails to undergo irreversible changes.

I wish to sincerely thank Prof. S. I. Sokolov for his constant interest in my work.

LITERATURE CITED

1. R. I. Fel'dman, Kolloid. Zhur. 21, No. 4, 499 (1959); 22, No. 3, 351 (1960).
2. R. I. Fel'dman, Kolloid. Zhur. 21, No. 2, 238 (1959).
3. R. I. Fel'dman, Kolloid. Zhur. 20, No. 2, 220 (1958).
4. R. I. Fel'dman and S. I. Sokolov, Kolloid. Zhur. 20, No. 3, 388 (1958).
5. K. H. Meyer and H. F. Mark, Structure of High Polymeric Natural Organic Compounds [Russian translation] (Goskhimtekhizdat, 1932); H. F. Mark, Physical Chemistry of Cellulose [Russian translation] (ONTI, 1935); K. Hess, Chemistry of Cellulose and Similar Substances [Russian translation] (Goskhimtekhizdat, 1934); H. Staudinger, High Molecular Organic Compounds [Russian translation] (ONTI, 1935); W. T. Astbury, The Fundamental Structure of Textile Fibers [Russian translation] (State Light Industry Press, 1936); J. R. Katz, Roentgenography of High Molecular Substances, Colloids, and Animal and Plant Tissues [Russian translation] (ONTI, 1937); P. P. Shorygin, Chemistry of Cellulose [in Russian] (GONTI, 1939).

6. V. A. Kargin, Vysokomolek. Soed. 2, No. 3, 467 (1960); V. A. Kargin and N. V. Mikhailov, Zhur. Fiz. Khim. 14, No. 2, 195 (1940); N. V. Mikhailov, V. A. Kargin, and V. M. Bukhman, Ibid., 14, No. 2, 205 (1940); V. A. Kargin and D. I. Leinunskaya, Ibid., 14, 312 (1940); 15, 1011 (1941); V. A. Kargin, P. V. Kozlov, and T. V. Zueva, Ibid., 17, Nos. 5-6, 318 (1943); N. V. Mikhailov, V. A. Kargin, and V. E. Elinek, Investigations in the Domain of High Molecular Compounds [in Russian] (Izd. AN SSSR, 1949), p. 281; Kh. U. Usmanov and V. A. Kargin, Chemistry and Physical Chemistry of High Molecular Compounds [in Russian] (Izd. AN SSSR, 1952), p. 169; V. A. Kargin, V. L. Karpov, Yu. S. Lipatov, G. S. Markova, and T. A. Koretskaya, Doklady Akad. Nauk SSSR 101, 707 (1955); V. A. Kargin and G. L. Slonimskii, Uspekhi Khim. 24, No. 7, 785 (1955); N. V. Mikhailov and É. Z. Fainberg, Doklady Akad. Nauk SSSR 109, No. 6, 1160 (1956); V. A. Kargin, P. V. Kozlov, and Van Nai-Chan, Ibid., 130 No. 2, 356 (1960).
7. V. N. Nikitin, Zhur. Fiz. Khim. 23, 775, 786 (1949).
8. A. L. Zaides and I. G. Stoyanova-Sinitskaya, Doklady Akad. Nauk SSSR 80, 213 (1951); 92, 601 (1953); 107, 711 (1956).
9. S. M. Lipatov, D. V. Zharkovskii, and I. M. Zagraevskaya, Kolloid. Zhur. 21, No. 5, 526 (1959).
10. A. I. Kitaigorodskii and D. Ya. Tsvankin, Vysokomolek. Soed. 1, 269, 279 (1959).
11. Advances in Chemistry and Technology of Polymers [in Russian] (Goskhimizdat), Coll. Vol. I, pp. 159 and 163 (1955); Coll. Vol. II, pp. 97 and 229 (1957).
12. F. W. Billmeyer, Introduction to the Chemistry and Technology of Polymers [Russian translation] (IL, 1958).
13. S. A. Glikman, Introduction to the Physical Chemistry of High Polymers [in Russian] (Saratov University Press, 1959).
14. Z. A. Rogovin, Vysokomolek. Soed. 2, No. 10, 1588 (1960); Z. A. Rogovin and N. N. Shorygina, Chemistry of Cellulose and Similar Substances [in Russian] (Goskhimizdat, 1953).
15. V. I. Sharkov, Vysokomolek. Soed. 2, No. 11, 1747 (1960); I. I. Korol'kov, V. I. Sharkov, and E. N. Garmanova, Doklady Akad. Nauk SSSR 109, 1140 (1956); Zhur. Priklad. Khim. 30, 586 (1957); V. I. Sharkov and V. P. Levanova, Vysokomolek. Soed. 1, 730, 1027, 1034 (1959); Doklady Akad. Nauk SSSR 130, 109 (1960).
16. Ya. K. Syrkin and M. E. Dyatkina, The Chemical Bond and the Structure of Molecules [in Russian] (Goskhimizdat, 1946).

All abbreviations of periodicals in the above bibliography are letter-by-letter transliterations of the abbreviations as given in the original Russian journal. *Some or all of this periodical literature may well be available in English translation.* A complete list of the cover-to-cover English translations appears at the back of this issue.

RADIOCHROMATOGRAPHIC SEPARATION OF MIXTURES OF SULFUR AND VULCANIZATION ACCELERATORS

I. V. Khodzhaeva and Yu. V. Kissin

M. V. Lomonosov Moscow Institute of Fine Chemical Technology
Translated from Kolloidnyi Zhurnal, Vol. 23, No. 3, pp. 322-326, May-June, 1961
Original article submitted November 30, 1959

The wide use of tagged atoms for studying the mechanism of chemical reactions and finding out the relation between reactivity and molecular structure gives the investigators a series of new problems connected with the separation of substances and radioactive isotopes. Since the type of isotopic exchange gives direct information on the mobility of the atoms in the molecule, isotopic exchange is one of the most widely used methods for investigating molecular structures.

Because the isotope must be isolated quantitatively from the reaction mixture, the separation of the substances studied and the radioactive isotopes is one of the most serious problems arising in the study of isotopic exchange. As a rule, this is done by binding chemically one of the components participating in the exchange, but usually, this operation is time consuming and, moreover, it is necessary to work with great amounts of radioactive substances.

In order to simplify this problem we attempted to separate the exchange products by the method of paper radiochromatography [1-3].

The separation of substances by means of distributive paper chromatography results from their different distribution coefficients in two immiscible liquid phases.

The travelling of the zones of the substances to be spearated is characterized by the coefficent R_f

$$R_f = \frac{\text{travelling speed of the zone}}{\text{travelling speed of the solvent front}}.$$

Each substance which can be distributed among both liquid phases has its constant R_f value. It is evident that the greater the distribution coefficient $\alpha = c_2/c_1$ (where c_1 and c_2 are the concentrations of the substance in the water phase and the organic solvent, respectively) the higher will be the travelling speed of the component along paper.

The following systems were studied:

1. Tetramethylthiuramdisulfide

$$(CH_3)_2N-\overset{\overset{S}{\|}}{C}-S-S-\overset{\overset{S}{\|}}{C}-N(CH_3)_2+S^{35}.$$

2. Diethyldithiocarbamates

$$[(C_2H_5)_2N-\overset{\overset{S}{\|}}{C}-S]_xMe+S^{35}.$$

3. Diethyldithiocarbamates + tetraethylthiuramdisulfide containing four S^{35} atoms.

These systems were chosen because tetramethylthiuramdisulfide (TMTD) and several diethyldithiocarbamates (carbates) are widely used as accelerators in rubber vulcanization.

The vulcanization activity of accelerators, obviously, is closely connected with the mobility of the sulfur atoms in their molecules. For this reason it was of interest to clarify the bond type and the ease of sulfur exchange entering the TMTD and carbate molecules. The isotopic exchange between TMTD and S^{35}, carbates and S^{35} was carried out by heating solutions of these substances in benzene or chloroform in sealed ampoules at 120-180° for varying durations of time. Besides, the exchange between TMTD and S^{35} was studied without solvent. The reaction conditions in the exchange of TMTD and carbates with S^{35} are given in Table 1.

TABLE 1. Isotopic Exchange of TMTD and Carbates with Elementary Radioactive Sulfur (S^{35})

Reacting compound	Temperature of exchange, °C	Reaction time, hr	TMTD:S^{35} of carbate:S^{35} ratio	Exchange, %
TMTD	126	6	1:4	73.0
TMTD	122	7	1:4	33.0
Pb Carbate	120	32	1:4	31.1
Cu Carbate	120	32	1:4	0
Co Carbate	150	20	1:6	0
Fe Carbate	150	20	1:6	0
Zn Carbate	150	14	1:4	47.6
Cd Carbate	150	14	1:4	23.4
Co Carbate	180	12	1:6	39.1
Fe Carbate	180	12	1:6	29.0
Ni Carbate	180	12	1:4	13.9
Cu Carbate	180	12	1:4	28.0

Note: The concentration of TMTD in benzene and Zn,Ni, Cu,Cd and Pb carbate in chloroform was 0.006 mole/liter, that of Co and Fe carbate in chloroform 0.004 mole/liter; the sulfur concentration in benzene and chloroform was 0.024 g-at/liter. In the case of TMTD the separation of the components was achieved by a methanol: water: acetic acid = 8:1:1 mixture, in the case of carbates by petroleum ether: water: acetic acid = 8:1:1.

The Co,Ni,Cu,Fe,Cd,Pb and Hg carbates were synthesized by precipitating them with the corresponding cations from a solution of Na carbate in water at a fixed pH [4]. To study the exchange between the carbates and tagged thiuram we have synthesized the radioactive tetraethylthiuramdisulfide (TETD*) $(C_2H_5)_2N-C(=S^*)-S^*-C(=S^*)-N(C_2H_5)_2$ by means of the method proposed by Rothstein and Binovic [5].

The exchange was carried out at 25° in chloroform at a TETD* concentration 0.04 mole/liter and the molar ratio:1:1.5 for Co and Fe Carbate:TETD* and 1:1 for Zn,Cd,Ni,Cu,Pb,Hg carbates: TETD*.

The reaction time and the degree of exchange are given in Table 2.

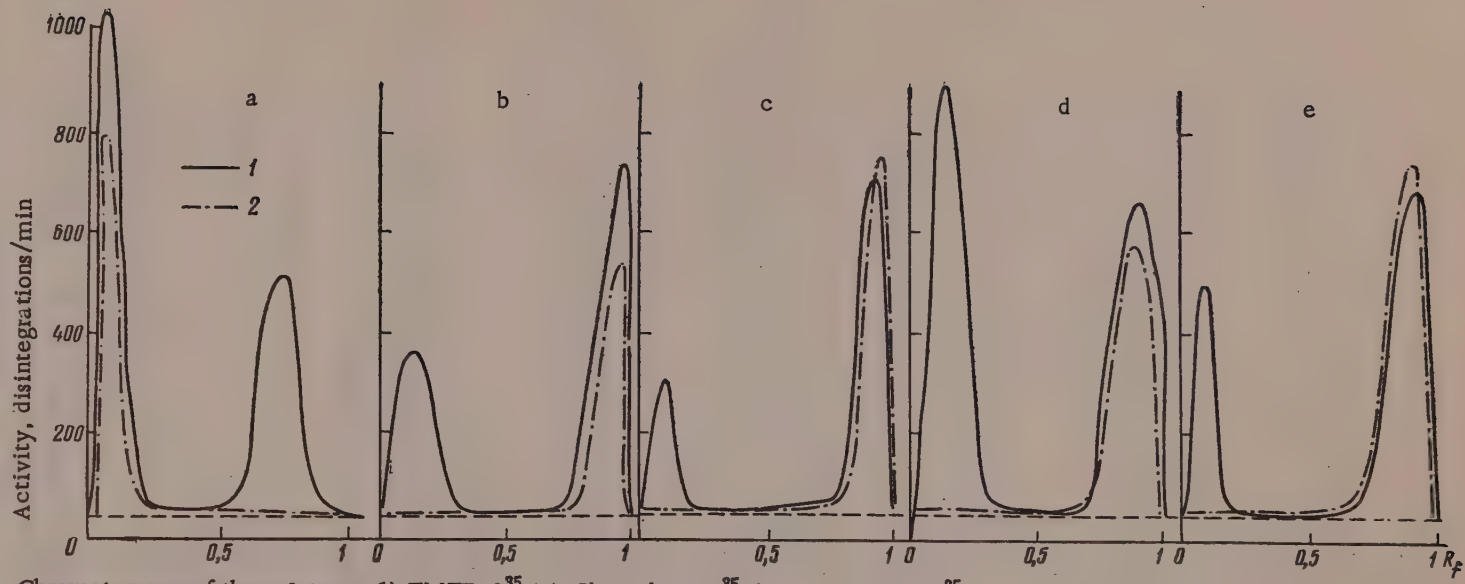
TABLE 2. Isotopic Exchange Between Metal Carbates and Radioactive TETD*

Carbates	Zn		Cd		Ni		Co		Fe		Cu		Pb		Hg	
Reaction time, min.	5	60	5	60	5	60	5	60	5	60	5	60	5	60	5	60
Exchange, %	100	100	100	100	61,0	100	0	1,0	35,4	82,3	100	100	100	100	100	100

When the ampoules with the solution of S^{35} and carbates were heated at temperatures above 100°, the latter compounds were found to decompose under precipitation of the metal sulfide.

In order to separate the components of the mixture, a small amount of solution (0.005-0.01 ml, which amounted to 10-30γ dissolved substance) was deposited in the form of a drop on a strip of special filter paper, 40 cm long and 4.5 cm broad; the activity of the original stain was 2000-3000 disintegrations per minute. After the drop had dried the end of the paper was placed in a dish with the organic solvent saturated with water and it was pressed between pieces of glass. The dish was fixed in a glass cell 50-cm high having a tightly fitting hood. The atmosphere in the cell was saturated with solvent and water vapor.

After the solvent had travelled over a certain distance (30-50 cm), the paper was taken out of the dish and the position of the solvent front was recorded. To interpret the chromatograms, the strip of paper was divided in small parts with a length of 1 or 2 cm along the path of the solvent and the activity of each part was measured by means of



Chromatograms of the mixtures: 1) TMTD-S^{35} (a); Pb-carbate-S^{35} (b); Cd-carbate-S^{35} (c); Cu-carbate-TETD (d) and Ni-carbate-TETD (e); 2) S^{35} (a,b,c) and TETD (d,e).

a window counter. The results were plotted in a graph of activity versus distance from the original stain. When the separation of the mixture is complete, a high activity is found in the original stain (if one of the components is insoluble in the travelling solvent), further on it drops to the background, then again a peak appears at the end of the chromatogram where the second component of the mixture is concentrated. By comparing the area under the peaks the ratio of the components in the mixture to be separated can be determined quantitatively. The area was measured by means of a planimeter or, more roughly, by summing up the activity of the separate 1-2 cm parts lying under the maxima. To calculate the degree of exchange we have used the following formula

$$\% \text{ обмена} = \frac{2\sum (I_1 - I_0)}{\sum (I_1 - I_0) + \sum (I_2 - I_0)},$$

where I_1 and I_2 are the activities of the 1-2 cm chromatogram parts under the activity maximum; I_0 the background activity.

The degrees of exchange between TMTD or carbates and S^{35} and those for carbates with TETD*, as are calculated in this way and given in the Tables 1 and 2, are the averages of data from 3-6 chromatograms. The relative error was 1-2%.

For the separation of the said mixtures we tested sixteen different organic solvents in combination with acetic acid and ammonia; from these, methyl and ethyl alcohol as the travelling phase and water as the immovable phase (in the presence of acetic acid to prevent the formation of "tails"), in the ratio 8:1:1 proved to be suitable for the separation of the system TMTD + S^{35} (Table 1).

In the Fig. we show typical cases of complete separation of this type of mixture. The initial high activity refers to S^{35}, which is not dissolved by alcohol and stays in the original stain, further on the activity drops to the background value and then rises again because of the active TMTD carried along by the travelling solvent. Separation of the mixtures: carbates + S^{35} was achieved by means of petroleum ether, water and acetic acid (8:1:1)—(Fig.1, b). In this case the original stain is characterized by the activity of the carbate and that at the end by S^{35}, which is washed out by petroleum ether.

The TETD + carbates mixtures were separated by ethyl alcohol, water and acetic acid (8:1:1)—(Fig. 1,c). The initial activity results from the carbate, that at the end from TETD* showed that all TETD* is concentrated in the stain at the end.

SUMMARY

1. We have synthesized Co,Ni,Fe,Cu,Cd,Pb,Hg-diethyldithicarbamates (carbates) and radioactive tetraethylthiuramdisulfied (TETD*).

2. We have carried out exchange between S^{35} and TMTD, S^{35} and the synthesized carbates, carbates and TETD* and the mixtures were separated by means of paper radiochromatography: S^{35} + TMTD by ethyl and methyl alcohol; TETD* + carbates by ethyl alcohol.

3. From the radiochromatographic data we have calculated the degrees of exchange.

LITERATURE CITED

1. V. V. Rachinskii, Uspekhi Khim. 19, 4, 445 (1950).
2. E. N. Gapon and V. V. Rachinskii, Transactions of the All-Union Conference on Chromatography, 1950 [in Russian].
3. N. P. Klimov, Collection: Chromatography [in Russian] (No. 1, 1956).
4. K. Greu, and R. Schwab, Angew. Chemie 62, 320 (1950).
5. R. Rothstein and K. Binovic, Recueil trav. chim. 73, 561 (1954).

INVESTIGATION OF THE STRUCTURATION AND RHEOLOGICAL PROPERTIES OF AQUEOUS DISPERSIONS OF BENTONITE CLAYS DURING THEIR REACTION WITH HUMATES

Chiang Lung, N. N. Serb-Serbina and

P. A. Rebinder

Institute of Physical Chemistry, Academy of Sciences, USSR
Translated from Kolloidnyi Zhurnal, Vol. 23, No. 3, pp. 327-333, May-June, 1961
Original article submitted August 19, 1960

In the previous communication [1] the principal laws of structuration were examined and the rheological characteristics of aqueous dispersions of humates were given. The present paper gives the results of investigations of the strength and rheological properties of dispersions of bentonite clays and their reaction with humates.

Two samples of Oglanlinsk bentonite, distinguished from each other by the different ratio of the cations in their exchange complex, were used for the investigations. Sample 1 of bentonite contained: Na^+ 45.6, Ca^{2+} and Mg^{2+} 14.5 mg-equiv per 100 g of clay; sample 2 contained: Na^+ 20.2, Ca^{2+} 33.9, Mg^{2+} 19.6 mg-equiv per 100 g of clay. The degree of dispersion of suspensions of bentonite sample 2 was therefore half that of sample 1, and the structure in its suspensions was weaker. Thus, the strength after the complete development of the taxotropic structure (P_m) of a 10% aqueous suspension of sample 1 was 1600 · dyne · cm^{-2}, while that of sample 2 was 250 dyne · cm^{-2}.

The Na humates added to bentonite suspensions and pastes were obtained from brown coal and were used in the form of solutions with pH 8.0-8.5. The reaction between humates and clay minerals has been studied by many investigators but this problem remains quite unclarified. It was recently [2-5] shown that adsorption of humates on the surface of clay particles is caused by Van der Waals forces and as a result of H-bonds formed by the reaction of humic acids with adsorbed cations on the surface of particles or resulting from the exchange capacity of clay minerals. The results obtained from our investigation of the structure strength and the rheological properties of aqueous dispersions of bentonites during their reaction with humates fully confirm this point of view.

We used the following apparatus for measuring the strength and rheological properties of aqueous dispersions of bentonites at low concentrations: 1. A Shvedov-type apparatus based on the principle of pure shear, with two coaxial cylinders with a 2 mm ring gap. 2. A Veiler-Rebinder elasticity gauge with a tangentially sliding corrigated plate in the middle of a closed vessel with fluted walls and with a gap of 2 mm between the walls and the plate. 3. Apparatuses of the capillary type—Ostwald and Ubelohde viscometer—with a set of capillaries of different diameter and length.

The following apparatuses were used for investigating dispersions of bentonite at high concentrations (in pastes): 1. A Tolstoi apparatus with pure shear stress applied was determined as $P = F/S$, where F is the applied tangential force; S is the working area of the plate. The shearing strain (relative shear) was calculated as $\epsilon' = \epsilon/h$, where ϵ is the absolute shear of one plate with respect to the other; h is the width of the gap between them. 2. A capillary-type apparatus consisting of a steel cylinder, open at both ends; metal tubular nozzles (corrigated on one side), the diameter and length of which varied widely, were screwed onto one end of the cylinder, while on the other end a piston was fitted to force the paste through at various pressures. After a constant plunge rate of the piston (volumetric consumption of the extruded paste) had been established (according to the indicator), the viscosity was calculated by Poiseuille's formula. 3. An MGU conical plastometer [6], in which the unit maximum shear stress (P_m) of the maximum-strengthened pastes was determined.

The $P_m = f(c)$ curves in Fig. 1,a indicate that in the case of 5% and 10% suspensions of sample 1 bentonite, additions of Na humates cause a reduction in the strength of the structure. At the same concentrations of the components

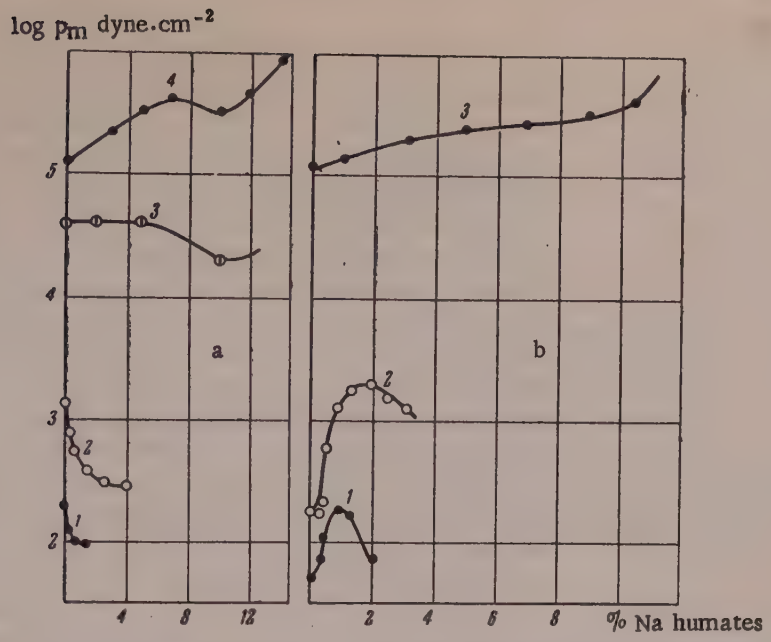


Fig. 1. Ultimate strength of a coagulational structure in suspension of Oglanlinsk bentonite of sample 1 (a) and sample 2 (b) in relation to the amount of Na humates introduced: 1) 5%; 2) 10%; 3) 20% (a) and 36% (b); 4) 36% suspensions of bentonite 1,2) by the plate method; 3 and 4) by the conical plastometer.

of the system, additions of Na humates to suspensions of the bentonite of sample 2 lead to a strengthening of the system (Fig.1, b). To cause a liquefaction of bentonite suspensions, larger amounts of humates must be added.

From the $P_m = f(c)$ curves it is evident that the maximum strength of the structure of a suspension of sample 2 with humates corresponds to the strength of bentonite of sample 1 in pure water. This confirms the laws previously found by the authors and other investigators in structuration processes in dispersions of bentonite clays in connection with the different degree of mosaic development of the structure of the surface layer of clay particles [7,8]. In the first case the optimum mosaic development of the structure of the surface layer on bentonite particles is determined by the ratio of Na and Ca cations in the exchange complex of bentonite, while in the second case it is caused by adsorption of humates in corresponding concentrations.

At high clay concentrations (in pastes) the structures strength in both bentonite samples increases with an increase in the amount of Na humates added. In these systems the adsorption layers of humates on bentonite particles assists their better compaction and leads to a stronger structure. But when the humate concentration in the dispersion medimum is fairly high, structuration affects all the system as a whole. An inflection is observed on the $P_m = f(c_{hum})$ curves when the humate concentration in the aqueous medium of the bentonite paste reaches 9-10%. This inflection indicates that at these ratios of the components there is a tendency to liquefaction of the paste. But with a further increase in the humate content in the dispersion medium the strength of the thixotropically strengthened structure increases still more.

Our previous data on the electrical conductivity of Na humate solutions confirm that at these concentrations micelle-formation commences, leading to structuration of the humates in the volume of the dispersion medium [1]. Therefore the structural-mechanical properties of aqueous bentonite pastes containing a fairly large amount of humates in the dispersion medium depend on the corresponding properties of the humates. During this process the bentonite particles play the role of an active filler; they carry a layer of adsorbed humates which assists their reaction with the structural elements of the humic substances in the medium and leads to an increase in the strength of the system as a whole.

We investigated the effect of electrolytes with polyvalent cations in the medium, using a 10% suspension of sample 1 bentonite. The experiments were carried out with bentonite pre-wetted with water to the state of maximum swelling, followed by treatment with Na humate solutions and the addition of $CaCl_2$.*

* To obtain suspension with given properties, the method used for their preparation is of great importance.

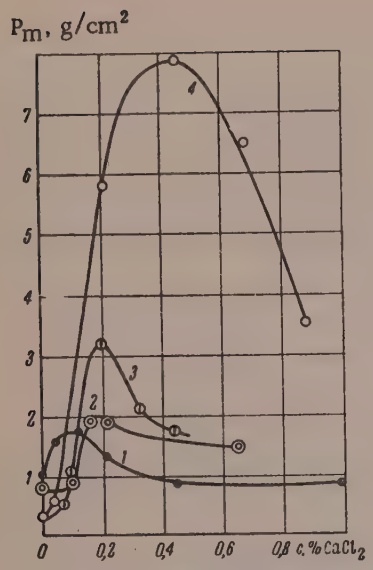


Fig. 2. Relation between the ultimate shear strength and the addition of $CaCl_2$ of thixotropically strengthened 10% suspensions of bentonite in Na humate solutions: 1) without humates; 2) in 0.7% Na humate solutions; 3) in 1.6%; 4) in 4.5%.

The results of the investigation show that on the $P_m = f(c,x)$ curves, where c and x are the concentrations of humates and electrolyte, there is a maximum which follows an increase in the amounts added. During this process the strength of the structure increases (Fig. 2). An investigation of the effect of an electrolyte on a suspension of sample 1 bentonite showed that the strength of the structural framework also increases to some extent when a small amount of $CaCl_2$ is added. An increase in the amount of $CaCl_2$ causes the appearance of compact coagulation and a decrease in the strength of the structure. The addition of the same amounts of electrolyte to aqueous dispersions of the same Na humates in the same concentrations leads to the precipitation of Ca humates. The observed increase in the strength of the structure when humates and electrolyte are present together in the system may be explained by the fact that the humates adsorbed by the clay particles react with the electrolyte added, exchanging cations, and thus increase the mosaicity development of their surface structure. Further reaction of the bentonite particles with each other and with the humates of the dispersion medium leads to a strengthening of the structural network by the forces of the hydrogen bond, by intermolecular cohesion and, at the sites of carboxyl groups, by chemical bonds, (possible linking macromolecules). With a further increase in the $CaCl_2$ content there is a regular reduction in the strength of the structure as a result of compact coagulation of the clay particles (local syneresis) and precipitation of Ca humates is possible.

An investigation of the rheological properties of aqueous bentonite dispersions with Na humates was carried out, using a 10% suspension and a 36% paste of sample 1 bentonite. The determination of the rheological curves for similar thixotropic systems presents great difficulties. In such dispersions, when a shear stress is applied or at a fixed strain rate the equilibrium state depends on the previous state of the suspension and can be attained, in principle, in two ways. The first way depends upon the fact that the investigation of the rheological properties is carried out under conditions of a thixotropically strengthened state of the suspension. In the second method, suspensions are investigated under conditions close to the ultimate standard strength.

During an investigation of the deformation kinetics at a constant and fairly low shear stress of a maximum-strengthened system the bonds between the individual elements of the system are broken but are restored within the period of measurement. The structure is retained practically unbroken until its disintegration rate is greater than the restoration rate. The period required to reach the equilibrium state, which depends on the relaxation time, i.e., the time for the transfer of the system from a thermodynamically unstable to a stable state, may be so great that it sometimes cannot be realized. Therefore at comparatively low stresses the effective viscosity values obtained are above the equilibrium values. But if the viscosity of the system is measured by the second method, i.e., under conditions close to the ultimate structural strength applying high gradients to the shear rate, and then changing-over to reduced rates, at fairly low values of the gradient the shear stress P will increase in time as a result of thixotropic strengthening of the structure. It must gradually reach the equilibrium value, which, however, is often unachieved in an experiment. Thus, for example, in our investigations the period required for complete strengthening of the structure in a 10% aqueous bentonite suspension, even under quiescent conditions, was three days. But if a system with an initially broken structure is strengthened in time, simultaneously undergoing deformation at even a relatively low velocity gradient, the time for the restoration of the structure increases considerably (to tens of days), which makes it practically impossible to attain an equilibrium (stationary) current. Therefore in this case the values obtained for the viscosity and the corresponding shear stress are less than their equilibrium values. This is the cause of the "break" in the experimental rheological curves for such systems. The true equilibrium rheological curve $\log\eta$-P must evidently lie between the curves obtained by the first and second methods of investigation.

The measured viscosity values are true, i.e., independent of time and corresponding to a stationary current with an equilibrium degree of disintegration of the structure [9], only in the two extreme cases of practically maximum-disintegrated structures (lower level of the effective viscosity η_m) and maximum strengthened and unbroken structures (upper level of the viscosity η_0 under conditions of low limiting shear rates).

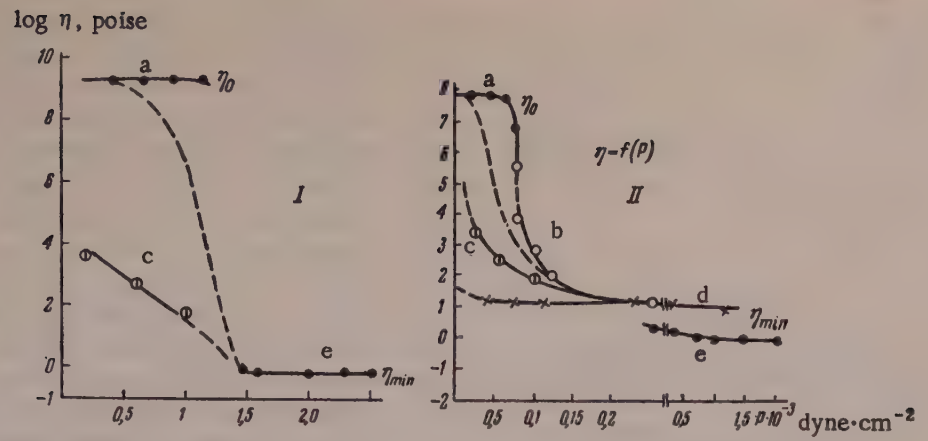


Fig. 3. Relation between the viscosity of a 10% bentonite suspension in water (I) and in a 2.4% solution of Na humates (II) and the shear stress.

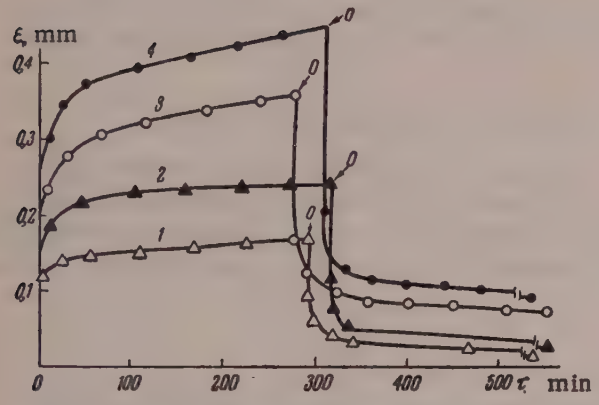


Fig. 4. Kinetics of the development and fall of deformation in a 10% suspension of natural Oglanlinsk bentonite; shear stress (P): 1) 433; 2) 650; 3) 866; 4) 1080 dyne·cm^{-2}.

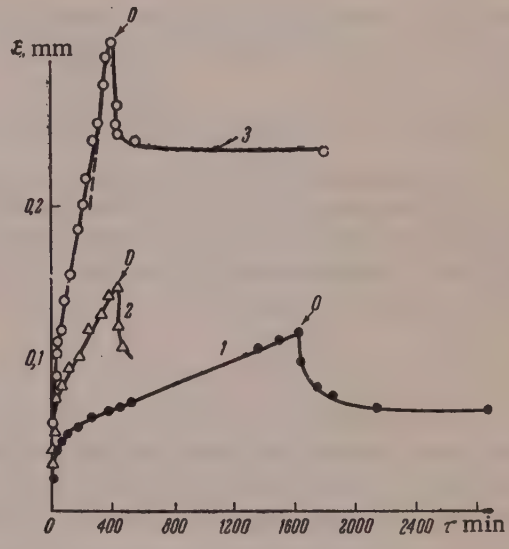


Fig. 5. Kinetics of the development and fall of deformation in a 10% suspension of natural bentonite in a 2.4% of Na humates; shear stress (P): 1) 47.7; 2) 63.7; 3) 79.6 dyne·cm^{-2}.

Fig. 3. gives the results of measurements of the viscosity of a 10% suspension of bentonite in water and in a 2.4% solution of Na humates. Measurements of the viscosity of practically unbroken, maximum-strengthened suspensions of bentonite of section a were carried out in a Shvedov apparatus under conditions of a predetermined constant shear stress (constant torque) (Figs. 4 and 5). At high shear stresses in the region close to disintegration of the structure a certain increase in the development of deformation can be observed on the curve $\epsilon = f(\tau)_p$ until a constant rate is attained.

The viscosity values in the intermediate part of the rheological curve $\log \eta = f(P)$ were measured in the same apparatus at a constant deformation rate. The steady state of the shear stress was determined. Section b of the rheological curve was obtained during an investigation of a pre-strengthened suspension under conditions of constant deformation rates. The c branch of the curve was obtained under the same measurement conditions but in suspensions with a preliminarily broken structure. Suspensions in conditions of a broken structure were also investigated in an Ubelohde viscometer with capillaries of different radii: 1.3 mm (section d of the rheological curve) and 0.5 mm section e of this curve).

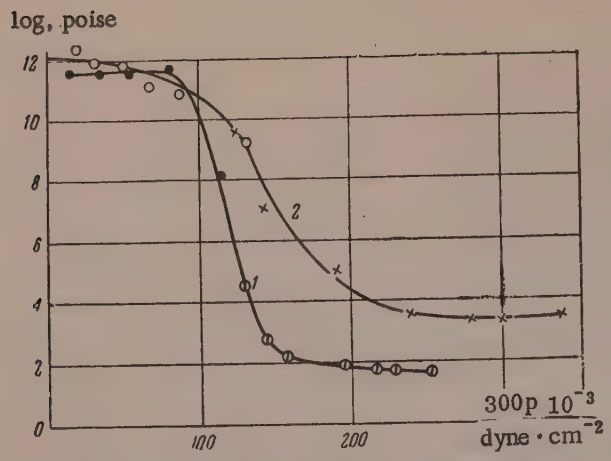


Fig. 6. Relation between the viscosity of a 36% aqueous bentonite paste and the shear stress: 1) in water; 2) in a 15% solution of Na humates.

An investigation of the rheological properties of a 36% bentonite paste without humates and in a 15% solution of Na humates showed that complete rheological curves (without a "break") can be obtained for these systems, which is explained by the inadequately high concentrations of both components and the considerable velocity of thixotropic restoration in their structure (Fig. 6). Both methods of measuring the viscosity in maximum-strengthened structurized pastes were used, followed by disintegration in the structure by the application of high shear stresses or high deformation rates, and in pastes with a practically maximum degree of broken structure, when the measurements were commenced at high gradients of the flow velocity and at corresponding equilibrium shear stresses. The rate of deformation and the corresponding shear stress were then gradually reduced. In both experiments the rate of deformation varied from 10^{-9} to 10^{2} sec^{-1}.

In the region of maximum viscosity the latter was measured in a Tolstoi apparatus and was calculated from the curves of the development of deformation at P = const; in the minimum viscosity region it was measured in a capillary (tubular) viscometer with extrusion through tubular nozzles.

Some points on the curves in the intermediate region were obtained in apparatuses of both types.

The measurements obtained showed that the viscosities η_0 and η_m differ by 10-fold in pastes without humates and by 9-fold in systems containing humates. These results and the increase in viscosity under conditions of a maximum degree of broken structure by two-fold in pastes with humates as against the viscosity of aqueous pastes indicate the effect of the structuration of the humates themselves in the dispersion medium, where the bentonite particles serve as an active filler in the dispersions.

SUMMARY

1. In aqueous bentonite dispersions of low concentration, Na humates cause liquefaction of suspensions, acting as a stabilizer. The more polyvalent cations in the complex of bentonite the higher is the concentration of the Na humates added, causing maximum liquefaction of the system. Additions of Na humates to concentrated dispersions of bentonite lead to strengthening of the system, by assisting the formation of a more compact structure.

2. By way of the example of aqueous dispersions of bentonite clays it was shown that at low concentrations of the system the measured viscosity values are true only in cases of practically unbroken and maximum-broken structures. The intermediate values do not generally correspond to the stationary state and are therefore conventional. In these cases a "break" is observed on the rheological curves. In bentonite pastes, as a result of rapid restoration of the thixotropic structure a "break" is not observed on the effective viscosity-shear stress curves.

3. The effect of electrolytes with a polyvalent cation ($CaCl_2$) on structuration processes in dispersions of bentonite clays with humates is similar to the effect of electrolytes in concentrated solutions of the humates themselves. In concentrated dispersions of bentonites in the presence of a fairly high humate concentration, bentonite is an active filler, and the properties of the dispersion medium are reflected in the properties of the system as a whole.

LITERATURE CITED

1. Chiang Lung, N. N. Serb-Serbina, L. E. Kuznetsova and V. S. Zhurina, Kolloid. zhur. 23, 2 (1961).
2. L. N. Aleksandrova, Pochvovedenie, 19, 23 (1954); L. N. Aleksandrova and M. Nad', Pochvovedenie, 10, 21 (1958).
3. I. V. Tyurin, Proc. Dokuchaev Soil Inst. [in Russian] (Acad. Sci. USSR Press, 1940), 23.
4. H. Beutelspacher, Z. Pflanzernähr, Dung. Bodenk. 69, 108 (1955).
5. M. M. Kononova, The Problem of Soil Humus and Present Aims of Its Investigation [in Russian] (Moscow, Acad. Sci. USSR Press, 1951).

6. S. Ya. Veiler and P. A. Rebinder, Doklady Akad. Nauk SSSR 49, 5 (1945); P. A. Rebinder, Proc. Conference on Eng.-Geol. Properties of Rocks and Methods of their Investigation [in Russian] (Moscow, 1956), 1, 31; P. A. Rebinder and N. A. Semenenko, Doklady Akad. Nauk SSSR 64 (1949).
7. N. N. Serb-Serbina, Kolloid. zhur. 20, 5 (1958).
8. O. M. Mdivnishvili and G. V. Vinogradov Kolloid. zhur. 20, 5 (1958).
9. L. A. Abduragimova, P. A. Rebinder and N. N. Serb-Serbina, Kolloid. zhur. 17, 3 (1955).

All abbreviations of periodicals in the above bibliography are letter-by-letter transliterations of the abbreviations as given in the original Russian journal. *Some or all of this periodical literature may well be available in English translation.* A complete list of the cover-to-cover English translations appears at the back of this issue.

INVESTIGATION OF THE INTERNAL STRESSES ARISING WHEN NITRO- AND ACETYLCELLULOSE FILMS ARE DEPOSITED ON GLASS

S. A. Shreiner, P. I. Zubov, and A. S. Arvan

Polymer Division of the Institute of Physical Chemistry,
Academy of Sciences USSR and the Leningrad Section of the
Scientific Research and Planning Institute
Translated from Kolloidnyi Zhurnal, Vol. 23, No. 3, pp. 334-337, May-June, 1961
Original article submitted July 25, 1960

We have previously [1,2] shown that the deposition of gelatin films on glass surface is accompanied by the development of stress at the phase boundary between the glass and film. The magnitude of the stress itself depends to a large extent on the conditions of film formation. In addition to this we established that as the thickness of the film becomes partially or entirely separated from the solid surface. We have proposed that these total critical stresses be used as a measure of the adhesive forces between the film and its solid support.

In the present communication we will present more data on the stresses arising at the phase boundary when films of nitro-cellulose (average mol. wt. = 2.12×10^5, 11.07% nitrogen, 0.13% sol) and acetylcellulose (average mol. wt. = 0.36×10^5, 50.2% acetic acid tied up, 0.064% sol) are deposited from various solvents. All solvents were thoroughly purified.

Films were at first deposited from 10% solutions of cellulose esters (as has already been described [12]) on the faces of rectangular glass prisms (at room temperature) over concentrated sulfuric acid. However, it soon became apparent that this method was not very satisfactory, particularly when highly volatile solvents were used, since the resulting films were uneven in thickness and also air bubbles would form in the films making our measurements irreproducible. In order to avoid these complications the films were initially formed under solvent pressures close to saturation and subsequently placed over concentrated sulfuric acid. The stress at the boundary between the film and the glass support were determined in the same way as before [1].

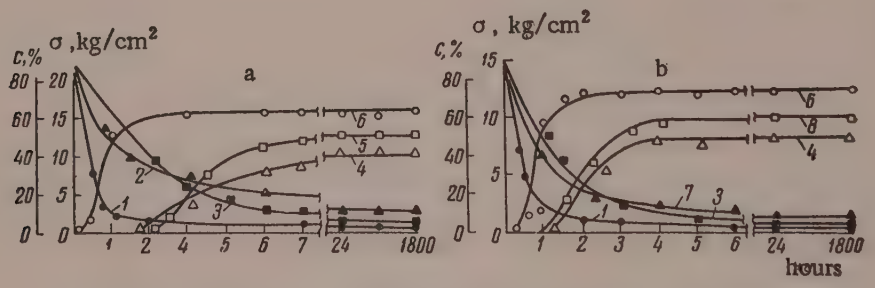


Fig. 1. Rate of evaporation and the rate at which stresses (σ) develop at the phase boundary between the glass and the films of a) nitrocellulose and b) acetylcellulose (deposited from various solvents) as a function of solvent concentration (c, %); the film was 80μ thick. 1 and 6) acetone; 2 and 5) butylacetate; 3 and 4) dioxane; 7 and 8) pyridine; 4,5,6, and 8) are pressure plots (kg/cm²); 1,2,3, and 7) are solvent concentration plots.

Figure 1 shows that stresses begin to appear when dilute gels become concentrated (as in the case of gelatin films) and the solvent content drops to 25-30%. The rate at which stress develops depends on the nature of the solvent.

The most rapid increase of stress is observed when films are formed from acetone solutions. Measurable stresses appear within 15 min after the film is allowed to dry and attain their ultimate strength after 2 hours. When butylacetate and dioxane are used stresses appear after 2 hrs and attain a constant value after 24 hrs. Our experiments have shown that these stresses remain practically unchanged even if the films are stored for 2.5 months over concentrated sulfuric acid. Figure 1,a also shows that the linear relationship between the rate of stress development and the solvent content of the film remains unchanged when films are stored for long periods of time (2-3 months). At first glance it would appear that the ultimate stress depends on the nature of the solvent, but under our experimental conditions the curves may be misleading since the solvent is not completely removed from the films.

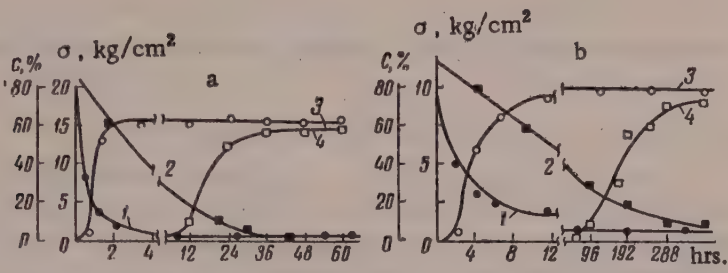


Fig. 2. The rate of growth of stresses (σ) at the interface between glass and nitrocellulose films deposited from acetone (a) and dioxane (b) at various vaporization rates as a function of solvent concentration (c, %). 1 and 2) solvent concentration plot (%); 3 and 4) pressure plot (kg/cm²).

Films deposited from acetone retain ~1.6% of solvent, those deposited from butylacetate retain 3.5%, and films deposited from dioxane 5.8%. The differences in the amount of solvent retained are apparently responsible for the variations in the ultimate stress of various films. Figure 1,b shows that acetylcellulose and nitrocellulose exhibit very similar rates of stress growth during the formation of films.

It was interesting to see what effect would variations in the evaporation rate of any one solvent have on the ultimate stress. In these experiments films were allowed to form inside rectangular cells 10 cm³ in volume with a small gap of fixed size between the cell walls and a ground cover.

The data plotted in Fig. 2 show that regardless of the evaporation rate stresses appear only after the solvent content of the film has dropped to 25-30%. These data indicate that in nitrocellulose films just as in the case of gelatin small relaxation periods appear only in concentrated gels when interaction between chains is strong. The curves plotted in Fig. 2 also show that the ultimate stress is independent of the solvent evaporation rate.

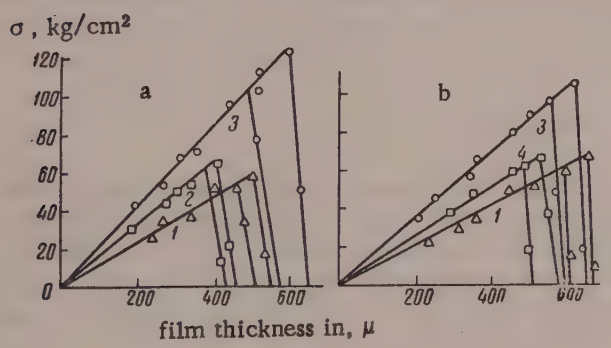


Fig. 3. The effect of final film thickness on the magnitude of stress at the phase boundary between the film and glass; a) nitrocellulose and b) acetylcellulose in various solvents. 1) Dioxane; 2) butylacetate; 3) acetone; 4) pyridine.

In Fig. 3 we have presented the results from our study of the effects of final film thickness on the development of stress. We increased the film thickness by pouring additional amounts of solution on films previously dried for 7 days over concentrated sulfuric acid.

One can see in Fig. 3 that the interface stresses increase linearly with increasing film thickness, attain their critical values then sharply decline; as in the case of gelatin [2] the observed effect may be due to a partial or total separation of the film from the glass support.

Cellulose ester films deposited from acetone break down under a stress of 100-135 kg/cm² before they can be separated from the glass. Films deposited from butylacetate, pyridine, or dioxane can be readily

separated from the glass surface by a force of 50-70 kg/cm^2. In the latter case the smaller adhesive force results from greater amounts of solvent retained in the films; the relative amounts of solvent retained are least in the case of acetone. Figure 3 shows that the formation of nitrocellulose films is accompanied by the development of greater stresses than is the formation of acetylcellulose films.

SUMMARY

1. We have investigated the rate at which stresses develop at the interface when nitrocellulose and acetylcellulose films are deposited from solution on glass surface at various evaporation rates.

2. The rate of internal stress development depends on the nature of the solvent.

3. The magnitude of the ultimate stress developed in cellulose ester films deposited from solution depends on the residual concentration of solvent in the film.

4. We have also determined the critical stresses leading to film break down.

LITERATURE CITED

1. S. A. Shreiner, and P. I. Zubov, Doklady Akad. Nauk SSSR, 124, 1102 (1959).
2. S. A. Shreiner, and P. I. Zubov, Kolloid. Zhur. 22, 497 (1960).

All abbreviations of periodicals in the above bibliography are letter-by-letter transliterations of the abbreviations as given in the original Russian journal. *Some or all of this periodical literature may well be available in English translation.* A complete list of the cover-to-cover English translations appears at the back of this issue.

THE HOMOGENEOUS FORMATION OF NUCLEI DURING VAPOR CONDENSATION AND THE ABSOLUTE (LIMITING) CRITICAL SUPERSATURATION

L. M. Shcherbakov, P. P. Ryazantsev, N. P. Fillipova

Tula Mechanical Institute

Translated from Kolloidnyi Zhurnal, Vol. 23, No. 3, pp. 338-344, May-June, 1961
Original article submitted January 4, 1960

According to the usually accepted scheme [1], the formation of nuclei during vapor condensation is a fluctuation process, in which the particles of the initial gaseous phase (vapor), come together and form droplets of the new (liquid) phase. The droplets become stable (in the sense of metastability) only on reaching a critical dimension, given, usually, by Kelvin's well known equation. The growth of a droplet to critical dimensions is accompanied by an increase in free energy of the whole system, which requires an expenditure of work A^*. This work is a characteristic energy barrier, which the nucleus must overcome, before it can maintain itself, and become a center of growth of the new phase.

The work, A^*, required to form the metastable nucleus, is an important parameter in the theory, which determines both the probability of formation of a nucleus $w \sim (A^*/kT)$ (where k is Boltzmann's constant), and the rate of production of the new phase. In calculating A^*, the nucleus following Gibbs and Volmer [1], is considered to be a micro-droplet, with the same, or slightly different, surface tension as in a large volume of liquid. On this assumption, the work of formation of the metastable nucleus A^* is equal to 1/3 of its free surface energy [1].

However, it is impossible not to be aware of some serious objections to the simple and effective method of calculation just described. For one thing, it leads to the conclusion that independent of the amount of supersaturation, $A^* > 0$. This would mean that it is, in principle, possible to produce arbitrary vapor supersaturation of any desired amount, which is at variance both with general thermodynamic considerations, and with the experimental data [2], which show the existance of rather easily reproducible limits to the values of supersaturation that can be obtained. In the present paper, an attempt is made to remove these objections by taking account of capillary effects of the second kind, the general theory of which has been worked out by one of the authors.

According to the theory of capillary effects of the second king [3], for sufficiently small dimensions of the object (small radius of drop, of small layer thickness), the deviations from the additive distribution of free energy can no longer be expressed by a single term proportional to the surface are of the interface, but some additional terms are required, which depend on the dimensions of the object. Accordingly, for the free energy of the system composed of a small drop of radius r (single prime ') and a vapor (double prine "), we have:

$$F = F' + F'' + 4\pi r^2 \sigma_\infty + f(r),$$

where F' and F" are the free energies of the phases, $4\pi r^2\sigma_\infty$, is the surface free energy of the boundary, and $f(r)$ is the additional free energy of a small drop, somewhat arbitrarily so called, since from direct calculations by Martynov and Deryagin, $f(r) < 0$. This energy comes from the whole drop, but to keep the original form of the deviation, it can be expressed formally per unit of surface of the interface, and included in the preceding term. Then, introducing the definition: $\sigma_\infty + f(r)/4\pi r^2 = \sigma(r)$, we obtain for the free energy of the system:

$$F = F' + F'' + 4\pi r^2 \sigma(r).$$

In this expression, $\sigma(r)$ may be considered formally as the specific surface free energy, but it has got to be kept in mind, that it is dependent on the dimensions of the drop.

Minimizing F, taking account of capillary effects of the second kind, with the additional conditions of thermal and mechanical isolation of the system, we find the thermodynamic conditions for the equilibrium of a small drop with its saturated vapor [4]:

$$\mu'(P', T) = \mu''(P, T); \quad P' - P = \Delta P = \frac{2\sigma}{r} + \frac{\partial\sigma}{\partial r}, \tag{1}$$

where $\mu^{(i)}$ is the chemical potential of the i'th phase, as related to one particle.

For the condensed phase, in very close approximation:

$$\mu'(P', T) = \mu'(P + \Delta P, T) \approx \mu'(P, T) + \frac{\partial\mu'}{\partial P'}(P' - P). \tag{1a}$$

But $\partial\mu'/\partial P' = v'$ is the volume occupied by one particle in the liquid phase. From the second condition of Eq. 1, we obtain:

$$\mu'(P', T) = \mu'(P, T) + v'\left(\frac{2\sigma}{r} + \frac{\partial\sigma}{\partial r}\right).$$

Similarly, $\mu'(P,T) = \mu'(P_S, T) + v'(P - P_S)$, where P_S is the pressure of the saturated vapor for a plane liquid surface. Substituting this value into the preceding equation, and expressing $\mu'(P_S,T)$ in terms of the chemical potential of the saturated vapor, we can rewrite Eq. (1) in the form:

$$\mu''(P_s, T) + v'(P - P_s) + v'\left(\frac{2\sigma}{r} + \frac{\partial\sigma}{\partial r}\right) = \mu''(P, T).$$

Hence, using the ideal gas approximation for the chemical potential of the vapor: $\mu'(P,T) = \mu^*(T) + kT\ln P$, we find, for the vapor pressure of a small drop

$$\frac{kT}{v'}\ln P/P_s - P_s(P/P_s - 1) = \frac{2\sigma}{r} + \frac{\partial\sigma}{\partial r}. \tag{2}$$

If we bear in mind that $v'P_S \ll v''P_S \approx kT$, then the second term on the left hand side is neglibible, and the equation takes on a form previously derived [3,5]:

$$P = P_s \exp\left[\frac{v'}{kT}\left(\frac{2\sigma}{r} + \frac{\partial\sigma}{\partial r}\right)\right]. \tag{2a}$$

This result shows that the calculation of capillary effects of the second kind cannot be reduced to simply replacing the tabulated value of the surface tension, σ_∞, in Kelvin's equation by a corrected value $\sigma = \sigma(r)$, but some additions to the equation itself are required. From data in the literature [6-8], σ decreases with decreasing r, i.e., the derivative $\partial\sigma/\partial r > 0$. Therefore the values of P, found from Eqs. (2) and (2a), will be somewhat higher than the values given by the usual Kelvin equation, in which σ_∞ is replaced by $\sigma = \sigma(r)$.

For any given degree of supersaturation $s = P/P_S$, the equilibrium radius of the drop is given by the equation:

$$\frac{2\sigma}{r} + \frac{\partial\sigma}{\partial r} = \frac{kT}{v'}\ln s - P_s(s - 1) \tag{3}$$

or, if we neglect the second term on the right hand side:

$$\frac{2\sigma}{r} + \frac{\partial\sigma}{\partial r} = \frac{kT}{v'}\ln s. \tag{3a}$$

The work of formation of a spherical nucleus of the liquid phase (single prime ') of radius r, in a homogeneous medium (double prime ") with vapor density P, may be expressed by the change in free energy of the system

$$A = F - F_0,$$

where

$$F_0 = \mu''(P, T)\, N - PV,$$

$$F = \mu'(P', T)\, g - P' \frac{4\pi}{3} r^3 + \mu''(P, T)(N - g) -$$

$$- P\left(V - \frac{4\pi}{3} r^3\right) + 4\pi r^2 \sigma(r).$$

Here, N is the total number of particles in the system, g is the number of particles in the nucleus ($g \ll N$), and V is the volume of the system. But $g = (4\pi r^3/v')/3$, and further, proceeding as in the derivation of Eq. (2), we have, for each phase:

$$\mu'(P', T) = \mu'(P_s, T) + v'(P - P_s) = \mu''(P_s, T) + v'(P' - P) + v'(P - P_s).$$

Using all these facts, along with the ideal gas approximation for the chemical potential of the vapor, we find, for the work of formation of nucleus of the liquid phase:

$$A = -\left[\frac{kT}{v'} \ln s - P_s(s - 1)\right] \frac{4\pi}{3} r^3 + 4\pi r^2 \sigma, \tag{4}$$

where $s = P/P_s$ is the given value of supersaturation. Since $kT \cong v''P_s \gg v'P_s$, the expression may be simplified by leaving out the term $P_s(s - 1)$, giving

$$A = -\frac{kT}{v'} \ln s \frac{4\pi}{3} r^3 + 4\pi r^2 \sigma. \tag{4a}$$

If at any given temperature, $P < P_s$ (i.e., the vapor is not saturated), both terms in Eq. (4a) are positive, and the work of formation of a new phase is a monotonically increasing function of r. Therefore, in the unsaturated vapor, the probability of forming a stable (metastable) nucleus is equal to zero. If the vapor is supersaturated ($P > P_s$), the first term in Eq. (4a) is negative, and as a result, the curve of A against r shows a well defined maximum. The same conclusion follows from the more exact Eq. (4). The maximum of the curve at $r = r^*$ corresponds to metastable equilibrium with the new phase. If $r < r^*$, any nuclei of the liquid phase which may be formed are unable to exist, and they decompose spontaneously; if $r > r^*$, the nucleus will grow spontaneously. Therefore, r^* may be taken as the critical radius for a nucleus of the liquid phase. The corresponding extreme value of the work, $A^* = A(r^*)$, is the activation energy which vapor particles must have to form permanent nuclei, capable of becoming centers of growth of the new phase, i.e., of becoming nuclei of the liquid phase in the strict sense of the word.

According to Frenkel', the process which precedes the formation of the nuclei is a chain of fluctuational associative processes between molecules, which leads to the formation, in the vapor, of associative complexes of varying degrees of complexity. The chain of fluctuations is finally brought to an end by the formation of a qualitatively new entity, which is the true nucleus of the liquid phase. The criterion by which the nuclei may be distinguished from the associative complexes is to be found from a consideration of the capillary effects of the second kind. The smaller the number of particles in the drop, the more the deviations from the additive distribution of free energy will tend to be evened out, and consequently:

$$\sigma(r) = \sigma_\infty + f(r)/4\pi r^2 \to 0.$$

We will recall that $\sigma(r)$ may be considered, formally, to be the specific surface free energy of the drop, but this quantity, as shown in Refs. [6-8], decreases with decreasing radius. Therefore, the value of $r = r_0$, at which $\sigma(r)$ goes to zero, may be taken as the dividing line between associative complexes ($r < r_0$), and nuclei ($r > r_0$)*.

*In connection with this idea, we must stop to consider the objections (raised, for example, in Ref. [9]) to extending concepts like "interface" and "surface tension" to objects as small as the condensation nuclei. Certainly, at $r \sim r_0$, the usual interpretation of these quantities, which assumes a physical boundary of some finite thickness between liquid and vapor, ceases to have any meaning. It is more to the point to adopt a purely formal treatment (as is done in the liquid drop model of the atomic nucleus [10]), in which the interface is considered to be the geometric surface defined by the relation: $4\pi r^3/3 = v'g$, and the specific surface free energy is defined as the measure of the deviation from additive distribution of free energy.

On the basis of these concepts, σ as a function of r may be represented in general form by the equation:

$$\sigma = \sigma_\infty \varphi(r/r_0) = \sigma_\infty \varphi(x), \tag{5}$$

where only two physically obvious assumptions are made with regard to the function $\varphi(x)$, namely

$$\lim_{x\to\infty} \varphi(x) = 1 \quad \text{и} \quad \lim_{x\to 1} \varphi(x) = 0$$

(holding only with respect to the translational energy of the molecules of the saturated vapor). Substituting this value of σ into Eqs. (4) and (4a) makes it possible to rewrite them in the form:

$$A = \alpha x^2 [\varphi(x) - a_s x], \tag{6}$$

where, for brevity, the following symbolism is introduced:

$$\alpha = 4\pi r_0^2 \sigma_\infty; \quad a_s = \frac{1}{3}\frac{r_0}{\sigma_\infty}\left[\frac{kT}{v'}\ln s - P_s(s-1)\right] \approx \frac{1}{3}\frac{r_0}{\sigma_\infty}\frac{kT}{v'}\ln s.$$

If we assume that in Eq. (6) $\varphi(x) = \text{const} = 1$, the equation takes on the well known Gibbs-Volmer form [1].

The sign of A will be determined by the sign of the square bracket in Eq. (6). The various cases which can occur are shown in Fig. 1. Here, the straight lines a, b, and c correspond with different values of the parameter a_s (which depends on the amount of supersaturation), the solid curve 1 is the graph of the function $y = \varphi(x)$, and the dotted line 1 corresponds with the Volmer-Gibbs theory.

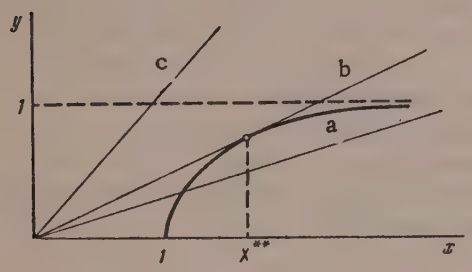


Fig. 1.

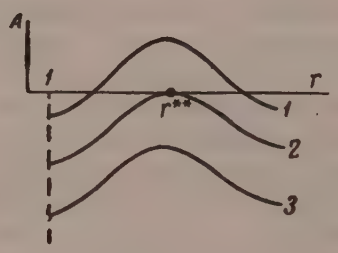


Fig. 2.

It is clear from Fig. 1, that according to the Volmer-Gibbs theory for any given straight line $y = a_s x$ (i.e., for any given amount of supersaturation), there always exists a certain range of values of x (from the origin of coordinates to the point of intersection with the dotted line), in which $A > 0$. Therefore, in the Volmer-Gibbs theory, the extreme value of the work of formation of a nucleus, A^*, can never become ≤ 0, which is equivalent to saying that it is possible to reach any, arbitrarily large value of supersaturation in the vapor, but this is in contradiction with experiment, and the general principles of thermodynamics.

In the treatment based on capillary effects of the second kind, where we calculate the functional relationship between σ and r, there is a range of values of x, for small values of supersaturation (straight line a, Fig. 1), where $A^* > 0$, no matter what the form of the functional relationship is, just as in the Volmer-Gibbs theory. But for larger values of supersaturation (line c, Fig. 1), the whole straight line $y = a_s x$ lies above the curve $y = \varphi(x)$, and the work of formation of a nucleus becomes negative, which means that, for practical purposes, it is impossible to achieve the values of supersaturation in question. The limit of realizable supersaturations is given by the straight line b of Fig. 1, for which the extreme value of the work of formation of a metastable nucleus, A^*, becomes zero. The variation of A with r, for the three cases considered, is shown schematically in Fig. 2.

In the current theories of the subject [11], the critical supersaturation is defined as the supersaturation at which the rate of nucleation reaches a prescribed value. This definition makes the whole concept of critical supersaturation somewhat arbitrary, since, obviously, a number of such values of supersaturation exist. It is therefore better to call the

quantity defined in this way the "relative critical supersaturation." It follows both from the general principles of thermodynamics and the experimental data [2] that the series of relative critical supersaturations must have an upper limit, which may be called the absolute (or limiting) critical supersaturation.

As distinguished from the Gibbs-Volmer theory, the theory being developed not only predicts the existence of the absolute critical supersaturation, it also provides a way of calculating its value thermodynamically. It follows from Fig. 1 that the limiting (absolute) critical supersaturation, s^{**}, must satisfy the conditions:

$$\frac{\varphi(x^{**})}{x^{**}} = \varphi'(x^{**}),\ a_s^{**} = \varphi'(x^{**}). \tag{7}$$

The first condition is similar to the one set up previously [5]:

$$\frac{\sigma(r^{**})}{r^{**}} = \left.\frac{\partial\sigma}{\partial r}\right|_{r=r^{**}}$$

and differs from it only in the introduction of the dimensionless parameter $x^{**} = r^{**}/r_0$, which corresponds with the absolute critical supersaturation. The second condition gives the absolute supersaturation itself. Finding the value of the derivative $\varphi'(x^{**})$ from the first condition, and substituting it in the second condition, we obtain:

$$\frac{r_0}{\sigma_\infty}\frac{kT}{v'}\ln s^{**} = 3\varphi(x^{**}), \tag{8}$$

which can be used to calculate the parameter r_0, if the form of the function $\varphi(x)$ is known.

We can assume that the function $\varphi(x)$ of the dimensionless parameter $x = r/r_0$ will have the same form for all liquids with the same type of intermolecular binding, and the same kind of thermal particle motion. Thermodynamic calculations of σ as a function of r lead to the same conclusion [6]. Hence the equation:

$$\frac{r_0}{\sigma_\infty}\frac{T}{v'}\ln s^{**} = \text{const},$$

which gives the relation existing between the absolute critical supersaturations of different substances. If we go from the radius of the nucleus to the number of particles in it, as given by the equation $4\pi r^3/3 = v'g_0$ and express v' interms of the molecular weight M and the density ρ, the equation takes the form:

$$g_0^{1/3}\left(\frac{\rho}{M}\right)^{2/3}\frac{T}{\sigma_\infty}\ln s^{**} = \text{const}. \tag{9}$$

Bearing in mind that, for every liquid, g_0 has a perfectly definite value, we obtain, from expression (9), the equation:

$$\left(\frac{\rho}{M}\right)^{2/3}\frac{T}{\sigma_\infty}\ln s^{**} = \text{const} = B, \tag{10}$$

which gives the absolute critical supersaturation as a function of temperature. Eq. (10) shows that if the temperature is lowered, the absolute critical supersaturation rises rapidly.

The calculations of Martynov and Deryagin show that g_0 is nearly the same, even for different substances, as long as they have the same type of intermolecular binding. Therefore Eq. (10) will be valid (but with reduced accuracy) even for different liquids.

The table shows the type of results obtained with the substances investigated by Bykov andTeverovskii [2]. The values of the limiting (absolute) critical supersaturation, and the values of the surface tension, σ_∞, are taken from Ref. [2], the values of the density are taken from Ref. [12].

It follows from the table, that the condition of constancy of B is fullfilled by each individual substance in a completely satisfactory way. The values of B for different substances do not agree quite so well.

SUMMARY

1. A calculation has been made of the work of homogeneous formation of a nucleus during condensation of a vapor, taking account of the role of capillary effects of the second kind.

Values of the constant B, calculated from the data of Ref. 2.

Substance	Temperature, °K	σ_∞ ergs/cm²	Density gm/cm³	Critical supersaturation s^{**}	B
Glycerine, M-92	340	61,6	1,231	121	0,65
	346	61,0	1,228	112	0,65
	353	60,2	1,222	101	0,66
	359	59,6	1,218	98	0,67
	368	58,9	1,211	80	0,66
	381	57,5	1,202	55	0,64
				Mean	0,65
Aniline, M-93	325	39,7	0,994	22,3	0,54
	332	38,9	0,988	18,2	0,52
	342	37,8	0,980	15,8	0,52
	361	35,7	0,964	13,7	0,55
	379	33,6	0,948	12,0	0,57
				Mean	0,54
Tetralin, M-132	344,5	28,5		16,4	0,56
	355	27,2		14,5	0,57
	364	26,2	~0,97	14,0	0,60
	371,5	25,3		13,2	0,62
	381	24,2		14,6	0,69
				Mean	0,61

2. It is shown that there are two kinds of critical supersaturation: relative and absolute. The latter represents the upper limit of achieveable supersaturations.

3. It has been found possible to calculate the absolute critical supersaturation thermodynamically, as it is the value of saturation which exists at the point at which the work of formation of a metastable nucleus goes to zero.

The authors wish to express their profound gratitude for the valuable discussions contributed by Corresponding Member of the Academy of Sciences, USSR, B. V. Deryagin.

LITERATURE CITED

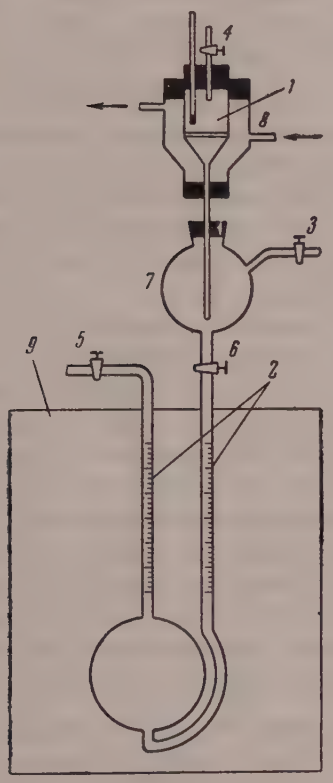
1. Josiah Willard Gibbs, Thermodynamic Papers [Russian translation] Moscow and Leningrad (1956); M. Volmer, A. Weber, Z. phys. Chem. 119, 227 (1925); R. Becker and W. Doring, Ann. Phys. 24, 719 (1935); P. I. Frenkel, Zhur. Experimental and Teor. Phys. 9, 199 (1939); P. B. Zelovnu, Zhur. Experimental and Teor. Phys., 12, 525 (1942).
2. A. G. Bykov, and E. N. Teverovskii, JETP 19, 328 (1949).
3. L. M. Shcherbakov, Phase Equilibria in Systems with Well Developed Interfaces [in Russian] Dissertation, Institute of Physical Chemistry Academy of Sciences, USSR, (1950). L. M. Shcherbakov, Tr. Tul'skogo mekhanicheskogo in-ta, 7, 17 (1955); 8, 173 (1958). L. M. Shcherbakov, Kolloid. Zhur. 22, 111 (1960). B. Deryagin and E. Obukhov, Kolloid. Zhur. 1, 385 (1935). B. Deryagin, and M. Kusakov, Izv. AN SSSR, seriya khim. No. 5, 734 (1936); No. 15, 1119 (1937).
4. L. M. Shcherbakov, Kolloid. Zhur. 20, 502 (1958); L. M. Shcherbakov, Uch. zap. Kishinevskogo un-ta 5, 117 (1952).
5. L. M. Shcherbakov, Kolloid. Zhur. 20, 759 (1958).
6. R. C. Tolman, J. Chem. Phys. 17, 333 (1949); I. J. Kirkwood and E. P. Buff, ibid, p. 338; V. K. La Mer, G. M. Pound, ibid, p. 1337.
7. F. P. Buff, ibid, 19, 591 (1951), 23, 419 (1955).
8. L. M. Shcherbakov, Kolloid. Zhur. 14, 379 (1952). L. M. Shcherbakov, and A. S. Bolotin, Uch. zap. Kishinevskogo un-ta, 11, 153 (1954).
9. S. V. Gorbachev and A. V. Shlykov, Zh. fiz. khimii 29, 1777 (1955).
10. Ya. I. Frenkel', JETP 9, 641 (1939).
11. M. Folmer and H. Flood, Z. phys. Chem. A. 170, 273 (1934); A. I. Barnard, Proc. Roy. Soc. A220, 132 (1953).
12. Handbook of Physical, Chemical and Engineering Constants [in Russian] edited by L. K. Martens, 1,2,10, Moscow (1929-1930).

APPARATUS FOR DETERMINING THE SWELLING OF GRANULATED MATERIALS AT VARIOUS TEMPERATURES

V. I. Gorshkov, V. I. Slovetskii and G. M. Panchenkov

Moscow University, Physical Chemistry Department
Translated from Kolloidnyi Zhurnal, Vol. 23, No. 3, pp. 345-346, May-June, 1961
Original article submitted January 19, 1961

When one studies the properties of granulated materials, in particular, those of ion-exchange resins, the problem of determining their degrees of swelling at various temperatures often arises. The apparatus propesed by Dogadkin [1], which is generally used for determining the swelling of gels, is not suitable in these cases. Methods based on measuring directly the weight or the volume of the swollen particles are no more suitable because of the troubles connected with thermostating. We suggest to determine the degree of swelling in the apparatus shown in the Fig. The lower part of the apparatus and the funnel with the porous bottom 1 into which a weighted portion of the material to be investigated is filled are thermostated. Before the determination the level of the water contained in the lower part of the apparatus is read on the scale 2. Then, with stopcock 3 closed, the water is forced by pressure into the funnel with the porous bottom. The funnel is closed by a plug containing a thermometer and stopcock 4, and with stopcocks 3,4,5 closed the substance is swollen during the time required (for ion-exchange resins this is 10-15 min). Thereafter stopcocks 4 and 5 are opened and the water flows to the lower part of the apparatus. The water lagging between the substance particles and in the filter is drawn off to the vessel 7 by a water-jet pump connected via stopcock 3, whereas stopcock 6 has been closed; then stopcock 6 is opened and, after the water has stopped flowing, its level is read on the scale 2.



Apparatus for determining the swelling of granulated materials at various temperatures: 1) funnel with a porous bottom; 2) scales; 3,4,5,6) stopcocks; 7) vessel; 8) jacket for thermostating the funnel with the porous bottom; 8) thermostat.

To estimate the loss of water caused by incomplete flow-back and evaporation occurring during the procedure described above, a blank experiment is done.

From the decrease in water volume corrected with the results of the blank test the amount of water consumed in the swelling is calculated. The degrees of swelling of the cation-exchanger KU-1 at 6, 25 and 50°, as found with this method were 97, 102 and 119% respectively, when referred to the weight of dry resin.

The degree of swelling of KU-1, as found from the difference in weight of the dry and the swollen cation-exchanger. was 102% at 25°, that is, the agreement is quite satisfactory.

LITERATURE CITED

1. B. A. Dogadkin, Kolloid. Zhur. 8, 31 (1946).

APPARATUS FOR MEASURING SWELLING AT ELEVATED TEMPERATURES

B. A. Dogadkin and A. A. Dontsov

M. V. Lomonosov Moscow Institute of Fine Chemical Technology
Translated from Kolloidnyi Zhurnal, Vol. 23, No. 3, pp. 346-347, May-June, 1961
Original article submitted February 10, 1961

Methods for measuring the degree of swelling at elevated temperatures have been developed insufficiently, however, nowadays such methods are ever more used for investigating the seaming of various polymers. So, in the case of polyethylene and other crystalline polymers of α-olefins, swelling of the samples must be carried out by heating to temperatures where the linear polymer dissolves completely.

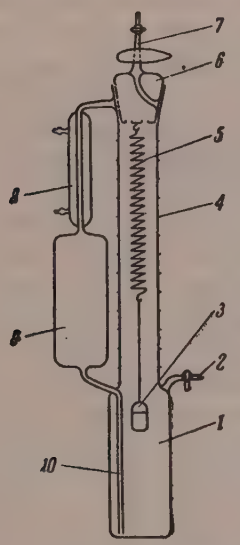


Fig. 1. Apparatus for measuring swelling at elevated temperatures.

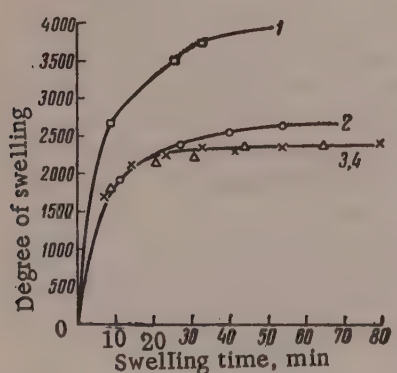


Fig. 2. Swelling kinetics of polyethylene, containing 7.74% sulfur after 3.5 hr at 230° for various weighed portions of polyethylene: 1) 0.016 g; 2) 0.021 g; 3) 0.032 g; 4) 0.038 g.

We have constructed a special apparatus (Fig. 1) enabling us to measure the swelling of porous and compact samples of any shape in a boiling solvent, in vapors, in an atmosphere of air or an inert gas. The apparatus constitutes a closed system.

To carry out swelling in a boiling solvent the sample, which has been weighed previously on a torsion balance, is suspended in the bag 3 made of fine steel gauze to the spring 5 and let down into the boiler 1 filled with solvent. The plug 6 is fixed in such a way that during the swelling the vapor formed passes through the aperture in the plug into the cooler 8 where it is condensed and via the siphon 10 it is returned to the cooler. When one wants to measure the degree of swelling, plug 6 is turned by 180°, whereby the compartment 4, heated by a coil from the outside in order to prevent the condensation of vapor onto the apparatus walls and the spring*, is isolated and the cooler 8 is connected to the atmosphere (for this purpose in the plug a special tube has been sealed to the bores). Via stopcock 2 excess pressure is applied to the compartment 4 so that via the siphon 10 such an amount of solvent is transferred to the container 9, as is required for weighing bag 3 by means of the spring. Stopcock 2 is closed, bag 3 is weighed (read by a catetometer) and the solvent is returned from the container 9 to the boiler 1. The weighing lasts until the sample weight is constant.

When one swells the sample in the solvent vapor, the bag is suspended above the boiling solvent and is weighed from time to time until the weight is constant. In order to work in an atmosphere of inert gas a device enabling us to give an excess pressure is connected to the stopcock 6. If the swelling is not carried out in a boiling solvent, the boiler 1 is placed in a thermostat giving the temperature desired.

We have used the apparatus for measuring in boiling toluene the swelling of the structural sulfur of high pressure polyethylene. From Fig. 2 it is evident that, when a greater amount is taken, at first the maximum swelling decreases,

*If condensation of vapors does not change the spring tension, heating by the coil is not obligatory.

until at a certain sample weight (0.03-0.04 g) it further stays unchanged. The accuracy of the weighing (using a calibration curve) is 0.003 g, which at a swelling of 500% corresponds to an error of 1.5-2%. If the maximum swelling is greater, the accuracy of weighing increases. The fact that at maximum swelling of polyethylene the weight is constant proves that during the swelling there is not destruction of the polyethylene, even when one works in air. If a constant weight is not attained, it may be advisable to add antioxidants to the solvent [2] or to carry out the swelling in an inert gas.

LITERATURE CITED

1. F. Waddington, J. Polymer Sci. 31, 221 (1958).
2. A. Charlesby, and S. H. Pinner, Proc. Roy. Soc. A249, 367 (1959).

All abbreviations of periodicals in the above bibliography are letter-by-letter transliterations of the abbreviations as given in the original Russian journal. *Some or all of this periodical literature may well be available in English translation.* A complete list of the cover-to-cover English translations appears at the back of this issue.

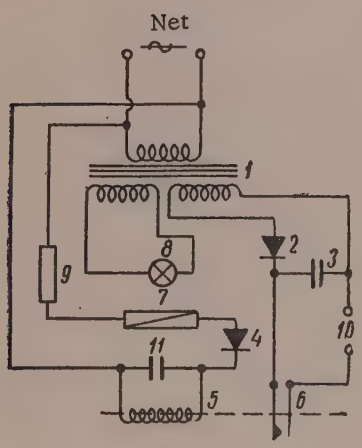
SURFACE TENSION MEASUREMENT WITH AN AUTOMATIC DROP COUNTING APPARATUS

S. A. Nikitina and A. B. Taubman

Institute of Physical Chemistry, Academy of Sciences, USSR, Moscow
Translated from Kolloidnyi Zhurnal, Vol. 23, No. 3, pp. 347-349, May-June, 1961
Original article submitted February 10, 1961

To measure the static equilibrium values of the surface tension of solutions containing soap-like micelle-forming surface-active substances (wetting agents, emulgators, detergents) with a low formation rate of adsorbed layers one must use either true static methods or semistatic ones, but the latter under conditions securing the formation of completely developed layers on the boundary surface (bubbles, drops) [1]. For this often much time is required and, for instance, in the method of drop counting one measurement takes one hour or more.

In such measurements we used automatic counting of the drops and this eliminates the said trouble. The electric equipment developed by us together with V. T. Avgul' and completed by N. P. Mitin works according to the scheme shown in the figure.



Scheme of the equipment for automatic drop counting: 1) transformer; 2) germanium diode, type DGTs-27; 3) electrolytic capacitor 20 μ farad, 300 v; 4) germanium diode, type DGTs-27; 5) coil of the polarization relay KZ 1956; 6) contacts of the polarization relay; 7) photoresistor FSK-1; 8) lamp 8v, 20 w; 9) resistor 11 kohm; 10) terminals of the electromagnetic counter SChZ; 11) paper capacitor, type KGB, capacity 4 μ farad.

Solution drops when falling from the stalagmometer intercept the light pencil emitted by a lamp and thereby they lower the illumination of a photosensitive resistor as a result of which the current in the circuit operating a relay is changed so that the circuit of an electromagnetic counter is closed and broken. The formation time of one drop is adjusted by choosing capillaries of various diameters, which by means of a rubber vacuum tube are connected to the upper part of the stalagmometer via a T-joint leading to a microstopcock, a normal stopcock and the atmosphere. The stalagmometer is placed in a closed compartment (a plan-parallel cuvet) saturated with vapor of the solution investigated so that evaporation from the drop surface is prevented.

The required thermostating of the apparatus to $\pm 0.5°$ is achieved by placing the stalagmometer in a box of plexiglas.

In the Table we give the results obtained when we measured the surface tension (σ) of solutions of a typical synthetic wetting agent—sodium dioctylsulfosuccinate (aerosol OT)—by means of this apparatus at a formation time of one drop equal to 2 minutes and for a comparison we give also those obtained by the strictly static method of the pending drop.

As is evident from the table, in the range $\sigma < 40$-50 erg/cm^2, which is the most important for testing the properties of solutions micelle-forming surface-active substances, the deviations between the results of the two methods do not exceed 1.5%; these are systematic deviations having always the same sign [both isotherms $\sigma = f(c)$ are parallel].

In the region of more diluted solutions the deviations increase and get a random character, which indicates that they are no longer related to the particularities of the method, but to ageing processes in the surface of the solution;

Method of measuring	Concentration of the solution, %						
	0,005	0,01	0,025	0,05	0,10	0,15	0,25
	Surface tension (σ), erg/cm²						
Stalagmometer	53,05	48,82	41,84	34,72	30,01	28,04	27,22
Pending drop	52,28	48,14	41,25	34,19	29,51	27,60	26,92

the latter effect has been studied in detail for many groups of soap-like compounds [2,3].

The data shown give reason to think that the apparatus proposed for measuring the static and the dynamic surface tensions of soap solutions by means of drop counting is quite suitable for obtaining reliable and sufficiently accurate results. Obviously, this accuracy may be enhanced in many cases by taking into account the corrections required according to the well-known tables of Harkins and Brown [4].

LITERATURE CITED

1. A. B. Taubman and S. A. Nikitina, Prevention of Silicose, Collection 2 [in Russian] (Acad. Sci. USSR Press, 1955), p. 61; S. A. Nikitina, A. B. Taubman and S. Kh. Zakieva, Prevention of Silicose, Collection 3 [in Russian] (Acad. Sci. USSR Press, 1959), p. 29.
2. W. D. Harkins, J. Amer. Chem. Soc. 62, 1946 (1940); 63, 84 (1941).
3. C. C. Addison and S. K. Hutchinson, J. Chem. Soc. 934 (1948); S. Fordham, Trans. Faraday. Soc. 50, 593 (1954).
4. W. D. Harkins and F. E. Brown, J. Amer. Chem. Soc. 41, 499 (1919); 38, 248 (1916), see also A. Weissberger, Physical Methods of Organic Chemistry, Vol. 1 [Russian translation] (Moscow, IL, 1950), p. 179.

All abbreviations of periodicals in the above bibliography are letter-by-letter transliterations of the abbreviations as given in the original Russian journal. *Some or all of this periodical literature may well be available in English translation.* A complete list of the cover-to-cover English translations appears at the back of this issue.

ON THE LAW OF FILTRATION OF A VISCOPLASTIC SUBSTANCE THROUGH A POROUS MEDIUM

A. M. Gutkin

Moscow Energetics Institute

Translated from Kolloidnyi Zhurnal, Vol. 23, No. 3, pp. 350-351, May-June, 1961
Original article submitted February 20, 1961

In order to calculate the filtration in highly dispersed clayey soils and certain peats in the presence of small pressure gradients, one sometimes uses the equation [1,2]

$$q = k(i - i_0)t, \tag{1}$$

where q is the amount of the substance being filtered flowing through a unit cross section of the porous medium in the time t; i is the pressure gradient in the substance being filtered; i_0 is the maximum value of this gradient for which filtration in the porous medium does not occur. It is supposed that Eq. (1) follows from the Shvedov* -Bingham equation

$$\tau = \tau_0 + \eta \frac{dv}{dt}. \tag{2}$$

However, an analysis of the laws of flow of a viscoplastic substance in capillaries leads to the conclusion that in case the pressure gradient i in the viscoplastic substance differs but little from the critical gradient i_0, that is, when

$$\frac{i - i_0}{i_0} \ll 1, \tag{3}$$

filtration should be described by a nonlinear filtration law

$$q = n(i - i_0)^2 t. \tag{4}$$

In Eq. (4), another coefficient n is introduced in place of the filtration coefficient k.

In order to obtain Eq. (4), it is sufficient to examine, for example, the formula for the flow of a viscoplastic material through a slit [3]

$$q = \frac{2}{3}\frac{ia^3}{\eta}\left[1 - \frac{3}{2}\frac{i_0}{i} + \frac{i_0^3}{2i^3}\right]t, \tag{5}$$

where a is the half-width of the slit; $i_0 = \pm\frac{\tau_0}{a}$ is the pressure gradient at which flow sets in.

When the condition (3) holds, Eq. (5) may be approximated to high precision by the equation

$$q = \frac{a^4}{\eta\tau_0}(i - i_0)^2\left[1 - \frac{4(i - i_0)}{3i_0}\right]t. \tag{6}$$

An analogous formula for a cylindrical capillary, derived from the formula of Buckingham, has the form

$$q = \frac{\pi r^5}{8\eta\tau_0}(i - i_0)^2\left[1 - \frac{5(i - i_0)}{3i_0}\right]t. \tag{7}$$

Neglecting the second term in the square brackets in Eqs. (6) and (7), we arrive at the law expressed by Eq. (4) in both cases.

The filtration law (4) follows also from simple qualitative considerations.

The gradient of the flow velocity of a material being filtered in pores is proportional to the quantity $(i-i_0)$. The length of the path over which the velocity increases is proportional to this same quantity. Therefore, the mean velocity is proportional to the square of the difference between the pressure gradient i and the critical gradient i_0.*

If slow filtration $[(i_0-i_0)<i_0]$ of a viscoplastic substance takes place under conditions such that at the surface of a cylinder of radius r_1 the pressure in the medium being filtered is p_1 and at the surface of a cylinder r_2 is p_2, where $r_1>r_2$ and $p_1>p_2$, then the application of Eq. (4) gives the following expression for the flow Q through unit length of the cylinder generators

$$Q=\frac{\pi}{2}n\frac{[(p_1-p_2)-i(r_1-r_2)]^2}{(\sqrt{r_1}-\sqrt{r_2})^2}t. \tag{8}$$

The expression

$$Q=4\pi n\left[\frac{(p_1-p_2)-i_0(r_1-r_2)}{\ln\frac{r_1}{r_2}}\right]t \tag{9}$$

gives the discharge through the surface of a sphere when there is spherical symmetry.

LITERATURE CITED

1. V. A. Florin, Fundamentals of Soil Mechanics [in Russian](Gosstroiizdat, 1959).
2. N. N. Kulakov, Introduction to the Physics of Peat [in Russian](Gosenergoizdat, 1947).
3. M. P. Volarovich and A. M. Gutkin, Zh. Tekhn. Fiziki 16, 321 (1946).

All abbreviations of periodicals in the above bibliography are letter-by-letter transliterations of the abbreviations as given in the original Russian journal. *Some or all of this periodical literature may well be available in English translation.* A complete list of the cover-to-cover English translations appears at the back of this issue.

---

* It should be kept in mind that the sign of the quantity i_0 agrees with the sign of the pressure gradient. Thus, in Eq. (4), the quantity q is determined by the difference of the absolute values of i and i_0.

SLOW FLOW OF A VISCOPLASTIC DISPERSED MEDIUM IN CONICAL AND PLANE DIFFUSORS WITH SMALL ANGLES OF DIVERGENCE

A. M. Gutkin

Moscow Energetics Institute
Translated from Kolloidnyi Zhurnal, Vol. 23, No. 3, pp. 352, May-June, 1961
Original article submitted February 20, 1961

The flow of a medium in a cylindrical tube, when the absolute value of the pressure gradient $i = (dp/dz)$ differs but little from the limiting value $i_0 = (2\tau_0/r)$, is expressed by the formula [1]

$$q = \frac{\pi r^5}{8\eta\tau_0}(i - i_0)^2 t. \tag{1}$$

Hence

$$\frac{dp}{dz} = \pm\left[\frac{2\tau_0}{r} + \left(\frac{8\eta\tau_0 q}{\pi r^5 t}\right)^{1/2}\right], \tag{2}$$

where the sign on the right side is chosen in accordance with the sign of the pressure gradient (plus sign if $dp/dz > 0$ and minus sign if $dp/dz < 0$).

After integration of Eq. (2), one can find the dependence of q on the pressure at the entrance and exit cross sections and on their radii

$$q = \frac{9\pi \operatorname{tg}^2\varphi}{32\eta\tau_0}\left[p_1 - p_2 - \frac{2\tau_0}{\operatorname{tg}\varphi}\ln\frac{r_2}{r_1}\right]^2 \frac{r_2^3 r_1^3 t}{(r_2^{3/2} - r_1^{3/2})^2}, \tag{3}$$

where p_1 and p_2 are the pressures at the entrance and exit cross sections; r_1 and r_2 are the radii of the larger and smaller cross sections; φ is the angle of divergence of the diffusor.

Equation (3) is applicable for small angles of divergence, i.e., for angles φ, when $\varphi^2 \ll 1$ and, in addition, if the difference standing in the square brackets of Eq. (3) is several times smaller than the difference $(p_1 - p_2)$.

For a plane diffusor, by an analogous method, one obtains the formula

$$q = \frac{\operatorname{tg}^2\varphi}{\eta\tau_0}\left[p_1 - p_2 - \frac{\tau_0}{\operatorname{tg}\varphi}\ln\frac{a_2}{a_1}\right]^2 \frac{a_1^2 a_2^2}{(a_2 - a_1)^2} t, \tag{4}$$

where $2a_1$ and $2a_2$ are the widths of the entrance and exit openings, and the remaining notation is the same as in Eq. (3). The limits of applicability of Eq. (4) are the same as for Eq. (3).

LITERATURE CITED

1. A. M. Gutkin, Kolloid. Zhur. 23, No. 3 (1961).

THE PROBLEM OF THE STABILITY OF COLLOIDAL SYSTEMS AND ITS PRESENTATION IN THE COURSE OF COLLODIAL CHEMISTRY

S. S. Voyutskii

Moscow

Translated from Kolloidnyi Zhurnal, Vol. 23, No. 3, pp. 353-358, May-June, 1961
Original article submitted November 26, 1960

Modern colloidal chemistry is passing through a critical period in its development [1]. The last decade has brought profound changes to almost every one of its sectors, altering not only the scope of material covered but also the principles which form the basis for interpretation of experimental results.

A clear-cut instance of this situation is found in the fact that those solutions of high molecular compounds (lyophilic colloids) which were treated theoretically as heterogeneous, non-equilibrium, systems even as late as the 1930's are now generally considered to be true solutions. This new aspect of the theory of solutions of high molecular compounds has been presented in numerous monographs, manuals, and text-books [2-4] and it is now entirely clear in principle how such systems should be treated in the modern course of colloidal chemistry.

Ther situation is considerably worse in regard to the theory of stability and coagulation although these problems are generally considered to occupy a central position in colloidal science. A satisfactory physical theory of stability and coagulation in colloidal systems was developed in the 1940's by Deryagin, Landau, Verwey, Overbeek, and others, and numerous monographs and reviews devoted to these matters have since appeared [5-14]. Nevertheless, the current text-books on colloidal chemistry treat stability, coagulation, and the closely related problem of the electrical properties of colloidal systems, at a level which is quite out of keeping with the present state of colloidal science.

What must this section of a text in colloidal chemistry contain in order to be compatible with current developments?

This question can be answered only after reaching a decision as to what is to be considered as the basic concept for interpreting colloidal stability. It is known that three factors are now adduced to explain the stability of those lyophobic sols whose study is the central problem of colloidal chemistry*.

1. The formation of an electrical double layer on the surface of the colloidal particle and the establishment of an energy barrier which keeps the particles from approaching close enough for the intensive forces of molecular attraction to come into play. Such a layer is generally externally diffuse and can arise either from selective adsorption of one of the ions of the electrolyte which is present in the system or from interaction between the dispersed phase and the dispersing medium with ionization of the resulting molecules.

2. The formation on the surface of the particle of a rather thick solvation layer of molecules of the dispersing medium. Such a solvation layer prevents the adhesion of particles on collision since it is elastic and these is no appreciable surface tension at its interface with the free dispersing medium.

3. The formation on the surface of the particle of an adsorbed layer which shows high structural viscosity at low velocity gradients and functions as a structural-mechanical barrier [15]. Nearly saturated adsorption layers of orientated surface active molecules showing two-dimensional structures similar to those found in crystals would fall under this heading. This theory predicts that an especially strong stabilizing action would be associated with those adsorbed colloidal layers which are designated as lyogels. These are peculiar gel films which are highly solvated by the dispersing medium and pass into the latter by diffusion. Proteins, alkali soaps and certain other substances which contain rather large organic ions, are capable of forming layers of this kind in hydrosols.

* No account will be taken of the effect of purely kinetic factors (the apparent elasticity of sap films (Maragon-Gibbs effect) and the reduction in the number of collisions of sol particles with dilution for example) on the stability of colloidal systems.

Rebinder [16] considers the stabilizing action of structured viscous (gel) adsorption layers to be due to the fact that the highly viscous film of stabilizer is not extruded from the space between the particles of the dispersed phase during the period of collisonal contact; he [17] further believes this to be the principal stabilizing factor, one which is invariably significant and indespensible for the preparation of such highly stable, concentrated, dispersed systems as technical foams, emulsions, and suspensions.

The ordinary lyophobic sols whose stability can be determined by some one of the above factors have recently begun to share interest with those thermodynamically stable colloidal systems which result from spontaneous dispersion. Such systems arise when the interfacial tension is quite low (< 0.1 erg/cm^2) and the thermal energy is sufficiently high to overcome the forces acting between the molecules of the dispersed phase. These systems can be truly designated as lyophilic*; they have been studied by Rebinder and his school [18], have great theoretical and practical significance, and must be treated in the course of colloidal chemistry. The stability of these systems has no direct relation to the stability of ordinary lyosols and is of quite different origin.

The first of these three stabilizing factors—the presence of an electrical double layer around each colloidal particle—is generally acknowledged to be of importance for stabilizing ordinary colloidal systems. This was brought out with special clarity in the International Discussion of Coagulation which was organized by the Faraday Society in Sheffield in 1954 [19]. The great majority of the papers read at this meeting interpreted hydrosol stability in terms of electrical forces of repulsions between particles carrying a diffuse electrical double surface layer. The fruitfulness of this approach to the problem of stability is confirmed by the fact that it gives a basis for the only quantitative physical theory of the stability of lyophobic colloidal systems which has been developed by either Soviet or foreign scientists. Finally, it should be noted that the stability of colloidal systems is treated in this manner in most journal articles and in the recent texts and monographs of the most competent scientists [5-7].

The only serious objection to the assumption that colloidal stability arises from the repulsive electrical forces between particles is based on the fact that certain silicic acid and metallic hydroxide sols are stable at zero electrokinetic potential. This objection must be considered as unfounded in the light of modern views concerning these systems. It has been shown, for example, that such sols are not true colloidal systems but solutions of high molecular compounds which contain giant chain molecules. The stability is determined here by high solvation and the entropy factor and is therefore of thermodynamic origin, specially in the case of the silicic acid sols [20,21]. Proof has been given in [21,22] that condensation and crystallization produce very minute crystals of silica in these latter sols and thereby give rise to true colloidal systems. An absorbed water layer can form on the polar surfaces of these crystallites to stabilize the system through particle solvation. In other words, stability in this particular case is due to the second of the above factors which is to be discussed below.

It should be noted that the electrical double layer theory is also applicable to the interpretation of lyosol stability in nonaqueous media. The belief that a high value of the dielectric constant of a non-aqueous medium makes the existence of an electrical double layer on the particle surface impossible [23,24] is one which must be abandoned. It has now been shown that ionization can occur even in nonpolar oils so that the presence of a suitable electrolyte will give rise to an outwardly diffuse electrical double layer at the interface and assure stability against aggregation [25, 26].

Modern theories have shown that the second of the possible stabilizing factors—the formation around the particle of a solvation film of molecules of the dispersing medium—cannot be of general significance for the stability of common colloidal systems.

1. Proof has not yet been given of the existence of molecular films which would be thick enough to prevent particle adhesion. Much data points to comparatively low solvation of most surfaces, even strongly polar functional groups interacting with only a few polar molecules [14]. Special surface films (solvation layers) can be formed in a non-polar medium only if the molecules of the latter are quite elongated and the system contains surface active molecules [27].

---

* Lyophilic systems of this kind should not be confused with systems which would be designated as lyophilic in the older sense of the word. The latter are known to be true solutions of high-molecular substances.

2. Protective solvation films can be formed only as the result of rather energetic interaction between the dispersing medium and the dispersed phase. It is clear that the lyophobic nature of the dispersed phase eliminates the possibility of such interaction in typical colloidal systems. The impossibility of such interaction is also indicated by the simple argument that it would invariably lead to the formation of a true solution in which the dispersed phase would be distributed through the dispersing medium in the form of individual molecules. The formation of particles of colloidal dimensions would then be possible only if the molecules themselves were of colloidal dimensions. This is exactly the situation which is met in solutions of high polymers but these should not be designated as colloidal in the light of modern views [1].

What has been said should not be understood as meaning that there can be no surface solvation without solution. Surface solvation certainly occurs but only if the molecules in question have a considerable affinity for the solvent and are bound firmly to one another either by chemical bonds or, at least, by strong hydrogen bridges. Glass, quartz, and cellulose are examples of substances whose surfaces can interact with water and undergo solvation without dissolution.

In speaking of the interpretation of the stability of colloidal systems in terms of the electrical double layer and the solvation film carried by the particle, it is in order to stop for a moment on one detail which is characteristic of Soviet texts on colloidal chemistry and which traces back to certain remarks of Peskov [10,11]. A number of these tests [9,28,29] acknowledge the significance of the electrical double layer for stabilizing lyophobic colloidal systems but base the actual interpretation of stability, not on the existence of an energy barrier between particles of like charge, but on the fact that the ions of the double layer are solvated and thus form a solvation film around the individual lyophobic particle. It is quite obvious that the ζ-potential is here no more than a measure of the depth of the stabilizing solvation layer.

We believe that there is no justification for presenting this theory of the stability of colloidal systems in texts of colloidal chemistry even though it appears at first glance to be quite reasonable and has found wide acceptance. We have pointed out earlier that such approach has one fundamental defect in that it does not permit a quantitative treatment of either stability or coagulation.

It is moreover clear that direct contradictions can arise in attempting to interpret the stability of colloidal systems in terms of solvation of the ions of the electrical double layer alone. Thus the prevention of particle adhesion on collison calls for the formation of dense, elastic, polymolecular solvation films similar to those formed by the attraction of polar water molecules to a polar solid and it is very difficult to see how such films could be produced by the action of solvation forces alone. Actually, solvation films of polar molecules of the dispersing medium are formed separately around each ion of the ionic atmosphere of the colloidal particle. The result must be that the polar molecules of the medium which are located in the interface between two neighboring counter-ions of like charge will themselves be so orientated as to oppose their ends of like charge and therefore repel one another. It should be remembered, moreover, that the microstructure of the film surrounding the particle will be altering continually because of the thermal movement of the ions. It is impossible to conceive of attraction and subsequent orientation of dipoles as giving rise to a continuum of medium molecules such as that required for assuring elasticity of the solvation layer surrounding the particle. The film elasticity which is responsible for stability can arise only from deformation of the ionic atmosphere and it is, therefore, determined by electrical forces alone.

The difficulty of explaining the existence of electrical effects still remains even if it is assumed that a dense, thick, elastic solvation film surrounds each colloidal particle. The high values of the mechanical constants of this film would tend to prevent micelle rupture along the slip plane which lies within the solvation layer surrounding the particle and is probably located much closer to the particle surface than to the outer fringe of the solvation film.

An explanation of the stability of colloidal systems in terms of solvation of the ions of the electrical double layer carried on the particle surface makes it also impossible to understand the mutual coagulation of similarly charged sols each of which is fully stable in its own right. Mutual coagulation can be given a strict quantitative treatment which is free of special assumptions if stability and coagulation in colloidal systems are assumed to result from electrical interaction.

The claim of universality for the third stabilizing factor—the presence of a structural-mechanical barrier at the particle surface seems rather open to question. It is, first of all, only possible to speak of structural-mechanical properties of the adsorbed layer in the case of stabilizers which have rather large molecules and are capable of forming two-dimensional gels. This is a special case, however. It is, moreover, impossible to see how the mechanical properties of the adsorbed layer could affect the stability of a suspension even if the system contained a stabilizer of the

type just mentioned. The dispersed phase would itself usually possess considerable rigidity while stability of the system calls, not for high mechanical strength of the adsorbed film, but for the ability of the particles to repel one another on collison; this can be assured only by having the particles carry identical charges or elastic solvation layers.

The stabilizing effect of the structural-mechanical factor is doubtful even in the case of many emulsions.

1. It is now firmly established that emulsion globules are covered with a layer of stabilizer which is far from saturation, regardless of whether stabilization has been achieved by a soap or by some other ionogenic or non-ionogenic substance [30-33]. It is also well known [31-34] that the molecules of surface active substances are so orientated at the interface that the hydrocarbon radical is dissolved in the oil droplet and only the polar ionogenic group is directed outward into the aqueous medium. Here it is scarcely possible to speak of the globule as being surrounded by a two-dimensional gel having structural-mechanical properties. This is in agreement with the fact that recent measurements [35,36] have failed to show the presence of structured layers of surface active substances such as ordinary soaps at a hydrocarbon—water interface, or even layers of enhanced viscosity.

2. Experiment shows that stable emulsions can be obtained by the use of emulsifiers which are clearly incapable of forming absorbed films of high mechanical strength. This applies to crystalline Nekals (alkali salts of alkylnaphthalene sulfonic acids), triethanolamine, and other widely used stabilizers.

3. The Schulze-Hardy Rule is known to apply to the electrolytic coagulation of emulsions, at least to those which have been stabilized by soaps [37,38]. It would be impossible to explain the validity of this rule if emulsion stability is due to the structural-mechanical factor.

The structural-mechanical factor would be of greatest significance in stabilizing foams. Even here, however, stability can be accounted for by other theories [39], while various observations indicate that the presence of a mechanical barrier at the surface of the air bubble does not invariably affect the stability [36,40].

The electrical double layer carried by the particle must then be made the basis for an understanding of the stability of lyophobic systems, and the content of the section of the modern course of colloidal chemistry devoted to stability and coagulation be determined accordingly.

The student must, at the outset, obtain a clear and rather complete picture of the origin of the stability of colloidal systems—the electrical double layer—and the effect of various factors on stability.

It is here not possible to be content with a dogmatic presentation of the views of Perrin, Gouy—Chapman, and Stern, on the structure of the electrical double layer but each theory must be subject to critical analysis. The presentation of the Gouy—Chapman theory must not only point out the inability to explain charge transfer among particles but must also bring out such other weaknesses as the failure to take account of the finite dimensions of the ion and differences in the coagulating ability of ions of the same valency. A discussion of the Stern theory must bring out the possibility that the slip surface will not, in general, be the same as the face of the Helmholtz layer. The mathematical aspects of the theory of the structure of the electrical double layer should be presented in a similar manner in the texts for universities and chemical institutes.

Most of our text-books consider only the effect of electrolytes on the depth of the electrical layer and it would seem that the time has come for the modern course to broaden this treatment to include such technically important factors as pH, temperature, and the dilution of the dispersed system. It is also necessary to give a general presentation of the concepts of electrophoretic retardation and electrical relaxation, with a brief indication of corrections in the calculation of electrokinetic potential necessitated by these factors. There must, finally, be a brief description of the determination of the electrokinetic potential by the Tiselius method and paper electrophoresis. It is a well known fact that these methods have found numerous applications in recent years.

Still more profound changes must be introduced in the presentation of material dealing directly with the stability and coagulation of colloidal systems. The prime need is for a detailed consideration of the forces of attraction and repulsion which act between the colloidal particles. It is well known that these forces are additive and that their dependence on distance in the case of the larger particles follows an entirely different law than that which is applicable to the force of interaction between individual molecules. It is also necessary to acquaint the student with the experimental proof of the validity of these concepts found in the work of Deryagin and Abrikosova [41] and to give at least an introduction into the Lefshitz theory of the attraction of two bodies separated by a narrow gap [42]. Some indication must be given of the conditions under which the Casimir-Polder retardation of electromagnetic waves can be observed.

At least brief mention should be given of Deryagin's[43] analysis of the interaction between colloidal particles which are surrounded by a counter ion atmosphere.

This presentation of the characteristics of the forces of attraction and repulsion which act betwen colloidal particles must be followed by a rather complete analysis of the over-all potential curve showing the alteration in the interaction energy with distance as the particles gradually approach one another, considering those conditions under which the particles will be unable to aggregate because of failure to overcome the energy barrier. Only on the basis of such an analysis is it possible to formulate general laws for the coagulation of colloidal systems and get away from the fetish of the older theories of the critical coagulation potential.

The course must take up in considerable detail those two basic types of coagulation—neutralization and concentration—which have been treated by physical theory. The older theories of coagulation (the chemical theory, the Freundlich theory, the electrostatic theory) must, of course, find a place in text-books, especially those intended for use in the universities and higher educational institutions, but in brief and rather critical form since they are of only historical interest.

It seems that the modern course in colloidal chemistry gives an adequate treatment of the kinetics of coagulation and that there is no need for amplification here. The technologist or researcher in colloidal chemistry is only rarely concerned with the problems of the kinetics of coagulation and it is therefore unnecessary to encumber the course with the mathematical apparatus which is required for an exact presentation of the Smoluchowski theory.

The course should also contain a rather detailed treatment of such coagulation effects as antagonism and syneresis of ionic action, irregular sequences, and the mutual coagulation of colloidal systems. It is impossible to be content here with a mere description of the effects, as is the case in many texts, and the mechanisms in question should be treated, at least in brief form. Special attention should be directed to the matter of colloidal protection. It is probably well to base the interpretation of this effect on the modern concepts which describe the increase of stability of a colloidal system resulting from the introduction of a high molecular material in terms of the entropy factor (thermal motion) and the mutual repulsion of flexible macromolecules which are only partially adsorbed by the particles of the lyphobic sol.

The course should also consider heterocoagulation, an effect which is of much practical importance for flotation, paper sizing, etc.. A generalized theory is now available which permits these effects to be treated in complete conformity with the physical theory of coagulation [45].

Finally, the colloidal chemistry text must give in its various chapters a rather detailed outline of other points of view on the stability of colloidal systems (solvation factor, structural-mechanical factor) and a presentation of the purely kinetic factors which come into play here (low collison frequency in diluted systems, Maragon—Gibbs effect). The factor responsible for stability must be pointed out in each concrete case as it is taken up.

LITERATURE CITED

1. S. S. Voyutskii and P. A. Rebinder, Kolloid. Zhur. 18, 253 (1956).
2. A. A. Tager, Solutions of High Molecular Compounds [in Russian] (State Chem. Press, 1951).
3. S. S. Voyutskii, Solutions of High Molecular Compounds [in Russian], (State Chem. Press, 1958).
4. S. A. Glikman, Introduction to the Physical Chemistry of High Polymers [in Russian] (Saratov University Press, 1959).
5. E. J. W. Verwey and J. T. G. Overbeek, Theory of the Stability of lyophobic colloids (Amsterdam, 1948).
6. J. T. G. Overbeek, Advances in Colloid Science 8, 97 (1950).
7. G. R. Kruyt, The Science of Colloids [Russian translation] (Moscow, Foreign Literature Press, 1955), vol. 1.
8. B. V. Deryagin, Contemporary State of the Theory of the Stability of Lyophobic Sols and Suspensions, Transactions of the Third All-Union Conference on Colloidal Chemistry (Moscow, Acad. Sci. USSR Press, 1956).
9. A. P. Tutskov, Brief Course in Colloidal Chemistry [in Russian] (Leningrad, State Chem. Press, 1958).
10. N. P. Peskov, Physical Chemical Principles of Colloidal Science (Moscow-Leningrad, State Chem. Press, (1932).
11. N. P. Peskov, Course of Colloidal Chemistry [in Russian] (Moscow-Leningrad, State Chem. Press, 1940).
12. H. R. Kruyt, Colloid Science, v. 2 (Elsevir Publ. Comp. 1949).
13. A. P. Pisarenko, K. A. Pospelova, and A. G. Yakovlev, Colloidal Chemistry [in Russian] (Moscow, 1958).
14. A. G. Pasynskii, Colloidal Chemistry, "High School" [in Russian] (Moscow, 1954).

15. P. A. Rebinder, Kolloid. Zhur. 20, 527 (1958).
16. P. A. Rebinder, Introductory article in the text of W. Clayton, Emulsions, Theory and Technical Applications [Russian translation] (Moscow, Foreign Literature Press, 1950).
17. P. A. Rebinder, Synopsis of a General Course in Colloidal Chemistry [in Russian] (Moscow University Press, 1949).
18. P. A. Rebinder, Transactions of Third All-Union Conference on Colloidal Chemistry [in Russian] (Moscow, Acad. Sci. USSR Press, 1956), p. 7; E. D. Shchukin and P. A. Rebinder, Kolloid. Zhur. 20, 645 (1958).
19. Coagulation and Flocculation, A general Discussion of the Faraday Society (The Aberdeen University Press. Ltd., 1954).
20. C. B. Hurd and P. C. Merz. J. Am. Chem. Soc. 68, 61 (1946).
21. W. Lewis, L. Squires and G. Braughton, The Chemistry of Colloidal and Amorphous Substance [Russian translation] (Moscow, Foreign Literature Press, 1948), p. 197.
22. Z. Ya. Berestneva and V. A. Kargin, Uspekhi Khim. 24, 249 (1955).
23. J. H. Schulman and E. G. Cockbain, Trans. Faraday Soc. 36, 661 (1940).
24. J. L. Moillet and B. Collier,Surface Activity, London (1951).
25. J. L. Fuoss and C. A. Kraus, J. Am. Chem. Soc. 55, 3614 (1933);W. A. Albers and J. T. G. Overbeek, J. Coll. Sci. 14, 501, 510 (1959).
26. H. Koelmans, and J. T. G. Overbeek, Coagulation and Flocculation, Discussion of the Faraday Society (The Aberdeen Univ. Press, Ltd, 1954), p. 52.
27. B. V. Deryagin, What is Friction [in Russian] (Moscow, Acad. Sci. USSR Press, 1952), p. 220.
28. N. P. Peskov and E. M. Aleksandrova-Preis, Course in Colloidal Chemistry [in Russian] (Moscow Leningrad, State Chem. Press, 1948); S. M. Lipatov, The Physical Chemistry of Colloids [in Russian] (Moscow-Leningrad, State Chem. Press, 1948).
29. S. A. Balezin and G. S. Parfenov, The Principles of Colloidal and Physical Chemistry [in Russian] (Moscow, Uchpedgiz, 1956).
30. E. K. Fischer and W. D. Harkins, J. Phys. Chem. 36, 98 (1932);L. Ya. Kremiev and S. A. Soskin, Zh. Obzhn. khimii 16, 200 (1946);L. Ya. Kremiev and P. I. Kagan, (1946); Kolloid. Zhur. 10, 436 (1948).
31. L. Ya. Kremnev and N. I. Kuibana, Kolloid. Zhur. 13, 38, (1951).
32. B. M. G. Zwicker, Ind. Eng. Chem. 44, 774 (1952).
33. R. M. Panich and S. S. Voyutskii, Kolloid. Zhur. 18, 326 (1956).
34. W. D. Harkins. The Physical Chemistry of Surface Films, N. Y.(Reinhold Publ. Corp., 1952), p. 83.
35. B. C. Blakey and A. S. Lowrence, Coagulation and Flocculation Discussion of the Faraday Soc. (The Aberdeen Univ. Press, Ltd, 1954). p.268, P. C. Blokker, ibid, p. 307.
36. K. Durham, and M. Camp, ibid, p. 308.
37. A. R. Martin, and R. N. Hermann, Trans. Faraday Soc. 37, 30 (1941);M.Van den Tempel, Rec. trav. Chim. 72, 419 (1953).
38. S. S. Voyutskiĭ and R. M. Panich, Kolloid. Zhur. 19, 268 (1957).
39. Faulk and Miller, Ind. Eng. Chem. 23, 1283 (1931);N. K. Adam, Phiz. and Khimii Surface (Gostenizdat., 1947), p. 190.
40. B. B. Deryagin, Kolloid. Zhur. 17, 149 (1955).
41. B. V. Deryagin and I. I. Abrikosova, Zhur. Eksp. i Teort. Fiz. 21, 945 (1951), 30, 993 (1956); see also, Doklady Akad. Nauk SSSR 90, 1055 (1953).
42. E. M. Lifshits, Doklady Akad. Nauk SSSR 97, 643 (1954).
43. B. V. Deryagin, Izvest. Akad. Nauk SSSR, OMEN, Ser, Khim. Nauk 5, 1153 (1937); Kolloid. Zhur. 16, 291 (1940); 7, 285 (1941).
44. Mackar and Van der Waals. J. Coll. Sci. 7, 535 (1952).
45. B. V. Deryagin and V. G. Levich, Doklady Akad. Nauk SSSR 98, 985 (1954); Kolloid. Zhur. 16, 425 (1954).

All abbreviations of periodicals in the above bibliography are letter-by-letter transliterations of the abbreviations as given in the original Russian journal. *Some or all of this periodical literature may well be available in English translation.* A complete list of the cover-to-cover English translations appears at the back of this issue.

REMARKS ON THE PROBLEM OF THE STABILITY OF DISPERSED SYSTEMS

P. A. Rebinder and A. B. Taubman

Institute of Physical Chemistry, Academy of Sciences, USSR, Moscow
Translated from Kolloidnyi Zhurnal, Vol. 23, No. 3, pp. 359-361, May-June, 1961
Original article submitted March 17, 1961

Although an abundance of experimental material on colloidal stability has been accumulated in industry and research, the treatment of this fundamental problem remains unsatisfactory and heated discussion continues to center around it [1].

The most characteristic dispersed system are those containing a liquid dispersing medium (emulsions, including foaming emulsions, gels, foams, suspensions, and the corresponding colloidal solutions) and it is on these that attention should be concentrated to the exclusion of the aerosols, since the latter occupy a special position as a result of peculiarities inherent in the gaseous dispersing agent.

It is useful to divide the former systems into two large groups, the lyophilic and the lyophobic, classification being based on a comparison of the specific free interfacial surface energy (σ_{12}) and a certain critical value (σ_m) which is fixed by the temperature and is proportional to the kinetic energy of thermal (Brownian) movement, kT [2,3]. Such comparison gives a new basis for classification and leads to what appears to be the only correct understanding of the difference between these groups.

A disperse, two-phase, micro-heterogeneous system is lyophilic when σ_{12} is rather low and either less than, or comparable with, the critical value σ_m. Conversely, the system is lyophobic when σ_{12} does not satisfy this condition. This natural classification will accomodate the limiting case of a lyophilic system which is a true (single phase) solution of either low or high molecular compounds with infinite mutual phase solubility ($\sigma_{12} = 0$). On the other hand, a lyophilic system involving a pair of stable, mutually saturated phases will form spontaneously when the conditions are such that $0 < \sigma_{12} < \sigma_m$, thus giving rise to an equilibrium curve showing the distribution of the dispersed phase as a function of the particle (drop) diameter in the sense of Volmer [4]. Such spontaneous dispersion is possible because the increase in entropy resulting from a more uniform distribution of the dispersed phase in the system over-compensates the inevitable rise in the surface energy [3].

Thus lyophilic dispersed systems are in stable thermodynamic equilibrium and require no further stabilization. Illustrations can be found in the formation of an emulsion in the neighborhood of the critical solution temperature (critical emulsions), in emulsions of soluble oils, and in still other emulsions which result from the introduction of rather large amounts of surface active components whose sole purpose is to reduce σ_{12} below the value σ_m. Colloidal suspensions of hydrophilic clays (Na and Li bentonites) in water and similar mixtures should be classified as lyophilic systems.

The lyophobic dispersed systems are known to differ from the lyophilic systems by being thermodynamically unstable, the stability of any such system being, in principle, a kinetic factor fixed by the time elapsing before breakdown.

Lyophobic dispersed systems require stabilization and the mechanism of this stabilizing action is usually the principal issue in any discussion of stability. Here it is necessary to underscore differences of great practical importance between dilute and concentrated systems, first in terms of the number of particles of the dispersed phase per unit volume and then in terms of degree of volume packing. Just as important, on the other hand, are the natural concepts of practically complete stability and relatively weak stability. The principal interest in each technological problem is invariably directed toward a rather concentrated (and sometimes saturated) dispersed system of maximum stability. Natural (biological) materials such as the products of plant and animal activity (rubber latex, milk, etc.) are systems of this type and the most interesting among these are the concentrated emulsions, foams, suspensions, and pastes which contain highly mobile liquid interfaces.

It should be noted in passing that foams, i.e., saturated emulsions whose cells are filled with a gaseous phase, differ from the usual emulsions in so far as they are essentially lyophobic, the value of σ_{12} at the two-phase interface being always much greater than σ_m even in cases where maximum stability has been attained by the use of a surface active foaming agent.

It is generally acknowledged that each such system (including concentrated suspensions) requires the existence of a mechanical (viscous or elastic) barrier to impede the approach of particles or the rupture of films of the liquid medium if it is to show maximum stability and be practically free of coalesence (coagulation, aggregation) over an extended period of time [5]. In itself, the electrical charge which arises in a homogeneous system is completely inadequate to assure practically complete stability and the same is true of a reduction in σ_{12} unless it is quite extensive.

It is well known that the general laws applying to maximum stabilization are the same in ionogenic systems (those involving water as the dispersing medium, for instance) and in non-ionogenic systems (those involving such nonpolar media as hydrocarbons). In neither case will the electrical charges assure practical stabilization. Stabilization invariably requires the application of some sort of protective colloid, i.e., a high molecular substance which will form a rather strong spatial structure, or net, of the gel type, either in the bulk of the dispersing medium or on the surface of the dispersed phase itself, this last as a result of surface activity and adsorption. It must be emphasized that the instances of this strong stabilization are extremely diversified and form a continuous spectrum ranging all the way from structuralization of the adsorption layer alone to structuralization of the entire volume of the dispersing medium. The high structural viscosity is the factor which impedes the approach of the particles toward one another; it is especially marked when the structured net is continuous even though it cannot always be detected experimentally due to structural breakdown in the course of the measurements themselves.

It is also generally known that a concentrated dispersed system cannot be stabilized in practice by the adsorption of a surface active (ionogenic or non-ionogenic) substance on the surface of the dispersed phase from the surrounding medium unless this substance can function as soap-forming detergent in aqueous media. The complex pattern of detergent action involves passage of the dirt particles into the dispersing medium with maximum stabilization and elimination of the possibility of re-adherence to the surface which is being washed. On the other hand, non-ionogenic soaps with the requisite degree of hydrophobic—hydrophilic balance in their molecules show marked detergent action and are just as capable of giving maximum stability to suspensions, emulsions and foams as the ionogenic soaps. In this respect they differ from the non-soap adsorbing electrolytes which are incapable of functioning as strong stabilizers. Every homologous series of surface active substances shows a sharp discontinuity in the ability to form structures (soaps) and stabilize dispersed systems as the length of the hydrocarbon chain is increased to 9-11 links, the exact number depending on the nature of the polar group. Cases of high stability in concentrated dispersions containing only ordinary electrolytes (bentonite suspensions, for example) always show marked lyophilic properties in the above sense of the word.

This same issue of the Kolloidnyi Zhurnal contains an article by Voyutskii [6] concerning the presentation of the problem of dispersed system stability in the course of colloidal chemistry. The appeal of this author for a detailed and (more important still) correct interpretation of the significance of electrical factors in determining the stability and coagulation of dispersed systems is naturally to be welcomed. In point of fact, however the classical work of Powis and Clowes has already shown that it is only in the absence of those other, incomparably more stronger, factors which have been pointed out above that electrical effects can be of significance for the stabilization and coagulation of dilute emulsions, suspensions, and sols. It is generally known that only structuralizing protective colloids can give the desired stability to concentrated colloidal preparations, emulsion concentrates, and similar systems, and that the electrical state of the phase interface then ceases to be a decisive factor.

Thus it would seem that an objective presentation of the problem of stability, both in the science of dispersed systems and in course work, would take all of these important details into consideration instead of refusing to consider them as S. S. Voyutskii does.

It does not follow from this that all aspects of the problem of stability have been solved or that they are all sufficiently clear for this is not true of even the basic ones among them. In fact there are many aspects of this problem that are not at all clear and we will now indicate some of these.

Despite the significance of the concept of the diffuse double layer as it is introduced in the work of the Dutch physical chemists and in the theory of B. V. Deryagin, it still does not exhaust all of the electrical factors which are related to stability. It is sufficient to recall the well known work of A. N. Frumkin and his school in the field of electrocapillary phenomena where the surface charge has been shown to rise from zero at the maximum on the capillary

curve to the value corresponding to its cathodic or anodic extremity when the electrolyte concentration is high, the compression of the double layer at a maximum, and all electrokinetic mobility has vanished. This fact can lead to a considerableincrease in the stability of those films of the medium which impede coalesence, the wetting of mercury by oil droplets in aqueous medium, and the adherence of hydrogen bubbles to a mercury surface.

There are many cases in which there is no direct parallelism between the stabilizing action of a surface layer and its structural-mechanical properties, although there are numerous others in which such parallelism is expressed clearly. An illustration is found in those emulsions which are stabilized by solid emulsifiers in the presence of surface active substances and electrolytes [8].

In the practically important problem of polymerization in emulsions, or in dispersions in general, the only stabilizers are substances which are soap-formers to a more or less pronounced degree. There is as yet no explanation of the predominance of the role of the soap-forming electrolytes here and in solubilization. It should be kept in mind that similar effects are also inherent in the non-ionogenic soaps.

It is impossible to conclude without noting that the foams are prime examples of systems in which maximum stability is assured by gradual transition from adsorptional (surface) structuralization to bulk setting. This fact is drawn on in the production of those stable foams which are employed in fire extinguishers, in phenoplasts, etc..

A critical review of the present state of the problem of the stability of dispersed sytems and the method of presentation of this problem in lectures and in text-books must not overlook the significance of maximum stability. This is the most important factor that comes into play in practice, and it is, at times, the only one.

LITERATURE CITED

1. P. A. Rebinder, Kolloid. Zhur. 20, 5, 527 (1958).
2. P. A. Rebinder, Transactions, Third All-Union Conference on Colloidal Chemistry [in Russian] (Acad. Sci. USSR Press, 1956); Discuss. Faraday Soc. No. 18, 151 (1954).
3. E. D. Shchukin and P. A. Rebinder, Kolloid. Zhur. 20, 5, 645 (1958).
4. M. Volmer, Z. phys. Chem. 125, 151 (1927); 155, 28 (1931).
5. V. G. Levich, Doklady Akad. Nauk SSSR 103, 3, 453 (1955).
6. S. S. Voyutskii, Kolloid. Zhur. 23, 3 (1961).
7. W. Clayton, Emulsions [Russian translation] (Moscow-Leningrad, Foreign Literature Press, 1950); P. Rebinder and A. Taubman, III. Kongress Oberflächenakt Stoffe, Köln (1960).
8. A. B. Taubman and A. F. Koretskii, Kolloid. Zhur. 20, 5, 676 (1958); A. F. Koretskii, Candidate's Dissertation, Institute of Physical Chemistry, Acad. Sci. USSR (1960).

All abbreviations of periodicals in the above bibliography are letter-by-letter transliterations of the abbreviations as given in the original Russian journal. *Some or all of this periodical literature may well be available in English translation.* A complete list of the cover-to-cover English translations appears at the back of this issue.

THE PROBLEM OF THE PRESENTATION OF COLLOIDAL STABILITY IN THE COURSE OF COLLOIDAL CHEMISTRY

B. V. Deryagin

Institute of Physical Chemistry, Academy of Sciences, USSR, Moscow
Translated from Kolloidnyi. Zhurnal. Vol. 23, No. 3, pp. 361-362, May-June, 1961
Original article submitted April 8, 1961

One can only welcome the initiative shown by S. S. Voyutskii in opening discussion of the unsatisfactory presentation of the problem of stability in the course of colloidal chemistry and the need for correction of the intolerable situation which has arisen here. I would like, at the outset, to give one more clear cut example of what is in question. The Kul'man text of physical and colloidal chemistry devotes two pages to the old Freudlich "theory" of sol stability which is now of no more than historical interest while treating the contemporary physical theory in a single sentence printed in small type.

There is no doubt that the material covered by text-books and, especially, programs for institutions of higher learning should be limited to well established facts which are of fundamental significance and quantitatively formulated theories which are applicable to a wide variety of phenomena. From this point of view one must certainly agree with S. S. Voyutskii in considering that it would be incorrect for the course in colloidal chemistry to present the structural-mechanical effect as a "strong" factor which is invariably involved in stabilizing colloids. This is a hypothesis and not a theory for it lacks a strict theoretical basis (such as the very general principles of solution theory and molecular physics upon which the modern theory of lyophobic colloidal stability rests) and cannot, at the same time, be empirically justified by direct comparison with experiment. Some of the available facts are even in direct contradiction with it. Thus the dissertation of Zotova has shown (Institute of Physical Chemistry, Academy of Sciences, USSR, 1960) that there is a million-fold difference in the two-dimensional viscosity of various brands of saponin which have the same foam life. It should be added that the concept of the structural -mechanical characteristics of the surface layer as a factor influencing colloid stability has not achieved quantitative precision, but has remained purely descriptive.

Under these circumstances, should it be considered the duty of the teacher or text-book author to convince the student that the "structural-mechanical" barrier is the most important and powerful stabilizing factor? Such statement is not generally accepted as valid; it is, in general, more than open to question and must be presented to the student dogmatically.

On the contrary, S. S. Voyutskii correctly notes that the theory of repulsive forces between diffuse ionic layers not only can, but must, be presented by derivation rather than by dogmatic statement, following the example of the very elementary Colloidal Chemistry of A. D. Sheludko which has recently been translated into Russian from the Bulgarian. It is also possible to call on direct experiments to demonstrate clearly the existence of well defined forces of electrostatic repulsion and molecular attraction.

It must be emphasized that the forces of electrostatic repulsion are capable of assuring practically complete stability not only of dilute, but also of concentrated, sols and suspensions. A special instance is found in the stable, highly concentrated, silver iodide sols which have been prepared by Verwey and Kruyt (Z. phys. Chem. 167A, 149, 1933). This property traces back to the fact that particle charge stabilized suspensions can form densely packed (at times, plastic) deposits or sheets which are free of secondary structure. Finally, the completely random distribution of flakes of Na montmorillonite clays in dilute NaCl solutions points to the extremely strong stabilizing effect of the thermodynamic fragmentation pressure even in the complete absence of an organic compound. These observations are in agreement with the theory of those repulsive forces which result from overlap of ionic atmospheres where it is shown that the stabilizing energy barrier in a colloidal system can be quite high and may even exceed the energy of thermal, or Brownian, movement, kT. Thus there is no valid reason for considering this to be a weak factor.

The presentation of these matters in the modern text-book should take account of the fact that the utility of the concept of electrostatic forces of repulsion between surfaces in ionic solutions extends beyond the confines of the theory of stability of lyophobic sols. It has been applied in conjunction with the mathematical methods proposed by the author to the treatment of a number of extensive and important branches of colloidal and surface chemistry such as swelling, thixotropy and other rheological properties of dispersed systems, elementary effects in flotation, water purification, and detergent action, the properties of clays and soils, tactoiddides, viruses, and periodic biological structures. Thus it is evident that it would be detremental to the development of science to fail to give a detailed presentation of the basic principles of the modern theory of colloidal stability (and not just final formulas).

It is generally known that the utility of this concept is limited to electrolyte concentrations which fall within the scope of the Debye-Huckel theory; this is, however, the principal,and essentially the only, limitation imposed on it, and it follows from the theory itself. The fact that there is no further change in the height of the energy barrier in moving by 150-200 mv from the null charge point into either the cathodic or anodic region was shown quite clearly by the model experiments of Voropaeva, Deryagin, and Kabanov (Doklady Akad. Nauk SSSR, 128, 981, 1959) where measurement was made of the force barrier for the adhesion of polarized platinum wires in solutions of electrolytes. This result is in complete agreement with theory.

The only definite modification of the theory which would follow from this work is the introduction of non-electrical repulsive forces, independent of the platinum potential and increasing rapidly with the concentration of the electrolyte, in the region where the diffuse double layer disappears along with its associated repulsive forces. The data of A. D. Sheludko on free films show the presence of these non-electrical forces in strong solutions of nonelectrolytes.

The existence of a second stabilizing factor, the non-electrostatic repulsive forces, is brought out quite clearly from these experiments on platinum wires and from others as well. It is, therefore, impossible to agree with S. S. Voyutskii in neglecting this (solvation) factor in the stabilization of colloidal systems, since it is especially significant when the surface carries lyophilic functional groups. The course of colloidal chemistry must give weight to the existence of this second stabilizing factor and to the need for a study of its theory and mechanism. In this manner the point would be emphasized, and correctly, that stabilization does not result from any universal factor or single type of force such as electrostatic repulsion.

Editorial Note: The editors considered the discussion of the problem of the presentation of the problem of stability in the course of colloidal chemistry to be closed with the articles of S. S. Voyutskii, P. A. Rebinder, A. B. Taubman and B. V. Deryagin which appear in the present number of the Kollodnyi Zhurnal.

ANGULAR SCATTERING FUNCTIONS FOR SPHERICAL PARTICLES

Detroit 2, Michigan, 226 pp.

William J. Pangonis and Wilfried Heller

Reviewed by K. S. Shifrin
Translated from Kolloidnyi Zhurnal, Vol. 23, No. 3, pp. 363-364, May-June, 1961

In recent years, extensive experimental and theoretical investigations of the scattering of light in colloidal solutions have been carried out under the direction of Professor Wilfried Heller in the chemistry department of Wayne State University in Detroit, Michigan, USA. The results of this work have been published systematically in the Journal of Chemical Physics and the Journal of Colloid Science. The exact diffraction equations have been used as a basis for certain very valuable calculations of the scattering of light by small particles which were carried out in the course of these studies. The results of the first calculations of W. Pangonis, W. Heller and A. Jacobson covering the amplitudes of the partial waves scattered by a spherical particle excited by an external plane wave were published by the Wayne State University Press in 1957 as Tables of Functions for the Scattering of Light by Spherical Particles. Various combinations of values of $\underline{m}$ and ρ ($\underline{m}$ is the relative coefficient of refraction $\rho = 2\pi a/\lambda$, $\underline{a}$ is the radius of the sphere, and λ is the wave length) were treated.

These tables gave not only the amplitudes of the partial waves but also values of the relative scattering coefficient, K_p, for these same values of $\underline{m}$ and ρ. This quantity is related to the "turbidity," or coefficient of scattering of a unit volume containing N particles, by the equation $\tau = \eta a^2 K_p N$.

Details concerning these earlier tables will be found in our review which appeared on page 134 of Vol. 21, No. 1, of the Kolloidnyi Zhurnal for 1959.

The new tables contain characteristic values of the scattering indicatrices, or angular dependence of the intensit of the scattered light. The theory of scattering leads to the following equations for the intensity of light scattered at the angle β by a particle illuminated by a bundle of parallel rays of natural light of intensity I_0

$$I_\perp = I_0 a^2 \frac{i_\perp(\rho, \beta)}{2\rho^2}, \qquad I_\parallel = I_0 a^2 \frac{i_\parallel(\rho, \beta)}{2\rho^2}. \tag{1}$$

Here $I_\perp$ and $I_\parallel$ are the intensities of rays in which the direction of vibration of the electrical vector is respectively perpendicular and parallel to the plane of scattering, and $i_\perp$ and $i_\parallel$ are the diffraction factors, quantities which are essentially dependent on ρ and β.

The total intensity, I, of the light scattered by the particle will be given by

$$I = I_\perp + I_\parallel = I_0 a^2 \frac{i_T(\rho, \beta)}{2\rho^2}, \quad i_T = i_\perp + i_\parallel, \tag{2}$$

while its degree of polarization, $\underline{p}$, can be calculated through the equation

$$p = \frac{i_\perp - i_\parallel}{i_T} \tag{3}$$

(see, for example, our book The Scattering of Light in Turbid Media, State Technical and Theoretical Literature Press, 1951). Tables of the indicatrices are usually set up in terms of $i_\perp$ and $i_\parallel$ and Eqs. (1)-(3) are then used to calculate the observed quantities $I_\perp$, $I_\parallel$, and $\underline{p}$.

In passing from the individual scattering particle to a unit volume containing a monodispersed sol with volume fraction of scattering material equal to Φ, one easily finds that

$$I_{\perp} = I_0 \Phi \frac{3}{4\lambda} \frac{i_{\perp}}{\rho^3}, \quad I_{\parallel} = I_0 \Phi \frac{3}{4\lambda} \frac{i_{\parallel}}{\rho^3}, \quad I = I_0 \Phi \frac{3}{4\lambda} \frac{i_T}{\rho^3}.$$

The tables under review are also set up in terms of $i_{\perp}/\rho^3$, $i_{\parallel}/\rho^3$ and i_T/ρ^3, which differ from the actually observed quantities only in a constant multiplying factor. Calculations have been carried out over the intervals: $\beta = 0(5)\ 180$; $m = 1.05(0.05)\ 1.30$ and $\rho = 0.2(0.2)\ 7.0$.

The accuracy of the results exceeds that which is called for in experiments with turbid media since most values are given to four or five significant figures.

The fact that these tables have been developed for a ρ interval of only 0.2 is especially valuable since this represents a radius interval of only 0.03 λ. A list of errata covering the earlier Tables of Scattering Functions is found at the end of the present tables on pages 222-223.

It is to be regretted that the results of these calculations on the scattering field are given in terms of scattering intensities alone. Here, the authors have followed what has not always been a happy tradition. In so doing a part of the information, namely, the phase difference between the perpendicular and parallel components, remains suppressed, even though these data were obtained in one step of the calculations for the table. It is true that the inclusion of such additional data would have markedly increased the volume of these tables but it would have also given a descripition of the so-called elipticity of the scattered light, a factor which is indispensable in experiments with polarizing instruments. The course of the authors can be justified by the fact that colloidal optics has no need of such data at the present time since full polarization measurements are practically never undertaken. This situation arises from the irregularity in the polarization characteristics for scattering which are already known and from the lack of clear and simple relationships (see, for example, Fig. 38 and Tables 20 and 21 in the text cited above).

These new tables represent a significant contribution to the optics of turbid media. They appreciably extend our knowledge of the fine details of the scattering of light by colloidal systems and will find extensive use in those most diversified investigations where the method of light scattering is penetrating more and more vigorously.

THE AUTOADHESION AND ADHESION OF HIGH POLYMERS

Scientific Technical Literature Press, RSFSR, 1960

Reviewed by V. E. Gul'

The latest book of S. S. Voyutskii is devoted to an extensive branch of the physical chemistry of polymers, namely adhesion and autoadhesion. This monograph is a survey of the contemporary theories and experimental facts which have been accumulated here. The author, himself, has contributed much to this sector of the science and the fact that he is able to present the factually rich material from a unified point of view which has recently won increasing recognition in the scientific community is one of the undoubted merits of the book. Acknowledging that the diffusion theory of adhesion is not universally valid, the author points out that it is capable of giving a good interpretation of an extensive body of phenomena connected with adhesion and autoadhesion.

The necessity of generalizing the work of Soviet and foreign scientists in the field of the physical chemistry of polymer gluing and the desirability of presenting the material from the point of view of the diffusion theory which he has proposed is brought out by the author in the introduction.

The first chapter outlines the physical chemical meaning of the "autoadhesion of high polymers" and describes methods which can be applied in its evaluation.

It is clearly impossible to overestimate the practical value of this and following chapters. The second chapter is devoted to the effect of various factors on autoadhesion. There is no doubt that the material presented here will serve as a powerful stimulant to the development of industrial processes for building up components from polymers.

The third chapter is devoted to the problem of autoadhesion and the formation of films from high polymer dispersions.

The fourth chapter outlines the role played by autoadhesion in the working of organic glasses and the preparation of articles by powder pressing.

Presentation of the material on the adhesion of high polymers begins with the fifth chapter where the concept of adhesion is defined and distinction drawn between two types of adhesion: specific, "which is the bonding force between the adhesive and the glued surface" and mechanical, "which is to be understood as the penetration of the adhesive into the pores of the glued material and the retention of the solidified adhesive in this material by mechanical wedging". It is useful to emphasize here that specific adhesion can give rise to electrostatic charges, to the appearance of dispersional forces, to the establishment of hydrogen bonds and so on. The material of this section is saturated with valuable facts and serves as a basis for the diffusion theory of adhesion, after being subjected to a scrupulous and impartial analysis.

The sixth chapter treats the effect of various factors on adhesion and a separate seventh chapter deals with the effect on adhesion of mechanical and chemical treatment of the substrate surface.

The eighth chapter is devoted to the problem of the adhesion of high polymers to metals, a matter of considerable practical and theoretical significance. It does not seem desirable to us to so single out one particular type of material, since the adhesion of high polymers to glass has also become a matter of no small interest.

The ninth chapter is devoted to the adhesiveness of high polymer solutions. Here, methods are given for the evalution of adhesiveness and a determination of its nature; the ropiness of high polymer solutions is also treated.

This summary makes it clear that the material contained in this book is quite diversified and should be of interest to a wide circle of readers.

In so extensive a work it is naturally quite difficult to completely avoid certain defects. I would like to point out the following among these.

The discussion of the polymer–polymer diffusion does not give sufficient weight either to the modern theory of the so-called bundle structure of high polymers which has been developed by V. A. Kargin and his collaborators or to the ideas of S. I. Sokolov and his coworkers concerning the various types of packing of macromolecules. Note should also be made of the almost complete lack of mathematical treatment of the adhesion and autoadhesion of high polymers.

It is to be hoped that those who are responsible for the development of the diffusion theory of adhesion will soon turn their attention to the development of the quantitative aspects of the phenomena in question. Despite these remarks it must be admitted that the text of S. S. Voyutskii is a valuable contribution to the science of high polymers and their applications; as such it will undoubtedly arouse much interest among a wide circle of readers.

CHEMISCHE TECHNOLOGIE, 1958, 768 pp.

K. Winnacker and L. Kuchler

V. Ksenzenko

The first part of the first volume of this text contains 10 chapters. The first three chapters are general and treat briefly the methods, apparatus and calculations which are used in chemical technology, as well as the principles upon which selection of optimal conditions for technological process is based, namely, a systematization of technological chemical processes, and data on equilibrium, kinetics, and catalysis.

The next eight chapters treat:

1. The recovery and preparation of water.

2. The reduction and separation of gases. This chapter contains theoretical principles and a description of technological systems for the reduction and separation of gases. Brief discussion is given of the properties and applications of the inert gases, and the preparation of hydrogen, nitrogen–hydrogen mixtures, and light hydrocarbons.

3. The recovery and treatment of potassium salts. The methods of preparing the most important components of the so-called natural potassium salts are treated in this chapter with citation of extensive theoretical, experimental, and technological material.

4. The technology of the compounds of boron. Preparations of boric acid, boron trioxide, salts of boric acid, and boro-halogen compounds are treated in this chapter.

5. The preparation of common salt, soda, and potash. This chapter is mainly devoted to a discussion of the methods used in the preparation of soda and the conversion of the latter into sodium hydroxide.

6. The technology of the preparation of chlorine and its most important compounds. Electrochemical preparations of chlorine and its oxygen compounds, the synthesis of hydrogen chloride and hydrochloric acid, and chemical methods for the production of chlorides, hypochlorates, bleaching powder, and phosgene are described here.

7. Fluorine and its inorganic compounds.

8. Methods of preparation of the most important peroxides.

In the introduction to the second edition the author indicates that this work was conceived as something intermediate between a text-book and an encyclopedia. The multiplicity of technological processes and methods and procedures for their realization which is characteristic of the present stage of technological development makes for complications in the development of a concise encyclopedia. The success of a work of this kind depends in considerable degree on the ability of the author to distinguish between principal and secondary technological processes. Moreover, selection for a mere encyclopedia must be made in such a manner as to take account of the importance of each particular product to the further development of material culture. On the other hand, publication of a work which would be both a text and an encyclopedia would necessitate a selection which would take account of the representativeness of the various methods and procedures which are applied in the technology of preparing the product in question.

It must be admitted that the authors of the present text have coped well with these difficulties so that the work suffers neither as a text nor as an encyclopedia.

The introduction of general problems of theory and equipment in the first two chapters makes it possible to become thoroughly familiar with the general principles of calculations, and selection of apparatus and optimal parameters for various technological processes. In many instances, however, these principles are not developed in the discussion of concrete technological problems. The simultaneous reading of two chapters, one general and the other special, and the analysis of various methods and procedures makes for difficulty in use of the book.

The theoretical material which has been accumulated in science and industry is not used to full advantage in certain chapters, such as those dealing with the production of soda, bromine and its salts, and common salt.

These remarks are in the nature of desiderata which might well be incorporated in a new edition of a timely and very interesting work which deserves to enjoy wide recognition among engineers and chemical technologists.

ISOTHERMS AND HEATS OF ADSORPTION OF ALCOHOLS ON CARBON BLACKS OF VARIOUS DEGREES OF GRAPHITIZATION

N. N. Avgul', A. V. Kiselev and I. A. Lygina

Institute of Physical Chemistry, Academy of Sciences of the USSR,
Surface Chemistry Group, Moscow
Translated from Kolloidnyi Zhurnal, Vol. 23, No. 4,
pp. 369-375, July-August, 1961
Original article submitted May 30, 1960

Investigation of adsorption on graphitized carbon blacks is of great theoretical interest, since these adsorbents possess one of the simplest crystalline lattices [1, 2]. In addition, the presence of a sufficiently large specific surface area of such adsorbents permits a detailed determination to be made both of the isotherms and of the heats of adsorption, as well as their theoretical treatment.

Since in the literature the results of an investigation of adsorption on carbon blacks differing in origin and degree of graphitization have been given, then it is of interest to carry out the comparison and to elucidate possible differences in the adsorption properties of different graphitized carbon blacks. The isotherms and heats of adsorption of argon on carbon blacks of different degrees of graphitization were studied in a previous paper [3]. Corresponding investigations of the adsorption of hydrocarbons were reported in papers [4-6], in the last of which graphitized carbon blacks of different origins were investigated. It was shown that with an increase in the degree of graphitization, the initial fall in the heat of adsorption, associated with the heterogeneity of the surface, decreased, and the rise in the heat of adsorption considerably increased near completion of compact monolayer coverage. Increase of the degree of graphitization of carbon blacks was revealed also by the shape of the adsorption isotherms which through this acquired a more distinct wave-like or even echelon form [7-11].

Comparison of the adsorption isotherms of alcohols on different graphitized carbon blacks and on graphite has only been made for methanol, in paper [12]. In this paper it was shown that the adsorption of methanol on graphite and on graphitized channel and thermal carbon blacks was very similar. However, the accuracy of such a comparison did not exceed 10%, owing to the absence in the literature of tabulated data and to possible errors both in the measurements and in the evaluation of the results from graphs given in the literature.

In the present work, we have made a detailed study of the isotherms and the differential heats of adsorption of methanol and n-butanol vapors on thermal carbon black graphitized at 3000°, and compared them with the corresponding characteristics which we had obtained earlier [13] for the channel black spheron-6, graphitized at 2800°.

We used the highly dispersed thermal black T1 (3000), graphitized at 3000° for 45 minutes in a CO atmosphere [13], which was prepared by P. A. Tesnera*. Its specific surface area was determined by the BET method from the low temperature adsorption of nitrogen [10, 11] and was 29.0 m^2/g. Purified methanol and n-butanol were provided for us by K. D. Shcherbakova*. Their properties were given in reference [13].

As in the studies [4, 5], the differential heat of adsorption was measured in a calorimeter with constant heat exchange (1953 model), and the values of the adsorption of alcohols by means of the vacuum capillary microburet for liquids [14]. All experiments were carried out at 20°.

The adsorption isotherms $\alpha\,(p/p_s)$ and the differential heat of adsorption $Q_a(\alpha)$ of methanol and n-butanol vapors on graphitized thermal black T1(3000) (fig. 1) were completely reversible down to small relative vapor pressures p/p_s. Several series of experiments were carried out for each vapor, the results of which agreed.

The initial portion of the adsorption isotherm of methanol as in [12, 13] was concave, then it passed through two points of inflexion. The differential heat of adsorption of the first portion of the methanol decreased, which is associated with some residual inhomogeneity of the surface; after that, only a very slight fall in the heat of adsorption was observed.

* The authors express their personal thanks.

The adsorption isotherm of n-butanol was initially concave; then it passed through not two points of inflexion as in the case of spheron-6 (2800) [13], but four points, forming clearly expressed waves. In agreement with this, two maxima were observed* on the isotherm of the differential heats of adsorption on the carbon black T1 (3000), during which the rise of the heat of adsorption in the region of predominant monolayer coverage from 0.5 to 4.0 micromole/$/m^2$ reached 1 kcal/mole.

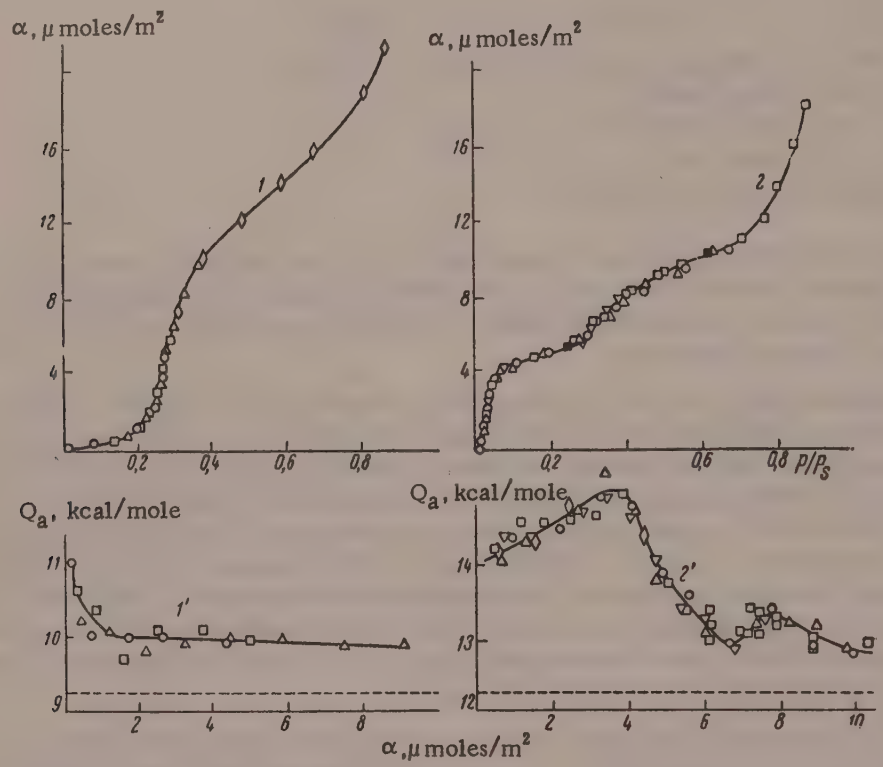


Fig. 1. Adsorption isotherms α (p/p_s) of methanol (1) and n-butanol (2) vapors, and the differential heats of adsorption $Q_a(\alpha)$ of methanol (1') and n-butanol (2') on thermal black T1 graphitized at 3000°. Black points – desorption. Here and further on, the value of the latent heat of condensation L is marked by a horizontal dotted line.

Comparison of Isotherms and Thermodynamic Characteristics of Adsorption of Different Graphitized Carbon Blacks: By comparison of the adsorption isotherms of methanol and n-butanol vapors on graphitized blacks (fig. 2), it was seen that although the difference in the amounts of adsorption by these isotherms did not exceed 5%, definite regularities could be discerned in them. In the case of methanol, the isotherm of adsorption on thermal black T1 (3000) was initially below that on the channel black spheron-6 (2800), then (in the region of a steep rise) the adsorption isotherms intersected and reached a maximum difference in the region of completion of the monolayer ($\sim\alpha = 10$ micromole/m^2); they then converged again and intersected a second time in the region of large p/p_s values approximately at the completion of the two layers. Such a variation in the course of the isotherms may be explained by the structure of the surface of these blacks. Thermal black by its mode of origin was more homogeneous than channel black. In the original thermal blacks, the dimension of the crystallites were several times greater than in the original channel blacks [7]. Also the thermal black, which we studied, was graphitized at a higher temperature and for a longer time. Consequently, the sample T1 (3000) had a more uniform surface than the sample spheron-6 (2800). Thus, on the more homogeneous black, the adsorption is initially less and the wave-like shape of the isotherm appears more distinctly.

* The initial values of the differential heats of adsorption with a 4-5% coverage of the surface were not measured owing to the considerable length of the adsorption experiment at low pressures.

An analogous regularity was also observed in the case of the adsorption of n-butanol, during which the shape of the isotherm within the range of measurements was even more complex. Owing to the small values of the equilibrium pressures at the beginning of the first wave, a difference in the isotherms did not develop; however, further on the adsorption isotherms of n-butanol on black T1(3000) and speron-6 (2800) intersected three times. In addition, the highest point of the adsorption isotherm on thermal black T1(3000) in comparison with channel black spheron-6 (2800) was observed in the region of predominant completion of the first (~5 micromole/m^2) and the second (9-10 micromole/m^2) layers. Thus, with adsorption on graphitized thermal black with a more homogeneous surface, there arises a sharper demarcation of the layers of adsorption, which in the case of adsorption on graphitized channel black is concealed by the greater inhomogeneity.

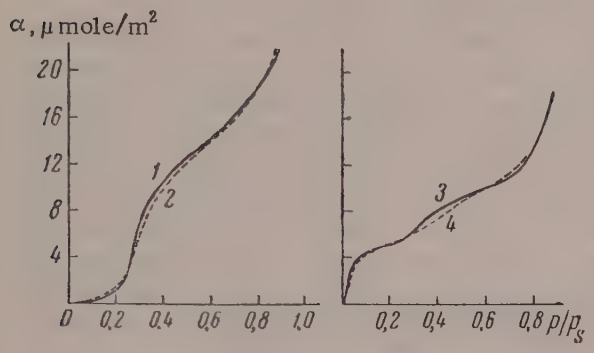


Fig. 2. Adsorption isotherms of methanol (left) and n-butanol (right) vapors. 1, 3) on thermal black T1 (3000); 2, 4) on carbon black, spheron-6 (2800).

The differential entropy of adsorption for the conversion of a substance from the liquid to the adsorbed state was calculated as in previous papers [1,4 – 6,13], with the liquid state taken as standard. By comparison of the differential heats and entropies of adsorption of n-butanol on the graphitized blacks T1(3000) and spheron-6 (2800) (fig. 6) it was seen that for a difference in the course of the isotherms of the heat and entropy of adsorption of n-butanol the same regularities were observed as for the adsorption isotherms themselves (fig. 2).*

Adsorption Isotherm Equations. Isotherms of the adsorption on a homogeneous surface measured in adequate detail are of great interest for the verification of the application of theoretical and semi-empirical equations introduced in order to describe adsorption on homogeneous surfaces. As recorded previously [13] the adsorption isotherm of methanol was not described by the BET equation, since the interaction of the adsorbed molecules of methanol with the graphite was small and in the adsorbed layer there is a strong interaction of the methanol molecules between themselves. Therefore, it was of interest to use for this isotherm approximate equations, which take into account not only the adsorbent-adsorbate interaction but also the adsorbate-adsorbate interaction.

From this the idea of localized and nonlocalized adsorption emerged [15, 16]. In order to describe localized adsorption on a homogeneous surface, an equation was introduced for polymolecular adsorption [17, 15] from which was approximately calculated the adsorbate-adsorbate interaction:

$$p/p_s = \frac{\theta\,(1-p/p_s)^2}{K_1\,[1-\theta\,(1-p/p_s)]\,[1+K_n\theta\,(1-p/p_s)]}, \qquad (1)$$

where $\theta = a/a_m = \alpha/\alpha\omega_m$ is the surface coverage; a is the relative (per 1 g) and α the absolute (per unit surface) values of adsorption; a_m and α_m are the corresponding values of the monolayer capacity; ω_m is the area occupied by a molecule in the completed monolayer; K_1 and K_n are the relative equilibrium constants for the adsorbate-adsorbent and adsorbate-adsorbate interactions.

To describe non-localized adsorption, Hill [18] introduced for polymolecular adsorption the approximate equation

$$p/p_s = \frac{\theta\,(1-p/p_s)^2}{K_1\,[1-\theta(1-p/p_s)]}\,e^{\frac{\theta(1-p/p_s)}{1-\theta(1-p/r_s)}-K_2\theta(1-p/p_s)}, \qquad (2)$$

where $K_2 = a_2/kTb_2$ is the adsorbate-adsorbate interaction constant; a_2 and b_2 the constants of the equation of a two dimensional state of the van der Waals type. Equations (1) and (2) can be represented in a linear form

* We made a comparison of the differential heats of adsorption of methanol vapor on these two blacks in an earlier paper [13]; the heats of adsorption of methanol in both blacks were practically coincident.

$$\frac{z(1-p/p_s)}{p/p_s(1-z)} = K_1 + K_1K_n z \qquad (3)$$

and

$$V(z, p/p_s) = \frac{z}{1-z} + \ln\frac{z}{1-z} - \ln\frac{p/p_s}{1-p/p_s} = \ln K_1 + K_2 z, \qquad (4)$$

where the symbol $z = \theta(1 - p/p_s)$ is introduced for brevity in writing.

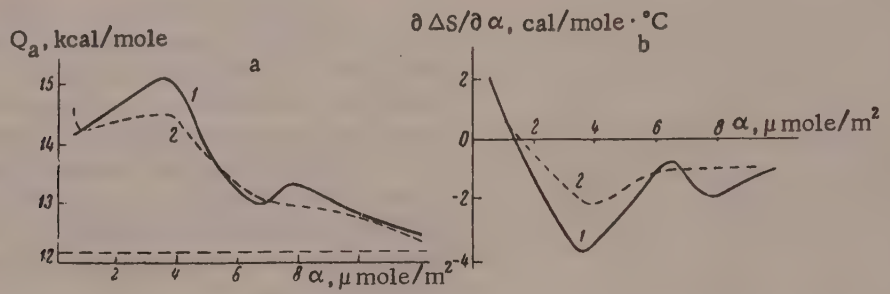


Fig. 3. Dependence of the differential heat of adsorption (a) and differential change of entropy of adsorption (b) on the amount of n-butanol vapor (α) adsorbed on thermal black T1(3000) (1) and on carbon black spheron-6 (2800)(2).

Equation (1) or (3) described very well localized adsorption of nitrogen at -195° [10, 11) and CO_2 at -79° [16] on graphitized thermal black. In reference [9] it was shown that equation (3) described very well the adsorption isotherm of methanol on channel blacks graphitized at 1700°. In reference [13] equation (3) was used to describe the adsorption isotherm of methanol on channel blacks graphitized at 2800°, but in this case the adsorption isotherm was described by this equation to a poorer degree. In this work we have carried out a treatment of the adsorption isotherm of methanol on thermal black by equation (3) for four values of the area occupied by one molecule in the completed monolayer $\omega_m = 1/\alpha_m$, equal to 16; 17; 18 and 20 Å^2, and we are satisfied that the adsorption isotherm of methanol on thermal black T1(3000) is not described by equation (3). This suggested that on the homogeneous basal plane of graphite, the adsorption of methanol is not localized and the successful description of the adsorption isotherm of methanol on channel black heated only at 1700° is connected with the restriction of the movements of the methanol molecules along the surface by the small regions of migration. Therefore, to describe the adsorption isotherm of methanol vapor which we obtained for thermal black T1(3000) with a very homogeneous surface, equation (4) for non-localized polymolecular adsorption in the first layer might be expected to be applicable. The calculation we carried out of the adsorption isotherm of methanol on channel blacks graphitized at 1700° [12] and at 2800° [13], and on thermal black graphitized at 3000°, with the values of $\omega_m = 1/\alpha_m$ equal to 16.0; 16.6; 17.0; 18 and 20 Å^2, showed that in the case of a channel black weakly graphitized at 1700°, this equation gave poor results; however, it described the adsorption isotherm of methanol on channel black, graphitized at 2800° (with ω_m = 16.6 Å^2) and the adsorption isotherm of methanol on thermal black T1 graphitized at 3000° (with ω_m = 17.0 Å^2) very well. Thus, according to the increase in the degree of graphitization of the surface, a transition from localized to non-localized adsorption takes place. In figure 4 is shown a comparison of the adsorption isotherms of methanol on graphitized thermal black T1 (3000) calculated from equation (4) and measured experimentally.

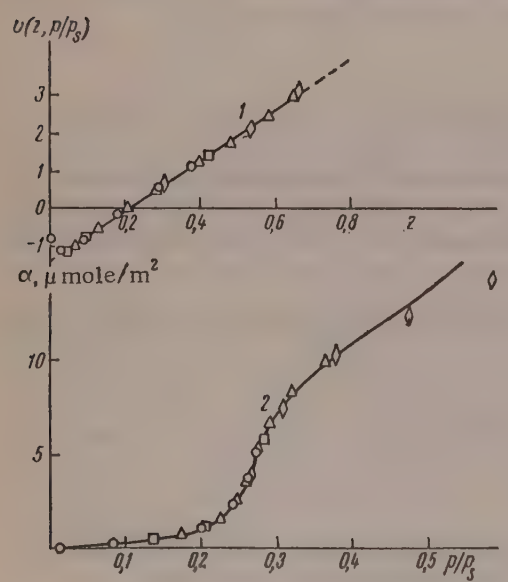


Fig. 4. Adsorption isotherm of methanol vapor on graphitized thermal black T1 (3000): 1) with equation (4) coordinates; 2) points – experimental results; line – calculated from equation (4).

A precise treatment of the adsorption isotherm of n-butanol by the equations mentioned above was difficult owing to the relatively large spread of points on the adsorption isotherm along the relative pressures axis connected with the very small values of the measured equilibrium pressures. However, it must be said that use of values of ω_m from 35 to 40 $Å^2$ in equations (3) and (4) still did not lead to a good description of this isotherm. At the same time equation (3) described the adsorption isotherm of n-butanol somewhat better than equation (4), i.e. in the present case, localization occurs more rapidly than non-localization. However, equation (3) described this isotherm only in the narrow range up to $\theta = 0.9$. Apparently this is connected with the fact that on the homogeneous surface of graphitized thermal black, the predominant adsorption of the first and second layers is demarcated more than on the less homogeneous surface of the black spheron-6 (2800), for which the adsorption isotherm of n-butanol was described by equation (3) up to $\theta = 2$ [13].

Thus, as yet a more general equation has not been obtained for the adsorption isotherm which takes into consideration the interactions in all the layers and their dependence on θ. In order to describe the wave-like adsorption isotherm, it is necessary to use the adsorption isotherm equations (3) and (4) separately for each layer [10, 11]. This example shows that for a description of the adsorption isotherm by some equation or other over a very wide range of θ, it is necessary to undertake its interpretation with caution. Thus it is possible that the better description by equation (3) of the adsorption isotherm of n-butanol on channel black graphitized at 2800° for first and second layer coverages in the region of the second layer coverages is connected with the spread of the sharp boundary between the first and second layer adsorptions caused by some residual inhomogeneity of the surface. From figure 2. it is seen that this spread is decreased on transition to the carbon black T1 (3000) with a more homogeneous surface. The isotherm in this case became wave-like and for a description of the second wave, it was also necessary to take into consideration the adsorbate-adsorbate interactions in the second level.

SUMMARY

1. The adsorption isotherms and the differential heats of adsorption of methanol and n-butanol vapors on thermal black T1 graphitized at 3000° were measured.

2. Transition from graphitized channel black to graphitized thermal black, i.e. increased degree of homogeneity of the surface, led to a small change in the adsorption isotherms, and at the same time, the wave-like form of these isotherms became more distinct.

3. With increase in the degree of surface homogeneity, two maxima appeared on the differential heats of adsorption isotherm, in the region of predominant completion of first and second layer coverage. The corresponding two minima were noted on the differential entropy curve, which indicated the predominantly layer sequence of surface coverage with n-butanol.

4. Adsorption of methanol vapors on transition from less to more highly graphitized blacks became mainly non-localized instead of mainly localized.

The authors thank G. I. Berezin for assistance in measuring the heats of adsorption.

LITERATURE CITED

1. A. V. Kiselev, Vestnik AN SSSR No. 10, 43 (1957).
2. N. N. Avgul', A. A. Isirikyan, A. V. Kiselev, I. A. Lygina and D. P. Poshkus, Izv. AN SSSR, Otd. Khim. n. 1314 (1957); N. N. Avgul', A. V. Kiselev, I. A. Lygina and D. P. Poshkus, same journal 1196 (1959).
3. R. A. Beebe and D. M. Young, J. Phys. Chem. 58, 95 (1954).
4. N. N. Avgul', G. I. Berezin, A. V. Kiselev, and I. A. Lygina, Zh. Fiz. Khimii 30, 2106 (1956).
5. N. N. Avgul', G. I. Berezin, A. V. Kiselev, and A. Ya. Korolev, Kolloidn. Zh. 20, 298 (1958).
6. A. A. Isirikyan and A. V. Kiselev, Kolloidn. Zh. 23, 281 (1961).
7. M. H. Polley, W. D. Shaeffer, and W. R. Smith, J. Phys. Chem. 57, 469 (1953).
8. S. Ross, and W. Winkler, J. Colloid Sci. 10, 330 (1955).
9. A. V. Kiselev, N. V. Kovaleva, V. A. Sinitsyn and E. V. Khrapova, Kolloidn. Zh. 20, 444 (1958).
10. A. V. Kiselev and E. V. Khrapova, Kolloidn. Zh. 23, 163 (1961).
11. A. A. Isirikyan and A. V. Kiselev, J. Phys. Chem. 65, 601 (1961).
12. A. V. Kiselev and N. V. Kovaleva, Izv. AN SSSR Otd. Khim. n. 989 (1959).
13. N. N. Avgul', G. I. Berezin, A. V. Kiselev and I. A. Lygina, Izv. AN SSSR, Otd. Khim n. 205 (1961).
14. N. N. Avgul', G. I. Berezin, A. V. Kiselev, I. A. Lygina and G. G. Muttik, Zh. Fiz. Khimii 31, 1111 (1957).
15. A. V. Kiselev, Kolloidn. Zh. 20, 338 (1958).

16. A. V. Kiselev, Zh. Fiz. Khimii 35, 233 (1961).
17. A. V. Kiselev and D. P. Poshkus, Izv. AN SSSR, Otd. Khim. n. 520 (1958).
18. T. L. Hill, J. Chem. Phys. 14, 441 (1946).

All abbreviations of periodicals in the above bibliography are letter-by-letter transliterations of the abbreviations as given in the original Russian journal. *Some or all of this periodical literature may well be available in English translation.* A complete list of the cover-to-cover English translations appears at the back of this issue.

COAGULATION OF LYOPHOBIC SOLS BY ELECTROLYTE MIXTURES

3. EFFECT OF COUNTER ION ADSORPTION

V. M. Barboi, Yu. M. Glazman and I. M. Dykman

Kiev Technological Institute of Light Industry
Translated from Kolloidnyi Zhurnal, Vol. 23, No. 4,
pp. 376-380, July-August, 1961
Original article submitted March 10, 1960

In our previous work [1, 2] the coagulation of lyophobic sols by electrolyte mixtures was examined from the point of view of Deryagin's theory of the stability of strongly charged lyophobic colloids [3]. It was established that [1] in the case of a mixture of two symmetrical electrolytes of the type 1 - 1 + 2 - 2 there should be synergism in almost all concentration regions. If the former of the components is unsymmetrical (for example, 1_2 - 2), then for such a pair of electrolytes (1_2 - 2 + 2 - 2) differing in the valence of the coagulating ions, an antagonism effect should be observed at least on the initial part of the curve [2]. The nature of this phenomenon differs in different cases. There is apparently the possibility of antagonism between the coagulating ions, which is connected with the competition for adsorption sites on the surface of the lyophobic colloidal particles, and antagonism caused by the electrostatic interaction of the ions in the bulk of the solution and in the electric field of the colloidal particles. We examined only the second of these types of antagonism in [1, 2], where sorption processes which always occur during coagulation were completely ignored.

The present investigation was devoted to the effect of counter ion adsorption on the coagulation of lyophobic sols by electrolyte mixtures. In contrast to previous calculations [1, 2], here it was profitable to examine first the opposite limiting case where, as a result of adsorption of the coagulating ions, the potential of the particles is reduced so much that the expression for the stability of weakly charged sols becomes applicable* [4]

$$\psi_a^2/\varkappa \geqslant a_1 = \text{const}, \tag{1}$$

where $\varkappa$ is the reciprocal thickness of the ionic atmosphere in the solution; ψ_a is taken as the potential at the boundary of the adsorption layer of the colloidal particles**.

The following assumptions are made to simplify the calculation.

1. The concentration of the particles of the colloidal system is assumed to be so low that the additional adsorption of potential-determining ions occurring during the introduction of indifferent (i.e., not containing ions determining the potential) electrolytes into the sol [5] has practically no effect on their concentration in the solution. In connection with this, it may be assumed that upon addition of the coagulating electrolytes, the potential ψ_0 on the surface of the disperse phase in accordance with the Nernst formula for electrode potential does not change***.

2. It is assumed that the adsorption of the coagulating electrolyte ions obeys the simplest Langmuir equation

$$\Gamma_i' = \Gamma_\infty \frac{c_i'/b_i}{1 + \sum_{i=1}^{n} c_i'/b_i}, \tag{2}$$

---

* Even if the adsorption of counter ions occurs, but the reduction in the potential of the particles produced by this is not sufficiently great and the sol remains strongly charged, neither the mechanism of coagulation of the colloidal solution nor the coagulating concentration of the electrolytes is changed.

** Expression (1), which was derived for coagulation by an individual electrolyte, remains accurate for coagulation of a sol by a mixture of electrolytes as the electrolyte concentration appears in this expression only in the form of the value $\varkappa$.

*** Here and later it is assumed that the activity of the electrolytes equals their concentration.

where Γ_i' is the adsorption of the i-th ion from the electrolyte mixture*; c_i' is the concentration of the i-th ion in the solution; b_i and Γ_∞ are the constants of the Langmuir equation. To simplify the subsequent calculations, we consider only the adsorption of counter ions and ignore the adsorption of indifferent ions bearing charges of the same sign as the colloidal particles [6, 7].

3. The potential ψ_a is determined by the value of the potential ψ_0, the concentration of the coagulating electrolytes in the solution, and their adsorbability; it is independent of the relative disposition of the particles.

4. As a first approximation, it is assumed that the potential ψ_a at the boundary of the adsorption layer changes linearly with the amount of adsorption of the coagulating ions of the electrolyte (Γ):

$$\psi_a = \psi_0 - k\Gamma z, \tag{3}$$

where z is the valence of the counter ions and k is constant at a given ionic strength of the solution.

Using Q_a and Q_0 to denote the electrical charge densities in electron units at the boundary of the adsorption layer and the surface of the disperse phases, respectively, after the addition of the coagulating electrolyte to the sol, we can obviously write the relation

$$Q_a = Q_0 - \Gamma z. \tag{4}$$

If it is considered that when $\Gamma z = Q_0$, $\psi_a = 0$, then by using formulas (3) and (4), the following expression is readily obtained:

$$\frac{Q_a}{Q_0} = \frac{\psi_a}{\psi_0}. \tag{5}$$

Hence it follows that relation (3) is equivalent to assuming that the adsorption of counter ions has a negligible effect on the capacity of the electrical double layer as a whole.

Since the capacity of the electrical double layer is inversely proportional to its thickness or, in the first approximation, the radius of the ionic atmosphere ($1/\varkappa$), which in its turn is inversely proportional to the square root of the ionic strength of the solution J [8], we may write

$$\frac{Q_0}{\psi_0} = \frac{Q_a}{\psi_a} = \alpha J^{1/2}, \tag{6}$$

where α is some constant.

For the coagulation of a sol by a mixture of two electrolytes, the potential ψ_a may be determined from formulas (4) and (6)

$$\psi_a = \psi_0 - \frac{\Gamma_1' z_1 + \Gamma_2' z_2}{\varkappa (J')^{1/2}}.$$

By substituting ψ_a from equation (1) in this expression and considering the relation of $\varkappa$ to the ionic strength of the solution, we obtain

$$\alpha\psi_0 (J_c')^{1/2} - \alpha a^{1/2} (J_c')^{3/4} = \Gamma_{1c}' z_1 + \Gamma_{2c}' z_2, \tag{7}$$

where the subscripts c here and later indicate the "critical" values of the corresponding magnitudes.

By substituting the values of Γ_{1c}' and Γ_{2c}' calculated from formula (2) in equation (7) and considering that $J' = \sum_{i=1}^{i=4} c_i' z_i^2$, we find the relation between the coagulating concentration of the two electrolytes in an explicit form:

* Here and later, all the values marked with a dash refer to the case where coagulation is produced by a mixture of electrolytes, while the absence of dashes corresponds to coagulation by individual electrolytes.

$$\alpha\psi_0\left(\sum_{i=1}^{i=4} c'_{1c}z_i^2\right)^{1/2} - \alpha a^{1/2}\left(\sum_{i=1}^{i=4} c'_{ic}z_i^2\right)^{3/4} = \Gamma_\infty \frac{c'_{1c}z_1/b_1 + c'_{2c}z_2/b_2}{1 + c'_{1c}/b_1 + c'_{2c}/b_2}. \tag{8}$$

In order to use equations (7) and (8) practically, it is advantageous to transpose them somewhat. We eliminate the values ψ_0, $\underline{a}$, α and Γ_∞ by expressing them in terms of the coagulating concentrations of the individual electrolytes. For this purpose we write out equation (7) for each of the electrolytes separately

$$\alpha\psi_0 J_{1c}^{1/2} - \alpha a^{1/2} J_{1c}^{3/4} = \Gamma_{1c}z_1,$$

$$\alpha\psi_0 J_{2c}^{1/2} - \alpha a^{1/2} J_{2c}^{3/4} = \Gamma_{2c}z_2$$

and determine the values of $\alpha a^{\frac{1}{2}}$ and $\alpha\psi_0$ from the equations obtained

$$\left.\begin{aligned} \alpha a^{1/2} &= \frac{\Gamma_{1c}z_1 (J_{2c})^{1/2} - \Gamma_{2c}z_2 (J_{1c})^{1/2}}{(J_{2c})^{3/4}(J_{1c})^{1/2} - (J_{2c})^{1/2}(J_{1c})^{3/4}}, \\ \alpha\psi_0 &= \frac{\Gamma_{1c}z_1 (J_{2c})^{3/4} - \Gamma_{2c}z_2 (J_{1c})^{3/4}}{(J_{2c})^{3/4}(J_{1c})^{1/2} - (J_{2c})^{1/2}(J_{1c})^{3/4}}. \end{aligned}\right\} \tag{9}$$

By substituting the expressions (9) in formula (7) we obtain

$$\frac{(J_{1c}/J_{2c})^{3/4} - \Gamma_{1c}z_1/\Gamma_{2c}z_2}{(J_{1c}/J_{2c})^{3/4} - (J_{1c}/J_{2c})^{1/2}}\left(\frac{J'_c}{J_{2c}}\right)^{1/2} - \frac{(J_{1c}/J_{2c})^{1/2} - \Gamma_{1c}z_1/\Gamma_{2c}z_2}{(J_{1c}/J_{2c})^{3/4} - (J_{1c}/J_{2c})^{1/2}}(J'_c/J_{2c})^{3/4} = \frac{\Gamma'_{1c}z_1 + \Gamma'_{2c}z_2}{\Gamma_{2c}z_2}. \tag{10}$$

Even in this form, equation (10) may be used for calculating the curve of the coagulating action of a mixture of two electrolytes if we know the coagulating concentrations of each of the electrolytes separately and the adsorbabilities (i.e., the constants b_i in the Langmuir equation) of the two coagulating ions.

As an illustration, we give the calculation of one of the points on the curve for the coagulation of a sol by a mixture of two 1 - 1-valent electrolytes, differing in their coagulating power by a factor of 16 ($c_1 = 16c_2$). This case corresponds to the experimental data of Freundlich [9] on the coagulation of As_2S_3 sol by ammonium chloride and aniline hydrochloride, respectively. Let us assume arbitrarily that for the electrolyte with the lowest coagulating power, coagulation begins when $^1/_2$ of the adsorption sites on the surface of a particle are filled by counter ions, i.e., $b_1 = c_1 = 16c_2$. Let us assume for the second electrolyte that coagulation begins when $^1/_4$ of all the adsorption centers are filled, i.e., $b_2 = 3c_2$.

By substituting the values of b_i and c_i in equation (9) we obtain

$$1{,}5\left(\frac{c'_1 + c'_2}{c_2}\right)^{1/2} - 0{,}5\left(\frac{c'_1 + c'_2}{c_2}\right)^{3/4} = \frac{c'_1/16c_2 + c'_2/3c_2}{1 + c'_1/16c_2 + c'_2/3c_2}\cdot 4.$$

However, from this equation it is not possible to express c'_2 as an explicit function of c'_1. The solution is obtained in the following way. Let us take some value of $(c'_1 + c'_2)^{1/4}$ in the range $c_1^{1/4}$, $c_2^{1/4}$. For example, let $(c'_1 + c'_2)^{1/4} = 1.2c_2^{1/4}$, then the left-hand part of the equation will equal

$$1{,}5\cdot 1{,}2^2 - 0{,}5\cdot 1{,}2^3 = 1{,}296.$$

By substituting this value in the equation given above, we obtain

$$\frac{c'_1}{16c_2} + \frac{c'_2}{3c_2} = \frac{0{,}324}{0{,}676}.$$

By solving this equation simultaneously with the equation

$$c_1' + c_2' = (1,2)^4 c_2,$$

we find

$$c_1' = 0,79c_2;\ c_2' = 1,28c_2.$$

Our calculations showed that depending on the individual characteristics of the electrolytes*, different types of interaction are possible: additive relations in coagulating action, synergism and antagonism. At the same time, it became obvious that a more detailed analysis of the equation derived was needed. A separate communication will be devoted to the examination of this problem.

SUMMARY

1. The effect of counter ion adsorption on the coagulation of lyophobic sols by the addition of a mixture of two electrolytes has been examined.

2. An equation was derived which makes it possible to calculate the coagulation curves for various electrolyte mixtures. The equation obtained applies to cases where the critical state of the sol is reached at quite low values of the colloidal particle potential as a results of counter ion adsorption.

3. Adsorption interactions between the electrolytes introduced into the sol and the colloidal particles may lead to different types of relation between the minimum coagulation concentrations of the two electrolytes in the mixture: additivity, synergism and antagonism.

The authors are very grateful to Corresponding Member Acad. Sci. USSR B. V. Deryagin for continuous interest in the work and discussion of the results.

LITERATURE CITED

1. Yu. M. Glazman and I. M. Dykman, Dokl. AN SSSR, 100, 299 (1955); Kolloidn. zh. 18, 13 (1956).
2. Yu. M. Glazman, I. M. Dykman and E. A. Strel'tsova, Dokl. AN SSSR, 117, 829 (1957); Kolloidn. zh., 20, 149 (1958).
3. B. V. Deryagin and L. D. Landau, Acta Phys. chim. 14, 633 (1941); Zh. éksperim. i teor. fiz., 11, 802 Izv. (1941); 15, 663 (1945); B. V. Deryagin, Transactions of the Third All-Union Conference on Colloid Chemistry [in Russian] (Izv. AN SSSR, p. 225 (1956)
4. B. V. Deryagin, Kolloidn. zh., 7, 285 (1941); Trans. Faraday. Soc. 36, 730 (1940).
5. Yu. M. Glazman, D. N. Strazhesko, E. F. Zhel'vis and L. L. Chervyatsova, Kolloidn. zh., 21, 263 (1959).
6. Yu. M. Glazman and D. N. Strazhesko, Dokl. AN SSSR, 75, 411 (1950); Yu. M. Glazman, D. N. Strazhesko and B. É. Tartakovksaya, Kolloidn. zh., 15, 161 (1953).
7. Yu. M. Glazman, D. N. Strazhesko and N. A. Bisikalova, Zh. neorg. khimii, 3, 115 (1958).
8. B. Galkenhagen, Electrolytes [Russian translation] ONTI, p. 133 (1935).
9. H. Freundlich, Collection "Coagulation of Colloids" [Russian translation] ONTI, p. 126 (1936)

All abbreviations of periodicals in the above bibliography are letter-by-letter transliterations of the abbreviations as given in the original Russian journal. *Some or all of this periodical literature may well be available in English translation.* A complete list of the cover-to-cover English translations appears at the back of this issue.

---

* It should be emphasized that the nature of the curves of the coagulating action of an electrolyte mixture depends both on the valence of each of the coagulating ions and on the ratio of their adsorbabilities.

COAGULATION OF LYOPHOBIC SOLS BY ELECTROLYTE MIXTURES

4. EFFECT OF COUNTER ION ADSORPTION

V. M. Barboi, Yu. M. Glazman and I. M. Dykman

Kiev Technological Institute of Light Industry
Translated from Kolloidnyi Zhurnal, Vol. 23, No. 4,
pp. 381-388, July-August, 1961
Original article submitted March 10, 1960

As in the previous communication [1], in the present work we examine the effect of counter ion adsorption on the coagulation of lyophobic colloids by electrolyte mixtures.

As our calculations were based on the assumption that there is a reduction in the potential of the colloidal particles as a result of the adsorption of coagulating ions, it is advantageous to investigate first how the potential ψ_a at the boundary of the adsorption layer changes in relation to the electrolyte concentration in solution. This relation was established by combining formulas (4) and (6) in [1]. As a result, we obtained the equation

$$\psi_a = \psi_0 \left(1 - \frac{\Gamma z}{\beta J^{1/2}}\right), \qquad (1)$$

where ψ_0 is the potential at the surface of the disperse phase; Γ is the amount of adsorption of the counter ion of the electrolyte; z is the valence of the counter ion; J is the ionic strength of the solution; β is constant for the given sol. In this formula, all the given values refer not only to the "critical" state, but also to the system containing any amount of electrolyte.

Analysis of equation (1) shows that the curve of the potential ψ_a against the concentration of coagulating electrolyte passes through a minimum (Fig. 1, curve 1), which corresponds to a concentration of the coagulating ion $c = b$ (b is the constant of the Langmuir equation).

It should be emphasized that the very fact that the curve of the potential ψ_a passes through a minimum and can then increase to the value ψ_0 with a further increase in the electrolyte concentration in the solution is of interest in itself. This increase in the potential ψ_a is apparently connected with further adsorption of potential-determining ions, which, in a definite range of electrolyte concentration ($c > b$), predominates over the reduction in potential produced by the adsorption of counter ions.

Consideration of both equation (1) and Deryagin's expression [2] for the stability of weakly charged sols (formula (1) in [1]), which corresponds to the line 2 in Fig. 1*, shows that under certain conditions, stable states of the colloidal system may be realized not only at very high dilutions of the electrolytes ($c < b$), but also in highly concentrated solutions ($c \gg b$), a fact which has sometimes been observed experimentally, but has never been explained, even qualitatively, up to now.

We will now limit ourselves to an examination of only one of the possible cases of sol coagulation, which occurs with a reduction in the potential at the boundary of the adsorption layer to a certain (critical) value, depending on the ionic strength of the solution. This corresponds to coagulating concentrations of the electrolyte $c \leq b$ at which the filling of the surface of the colloidal particles by the coagulating ions is limited by the condition

$$\Gamma \leqslant \frac{1}{2}\Gamma_\infty. \qquad (2)^{**}$$

* It should be remembered that proportionality between ψ_a and $J^{1/4}$ exists only in the region where the surface potential is not too high. With a further increase in it, the stability of the colloidal solution becomes completely independent of the potential.

** Coagulation of the sol at high fillings of the adsorbing surface ($c > b$) evidently is also possible. A separate communication will be devoted to the examination of this case.

It is readily shown that the coagulating concentration of the electrolyte is related to the adsorbability of the counter ion not only by the inequality (2), but also by the equation

$$\frac{\left(1-\frac{\psi_{a1}}{\psi_0}\right)\left(\frac{\psi_{a1}}{\psi_0}\right)^2}{\Gamma_1 z_1} = \frac{\left(1-\frac{\psi_{a2}}{\psi_0}\right)\left(\frac{\psi_{a2}}{\psi_0}\right)^2}{\Gamma_2 z_2} = \frac{a}{\beta\psi_0^2} = \text{const}, \tag{3}$$

which is obtained by combining formula (1) with Deryagin's expression for the stability of weakly charged sols, written in the form $\psi_a^2 = \alpha J^{\frac{1}{2}}$; the subscripts refer to coagulation of the sol by the individual electrolytes 1 and 2, respectively. The numerical value of the constant in equation (3) may be estimated by considering that the numerator of the left-hand part of this equation has a maximum when $\psi_a/\psi_0 = 2/3$. Assuming that among the many electrolytes with monovalent coagulating ions it is possible to find one which satisfied this condition $\psi_a/\psi_0 = 2/3$, we find that in this case the constant equals $4/27\,\Gamma$.

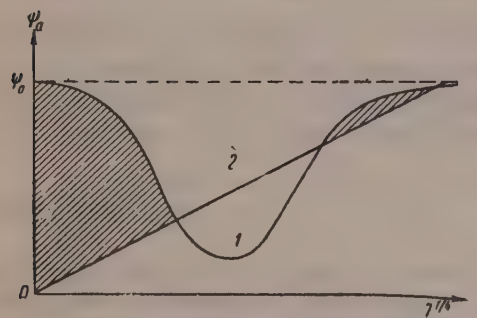


Fig. 1. Change in potential of a colloid particle (ψ_a) in relation to the ionic strength of the solution. The shaded portions correspond to stable states of the colloidal system.

Considering the inequality (2), we obtain

$$\text{const.}\,\Gamma_\infty \geqslant 8/27. \tag{4}$$

The subsequent analysis is carried out with the assumption that $\Gamma_\infty = 8/27 = \gamma$; the rules of the coagulating action of a mixture of two electrolytes remain the same qualitatively when const. $\Gamma_\infty > 8/27$.

To establish the nature of the rules of the coagulating action of an electrolyte mixture, it is possible to limit ourselves to determining the values

$$\Phi = \lim_{c_1'=0} \frac{dc_2'}{dc_1'} \quad \text{and} \quad F = \lim_{c_2'=0} \frac{dc_2'}{dc_1'},$$

where c_1' and c_2' are the concentrations of the first and second electrolyte, respectively, in the mixture at the moment of coagulation.

By differentiating the equation

$$\frac{1}{1-(\psi_{a2}/\psi_0)}\left(\frac{J'}{J_2}\right)^{1/2} - \frac{\psi_{a2}/\psi_0}{1-(\psi_{a2}/\psi_0)}\left(\frac{J'}{J_2}\right)^{3/4} = \frac{\Gamma_1' z_1 + \Gamma_2' z_2}{\Gamma_2 z_2}, \tag{5}$$

which was obtained by transposing equation (10) in [1], we obtain

$$\frac{c_1}{c_2}\Phi = \frac{(2-3K_2)\left(\frac{K_1}{K_2}\right)^2 \gamma z_2 - \frac{\gamma z_1 - K_2^2(1-K_2)}{\gamma z_1 - K_1^2(1-K_1)} 4(1-K_1)[\gamma z_2 - K_2^2(1-K_2)]}{\gamma z_2 (2-K_2) - 4K_2^2(1-K_2)^2}\left(\frac{K_1}{K_2}\right)^2, \tag{6}$$

$$\frac{c_1}{c_2}F = \frac{\gamma z_1 (2-K_1) - 4K_1^2(1-K_1)^2}{(2-3K_1)\left(\frac{K_2}{K_1}\right)^2 \gamma z_1 - \frac{\gamma z_2 - K_1^2(1-K_1)}{\gamma z_2 - K_2^2(1-K_2)} 4(1-K_2)[\gamma z_1 - K_1^2(1-K_1)]}\left(\frac{K_1}{K_2}\right)^2, \tag{7}$$

where $K_1 = \psi_{a1}/\psi_0$ and $K_2 = \psi_{a2}/\psi_0$, and the values marked with a dash refer to the case where coagulation is effected with a mixture of the electrolytes.

By taking various values of the potential drop in the adsorption layer, i.e., the values of ψ_a/ψ_0 for each of the electrolytes separately, it is possible to calculate from equations (6) and (7) the values of the given limits of the

• Here and in subsequent equations all the values refer to the critical state of the system; the subscript c is omitted for brevity.

derivatives Φ and F. Table 1 and Fig. 2 give the conceivable variants of the rules for the coagulating action of electrolyte mixtures in relation to the numerical values of these derivatives*. However, it should be noted that when $\gamma \geq 8/27$, not all of the given cases can be obtained from the equation derived (5). In particular, it is not possible to realize curves 1 and 2 in Fig. 2a and curve 1 in Fig. 2c at any values of K_1, K_2, z_1, and z_2, as is shown by Table 2.

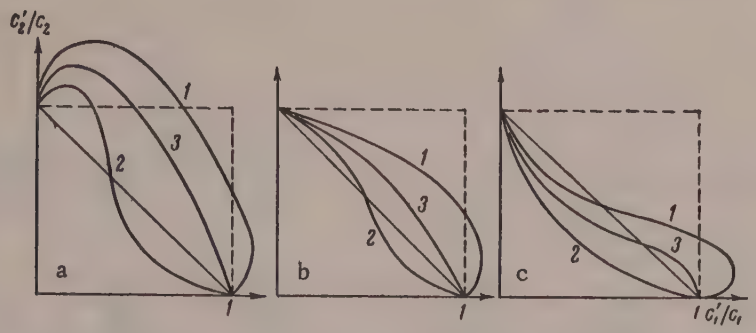


Fig. 2. Types of coagulation curves for different electrolytic mixtures.

TABLE 1. Rules for the Coagulating Action of Electrolytic Mixtures

	$\Phi\frac{c_1}{c_2} > 0$ (Fig. 2a)	$-1 < \Phi\frac{c_1}{c_2} < 0$ (Fig. 2b)	$\Phi\frac{c_1}{c_2} < -1$ (Fig. 2c)
$F\frac{c_1}{c_2} \geqslant 0$ (curve 1)	Antagonism—double	Superadditivity, changing into antagonism	Synergism, changing into antagonism
$-1 < F\frac{c_1}{c_2} \leqslant 0$ (curve 2)	Antagonism, changing into synergism	Superadditivity, changing into synergism	Synergism in all concentration regions
$F\frac{c_1}{c_2} < -1$ (curve 3)	Antagonism, changing into superadditivity	Superadditivity in all concentration regions	Synergism, changing into superadditivity

Some Cases of Coagulation by Different Electrolytic Mixtures.

1. Each of the electrolytes examined contains strongly adsorbed coagulating ions, as a result of which the reduction in potential in the adsorption layer is large. In this case

$$\Phi\frac{c_1}{c_2} \approx \left(\frac{K_1}{K_2}\right)^4 - 2\left(\frac{K_1}{K_2}\right)^2$$

and

$$F\frac{c_1}{c_2} = \frac{1}{(K_2/K_1)^4 - 2(K_2/K_1)^2}.$$

When $(K_1/K_2) > \sqrt{2}$ (i.e., $J_1/J_2 > 4$) $\Phi\frac{c_1}{c_2} > 0$, i.e., there is antagonism (curves 2 and 3, Fig. 3), which is expressed more strongly, the greater the ratio K_1/K_2. When $(K_1/K_2) < \sqrt{2}$ (curve 1, Fig. 3), $-1 < \Phi\frac{c_1}{c_2} < 0$, and consequently there is superadditivity. In both cases $F\frac{c_1}{c_2} < -1$, and therefore the coagulation curve does not intersect the additivity line.

* Here and later the subscript 1 refers to the electrolyte with the lower coagulating power ($c_1 > c_2$).

In the case of strongly adsorbed counter ions, not only the nature of the curves, but also the degree of deviation of the coagulating action of the electrolytes from additivity depends little on the valence of the counter ions. In this connection, we give only the corresponding curves for monovalent coagulating ions in Fig. 3.

TABLE 2. Calculated values of $c_1/c_2\,\Phi$ and $c_1/c_2\,F$

K_1	K_2	$\frac{c_1}{c_2}\Phi$	$\frac{c_1}{c_2}F$	K_1	K_2	$\frac{c_1}{c_2}\Phi$	$\frac{c_1}{c_2}F$
	$z_1 = z_2 = 1$				$z_1 = 1,\ z_2 = 2$		
0,055	0,05	—0,94	—1,04	1	0,80	—0,97	—0,95
0,10	0,05	+8,0	—2,2	1	0,67	0,00	—1,00
0,15	0,05	+80	—4,3	1	0,33	+6,1	—2,6
0,20	0,18	—0,95	—1,03		$z_1 = 1,\ z_2 = 3$		
0,20	0,10	+8,0	—2,2	0,67	0,33	+6,0	—3,3
0,33	0,30	—0,94	—1,05	1	0,80	—0,92	—1,0
0,33	0,11	+80	—4,4	1	0,67	0,00	—1,1
0,60	0,30	+9,0	—2,2	1	0,33	+5,6	—3,0
0,67	0,60	—0,94	—1,05		$z_1 = z_2 = 2$		
0,67	0,50	+0,11	—1,9	0,06	0,05	—0,92	—1,1
0,67	0,33	+10	—4,5	0,10	0,05	+9,4	—2,8
0,74	0,67	—0,92	—1,03	1	0,80	—0,97	—0,95
0,88	0,70	—1,01	—0,98	1	0,67	0,00	—1,0
0,90	0,30	+78	—4,0	1	0,33	+6,1	—2,9
0,99	0,90	—1,06	—0,92		$z_1 = 2,\ z_2 = 3$		
1	0,90	—1,11	—0,91	1	0,80	—0,92	—1,00
1	0,80	—1,19	—0,80	1	0,67	0,00	—1,09
1	0,67	0,00	—0,70	1	0,33	+5,6	—2,98
1	0,50	+7,0	—1,1		$z_1 = 2,\ z_2 = 1$		
1	0,33	+81	—2,5	0,33	1	—0,41	+0,01
	$z_1 = 1,\ z_2 = 2$			0,67	1	—1,4	∞
0,055	0,05	—0,94	—1,05	0,85	0,67	—0,75	—900
0,33	0,30	—1,01	—4,5	0,47	0,67	—0,15	—25
0,44	0,40	—1,03	—5,0		$z_1 = 3,\ z_2 = 1$		
0,67	0,33	+6,7	—3,5	0,05	0,08	—0,83	+4,3
0,80	1	—0,84	+2,7				

2. Neither coagulating ion is adsorbed. Analysis of expressions (6) and (7) shows that

$$\lim_{K_1=1,K_2=1} \Phi\,\frac{c_1}{c_2} = -1$$

and

$$\lim_{K_1=1,K_2=1} F\,\frac{c_1}{c_2} = -1$$

It should be noted that it is only in the complete absence of adsorption of the counter ions ($K_1 = K_2 = 1$) that the coagulation curve for an electrolyte mixture merges with the additivity line over its whole length.

3. One of the coagulating ions is hardly adsorbed. Then

$$\lim_{K_1=1} \Phi\,\frac{c_1}{c_2} = \frac{(2-3K_2)\,(1/K_2)^4\gamma z_2}{\gamma z_2\,(2-K_2) - 4K_2^2\,(1-K_2)^2}.$$

It may be shown that the denominator of this expression is always positive and, consequently, when $K_2 < {}^2/_3$ there is antagonism (Fig. 4, curve 4), whose nature in this case is evidently not connected with mutual suppression of the adsorption of the coagulating ions. The antagonism here probably results from the fact that on addition of electrolytes to a sol, there is additional adsorption of the ions determining the potential of the colloidal particles as well as adsorption of the counter ions [3].

As K_2 increases above the given limit, antagonism gives way to superadditivity (Fig. 4, curve 3). Over a certain range of values of K_2 (Table 2) there is synergism, which actually is not expressed very strongly (Fig. 4, curves 1 and 2).

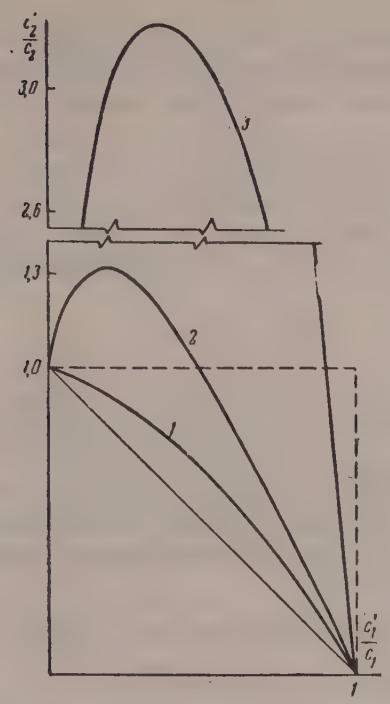


Fig. 3. Theoretical coagulation curves for mixtures of electrolytes containing monovalent, strongly adsorbed counter ions:
1) $K_1 = 0.055$, $K_2 = 0.050$;
2) $K_1 = 0.10$, $K_2 = 0.050$;
3) $K_1 = 0.15$, $K_2 = 0.050$.

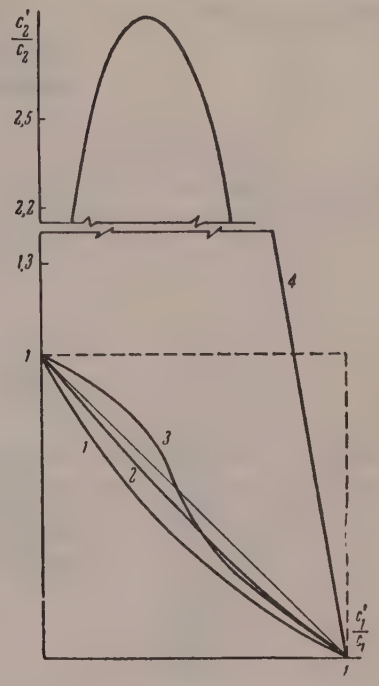


Fig. 4. Theoretical coagulation curves for mixtures of electrolytes containing monovalent counter ions, one of which is not adsorbed:
1) $K_1 = 1$, $K_2 = 0.80$; 2) $K_1 = 1$, $K_2 = 0.90$; 3) $K_1 = 1$, $K_2 = 0.70$; 4) $K_1 = 1$, $K_2 = 0.50$.

It should be emphasized that in the present work we investigated only cases of coagulation where the expression for the stability of weakly charged sols applies. As the calculations presented show, synergism can occur only at values of $K = \psi_a/\psi_0$ close to unity. This means that if coagulation begins with a reduction in the potential ψ_a (in the region where $c < b$), then synergism may be observed only if the potential of the colloidal particles is sufficiently low not only at the moment of coagulation of the sol, but also in its initial state.

The different combinations of electrolytes given indicate that the equation derived reflects experimentally observed types of rules of coagulation by electrolyte mixtures, namely, antagonism, superadditivity and synergism.

Relation of the Rules of Coagulation to the Valence of the Electrolytes.

1. A mixture of two 1 – 1-valent electrolytes with coagulating ions of the same adsorbability.

From equations (3) and (6) it follows that in this case $\Phi \frac{c_1}{c_2} = F \frac{c_1}{c_2} = -1$, i.e., there must be additive relations in coagulation. This, however, is almost self-evident.

2. A mixture of two electrolytes of the type 1 - 1 + 1_2 - 2, where the coagulating ions are monovalent and have the same adsorbability. The subscript $_1$ refers to the symmetrical electrolyte and the subscript $_2$ to the electrolyte 1_2 - 2. In this case, equation (6) may be presented in the form

$$\Phi = -\frac{K_2^2 (1 - K_2)/\gamma - (4 - 3K_2)/6 (1 - K_2)}{K_2^2 (1 - K_2)/\gamma - (2 - K_2)/4 (1 - K_2)} .$$

Hence it follows that if $K_2 < {}^2/_3$, then $\Phi < -1$; when $K_2 > {}^2/_3$, $\Phi > -1$. This means that in contrast to the previous case, additive relations cannot be observed here.

3. A mixture of two electrolytes differing in the valence of the coagulating ions.

a) 1 - 1 + 2 - 2. Let us assume, as an example, that the coagulating concentration of the 1 - 1 -valent electrolyte c_1 is 64 times greater than the concentration of the 2 - 2-valent electrolyte c_2. Consequently

$$\frac{K_1}{K_2} = \left(\frac{J_1}{J_2}\right)^{1/4} = 2.$$

By substituting the values of K_1/K_2 and c_1/c_2 in equation (6) we obtain

$$\Phi_{\frac{c_1}{c_2}} = 16 \times$$

$$\frac{2\gamma(2-3K_2)[\gamma - K_1^2(1-K_1)] - (1-K_1)[\gamma - K_2^2(1-K_2)][2\gamma - K_2^2(1-K_2)]}{[\gamma - K_1^2(1-K_1)][2\gamma(2-K_2) - 4K_2^2(1-K_2)^2]}$$

When $K_1 < {}^2/_3$ and consequently $K_2 < {}^1/_3$, there must be antagonism. When $K_1 > {}^2/_3$ and consequently ${}^1/_2 > K_2 > {}^1/_3$, there must be superadditivity. In both the cases examined, the coagulation curve does not intersect the additivity line (Fig. 5, curves 1 and 2).

b) 1_2 - 2 + 2 - 2. Let us assume that here also $c_1 = 64c_2$. In this case

$$K_1/K_2 = (J_1/J_2)^{1/4} = 2\sqrt{1{,}5}.$$

As above, it is not difficult to draw the conclusion that the relations in the coagulating action are qualitatively the same as for symmetrical electrolytes. However, as Fig. 5 shows (curves 3 and 4), antagonism is expressed much more strongly here (also [4]); in addition, in this case superadditivity changes into antagonism at higher values of K_1.

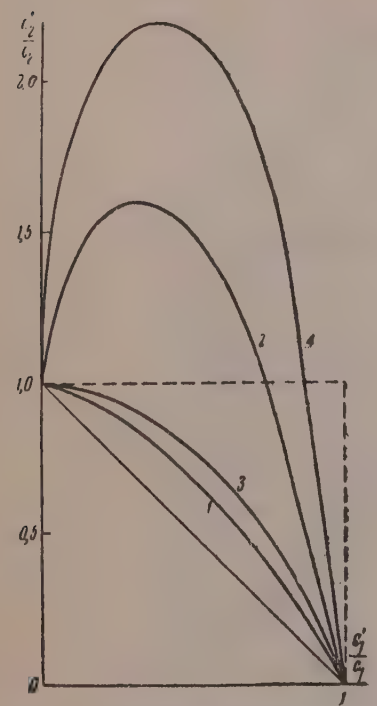


Fig. 5. Theoretical coagulation curves for mixtures of electrolytes containing coagulating ions of different valences:
1) $K_1 = 0.80$; 2) $K_1 = 60$ — electrolyte of the type 1 - 1 + 2 - 2;
3) $K_1 = 0.80$; 4) $K_1 = 0.60$ — electrolyte of the type 1_2 - 2 + 2 - 2.

The case of coagulation by a mixture of two symmetrical electrolytes 1 - 1 + 2 - 2 where their critical concentrations are similar is of particular interest. For example, let the critical concentration of the 1 - 1-valent electrolyte be only slightly greater than the concentration of the 2 - 2-valent electrolyte: $c_1 \approx c_2$. Then $(K_1/K_2) = 0.5\sqrt{2}$. When $K_2 \ll 1$, there is strongly expressed antagonism at low concentrations of the divalent coagulating ion. On the other hand, when $K_2 \approx 1$, there must be the opposite effect, namely, synergism.

SUMMARY

1. A relation has been found between the potential of colloidal particles and the electrolyte concentration of the solution. On the basis of this, it has been shown that stable states of the sol exist both at very low concentrations of the electrolytes in the system (lower than the coagulation threshold normally found) and in relatively concentrated electrolyte solutions.

2. An analysis has been made of the equation relating the minimal coagulating concentrations of the two electrolytes in the mixture. One of the two possible cases of coagulation where the potential of the colloidal particles is decreased on addition of the electrolyte to the sol has been examined.

3. Positive deviations from additivity of the coagulating effects (antagonism or superadditivity) occur when the critical ionic strengths of the solution for each electrolyte separately differ substantially; if these differences are very great, superadditivity always changes into antagonism.

Synergism is observed only when the potential of the colloidal particles is sufficiently low not only in the critical, but also in the initial state of the sol.

4. Antagonism in the coagulation of lyophobic sols may occur even when one of the counter ions added to the colloidal solution of electrolytes is not adsorbed at all. Antagonism in this case evidently is not connected with mutual suppression of the adsorption of the coagulating ions; it is caused by additional adsorption of potential-determining ions.

The authors would like to thank Corresponding Member Acad. Sci. USSR B. V. Deryagin for a critical examination of the manuscript and a series of valuable comments.

LITERATURE CITED

1. V. M. Barboi, Yu. M. Glazman and I. M. Dykman, Kolloidn. zh., 23, 376 (1961).
2. B. V. Deryagin, Kolloidn. zh., 7, 285 (1941); Trans. Faraday. Soc. 36, 730 (1940).
3. Yu. M. Glazman, D. N. Strazhesko, E. F. Zhel'vis and L. L. Chervyatsova, Kolloidn. zh., 21, 263 (1959).
4. Yu. M. Glazman, I. M. Dykman and E. A. Strel'tsova, Dokl. AN SSSR, 117, 829 (1957); Kolloidn. zh., 20, 149 (1958).

All abbreviations of periodicals in the above bibliography are letter-by-letter transliterations of the abbreviations as given in the original Russian journal. *Some or all of this periodical literature may well be available in English translation.* A complete list of the cover-to-cover English translations appears at the back of this issue.

ISOTHERMS AND HEATS OF ADSORPTION OF PROPANE AND PROPYLENE ON GRAPHITIZED CARBON BLACK. THE ENERGY OF THE ADSORPTION FORCES

A. G. Bezus, V. P. Dreving and A. V. Kiselev

Moscow University, Chemistry Dept., Adsorption Laboratory
Translated from Kolloidnyi Zhurnal, Vol. 23, No. 4,
pp. 389-398, July-August, 1961
Original article submitted March 29, 1960

To calculate the energy of adsorptional forces, it is necessary to know both the structure and properties of the adsorbate molecules, and the structural properties and the degree of chemical and geometric homogeneity of the surface of the adsorbent. Therefore, definite theoretical advances have been attainable only through the study of simpler types of systems.

The experimental determination of heats of adsorption is a matter of great importance in this work, since the heat of adsorption can serve as a check on the results of calculations of the energy of the adsorptional forces [1-5]. At the same time, experimental values of heats of adsorption enable one to set up empirical laws which can be of aid in the solution of special problems. Thus, from calorimetric measurements of the heats of adsorption of the vapors of normal butane, pentane, hexane, heptane and octane on graphitized carbon black [6-10] a linear relation was established between the standard heat of adsorption (at surface filling $\theta = 0.5$) and the number of carbon atoms n in the hydrocarbon chain. Similar relations have been set up for the heats of adsorption of a number of normal alkanes on magnesium oxide [3] and on large pore silicagel [11]. An additive method of calculating the standard heats of adsorption of some isoalkanes, naphthenes and aromatic hydrocarbons on graphitized carbon black was used in [12] and [13].

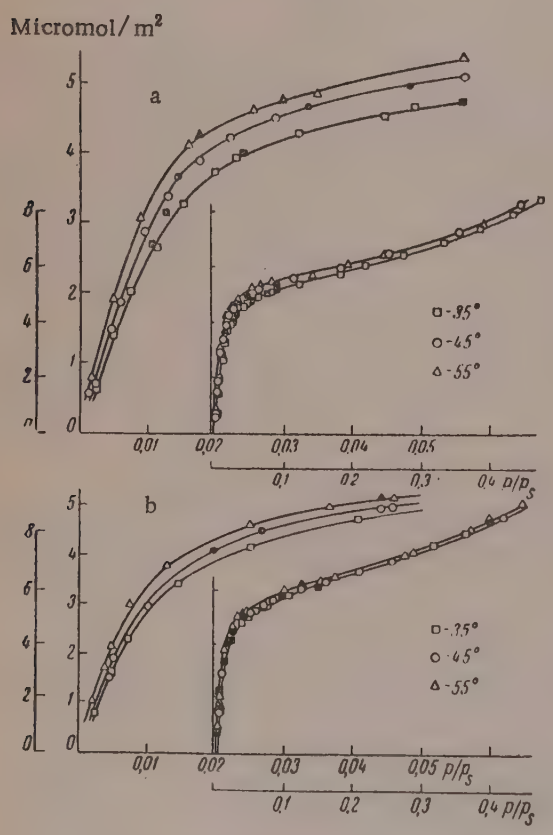


Fig. 1. Absolute adsorption isotherms of propane (a) and propylene (b) on graphitized carbon black at different temperatures. Here, and subsequently, the black points represent desorption.

For comparison with theoretical and semiempirical calculations, the heats of adsorption and adsorption isotherms on homogeneous surfaces, in particular on carbon black, graphitized at ~3000°, are particularly useful. The surface of such a black is formed almost completely by the basal planes of the graphite lattice [14, 15] and is very stable chemically. In the previous papers of this series, calorimetric measurements of the heats of adsorption were made for different hydrocarbons on graphitized blacks [1, 7-9, 13, 16, 17], including n-alkanes beginning with n-pentane [7-9]. The heats of adsorption of n-butane [6, 10] and butene-1 [6] were also measured on graphitized blacks. The lower hydrocarbons present special interest, since it is to be expected that the adsorptional properties of compounds with short hydrocarbon chains will be the ones that most clearly reflect changes in the molecular structure (for example, the appearance of multiple bonds or the presence of some substituent). The present paper gives isotherms and heats of adsorption of propane and propylene on graphitized black.

For the normal hydrocarbon series studied in our calorimetric papers [7-9], the vapor pressure at 25° lies within the limits 760 to 14 mm Hg. This enables us to obtain the whole adsorption isotherm, with the parallel change in the heats of adsorption, working with the usual glass vacuum apparatus in our ordinary calorimeter with constant heat exchange, as calculated from measurements near room temperature [18]. However, in the case of the more volatile lower members of the homologous series, the temperature had to be lowered correspondingly in order to get higher degrees of surface filling. Since we did not have a low temperature calorimeter at our disposal, we established conditions such that the equilibrium pressure could be measured with an accuracy sufficient for the determination of the heat of adsorption from the isosteres.

In measuring the adsorption isotherms of propane and propylene, we used a volume apparatus [19], provided with cryostats for cooling the ampules containing the adsorbent to different temperatures. With this setup, we measured the adsorption isotherms of propane and propylene vapor on graphitized black at -35, -45 and -55° up to a relative vapor pressure $p/p_s = 0.5$. This range of relative pressure was sufficient to calculate the heats of adsorption in the monolayer filling range and the transition to polymolecular adsorption.

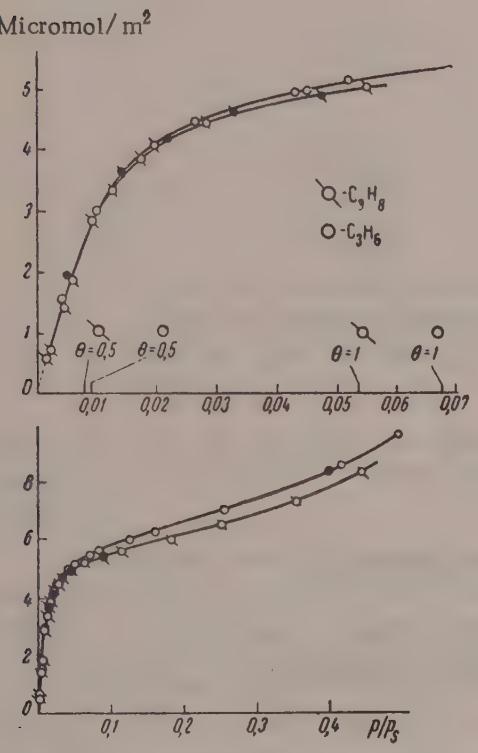


Fig. 2. Absolute adsorption isotherms of propane and propylene on graphitized carbon black at -45°.

As adsorbent, we used Spheron-6 black, graphitized at 2800°, as in [17], with the specific surface 89 m^2/g. Before the work was started, the charcoal layer was degassed in another setup for twenty hours at 250°, and for twenty hours at 350°, down to 10^{-5} mm Hg. The weight loss after degassing was 0.23%. The propane and propylene were the same as in [19].

Adsorption Isotherms. Figure 1 shows the absolute adsorption isotherms of propane and propylene on graphitized black, calculated per unit of surface. The slope of the isotherms in the initial region is greater, the lower the temperature. This indicates a positive value for the pure heats of adsorption. On going over from the predominantly monomolecular to the predominantly polymolecular adsorption, by the time the second layer is formed the interaction of the hydrocarbons with the surface of the adsorbent is considerably weakened.

Comparison of the absolute adsorption isotherms of the two hydrocarbons at one temperature, for example at -45° (Fig. 2) shows that both hydrocarbons are adsorbed on the carbon black in approximately identical quantities.

All the isotherms obtained linearize satisfactorily in the coordinates of the BET equation, within the limits of p/p_s from 0.1 to 0.25–0.35 (Fig. 3). Right at the start of these isotherms (up to $p/p_s = 0.01$) we observe a deviation from linearity in the upward direction which corresponds with lowering the energy of adsorption of the first portions of hydrocarbon adsorbed compared with the following portions. However, in the present paper, we did not set ourselves the problem of investigating the adsorption isotherms in detail in the smallest relative pressure region, since for this purpose, one must use carbon blacks with an even more homogeneous surface, such as graphitized thermal black [9, 20-24].

The Table shows the constant C in the BET equation obtained from the curves of Fig. 3, and the absolute values of the capacity of the monolayer α_m. The values of the areas ω_m occupied by the molecules of propane and propylene in the continuous monolayer on carbon black were found by three methods: 1) from the values of α_m in the formula $\omega_m = 1/\alpha$ (here α_m is expressed as the number of molecules on 1 $Å^2$); 2) from the values of the densities of liquid propane and propylene $d^{-44.5} = 0.5853$ and $d^{-47} = 0.6095$, [25], using the formula $\omega_m = M/dN\tau$, where M is the molecular weight, N is Avogadro's number, the thickness of the molecules, τ being taken equal to 4.0 Å [26] and 3.8 Å [12] respectively; 3) from the value of the van der Waals dimensions of the molecules. Figure 4 shows the projections of the molecules of propane and propylene on the surface of the adsorbent. The outlines of these projections were constructed starting with structural models of the molecules having interatomic distances:

C–C 1.54; C = C 1.34; C–H with a double bond 1.07 Å [27]. From the centers of the carbon atoms with a double bond and from the centers of the hydrogen atoms bound to them, circles were drawn with radii equal respectively to 1.8 and 1.2 Å [26]. These values represent the van der Waals radii of the carbon and hydrogen atoms. Since the methyl group can rotate, circles of radius 2.0 Å [26] were drawn from the centers of the carbon atoms in the methyl groups. The area of the projection for propylene is equal to 27 $Å^2$. The propylene molecule is plane, like the benzene molecule. This makes it improbable that it will rotate around a longitudinal axis on the surface of the adsorbent, at least at sufficiently low temperatures. The form of the outline of the propylene molecule is rather complicated; therefore, even at the closest packing on the adsorbent surface, each of the molecules occupies not 27 but about 30 $Å^2$. The projectional area for propane is only equal to 26 $Å^2$. But it must be kept in mind that without substantial change in the energy of interaction with the surface, the adsorbed propane molecule can rotate around its longitudinal axis; therefore, the surface area occupied by one propane molecule in calculating the packing factor can be approximately represented by the rectangle drawn around the outline shown in Fig. 4. This rectangle is shown dotted in the figure, and its area is equal to 32 $Å^2$. The values of the areas ω_m found by these three methods are in good agreement with one another.

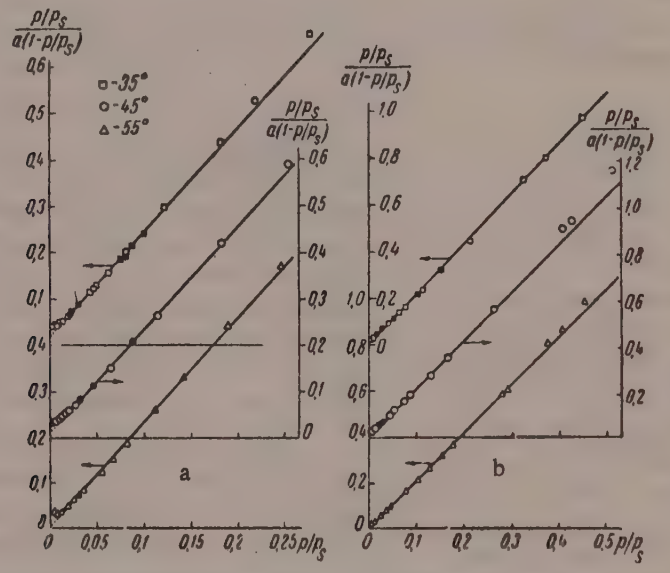


Fig. 3. Adsorption isotherms on graphitized carbon black in the coordinates of the BET equation: propane (a) and propylene (b) at various temperatures.

Thus, the value of ω_m for propane, at all three temperatures, found by the first method is 33 by the second 31, and by the third 32 $Å^2$. For propylene the values are 31, 29 and 30 $Å^2$.

Value of the Constants in the BET Equation – Equilibrium Constant C and Monolayer Capacity α_m *

Constants	Temperature, C°					
	–35	–45	–55	–35	–45	–55
	Propane			Propylene		
Micromol/m^2	140 5,0	185 5,0	320 5,0	140 5,4	170 5,4	235 5,4

* The specific surface of the carbon black was measured from nitrogen adsorption at -195.8° and $\omega_m N_2$ = 16.2 $Å^2$.

Knowing the values of the areas ω_m (33 Å^2 for propane and 31 Å^2 for propylene) we will find from the isotherms of Fig. 3 that the fraction of the surface θ occupied by each of these adsorbates at the same relative pressures are practically identical. For example, at $p/p_s = 0.028$ and -45°, $\theta = 0.83$ for propane and $\theta = 0.84$ for propylene.

Heats of Adsorption. The differential heats of adsorption of propane and propylene were calculated from the isosteres of Fig. 5, constructed from three isotherms (-35, -45 and -55°). The differential heats of adsorption as a function of the surface filling θ are given in Fig. 6.

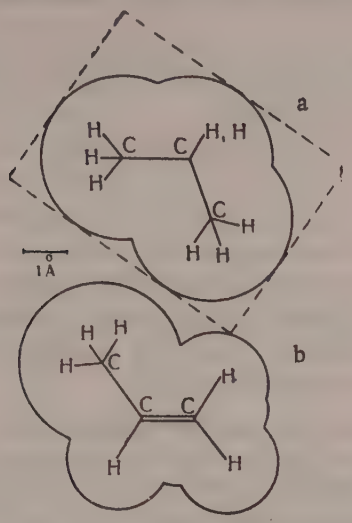


Fig. 4. Van der Waals' projections of the molecules of propane (a) and propylene (b) on the carbon black surface.

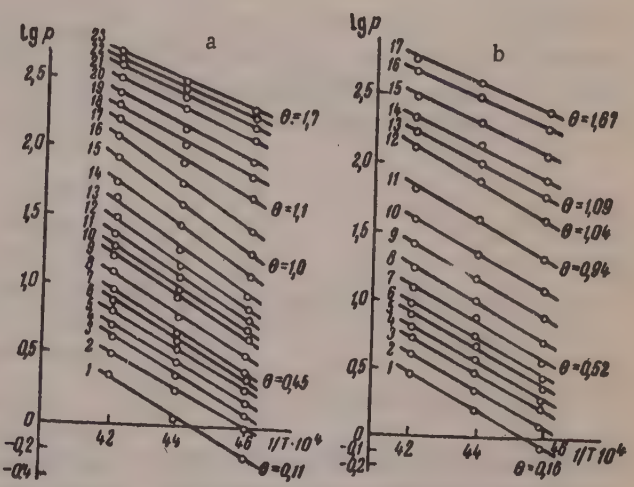


Fig. 5. Adsorption isosteres on graphitized carbon black. Propane (a) and propylene (b). Some isosteres show the values of surface filling.

The vertical lines show the values of possible error in determining the heats of adsorption, evaluated as in [28]. Both curves drop off sharply near $\theta = 1$. When θ approaches 1.5, the heat of adsorption is already near the heat of condensation.

In the predominantly monomolecular filling region directly behing the initial dropoff, due to the residual nonhomogeneity of the surface of the 2800° Spheron-6 black, the curve of the differential heats of adsorption of propane begins to rise, and near $\theta = 1$, it goes through a maximum. This increase in the heat of adsorption is caused by an increase in interaction of the molecules of the adsorbate as they get closer together in filling up the monolayer [2, 7, 8, 9, 13]. In contrast, the differential heat of adsorption of propylene on graphitized black remains approximately constant up to $\theta \approx 1$. This difference is similar to the corresponding difference in the curves for the differential heats of adsorption of n-hexane and benzene on graphitized black [16, 17], and arises, probably, from analogous causes. The weakening of the attraction between propylene molecules as compared with propane molecules can be caused by the large dimensions of the propane molecules in a direction perpendicular to the surface of the adsorbent as the electrokinetic (dispersional) attraction is balanced by the electrostatic repulsion from the interaction of the quadrupoles formed by the π-electrons of propylene and the CH dipoles lying in the plane of the molecule at the double bond.

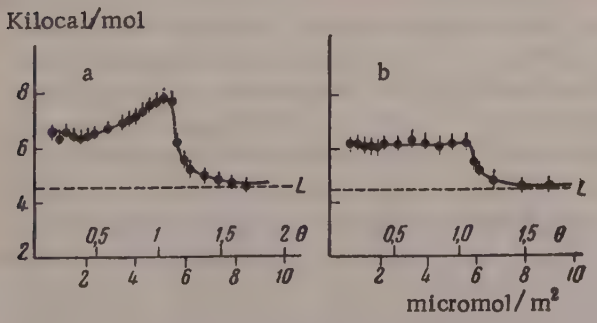


Fig. 6. Differential heat of adsorption Q_a as a function of the adsorption value α and the surface filling θ of graphitized carbon black for propane (a) and for propylene (b).

The standard (at $\theta = 0.5$) heats of adsorption Q_a^0 of propane and propylene on graphitized charcoal are almost identical (6.5 and 6.2 kcal/mole). The excess in the heat of adsorption of propane over the heat of adsorption of propylene (~0.3 kcal/mole) is very small. It is very much less than the corresponding excess of the heat of adsorption of

n-hexane over the heat of adsorption of benzene (~ 2 kcal/mole) [7, 16]. Since at $\theta = 0.5$, the interaction between the adsorbent and the adsorbate is still not large, even in the case of propane, the difference in the heat of adsorption can be explained only by a difference in the interaction between the adsorbate and the adsorbent, due to the somewhat lower polarizability of propylene as compared with propane.

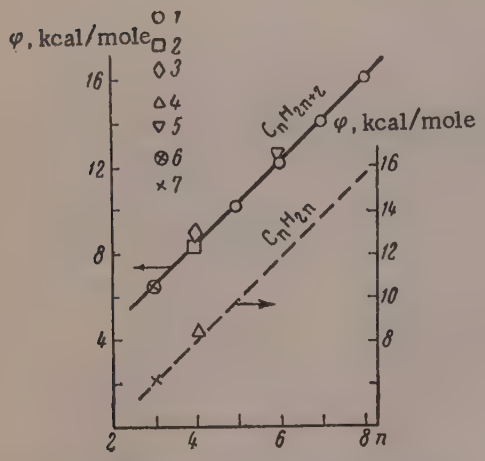


Fig. 7. Standard heats of adsorption Q^0_α of n-alkanes and olefins on graphitized carbon black as a function of the number of carbon atoms in the molecules. Straight lines – theoretically calculated adsorption energies at $\theta = 0.5$ as a function of the number of carbon atoms in the hydrocarbon molecule: 1) [8]; 2) [6]; 3 [10]; 4) [6]; 5) [9]; 6 and 7) data obtained in the present paper.

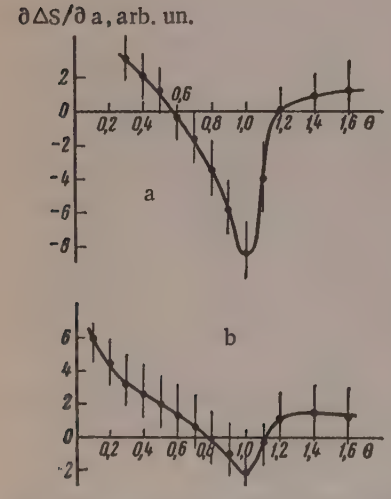


Fig. 8. Differential entropy of the adsorption of propane (a) and propylene (b) as a function of the surface filling θ of graphitized carbon black.

Figure 7 shows the standard heats of adsorption of n-alkanes on graphitized black as a function of the number of carbon atoms in the molecule [6-10], including the value for propane found in the present paper. The experimental values of Q^0_a give a good fit to the straight line corresponding with the equation

$$Q^0_a = 0{,}7 + 1{,}9n, \qquad (1)$$

where n is the number of carbon atoms in the n-alkane chain [8]. Thus, the standard heat of adsorption of propane found from the isosteres in this paper gives a good fit to the straight line found previously [8], extrapolated to n = 3. The linear variation with n of the Q^0_a values of normal hydrocarbons on graphitized black is maintained even when three carbon atoms are present in the chain.

The standard heat of adsorption of propylene found in this paper, 6.2 kcal/mole may be compared with the heat of adsorption of butylene measured calorimetrically in [6] and equal, at $\theta = 0.5$, to 8.4 kcal/mole. The difference between these values is ~ 2.2 kcal/mole. It is near the difference between the adsorption energies of neighboring members in the normal alkane series (~2 kcal/mole). This enables us to make an approximated calculation of the standard heats of adsorption for other similar olefins from the simple additive formula

$$Q^0_a = 0{,}2 + 2{,}0n. \qquad (2)$$

Adsorption Entropy. Figure 8 gives the entropy curves for adsorbed propane and propylene found at -45° from the adsorption isotherms of Fig. 1, b and Fig. 2, and the heat of adsorption curves of Fig. 6, evaluating the error as in [28]. The curves show the variation in the differential values of the differences between the entropies of the adsorbed substance and the entropies of the corresponding liquid, ΔS, as the surface is filled. At the start of formation of the monolayer on the carbon black, ΔS is positive, i.e., the molecules of propane and propylene and less tightly bound than in the liquid phase. As the monolayer is filled up, the differential values of ΔS for both adsorbates drop off, and in the vicinity of $\theta = 1$, they go through a minimum which corresponds with stronger binding of the molecules. The mean molar values of ΔS show that at $\theta = 1$, the propane molecules are considerably more strongly bound than the propylene molecules, which as was shown above, can experience mutual electrostatic repulsion when they are close together. When the second layer is being filled, the mobility of the molecules is again increased, but apparently it only slightly exceeds the mobility in the liquid state. This picture is completely analogous to the one obtained previously from comparing the entropy curves of the normal and aromatic hydrocarbons, n-hexane and benzene [7, 16].

The whole entropy curve of propylene lies above the corresponding curve for propane. At $\theta = 0.5$, the standard values of ΔS^0 for

propane and propylene are respectively equal to 1.2 and 2.1 entropy units, i.e., the propylene molecules are partially in a less bound state than the molecules of propane, due to the repulsive forces mentioned.

Free Energy of Adsorption. The standard values of the free energy of adsorption on graphitized carbon black (the differences between the chemical potentials in the adsorbed state at $\theta = 0.5$ and in the liquid state [7]) are 2.17 kcal/mole for propane and -2.16 kcal/mole for propylene, i.e, the free energy on going from the liquid state to the adsorbed state in both cases at standard filling, drops off almost identically. This corresponds to the above mentioned closeness in the values of θ for both hydrocarbons at the same values of p/p_s.

Theoretical Calculation of the Energy of the Adsorptional Forces. The interaction energy Φ_i of the individual links of the hydrocarbon molecules with the graphite lattice has been calculated by us, using the method described in preceding papers [2, 3]. The adsorption energy of a complex molecule consisting of several strong centers, for example, the links of a hydrocarbon chain, is expressed by an additive function of the adsorption energy of the individual centers [1-3, 7]

$$\Phi = \sum_i \Phi_i. \tag{3}$$

Therefore, the adsorption energy of n-alkanes was claculated as an additive function of the adsorption energy of the CH_3 and CH_2 groups [2, 3, 7]

$$\Phi = 2\Phi_{CH_3} + (n-2)\,\Phi_{CH_2} = 2\,(\Phi_{CH_3} - \Phi_{CH_2}) + n\Phi_{CH_2} = a + bn. \tag{4}$$

This function is a linear function of the number of carbon atoms, n in the n-alkane molecule. The individual links of the normal alkanes may fall into different positions relative to the basal plane of graphite. Therefore, in order to compare the calculated adsorption energy with the heat of adsorption found calorimetrically, we must use a mean value $-\overline{\Phi}'$ [2].

$$-\overline{\Phi}_0' = 0{,}85 + 1{,}88n. \tag{5}$$

With this value of $-\overline{\Phi}_0'$, we must compare the initial heats of adsorption at $\theta = 0$, which is not always convenient, since, because of the residual nonhomogeneity of the surface of the graphitized carbon black, on which the heat of adsorption measurements are being carried out, we cannot accurately determine the correct heat of adsorption curve for a homogeneous surface in the initial region. Extrapolation of this curve to $\theta = 0$ in the case of propane (Fig. 6, a) does not give completely valid results. Therefore for comparison, it is convenient to go to the standard values $-\overline{\Phi}^0$ at $\theta = 0.5$. To transform $\overline{\Phi}_0$ to $\overline{\Phi}^0$, we must take account of the interaction energy between the adsorbate molecules in the adsorbed layer [2, 3]. An approximate calculation made for normal alkanes and α-mono olefins at a degree of filling $\theta = 0.5$ gave the following linear relationships for Φ^0 as a function of the number of carbon atoms, n in the chain.

$$-\Phi^0 = 1{,}0 + 1{,}9n \quad \text{(for n-alkanes)} \tag{6}$$

$$-\Phi^0 = 0{,}35 + 1{,}88n \quad (\text{for } \alpha\text{-mono olefins}^*) \tag{7}$$

In these calculations, the distance between the centers of the hydrocarbon links and the centers of the carbon atoms in graphite was taken equal to 3.7 Å for all links in a saturated chain and 3.6 Å for links near double bonds [12].

In Figure 7, the solid straight line for alkanes and the dotted line for olefins are given on the basis of values of $-\Phi^0$ calculated theoretically from Eqs. (6) and (7). The heats of adsorption measured calorimetrically are marked in the same diagram by points, and those calculated from the isosteres in this paper are marked with x's. Figure 7 clearly shows the good agreement between the theoretically calculated values of the adsorption energy and the values of the heats of adsorption found experimentally for all the n-alkanes from C_3 to C_8 and for the two α-mono olefins C_3 and C_4.

* In [12] an approximate calculation gave a somewhat different expression $-\Phi = 0.1 + 1.85\,n$. In the present paper, Eq. (7) was derived taking account of the higher terms in the electrostatic attration energy as in [2, 3].

SUMMARY

1. The adsorption isotherms of propane and propylene have been measured at -35, -45 and -55° on Spheron-6 black, graphitized at 2800°.

2. With the exception of the initial part, which exhibits interaction between adsorbate and adsorbate, all the isotherms are well described by the BET equation. A BET calculation of the areas occupied by the molecules of these hydrocarbons on the surface of the graphitized black in a continuous layer gives values near those calculated from the density of the liquid, and from the van der Waals dimensions of the molecules, allowing for the packing probability.

3. The isoteres were used to find the differential heats of adsorption of propane and propylene as a function of the degree of filling, θ, of the graphitized carbon black surface. Near $\theta = 1$, these curves drop off sharply to values which are close to the heats of condensation. In the case of propane, the heat of adsorption in the vicinity of $\theta = 1$ goes through a well defined maximum due to the appearance of adsorbate-adsorbate attraction when the monolayer is filled up.

4. Standard values of heat, entropy and free energy of adsorption have been found. The standard heat of adsorption of propane agrees well with the previously found linear dependence on the number of carbon atoms n in the n-alkane molecules. A similar dependence has been noted for α-monoolefins as well.

5. The curve of the heats of adsorption of n-alkanes and α-monoolefins as a function of n are very close to the theoretically calculated curves of the energy of the adsorptional forces as a function of n.

LITERATURE CITED

1. A. V. Kiselev, Vestn. AN SSSR No. 10, 43 (1957).
2. N. N. Avgul', A. A. Isirikyan, A. V. Kiselev, I. A. Lygina and D. P. Poshkus, Izv. AN SSSR, Otd. Khim. n., 1314 (1957); N. N. Avgul', A. V. Kiselev, I. A. Lygina and D. P. Poshkus, ibid. 1196 (1959).
3. A. V. Kiselev, D. P. Poshkus, Zh. fiz. khimii, 32, 2824 (1958).
4. E. L. Pace, J. Chem. Phys. 27, 1341 (1957).
5. E. L. Pace and A. R. Siebert, J. Phys. Chem. 63, 1398 (1959).
6. R. A. Beebe, M. Polley, W. R. Smith and C. B. Wendel, J. Amer. Chem. Soc. 69, 2294 (1947).
7. N. N. Avgul', G. I. Berezin, A. V. Kiselev and I. A. Lygina, Zh. fiz. khimii 30, 2106 (1956).
8. N. N. Avgul', G. I. Berezin, A. V. Kiselev and I. A. Lygina, Izv. AN SSSR, Otd. khim. n. 1021 (1957).
9. A. A. Isirikyan and A. V. Kiselev, Kolloidn. Zh., 23, 67 (1961).
10. J. W. Ross and R. J. Good, J. Phys. Chem. 60, 1167 (1956).
11. A. A. Isirikyan, A. V. Kiselev and B. A. Frolov, Zh. fiz. khimii. 33, 389 (1959)
12. N. N. Avgul' and A. V. Kiselev, Dokl. AN SSSR 112, 673 (1957).
13. N. N. Avgul', G. I. Berezin, A. V. Kiselev and I. A. Lyginia, Izv. AN SSSR, Otd. khim. n. 787 (1958).
14. R. A. Beebe and D. M. Young, J. Phys. Chem. 58, 93 (1954).
15. W. D. Schaffer, W. R. Smith and M. H. Polley, Industr. and Engng. Chem. 45, 1721 (1953).
16. N. N. Avgul', G. I. Berezin, A. V. Kiselev and I. A. Lygina, Izv. AN SSSR, Otd. khim. n. 1304 (1956).
17. N. N. Avgul', G. I. Berezin, A. V. Kiselev and I. Ya. Korolev, Kolloidn. Zh. 20, 298 (1958).
18. N. N. Avgul', G. I. Berezin, A. V. Kiselev, I. A. Lygina and G. G. Muttik, Zh. fiz. khimii 31, 1111 (1957).
19. A. G. Bezus, V. P. Dreving and A. L. Klyachko-Gurvich, Kolloidn. Zh. 23, 241 (1961).
20. A. V. Kiselev, N. V. Kovaleva, V. A. Sinitsyn and E. V. Khrepova, Kolloidn. Zh. 20, 444 (1958).
21. A. V. Kiselev and E. V. Khrapova, Kolloidn. Zh. 23, 163 (1961).
22. S. Ross and W. Pultz, J. Colloid. Sci. 13, 397 (1958).
23. S. Ross, W. Winkler, Ibid. 10, 319, 330 (1955).
24. W. B. Spenser, C. H. Amberg and B. A. Beebe, J. Phys. Chem. 62, 719 (1958).
25. C. P. Hodgman, "Handbook of Chemistry and Physics", Chemical Rubber Publishing Co., 33 ed., Cleveland, Ohio (1951-1952).
26. M. Pauling, Nature of the Chemical Bond [in Russian] Goskhimizdat, Moscow and Leningrad (1947).
27. M. V. Vol'kenshtein, Structure and Physical Properties of Molecules [in Russian] Izd. AN SSSR (1955).
28. A. V. Kiselev and D. P. Poshkus, Kolloidn., Zh. 22, 25 (1960).

COMPARATIVE STUDY OF MECHANICAL AND CHEMICAL METHODS OF VARYING THE DISPERSITY OF PEAT*

M. P. Volarovich, I. I. Lishtvan and N. V. Churaev

Kalinin Peat Institute

Translated from Kolloidnyi Zhurnal, Vol. 23, No. 4,
pp. 399-403, July-August, 1961
Original article submitted December 19, 1960

With the existing technology of peat production, the structure of raw peat is varied by dispersion and forming in various processing machines. This treatment of peat leads to the disruption (dispersion) of its coarse particles and more uniform distribution of them through the volume of the peat system as a result of mixing [1, 2]. The mechanical treatment leading to the disruption of the plant residues and an increase in the plasticity of peat as a result of liberation of the intracellular water does not substantially affect its colloidal fraction. The alteration of the properties of the latter requires chemical treatment [3], which essentially changes its hydrophilicity and dispersity and also produces a corresponding change in the physicochemical properties of the peat. In this connection it seemed interesting to study not only mechanical, but also chemical methods of varying the dispersity of peat (peptization and coagulation).

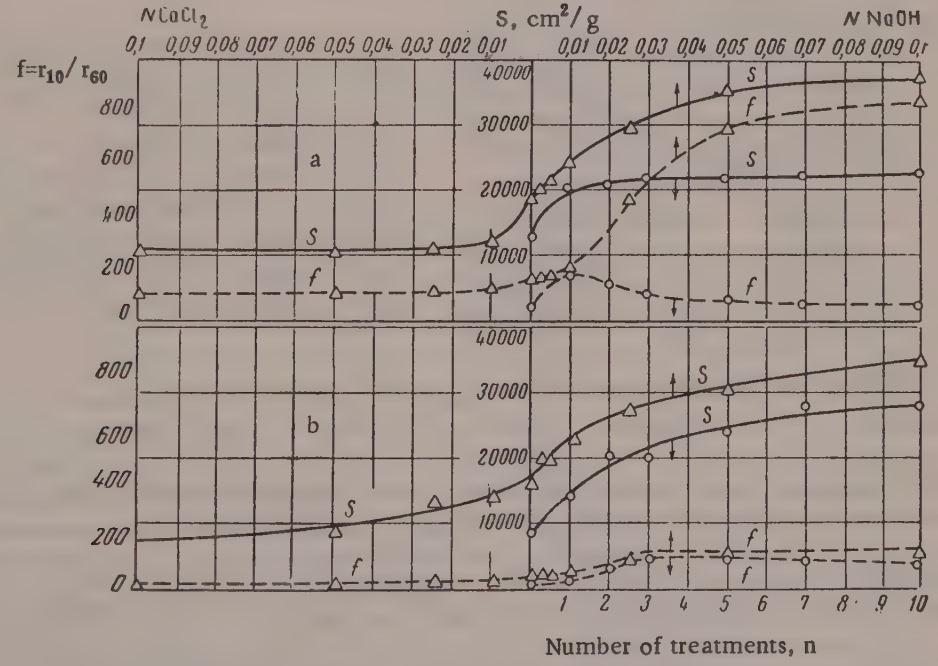


Fig. 1. Relation of specific surface s and heterogeneity factor f to the number of treatments n and the concentration of added electrolytes N for high (a) and low (b) peats.

* In the article of M. P. Volarovich, N. I. Gamayunov and N. V. Churaev, "Investigation of the Moisture Conductivity of Peat," which was published in the Kolloidnyi Zhurnal, Vol. 22, No. 5, 1960, on p. 536, the legend of Table 1 should read: u – moisture content; γ – density; Φ – moisture transfer potential; t – temperature; q – heat output from unit surface of the probe...etc. in accordance with the text.

The effect of mechanical and chemical treatment methods was studied on two peat samples: high medium peat (degree of decomposition 25%) and low sedge peat (degree of decomposition 35%). The peat was dispersed mechanically in a meat grinder. The preliminarily treated peat was coagulated and peptized by the addition of $CaCl_2$ and NaOH solutions, whose concentrations in the dispersion medium were varied from 0.0025 to 0.1 N. The dispersion analysis of the samples and processing of the experimental data were carried out by the procedure developed previously [4, 5] with allowance for the above content of electrolytes in the dispersion medium.

Change in Dispersity Parameters as a Result of Mechanical Treatment and the Action of Electrolytes

Peat samples	Content of highly disperse peat fraction, %		Weighted-average diameter of particles of coarse peat fraction d_1, μ.		Amount of dispersed particles (relative to original), %	
	low	high	low	high	low	high
Mechanical treatment						
Original	12,60	11,36	663,0	411,0	—	—
Treated once in a meat grinder	21,90	22,10	260,0	234,0	+32,8*	+28,0
The same 2 times	27,00	24,10	166,0	173,0	+40,0	+32,3
The same 3 times	27,59	24,40	153,0	160,0	+47,2	+33,4
The same 5 times	32,38	25,20	85,0	89,6	+58,4	+33,4
The same 7 times	38,64	25,70	83,6	77,0	+58,8	+34,0
The same 10 times	39,28	26,42	79,3	67,0	+60,2	+34,0
Chemical treatment						
$CaCl_2$ Concentration in peat dispersion medium						
0.1N	8,25	6,02	102,0	194,1	−23,2	−22,6
0.05N	8,71	6,74	90,5	176,9	−22,4	−23,6
0.25N	12,24	7,72	86,0	166,0	−19,2	−23,6
0.01N	14,22	12,64	76,4	166,0	−17,4	−21,1
Original	17,85	22.27	76,4	191,0	0	0
NaOH Concentration in peat dispersion medium						
0.0025N	21,72	25,66	79,5	194,0	+12,8	+9,4
0.005N	23,54	28,19	82,0	194,0	+15,6	+9,6
0.01N	29,35	33,92	82,0	195 0	+19,9	+15,4
0.025N	37,90	44,84	89,8	210,0	+27,4	+25,4
0.05N	46,58	57,16	91,0	277,0	+30,1	+34.9
0.1N	56,15	63,28	103,0	333,0	+38,3	+43,9

* The sign (+) indicates an increase in the degree of dispersity, while (-) indicates a decrease.

The experimental results are given in the Table and in Fig. 1. Mechanical dispersion led to an increase in the content of the fraction less than 1 μ in size (k) and the specific surface (s), while the weighted-average diameter of the particles of the coarse fraction (d_1) decreased. Chemical treatment also led to a substantial change in the dispersion characteristics. The addition of $CaCl_2$ solutions reduced the degree of dispersion, while NaOH solution increased it. The peptizing effect on treated peat with an NaOH concentration of 0.0025 N in the dispersion medium was equivalent (as regards the increase in the specific surface and the content of the highly disperse fraction) to a further five mechanical treatments of this peat in a meat grinder. With a further increase in the NaOH concentration in the solvent, there was a sharp increase in the content of the fraction less than 1 μ in size while the specific surface increased to more than twice the original value.

The increase in the specific surface of high (a) and low (b) peats (Fig. 2, I) occurred as a result of the chemical reaction of their highly disperse fractions with NaOH solutions. Thus, even with an NaOH concentration of 0.025 N, the content of this fraction was 37.9% of the total mass of particles for low peat and 44.8% for high peat, i.e., increases of 55 and 51%, respectively, in comparison with the content in the original peats. This increase is equivalent to a single treatment of the peat, which is known to be the most effective.

As the graphs of the spread by dispersion presented in Fig. 2, II show, mechanical treatment produces much less increase in the content of the fraction < 1 μ and consequently, in the specific surface. A characteristic of this type of treatment is the appearance of a considerable amount of fractions > 1 and even 10 μ, which does not occur during chemical treatment, for example.

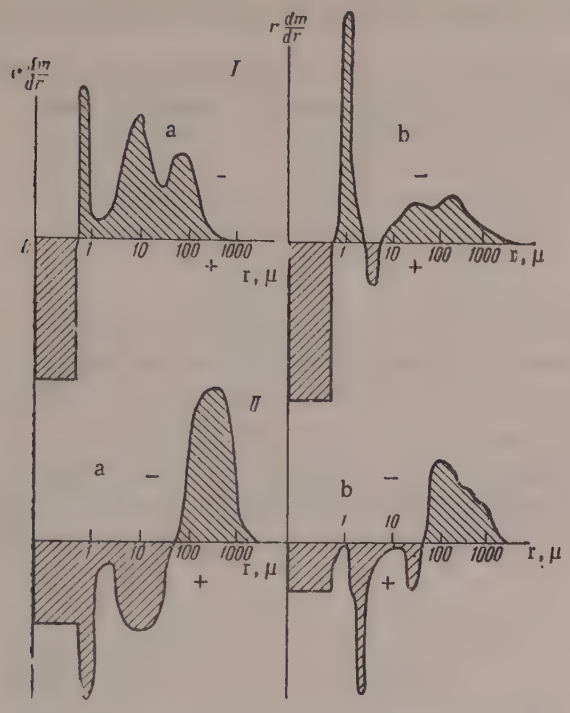


Fig. 2. Spread from chemical (peptization) I and mechanical II dispersion of low (a) and high (b) peats. The mechanical dispersion consisted of five passes of the peat through a meat grinder and the chemical dispersion consisted of treatment of processed peat with 0.1 N NaOH solution.

The dispersity of high and low peats is changed differently by chemical additives. In high forms of peat, there is an increase in the content of only the colloidal fraction < 1 μ, while in low peats, chemical treatment also results in the formation of coarser particles 1-5 μ in size. The presence of aggregated particles in the peat suspension is caused by their capacity to exchange hydrogen ions and polyvalent cations and the peptization is based on the displacement of these by monovalent cations (Na^+) and the increase in the pH of the medium, which changes the absorption capacity. The action of electrolytes on plant residues, namely, high polymers of the cellulose type, is considerably less. For this reason, the heterogeneity factor $f = r_{10}/r_{60}$, which characterizes the polydispersity of the system, changes considerably on the addition of electrolytes. On the addition of NaOH solutions, f increases from 160 to 840 for high peat and from 54 to 120 for low peat. During mechanical treatment of peat, the heterogeneity factor changes to a considerably smaller extent (Fig. 1) and passes through a maximum with an increase in the number of treatments. This indicates a change in the system from a homogeneous coarsely dispersed state, through a maximum of heterogeneity, to a homogeneous highly disperse state. Analysis of the table shows that mechanical treatment of peat produces a considerable change in dispersity in the initial stage of this process and then its effect tails off. After the first treatment, 32.8% of the particles of low peat and 28% of those of high peat are dispersed, while after five treatments the coresponding values are 58.4 and 33.4%. Further treatment of peat in a meat grinder has little effect on these values, while chemical treatment produces a change in the dispersity of a considerably larger number of particles (38% for low peat and 44% for high peat).

$CaCl_2$ solutions, which produce coagulation of peat, reduce its degree of dispersity mainly by reducing the content of the fraction < 1 μ as a result of association and aggregation of particles of the disperse phase. Progressive aggregation with an increase in the concentration of $CaCl_2$ solutions added leads to a displacement of the maximum on the distribution curves toward larger particles. The heterogeneity factor is then decreased.

The results obtained indicate the fundamental possibility and efficiency of chemical treatment of peat, which results in either peptization or coagulation and changes the dispersion parameters and physicochemical properties and, consequently, the quality of the finished product. An improvement in the quality of peat as a result of the addition of a series of chemical reagents has also been reported by other authors [6]. The results presented indicate the advantages of combining mechanical processing with chemical treatment.

SUMMARY

1. The peptizing action of NaOH solutions on processed peat increases the dispersity by a factor of more than two, while mechanical dispersion becomes increasingly inefficient. The addition of $CaCl_2$ solutions decreases the dispersity of peat.

2. The combination of peptization of peat with mechanical dispersion makes it possible to improve the quality of the finished product.

LITERATURE CITED

1. S. G. Solopov, Tr. Moskovskogo torfyanogo inst. 8, (1958); Doctor's dissertation [in Russian] Moscow (1955).
2. M. P. Volarovich and N. V. Churaev, Kolloidn. zh. 17, 3 (1955; Transactions of the Third All-Union Conference on Colloid Chemistry [in Russian] Izd. AN SSSR (1956).
3. M. P. Volarovich, I. I. Lishtvan and N. V. Churaev, Kolloidn. zh. 22, 5 (1960).
4. N. V. Churaev, Collection of articles, New Physical Methods of Studying Peat, edit. by M. P. Volarovich and N. V. Churaev [in Russian] Gosénergoizdat (1960).
5. M. P. Volarovich and N. V. Churaev, Kolloidn. zh. 16, 4 (1954); N. V. Churaev, Kolloidn. zh. 16, 3 (1954).
6. S. V. Kurdyumov, Transactions of the Ukr. Scientific Inst. of Local and Fuel Industry [in Russian] (1956); G. Ya. Voronkov, Torfyanaya prom-st', 3 (1961).

THE EFFECT OF FREEZING ON THE PROPERTIES OF METAL HYDROXIDE COAGULATES

4. MANGANESE DIOXIDE COAGULATE

V. V. Vol'khin, V. L. Zolotavin and S. A. Tipikin

S. M. Kirov Urals Polytechnical Institute, Sverdlovsk
Translated from Kolloidnyi Zhurnal, Vol. 23, No. 4,
pp. 404-407, July-August, 1961
Original article submitted February 8, 1960

We have already published [1-3] the results of studies on the influence of conditions of freezing, thawing and electrolyte concentration on the change in properties of iron hydroxide coagulates and have proposed a mechanism for the action of freezing on the coagulates.

It was considered of interest to verify the accuracy of the proposed mechanism of action of freezing for the case of hydrated oxides of other metals. An analogous study was therefore carried out with manganese dioxide coagulate. We chose manganese dioxide for the present studies because of its application as sorbent for the extraction, concentration and separation of radioactive isotopes [4-6].

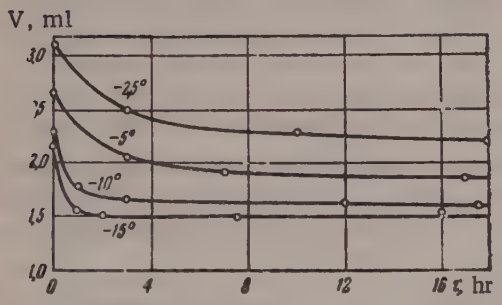


Fig. 1. The influence of freezing temperature and time of storage of coagulate in the frozen state on the volume of the precipitate after thawing.

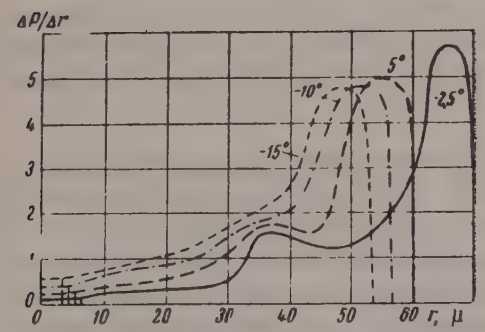


Fig. 2. The influence of the temperature of freezing of an MnO_2 precipitate on its particle size after thawing.

It was also hoped that the method of freezing, by making it possible to improve considerably the properties of manganese dioxide gels without the introduction of foreign substances, could increase considerably its possible applications for these purposes.

The effect of freezing on the properties of manganese dioxide. Manganese dioxide coagulate was prepared by the reaction of potassium permanganate with hydrogen peroxide [7]. The resulting colloidal manganese dioxide was coagulated with sodium chloride and washed by decantation to pH 6.5-7.0. The residual concentration of sodium chloride in the coagulate amounted to ~0.5 mg/liter. Further treatment of the precipitate was carried out by the method described earlier [1-3]. The experiments were carried out with 125 ml specimens of coagulate (~240 mg Mn), which corresponds to 100 ml of coagulate when this has been left to stand until the level remains unchanged.

The effect of freezing on the change in volume of the MnO_2 precipitate was studied at temperatures of -2.5, -5, -10 and -15° (Fig. 1). Specimens of the coagulate were kept at each of these temperatures in the frozen state for different periods of time. The first specimens of frozen coagulate were removed from the refrigerated thermostat [8] at the moment when the distilled water in control specimens had frozen completely.

The data obtained show that the lower the freezing temperature, the smaller the volume of the MnO_2 precipitate after thawing. In addition, there is a decrease in the volume when the precipitate is kept in the frozen state, and this process takes place more rapidly and is completed earlier at low temperatures.

Comparison of the extent of the decrease in volume of the manganese dioxide precipitate with the corresponding data for iron hydroxide [1] shows that in the two cases the effect of the factors considered above is identical but that there is a considerable difference in the quantitative aspect. Thus in the case of manganese dioxide, the volume of the precipitate after freezing and thawing decreases by a factor of 40-65, compared with a factor of 15-25 for iron hydroxide. This difference in the effect of freezing on the change in volume of the metal hydroxide coagulates is apparently due to a number of factors, but primarily to a difference in the concentration of solid phase present in the coagulate when this has been left to settle completely (80 mm/liter Fe_2O_3 and 43 mm/liter MnO_2) and a difference in the degree of hydrophilic nature of the coagulates.

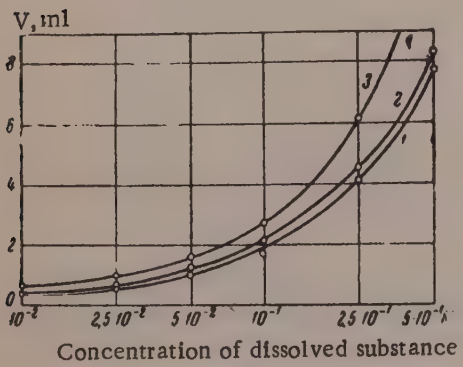


Fig. 3. The influence of ethyl alcohol (1), glycerol (2) and sodium chloride (3) on the volume of MnO_2 precipitate after freezing and thawing.

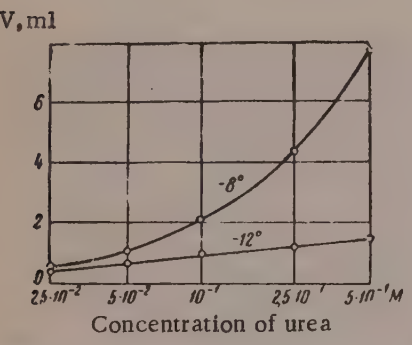


Fig. 4. The influence of urea on the volume of the MnO_2 precipitate after thawing. Temperatures of freezing -8 and -12°.

Sedimental analysis of the manganese dioxide precipitates after thawing showed an increase in their degree of dispersion (Fig. 2). Moreover, for identical conditions of preparation, the manganese dioxide precipitate has a lower degree of dispersion than the iron hydroxide precipitates. The reason for the observed phenomena is probably the difference in the degree of aggregation of the particles of the original coagulate during freezing. At temperatures close to the freezing point, ice is formed slowly, the particles of coagulate are concentrated towards the center of the specimen and when freezing goes to completion, a large-grained precipitate is formed after thawing. At lower freezing temperatures, the rate of crystallization of water is higher, the coagulate precipitate is entrained by the ice phase at lower concentrations, and the particles of the MnO_2 precipitate obtained are smaller.

Experiments showed that the tendency of the different precipitates to concentrate depends not only on the freezing temperature but also on the properties of the precipitates themselves. Thus for the same freezing conditions, manganese dioxide undergoes more efficient concentration than the more lyophilic iron hydroxide and the manganese hydroxide particles obtained after thawing are larger. As a result, the manganese hydroxide precipitates also exhibit a higher filtering capacity. Under identical conditions, the rate of filtration through the manganes dioxide precipitates was 10-15 times the value for iron hydroxide.

The effect of freezing on the properties of manganese dioxide in the presence of electrolytes. Study of the influence of electrolytes on the change in volume, particle size and filtering capacity of manganese dioxide precipitates after freezing showed that for all these properties there is complete analogy with the corresponding data for iron hydroxide [2, 3]. For the sake of brevity, therefore, the results of these experiments are not given in the present work. We would merely point out that this analogy is not accidental, since these properties depend to a considerable extent on the nature of the freezing of the liquid phase of the coagulate.

The effect of freezing on the properties of manganese dioxide coagulate in the presence of nonelectrolytes and lyophilic colloids. Solutions of weak electrolytes and nonelectrolytes are little dissociated and exhibit a lower molar depression of the freezing point than strong electrolytes. For identical conditions and freezing temperatures above the eutectic therefore, weak electrolytes reduce the effect of freezing on the decrease in volume of the precipitates to a smaller extent than strong electrolytes. Experiments carried out with the addition of ethyl alcohol, glycerol and urea to manganese dioxide coagulates confirmed this assumption (Figs. 3, 4). Increase in the concentration of ethyl alcohol or glycerol in the original MnO_2 coagulate leads to a corresponding increase in the volume of the precipitate after freezing, since these compounds do not form a cryohydrate at $-10°$; their influence on the volume of the precipitate is less marked than that of strong electrolytes (Fig. 3).

In the case of urea, it is convenient to follow the influence on the coagulate of the quantity of substance dissolved in the liquid phase for cases where freezing leads to the formation of a cryohydrate and for cases where a cryohydrate is not formed. For this purpose, the freezing of manganese dioxide coagulate with added urea was carried out at -8 and -12° (Fig. 4), since the eutectic temperature for solutions of urea in water is equal to -11.6° [9]. These data correspond to the data obtained earlier for strong electrolytes. Study of the influence of electrolytes on the particle size of the precipitate showed that the nature of this influence also corresponds completely to that for strong electrolytes. Quantitatively, however, discrepancies are observed, due to differences in the influences of the substances on the crystallization of the solutions [10, 11].

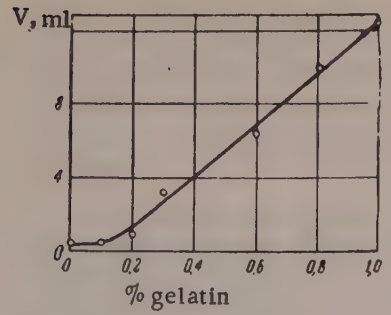


Fig. 5. The influence of gelatin on the volume of the MnO_2 precipitate after thawing. Temperature of freezing -10°.

A study was also made of the effect of freezing on the change in properties of metal hydroxides in the presence of lyophilic colloids. It is known that lyophilic colloids weaken the coagulating effect of freezing on sols [12] and that in a gel of gelatin, for example even at -192°, ~35% water remains in the liquid state [13, 14]. Consequently, the addition of a lyophilic colloid to metal hydroxide coagulates should prevent complete freezing of their liquid phase and thus weaken the effect of freezing. Lyophilic colloids can probably also hinder the process of aggregation of the metal hydroxide particles.

Experiments on the freezing of manganese dioxide coagulates in the presence of gelatin (freezing temperature -10°) confirmed this assumption. A marked influence on the volume of the MnO_2 precipitate was observed at a gelatin concentration in the original coagulate of only 0.1%, and at concentrations of ~1% the effect of freezing was reduced by a factor of approximately 35 (Fig. 5). Higher concentrations of gelatin could not be studied because in these cases the solutions become so viscous that the manganese dioxide particles do not settle.

SUMMARY

1. A study has been made of the effect of freezing and the influence of dissolved substances on the change in properties of pure manganese dioxide coagulate.

2. The manganese dioxide precipitate decreases in volume on freezing and subsequent thawing by a factor of 45-65, due to the increase in the diameter of the particles to 80-140 μ; the filtering capacity of the precipitate increases considerably at the same time.

3. Weak and strong electrolytes, nonelectrolytes, and lyophilic colloids reduce the effect of freezing on the manganese dioxide coagulates, since at temperatures above the eutectic they restrict the degree of freezing of the liquid phase of the coagulates.

LITERATURE CITED

1. V. L. Zolotavin, V. V. Vol'khin and V. V. Rezvushkin, Kolloidn. Zh., 22, 305 (1960).
2. V. V. Vol'khin and V. L. Zolotavin, ibid., 23, 134 (1961).
3. V. L. Zolotavin and V. V. Vol'khin, ibid., 23, 276 (1961).
4. E. V. Alekseevskii, Active Manganese Dioxide [in Russian] Khimteoret (1937).
5. T. Gerevini and E. Lazzarini, Energia nucl. 5, 831 (1958).
6. D. Cvjeticanin and N. Cvjeticanin, Jener, Report., No. 54 (1958).
7. Yu. V. Karyakin and I. I. Angelov, Pure Chemical Reagents [in Russian] Goskhimizdat, Moscow, p. 334 (1955).
8. V. V. Vol'khin and V. L. Zolotavin, Khologil'naya Tekhnika, No. 5, 54 (1959).
9. A. P. Rollet and R. Cohen-Adad, Compt. rend. 227, 554 (1948).
10. B. P. Veinberg, Ice [in Russian] Gostekhizdat, Moscow-Leningrad, p. 155 (1940).
11. J. Arakawa and Keiji Higuchi, Low Temperat. Sci. (Japan) No. 12A, 73 (1954).
12. Shohei Uno and Naoji Ichiji, J. Chem. Soc., Japan, Pure Chem. Sect. 72, 607 (1951).
13. T. Moran, Proc. Roy. Soc. (London) 112A, 30 (1926).
14. T. Moran, Kolloid.-Z. 59, 217 (1932).

DIFFUSION-ELECTROKINETIC THINNING OF LIQUID FILMS

S. S. Dukhin

Caucasian Institute of Mineral Raw Material, Tbilisi
Translated from Kolloidnyi Zhurnal, Vol. 23, No. 4,
pp. 408-417, July-August, 1961
Original article submitted September 8, 1959

It was indicated in [1] that the thinning of a liquid layer between a bubble and a mineral particle under conditions of flotation, and also in experiments simulating flotation conditions, is caused by desorption of the reagent from the mineral particle surface, diffusion to the water–air interface, and adsorption at this interface. The diffusion under these conditions is caused by movement of the medium, and the electrical field which appears is caused by the diffusion; hence, a similar mechanism of film thinning should be termed diffusion-electrokinetic. In the present work, the theory of this effect is presented in conformity with the experimental conditions of L. F. Evans and V. E. Ewers [2].

Let a liquid film of thickness h_0 be flowing along an inclined plane surface of a solid body, which for simplicity we will consider as infinitely extended. Let us introduce a rectangular coordinate system with the x-axis oriented along the direction of movement of the film, and the y-axis perpendicular to the surface. We will consider that prior to the formation of the film there has been applied to the surface a polymolecular* layer of a soluble ionogenic surfactant, the upper boundary of which coincides with the line x-o. For a strictly stationary course of the diffusion-electrokinetic process, it is necessary that surface diffusion should be absent. In the opposite case, the boundary of the polymolecular layer will migrate; this, however, only complicates the analysis, but does not change the essence of the situation.

It was demonstrated previously [3] that the distribution of electric potential $\varphi(x', y')$ is expressed in terms of the distribution of concentration $c(x', y')$

$$\varphi(x', y') = \Phi \ln c\ (x', y')/c_0], \tag{1}$$

where $\Phi + R_0T(D^+ - D^-)/F(Z^+D^+ + Z^-D^-)$, c_0 is the concentration over the applied layer of the reagent, R_0 is the universal gas constant, T is the absolute temperature, and z^+ and z^-, D^+ and D^- are the valence and diffusion coefficients respectively of the positive and negative ions. Later we will need expressions for the normal and tangential components of the electric field, $E_y(x', y')$ and $E_x(x', y')$, and also for the bulk and surface electric charge density, $\rho_e(x', y')$ and $\sigma_e(x')$, which are readily worked out according to well-known formulas of electrostatics

$$E_x = \partial\varphi/\partial x' = \Phi\partial \ln c/\partial x';\ E_y = \partial\varphi/\partial y' = \Phi\,\partial \ln c/\partial y' \tag{2}$$

$$\rho_e = -\frac{\varepsilon}{4\pi}\Delta\varphi = -\frac{\varepsilon\Phi}{4\pi}\Delta \ln c;\quad \sigma_e = \frac{\varepsilon}{4\pi}E_y(x', h) = \frac{\varepsilon\Phi}{4\pi}\frac{\partial \ln c(x', h)}{\partial y}, \tag{3}$$

where ϵ is the dielectric constant.

The action of the electric field on the surface charges causes a force acting along the normal to the liquid–gas interface and tending to thin the film

$$F_{ey}(x') = \sigma_e(x')\,E_y(x', h) = \frac{\varepsilon\Phi^2}{4\pi}\left[\frac{\partial \ln c(x', h)}{\partial y}\right]^2. \tag{4}$$

* The consideration of a monomolecular layer is not expedient, since in this case the concentration at the surface changes with time.

If the movement of the film is neglected and it is attempted to determine its profile at the place of its thinning statically, it should be taken into account that the action of the electrical force on the surface of the film that leads to its thinning must be balanced by the capillary pressure arising as a result of distortion of the liquid–gas interface on thinning of the film $F_{ey}(x') + \sigma(x')/R(x') + p_0 = \text{const}$, where $\sigma(x)$ is the surface tension, which being a function of concentration, varies with the concentration along the surface, R_x is the radius of curvature of the liquid–gas interface, and p_0 is the pressure in the film far from the place of thinning, where the film surface is plane. However, as shown by a detailed analysis of the problem, a static analysis of the phenomenon of film thinning is entirely inadequate. In addition to the electrical and capillary forces, account should be taken of gravitational and viscous-drag forces.

The dynamic analysis of the diffusion-electrokinetic thinning of a film leads to problems which are similar to those examined in the hydrodynamics of thin films [4]. The essential difference is that along with the capillary pressure one should take into account electrostatic pressure, and in place of $p_\sigma(x') = \sigma(x')/R(x')$ in the hydrodynamic equation of motion one should substitute

$$p_{\sigma e} = \sigma(x')/R(x') = (\varepsilon\Phi^2/4\pi)\,[\partial \ln c(x', h)/\partial y]^2. \tag{5}$$

One of the essential simplifications in the hydrodynamics of thin films is the fact that movement in the normal direction can be neglected in comparison with movement in the tangential direction, in connection with which the equation of motion is written only for the tangential component of velocity $u(x', y')$

$$\eta \partial^2 u/\partial y'^2 + Q = \partial p/\partial x', \tag{6}$$

where Q is the tangential component of the bulk forces acting on the film and η is the viscosity.

If only forces of gravity are usually taken into account as the bulk forces acting on the film, then in the case of interest to us there should also be taken into account the force caused by the action of the tangential component of the electrical field $E_x(x', y')$ on the bulk charges $\rho_e(x', y')$

$$\eta \frac{\partial^2 u}{\partial y'^2} + \rho g \sin\theta - \rho_e(x', y') E_x(x', y') =$$
$$= \eta \frac{\partial^2 u}{\partial y'^2} + \rho g \sin\theta - \frac{\varepsilon\Phi^2}{4\pi} \Delta \ln c \frac{\partial \ln c}{\partial x'} = \frac{\partial p}{\partial x'}, \tag{7}$$

where θ is the slope angle of the surface, ρ is the density of the liquid, and g is the acceleration of gravity. As regards the normal constituent of the electrical field, its action on the bulk electrical charges is taken into account in the pressure.

The second equation of motion of a thin film, as is well known, expresses the condition of constancy of pressure along a section of the film

$$\partial p/\partial y' = 0, \tag{8}$$

whence it follows that

$$p = p_0 - p_{\sigma e}, \tag{9}$$

Substituting Eq. (9) with regard for (5) into Eq. (7), we transform the latter into the following form

$$\eta \frac{\partial^2 u}{\partial y'^2} = -\rho g \sin\theta + \frac{dp_{\sigma e}}{dx'} + \frac{\varepsilon\Phi^2}{4\pi} \Delta \ln c \frac{\partial \ln c}{\partial x'}. \tag{10}$$

The boundary conditions for the velocities must take into account the adhesion of the liquid to the surface of the solid body and the viscous drag at the liquid–gas interface caused by the tangential component of the electrical field and the change in surface tension along the surface

$$u|_{y'=0} = 0; \quad \eta \frac{\partial u}{\partial y'}(x', h) = \frac{\partial \sigma}{\partial x'} + \sigma_e(x') \frac{\partial \varphi}{\partial x'}(x', h). \tag{11 and 12}$$

Utilizing the Gibbs formula $\partial\sigma/\partial c = RT\Gamma/c$, where Γ is the adsorption, and considering the ratio Γ/c as invariant along the surface (which will be correct if the adsorbed layer is far from saturation), we may represent $\partial\sigma/\partial x'$ in the following manner

$$\partial\sigma/\partial x' = \partial\sigma/\partial c \cdot \partial c/\partial x' = RT\alpha\,\partial c/\partial x';\ \alpha = \Gamma/c.$$

Then condition (12) assumes the form

$$\eta\frac{\partial u}{\partial y}(x', h) = \left[RT\alpha\frac{\partial c}{\partial x'} + \frac{\varepsilon\Phi^2}{4\pi}\frac{\partial \ln c}{\partial x'}\frac{\partial \ln c}{\partial y'}\right]_{y'=h}. \tag{13}$$

In the integration of Eq. (10) we take into account that the first two items on the right are independent of y. It is not difficult to be convinced that the expression shown below satisfies both Eq. (10) and the boundary conditions (11) and (13)

$$\eta u(x', y') = \frac{Ay'^2}{2} + \left(f(x') - Ah - \frac{\varepsilon\Phi^2}{4\pi}\int_0^h \Delta\ln c\frac{\partial \ln c}{\partial x'}dy'\right)y' + \\ + \frac{\varepsilon\Phi^2}{4\pi}\iint \Delta\ln c\frac{\partial \ln c}{\partial x'}(dy')^2, \tag{14}$$

where

$$A = -\rho g\sin\theta + \frac{dp_{\sigma e}}{dx'};\ f(x') = \left[RT\alpha\frac{\partial c}{\partial x'} + \frac{\varepsilon\Phi^2}{4\pi}\frac{\partial \ln c\,\partial \ln c}{\partial y'\ \partial x'}\right]_{y'=h}.$$

In the stationary state, the flow of liquid Q taking place through every section of the film perpendicular to the direction of its motion is constant and can be calculated according to the formula

$$Q(x') = \int_0^{h(x')} u(x', y')\,dy' = Q_\infty, \tag{15}$$

where Q_∞ is the flow of liquid far from the region of thinning, where the second and third items on the right in Eq. (10) and the right-hand portion of the boundary condition (13) may be neglected. Omitting the corresponding items in Eq. (14), it is not difficult to be convinced that

$$u(y')|_{x'\to-\infty} = u_1(y') = y'(h - y'/2)\rho g\sin\theta/\eta \tag{16}$$

and consequently

$$Q_\infty = h_0^3\rho g\sin\theta/3\eta. \tag{17}$$

Substituting $u(x', y')$, expressed in accordance with Eq. (14), into the integral of (15) and carrying out the integration, we obtain

$$-\frac{Ah^3}{3} + f(x')\frac{h^2}{2} - \frac{\varepsilon\Phi^2h^2}{2\cdot4\pi}\int_0^h \Delta\ln c\frac{\partial \ln c}{\partial x'}dy + \\ + \frac{\varepsilon\Phi^2}{4\pi}\iiint_0^h \Delta\ln c\frac{\partial \ln c}{\partial x'}(dy')^3 = h_0^3\rho g\sin\theta/3. \tag{18}$$

Substituting the values for A and f(x) into this equation, and taking into account that with a low degree of curvature of the film surface the curvature can be related approximately to the film thickness by the simple relationship $1/R(x') \simeq d^2h/dx'^2$, we reduce Eq. (18) to the form

$$-\sigma(x')\frac{h}{3}\frac{d^3h}{dx'^3} + \frac{d\sigma}{dx'}\left(\frac{h}{3}\frac{d^2h}{dx'^2} + \frac{1}{2}\right) + \frac{\varepsilon\Phi^2}{4\pi}\left[\frac{h_0}{3}\frac{d}{dx'}\left(\frac{\partial \ln c}{\partial y'}\right)^2 + \right.$$

$$\left. + \frac{1}{2}\frac{\partial \ln c}{\partial x'}\frac{\partial \ln c}{\partial y'} - \frac{1}{2}\int_0^h \Delta\ln c\frac{\partial \ln c}{\partial x'}dy + \frac{1}{h_0^2}\iiint_0^h \Delta\ln c\frac{\partial \ln c}{\partial x'}(dy')^3\right] = \rho g\sin\theta(h_0^3 - h^3)/3h^2. \tag{18'}$$

This nonlinear differential equation, which is impossible to solve exactly, can be simplified considerably with the condition of relatively low degree of curvature of the film, i.e., with $R(x') \gg h(x')$, owing to which $h_0 d^2h/dx'^2 \ll \ll 1$. Therefore, if the drop of surface tension in the film is not too small, i.e., if the condition is fulfilled that

$$\sigma(x')\, h_0 d^3h/dx'^3 \ll d\sigma/dx', \tag{19}$$

it is sufficient to take into account in Eq. (18') the action of capillary forces by the item of largest magnitude, $\frac{1}{2}\partial\sigma\ \partial x'$. Moreover, we will limit the analysis to the condition of relatively low degrees of thinning

$$(h_0 - h)/h_0 \ll 1, \tag{20}$$

the necessity of which becomes clear from the following. Then we obtain

$$h_0 - h(x') = \frac{1}{\rho g \sin\theta}\left\{\frac{R_0 T\alpha}{2}\frac{\partial c}{\partial x'} + \frac{\varepsilon\Phi^2}{8\pi}\left[\frac{\partial \ln c}{\partial y'}\frac{\partial \ln c}{\partial x'} + \frac{2h}{3}\frac{d}{dx'}\left(\frac{\partial \ln c}{\partial y'}\right)^2 - \right.\right.$$

$$\left.\left. - \int_0^h \Delta \ln c \frac{\partial \ln c}{\partial x'}\, dy' + \frac{2}{h_0^2}\int_0^h\int\int \Delta \ln c \frac{\partial \ln c}{\partial x'}\, dy'^3\right\}. \tag{21}$$

For determining the field of concentrations, it is necessary to examine the diffusional migration of the surfactant from the surface of the solid body through the moving film to the liquid–gas interface on the basis of the equation of convective diffusion

$$D_e(\partial^2 c/\partial x'^2 + \partial^2 c/\partial y'^2) = u(y')\,\partial c/\partial x', \tag{22}$$

where $D_e = D^+D^-(z^+ + z^-)/(z^+D^+ + z^-D^-)$ the so-called effective diffusion coefficient of the ions. It is essential to emphasize that for determining the field of concentrations according to Eq. (22) it is necessary to compute the given field of velocities, and for determining the field of velocities according to Eq. (10) it is necessary to compute the given field of concentrations. Meanwhile, the joint solution of Eqs. (10) and (22) on the basis of utilizing the distribution of velocities and concentrations at minus infinity entails insurmountable difficulties. Therefore, one must be limited to an investigation of the case of relatively low degrees of thinning [condition (20)], with which the field of velocities at the site of thinning of the film is not deformed significantly

$$u(x', y') = u_1(y') + u_2(x', y'),\ u_2(x', y') \ll u_1(y'). \tag{23}$$

Under these conditions, when the conditions (20) and (23) are fulfilled in Eq. (22) the field of velocities can be considered to be given approximately as

$$D_e(\partial^2 c/\partial y'^2 + \partial^2 c/\partial x'^2) = u_1(y')\,\partial c/\partial x'. \tag{24}$$

The boundary condition at the surface of the solid body must take into account saturation of the solution over the adsorbed layer

$$c|_{y'=0} = c_0. \tag{25}$$

In order not to take into account extraneous ions, we assume that in the film there previously has been dissolved a fixed quantity of that same surfactant, which gives the following boundary condition

$$c|_{x'\to-\infty} = c_1. \tag{26}$$

It is evident that the remaining ions can be disregarded if their concentration is much less than c_1.

The increase in adsorption with a shift of the film surface by a distance dx' can be expressed on the one hand in terms of the normal component of the flow of diffusion, and on the other hand, on the assumption of adsorption equilibrium, in terms of $c(x', h_0)$

$$d\Gamma(x') = \alpha dc(x', h_0) = -D\frac{\partial c}{\partial y}(x', h_0)\,dt = -D\frac{\partial c}{\partial y}(x', h_0)\frac{dx'}{u(h_0)}.$$

Hence follows the boundary condition

$$\partial c(x', h_0)/\partial x' = -\gamma \partial c(x', h_0)/\partial y', \tag{27}$$

where $\gamma = D/\alpha u(h_0)$.

An exact solution of Eq. (24) is difficult to obtain, in connection with which we are limited to approximate solutions, which are adequate for describing the thinning process in certain limited cases.

We will limit the analysis to the condition under which diffusion of ions along the film may be neglected

$$\partial^2 c/\partial x'^2 \ll \partial^2 c/\partial y'^2. \tag{28}$$

The values of the parameters to ensure fulfilling this condition will be determined below. In addition, it is necessary to give up considering the change in velocity along a section of the film and to assume it as a constant. Since the boundary condition (27) is most important, such that it is desirable to describe as accurately as possible the diffusion process at the liquid–gas interface, we adopt, as the constant value of velocity along a section of the film, the velocity of movement of the surface of the film $u(h_0)$. Even though the errors caused by this simplification do not tend toward zero at any values of the parameters, the adopted simplification cannot affect either the qualitative character of the results obtained below or the order of magnitude of the thinning.

In the dimensionless variables $x = x'/h_0$, $y = y'/h_0$ Eq. (24) with the adopted simplification reduces to the form

$$\partial^2 c/\partial y^2 = Pe\, \partial c/\partial x, \tag{29}$$

where

$$Pe = u(h_0) h_0 D^{-1} = g \sin 0 \,(2\nu D)^{-1} h_0^3 \sim 10^{10} h_0^3. \tag{30}$$

For the solution of Eq. (29) together with the boundary conditions (25), (26) and (27) we will apply an operational method. Utilizing a standard procedure of operational calculus, we obtain a differential equation and boundary conditions for the transform $C(s, y) = \int_0^\infty c(x, y)\, e^{-sx}\, dx$,

$$\frac{\partial^2 C(s, y)}{\partial y^2} = Pe \cdot sC(s, y) - c_1, \tag{31}$$

$$C(s, y)|_{y=0} = \frac{c_0}{s}; \quad \gamma \left.\frac{\partial C(s, y)}{\partial y}\right|_{y=1} = sC(s, y)|_{y=1} - c_1. \tag{32) and (33)}$$

The solution of the differential equation (31) satisfying the boundary conditions (32) and (33) has the form

$$C(s, y) = \frac{c_1}{s} + \frac{\Delta c \{(\gamma Pe^{1/2} - s^{1/2})(\gamma Pe^{1/2} + s^{1/2}) \exp[-(Pes)^{1/2}(2 - y)] + \exp[-(Pes)^{1/2} y]\}}{s\{1 + \exp[2(as)^{1/2}](\gamma Pe^{1/2} - s^{1/2})(\gamma Pe^{1/2} + s^{1/2})\}}, \tag{34}$$

where $\Delta c = c_0 - c_1$.

For reestablishing the approximate value of the original in the region of not too large values of x, one can take advantage of an approximate expression for the transform which is obtained from Eq. (34) with $s \gg 1$ and $\gamma \ll 1$

$$C'(s, y) = \frac{c_1}{s} + \frac{\Delta c}{s}\left\{\left(1 - 2\gamma \sqrt{\frac{Pe}{s}}\right) \exp[(sPe)^{1/2}(y - 2)] - \exp[-(Pes)^{1/2} y]\right\}. \tag{34'}$$

The original for the transform (34) has the form

$$c'(x, y) = c_1 + \Delta c \left\{erfc \sqrt{\frac{Pe}{4x}}\, y - erfc\left[\sqrt{\frac{Pe}{4x}}(2 - y)\right] + \right.$$

$$\left. + 4\gamma \sqrt{\frac{Pex}{\pi}}\, e^{-(2-y)^2 \frac{Pe}{4x}} - 2\gamma Pe \cdot erfc\left[\frac{(2 - y)}{2}\sqrt{\frac{Pe}{x}}\right]\right\}. \tag{35}$$

Now it is possible to establish that condition (28) is fulfilled, if $x \gg 1$. On the other hand, the approximate solution satisfies the boundary condition (25) if $Peh/x \gg 1$, boundary condition (27) if $4\gamma x \ll 1$. Thus, the function (35) can be utilized in the interval values of $\underline{x}$

$$1 \ll x \ll Pe, \quad 1 \ll x \ll (4\gamma)^{-1} = Pe\alpha/4h. \tag{36}$$

But under these conditions and with $\underline{y}$ differing substantially from zero, it can be written in the following form

$$c'(x, y) = c_1 + \Delta c\,[f_1(x, y) + f_2(x, y)],$$

$$\text{where} \quad f_1(x, y) = \left(\frac{4x}{Pe\pi}\right)^{1/2}\left\{\frac{e^{-y^2 Pe/4x}}{y} - \frac{e^{-(2-y)^2 Pe/4x}}{2-y}\right\},$$

$$f_2(x, y) = \frac{4\gamma x}{2-y}\sqrt{\frac{4x}{Pe\pi}}\, e^{-(2-y)^2 Pe/4x} \tag{35'}$$

We also transform the basic formula (21) into dimensionless variables $\underline{x}$ and $\underline{y}$, the integrals which figure in it being transformed by means of integration by parts. At the same time, we utilize conditions (25) and (28), whence it follows that

$$\partial \ln c/\partial x|_{y=0} = 0, \quad \Delta \ln c \simeq \partial^3 \ln c/\partial y^2. \tag{37}$$

As a result, we obtain

$$\int_0^1 \Delta \ln c \frac{\partial \ln c}{\partial x}\,dy \simeq \frac{\partial \ln c}{\partial y}\frac{\partial \ln c}{\partial x}\bigg|_{y=1} - \int_0^1 \frac{\partial \ln c}{\partial y}\frac{\partial^2 \ln c}{\partial y \cdot \partial x};$$

$$\iiint_0^1 \Delta \ln c \frac{\partial \ln c}{\partial x}(dy)^3 \simeq \iint_0^1 \frac{\partial \ln c}{\partial y}\frac{\partial \ln c}{\partial x}(dy)^2 - \iiint_0^1 \frac{\partial \ln c}{\partial y}\frac{\partial^2 \ln c}{\partial x \cdot \partial y}(dy)^3;$$

$$\Delta h(x) = (\rho g \sin\theta)^{-1}\left\{\frac{R_0 T\alpha}{2h_0}\frac{\partial c}{\partial x} + \frac{\varepsilon\Phi^2}{8\pi h_0^2}\left[\frac{2}{3}\frac{\partial}{\partial x}\left(\frac{\partial \ln c}{\partial y}\right)^2 + \right.\right. \tag{21'}$$

$$\left.\left. + \int_0^1 \frac{\partial \ln c}{\partial y}\frac{\partial^2 \ln c}{\partial y \cdot \partial x}\,dy + 2\iint_0^1 \frac{\partial \ln c}{\partial y}\frac{\partial \ln c}{\partial x}(dy)^2 - 2\iiint_0^1 \frac{\partial \ln c}{\partial y}\frac{\partial^2 \ln c}{\partial y \cdot \partial x}(dy)^3\right]\right\}_{y=1}.$$

For overcoming the difficulties connected with computation of the integrals figuring in formula (21), it is necessary to carry out a further simplification of the function c'(x, y). The function c'(x, y) and its derivatives can be simplified if there is excluded from consideration the vicinity of the points y = 0 and y = 1, i.e., if it is considered in the interval $\epsilon_0, 1 - \epsilon$

$$c'(x, y) \simeq \frac{\Delta c}{\sqrt{\pi y}}\left(\frac{4x}{Pe}\right)^{1/2}\exp(-y^2 Pe/4x),$$

$$\frac{\partial c'}{\partial x}(x, y) \simeq \frac{\Delta c y}{\sqrt{\pi x}}\left(\frac{Pe}{4x}\right)^{1/2}\exp(-y^2 Pe/4x), \quad \frac{\partial c'(x, y)}{\partial y} = -\frac{2\Delta c}{\sqrt{\pi}}\left(\frac{Pe}{4x}\right)^{1/2}\exp(-y^2 Pe/4x). \tag{38}$$

In setting up the approximate expression for c'(x, y) we introduced the additional condition

$$c_0/c_1 \geqslant (Pe/4x)^{1/2}\exp(Pe/4x), \tag{39}$$

which ensures reduction of the exponent in the subintegral expressions. These formulas can be utilized in setting up the subintegral expressions, since their magnitude at least does not increase in the vicinity of these points, while with condition (36) $\epsilon_0 \ll 1$ and $\epsilon_1 \ll 1$

$$\frac{\partial \ln c'}{\partial y} = -2y\left(\frac{Pe}{4x}\right); \quad \frac{\partial \ln c'}{\partial x} = \frac{y^2}{x}\left(\frac{Pe}{4x}\right); \quad \frac{\partial^2 \ln c'}{\partial x \cdot \partial y} = \frac{2y}{x}\left(\frac{Pe}{4x}\right);$$

$$\int_0^1 \frac{\partial \ln c'}{\partial y}\frac{\partial^2 \ln c'}{\partial y\cdot\partial x}dy + 2\iint_0^1 \frac{\partial \ln c'}{\partial y}\frac{\partial \ln c'}{\partial x}(dy)^2 - 2\iiint_0^1 \frac{\partial \ln c'}{\partial y}\frac{\partial^2 \ln c'}{\partial x\cdot\partial y}(dy)^3 =$$

$$= x^{-1}(Pe/4x)^2(4/3 + 2/10 - 2/15) \simeq 4/3x(Pe/4x)^2. \tag{40}$$

In computing the remaining two items in formula (21') it should be taken into account that $f_1(x, 1) = 0$, and $\partial f_1(x, 1)/\partial x = 0$, as a consequence of which

$$c'(x, 1) \simeq \Delta c(4x/\pi Pe)^{1/2}\cdot 4\gamma x\cdot\exp(-Pe/4x) \tag{41}$$

$$\partial c'(x, 1)/\partial x = -\gamma\partial c'(x, 1)/\partial y = 4\gamma\Delta c(Pe/4\pi x)^{1/2}\exp(-Pe/4x). \tag{42}$$

$$\frac{\partial \ln c'}{\partial y} = \frac{Pe}{4x\gamma};\quad \frac{\partial}{\partial x}\left(\frac{\partial \ln c'}{\partial y}\right)^2 = 2\frac{\partial \ln c'}{\partial y}\frac{\partial^2 \ln c'}{\partial x\cdot\partial y} = \left(\frac{Pe}{4x}\right)^2\frac{4}{\gamma^2 x}. \tag{43}$$

In obtaining formula (41) we actually introduced a condition more rigid than (39)

$$c_0/c_1 \gg (Pe/4x)^{1/2}(4\gamma x)^{-1}\exp(Pe/4x).$$

Utilizing the obtained results of formulas (40), (41) and (42) we obtain the final expression for the magnitude sought

$$\Delta h(x) = (\rho g\sin\theta)^{-1}\left\{\frac{2R_0T\Delta c}{(\pi Pex)^{1/2}}e^{-\frac{Pe}{4x}} + \frac{\varepsilon\Phi^2}{3\pi h^2}\left(\frac{Pe}{4x}\right)^2\frac{2Pe^2}{x}\left(\frac{\alpha}{h}\right)^2\left[1 + \frac{1}{2}\left(\frac{h}{\alpha Pe}\right)^2\right]\right\}. \tag{44}$$

Let us establish the values of the parameters approximately meeting all Pe for the limits introduced above. Values of the criterion Pe which are too large, as will be evident from the following, prove to be inadmissible. In order to satisfy the conditions (36) it is necessary to adopt the following numerical values of the parameters: x = 5, $Pe = 10^2$, $h_0 \sim 10^{-3}$ cm, $\alpha = h_0$.

Taking into account the numerical value adopted for fulfilling the condition of relatively slight thinning of the film, it should be required that the expressions in the braces of formula (44) should be much smaller than unity. However, it is not difficult to be convinced that the second item in the braces, taking into account diffusion-electrokinetic thinning, with the values of the parameters adopted above, is much greater than unity ($\Phi^2 = 10^{-9}$). The first item, which reflects the thinning of the film on account of the drop of surface tension along the surface, on substitution of the corresponding parameters can prove to be on the order of unity or much smaller.

Thus, the solution obtained can be utilized for the case of a nonionogenic surfactant, in which electrical effects, which are accounted for by the second item in the braces, are absent

$$\Delta h(x) = 2(\rho g\sin\theta)^{-1}R_0T(c_0 - c_1)(\pi Pex)^{-1/2}\exp(-Pe/4x). \tag{44'}$$

One must also conclude that with an ionogenic character and high surface activity of the reagent, expressed by a value of α equal to 10^3 cm, the thinnings are so substantial that their quantitative description presents great difficulties. On the other hand, the possibility is not excluded that reagents characterized by so high a surface activity of the ions are in general not encountered.

In this connection, it is advisable to attempt to evaluate the film thinning with relatively low values of α, which correspond to low values of γ.

For reestablishing the approximate expression of the original, in this case one can take advantage of an approximate expression for the transform obtained from Eq. (34) with $\alpha/h \ll (Pes)^{-\frac{1}{2}}$

$$C''(s, y) = \frac{c_1}{s} + (c_0 - c_1)\left[e^{-\sqrt{Pes}y} + e^{\sqrt{Pes}(y-2)}\left(1 + \frac{2\alpha}{h}\sqrt{Pes}\right)\right]. \tag{34''}$$

The original for the transform (34") has the form

$$c''(x, y) = c_1 + \Delta c[f_1(x, y) + f_2(x, y)],$$

$$f_1(x, y) = erfc \sqrt{\frac{Pe}{4x}}\, y + erfc \sqrt{\frac{Pe}{4x}}\,(2 - y);\quad f_2(x, y) = \frac{2\alpha}{yh}\left(\frac{Pe}{4\pi x}\right)^{1/2} e^{-\frac{Pey^2}{4x}}. \tag{35''}$$

In this case, condition (28) is also fulfilled if $x \gg 1$. The solution obtained satisfied approximately the boundary condition (27) if $\alpha/h \ll x/Pe$ and boundary condition (25) if $(Pe/4x)^{\frac{1}{2}} \gg 1$. Thus, the function (35") can be utilized in the interval of x-values determined by the conditions

$$1 \ll x \ll Pe/4 \tag{45}$$

with the ratio α/h required to satisfy the condition

$$\alpha/h \ll x/Pe \ll 1/4 \tag{46}$$

On comparing formulas (35") and (35') it is not difficult to be convinced that in computing the integrals in this case the same simplifications are possible as those utilized previously, and that the simplified expressions for the function c"(x, y) and its derivatives may have the same form as for the function c'(x, y), i.e., may be expressed by the equations (38); however, this signifies that the approximate values of the integrals are also obtained the same, i.e., also in the distribution of concentrations c"(x, y), formula (40) is correct.

The function c"(x, y) and its derivatives with y = 1 can be simplified if account is taken of the conditions (45) and (46) and the circumstance that $\partial f_1(x, 1)/\partial y = 0$

$$c''(x, 1) = 2\Delta c \left(\frac{4x}{\pi Pe}\right)^{1/2} e^{-\frac{Pe}{4x}};\quad \frac{\partial c''(x,1)}{\partial y} = \frac{4\alpha\Delta c}{\pi^{1/2}h}\left(\frac{Pe}{4x}\right)^{3/2} e^{-\frac{Pe}{4x}},$$

$$\frac{d}{dx}\left[\frac{\partial \ln c''(x, 1)}{\partial y}\right]^2 = \frac{16}{x}\left(\frac{\alpha}{h}\frac{Pe}{4x}\right)^2\left(\frac{Pe}{4x}\right)^2;\quad \frac{\partial c''(x, 1)}{\partial x} = \frac{\Delta c}{x}\left(\frac{Pe}{4\pi x}\right)^{1/2} e^{-\frac{Pe}{4x}}. \tag{47}$$

Substituting into formula (21') the values of the integrals according to formula (40) and the values of the derivatives according to the formulas (47), we obtain the final expression for the profile of thinning of the film with sufficiently low values of surface activity α, satisfying condition (46),

$$\Delta h(x) = (\rho g \sin\theta)^{-1}\left\{\frac{R_0 T\alpha\Delta c}{2h_0 x\pi^{1/2}}\left(\frac{Pe}{4x}\right)^{1/2} e^{-\frac{Pe}{4x}} + \frac{\varepsilon\Phi^2}{6\pi h^2 x}\left(\frac{Pc}{4x}\right)^2\left[\frac{1}{}+ 8\,\frac{\alpha}{h}\,\frac{Pe}{x}\right)^2\right]\}. \tag{48}$$

Comparing the values obtained for the first and second items in the braces, we arrive at the conclusion that with a sufficiently high surface activity of the reagent, the thinning is accomplished on account of the change in surface tension along the film surface. The diffusion-electrokinetic mechanism of thinning prevails at values of α that are not too large. However, it should be kept in mind that these conclusions apply only to the case characterized by the conditions (45) and (46), which had to be assumed in order to overcome the mathematical difficulties. In the more general case, the relative roles of thinning the mechanisms which were examined may be changed.

SUMMARY

1. For films of thickness exceeding 10^{-3} cm and with sufficiently low surface activity of an ionogenic reagent at the liquid–gas interface [satisfying condition (46)] it has been established that the profile of film thinning is determined by the diffusion-electrokinetic effect with sufficiently low solubility and surface activity of the reagent. With higher values of solubility and surface activity of the reagent, the film thinning profile is determined by the change in surface tension along the surface of the liquid–gas interface.

2. A marked thinning of a film with thickness on the order of 10^{-3} cm can be caused also by a nonionogenic surfactant, on account of the change in surface tension of the film. However, for ensuring a marked thinning by means of a nonionogenic reagent, considerably higher values of solubility and surface activity are required than in the case of an ionogenic material.

LITERATURE CITED

1. S. S. Dukhin, Dokl. AN SSSR 130, 1298 (1960); B. V. Deryagin and S. S. Dukhin, Bulletin of the Institute of Mining and Metallurgy, 70, part 5, 221 (1961).

2. K. L. Sazerlend and I. V. Uork, Principles of flotation, Metallurgizdat, Moscow (1958); L. F. Evans and W. E. Ewers, Recent Developments in Mineral Dressing, Institute of Mining and Metallurgy, London, 457 (1953).
3. S. S. Dukhin and B. V. Deryagin, Dokl. AN SSSR 121, 503 (1958); B. V. Deryagin, S. S. Dukhin and V. A. Lisichenko, Zh. fiz. khimii, 33, 2280 (1959).
4. B. V. Deryagin, Dokl. AN SSSR 39, 11 (1943); V. G. Levich, Physicochemical Hydrodynamics, Acad. Sci. USSR Press, Moscow (1959); B. V. Deryagin and S. M. Levi, Physical Chemistry of the Application of Thin Layers on a Moving Sublayer, Acad. Sci. USSR Press, Moscow (1959).

All abbreviations of periodicals in the above bibliography are letter-by-letter transliterations of the abbreviations as given in the original Russian journal. *Some or all of this periodical literature may well be available in English translation.* A complete list of the cover-to-cover English translations appears at the back of this issue.

DETERMINATION OF INTERNAL STRESSES DURING FORMATION OF GELATIN FILMS

P. I. Zubov and L. A. Lepilkina

Institute of Physical Chemistry, Academy of Sciences, USSR, Moscow
Translated from Kolloidnyi Zhurnal, Vol. 23, No. 4,
pp. 418-422, July-August, 1961
Original article submitted November 1, 1960

As had been shown previously [1], during the formation of polymeric films on solid substrates, internal stresses arise in the films, causing crack formation and in the limiting case spontaneous peeling of the films from the substrate. Since these stresses are transmitted to the substrate, the stresses in the film can be judged by the magnitude of birefringence in the substrate. The visual method, however, is very time-consuming, especially in measuring the stresses in various planes.

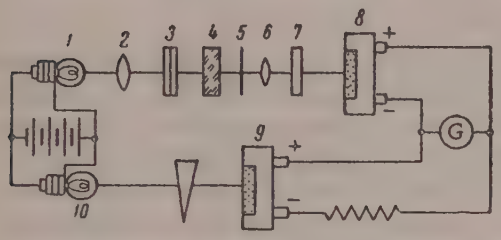


Fig. 1. Scheme of electro-optical apparatus

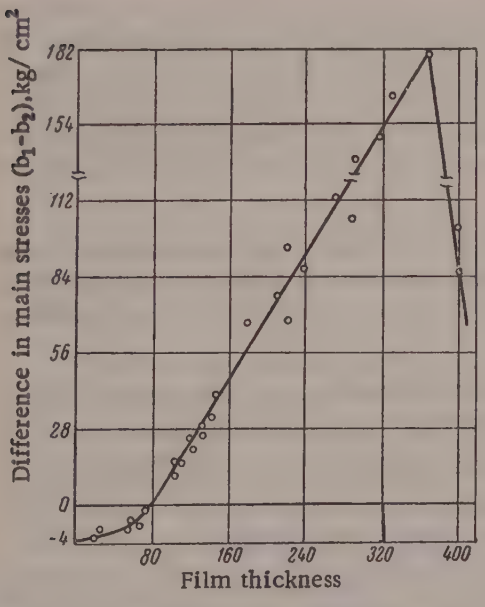


Fig. 2. Dependence of internal stresses at glass-film interface on film thickness.

For rapid measurments, we used an apparatus which we had developed, with automatic recording of the optical density The scheme of the apparatus is shown in Fig. 1.

The measurement of stresses was carried out in the following manner. A light beam from the incandescent lamp 1 is directed first through the condenser lens 2, then through the polarizer 3 to the test sample 4. Through the aperture 5 (size 0.5 × 5 mm) and objective lens 6, the polarized light strikes the analyzer 7, crossed with the polarizer 3, and passes to the measuring photoelement 8. In parallel with the measuring photoelement, there is connected the compensating photoelement 9, on which there falls a light beam from the source 10, having a diaphragm and neutral-wedge system. The compensating portion of the scheme, connected to meet the measuring photoelement, served for accurate adjustment of the null position of the electrical scheme. Plates are introduced into the optical system with the additional opacity necessary for creating an approximately linear relationship between the intensity of light passing through the sample and the birefringence in the substrate.

The recording apparatus which registers the photocurrent is an EPP-09 electronic potentiometer. The measurement of the internal stresses in various planes was accomplished by means of automatic travel of the sample stage at a rate of 4 mm/min.

The method of measuring optical density is more sensitive than the visual method. It permits detailed investigation of the change in internal stresses during film formation.

In the present work, the internal stresses in gelatin films and in the substrate were investigated. The formation of the films, as was done previously [1], was carried out on glass prisms (10 × 20 × 20 mm parallelopipeds). A film of a 10% aqueous solution of gelatin was deposited on one of the faces of the prism. The stage with the prism was placed in a chamber where the film was dried at 18-20° and rate of air movement 3 m/sec. The thickness of the films was measured with a micrometer with scale division 0.01 mm.

The magnitude of the internal stresses was calculated according to a calibration line obtained as a result of preliminary calibration of the glass prisms.

Figure 2 shows the dependence of the magnitude of internal stress on film thickness. With thin films (up to ~80 μ) the internal stresses are negative (compressive stresses). In thicker films (>80 μ) the stresses have a positive sign, and are linearly dependent on film thickness up to the limiting (critical) stress at which spontaneous breakoff of the film from the substrate occurs.

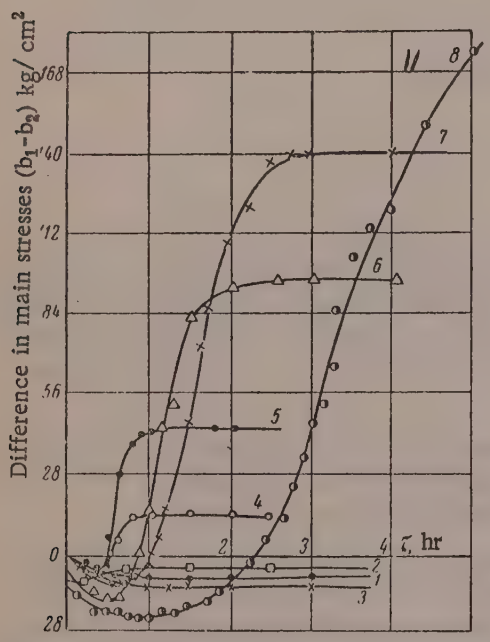


Fig. 3. Kinetics of growth of internal stresses in films of different thicknesses: 1) 20 μ; 2) 40 μ; 3) 70 μ; 4) 90 μ; 5) 140 μ; 6) 220 μ; 7) 290 μ; 8) 390 μ.

The kinetic data (Fig. 3) show that the negative stresses which we detected in the glass at the boundary with the film are manifested not only in thin, but also in thick films. The essential feature of the thin films (Curves 1-3) consists of the fact that during their formation the internal stresses are established very rapidly (30 min), have a small magnitude and retain the negative value throughout the entire process of film formation. During the formation of thicker films (Curves 4-8) the internal stresses are characterized by change of sign. In the initial period of formation (drying) of the film, the internal stresses are negative, but subsequently pass through zero and increase up to a certain positive value which depends on the film thickness. Apparently the internal stresses in thick films are distributed nonuniformly with respect to the thickness of the film.

This hypothesis was checked by investigating the distribution of internal stresses through the thickness of the films. Experiments were conducted with films of thickness up to 3000 μ. The preparation of the thicker films was accomplished by pouring the solution into a glass cuvette, the walls of which were wetted with white oil. The measurement of the stresses through the thickness of the film was carried out by the method used for measuring the stresses on the prism.

Indeed, the internal stresses were distributed nonuniformly through the thickness. However, the magnitude and distribution of the internal stresses depends not only on the film thickness, but also on the time of its formation. In the initial period of formation (24 hours after application of the solution to the surface of the glass, Curve 1, Fig. 4a) the internal stresses at the surface of the film in contact with the substrate are negative, and at the outer surface are positive. After 96 hours of drying (Curve 2, Fig 4a) the stresses at the surface of the film become negative, and at the glass-film boundary become positive. In absolute magnitude, the positive stresses exceed considerably the stresses arising in the initial period of film formation.

The sign-changing character of the distribution of internal stresses, which is related to nonuniformity of water distribution through the thickness of the sample, and the change in sign of the stresses in the process of drying have also been observed by other investigators [2, 3]. Such a distribution of stress takes place not only through the thickness of the film, but also through the thickness of the substrate.

The maximum positive stresses in the prism arise at the glass–film interface (Fig. 4b). The stresses drop off sharply with distance from the interface, and then pass through zero and change their sign to negative.

Nonuniform distribution of internal stresses is observed not only through the thickness of the film, but also through its area. The maximum stresses arise at the end of the drying process along the edges of the film (Fig. 5). In the middle portion of the film, the stresses are relatively low and have a sign opposite to that of the edge stress.

The kinetic curves of the growth of internal stresses at different points in the area of the film (Fig. 6) show that in the initial period of film formation, the maximum internal stresses arise in the middle portion of the film surface. At the end of the process of film formation, the zone of maximum stresses is shifted to the edge of the film at the glass–film interface.

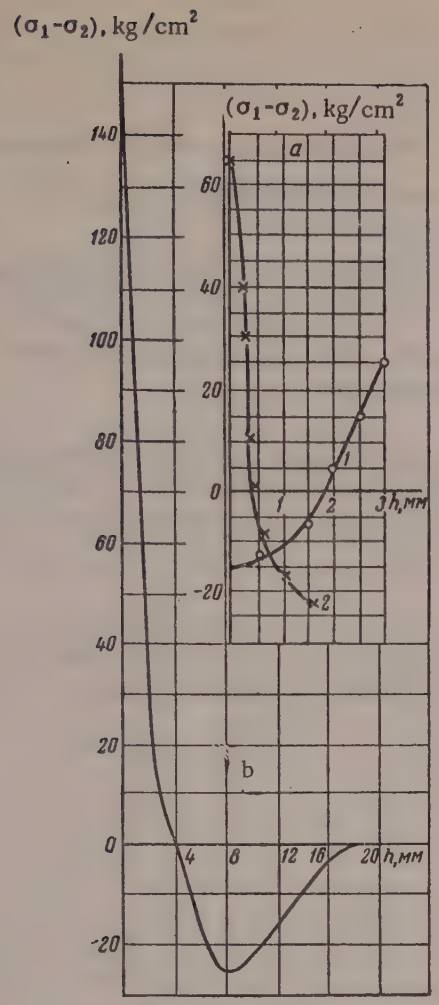


Fig. 4. Distribution of internal stresses: a) through thickness of film during its formation, in 24 hrs (1) and 96 hrs (2); b) through thickness of prism for film thickness 390 μ in 5 hrs drying.

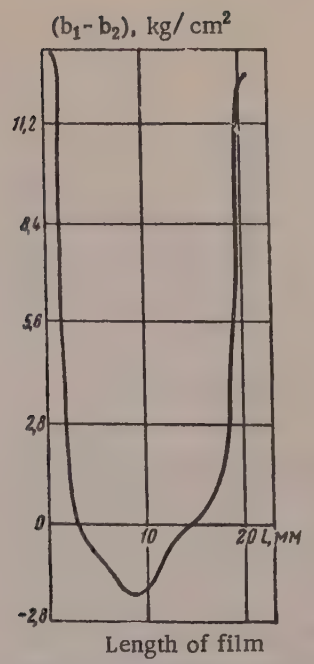


Fig. 5. Distribution of internal stresses along the length of film with 240 μ thickness.

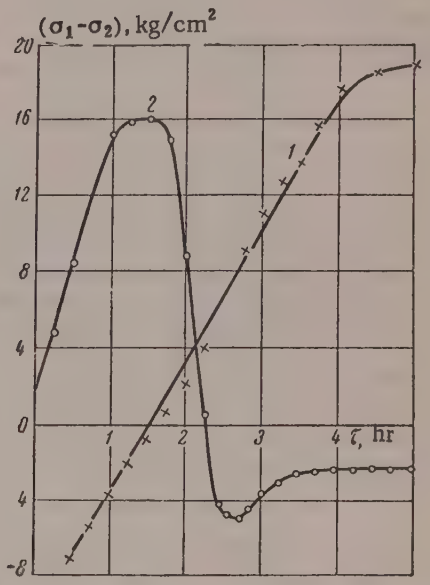


Fig. 6. Kinetics of growth of internal stresses at a distance of 1 mm (1) and 5 mm (2) from edge of film.

The magnitude of the internal stresses can be reduced not only as a result of a decrease in film thickness, but also on account of an increase in the concentration of the initial solution.

Kinetic curves are shown in Figure 7 for the growth of internal stresses in the substrate at the film boundary, obtained from solutions of differing initial concentration. Identical final thicknesses were attained by selection of the solution volumes.

From the data of Fig. 7, it is evident that with an increase in concentration of the initial solution the limiting values of internal stresses are decreased. An especially significant difference in magnitudes of the internal stresses with a change in initial concentration is observed with large film thicknesses. The internal stresses of the films obtained from the more concentrated solutions relax more slowly and retain the negative sign through a longer time interval.

These results are in accord with previously published data [3], from which it follows that with an increase in initial solution concentration, the strength of adhesion is increased.

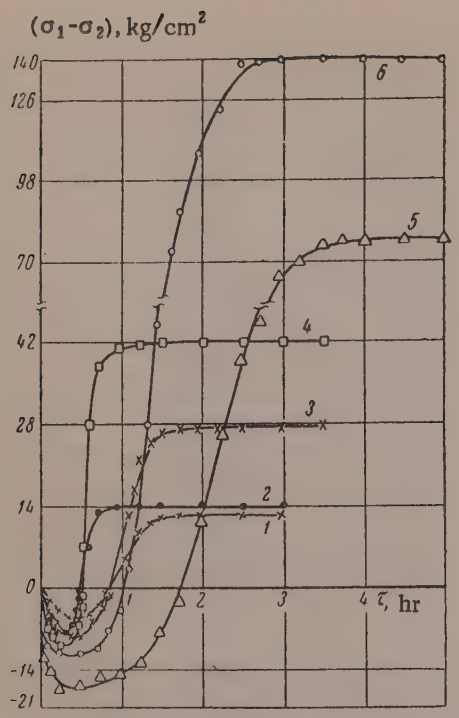


Fig. 7. Influence of initial solution on the kinetics of growth of stresses in films of differing thicknesses: 1, 3, 5) for 40% solution; 2, 4, 6) for 10% solution, with film thicknesses respectively of 100, 150 and 300 μ.

SUMMARY

1. A new system of an optical apparatus with automatic recording has been proposed for measuring internal stresses in polymeric coatings.

2. The limiting stresses in thick and thin films differ in sign.

3. The internal stresses are distributed nonuniformly through the thickness and area of the films.

4. In the process of film formation, a change in sign of the internal stresses is observed.

5. The internal stresses arising in the films depend on the initial solution concentration.

LITERATURE CITED

1. S. A. Shreiner, P. I. Zubov, Dokl. AN SSSR 124, 1102 (1959); Kolloid. Zh. 22, 496 (1960).
2. B. N. Ugolev, Zavodsk. laboratoriya 18, No. 12, 1505 (1952); 21, No. 10 (1955); I. V. Krechetov, Wood Drying, Moscow (1956).
3. A. V. Lykov, Heat and Mass Exchange in Drying Processes, State Power Engineering Press, Moscow (1956).
4. S. A. Shreiner, and P. M. Shchubov, Kolloid. Zh. 5, 651 (1957).

All abbreviations of periodicals in the above bibliography are letter-by-letter transliterations of the abbreviations as given in the original Russian journal. *Some or all of this periodical literature may well be available in English translation.* A complete list of the cover-to-cover English translations appears at the back of this issue.

FLOCCULATION IN THE ELECTROPHORETIC DEPOSITION OF CARBONATE SUSPENSIONS

I. S. Lavrov

Lensovet Leningrad Technical Institute

Translated from Kolloidnyi Zhurnal, Vol. 23, No. 4,
pp. 423-427, July-August, 1961
Original article submitted February 10, 1960

The electrophoretic deposition of suspensions to form coatings, for example, on the surface of the heating elements and on the cathode emitters of radio tubes is widely used industrially. The formation of a coating by the electrophoretic method depends to a considerable degree on the aggregational stability of the suspensions [1-4].

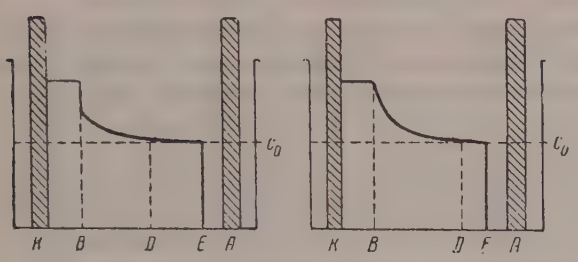


Fig. 1. Change in concentration of suspensions in the interelectrode volume as given by Hamaker and Verwey: K) cathode; KB) deposited layer; BD) layer of suspension with increased concentration; DE) layer of constant concentration; EA) epi-anode layer; C_0) initial concentration of suspension; A) anode.

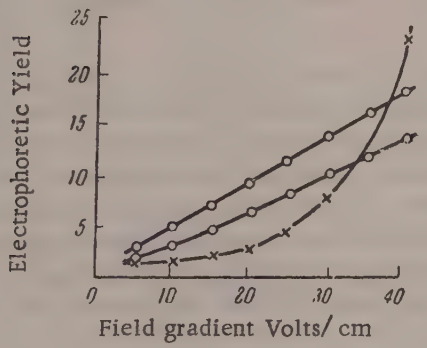


Fig. 2. Electrophoretic yield as a function of the voltage gradient in the field: 1 and 2) stable suspensions; 3) unstable suspensions.

Hamaker and Verwey [1] point out the analogy with the formation of a deposit in the sedimentation of electrophoretic deposition of particles, noting that in both cases the unstable suspensions give loose deposits, while stable suspensions give dense deposits. It is also recognized that the principal role of the electric field consists of transferring the suspended particles to the electrode surface and compressing the deposit: with unstable suspensions, the particles collect into flakes, and these are what form the deposit. Interaction of the particles prevents packing of the precipitate.

Investigators in the field point out that there are two possible forms for the variation in concentration of particles in the interelectrode volume (Fig. 1, a, b). After the electrophoretic deposition of the particles has been going on for some time, a layer of deposit of approximately constant concentration is formed on the electrode. After the layer of deposit follows a layer of suspension in which the concentration of particles drops off gradually and reaches a practically zero value in the layer adjacent to the opposite electrode. A particle concentration distribution of this sort can occur when using stable suspensions, but if insufficiently stable suspensions are used, the picture of the variation in concentration in the layers follows the scheme shown in Fig. 1, b.

Stable suspensions are usually used to prepare high quality electrophoretic coatings. It has been shown that the yield, i.e., the weight of deposits per unit surface of the electrode, is directly proportional to the concentration, the deposition time and the intensity of the field [3]. For slightly stable and unstable suspensions, no such law exists. The reason for the absence of any such law must be sought, in our opinion, not so much in the polarization of the electrode [1], as in the complicated processes involved in coagulting the suspensions. The mechanism of formation of the electrophoretic deposit must be very complicated and closely bound up with the coagulation process, since, in electrophoresis, electrolysis of the dispersing medium occurs, along with a change in the ionic concentration in the epi-electrode volume which accelerates the flocculation. From this point of view, any idea of

the electrophoretic deposit being formed by particle sedimentation is unsatisfactory, and so we have made visual observations on the behavior of the particles in the interelectrode volume during the electrophoretic deposition of particles from stable, slightly stable and unstable suspensions.

The suspension subjected to electrophoresis was a triple carbonate of alkaline earth metals [$(BaSrCa)(CO_3)_3$] in methanol, acetone and mixtures of the same. The suspensions were prepared by pulverizing the thoroughly baked carbonate powder in a porcelain ball-mill in the presence of the dispersing medium. The relative stability of the suspensions was estimated from the volume of the deposits ultimately formed on sedimentation. The suspension in methanol was the most stable, in (1:2) methanol acetone mixture it was moderately stable, and in acetone it was unstable. The ratio by weight of carbonate to medium was kept constant at 1:1.5 in all cases. The deposition was carried out on a nickel electrode at potential gradients from 5 to 40 volts/cm. The source of direct current was a voltage stabilized vacuum-tube rectifier provided with a time relay.

The yield as a function of voltage (Fig. 2) shows that the yield is directly proportional to the potential gradient in the field for the first and second (that is, for the relatively stable) suspensions. However, in the acetone suspension, the yield changes very little when the gradient is increased to 25 volts/cm and then rises sharply, exceeding the yield reached by the stable suspensions.

Since the sedimentation of the particles in the acetone suspension results in a loose deposit, we should also expect unpacked loose deposits from the electrophoretic deposition of such suspensions.

We determined the density of the dry coatings on an emitter prepared by three seconds electrophoresis from suspensions in methanol and methanol acetone mixture at gradients of 30 volts/cm and in acetone at 40 volts/cm for two seconds. After drying in air for fifteen minutes, the deposits were weighed and the geometric dimensions of the deposits were determined with an IZA-2 horizontal comparator.

The greatest density (2.9 g/cm^3) was found for the deposit prepared from the methanol suspension. The methanol-acetone-carbonate suspension has nearly the same stability; nevertheless, the density of the deposit was considerably less (2.2 g/cm^3). In our opinion, this may be explained if we recognize that the electric field accelerates the coagulation of the suspensions. This most probably occurs because of the considerable change in concentration of ions in the epi-electrode layers resulting from electrolysis of the dispersing medium.

The suspension of the triple carbonate in acetone is flocculant, but on mixing with a stirrer or by supersonic vibration, the flocs are destroyed and appear in appreciable quantity again only after fifteen to twenty minutes undisturbed standing of the suspension. Since the electrophoresis of the suspension was carried out immediately after the mixing, the flocculation could not be very considerable unless the electric field had some effect on the process. Apparently, the loose electrolytic deposit (density 1.8 g/cm^3) again, in this case, is caused by accelerated coagulation of the suspension under the influence of the change in ionic concentration in the epi-electrode layers. It seemed as though the electrophoretic deposition of the methanol suspension, with some electrolyte added to it, was accompanied by a lowering in the density of the deposit, the more so, the higher the concentration of electrolyte in the dispersing medium.

Visual observation of the behavior of the particles in the interelectrode volume was carried out in these same suspensions. The electrophoresis was done in a narrow vertical glass cell with plain parallel walls (3 × 20 × 25 mm). Observation of the motion of the particles in an interelectrode space was accomplished by means of a horizontal microscope. On passing the current through the suspension, the accelerated sedimentation of the particles was readily discerned. This fact is confirmed by the change in concentration of particles with time in suspensions subjected to the action of an electric current. Table 1 shows the results of measuring the concentrations during the sedimentation of a methanol suspension in a larger cell (20 ml). The samples were taken out of the suspension from a depth of 10 mm with micropipettes previously dipped into the suspension. The carbonate content of the samples was determined by a gravimetric method.

The accelerated settling of the particles to the bottom of the cell in the electric field as compared with ordinary sedimentation is a direct indication of the coagulating action of the current on the suspension. Comparison of the density of the deposits obtained also indicates coagulation of the suspension in the electric field. The deposit from ordinary sedimentation has a density of 1-1.1 g/cm^3 while the density of deposit prepared from passing current through the suspension is 0.7-0.8 g/cm_3. A deposit of this sort is easily loosened up by agitation and peptized. The instability of the bond between particles which leads to the formation of reversible coagulated structures permits us to assume that the asymmetric particles are oriented in a definite fashion in the electric field.

Using the method and tha apparatus developed by Tolstoi and Apartakov [5], we observed the phenomenon of undulant modulation of polarized light going through the suspension perpendicular to the direction of an electric field formed by rectangular electrical pulses. This phenomenon shows that the particles in suspension of all more or less polar media have a a stiff dipole moment (this is not observed in xylol suspensions of carbonate) and consequently, they are oriented in an electric field.*

TABLE 1. Change in Concentration of a Methanol Suspension during Particle Sedimentation

Time from beginning of experiment, min.	Carbonate concentration in the suspension, g/cm^3	
	without current	with current
0.0	0.9901	0.9901
0.5	0.9582	0.5489
1.0	0.7670	0.4927
2.0	0.7416	0.1109

The orientation of the particles and their concentration in the epi-electrode volume can lead to the formation of chains of particles or more complex space structures. Thus, in studying the action of the electric field on suspensions of metals, cuprous oxide and boron carbite in benzene, nitrobenze and other media, Gindin and Putilova [6] were able to observe the formation of chains and more complex space structures of particles, forming continuous bridges between the electrodes. We did not observe any structural formations of this sort in our suspensions under the deposition conditions used. However, the visual observation of the electrophoretic motion of the particles of the triple carbonate in methanol-acetone mixtures, and consequently in suspensions of different stability, enabled us to observe considerable differences in their behavior.

As a result of the electrophoresis of stable suspensions at a gradient of 30 volts/cm, and with long continued passage of current, we observed a concentration of positively charged particles at the cathode, and the formation of a dense deposit on the electrode surface. As we leave the cathode, the concentration of particles drops off and in the epi-anode layer there is a marked rarification of the suspension, i.e., in this case, the electrophoretic deposition process follows the schemes discussed above [1]. However, the electrophoresis of these same suspensions at gradients of 100 volts/cm and higher is much more complicated, and even more obviously so in suspensions which are not particularly stable. In analogy with Hamaker and Vewey's views [1], the process may in this case be represented by a more complicated scheme (Fig. 3). A dense coating is formed on the cathode which changes suddenly into a layer of rarified suspension 1-2 mm wide. Adjoining this layer, we find, first, layers with increasing concentration, then, layers with decreasing concentration, as we approach the anode. Near the anode, as in the first case, a layer of rarified suspension is maintained. When the electrophoresis has got itself going, we observed particle currents at the cathode and anode surface moving from bottom to top of the cell, which pile up into a more concentrated suspension over the whole surface of the suspension in the interelectrode space. In the middle part of the interelectrode volume, the concentrated suspension moves down and leaves a considerable quantity of adherent particles on the bottom of the cell, and subsequently moves either to the cathode or to the anode. On the bottom of the cell, the deposit is not laid down uniformly and there is always a greater quantity of it at the middle part of the bottom of the cell.

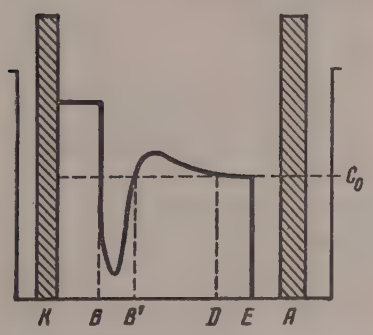


Fig. 3. Change in concentration of suspension in the interelectrode volume: K) cathode; KB) layer of deposit; BB') epi-anode layer; B'D) layer of increased concentration; DE) layer of constant concentration; EA) epi-anode layer; C_0) initial concentration of suspension; A) anode.

* As was shown by the calculations in [5] the dipole moment of the particles of the suspension is very large and may be a million times larger than the dipole moment of simple molecules.

The qualitative picture of the distribution of particles in the interelectrode volume during electrophoresis is confirmed quantitatively by the relation between the concentrations of the suspensions and the vertical epi-cathode, middle, and epi-anode layers. Samples of the suspensions were taken out with micropipettes, immersed to a depth of 15 mm, from all the layers simultaneously after two minutes electrophoresis (Table 2).

The picture which we are considering of the electrophoretic deposition of particles in slightly soluble suspensions is apparently correct for all suspensions, since the destruction of aggregational stability during electrophoresis at medium and high gradients occurs even in stable suspensions. The flocculation which develops here is reflected by the porous structure of the electrophoretic deposits.

TABLE 2. Concentration of Suspension During Electrophoresis

Medium	Concentration of suspension in the layers		
	near cathode	in intermediate layer	near anode
Acetone 92% + methanol 8%	0.404	0.660	0.432
Acetone 50% + methanol 50%	0.668	0.666	0.473

The new experimentally discovered scheme of particle distribution in the interelectrode volume during the deposition process adds substantially to Hamaker and Verwey's theory. Proof of the existence of coagulational processes in the electrophoretic deposition of suspensions makes it possible to introduce a number of important changes into the practical production of electrophoretic coating.

SUMMARY

1. Under the influence of an external electric field in suspensions subjected to electrophoresis one observes not only electrophoretic displacement of the particles to one of the electrodes, but acceleration of particle sedimentation as well, the more so, the less the aggregational stability of the suspensions.

2. From the experimental data on the change in concentration of the suspension during electrophoresis, and from observation of the displacement of the suspended particles, a new scheme has been formulated for the distribution of particles in the interelectrode volume of the suspension, which takes account of coagulation.

3. The formation of the electrophoretic deposit has a coagulational character.

LITERATURE CITED

1. H. C. Hamaker and E. J. W. Verwey, Trans. Faraday Soc. 36, 180 (1940).
2. S. A. Troelstra, Philips techn. Rundschau 12, 297 (1951).
3. J. Th. Overbek and H. Koelmans, Disc. Faraday Soc. 18, 52 (1954)
4. G. A. Egerer, G. Landsberg, Z. Elektrochem. 59, 3, 207 (1955).
5. N. A. Tolstoi and A. A. Spartakov, Dokl. AN SSSR 100, 5 (1955).
6. L. G. Gindin, I. N. Putrlova Kolloidn Zh. 16, 325 (1954).

All abbreviations of periodicals in the above bibliography are letter-by-letter transliterations of the abbreviations as given in the original Russian journal. *Some or all of this periodical literature may well be available in English translation.* A complete list of the cover-to-cover English translations appears at the back of this issue.

MECHANISM OF RUBBER REINFORCEMENT

A. I. Lukomskaya

Scientific Research Institute of the Tire Industry, Moscow
Translated from Kolloidnyi Zhurnal, Vol. 23, No. 4,
pp. 428-437, July-August, 1961
Original article submitted March 26, 1960

In spite of the present day technical importance of reinforcement with resin fillers and the exceptionally wide distribution of this phenomenon in everyday technological practice, the essence of the phenomenon cannot, at the present time, be considered satisfactorily explained, in any sense of the word. Numerous experimental facts accumulated from practical experience and from special investigations carried out to discover the laws governing the mechanism of reinforcement, have led to contradictory conclusions in more than one case. As a result, there is no unity of opinion as to the basic causes of reinforcement. Meanwhile, the time has come to shift attention from the study of the separate aspects of this complicated process to the job of finding out how they interact to give the one final result of reinforcement. One reason for this is to be found in the investigations of recent years, the value of which becomes evident if we consider the logical ways in which the ideas relative to the reinforcement mechanism have developed.

The reinforcement of resins results in increased rigidity and increased strength indexes. The most reinforcing, or most active fillers, are found to be some types of carbon black [1].

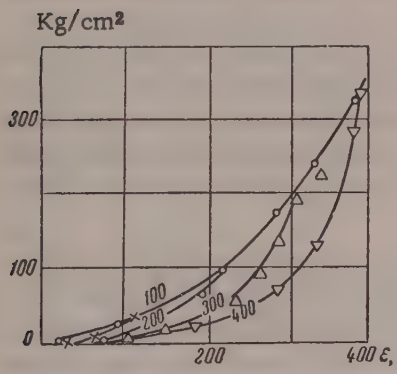


Fig. 1. Extension curves of previously worked SKB samples containing 40% by weight of channel black (the numbers on the curves are the numbers of previous deformations) [23].

Unquestionably, the basic condition for reinforcement is that the rubber must be brought into direct interaction with the reinforcing filler. Thus, for example, there is no reinforcing effect in a latex, since the globules are protected by a coating of nonrubber constituents and reinforcement appears only under the action of destabilizing agents, which give the fillers free access to the rubber hydrocarbon [2]. A natural consequence of the above fact is that the majority of investigators consider that a stable bond must be formed between the rubber and the filler [3-8].

Previous papers dealing with the reinforcing mechanism [4-6] have pointed out the analogy between the strengthening of rubber by vulcanization with sulfur and reinforcement with fillers. It has been shown that the chemisorption of the rubber and the other constituents of the mixture occurs on the surface of the filler particles. Therefore, the more active the filler, the greater the fraction of the rubber which it converts into the film state as such [7]. In this state, the rubber shows the properties of increased rigidity and strength. The anomalous mechanical properties of rubber films have been described in several papers [9]. It is also known that after the addition of carbon black, a fibrous x-ray structure diagram of the vulcanizate is found at low degrees of extension [10], which shows the orientation of the rubber in the presence of the filler. The inconsistency of the adsorptional theory of vulcanization is completely obvious at the present time [11].

If we stop to consider the fact, that, at temperatures above 180°, filled resinous mixtures made of sodium, butadiene rubber (SKB), heated for about forty minutes, have a limiting tearing strength of 44 kg/cm^2, instead of 10 kg/cm^2 as for unfilled SKB heated under the same conditions, we are apt to come to the conclusion, [5], that heating SKB mixtures at high temperatures is a vulcanization process. However, this conclusion has little foundation, since filled sulfur vulcanizates made from SKB have substantially higher strength, of the order of 100 - 150 kg/cm^2. The filled unvulcanized mixtures are also considerably stronger than the unfilled ones, i.e., the reinforcement takes place without vulcanization or heating. Finally, SKB rubber structurizes at high temperatures under the influence of oxygen, giving increased strength even in the absence of carbon black, [12] and [13]. This is not observed on heating a sulphur-free, filled mixture, made from NK, which destructurizes under the influence of oxygen.

The idea that the polymeric molecules of rubber are bound to the carbon black through sulfur "bridges" [4] is in contradiction to the data which shows that the dipole moments of filled and unfilled vulcanizates are equal [14-16]. In addition, if we are to some degree willing to recognize the usefulness of studies in which the behavior of the low molecular analogs of rubber serves as a model, it is interesting to note that the reaction of squalene with carbon black is independent of the presence of sulfur in the system [17]. Bringing up the analogy between vulcanization and filling must be considered unfortunate. For one thing, the quantity of filler which must be added to produce noticeable strength and rigidity is considerably greater than with sulfur. Further, the effect of the sulfur shows up only after vulcanization. Here the sulfur reacts chemically with the rubber, as is shown, for example, by the appearance of dielectric dipole losses, caused by the presence of sulfur dipoles [18] which line up in the electric field. The presence of "bridging" sulfur, which in vulcanization unites the individual rubber molecules into a single space network, is confirmed by the absence of flow in the vulcanizates, i.e., they do not show unlimited increase in deformation under the action of a constant stress at moderate temperatures. Adding carbon black does not stop flow of the resin mixture, but only produces a substantial increase in the viscosity of the material. Consequently, the theory of reinforcement with fillers in which the carbon black particles are stable nodes of the rubber space network is not immediately confirmed.

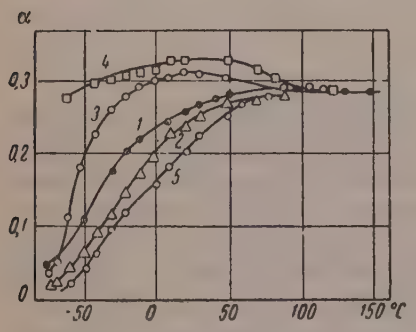


Fig. 2. Temperature dependence of the relaxation time distribution parameter α for rubber vulcanizates without carbon black (1) and containing 10 (2), 15 (3) and 20 (4) volumes of channel gas black or 10 (5) volumes of thermal black.

The adsorptional theory is more realistic. However, this theory does not touch on the question of the nature of the interaction, i.e., whether it is of chemical or physical nature.

Watson [19], from data on the formation of free radicals by mechanical treatment of the rubber, interprets the reinforcement of the latter as the result of the interaction of the radicals with the surface of the carbon black particles. As against this point of view, practically equivalent reinforcement [2] may be achieved even in the absence of mechanical working on rolls, by adding fillers to a de-stabilized latex, for example. Watson's data also shows that the carbon black maintains its reinforcing properties to a considerable degree, even after suppressing the acceptor functions of the surface groups (relative to the free radicals) by special chemical modification of the surface.

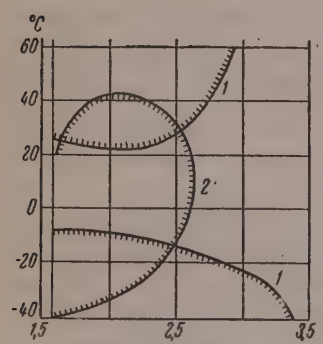


Fig. 3. Nodal tearing regions (inside the curves, the direction is shown by hatching) of filled vulcanizates made from SKB: 1) with 60 parts by weight of channel, and 2) with 60 parts by weight of thermal black from tests according to ASTM D 624-54 on type B samples with 1 mm cut.

It should be noted that the only convincing proof of the existence of stable bonds between the rubber and the filler is the formation of insoluble carbon black-rubber jells [12] by rolling and heating the carbon black mixtures. Also, as follows from what we have said, rolling and heating are not indispensable to reinforcement. At the same time, a number of experimental facts can be grasped only in the light of the idea that the deformation of filled resins is accompanied by destruction of the rubber–filler interphase boundary. A substantial reduction is shown in the rigidity of filled resins after preliminary deformation [20-23]. Figure 1 shows the data of [23]. Similar results of Mullins show that on repeated deformation, the stress–deformation curves approach the curve which is found for unfilled vulcanizate. The effect of the previous deformation history applies only to such degrees of deformation as were limiting in the previous history [21-23]. Depending upon conditions, the equilibrium modulus for static and dynamic deformations approaches asymptotically, with increase in the maximum previous deformation, to the equilibrium modulus of the corresponding unfilled vulcanizate [23]. The more the filler increases the rigidity of the resin, the more the modulus is reduced after previous extension. If the resin is allowed to rest, some of the rigidity lost by previous stretching is recovered. It has been found that the tearing resistance of previously stretched samples is reduced considerably in a direction parallel to the previous stretching [24]. The value of the tearing resistance of filled vulcanizates is in this case likewise close to that of the corresponding unfilled

vulcanizates [24, 25]. Since the reinforcement occurs only under conditions in which the rubber interacts directly with the filler [2], we may assume that the previous deformation, which lowers the reinforcing effect, destroys the rubber–filler bonds. Consequently, the rubber–filler interface region is a weak spot in the structure of the filled vulcanizates.

The destruction of the rubber–filler bonds occurs not only on complete failure of the filled resins, but even at deformations lower than the tearing value. It is also observed under the influence of thermal action. Thus, for example, in unfilled vulcanizates, the range of dipole relaxation times [16] becomes smaller with increasing temperature, reaching a constant value at 100-120°. This is treated as a gradual elimination of the role of the weaker intermolecular bonds in the dipole orientation process.

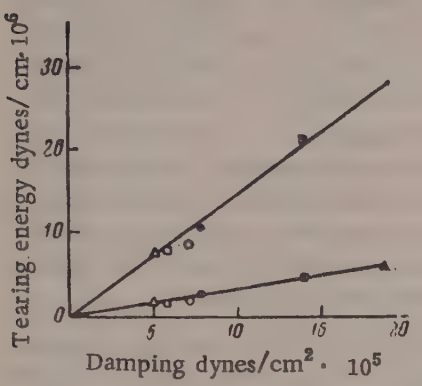


Fig. 4. Characteristic tearing energy as a function of damping [29].

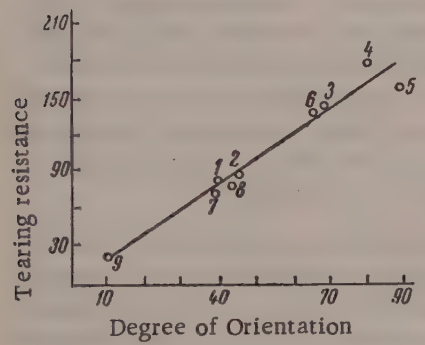


Fig. 5. Tearing resistance as a function of the degree of molecular orientation in resins made from sodium butadiene rubber with the following fillers: 1) channel black; 2) spray black; 3) stove black; 4) lamp black; 5) thermal black; 6) athracene black; 7) and 8) silicic acid; 9) without filler.

With filled vulcanizates, independent of the type or content of carbon black, at 100-120°, the parameter giving the range of relaxation times is always the same, and equal to the value for an unfilled vulcanizate made from the same starting material (Fig. 2). Hence it follows that in dipole orientation, the stable rubber–filler bonds (if there are any such) play no role, as is the case in mechanical deformation [20-23], since after rupture of the weak rubber–filler bonds, the filled vulcanizates behave as though they contained no filler.

The most convincing proof of the destruction of the rubber–filler interface boundary was the direct observation of the tear in the surface of filled vulcanizates with an electron microscope [26]. It was shown that the concentration of carbon black particles on the failure surface was greater than in the volume. Consequently, the tearing proceeds in a direction going from one filler particle to another.

It is a well known fact that the reinforcing action of fillers shows up especially clearly with an uneven failure surface (rough or even nodal tearing) [25-27]. In nodal tearing, the direction of failure does not follow the regions of maximum stress concentration, which arise from the form of the sample being torn or from the method of applying the deforming force.

Figure 3 shows the location of the regions mentioned for vulcanizates made of sodium butadiene rubber (SKB) with channel and thermal blacks [25]. Usually, the nodal tearing regions are found at higher velocities and higher temperatures. In all cases, the increase in strength due to the presence of the carbon black is observed to occur at the lower velocities, and becomes considerably less at the higher velocities [25-27].

Under adiabatic deformation, the filled and unfilled resins show the same thermal effect per unit of deformation work [28]. This shows that the reinforcing role of the filler is absent in rapid processes.

The data given indicate that the occurrence of nodal tearing, and the maximum reinforcement effect in tearing appearing with it are possible only in case the deformation time is sufficient to allow it to develop. Consequently, the reinforcement is caused by processes which take time. When the rate of the processes in question is comparable with the deformation processes, reinforcement is possible.

The data of [29] also show the role of the time factor from the linear dependence between the tearing energy and the hysteresis properties shown in Fig. 4. The resins with the greater hysteresis also have greater resistance to tearing. On samples deformed by tearing "of simple stretching type" it has been shown theoretically and experimentally [30] that the characteristic tearing energy (H) is related to the energy of stretching the rupture (E) by the simple

formula: $H = dE$, where d is the effective diameter of the top of the cut in the sample being torn, which represents the dimensions of the place where the failure occurs. It has been shown [27] that nodal tearing is related to an increase in the effective diameter of the top of the cut.

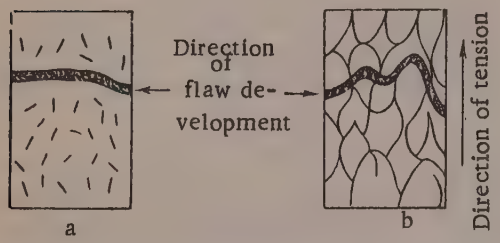


Fig. 6. Scheme of development of a flaw in rupturing resins with different filler distributions: a) a mixture containing inactive filler; b) a mixture containing active filler chain structures.

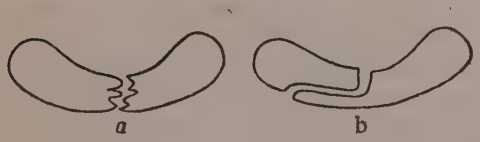


Fig. 7. Nodal tearing of filled vulcanizates using a) thermal black and b) channel blacks.

Comparing the facts relative to the mutual relationship between the tearing energy and hysteresis losses, the reduction in rigidity after previous stretching and the increase in diameter of the top of the cut with growth of the cut in rough tearing along the rubber–filler interface surface, a very probable and convincing explanation has been found for the reinforcement effect, according to which considerable stress relaxation occurs in filled vulcanizates under constant deformation. As a result of the relaxation in the highly deformed zone near the top of the spreading cut, a local reduction in modulus occurs, and along with it an increase in the diameter of the top of the cut. Since the stress concentration is thus lowered, higher mean stresses have to be applied to the sample to enlarge the cut any further. The relaxation is again repeated, along with an increase in diameter of the top of the cut, and the tearing occurs in jumps.

The reinforcement mechanism considered must be refined from the point of view of molecular concepts, in view of the numerous data on the effect of structure [14-16, 27, 31-37], dispersion [3, 5] and the surface activity of the filler [14, 38].

A characteristic property of the reinforcing fillers is their ability to form chainlike structures in the rubber medium [14, 31, 34]. The degree of structure formation has been evaluated for carbonatious blacks from the electrical resistance [31, 34] and from the dielectric properties [15, 16] as well as from electron microscope studies [34, 35], for bentonites by the method of swelling [31], for colloidal silicic acid by alkaline extraction [34]. In these papers, it was shown that the increase in the limiting rupture strength [31, 34] and the tearing resistance [27, 37] are parallel with the degree of structurization.

From data on the measurement of electrical conductivity [32, 33] and dielectric losses [39], heating and deformation lead to destruction of the carbon black structures, while resting the sample reestablishes them, but in the case of active blacks, the most stable distribution seems to be the distribution in chains [33]. The difference in stability of the carbon black structures is reflected in the curves of mechanical properties as a function of temperature for carbon black vulcanizates given in [33, 37].

For filled vulcanizates made from SKB and SKS-30 containing channel black in quantities sufficient to form carbon black structures, two regions of nodal tearing have been observed in [25]: the one, at relatively high temperatures and low velocities, and the other at lower temperatures and high velocities, Fig. 3. Lowering the channel black content causes the disappearance of the high temperature region and displacement of the low temperature region to higher temperatures and velocities.

The first nodal tearing region for filled resins made of SKB and SKS-30 containing channel blacks is caused by the presence of carbon black chains, while the second region, occurring also in resins with thermal blacks, comes from the presence of isolated carbon black particles.

The presence of filler chain structures is the basic factor in reinforcement [14]. The chain structures serve as the matrix on which the molecular rubber chains are laid down and orient themselves. The more developed the chain structure is, the greater the degree to which the rubber is oriented even in lengthening the size of the tear. This was confirmed in [36] by x-ray data, Fig. 5. The effect of orientation (in the limit of crystallization) is to cause increased strength of the rubber. The chain structures determine the topography of the development of flaws in tearing, since the presence of the filler structure prevents the development of a tear in the direction normal to the applied force. The path of development of the flaw is enlarged. The effective surface of the tear increases

which causes an increase in strength of the sample, Fig. 6. In addition, the presence of thixotropic chain structures increases the viscosity of the system, and favors the development of relaxational processes.

In its time, an interesting paper [40] was published, in which the authors divided rubbers into those which crystallize on stretching, and those which do not so crystallize. The first of these are sufficiently strong without filler and are only slightly reinforced by filler, while the second kind requires reinforcement. In the opinion of the authors, the crystals formed by stretching rubbers in the first group play the role of an active filler and increase the strength of the resin. The role of the filler is to promote equalization of the stresses in the resin sample.

We can imagine the following picture of deformation and failure of filled resins. Under stress, the rubber–carbon black bonds formed in chaotic disorder during mixing are broken and again reestablished in new positions, fastening onto the surface of the filler of the rubber molecules, which are partly straightened out (oriented) in the direction of the acting forces. As a result of this, in stretched filled resins, we can observe the increased content of oriented rubber phases by means of x-rays.

As a result of the processes mentioned, equalization of the local over-stresses or local relaxation of the stress occurs. It is understandable that the greater the strength of the rubber–filler bonds, the greater the increase in stress which occurs on subsequent increase of the deformation along with the further orientation of the rubber molecules which accompany it. However, the strength of the rubber–filler bonds cannot be infinitely large because otherwise we could not have the advantageous rupture of these bonds and we would not have the mechanism described, which leads to such substantial increase in the required deformation force.

The presence of carbon black structures in the resin increases the number of bonds broken in one desorption event, since the carbon black particles, the surface of which is a weak part of the material, are in the immediate vicinity of one another. This simplifies the transition from one weak rubber–filler bond to another.

The total deformation energy (for deformations below failure), either the energy of rupture or the energy of tearing (in failure) is given by the product of the number of ruptured bonds by the energy of a single bond. Therefore, increasing the size of the failure region (number of bonds being ruptured) causes the energy to increase. Thus, in the presence of carbon black structures, we should observe a substantial increase in the rigidity and strength. As one of the important facts which confirm the role of the carbon black structures in lengthening the failure path, it should be noted that the nature of the nodal tearing of the vulcanizates is different, depending upon whether they are made with thermal (unstructures) blacks or channel black (of the sort which forms chains). See Fig. 7.

With vulcanizates made of thermal blacks, the failure line returns one or more times to its original direction, which corresponds with the largest stress concentration. However, with vulcanizates made with channel blacks, the failure line may wander far off without returning to its original direction. This is explained by the fact that in the first case the tear goes from one filler particle to another, the particles being separated from one another by a considerable volume of the rubber phase. The failure oscillates around the region of maximum stress concentration (the axis of the sample being torn). In the second case, leaving the region of concentration, the failure encounters an extensive region of weakened bonds which follow along the carbon black chains.

The basic causes of reinforcement obviously follow from the deformation and failure mechanism which we have just considered. The fillers and in particular, the chain structures which they form, provide the topography followed by the development of flaws and the failure path of the material. They favor an increase in the effective surface of the tear. The development of flaws proceeds in directions where the interaction forces between the structural elements are smallest.

The stress relaxation which occurs from the rupture of the weak rubber–filler bonds necessarily produces an increase in the deforming forces required to produce failure of the material. Thus, the equalization of stresses in the deformation process and the enlargement of the failure path are the reasons for the increase in the total stress in rupture tearing or in the limiting strength of the filled resins. Along with this, orientation of the rubber molecules occurs, which is more effective in the presence of fillers, and especially of filler chain structures, as a result of the fixing of the oriented molecules by newly formed rubber–filler bonds. Orientation (alignment) of the rubber molecules causes increased rigidity of the material. It is natural that the more dispersed fillers will show more reinforcing action, since, having a more widely developed surface, they give a larger number of rubber–filler bonds. However, excessively stable bonds cannot play a role in the reinforcement mechanism just described since they cannot be ruptured. Also, this mechanism cannot occur at high deformation rates (during times which are too short for it to occur). Thus, both deformation and failure of the material proceeds, in the first instance, by rupture of the weakest

(intermolecular) bonds. A similar treatment of the deformation mechanism has already been presented in [41], in which the vulcanizates were considered as a space network made up of primary chemical and secondary intermolecular bonds, and it was assumed that the equilibrium value of the modulus is reached as soon as the rupture of the secondary bonds is completed.

Similar assumptions lie at the basis of [42], in which the reinforcement mechanism is considered in the light of the theory of the strength of unfilled noncrystallizable vulcanizates, which was worked out by the author. The latter is based on the assumption that in unfilled vulcanizates, during deformation, the portions of the molecular chains which are located between nodes of the space network are nonuniformly stressed. Failure begins with the rupture of over-stressed portions of the chains. The force, first taken up by the ruptured portions, is transmitted through the nodes of the space network to the neighboring portions.

Bueche has made a calculation of strength as a function of the degree of cross linking and other parameters, in particular, the factor q, which shows to what extent the remainder of the force, formerly acting on the ruptured element, is transferred to neighboring parts of the chain.

The curve of strength as a function of the degree of cross-linkage goes through a maximum, which is in good agreement with the following trivial fact: the strength of insufficiently vulcanized and overvulcanized resins is less than the optimum.

The role of the filler as well as the crystals formed by stretching some rubbers, in Bueche's opinion, consists in the fact that they favor the spread of the excess force occurring at the tear over more widely distributed neighboring regions. In unfilled vulcanizates, the factor q is close to 0.5. This shows that the excess stress is approximately divided in half between two neighboring parts of the chain. In filled vulcanizates $q \approx 0.32 - 0.35$, i.e., through the relatively large filler particles which are the actual transmitting links, as well as through the nodes of the space network, the torn portion is connected with a number of neighbors greater than 2. Unfortunately, the treatment given is not confirmed by any auxilliary experiment.

The theory of rupture of the over-stressed sections proposed by Bueche is completely adequate for an isotropic material. However, if the strength is anisotropic, as for example in a filled resin, where there are more stable bonds acting in the molecular chains of the rubber and less stable bonds between the rubber and the filler, the rupture may occur not only in the overstressed parts, but in the relatively weaker parts as well, depending on where the previous local stress reached the limiting value of local strength for the portion in question.

As follows from the facts presented earlier, the less stable rubber–filler bonds tear, not only in failure, but during deformation of the resin. Here, naturally, the effective degree of cross linking changes, as had been established by Bueche.

The mechanism of deformation in failure presented above, based on the idea of the equalization of stresses in the presence of the particles by a desorption-adsorption process (according to Alekandrov) does not contradict Bueche's data on the lowering of the q factor caused by the filler, but makes a substantial correction to Bueche's ideas on the reinforcement mechanism. The filler will not actually equalize the stresses unless it interacts with the rubber, but the rubber–filler bond is not as strong as the nodes of the space network, and thus is not able, under all conditions, to transmit the stresses from the ruptured portions of the rubber chains to the neighboring portions. It is more probable that the rupture of the rubber–filler bonds occurs by taking up the overstress from portions of the rubber chains.

In the light of this presentation, some interest is presented by investigations directed toward explaining the causes of structure formation by the carbon black in the resin mixtures. One of the ways to solve this problem is to study the structure of different types of carbon black and the surface activity produced by them [17, 43].

LITERATURE CITED

1. K. A. Pechkovskaya, N. A. Shedin-Khuzemi, P. N. Orlovskii, F. B. Livshits, et al. Kauchuk i resina, No. 6, 8 (1958).
2. B. A. Dogadkin, L. G. Senatorskaya, V. I. Guseva, A. V. Suslyakov and P. I. Zakharchenko, Kolloidn. Zh., 18, 528 (1955).
3. A. F. Blanchard, D. Parkinson, Proceed. 2. Rubber Technol. Confer., London, p. 414 (1948); Trans. IRI 23, 259 (1948); A. F. Blanchard, Ibid., 32, 124 (1951).
4. R. S. Stearns and B. L. Johnson, Industr. and Engng. Chem. 43, 146 (1951).
5. A. B. Kusov, Kauchuk i. Resina, No. 9, 26 (1940).

6. P. A. Rebinder and V. B. Margaritov, Zh. rezin. prom-sti 12, 991 (1935).
7. R. Spear, Indian. Rubber. Rev., No. 6 (1924).
8. E. Guth, Rubber Age 63, 462 (1948); Proceed. 2, Rubber. Technol. Confer., London, p. 353 (1948).
9. A. A. Trapeznikov, Dokl. AN SSSR 22, No. 284 (1939).
10. G. I. Clark, Rubber Age, April, 28 (1941).
11. B. A. Dogadkin, Study of Rubber [in Russian] Moscow, p. 295 (1938); Chemistry and Physics of Rubber [in Russian] Goskhimizdat, Chapter 13 (1947).
12. B. A. Dogadkin and M. S. Fel'dshetin, Kachuk i Resina, No. 12, 14 (1939).
13. B. K. Karmin, Dissertation [in Russian] Moscow (1943).
14. A. I. Lukomskaya, Dissertation [in Russian] Moscow (1951); B. A. Dogadkin and A. I. Lukomskaya, Transactions of the Third International Conference on Colloid Chemistry [in Russian] Izd. AN SSSR, p. 363 (1956).
15. B. A. Dogadkin and A. I. Lukomskaya, Dokl. AN SSSR, 88, 1915 (1953); Kolloidn. Zh. 15, 183 (1953).
16. A. I. Lukomskaya, B. A. Dogadkin, Kolloidn. Zh. 15, 259 (1953); 16, 34 (1954).
17. M. L. Studebaker and L. G. Nabors, Rubber Age 80, 1027 (1957).
18. A. M. Zolotareva, Zh. Tekhn. fiz, 16, 937 (1946).
19. W. F. Watson, Industr. and Engng. Chem. 47, 1281 (1955); Proceed. 3, Rubber Technol. Confer., London, p. 553 (1954).
20. General Chemical Technology [in Russian] Vol. 9, Edited by. S. I. Vol'fkovich, Goskhimizdat, Chapter 12 (1946).
21. L. Mullins, J. Rubb. Research 16, 275 (1947); IRI Trans. 23, 6 (1948); 26, 27 (1950); 32, 231 (1956); J. Phys. a. Colloid. Chem. 54, 239 (1950).
22. L. Mullins and N. R. Tobin, Proceed. 3, Rubber Technol. Confer., London, p. 397 (1954).
23. M. M. Reznikovskii, L. S. Priss and B. A. Dogadkin, Kolloidn. Zh. 16, 211 (1954).
24. H. J. T. Janssen, Proceed. 3, Rubber Techol. Confer., London, p. 351 (1954).
25. A. I. Lukomskaya, Vysokomolekulyarnye Soedineniya 1, 1287 (1959).
26. E. H. Andervs and A. Walsh, J. Polymer Sci. 33, 39 (1958).
27. H. W. Greensmith, J. Polymer Sci. 21, 175 (1956); The Rheology of Elastomers, Proceedings of a conference, BRPRA, p. 113 (1957).
28. M. P. Votinov and E. V. Kuvshinskii, Zh. Tkhn. fiz. 25, 2151 (1955); 27, 2303 (1957); 28, 2022 (1958); M. P. Votinov and L. L. Sul'shenko and E. V. Kuvshinskii, Ibid., 27, 2308 (1957).
29. L. Mullins, International Rubber Conference, Washington, November, p. 8 (1959).
30. A. G. Thomas, J. Polymer Sci. 18, 177 (1955).
31. B. A. Dogadkin, K. A. Pechkovskya, and L. A. Chernikina, Kolloidn. Zh. 8, 31 (1946); B. Dogadkin, K. Pechkovskaya and M. Dashevskii, Kolloidn. Zh. 10, 357 (1948).
32. B. A. Dogadkin, K. A. Pechsovskaya and Ts. Mil'man, Kolloidn. Zh. 14, 250 and 346 (1952).
33. B. A. Dogadkin and K. A. Pechkovskaya, Transactions of the Third International Conference on Colloid Chemistry [in Russian] Izd. AN SSSR, p. 371 (1956); Aging and Fatigue of Rubbers in Resins and Increasing Their Endurance (Second Scientific Technological Conference VNITO of Resin Specialists, 1953) [in Russian] Goskhimizdat, p. 53 (1955).
34. B. Dogadkin, K. Pechkovskaya, et al, Studies on the Physics and Chemistry of Rubber and Resin [in Russian] Goskhimizdat, pp. 103, 120 and 134 (1950).
35. K. Pechkovskaya, S. Pupko and B. Dogadkin, Kolloidn. Zh., 12, 367 (1950).
36. V. I. Kasatochkin and B. V. Lukin, Zh. Tekhn. Fiz. 19, 76 (1950).
37. V. G. Épshtein, Kauchuk i Resina, No. 1, 27 (1959).
38. D. Parkinson, Trans. IRI 19, 131 (1943); 21, 7 (1945); Advances in Colloid Sci., N. J., 2, 389 (1946).
39. P. Thirion and R. Shasset, Trans. IRI 27, No. 6, 364 (1951).
40. A. P. Aleksandrov and U. S. Lazurkin, Dokl. AN SSSR 45, 308 (1944).
41. B. A. Dogadkin, G. M. Bartenev and M. M. Resinkovskii, Kolloidn. Zh. 11, 314 (1949); Dokl. 6 Reports of the Sixth Conference on High Molecular Compounds [in Russian], Academy of Sciences Press, USSR p. 297 (1949).
42. F. Bueche, J. Polymer Sci. 33, 249 (1958).
43. M. L. Studebaker, Rubber Chem. Technol. 32, No. 5 (1959); B. A. Dogadkin, Z. V. Skorodumova and M. S. Fel'gshtein, Kolloidn. Zh. 22, 663 (1960).

EXPERIMENTAL STUDIES OF LAMINAR SYSTEMS

26. THE FORMATION OF ULTRATHIN FILMS OF CADMIUM SULFIDE AT A SOLID–SOLUTION INTERFACE

S. G. Mokrushin and Yu. D. Tkachev

S. M. Kirov Urals Polytechnical Institute, Sverdlovsk
Translated from Kolloidnyi Zhurnal, Vol. 23, No. 4,
pp. 438-441, July-August, 1961
Original article submitted February 10, 1960

The formation of ultrathin films of metal sulfides on a solution–gas interface was regarded by the authors [1] as the result of coagulation of colloidal sulfide particles on the surface of the solutions. The formation of ultrathin films or layers on a solid–solution interface can be regarded, in accordance with Svedberg's views [2], as a process of adsorption of primary colloidal particles on the surface of the solid. The phenomenon of the formation of thin layers of lead sulfide on a glass surface in alkaline solutions of thiourea and a lead salt has been studied by a number of authors [3]. Thin layers of silver sulfide have been obtained [4] on the surface of various insulating materials by the reaction of thiourea, silver nitrate and ammonia. The study of the conditions of formation of ultrathin films of cadmium sulfide on a solid surface in alkaline solutions of cadmium salts with thiourea is of considerable interest, since thin films of cadmium sulfide are used as photoresistors [5]. Cadmium sulfide films have been obtained from a reaction mixture prepared as follows: 0.3 ml of 1 M cadmium acetate solution, 4.2 ml of 11.4 M ammonia, 2.5 ml of 0.23 N caustic soda solution (added dropwise with continuous stirring), 1.2 ml of 0.25 M thiourea solution and 91.8 ml of distilled water (in one portion) were added successively to a beaker of 150 ml capacity*. After the addition of the water, the reaction was stirred vigorously and a wet 9 × 4 cm glass plate was placed in the beaker. After 14-20 hours (different experiments), the plate was removed from the solution and rubbed with a plug of moist cotton wool to remove the coarse particles from the surface of the fine film which had formed on the glass. This film was yellow in color with a mirror-like gloss and was very firmly attached to the glass surface. Similar films were obtained on different varieties of glass, porcelain, plexiglass and quartz.

The films exhibit photoelectric properties and absorb the spectral range from 4200 to 5200 Å. In the experiments on the study of the kinetics of formation of the films, we used battery dishes of 2 liters capacity. In this case, 8-12 plates were suspended from glass hooks simultaneously or at definite time intervals, depending on the requirements of the experiment. The thickness of the films was determined gravimetrically. The density of CdS was taken as equal to 4.5 g/cm^3, and the films were arbitrarily assumed to be compact [6]. The thickness of the films varied from 25 to 75 mμ, depending on the experimental conditions**.

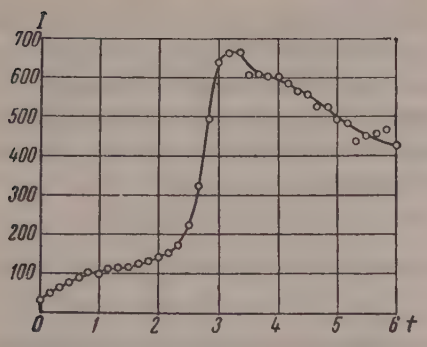
It was established experimentally that cadmium sulfide can be prepared by shaking freshly precipitated cadmium hydroxide with thiourea for ~30 minutes. Cadmium sulfide films are formed, however, only in the presence of ammonia.

The mirror-like gloss of the film is intensified with increase in the concentration of caustic soda in the reaction mixture; at the same time the color of the film also changes slightly: it becomes similar to that of polished brass. In solutions containing a large quantity of cadmium salt (30 ml of 1 M solution instead of 0.3 ml), cadmium sulfide is not formed, even after 8-10 days. Increase in the NaOH concentration by a factor of 10 (25 ml of alkali solution instead of 2.5 ml per 100 ml of reaction mixture) accelerates the formation of the cadmium sulfide. The

* Films can also be prepared from a mixture containing no alkali, in which case the quantity of ammonia should be decreased to 2.5 ml and the quantity of water correspondingly increased.

** In the determination of the thickness, two plates were weighed simultaneously. When the plates had been weighed, the film was removed from the plates with chromic mixture and the plates were weighed again. This gave the weight of four films by difference (since the film was formed on both sides of each plate). The error in the determination of the weight amounted to ±25% for the thinnest plates and ±6% for the thickest plates.

precipitate becomes bright orange, but no film is formed. The introduction of twice the quantity of thiourea (2.4 ml instead of 1.2 ml) has no influence on the outward appearance of the film and the nature of the process of film-formation. It was established that the films are formed for the most part during the first 4-6 hours. At the end of this time, the reaction mixture becomes transparent and contains practically no cadmium ammine.



Change in the opalescence of the reaction mixture with time: I is the intensity of scattered light expressed as divisions of the galvanometer scale; t is the time from the moment when the reagents of the mixture were mixed (hr).

From the relationships between the concentrations of the components of the reaction mixture, the solubility products of cadmium hydroxide and cadmium sulfide, and the instability constant of the tetrammine complex ion, it follows that before dilution with water the reaction mixture contains practically no cadmium ions. On rapid dilution of the reaction mixture the concentration of cadmium ions becomes sufficient for the formation of hydroxide. When sulfur ions are present, the formation of sulfide will be more probable. When insufficient sulfur ions are present, the hydroxide produced is converted gradually to the sulfide. The opalescence observed immediately after dilution of the reaction mixture indicates the formation of a colloidal solution. The resulting solution is extremely unstable, since the high concentration of primary particles and the high electrolytic content of the reaction mixture facilitate rapid coagulation with the formation in Svedberg's terminology [7], of larger particles of the secondary degree of dispersion. The coagulation is accompanied by adsorption of the primary, highly-dispersed mobile particles on the solution – gas and solution – solid interfaces. The primary particles attached to the glass plate and the walls of the vessel form a thin strong film with a mirror-like gloss. This process can be regarded as the primary stage of film formation.

As a result of the adsorption and more particularly the bulk coagulation, the quantity of primary mobile particles decreases very rapidly. The larger secondary particles are adsorbed on the film and form a loose, thick matt secondary layer. This layer (or deposit) can be regarded as the result of the second stage of the process – the adhesion of dispersed particles. The adhesion of the secondary particles stops, according to Buzagh [8], when the dimensions of the particles reach ~10 μ and the influence of gravity forces becomes appreciable. The formation of the film is complete 4-6 hours after the plates are immersed in the reaction mixture, but when the film is kept for a longer period (up to 14-20 hours) in the reaction mixture the external appearance of the film is improved: it becomes more uniform, yellow and transparent, as a result of recrystallization of the particles of the primary film or the formation of particles of the tertiary degree of dispersion [7].

These theories of the mechanism of formation of the film explain the extreme sensitivity of the reaction mixture to the method by which the water is added, since the latter determines the rate of formation of the centers of crystallization or primary colloidal particles. It also explains the part played by ammonia, since with even a small excess of the latter the rate of formation of the primary particles is low, leading to the formation, by the particles of the secondary degree of dispersion, of a stable deposit which cannot be removed without damaging the main film. When insufficient ammonia is present, the rate of coagulation is much greater than the rate of adsorption of the primary particles. The greater part of the cadmium is then precipitated as the hydroxide and a very thin film is formed (apparently produced by that fraction of the cadmium which was combined in the form of the ammine after the precipitation of the main bulk of the product). In open vessels, the concentration of ammonia in the reaction mixture decreases continuously as a result of desorption and the concentration of free cadmium ions gradually increases, creating spontaneously conditions for the formation of cadmium sulfide. The formation of the latter displaces the equilibrium

$$[Cd(NH_3)_4]^{2+} \rightleftarrows Cd^{2+} + 4NH_3.$$

to the right.

The addition, to the reaction mixture, of a large excess of soluble cadmium salts (100 times more than indicated in the composition of the reaction mixture) decreases the hydroxide ion concentration to such an extent that the decomposition of the thiourea stops, causing the formation of cadmium sulfide to stop simultaneously. Increase in the concentration of sodium hydroxide in the reaction mixture favors the formation of cadmium sulfide or, more

accurately, the conversion of cadmium hydroxide to cadmium sulfide. The cadmium sulfide precipitates formed in more alkaline reaction mixtures have an orange color, indicating their comparitively low degree of dispersion, since the highly-dispersed cadmium sulfide coagulate has a lemon-yellow color [9].

These views are confirmed by the change in the opalescence of the reaction mixture with time. As shown in the Figure, the opalescence increases, reaching a maximum 3-3.5 hours from the moment when the reacting components are mixed. The experiments show that for 2.5 hours the predominant reaction taking place in the reaction mixture is the formation of the primary colloidal particles, which as a result of their adsorption produce a compact, mirror-like primary film. After 2.5 hours, the process of coagulation, i.e. the formation of the secondary particles giving a loose readily-removed layer (or deposit) on the primary film, predominates. The primary mirror-like films are formed on glass plates placed in the reaction mixture only if these are introduced during the first two hours after its preparation, the films being thinner, the later the plates are immersed in the mixture.

SUMMARY

1. Mirror-like thin films (25-75 mμ) of cadmium sulfide have been prepared on the surface of glass and other materials.

2. The influence of the concentration of the individual components (ammonia, caustic soda, etc.) on the conditions of formation of the films and the properties has been examined.

3. The mechanism of formation of the films has been examined on the basis of theories regarding the production of colloidal cadmium sulfide particles of primary, secondary and tertiary degrees of dispersion and their adsorption.

4. The films absorb most strongly the spectral region from 4200 to 5200 Å and exhibit photoconductivity.

LITERATURE CITED

1. S. G. Mokrushin, Yu. D. Tkachev and O. K. Shabalina, Kolloid. Zh., 19, 597 (1957).
2. T. Svedberg, The Formation of Colloids [Russian translation] Khimtekhizdat, Leningrad, p. 21 (1927).
3. J. G. Brückman, Kolloid.-Z. 65, 1 (1933); F. Kicinski, Chemistry and Industry 4, 54 (1948); H. Pick, Z. Phys. 126, 12 (1949).
4. K. K. Demidov and E. A. Pozigun, Tr. Odesskogo Univ., 16, 105 (1952)
5. B. T. Kolomiets, Dokl. AN SSSR 83, 561 (1952).
6. G. V. Rozenberg, The Optics of Thin Coatings [in Russian] Fizmatgiz, Moscow, p. 15 (1958).
7. T. Svedberg, The Formation of Colloids [Russian translation] Khimtekhizdat, Leningrad, p. 8 (1927).
8. A. Buzagh, Kolloid.-Z., 51, 109 (1930).
9. B. G. Zaprometov and N. E. Prikhod'ko, Kolloid. Zh., 10, 15 (1948).

All abbreviations of periodicals in the above bibliography are letter-by-letter transliterations of the abbreviations as given in the original Russian journal. *Some or all of this periodical literature may well be available in English translation.* A complete list of the cover-to-cover English translations appears at the back of this issue.

CONDITIONS FOR THE FORMATION OF COLLOIDAL PARTICLES OF INTERMETALLIC COMPOUNDS

E. M. Natanson, V. V. Bushin and N. N. Kozachek

Colloidal Metals Laboratory, Kiev General and Inorganic Chemistry Institute,
Academy of Sciences, Ukrainian SSR
Translated from Kollodnyi Zhurnal, Vol. 23, No. 4,
pp. 442-447, July-August, 1961
Original article submitted May 16, 1960

The ferromagnetic properties of manganese-bismuth alloys [1] are due to the formation of the intermetallic compound MnBi in these alloys [2]. Manganese-bismuth alloys containing a high concentration of this compound exhibit a high coercive force and other valuable properties, which increase sharply with increase in the degree of dispersion of the alloy. Thus, for example, the coercive force increases from 3500 to 9000 oe when the particle size is decreased from 7 to 3 μ. The preparation of the intermetallic compound MnBi in compact form by fusing together powdered specimens of the corresponding metals [4, 5] is complicated by the fact that its formation never goes to completion, irrespective of the original ratio of the components. If the atomic ratio of Mn to Bi in the original mixture corresponds to the compound MnBi, the melt always contains, in addition to the MnBi, some unreacted manganese in fused bismuth [4, 5].

Since the method of preparing the intermetallic compound MnBi in the highly-dispersed state has not yet been studied, we have carried out investigations to examine the possibility of preparing this compound in a highly-dispersed state by the simultaneous deposition of manganese and bismuth on a cathode by an electrolytic method under the conditions of a two-layer bath.

Conditions for the formation of colloidal particles of the intermetallic compound MnBi. In the combined deposition of manganese and bismuth from aqueous solutions on a cathode, considerable difficulties are encountered, due chiefly to the fact that these two elements differ considerably from one another in chemical and electrochemical properties.

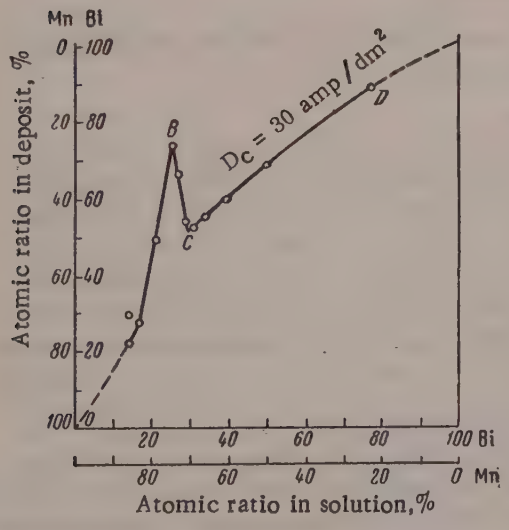


Fig. 1. Relationship between the composition of electrolytic deposits of manganese-bismuth alloy and the atomic ratio of the components of the electrolyte at constant current density.

It is well known that the simultaneous deposition of different metals at a cathode is possible only if the difference between their deposition potentials is slight. The formation of the alloys then takes place predominantly with a fairly high cathode polarization.

The deposition potentials of manganese and bismuth can be brought closer to one another in electrolysis under the conditions of a two-layer bath, where there is a particularly high polarization of the cathode, which rotates continuously at the water–hydrocarbon phase interface.

The general principles of the formation of organosols of metallic alloys at a cathode under two-layer bath conditions have been examined in [6], where it was also pointed out that, as a result of the formation of saturated adsorption layers of surface-active substances on the cathode, there takes place a retardation of the discharge of the ions, for the most part, of those metals whose equilibrium potentials correspond to stability of these adsorption layers. It is also necessary to take account of the depolarizing influence of electropositive metals, which often decreases the deposition potential of other less positive components of the mixture.

The composition of the bath has a considerable influence on the process of deposition of the alloys. Usually, solutions of complex salts of the corresponding metals are used. The assist in bringing the equilibrium potentials of the metals closer to one another. The ratio of the components in the alloy is to a great extent determined by the nature and relative position of the polarization curves for each metal separately under the given electrolysis conditions and by the concentration of these components in the electrolytic bath.

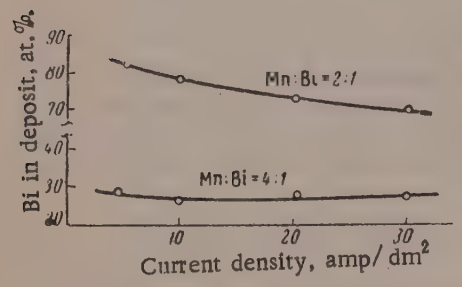


Fig. 2. Relationship between the composition of electrolytic deposits of manganese-bismuth alloy and the current density for different Mn: Bi ratios in the electrolyte.

In addition to these general considerations, in the case of the preparation of manganese-bismuth organosols it is also necessary to take account of features related to the specific properties of the components of the electrolytic bath used for the deposition of this alloy.

As a result of the marked tendency of bismuth salts to undergo hydrolysis, it is necessary to carry out the electrolysis in strongly acid media, in order to avoid the formation of oxides. This factor decreases considerably the current efficiency of the highly-dispersed manganese deposited simultaneously, since the latter dissolves comparitively rapidly in a strongly acidic medium.

In this connection, the composition of the cathodic deposit of manganese-bismuth alloy obtained differs considerably from the ratio of the components to the electrolyte. In this case, in order to decrease the solubility of the manganese deposited, it is advantageous to make use of results obtained in the study of the process of deposition of pure manganese.

To decrease the solubility of the manganese, it has been suggested [7] that 10 g of ammonia be added per liter of electrolyte and that a lead anode covered with a compact layer of precipitated manganese dioxide be used as anode.

The use of anodes of a lead-silver alloy and aluminum cathodes which have a higher electrical conductance and are more easily purified than stainless steel cathodes, has also been recommended for improving the process of electrolytic preparation of manganese.

The addition of carefully controlled quantities of ammonium sulfate has a favorable influence on the deposition of pure manganese.

In selecting the composition of the electrolyte for the deposition of highly-dispersed manganese-bismuth alloy at a cathode under two-layer bath conditions, we took account of the results of our earlier studies of the process of formation of organosols of nickel-chromium alloys at a cathode [6] and also of literature data characterizing the process of electrodeposition of the pure components of this alloy separately.

As a result of the experiments, we chose an electrolyte for the lower aqueous layer, which proved to be stable on storage and, when the acidity was sufficiently high, on prolonged electrolysis.

The electrolyte was prepared by mixing the following solutions:

Bismuth chloride	different concentrations (Figs. 1 and 2)
Manganese chloride	" "
Ammonium chloride	25 g/liter
Urea	30 "
Hydrochloric acid (concentrated)	15-20 ml/liter

The bismuth chloride was prepared by dissolving the calculated quantity of Bi_2O_3 in concentrated hydrochloric acid and diluting to the required volume.

As in the previous studies, a 0.2-0.4% solution of oleic acid in toluene was used as the upper organic layer. Higher concentrations of oleic acid led to marked screening of the cathode surface with simultaneous particularly intense evolution of hydrogen. The evolution of hydrogen has a marked influence on the size and shape of the particles of the cathodic deposit produced [9] and also favors the production of hydrophobic properties on the surface of its particles and their transfer to the organic layer of the bath, due to the intense agitation of the latter by hydrogen bubbles in direct proximity to the cathode surface. The intense evolution of hydrogen is also accompanied by a considerable decrease in the current efficiency. It is therefore very important, in the production of highly-dispersed

powdered cathodic deposits under two-layer bath conditions, to establish the limiting current density below which the evolution of hydrogen is desirable in order to influence favorably the process of formation of the particles of these deposits.

When the electrolysis was complete, the resulting organosols of manganese-bismuth alloy were rapidly and thoroughly separated from the lower layer of electrolyte and immediately centrifuged for a prolonged period. The deposits obtained after centrifuging were washed repeatedly with benzene, acetone containing 2-3% formaldehyde, and then 2-3 times with a solution of oleic acid in benzene. After treatment in this way the dispersed phase of the manganese-bismuth alloy organosols were not oxidized on prolonged storage under benzene or in the air-dry state.

TABLE 1. The Influence of Glycerol on the Yield of Ferromagnetic Fraction at Different Mn:Bi Ratios in the Electrolyte.

Concentration in electrolyte, M		Ratio in electrolyte, %				Yield of magnetic fraction, % of the weight of the dispersed phase of the MnBi organosol		
		wt. %		at. %		with glycerol	with glycerol, g/liter	
$BiCl_3$	$MnCl_3$	Bi	Mn	Bi	Mn		33	66
0,264	0,119	80	20	51,1	48,9	—	1,4	2,97
0,198	0,238	60	40	28,6	71,4	0,13	2,09	7
0,148	0,35	40	60	15	85	0,26	2,7	50
0,074	0,478	20	80	4,9	95,1	0,17	1,4	4,7

TABLE 2. Values of the Interplanar Spacings (d) of the Crystal Lattices of the Components Present in the Magnetic Fraction of the Dispersed Phase of the MnBi Organosol Obtained in an Electrolyte with Mn:Bi = 85:15 and the Crystal Lattic Parameters of the Intermetallic Compound MnBi

Phase composition of the magnetic fraction of the organosol	τMnBi		MnBi		τMn		MnBi	Bi	
Values of d, experimental	3,66	2,33	2,09	2,04	1,92	1,64	1,56	1,51	1,47
Values of d, calculated	3,65	2,35	2,06	2,02	1,95	1,65	1,58	1,51	1,48

Crystal lattice parameters of the intermetallic compound

	a	*c*	*c/a*
Experimental data	4,27	6,15	1,44
Literature data	4,26	6,12	1,44

The bismuth in the dispersed phases of the organosols of the alloys was determined gravimetrically as $BiPO_4$ and the manganese by the permanganate method. The changes in the composition of the manganese-bismuth cathodic deposits with change in the ratio of the components of the electrolyte and the current density at the cathode (the current efficiency amounted to 5-6%) show (Figs. 1 and 2) that in almost all cases, the Mn:Bi ratio in the dispersed phases of the organosols of these alloys is lower than that in the corresponding electrolytes. This is particularly marked when the Mn:Bi ratio in the electrolyte lies between 3:1 and 1:3. This marked difference between the composition of the dispersed phases of the manganese-bismuth organosols and the composition of the corresponding electrolytes in this concentration range was due chiefly to the comparatively ready solubility of the free highly-dispersed manganese at the moment of its deposition in strongly acidic medium.

The maximum on the curve at the point B (Fig. 1) apparently corresponds to the start of formation of the intermetallic compound, which is fairly stable in acid medium. In this connection, the section of the curve BC shows a comparitively rapid increase in the relative manganese concentration in the dispersed phases of these organosols up to the point C. The clearly-defined minimum at the point C corresponds to an Mn:Bi atomic ratio of 1:1 in the cathodic deposit and 3:1 in the electrolyte. This ratio of the components in the electrolyte favors the deposition, at the cathode, of deposits whose composition is close to that of the manganese-bismuth intermetallic compound.

Along the length of section CD there is again observed a decrease in the relative manganese content of the dispersed phases of the organosol, due chiefly to the marked increase in the relative concentration of bismuth in the electrolyte. In this case, the manganese is apparently present chiefly in the combined state.

The current density, in the range 5 to 30 amp/dm^2, has no significant influence on the composition of the dispersed phases of the manganese-bismuth organosols, particularly at ratios of these components in the electrolyte equal to 4:1 (Fig. 2).

The dispersed phases of the manganese-bismuth organosols were subjected to magnetic separation. In almost all cases, the yield of ferromagnetic fraction was very small. Studies showed that the presence of glycerol in the electrolyte bath favors an increase in the yield of the ferromagnetic fraction (Table 1). This is particularly true at an Mn:Bi atomic ratio in the electrolyte equal to 85:15, when the Mn:Bi ratio in the dispersed phase deposited at the cathode is 1:1.

X-ray diffraction studies of the dispersed phases of the manganese bismuth organosols. The magnetic fractions of the dispersed phases of the manganese-bismuth alloy organosols were dehydrated and mixed with a solution of pure paraffin in ethyl ether (approximately 0.2-0.3 parts by weight of metal). After evaporation of the ether, the resulting paste was transferred in small portions to a glass capillary of 0.75 mm diameter. One-third of the paste was pressed out of the capillary onto the stage of an RKD x-ray camera. The x-ray diagrams were recorded with iron radiation from a tube of the BSV_{Fe} type. "Agfa" film was used to record the patterns. The developer was standard. The film mounting was asymmetrical.

The exposure time, established on several specimens amounted to 3.5 hours, with tube operating conditions of I = 9 ma nd V = 36 kv. The lines on the resulting x-ray diagrams were measured with an accuracy of up to 0.01 mm by means of an "IZN-2" comparator. The calculation of the x-ray diagrams was carried out by the analytical method.

The results of the x-ray analysis (Table 2) show that the magnetic fraction of the dispersed phase of the Mn-Bi organosols studied consists of metallic bismuth, the γ-modification of manganese, and the intermetallic compound MnBi. The crystal lattice parameters of these substances agree closely with the literature data [10].

The x-ray diagrams for the dispersed phases of the MnBi organosols obtained at different ratios of these components have partly blurred lines, indicating the high degree of dispersion of these specimens.

SUMMARY

1. A study has been made of the processes of formation of colloidal particles of manganese-bismuth alloy in a two-layer bath with a lower aqueous layer containing the manganese, bismuth and ammonium chlorides, urea and hydrochloric acid.

2. The Mn:Bi atomic ratio in the cathodic deposit is less than that in the electrolyte. The curve giving the relationship between the composition of the colloidal particles of the alloy and the ratio of the components in the electrolyte has a clearly-defined minimum corresponding to an Mn:Bi atomic ratio of 1:1 in the deposit and 3:1 in the electrolyte. This ratio of components in the electrolyte favors the deposition at the cathode of deposits with compositions close to that of the manganese-bismuth intermetallic compound.

3. The presence of glycerol in the electrolyte bath favors an increase in the yield of the ferromagnetic fraction.

4. The x-ray diagrams of almost all the magnetic fractions of the dispersed phases of the MnBi alloy organosols show partly blurred lines, indicating the high degree of dispersion of the test specimens. The dispersed phase of the organosol contains the intermetallic compound MnBi, bismuth and the γ-modification of manganese. The qualitative composition of this phase remains constant over a wide range of electrolysis conditions.

LITERATURE CITED

1. F. Heisler, Z. angew. Chem. 17, 260 (1904).
2. C. Guilland., Cahiers phys. p. 15 (1945).
3. E. Adams, W. Hubbard and A. Syeles, Problemy Sovremennoi Metallurgii, No. 3, p. 114 (1953).
4. M. Hansen, The Constitution of Binary Alloys [Russian translation] Metallurgizdat, Vol. 1, p. 305 (1941).
5. G. Siebe., Z. anorgan. und allgem. Chem. 108, 161 (1919).
6. E. M. Natanson and N. N. Kozachek, Kolloid. Zh. 19, 698 (1957).
7. S. A. Zaretskii, Dokl. AN SSSR 56, No. 2, 181 (1947).

8. S. A. Zaretskii, Z. Prikl. Khim., 13, 796 (1940); P. V. Zhivotinskii and S. A. Zaretskii, ibid., 12, 200 (1939).
9. N. N. Kozachek, "Organosols of Alloys", Candidate's Thesis, IONKh AN Ukr. SSR (1958).
10. G. V. Bokii, Introduction to Crystal Chemistry [in Russian] Izd. Mosk. Univ., p. 354 (1954).

All abbreviations of periodicals in the above bibliography are letter-by-letter transliterations of the abbreviations as given in the original Russian journal. *Some or all of this periodical literature may well be available in English translation.* A complete list of the cover-to-cover English translations appears at the back of this issue.

SOME FEATURES OF EMULSION FORMATION BY ULTRASONICS

S. A. Neduzhii

Acoustics Laboratory, Scientific Research Cinephoto-Institute, Moscow
Translated from Kollodnyi zhurnal, Vol. 23, No. 4,
pp. 448-453, April, 1961
Original article submitted July 21, 1960

The nature of the formation of W/O and O/W types of emulsion by ultrasonics as a function of the intensity and duration of irradiation has been investigated. A study has also been made of the relation between the particle size of the disperse phase at the moment of formation of O/W emulsion and ultrasonic intensity. The experiments were carried out on the system dibutyl phthalate-water in a glass vessel in a standing-wave field of frequency 22 kcps. It has been found that: 1) each type of emulsion has different threshold values of intensity for its formation; 2) the nature of the emulsification process is different for the two types of emulsion; 3) limit concentration values exist for corresponding intensity values and 4) the particle size of the disperse phase at the moment of formation of the emulsions is independent of the irradiation intensity.

Chemically pure, highly disperse, homogeneous and concentrated emulsions are currently of special interest for a number of technical processes. The production of such emulsions in an industrial scale is possible only by means of ultrasonics. Although this possibility has been known for a comparatively long time [1], there is still no clear conception of the way in which the qualitative and quantitative characteristics of the resulting emulsions depend on the fundamental parameters of the acoustic field, the physical condition of the boundary surfaces and the nature of the starting components. Such a situation does not permit the choice of optimum conditions for carrying out the process, reduces the efficiency of the working apparatus and, accordingly, retards any extensive introduction into industry of this method of producing an emulsion. The study of the formation of emulsions by means of ultrasonics is a pressing problem of considerable interest.

The present work was undertaken with a view to studying the nature of the process of emulsion formation and the state of the disperse phase of an emulsion at the moment of its formation as a function of the ultrasonic intensity.

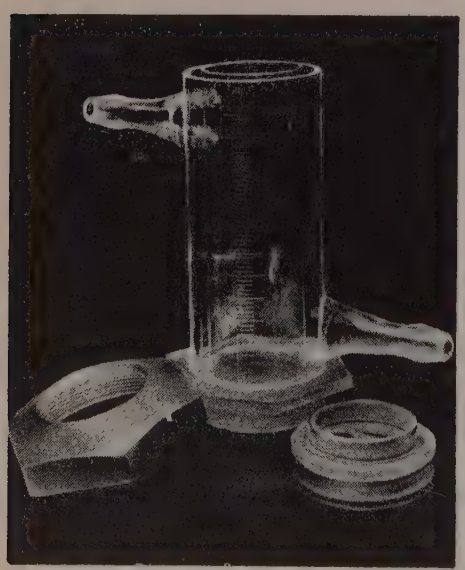


Fig. 1. External view of reaction vessel.

The starting components employed were distilled water (speed of sound in it c = 1497 m/sec at 25°C) and dibutyl phthalate (DBP) (c = 1604 m/sec at 25°C). The results given below were obtained in a standing-wave field of frequency 22 kcps. A detailed description of the apparatus and the experimental technique are given in [2]. Ultrasonic irradiation was carried out in a glass vessel with an internal diameter of 29 mm and a wall thickness of 1.5 mm (Fig. 1). The bottom of the vessel was formed by a resiliently stretched film of polyethylene terephthalate ("Lavsan"), 10-25μ thick. The apparatus is shown diagrammatically in Fig. 2. The transducer, intermediate liquid and reaction vessel were thermostat-controlled at a temperature of 25°C. The height of the layer of each liquid phase was equal to half a wavelength. It was thus possible to reduce coagulation to a minimum, since coagulation occurs very intensely in a standing-wave field, depending on the number of nodes and antinodes per unit height of the column of liquid [3]. In addition, with the relative excess of each of the components present, it was possible to observe simultaneously the process of formation of both types of emulsion, this being of considerable interest, since the opinion is held [4] that the acoustic conditions influence the type of emulsion formed. Such a possibility is not provided if the choice of starting quantities is based on considerations of recipes. Investi-

gation of the process of emulsion formation in the low-frequency part of the ultrasonic range permits the production of sufficient volumes of emulsion for qualitative and quantitative analysis, while retaining the above-mentioned advantages of half-wave volumes.

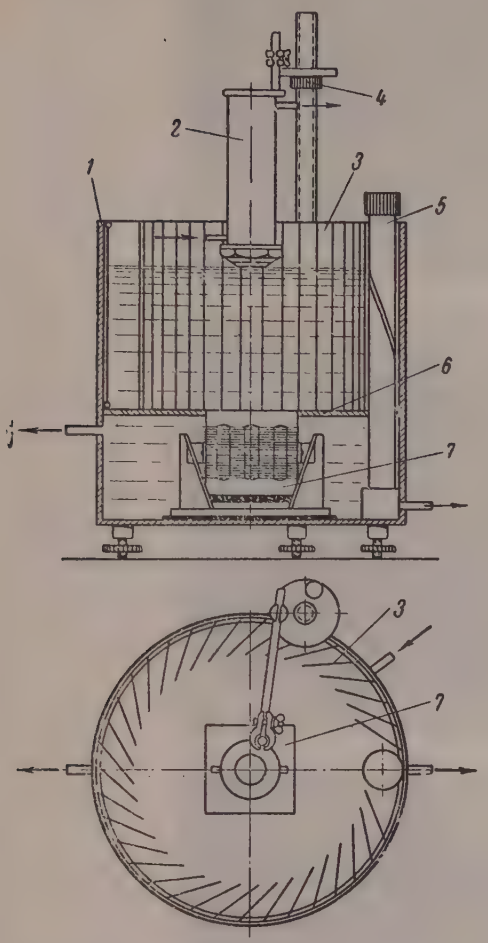


Fig. 2. Diagram of ultrasonic irradiation apparatus: 1) Tank with transducer operating in it; 2) reaction vessel; 3) acoustic "louver" type lining of tank; 4) stand for carrying reaction vessel; 5) device for smooth regulation of level of liquid in tank; this liquid formed the intermediate layer; 6) screen; 7) magnetostriction transducer.

In the course of the experiments, the formation of both types of emulsion was observed. Formation of the oil-in-water (O/W) type of emulsion occurred at the boundary with the wall of the reaction vessel in the plane of separation of the two liquid phases. The initial moment of the process of formation of this emulsion will be seen in Fig. 3, showing the development of the process at 10 sec intervals, from the moment of the commencement of the formation. Photography was carried out from above the reaction vessel, so that the focal plane of the image was situated in the plane of the boundary of separation of the two liquid phases. Formation of the water-in-oil (W/O) type of emulsion occurred over the entire plane of separation. The character of the emulsion formation at intensities at the transducer of up to 4 w/cm^2* was verified by periodical measurement of its relative concentration nephelometrically from the coefficient of light transmission τ with blue, green and red light filters using an instrument of type FEK-N-57; the results are shown in Fig. 4. It was found that emulsion of either type commences to form after the ultrasonic intensity has reached a definite (threshold) value, which in our case for the formation of the O/W type of emulsion is below the threshold of intensity for the formation of W/O type of emulsion, the values being respectively 0.5 and ~1.5 w/cm^2. With further increase in the intensity, the rate of emulsion formation increases, and the value of the limit concentration of the emulsion formed varies accordingly. The dependence of limit concentration on intensity is more pronounced for the O/W type of emulsion than for the W/O type (Fig. 5). The existence of different values for the limit concentration indicates that the processes of emulsification and coagulation are intensified differently with increase in ultrasonic intensity. This is evidently due to the difference in character of the processes taking place. Coagulation has a volume character, while emulsification occurs only at the interface of the two liquid phases. Despite the fact that the processes of the formation of emulsions of both direct and reverse types obey the same general laws (increase in the rate of emulsification with increase in intensity, and the existence of limit concentrations of the emulsions for each value of the intensity), comparison of the curves for the same intensity values (Fig. 4) shows the difference in character of the course of these two processes. Thus, if the process of the formation of emulsion of O/W type occurs immediately after the commencement of irradiation, emulsion of W/O type begins to form only after a certain interval of time, corresponding to a definite value for the concentration of emulsion of O/W type at the boundary of the two phases. This value of the concentration, expressed in units of the coefficient of light transmission τ, lies within the limits of 40-60%. This may evidently be explained by the variation in surface tension at the water-DBP interface to values at which the formation of emulsion of W/O type commences. This difference in the course of the processes of formation of the two types of emulsion and the fact that emulsion of

* In view of the fact that to speak of ultrasonic intensity as of a flow of energy in a standing-wave field would be incorrect from the physical point of view, the term employed here bears an arbitrary character. In our experiments, the intensity was determined from the current and voltage at the transducer. Cos φ was determined by the three voltmeter method. In calculating the intensity, the loss of efficiency of the transducer due to cavitation was ignored [5]. In addition, the relative constancy of the established working conditions was verified acoustically by means of a pressure-pick-up probe.

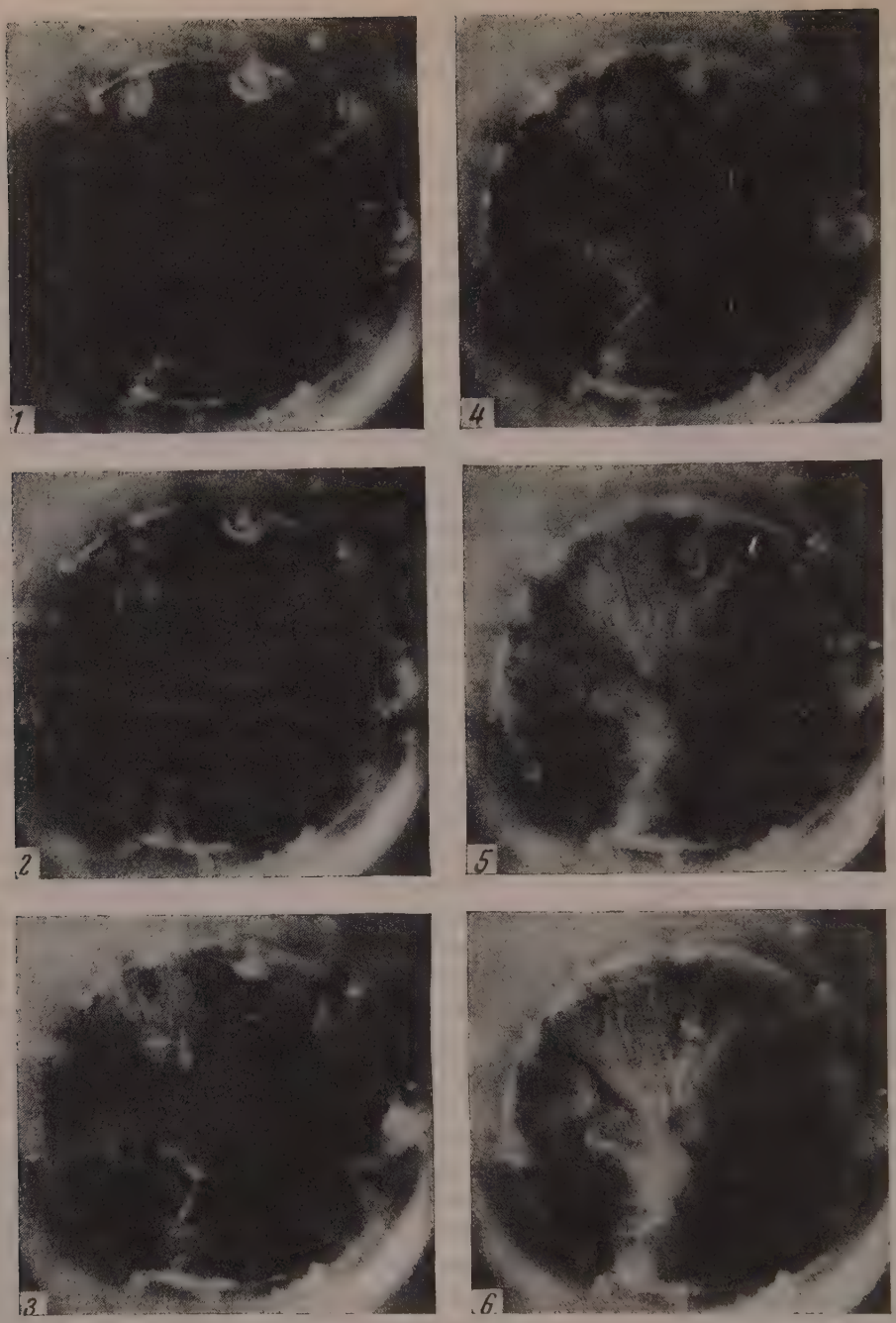


Fig. 3. Photographs of the start of the process of emulsion formation, taken at 10 seconds intervals.

W/O type is formed over the entire interface of the two liquid phases gives rise to the supposition that there is some differences in the character of the mechanism of formation of emulsion of W/O type from that of emulsion of O/W type.

The mechanism of the conversion of one of the starting components into the disperse state has not been studied with sufficient clarity for any of the known methods of producing an emulsion, including emulsification produced by the action of ultrasonics. Until recently, there has not yet been sufficient clarity in the question as to the factor which causes the process of formation of an emulsion. Primarily, two points of view are deserving of attention. According to the first, emulsification is due to a process of cavitation occurring on the boundary surfaces; according to the second, the transformation of a component into the disperse state is the result of the formation of surface capillary waves. For forming a definite opinion in this question, the results of an investigation of the state of the disperse phase of an emuls-

ion would appear to be decisive, particularly an investigation of the dependence of the particle size of the disperse phase at the moment of its formation on the fundamental parameters of the acoustic field (intensity and frequency). At this stage in the process of emulsion formation, the effect of coagulation is practically absent, and the size of the particles will be determined by the forces producing their formation, the physical condition of the boundary surfaces and the nature of initial components. There are no data in the literature directly bearing on such a dependence.

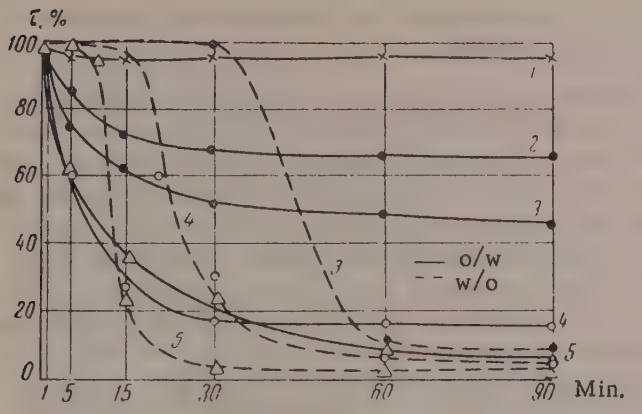


Fig. 4. Curves characterizing the process of formation of both types of emulsion as a function of the duration of irradiation for the different intensities (w/cm^2): 1) 0.5; 2) 0.9; 3) 1.6; 4) 2.5; 5) 3.0

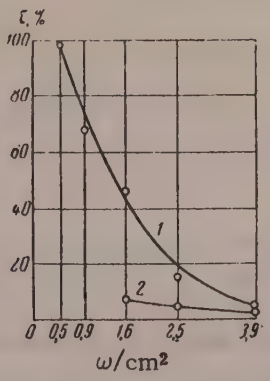


Fig. 5. Dependence of limit concentration of emulsions of O/W type (1) and W/O type (2) on ultrasonic intensity.

An investigation of the dependence of particle size on ultrasonic intensity was carried out on an emuls-

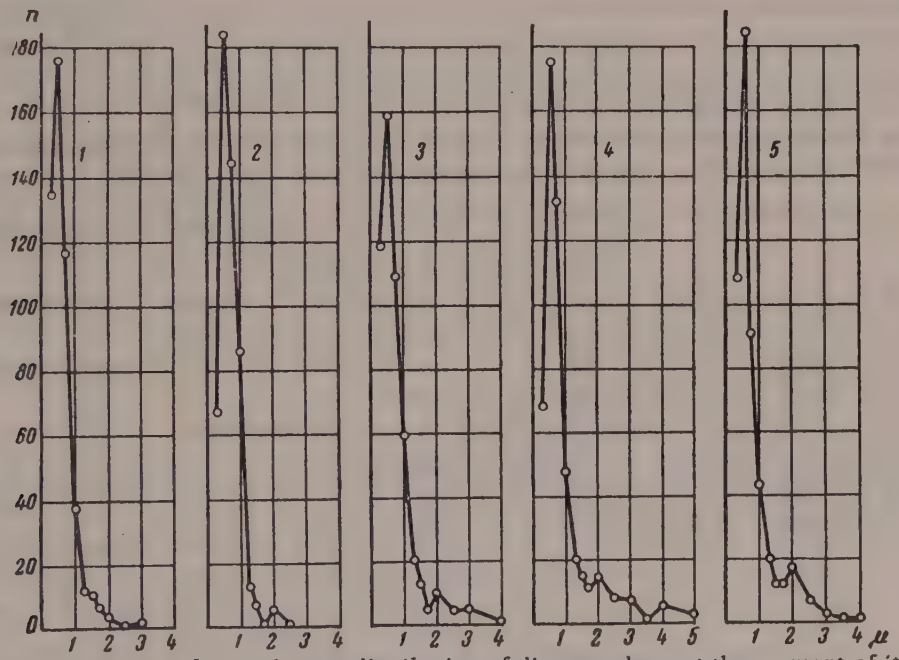


Fig. 6. Curves of particle size distribution of disperse phase at the moment of its formation at intensities (w/cm^2) of: 1) 0.4; 2) 2; 3) 3.3; 4) 7; 5) 8.

ion of O/W type. The dispersion analysis was made by means of an MBI-1 microscope fitted with an AU-12 binocular tube. The magnification adopted and the eyepiece micrometer scale used permitted classification of the particles by sizes, commencing with 1/3 μ upward. To eliminate Brownian motion of the particles during their examination in the microscope, the specimens of emulsion were fixed by a 10% gelatin solution. The layer of fixed emulsion on the object glass was covered by a cover glass, since an oil-immersion microscope objective was used. In the final preparations, the average thickness of the layer was 300μ.

Samples were taken from the reaction vessel every 15-60 sec after the commencement of the formation of emulsion. Measurements were made on 500 particles in each sample. Fig. 6 shows the curves characterizing the distribution by size of the disperse phase, produced at ultrasonic intensities at the transducer of from 0.4 to 8 w/cm^2. As will be seen from Fig. 6, the size of the particles at the moment of their formation does not depend on the intensity, despite the intensification of disperse phase formation with increase in intensity. This is indicative of the constancy of the forces producing the transformation of one of the components into the disperse state.

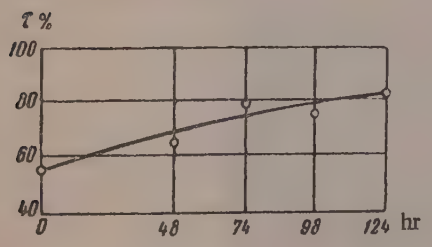


Fig. 7. Curve characterizing the stability of O/W type of emulsion.

In this connection, special interest attaches to the reference made by the authors of article [6] to the fact that the force of destruction of a cavitation bubble does not depend on increase in intensity; only the number of cavitation bubbles increases with increase in intensity. Bearing also in mind the fact that the formation of emulsion of O/W type occurred at the boundary of separation of the two liquid phases with the wall of the reaction vessel, i.e. at places which from the energy standpoint were more favorable for the production of cavitation [7], it is impossible not to conclude that the emulsification in our experiments was the result of cavitation.

In the experiments made, the problem of investigating the stability of the emulsions produced did not arise particularly. It should be noted, however, that although no surface-active reagents were used, the emulsion of O/W type produced was fairly stable (Fig. 7). The emulsion of W/O type was less stable, which gave rise to inconvenience in making the nephelometric measurements of relative concentration, especially at low values of the latter.

SUMMARY

1. Emulsions of O/W and W/O type were produced in a cylindrical glass vessel in a field of standing waves of frequency 22 kcps.

2. For the commencement of the formation of each type of emulsion, a different threshold value of the ultrasonic intensity is necessary, below which emulsification does not take place.

3. A definite value of the limit concentration corresponds to each intensity level.

4. The particle size of the disperse phase at the moment of its formation does not depend on the ultrasonic intensity. This is indicative of constancy of the forces causing the formation of such particles.

The author is deeply indebted to V. M. Uvarova for assistance in carrying out the dispersion analysis.

LITERATURE CITED

1. R. W. Wood and A. L. Loomis, Philos. Mag. (7), 4, 22 417, 1927; W. T. Richards, J. Amer. Chem. Soc. 51, 6, 1724, 1929; S. N. Rzhevkin and E. L. Ostrovskii, Zh. fiz. khimii 6, 1, 73, 1935.
2. S. A. Neduzhii, Akusticheskii sb. 1, 85, 1960.
3. K. Söllner, and V. Bondy, Trans. Faraday Soc. 32, 616, 1936.
4. A. Audouin, and G. Levavasseur, Oleagineux 4, 95, 1949; Food, 18, 190, 1949.
5. L. D. Rozenberg and M. G. Sirotyuk, Akust. zh. 6, 478, 1960.
6. R. Esche, and P. Wenk, Elektrotechn.-Z., B12, 97, 1960.
7. K. Söllner, Trans. Faraday Soc. 32, 1537, 1936.

SYNTHESIS OF ARTIFICIAL ZEOLITES AND INVESTIGATION OF THEIR ADSORPTION PROPERTIES

I. E. Neimark, M. A. Pionkovskaya, A. E. Lukash and R. S. Tyutyunik

L. V. Pisarevskii Institute of Physical Chemistry, Academy of Sciences of the Ukranian SSR, Kiev

Translated from Kolloidnyi Zhurnal, Vol. 23, No. 4, pp. 454-461, July-August, 1961
Original article submitted May 27, 1960

Some sorbents have pores the diameters of which are commensurable with the dimensions of molecules. Inasmuch as only molecules of small dimensions can pass through these pores, they act as molecular sieves. Molecular sieves make it possible to separate various gaseous and liquid mixtures by making use of the differences in size and shape of the molecules of which they are composed.

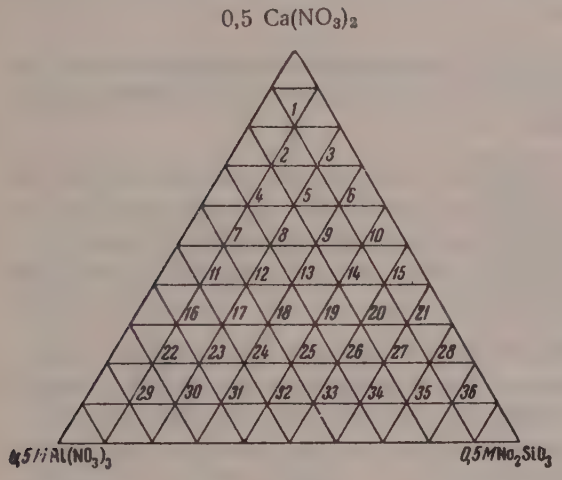


Fig. 1. Triangular diagram of $Ca(NO_3)_2$, $Al(NO_3)_3$ and Na_2SiO_3.

The zeolites, which are polyhydrates of aluminum silicates, behave as molecular sieves. Their general composition may be expressed by the formula $(R'_2, R)\,O \cdot Al_2O_3 \cdot nSiO_2 \cdot mH_2O$, in which R' designates the monovalent cation (Na^+, K^+, Li^+) and R a divalent cation (Ca^{2+}, Ba^{2+}, Sr^{2+} etc.).

In all zeolites, weakly adsorbed water molecules are present which may be reversibly removed. In place of the water removed, the zeolites may adsorb other substances. Because of the uniform dimensions of the zeolite pores, only those molecules are easily adsorbed which, as a result of their shape and dimensions, can penetrate into the narrowest parts of these channels.

The properties of the natural zeolites as molecular sieves have been known ever since Weigel and Steinhaff [1] discovered the ability of the mineral chabazite to adsorb selectively. These authors found that the vapors of water, methyl and ethyl alcohols and formic acid are rapidly adsorbed on chabazite, while acetone, ether and benzene are not taken up by it at all. However, the natural zeolites are not used in practice for the separation of mixtures. Inasmuch as the deposits of natural zeolites are rare and poor, a great deal of attention is being given to synthetic zeolites. The methods of preparing synthetic zeolites [2] imitate the natural geochemical processes, since it has been found that zeolites and clays are formed in superheated aqueous solutions under pressure. The Linde Company (USA) produces molecular sieves of type 4A and 5A (pore diameter 4 and 5 Å) and 13X. A great deal of research work [3] preceded getting molecular sieves into production.

Because of their high adsorption capacity at low concentrations and high temperatures, and because of their great affinity for water, unsaturated organic compounds and other polar molecules, artificial zeolites have found wide use for drying and purifying gases, for the removal of unsaturated hydrocarbons from waste gases, for the separation of hydrocarbons, for the absorption of isotopes from aerosols and as ion-exchangers carrying vulcanizing agents for rubber plastics, etc. [4].

The purpose of this study was to synthesize artificial zeolite and to investigate their adsorptive properties and their properties as molecular sieves.

The artificial zeolites were prepared by the crystallization of gel-form aluminum silicates under mild conditions (in a water bath at 60-80°) or in autoclave-like bombs under water vapor pressure at 150, 170, 220, 250 and 300°. In some cases, crystallization under mild conditions preceded hydrothermal treatment of the aluminum silicate gels.

TABLE 1. Adsorption Volume of Samples of Sodium Aluminum Silicate (crystallized at 60°).

Sample	294	295	296	297	298	299	300
Length of crystallization, hours	0	1	3	5	10	24	48
Adsorption volume for water vapor at P/P_s = 0.1 mmole/g.	0.7	0.4	12.4	13.3	12.95	11.6	11.3

To begin with, we synthesized gel-form aluminum silicates of calcium; this was done by mixing solutions of the nitrates of aluminum and calcium and sodium silicate in ratios that correspond to the equilibrium points on the diagram (Fig. 1) [5].

Heating at 60° in a water bath, and even hydrothermal treatment failed to bring about the crystallization of gel-form calcium aluminum silicate even at 400° over a long period. X-ray photographs showed the absence of diffraction peaks and diffuse rings were observed. The adsorptive activity of the samples prepared in this way for water vapor was equal to 3-6 mmoles/g at P/P_s = 0.1. It was characteristic that the activity of samples subjected to hydrothermal treatment was lower than that of samples heated at 60°.

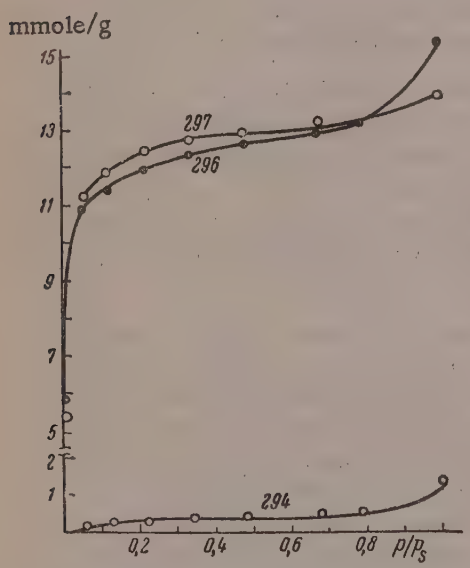


Fig. 2. Sorption isotherms of water vapor at 20° on various samples of sodium aluminum silicate (Table 1).

The easiest way to obtain crystalline calcium aluminum silicate is from crystalline sodium aluminum silicate by exchanging sodium ions for calcium ions.

The raw material from which sodium aluminum silicate was prepared included solutions of aluminate and water glass with an excess of alkali. Crystalline gel-form sodium aluminum silicate was formed in from 3-6 hours at 60°. The time required for ripening the precipitate varied up to 48 hours.

From the data of Table 1 and Figure 2, it can be seen that samples with a high water vapor capacity are prepared by heating the sodium aluminum silicate gel under mild conditions for 3-6 hours. X-ray structural studies showed that sodium aluminum silicate gels, ripened in the mother solution for 3-6 hours at 60°, had a crystalline structure identical with Linde 4A molecular sieves.

On prolonged ripening of the precipitate (~24 hours), the adsorption volume of crystalline sodium aluminum silicate decreases which, apparently, is connected with the recrystallization of the product.

Independent experiments showed that the adsorption volume of sodium aluminum silicate at low concentrations of water vapor (P/P_s = 0.1) increases with increasing alkalinity of the aluminum silicate solution.

Since gels containing calcium cations crystallize very slowly both at low temperatures and during hydrothermal treatment, we prepared calcium zeolites by exchanging sodium ions in sodium zeolite by calcium. This was done by repeatedly treating crystalline sodium aluminum silicate with solutions of calcium salts and washing out the occluded salts with distilled water until a test for the calcium ion was negative. Chemical analysis showed that at room temperature, calcium easily passes from the solution into the zeolite. The corresponding lithium (LiA) and potassium (KA) zeolites were synthesized by exchanging sodium ions in type 4A zeolite by lithium and potassium ions. The lithium zeolite was prepared by treating crystalline sodium aluminum silicate in the cold with a solution of lithium sulfate. For the potassium zeolite, a solution of potassium chloride was used. It is interesting to note that in addition

to the method of ion exchange, the possibility of preparing potassium zeolite from gel-form potassium aluminum silicate was also studied. Gel-form potassium aluminum silicate of composition $K_2O \cdot Al_2O_3 \cdot 2SiO_2 \cdot xH_2O$ was prepared by the reaction of solutions of potassium aluminum silicate and potassium silicate. Crystallization was carried out at 60-80°, and at increased alkalinity of the solution. The experiments showed that the crystallization of gel-form potassium aluminum silicate of the composition $K_2O \cdot Al_2O_3 \cdot 2SiO_2 \cdot xH_2O$ proceeds at an appreciable rate; this rate, however, is much less than the rate of crystallization of the corresponding sodium aluminum silicate. X-ray spectra of potassium aluminum silicate clearly showed diffraction lines.

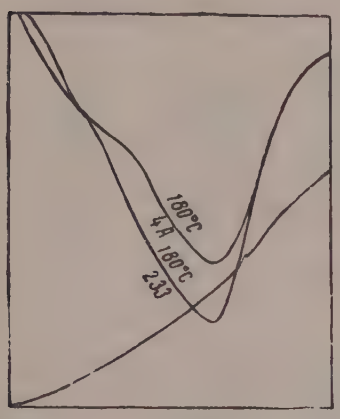


Fig. 3. Thermograms of artificial zeolites NaA(233) and 4A.

The samples of artificial zeolites which we prepared were subject to chemical analysis, and to X-ray and thermographic study.* Samples of American molecular sieves, type 4A and 5A, were also studied for comparison. The x-ray spectra were taken on a URO-70 apparatus with copper (λ_k = 1.5734 kX) and in some cases chromium (λ_k = 2.2850 kX) emission at a current of 15 ma at 35,000 v and an exposure of two hours.

On the x-ray spectra of sample 213 and a sample of American sieve 4A, good coincidence of the intervals and intensities of lines is observed, which shows that the crystalline structure of both zeolites is similar.

In the thermograms (Fig. 3) a diffuse endothermic maximum for our sample and for zeolite 4A can be observed at the same temperature, which indicates that they are close to each other in composition.

The results of chemical analysis (Table 2) also show that the zeolites we prepared and the American molecular sieves are close to each other in chemical composition. The only difference is in moisture content.

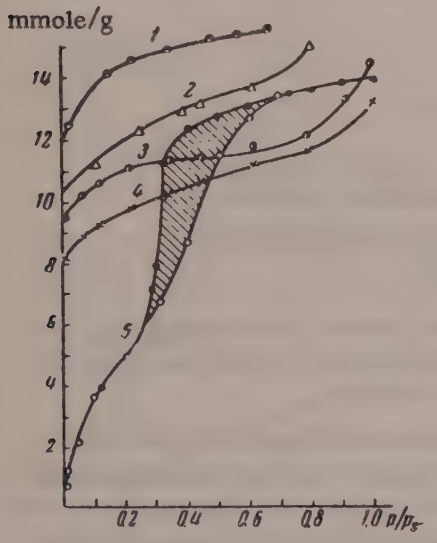


Fig. 4. Sorption isotherms of water vapor at 20° on sodium (1) and calcium (2) zeolites; on American 4A (3) and 5A (4) sieves and on silica gel (5).

Figure 4 shows the sorption isotherms of water vapor on the zeolites we synthesized, on American 4A and 5A sieves and on silica gel. Since the pores of all samples are accessible to water molecules, water vapor is adsorbed well on zeolites. The isotherm curves at very low vapor pressures turn abruptly, while on further increasing the vapor pressure the amount of water vapor adsorbed changes only slightly. The activity of zeolites for water vapor at low values of relative pressure exceeds the activity of small-pored silica gel by six to seven times. The sorption isotherms of our samples lie somewhat higher than those of the American ones because of their higher moisture content (Table 2).

The sorption isotherms of ammonia on our sodium (NaA) and calcium (CaA) zeolites at 20° (Fig. 5) show that molecular sieves NaA and CaA have a very large capacity for ammonia. It is characteristic that in this case a sharp rise in the sorption isotherms is observed at low relative pressures.

In order to demonstrate that as the result of ion exchange of sodium by other cations, a change in the molecular-sieve properties of zeolite occurs, the method of "molecular probes" was used. The sorption isotherms of the vapors of water, methyl alcohol, n-hexane, benzene, propane and of carbon dioxide gas were studied.

Table 3 shows which of the adsorbates is adsorbed by one or another of the types of zeolite at their low relative pressures. Adsorption on secondary structure, which occurs when P/P_s approaches unity [6], was not taken into consideration in assembling the table.

As was to be expected, benzene molecules, because of their shape and dimensions could not penetrate the pores of type A zeolites (NaA, KA, LiA, CaA), which was confirmed by experimental data. The sorption isotherm curves for benzene vapor at low relative pressures are concave and squeezed against the pressure axis.

* The chemical analysis was done by A. I. Kazantseva and E. V. Koryakina. The x-ray and thermographic studies were done by A. E. Voitsekhovskii. The authors express their thanks to these persons.

Potassium, sodium and lithium zeolites, for all practical purposes, do not adsorb n-hexane and propane. The sorption isotherms of propane on dehydrated samples of potassium, sodium and lithium zeolites showed no increase in weight of the adsorbent when the pressure of propane in the system was 13 mm.

TABLE 2. Chemical Composition of Artificial Zeolites, %

Sample	Moisture			SiO_2	Al_2O_3	CaO	MgO	Na_2O	K_2O	Sum
	hygroscopic	loss at 1100°	total							
4A	5,95	11,35	17,30	35,44	31,60	0,84	0,62	14,0	—	99,80
5A	5,67	12,9	18,57	35,08	32,20	10,66	0,58	2,66	—	99,75
NaA	12,66	10,86	23,52	32,10	28,9	—	—	15,5	—	100,02
CaA	6,30	17,40	23,70	33,40	28,80	12,4	—	1,8	—	100,10
Na Атаб	3,86	14,80	18,66	35,86	30,78	0,62	—	14,1	—	100,02
KA	5,46	10,35	15,81	32,60	28,53	—	—	—	22,60	99,54

TABLE 3. The Properties of Type A Zeolites as Molecular Sieves

Zeolites	Radius of cation, A	Approx. pore dimension, A	Adsorbates					
			H_2O (2,6 Å)	CH_3OH	CO_2 (3,3 Å)	C_3H_8 (4,89 Å)	n-C_6H_{14} (4,9 Å)	C_6H_6 (5,6 Å)
KA	1,33	3,3	+	weak	—	—	—	—
NaA	0,98	4,0	+	+	+	—	—	—
LiA	0,78	4,4	+	+	+	—	—	—
CaA	1,06	5,0	+	+	+	+	+	—
4A	0,98	4,0	+	+	+	—	—	—
5A	1,06	5,0	+	+	+	+	+	—

Note. The adsorbate molecules are arranged from left to right in order of magnitude of their molecular dimensions (the critical diameters of the sorbate molecules are shown in the parentheses); the zeolites are arranged from top to bottom in order of increasing size of the openings in the elementary voids in the crystalline structure.

The sorption isotherms of n-hexane and propane vapor on sodium (NaA) and calcium (CaA) zeolites (Fig. 6, 7) show that crystalline sodium aluminum silicate does not adsorb n-hexane practically at all. The sorption isotherms of n-hexane and propane on calcium zeolite turn up sharply even at low relative pressures.

Complete substitution of sodium by calcium in sodium zeolite sharply reduces the adsorption of methanol (Fig. 8), and the adsorption of such an adsorbate as CO_2 is reduced to zero. It is interesting to note that potassium zeolite, synthesized from gel-form potassium aluminum silicate is analogous to potassium zeolite prepared by cation exchange from sodium aluminum silicate in its adsorption properties (adsorption of methyl alcohol and carbon dioxide).

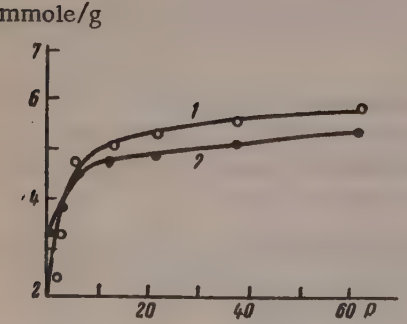


Fig. 5.

The sorption isotherms of carbon dioxide gas on sodium (NaA) and calcium (CaA) zeolites, American 4A and 5A molecular sieves, and silica gel show that the openings of the elementary voids in these samples are accessible to molecules of carbon dioxide gas and that zeolites, in comparison to silica gel, are sorbents with greater adsorptive capacity for carbon dioxide.

The dimensions of the openings of the elementary voids of the crystalline structure of all the zeolites shown in Table 3 are accessible to water molecules. This was to be expected on the basis of a comparison of the critical diameter of water molecules and the dimensions of the entrance to the adsorption voids of the synthetic crystalline aluminum silicates.

Thus, it was shown by the molecular probe method that the diameter of the openings of the elementary voids is changed by the exchange of sodium ions by other cations. Consequently, the cation exchange reaction may be utilized for the modification of the molecular sieve properties of artificial zeolites.

The molecular sieve properties of artificial zeolites may be changed by the exchange of sodium ions in sodium aluminum silicate by other cations. Since the sodium ion is only slightly smaller than the calcium ion (their radii are 0.98 and 1.06 A) and in the exchange reaction two ions of sodium are replaced by one ion of calcium, the dimensions of the pores in calcium zeolite become larger. If in sodium zeolite the dimension of the openings of the elementary voids in the crystalline structure is ~4 A, then it will reach ~5 A in calcium zeolite. In similar fashion one may calculate approximately the dimension of the pores of artificial zeolites (LiA, KA) synthesized from sodium aluminum silicate (Table 3).

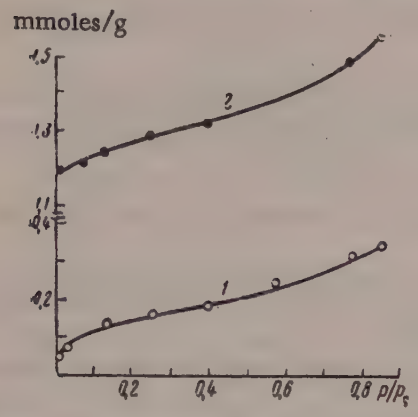


Fig. 6. Isotherms of the adsorption of vapors of n-hexane at 20° on sodium (1) and calcium zeolites (2).

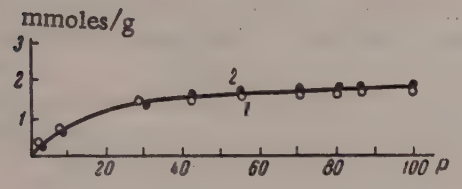


Fig. 7. Isotherms of the adsorption of propane at 20° on calcium zeolite CaA (1) and on 5A (2).

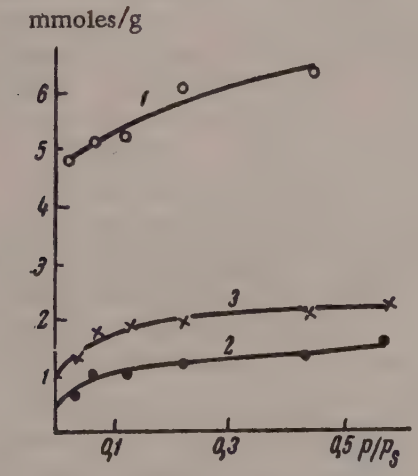


Fig. 8. Isotherms of the adsorption of vapors of methyl alcohol at 20° on sodium zeolite (1) and potassium zeolites synthesized by cation exchange (2) and by the crystallization of gel-form potassium aluminum silicate (3).

Studies of the amount of adsorption of molecules of various dimensions confirmed that the diameter of the pores changes on replacing a sodium ion by ions of other metals. Thus, for example, n-hexane and nitrogen are adsorbed on calcium zeolite, while sodium zeolite practically does not adsorb them at all.

The poor adsorptive capacity of sodium aluminum silicate for nitrogen is not related to the inaccessibility of the pores to the nitrogen molecule, but rather to the fact that the dimensions of the pores and the critical diameter of the nitrogen molecule are very close. As Barrer [3] and Dubinin [6] showed, the activation energy which determines the kinetics of sorption reaches a considerable magnitude, and the rate of sorption at low temperatures becomes fairly small. Nitrogen is adsorbed on sodium zeolite at high temperatures and on calcium zeolite at low temperatures.

Benzene molecules which have a critical dimension exceeding 5A are not adsorbed on type A zeolites (NaA, KA, LiA, CaA).

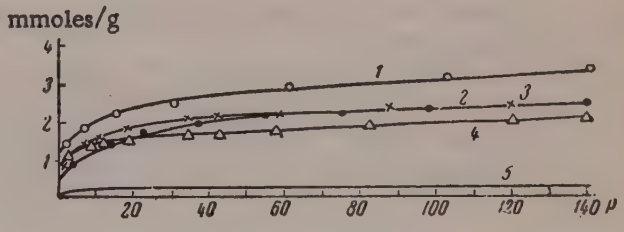


Fig. 9. Isotherms of the sorption of carbon dioxide gas at 20° on sodium (1) and calcium (2) zeolites; on American molecular-sieves 5A (3) and 4A (4) and on silica gel (5).

Adsorption on zeolite differs essentially in a number of respects from adsorption on other sorbents. Interaction between molecules of the sorbate, in this case, is reduced to a mininum since they are separated from one another by the atoms of aluminum silicate. However, the interaction of the molecules of the sorbate with the sorbent is greatly increased as a result of the fact that the sorbate molecules are sorrounded by the sorbent on all sides. Because of the superposition of the margins of the opposite walls in the narrow pores of the zeolites, the adsorption potential increases sharply and as a result of this the zeolite has a very high adsorptive volume at low sorbate concentrations (see sorption isotherms in

Fig. 4). The dispersional energy of the van der Waals interaction in the narrow pores may be six times greater than on a flat surface [7].

Since the zeolites are polar sorbents, they have a great affinity for polar molecules, and especially for water (Fig. 4); therefore the artificial zeolites are highly efficient drying agents. Drying a gas by means of molecular sieves is eight times more effective than successive drying by means of magnesium perchlorate and phosphorus pentoxide [8].

SUMMARY

1. A method for preparing artificial zeolites without the use of an autoclave was described. Crystalline sodium aluminum silicate may be prepared from solutions of sodium aluminate and water glass in the presence of excess alkali at 60-80°C.

2. Crystalline calcium aluminum silicate cannot be prepared either at low crystallization temperatures nor by hydrothermal treatment of a gel of calcium aluminum silicate. Crystalline calcium aluminum silicate is most easily prepared by the exchange of the sodium ion in sodium zeolite by calcium.

3. Potassium and lithium aluminum silicates may also be prepared from sodium zeolite by cation exchange with the corresponding metal ions.

4. The zeolites which we synthesized had a high adsorptive capacity for water vapor at low relative pressures, exceeding the adsorptive capcity of fine-pored silica gel by six to seven times.

5. By using the molecular probe method it was shown that sodium, calcium, potassium, and lithium zeolites have differing molecular-sieve properties.

LITERATURE CITED

1. D. Weigel and E. Steinhaff, Kristallogr. 61, 125 (1925); D. V. Mak-Ben, "Sorption of Gases and Vapors on Solids," ONTI, Goskhimizdat, M. L. [in Russian] (1934).
2. R. M. Barrer, English pat. 574911 of January 25, 1946; ref. Chem. Abstr. 43, 1618 (1949); German pat. 1041020 of February 27, 1957; ref. Chem. Zbl. 33, 1068 (1950); E. E. Sensel, US pat. 2841471 of October 23, 1956; ref. Chem. Zbl. 24, 7919 (1959).
3. R. M. Barrer, Brit. Chem. Engng. 4, No. 5 (1959); R. M. Barrer, et al., J. Chem. Soc. 195 (1959).
4. P. R. Scarre, Chem. Age India 8, 81 (1957).
5. F. M. Shemyakin, E. S. Mitselovskii, and L. V. Romanov, "Chromatographic Analysis," Goskhimizdat, M. [in Russian] (1955).
6. M. M. Dubinin, I. M. Vishnyakova, E. D. Zaverina, E. G. Zhukovskaya, E. A. Leont'ev, V. M. Luk'yanovich, and A. I. Sarakhov, Izv. AN SSSR, Otd. Khim. n. No. 3, 396 (1961).
7. I. H. de Boer and I. F. H. Custers, Z. Phys. Chem. Abt. B. 25, 225 (1934).
8. C. C. Addison, E. Iberson, and I. B. Raynor, Chemistry and Industry 96 (1958).

All abbreviations of periodicals in the above bibliography are letter-by-letter transliterations of the abbreviations as given in the original Russian journal. *Some or all of this periodical literature may well be available in English translation.* A complete list of the cover-to-cover English translations appears at the back of this issue.

REINFORCING OF RUBBER IN LATEX*

3. ELECTRON MICROSCOPE STUDY OF FILLED LATEX MIXES

K. A. Pechkovskaya, L. G. Senatorskaya, B. Z. Berman

and B. A. Dogadkin

Scientific Research Institute of the Tire Industry, Moscow
Translated from Kolloidnyi Zhurnal, Vol. 23, No. 4,
pp. 462-463, July-August, 1961
Original article submitted November 21, 1960

The usual resin mixtures are prepared by the addition to solid rubber of vulcanizing agents, carbon black reinforcers, and other ingredients. The process is carried out on open rolls, or in a closed resin mixer, and is, in essence a process of rubbing the ingredients into the polymer. This mechanical action in the presence of air, leads to the result that the fundamental process is inevitably accompanied by side effects, principally mechanical and oxidational rupture of the molecular chains of the polymer, and recombination of the breaks into new, more branched chains. As a result, the structure of the polymer is changed.

Change in structure of the polymer on mixing can be avoided if all the ingredients are added, not to the solid polymer, but to a dispersion in water, namely, a latex. However, it was found that when carbon black is added to the latex, the reinforcing action on the polymer is markedly reduced in its effect.

The investigations of Dogadkin and his co-workers [1], have shown that reinforcement can be effected if a substance such as casein is added to the latex, which produced destabilization and co-deposition of the components of the latex mixture. In the presence of casein, the mechanical strength of a vulcanized sheet of butadienestyrol latex containing carbon black is increased from 25 to 200 kg/cm^2, [1].

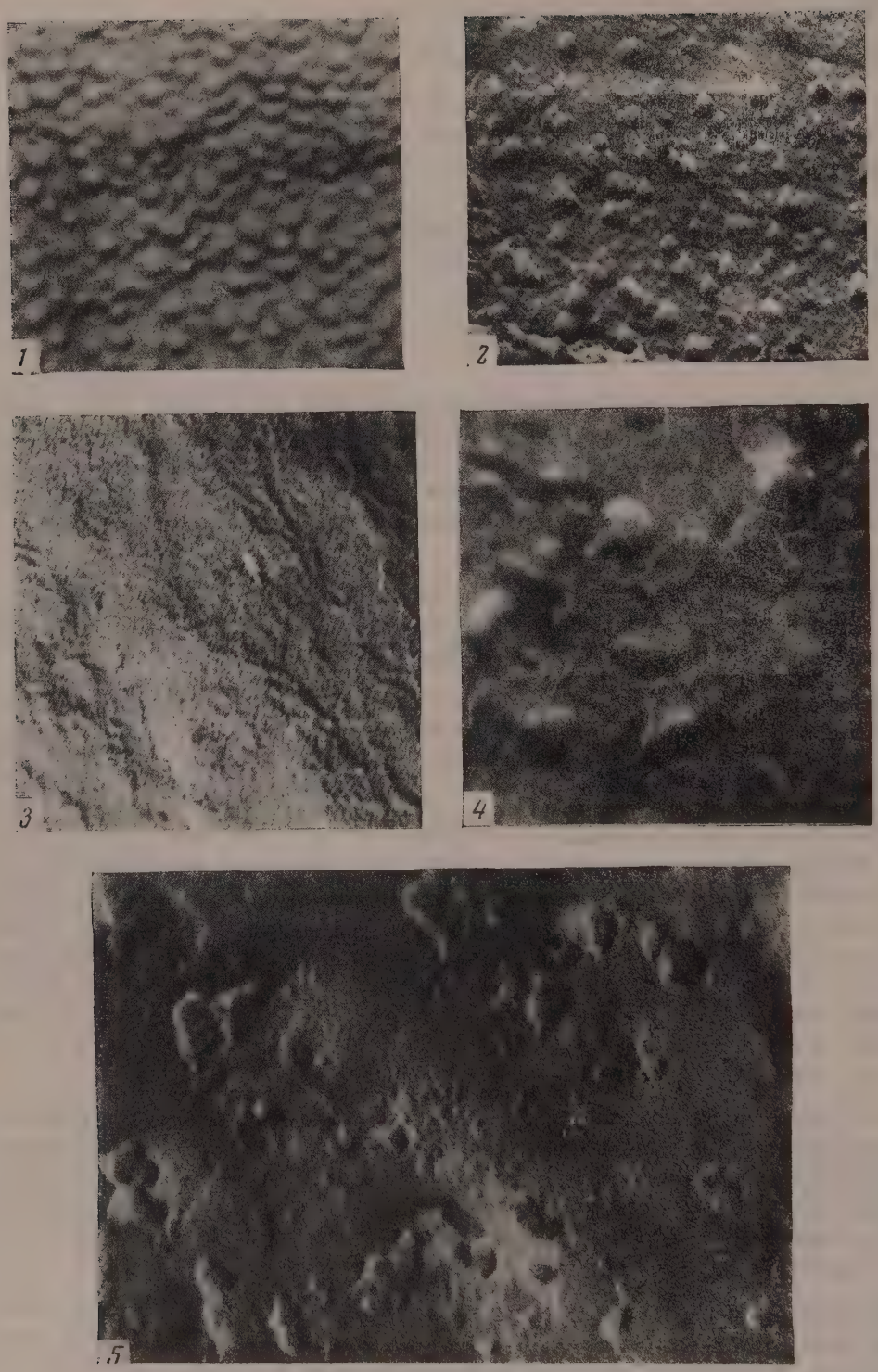
In order to study the changes in the structure in the presence of carbon black and casein, and to investigate the reinforcing action, the latex films were subjected to an electron microscope study. The microscopic preparations were made by the method of one stage collodion, quartz, and charcoal replicas. After depositing the replica on the object, the film formed is strengthened by a thicker layer of some readily soluble plastic substance, most often gelatin. Before taking off the replica, the object was frozen in liquid nitrogen, since otherwise the replica would take a rather thick layer off of the surface of the object. Then, as usual, the gelatin was dissolved off with hot water, the replica was washed and dried, and, in the case of collodion, was stained with chromium. Photographing the replicas was done on a modernized ÉM-100 electron microscope with an illuminating diaphram in the condenser lens, 0.25 mm in diameter and an aperture diaphram 0.05 mm in diameter, at an electron magnification ~ 20,000.

In a film which contains neither carbon black or casein, a continuous globular structure is observed (photograph 1). If casein is present (photograph 2) the structure of the film changes; part of the globules disappear and are replaced by the grain structure described previously [2], which is characteristic of many polymeric materials in mass. Obviously, the casein partially replaces the protective substance on the surface of the globules, thus causing them to be destabilized. The destabilized globules, coalescing with one another, form a continuous polymer phase. The destabilizing action of casein has also been shown by other independent methods [1].

The liberated polymer molecules find it possible to interact directly with the carbon black, whereas, previously, the interaction was limited to the surface of the globules. On the whole, the area of contact of the rubber with the carbon black is increased, which leads to an increase in the reinforcement, and to an increase in the mechanical strength of the film.

If an unvulcanized, filled film is subjected to mechanical working on the rolls, the globules that have remained intact are destroyed. The electron microscope picture of a film of this sort shows characteristic grain structure and

* Presented at the Third All Union Conference on theElectron Microscope in October, 1960 in Leningrad. The second communication of this series was pringed in he Transactions of the Second Conference on Latex, Leningrad, 1958.



Photographs of the beginning of the emulsion forming pocess taken at intervals of 10 seconds.

complete absence of globules (photograph 3). It is very important, that after vulcanization, a film of this sort is somewhat stronger than the film which has been destabilized but not subjected to mechanical working. The increase in strength in this case may be explained by a new increase in the area of contact of the rubber with the carbon black from the interaction of the latter with the additional liberated rubber molecules. It is interesting to notice that the carbon black also exhibits some desorptional action on the protective membrane of the globules. A latex film containing carbon black without casein consists of larger and more widely spread globules (photograph 4). If casein and carbon black are both present, the fraction of globules remaining is still smaller (photograph 5).

The electron microscope study here given made it possible to observe one of the mechanisms by which the destabilizing agents affect the reinforcement of the polymer in the latex, and the mechanical strength of the latex systems. This mechanism consists in the liberation of polymer molecules which had formerly been confined in the globules. The liberated molecules find it possible to interact with the carbon black, which favors an increase in the area of contact of the rubber with the carbon black, and consequently an increase in the reinforcing effect and the mechanical strength of the system.

Along with these added substances, other factors have an effect on the way the carbon black is distributed in the latex. These factors have been discussed in a previously published paper, [1], and they have likewise been found to have an effect on the reinforcement of the rubber in the latex.

SUMMARY

Electron microscope photographs show that when agents which promote the reinforcement of rubber by fillers are added to latex, the globules are observed to coalesce forming a continuous rubber phase, as a result of which the rubber comes into direct contact with particles of the filler. This confirms the idea developed previously in Ref [1] concerning the conditions under which the rubber and the latex is reinforced.

LITERATURE CITED

1. B. A. Dogadkin, and L. G. Senatorskaya, et al., Kolloidn. Zh. 18, No. 5, 528, 1956: B. A. Dogadkin and L. G. Senatorskaya, Transactions of the Second Conference on Latex, Leningrad, 1958.
2. A. S. Lykin, and K. A. Pechkovskaya, Izv. AN SSSR, Physics Series, 23, 725 1959.

All abbreviations of periodicals in the above bibliography are letter-by-letter transliterations of the abbreviations as given in the original Russian journal. *Some or all of this periodical literature may well be available in English translation.* A complete list of the cover-to-cover English translations appears at the back of this issue.

INVESTIGATION OF LONG-RANGE DIFFUSION FORCES BETWEEN WATER DROPLETS AND NONVOLATILE PARTICLES

P. S. Prokhorov, and L. F. Leonov

Institute of Physical Chemistry of the Academy of Sciences,
USSR, Moscow
Translated from Kolloidnyi Zhurnal, Vol. 23, No. 4,
pp. 464-468, July-August, 1961
Original article submitted May 12, 1960

Working out the theoretical bases of the dissipation of natural and artificial fogs requires some knowledge of the physical chemical processes which take place in them. One of the most important problems awaiting solution is the further investigation of the factors which affect the coagulation of droplets in the fog, and in particular, refining the value of the capture coefficient. In addition to purely hydrodynamic forces, the capture coefficient may be influenced by forces of diffusional origin, which appear as a result of the diffusion of water vapor from the evaporating drop. Thus, in the presence of a humidity deficiency, repulsive forces of diffusional origin arise between the droplets as they approach one another, which prevent them from coming any closer and coalescing.

In the theory developed by Deryagin and Dukhin, [1], it has been shown that the diffusional repulsive forces between water droplets and nonvolatile particles at a distance much greater than their radii are small, but fall off inversely proportional to the square of the distance between them, i.e., relatively slowly, in particular in comparison with the law governing the decrease of molecular forces.

In our paper we give quantitative measurements of the long-range diffusional forces which arise between water droplets and solid particles carried out by a specially developed technique. The measurements were made with a torsion balance having a sensitivity of $0.4 \cdot 10^{-9}$ grams, incorporating a photoelectric amplifying circuit and a self-collimating grating photo-relay* (Fig. 1).

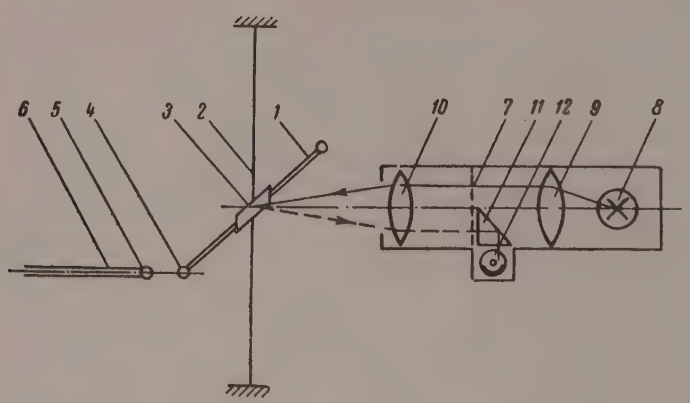


Fig. 1. Diagram of torsion balance.

The silvered glass beam 1, of the torsion balance, Fig. 1, is held by the suspensions 2, made of phospher bronze ribbon with a cross section $10 \times 50\mu$ 4.6 cm long with a displacement modulus $q \approx 0.435 \cdot 10$ g/cm^2. A rectangular mirror 3 is attached to the middle of the beam, and on the ends are silvered glass spheres 4. The whole movable

* The circuit of the self-collimating grating photo relay was proposed by Deryagin. It may also be used to shorten the period of oscillation of the suspension by means of a feed-back connection, as shown in the diagram given previously in [2].

part of the torsion balance is mounted on a base with leveling screws, and is enclosed in a hermetically sealed copper box. The walls of the box have glass windows for illumination, observation, and transmission of the light beam from the grating photo-relay. The drop 5 was pressed out of the silvered glass tube 6 and brought up gently to the sphere 4 by means of an electric motor. In order to set the drop and the sphere in the proper relation to one another, the tube 6 is mounted on a positioning mechanism, which enables it to be moved in two mutually perpendicular directions, at the same time keeping the chamber hermetically sealed. Through a packing gland in the top of the box, a small stirrer is admitted to agitate the air inside the chamber before the experiment.

To avoid external vibration, a special shock absorbing device was used which consists of an upper plate of thin sheet steel with stiffening ribs on which the torsion balance is mounted. The plate is supported by the leveling screws on four resin pillows, to which, during the time the shock absorber is operating, air is admitted at a pressure of 0.4 – 0.5 atmospheres. All the pillows are united to one another by flexible vacuum hose, therefore, they are all at the same pressure. Rigidly suspended from the plate is a massive weight (200 kg) one meter below the level of the plate. Thus, the center of gravity of the system is considerably lower than its support. The low position of the center of gravity and the combined effect of all the elastic supports (pillows), makes for good stability of the system, and the elasticity of the supports and the large mass increase the period of vibration of the system, which considerably reduces the effect of external vibrations on the operation of the torsion balance.

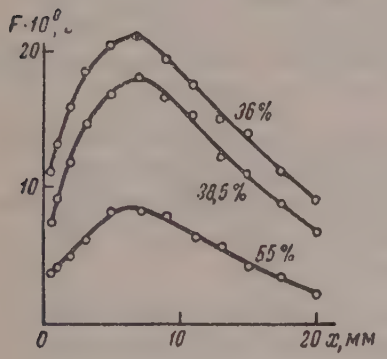


Fig. 2. Attractive forces between drop and sphere, as a function of the distance, in the presence of convection, at various values of relative humidity.

The self-collimating grating photo-relay (Fig. 1) consists of the grating 7 (6.2 lines per cm), illuminated by the lamp 8, fed by a storage battery, two wide aperture "Zonnar" objective lenses 9 and 10, the right angular prism 11 and the STsV-3 photocell 12. The parts are mounted in a tube which may be positioned with respect to the optical path in three mutually perpendicular directions in such a way that its inclination can be varied. The grating photo-relay operates in the following way: to obtain a beam of parallel light the filament of the lamp 8 is placed at the focus of the objective lens 9. The beam of parallel light goes through one-half of the grating 7 and falls on the objective 10. The lens focuses the lamp filament on the mirror 3 fastened to the moving beam. After reflection from the mirror, the light beam again falls on the lens 10, emerges from it parallel and goes through the other half of the grating 7 and is reflected by the prism 11 onto the photocell 12. Thus, a sharp image of half of the grating 7 is projected on the other half of the same grating. Since the axis of rotation of the mirror 3 is parallel with the lines of the grating, as the mirror turns through some angle, the image of the first half of the grating is superimposed on the plane of the second half of the grating. The lines of both halves of the grating are parallel to one another. Thus, as the mirror rotates under an external force, the lines of both halves of the grating overlap which causes a sharp change in the illumination of the photocell over the whole field, which causes a change in current in the cathode circuit of the amplifier. The torsion balance was calibrated by the torsional vibration method which measures the torsional restoring moment of the elastic suspension. The angle of rotation of the beam was determined as a function of the change in indication of an EPP-09 electronic potentiometer connected in the cathode circuit of the amplifier.

The torsion balance just described was used to make a series of measurements of the interaction between a drop 1 mm in diameter brought up to the 1 mm diameter silvered glass sphere shown in Fig. 1. To eliminate the possibility of producing electrostatic charges on the drop, the sphere and the cabinet of the torsion balance were grounded.

During the study of the interaction between the evaporating drop and the glass sphere, we observed forces of clearly nondiffusional origin. Subsequently, it became clear that these forces were caused by convection currents arising in the chamber of the apparatus. The horizontal temperature field was measured under the drop at a distance of 4 mm from the center. Directly under the drop, at a relative humidity of 50%, the ambient temperature was reduced by 1.5°. The presence of a temperature field of this sort produced a vertical convection current directly downward. These convection currents not only reduced the force of repulsion between the drop and the sphere but could reverse its sign.

A torsion balance was used in [3] to observe the repulsion between evaporating water drops at relatively large distances from one another. With a drop radius of 1 mm and a distance of 0.1 mm between them, the repulsive force in air with 55-60% humidity was $1.6 \cdot 10^{-4}$ dyne. The large disparity between the experimentally measured and the theoretically calculated long-range diffusional forces in [3] was obviously caused by convection currents in the air in the balance chamber.

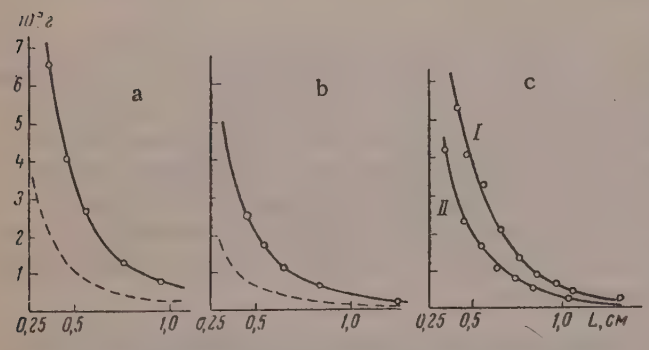


Fig. 3. Curves showing the change in long-range diffusional forces between drop and sphere: a) R = 0; r_s = 0.1 cm; r_d = 0.15 cm; b) R = 40%. r_s = 0.1 cm; r_d = 0.15 cm; c) R = 40%. r_d = 0.15 cm; r_s = 0.22 cm (I) and 0.1 cm (II) (dotted — theoretical curve).

In order to avoid the effect of convection currents, it was necessary to equalize the temperature of the surface of the evaporating drop with the ambient. A miniature heater made of 20μ diameter tungsten wire was placed inside the drop and alternating current was passed through it. A differential thermo-couple was set up near the surface of the drop and the other junction was placed in the chamber, but at a distance of 8 — 10 mm from the drop. Thus, the ambient temperature could be equalized with an accuracy of 0.01°. When the drop is overheated relative to the ambient, convection currents arise, directed upward, but the effect of this is similar to that of the convection directed downward. Therefore, the absence of convection currents may also be monitored by finding the maximum in the repulsive force between the drop and the sphere.

The measurements of the diffusional forces (after eliminating the effect of convection currents) were carried out at different ambient humidities and different distances. When the ambient medium was completely saturated with water vapor, no diffusional forces were observed. The long range diffusional forces were measured at relative humidities of 0 and 40%, with a drop radius r_d = 0.15 cm, and a sphere radius r_s = 0.1 cm.

At zero humidity the diffusional forces show up to a considerable extent, and the magnitude depends on the distance, Fig. 3. At 40% humidity, the diffusional forces have a considerable magnitude, but they clearly drop off much more sharply than at zero humidity (Fig. 3 b), which is not at variance with the data obtained previously in [1] and [2].

Increasing the radius of the sphere to 0.22 cm produces a 1.5 — 2 fold increase in the long-range diffusional forces, which is also in agreement with theory, (Fig. 3c).

It was not possible to measure the diffusional forces at very small distances since moving the drop up to the sphere displaced the beam from its working position.

It has been established from the measurements given that the magnitude of the diffusional forces is inversely proportional to the square of the distance in the range 12 to 5 mm, which agrees with the theory of the attenuation of the forces with distance. However, the experimental value of the proportionality constant in this region is approximately 2.5 times greater than the theoretical. The order of magnitude of the repulsive forces in this region is $1 \cdot 10^{-9}$g. If the drop is brought up closer, the square law is departed from and the forces increase less rapidly. This discrepancy may be interpreted in the following way. The theory of Ref. [1] considers the force which arises from the sphere being surrounded by a Stefan current, i.e., from the relative velocity of the sphere and the center of mass of the surrounding vapor air mixture. Here, Stokes' law, which assumes that there is no slip on the boundary between the sphere and the surrounding medium is used. At the same time, the presence of concentration gradients in the medium, tangential to the surface of the sphere, ought to cause slip of the gas relative to the latter and, consequently, an additional force, which explains the discrepancy, Ref. [6].

SUMMARY

1. A type of torsion balance has been developed, with a high degree of sensitivity ($0.4 \cdot 10^{-9}$ g), and a short period of oscillation, by using a photo electric amplifier circuit with a self-collimating grating photo-relay.

2. The long-range diffusional forces between water drops and silvered glass spheres at 0 and 40% relative humidity are inversely proportional to the square of the distance, or distances from 12 to 5 mm, which is in agreement

with the theoretical calculations for the case, but the proportionality constant is 2 – 2.5 times larger than the theoretical value derived only from the Stefan current.

3. The fundamental cause of the quantitative discrepancy between the theoretically calculated and experimentally measured long-range diffusional forces is the presence of slip of the gas on the boundary between the sphere and the surrounding medium, which causes an increase in the repulsive forces.

We express our gratitude to corresponding member of the Academy of Science, USSR, B. V. Deryagin for the interest shown in the present work, which, in considerable degree, encouraged us to carry out the experiments.

LITERATURE CITED

1. B. V. Deryagin, and S. S. Dukhin, Dokl, AN SSSR, 106, 851, 1956; 111, 613, 1956; 112, 3, 1957.
2. B. V. Deryagin, Dokl. AN SSSR, 61, 2, 1948.
3. V. A. Fedoseev, and A. I. Polyanskii, Odessa University Bulletin, Collection of the Physics and Mathematics Dept. and the Scientific Research Institute of Physics, 5, 95, 1954 [in Russian].
4. B. V. Deryagin and P. S. Krokhorov, Dokl. AN SSSR, 54, 6, 1946; Collection of Reports "New Ideas in the Field of Aerosol Studies", Izd. AN SSSR, 1949 [in Russian].
5. P. S. Prokhorov, Zh. Fiz. khimii 21, 9, 1947; Kolloidn Zh. 2, 2, 1948.
6. B. Derjaguin, and S. Bakanov, Trans. Faraday Soc. (in press).

All abbreviations of periodicals in the above bibliography are letter-by-letter transliterations of the abbreviations as given in the original Russian journal. *Some or all of this periodical literature may well be available in English translation.* A complete list of the cover-to-cover English translations appears at the back of this issue.

ELECTROCHEMICAL STUDY OF BENTONITE SUSPENSIONS

6. POTENTIOMETRIC TITRATION OF AMINOBENTONITE COMPLEXES

I. A. Uskov and E. T. Uskova

T. G. Shevchenko Kiev University, Kiev Technological Institute of the Food Industry

Translated from Kolloidnyi Zhurnal, Vol. 23, No. 4, pp. 469-474, July-August, 1961
Original article submitted June 2, 1960

The cation exchange properties of clays [1] – [3], are caused by the considerable negative charge which is present on the clay particles. Recently, clays have been used in which the exchange cations are replaced by organic ions [3]. The result of a substitution of this sort is a radical change in the surface of the clay particles, which changes from hydrophilic to hydrophobic.

When clays of the montmorillonite group react with salts of high molecular amines, stable aminobentonite complexes are formed [4] and [5]. In this case intermolecular attraction forces [6] and [7], are acting in addition to the electrostatic forces.

If we are going to prepare active fillers with definite properties for resins [8], and plastics [9]–[10], we must be able to explain the mechanism by which the aminobentonite complexes are formed. One of the most highly recommended and promising methods of studying the surface properties of colloids, [11], and in particular, bentonite suspensions, [12] and [13], is the potentiometric titration method. In the present paper, this method has been used to study the formation of aminobentonite complexes and the nature of the products formed.

In organizing the study, we started from the fact, that, when electrodialyzed bentonite reacts with a salt of an amine, an undissociated aminobentonite complex, [7], is formed, which is insoluble in water, and an equivalent quantity of free acid, or aluminum chloride, [6] and [12] is split off according to the reaction

$$H_nM + mRNH_3Cl \rightarrow H_{n-m}(RNH_3)_mM + mHCl, \quad (1)$$

where M designates the n-valent montmorillonite anion, and R designates the hydrocarbon radical of the amine.

After the precipitate is washed, the free acid (or aluminum salt) is removed, and the only thing that is titrated is the aminobentonite complex. The residual unsubstituted hydrogen (or aluminum) ions may be titrated out with alkali according to the reaction

$$H_{(n-m)}(RNH_3)_mM + (n-m)NaOH \rightarrow Na_{(n-m)}(RNH_3)_mM + (n-m)H_2O \quad (2)$$

If the amine salt is added in quantities which exceed that equivalent to the cation exchange capacity of the bentonite, adsorption of the excess amine salt, Ref. [14] occurs according to the reaction

$$(RNH_3)_nM + mRNH_3Cl \rightarrow (RNH_3)_n(RNH_3Cl)_mM \quad (3)$$

It is to be expected that the aminized bentonite will be titrable with alkali just like the pure amine salt according to the reaction

$$(RNH_3)_n(RNH_3Cl)_mM + mNaOH \rightarrow (RNH_3)_n(RNH_2)_mM + mNaCl + mH_2O \quad (4)$$

Thus, the alkaline titration of aminobentonite complexes, in which the organic cation content is less than the equivalence value, ought to proceed just as though the concentration of electrodialyzed bentonite in the system had simply been reduced by an amount equal to the amount of acid and aluminum salt replaced and removed in washing,

or, what is the same thing, if the acidity of the preparation had been reduced accordingly. However, in the titration of hyperaminated preparations, we ought to get the quantity of amine salt added over and above the cathode exchange capability of the amount of bentonite taken. With bentonite aminated in the stoichometric relation the acidity should be absent.

The deviations of the exchange capacity from the additive values of acidity, calculated from the equations which apply to the case, should stand in direct relation to the mechanism of the reaction of the amine in question, and its salts, with bentonite.

The electrodialyzed ascangel was prepared as in [13], and was kept for a year after electrodialysis in order to reach a state of equilibrium. The amination was carried out by the exchange reaction of this preparation with octadecylamine hydrochloride. The latter was prepared from octadecylamine by treating with an excess of hydrochloric acid in alcohol solution and was purified by recrystallizing twice from alcohol.

The dilute suspension of the electrodialyzed ascangel (about 0.5%) was mixed with a definite quantity of 0.1% solution of octadecylamine hydrochloride at 70-72°. The resulting flocculent precipitate was washed with water and after centrifuging was diluted to give an approximately 0.5% suspension.

The titration samples were taken out with a pipette which had a high rate of runout so as to avoid settling of the suspension on the walls of the pipette. The samples were titrated with continuous agitation by a constant velocity magnetic mixer. For the pH measurement, an antimony electrode with constant surface of contact [13], was used with a calomel electrode attached to the titrating system through a neck with a ground in cover. E. M. F. readings were made every 60 seconds. The next portion of alkali was added immediately after balance had been reached.

After the titration was finished, the concentration of the suspension was determined by a gravimetric method, allowing for the quantity of amine salt added and the amount of alkali run in. From these data the potentiometric curves were calculated, which gave the pH values as a function of the quantity of sodium hydroxide added in microequivalents per gram of dried electrodialyzed bentonite.

The initial solution of octadecylamine hydrochloride titrates like an acid of moderate strength (Fig. 1). These

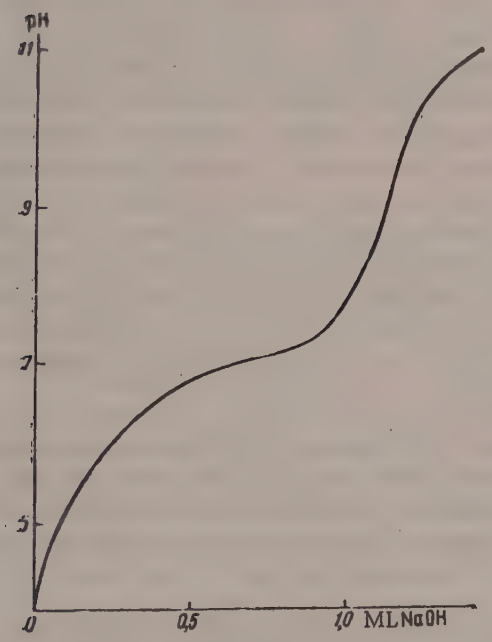


Fig. 1. Potentiometric titration curve of 5 ml of 0.34% octadecylamine hydrochloride with 0.05 N caustic soda.

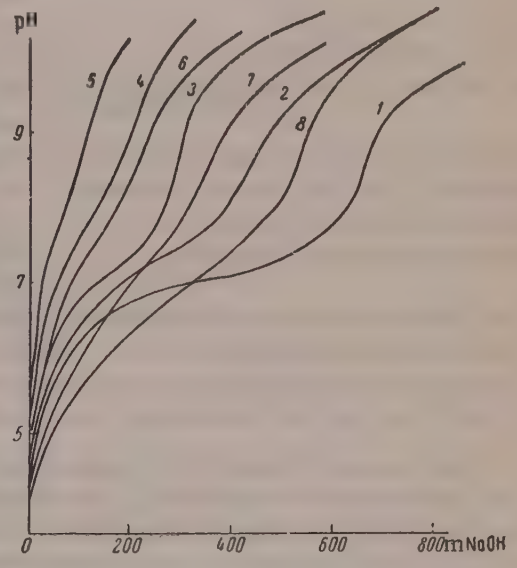


Fig. 2. Potentiometric titration curves of aminobentonite complexes containing different quantities of octadecylamine in microequivalents per gram of electrodialyzed bentonite: 1) 0; 2) 155; 3) 320; 4) 540; 5) 660; 6) 920; 7) 1080; 8) 1320.

data were used to calculate the concentration of the amine salt from which the aminated bentonite preparations were originally prepared.

The more the amine concentration in the aminobentonite complex is increased, the less marked the inflection point in the neutralization region of the titration curves becomes, and the curves themselves are displaced to the left as in Fig. 2. For completely aminated bentonite the exchange capacity, or, more accurately, the acidity of the preparation, is not equal to zero, as might be expected from the principal of equivalent substitution of exchanged cations by the amine radical.

If we continue to add amine salt over and above the equivalent quantity, even this does not give a preparation with zero exchange capacity. More than that, the acidity of the preparations again begins to increase, and the form of the curves more and more suggests the titration curve of an amine salt. This similarity appears in particular, from the fact that the equivalent neutralization region lies higher than in the case of preparations having residual acidity from the electrodialized bentonite where the values lie closer to the pH value for the pure amine.

If we draw the curve which fits the conditions (2) and (4), it will take the form of two branches diverging symmetrically from a point on the axis of the quantity of amine salt added, which corresponds with the cation exchange capability of the bentonite (dotted curve of Fig. 3). The experimentally determined points (Fig. 3, solid line) lie on a curve which does not fit the theoretically calculated one.

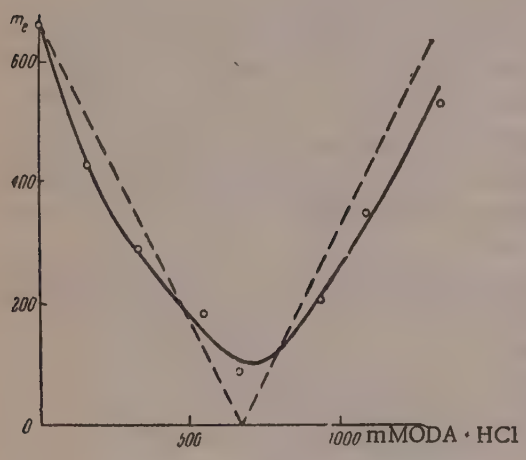


Fig. 3. Titrated acidity of aminobentonite complexes, m_e, as a function of the quantity of octadecylamine hydrochloride added per gram of electrodialyzed bentonite.

Adding relatively small quantities of an organic cation to the bentonite exchange complex causes a more considerable lowering of the acidity than might be expected from Eq. (2). At the same time, the samples with nearly the equivalent ratio of amine salt to bentonite have a higher acidity than might be expected. Further addition of amine salt, however, gives preparations with a lower acidity than that required by Eq. (4). As is the case with under-aminated samples, the over-aminated preparations have equivalence points which lie below the theoretical curve.

The observed phenomenon may be explained by the fact that the first portions of organic cation added cause shielding of part of the exchange-active points on the bentonite particles. As a result, the acidity of the preparations does not drop by an amount equivalent to the quantity of amine salt added, but to a somewhat higher value. The appearance of the groups being titrated with alkali, when the bentonite is overaminated, indicates that a secondary adsorption process is taking place, which obviously consists in the adsorption of amine salt molecules on the already aminated surface of the bentonite particles [14]. Actually, this salt is dissociated and may be titrated out just like the free amine salt. Apparently, the adsorption occurs on the hydrocarbon radicals of the amine and has no effect on the properties of the octadecylamine hydrochloride. But here, nevertheless, not all the excess amine salt gets titrated out but only the greater part of it. This may be explained either by the formation of a polymolecular layer of amine salt on various portions of the surface of the bentonite, or by the titration of new exchange adsorption centers which up to that time had taken no part in the neutralization reaction.

Of all the ideas which we have considered on the acidic character, [13] exhibited by electrodialyzed bentonite, the last one seems the most probable. At the same time, if some of the acid forming groups lie sufficiently deep inside the packets of themontmorillonite crystal lattice, the large octadecylamine ion will have trouble getting at them. This does not exclude the possibility that aluminum ions may migrate out and encounter hydrochloride ions or the other way around.

However, we must not reject the idea that a polymolecular layer of amine salt is formed. The formation of a layer of this sort, [15], ought to be accompanied by a more or less strong shielding of the positive charge on the organic cation. This shielding may be considered as a special type of steric hindrance even for the mobile hydroxyl ions of the alkali.

It must be emphasized that in the region where equivalent quantities of amine salt are added to the bentonite the preparations maintain a considerable acidity. This comes from the fact that we are titrating both the acidifying

groups of the electrodialyzed bentonite and the amine salt molecules adsorbed on the organophilic surface of the bentonite particles.

The study, which we have made, enables us to explain the interesting phenomena observed previously, which, up to the present, had remained without explanation. Hendricks [6] found that large organic cations lower the cation exchange capability of montmorillonite while small ones do not affect it. This is completely comprehensible if we accept the shielding effect of large organic cations on the cation exchange localities. Francen [15] has shown that cetyltrimethylammonium bromide is adsorbed on montmorillionite in an amount which is 2.4 times greater than the cation exchange capability of the mineral. From our study, this conception of the adsorption of bromine ions may be considered proven.

In the study of the equilibrium in bentonite – soda – amine salt systems, Cowan and White, [14] found that the equilibrium constant changes in the initial stages of the exchange. They ascribe this to changes in the montmorillonite structure which can occur when it reacts with an amine salt. Now it may be asserted that the cause of this is to be found in the appearance of van der Waals forces, and the shielding of the exchange localities occupied by sodium through the aliphatic amine chains.

Kurilenko and Mikhailyuk, [16], studying the effect of different amounts of trimethyloctadecylammonium chloride bound with an ascangel, found, from the heat of wetting of the latter with water, that even with equivalent replacement of the exchange cations by an organic ion (more accurately for an equivalent amount of amine salt taken), the heat of wetting of the ascangel by water remains considerable (1/10 of the heat of wetting of the hydrophilic bentonite soda). This becomes clear if we keep in mind that the competitive effect of several simultaneously occurring processes causes physical adsorption of the amine salt right up to the point where all the resources of cation exchange are used up.

In the final count, the data presented may be explained by steric effects arising from the interaction of bulky organic cations with the partially aminated surface of the bentonite particles.

SUMMARY

1. The reaction of electrodialyzed bentonite with a salt of a high molecular amine has been investigated by potentiometric titration.

2. It has been found that no completely neutral aminobentonite complexes are found at any degree of amination. If the amine is added to the complex in quantities greater or less than that equivalent to the cation exchange capability of the bentonite, the acidity of the preparations deviates from the additive values.

3. The observed phenomena are explained by the shielding action of the adsorbed organic cations and the steric hindrance arising from this.

LITERATURE CITED

1. K. K. Gedroits, Selected Works, Vol. 1, [in Russian] Sel'khozgiz, Moscow, 1955.
2. S. Mattson, Soil Colloids [in Russian] Sel'khozgiz, Moscow, 1938.
3. R. E. Grim, Mineralogy of Clays [Russian translation] IL, 1956.
4. E. A. Hauser, Colloid. Chem. 7, 431 1950.
5. J. W. Jordan, J. Phys. Colloid. Chem. 53, 294, 1949.
6. S. B. Hendricks, J. Phys. Chem. 45, 65, 1941.
7. R. E. Grim, W. H. Allaway, and F. L. Cuthbert, J. Amer. Ceram. Soc. 30, 137, 1947.
8. E. A. Hauser, and J. W. Jordan, Silicates Industry 17, 9, 1952.
9. I. A. Uskov, Vysokomolek soed, 2, 200, 1960.
10. I. A. Uskov, and T. A. Kusnitsyna, Vysokomolek, soed, 2, 728 1960.
11. W. Pauli and E. Walko, Electrochemie der Kolloide, Wien, 1929; A. I. Ravinovich, and V. A. Kargin, Zh. fiz. khimii, 1, 1930.
12. J. N. Muckerjee, and R. P. Mitra, J. Colloid Sci. 1, 141, 1946; V. A. Chernov, The Nature of Soil Acidity [in Russian] Academy of Sciences Press, USSR, 1947; C. E. Marshall, and C. A. Krinbill, J. Phys. Chem. 46, 1077, 1942, S. N. Papuashvili, M. E. Shishniashvili, and L. D. Agladse, Transactions of the Institute of Chemistry of the Academy of Sciences of the Georgian SSSR, [in Russian] 12, 23, 1956; I. A. Uskov, Scientific Reports of the Kiev University [in Ukrainian] 16, 55, 1957.
13. I. A. Uskov, and E. T. Uskova, Kolloidn Zh. 19, 381, 1957; 20, 487, 1958, 21, 231, 492, 1959.

14. C. T. Cowan, and D. White, Trans. Faraday Soc. 54, 691, 1958.
15. P. Franzen, Clay Minerals Bull. 2, 233, 1955.
16. O. D. Kurilenko, and R. V. Mithalyuk, Kolloidn Zh. 21, 195, 1959.

All abbreviations of periodicals in the above bibliography are letter-by-letter transliterations of the abbreviations as given in the original Russian journal. *Some or all of this periodical literature may well be available in English translation.* A complete list of the cover-to-cover English translations appears at the back of this issue.

STATES OF AGGREGATION OF HIGH-MOLECULAR COMPOUNDS

9. THERMODILATOMETRIC INVESTIGATIONS OF POLYCHLOROPRENE AND NATURAL RUBBER

R. I. Fel'dman

N. K. Krupskaya Moscow Regional Pedagogical Institute
Translated from Colloidnyi Zhurnal, Vol. 23, No. 4,
pp. 475-481, April, 1961
Original article submitted February 18, 1960

Natural rubber, gutta-percha, balata, and synthetic polychloroprene are polymers which are capable of crystallizing over a certain temperature range and on being stretched. The literature [1-6] contains numberous data on the determination of the transition points and regions of polychloroprene and natural rubber, though the results from different methods are often different.

Thermodilatometric investigations of gutta-percha, polyethylene, and other crystallizable, high-molecular compounds showed that in many respects they behave similarly to noncrystalline compounds, but also show their own specific characteristics [7-9]. In the present communication we describe the properties of polychloroprene and natural rubber (smoked sheet) at a varying temperature, which were determined by the procedure developed previously [8]. The data obtained were compared with data we obtained for other polymers [7-9].

Polychloroprene. As x-ray investigations have shown, the structure of polychloroprene is similar to that of β-gutta-percha. The difference consists of a different relative disposition of the units of the molecular chains in the crystalline regions as a result of differences in the volume and polarity of the side methyl groups and chlorine atoms. Because of this, the distance between the molecular chains of the polymers is different and the elasticity of polychloroprene at room temperature is greater than that of gutta-percha [1,2]. Polymerization of chloroprene under different conditions and with the introduction of different stabilizers yields polychloroprenes with different properties, which determine the name or grade of this widely-used polymer [1-4, 10]. Polychloroprenes of different grades crystallize on stretching by 400-500% [2] in the temperature range from ~ -35 to $+32°$ [3]. The crystallization rate depends on the temperature and is maximal at $t \approx 0°$ [3]. The lower the chloroprene polymerization temperature, the higher is the polychloroprene crystallization rate [4].

In the present work we used Soviet industrial polychloroprene. The temperature dependences of the length and volume were determined for samples in the form of films and blocks with various histories (preliminary thermal treatment and preparation method). The films from which strips were cut for determination of the temperature dependence of the length (linear dilatometry) were prepared on a mercury surface from a solution of polychloroprene in dichloroethane. The solvent was evaporated at 15-20° in the dark. The evaporation of the solvent and the completeness of its removal were checked gravimetrically as in the preparation of films of other polymers [7,8]. The thickness of the films did not exceed 0.1 cm. The length of the strip was varied from 5 to 10 cm and the width from 0.5 to 1.3 cm. Figure 1 a* shows the temperature dependence of the length of one of the polychloroprene samples, which was obtained with a load $P = 2.3$ g/mm^2. The temperature was varied at a rate of 1° in 3-5 min. The linear expansion coefficient α [cm/°C cm] over the temperature range from 0 to 18°, $\alpha_{0-18°} = 2.91 \cdot 10^{-4}$. The elongation on heating from 0 to 36° (from point A to point B) $\approx 17\%$.

If we consider the differences in the structure and properties of gutta-percha and polychloroprene given above, then the value of the linear expansion coefficient of polychloroprene films agrees completely with that calculated for films of gutta-percha "P" prepared from a solution in dichloroethane on a mercury surface, which $\alpha_{5-23°} = 2.28 \cdot 10^{-4}$, at $P = 10.9$ g/mm^2 [7]. As a result of yield which occurred to some extent at ~37°, after cooling the samples showed a considerable residual elongation, which depended on the rate of temperature change, the final heating and cooling temperatures, the time at the final test temperature, the load, the method of preparing the films, the form and dimensions of the samples, and other factors.

* The scales of the individual curves in Figs. 1 and 3 are different. The absolute values of the sample lengths should not be compared from these figures.

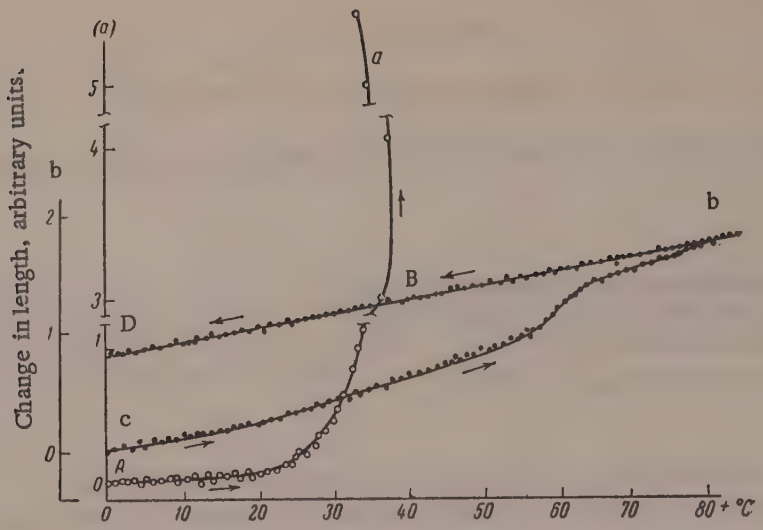


Fig. 1. Temperature dependence of the length of polychloroprene films that had not been heated (a) and that had been heated to 160° (b).

To establish the effect of thermal treatment on polychloroprene films, we heated them for 4 hr in an air thermostat at 130 and 160°. The thermal treatment caused the films to darken, decrease in volume considerably, and lose their solubility in dichloroethane, though they retained the capacity for limited swelling in it. The swelling of films heated to 160° was less than that of films heated to 130°. For example, Fig. 1 b shows the temperature dependence of the length of a film heated at 160° when P = 5 g/mm^2.

The linear expansion coefficients calculated from the linear sections of the dilatometric curve were as follows: $\alpha_{0-20^\circ} = 2.65 \cdot 10^{-4}$; $\alpha_{20-52^\circ} = 5.77 \cdot 10^{-4}$; $\alpha_{64-82^\circ} = 6.04 \cdot 10^{-4}$, and $\alpha_{82-0^\circ} = 3.0 \cdot 10^{-4}$.

When the sample was heated from 0 to 82°, its length increased by ~ 5%, while the increase in length from the beginning to the end of testing (from point C to point D) was 2.5%. Films heated at 130° had $\alpha_{0-21^\circ} = 1.97 \cdot 10^{-4}$ and lengthened by ~ 7.5% from 0 to 82° and ~ 9.0% from 0 to 95° with P = 4.1 g/mm^2. The data obtained indicate an increase in the thermal stability of polychloroprene films after thermal treatment (thermal vulcanization).

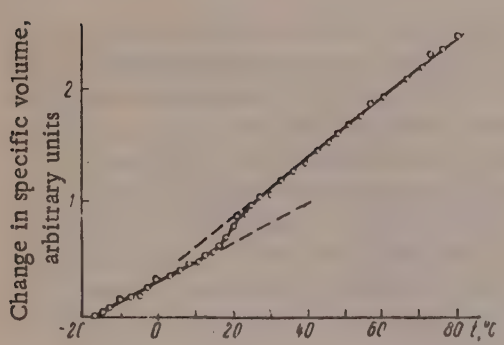


Fig. 2. Temperature dependence of the specific volume of a polychloroprene sample.

The yield, which was observed at 37° with films that had not undergone thermal treatment, was displaced toward higher temperatures with thermally treated films. This is explained by cross-linking of the polymer during thermal treatment, reducing the mobility of the structure.

The smoothness of the cooling sections of the temperature dependences of length and the absence of transition points, which are noticeable on the heating sections, are most likely connected with a normal lag effect as all the transitions are of the relaxation type. We demonstrated this type of phenomenon previously on other high-molecular materials [7-9].

Under our testing conditions, the temperature dependences of the length of samples that had not undergone thermal treatment showed breaks in the temperature ranges from ~ 18 to ~20° and from ~ 33 to ~ 37°. The transition point at t ≈ 20° remained in the same position on the temperature dependences of the length of thermally treated samples, while the other points indicated the transition of polychloroprene from a highly elastic to an elastic yield and then to a viscous yield state of aggregation. It is noteworthy that over the temperature range investigated, the position of the first transition point at ~20°, which was found for untreated and thermally treated polychloroprene, is close to the breaks found on the thermodilatometric curves of gutta-percha [6] and natural rubber.

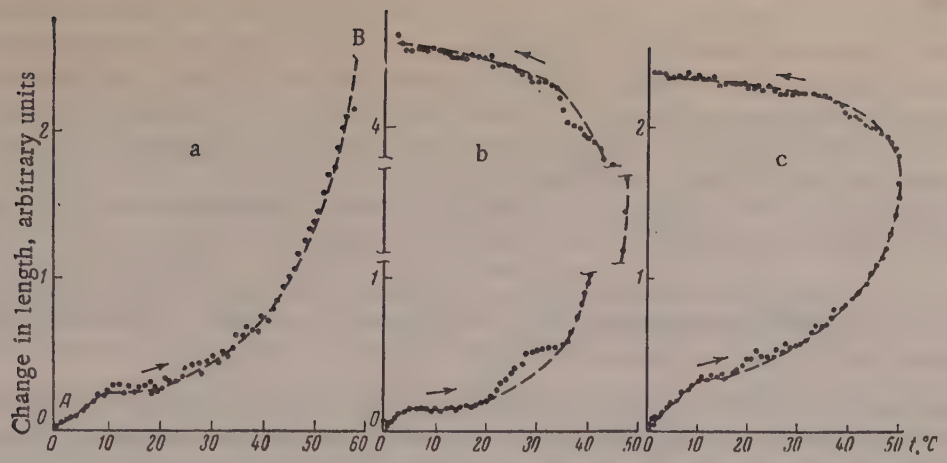


Fig. 3. Temperature dependence of the length of smoked sheet samples: a) Film obtained from benzene solution; b and c) sheets which were first cooled to -15° and + 4°, respectively.

The temperature dependence of the specific volume of a polychloroprene sample cut from an industrial block is given in Fig. 2. The specific volume was measured over the range from -17 to + 80°. The filling liquid in the glass dilatometer was mercury. The relation shown in Fig. 2 is analogous to that obtained for natural rubber samples [6] in the parts where there is a nonlinear change in the specific volume with a change in temperature, which may be connected with disordering of the structure. A comparison of the temperature dependences of length and volume (Figs. 1 and 2) indicates that the former (Fig. 1) has great advantages as regards sensitivity in the determination of transition points and regions for high-molecular compounds.

Natural rubber. It is difficult to obtain thermodilatometric curves for natural rubber by the procedure we adopted as the "equilibrium" length of samples under load is reached extremely slowly. As was shown in previous work [7 - 9], the length of samples of such materials as natural rubber should not be measured with the samples in an unloaded state. The results of the experiments described below showed that despite these difficulties, the thermodilatometric method may be used to determine the transition points and regions of natural rubber.

We examined films obtained from a benzene solution of smoked sheet by evaporation on a glass surface, strips of smoked sheet, and vulcanized latex films prepared industrially.

Samples in the form of strips cut from unvulcanized films prepared from a solution had a mean thickness of 0.65 mm, a width of 1 cm, and a length of 5 to 10 cm. Figure 3 a gives the results of tests on one sample with P = 1 g/mm^2. The length of the sample increased by 5.4% from the beginning (point A) to the end of testing (point B). The thermodilatometric curves showed a transition region from ~ 10 to ~ 40°. The general form of the relation was similar to that described previously for samples of gutta-percha film "C" obtained from dichloroethane solution on a glass surface [7]. The "plateau" on the thermodilatometric curve of the natural rubber film from ~ 10 to ~ 20°, where the length of the sample remained practically constant with an increase in temperature (Fig. 3,a) was at lower temperatures than the "plateau" on curves for films of gutta-percha "C" (from ~ 27 to ~ 42° when P = 19 g/mm^2). For natural rubber films, $\alpha_{1-10^\circ} = 3.95 \cdot 10^{-4}$ at P = 1 g/mm^2 and for films of gutta-percha "C" at P = 19 g/mm^2, α_{8-27° varied from $1.6 \cdot 10^{-4}$. The difference in the linear expansion coefficients is in complete agreement with the known elastic properties of the materials compared.

As a check on the temperature dependence of the length established, natural rubber samples were kept at various temperatures for a longer time than with the heating rate of 1° in 3-5 min which we had used. It is noteworthy that there was much more scatter of the experimental points and more marked steps on the thermodilatometric curves over the range of ~ 10 to ~ 40° than in other temperature regions. In anisotropic polymeric materials with crystalline regions, two processes apparently occur simultaneously with an increase in temperature, namely, expansion and contraction of the samples [7]. After the disappearance of the crystalline regions and the orientation of the long-chain molecules in the material under the influence of thermal motion, there is normal thermal expansion and then yield.

For determination of the effect of thermal crystallization, samples cut from a smoked sheet in the form of strips from 8 to 12 cm in length, 1.5 cm in width, and 0.3 cm in thickness were kept for 33 days in air at a temper-

ature of -15 to -9°. The results of one cycle of tests (1° → 48° → 1°) at P = 1.4 g/mm^2 are illustrated in Fig. 3 b. The samples expanded with an increase in temperature to 4°. From 4° to ~ 13-15°, the length of the samples remained practically unchanged. The length of the samples increased in all subsequent heating and cooling cycles. For example, after four cycles over the temperature range from 1 to 51° with intervals between them of a few days and a total duration of the observations equal to 20 days, the final length of the samples was ~ 13% greater than the original length. The point at which the length began to remain practically constant (the "plateau" on the temperature dependence of the length), which lay at 4° in the first cycle, was displaced to ~ 10° in subsequent cycles with heating (Fig. 3 c), i.e., to the temperature for films that had not been cooled previously to -15° (Fig. 3 a).

A "plateau" from ~ 11 to ~ 16° was observed on temperature dependences of the length for vulcanized latex samples with P = 92.6 g/mm^2. The samples contracted when heated from ~ 16 to ~ 30° and expanded above 30°. Films that had been stretched first began to contract at lower temperatures.

The temperature dependences of the length obtained for all the natural rubber samples are of definite interest despite their complex form as they describe the behavior of the materials over various temperature ranges under load. The form of the thermodilatometric curves and the presence of strongly developed hysteresis may be explained on the basis of the following considerations.

Even with P = 1 g/mm^2, samples of unvulcanized natural rubber show clearly expressed hysteresis and the original length is not recovered as a result of changes in temperature. Consequently, under the influence of this relatively low external force, the long-chain molecules of natural rubber slip relative to each other despite a reduction of the temperature impeded by the parallel processes of crystallization and fusion, as a result of which the thermodilatometric curves are not smooth. Over a relatively wide and definite temperature range, two processes may occur simultaneously, namely, the "fusion" of some crystalline regions, which were formed at lower temperatures, and the formation of others under the existing conditions. It should also be remembered, that with certain internal stresses, in natural rubber their begins oriented crystallization, which hampers yielding [11]. The application of a load to a sample during thermodilatometric testing, on the one hand, produces orientation of the long-chain molecules and their units in the direction of its application and, on the other hand, disruption of crystalline regions oriented in other directions and promotes yielding. The creep of natural rubber is known to decrease with an increase in the degree of crystallinity. If the crystalline regions in samples of unvulcanized natural rubber are scattered without any predominating direction, a small external force cannot produce reorientation, but must promote their disruption ("fusion").

Samples under a small load must expand partly as a result of straightening of folds occurring both in the crystalline and amorphous regions [12]. When the magnitude of the external force is sufficient for reorientation, the ordered regions of one orientation may change into regions with another orientation (along the stretching axis).

The orientation which is obtained in preparing rubber films on a glass surface and which was observed for guttapercha films [7] also affects the course of the thermodilatometric curve and the "plateau."

In tests with a relatively large load, simultaneously with thermal crystallization there was oriented crystallization, which could occur in a fraction of a second [11].

The complexity of the thermodilatometric curves is explained by the fact that they reflect a combination of the processes described. For example, the curve illustrated in Fig. 3 b must reflect the fusion of crystals formed at temperatures below 0° and the simultaneous formation of crystals at higher temperatures. Judging by the nature of the curve, the "fusion" process is complete at ~ 35°. The steps on the cooling curve may be a reflection of the formation of crystalline regions (ordered regions) with different "fusion" temperatures, entropies, and other thermodynamic characteristics and a lag in the establishment of "equilibrium" states. The degree of crystallization during cooling under our experimental conditions was naturally low. Therefore, if samples of smoked sheet are kept for 13 days in the temperature range from ~ 4 to ~ 6°, then crystalline regions are formed in them at a higher temperature than in the original samples. The melting points of the "higher-temperature" crystals is higher than that of the "low-temperature crystals and therefore their characteristic points are displaced correspondingly toward higher temperatures (cf. Figs. 3 b and 3 c). As the crystallization conditions in films obtained from solutions and strips of smoked sheet kept for a long time at temperatures above zero are quite similar, the thermodilatometric curves of these samples are similar (Figs. 3 a and 3 c).

The thermodilatometric curves for samples of stretched and unstretched vulcanized natural rubber are even more complex than for samples of unvulcanized rubber as a result of the tendency of the strained, cross-lined structure to return to its previous morestable state on heating (entropy effect).

SUMMARY

1. The behavior of polychloroprene and natural rubber (smoked sheet) samples with various histories during heating and cooling has been investigated dilatometrically. The transition points and regions found and also the linear expansion coefficients have been compared with those for gutta-percha films.

2. Thermal treatment of polychloroprene films has a characteristic effect on their properties and the position of the transition regions. The displacements of the transition points and regions after thermal treatment is connected with cross-linking of the polymer by thermal vulcanization.

3. The position of the transition points and regions for various samples of natural rubber is explained by the presence of crystalline regions formed at different temperatures.

The author would like to thank Prof. S. I. Sokolov for interest in the work.

LITERATURE CITED

1. C. Bunn, Chemistry of Large Molecules, Collection 2 [Russian translation] (IL, 1948).
2. E. Kirchhof, Gummi und Asbest, 4, 51, 84, 121, 159, 1951; Coll. Rubber [Russian translation] (IL, 1952), p. 49.
3. L. Wood, Chemistry of Large Molecules, Collection 2 [Russian translation] (IL, 1948).
4. Synthetic Rubber, edited by G. Whitby, C. Davis and R. Danbrook [Russian translation] (Goskhimizdat, 1957).
5. I. Katz, Radiography of High-Molecular Substances, Colloids, and Animal and Plant Tissues, [in Russian] (ONTI, 1937); B. A. Dogadkin, Chemistry and Physics of Rubber [in Russian] (Goskhimizdat, 1947); R. Fuss, Chemistry of Large Molecules, Collection 2 [Russian translation] (IL, 1948); S. I. Sokolov, N. A. Krotova, cited by B. B. Deryagin and N. A. Krotova, Adhesion [in Russian] (Izd. AN SSSR, 1949); A. I. Marei, Chemistry and Physical Chemistry of High-Molecular Compounds, [in Russian] (Izd. AN SSSR, 1952); N. I. Smirnov, Synthetic Rubbers [in Russian] (Goskhimizdat, 1954); V. Cimril, J. Polymer. Sci. 2, No. 2, 142, 1947; G. Kohman, and R. Peak, Industr. and Engng. Chem. 20, 81, 1928; N. Bekkedahl and L. Wood, Industr. and Engng. Chem. 33, 381 (1941) ; M. Selker, G. Winspear, and A. Kemp, Industr. and Engng. Chem. 34, 157 (1942); E. King, Industr. and Engng. Chem. 35, 949 (1943); N. Bekkedahl and H. Matheson, J. Res. Nat. Bur. Standards 15, 503 (1935); G. Clark, S. Gross, and W. Swith, J. Res. Nat. Bur. Standards 15, 503 (1935); G. Clark, S. Gross, and W. Swith, J. Res. Nat. Bur. Standards 22, 105 (1939); W. Gibons, R. Gerke, and H. Tingey, Rubber Chem. and Technol. 6, 525 (1933); W. Holf and A. McPherson, Rubber Chem. and Technol. 10, 412 (1937); W. Swith and H. Wing, Rubber Chem. and Technol. 12, 789 (1939); L. Wood, N. Bekkedahl, and C. Peters, Rubber Chem. and Technol. 13, 290 (1940); J. Fild, Rubber Chem. and Technol. 14, 555 (1941); E. Koch, Rubber Chem. and Technol. 14, 799 (1941); W. Barnes, Can. J. Research B. 15, 156 (1937).
6. N. Bekkedahl, J. Res. Nat. Bur. Standards 13, 411 (1934); Rubber Chem. and Technol. 8 , 5 (1935).
7. R. I. Fel'dman and S. I. Sokolov, Kolloidn. Zh. 20, 388 (1958); Chemistry and Physical Chemistry of High-Molecular Compounds [in Russian] (Izd. AN SSSR, 1952) p. 159; Abstracts of Proceedings of the Ninth Conference on General Problems on the Chemistry and Physics of High-Molecular Compounds [in Russian] (Izd. AN SSSR, 1957) p. 97.
8. R. I. Fel'dman, Kolloidn. Zh. 20, 220 (1958).
9. R. I. Fel'dman, Kolloidn. Zh. 21, 238, 499 (1959).
10. H. Barron, Modern Synthetic Rubbers [Russian translation] (Goskhimizdat, 1948); N. Katton, Khimiya i Tekhnologiya polimeroy, No. 3, 46 (1957); N. P. Fedorenko and G. F. Borisevich, Khimicheskaya promyshlennost', No. 3, 202 (1959).
11. T. Alfrey, Mechanical Properties of High Polymers [Russian translation] (IL, 1957); L. Treloar, Physics of Rubber Elasticity [Russian translation] (IL, 1953).
12. S. I. Sokolov and R. I. Fel'dman, Kolloidn. Zh. 21, 630 (1959).

All abbreviations of periodicals in the above bibliography are letter-by-letter transliterations of the abbreviations as given in the original Russian journal. *Some or all of this periodical literature may well be available in English translation.* A complete list of the cover-to-cover English translations appears at the back of this issue.

MECHANISM OF DISINTEGRATION OF QUARTZ IN SURFACE ACTIVE MEDIA

G. S. Khodakov and P. A. Rebinder

Institute of Physical Chemistry Academy of Science, USSR,
Department of Dispersed Systems
Scientific Research Institute for New Structural Materials
Translated from Kolloidnyi Zhurnal, Vol. 23, No. 4,
pp. 482-490, July-August, 1961
Original article submitted January 6, 1961

The fine disintegration of solids usually accomplished by successive breakdown to smaller and smaller particles, is one of the most widespread technological processes. The study of these processes, important both practically and scientifically, is concerned to a great degree with elucidating the connection between dispersion and energy expenditure in the disintegration of materials [1-10]. Various relationships are known which accurately describe the kinetics of disintegration only within a narrow range of relatively coarse dispersions, but the derivation of an equation based on adequate theoretical or experimental considerations which accurately applies over a wide range of dispersion has not yet been established. One reason for this lies in the fact that earlier the irreversible deformation of the particles preceding their breakdown [11] was not considered. Meanwhile it is known [11-15] that disintegration of even such a friable mineral as quartz results in amorphization of the fine surface layers. Similar effects of amorphization, dislocations or subsequent reorganization of the crystalline structure are also observed during disintegration of other solids [16]. The possibility that irreversible deformations have a substantial effect on the breakdown of very small particles also follows from certain general considerations of the theory of strength of materials [17]. In this connection a study of the role of the irreversible deformations during disintegration of solids is of interest, especially in determining the effect of the medium. Since in general such investigations encounter considerable difficulties, we have studied the most favorable material in this respect – quartz.

Amorphization of Quartz During Its Disintegration in Surface-Active Media. In our experiments the amorphization of quartz sand, containing not less than 98% of crystalline quartz of the low temperature α-modification, was investigated during its disintegration in a laboratory eccentric vibromill. The amount of the amorphized phase was determined by the differential thermal analysis method from the magnitude of the temperature peak of the $\beta \rightarrow \alpha$ conversion at 574°. The dispersion was characterized by the value of the specific surface area, measured by low temperature adsorption of nitrogen (by the BET method) for which all the powders were subjected to disaggregation [18].

Since the quartz particles during disintegration are amorphized in surface layers [12,13] then comparison of the amorphous phase content (Q) with the specific surface area of the same powders (S, cm^2/g) permits calculation of the average thickness of the amorphous layer on the crystalline cores, which for not very finely divided particles is equal to $Q/\rho S$ (ρ is the density of the layer). As follows from fig. 1, the thickness of the amorphous layer on the quartz particles, disintegrated in dry air changed very sharply – from ~ 20 A for a coarse dispersion to several hundred angstroms for a sufficiently lengthy grinding. During disintegration in an active medium (water) the thickness of the amorphous layer remained constant (20 A) in the range of specific surface area up to 50-60 m^2/g and somewhat increased only on further increase of the dispersion. The depth of amorphization of coarse particles arising on grinding with 1.2% water was the same as on grinding with 80% water, but with an increase in the specific surface area to 30-50 m^2/g the thickness of the amorphized layer in this case increased rather sharply. The sudden transition corresponded to a decrease in the surface concentration of the liquid medium from 1 to 0.5 of a saturated monomolecular layer. From the data presented it is seen that the thickness of the amorphous layer on the crystalline granules of disintegrated quartz does not remain constant but depends in a regular way both on the duration of grinding and, especially, on the medium in which the grinding is carried out.

The thickness of the amorphous layer on quartz particles by dry grinding determined thermographically [12], is several times greater than our determination. This is explained by the fact that in reference [12] the specific sur-

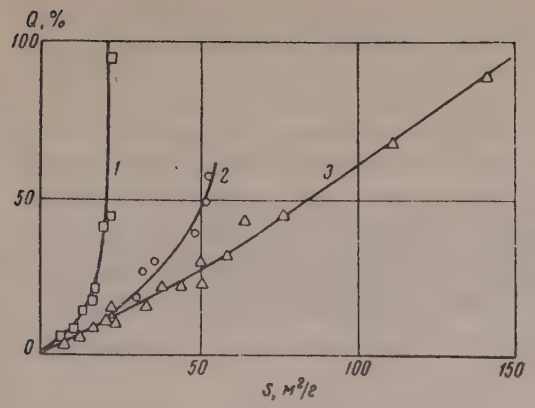


Fig. 1. Comparison of dispersion and amorphization of quartz. 1) Grinding in dry air; 2) grinding with 1.2% water; 3) grinding with 80% water.

face area was measured by an air-porosity method, which, allowing for the effect of aggregation during disintegration [18], gives 4-7 times lower values in comparison with the actual values. Consequently the thickness of the amorphous layer was increased by as much again.

In order to elucidate the nature of the amorphization of quartz an X-ray examination of powders of different degrees of disintegration was carried out. We have shown [11] that with increased duration of grinding, the background density of the blackening of the X-ray photograph gradually increased and the diffraction maxima, characteristic for the quartz lattice, remained perfectly clear, without appreciably broadening. Consequently it is not possible to ascribe the amorphization of quartz during disintegration to a gradual decrease in the size of the individual crystallites as can occur for example during disintegration of graphite [16].

The amorphous structure of the surface layers of pulverized quartz was confirmed by experiments in which the effect of the disintegration process on the solubility of the quartz in water [15] was studied. Increase in temperature to 100° caused a sharp increase of the equilibrium solubility of the pulverized quartz, which is characteristic for amorphous silica. However in the case of crystalline quartz an increase in temperature even to 150° resulted in only a negligible increase in the solubility [19]. These results also confirm that the amorphized quartz is not a conglomerate of submicroscopic accretions between the crystallites themselves.

Taking into consideration that the high temperature needed for fusion of quartz (~ 1700°) does not arise in the mill, the plastic deformations of the particles during their breakdown may be considered the most probable cause of amorphization. Such deformation can arise in the fine layers adjoining the surfaces along which at the moment of breakdown are concentrated the maximum shear stresses. The depth of these layers is very small and in any case is not greater than the thickness of the amorphous layer which is 20 A for coarse grinding. Therefore the role of plastic deformations during breakdown of coarse particles is also small, but increases during fine grinding, when the particle size becomes comparable with the depth of the amorphous layer.

Comparison of the intensity of blackening curves of the X-ray photographs of fused quartz and quartz amorphized in a vibromill to near complete destruction of the crystalline phase shows the expected similarity of structures in the sense of complete absence of far order in the arrangement of the atoms [11]. On this basis it can be assumed that the density of energy expended in irreversible deformations in every case is not less than the specific heat of amorphization of quartz, equal to $4.4 \cdot 10^9$ ergs/cm^3 [19]. Such a value for the work density of the limiting irreversible deformations also follows from a theoretical basis for the condition that the limiting shear stress $P \approx 0.1\,G$, where G is the shear modulus. The theoretical value for P lies within the limits $G/2\pi$ to $G/30$ [17].

The limiting density of the elastic energy of quartz in the absence of an appreciable measure of hardening is considerably less (~ $2 \cdot 10^6$ ergs/cm^3). In support is the fact that during mechanical dispersion there is no appreciable development of a measure of hardening which substantiates for example, the fact of amorphization of quartz and the very large effects of the media, which do not lessen with increase of dispersion [18]. During breakdown of solids the divided fragments are subjected to stresses close to the limiting stresses. Such stresses cannot avoid causing the development and generation of defects which in the presence of a liquid medium become unstable by the repeated actions. We have also observed other cases where a decrease in the dimensions of the solids is not accompanied by their hardening [20].

Kinetics of Disintegration of Quartz. From general ideas of the nature of the breakdown of solids [1] an equation has been obtained for the energy expended in the breakdown of the solid of volume v, which is accompanied by a Δs increase of the surface area.

$$\Delta u = ev + A\Delta s, \qquad (1)$$

where e is the density of energy of limiting eleastic deformations. A is the surface density of the total work required to form new surfaces.

The value of A is determined by the work required to increase the separation surface of the phases, the density of energy of the limiting irreversible deformations, and by other expenditure of energy (frictional work and energy of formation of aggregates), the contribution of which is increased with increase in dispersion. Calculation of all these factors by means of an equation for the kinetics of disintegration does not seem possible because of the inadequacy of the experimental investigations on the mechanism of the effect of the medium, the dependence of the magnitude of adsorption effects on the concentration of the active ingredients, on the temperature of the medium and on the nature of the solids. The effects of aggregation and coagulated structure formation during disintegration [18] have been still less studied. In this connection it is helpful to examine a particular case – the disintegration of quartz in an active medium, in which it is possible to neglect aggregation of particles and coagulated structure formation, and where the layer thickness of the plastic deformation does not depend on the dispersion of the powders.

In order to deduce a relationship between the energy expenditure during disintegration and the dispersion we will make the following assumptions:

1. It has been shown by the experiments of Kick and others [2] that solids of different particle sizes, but of the same composition and structure, during attainment of the limiting stressed state are broken down in a similar way (for example to an equal number of fragments). We will assume also that in the region of very small particle sizes such a similarity will be maintained. We will write this condition in the form: $\Delta s = ax^2$, where Δs is the increase of the surface area as a result of breakdown of a particle of size x; a is a constant.

2. During successive breakdown the strength of the quartz particles does not depend on their volume (bx^3), and the density of energy of the limiting elastic deformations is equal to $e = P_n^2/2E$, where P_n is the strength of quartz, E is the modulus of elasticity.

3. Since quartz is amorphized in surface layers, the thickness of which (l) during disintegration in water does not depend on the particle sizes, then the energy which is expended to give the limiting plastic deformations (with $x \gg l$) is equal to $\beta a x^2 / l$ where β is the average volume density of energy of the limiting plastic deformations according to the thickness of the amorphous layer. Allowing for the limiting elastic and plastic deformations, the expenditure of energy in disintegrating a particle is equal to

$$\Delta u = bex^3 + a(\beta l + \sigma) x^2, \tag{1a}$$

where σ is the unit surface area free energy of silica. From expression (1a) it follows that the density of the energy expenditure in breakdown $\Delta u/bx^3$ increases with decrease in particle sizes. Meanwhile the maximum energy density (W_m) which can be imparted to the particle in a single act, is limited and is a constructive parameter of the disintegration [7].

The condition $W_m = e + \frac{a(\beta l + \sigma)}{b x_m}$ determines the limiting size of the non-disintegrated particles

$$x_m = \frac{a(\beta l + \sigma)}{b(W_m - e)}. \tag{2}$$

Strictly speaking, particles of size $x < x_m$ will be disintegrated as a result of fatigue breakdown. But the total expenditure of energy in disintegration sharply increases for $W_m < \Delta u / bx^3$ and therefore the increase in the dispersion resulting from this process when sufficient number of particles of size $x > x_m$ are present can be disregarded. As follows from expression (2), in order to attain the maximum fine disintegration it is necessary that the condition $W_m > \beta l + e + \sigma$, be fulfilled which can be attained by an increase in the energy intensity of the mill. Another way to increase the fineness of grinding is to decrease the depth of plastic deformation, which can be achieved in a number of cases by using surface-active substances.

In the deformation of particles of size $x < x_m$ formed as a result of breakdown of coarser particles of size $x > x_m$ a certain amount of energy is expended. Consequently the energy density expended directly in disintegration (W), leading to increase in dispersion is only part of the energy expended (ϵ). This part is determined by the ratio of the total volume (V_m) of particles of size $x < x_m$ to the total volume of the particles (V).

The value V_m/V is small in the initial grinding and tends to unity after a sufficiently long period of grinding. Taking into consideration that the value S/S_m (S is the specific surface area of the powder, S_m is the specific surface area of the fully disintegrated powder with all particles sizes $x < x_m$) has the same limiting value at the same

points and taking into account the experimentally observed proportionality between the content of particles of sizes less than that given by the ratio S/S_m, it is possible to assume with some degree of approximation:

$$V_m/V = S/S_m;\ dW = kd\varepsilon\,(1 - S/S_m), \tag{3}$$

where k is the efficiency coefficient (EC) of the disintigrator.

For the disintegration of a considerable quantity of an adequately dispersed substance the average expenditure of energy in disintegration of one particle, and the average increase in the surface area as a result of its disintegration are small in comparison with the total consumption and total surface area. Therefore by considering the expressions (1a) and (3) it is possible to write

$$\frac{dW}{dS} = \frac{d\bar{u}}{d\bar{s}} = \frac{\Delta\bar{u}}{\Delta\bar{s}} = \frac{kd\varepsilon\,(1 - S/S_m)}{dS} = \frac{be\Sigma x_i^3}{a\Sigma x_i^2} + (\beta l + \sigma) = \frac{ec}{aS} + (\beta l + \sigma). \tag{4}$$

For spherical particles the constant has the form $c = \pi$, and for cubic particles $c = 6$.

Expression (4) after separating out the variable becomes

$$kd\varepsilon = \left[\frac{ec}{a\,(1 - S/S_m)\,S} + \frac{\beta l + \sigma}{(1 - S/S_m)}\right] dS. \tag{5}$$

Integration of expression (5) within the limits S_0 – the specific surface area of the original material and S, gives a relationship for the energy expenditure in disintegration ($\Delta\epsilon$).

$$k\Delta\varepsilon = \frac{ec}{a}\ln\frac{S}{S_0} + \left[\frac{ec}{a} + (\beta l + \sigma)\,S_m\right] \cdot \ln\frac{S_m - S_0}{S_m - S}. \tag{6}$$

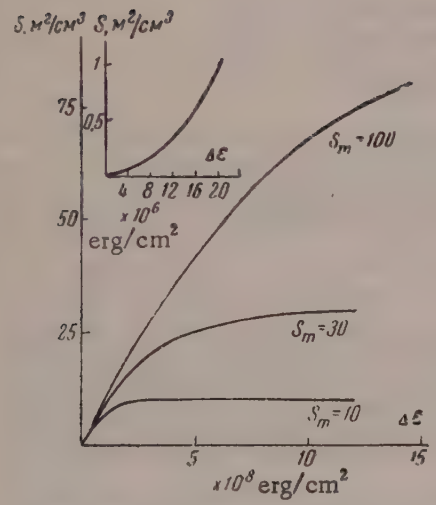


Fig. 2. Kinetic curves for the disintegration according to equation (7).

For the condition that during disintegration the particles break down into 8 parts, $a \approx 3$. The value c can be put equal to 4. By considering that for amorphous silica in water $\sigma = 100$ ergs/cm^2 [19]; for quartz $e \approx 2 \cdot 10^6$ ergs/cm^3 and by taking the value of the energy density of the limiting plastic deformations equal to the heat of amorphization $\beta = 4.4 \cdot 10^9$ ergs/cm^3, the expression (6) can be written in the form

$$k\Delta\varepsilon = 2{,}7 \cdot 10^6 \ln\frac{S}{S_0} + [2{,}7 \cdot 10^6 + (4{,}4 \cdot 10^9 l + 100)\,S_m] \cdot \ln\frac{S_m - S_0}{S_m - S}. \tag{7}$$

From the results calculated from equation (7) with $S_0 = 0.01$ m^2/cm^3 and different values of S_m, and with $l = 20$ A (Fig. 2) it follows that the relationship $S = f(k\Delta\epsilon)$ is substantially different for small, medium and large values of S and $k\Delta\epsilon$. In the region $S \ll S_m$ it is correct to put $\frac{S_m - S_0}{S_m - S} \approx \frac{S - S_0}{S_m - S} \approx \frac{S - S_0}{S_m}$ With the values $\frac{S - S_0}{S_m} \sim 0{,}01$ $lS_m \leqslant 0{,}1$ and $S < \sim 100\ S_0$ (very coarse grinding) in equation (7) it is possible to neglect the second term in comparison with the first and the equation becomes identical with the relationship resulting from the known Kirpichev-Kick law and experimentally proved for the disintegration processes [2,10]:

$$\Delta\varepsilon = k' \ln\frac{S}{S_0}, \tag{8}$$

where k' is a constant. The relationship (8) only gives the expenditure of energy in an elastic deformation.

With $S_0 \ll S \ll S_m$ in equation (7) the first term is small compared to the second, consequently this equation can be written in the form

$$k\Delta\varepsilon \approx (S - S_0)(\beta l + \sigma). \qquad (9)$$

The relationship (9) is analogous to Rittinger's law, the correctness of which has been shown for relatively fine (medium-fine) disintegration [4,5].

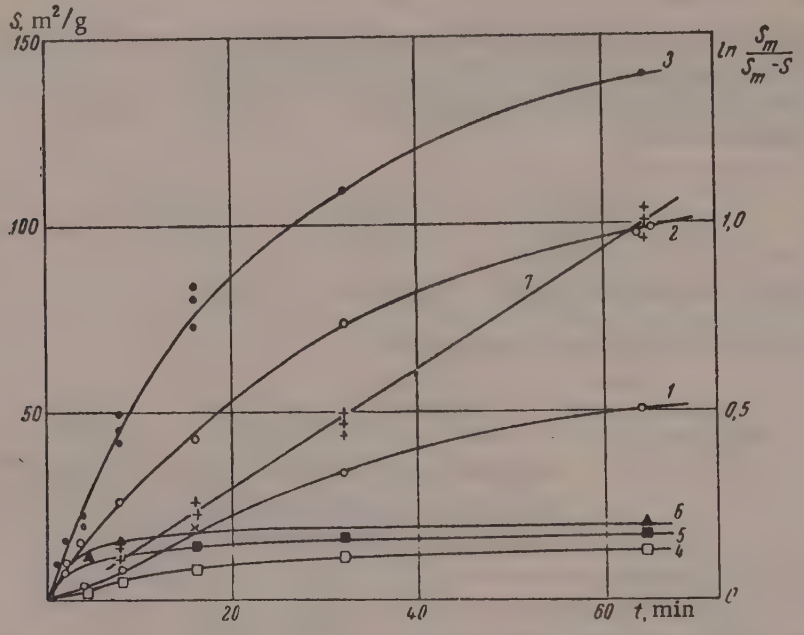


Fig. 3. Disintegration of quartz in an eccentric vibromill. 1, 2 and 3: in water with a vibration amplitude of 3, 4 and 5 mm respectively; 4, 5 and 6: in air with amplitudes of 3,4 and 5 mm; 7: kinetics of the disintegration in water with coordinates t, $\ln \frac{S_m}{S_m - S}$

The value βl, being the surface density of the energy of the limiting plastic deformations; is approximately an order greater than the surface energy of silica [19] both for wet and for dry milling. Therefore Rittinger's equation cannot be used to reckon, as sometimes is done [4,6], the specific expenditure of energy required in generating new surfaces only. Actually it indicates mainly the expenditure required in the limiting irreversible deformation of particles during disintegration.

In a wider range of dispersion, with $S \gg S_0$, the first term in equation (7) can be neglected in comparison with the second, which allows it to be written in the form

$$k_1\Delta\varepsilon = \ln\frac{S_m}{S_m - S} \quad \text{or} \quad S = S_m[1 - \exp(-k_1\Delta\varepsilon)], \qquad (10)$$

where $$k_1 = k/(2{,}7\cdot 10^6 + 4{,}4\cdot 10^9 l S_m).$$

For a constant disintegration regimen $\Delta\epsilon = Nt/V$ where N is the power output of the disintegrator, t is the duration time of the process, which permits an equation for the kinetics of disintegration to be obtained

$$k_2 t = \ln\frac{S_m}{S_m - S} \quad \text{or} \quad S = S_m(1 - e^{-k_2 t}). \qquad (10a)$$

The value $k_2 = k_1 N/V$ is in effect the rate constant of dispersion.

The results presented in Fig. 3 show that for wet grinding of quartz in an eccentric vibromill with a 3-5 mm amplitude, equation (10a) is fulfilled completely satisfactorily within the accuracy of the coefficient of efficiency (CE) of the disintegrator. It is characteristic that the values of S_m, calculated by extrapolation of the curves prove

to be proportional to the values of the power expended by the mill which in turn are proportional to the square of the vibration amplutide. Therefore the dispersion rate constants for different disintegration regimens are in agreement.

Role of Active Media In Disintegration: As seen from our experiments, the action of media on the disintegration leads to a decrease in thickness of the amorphous layer, and consequently to a decrease of the depth of plastic deformation.

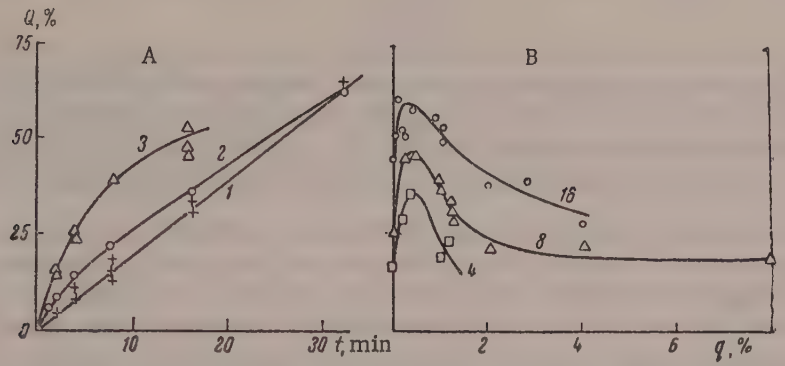


Fig. 4. Effect of a medium on the amorphization of quartz: A) Kinetics of amorphization for disintegration with 80% water (1), in dry air (2), and with 1.2% water (3); B) Effect of small additions of liquid on the amorphization for 4, 8 and 16 min. grinding.

As a result of this the density of the energy expenditure required in the disintegration of the particles is decreased and since the expenditure required for the limiting plastic deformation is the determining factor during fine grinding, the effectiveness of dispersion is also increased in corresponding degree. The mechanism of the effect of water and other liquids is apparently analogous to the "brittle-growing" effect of fine layers of active low melting metals [21]. The possibility of a brittle growing effect follows from the over twofold reduction of the surface energy of quartz and of amorphous silica in water in comparison within a vacuum [19]. About the same reduction in the surface energy of silica occurs in acetone, alcohol and benzene [19, 22, 23]. The increase in thickness of the amorphous layer during dry milling and during milling with 1.2% water with increasing dispersion (Fig. 1) arises in agreement with the reported increase of the average depth of the layer of the limiting plastic deformation associated with a decrease in the surface concentration of moisture or other active liquids. The role of the medium in disintegration does not only limit the decrease in depth of the limiting plastic deformations. It was established [18] that the effectiveness of dispersion materially depended on the surface concentration of water, which arises through a change in the mechanical properties of the system, comprising solid particles with layers of liquid between them, and in the thickness of such layers. Associated with this the kinetics of amorphization (Fig. 4) also markedly depend on the concentration of the liquid medium. The greater amount of amorphous phase during grinding with small amounts of liquid compared with wet or dry milling is explained by the greater effectiveness of dispersion with a surface concentration of liquid close to a saturated monolayer [18].

For coarse milling the kinetic curves for the disintegration of quartz (Fig. 3) in dry air are close to the curves for disintegration of quartz in water. Later on the curves for wet and dry milling are sharply separated which is explained by the rapid decrease in the surface concentration of the active contaminants with increase in dispersion. As a result of this the depth of plastic deformations preceding disintegration, is increased, the energy expenditure required for disintegrating the particles is increased and the rate of disintegration is sharply reduced. Consequently use of equations (7), (9) and (10) to describe "dry" milling is not possible.

The presence of contaminants (traces of moisture) does not permit measurement of the thickness of the amorphous layer on quartz particles, corresponding to absolutely dry milling. The moisture impedes amorphization of the very fine non-disintegrated particles. However with a sufficiently high dispersion of the dry-milled powders the surface concentration of contaminants becomes very small. The comparison of the limiting values of the specific surface area by wet and dry milling ($l\ S_m$ = const), makes possible the evaluation of the thickness of the amorphous

layer of quartz during its disintegration in absolutely dry air. Taking into account that for milling in water $l \approx 20$ A; $S_m = 150$ m^2/g, and in dry air $S_m \approx 19$ m^2/g a value of around 150-160 A is obtained for absolutely dry milling.

From equation (7) (Fig. 2) as well as from the data of Fig. 3, it also follows that in the region of applicability of the Kirpichev-Kick law the specific expenditure in disintegration does not depend on the energy output of the disintegrator which determines the values of S_m. In contrast to this, during the transition to fine grinding the specific expenditure of energy is the less the greater the energy output of the machine (larger W_m and S_m). These results point to the necessity for a rational construction and utilization of different types of disintegrators.

SUMMARY

1. Dispersion of quartz is accompanied by amorphization of its surface layers, the thickness of which is sharply changed under the action of a medium. By grinding in an active medium (water) the thickness of the amorphous layer remains constant at ~ 20 A, up to values of the specific surface area of 50-60 m^2/g, and in dry air the thickness of the amorphous layer owing to the decrease in the surface concentration of active contaminants is changed from ~ 20 A for coarse dispersion up to some hundred angstroms for a sufficiently dispersed powder.

2. The specific expenditure of energy in amorphization during disintegration of quartz exceeds the increase in surface energy by approximately ten times, and becomes the determining factor compared with the energies of the limiting elastic deformations for particles below 1-2 microns in size. An equation for the kinetics of disintegration introduced and making allowance for the energy expenditure in irreversible deformations, as well as for the effect of the medium, the energy output of the disintegrator and the dispersion of the powder, describes very well the experimental results for wet grinding of quartz. This equation also applies accurately in the region of high dispersion, taking as an extreme case the known Kirpichev-Kick and Rittinger relationships respectively for coarse and medium-fine grinding.

3. The decrease in the depth of amorphization in the presence of active media which may be treated as a "brittle-growing" effect, leads to a proportional (for small particles) reduction in the specific expenditure of energy and consequently to an increase in the effectiveness of disintegration.

LITERATURE CITED

1. P. A. Rebinder, L. A. Shreiner and K. F. Zhigach, Hardness-Reducing Solutions for Rock Drilling [in Russian] (Acad. Sci. USSR Press, 1944).
2. F. Kick, Das Gesetz der proportionalen Widerstand und seine Anwendung, Leipzig, 1885; H. Stadtler, Trans Instn. Mining. and Met. 19, 471, 1910; 20, 420, 1922; cited in collect. edited by G. G. Egorov, The Theory and Practice of Grinding and of Fine Disintegration [in Russian] (GNTI, Mines Engineer, Moscow-Leningrad-Novosibirsk, 1932).
3. R. I. Charles, Mining Enging. No 1, 80, 1957.
4. J. Gross, and S. R. Limmerley, Trans. Amer. Inst. Mining. and Met. Techn. Pab. No 127, 1928.
5. I. W. Axelson, and E. L. Piret, Industr. and Enging. Chem. 42, No. 4, 665, 1950; J. N. S. Kwong, J. T. Adams, J. T. Jonson, and E. L. Piret, Chem. Enging. Progr. 45, No. 8, 508, 1949; J. T. Adams, J. F. Jonson and E. L. Piret, same journal 45, No. 11, 708, 1949.
6. V. I. Akunov, Modern Vibration Disintegrators without Pulverizers [in Russian], (Promstroiizdat, 1957); Conventional Disintegrators [in Russian], (Gosstroiizdat, 1958).
7. L. A. Lesin, Basic Theory and Methods of Calculation of Fundamental Parameters of Vibromills, [in Russian], (Promstroiizdat, 1957).
8. E. B. Matskevich and P. Yu. Butyagin, Kolloidn. Zh. 20, 665 (1958).
9. M. Andreasen, and H. Zeusen, VDI-Zeitschrift 96, No. 33, 1127, 1954.
10. A. F. Taggart, Handbook on Benefication of Minerals [in Russian] (Vol. 2, Moscow, Metallurgizdat 1950).
11. G. S. Khodakov and P. A. Rebinder, Dokl. AN SSSR, 131, 1316 (1960).
12. P. D. Dempster, and P. D. Ritchie, J. Appl. Chem. 3, 182, 1952.
13. J. G. Gibb, P. D. Ritchie, and J. W. Sharpl, J. Appl. Chem. 3, 213, 1953.
14. D. W. Clelland, W. M. Cumming, and P. D. Ritchie, J. Appl. Chem. 2, 31, 1952.
15. G. S. Khodakov and E. R. Plutsis, Dokl. AN SSSR, 123, 725 (1958).
16. L. A. Geigin, same journal, 127, 313 (1959).
17. R. I. Garber and I. A. Gindin, Uspekhi Fiz. n. 70, 11 (1960); V. I. Likhtman and E. D. Shchukin, same journal 66, 213 (1958).
18. G. S. Khodakov, P. A. Rebinder, Dokl. AN SSSR, 127, 1070 (1959) Kolloidn. zh. 22, 365 (1960).

19. R. K. Ailer, Colloid Chemistry of Silicates and Silica [in Russian] (Gosstroiizdat, Moscow 1959).
20. E. P. Shchukin and P. A. Rebinder, Kolloidn Zh. 20, 645 (1958).
21. E. P. Shchukin and P. A. Rebinder, Kolloidn Zh. 20, 645 (1958).
22. S. Brunauer, Adsorption of Gases and Vapors [Russian translation] (For. Lit. Press, Moscow-Leningrad 1948).
23. B. S. Shvetsov, Introduction to Silicon Chemistry [in Russian] (Moscow-Leningrad, Goskhimizdat, 1933).

All abbreviations of periodicals in the above bibliography are letter-by-letter transliterations of the abbreviations as given in the original Russian journal. *Some or all of this periodical literature may well be available in English translation.* A complete list of the cover-to-cover English translations appears at the back of this issue.

CHANGES IN THE MECHANICAL PROPERTIES OF PRINTING INKS DURING AGEING

B. N. Shakhkel'dyan, L. F. Kalyavina,

and A. A. Sinegub-Lavrenko

Scientific Research Chemical Institute of the Local Service Industry, Moscow
Translated from Kolloidnyi Zhurnal, Vol. 12, No. 4,
pp. 491-494, July-August, 1961
Original article submitted March 30, 1960

This paper deals with a study of stability in the mechanical properties of inks*, made of the pigments: light-resistant yellow (ink I) phthalocyanine blue (ink II) and red lake ZhB, mixed with bright red 4Zh (ink III). All three inks were spread on a binder consisting of a mixture of the active resins GFL-300, and KMPL-300 diluted with the kerosene fraction, b.p. 260-290°, to give a viscosity of 12 poise. The measurements were made on a conic plastometer [1] constructed from analytical weights**, which insured high sensitivity, and made it possible to impose small loads on the samples. Since the usual printing inks seldom form a structure with a sharply marked flow limit, and since such systems are, to a large degree, distinguished by structural viscosity, it is possible, with a conic plastometer, to make an actual determination of the conventional flow limit, as calculated from the depth of immersion which corres ponds with sudden slowing down of the motion of the cone. However, this technique is unreliable, since in printing inks it is often difficult to fix exactly either the stoppage of the immersion with decreasing weight or the transition from rapid to slow immersion.

The difficulties indicated may be avoided, if, from the kinetics of immersion of the cone, we calculate and draw conventional flow curves, giving the rate of immersion of the cone as a function of the force, which drops off continuously as the cone is immersed under the influence of a constant load, Ref. [1]. These curves (see figure) are invariant and satisfactorially reproduceable when the cone is immersed under loads of different size. This simplified method is not to be recommended for the detailed study of the rheological properties of inks, but it is useful for solving a limited range of problems, in particular for the study of changes in the mechanical properties of inks during prolonged storage.

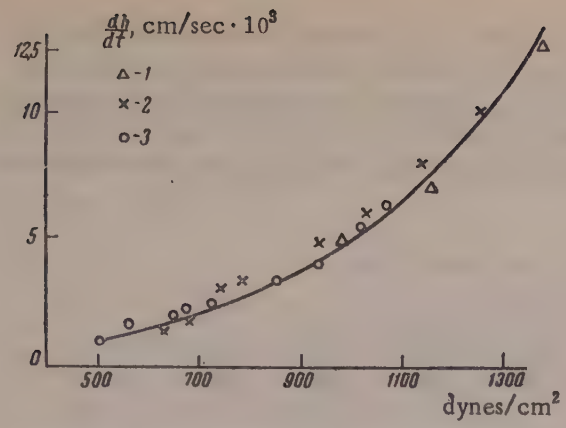
The depth of immersion of the cone was measured immediately after preparation of the inks on the ink mixing machines in the laboratory, and then was repeated periodically until the limiting value of strength of the thixotropic structure was reached. Then the inks were carefully stirred for five minutes to destroy the structure, and the whole course of strength build-up with time was again studied.

The strength of the thixotropic structures formed in inks, directly after preparation, reaches a limiting value after several days, and these initial structures have a greater strength than the structures which are reformed after mixing, Table 1.

Similar results were obtained in [2] from a study of the kinetics of structure formation of a carbon black ink dispersed on polymerized lindseed oil. Consequently this effect is not specific for the sytems being studied, but has general significance for pigments suspended in different oily media. The reduced strength of the secondary structures is similar to the difference between condensed and dispersed coagulational structures [3]. In the present case, apparently, a time change in the conditions governing the adsorption of the stabilizing surface acting substances also takes place.

* The formulas for these inks were developed at the Gosplan Scientific Research Chemical Institute, RSFSR, for printing on sheet metal, with subsequent stamping out of the letters.

** The construction of the apparatus was borrowed from M. A. Gil'debrant.



Invariance of the conventional flow curves of ink, (phthalocyanine blue pigment) at different cone loadings. 1) 1.5 g; 2) 1 g; 3) 0.5 g.

The reduction in strength of the structure is bound up with the considerable increase in the length of time required to determine the flow limit, because of the necessity of reaching lower values of stress, and with the constantly decreasing rate of change in stresses with immersion of the cone. In individual cases, the deceleration in immersion of the cone continued up to an hour or more, with the result that one could not be sure whether the equilibrium depth of immersion had been reached or not. In such cases, the experiments can be speeded up, if, without waiting for the cone to stop, we construct conventional flow curves, and determine the flow limit by extrapolating one curve to the axis of the stress coordinates. The values of the flow limit found in this way are in complete agreement with the values calculated from the limiting depth of immersion. The length of time of the measurement is reduced from 60-70 to 15-20 minutes. In those cases where the limiting depth of immersion is not reached at all, the method of extrapolating the conventional flow curves makes it possible to obtain conventional, but objectively meaningful values for the properties of the structurally viscous material.

TABLE 1. Flow Limit (dynes/cm²) of Thixotropic Structures Formed After a Series of Destructions

Inks	Aging time, 24-hour periods							
	13	16	25	32	36	43	52	62
	Fixing time, 24-hour periods							
	13	3	9	7	4	7	10	9
	Primary structure	Secondary structure						
I	5200	—	3000	2300	2100	2400	2300	2100
II	5200	—	2500	1850	1800	2050	1900	1800
III	11 000	8000	4600	2500	2800	2650	2700	2500

TABLE 2. Change with Time of Flow of Inks With a Destroyed Structure from the Mean Rate of Immersion of the Cone (cm/sec)

Inks	Aging time, 24-hour periods						
	0	9	15	18	23	30	34
I	0,008	0,01	0,016	0,024	0,020	0,033	0,055
II	0,008	0,072	0,082	0,082	0,082	0,082	0,115
III	0,016	—	0,014	0,020	0,019	0,023	0,022

The aging processes also lead to a gradual fluidizing of the inks in a state where the thixotropic part of the structure has been destroyed, Table 2.

Since, after stirring, the inks do not have a flow limit, and the cone sinks into them too fast, the conventional measure of the change in flow was taken to be the mean velocity of immersion of the cone at the limiting depth of the present apparatus (0.575 cm).

There is a false idea about inks to the effect that, for some time after they are made, they thicken, until their properties become stable. What is in mind here is measuring the consistency, after the destruction of the thixotropic part of the structure. All these ideas are based on measurements of the fluidity of the ink – the standard test for thickness as the diameter of the spot formed by spreading out a given volume of ink on a horizontal surface under a constant load.

The confusing thing is that although All Union State Standard (7346 – 55) points out the necessity of carefully mixing the ink sample before measuring the fluidity, no precise method of mixing the ink is specified. Therefore, when the fluidity is measured, the thixotropic structure of the ink is not completely destroyed, and the characteristic constant minimum viscosity state of such systems, [4], is not reached. This fact is confirmed by the data of Table 3, which compares the fluidity indices of ink measured by the usual standard method with the express destruction of the structure as observed in carrying out the present work.

TABLE 3. Change in "Fluidity" (mm) of Inks During Aging

Inks	Measurement by All Union State Standard				Measurement with destruction of structure		
	Aging time, 24-hour periods						
	1	4	20	36	1	20	36
I	20	20,5	20,5	20,5	20	26	26,5
II	31	28	28	28	31	33	34
III	24	22	22	22	24	26	26

Since, in printing machines, the inks are subjected to mechanical forces, which beyond any doubt, destroy the thixotropic structure, there is practical value in knowing the thickness index when the structure has been destroyed to a sufficient extent.

SUMMARY

1. In the study of slightly structurized systems (printing inks) with a conic plastometer, the flow limit was determined by extrapolation of conventional flow curves. This method reduces the time required for the experiment, and makes it possible to calculate the flow limit when the immersion of the cone has practically not slowed up at all.

2. During ageing, printing inks become more fluid which appears as increased flow in the state where the thixotropic structure has been destroyed, as well as in lower strength of the secondary structures.

LITERATURE CITED

1. P. A. Rebinder, and N. A. Semenko, Dokl. AN SSSR, 44, 835, 1949; B. Ya. Yampol'skii, and P. A. Rebinder, Kolloidn. Zh. 10, 467, 1948.
2. B. N. Shakhkel'dyan, Nauchnye trudy, MPI, 4, 137, 1956.
3. E. E. Segalova, and P. A. Rebinder, Kolloidn. Zh. 10, 223, 1948.
4. N. V. Mikhailov, and P. A. Rebinder, Kolloidn. Zh. 17, 107; 1955; T. I. Gudkova, L. A. Kozarovitskii, and N. V. Mikhailov, Dokl. AN SSSR, 131, 890, 1960.

DETERMINATION OF THE SPECIFIC SURFACE OF CLAYS AND KAOLINS BY MEANS OF RADIOACTIVE TUNGSTEN

D. M. Shakhtin and E. V. Levintovich

Ukrainian Scientific Research Institute of Refractories, Khar'kov
Translated from Kolloidnyi Zhurnal, Vol. 23, No. 4,
pp. 495-498, July-August, 1961
Original article submitted January 14, 1960

There exist various methods for determining the specific surface of clays, kaolins, and other disperse materials. The possibility of carrying out such determinations by using radioactive isotopes is pointed out in the literature [1,2]. However, despite the great number of different methods, it still is necessary to improve and to develop them further. The procedure described here is based on the phenomenon of adsorption of a dissolved substance on the surface of a powder. Sodium tungstate, tagged with W^{185}, is adsorbed by argillaceous materials from an aqueous-alcoholic solution (water-alcohol ratio 1 : 3). The specific surface is evaluated from the adsorption capacity of the material, i.e., the quantity of the substance adsorbed by 1 g of the powder under investigation. The adsorption capacity was determined experimentally. The quantity of the substance adsorbed was determined by the difference in activities before and after adsorption.

Results of the measurements are given in Fig. 1. The parallel portions of lines 1 and 2 correspond to sodium tungstate concentrations in the solution, at which adsorption equilibrium sets in. The dependence of the adsorption capacity (A) on the time (t) of contact of the solution with the clay, is given in Fig. 2. The time of the experiment was chosen on the basis of the data obtained.

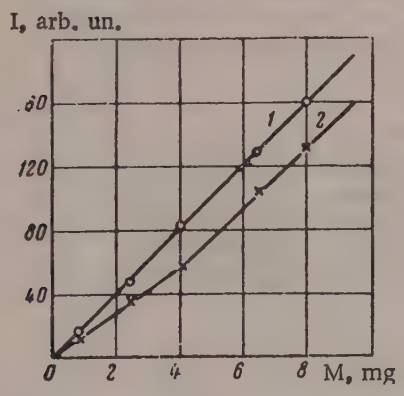


Fig. 1. Saturation kinetics of the adsorption layer of clay. 1) Solution of radioactive sodium tungstate; 2) same in the presence of the adsorbent, clay; I) relative activity of the solution; M) quantity of sodium tungstate in the solution.

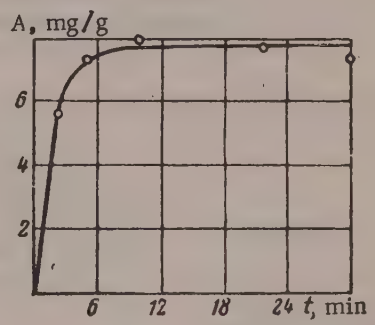


Fig. 2. Dependence of the adsorption capacity on the time of contact of the solution with the clay.

For determination of the adsorption capacity of argillaceous materials 0.2-0.3 g of the clay is added to 10 ml of an aqueous-alcoholic solution of sodium tungstate (0.6-0.8 mg/ml), whose activity has been measured beforehand. The solution containing the clay is stirred by means of a mechanical stirrer for 10 min and left to stand for 20 min. Since the clay does not settle out within this time, the solution is filtered. Filtration errors, due to adsorption on the filter (20 mm diameter), are practically absent. After filtration the solution activity is measured again.

The activity determination was carried out with 0.05 ml samples, which were placed in cuvets by means of a micropipet, and completely dried. Sufficient accuracy of measurement of the solution activity was secured by taking at least five parallel sample. Cuvets 18 mm in diameter and 2 mm high were stamped from aluminum foil. The activity of the samples was measured in a Type "B" radiometric instrument by means of a Type T-25-BFL end-type counter. The cuvets were placed under the counter in an absolutely fixed position.

The adsorption capacity A (mg/g) was calculated by the following formula:

$$A = \frac{(1 - I/I_0)\, cV}{P},$$

where I_0 and I are the intensity of radioactive radiation of the solution before and after adsorption (imp/min), c is the concentration of sodium tungstate in the solution (mg/ml), V is the solution volume (ml), and P is the quantity of clay (g).

Analysis of possible sources of error in determination of the adsorption capacity, showed that the maximum error is about ± 20%. The mean square deviation from the average value, characterizing the experimental error and reproducibility of results, is ± 5-6%. A single determination of the adsorption capacity requires 1.5-2 hr. The presence of a relation between the adsorption capacity and the specific surface was checked in the case of clay and kaolin samples, divided into fractions by elutriation. Results of the investigation (Table 1) show that the adsorption capacity depends on the dispersity of the material or its specific surface. This same dependence was found in kaolins.

TABLE 1. Adsorption Capacity of Clay Fractions from the Kirov Formation

Sample	Diameter of clay particles*, μ							Adsorption capacity, mg/g
	>60	60–40	40–20	20–10	10–4	4–2	2	
	Particle content in fractions, %							
Original	10	8,8	6,5	3,9	11,8	6,7	52,3	6,9
Enriched	—	—	—	1,8	4,2	6,5	87,5	10,8

*A. P. Kochetova carried out the determination of particles according to size by the Figurovskii method [3].

TABLE 2. Adsorption Capacity of Various Clays and Kaolins

Material	Particle diameter, μ						Adsorption capacity, mg/g	Specific surface, m^2/g	
	40	40–20	20–10	10–4	4–2	<2		by nitrogen sorption	by sodium tungstate adsorption
	Particle content in fractions, %								
Kaolin from the Vladimir formation									
1st kind	7,5	11,4	5,9	10,4	17,3	47,5	8,4	—	16,2
2nd kind	11,3	11,8	6,8	10,1	18,3	41,7	6,9	—	13,3
Kaolin from the Murzinka formation									
sample 1	5,8	8,6	4,7	14,5	2,4	64,0	9,8	18,0	18,9
sample 2	5,8	3,5	3,5	5,5	6,4	75,3	15,4	26,6	29,7
Kaolin from the Pologi formation									
1st kind	7,9	16,5	12,9	15,2	14,3	33,2	7,5	—	14,5
2nd kind	15,7	14,2	14,2	16,3	11,4	28,2	6,8	15,7	13,1
Clay from the Pologi formation									
1st kind	2,3	10,8	1,2	5,6	8,2	71,9	12,3	24,2	23,7
Clay from the Kirov formation									
2nd kind	19,5	7,2	3,7	9,1	11,9	48,6	7,5	14,2	14,5
3rd kind	33,2	7,9	8,6	12,2	4,9	33,2	8,2	15,2	15,8
sample 3	3,7	7,9	7,8	13,2	13,2	54,2	9,9	19,9	19,1

Results, obtained in the study of clays and kaolins from a number of formations, are given in Table 2, in which the adsorption capacity is compared with the particle distribution according to size. Values of specific surface, measured by nitrogen sorption* [4], also are given for a number of samples.

The coefficient of proportionality between the adsorption capacity of clays and kaolins, determined with sodium tungstate, and the specific surface, determined by nitrogen sorption, was calculated from the data of Table 2; specific-surface values were calculated in turn by means of this coefficient. From the data of Table 2 it is evident that there is a correspondence among the adsorption capacity, nitrogen-sorption data, and the particle distribution according to size.

It should be pointed out that there are discrepancies between the method used here and the nitrogen-sorption method, amounting to ± 15% in some cases. This may be explained both by the errors of the procedures being compared, and the composition of the materials. The clays and kaolins investigated, differ somewhat in their mineralogical and chemical compositions. However, the fine fractions, which determine the specific surface, consist mainly of kaolinite.

SUMMARY

The specific surface of kaolinite-type argillaceous materials may be evaluated by the method of measuring the adsorption capacity by means of a radioactive tungsten isotope.

LITERATURE CITED

1. V. G. Khlopin and M. S. Merkulova. Zh. Fiz. Khimii 8, 9 (1939).
2. G. I. Loginov and O. M. Khusainova. New Methods of Physicochemical Investigation [in Russian] (Moscow, Acad. Sci. USSR Press, 1957), p. 140.
3. N. A. Figurovskii. Sedimentometric Analysis [in Russian] (Moscow-Leningrad, Acad. Sci. USSR Press, 1948).
4. Vibration Pulverization of Materials (Information Report) No. 21 [in Russian] (Moscow, Promstroiizdat, 1956).

All abbreviations of periodicals in the above bibliography are letter-by-letter transliterations of the abbreviations as given in the original Russian journal. *Some or all of this periodical literature may well be available in English translation.* A complete list of the cover-to-cover English translations appears at the back of this issue.

---

*At the All-Union Scientific Research Institute of New Building Materials.

ELECTROKINETIC PROPERTIES OF MONOCARBOXYCELLULOSE AND SOME CELLULOSE ACID ESTERS

V. I. Yur'ev and S. S. Pozin

S. M. Kirov Wood Technology Academy
Department of Physical and Colloid Chemistry, Leningrad
Translated from Kolloidnyi Zhurnal, Vol. 23, No. 4,
pp. 499-503, July-August, 1961
Original article submitted June 16, 1960

The electrokinetic properties of solids depend on both the composition of the surrounding liquid medium and the chemical nature of the actual surface of the solid. Many investigations on a variety of solids have been devoted to determining the effect of the liquid medium composition on the electrokinetic properties. There is very little information on the effect of the chemical composition of the solid phase in its electrokinetic properties [1].

Preparation of monocarboxycellulose and some acid esters of cellulose were investigated for determining the effect of functional groups present in technical cellulose materials on their electrokinetic properties and in particular the effect of carboxyl groups.

Treatment of cellulose with nitrogen dioxide results in preferential oxidation of the primary hydroxyl groups in the basic unit of the cellulose macromolecule [2]. Oxycellulose preparations of this type have become known as "monocarboxycelluloses".

In the present work we studied three sample of monocarboxycellulose obtained by oxidation of cotton cellulose (absorbent cotton), which contained 0.35, 4.45, and 7.76% of carboxyl groups (samples 1, 2, and 3), and three samples obtained by oxidation of bleached sulfite wood cellulose, which contained 1.16, 2.52, and 4.36% of COOH groups (samples 4, 5, and 6).

The acid esters of cellulose were prepared by esterification of cotton cellulose with the appropriate acid anhydride in glacial acetic acid in the presence of anhydrous sodium acetate [3]. By varying the esterification temperature and time, we obtained samples of cellulose acid phthalates containing 2.7 and 8.9% of free carboxyl groups and cellulose acid maleate with 6.6% of COOH groups. To study the electrokinetic properties we used the streaming potential method, which has a number of advantages over the electro-osmosis method [4]. The procedure for using the streaming potential to study the electrokinetic properties of fibrous cellulose materials has been described in detail in a previous paper by the authors [5]; it was shown that the electrokinetic potential of various fibrous cellulose materials, determined with allowance for the surface conductivity ($\varkappa_s$), is independent of the diaphragm density and is practically a constant value characterizing the state of the surface of the cellulose fibers.

The electrokinetic potential (ζ) was calculated from the following formula:

$$\zeta = \frac{4\pi\eta\varkappa_0 E}{DP} = 1{,}05 \cdot 10^5 \frac{\varkappa_0 E}{P}, \qquad (1)$$

where ζ is the potential (mv), $\pi = 3.1416$, $\eta = 0.01$ and $D = 81$ are the coefficient of viscosity and dielectric constant of pure water, P is the pressure at which the liquid is forced through the cellulose diaphragm (cm Hg), and E is the streaming potential (mv) determined directly from the experiment. The specific electrical conductivity of the diaphragm ($\varkappa_V$) and the surface conductivity ($\varkappa_S$). $\varkappa_0$ and $\varkappa_V$ were measured experimentally, while the surface conductivity was calculated from the following equation

$$\varkappa_s = \varkappa_0 - \varkappa_V. \qquad (2)$$

For conductimetric characterization of the diaphragm with allowance for its nonconducting part (skeleton), we introduced the coefficients α, β, and α/β [6]. The efficiency factor of the diaphragm $\alpha = \varkappa_0 / \varkappa_V$, which reflects the role of surface conductivity; β characterizes the skeleton of the diaphragm and is determined from the electrical

TABLE 1. Change in Electrokinetic Properties of Monocarboxycellulose Diaphragm
Density d = 0.360 g/cc

Samples	COOH in original sample, %	Medium	$\varkappa_0 \cdot 10^6$, ohm^{-1}. cm^{-1}	$\varkappa_S \cdot 10^6$, ohm^{-1}. cm^{-1}	$\frac{E}{P}$, mv/cm Hg	ζ, mv	α	β	$\frac{\alpha}{\beta}$
In H-form									
Cotton cellulose	0,04	H_2O	5,0	3,3	26,75	—14,0	2,9	2,2	1,3
Monocarboxy-cellulose 1	0,35	H_2O	15,6	13,5	8,30	—13,6	7,4	2,4	3,1
2	4,45	H_2O	34,1	32,4	4,13	—14,8	20.0	1,9	10,5
3	7,76	H_2O	60,3	58,5	1,58	—10,(	33,5	1,8	18,6
Bleached sulfite cellulose	0,30	H_2O	29,6	27,3	4,11	—12,8	12,9	2,5	5,2
Monocarboxy-cellulose 4	1,16	H_2O	53,2	50,1	2,10	—11,7	17,2	2,1	8,2
5	2,52	H_2O	63,5	60,1	1,16	—7,7	18,7	1,9	9,8
6	4,36	H_2O	77,8	74,2	0,92	—7,5	21,6	1,8	12,0
In salt form									
Monocarboxy-cellulose 2, K-f	4,45	H_2O	260,3	254,1	0,84	—23,0	42,0	1,6	26,2
	4,45	10^{-4} *N*KCl	381,9	361,9	0,31	—12,4	19,1	1,6	11,9
	4,45	10^{-3} *N*KCl	816,3	690,2	0,10	—8,6	6,5	1,6	4,1
	4,45	10^{-2} *N*KCl	2811	1578	—	—	2,3	1,6	1,4
Monocarboxy-cellulose 2, Ca-f	4,45	H_2O	24,3	22,0	4,69	—12,0	10,6	1,6	6,6
	4,45	10^{-4} *N*$CaCl_2$	69,3	44,9	1,34	—9,8	2,8	1,6	1,7
	4,45	10^{-3} *N*$CaCl_2$	220,3	50,7	0,29	—6,7	1,3	1,6	0,8
	4,45	10^{-2} *N*$CaCl_2$	1021	—114	—	—	0,9	1,6	0,6
	4,45	$5 \cdot 10^{-2}$ *N*$CaCl_2$	3591	—971	—	—	0,8	1,6	0,5
	4,45	10^{-1} *N*$CaCl_2$	6535	—2149	—	—	0,8	1,6	0,5
Monocarboxy-cellulose 3, K-f	7,76	H_2O	567,9	561,0	0,46	—27,4	82,3	1,3	63,3
	7,76	10^{-4} *N*KCl	583,9	564,9	0,13	—8,0	30,7	1,3	23,6
	7,76	10^{-2} *N*KCl	3430,7	2242,4	—	—	2,9	1,3	2,2
Monocarboxy-cellulose 3, Ca-f	7,76	H_2O	37,3	35,2	1,82	—7,1	17,8	1,4	12,7
	7,76	10^{-4} *N*$CaCl_2$	72,5	55,7	0,64	—4,9	4,3	1,4	3,1
	7,76	10^{-3} *N*$CaCl_2$	219,3	93,6	0,16	—3,7	1,7	1,4	1,2
	7,76	10^{-2} *N*$CaCl_2$	941,7	—139,2	—	—	0,9	1,4	0,6
	7,76	10^{-1} *N*$CaCl_2$	5263	—3185	—	—	0,6	1,4	0,4
Monocarboxy-cellulose 3, Al-f	7,76	H_2O	17,5	15,8	13,33	—24,5	10,3	2,1	4,9
	7,76	10^{-4} *N*$AlCl_3$	57,1	22,9	2,26	—13,5	1,7	2,1	0,8
	7,76	10^{-3} *N*$AlCl_3$	219,1	—49,3	0,15	—3,5	0,8	2,1	0,4
	7,76	10^{-2} *N*$AlCl_3$	1065,3	—94,0	—	—	0,9	2,1	0,4
	7,76	10^{-1} *N*$AlCl_3$	8058,0	—216,5	—	—	0,9	2,1	0,4

*K-f, Ca-F, and Al-F represent the K-, Ca-, and Al-forms.

capacities of a cell with the diaphragm material (C_D) and without it (C_O) ($\beta = C_D/C_O$); α/β characterizes the conductivity of the diaphragm as a whole.

Tables 1 and 2 give the corresponding electrokinetic values obtained by studying the samples of monocarboxycellulose and acid esters of cellulose. Preparations both in the acid form (H-form) and saturated with potassium, calcium, and aluminum ions (salt forms) were investigated.

The data presented show that for the H-forms of both monocarboxycellulose and the acid esters of cellulose, the streaming potential (E/P) decreases and the surface conductivity ($\varkappa_s$) increases with an increase in the content of COOH groups. As regards the ζ-potential, in general, its negative value tends to decrease with an increase in the amount of COOH groups in the cellulose material. An analogous phenomenon, namely, a decrease in the ζ-potential and an increase in the surface conductivity has been observed with unbleached sulfite cellulose with an increase in rigidity (a decrease in the boiling of the cellulose). Rigid sulfite wood celluloses contain a large amount of solid lignosulfonic acid, which is strongly acidic [7].

Thus, we may draw the general conclusion that in cellulose materials, an increase in the content of acid groups (in the H-form) both in the cellulose macromolecule itself and in the molecules of associated substances is accompanied by a decrease in E/P and the ζ-potential, while $\varkappa_s$ increases. The increase in the surface conductivity under

TABLE 2. Electrokinetic Properties of Acid Esters of Cellulose Diaphragm Density d = 0.360 g/cc

Samples	COOH in original sample, %	Medium	$\varkappa_0 \cdot 10^6$, ohm$^{-1}\cdot$cm^{-1}	$\varkappa_S \cdot 10^6$, ohm$^{-1}\cdot$cm^{-1}	$\frac{E}{P}$ mv/cm Hg	ζ, mv	α	β	$\frac{\alpha}{\beta}$
Cotton cellulose	0,04	H_2O	5,0	3,3	26,75	—14,0	2,9	2,2	1,3
Phthalate 1, H-form	2,7	H_2O	10,0	7,2	13,50	—14,2	3,6	1,8	2,0
Phthalate 1, K-f	2,7	H_2O	63,7	56,1	0,78	—5,2	8,4	2,0	4,2
	2,7	10^{-4} *N*KCl	93,2	75,9	0,92	—9,0	5,4	2,0	2,7
	2,7	10^{-3} *N*KCl	278,2	150,7	0,41	—12,0	2,2	2,0	1,1
	2,7	10^{-2} *N*KCl	1528,2	335,1	0,03	—5,3	1,3	2,0	0,7
Phthalate 1, Ca-f	2,7	H_2O	54,9	50,1	1,02	—5,9	11,4	1,8	6,3
	2,7	10^{-4} *N*$CaCl_2$	88,6	72,0	0,47	—4,4	5,3	1,8	3,0
	2,7	10^{-3} *N*$CaCl_2$	276,5	151,4	0,13	—3,9	2,2	1,8	1,2
	2,7	10^{-2} *N*$CaCl_2$	1220,9	195,8	—	—	1,2	1,8	0,7
Phthalate 2, H-f	8,9	H_2O	11,9	8,0	10,01	—12,5	3,1	2,2	1,4
Phthalate 2, H-f	8,9	H_2O	51,7	44,1	2,69	—14,6	6,8	2,2	3,1
	8,9	10^{-4} *N*KCl	93,8	65,2	1,30	—12,8	3,3	2,2	1,5
	8,9	10^{-3} *N*KCl	276,4	132,2	0,36	—10,6	1,9	2,2	0,9
	8,9	10^{-2} *N*KCl	1513,7	288,6	0,03	—5,2	1,2	2,2	0,5
Maleate 1, H-f	6,6	H_2O	17,0	14,2	4,79	—8,6	6,1	2,3	2,7
Maleate 1, K-f	6,0	H_2O	43,5	35,0	2,90	—13,2	5,1	2,3	2,2

*H-f, K-f, and Ca-f represent the H-, K-, and Ca-forms.

these conditions is apparently connected with an increase in the highly mobile hydrogen ions in the electrical double layer on the surface of the cellulose fibers. At the same time, there is a decrease in the diffuse part of the outer envelope of the double layer and this produces a fall in the streaming potential and the ζ-potential.

The increase in the surface conductivity with an increase in the content of COOH groups is clearly illustrated by the corresponding increase in the diaphragm efficiency factor (α). The coefficient β changes very little in these cases, indicating that the skeletons of all the cellulose diaphragms are practically equally nonconducting. For the salt forms of monocarboxycellulose, with an increase in the content of carboxyl groups the streaming potential (E/P) decreases for the K-form and increases for the Ca- and Al-forms in comparison with the H-form for distilled water. The surface conductivity increases sharply for the K-form and decreases for the Ca- and Al-forms in comparison with the H-form of the corresponding samples (Table 1). With an increase in the concentration of the corresponding chlorides, $\varkappa_S$ increases for the K-form and passes through a maximum and then falls to negative values for the Ca- and Al-forms. The salt forms of the acid esters of cellulose show behavior that is generally analogous to that of the corresponding forms of monocarboxycellulose, though in some cases there is a difference, such as in the case of the Ca-form of cellulose phthalate, which does not show an increase, but a decrease in the streaming potential. However, it should be noted that all these changes with an increase in the content of COOH groups are expressed less strongly in the case of acid esters of cellulose in comparison with monocarboxycellulose preparations. This behavior of acid phthalates and maleates of cellulose is apparently due to the lower value of the dissociation constants of the carboxyl groups of these compounds in comparison with the corresponding value for monocarboxycellulose samples [8].

SUMMARY

1. With an increase in the amount of COOH groups in samples of monocarboxycellulose and acid phthalates and maleates of cellulose in the H-form, the streaming potential and the ζ-potential decrease, while the surface conductivity increases and this is connected with an increase in the concentration of highly mobile hydrogen ions in the electrical double layer and contraction of the diffuse part of the outer envelope of this layer.

2. With the salt forms of the preparations studied, the streaming potential and the ζ-potential decrease with an increase in the concentration of the equilibrium solution.

LITERATURE CITED

1. J. J. Bikerman, Surface Chemistry. Theory and Application. Second Edition, N. Y., 1958; G. Robinov, and E. Heymann, J. Phys. Chem. 47, 655, 1943.

2. Z. A. Rogovin and N. N. Shorygina, Chemistry of Cellulose and Its Associated Compounds [in Russian] (Moscow-Leningrad, 1953), p. 285; G. M. Skurikhina and V. I. Yur'ev, Zh. prikl. khimii, 31, 931, 1958.
3. F. C. McIntire, and J. R. Schenck, J. Amer. Chem. Soc. 70, 1193, 1948.
4. O. N. Grigorov, Z. P. Koz'mina, A. V. Markovich, and D. A. Fridrikhsberg, Electrokinetic Properties of Capillary Systems [in Russian] (Izd. AN SSSR, 1956), p. 124.
5. V. I. Yur'ev and S. S. Pozin, Materially Tsentral'nogo nauchn. inst. bumagi, No. 38, 58 (1950).
6. I. I. Zhukov, Vestnik Leningradskogo Univ., No. 5, 34, 1949; V. I. Yur'ev and S. S. Pozin, Nauchn. dokl. vyssh. shk. Lesoinzhenernoe delo, No. 4, 215, 1958.
7. V. I. Yur'ev, S. S. Pozin, and G. M. Skurikhina, Izv. vyssh. uch. zaved., Lesnoi zh., No. 5, 147, 1958.
8. V. I. Yur'ev and G. M. Skurikhina, Zh. prikl. khimii, 33, 2803, 1960.

All abbreviations of periodicals in the above bibliography are letter-by-letter transliterations of the abbreviations as given in the original Russian journal. *Some or all of this periodical literature may well be available in English translation.* A complete list of the cover-to-cover English translations appears at the back of this issue.

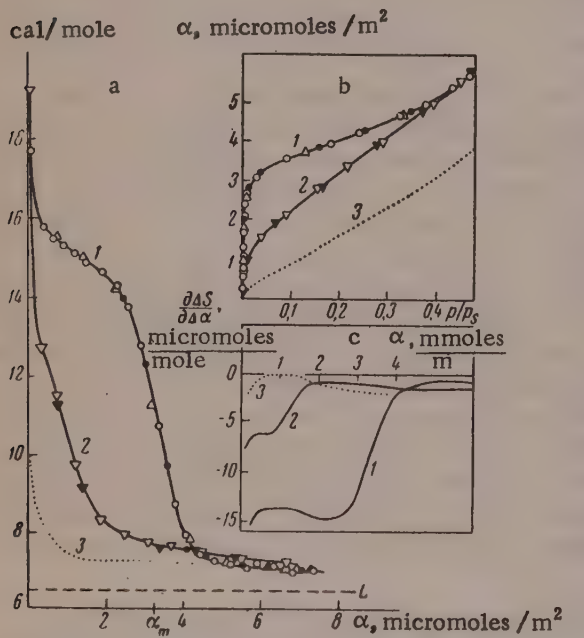
HEATS OF ADSORPTION OF DIETHYL ETHER VAPORS ON SILICA GEL

O. M. Dzhigit, A. V. Kiselev, and G. G. Muttik

M. V. Lomonosov Moscow University

Translated from Kolloidnyi Zhurnal Vol. 23, No. 4,
pp. 504-505, July-August, 1961
Original article submitted April 6, 1961

The adsorption of water on silica gel is basically determined by the interaction of the hydrogen bonds of its molecule with the hydroxyls of the surface and with each other [1]. Ether molecules can form hydrogen bonds only with the hydroxyls of the surface, but not with each other. The differential heat of adsorption Q_a* of the ether on a hydrated surface of silica gel in the middle range of filling the monolayer, unlike water [1], changes slowly, and on completion of the ($\alpha = \alpha_m$) falls sharply (Figure, a). A small decrease in the heat of adsorption on completion of the monolayer on a hydrated surface is caused by its geometric and chemical heterogeneity. This heterogeneity appears most markedly on a dehydrated surface which still partially retains a silanol group along with a siloxane group. Inasmuch as an ether cannot form a hydrogen bond, Q_a on a dehydrated sample falls sharply at first, while on further adsorption it diminishes slightly and is close to the heat of adsorption of n-pentane [3] (the magnitudes of Q_a of n-pentane and ether on graphite are close [4]). In the vicinity of $\alpha = \frac{1}{2}\alpha_m$ on a hydrated surface, Q_a is 6.2 Cal/mole larger than on a dehydrated one, and 7.5 Cal/mole larger than the Q_a of n-pentane [3]. As in the case of water [1], an atom of oxygen of the ether molecule may interact with two favorably located hydroxyls. Since these hydroxyls may be joined to each other by a weak hydrogen bond [5], the molecule of ether adsorbed on them breaks this bond. Therefore the energy of interaction of a molecule of ether with the hydroxyls of the surface is larger than the difference in the heats of adsorption mentioned above by the magnitude of the energy of the bond broken between the hydroxyls and amounts to ~9-11 Cal/mole, which corresponds with two hydrogen bonds.



a) Heats; b) isotherms and c) entropies of adsorption of ether (I) and n-pentane (3) on silica gel with a hydrated surface, and of ether (2) on silica gel with a dehydrated surface; L) heat of condensation of the ether.

The strong influence of dehydration of the surface on adsorption and differential entropy of adsorption is evident from the figure b and c. The entropy of the ether on hydrated silica gel in comparison with the liquid state falls much more than in other adsorption systems; this is connected with the presence of hydrogen bonds of the adsorbed ether with silica gel, and to their absence in the liquid ether.

LITERATURE CITED

1. O. M. Dzhigit, A. V. Kiselev, and G. G. Muttik, Kolloidn. zh., 23, (1961).
2. A. V. Kiselev, and G. G. Muttik, Zh. fiz. khimii (1961).
3. A. A. Isirikyan, A. V. Kiselev, and B. A. Frolov, Zh. fiz. khimii, 33, 389 (1959).
4. A. V. Kiselev, Zh. fiz. khimii, 35, 233 (1961).
5. A. V. Kiselev, and V. I. Lygin, Kolloidn. zh., 21, 581 (1959).

* The silica gels and the calorimeter were the same as in [1]. The measurements were carried out under isothermic conditions by the compensation method [2].

THE QUESTION OF PRIORITY IN THE DEVELOPMENT OF THE THEORY OF THE DIFFUSIOPHORESIS AND THERMOPHORESIS OF SMALL AEROSOL PARTICLES

B. V. Deryagin and S. P. Bakanov

Institute of Physical Chemistry of the Academy of Sciences
USSR, Moscow
Translated from Kolloidnyi Zhurnal Vol. 23, No. 4,
pp. 505-507, July-August, 1961
Original article submitted May 17, 1961

In the paper "The Theory of the Motion of Small Aerosol Particles in a Diffusion Field", [1] we showed that for the case where the radius of the aerosol particle is much less than the mean free path of the gas molecules, it is possible to make a rigorous calculation of the forces acting on the particles in the nonhomogeneous gas mixture, using the distribution of velocities of the gas molecules, given by the Chapman – Enskog formula, which is not disturbed materially by the presence of the aerosol particles.

By this method we calculated both the force arising in the presence of a concentration gradient and the diffusiophoresis rate of an aerosol particle. It was natural to use the same approach to calculate the thermophoretic force and thermophoresis rate of small aerosol particles. Proof of the correctness of this approach was given by the agreement between the formula which we obtained and the one which we had obtained from considering thermophoresis as a special case of thermal diffusion, when one of the components of the mixture has a very large mass. The paper in question, [2], was submitted to the Kolloidnyi Zhurnal on July 15, 1958.

The paper by Waldmann [3] appeared in 1959. It also deals with the calculation of the thermophoresis and diffusiophoresis rate of small aerosol particles and was submitted on March 23, 1959. The approach which he used is identical with the one we used in [1], and is based on the Chapman-Enskog distribution, undisturbed by the presence of a small aerosol particle. Therefore, it is natural that the calculations of thermophoresis themselves, although made independently of our second paper, do not differ from the ones which we published in any way, except in the substitution through the well-known Chapman formulas, of the coefficient of heat conduction in place of some of the molecular constants.

As for the part of Waldmann's paper which deals with the calculation of the diffusiophoreis rate by the same method, it was published two years after our [1] and is, likewise, in essence, completely identical with our paper except for the fact that the calculations were made to a lower degree of approximation, no account being taken of the molecular radii of the two gases. This being the state of affairs, it is pointless to speak of Waldmann's calculations as being independent and, in accordance with established international tradition, the question is exhausted by the statement that the priority of the rigorous (and in addition, more accurate) calculation of the diffusiophoresis and thermophoresis of small aerosol particles belongs to us. The fact that our 1957 paper on diffusiophoresis was not cited in this, or in Waldmann's further work, [4], is without objective reason, and cannot fail to produce astonishment. This failure to cite our work has already caused some foreign authors, [5], to be ignorant of our priority in this field.

It is even more surprising that N. A. Fuks, in a recently published review, [6], not only does not notice that Waldmann's paper is essentially only a repetition of our paper, but he quotes as "Waldmann's" formulas for the diffusiophoresis and thermophoresis rates. Here, N. A. Fuks emphasizes the difference between the numerical coefficient in Bakanov and Deryagin's formula and the coefficient in Waldmann's form. Actually, the two formulas for the thermophoresis rate are completely indistinguishable from one another. The difference in coefficients between the Waldmann formula and the Deryagin – Bakanov formula is the fruit of the incorrect calculations which Fuks himself made. The Waldmann formula (Fuks, p. 16 (2,9) first part of formula) is absolutely identical with Formula (36) (Kolloidn. zh. Vol. 21, No. 4, p. 383, 1959). It cannot be otherwise, since both formulas were derived by an absolutely identical

method, to the same degree of approximation. The second part of formula (2,9) had already been derived by N. A. Fuks, who substituted in it the value $\eta = 0.499\, c\lambda\rho$ although to this degree of approximation (where the relation holds that $\varkappa a = (15/4)(k\eta/m)$, as used by N. A. Fuks)

$$\eta = \frac{5\pi}{32} \bar{c}\lambda\rho \simeq 0{,}490\bar{c}\lambda\rho.$$

Futher quoting Waldmann's formula for the diffusiophoresis rate, N. A. Fuks limits himself to noting the, as it were, greater complexity of Deryagin and Bakanov's formula. This completely twists the essence of the matter, which consists in the fact that, in the paper published by Bakanov and Deryagin two years earlier than Waldmann, the diffusiophoresis rate had been more accurately calculated to the second order of approximation, we obtain, as a special case, the formula of [7] which differs from the formula which Waldmann published, without reference to our work, only in the use of another system of coordinates, fixed relative to the center of gravity of the gaseous mixture. Therefore, quoting in the review only Waldmann's formula, whatever the intentions of the author of the review, N. A. Fuks, may have been, leads the reader into error and in an objective way transfers the factual priority of the diffusiophoresis formula to a scientist of the German Federal Republic. This simplified formula unfortunately is not very accurate since it takes no account of the dimensions of the molecules and thus arrives at the false conclusion that there is no diffusiophoresis in a mixture of gases of the same molecular weight but different molecular radii. The damage grows still more in case the author does not make the necessary correction when his work is translated into foreign languages.

LITERATURE CITED

1. B. V. Deryagin and S. P. Bakanov, Doklady, AN SSSR, 117, No. 6, 1957.
2. S. P. Bakanov, and B. V. Deryagin, Kolloidn. Zh. 21, 377, 1959.
3. L. Waldmann, Z. Naturforsch. 14a, No. 7, 1959.
4. L. Waldmann, Z. Naturforsch. 15a, No. 10, 1960.
5. See, for example, R. D. Cadle, Disc. Faraday. Soc. and on the Physical Chemistry of Aerosols (preprint), 1960.
6. N. A. Fuks, Advances in the Mechanics of Aerosols, [in Russian] Academy of Sciences Press, USSR, Moscow, 1961.
7. S. P. Bakanov, Dissertation, [in Russian] Institute of General and Inorganic Chemistry (n. S. Kurnakov) AN SSSR, 1957.

All abbreviations of periodicals in the above bibliography are letter-by-letter transliterations of the abbreviations as given in the original Russian journal. *Some or all of this periodical literature may well be available in English translation.* A complete list of the cover-to-cover English translations appears at the back of this issue.

COLLOID CHEMISTRY - A. Sheludko

Reviewed by Yu. M. Glazman
Translated from Kolloidnyi Zhurnal, Vol. 23, No. 4,
pp. 508-509, July-August, 1961

At the present time an urgent need is being felt for new handbooks of colloid chemistry. This is due to the rapid development in the study of colloids, which has changed substantially in nature and content. The greater part of the existing monographs, teaching aids, and text books are out of date and do not meet present day needs. In view of this state of affairs, the publication of the Russian translation of A. Sheludko's book "Colloid Chemistry" is to be welcomed unconditionally.

A. Sheludko's monograph is an original work, which is similar to none of the existing handbooks, either in content, or in method of presenting the material. A. Sheludko's book is completely up to date— it was written from the point of view of the "New" colloid chemistry, and, in general, reflects the fundamentals of the subject, although not always with due completeness. The serious omission in this respect is that as important a part of colloid science as the reological properties of disperse systems is treated in a completely unsatisfactory fashion. This defect, moreover, is noted both by the author himself, and by the editors of the Russian translation—B. V. Deryagin and S. S. Voyutskii.

The questions treated most extensively in A. Sheludko's book are those dealing with the coagulation of colloidal solutions. This is in complete accord with the fact that the problem of the aggregational stability of disperse systems rightfully occupies a central position in contemporary colloid chemistry.

We must note particularly that the usually "forgotten" part of colloid chemistry courses, the part dealing with aerosols, is excellently described in A. Sheludko's monograph.

Along with the unquestionable achievements of A. Sheludko's book there are some defects too. The most important of these (in addition to the above mentioned section on the reological properties of disperse systems) have to do with the properties of lyophobic and lyophilic colloidal solutions, as well as the question of the stability and the coagulation by electrolytes of lyophobic colloids.

1. Confusion is caused by the definition of lyophobic colloid systems which is given on page 13. It also remains unclear whether or not lyophilic sols exist at all, and if they exist, what meaning the author attaches to the concept.

2. The enormous amount of factual material dealing with the laws which have been established for the coagulation of lyophobic sols by electrolytes has not received adequate treatment in the book. Meanwhile, a number of facts, and in particular, the ion exchange reactions occurring in the external part of an electric double layer and likewise, all the data, direct and indirect, on the adsorption of counter-ions and of electrolytes added to colloid systems are of great importance for the further development of the theory of the stability of lyophobic colloids. It must be emphasized—and this should in our opinion, have been noted in the monograph, that up to the present time, the question of the importance of the adsorption factor in the mechanism of the coagulation of lyophobic sols by electrolytes remains essentially unresolved; it needs profound study from every angle. Another defect of this section is that it completely ignores some of the views held on the nature of the stability of colloidal solutions. We are all familiar with the ideas developed by P. A. Rebinder on the structural mechanical barrier as one of the more important factors in the stability of disperse systems. Whatever the author himself may think, it seems unquestionable to us that a present-day handbook of colloid chemistry ought to reflect different points of view on this very important and presently discussed question. This becomes all the more evident if we realize that A. Sheludko's monograph can also be sucessfully used as a teaching aid with students in the chemistry departments of our institutions of higher learning.

Of the lesser defects, we can note the following:

1. In recounting the experimental data on the properties of the ξ potential (p. 102) there is no indication of the predominant influence exerted on the ξ potential by electrolyte ions which are oppositely charged with respect

to the sign of the ξ potential.

2. Although ultrafiltration can be used for purifying sols, nevertheless, it is scarcely correct to define ultrafiltration as "a method of purifying colloidal solutions" or as "dialysis under pressure."

3. It would be more rational to place the chapter dealing with optical properties (this is the least successfully written chapter in the book) after the treatment of Brownian motion. In spite of a relatively detailed treatment of the theory of optical scattering, Rayleigh's formula for the total intensity of the scattered light is not only not derived, but for some reason, it is not given at all. The principle of nephelometry is not presented with sufficient clarity. The cause of the phenomenon of flicker is not explained. The question of opalescence in molecularly disperse systems is not discussed.

The book contains some unfortunate expressions: "metallic solls" (pp. 41, 42), "colloidal sols" (pp. 41, 45), "valence of the electrolyte" (p. 107), and a number of others.

It is, of course, to be understood that the comments that have been made in no way reflect on the high rating which A. Shuludko's compendious book deserves, as it is written in an interesting an original fashion.

Yu. M. Glazman

COLLOID CHEMISTRY - Higher School Edition

A. G. Pasynskii

Reviewed by V. A. Pchelin
Moscow, 1959
Translated from Kolloidnyi Zhurnal, Vol. 23, No. 4,
p. 509, July-August, 1961

The physical chemistry of disperse systems, or, in the old terminology, "Colloid Chemistry" is gaining great scientific and practical importance. Nevertheless, at the present time a lack of educational literature in colloid chemistry is being felt and the publication of A. G. Pasynskii's "Colloid Chemistry" must, without a doubt, be welcomed.

The book consists of ten chapters, including material typical of the present state of colloid chemistry, as well as the physical chemistry of polymers. The first chapter speaks of the practical importance of colloid systems and gives an historical outline of the development of colloid chemistry. The following chapters discusss: molecular kinetic properties, optical and surface phenomena, electro-chemistry, stability and coagulation of colloids, the properties of foams, emulsions and aerosols, the physical chemical properties of solutions of polymers, the properties of gels and membranes, and finally, the properties of solid polymers.

A. G. Pasynskii's books is completely in line with contemporary conceptions in the field of colloid chemistry, and differs happily from previously published books in that the author has included a description of a number of new contemporary ideas and methods. These have to do with the fields which are indispensable as teaching aids for the biological specialties: the phenomenon of rotational diffusion, the determination of molecular weight by optical scattering, the methods of infrared and ultraviolet spectroscopy, the method of electrophoresis on paper, the chromatographic method, et al.

In every chapter of his book, the author tries to establish a connection between the theoretical material presented and contemporary biological problems. This gives the book a sense of purpose and practical importance.

The test questions and short conclusions at the end of each chapter are quite useful.

In such a small book, it is difficult to lay out the course being followed by contemporary colloid chemistry and the still completely new course being followed by the physical chemistry of polymers in the required detail. Therefore, A. G. Pasynskii's books is written in too compressed a fashion, and this, it appears to us will hinder the study of the subject by persons who are coming into contact with this branch of knowledge for the first time. Some important branches are treated too briefly, for example, the matter of the structural mechanical properties of disperse systems and the mechanism of floculation.

In future editions of A. G. Pasynskii's certainly useful book, its size should be increased, which will make it possible for the author to present the material of this important branch of science in more detail.

V. A. PCHELIN

V. I. Klassen and V. A. Mokrousov

Introduction to Flotation Theory, MINING LITERATURE PRESS, Second Edition
Moscow, 1959, 636 pages
Reviewed by A. B. Taubman
Translated from Kollodnyi Zhurnal
pp. 509-510, July-August, 1961

Four years have passed since the appearance of the first edition of this monograph (see our review in Kolloidn. Zh. 17, No. 1, 1955). Since this time, many important investigations have appeared in the rapidly developing field of the flotation enrichment of useful ores, which have greatly advanced the theory and practice of the process. Therefore, there is every reason to take note of the reappearance of this monograph in a new, enlarged and revised edition.

The second edition of the book is a capital work, containing not only extensive material on experimental studies in the field of flotation (more than 500 references are given in the bibliography), but, as in the first edition, numerous generalizations and conclusions by the author on a number of the most important as yet unsolved problems in the theory and on many special open questions.

While retaining the original arrangement of material, a particularly extensive revision was undertaken in the chapters of the monograph dealing with flotation reagents, and a discussion of the laws and mechanism governing their interaction with mineral surfaces. It should be noted that in presenting the subject of the collecting action of reagents, the authors correctly emphasize the role of adsorbtional (chemoadsorbtional) processes, which was not done in the first monograph.

Among the most interesting additions to this section of the book, the presentation of the following subjects should be noted:

1. Some peculiarities of the mechanism by which the reagents become attached to the surface of the particles of the undergoing flotation and, in particular, of collectors of non-polar type acting by selective wetting.

2. The nature and mechanism of "salt" flotation in solutions of inorganic electrolytes without the aid of organic surface active substances.

3. The collecting action of the products formed in statu nascendi by chemical reactions between the reagents and the inevitable ions in the flotation bath.

4. The role in the adsorbtive interactions of the reagents played by the correspondence between the dimensions of the adsorbing ions (molecules) of the collectors and the geometric parameters of the crystal lattice of the minerals.

5. The effect of foam forming reagents on the collecting action.

6. New types of anion and cation active collectors and organic reagents such as regulators, etc.

Considerable attention is also given to the description of the results of studies that have been carried out in recent years on adsorbtional interactions on mineral surfaces using tracer atoms and radiography, which enable the authors to enlarge the treatment of the much discussed question of the structural details of the layers adsorbed on floated particles as related to the homogeneity of their surface structure.

A number of additions have also been made in other sections of the book. Thus, a considerably more detailed critical discussion is given of K. F. Beloglazov's ideas on the thermodynamics of the adhesion to air bubbles of mineral particles covered by an absorbing layer of collector; more detailed consideration is given to the growth kinetics of the bubbles as they separate from solution, and the mineralization kinetics under cohesion conditions with mineral particles, including all the new experimental data obtained from high speed micro-motionpictures.

Along with this, it is impossible not to notice some deficiencies in presentation which have been retained in the text of the present edition. Thus, for example, on pages 549 to 550, the author is unsuccessful in his presentation

of the essence of Kelvin's well-known law for the increased vapor pressure and solubility of particles of small dimensions. In presenting B. V. Deryagin's work on the splitting pressure of thin liquid layers, no mention is made of the special role of coulomb forces in the ionic interactions (in the repulsion of diffuse double layers) when particles covered with them are brought together. In this particular case, however, the mechanism and theory of the positive splitting action is completely explained, which makes it possible to use them to intepret the effect of modifier electrons on the flotation process.

In comparison with the first edition, the second edition of the book gives a fuller presentation of the contemporary state of the theoretical problems of the flotation process along the most up-to-date lines open to further study.

The book is well executed and richly illustrated but, unfortunately, it has no subject or author index.

The great importance of this monograph, not only for the theory and practice of flotation, but for the associated fields of the physical chemistry of surface phenomena is beyond question.

SIGNIFICANCE OF ABBREVIATIONS MOST FREQUENTLY ENCOUNTERED IN SOVIET PERIODICALS

FIAN	Phys. Inst. Acad. Sci. USSR
GDI	Water Power Inst.
GITI	State Sci.-Tech. Press
GITTL	State Tech. and Theor. Lit. Press
GONTI	State United Sci.-Tech. Press
Gosenergoizdat	State Power Press
Goskhimizdat	State Chem. Press
GOST	All-Union State Standard
GTTI	State Tech. and Theor. Lit. Press
IL	Foreign Lit. Press
ISN (Izd. Sov. Nauk)	Soviet Science Press
Izd. AN SSSR	Acad. Sci. USSR Press
Izd. MGU	Moscow State Univ. Press
LEIIZhT	Leningrad Power Inst. of Railroad Engineering
LET	Leningrad Elec. Engr. School
LETI	Leningrad Electrotechnical Inst.
LETIIZhT	Leningrad Electrical Engineering Research Inst. of Railroad Engr.
Mashgiz	State Sci.-Tech. Press for Machine Construction Lit.
MEP	Ministry of Electrical Industry
MES	Ministry of Electrical Power Plants
MESEP	Ministry of Electrical Power Plants and the Electrical Industry
MGU	Moscow State Univ.
MKhTI	Moscow Inst. Chem. Tech.
MOPI	Moscow Regional Pedagogical Inst.
MSP	Ministry of Industrial Construction
NII ZVUKSZAPIOI	Scientific Research Inst. of Sound Recording
NIKFI	Sci. Inst. of Modern Motion Picture Photography
ONTI	United Sci.- Tech. Press
OTI	Division of Technical Information
OTN	Div. Tech. Sci.
Stroiizdat	Construction Press
TOE	Association of Power Engineers
TsKTI	Central Research Inst. for Boilers and Turbines
TsNIEL	Central Scientific Research Elec. Engr. Lab.
TsNIEL-MES	Central Scientific Research Elec. Engr. Lab.-Ministry of Electric Power Plants
TsVTI	Central Office of Economic Information
UF	Ural Branch
VIESKh	All-Union Inst. of Rural Elec. Power Stations
VNIIM	All-Union Scientific Research Inst. of Metrology
VNIIZhDT	All-Union Scientific Research Inst. of Railroad Engineering
VTI	All-Union Thermotech. Inst.
VZEI	All-Union Power Correspondence Inst.

NOTE: Abbreviations not on this list and not explained in the translation have been transliterated, no further information about their significance being available to us. —Publisher.

ADSORPTION AND HEAT OF ADSORPTION OF ISOMERIC BUTANOLS ON GRAPHITIZED CARBON BLACKS

N. N. Avgul', A. V. Kiselev, and I. A. Lygina

Institute of Physical Chemistry, Academy of Sciences USSR, Group Surface Chemistry, Moscow

Translated from Kolloidnyi Zhurnal, Vol. 23, No. 5, pp. 513-520, September-October, 1961
Original article submitted June 30, 1960

In a series of papers [1] we have studied the adsorption and the differential heat of adsorption of various hydrocarbon vapors (normal and branched alkanes, several cyclic and aromatic hydrocarbons) on the homogeneous surface of a graphitized carbon black. In the most recent studies of this series [2, 3] we have investigated on a graphitized carbon black the adsorption of a series of normal alcohols: methanol, ethanol, propanol and butanol. In the paper [2] it has been shown that upon passing from the normal alkanes to the corresponding normal alcohols the adsorption energy on the channel black Spheron-6 graphitized at 2800° sharply increases and this was explained by a strong mutual interaction between the alcohol molecules in the adsorbed layer. The interaction between the alcohol molecules is still more clearly manifested [3] in their adsorption on a graphitized thermal black with a more homogeneous surface. In the present study, which is a continuation of the said series, we have investigated on a graphitized thermal carbon black the adsorption and the heat of adsorption of branched alcohols, namely, those of the isomeric butanols: isobutanol (2-methylpropanol-1), secondary butanol and tertiary butanol.

As adsorbent we used the thermal carbon black T1, graphitized at 3000° during 45 min in an atmosphere of CO, which has a specific surface area s = 29.0 m^2/ g and was also used in the studies [2-6]. The purified secondary butanol we obtained from E. A. Mikhailova and the isobutanol and tertiary butanol from V. L. Foss.* The constants of the alcohols used are given in the table.

Constants of the Alcohols Used

Alcohol	d_4^{20}	n_D^{20}	Vapor pressure p_s, mm
2-Methylpropanol-1	0.801	–	6.7 (at t = 17.2°)
Secondary butanol	0.8067	1.3971	9.6 (at t = 16.5°)
Tertiary butanol	–	–	23.2 (at t = 16.5°)

Just as previously, the differential heat of adsorption was measured in a calorimeter with constant heat exchange (the model of 1953) and the amount of methylpropanol and secondary butanol adsorbed was determined by means of capillary liquid microburets [7] in a vacuum equipment. Because tertiary butanol is a solid at room temperature but has a quite high vapor pressure, for this substance the amount adsorbed was measured by the volumetric method. All experiments were carried out at 20°.

Isotherms of the amounts adsorbed α expressed in absolute units (per unit surface area) and the differential heats of adsorption Q_a on the graphitized thermal black T 1(3000) are shown in Fig. 1; the values for n-butanol were taken from the paper [3] and those of 2-methylpropanol-1, secondary and tertiary butanol were obtained in the present study. For each alcohol we carried out two series of experiments and their results coincided. The isotherms were reversible up to small values of the relative vapor pressure p/p_s.

* The authors express their gratitude to these persons.

As has been noticed previously [3], the adsorption isotherm of n-butanol starts with a convex region, passes through four points of inflection and forms two clearly developed waves. The adsorption isotherm of methylpropanol has the same shape, but in this case the second wave is still more sharply developed. Although upon passing to secondary butanol all four points of inflection on the isotherm are preserved, the second wave is very near to the first one. In the adsorption of tertiary butanol both these waves of the adsorption isotherm have completely coalesced and the adsorption isotherm of tertiary butanol, which at its start is convex too, passes only through two points of inflection in the range embraced by the measurements.

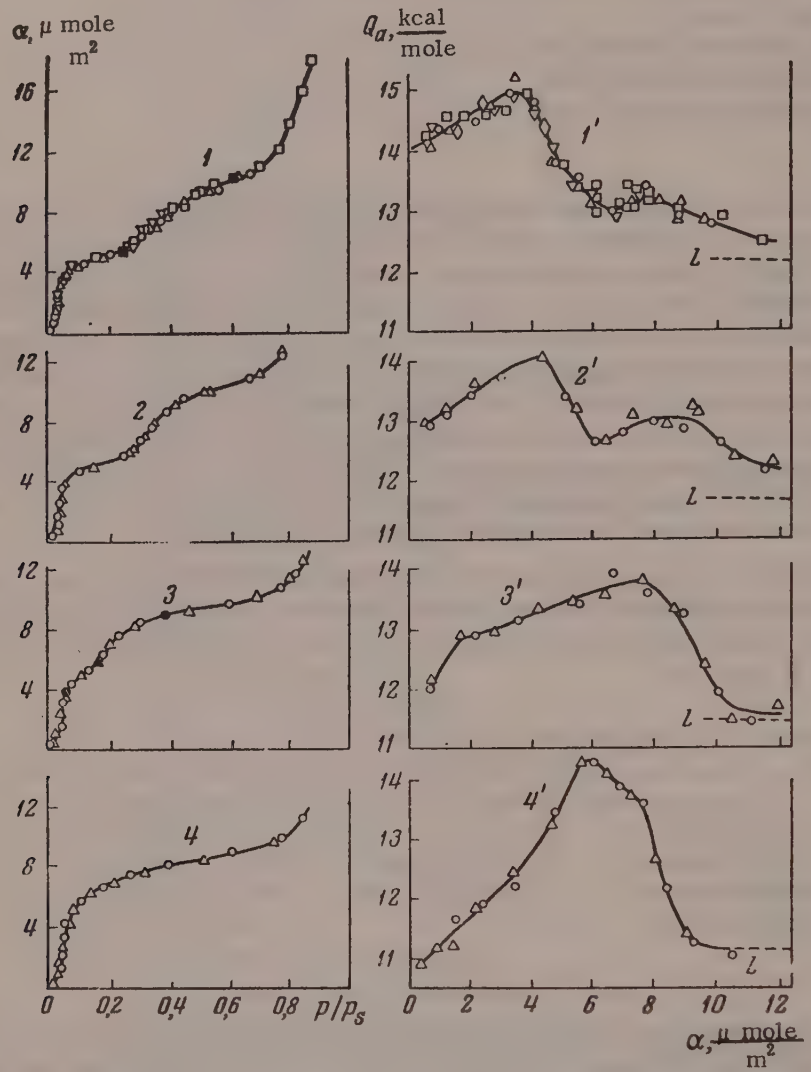


Fig. 1. Adsorption isotherms (left) and differential heats of adsorption (right) of n-butanol (1, 1'), 2-methylpropanol-1 (2, 2'), secondary butanol (3, 3') and tertiary butanol (4, 4') vapors on the graphitized thermal black T1(3000). Filled marks denote desorption. The latent heats of condensation L are designated by the horizontal dashed lines.

Similar regularities are found in the curves for the differential heats of adsorption (Q_a). The curve of the isothermal differential heat of adsorption for n-butanol passes through two maxima corresponding to the two waves of the adsorption isotherm, while the heat of adsorption in the first maximum surpasses that at the start of the isotherm (at $\alpha = 0.05$ μmole/m²) by an amount of ~1 kcal/mole, then it falls by about 2.0 kcal/mole, hereafter it rises again by about 0.2-0.3 kcal/mole and passes through the second maximum. In the adsorption of methylpropanol

the entire curve of the heats of adsorption lies lower, but both maxima on this isothermal curve are preserved and the rise in heat of adsorption from $\alpha = 0.05$ μmole/m^2 to the first maximum is somewhat greater (it attains the value 1.2 kcal/mole), further on the heat of adsorption falls by about 1.5 kcal/mole, passes through a minimum, then rises again by approximately 0.5 kcal/mole to the second maximum. In the case of secondary butanol, obviously, the two maxima coalesce and on the curve of the isothermal heat of adsorption only one sloping bulge is found, whereas the rise in heat of adsorption from $\alpha = 0.05$ μmole/m^2 to the maximum is ~ 2 kcal/mole. The curve of the isothermal heat of adsorption for tertiary butanol has one sharply developed maximum, whereas the rise in heat of adsorption from $\alpha = 0.05$ μmole/m^2 to this maximum already amounts to 3.5 kcal/mole.

Comparison of the isotherms and the heats of adsorption. Equations which describe the adsorption isotherms. In the preceding papers [2, 3] the great role of mutual hydrogen bonds in the adsorption of alcohols was proved. Owing to this interaction, in the adsorption of normal alcohols, in particular, n-butanol, on the surface of a graphitized carbon black even at small degrees of coverage there are adsorbed not separate molecules but their associated complexes, as it were, "strings" from n-butanol molecules, mutually united by hydrogen bonds. By this it was explained why the amount adsorbed and the heat of adsorption are higher for n-butanol than for n-butane [2]. Owing to the presence of these strong bonds, n-butanol is very densely packed in a monolayer so that the area occupied by one molecule in a compact monolayer, ω_m, amounts to ~ 35 A^2 and, correspondingly, the capacity of a compact monolayer is equal to 4.7 μmole/m^2 [2].

From Fig. 2, in which the adsorption isotherms of Fig. 1 (this time plotted versus the absolute vapor pressure p) and the heats of adsorption for the isomeric butanols are compared, it is evident that the adsorption isotherm of n-butanol forms two waves corresponding to the fact that the first layer is preferentially filled before the second layer starts. The two maxima in the curve for the heat of n-butanol adsorption lie close to the points where the first and

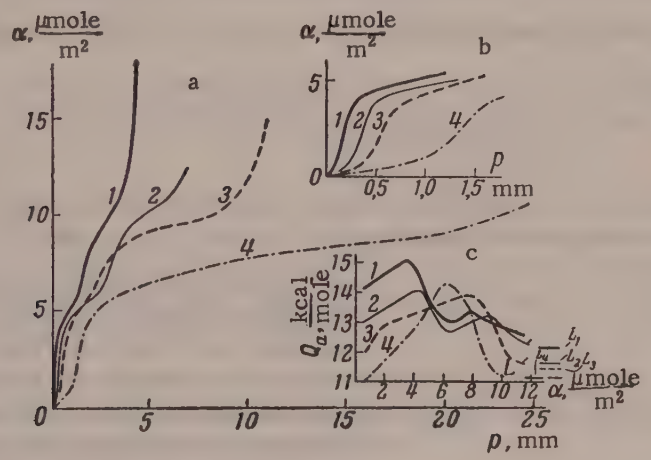


Fig. 2. Adsorption isotherms (a) and (b) plotted versus absolute vapor pressure p (at two different scales) and the differential heat of adsorption Q_a as a function of the amount α (c) of n-butanol (1), 2-methylpropanol-1 (2), secondary (3) and tertiary butanol (4) adsorbed on the graphitized thermal black T1 (3000). In Fig. (c) the values of the latent heats of condensation L are indicated by the horizontal lines.

the second layer, respectively, are completed and they are mainly connected with the electrokinetic (dispersional) interaction in these layers between neighboring strings of associated n-butanol molecules. Upon passing to 2-methylpropanol-1 the adsorption isotherm is shifted to the right, although it also forms two waves, just as is the case for n-butanol, but completion of these waves takes place at a somewhat higher value of α and this indicates that the 2-methylpropanol-1 molecules occupy a smaller area in a compact monolayer. Obviously, in adsorption the 2-methylpropanol-1 molecules too form associated complexes (strings) where the entire molecule, except the branched methyl group, lies flat on the surface and the said side group somewhat protrudes from the surface. This is confirmed by the

magnitude of the heat of adsorption. From Fig. 2, c it is evident that the heat of adsorption in the first layer of 2-methylpropanol-1 is by 1 kcal/mole smaller than that of n-butanol. The somewhat higher value of the second maximum in the heat of adsorption, as is found upon passing from n-butanol to 2-methylpropanol-1, may be caused by a decreased dispersional interaction between adjacent strings of associated 2-methylpropanol-1 molecules.

Upon passing to secondary and tertiary butanol the amount adsorbed and the heat of adsorption continue to decrease. In this case a stringlike arrangement of associated alcohol molecules on the surface so that each molecule is engaged in one hydrogen bond is already impossible. In the case of the secondary and the tertiary butanol the adsorbed molecules form more locked associates on the surface, while, probably, at an increase of the amount adsorbed the orientation of these alcohol molecules also changes. Obviously, this is particularly clearly manifested in the adsorption of tertiary butanol.

Since in the adsorption of the butanol isomers there is a strong mutual interaction between the adsorbate molecules in the adsorbed layer, in order to describe the adsorption isotherms we have used equations which approximately take into account both adsorbent-adsorbate and adsorbate-adsorbate interactions.

For the description of localized polymolecular adsorption we have derived [8, 9] the following approximate equation:

$$p/p_s = \frac{\theta\,(1-p/p_s)^2}{K_1\,[1-\theta\,(1-p/p_s)]\,[1+K_n\theta\,(1-p/p_s)]}\,, \qquad (1)$$

where $\theta = \alpha/\alpha_m = \alpha\,\omega_m$ represents the degree of surface coverage; α the amount adsorbed; α_m the capacity of a compact monolayer; ω_m the area occupied by one molecule in the compact monolayer; K_1 and K_n the relative equilibrium constants for adsorbate-adsorbent and adsorbate-adsorbate interaction, respectively.

For nonlocalized polymolecular adsorption the following equation [10] has been given:

$$p/p_s = \frac{\theta\,(1-p/p_s)^2}{K_1\,[1-\theta\,(1-p/p_s)]}\,e^{\frac{\theta(1-p/p_s)}{1-\theta(1-p/p_s)}-K_2\theta(1-p/p_s)}\,, \qquad (2)$$

where $K_2 = a_2/kTb_2$ is the constant of the adsorbate-adsorbate interaction, whereas a_2 and b_2 are the constants of the two-dimensional equation of state of van der Waals' type.

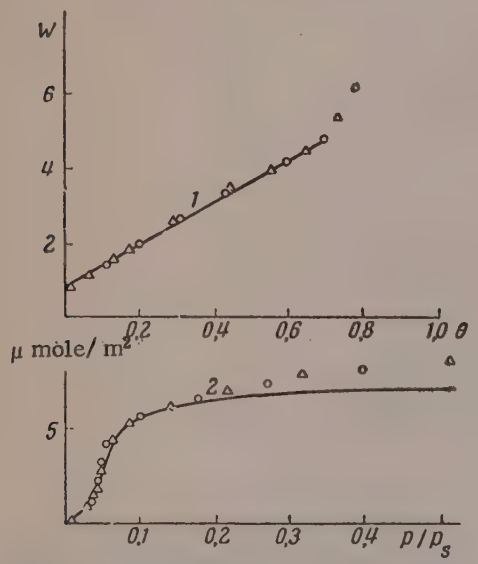


Fig. 3. Adsorption isotherm of tertiary butanol on the graphitized thermal black T1 (3000) plotted in the coordinates of equation (4) for monomolecular nonlocalized adsorption (1) and as α versus p/p_s (2): The points represent experimental data, the curve and the straight line were calculated by means of Hill's equation.

In the paper [3] the adsorption isotherm of n-butanol on the carbon black T1 (3000) was treated by means of these equations and it was shown that equation (1) somewhat better describes the isotherm than equation (2) does, that is, in that case there is rather localized than nonlocalized adsorption. In the present study while varying ω_m from 35 to 28 A^2 we applied the said equations to the adsorption isotherm of 2-methylpropanol-1. It was found that at ω_m = 28 A^2 the first wave in the adsorption isotherm for 2-methylpropanol-1 is satisfactorily described by the approximate equation (2) for nonlocalized polymolecular adsorption. But in this case equation (1) was found to be unsuitable, that is, in the adsorption of 2-methylpropanol-1 where when compared with n-butanol the mutual interaction between the absorbate molecules in the surface layer is somewhat higher but that between an adsorbate molecule and the adsorbent surface is somewhat lower, there is already rather nonlocalized than localized adsorption.

In its shape the adsorption isotherm of secondary butanol takes an intermediary position between the isotherm of 2-methylpropanol-1 and that of tertiary butanol and, therefore, it was not tested. The absorption isotherm of tertiary

butanol on the graphitized black up to $p/p_s \approx 0.5$ in its appearance looks like an isotherm of monomolecular adsorption, as is found, when adsorbate-adsorbate interaction does occur. At the same time the initial heat of adsorption, which is characteristic for the adsorbate-adsorbent interaction, is small in this case. Therefore, in order to describe this adsorption isotherm we used the equation for monomolecular nonlocalized adsorption, as was given by Hill [10] and De-Boer [11].

$$p/p_s = \frac{\theta}{K_1(1-\theta)} e^{\frac{\theta}{1-\theta} - K_2\theta} \tag{3}$$

When linearized this equation becomes of the form [12, 9]:

$$W(\theta, p/p_s) = \frac{\theta}{1-\theta} + \ln\frac{\theta}{1-\theta} - \ln p/p_s = \ln K_1 + K_2\theta. \tag{4}$$

In Fig. 3 the adsorption isotherm of tertiary butanol on the graphitized thermal black is plotted according to this equation: the best fit to this isotherm is obtained by taking $\alpha_m = 9.5$ mole/m^2, that is, $\omega_m = 17.5$ A^2. Such a small value of ω_m has no physical sense for a single tertiary butanol molecule, but such a "monolayer" may be considered to consist of two compact layers of these alcohol molecules mutually connected in pairs by hydrogen bonds perpendicularly to the surface of the carbon black with a strong interaction along the surface.

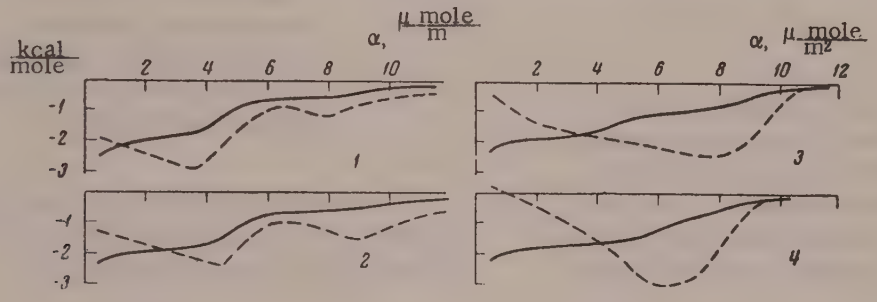


Fig. 4. The differential changes in energy $\frac{\partial \Delta U}{\partial \alpha}$ (dashed) and free energy $\Delta\mu$ (drawn curves) plotted as a function of the amount of n-butanol (1), methylpropanol (2), secondary butanol (3) and tertiary butanol (4) adsorbed on the graphitized thermal black T 1(3000).

By applying the equation of monomolecular localized adsorption [9] to the isotherm of tertiary butanol it was shown that the said equation is not appropriate for this isotherm.

Energy, free energy and entropy of adsorption. From the adsorption isotherm $\alpha(p/p_s)$ and the differential heats of adsorption $Q_a(\alpha)$ we calculated, just as was done in the papers [1-3], the differential changes in the free energy $\Delta\mu = RT \ln p/p_s$, the energy $\partial\Delta U/\partial\alpha = -(Q_a - L)$ (Fig. 4) and the entropy of adsorption $\partial\Delta S/\partial\alpha = \frac{1}{T}(\partial\Delta U/\partial\alpha - \Delta\mu)$ (Fig. 5) for the transition of these alcohols from the pure liquids to the adsorbed layer. In the case of tertiary butanol these changes may be taken to refer as well to the liquid as to the solid state, since the latent heats of its condensation and sublimation differ only by 0.2 kcal/mole.

From the entropy curves of Fig. 5 it is evident that at a small degree of coverage the mobility of the butanol molecules is higher than that in the liquid, while this mobility increases upon passing from n-butanol to the tertiary butanol. In the regions where mainly the first or the second layer is completed, minima are found in the entropy curves for the adsorption of n-butanol and methylpropanol. In the adsorption of the secondary and the tertiary butanols the curves of the differential adsorption entropy have a particularly deep minimum. So, in this series of alcohols, as the structure of the molecules becomes more complex, both at small θ and at θ values close to one an ever greater difference is found between the state of the substance in the adsorbed layer and that in the liquid.

It is also of interest to compare the mean molar (integral) changes in entropy at increasing amounts adsorbed and the results obtained by calculating $\frac{1}{\alpha}\int_0^{\alpha} \frac{\partial \Delta S}{\partial \alpha} d\alpha$ are shown in Fig. 6. At small amounts adsorbed the mobi-

lity of all alcohols is much higher in the adsorbed state than in the liquid. However, the mean molar entropy change falls gradually. At about two layers adsorbed, the molecules of n-butanol, methylpropanol and secondary butanol are already somewhat less mobile than they are in the liquid. The entropy curve shows that in a double layer the mobility of the tertiary butanol molecules is close to that in the solid state.

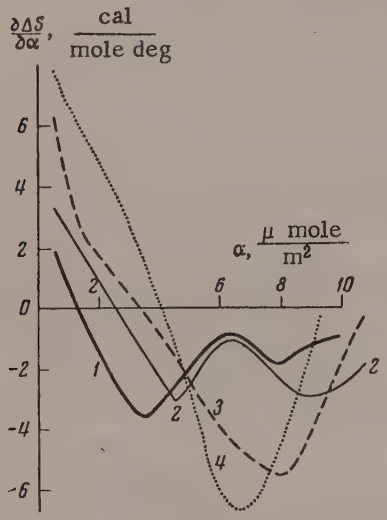


Fig. 5. The differential change in adsorption entropy $\partial\Delta S/\partial\alpha$ plotted versus the amount α of n-butanol (1), methylpropanol (2), secondary (3) and tertiary butanol (4) adsorbed on the graphitized thermal black T 1 (3000).

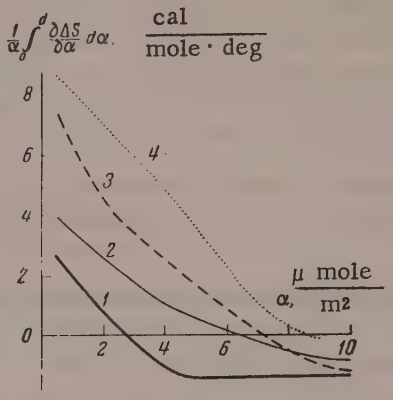


Fig. 6. The integral molar change in adsorption entropy plotted versus the amount of n-butanol (1), methylpropanol (2), secondary (3) and tertiary butanol (4) adsorbed on the graphitized thermal black T1 (3000).

A theoretical estimate of the adsorbate-adsorbent and adsorbate-adsorbate interaction energies in the adsorption of alcohols on graphite has been given in the paper [13].

SUMMARY

1. Adsorption isotherms and differential heats of adsorption of 2-methylpropanol-1, secondary- and tertiary butanol vapors on a graphitized carbon black have been measured in a calorimeter with constant heat exchange. The adsorption isotherms of the butanols are wave-like; in the case of n-butanol and 2-methylpropanol-1 there are two waves in the adsorption isotherm and two corresponding maxima in the curves for the heat of adsorption. Upon passing to secondary and especially to tertiary butanol the two waves in the adsorption isotherm and the two maxima in the curve of the heat of adsorption merge into one wave and one maximum, respectively.

2. As one passes from n-butanol to tertiary butanol, the amount adsorbed and the heat of adsorption at low vapor pressures decreases.

3. Calculations of the adsorption entropies of the butanols show that these substances when adsorbed on a graphitized carbon black are in a state quite different from that of the normal liquid.

The authors thank G. I. Berezin for his assistance in measuring the heats of adsorption.

LITERATURE CITED

1. N. N. Avgul', G. I. Berezin, A. V. Kiselev, and I. A. Lygina, Zh. fiz. khimii, 30, 2106 (1956); Izv. AN SSSR, Otd. khim. n. 1956, 1304; 1957, 1021; 1959, 787; N. N. Avgul', G. I. Berezin, A. V. Kiselev, and A. Ya. Korolev, Kolloidn. zh. 20, 298 (1958).
2. N. N. Avgul', G. I. Berezin, A. V. Kiselev, and I. A. Lygina, Izv. AN SSSR, Otd. khim. n. 1961, 205.
3. N. N. Avgul', A. V. Kiselev, and I. A. Lygina, Kolloidn. zh. 23, 369 (1961).
4. A. V. Kiselev and E. V. Khrapova, Kolloidn. zh. 23, 163 (1961).
5. A. A. Isirikyan and A. V. Kiselev, Kolloidn. zh. 23, 281 (1961).
6. A. V. Kiselev and A. A. Isirikyan, J. Phys. Chem. 65, 601 (1961).

7. N. N. Avgul', G. I. Berezin, A. V. Kiselev, A. I. Lygina, and G. G. Muttik, Zh. fiz. khimii, 31, 1111 (1957).
8. A. V. Kiselev and D. P. Poshkus, Izv. AN SSSR, Otd. khim. n. 1958, 520.
9. A. V. Kiselev, Kolloidn. zh. 20, 338 (1958)
10. T. L. Hill, J. Chem. Phys. 14, 441 (1946).
11. J. H. De - Boer, The Dynamical Characters of Adsorption, Oxford, 1953.
12. S. Ross and W. Winkler, J. Coll. Sci. 10, 319, 330 (1955).
13. N. N. Avgul', A. V. Kiselev, and I. A. Lygina, Izv. AN SSSR, Otd. khim. n. 1961, 1404.

All abbreviations of periodicals in the above bibliography are letter-by-letter transliterations of the abbreviations as given in the original Russian journal. *Some or all of this periodical literature may well be available in English translation.* A complete list of the cover-to-cover English translations appears at the back of this issue.

EMULSION METHOD OF EXTRACTING COLLOIDAL MIXED URANYL FERROCYANIDE FROM ITS HYDROSOLS

V. I. Borisikhina, L. D. Skrylev, and S. G. Mokrushin

Sverdlovsk Ural Polytechnic Institute
Translated from Kolloidnyi Zhurnal, Vol. 23, No. 5,
pp. 521-523, September-October, 1961
Original article submitted July 9, 1960

In the work of Mokrushin and his co-workers[1,2] it was established experimentally that an emulsion method is feasible for complete extraction of colloidal metals, sulfides, hydroxides, and pigments from their hydrosols, and it was also shown that the colloid extraction process is improved considerably by the presence of small quantities of gelatin. The favorable influence of gelatin is explained by the formation of a surface-active complex from the colloidal particles being extracted and the gelatin micelles, as a result of which the colloidal particles acquire surface activity and migrate readily to the hydrosol– organic liquid phase boundary.

The present investigation was aimed at studying the possibility of utilizing an emulsion method for recovering colloidal mixed uranyl ferrocyanide from aqueous solutions.

A colloidal solution of mixed uranyl ferrocyanide was prepared by mixing solutions of potassium ferroxyanide and uranyl nitrate. The reagents were added in amounts calculated to give 100 mg of solid phase per liter, with the composition $K_2(UO_2)_3[Fe(CN)_6]_2$ [3], using a 50% excess of potassium ferrocyanide, which played the role of a peptizing agent. The resulting electronegative sol had an intense red-brown color and was completely transparent. The sols were not dialyzed. Freshly distilled carbon tetrachloride was used as the organic liquid for obtaining the emulsion.

Our first investigations demonstrated that it was impossible to achieve any appreciable extraction of the solid phase by direct shaking of the sol and carbon tetrachloride; therefore, an attempt was made to improve the extraction process by introducing small quantities of gelatin into the sol.

Influence of Gelatin. The experiments on studying the influence of gelatin on the process of emulsion extraction of colloidal mixed uranyl ferrocyanide were performed in the following manner. A 75-ml quantity of the sol and 25 ml of carbon tetrachloride were poured into a 200-ml separatory funnel, and then 0.1 ml of 0.5% aqueous gelatin solution was introduced from a microburette. The mixture was shaken thoroughly (2 min) by a standard method [4]. After the resulting emulsion had stood for 20 min, the degree of extraction of the colloid was determined colorimetrically on the aqueous phase. If it turned out that the disperse phase had been incompletely extracted, then a fresh portion of gelatin was introduced into the sol and the shaking was repeated. This procedure was continued until practically complete recovery of the disperse phase was achieved.

With an increase in the quantity of gelatin introduced into the sol, the degree of extraction of the colloid is increased and reaches 100% at a certain concentration of gelatin in the sol:

Quantity of 0.5% aqueous gelatin solution, ml	0.0	0.1	0.2	0.3	0.4	0.5
Degree of extraction of colloid, %	2.1	28.7	53.1	73.4	94.7	~100

The emulsion which settles from the system on standing contains 75-80% carbon tetrachloride, and is not broken in the course of several months. The volume of emulsion settling out varies from 32 to 33 ml.

The extremely low (~2%) extraction of the colloid observed on emulsifying carbon tetrachloride and gelatin-free sols is explained by the negative charge of the ferrocyanide particles, which undoubtedly hampers their migration to the hydrosol – organic liquid phase boundary, which is charged negatively [5].

Influence of Electrolytes. As electrolytes we utilized potassium, barium, and aluminum nitrate solutions, which were introduced in small portions into a test system consisting of 75 ml of the sol and 25 ml of carbon tetrachloride, after adding 0.1 ml of 0.5% aqueous gelatin solution to the system and emulsifying vigorously for two minutes. The periods of emulsifying, standing, and colorimetric examination of the aqueous phase were repeated after each addition of electrolyte.

Influence of Additions of Electrolytes on Degree of Extraction of Colloidally Dissolved Mixed Uranyl Ferrocyanide by the Emulsion Method

Electrolyte	Quantity of electrolyte added to sol, ml	Degree of extraction of colloid, %
0,01*N* Al $(NO_3)_3$	0,0	28,5
	0,5	42,0
	1,0	50,6
	1,5	69,4
	2,0	88,0
	2,5	95,0
	2,8	100,0
0,7*N* Ba $(NO_3)_2$	0,0	29,0
	0,1	63,2
	0,2	80,0
	0,3	95,0
	0,35	100,0
1,0*N* KNO_3	0,0	29,1
	0,1	46,0
	0,2	54,0
	0,3	60,0
	0,4	68,0
	0,5	75,0
	0,6	82,0
	0,8	98,0

The results of the investigations which were conducted are presented in the table.

From the table it is evident that the degree of extraction of the colloids shows a progressive increase with an increasing quantity of electrolyte introduced into the sol, the greater effect being shown by the higher-valence cations. The favorable influence of electrolytes on the process of emulsion extraction of colloids is explained by their effect in decreasing the negative charge of the ferrocyanide particles. This point of view is supported by the circumstance that the electrolytes investigated are rated in the order $Al(NO_3)_3 > Ba(NO_3)_2 > KNO_3$ (taking their normality into account) in the intensity of their effect on the colloid emulsion-extraction process; this is in complete agreement with the well-known Schulze-Hardy rule.

The emulsification of systems which do not contain gelatin but contain ever-increasing quantities of electrolytes (right up to the threshold of coagulation) does not give the desired results, since the ferrocyanide particles do not migrate to the phase boundary, and the emulsion formed on shaking is broken rapidly.

Breaking of Emulsion Settled from the System on Standing. It is necessary to break the highly concentrated emulsion of carbon tetrachloride with surface-adsorbed uranyl ferrocyanide particles which results from the extraction of the colloid. Breaking of the emulsion is necessary both with a view to subsequent concentration of the disperse phase and with a view to regeneration of the oil [recovery of the carbon tetrachloride].

According to the views of Rebinder [6], the main factor in emulsion stability is the structural viscosity (strength) of their stabilizing films. For destroying these films, we took advantage of the displacing action of monobasic alcohols, which possess high surface activity and at the same time are not capable of forming strong stabilizing films.

The experiments on breaking the emulsion were conducted in the following manner: A 25-ml quantity of emulsion obtained in the process of extracting mixed uranyl ferrocyanide was poured into a 100-ml separatory funnel, and fractional portions of alcohol were added. After each alcohol addition, the contents of the funnel were shaken thoroughly for one minute and then allowed to stand. On standing, the volume of oil separated was determined. Usually the first portions of alcohol do not break the emulsion, but increase the viscosity of the system markedly; however, on reaching a certain concentration of alcohol in the system, the emulsion is broken rapidly.

The minimum quantity of alcohol necessary for complete breaking of the emulsion is 0.25 ml in the case of ethyl alcohol, 3.0 ml for isopropyl, 0.75 ml for isobutyl, and 0.82 ml for isoamyl.

One can also take advantage of the demulsifying action of acetone for breaking the emulsion. Under analogous conditions in emulsion-breaking experiments, only 0.4 ml of acetone is required.

After breaking the emulsion, the system in the funnel consists of two layers, an upper aqueous phase and a lower oil phase, with a thin interlayer band of coagulum of mixed uranyl ferrocyanide and gelatin. The coagulum can be recovered readily in pure form from this interlayer.

SUMMARY

1. Colloidally dissolved mixed uranyl ferrocyanide can be recovered from its hydrosols containing a small quantity of gelatin, at a hydrosol – organic liquid phase boundary.

2. Small quantities of electrolytes [$Al(NO_3)_3$, $Ba(NO_3)_2$, and KNO_3] introduced into a system of 75 ml sol, 25 ml carbon tetrachloride, and 0.1 ml of 0.5% gelatin solution promote the process of colloid recovery.

3. The highly concentrated gelatinized emulsions of carbon tetrachloride stabilized with colloidal mixed uranyl ferrocyanide can be broken by the addition of alcohols or acetone.

LITERATURE CITED

1. S. G. Mokrushin, V. I. Borisikhina, Tr. Ural'skogo politekhnicheskogo inst., Coll. 69. 1957, pp. 4 and 9.
2. S. G. Mokrushin, Soobshch. o nauchnykh rabotakh Vses. obva. im. D. I. Mendeleeva 2, 27, 1953.
3. I. V. Tananaev, Izv. AN SSSR. Otd. khim. nauk, 1957, 12, 1421.
4. S. G. Mokrushin, V. I. Borisikhina, Kolloidn.zh.20, 736, 1958.
5. V. Clayton, Emulsions [Russian translation] (IL, Moscow, 1950), p. 208.
6. P. A. Rebinder, Kolloidn. zh. 8, 15, 1946; 20, 527, 1958.

All abbreviations of periodicals in the above bibliography are letter-by-letter transliterations of the abbreviations as given in the original Russian journal. *Some or all of this periodical literature may well be available in English translation.* A complete list of the cover-to-cover English translations appears at the back of this issue.

DETERMINATION OF THE DISCHARGE AND RATE OF MOVEMENT OF WATER IN POROUS MEDIA BY MEANS OF RADIOACTIVE TRACERS

M. P. Volarovich, N. I. Il'in, and N. V. Churaev

Kalinin Peat Institute

Translated from Kolloidnyi Zhurnal, Vol. 23, No. 5,
pp. 524-527, September-October, 1961
Original article submitted March 23, 1961

The problem of determining the discharge and rate of movement of water in porous media, in particular, in peat, up to now has not been studied adequately. It appeared of interest to compare the results of determinations of discharge and rate of movement of water by methods developed previously with data from direct measurements by means of the apparatus depicted in Fig. 1. The glass tube 1 is charged with samples 2 of the test material, which is either lowland sedge-clay peat with degree of decomposition R = 35%, or 0.25-0.10 mm washed river sand. Spaces are maintained between the samples of material by means of Plexiglas filters; these spaces are the chambers 3, simulating wells in the ground. Samples for radiometric analysis are withdrawn from these chambers through the tubes 4 by the pipettes 5. The water level in the system can be regulated by the device 6 with the leveling flask 7, and the water discharge in the system can be regulated by the stopcock 8. The solution of radioactive tracer Na_2SO_4 in a quantity of 0.02-0.05 μ is introduced into the upstream chamber (primary) and is picked up in the downstream chamber (observation). The tracer concentration is measured by a T-25-BFL end-window counter in a B-2 unit by methods described previously [1].

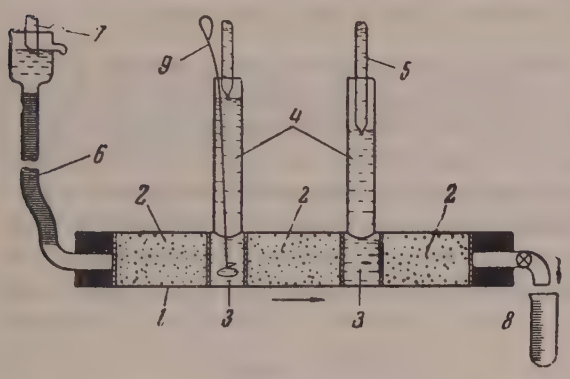


Fig. 1. Diagram of apparatus for checking methods of determining discharge of water in soil by means of radioactive tracers.

In conducting the experiments, the volume of samples withdrawn did not exceed 0.2 cm^3 (with a water volume in the chamber of 12-18 cm^3), in order to avoid variation of the water level in the chambers and the effect of additional removal of tracer. The water in the chambers was mixed by the stirrer 9, continuously when sand was in the tube 2, and once or twice a day when peat was in the tube 2. As demonstrated by the results of special investigations, this stirring ensured uniform distribution of the tracer in the chamber volume, which underlies the theory of the method [2].

As a result of the experiments, curves were obtained for the change in tracer concentration for the primary and observation chambers with various values of the water discharge in the system Q, which was measured volumetrically. The data obtained were compared for the primary chamber with the results of calculations according to a formula proposed previously [2].

$$Q_p = \frac{V_p}{\tau} \ln \frac{N_i}{N}, \quad (1)$$

where V_p is the water volume in the primary chamber; N_i is the initial radiotracer concentration in it; N is the tracer concentration at the end of time τ after the start of the experiment.

For calculating the water discharge on the basis of tracer concentration change in the observation chamber, no comprehensive recommendations were available [3]. Therefore, we will give a brief derivation of the computational formula propounded for these purposes.

The balance of change in radiotracer concentration (M) in the observation chamber for a time interval $d\tau$ can be written in the form

$$dMV_o = N\,dV - M\,dV, \tag{2}$$

where dMV_o is the change in total supply of tracer in the observation chamber (V_o is the water volume in it); NdV and MdV are, respectively, the quantity of tracer which entered from the primary chamber and which was taken out from the observation chamber. Taking into account the exponential law of concentration change of the tracer N in the primary chamber [2], the solution of Eq. (2) with Q constant has the form:

$$M = \frac{BN_i}{B - A}\left(e^{-At} - e^{-Bt}\right), \tag{3}$$

where $A = Q/V_p$, $B = Q/V_o$; t = time reading from the point where M = O.

With sufficiently high rates of movement of the water in the system, when the effect of diffusion can be neglected [4], the point t = O on the τ-axis determines the average rate of water movement and can be designated as τ_r. In Fig. 2 an experimental curve is shown for one of the experiments with sand and a theoretical curve calculated according to Eq. (3). The observed deviation of the experimental curve from the theoretical, which is most marked in the initial section (6-10 min), is related to nonuniformity of water movement rate in the sample pores [1].

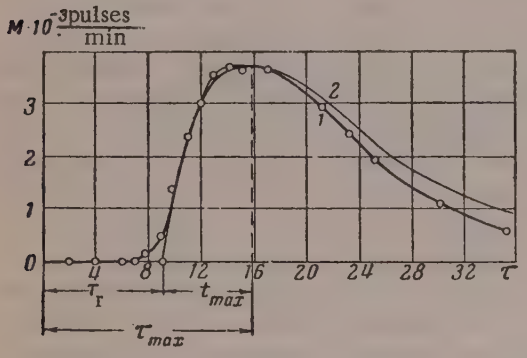


Fig. 2. Change in radiotracer concentration (M) with time (τ) with passage of the flow through the observation chamber: 1) Experimental data; 2) theoretical relationship plotted according to Eq. (3).

Analysis of the experimental data obtained, analogous to those shown in Fig. 2, for various samples, shows that the position of the point of maximum tracer concentration M in the observation chamber shows sufficiently good agreement for the experimental and theoretical curves. This circumstance permits calculating the value τ_r starting from the position of the point τ_{max} on the experimental curves. After simple transformations of Eq. (3), taking into account that

$$\tau_r = L/v^* = L\omega m/Q,$$

where ω is the cross-sectional area of the sample in the tube, m is the active porosity of the material, v^* is the actual water movement rate in its pores, and L is the distance between the walls of the chambers (length of sample), we obtain a formula for determining the water discharge through the sample

$$Q_o = \frac{L\omega m\,(V_p - V_o) + V_p V_o \ln V_p/V_o}{\tau_{max}\,(V_p - V_o)}, \tag{4}$$

which with $V_p \to V_o$ assumes the form

$$Q_o = \frac{L\omega m + V_p}{\tau_{max}}. \tag{5}$$

Utilizing expressions (4) and (5), it is not difficult to find the corresponding relationships for determining the actual water movement rate in the pores of the sample.

From the formulas obtained, it is evident that in comparison with the formula $v^* = L/\tau$ (which is generally accepted in hydrogeological investigations), the accounting for the exponential law of tracer concentration change in the primary chamber leads to the appearance of an additional term, the magnitude of which depends on the geometry of the experiment. The influence of this term is especially great in those cases in which the dimensions of the chamber are rather large in comparison with the distance L between them.

The results of experimental verification of the proposed formula are shown in the table, including the characteristics of the samples investigated and a comparison of the actual values of water discharge in the system Q_{meas} with the values calculated according to formulas (1) and (4), obtained on the basis of observations of the change in tracer concentration in the primary chamber Q_p and in the observation chamber Q_o. For each measurement, the relative errors δ_p and δ_o are computed.

Results of Comparison of Measured Water Discharges through Samples with the Values Calculated by Radiotracer Methods

Filtering medium	V_p cm³	V_o cm³	L, cm	τ_{max}, hr	Q_{meas}, cm³/hr	Q_p, cm³/hr	Q_o, cm³/hr	δ_p %	δ_o, %
Sand, 0.25-0.10 mm,									
m = 0.41	12,17	12,04	6,0	0,266	103	108	107	—5,2	—4,1
Same	12,47	12,58	14,0	0,584	85	80,5	88,1	+5,5	—3,5
Same	17,35	13,51	22,0	0,584	136	126	131	+7,5	+3,9
Peat, sedge-clay, R=35%,	18,0	12,9	6,4	28,0	1,28	1,37	1,34	—7,9	—5,5
m = 0.50	18,0	12,9	6,4	151,0	0,225	0,232	0,218	—3,1	+3,1
						Average deviation		5,8	4,0

In the calculations according to formulas (4) and (5) the values of active porosity of the sand, determined by methods set forth in [1], proved equal to m = 0.41; for the peat, according to the recommendations of [1, 2], it was assumed that m = 0.5.

From the table it is evident that the determination of discharge by the proposed methods proved to have a sufficiently high level of accuracy. At the same time, notwithstanding the considerable difference of rates and discharges in the sand and in the peat, no differences were observed in the values of the relative error δ for the experiments with the two materials. Thus, the relationships obtained are correct, in all probability, for all porous materials which do not absorb the radioactive tag.

SUMMARY

1. A procedure has been developed for experimental checking of methods of measuring the discharge of water in porous media by means of radioactive tracers in a model consisting of a filtration tube with chambers left between the samples, simulating wells in the ground. Sand and peat were tested as filter media.

2. Computational formulas have been obtained for determining water discharge in porous materials on the basis of observations during the passage of the tracer through the observation chamber.

3. The experimental verification of radiotracer methods for the primary and observation chambers showed that the relative error of measurement of water discharge by these methods does not exceed 4-6%.

LITERATURE CITED

1. M. P. Volarovich, N. V. Churaev, and B. Ya. Minkov, Kolloidn. zh. 19. 159, 1957; M.P. Volarovich, N. I. Gamayunov, Z. A. Starikova, and N. V. Churaev, Kolloidn. zh, 21, 257 (1959).
2. M. P. Volarovich and N. V. Churaev, Investigation of Peat Properties and Processes Taking Place in Peat by means of Radioactive Isotopes [in Russian] (USSR Acad. Sci. Press, Moscow, 1960).
3. G. N. Kamenskii, Principles of Underground Hydrodynamics [in Russian] (State Geological Literature Press, Moscow, 1943).
4. N. V. Churaev, Tr. Kalininskogo torfyanogo inst. [Transactions of Kalinin Peat Institute], No. 11 (1960).

EFFECT OF ELECTROLYTES ON CRITICAL MICELLE CONCENTRATION AND SOLUBILIZING CAPACITY OF SODIUM LAURATE SOLUTIONS

P. A. Demchenko

Institute of General and Inorganic Chemistry, Academy of Sciences, UkrSSR, Kiev
Translated from Kolloidnyi Zhurnal, Vol. 23, No. 5,
pp. 528-530, September-October, 1961
Original article submitted April 28, 1960

It is of practical value to study the various factors affecting the bulk properties of solubilized systems and the ratio of components in systems of soap–hydrocarbon–water and of emulsifier (solubilizer)–monomer–water [1]. No systematic investigations have been conducted in this area, and no study has been made of the effect of electrolytes on the critical micelle concentration (CMC) and solubilizing capacity of detergents of differing molecular weight, structure, and ionic properties.

In this article results are presented of an investigation of the effect of neutral electrolytes on the solubilization of hydrocarbons and the CMC in solutions of sodium laurate. The samples for the investigations were prepared by a method described previously [2].

The change in solubilizing capacity of sodium laurate solutions under the influence of electrolytes was determined volumetrically [3] (reproducibility of results ~ 3%). In the absence of electrolytes in a 0.1 M solution of sodium laurate, toluene and heptane are solubilized in amounts of 0.14 and 0.56 mole per mole of soap, respectively. The addition of increasing quantities of sodium chloride, nitrate, and sulfate to the 0.1 M sodium laurate solution causes a sharp increase in its solubilizing capacity for toluene and heptane (Fig. 1). For example, on adding 1.0 and 2.5 moles of sodium chloride, the solubilization of toluene and heptane increases by 1.3 and 1.8 times (toluene) and 1.7 and 3.1 times (heptane), respectively, in comparison with the solubilization in the absence of added electrolyte. With further increase of sodium chloride concentration the solubilization of the hydrocarbons increases less sharply (Fig. 1, curves 3 and 6). Sodium nitrate shows an analogous effect (Fig. 1, curves 2 and 5). A more marked increase in the solubilization of toluene and heptane is observed on the addition of sodium sulfate to the soap solution (Fig. 1, curves 1 and 4). The neutral electrolytes are arranged in the following order of capability of increasing solubilization of hydrocarbons in sodium laurate solutions: Sodium sulfate > sodium nitrate > sodium chloride.

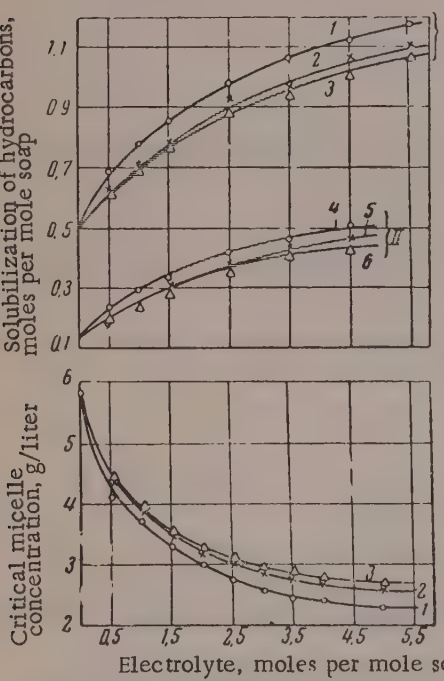


Fig. 1. Effect of electrolytes on solubilization of toluene (I) and heptane (II) in 0.1 M sodium laurate solution and on the critical micelle concentration of sodium laurate: 1,4) Na_2SO_4; 3,6) NaCl; 2,5) $NaNO_3$.

The effect of electrolytes on the CMC of sodium laurate was determined by titration. In an investigation of the CMC of saturated fatty acid soap homologs it had been established that sodium laurate in the absence of electrolytes and organic polar substances has a CMC equal to ~ 5.9 g/liter [4]. The addition of increasing quantities of sodium chloride, nitrate, and sulfate causes the formation of micellar structures at a lower soap content in the solution (Fig. 1); small quantities of these salts cause a sharper decrease of the sodium laurate CMC than does the further addition of large quantities.

In their capability of reducing the CMC, the electrolytes are arranged in the reverse order, i.e., antibatically, to their effect on the increased solubilizing capacity of sodium laurate (Fig. 2).

The observed reduction in CMC and increase in solubilization can be explained by a comparison of the balance of forces acting in the formation of micelles in solutions of surface-active substances [5]. The addition of electrolytes to a soap solution reduces the CMC sharply and shifts the equilibrium between the molecularly dispersed and the associated part of the molecules of the detergent toward the formation of micellar structures with more oleophilic properties. Antibatic change of CMC and solubilization of hydrocarbons is observed on increasing the length of the hydrocarbon chain in the homologous series of saturated fatty acid soaps [4]. Electrolytes exert an analogous influence on the properties of detergent solutions. On the basis of the change in CMC is has proven possible to calculate the ratio between the micellar and the molecularly dispersed part of the detergent in the solution and to establish the limiting concentrations of transition of the solution from a true solution to the colloidal state with various contents of electrolytes and other additives. The bulk colloid chemical properties of detergents can be changed not only by changing the length and structure of the hydrocarbon chains of the detergents [6,7], but also by the addition of electrolytes and polar compounds. The present investigation points out the possibility of regulating the lyophilic properties of micellar structures in the solution and the preparation of detergents with optimum bulk properties.

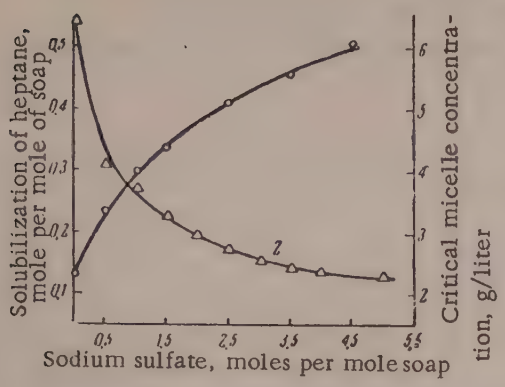


Fig. 2. Effect of sodium sulfate on solubilizing capacity (1) and critical micelle concentration (2) of sodium laurate.

SUMMARY

1. On the addition of increasing quantities of sodium chloride, nitrate, and sulfate to a sodium laurate solution, the critical micelle concentration (CMC) is decreased sharply, and the solubilizing capacity increases regularly.

2. Identical quantities of sodium sulfate cause a greater decrease in CMC and a sharper increase in solubilizing capacity of the soap solution, in comparison with equimolal quantities of sodium chloride or nitrate.

3. In the presence of electrolytes, more oleophilic micellar structures are formed; this is equivalent to lengthening the hydrocarbon chain of the soap.

4. It is suggested that by means of additions of various electrolytes and polar compounds, it is possible to regulate the colloid chemical properties of detergents.

LITERATURE CITED

1. P. A. Rebinder, Khim. nauka i prom. 4, 554 (1959); A. B. Taubman, Khim. nauka i prom. 4, 556 (1959); P. M. Khomikovskii, Uspekhi khimii 27, 1025 (1958).
2. A. V. Dumanskii and P. A. Demchenko, Dokl. AN SSSR 78, 277 (1951).
3. P. A. Demchenko, Masloboino-zhirovaya prom., No. 10, 22 (1959).
4. P. A. Demchenko, Masloboino-zhirovaya prom., No. 7, 36 (1959).
5. H. B. Klevens, Chem. Rev. 47, 1 (1950).
6. P. A. Demchenko, Reports of Proceedings, Colloid Chemistry Section of 8th Mendeleev Conference [in Russian] (USSR Acad. Sci. Press, Moscow, 1959), p. 111.
7. P. A. Demchenko and A. V. Dumanskii, Kolloidn. zh. 22, 272 (1960).

All abbreviations of periodicals in the above bibliography are letter-by-letter transliterations of the abbreviations as given in the original Russian journal. *Some or all of this periodical literature may well be available in English translation.* A complete list of the cover-to-cover English translations appears at the back of this issue.

EFFECT OF MOLECULAR WEIGHT OF SODIUM NAPHTHENATES AND SALTS OF SYNTHETIC FATTY ACIDS ON THE SOLUBILIZATION OF HYDROCARBONS

P. A. Demchenko

Institute of General and Inorganic Chemistry, Academy of Sciences,
UkrSSR, Kiev
Translated from Kolloidnyi Zhurnal, Vol. 23, No. 5,
pp. 531-534, September-October, 1961
Original article submitted June 30, 1960

In the alkali treatment of petroleum and in the technology of producing synthetic fatty acids, the soaps which are formed from the naphthenic and fatty acids carry into the aqueous phase a considerable quantity of hydrocarbons and other unsaponifiable contaminants, which entail great difficulty in their removal [1, 2, 3]. The factors affecting this process still have not been explained adequately, and no study has been made of the interdependence of the components in systems of soap–hydrocarbon–water and of soap–hydrocarbon–polar compound–electrolyte–water. This is hindering the development of effective methods of purifying soaps of naphthenic and synthetic fatty acids from the indicated contaminants.

In the present article results are presented from an investigation of the solubilization of hydrocarbons in 0.3 M solutions of sodium naphthenates of various molecular weights and of several soaps of saturated fatty acids. The samples for the investigation of sodium naphthenates were prepared from narrow fractions of pure naphthenic acids. Technical-grade naphthenic acids of the Baku deposit were first freed from dark-colored tarry contaminants by vacuum distillation. Then the distilled naphthenic acids were converted to the methyl esters by boiling with methanol in the presence of sulfuric acid. The resulting methyl naphthenates were washed with 1% sodium hydroxide solution for removal of phenolic compounds, and then separated into five fractions by vacuum distillation. The individual ester fractions were saponified by boiling with alkali. The soap solutions were diluted with methanol in 1 : 1 ratio and extracted several times with petroleum ether for removal of hydrocarbon impurities. Then the methanol and the colloidally dissolved petroleum ether were boiled off, and the soap was decomposed with sulfuric acid. The liberated naphthenic acids were washed, vacuum distilled, and used for preparing the naphthenic acid soaps. Neutralization of the naphthenic acids was accomplished with an equivalent quantity of alkali in alcoholic medium. The alcohol was distilled off, and the soap was vacuum dried at steam-bath temperature. The naphthenic acid soaps, free of contaminants and of moisture, proved to be solid clear substances with a weak characteristic odor.

We did not confirm the indications in the literature to the effect that the sodium soaps of naphthenic acids are greaselike [2]. The low molecular weight soaps have a white color and are readily pulverized. The soaps obtained from the narrow fractions of high molecular weight naphthenic acids have a light yellow color and a waxy consistency. The purified alkali soaps of naphthenic acids of various molecular weights are readily soluble in water, and over a wide range of concentrations form transparent, stable colloidal solutions, suitable for investigating their solubilizing capacity and other bulk properties.

The investigation of the solubilizing capacity of solutions of sodium naphthenates of various molecular weights was conducted by a direct method which gives good reproducibility of the experiments [3]. The experimental data are shown in Fig. 1. From these data it follows that the solubilization of hydrocarbons increases with an increase in molecular weight of the naphthenic acids. On addition of small portions of toluene, styrene, heptane, and isooctane to micellar solutions of the soaps, their solubilization is not accompanied by any significant change in transparency of the solutions. The formation of emulsion is observed after reaching the hydrocarbon solubilization limit.

In capacity for being solubilized in sodium naphthenate solutions of various molecular weights, the hydrocarbons examined are arranged in the order toluene > styrene > heptane > isooctane. The low molecular weight homologs (164-192 and below) have no solubilizing capacity, which points out the absence of micellar structures in the solution.

This value of molecular weight of the naphthenates can be termed critical. In the critical region the energy of attraction with respect to the hydrocarbon radicals is close in magnitude to the forces of repulsion of the similarly charged hydrophilic groups. With an increase in molecular weight of the sodium naphthenates above the critical value, the energy of bonding with respect to the hydrocarbon radicals begins to predominate, which leads to the formation of micellar structures. Thereby the bulk properties of the soap solutions are changed, and there appears the solubilization effect for hydrocarbons and polar substances.

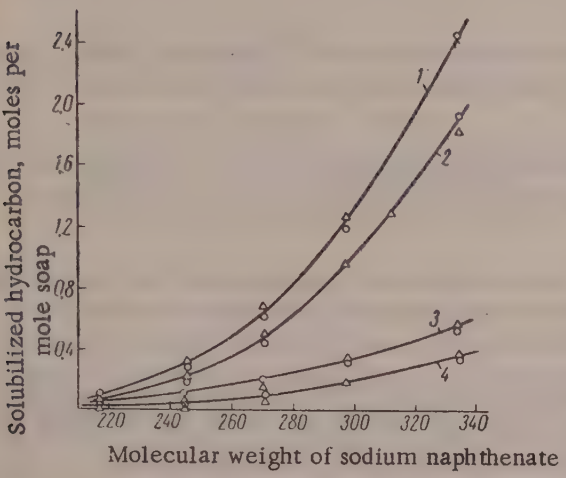


Fig. 1. Effect of molecular weight of sodium soaps of naphthenic acids on solubilization of toluene (1), styrene (2), heptane (3), and isooctane (4): Experimental and calculated points based on formula.

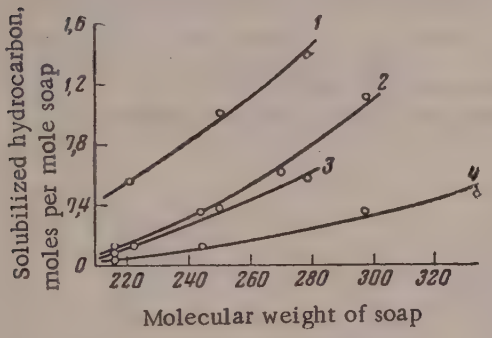


Fig. 2. Comparative solubilizing capacity of 0.3 M solutions of sodium soaps of naphthenic and synthetic fatty acids: 1) Toluene and 3) pentane in solutions of fatty acid soaps; 2) toluene and 4) heptane in solutions of sodium naphthenates.

If the critical value of sodium naphthenate molecular weight is deducted from the molecular weight of the homolog under consideration, we obtain a value defining the oleophilicity of the micellar structures and the solubilizing capacity of the solution. Using the relationships found, one can compute the solubilization of hydrocarbons in soap solutions (L, moles per mole of soap) according to the formula:

$$L = K (M - M_{cr})^2,$$

where K is a constant which accounts for the nature and concentration of the soap and the structure of the hydrocarbon being solubilized (in the solubilization of toluene, styrene, heptane, and isooctane in 0.3 M sodium naphthenate solutions, K is respectively $1.2 \cdot 10^{-4}$, $9 \cdot 10^{-5}$, $3 \cdot 10^{-5}$ and $2 \cdot 10^{-5}$); M is the molecular weight of the soap forming the colloidal solution; M_{cr} is the critical value of sodium naphthenate molecular weight, equal to 192.

The solubilization effects computed from this empirical formula for toluene, styrene, heptane, and isooctane in 0.3 M solutions of sodium naphthenates of various molecular weights agree closely with the experimental data which were obtained (Fig. 1).

It had been shown previously that the bulk properties of detergent solutions depend on the structure of their hydrocarbon radicals [4]. In the present work, new experimental data are cited, supplementing this concept. In Fig. 2 comparative data are shown for the solubilizing capacity of solutions of sodium soaps of naphthenic acids and sodium soaps of synthetic fatty acids with respect to toluene and heptane. The purification of the synthetic fatty acids and the preparation of the soap samples for the investigation was carried out by a method described previously [3]. From the course of the curves in Fig. 2 it follows that the fatty acid soaps, which have a chain-like radical, have a greater solubilizing capacity than the naphthenates of similar molecular weight. The solubilization is affected not only by the molecular weight and structure of the soap radicals, but also by the structure of the hydrocarbons being solubilized (Figs. 1 and 2). In the detergent solutions investigated, the aromatic hydrocarbons are solubilized in greater amounts than the aliphatic hydrocarbons. The micellar structures of the soaps studied have a smaller effective volume for the solubilization of aliphatic hydrocarbons. This phenomenon is explained, apparently, by the fact that the aromatic hydrocarbons on solubilization are located not only between the ends of the hydrocarbon radicals of the soaps associated in the micelles [in the micelle interior] [5], but also in the lateral space between the hydrocarbon radicals.

The partial pressure of solubilized hydrocarbons is considerably lower than when emulsified in an aqueous medium, which indicates the establishment of a close bond between the soap and the hydrocarbon in soap–hydrocarbon–water systems. The quantitative difference of solubilization depends on the energy of the bond of the hydrocarbons

with the soaps [6]. An analogous relationship was observed for chlorinated hydrocarbons on solubilizing them in solutions of saturated fatty acid soaps [7], and for o-xylene, octane, and synthine in solutions of synthetic fatty acid soaps [3].

Solubilization effects may be utilized for the comparative characterization of the lyophilic properties of detergents and the micellar structures formed from them in various concentration regions and in the presence of added electrolytes and polar substances.

SUMMARY

1. The solubilization of toluene, styrene, heptane, and isooctane has been studied in solutions of sodium soaps of naphthenic and fatty acids. It has been shown that the low molecular weight homologs of the soaps do not form micellar solutions and do not have any solubilizing capacity.

2. An increase of molecular weight of the sodium naphthenates above the critical value is accompanied by an increase in the oleophilicity of the micellar structures formed and an increase in the solubilizing capacity of their solutions.

3. Aromatic hydrocarbons and styrene are solubilized in the soap solutions to a greater extent than are aliphatic hydrocarbons. The hydrocarbons are arranged in order of capacity for being solubilized: Toluene > styrene > heptane > isooctane.

4. An investigation was made of the comparative solubilizing capacity of 0.3 M solutions of sodium laurate, myristate, and palmitate and of sodium naphthenates with respect to toluene and heptane. It was shown that the fatty acid soaps are more effective solubilizers than the sodium naphthenates with similar molecular weights.

LITERATURE CITED

1. L. G. Gurvich, "Scientific Principles of Petroleum Processing" [in Russian] (State Tech. and Theor. Literature Press, Moscow, 1940).
2. B. M. Rybak, "Naphthenic Acids" [in Russian] (State Tech. and Theor. Literature Press, 1948).
3. P. A. Demchenko, Masloboino-zhirovaya prom., No. 10, 22 (1959); No. 7, 36 (1959).
4. P. A. Demchenko, Theses of Proceedings of Fourth All-Union Conference on Colloid Chemistry [in Russian] (USSR Acad. of Sci. Press, Moscow, 1958), p. 255.
5. H. B. Klevens, Chem. Rev. 47, 1 (1950).
6. P. A. Demchenko, A. V. Dumanskii, and L. G. Demchenko, Kolloidn. zh. 14, 164 (1952).
7. P. A. Demchenko, Doklady Akademii Nauk URSR, No. 5, 494 (1959); Ukr. khim. zh. 24, 746 (1959).

All abbreviations of periodicals in the above bibliography are letter-by-letter transliterations of the abbreviations as given in the original Russian journal. *Some or all of this periodical literature may well be available in English translation.* A complete list of the cover-to-cover English translations appears at the back of this issue.

DISJOINING PRESSURE OF ELECTROLYTE SOLUTIONS ON POLARIZED MERCURY

B. V. Deryagin, A. V. Gorodetskaya, A. S. Titievskaya, and V. N. Yashin

Institute of Physical Chemistry of the Academy of Sciences, USSR, Surface Phenomenal Laboratory, Moscow

Translated from Kolloidnyi Zhurnal, Vol. 23, No. 5. pp. 535-543, September-October, 1961
Original article submitted February 25, 1960

Studies on the behavior of thin wetting films, formed by pressing a bubble onto the flat surface of a solid body (for example, glass), have made it possible to establish the existence of an equilibrium disjoining pressure [1], and to study its functional relationship with equilibrium thickness of the film, i.e. the isotherm of the equation of state of the thin layer. Here, in the study of the equation of state of thin films of aqueous solutions of electrolytes, a functional dependence on the concentration was observed, which can be interpreted from a consideration of the repulsive forces between the film surfaces arising from deformation of an ionic double layer located near the solvent wall.

However, a complete check of the theory was rendered difficult by the fact that the surface charge was unknown and could not be changed at will. In this respect, great advantages would be presented in the case of a film which wets the surface of a liquid metal, for example, mercury. Here, by polarizing the surface of the mercury it would be possible to change its potential and charge, the latter being calculated from Lipman's equation. However, with a liquid substratum the surface of the wetting film under the drop would not remain plane, which would make it difficult to get an accurate measurement of its thickness by optical methods. This difficulty can be overcome by replacing the liquid metal by a solid with a plane surface, but here it would be hard to measure the charge on the surface and to keep the surface clean.

We decided to conduct the study on a thin liquid film, pressed between a plane glass surface and a mercury meniscus.*

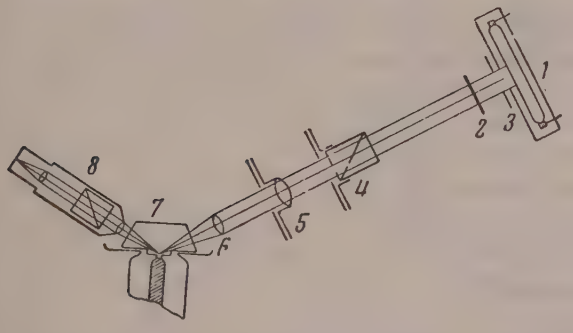


Fig. 1. Optical diagram of the method for measuring the thickness of the film between mercury and glass.

Technique of measurement. To measure the disjoining pressure isotherm of electrolyte solutions on polarized mercury over a wide range of pressures, it did not seem convenient to use optical interference methods for determining the thickness of the films as we had done previously, since the films were often thicker than 100 mμ, and the light intensity reflected from the film did not reach to the first minimum over the whole visible part of the spectrum. For this purpose we used an optical micro-polarization method.

The diagram of the optical part of the apparatus is given in Fig. 1.

The light from a monochromatic source (the 5461 A line from the mercury lamp 1, filtered by the neodymium, yellow and blue-green glasses 2) passes through the slit 3, the polarizer 4, the plate 5, and the lens 6, which focuses an image of the slit on the object (the film) through the prism 7. The beam reflected from the film passes through a polarizing miscroscope, in which the analyzer is fastened

* A study of the adhesion phenomena of mercury to glass in the presence of an intermediate layer of an aqueous solution of an electrolyte was made in [2] but without measuring the equilibrium thickness of the layer.

at an angle of 45° to the point of incidence. The polarizer 4, and the plate 5, are provided with vernier degree circles, on which their angular rotation may be measured with an accuracy of 3'.

The plane-polarized light from the polarizer passes through the plate 5. The light leaves the plate elliptically polarized, since, with a path difference equal to $\pi/2$, the light oscillation follows around an ellipse, and the ratio between the semi-axes of the ellipse depends on the angle of rotation between the polarizer and the axis of the plate 5. Here the axes of the ellipse are parallel to the axes of the plate 5. As was stated above, the light from the plate 5 is focused on the film between the glass and the mercury, which is what we want to measure.

The light reflected from this plane will also in general be elliptically polarized, but for the particular setting 5, at which on reflection, the phase difference of the components of the light polarized in, and perpendicular to, the plance of incidence is reduced to 0 or 180°, the light reflected from the film will be plane polarized, and if the direction of vibration of the reflected light and analyzer are mutually perpendicular, the light will be extinguished by the analyzer. Different angular settings of the plane 5 and the polarizer 4 make it possible to fulfill this second condition. Knowing the angular settings of the polarizer 4 and the plane 5, it is possible to find both the phase shift, and the ratio of the reflection coefficients of the two components of the light reflected from the film.

The polarized light was incident and reflected at an angle of 60° on the plane of the film. To prevent the ray reflected from the glass surface from falling on the analyzer, a special trapezoidal prism (7), with a 60° angle at the lower edge and with a horizontal polished surface, having underneath a disc form projection "five-cent piece" for pressing onto the convex mercury meniscus. The "five-cent piece" on the prism is 14 mm in diameter, and its flat boundary is polished to an accuracy of 0.1 interference fringe. The prism is pressed down from above by a lever, which was fastened to a micromanipulator (the lever is not shown in Figs. 1 and 2).

By means of the micromanipulator the prism could be moved in a horizontal direction. The maximum possible displacement of the prism from the center was 5 mm, which was sufficient to change, if necessary, the place where the mercury meniscus is pressed onto the prism.

Our aim was to study the disjoining action of electrolytes on polarized mercury, both as a function of pressure at constant potential, and as a function of potential at constant pressure. With this aim in mind, we constructed a special glass apparatus (Fig. 2).

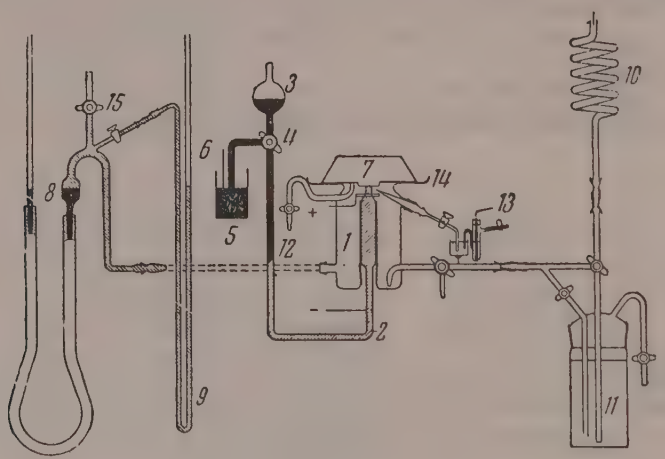


Fig. 2. Diagram of apparatus.

Description of Apparatus. The apparatus consists of a central vessel 1 into which the test solution was poured. Into a ground cylindrical tube in this vessel was fastened the tube 2, filled with mercury. The end of the tube which is in the vessel is terminated by a 1.4 mm diameter capillary. The mercury meniscus in the capillary, in contact with the solution, was pressed onto the lower polished surface of the "five-cent piece" of the prism 7. By means of the cylindrical ground glass tube the mercury meniscus could be moved up and pressed on the glass. The tube 2 was filled with mercury from the reservoir 3 by means of the three way cock 4. The mercury in the vessel 5 served to keep the meniscus at the desired level, this level being fixed by the platinum needle 6. The required pressure in the vessel 1 was produced and measured by means of the mercury manometer 8, which served to produce and measure

large pressures, while for the measurement of small pressures the water manometer 9 was used [3]. Hydrogen was admitted through the glass spiral 10 and the vessel 11. The hydrogen was prepared by electrolysis and purified by the usual method of passing it through heated platinized asbestos and an alkaline solution of plumbite. The hydrogen was drawn from the apparatus through tube 12.

The cathode polarization of the mercury meniscus was accomplished by means of a platinum contact (minus sign, Fig. 2), sealed into the tube 2. The anode was a wide platinum ring, sealed into the vessel (plus sign, Fig. 2).

To achieve small mercury meniscus pressures inside the tube 2, a small ring of platinum foil 1.4 mm in diameter, was placed near the mouth of the capillary end, and then after cathode polarization the ring was well wetted with mercury, giving a flat meniscus. The voltage for polarizing the mercury was taken from a storage battery and was adjusted by means of a rheostat. The mercury potential was measured by a null method against a standard calomel electrode 13 (Fig. 2). The end of the siphon 14 was placed close to the mercury surface. A galvanometer with a sensitivity of 10-8 amp was used as a null indicator.

Measurement procedure. Before the measurement all the parts of the apparatus were stored in a chromic acid mixture for not less than 20-22 hours, after which they were washed in running water for not less than 30-40 minutes. They were then washed with distilled water, and, finally, with doubly distilled water. A freshly prepared solution of the necessary concentration was added to vessel 11 (Fig. 2). To remove traces of oxygen from the solution, hydrogen from an electrolysis apparatus was drawn into vessel 11 through spiral 10 for 20-24 hours. After this, the whole apparatus was washed with hydrogen for several hours. From vessel 11, the solution was pumped into vessel 1. The hydrogen, which filled the whole system, flowed out through the exit tube 12 (Fig. 2).

Before measuring the film thickness, the cathode polarization (minus 0.8–1 v) was put on the mercury for 30 minutes to provide some additional cleaning of the mercury meniscus from traces of oxides and other impurities which might possibly be on it. Then the end of the capillary was brought up to the horizontal surface of the prism 7, in such a way, that the mercury meniscus just barely touched it. The position of the water meniscus and the manometer 9 then corresponded with no mercury pressure. The level of mercury in the beaker 5 was fixed, as has been said above, by the platinum needle 6. Now, the moveable scales were brought up to the mercury and water levels in the manometers 8 and 9 with the apparatus at zero pressure. The thickness of the electrolyte film between the glass and the mercury meniscus was measured with no mercury pressure. For this purpose, readings were taken of the settings of the polarizer 4 in the plate 5 (Fig. 1) at which the light reflected from the film is completely extinguished. Then the pressure in the vessel 1 was lowered by dropping the moveable mercury column in the manometer 8, which gave a corresponding increase in the capillary pressure of the mercury meniscus, which was in equilibrium with the disjoining pressure of the electrolyte film, and by these procedures the thickness of the film was determined which corresponded with a given increased pressure.

The capillary pressure of the mercury meniscus on the film is determined, for small pressures, by the change in liquid level in the water manometer 9 before and after applying pressure. At high pressures, the cock 15 was closed, and the pressure of the mercury meniscus was fixed by lowering the mercury in the lefthand moveable column of the manometer 8. While measuring the thickness of the film as a function of the polarization, the pressure was kept constant. In measuring the metallic reflection constant of light, at the mercury–glass boundary with no electrolyte, the clean apparatus was dried in a current of clean dry hydrogen, and the measurements made in these experiments were also taken in a stream of hydrogen.

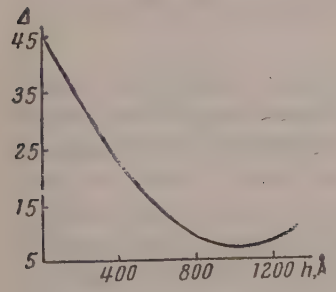


Fig. 3. Phase shift Δ when light is reflected from a film of thickness h.

As the electrolyte, we used Na_2SO_4 (Anal.) solutions of various concentration. The salt was recrystallized and before the measurement it was baked. The solvent used was doubly distilled water.

Calculations. In calculating the thicknesses of the films on the mercury, it was necessary to know the index of refraction of the film and the optical constants of the mercury. We determined the indices of refraction of the test solutions using an Abbe refractometer with an hemisphere for $\lambda = 5461$ A.

The optical constants of the mercury, i.e., the index of refraction and the absorption coefficient of the mercury for the same wave length, were taken from the paper by Tronstad [4] who had made measurements for angles of incidence from 36° to 85° 30'.

In our case, the light emerged from glass with an index of refraction $n_o = 1.516$, and was incident on the mercury. The angle of incidence of the light from the glass onto the mercury was $\varphi = 60°$ ($n_o \sin\varphi = 1.3129$). The optical constants of the metal, n and k, were recalculated for these conditions, and a calculation was made of the phase shift between the components of the light factor, parallel and perpendicular to the plane of incidence, reflected from the mercury covered by the film. The method of recalculating the constants is given in a paper by Vasicek [5]. Taking different values of film thickness, we calculated the phase shift and constructed the graph (Fig. 3) showing the phase shift Δ as a function of the thickness of the film between the glass and the mercury h. Then, using the graph in reverse we found the film thicknesses from the measured values of the phase differences.

Results of measurements. Measurements were made on the thickness of films of 1, 10^{-1}, 10^{-2}, and 10^{-3} N aqueous solutions of Na_2SO_4 as a function of pressure and polarization. In the pressure measurement, as well as in the potential measurement, an equilibrium thickness of the film was allowed to establish itself for 10-15 minutes, and sometimes longer. As a check, in each individual case, we took several angular ratings on the polarizer 4 and the plate 5 (Fig. 1) at short intervals, and compared them. If the readings changed systematically in a definite order (monotonic increasing or decreasing), this showed that equilibrium had not been established in the film, and that it was necessary to wait awhile longer before the final equilibrium thickness of the film was established. After equilibrium had been established, we made 6-8 measurements of angle on the polarizer 4 and the plate 5, giving complete extinction of the light reflected from the film, and took the main value.

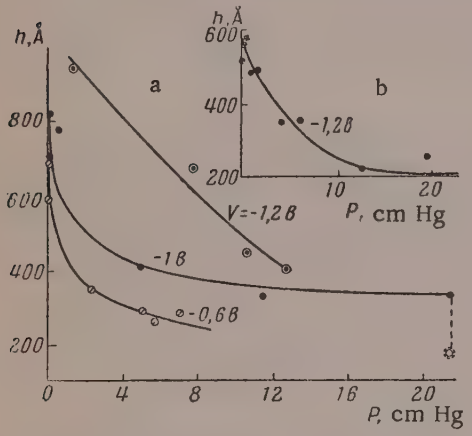


Fig. 4. Film thicknesses of 10^{-3} N (a) and 10^{-2} N (b) aqueous solutions of Na_2SO_4 as a function of disjoining pressure at different polarizations, V.

The pressure of the mercury on the film was changed from 0 to ~ 20 cm Hg. Figures 4 and 5 give the results of the measurements of film thickness as a function of pressure for different Na_2SO_4 concentrations. For all Na_2SO_4 concentrations a considerable attenuation of the film was observed with increasing pressure. In the 10^{-3} N Na_2SO_4 solution (Fig. 4a) at different polarization potentials and an increase in pressure up to 21 cm Hg, the thickness of the film was attentuated from the order of 800 A down to about 300 A but here it became very unstable, and was easily broken. After it was broken (Fig. 4a, polarization -1 volt, pressure 21 cm mercury) a film remained with the thickness of 180 A. In the more concentrated solutions (Fig. 4b and 5) the thickness of the film was initially 400-600 A, but when the pressure was increased to 20 cm mercury, the film was attentuated and compressed down to almost 200 A. It was not possible to produce higher pressures because the joints in the apparatus were not tight.

In the 10^{-1} N solution of Na_2SO_4 (Fig. 5) a measurement was made on the thickness of the film and the process of letting the pressure back down from 12 cm mercury to 0. Here the initial thickness of the film was 550 A, but after increasing the pressure to 12 cm mercury (curve 1) and subsequently reducing the pressure from 12 cm mercury to ~ 0 (curve 2), the thickness of the film reached a value of 320 A, in other words the disjoining pressure isotherm showed hysteresis.

In measuring the film thicknesses of the function of polarization, the polarization was changed in 0.1 volt steps from −1.46 to 0.3 volts (measured against a calomel half-cell). Near the point of zero charge on the mercury (−0.48 volt), the polarization was changed in 0.05 volt steps. The results of the measurement of film thickness as a function of mercury polarization for different electrolyte concentrations are given in Fig. 6 and 7, where the abscissas are the mercury potential measured against a standard calomel electrode, and the ordinates are the film thicknesses in A. Fig. 7 gives the measurements at the lowest pressure (small compression), equal to 2 cm water (curve one), at a pressure of 10 cm mercury (curve two), and at 12 cm mercury (curve three). The general form of the curve of film thickness against mercury potential is the same for all concentrations of the solution. At a potential close to the point of zero charge on the mercury (but, apparently, not coincident with it), the film thickness goes through a sharp minimum, near which the film becomes extremely unstable and inclined (from observations under a microscope) to break.

In 10^{-3} N solution, after the film breaks, there remains an intermediate liquid layer with a thickness of ~140 A, which does not change with further change in the potential from + 0.2 to −1.0 volt (Fig. 6, curve 1). At an anode

polarization of + 0.5 volt, the thickness of the "residual" layer is reduced to 50-80 A. In the more concentrated solutions breakdown of the film usually does not occur, but in the range near zero charge, the film is noticeably attentuated (for example for 1 Nsolution at low pressure, on changing the potential from −0.80 to −0.55 volts the thickness changes from 800 to 550 A, Fig. 7, curve 1).

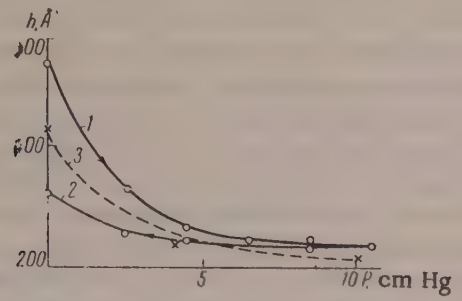


Fig. 5. Film thickness of 10^{-1}N (1,2) and 1 N (3) aqueous solutions of Na_2SO_4, as a function of disjoining pressure at the polarizations −1 volt (1, 2) and 0.7 volt (3).

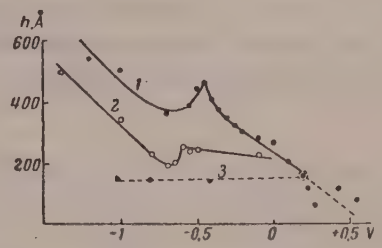


Fig. 6. Film thicknesses of 10^{-3}N (1) and 10^{-1}N (2) aqueous solutions of Na_2SO_4 as a function of the polarization V.

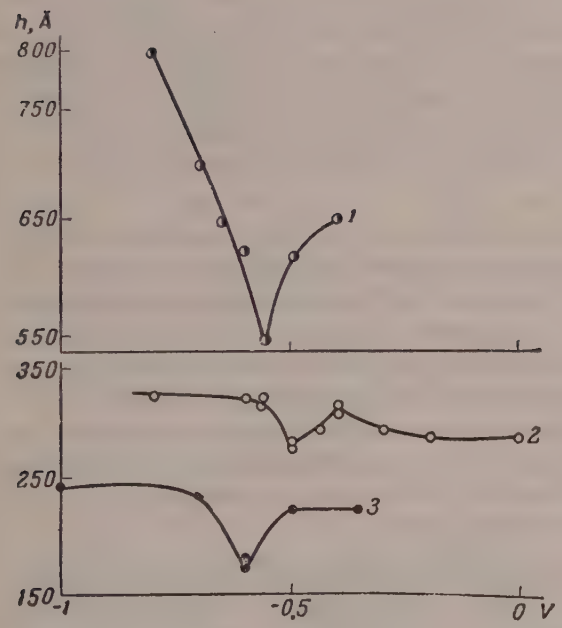


Fig. 7. Film thicknesses of a 1N aqueous solution of Na_2SO_4 as a function of the polarization V, at disjoining pressures P (cm mercury): 1 −< 1: 2−10: 3−12.

It may be seen from Fig. 8, that the film thickness at all polarizations is the minimum for the 10^{-1}N Na_2SO_4 solution. This minimum thickness increases as the cathode potential is increased. In 1N solution the film thickness is only slightly dependent on the polarization, and is greater for all polarizations, than in 10^{-1}N solutions [6].

The results obtained show that equilibrium film thicknesses of water solutions exist for essentially unsymmetric mercury−film−glass conditions. The equilibrium film thickness (h) is a function of the capillary pressure acting on it, which comes to equilibrium with the disjoining pressure of the film (P). The curves h = h (P) thus represent disjoining pressure isotherms. A special feature of the object studied in the technique used, is that it is possible to study the disjoining pressure isotherm as a function not only of the electrolyte concentration, but of the potential as well, and consequently of the charge on the film−mercury interface.

In the general case the equilibrium disjoining pressure may be set equal to the sum of three terms

$$P = P_A + P_E + P_S,$$

where P_A is a term depending upon the balance between the forces of interaction between the molecules [7] of mercury [1], glass [2], and water [3]. P_E is a term depending on the interaction arising from the overlap of the ionic atmospheres formed at the surfaces of the mercury and glass [8]. P_S is a term arising from the formation of polymolecular hydrated layers on the hydrophil glass surface (boundary phase) [9]. In contrast to the first two terms, there is not only no quantitative theory of the last component of the disjoining pressure, but even the mechanism of how it arises has not been studied. There are, however, strong indications that it is caused by structural changes in the boundary layers of water [10], as compared with the volume properties of water.

The existence of such hydrated boundary layers is supported by the fact, that at no electrolyte concentration or at no value of mercury polarization, does the thickness of the equilibrium water layer fall below 120-130 A (with

the exception of polarizations greater than +0.25 volts with 10^{-3}N Na_2SO_4 solutions, see Fig. 6, curve 1), even at the potential corresponding with zero charge on the mercury, and at concentration so high that the double layer is known to be no longer diffused. Here, even in concentrated solutions, the equilibrium layer thickness increases substantially as the pressure is reduced (Fig. 5). Hence, it is clear that the deductions of the quantitative theory based on the terms P_A and P_E alone is capable of only a partial representation of the experimental results which we have obtained.

The theory leads first of all to the conclusion, that the equilibrium film thickness must decrease systematically with increase in the pressure, P, while at equal pressures it must decrease according to a definite law as the electrolyte concentration is increased. This conclusion is justified at concentrations less than 10^{-1}N (Fig. 8). The concentration 10^{-1}N corresponds with the minimum thickness, and the fact that this thickness is different from zero can only be interpreted in terms of P_S, which is the term containing the disjoining pressure. The increase in equilibrium thicknesses with further interpretation (Fig. 8) shows that the term P_S is affected by the added electrolyte, in any case in the concentrated solution region.

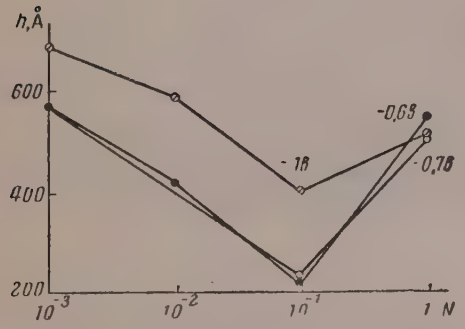


Fig. 8. Film thicknesses as a function of molar concentration (N) at various polarizations (V).

The relation between the film thickness and the polarization does not fit very well into the usual electrostatic ideas on the subject (Fig. 6 and 7). According to the theory of the interaction between two surfaces of unlike charge, [11] (assuming the term P_A small in comparison with the term P_E, which, apparently, is true for h > 200 A), as the potential is of one surface is changed (in our case the mercury), for P_E,= const, the layer of thickness should fall off monotonically as the potential approaches the isoelectric point. If, after going through the isoelectric point, the potentials of the two surfaces become of opposite sign, the electrical interaction for any thicknesses will change from repulsive to attractive (see Ref. [11] Figs. 3 and 3a). But this conclusion is not even in qualitative agreement with the solid curve 1 of Fig. 6.

In the region of the point where the charge on the mercury is zero (V ≈ − 0.5 volt) there is a thickness minimum, although not a very deep one. A minimum of this sort might be explained in a way similar to the theory of the interaction of diffuse ionic layers in wetting films [12], if it is assumed, that the surface charge on the glass is always equal to zero. However, this is counteracted by the behavior of curve 1 of Fig. 6 to the right of the sharp maximum located at V = − 0.48 volt. Thus, the picture as a whole fails to agree either with the assumption of constant potential, or with the assumption that the charge on the glass is equal to zero. It is possible to assume some sort of intermediate boundary condition on the glass surface, however, the quite similar form of curve 2 Fig. 8, for the concentrations of 10^{-1}N, when the ionic double layer is compressed as far as possible, makes it more natural to try to explain the relation between the thickness of the water layer and the polarization not merely in terms of the term P_E but, above all, in terms of the properties of the hydrated boundary layers.

The fact that these layers are there, along with their properties, shows up exceedingly clearly in the "breakdown" phenomena of water films which lead to the formation of a layer, whose thickness is completely independent on the polarization of the mercury, as is shown by the dotted curve of Fig. 6 (see also Fig. 4a, the low point on the right). This shows that the term P_S is independent of the surface charge, although it depends on the electrolyte concentration. This last conclusion as well as the relation between the thickness and the electrolyte concentration itself agrees with the results obtained from the method of crossed metal filaments [6].

Finally, the properties of the hydrated boundary film are obviously the cause of the hysteresis (double valuedness) of the film thickness (Fig. 4a, Fig. 5, curves 1 and 2, Fig. 6 curve 1) and the associated instability of films with a thickness somewhat greater than the thickness of the boundary layers (200 A) explains [13] the edge angle at the glass−mercury−aqueous solution boundary [2], formed after certain jump−attenuation of the film.

SUMMARY

1. A method has been worked out which makes it possible to make a simultaneous measurement of the equilibrium thickness and the disjoining pressure of a water film between a plane optical glass surface and a mercury meniscus, the potential of which is varied by a polarizing current.

2. The equilibrium thickness of films of aqueous solutions of Na_2SO_4 falls within increasing disjoining pressure for all electrolyte concentrations from 10^{-3}N to 1 N.

3. The equilibrium film thickness for all Na_2SO_4 concentrations depends in a similar way on the potential. A sharp minimum is observed near the point of zero charge on the mercury. And a concentration of 10^{-3}N, the film is only slightly stable at high pressures or near the zero charge point. It easily undergoes a jump type attentuation to a thickness of 140 A, which does not change if the potential is subsequently changed from + 0.2 to -1.0 volts. If the concentration of the solution is increased, the instability of the film disappears.

4. If the concentration of the Na_2SO_4 solution is increased, the thickness of the film decreases for all polarizations, going through a minimum at 10^{-1}N, and then increasing.

5. The results obtained admit of only a partial qualitative explanation at low electrolyte concentrations in terms of the action of the electrostatic and Van der Walls forces. If the sum total of the facts is to be explained, account must be taken of forces of another sort, apparently involving the ability of the hydrophilic glass surface to form hydrated boundary layers, with a special structure $\sim 10^{-6}$ cm thick.

The authors express their gratitude to Academician A. N. Frumkin for comments and discussion of the results, and to Z. M. Zorin for valuable advice and aid in calculating the film thicknesses.

LITERATURE CITED

1. B. V. Deryagin, M. M. Kusakov, Izv. AN SSSR, Otd. Khim n 1937, No. 5, 1119; Acta Phys. Chim. URSS 10, 25, 1939; 10, 153, 1938; B. V. Deryagin, M. M. Kusakov and L. S. Lebedeva Dokl. AN SSSR. M. M. Kusakov, A. S. Titievskaya, Ibid, 83, No. 4, 1940.
2. A. V. Gorodetskaya, A. N. Frumkin, and A. S. Titievskaya, Zh. Fiz khimii, 21, 675 (1947).
3. B. V. Deryagin and A. S. Titievskaya, Kolloidn, Zh. 15, 416 (1953); Disc. Faraday Soc., No. 18, 24 (1954); Proc. of the II Congress of Surface Activity, Vol. 1, p. 211 (1957); Dokl. AN SSSR 89, 2041 (1952).
4. L. Tronstad, Proc. Roy. Soc. 145, 115 (1934).
5. Vasicek, Optika tenkych vrstev, Praha, 1955.
6. T. N. Voropaeva, B. V. Deryagin, and B. N. Kabanov, Dokl. AN SSSR, 128, 981, 37, 229 (1959).
7. I. E. Dzyaloshinskii, E. M. Lifshits, and L. P. Pitaevskii, Zh. Eksperim. i Teor fiz, 1959.
8. B. V. Deryagin, Izv. AN SSSR, Seriya, Khim n, 1937, No. 5, 1153; Acta Phys. Chim. URSS 10, 333, 1939; Trans. Faraday Soc. 36, 1, 203, 1940; 36, 11, 730, 1940; Kolloidn. Zh. 6, 291, 1940, 7, 285, 1941, B. V. Deryagin, L. D. Landau, JETP, 2, 802, 1941, 15, 662, 1945; Acta Phys. Chim. URSS, 14, 633, 1941; B. V. Deryagin, V. G. Levich, Dokl. AN SSSR 98, No. 6, 1954, B. V. Deryagin, Kolloidn. Zh. 16, 425, 1954; Disc. Faraday Soc. No. 18, 95, 1954.
9. B. V. Deryagin, Transactions of the all-union conference on colloid chemistry [in Russian], 1952 Kiev, p. 26.
10. B. V. Deryagin, Z. S. Zorin, V. V. Karasev, Transactions of the conference on the nature of the liquid state [in Russian] Kiev, Academy of Sciences Press, USSR, 1954, collection of memoirs of academician P. P. Lazarev [in Russian], Moscow Academy of Sciences Press, USSR, 1956, p. 65, B. V. Deryagin, Z. M. Zorin, Dokl. AN SSSR 98, 93, 1954, Zh. Fiz khimii, 29, 1010, 1755, 1955; Trans. of the Congr. Surface Activ., Vol. 2, 1957, p. 145; Everett, Disc. remark, Ibid, p. 244; B. V. Deryagin, V. P. Karasev, Ibid, 3, 531, Dokl. AN SSSR, 62, 761, 1948, 101, 289, 1955, Kolloidn. Zh. 15, 365, 1953.
11. B. V. Deryagin, Kolloidn, Zh. 16, 425, 1954; Disc. Faraday Soc., No. 18, 85, 1954.
12. A. N. Frumkin, A. V. Gorodetskaya, Acta phys. Chim. URSS 9, 357, 1938.
13. A. N. Frumkin, Zh. Fiz khimii, 12, 337, 1938.

All abbreviations of periodicals in the above bibliography are letter-by-letter transliterations of the abbreviations as given in the original Russian journal. *Some or all of this periodical literature may well be available in English translation.* A complete list of the cover-to-cover English translations appears at the back of this issue.

ADHESION OF POWDER PARTICLES TO PLANE SURFACES

B. V. Deryagin and A. D. Zimon

Moscow

Translated from Kolloidnyi Zhurnal, Vol. 23, No. 5,
pp. 544-552, September-October, 1961
Original article submitted February 9, 1961

The adhesion of particles of powdered substances to solid surfaces is a matter of great theoretical and practical importance.

Thermodynamic theory [1] considers the adhesion of convex powder particles to be a thermodynamic equilibrium and a reversible process. Here the total adhesion force (N_0) is given by the formula

$$N_0 = -\frac{2\pi}{\sqrt{\varepsilon\varepsilon'}} f(0), \tag{1}$$

where ε and ε' are the curvatures of the tangent surfaces, $f_0 = \sigma_{12} - \sigma_{13} - \sigma_{23}$, σ_{12} is the surface tension at the boundary between phases 1 and 2 (the particles in the plane), σ_{13} and σ_{23} are the surface tensions at the boundary between the solid and the surrounding phase 3. For adhesion of a sphere to a plane

$$N_0 = -2\pi r f(0). \tag{2}$$

where r is the radius of the spherical particle. Experiments [2 and 3] made on small spheres 0.4–1 mm in diameter have demonstrated the correctness of formulas (1), (2). Thus, formulas (1) and (2) are not merely of theoretical interest, but they make it possible in some cases [2 and 3] to calculate the adhesion forces. However, for powdered substances consisting of particles with dimensions 100 μ and less, formulas (1) and (2) have not been checked. Subsequently, some attempts were made to elucidate the mechanism of powder particle adhesion and to obtain some quantitative results [4].

The present paper presents methods of measuring the adhesion of small particles (< 100 μ) and the results obtained from the methods.

The magnitude of the adhesion of powder particles to solid surfaces may be expressed either in terms of the adhesive force or in terms of the adhesion number (γF), which gives the ratio of the number of particles remaining to the initial number of particles for a given force applied to tear them loose.

Existing methods make it possible to measure the force of interaction between two contacting bodies, and to make a direct measurement of the force of adhesion by tearing the powder particles loose from various surfaces.

Thus, Bradley [2] has measured the force of interaction between two spheres with dimensions from 0.4 to 1 mm by means of quartz spiral microbalances, which he constructed specially. In the crossed filament method [5], one of the filaments serves as the dynamometer, and the adhesive force is measured from how much this filament is bent when they are torn apart. A feedback microbalance [6] has been developed to measure the molecular forces arising between two solid bodies as a function of the width of the space separating them.

We shall now discuss methods of measuring the adhesive forces based on tearing the powder particles off under rotation or vibration.

Fuks [7] has measured the adhesive force of powder particles by rotating a cylindrical rod covered with powder around a horizontal axis. Here the maximum disruptive force (when the directions of the centrifugal force and the force of gravity coincide) is given by the equation

$$F = m(\omega^2 x + g), \tag{3}$$

where m is the mass of the particles, ω is the angular velocity, $\omega = 2\pi n/60$, n is the rotational speed, x is the distance between the surface of adhesion and the axis of rotation. To measure the disruptive force when the directions of the centrifugal force and the force of gravity do not coincide, it is necessary to make a vector addition of the accelerations occurring in Eq. (3). For $\omega^2 \chi \gg g$, g may be taken equal to zero. In Ref. [7] a study was made of the adhesion of particles in liquid media using relatively small disruptive forces (up to 100 grams).* The method

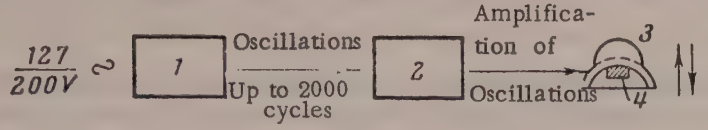


Fig. 1. Diagram of acoustic measurement of adhesion forces: 1) 3G-10 or 3G-12 sound generator; 2) U-50 amplifier; 3) R-10 dynamic speaker; 4) dusted test plate.

of measuring the adhesive force by rotating the dusted surface is simple and reliable, but the physical realization of the method requires some further improvement, one of the directions of which, in particular, is the use of centrifuges, which make it possible to reach disruptive forces of thousands of g's [8].

To measure the adhesion of films vibrationally, [9] the film of the material being studied is put on a cylindrical rod base, which is vibrating at supersonic frequency. The accelerations thus produced tore the film loose. Attempts have also been made to observe spherical dust particles being torn off fibers oscillating at a frequency of 10 or more cycles per second [10]. We have used the vibrational method to measure the adhesion of dust to plane surfaces. The method consists essentially in letting a dusted surface vibrate at a definite frequency. The dust particles are thus accelerated, and are consequently subjected to the action of an alternating force. Knowing the frequency of oscillation (ν) and the amplitude of oscillation (Y), we can calculate the maximum acceleration which the particles receive. The value of the disruptive force for $j \gg g$ will be given by the formula

$$F = m \cdot j, \tag{4}$$

where j is the maximum acceleration from the oscillatory motion ($j = 4\pi^2\nu^2 Y$). The use of sonic and supersonic vibrations gives a large range of values for the disruptive force (tens of thousands of g's).

To measure the adhesion numbers as well as the effect of various disruptive forces we must have some way of counting the dust particles on the different surfaces. Visual counting of the particles under a microscope with statistical treatment of the resulting data have been used in a number of investigations,[7 and 8]. This method is simple but laborious. Using powders with "marked" atoms [11], the initial and final number of particles is proportional to the number of pulses given by the counters. It must be noted, that particle counting techniques using "marked" atoms are applicable only to powders which are dispersed to more or less the same degree.

In our work we used two setups. In the first setup (see diagram fig. 1), sonic oscillations after passing through the U-50 amplifier, are converted into vibrational motion of a dynamic loudspeaker cone provided with an arrangement for holding the dusted plates. The vibrational frequency of the plates did not exceed 2000 cycles per second. The particle count was made visually with a microscope. This setup gives a disruptive force of up to 2500 g.

The amplitude of the vibrations was made in two different ways.

1. Using the micrometer adjustment the microscope was focused on the test plate, which had a cross mark on it. From the scale in the microscope tube the distance between the two extreme positions of the vibrating plate was determined, which gave twice the amplitude.

2. A needle was fastened onto the loudspeaker cone, which left the trace of the vibration on a piece of smoked glass.

---

*Here and subsequently the expression "disruptive force in g's" is taken to mean the force, which is experienced by unit mass of powder particles at the instant in which they are torn loose (or the acceleration acting on a powder particle at the instant in which it is being torn loose).

Thus, the vibrational frequency ν was fixed by the generator, the amplitude Y was measured, the mass of the particles had been determined previously, and we had all the data needed to calculate the disruptive force from Eq. (4).

The second setup provided considerably larger disruptive forces than the first.

To increase the range of the disruptive forces we used a supersonic setup with striction reproducers operating at 10 and 20 kilocycles per second. Here the disruptive force was equal to ten thousand and 24,000 g respectively.

To study the effect of the disruptive forces at different angles to the dusted surface we used a special holder shown in Fig. 2, which made it possible to give the surface various angles with respect to the axis of rotation of the centrifuge. This holder was fastened into the test cell of the centrifuge. The rotational speed (n) was measured along with the distance between the dusted surface and the axis of rotation (x). The disruptive force was calculated from Eq. (3). A more exact technique for measuring the adhesional forces with the centrifuge was described previously in [8]. A centrifuge was used to study the slip and flight paths of the dust particles torn off by catching them in a sticky substance. To get a record of the slipping and jumping of the particles, the sticky substance was placed at different distances from the dusted surface (0.5, 1.0, 1.5 mm etc.). Catching the particles made it possible to determine the distance corresponding with the slip and jump path of the particles on the surface. In order to record the flight path of the particles torn off, a plate which caught the flying particles was set up perpendicular to the dusted plate at a distance of 17 mm from it.

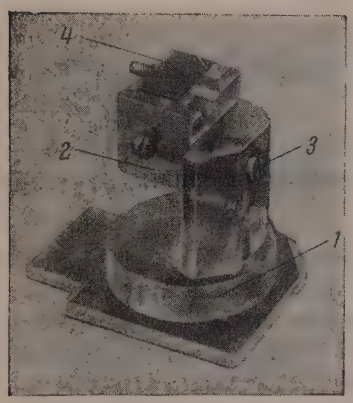


Fig. 2. Plate holder: 1) base; 2) rotating head; 3) aligning screw; 4) dusted test plate.

In this case, as well as when the supersonic setup was being used, the number of particles was counted with a microscope. For this purpose the holder was fastened to the mechanical stage and the number of particles was counted in a strip equal to about one-fifth of the area of the whole plate. To investigate the magnitude and sign of the charges formed in carrying the particles from the surface, we used a SG-1M electrometer with a screening chamber, which prevented any effect of external fields on the charge of the test surface. A measurement was made of the total charge remaining on the plate after the dust particles had been torn from it, and the mean mass of the dust particles in the given faction was calculated. The amount of powder being known, the number of powder particles was determined, along with the mean charge, occurring on one particle.

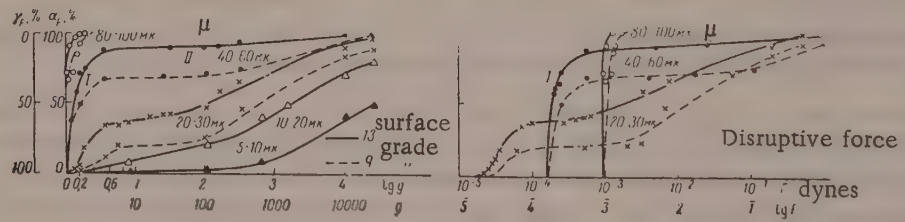


Fig. 3. Integrated adhesion curves in g's (a), and absolute values (b).

The system chosen for study was glass powder made up of spherical particles, previously sorted by air separation into more or less monodispersed fractions and steel plates finished to grade 9 and 13, prepared in the calibrating shop. Before each experiment the plates were given a treatment with purified benzene, distilled water, activated charcoal, and ethyl alcohol to remove grease and surface active matter. The surfaces were dusted by free settling. Every experiment was repeated 10-20 times. The deviation from the mean of the adhesion numbers did not exceed 12%.

To study the effect of atmospheric humidity on the adhesion of the powder, an MI-2 microanaerostat was used, which made it possible to maintain an air pressure of 10 mm Hg. The dusted samples could be kept in the microanaerostat either under conditions approximating absolute air dryness (using P_2O_5) or approximating 100%

humidity (a vessel of water was placed in the microanaerostat). The vacuum produced in the microanaerostat in the first case facilitated removal of water vapor, in the second case it facilitated evaporation of the water and establishment of the equilibrium vapor pressure.

The adhesional forces were investigated as a function of the state of dispersion of the powder, the surface roughness, the length of time the powder was in contact with the surface, the humidity of the surrounding medium, and the direction of the disruptive force.

TABLE 1. 40–60 μ Powder Particles Torn from Grade 9 Surfaces by Vibration or Centrifuging

Disrupting method	Disruptive force, dynes						
	$2{,}54\cdot10^{-4}$	$5{,}71\cdot10^{-4}$	$4{,}23\cdot10^{-3}$	$1{,}72\cdot10^{-2}$	$5{,}90\cdot10^{-2}$	1,64	3,94
	Number of particles remaining, %						
Vibration	51,7	32,0	31,4	28,5	25,5	4,9	0,3
Cetrifuging	60,2	—	37,3	30,1	21,2	1,2	0,6

In the first series of experiments the adhesive forces were measured immediately (not more than 10 minutes) after dusting. Here the temperature of the air surrounding the dusted surface was 16-20°, and its relative humidity was 50-65%. Even for particles of the same powder fraction (5-10, 10-20, 20-30, 40-60, and 80-100 μ), the adhesive forces are not the same. There is a statistical distribution of adhesive forces (Fig. 3). The integral adhesive force distribution curves of the particles, given in semilogarithmic coordinates, expressed the fraction of residual particles (aggregation number γ_F) or of particles torn off (α_F) as a function of the disruptive force (exclusive of the weight of the particles), expressed in g's (Fig. 3,a), as well as in absolute values (Fig. 3,b). The curves given in Figs. 3,a and 3,b for different fractions and surfaces show the effect of particle dimensions and surface roughness on the adhesive forces.

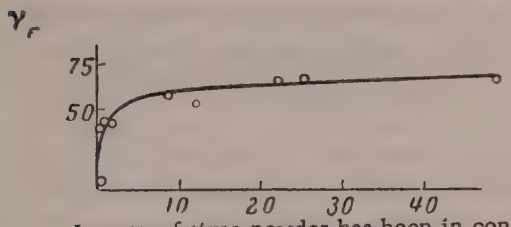


Fig. 4. Adhesion as a function of the length of time the powder has been in contact with the surface, 60-90 μ particles, grade 9 surface, disruptive force $2.76 \cdot 10^{-1}$ dynes.

The advantage of the vibrational method of measuring the disruptive forces, as compared with other methods, is that it makes it immediately possible to take inequal curves of the adhesive force distribution of the particles.

Comparative data on tearing off the dust particles by vibrational and centrifugal methods are given in Table 1.

It may be seen from Table 1 that the two techniques used give the same results within the limits of experimental error.

The results of the experiment show that the adhesive forces increase with the length of time the powder has been on the solid surface (Fig. 4). The phenomenon observed is called aging, since the adhesive forces increase for 30-60 minutes of contact and then reach a constant value about 24 hours after the dust particles have been on the surface.

A study was made of the effect of atmospheric humidity on the adhesion of a powder (60-90 μ) to a grade 9 surface at a disruptive force of $2.75 \cdot 10^{-1}$ dynes, with one hour contact time between the powder and the surface. The following data was obtained:

Relative humidity of air, %	0	50–65	100
Number of residual particles in per cent of initial number (adhesion number γ_F)	50	62	100

An important question is the functional relationship between the adhesive force and the direction of application of a disruptive force. If for each direction of application of the disruptive forces as an axis we lay out the number of residual particles in percent, we obtain a figure which may be described as a polar diagram or directional

chart for the adhesion. The polar diagram of the adhesion for 20-30 μ particles on a grade 13 surface and a disruptive force of $4.1 \cdot 10^{-4}$ dynes is given in Fig. 5.

In measuring the effect of disruption by forces applied at various angles to the dusted surface, a sticky substance was used to trap the dust particles as they were torn off. If the forces are applied at angles of 30, 60, 90, 120, and 150° to the dusted surface (positions 2-6, Fig. 5), the particles torn off leave the surface directly. If the disruptive

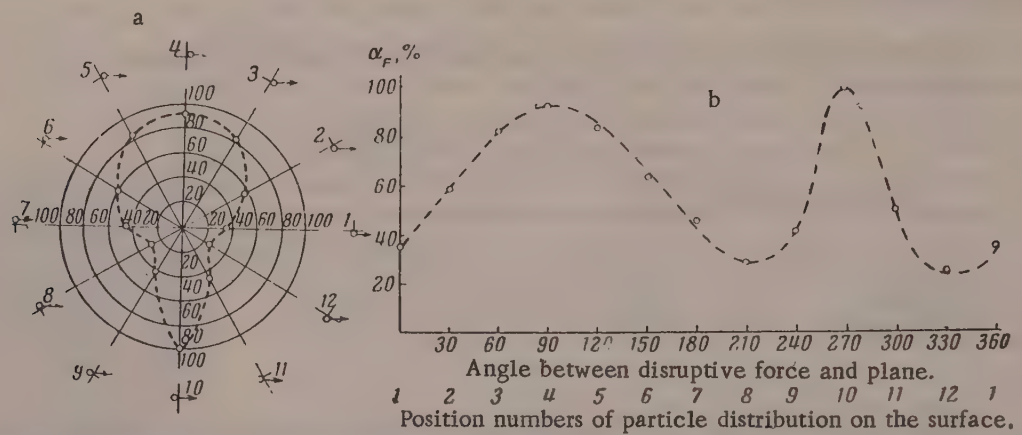


Fig. 5. Polar diagram of adhesion (a) and developed curve (b) (20-30 μ particles grade 13 surface, disruptive force $4.1 \cdot 10^{-3}$ dynes).

forces act at angles of 180, 210, and 240° (positions 7-9), the particles torn off move over the whole surface, and in their motion they can "hook" particles that have not been torn loose yet. A similar effect is observed in the tearing off of particles by a force acting at angles of 300, 330, and 360° (positions 11, 12 and 1). Thus, for example, the particles torn off by a force directed parallel to the dusted surface (position 1) may, in their flight, hook as yet undisrupted particles at a distance of 7-10 mm from their original position (the motion of the particles is considered to be in a straight line). In order to eliminate any secondary phenomona involving particle collision, the dusting of the plates was confined to a narrow strip 1 mm wide. However, it was not possible to avoid the secondary phenomena completely. Finally the electrical properties of the powder were studied. The following data were obtained on the electrical charges produced by tearing 40-60 μ dust particles loose from a grade 9 surface as a function of the time they had been in contact:

Time particles and surface had been in contact, hours	0.2	24	48
Mean charge on a particle in cgs units	$1.47 \cdot 10^{-7}$	$1.74 \cdot 10^{-7}$	$4.35 \cdot 10^{-7}$
The same, in unit charges	306	363	914

Table 2 gives the charges on dust particles blown off, in order, by a stream of air when the velocity was increased in steps.

TABLE 2. Charge on 40-60 μ Dust Particles in Order of Blowing off from a Grade 9 Surface. 48 Hours Contact between Particles and Surface.

Number of particles blown off%	Mean particle charge	
	cgs units	Unit charges
23,0	$3,43 \cdot 10^{-7}$	723
36,0	$3,62 \cdot 10^{-7}$	770
30,0	$3,78 \cdot 10^{-7}$	778
11,0	$1,2 \cdot 10^{-6}$	2500

TABLE 3. Effect of Particle Diameter on the Disruptive Force ($F_{1/2}$) Required to Tear Half the Particles off of a Grade 13 Surface.

Particle diameter, μ	Disruptive force	
	in g's	in dynes
40—60	1,3	$2,13 \cdot 10^{-4}$
20—30	107	$2,15 \cdot 10^{-3}$
10—20	1400	$6,12 \cdot 10^{-3}$
5—10	24000	$1,33 \cdot 10^{-2}$

It can be seen from Table 2, that the charge on the particles blown off at the highest air velocities, i.e., those particles which adhered more solidly, is higher than for the three smaller air velocities.

Two regions may be distinguished in the integral curve for particles with grain diameter > 20 μ (Fig. 3, a and 3, b for 40-60 μ particles).

Region 1. The adhesive force is comparable with the weight of the particles. Here there is a sharp increase in the number of particles torn off in a narrow range of applied force.

Region 2. The adhesive force is greater than the weight of the particles. With considerable increase in the disruptive force the number of particles torn off increases slowly.

If the diameter of the particles is decreased, the difference between the two parts of the adhesion curves becomes much less pronounced. What happens mainly is that the first region disappears (Fig. 3,a). There is a minimum disruptive force at which the last particles are pulled off. Since the present technique does not provide disruptive forces greater than 24,000 g, and forces of this size cannot pull off particles with a diameter < 20 μ, it is convenient to consider what force is required to pull off half the particles. These data are given in Table 3.

As can be seen from Table 3, a reduction in grain diameter from 40-60 μ to 5-10 μ means an increase in the disruptive force ($F_{1/2}$) from $2.13 \cdot 10^{-4}$ to $1.33 \cdot 10^{-2}$ dynes, i.e. about 100 fold. In regard to the reduction in mass of the particles, the disruptive force in g's is increased from 1.3 to 24,000 i.e. more than 10,000 times.

The distribution of adhesive forces is explained by the fact that the charges on the particles are not always the same size, and by the difference in dimensions of the particles, and the actual contact area. The difference in particle dimensions plays some role in the distribution of the adhesive forces. However, decreasing the range of particle dimensions in a powder fraction does not put an end to the distribution. Direct measurements of the diameters of the initial and final powder fractions show that for one and the same disruptive force, not all the particles of a given diameter are torn off. It is to be assumed that the micro-roughness of the contacting bodies exerts an influence on the adhesive forces, since when the dust particles are in contact with the surface, the actual contact area will be determined by the microrelief structure of the surface and the particles, and will be a function of the roughness of the former.

However this does not seem to be a basic factor in rupturing the adhesive forces, since the adhesion remains very large even on grade 13 surfaces.

The distribution of adhesive forces may be explained by the fact that, when the dust particles are in contact with the surface, the charges on the different particles are not the same. This point of view is supported by the data of Table 2, which show (in the case of a metallic surface that there is a parallelism, consisting in the fact, that strongly charged particles correspond with the greatest adhesive forces. On this basis, we can assume that the increase in the adhesive forces with time is, to a considerable degree, to be explained by the increase with time of the charges on the particles as a result of constant contact electrification.

The effect of atmospheric humidity on the adhesive force found between the dust particles and the surface, may be explained by the fact that in the space between the contacting bodies a water film is formed by capillary condensation of water vapor. A rigorous thermodynamic theory of the effect of capillary condensation on the adhesive force of particles with a spherical surface was worked out recently by one of the authors [12]. Apparently, the capillary condensation of water vapor plays a very definite role in increasing the adhesive forces during the time the dust particles are in contact with the surface.

It may be seen from Fig. 5, a, that the adhesive forces are a function of the direct application of the disruptive force. A normal force (position 4) tears off a smaller number of particles than tangential forces do (positions 1 and 7). It is possible that when tangential forces are acting the disruption of the particle is preceded by some sort of oscillation under the influence of the centrifugal force. In other cases, for example using quartz filaments [5], a disruptive force applied perpendicular to the surface of contact is approximately equal to the tangential force, corresponding to static friction. The most favorable direction for the force to tear off the particle is the tangential direction (parallel to the dusted surface or close to this direction, Fig. 5, positions 1, 7, 8, and 12).

Naturally, a compressive force (position 10), directed inward to the surface cannot tear off any particles. The force of gravity helps to tear off hanging particles (positions 1, 2, and 3), and makes it somewhat harder to tear off particles that are sitting down (positions 5, 6, and 7). This fact explains the slight asymmetry of the upper half of the

polar diagram of adhesion relative to the vertical axis. In addition, some effect is exerted on tearing off the particles by collisions between particles torn loose from positions 1, 7-9, 11, 12 (Fig. 5) with particles that are still adhering, and have not yet been torn loose.

It should be noted that the integral adhesion curves (Fig. 3,a, and 3, b), obtained by the vibrational method, give data for normal adhesive forces.

SUMMARY

1. A vibrational method for measuring adhesive forces has been presented and tested, which uses a sonic and a supersonic setup, giving disruptive forces up to 24,000 g's.

2. The forces of adhesion of particles of approximately the same size to a given surface are not the same, and give integrated adhesion curves, which represent the statistical distribution of particles having different adhesive forces.

3. The difference in the adhesive forces is explained by the difference in diameter of the powder particles and the difference in actual contact areas between the particle and surface, as well as by different values of charge, which shows the importance of electrical forces when the particles are torn loose from the surface.

4. An experimental determination has been made of the adhesive force between spherical particles of different sizes and grade 9 and grade 13 metal surfaces. As the diameter of the particle is reduced, the adhesive forces increase.

5. If the time during which the powder is in contact with the surfaces lengthened, the adhesive forces increase, which is explained, in particular, by the increase in charge on the particles with time. The increase in the adhesive force comes to an end 20-24 hours after the moment of contact.

6. Atmospheric humidity affects the adhesive force. With the atmospheric humidity near 100%, a considerable increase in the adhesive forces is observed on account of capillary condensation in the space between the particles and the surface.

7. The ease with which the powder particles are torn loose depends on the direction of application of the disrupting force. The polar adhesion diagram obtained gives evidence that a disruptive force tangential to the dusted surface is the most effective from the standpoint of tearing off the particles.

LITERATURE CITED

1. B. V. Deryagin, Zh. Fiz khimii 6, 1306 (1935); Kolloid. -Z. 69, 155 (1934).
2. R. S. Bradley, Philos. Mag. 13, 853 (1932); Trans. Faraday Soc. 32, 1088 (1936).
3. H. C. Hamaker, Physica 4, 1058 (1937).
4. D. W. Jordan Brit. J. Appl. Phys. Suppl. 3, 194 (1954).
5. B. V. Deryagin, N. I. Moskovitin, M. F. Futian, Transactions of the third all union conference on colloid chemistry [in Russian] Academy of Sciences Press, USSR, 1956, p. 285; A. D. Malkina, B. V. Deryagin, Kolloidn, Zh. 12, 431 (1950).
6. B. V. Deryagin, I. I. Abrikosova, E. M. Lifshits, Uspekhi fiz, Nauk 64, 493 (1958).
7. G. I. Fuks et al. Collection of papers on Tech. Rat. of Petroleum [in Russian] No. 1, 266 (1948); G. I. Fuks, E. V. Tsygnova, and V. M. Kychkov, Dokl. AN SSSR 65, 307 (1949); G. I. Fuks and V. M. Kychkov, Transactions of VIUAA 29, 186 (1959).
8. A. D. Zimon, Yu. N. Petunin, Lacquer Coloring Materials and their Application [in Russian], No. 2, 63 (1961).
9. S. Moses, Industr. and Engng. Chem. 41, 2339 (1949).
10. R. I. Larsen, J. Amer. Industr. Hyg. Assoc. 19, 265 (1958).
11. R. Challande, Compt. rend. 237, 35 (1953).
12. B. V. Deryagin, Report presented to the Symposium on Powders in Industry held in the Royal Institution, London; 29-30 September, 1960.

THE HEAT OF ADSORPTION OF WATER VAPOR ON HYDRATED AND DEHYDRATED SILICA GELS

O. M. Dzhigit, A. V. Kiselev, and G. G. Muttik

Adsorption Laboratory, Chemistry Department, Moscow University
Translated from Kolloidnyi Zhurnal, Vol. 23, No. 5.
pp. 553-562, September-October, 1961
Original article submitted July 17, 1960

The determination of adsorption heats and equilibria for the adsorption of various non-polar compounds which either have a very small quadrupole moment (for example, inert gases and saturated hydrocarbons) or very large quadrupole moment (for example, nitrogen, aromatic and unsaturated hydrocarbons), or else compounds with a large peripheral dipole moment (such as, water, and alcohols), on the surface of hydroxides is of considerable interest. There is already a large amount of experimental data available dealing with the energy and mechanism involved in interactions of hydrated silica gel surfaces with saturated and unsaturated hydrocarbons and benzene [1-6]. The heat of adsorption of methanol vapor on silica has been measured directly [7] and also calculated from the isosteres [8]. The partial molar heats of adsorption of water on hydrated rock crystal have also been calculated from the isosteres [8]. On silica gels they were determined chiefly from the wetting heats [9, 10], and only on a silica gel with an intermediate degree of hydration (6 μ moles of OH/ m^2) were they determined directly [10]. The effect of surface hydration on the heat of adsorption of vapors on silicas has only been examined over a narrow range of surface coverages (between 5.2 and 8.3 μ moles of OH/ m^2) [10]. Thus the available experimental data on the differential heats of adsorption of water remain uncorrelated. Moreover a detailed investigation of these heats and of adsorption equilibria together with a study of the heat capacities [11] and infrared spectra [12, 13] of the adsorption complexes will not only provide a detailed picture of the surface properties of silicas and the adsorption mechanism but also enable us to explain the chemical features of the surface and the likelihood of chemisorption leading to the formation of new surface compounds and also show how these factors depend on the past history of a silica sample.

We have therefore conducted a simultaneous investigation of the isotherms and partial molar heats of adsorption of water vapor on coarsely porous silica gels with surfaces in various degrees of hydration.

The calorimeter and materials. The isotherms and heats were determined using an apparatus designed for measuring very slow evolution of heat in a calorimeter. The working of the calorimeter was stabilized by placing the apparatus in two separate air-conditioned basement rooms protected from vibrational and electromagnetic interference. The calorimeter was located inside the main room in which the air temperature was maintained constant to within $\pm 0.2^\circ$ and relative humidity at 60 ± 10%. The galvanometers and the equipment for the introduction of gas samples were placed on a foundation separate from that of the building. The equipment was operated by remote control from an anteroom in which the temperature was maintained constant to within ± 0.4°C; inside it we kept all the auxiliary equipment (recorders, stabilizers, a relay, and the control panel) as well as the resistance boxes for the measuring and regulating bridges.

The design of our adiabatic calorimeter was similar to that shown before [14]. Since prolonged experiments require that the heat transfer from the calorimeter to the jacket be regulated with a high degree of stability for the bridge regulating the first jacket we selected a galvanometer with a quartz suspension (Cernike, type E, made by Kipp) since it can stabilize the zero point position better than any other kind. Since the second operating calorimeter jacket [14] was at a slightly lower temperature than the calorimeter itself, we wound a nichrome wire around the part of the adsorption shell located at the neck of the jacket and heated it with current from a storage battery. The heater was turned on whenever we worked at high relative pressures to prevent the condensation of water vapor on the inside walls of the shell.

The calorimeter readings were recorded automatically on a ÉPP-09 recorder the slide wire of which was connected in series with the resistance box of the measuring bridge. The recorder amplifier was regulated by a differ-

ential photorelay (see Fig. 1). To eliminate galvanometer oscillations during the automatic balancing of the measuring bridge the reversing motor of the recorder pen was only switched on for 0.1-0.2 sec every 3 sec by means of a special circuit breaker.

The apparatus for introducing vapors into the calorimeter was inclosed in an air-cooled thermostat in which the temperature was maintained constant to within ±0.08° C. The water samples to be introduced into the calorimeter could be measured either as vapor in a gas burette (up to 500 moles) or as liquid in a capillary microburette [2, 14]. In the case of volatile liquids such as water it is rather difficult to measure the volume in a vacuum microburette with a high degree of precision mainly due to the fact that the amount of water remaining on the burette walls above the meniscus is not constant. We have therefore tried to keep parts of the burette above the water level and the tube connecting the apparatus with the burette at 35-40° by heating. Whenever the water level was changed during an experiment the burette heater was lowered by means of a crank operated by a Warren motor. The heaters reduced wall adsorption to the extent that its effects on the final results could be disregarded.

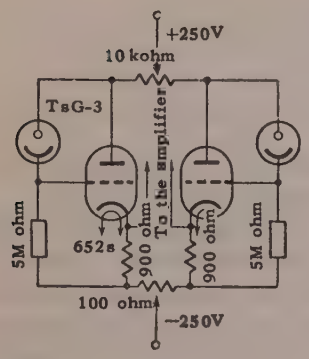


Fig. 1. A schematic diagram of the differential photorelay.

To eliminate the adsorption of grease vapor on the sample, the surface of water, and microburette walls we used tefloncoated magnetic valves throughout the operating part of our apparatus [15]. They are more convenient to use than mercury seals [14] and also have the same small volume whether open or closed.

In experiments with silica gels having a large specific surface s the accuracy with which the partial molar heats of adsorption can be determined will actually depend only on how well the capillary is calibrated and how good is the extrapolation of the terminal calorimetric data. Water aliquots introduced into the calorimeter from a ~ 3 mm capillary can be measured with an accuracy of ±10μ moles (for the entire sample). Since a large amount of heat is evolved in all the experiments with silica gels errors in the determination of heat do not exceed ±0.5%. In most of our experiments, though, the error was less than 0.2%.

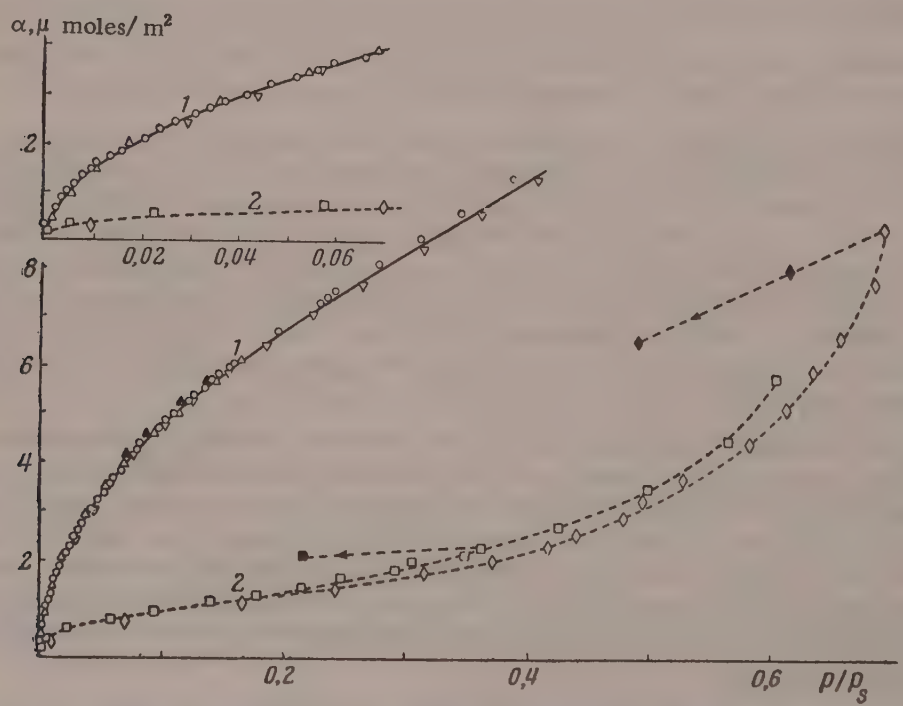


Fig. 2. Adsorption isotherms of water vapor on silica gels: 1) KSK-2 (150°) and 2) KSK-2 (900°). The upper left corner shows the initial portions of the isotherms. Here and in later figures the solid markings represent desorption. The squares denote the first set of experiments.

We used in our work coarsely porous silica gel of the same type, KSK-2, as that used in a number of other experiments [2, 4, 5, 16]. A sample of this silica gel denoted by KSK-2(150°) was heated in vacuo for 100 hrs at 150° C before the experiment. The weight loss observed after it was further heated at 115° was 3.35% which would correspond to hydroxyl group concentration of α_{OH} = 11.2μ moles/m^2 = 6.75 OH/100A^2 (assuming that all the water lost after the heating at elevated temperature was originally on the surface in the form of hydroxyl groups). Another sample of this silica gel, denoted by KSK-2(900°), was fired before the experiment under conditions which would provide the most complete surface dehydration at a minimum change in the structural properties of the original sample. Since firing of silica gel above 900° in vacuo drastically reduced s [4] we settled for a 45 hr heating of KSK-2 at 900° with pumping.* Such a treatment produced only insignificant changes in the porosity of the silica gel [4]. The concentration of structural water in a sample thus treated did not exceed 0.3-0.6%, which represents an α_{OH} = 1-2 μ moles/m^2 = 0.6-1.2 OH/100A^2.

We thus used two samples of coarsely porous silica gel with about the same pore structure but radically different surface hydration. The isotherms and the partial molar heats of adsorption of water vapor were determined on these two samples.

EXPERIMENTAL RESULTS AND DISCUSSION

To facilitate the comparison of results obtained in various experiments we have expressed all the pertinent data per unit area of silica gel; the surface area calculated by the BET method from the adsorption of nitrogen vapor was 330 m^2/g for KSK-2 (150°) and 275 and 282 m^2/g for KSK-2(900°).**

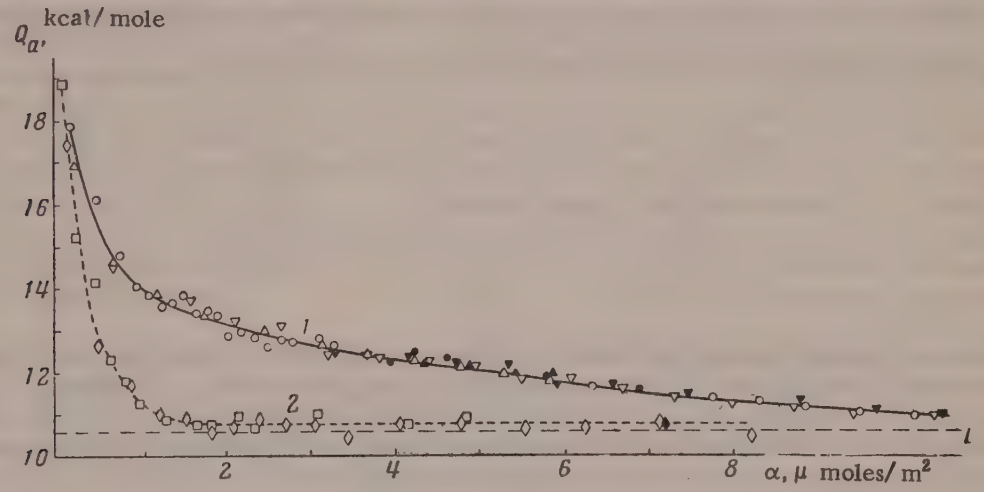


Fig. 3. The plots of partial molar heat of adsorption as a function of the amount of water vapor adsorbed on: 1) KSK-2(150°) and 2) KSK-2(900°).

In Fig. 2 we have plotted our adsorption isotherms. On curve 1, which represents the isotherm on KSK-2(150°), the markings represent the results of three sets of experiments while the solid line represents a previously obtained [16] and interpolated reversible adsorption isotherm of water vapor on a KSK-2(200°) sample on several other kinds of coarsely porous silica gels with hydrated surfaces.*** Curve 2 (Fig. 2) shows how much the adsorption of water

* After the tube with adsorbent was evacuated dry air was let in, the silica gel was quickly shaken out into the cups inside the calorimeter shell [14], weighed, and the shell sealed off with all due precautions taken to keep water vapor away from the silica gel. Prior to each experiment this silica gel was heated for 12 hrs at 400° with pumping. Another sample of KSK-2 was dehydrated under similar conditions but the transfer into the cups and placement in the shell were done inside a dry box; we determined the partial molar heats of adsorption of benzene vapor [14] on this sample first and then the heat of adsorption of water vapor.

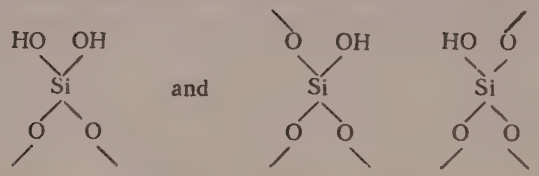
** We would like to thank L. D. Belyakov and B. G. Aristov for the determination of specific surface areas.

*** Zhdanov [17] has shown that the same absolute isotherm is valid for other silicas (porous glass, rock crystal) if their surface is hydrated to about the same extent.

decreases when the temperature of preliminary firing is raised from 150 to 900°. The adsorption isotherm of KSK-2 (900°) looks convex only at the beginning (up to $p/p_s = 0.05$), which can, of course, be attributed to a small number of hydrozyl groups (α_{OH} = 1-2 moles/m^2) retained on the surface of this sample. At all higher relative pressures the adsorption isotherm of water vapor is concave.* It should be noted that curve 2 is not an equilibrium isotherm for the physical adsorption of water vapor on dehydrated silica gel KSK-2(900°), since in addition to the physical adsorption irreversible chemisorption also takes place. The chemisorption rate of water increases rapidly with increasing p/p_s [15], while the amount of chemisorbed water will greatly depend on how long the adsorbent had been exposed to water vapor. To minimize chemisorption we carried out our measurements around the clock trying to reduce the time intervals between experiments while making sure that the rapid physical adsorption stage is completed. Nevertheless, when after 85 hrs we reached $p/p_s = 0.69$ and subsequently tried desorption some of the water remained adsorbed irreversibly. Another evidence of chemisorption is the fact that as p/p_s increases the amount of material adsorbed when determined in two independent sets of measurements comes out different. The first set was carried out slower than the second, i.e., in the first case the adsorbent was exposed to water vapor for longer periods of time. And as one would expect the isotherm obtained in the first set of experiments lies above that obtained in the second. For example, in the first set we reached $p/p_s = 0.6$ after 101 hrs while in the second after 68 hrs. By extending the exposure time by 33 hrs we increased the adsorption by 0.6 μmoles/m^2.

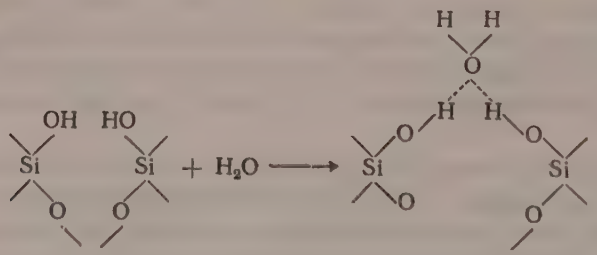
In Fig. 3 we have plotted the partial molar heats of adsorption of water vapor as a function of water adsorbed on the two investigated silica gels. Initially the adsorption of water on the hydrated surface of KSK-2(150°) is accompanied by the evolution of a fairly large amount of heat (~ 18 kcal/mole, see curve 1). As the first 10-15% of the surface area becomes covered the evolution of heat sharply declines. The observed effect is caused by the fact that in places where the component particles of the silica gel structure either adhere to each other or are fairly close to each other [19, 1] the hydrozyls are most favorably oriented for strong bonding to water molecules.

The hydrated surface contains two main types of silanol groups [1, 16, 20].



These hydroxyls are located close enough to permit a slight interaction between them [13]. As a consequence the surface is chemically and geometrically inhomogeneous which explains why the heat of adsorption of water decreases with increasing surface coverage. Moreover the rapid decline in the adsorption heat occurs within a fairly narrow region extending to $\alpha \approx 0.5$ molecules/100 A^2. Beyond that point the heat of adsorption declines quite slowly: between $\alpha \approx 0.5$ and $\alpha \approx 4$ molecules/ 100A^2 the drop is only 2.7 kcal/mole.

The main initial interaction between the adsorbed water and the hydrated surface can be schematically represented by the sequence shown below:



* A concave isotherm for the adsorption of water vapor on silica was first reported in [18].

where a pair of favorably oriented hydroxyls constitute an active center for the adsorption of a water molecule [1, 16, 20]. The average heat of 12.5 kcal/mole observed in this region is probably produced in this reaction. It should be noted that the monolayer surface density α_m = 6.5 μ moles/m^2 = 3.9 molecules/100A^2 [16] determined by the BET method is a strictly formal figure, since, in the first place, the surface is not homogeneous and, in the second, one can not disregard here the adsorbate–adsorbate interaction (neither in the case of water nor in the case of nitrogen adsorption, on which the BET method is based). This α_m represents an average area of ω_m = 25A^2 (as in the case of methanol [21]). Since a water molecule occupies a much smaller area (10.6A^2), the value of α_{mBET} = 3.9 molecules/100A^2 must correspond to only the first stage of surface coverage, i.e., the water molecules are attached primarily to the favorably oriented hydroxyls on the silica surface. This stage is subsequently overlapped by another in which the water molecules become attached to the surface both directly through the hydroxyls and through the already adsorbed molecules. And finally we get adsorption over a completely filled layer of adsorbed water molecules, i.e., polymolecular adsorption. The overlapping of these processes leads to a gradual decline in the heat of adsorption.

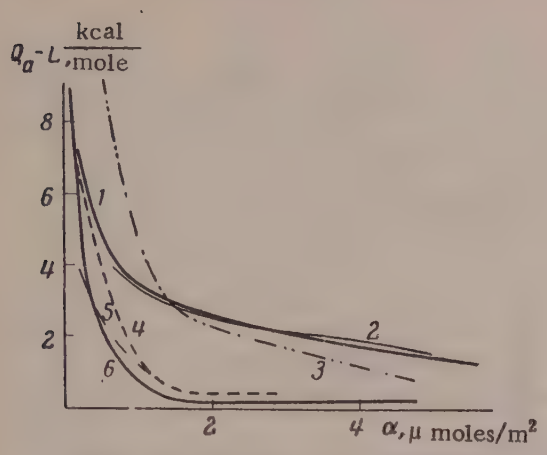


Fig. 4. Net partial molar heat of adsorption of water vapor as a function of the amount of water already adsorbed on silicas with various average concentrations of surface hydroxyls: 1) Silica gel KSK-2(150°), α_{OH} = 11.2 μ moles/m^2; 2) rock crystal, α_{OH} = 11.2 μ moles/m^2 [8]; 3) silica gel KSK-3(300°), α_{OH} 8.3 μ moles/m^2 [10]; 4) silica gel K-2(300°), α_{OH} = 6 μ moles/m^2 [10]; 5) silica gel K-2(700°), α_{OH} = = 5.2 μ moles/m^2 [10]; 6) silica gel KSK-2 (900°), α_{OH} = μ moles/m^2.

When the heat of adsorption is plotted as a function of the amount of water vapor adsorbed on the dehydrated silica gel KSK-2(900°) the curve looks somewhat different (see curve 2 in Fig. 3). Though the adsorption of the first few aliquots of water yields about the same amount of heat as in the case of a hydrated surface the heat of adsorption declines much more sharply in this region. The sharp drop in the heat curve occurs in the region represented by the initial convex section of the adsorption isotherm (curve 2, Fig. 2). In fact the heat of adsorption becomes practically constant α = 1 μ moles/m^2 = = 0.6 molecule/100A^2 and exceeds the heat of condensation by only about 0.2 kcal/mole. Apparently in this case where 85% of the surface is free of hydroxyls adsorption proceeds mainly through the interaction of water molecules with oxygen ions at the surface and by the formation of a two-dimensional film of hydrogen-bonded water molecules which are anchored to the silica gel surface in the few places where some hydroxyl groups remain attached to the surface.

Except for the initial segment and the value of the heat of adsorption on KSK-2(900°) curve 2 in Fig. 3 resembles very much in its shape the corresponding curve for carbon lampblack with an oxidized surface [22]. It is quite likely that the physical adsorption of water on dehydrated silica has a lot in common with a similar adsorption on oxidized but dehydrated hydrocarbon adsorbents and other oxides.

In Fig. 4 we have plotted the net partial molar heat of adsorption ($Q_a - L$) as a function of the amount of water vapor adsorbed per unit area of various silicas. Our experimentally determined heats of adsorption of water vapor on a hydrated silica gel (curve 1) with an average concentration of surface hydroxyls α_{OH} = 11.2 μ moles/m^2 almost coincide with heats calculated by Stober[8] from the isosteres for a hydrated* rock crystal with the same α_{OH} = 11.2 μ moles/m^2 (curve 2). The partial molar heat calculated in [10] from the wetting heats of a silica gel with α_{OH} = 8.3 μ moles/m^2 at α_{H_2O} > 1.3 μ moles/m^2 is slightly smaller** (curve 3). And even lower lie the two curves obtained in [10] for silica gels with a smaller degree of hydration, α_{OH} = 6.0 μ moles /m^2 (curve 5). The lowest of all is curve 6, which was obtained by us for KSK-2(900°) where α_{OH} < 2 μ moles /m^2.

---

* After prolonged washing with nitric acid and water the powdered rock crystal was dried by Stober in vacuo at 150° C.

** The much higher heats at lower surface coverages reported in [10] for this sample seem to result from errors in the calculation of partial molar heats of adsorption from wetting heats.

Thus the heat of adsorption of water vapor on silica gels depends very much on α_{OH}. As α_{OH} decreases so does the heat of adsorption. A complete dehydration of a silica surface would result in even smaller net heats of adsorption of water.

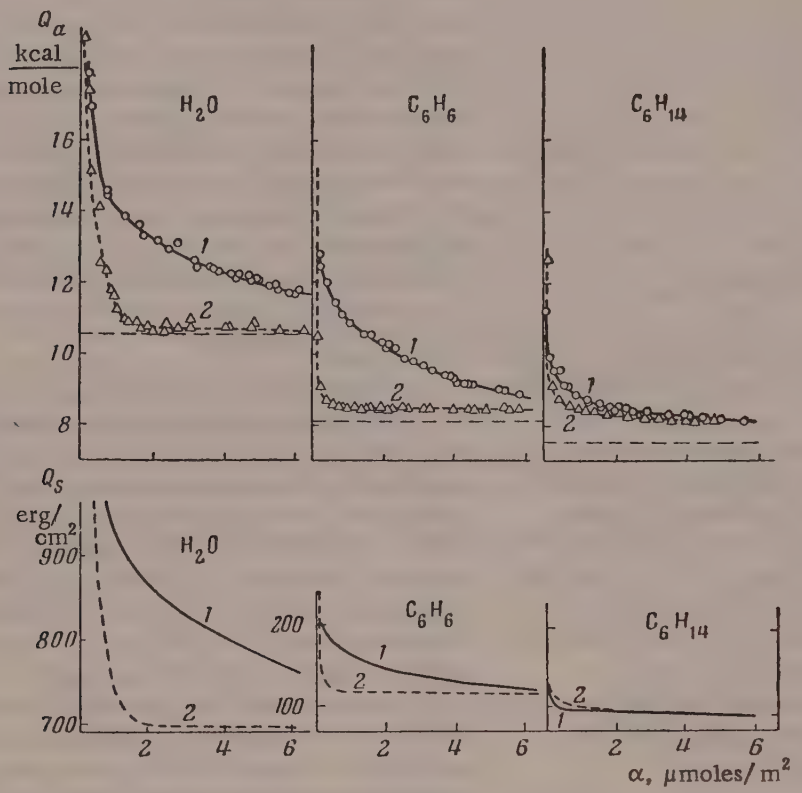


Fig. 5. A comparison of the partial molar heats of adsorption of water vapor, benzene, and n-hexane on a KSK-2 silica gel with a hydrated (1) and dehydrated (2) surface. On top Q_a is given per mole of adsorbate; below Q_s is given per unit area of the surface occupied by the adsorbate molecules.

In the three upper graphs of Fig. 5 we have compared the differential molar heats of adsorption of water, benzene, and n-hexane vapors (Q_a in kcal/mole) plotted against the surface coverage on a dehydrated and hydrated silica gels. Whereas dehydration has practically no effect on the heat of adsorption of hexane [2, 4], in the case of benzene and water not only do we observe a pronounced and roughly similar effect of dehydration but we also find that the respective heats of adsorption change by about the same amount. This confirms an earlier conclusion, based on a comparison of adsorption isotherms [4], that the presence of a dense hydroxyl layer on a silica surface greatly promotes the adsorption of both benzene and water [3].

The curves plotted in the upper half of Fig. 5 show the molar heats of adsorption Q_a of molecules occupying different areas on the adsorbent surface. That is why it is also necessary to show alongside the partial molar heats of adsorption $Q_a = \partial Q/\partial_a$ the corresponding partial heats per unit area of the covered surface $Q_s = \partial Q/\partial_s$. We tried to get the latter by dividing the partial molar heat Q_a by the area occupied by the respective molecules, ω_m. * However, the correct choice of ω_m presents certain difficulties, since the values determined by the BET method from adsorption on inhomogeneous surfaces are strictly formal, as we have already pointed out. We finally calcu-

* This method was proposed by L. D. Belyakova.

lated Q_s by using values of ω_m determined from the bulkproperties of the corresponding compounds and their adsorption on a homogeneous surface such as graphitized carbon black; for water we get $10.6A^2$, for benzene $40A^2$ [23], and for n-hexane $51A^2$ [23]. The plots of $Q_s = Q_a/N\omega_m$ (where N is Avogadro's number) against surface coverage on hydrated and dehydrated silica gels are shown in the lower half of Fig. 5. When we switch from water to hexane the value of Q_s on a hydrated surface declines sharply. Dehydration of the surface also reduces the value of Q_s with the reduction being most pronounced for water, less so for benzene, and practically negligible for hexane.

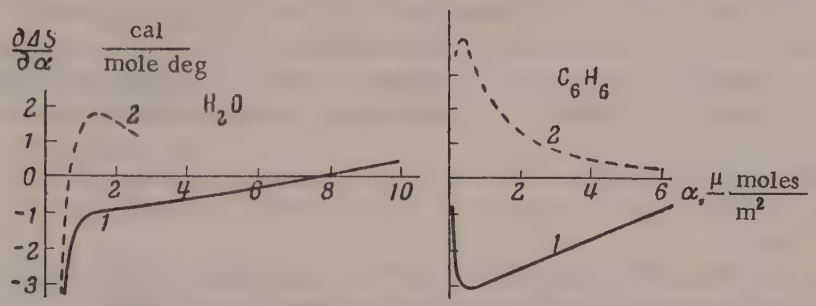


Fig. 6. Change in the partial molar entropy during the adsorption of water and benzene vapors on hydrated (1) and dehydrated (2) silica gel KSK-2.

From adsorption heats and isotherms we calculated the change in the total energy, free energy, and entropy for the adsorption of water vapor. For the highly dehydrated silica KSK-2(900°) we assumed that at $p/p_s < 0.25$ the rate of chemisorption is still negligibly small, or in other words, that in this region curve 2 in Fig. 2 practically coincides with the reversible physical adsorption isotherm for water on dehydrated silica.

In Fig. 6 we have shown how the partial molar entropy of adsorption depends on the surface coverage of hydrated (curve 1) and dehydrated (curve 2) silica gels. Liquid water was taken as a standard state. The first few water molecules are always the most rigidly held by the activated sites on either sample. On the hydrated surface the entropy remains below the zero line (see Fig. 6, curve 1) until a monolayer is completed, which means that water molecules are less mobile in the adsorption layer than in pure liquid water, apparently due to strong hydrogen bonding to the surface hydroxyl groups. The shape of curve 2 (representing KSK-2(900°)) seems to indicate that once the few remaining activated sites are covered up the water molecules adsorbed on the dehydrated surface are more mobile than in the liquid phase.

Benzene yields similar results (Fig. 6); when adsorbed on a hydrated surface the molecules in the first layer are less mobile than in liquid benzene, while on a dehydrated surface the mobility is greater than in the liquid phase [4].

SUMMARY

1. We have determined the adsorption isotherms and the partial molar heats of adsorption of water vapor on two kinds of coarsely porous silica gels, one with a hydrated and one with strongly dehydrated surface. The adsorption heat of water on a hydrated surface declines smoothly and becomes ~ 12.5 kcal/mole in the region of medium surface coverage. On a dehydrated surface the heat of adsorption at first declines sharply then becomes constant and close to the heat of condensation.

2. With increasing surface dehydration the reversible adsorption of water vapor on silica gel declines.

3. We have compared the heats of adsorption of water, benzene, and n-hexane expressed both per mole and per unit area of surface occupied by the respective compounds. The effects of surface dehydration diminish in importance as one proceeds from water to benzene to hexane.

The authors would like to thank E. G. Boreskova and K. N. Mikos for their assistance in the measurements.

LITERATURE CITED

1. A. V. Kiselev, in Coll. Chemical Surface Compounds and Their Role in Adsorption [in Russian] Izd. MGU, 1957, p. 90; Dokl. AN SSSR, 106, 1046 (1956); Uspekhi Khimii, 25, 705 (1956); ZhFKh, 35, 233 (1961).

2. A. A. Isirikyan and A. V. Kiselev, ZhFKh, 31, 2127 (1957); 32, 639 (1958); Dokl. AN SSSR, 110, 1009 (1956); 115, 343 (1957); A. A. Isirikyan, A. V. Kiselev, and B. A. Frolov, ZhFKh, 33, 389 (1959).
3. A. V. Kiselev and D. P. Poshkus, Dokl. AN SSSR, 120, 834 (1958); A. V. Kiselev, Ya. Kutetski, and I. Chizhek, Dokl. AN SSSR, 137, 638 (1961).
4. L. D. Belyakova and A. V. Kiselev, Dokl. AN SSSR, 119, 298 (1958); in Coll. Preparation, Structure, and Properties of Adsorbents [in Russian], Goskhimizdat, 1959, p. 180.
5. A. G. Bezus, V. P. Dreving, and A. L. Klyachko-Gurvich, Kolloidn. Zh. 23, 241 (1961).
6. A V. Kiselev, and V. I. Lygin, Kolloidn. Zh. 23, 574 (1961).
7. N. N. Avgul', O. M. Dzhigit, A. A. Isirikyan, A. V. Kiselev, and K. D. Shcherbakova, Dokl. AN SSSR, 77, 625 (1951); O. M. Dzhigit, A. V. Kiselev, N. N. Mikos-Avgul', and K. D. Shcherbakova, Dokl. AN SSSR, 70, 441 (1950).
8. W. Stober, Kolloid. Z. 145, 17 (1956).
9. A V. Kiselev, K. G. Krasil'nikov, N. L. Pokrovskii, N. N. Avgul', O. M. Dzhigit, and K. D. Shcherbakova, ZhFKh, 26, 986 (1952).
10. T. S. Egorova, V. F. Kiselev, and K. G. Krasil'nikov, Dokl. AN SSSR, 123, 1060 (1958).
11. G. I. Berezin, A. V. Kiselev, and V. A. Sinitsyn, Dokl. AN SSSR, 135, 638 (1960).
12. A. N. Terenin, in Coll. Chemical Surface Compounds and Their Role in Adsorption [in Russian], Izd MGU, 1957, p. 206.
13. A. V. Kiselev and V. I. Lygin, Kolloidn. Zh. 21, 581 (1959); 22, 403 (1960); 22, 157 (1960).
14. N. N. Avgul', G. I. Berezin, A. V. Kiselev, I. A. Lygina, and G. G. Muttik, ZhFKh 31, 1111 (1957).
15. A. V. Kiselev and G. G. Muttik, Kolloidn. Zh. 19, 562 (1957).
16. L. D. Belyakova, O. M. Dzhigit, and A. V. Kiselev, ZhFKh, 31, 1577 (1957).
17. S. P. Zhdanov, Coll. Preparation, Properties, and Structure of Adsorbents [in Russian] Goskhimizdat (1959), p. 166.
18. S. P. Zhdanov, Dokl. AN SSSR, 68, 99 (1949).
19. A. V. Kiselev, Dokl. AN SSSR, 98, 427 (1954).
20. S. P. Zhdanov, ZhFKh, 32, 699 (1958).
21. A. V. Kiselev and L. N. Soboleva, ZhFKh, 32, 49 (1958).
22. N. N. Avgul', O. M. Dzhigit, A. V. Kiselev, K. D. Shcherbakova, Dokl. AN SSSR, 92, 105 (1953).
23. A. A. Isirikyan and A. V. Kiselev, ZhFKh (in Print); J. Phys. Chem. 65, 601 (1961).

All abbreviations of periodicals in the above bibliography are letter-by-letter transliterations of the abbreviations as given in the original Russian journal. *Some or all of this periodical literature may well be available in English translation.* A complete list of the cover-to-cover English translations appears at the back of this issue.

INVESTIGATION OF INTERNAL STRESSES ON HARDENING OF POLYESTER RESIN

P. I. Zubov, L. A. Lepilkina, T. P. Gil'man, and A. Z. Leites

Polymer Division, Institute of Physical Chemistry
Academy of Sciences, USSR
Translated from Kolloidnyi Zhurnal, Vol. 23, No. 5
pp. 563-567, September, 1961
Original article submitted March 13, 1961

Unsaturated-polyester resins are widely used as film-forming agents in polymeric coatings, and also as binders in reinforced plastics [1]. It is well known from literature data that the strength of polyester-resin samples is greatly affected by the amounts of polymerization initiator and accelerator added in cold setting; the authors of these works explain this by a variable degree of hardening.

As is also well known [2], the greater the rate of hardening of polyester resins, the greater is their initial strength, and the less is their strength after aging. Presumably, however, the degree of hardening of the polyester resin is not the only factor determining the strength of the structure. From the experimental data given below, it follows that the strength properties of polyester resins are connected with internal stresses arising and relaxing during the formation and aging of these resins.

Dependence of Internal Stress in Hardened Slabs of Polyester Resin on the Material of the Form

Amount of accelerator, %	Amount of initiator, %	Internal stress, kg/cm²			Hardening time, days
		metal	glass	Ftoro-plast	
8	3	62.4	38.4	7.6	1.5
6	3	105.0	50.4	5.6	1.5
8	1	36.0	–	18.0	3.0
8	2	76.0	–	39.0	3.0
8	3	40.0	–	28.0	3.0
8	4	16.1	–	20.1	3.0

The effects of the initiator and accelerator concentrations on the magnitude of internal stresses and the physicomechanical parameters (modulus of elasticity, hardness, and tensile and bending strengths) of a polyester resin, were investigated in the present work.

In preparing the samples polyester resin with a variable content of initiator and accelerator was poured into 5 × 50 × × 120 mm forms and then hardened in air at 18-20°. After 3 days the samples were removed from the forms and examined. The samples were prepared from Type PN-1 polyester resin, synthesized from ethylene glycol and phthalic and maleic anhydrides and containing a polymerized solvent (styrene). Cumene hydroperoxide was used as polymerization initiator. An 8% solution of cobalt naphthenate was added to accelerate the reaction.

The first experiments showed that the maximum value of internal stress depends on the material of the forms; this is due to adhesion (table). The internal stresses were measured by means of an automatically-recording optical instrument, as before [3].

As is evident from the table, the lowest internal stresses arise in the case where the resin hardens in "Ftoroplast"-lined forms. In order to minimize stresses due to adhesion of the resin to the form, all subsequent experiments were performed with slabs of polyester resin hardened in Ftoroplast-lined forms. Adhesion of polyester resin to Ftoroplast is slight, and hence unformed slabs are easily peeled from the walls of the form.

The effect of the amount of accelerator, in the presence of a constant initiator content, on internal stresses in the resin samples is shown in Fig. 1. As is evident from Fig. 1a, the maximum internal stress is observed when the system contains 10-12% accelerator. For different lots of resin, differing in styrene content, the maximum is shifted toward a lower accelerator content.

An analogous dependence is observed for the modulus of elasticity of the resin (E) (Fig. 1b), which we deter-

mined by a dynamic method—through the velocity of ultrasonic waves therein, C. This was measured with an ultrasonic pulse apparatus (a modernized IKL-5 instrument). The vibration frequency was 800 kc, and the multiplying factor in scanning was 0.2 μsec.

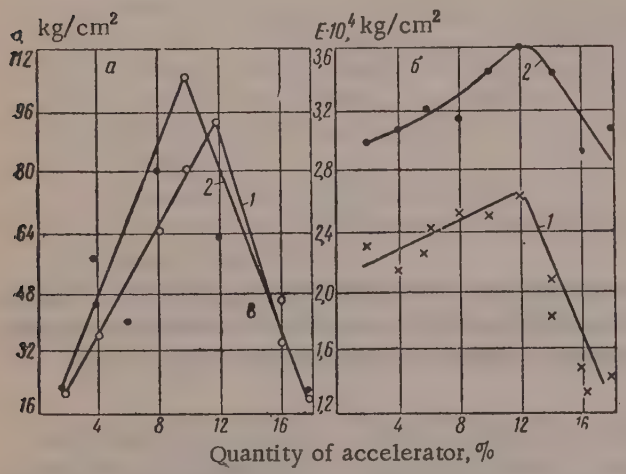


Fig. 1. Dependence of internal stress (a) and modulus of elasticity (b) in polyester resin samples on the amount of added accelerator for 3% initiator content: 1) After 3 days of hardening; 2) after 30 days.

The modulus of elasticity was calculated by the formula [4]

$$E = C^2\rho\frac{(1+\mu)(1-2\mu)}{1-\mu},$$

where μ is Poisson's coefficient and ρ is the density.

The dependence of the final modulus of elasticity of the resin on the accelerator content, shown in Fig. 1b, has a maximum at an accelerator content of about 12%. In this case the maximum stress corresponds to the maximum final modulus of elasticity (see Figs. 1a and 1b).

Curves of dependence of the internal stress of the resin on the amount of initiator for an accelerator content of 8% (Fig. 2) display maxima at 3% initiator content in the system. This occurs also for other mechanical characteristics: modulus of elasticity (Fig. 3), hardness (Fig. 4), tensile strength (Fig. 5), and bending strength (Fig. 6).

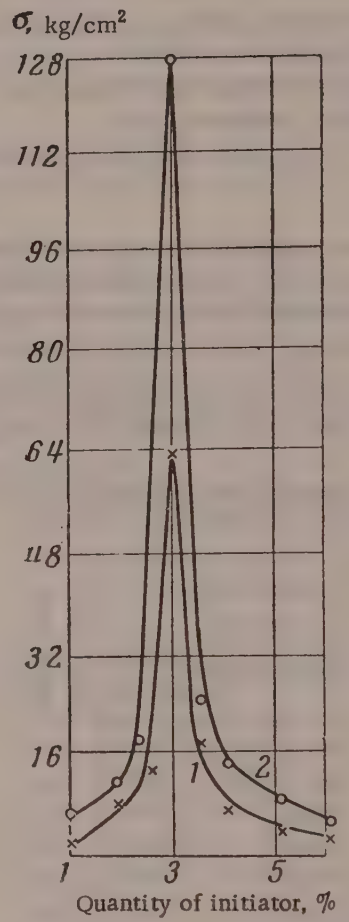


Fig. 2. Dependence of internal stress in polyester resin samples on the amount of added initiator for 8% accelerator content: 1) After 3 days of hardening; 2) after 120 days.

The hardness of the resin was measured in a super-Rockwell instrument at a load of 1.5-9 kg. The measurement was made after the indicator needle had come to rest (the load was maintained for 10-15 min; i.e., until the sphere completely stopped sinking in). The hardness was recorded both under load and after removing the load; the elastic and plastic deformations were measured.

The bending strength of the resin was tested in a Type 3F-25 instrument with a maximum load of 30 kg and a multiplying factor of 20 g and a breaking machine with 10-ton capacity. The data given in Figs. 3-6 correlate with the change of internal stress. The greatest tensile and bending strengths correspond to the maximum stresses, which are compressive ones. These data agree with the observations of other investigators [4], according to whom compressive stresses in materials promote increase in tensile and bending strengths. It follows from our data, however, that more-highly stressed samples of hardened polyester resin are less stable to aging than less-stressed ones.

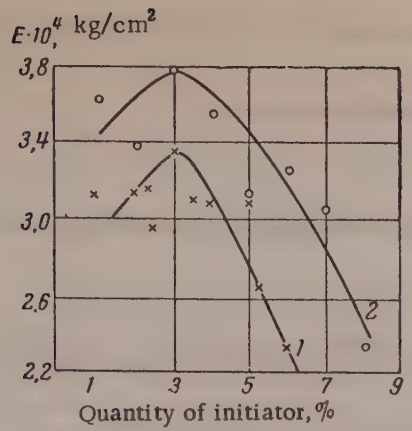


Fig. 3. Dependence of the modulus of elasticity of the resin on its initiator content: 1) After 3 days; 2) after 30 days.

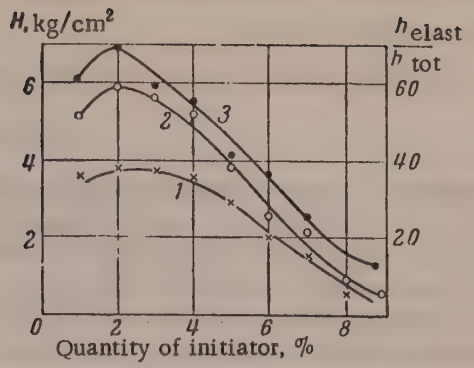


Fig. 4. Dependence of the hardness (H) after 30 days (1) and 15 days (2) of hardening, and the ratio h_{elast}/h_{tot} after 30 days of hardening (3) on the initiator content.

The presence of great stresses, amounting to 25-35% of the bending and tensile strengths, leads to the appearance of visible cracks at the edges of the resin samples. Relaxation of stresses, which takes place when the resin samples are heated (Fig. 7), increases the stability to aging.

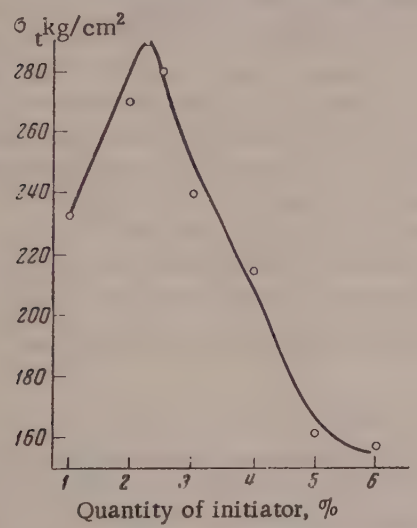


Fig. 5. Dependence of tensile strength on the initiator content in the resin after 30 days of hardening.

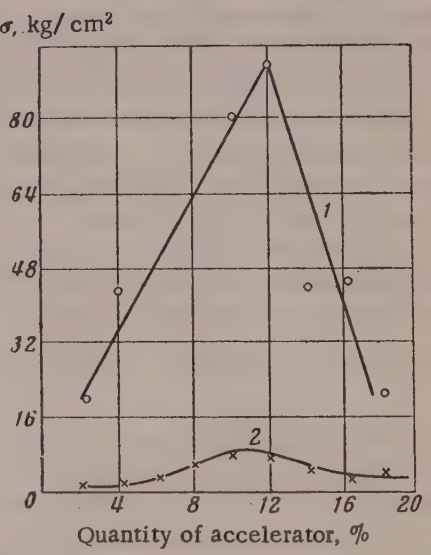


Fig. 7. Effect of annealing on internal stress: 1) After 30 days of hardening at 20°; 2) after heating for 3 hr at 75°.

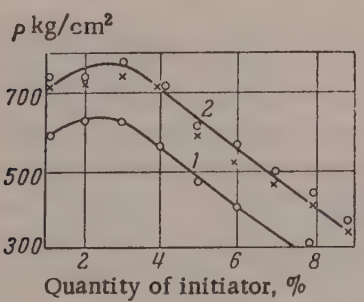


Fig. 6. Dependence of bending strength on the initiator content in the resin: 1) After 3 days; 2) after 30 days.

SUMMARY

1. The internal stresses and mechanical characteristics (modulus of elasticity, hardness, tensile and bending strengths), developed on hardening of polyester resins, depend on the conditions of hardening and display pronounced maxima on increase of the initiator and accelerator contents in the system.

2. The internal stresses and physicomechanical characteristics of polyester resins vary in parallel fashion, displaying maxima at the same initiator and accelerator concentrations.

3. More-stressed resin samples are less stable to aging: Stresses, amounting to 25-35% of the tensile strength, cause cracks to appear on aging.

4. Relaxation of internal stresses in polyester resins increase their stability to aging.

LITERATURE CITED

1. B. Berdtsson, L. Turunen, Kunststoffe 46, 1, 9, 1956; B. Parkyn, British Plastics 28, 1, 23, 1955; R. Kraft, VDI-Z 99, 12, 511, 1957; I. Cynisky, British Plastics 30, 10, 449, 1957.
2. I. Brydson, C. Weleh, Plastics 21, 229, 282, 1957.
3. P. I. Zubov and L. A. Lepilkina. Kolloidn. zh. 23, 418 (1961).
4. V. A. Kuz'menko. Zavodsk. labor. 14, 11, 1407 (1958); V. V. Bogorodskii. Transactions of the Seminar on Physics and the Use of Ultrasonics [in Russian] (1958), p. 76.
5. B. B. Pusey, Plastics Technology 3, 9, 721 (1957); N. Kylvert, The Engineer 10, 2, 522 (1957).

All abbreviations of periodicals in the above bibliography are letter-by-letter transliterations of the abbreviations as given in the original Russian journal. *Some or all of this periodical literature may well be available in English translation.* A complete list of the cover-to-cover English translations appears at the back of this issue.

FORMATION OF POROUS STRUCTURES IN ALUMINA-SILICA GELS

1. THE ROLE OF SYNERESIS IN THE FORMATION OF POROUS ALUMINOSILICATES

E. M. Kaganova, T. E. Shakhova and A. E. Panitkova

All-Union Scientific Research Institute of Petrochemistry, Leningrad
Translated from Kolloidnyi Zhurnal, Vol. 23, No. 5
pp. 568-573, September-October, 1961
Original article submitted May 22, 1960

The rate of reaction and the composition of the reaction products are largely dependent on the pore structure of the catalysts or adsorbents. To make a catalyst with a given pore structure the laws governing formation of gels must be known.

The connection between formation conditions and pore structure obtained in silica gels has been repeatedly emphasized by the authors of [1]. Similar studies have been made with alumina-silica gels [2]. According to one of the most widely held view [3], the formation of glassy silica gels proceeds by drying, and depends in the final analysis on the relation between the strength and elasticity of the gel skeleton and on the surface tension of the intermicellar liquid. The formation of glassy alumina-silica gels appears to take place in the same way. From this point of view, under conditions of constant drying and equal surface tension of the intermicellar liquid, the type of pore structure obtained depends only on the strength of the gel skeleton. The strength of the skeleton is dependant on the processes of dehydration and condensation occurring during syneresis of the silica and alumina gel micelles. Molecules, which when first formed are highly hydrated, are gradually condensed and lose water, and the bonds between molecules become stronger. Therefore syneresis determines the strength of the gel skeleton and must obviously play a decisive part in the formation of porous gel structures. Nonetheless, up to the present time little attention has been devoted to this process. In studies [4] of syneresis in silica gels, the effect on the final structure was not investigated.

The present communication is devoted to the part played by syneresis in formation of porous alumina-silica gels.

A glassy alumina-silica gel was prepared by continuous mixing of a stream of water glass with a stream of aluminum sulfate solution in sulfuric acid. The resulting sol was divided into streamlets which passed into a column filled with mineral oil, where they were broken up into droplets. After gelling the gel was in the form of spheres of diamter 8-9 mm. The gel was subjected to syneresis by heating in a closed vessel on a water bath. After syneresis the gel was activated with a solution of aluminum sulphate, washed, and dried in a drying oven at 110°, then calcined at 550° for four hours.

The specific surface was calculated from benzene adsorption isotherms. The distribution of pore radii was calculated from the desorption branch of the isotherm.*

As syneresis is accompanied by the expulsion of liquid** from the gel, the depth of penetration of syneresis could be taken as proportional to the total volume of liquid expelled, and the rate of syneresis derived from the slope of the graph of liquid expelled against time. By using these properties we have been able to show that the porous structure of aluminosilicates, under constant drying and calcination conditions, depends only on the depth of syneresis and is independant of formation conditions and treatment of the gel. This is to say that gels having identical structures can be derived by methods which differ greatly both in individual operations and in over-all method, so long as the syneresis conditions are chosen so that the depth of syneresis attained is the same in all cases. The many effects of different formation conditions of alumina-silica gels on their structure can be attributed to their effect on syneresis rate.

---

* Adsorption measurements were supervised by D. P. Dobychin.

** The liquid expelled from the alumina-silica gel or syneresis contained Na_2SO_4, SiO_2 and Al_2O_3. Depending on the initial concentration, Na_2SO_4 varied between 5 and 7%, SiO_2 between 0.01 and 0.02%, and Al_2O_3 between 0.001 and 0.005%.

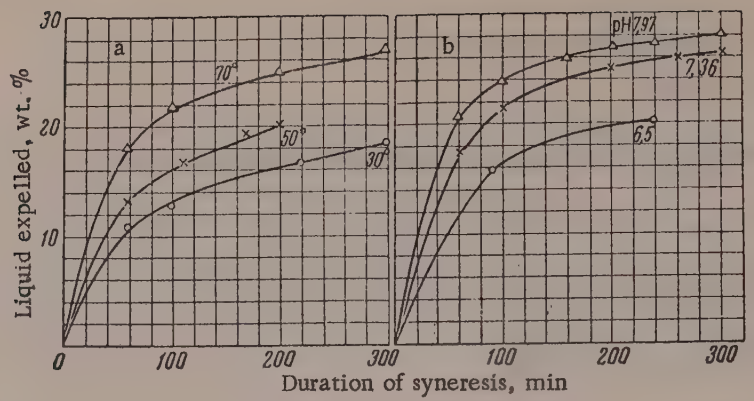


Fig. 1. Effect of temperature and pH of the sol on expulsion of liquid during syneresis.

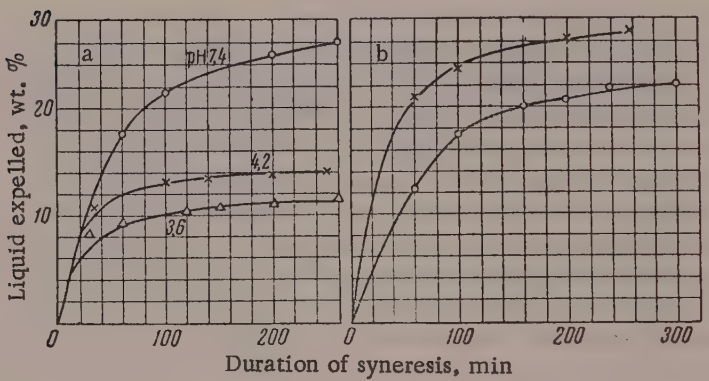


Fig. 2. Effect of (A) pH of medium in which syneresis takes place, and (B) Al_2O_3 content in the aluminosilicate, on amount of water expelled during syneresis. In (B), for X, Al_2O_3 = 5.7%; for O, Al_2O_3 = 7%

Increasing temperature (Fig. 1, A) and pH (Fig. 1, B) hastens expulsion of liquid. Rate of syneresis depends not so much on the pH of preparation of the gel as on the pH of the medium in which syneresis takes place. Normally, heating of the gel during syneresis takes place in the liquid which is expelled during this process and which has the same pH as the gel. If the gel is immersed in a liquid of different pH, after a while the rate of syneresis changes to correspond with the pH of the medium. The time for the new rate of syneresis to establish itself varies somewhat according to the size of the gel spherules, and appears to be equal to the time taken for the solution to diffuse through into the inside of the gel spherules. A gel which was prepared at pH 7.4 was immersed in liquids having pH 4.2 and 3.6. In both cases, within 15-20 minutes the separation of liquids slowed down, and the syneresis rate changed to correspond with the immersion medium (Fig. 2, A). To lower the pH to 4.2, the liquid expelled during syneresis was acidified with sulfuric acid, and to reduce the pH to 3.6, the gel was immersed in an aluminum sulfate solution.

We used this property of gels of changing the syneresis rate in accordance with the pH of the medium to stop syneresis at the desired stage. To arrest syneresis at a given depth, it was enough to immerse the gel in a solution of pH 3.2-3.6, after the appropriate quantity of liquid had been expelled.

Increasing the amount of alumina in the alumina-silica gel greatly slowed down liquid separation (Fig. 2, B). Increasing the concentration of the initial solution, which leads to an increase in the $SiO_2 + Al_2O_3$ content in the gel, but leaves the SiO_2-Al_2O_3 ratio constant, leads to an increase in total liquid expelled during syneresis under constant conditions (Fig. 3). This agrees with the results of Lipatov [5], who established that the quantity of liquid expelled during syneresis increased with increasing concentration. If the weight of expelled liquid is related, not to the

initial weight of the gel, but to the sum of weights of $SiO_2 + Al_2O_3$ in the gel, then it appears that expulsion of liquid is identical under the same conditions of syneresis from gels derived from solutions of differing concentrations and containing different weights of $SiO_2 + Al_2O_3$ (Fig. 3, curve 3). The structure of alumina-silica gels prepared from sols with different $SiO_2 + Al_2O_3$ concentrations is the same if the same amount of liquid, expressed as a percent-

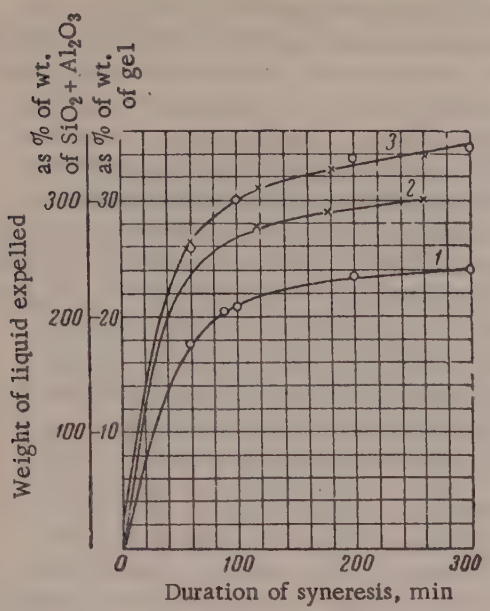


Fig. 3. Effect of $SiO_2 + Al_2O_3$ concentration in the gel on expulsion of water during syneresis. 1) $SiO_2 + Al_2O_3$ = 6.9% of weight of initial gel; 2) the same but = 9%; 3) weight of water expelled from specimens 1 and 2 during syneresis, expressed as a percentage of the weight of $SiO_2 + Al_2O_3$ in the gel.

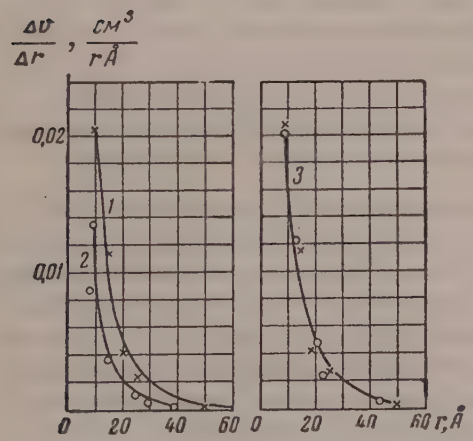


Fig. 4. Effect of concentration of $SiO_2 + Al_2O_3$ (with $SiO_2 : Al_2O_3$ ratio constant) in alumina-silica gels on pore structure. 1) $SiO_2 + Al_2O_3$ = 6.9%; 2) $SiO_2 + Al_2O_3$ = = 9%; 3) as 1 and 2 6.9 and 9% equals amounts of liquid, expressed as a percentage of $Al_2O_3 + SiO_2$ in the gel, were expelled during syneresis.

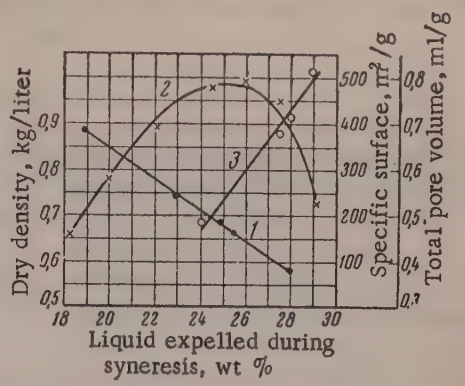


Fig. 5. Effect of depth of syneresis on aluminosilicate structure. 1) Dry bulk density; 2) specific surface; 3) total pore volume.

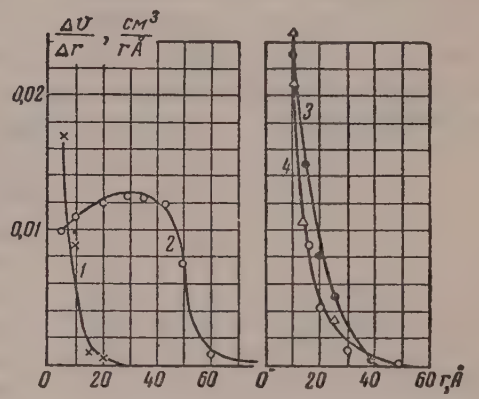


Fig. 6. Effect of syneresis temperature on pore structure of alumina-silica gels. d = = dry density, kg/liter; s = specific surface, m^2/g. 1) 20°, d = 0.86, s = 230; 2) 70°, d = = 0.54; 3) 70°, d = 0.68, s = 500; 4) 30° and 50°, d = 0.74, s = 455 and 445.

age of the sum of SiO_2 and Al_2O_3 in the gel, separated during syneresis (Fig. 4, curve 3). If syneresis takes place in gels with differing $SiO_2 + Al_2O_3$ concentrations, in such a way that the liquid expelled makes up the same percentage of the initial weight of the gel, then the aluminosilicates will have different structures (Fig. 4, curves 1 and 2). This shows that the property which we took tentatively as expressing depth of syneresis, i.e., percentage of liquid expelled during syneresis expressed as a percentage of the initial weight of the gel, does not reflect the true nature of processes occurring during syneresis. It is more correct to relate liquid expelled to the weight of $SiO_2 + Al_2O_3$ in the gel. However for gels derived from solutions with the same initial concentrations (those most frequencly met with in practice), it is convenient to express expelled liquid as a percentage of total gel weight.

Fig. 5 shows the relation between depth of syneresis and structure of the aluminosilicate. The smaller the depth of syneresis, the higher the density and the finer the pores. The specific surface passes through a maximum at a density of 0.6-0.7. On further increasing depth of syneresis, formation of coarse pores is accompanied by a drop in specific surface. It does not appear possible to make a coarse-pored alumina-silica gel with a high specific surface by increasing the depth of syneresis. To achieve this the surface tension os the intermicellar liquid must be lowered during drying. Using these results we can explain satisfactorily the changes in pore structure observed in aluminosilicates on changing formation conditions. An increase in syneresis temperature, keeping all other conditions constant, leads to a coarse-pored structure. Since syneresis rates increase with temperature, the same time of syneresis at different temperatures causes different depths of syneresis and the gel specimens have different pore structures (Fig. 6, curves 1 and 2). If the times of syneresis at different temperatures are chosen in such a way that the same depth of syneresis is obtained, then the specimens will have practically identical pore structures (Fig. 6. curves 3 and 4).

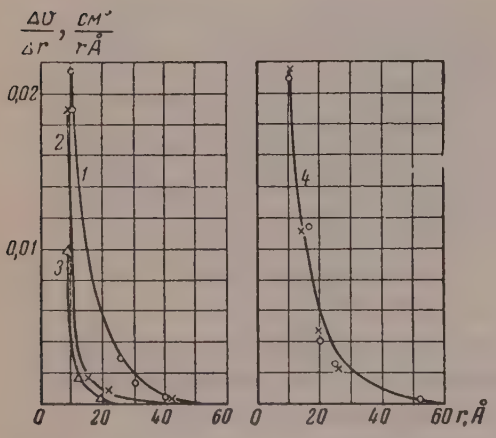


Fig. 7. Effect of pH on alumina-silica gels. d = dry density, kg/liter. s = specific surface, m^2/g. 1) pH = 7.4, d = 0.75, s = 360; 2) pH = = 6.5, d = 0.9, s = 240; 3) pH = 5.9, d = 0.92, s = 160; 4) pH = 7.4, 6.5 and 5.9, syneresis continued to the same depth.

A number of investigators have studied the effect of pH during gelling, and the effect of the pH of water used to wash silica gel, and have established that increase in pH leads to a more coarsely-pored structure [6]. We have observed that pH has the same effect on alumina-silica gels.

The volume distribution is plotted against effective radius in Fig. 7 for alumina-silica gels obtained at various pH values, and shows that an increasing pH the larger diameter pores increase in volume. Syneresis of these specimens was carried out under identical conditions, so the changes in syneresis rates due to different pH values leads to different depths of syneresis. Using the water expulsion curves for syneresis at various pH values (Fig. 1), syneresis times can be chosen for gels made at different pH values so that all achieve the same syneresis depth. In this case pH appears to have no effect on alumina-silica gel structure. Specimens made at different pH have identical structures (Fig. 7, curve 4). The same effect is observed when constant syneresis depth is achieved, in specimens made at different pH, by altering syneresis temperatures or by immersion in a medium of diferent pH.

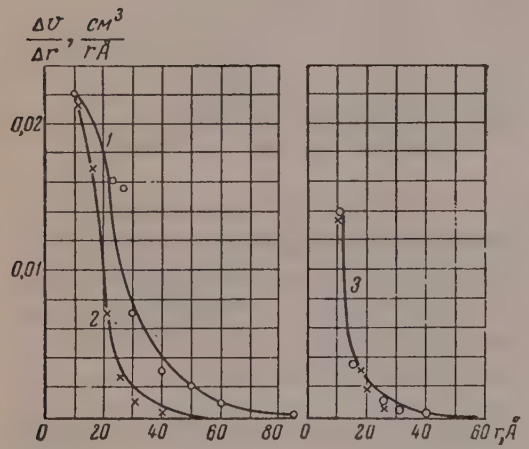


Fig. 8. Effect of Al_2O_3 content on pore structure in aluminosilicates $SiO_2 + Al_2O_3 = 100\%$. 1) 9.2% Al_2O_3, d = 0.57, s = 168; 2) 12.8% Al_2O_3, d = 1.0, s = 26; 3) 9.2 and 12.8% Al_2O_3, syneresis continued to the same depth.

Increasing alumina content in the aluminosilicate while keeping constant syneresis conditions leads to a fine-pored structure (Fig. 8). We noted above that the liquid expulsion rate falls with increasing Al_2O_3 content (Fig. 2, B). Thus under identical syneresis conditions, increasing alumina content in the alumina-silica gel will decrease the depth of syneresis, and the resulting structure will become more finely-pored. However, the gels will have identical structures if syneresis conditions bring about the same depth of syneresis (Fig. 8, curve 3).

SUMMARY

1. The role of syneresis in the formation of porous alumina-silica gel structures was studied, and it was shown that under constant conditions of drying and calcination the pore structure is determined by the depth of syneresis.

2. The depth of syneresis is satisfactorily expressed by the weight of expelled liquid given as a percentage of the initial weight of the gel or of the weight of $SiO_2 + Al_2O_3$ in the gel.

3. On increasing the depth of syneresis, the dry bulk density decreases, and the total pore volume and coarse pore volume increase. The specific surface passes through a maximum at a dry bulk density value of 0.6-0.7 kg/liter, as the depth of syneresis changes.

4. Syneresis rates increase with increase in temperature, pH of the gel, or pH of the medium in which the gel is immersed during syneresis, but decrease as the alumina content is raised.

LITERATURE CITED

1. M. O. Kharmadar'yan, V. K. Markov, Zhur. Fiz Khimii, 5, 165, (1934); I. E. Neimark, I. B. Slinyakova, Kolloidn. Zhur, 15, 277 (1953); K. S. Sing, J. D. Modeley, J. Appl. Chem. (London), 3, 549 (1953); K. Gartner, R. Griessbach, Kolloid. Zeit., 160, 21, (1958); F. Wolf, H. Beyer, Kolloid. Zeit., 165, 151, (1959).
2. G. J. Plank, L. C. Drake, J. Colloid. Sci. 2, 399, (1947).
3. V. S. Veselovskii, N. A. Selyaev, Zh. Fiz. Khimii, 6, 1171, (1935); I. E. Neimark, F. I. Khatset, Kolloidn. Zhur., 9, 289, (1947); G. K. Boreskov, M. S. Borisova, O. M. Dzhigit, V. A. Dzis'ko, V. P. Dreving, A. V. Kiselev, O. A. Likhacheva, Zhur. Fiz Khimii, 22, 603, (1948).
4. J. Fergusen, M. P. Applebey, Trans. Faraday Soc. 26, 642, (1930); H. Freundlich, J. Phys. Chem. 41, 901, (1937).
5. S. M. Lipatov, High polymer compounds [in Russian] (Acad. Sci. Belorus. SSR, 1943).
6. I. E. Neimark, P. Ya. Sheinfain, Kolloidn. Zhur., 15, 45, (1953); I. E. Neimark, I. B. Slinyakova, Kolloidn. Zhur., 18, 219, (1956); 20, 84, (1958).

All abbreviations of periodicals in the above bibliography are letter-by-letter transliterations of the abbreviations as given in the original Russian journal. *Some or all of this periodical literature may well be available in English translation.* A complete list of the cover-to-cover English translations appears at the back of this issue.

INFRARED STUDY OF THE ADSORPTION OF BENZENE AND HEXANE ON SILICA

A. V. Kiselev and V. I. Lygin

Moscow University Chemical Department
Institute of Physical Chemistry, Academy of Sciences USSR
Translated from Kolloidnyi Zhurnal, Vol. 23, No. 5,
pp. 574-581, September-October, 1961
Original article submitted June 30, 1960

For some time past, infrared spectroscopy finds an ever wider application for studying physical and chemical adsorption (see the reviews [1, 2]). The results of spectral investigations may be used both for conjecturing the structure of chemical surface compounds and for calculating the thermodynamic functions in connection with the problem of determining adsorption equilibria only from properties of the adsorbent-adsorbate system [3, 4]. In order to calculate the thermodynamic functions of adsorbed substances one must know the characteristics of the motion of the adsorbate molecule on the surface or, more accurately speaking, the characteristics of the motion in the adsorbed complex of adsorbate-adsorbent. In the case of localized adsorption one must know the frequencies of the molecular vibrations and rotations in the adsorptive complex and also have information on the distribution of the adsorbate molecules over the surface. In the case of nonlocalized adsorption one must know those same frequencies and at the same time have information on the migration of molecules along the surface. In the presently existing papers [5] the entropy calculations have only been based on quite arbitrary assumptions on the character of the molecular motion along the surface and on the possible vibration and rotation frequencies of adsorbed molecules. There are only individual attempts to estimate the vibration frequencies of adsorbed molecules from the theoretically calculated functions of their potential energy on the surface [6, 7].

Besides from the direct spectrum of adsorbed molecules, some information on the state of the molecules may also be obtained from the changes, as are observed in adsorption, in the spectra of the chemical functional groups in the surface of the adsorbent. In this the displacement of the adsorption band of the superficial functional groups in adsorption may indicate that these groups participate in the formation of adsorptive complexes and the magnitude of the shift gives an indication on the strength of the bond in these complexes. The spectrum of the adsorbed molecules themselves may point out which part is bonded to the superficial group. The very fact that in the infrared spectrum of adsorbed molecules there appear adsorption bands which usually are only active in combined excitation enables one to draw conclusions on the character of the perturbation in the adsorbed molecule, the redistribution of its charge and the change of its symmetry. One may get information on the nature of the rotations of the adsorbed molecules in the field of the adsorbent by investigating the fine structure of the adsorption bands. The study of the spectrum in the far infrared allows one to determine the vibration and rotation frequencies of the molecules with respect to the adsorbent surface.

The majority of the presently published spectral studies is devoted to investigating the nature of the interaction between the adsorbed molecules and the superficial hydroxyl groups of silica [1, 8-10]. In a smaller number there are published studies on the change in the molecular spectra observed in adsorption [11-13]. The fine structure of the adsorption bands of adsorbed molecules has only been studied for a very limited number of molecules [14]. As yet, the problem of investigating the spectra of molecular vibrations and rotations with respect to the surface has only been raised [4, 15]. Moreover, in most cases the spectral investigations were carried out isolatedly and were not compared with the results of a determination of adsorption equilibria and adsorption heats.

We have already noted [4] that nowadays it is necessary to study systematically the state of the adsorbed complexes by the methods of statistical thermodynamics (see [7]) while attracting the results of spectral studies. In the paper [4] we attempted to estimate from spectral data the entropy of water adsorbed on hydrated silica surfaces.

In the present study we undertook to investigate the state of adsorbed benzene and hexane, which, although they contain an equal number of carbon atoms, have very different chemical structures and different adsorptive

properties. For this purpose we investigated the change in the spectrum of superficial OD groups of aerosil at various surface coverages and estimated the entropy of adsorbed benzene and hexane. The observed perturbative action of the adsorbed molecules on the superficial OD groups was compared with the heats of adsorption. The study is an extension of our spectral investigation into the structure of superficial chemical compounds [16] and the nature of the adsorption bond [17, 18].

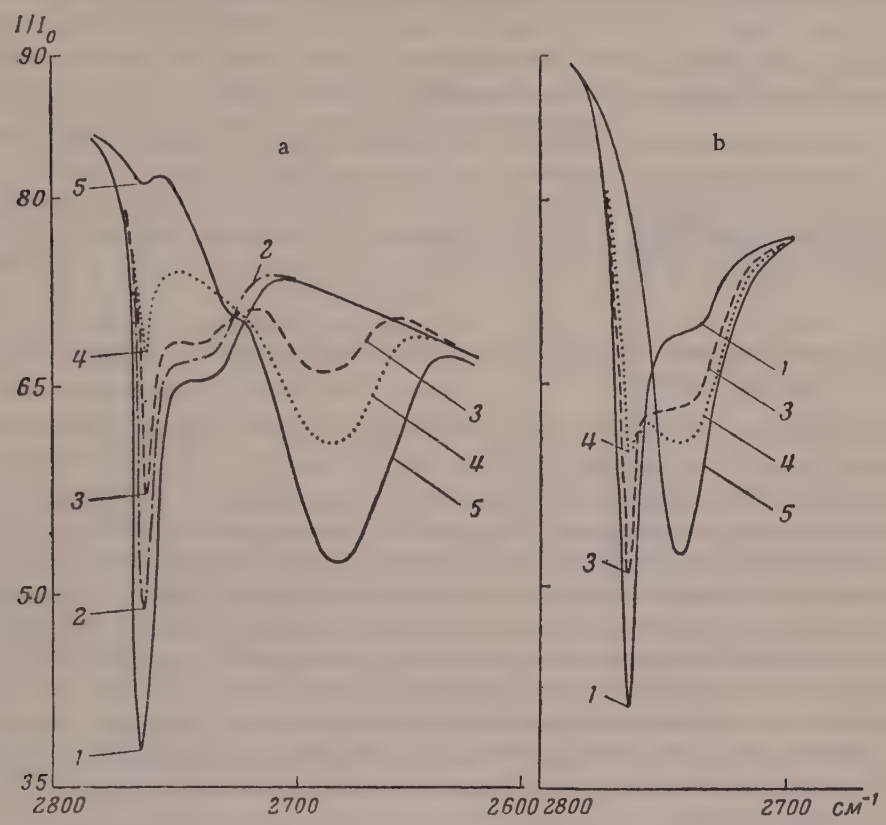


Fig. 1. Spectrum of aerosil containing OD groups on its surface and outgassed at 200° during six hours (1); that after adsorption of benzene (a) and hexane (b) to coverages of 0.1 monolayer (2), 0.5 monolayer (3) and a complete monolayer (4); that for capillary condensation (5).

As adsorbent we chose aerosil with a specific surface area of 170 m^2/g. By applying saturated vapor pressures and using the adsorption isotherms obtained in the papers [19, 20] the aerosil surface was covered to the required degree with hexane or benzene molecules. The aerosil samples for the spectral investigation were prepared in the form of discs with 25 mm diameter and 20 mg/cm^2 weight and were obtained by pressing aerosil at a pressure of 20 kg/mm^2. The vacuum treatment of the sample, the adsorption of vapors and the taking of the spectrum were done in the vacuum cell (which was described previously in the papers [17, 21]) in the single beam spectrometer IKS-12 with a LiF prism.

Adsorption of infrared radiation by water vapor in the atmosphere encumbers the study of the changes in the spectra of the superficial hydroxyl groups of aerosils. Therefore, we investigated the interaction between benzene or hexane and the OD groups of a completely deuterated aerosil sample. Aerosil was deuterated by repeatedly admitting D20 vapor to the cell and pumping it off. The extent to which the OH groups were replaced by OD was checked spectrally. In the 2600 cm^{-1} range the slit width was 4 cm^{-1}.

The interaction of adsorbed benzene and hexane molecules with hydroxyl groups in the surface of silicas. In Fig. 1, a the adsorption specta of superficial OD groups of aerosil at various coverages of the surface by adsorbed benzene molecules are shown. In the spectrum of the original aerosil sample outgassed at 200° in a vacuum of 10^{-5} mm Hg during six hours (Fig. 1, a, curve 1) the sharp intensive 2760 cm^{-1} band of free OD groups in the surface of

aerosil is observed [16-18]. The asymmetric absorption band on the long-wave side is explained by the superposition of the band originating from superficial OD groups mutually interacting under the formation of a weak hydrogen bond [16-18]. Adsorption of benzene to a degree of coverage of ~ 0.1 monolayer results in a lowered intensity of the 2760 cm^{-1} band (Fig. 1, a, curve 2). Raising the adsorption of benzene to a degree of coverage of about 0.5 still further decreases the intensity of the 2760 cm^{-1} band and gives rise to the appearance of a broad band at 2670 cm^{-1}. (Fig. 1, a, curve 3). When the surface is covered by a monolayer of benzene molecules, only a weak adsorption band is left at 2760 cm^{-1} (Fig. 1, a, curve 4), but the intensity of the 2670 cm^{-1} band increases still further. In polymolecular adsorption and capillary condensation of benzene in the spaces between the particles of the pressed aerosil one observes only the broad 2670 cm^{-1} band (Fig. 1, a, curve 5).

A qualitatively similar change in the spectrum of the superficial groups is observed, when hexane is adsorbed on aerosil (Fig. 1, b). When the surface is covered by ~ 0.5 monolayer (Fig. 1, b, curve 3) or by a complete monolayer of hexane (Fig. 1, b, curve 4) the intensity of the 2760 cm^{-1} band of the free groups in aerosil is lowered, a band at 2734 cm^{-1} appears and gets a higher intensity, respectively. At coverages corresponding to polymolecular adsorption and capillary condensation of hexane vapor, only the band at 2734 cm^{-1} is left in the spectrum (Fig. 1, b, curve 5).

In all cases pumping off the adsorbed vapors has the result that the new bands disappear and the original intensity of the 2760 cm^{-1} band is reestablished.

Thus, the data obtained show that the shift of the OD absorption band at the adsorption of benzene amounts to 90 cm^{-1} and considerably surpasses the band shift at the adsorption of hexane, which is only 26 cm^{-1}.* The fact that adsorbed benzene and hexane molecules have a different effect on the superficial hydroxyl groups is explained by the difference in the character and the energy of the interaction between these molecules and the hydroxyl groups. In the case of hexane, just as for other saturated hydrocarbons and for molecules with a spherically symmetric shell, the small band shift is essentially caused by electrokinetic (dispersion) forces. This is indicated by the fact that the heat and the isotherm of n-hexane remains unchanged, when the silica surface is dehydrated [19]. However, the heat and isotherm of benzene adsorption drop sharply, when the silica surface is dehydrated; on a hydrated silica surface the heat of benzene adsorption is higher than that of hexane [19]. The high adsorption heat and the greater perturbation of the superficial hydroxyl groups by the adsorption of benzene may be explained by the strong interaction between the dipoles of the superficial hydroxyl groups and mainly the π-electrons of the benzene molecule, which together with the carbon ring form a three-dimensional quadrupole [23].**

However, this interaction is much weaker than the normal hydrogen bond which adsorbed water molecules form with the superficial hydroxyl groups. The adsorption band shift of the superficial OD groups of silica at the adsorption of water amounts to ~ 260 cm^{-1}.

There is a certain parallelism between the adsorption band shifts of the superficial OD groups of silica and the heats of adsorption for the vapors of water, benzene and n-hexane. These values are compared in Table 1 where the differential heat of adsorption at mean coverage of the surface is given both per mole (Q_a) and per unit surface area occupied (Q_a) [25].

The conformity between the sequence of the adsorption band shifts $\Delta\nu$ of the superficial groups and that of the adsorption heats of water, benzene and n-hexane is particularly clearly manifested, if the shifts $\Delta\nu$ are compared with the differential heats of adsorption not calculated per mole (Q_a) but expressed per unit surface area occupied by these molecules (Q_a). The determination and the interpretation of the quantitative relation between $\Delta\nu$ and the adsorption energies should be the object of further studies.

Estimation of the extent to which the adsorbed molecules are localized on the silica surface. A further examination of the extent to which the molecules of benzene and hexane are localized on the hydroxyl groups of the silica surface is of great interest. It has been established previously [4] that, in accordance with spectral data and an ap-

---

* The adsorption band shift in the overtone region for the OH groups of porous glass at adsorption of benzene and n-hexane amounts to 236 cm^{-1} and 70 cm^{-1} [1]; in the main spectral region at the adsorption of benzene on porous glass [11] and on aerosil [9] it amounts to 110 cm^{-1}, but the adsorption band shift at the adsorption of cyclohexane on aerosil is 34 cm^{-1} [9].

** On a dehydrated silica surface and, particularly, on a graphite surface the adsorption heat of benzene is smaller than that of hexane [22].

proximate estimate of the adsorption entropy, adsorbed water molecules may be considered to be localized on the superficial hydroxyl groups. As long as there are no direct data on the character of the vibrations and rotations on the silica surface, the solution of the problem to which degree benzene and hexane are localized may help to estimate the entropy of these substances for their various degrees of freedom in the adsorbed state. The mean molar entropy change, as was obtained experimentally in the papers [9], for benzene at the completion of half a monolayer amounts to 20,7 eu, when it is referred to the standard state of an ideal gas (P° = 1 atm; T = 298° K). Since under

TABLE 1. Comparison of the Adsorption Band Shifts for the Superficial OD Groups of Silica with the Differential Heats of Adsorption per Mole Q_a and Those per Unit Surface Area Covered by the Molecules Q_s in Half a Monolayer

Substance adsorbed	Water	Benzene	n-hexane
Differential heat of adsorption on the hydrated silica surface, Q_a. kcal/mole	12.5	10.2	8.5
For the same surface, Q_s, erg/cm^2	800	150	100
Shift of the adsorption band of the superficial hydroxyl groups at adsorption, $\Delta\nu$, cm^{-1}	260[17]	90	26

standard conditions the entropy of gaseous benzene is 64.4 eu [26], the molar entropy of adsorbed benzene at half a monolayer coverage amounts to 43.7 eu. Taking into account that a benzene molecule has the principal moments of inertia $J_A = 2.906\ 10^{-38}$ g cm^2, $J_B = J_C = 1.453\ 10^{-38}$ g cm^2 and the symmetry number 12 [26] one may calculate the entropy pertaining to the various degrees of freedom for the molecular motion when one uses the formulas given in the review paper by Kemball [5]. In this we confine ourselves to a calculation for nonlocalized adsorption, since an estimate for localized adsorption gives a too small entropy value for adsorbed benzene and hexane.

TABLE 2. Estimated Entropies of Benzene Adsorbed on a Silica Surface at the Standard Degree of Coverage $\theta = 0.5$ (P° = 1; T = 298° K).

Kinds of molecular motions	Entropy values, eu			
	translational	rotational	total	loss
Three-dimensional translation and rotation around three axis	38.5	21.0	59.5	0.0
Two-dimensional translation without rotation	30.9	0.0	30.9	28.6
Two-dimensional translation with rotation in the plane of the ring	30.9	4.0	34.9	24.6
Two-dimensional translation, rotation in the plane of the ring and around one of the axis lying in this plane	30.9	11.8	42.7	16.8
Two-dimensional translation with rotation around all three axis (unhindered)	30.9	21.0	51.9	7.6

In the calculation of the translational entropy the area occupied by an adsorbed molecule was taken to be 49 A^2 [19].*

* This value was determined [19] by formally applying the BET method. In the strong adsorption on a graphitized carbon black W_m for benzene is 40 A^2 and for hexane 51 A^2 [27].

For rotation of a benzene molecule only in the plane of its ring the symmetry number should be taken equal to six [26].

The results of the calculations are given in Table 2.

The experimental entropy loss at adsorption 20.7 eu lies between the value calculated for molecules showing two-dimensional translation and rotation only in the plane of the ring and that for molecules which, moreover, rotate around one of the axis lying in the plane of the ring. But as yet, the accordance noted is very rough, because approximate formulas were used, the surface is inhomogeneous, other kinds of motions (not taken into consideration) exist and the rotations may even be hindered. In particular, the vibration of benzene in the direction perpendicular to the surface has not been taken into account. If, on the contrary, this is done, one comes to the conclusion that the molecular motions considered above and, in particular, the rotation around the axis lying in the plane of the ring are hindered.

The motion of adsorbed hexane molecules on the silica surface is less hindered than that of benzene molecules. The mean molar adsorption entropy which we obtained experimentally in [19] for hexane on silica gel at half a monolayer coverage and referred to the standard state (P° = 1 atm; T = 298°K) amounts to 21.1 eu. The entropy of hexane in its standard state is 92.4 eu [28]. Hence it follows that the molar entropy of adsorbed hexane is equal to 71.3 eu, that is, it surpasses considerably the entropy of adsorbed benzene (43.7 eu). This indicates that the hexane molecules are more mobile on the hydrated surface of silica. The observed difference in the entropy values (and consequently, in the mobility) of adsorbed benzene and hexane will be still greater, if from the obtained value for hexane one excludes the entropy loss connected with the hindering of the internal vibrations and compares such entropies of adsorbed molecules, as originate only from external motions of the molecules as a whole along the surface. At present it is impossible to estimate that part of the adsorption entropy which pertains to the internal rotations of hexane. It is only possible to estimate the total adsorption entropy pertaining to the external rotations of the molecules and to the internal rotations of the groups.

The molar entropy of n-hexane (at $\theta = 0.5$) pertaining to one translation degree of freedom, as is found by subtracting the calculated (under the assumption that the area occupied by a n-hexane molecule is equal to 70 A^2 [19]) entropy for two-dimensional translation (31.9 eu) from that for three-dimensional translation (39.2 eu), amounts to 7.3 eu. This latter value does not give the experimentally found molar loss in entropy at the adsorption of half a monolayer (21.1 eu). Since the small absorption band shift of the hydroxyl groups at adsorption of hexane and the low heat of adsorption indicate that the interaction of hexane with the surface is weak and, consequently, the two-dimensional translation is very free, the rest of the entropy loss, namely 13.8 eu, is connected with a change in the external and internal rotations. As yet, it is impossible to make out which is the hindering effect of the surface forces on the external rotations of the entire molecule and the internal rotation of the CH_3 groups of hexane. But it is quite arbitrary to explain, as is done in [26], the entropy loss at adsorption of molecules with a long chain by coiling, since the adsorptive field would rather uncoil these molecules.

Our study of the state of the adsorbed molecules on silica surfaces is quite rough, because we use approximate formulas, choose simplified models and do not take into account the molecular vibrations on the surface, the inhomogeneity of the surface and the mutual interaction between the molecules. A further study on the molecular motions on the surface should be directed to deepen our knowledge of the adsorbent surface structure and improve theory as well as to get more accurate data on the mobility of adsorbed substances, chiefly by means of infrared spectroscopy. For this purpose we hope to investigate in the future the spectrum of adsorbed benzene and hexane molecules themselves.

An investigation into the spectrum of the skeleton vibrations of hexane would give information on the change in the molecular shape caused by adsorption and a study of the torsion vibrations of the methyl groups would give information on the effect of the force field on internal vibrations. On the effect which the force field of the surface has on the external rotations one might get insight by comparing experimental and calculated adsorption entropies for a homologous series of compounds with ever more complex structures so that internal rotations become involved. In the case of benzene, which has a stronger interaction with the superficial hydroxyl groups, the study of the spectrum enables one to get information on the change in its internal structure, as was observed at the adsorption of benzene on ionic adsorbents [13].

SUMMARY

1. The change in the infrared spectrum of the superficial OD groups of aerosil has been studied in the main

spectral region for various coverages of the surface by adsorbed benzene and hexane molecules. The shift in the absorption band of free OD groups considerably exceeds that found at adsorption of hexane.

2. A correspondence has been noted between the sequence of the shifts in the absorption bands of OD groups at adsorption of water, benzene and hexane and the sequence of their differential heats of adsorption.

3. For various mobility models of nonlocalized adsorbed molecules the entropies of benzene and hexane on a hydrated silica surface have been estimated. The values obtained have been compared with the experimental data. It has been noted that in the sequence: hexane, benzene, and water, the mobility of the adsorbed molecules is lowered ever more.

LITERATURE CITED

1. A. N. Terenin, Collection: Superficial Chemical Compounds and Their Role in Adsorption Phenomena [in Russian] (Moscow State University Press, 1957), p. 206; Collection: Problems of Kinetics and Catalysis Vol. 10 [in Russian] (Acad. Sci. USSR Press, 1959), p. 214
2. R. P. Eischens, W. A. Pliskin, Advances in Catal. and Related Subject 10, 2, (1958); N. Sheppard, Spectochim. acta 14, 249 (1959).
3. A. V. Kiselev, Vestnik AN SSSR, 10, 43 (1957); Zh. fiz. khimii, 35, 233 (1961).
4. A. V. Kiselev and V. I. Lygin, Kolloidn. Zh. 23, 157 (1961)
5. C. Kemball, Collection: Catalysis. Problems and Investigation Methods [Russian translation] (IL, 1955), p. 256; T. Nayakawa, Bull. Chem. Soc. Janan, 30, 124, 236, 243 (1957).
6. A. D. Crowell, J. Chem. Phys. 26, 1407 (1957).
7. A. V. Kiselev and D. P. Poshkus, Dokl. AN SSSR, 132, 876 (1960); 139, 1145 (1961).
8. L. N. Kurbatov and G. G. Neuimin, Dokl. AN SSSR, 68, 341 (1949); N. G. Yaroslavskii and A. N. Terenin, Dokl. AN SSSR, 66 , 885 (1949); N. G. Yaroslavskii, Vestnik LGU, No. 3, 55 (1950); N. G. Yaroslavskii and A. V. Karyakin, Dokl. AN SSSR, 85, 1103 (1952); V. N. Filimonov, Optika i spektroskopiya, 1, 490 (1956); V. A. Nikitin, A. N. Sidorov and A. V. Karyakin, Zh. fiz. khimii, 30, 117 (1956).
9. R. S. McDonald, J. Amer. Chem. Soc. 79, 850, (1957); J. Phys. Chem. 62, 1168, (1958).
10. D. J. C. Yates, N. Sheppard, C. L. Angell, J. Chem. Phys. 23, 1980, 1955; M. Folman, D. J. C. Yates, Proc. Roy. Soc. A246, 32, (1958); Trans. Faraday. Soc. 54, 11, (1958); J. Phys. Chem, 63, 183, (1959); H. A. Benesi, A. C. Jones, J. Phys. Chem. 63, 179, (1959).
11. A. N. Sidorov, Dokl. AN SSSR, 95, 1235 (1954); Zh. fiz. khimii, 30, 995 (1956); A. N. Sidorov and A. N. Terenin, Optiko-mekhanicheskaya prom-st', 1, 1 (1959).
12. T. Yoshino, J. Chem. Phys. 23, 1564, (1955).
13. G. Karagonnis, O. Peter, Z. Electrochem, 61, 827, (1955); 63, 1120, (1959).
14. N. Sheppard, D. J. C. Yates, Proc. Roy. Soc. A238, 69, (1956); R. P. Eischens, W. A. Pliskin, Advances in Catal. and Related Subject 9, 662, (1957).
15. G. L. Kington, "The Structure and Properties of Porous Materials", London (1958); p. 247; G. J. Frohnsdorf, G. L. Kington, Proc. Roy. Soc. A247, 469, (1958).
16. A. V. Kiselev and V. I. Lygin, Proc. of the Second Intern. Congr. on Surf. Activity, London, Vol. 2, (1957), p. 204; V. I. Lygin, Vestnik Moskovskogo univ. No. 1, 223, (1958); V. I. Lygin, N. V. Kovaleva, N. N. Kavtaradze and A. V. Kiselev, Kolloidn. zh. 22, 334 (1960); A. V. Kiselev and V. I. Lygin, Kolloidn. zh. 21, 581 (1958).
17. A. V. Kiselev and V. I. Lygin, Kolloidn. zh. 22, 403 (1960).
18. V. I. Lygin and A. V. Kiselev, Kolloidn. zh. 23, 299 (1961).
19. A. A. Isirikyan and A. V. Kiselev, Dokl. AN SSSR, 115, 343 (1957); A. A. Isirikyan and A. V. Kiselev, Zh. fiz. khimii, 32, 679 (1958); L. D. Belyakova and A. V. Kiselev, Dokl. AN SSSR, 119, 298 (1958).
20. I. Yu. Babkin, V. S. Vasil'eva, I. V. Drogaleva, A. V. Kiselev, A. Ya. Korolev and K. D. Shcherbakova, Dokl. AN SSSR, 129, 131 (1959); I. Yu. Babkin, A. V. Kiselev and A. Ya. Korolev, Dokl. AN SSSR, 136, 373 (1961); A. V. Kiselev, A. Ya. Korolev, R. S. Petrova and K. D. Shcherbakova, Kolloidn. Zh. 22, 671 (1960).
21. N. N. Kavtaradze and V. I. Lygin, Zh. fiz. khimii, 34, 462 (1960).
22. N. N. Avgul', G. I. Berezin, A. V. Kiselev and I. A. Lygina, Izv. AN SSSR, Otd. Khim. n. 1956, 1304.
23. A. V. Kiselev and D. P. Poshkus, Dokl. AN SSSR, 120, 834 (1958); A. V. Kiselev, Ya. Kutetski and I. Chirek, Dokl. AN SSSR, 137, 638 (1961).

24. G. J. C. Frohnsdorff, G. L. Kington, Trans. Faraday Soc. 55, 1173, (1959).
25. O. M. Dzhigit, A. V. Kiselev and G. G. Muttik, Kolloidn. zh. 23, 553 (1961).
26. G. Kemball, Proc. Roy. Soc. 187, 73 (1946); Physicochemical Properties of Separate Hydrocarbons [in Russian] (Gostoptekhizdat, 1947), p. 266.
27. A. A. Isirikyan and A. V. Kiselev, Zh. fiz. khimii (in press).

All abbreviations of periodicals in the above bibliography are letter-by-letter transliterations of the abbreviations as given in the original Russian journal. *Some or all of this periodical literature may well be available in English translation.* A complete list of the cover-to-cover English translations appears at the back of this issue.

ADSORPTIVE PROPERTIES OF OXIDIZED CARBON BLACKS

1. OXIDATION OF CHANNEL BLACK IN WATER

A. V. Kiselev, N. V. Kovaleva and A. Ya. Korolev

Institute of Physical Chemistry, Academy of Sciences USSR,
Group Surface Chemistry, Moscow
Translated from Kolloidnyi Zhurnal, Vol. 23, No. 5,
pp. 582-591, September-October, 1961
Original article submitted June 16, 1960

Carbon black finds a wide application as a reinforcing filler in rubber, as a pigment in lac dyes and typographic paints, as coloring substance in Indian and other inks and so on. Together with the degree of dispersity, the nature of the surface of the carbon particles, which is characterized by the chemical composition of the surface layer, is the important property determining the behavior of carbon black as an active filler in polymeric materials. Carbon black particles (if they have not been heated at a temperature above 1000°) constitute irregular agglomerates of aromatic polymeric molecules, which contain on their perimeter disordered graphite-like networks condensed from hydrocarbon chains and functional groups, in particular, those with double bonds of the olefinic type, hydroxyl, carboxyl, quinone, peroxide, aldehyde and other groups [1-7].

The difference in the chemical composition of those carbon blacks which are manufactured nowadays lies mainly in the content of oxygen chemisorbed on the surface. Among the blacks manufactured by our Soviet industry, the thermal, the acetylenic and the gas furnace blacks, [8] which have sharply developed hydrophobic properties, are distinguished by their low oxygen content (0.1-0.5%) and small polarity. Comparitively more oxidized are channel blacks, which usually contain 3-5% chemically bound oxygen. These blacks have already a certain hydrophilic character and are better dispersed in water. However, for several applications the channel black is not sufficiently hydrophilic. In the first place this concerns the use of carbon black dispersed in water, for instance, for reinforcing rubber in latex [9], for pigmenting emulsified paints, Indian and other inks and so on. Obviously, it is desirable to raise the degree of oxidation of channel blacks even in those cases where it is used as a filler or pigment in organic media containing carbonyl, hydroxyl, acrylnitril, amine and other polar functional groups.

Until now, usually, surface active substances (adsorptive, that is, physical modification) are employed in order to raise the stability of carbon black suspensions in water. A much more effective way of enhancing the hydrophilic nature is to form on the surface of the carbon black a layer of a natural dispergator consisting of functional groups grafted to the carbon particles by covalent bonds (chemical modification) and very strongly retained on the surface of the carbon black particles. The enhanced stability in water and in many cases also the raised thermostability of polymeric materials (rubbers, lac paint coatings, lubricants and other filled or reinforced materials) prepared by means of such modified blacks is the advantage of a chemical modification of the surface of carbon blacks and other fillers and pigments [10, 11].

It is of great interest to study the adsorptive properties of highly disperse fillers and, in particular, of carbon black, since adsorption is an important and often decisive stage in the formation of a phase separation boundary in filled polymeric materials. It was studied by many authors and discussed in detail in the papers [12] how the adsorption of various vapors changes, if carbon black is modified by a thermal treatment so that its surface becomes more hydrophobic.

In the present study we investigated the adsorptive properties of carbon black samples which were modified in such a way that they became more hydrophilic. A nongraphitized carbon black is able to enter into various chemical reactions. This is connected with the fact that under known conditions there are free valences on the surface of the particles [4, 13] and that during the preparation there are formed oxygen containing functional groups on the surface; these groups may further enter with the surrounding medium into chemical reactions innate to the said groups. The reactivity of carbon blacks enables one to carry out a variety of chemical reactions on the surface of its particles

and to modify thus its properties into the direction required. The reactivity of carbon black should also be taken into account in the formation of polymeric materials filled with carbon blacks, since on the boundary between the carbon particle and the high-polymer not only adsorptive but also chemical bonds are formed. The chemical activity of the particles even plays a considerable role in the ageing and wear of filled polymeric materials during storage and use.

Methods of oxidizing carbon black by gaseous oxygen at high temperatures are known. For some time past it was established [10, 14, 15] that oxidation of carbon black can even be carried out in water without heating and, in this case, samples with new and very interesting properties are obtained. To oxidize carbon black we used sodium hypochlorite, hydrogen peroxide and a mixture of nitric and sulfuric acid. The study was done with a gas channel black having a specific surface area of ~ 150 m^2/g and an oxygen content of 4.4%. *

Oxidation of carbon black by sodium hypochlorite. Into a porcelain vessel provided with a stirrer and a thermometer 1.7 kg black was poured and then under stirring 12 liters of a 9% solution of sodium hypochlorite was added in portions. During the addition of the solution, gas was liberated and the suspension rose in temperature to 75°. When the evolution of gas had stopped, the suspension was acidified by a solution of hydrochloric acid and filtered through a folded paper filter. To remove the electrolyte the residue was repeatedly rinsed with distilled water. The oxidized black obtained was dried at 100°.

Oxidation by sodium hypochlorite [15] did not only oxidize the surface but also resulted in penetration of oxygen into the carbon black particles via the parcels of irregular graphitic networks and possibly also into the voids of the latter, just as is the case for carbon blacks derived from graphite oxide [6]. This caused the irreversible sorption of a great amount of water. Therefore, we also undertook a more mild oxidation by means of hydrogen peroxide or a mixture of concentrated nitric and sulfuric acid.

Oxidation of carbon black by hydrogen peroxide. Into the porcelain vessel 2 kg carbon black and 4 liters of a 13.1% solution of hydrogen peroxide in water were poured and then stirring was started. After the suspension had been stirred during ten minutes, 500 ml of 0.5% solution of ammonia was gradually added. During this the temperature of the reacting mixture rose to 95°. Stirring the suspension was continued until the evolution of gas stopped. After the reaction had been completed, the water from the suspension was evaporated and the oxidized carbon black thus obtained was dried at 100°.

Oxidation of carbon black by a mixture of nitric and sulfuric acid. To 100 g carbon black in a porcelain vessel a 200 ml mixture of concentrated nitric and sulfuric acid (1 : 2) was added stepwise under stirring and during this the suspension was found to heat up to 100° and nitrogen oxides were liberated. After the reaction mixture had been cooled to room temperature, 500 ml distilled water was added and the carbon black suspension was filtered through a paper filter. The carbon black was rinsed with distilled water until it started to pass through the filter, because the coagulating electrolytes had been removed. At this instant the washing was stopped and the carbon black was dried at 100°.

We have proved [15] that oxidation in water enables one to raise the content of chemisorbed oxygen and to change considerably the colloid-chemical and technological properties of carbon black. By this treatment the hydrophilic nature and the wettability of carbon black by polar organic liquids is enhanced and the black acquires an unusual tendency to spontaneous peptization in water under the formation of highly disperse colloidal hydrosols without addition of organic wetting agents. An investigation into the sedimentation of such carbon black hydrosols proved that they were very stable. The oxidative treatment in water also improves the properties of the gas channel black when used as a pigment in printing inks [16]. By this the carbon black is more easily wetted by the binding agent, the capacity to oil is lowered, the peptization and the rheological characteristics of the prepared printing inks are improved. Inks obtained from thus oxidized carbon black have a high coloring strength and good printing properties. So, the coloring strength of an ink made from the carbon black modified by sodium hypochlorite attained 160% of the value for the original gas channel black. Tests which we carried out showed that the thus modified black has advantages not only with respect to the original one but also to blacks additionally oxidized by gaseous oxygen at high temperatures.

---

* G. M. Lyulina took part in the modifying of carbon black by means of the various oxidizing agents and the authors are greatly indebted for her assistance.

The samples of oxidized carbon black prepared by the methods described above were analyzed chemically and this was done, after the modified samples had been dried and then further outgassed at 150°, which secured that the substances adsorbed on the black were removed practically completely. To determine the carbon and hydrogen content an elementary analysis in a micro-equipment was done on the samples thus prepared. The total amount of oxygen in the samples was calculated from the difference between the sample weight and the sum of the carbon and hydrogen contents. An indication on the presence of active hydrogen in the carbon black samples was found from the adsorption of sodium hydroxide in water [12] and from the amount of hydroxyl (phenolic) groups; the latter were determined by using an analysis according to Grignard [2]. The content of volatile components was determined by heating the carbon black at 800-820° in a standard procedure [17]. When being modified by the mixture of nitric and sulfuric acid, the carbon black, obviously is nitrated under formation of surface compounds containing nitro groups. To check this in the sample thus modified we also analyzed nitrogen by Kjeldahl's method. The amount of nitrogen was found to be 0.27%. The specific surface areas of the samples were determined by the BET method from the adsorption isotherms of nitrogen vapor at its boiling point.* The data on the specific surface area and the chemical composition of the carbon blacks oxidized by the various methods are assembled in the table.

The Effect Which an Oxidizing Treatment Has on the Chemical Composition and the Properties of a Channel Black

Carbon Black	Specific surface area, m^2/g	Content, %						Adsorption of NaOH, mg-eq/g	Amount of OH groups		h_2/h_1
		C	H	O	OH groups	volatile substances	Sol		from Grignard's reaction, h_1	from NaOH adsorption, h_2	
Original	148	94.84	0.75	4.40	0.4	5.0	0.15	0.32	1.0	1.3	1.35
Oxidized by H_2O_2	146	93.94	0.64	5.43	0.7	6.1	0.09	0.56	1.7	2.3	1.35
" " NaClO	80	81.87	0.83	17.27	1.7	16.7	0.5	1.70	9.4	12.7	1.35
" " HNO + + H_2SO_4	148	84.65	1.04	14.03	1.5	14.0	0.14	1.25	3.6	5.1	1.4
Treated at 1700° [12]	100	99.65	0.30	0	0	—	—	0	—	—	—

From the results obtained it is evident that all treatments of carbon black with the various oxidantia result in raised oxygen content. Upon modifying by hydrogen peroxide a moderate growth of the oxygen content in carbon black is observed. A much more considerable oxidation takes place in the treatment with sodium hypochlorite and with the mixture of nitric and sulfuric acid.

In all probability, the chemisorbed oxygen becomes part of carboxyl, carbonyl and hydroxyl groups, as is pointed out by investigations into the infrared spectra of carbon blacks made from graphite oxide or obtained by oxidizing with sodium hypochlorite [6]. The data obtained in elementary analyses of the various channel black samples are in agreement with the content of volatile substances; the latter mainly are the products formed by the thermal destruction of the oxygen containing complexes on the carbon black surface. The hydroxyl content found by a Grignard analysis and that determined from the adsorption of sodium hydroxide on the carbon black** are nearly proportional to each other and are directly related to the total amount of oxygen chemisorbed on the carbon black, as is found from the elementary analysis.

As is evident from the table, the specific surface area of the samples, except that for the carbon black oxidized by sodium hypochlorite, is not changed by the oxidation. Here it should be kept in mind that the surface of the original black and that of all additionally oxidized samples are chemically and geometrically inhomogeneous,

---

* The nitrogen adsorption isotherms were measured by N. N. Avgul' and the authors thank her sincerely.

** In all probability, the adsorption of NaOH takes place on the carboxyl and phenolic groups present on the surface of the carbon black particles [6].

be it to a different extent; therefore, the determination of the surface area from nitrogen adsorption by the BET method has a somewhat formal character; moreover, the packing of nitrogen molecules and, consequently, the mean area occupied by a nitrogen molecule in a complete monolayer may vary somewhat dependent upon the nature of the surface of the sample [18].

On the samples obtained we studied adsorption from the vapor phase of substances with sharply differing properties: water, methanol, benzene and n-hexane.*

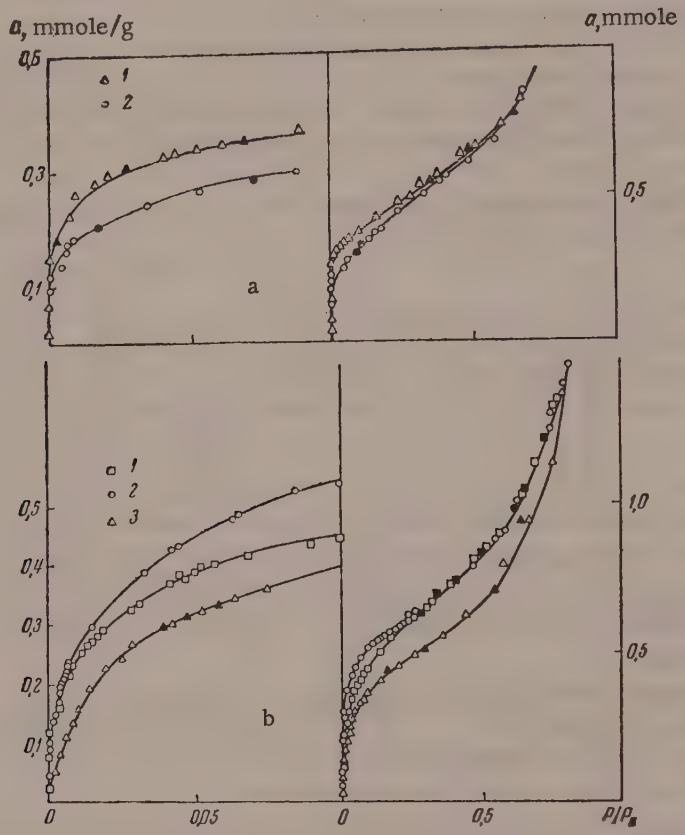


Fig. 1. Adsorption isotherms of n-hexane (a) and benzene (b) vapors on the carbon blacks: the original black (1), that oxidized by the mixture of nitric and sulfuric acid (2) and the graphitized sample (3). Here and further the filled points designate desorption.

The adsorption isotherms of water vapor were measured at 30° in a vacuum apparatus according to Mac Bain-Bakr having three spring balances with an accuracy of $5 \cdot 10^{-4}$ g [12]; the adsorption isotherms of methanol, benzene and hexane vapors were measured with an accuracy of $5 \cdot 10^{-6}$ g in vacuum equipment with a capillary liquid microburet [12]. Before each series of measurements the samples were outgassed for a long time to a pressure of 10^{-5} mm Hg at room temperature and then at 200°. In nearly all cases, 2-3 series of independent determinations were carried out.

Results obtained upon measuring adsorption on the carbon blacks. In Fig. 1, a the measured adsorption isotherms of n-hexane vapor on the original black and on that oxidized by the mixture of nitric and sulfuric acid are given, while two scales are used along the axis of the relative pressure p/p_s. As is evident from Fig. 1, a, oxidizing the carbon black surface resulted in a lowered adsorption of hexane vapor. Clearly, this is connected with the fact

* A. P. Arkhipova took part in the adsorption measurements and the authors are much indebted for her assistance.

that the surface of the oxidized samples is quite completely covered by oxygen containing groups so that the free sites on the surface of the carbon black are inaccessible for the big hexane molecules. Perhaps, the electrokinetic (dispersion) interaction between hexane and the carbon black surface is weakened because the molecules are at a greater distance from the hydrocarbon part of the said surface.

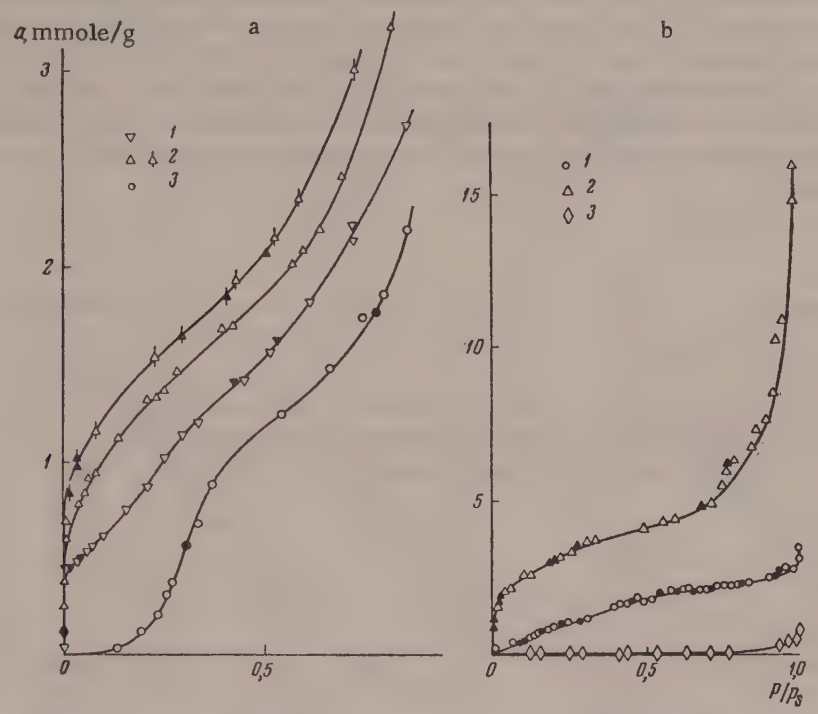


Fig. 2. Adsorption isotherms of methanol (a) and water (b) vapor on the carbon blacks: the original black (1), that oxidized by the mixture of nitric and sulfuric acid (2) and the graphitized sample (3). Here and further the points with lines across designate a second series of measurements.

In the case of benzene adsorption the opposite effect is found: When the surface of carbon black is oxidized to a greater extent, the adsorption of benzene vapor rises somewhat in the region of small p/p_s values, as is visible in Fig. 1, b where the adsorption isotherms of benzene vapor on the graphitized, the original and the oxidized carbon black are shown. In all probability, this rise is connected with an increase in the additional interaction of the π-bonds in the benzene molecule with the hydroxyl groups on the surface of the oxidized carbon blacks, just as is found in the adsorption of benzene on a hydrated surface of silica gel [19].

Adsorption of methanol vapor is still more sensitive to oxidation of the carbon black surface. The adsorption isotherms of methanol vapor on those same samples are shown in Fig. 2, a. For the graphitized sample the isotherm is concave in the region of small p/p_s, then the adsorption rises sharply and the isotherm passes through two points of inflection; the isotherm is reversible. On the original carbon black, which has oxidic groups on its surface, the adsorption isotherm of methanol vapor is already convex in the region near the origin. Still more sharply convex is the adsorption isotherm of methanol vapor on the oxidized carbon black; this isotherm is irreversible. Even after a long lasting evacuation (12 hr) at room temperature part of the methanol (0.15 mmole/g) is kept by the carbon black. Probably, in this case there is chemisorption of methanol and this is confirmed by the further course of the measurements. In the second series of measurements, which was carried out, after the carbon black had been pumped out for a long time at room temperature, the adsorption and the desorption branch coincided with each other and with the desorption branch of the first series of measurements. Only by pumping off at 100° during 16 hr could methanol be completely desorbed. In the third series of measurements, which was carried out after pumping off the sample at 200°, both the adsorption and the desorption branch coincided with the corresponding branch of the first series of measurements. So, the hysteresis found in the first isotherm in the region of small p/p_s is connected with chemisorp-

tion (obviously, by methoxylation of hydroxyl groups on the surface of carbon black*). The hysteresis in the region of high relative pressure, probably, is connected with capillary condensation in the free spaces between the particles of the oxidized carbon blacks.

Oxidizing carbon black has the sharpest effect on the adsorption of water vapor (Fig. 2, b). On the graphitized sample the adsorption of water vapor is trifling low and, even in the region of relative pressure close to one, completion of a monolayer is not attained [20]. The adsorption isotherm of water vapor on the original sample has the usual shape with a concave start and two points of inflection. But the adsorption isotherm on the oxidized sample is already sharply convex in the region of small p/p_s and it rises very steeply upwards. On the oxidized sample part of the water (1.05-1.2 mmole/g) is irreversibly kept by the carbon black; this water, just as methanol on this same sample, could not be removed by pumping during a long time at room temperature. Only by pumping during 15-20 hr at 100° can this water be completely desorbed. Probably, the irreversibly adsorbed water is chemisorbed by hydrating the superficial oxides.

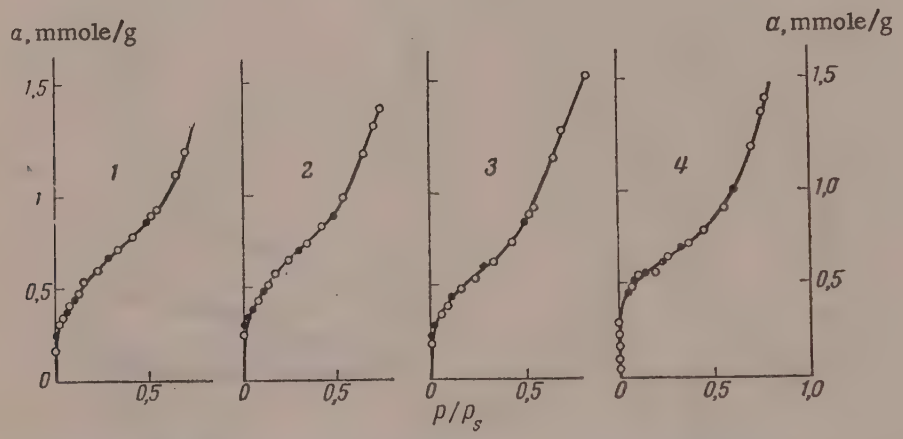


Fig. 3. Adsorption isotherms of benzene vapor on the carbon blacks: the original black (1) and those oxidized by hydrogen peroxide (2), by sodium hypochlorite (3), by the mixture of nitric and sulfuric acid (4).

So, by modifying the surface of carbon black by graphitization or oxidation so that it becomes strongly hydrophobic or hydrophilic, respectively, the amount of vapor adsorbed by it may be varied by ten or even a hundred times.

Above we have compared the effects which graphitization and one of the oxidation methods have on adsorption of vapors by carbon black. It is interesting to examine the effect which the various methods of oxidizing carbon black have on the adsorption of those same vapors.

In Fig. 3 the adsorption isotherm of benzene vapor on the original sample is compared with those for the samples oxidized by hydrogen peroxide, sodium hypochlorite and the mixture of nitric and sulfuric acid. In all cases the adsorption of benzene increases very little, when one passes from the original sample to the oxidized ones. The highest adsorption in the region of small p/p_s is found for the sample oxidized by the mixture of nitric and sulfuric acid.

From Fig. 4 it is evident that, when one passes from the original black to the oxidized samples, the adsorption of methanol rises. The highest adsorption is observed for the sample oxidized by the mixture of nitric and sulfuric acid, although the latter sample contains less oxygen in its elementary composition than does the sample oxidized by sodium hypochlorite. Obviously, the action of sodium hypochlorite in water not only results in strongly oxidizing the external surface of the crystallites from which the carbon black particles are built up (mainly at the sites where the hydrocarbon radicals left undecomposed in the formation of the channel black are connected and at the carbon sites too of the prismatic faces and edges of the crystallites), but also causes a partial penetration of oxygen into the space between the crystallites and, possibly, even into the interplanar voids inside the crystallites themselves. The

* In the case of the original carbon black this effect was not detected, because the surface of this black is considerably less oxidized.

fact that the adsorption isotherm of water on the said black is similar to that on the carbon black prepared from graphite oxide [6] is to the advantage of our assumption. When carbon black is oxidized to a greater extent, water adsorption rises sharply (Fig. 5). Here, just as in the case of methanol adsorption, the sample oxidized by sodium hypochlorite forms

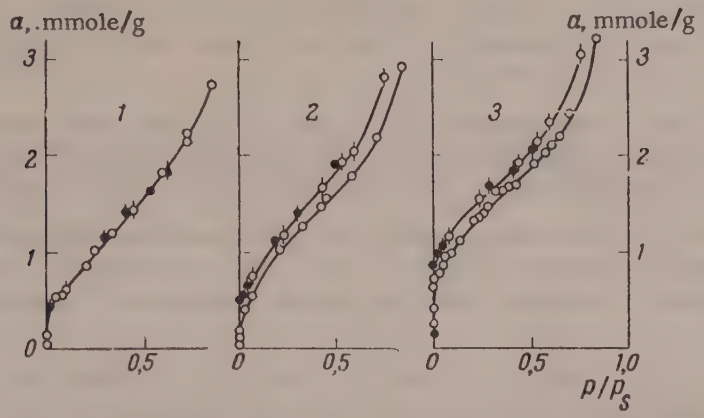


Fig. 4. Adsorption isotherms of methanol vapor on the carbon blacks: the original sample (1) and those oxidized by sodium hypochlorite (2), the mixture of nitric and sulfuric acid (3).

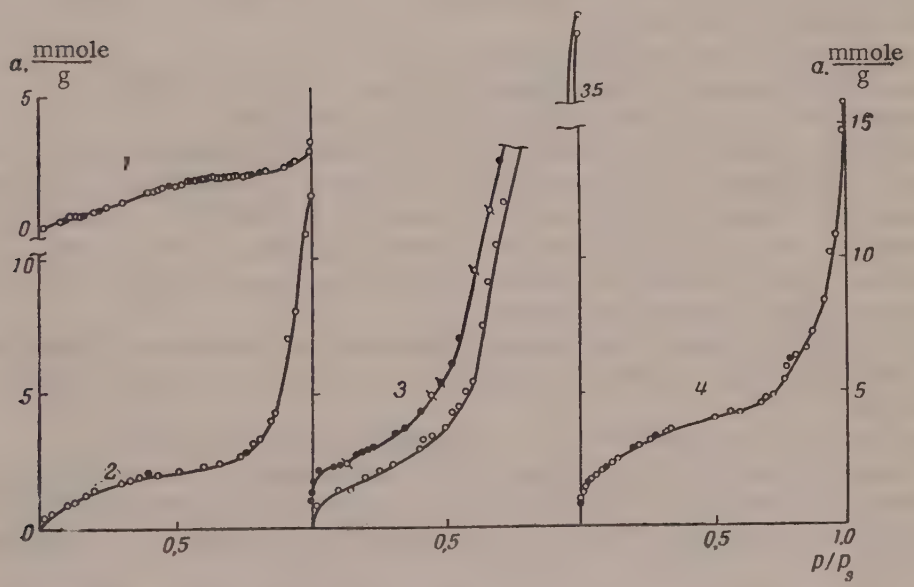


Fig. 5. Adsorption isotherms of water vapor on the carbon blacks: the original sample (1) and those oxidized by hydrogen peroxide (2), sodium hypochlorite (3), the mixture of nitric and sulfuric acid (4).

an exception. Obviously, not all oxygen located between the crystallites from which the carbon black particles are built up is accessible for water adsorption. Probably, the hysteresis on this sample in the region of small p/p_s is connected with chemisorption, just as is the case for adsorption of methanol vapor, but also with penetration of water to the oxidized sites between the crystallites of this carbon black [6]. The hysteresis in the region of high p/p_s, obviously, results from capillary condensation in the free spaces between the particles of this carbon black. It is interesting to note that, after this black has been heated at 950° in vacuum during 12 hr, the adsorption of water vapor in

the region of small coverages drops sharply and becomes nearly equal to the adsorption of water vapor on the original carbon black. This is connected with the fact that by the heating, the superficial "carbon-oxygen" complexes are destroyed (after heating at 950° the amount of oxygen on this carbon black was sharply lowered).

SUMMARY

1. We have developed methods of modifying chemically the surface of a channel black by treating it with various oxidizing agents in water without heating. This treatment gives an increase in the content of various oxygen containing functional groups in the carbon black.

2. Oxidation in water causes a considerable change in the nature of the surface and the colloid-chemical properties of the black; the latter becomes hydrophilic and more wettable by polar organic liquids. The thus modified carbon black forms stable colloidal dispersons in water without addition of surface active substances.

3. After the oxidation of the carbon black the adsorption of hexane vapor in the region of low relative pressures was somewhat lowered because the distance to the actual carbon surface was increased, whereas the adsorption of benzene rose somewhat as a result of additional interaction between the π-bonds of benzene and the oxygen-carbon complexes.

4. When the carbon black is oxidized to a higher extent, adsorption of methanol and, particularly, water vapor rises sharply, because on the surface of these blacks the number of oxygen complexes, which strongly adsorb the said polar substances, is raised.

The authors express their sincere gratitude to L. I. Doroshina and M. G. Kuz'mina for assistance in the chemical analysis of the carbon black samples.

LITERATURE CITED

1. R. S. Stearns, B. L. Johnson, Industr. and Engng. Chem. 43, 146, (1951); W. R. Smith, W. D. Schaeffer, Rubber, Chem. and Technol. 23, 625, (1950).
2. D. S. Villars, J. Amer. chem. Soc. 70, 3655 (1948).
3. B. C. Barton, H. M. Smalwood, G. H. Ganzhorn, J. Polimere Sci. 13, 487, (1954).
4. N. N. Lezhnev and A. S. Kuz'minskii, Dokl. AN SSSR, 110, 108 (1956).
5. M. L. Studebaker, E. Hoffman, A. C. Wolfe, L. G. Nabors, Industr. and Engng. Chem. 48, 162 (1956).
6. V. I. Lygin, N. V. Kovaleva, N. N. Kavtaradze and A. V. Kiselev, Kolloidn. zh. 22, 334 (1960).
7. V. A. Garten, D. E. Weiss, J. B. Willis, Austral. J. Chem. 10, 295, (1957); V. A. Garten, D. E. Weiss, K. Eppinger, Austral. J. App. Sci. 7, 148, (1956); V. A. Garten, D. E. Weiss, Austral. J. Chem. 8, 68, (1955); Revs. Pure and Appl. Chem. 7, 69 (1957); D. Hadzi, V. Novak, Trans. Faraday Soc. 51, 1614 (1955); J. V. Hallum, H. V. Drushell, J. Phys. Chem. 61, 110, (1958).
8. V. V. Kel'tsev and P. A. Tesner, The Properties, Manufacture and Application of Carbon Black [in Russian] (Gostopizdat, 1952); V. P. Zuev and V. V. Mikhailov, The Manufacture of Carbon Black [in Russian] (Goskhimizdat, 1953).
9. B. A. Dogadkin, B. A. Senatorskaya and V. I. Guseva, Kolloidn. zh. 18, 528 (1956).
10. A. V. Kiselev, N. V. Kovaleva, A. Ya. Korolev and K. D. Shcherbakova, Dokl. AN SSSR, 124, 617 (1959).
11. I. Yu. Babkin, V. V. Vasil'eva, I. V. Drogaleva, A. V. Kiselev, A. Ya. Korolev and K. D. Shcherbakova, Dokl. AN SSSR, 129, 131 (1959); A. V. Kiselev, A. Ya. Korolev, R. S. Petrova and K. D. Shcherbakova, Kolloidn. zh. 22, 671 (1960).
12. A. V. Kiselev and N. V. Kovaleva, Izv. AN SSSR, Otd. khim. n. 1959, 989; A. A. Isirikyan and A. V. Kiselev, Kolloidn. zh. 23, 231 (1961).
13. V. A. Garten, Nature 173, 997 (1954).
14. G. Genin, Peintures, pigments, vernis 30, 639 (1954); L. Vanuto, Paint Manafact. 24, 227 (1954).
15. A. Ya. Korolev, Abstracts of the Proceedings of the Fourth All-Union Conference on Colloid Chemistry [in Russian] (Acad. Sci. USSR Press, 1958), p. 113.
16. A. Ya. Korolev, T. N. Malova and V. I. Romanova, Poligrafitseskoe proizvodstvo, 7, 25 (1957).
17. Gost 7885-56.
18. A. V. Kiselev and A. A. Isirikyan, zh. fiz. khimii, 34, 2817 (1960).
19. A. V. Kiselev and L. D. Belyakova, Dokl. AN SSSR, 119, 298 (1958); Collection: Preparation, Structure and

Properties of Sorbents [in Russian] (Goskhimizdat, 1959), p. 180; A. V. Kiselev and D. P. Poshkus, Dokl. AN SSSR, 120, 834 (1958).

20. N. N. Avgul', O. M. Dzhigit, A. V. Kiselev and K. D. Shcherbakova, Dokl. AN SSSR, 92, 105 (1953); A. V. Kiselev and N. V. Kovaleva, Zh. fiz. khimii, 30, 2775 (1956).

All abbreviations of periodicals in the above bibliography are letter-by-letter transliterations of the abbreviations as given in the original Russian journal. *Some or all of this periodical literature may well be available in English translation.* A complete list of the cover-to-cover English translations appears at the back of this issue.

RADIOTRACER METHOD OF DETERMINING THE ADSORPTIVE CAPACITY AND SPECIFIC SURFACE AREA OF PHOSPHATE COATINGS

V. S. Lapatukhin, Yu. M. Ovchinnikov

Scientific Research Institute of the Polygraphic Industry, Moscow
Translated from Kolloidnyi Zhurnal Vol. 23, No. 5,
pp 592-595, September-October, 1961
Original article submitted June 9, 1960

Phosphate coatings are used to give antifrictional and anticorrosive properties to metal surfaces. In practice phosphated metal surfaces are seldom used alone. In almost all cases they are covered either with lubricants or with additional protective and decorative lacquers. The ability of phosphate coatings to take up oils and pigments is considerably greater than that of the same metals unphosphated. From the data of Darcy [1] and Machu [2], phosphated steel holds 1.5-1.7 times as much pigment and twice as much oil as unphosphated steel. This cannot be explained merely by the porous spongy structure of the coating [1]. An important role is played by the molecular surface properties of these coatings, which predetermine their special behavior with respect to various reagents contained in the protective greases, lacquers or pigments. These properties of phosphated metals, their molecular nature, and their adsorptive capacity, have been studied previously in [3] by selective wetting methods (after Rebinder) as a function of the composition and method of preparation of the coatings and subsequent treatment with surface active agents. In particular, this method has been used to measure the adsorptive capacity of various phosphate coatings with respect to oleic acid and hydrophilic colloids. However, the test of the surface properties used in these papers, based on the change in wettability is an indirect method and therefore does not give any direct information on the mechanism of fatty acid adsorption or the actual role played by the hydrophilizing agent used as a depressant of the oleophilic adsorptive film. For the purpose of investigating the adsorptive capacity of phosphate films by direct measurement of the amount of fatty acid adsorbed, and of the stability of the adsorbed layers, we used a tracer technique, the adsorbate being tridecylic acid $CH_3(CH_2)_{11}COOH$, with the radioactive isotope C^{14} in the carboxyl group.

The tridecylic acid was dissolved in nonpolar vaseline oil to various concentrations, and was used to treat coatings on zinc, phosphatized at room temperature in a solution containing Mazhef's reagent (60 g/liter), sodium fluoride (8 g/liter) and zinc nitrate (50 g/liter).

Preliminary tests showed that to reach saturated equilibrium volume adsorption the samples had to be treated with the radioactive solution for not less than five minutes. The excess solution was then removed from the surface with filter paper, and the sample was washed in benzene to constant counting rate, which showed that all the tridecylic acid had been washed off with the exception of what was irreversibly adsorbed on phosphatized surface. The sample prepared in this way was treated with a 2% aqueous solution of starch.

The whole cycle of treatment and activity changes is shown schematically in Fig. 1.

It follows from the adsorption isotherms of tridecylic acid that saturated adsorption occurs on the surface at 10% tridecylic acid concentration in the solution. A comparison of the saturated activities at the saturated adsorption point before (curve 1), and after treatment with a depressant (curve 2), shows that the starch solution has large surface activity and considerable depressant action on the adsorbed oleophilic film of fatty acid. After treatment with starch the surface activity falls to 25% of its original value.

Considering the irreversibility of the tridecylic acid adsorption, it may be assumed that the observed reduction in activity is a result of the shielding action of the secondary film of starch which has not been washed out by the water and absorbs 3/4 of the radiation. To test this assumption, a sample treated with starch for one hour was subjected to the action of hot water (90-95°C) to break up the starch film. However, no appreciable

increase in activity was observed as a result of the treatment. To explain the absorbing action of the starch film on the surface activity of the sample a relatively thick starch layer (0.3 mg/cm^2) was put on without any further washing with water. As might be expected, no appreciable change in the activity was observed in this case either . Calculations show that to reduce the radiation four times requires a starch layer 20 times thicker than the one we used.

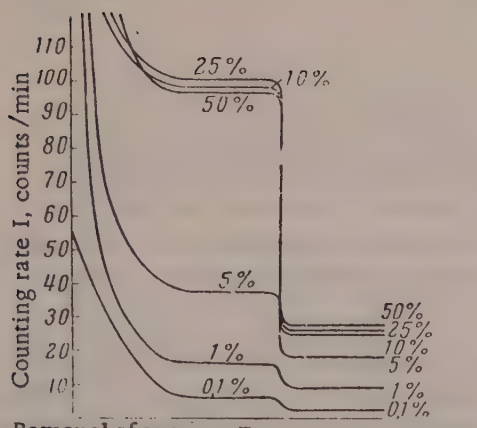


Fig. 1. Change in radioactivity of samples at various stages of treatment.

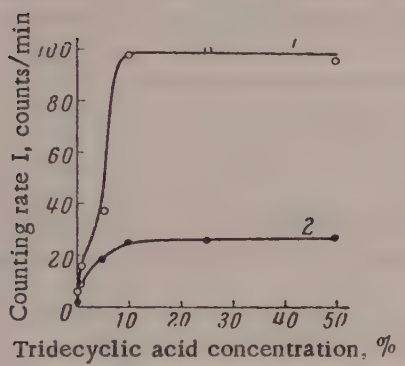


Fig. 2. Adsorption isotherms of radioactive tridecylic acid on phosphated zinc, (1) before, and (2) after depressant treatment.

All these facts completely eliminate the assumption of any shielding action of the starch film, and gives support to the idea that the starch displaces part of the tridecylic acid from the surface of the phosphate coating.

It might be assumed that the adsorbed acid molecules which are solidly attached by chemical bonds to the coating surface are not the ones that are displaced, but rather the molecules in the following layers, which have survived the benzene treatment. However, under the present experimental conditions, this mechanism is not very probable.

Finally, we can make another assumption to the effect that the change in activity after the starch treatment is due to washing out from the surface of part of the tridecylic acid, which has reacted with the phosphates to form water soluble soaps. No water soluble soaps can be observed from washing with benzene but it can happen during treatment with water soluble reagents.

Experimental check confirmed this assumption. Prolonged (10 minute) waterwashing of a sample with an adsorbed tridecylic acid layer reduced its activity. In the presence of starch the activity drops off even more.

These results for the adsorption of tridecylic acid by a phosphate coating on zinc enable us to calculate the specific surface of the phosphate coating.

The specific surface of the coating (s) may be calculated from the equation

$$s = s_0 n/P ,$$

where s_0 is the area occupied by one molecule of tridecylic acid, which we took equal to 20 A^2, $\underline{n}$ is the number of molecules adsorbed per cm^2 of coating and P is the weight of one square meter of coating in grams.

The value of $\underline{n}$ may be found from the equation

$$n = mN/M,$$

where $\underline{m}$ is the mass of tridecylic acid adsorbed by one square centimeter of coating, N is Avogadro's number, M is the molecular weight of tridecylic acid (M = 214.34).

The mass of tridecylic acid adsorbed, $\underline{m}$, is proportional to the measured activity

$$m = kI,$$

and $\underline{k}$ is a proportionality constant.

The constant $\underline{k}$ may be found from the equation

$$k = 1/I_0 \omega \varepsilon pq ,$$

where I_0 is the specific activity of tridecylic acid, ω is a coefficient taking account of the geometry of the measurements setup, ϵ is the counting efficiency, p is the β-ray self-adsorption factor in the sample, q is the self scattering and reflection factor from the base plate.

The product $\omega\epsilon pq = I/I_{act}$, which is known under the general name of counting efficiency, may be measured with standard sources, which are similar in form to the test samples.

Using the equations given we can write finally

$$s = s_0 NI/PMI_0\omega\varepsilon pq \quad \text{or} \quad s = s_0 NI_{act}/PMI_0.$$

A similar equation for determining this specific surface of structural materials was used in the paper by Loginov and Khusainova, [4].

If we make a calculation from the activity corresponding with the saturated adsorption of the surface before treatment with the depressant, the specific surface area of a phosphate coating on zinc (9.6 gram/m^2 coating) comes to 24 m^2/g.

We are not making any attempt here to compare our specific surface values with the data of other authors, since there is no information of this sort on phosphate coatings in the literature. Comparing these data with this specific surface of oxide coatings on aluminum and magnesium as determined sorptionally by Nabokov, Paleolog, and Tomashov [5] shows that phosphate and oxide coatings have specific surfaces of the same order of magnitude.

Thus, the experiments have shown that using an absorbate in the form of a radioactive indicator which forms a chemisorbed layer on the surface under investigation makes it possible to study the adsorptive capacity of this surface, and to measure the specific surface area of phosphate coatings. The technique described using labeled tridecylic acid is recommended for use in all work which presents the similar problem of measuring the adsorptive capacity of a solid surface (pure metals or coated metals) relative to fats. Use of this technique to measure the adsorptive capacity of various phosphate coatings on various metals, together with the technique based on wetting measurements, will, beyond any doubt, provide very valuable practical information on these coatings.

SUMMARY

1. A technique is described for measuring the adsorptive capacity and specific surface area of phosphate coatings, based on measuring the radioactivity of the adsorbent after treatment with a solution of tridecylic acid labeled with C^{14}.

2. This specific surface area of a phosphate coating on zinc from cold phosphatizing is 24 m^2/g.

LITERATURE CITED

1. V. Darcy, Collection "Corrosion of Metals", Vol. 2 [Russian translation from English] Goskhimizdat (Leningrad 1952) p. 938.
2. W. Machu, Die Phosphatierung. Wisenschaftliche Grundlagen und Technik (Weinheim) Bergstr. Verlag Chemie, 1950, Gmbh.
3. V. S. Lapatukhin, Phosphatizing Metals [in Russian] Mashgiz (Moscow, 1958).
4. G. I. Loginov, O. I. Khushinova, "New Method of Physicochemical Investigation" No. 2, Issue VI, [in Russian] Academy of Sciences Press, USSR, 1957, p. 140.
5. V. S. Nabokov, E. N. Paleolog, N. D. Tomashov, Collection "Methods for the Study of Structure of Highly Dispersed and Porous Bodies" [in Russian] Academy of Sciences Press, USSR, 1958, p. 137; Zh. fiz. khimii 30, 2705, 1956; Collection "New Methods of Physicochemical Investigation", Transactions of the Institute of Physical Chemistry of the Academy of Sciences, USSR, Vol. 2, Issue 6 [in Russian] Academy of Sciences Press, USSR, 1957, p. 39.

STRUCTURATION PROCESSES IN CEMENT-REINFORCED TERRAINS

T. Yu. Lyubimova, T. V. Yagodovskaya

All Union Scientific Research Highway Institute, Moscow
Translated from Kolloidnyi Zhurnal, Vol. 23, No. 5,
pp 596-604, September-October, 1961
Original article submitted September 16, 1960

The structure of terrains, reinforced with cement, as follows from the fundamental concepts of physico-chemical mechanics [1] arises as a result of the formation of two types of bonds: coagulational bonds (between soil particles) and crystallizational bonds (from hydrational hardening of the binder) [1-9]. Since the strength of the bonds of the second type is several orders of magnitude higher than the strength of bonds of the first type, and less dependent on external conditions, the properties and constants of the crystallizational component of the structure determine all the important engineering properties of cement terrains as structural materials. Therefore, if cement terrains are going to last for a long time, we must look into the optimum conditions for the formation and stable existence of the crystallizational binder structure.

The coagulational component of the structure may also have a substantial effect on the properties of cement terrains, but, since the effect of the two components is known to be opposite, the specific properties of the soil will be reflected in the properties of the reinforced terrain to a higher degree, the less effective the method of reinforcement is.

In addition to the coagulational and crystallizational bonds which are formed in cement reinforcement of terrains, the particles in the microaggregates of the soil may be solidly bound by condensational bonds, previously formed under natural conditions. The role of the solid microaggregates in cement soil structure is in some degrees similar to the role of the aggregate in concrete.

The conditions under which the crystallizational binding structure of cement terrains arises and continues to exist, have a number of peculiarities which are different from the "normal" conditions in cement concretes as a result of: a) the extremely high specific surface and the hydrophilic properties of the reinforcing material, b) the small concentration of binder in the mixture, c) the high adsorptional and chemical activity of the soil.

The high specific surface of the soil together with the low concentration of cement in the mixture, forms exceedingly thin walled "azure" (transparent) cement stone structures, distributed among the microaggregates of soil in the form of thin layers, possibly discontinuous in spots. The less the cement concentration, the less the thickness of the cement stone layers, and the greater the probability that its density and continuity will be disturbed in spots. If the humidity of the cement soil mixtures oscillates about its optimium value, as occurs under actual conditions, the hydrates in the cement are in intimate contact with the moist hydrophilic soil, which is a constant source of moisture for the cement stone structure " from inside" and favors the recrystallization processes caused by the thermodynamic instability of the crystallizational hardening structures [1 and 7].

These processes must be accompanied by a gradual loss in strength. According to P. A. Rebinder structural degeneration of this sort can be prevented completely if three conditions are observed: High density of material, absence of water in the pores, and, for practical purposes, complete insolubility in the liquid phase of the hydrates in the binder forming the structure [7]. The last condition is a decisive one and is apparently fulfilled as far as the silicate minerals in the cement are concerned. In concretes, the dense layers of cement stone unite the grains of rock and sand into a monolithic structure. With the high density of concrete as a whole provided by present day technology, the recrystallization reactions occur at an infinitesimal rate. The crystallizational structures formed in cement soil mixtures find themselves in considerably less favorable circumstances. Therefore, one of the first conditions required to increase the life of a cement soil mixture is getting the highest possible degree of density in the cement soil mixtures. This may be achieved by a stepup and thoroughgoing revision of the den-

sifying procedures (by using vibrational methods), or by adding very small quantities of of surface active hydrophobic agents to the mixtures, thus reducing the optimum humidity, [5], or by a combination of both methods, [1].

A third peculiarity of the formation of crystallizational structures in cement soil mixtures has to do with the absorption by the soil of lime formed in the hydrolysis of alite (tri-calcium silicate).

The most important and informative property of the structuration process in the hydration hardening of mineral binders is the supersaturation kinetics of the structure forming substance, which regulates the process [7-10]. In the hardening of cement under "normal" conditions (in concrete), one of the characteristic features is the existence in the liquid phase of isothermal supersaturation with respect to $Ca(OH)_2$, and the presence of an excess of free lime in the solid phase of the system for a long period of time. A stable form of the calcium hydrosilicates crystallizing under these conditions is the compound with the ratio $CaO:SiO_2 \approx 2$ (various data gives 1.5-1.8). In contact with less concentrated solutions of $Ca(OH)_2$ hydrosilicates are formed with a lower concentration of CaO. At a concentration of $Ca(OH)_2$ less than 2 millimoles/liter, no hydrosilicates are formed [11-13]. Therefore, the dicalcium hydrosilicate is unstable in contact with unsaturated $Ca(OH)_2$ solutions, and goes over, with formation of free lime, into less basic forms. The rate of these reactions is usually infinitesimal for the dense cement stone structures in concrete, which always contain an excess of $Ca(OH)_2$ in the solid phase. With no lime in the solid phase, and a low density of the structure, as occurs in cement soil mixtures, reduction of $Ca(OH)_2$, concentration in the liquid phase may bring about a lowering of basicity of the hydrosilicates with time.

Indications have been found that the conditions for hardening cement in cement soil mixtures are made worse in comparison with the conditions for hardening in concrete because of the absorption by the soils of Ca^{2+} or lime [14-16]. The desirability has been noted of adding Ca^{2+} to the cement soil mixtures in the form of small quantities of $CaCl_2$ or $Ca(OH)_2$ [14,16], which has resulted in increased strength, [14].

The results obtained in the present paper have made it possible to evaluate what importance the interaction of the components of the cement soil mixture has for the life of the materials, to discuss the mechanism involved, and to show the reason why it is necessary to add even large quantities of lime when reinforcing argillaceous soils with cement.

In mixtures of different soils, argillaceous minerals, and sand with cement, a study was made of the effect of the nature of the mineral material on the structuration of the binder, by making a parallel measurement of the change with time (kinetics of the following factors: 1) the total concentration of free lime in the system, 2) the concentration of Ca_{2+} and H+ ions and silicic acid in the liquid phase, and 3) the structuration or hardening. Here the concentration of the basic structure forming substances, lime and silicic acid, could not be used to calculate the composition of the hydrosilicates [13], because they depend on the nature of the absorbing complex in the soil. However, the kinetics and the limits of change in the concentration of $Ca(OH)_2$ and silicic acid were given by the tendency of the reactions occurring in the system, and the conditions of formation and existence of the crystallizational structure. The composition of the liquid phase of cement-mineral material-water systems was studied in suspensions with S/L from 1:1 to 1:5, kept in hermetically sealed vessels. The suspensions were stirred periodically, and the liquid phase was removed by centrifuging. The Ca^{2+} concentration was measured by the trilonometric method, the silicic acid was measured by a colorimetric method [17], the free lime content was measured by the glycerate method in beam samples prepared by packing the cement mineral mixtures at optimum humidity [5 and 6]. To prevent carbonation, the samples were covered with paraffine.

The following mineral materials were used:

Mono-mineral clays of basic types: Prosyanaya kaolinite; Chasov Yar and hydro-schist clays; Oglanly, Kiel, and Gumbrin bentonite.

Soils: protective clay (Cheremushki), Krasnodar black earth; Central-Asiatic and Ukrainian loess.

Vol'sk quartz sand (washed): unground with specific surface (after Tovarov), s = 500 cm^2/g; and ground s = 2000 and s = 9000 cm^2/g.

Binders: tri-calcium silicate (alite), s = 5000 cm^2/g, and cement from the Belgorod factory with 3% gypsum, s = 4000 cm^2/g.

For mixtures of various mineral materials with cement under otherwise identical conditions, one observes that there is a difference in the change with time (kinetics) of the concentration of lime and silicic acid in the

liquid phase, the overall free CaO concentration in the system, and consequently in the structurization kinetics, that is, the increase in strength of the structures being formed.

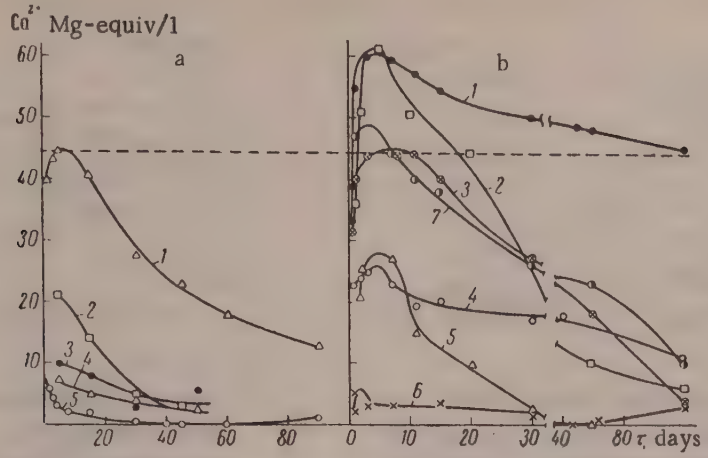


Fig. 1. Kinetics of Ca^{2+} concentration in the liquid phase of the systems: cement-mineral material-water, S/L = 1/5, cement concentration in the solid phase 10%, t = 20°. a) Mixture of cement with clay minerals: 1) Prosyanaya kaolinite; 2) Chasov Yar clay (hydroschist); 3) Kiel; 4) Gumbrin; 5) bentonite. b) Mixtures of cement with soils, minerals and sand: 1) Normal Vol'sk sand (s = 500 cm^2/g); 2) Ukrainian loess; 3) Prosyanaya kaolinite; 4) Moskva clay (Cheremushki); 5) Krasnodar black earth; 6) Oglanly bentonite; 7) ground Vol'sk sand (s = 9000 cm^2/g).

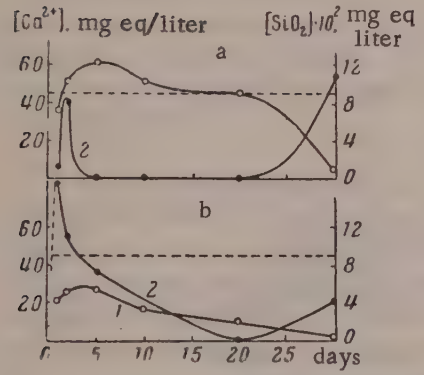


Fig. 2. Kinetics of the concentration of Ca^{2+} (1) and SiO_2 (2) in the liquid phase of cement soil suspensions with S/L = 1/5. Cement concentration in the solid phase 10%, t = 25°: a) central asiatic loess; b) Krasnodar black earth.

Fig. 1 shows the kinetics of the Ca^{2+} concentration in the liquid phase for systems with S/L = 0.2. Experiments made at different values of S/L (1; 0.5; 0.33; etc.) made it possible to find, by extrapolation, the concentration of lime in the liquid phase of actual cement soil mixtures, packed at optimum humidity. The more the S/L ratio is increased, the more the lime concentration is decreased, because here the relative reduction of $Ca(OH)_2$ in liquid phase is stepped up.

In accordance with current conceptions on the structure and properties of argillaceous minerals, the lowest lime concentrations corresponds to mixtures of cement with clays of the montmorillionite group, while the highest concentrations correspond to mixtures of cement with kaolinite. A mixture of cement with unground quartz sand may be regarded as a standard for the "normal" conditions of binder structuration (Fig. 1).

In suspensions of sands with cement, one observes a reduction in the lime concentration in the liquid phase below the standard, the more so, the higher the degree of disperseness of the sand. This is to be explained by chemical absorption of the lime by ground quartz sand, which has been established for ordinary temperatures in [18 and 19]. Among the soils investigated, relative to their absorptive capacity, the smallest lime concentrations in the liquid phase were observed in suspensions of cement with black earth and clay, and the highest concentrations were observed in suspensions with loess.

By extrapolating the data obtained from the suspensions to actual cement soil mixtures, it was shown that, for example, in cement soil mixtures made from protective clay, the lime concentration in the liquid phase 7-10 24 hour periods after packing becomes close to zero. The greater the concentration of argillaceous material in the soil, and the greater its absorptional capacity, the quicker the liquid phase becomes depleted in lime. The kinetics

of the silicic acid concentration in the liquid phase of the suspension for weakly absorbing loess and strongly absorbing black earth (Fig. 2) confirms what has been said.

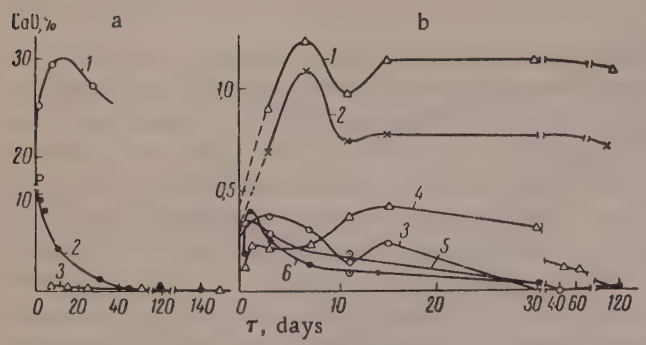


Fig. 3. Kinetics of the concentration of free lime in samples of soils and minerals, reinforced with cement at optimum humidity: a) Sample of alite (C_3S) (1) Gumbrin (2) and bentonite (3) reinforced with 15% alite (CaO % with respect to C_3S). b) Samples with 10% cement from normal Vol'sk sand (1) ground to s = 2000 cm^2/g (2) and 9000 cm^2/g (3) kaolinite (4) bentonite (5) and Cheremushki clays (6) (CaO, % with respect to dry mixture).

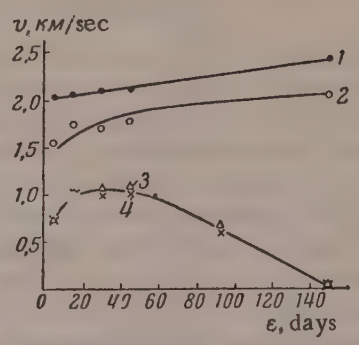


Fig. 4. Structuration kinetics—hardening of cement mineral mixtures densified at optimum humidity. Cement concentration 15% (v-supersonic velocity): 1) kaolinite, W/WS = 0.34; 2) hydroschist clay W/S = 0.22; 3) Kiel, W/S = 0.42; 4) Gumbrin, W/S = 0.42.

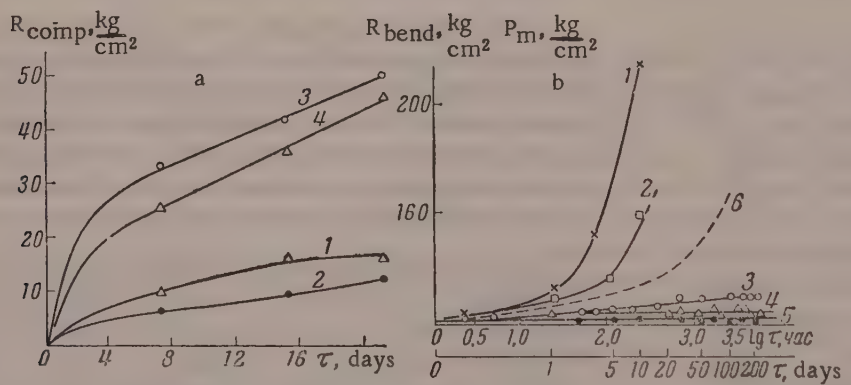


Fig. 5. Hardening kinetics of cement sand and cement soil mixtures. Cement concentration 10% of mineral material. a) Strength of samples: 1, 2—Vol'sk normal sand, s = 500 cm^2/g W/S = 0.10; γ_{skel} = 2.04 g/cm^3; 3, 4—Vol'sk sand ground, s = 9000 cm^2/g, W/S = 0.23 γ_{skel} = 1.73 g/cm^3; 2, 3—compression strength R_{comp}; 1, 4—bending strength R_{bend}. b) Plastic strength of pastes: 1) Vol'sk sand ground, s = 9000 cm^2/g W/S = 0.27; 2) the same, s = 2000 cm^2/g, W/S = 0.15; 3) protective clay W/S = 0.30; 4) Prosyanaya kaolonite, W/S = 0.57; 5) Oglanly bentonite W/S = 0.70; 6) normal Vol'sk sand, s = 500 cm^2/g, W/S = 0.11.

Since at very low lime concentrations in the solution, the hydrosilicates are either not formed or become unstable, and in cement soil mixtures made of clay soils not saturated with Ca^{2+}, the lime depletion of the solution

occurs in the first few days; it is to be expected that under these conditions there will probably be an anomalous development or degeneration of the initially formed binder structure, as a result of conversion of the strongly basic forms. There will be no filling of the liquid phase with lime by solution from the solid phase, since for all the cement soil mixtures investigated the total concentration of free lime after 1.5–2 months is close to zero (Fig. 3).

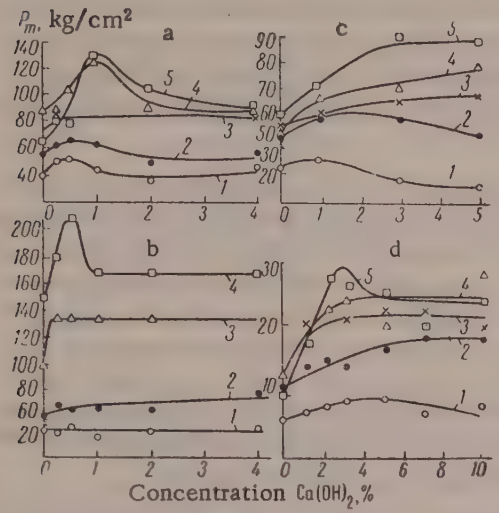


Fig. 6. Plastic strength of cement soil pastes as a function of the quantity of lime added: a) protective clay (Cheremushki) + 10% cement, W/S = 30. Age of samples (24 hour periods): 1-5; 2-15; 3-60; 4-70; 5-110. b) central asiatic loess + 10% cement, W/S = 0.25. Age of samples (24 hour periods): 1-1; 2-15; 3-30; 4-150. c) Krasnodar black earth + 14% cement, W/S = 0.40. Age of samples (24 hour periods): 1-1; 2-20; 3-40; 4-60; 5-95. d) oglanly bentonite + 14% cement, W/S = = 0.70. Age of samples (24 hour periods): 1-1; 2-15; 3-45; 4-65; 5-150.

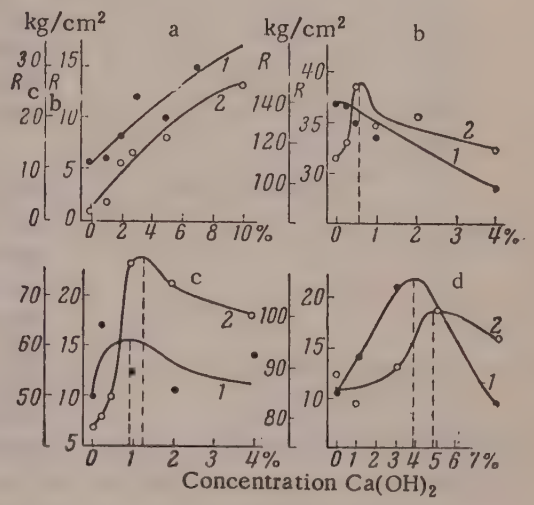


Fig. 7. Strength of cement terrains as a function of the amount of lime added in compression (1) and bending (2). Age of samples 6 months, experiment at humidity maintained in samples with hardening without evaporation: a) Oglanly bentonite + 14% cement, W/S = 0.42; b) central asiatic loess + 10% cement, W/S = 0.15; c) proclay + 10% cement, W/S = 0.18; d) Krasnodar black earth + 10%, W/S = 0.25.

Actually, experiments have shown that in reinforcing one-mineral clays of the montmorillonite group with cement, the samples fall apart themselves 3–6 months after preparation. For samples of one-mineral kaolinite and hydroshist clays, reinforced by the same quantity of cement, no loss in strength is observed (Fig. 4). For soils, satisfactory (according to the classification made) for cement reinforcing, the absorption of lime by the soil can apparently exert a negative influence on the mechanical properties of the cement soil mixtures, by slowing up the growth in strength, or in its maximum value, and with very large absorption even lowering the strength with time.

A large concentration of coarse sand particles in the soil brings the conditions under which the cement stone structure is formed close to the conditions under which cement hardens in dilute solutions. The thinly dispersed silicatious particles, just like ground sand, react chemically under the usual conditions with $Ca(OH)_2$, with the formation of calcium hydrosilicates on the surface of contact between the binder and the mineral particle [18 and 19], which favors densifying and strengthening the structure as a whole. These processes go rather intensively (Fig. 1), but the lime concentration in the liquid phase is here rather high, and, for a long time after laying, it corresponds with the conditions for the stable existence of monocalcium hydrosilicate. The chemical binding of lime is an element in the overall process of forming and reinforcing the structure. Therefore, in a number of cement sand mixtures using sand of various degrees of fineness, the strength of the samples packed at a humidity optimum for the grade of sand used, increases proportional to a specific surface, in spite of the parallel increase in water requirement (Fig. 5, a). A similar effect is observed with lime sand mixtures using various grades of sand [19].

Thus, the degree of dispersion of the soil being reinforced is not in itself the decisive factor in the formation kinetics and final properties of the structure. An additional feature is the nature of the interaction between the

material being reinforced and the binder. If there is chemical interaction increasing the degree of dispersion over wide limits can cause an increase in strength. As distinct from chemical interaction, the adsorptional absorption of lime, which is characteristic of clay minerals, can cause weak development of the crystallizational structures and instability of the hydrosilicate composition. This fact together with the high degree of dispersion and the hydrophilic properties of the clays, which cause an increase in the water requirement of the cement soil mixtures and a reduction in density of the crystallizational structure, is the cause of the low strength and retarded reaction kinetics in the structuration of cement clay mixtures as compared with cement sand mixtures (Fig. 5, b).

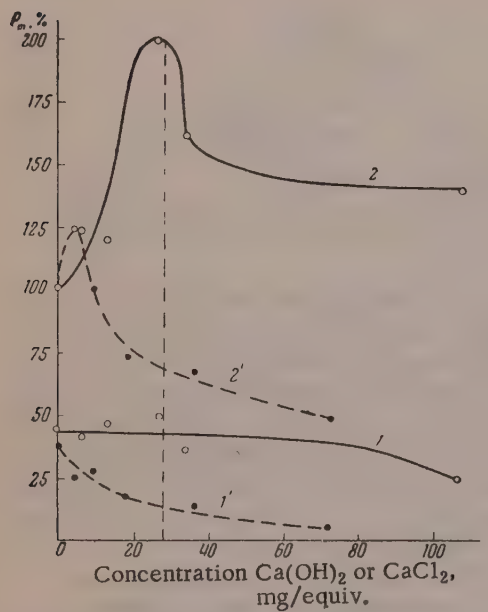


Fig. 8. Plastic strength of cement soil pastes as a function of the quantity of $Ca(OH)_2$ and $CaCl_2$ added (1', 2'). Protective clay + 10% cement, W/S = 0.30. Age of samples (24 hour periods): 1'–1, 2 and 2'–70. p^{70}_m of cement terrain without additive taken as 100%.

To increase the stability of the crystallizational binder structures in cement earth mixtures, and to stabilize the engineering properties of the latter in time, it its necessary to add small quantities of lime along with the cement in reinforcing soils having a large concentration of clay minerals and a large absorptive capacity. The optimum amount added obviously depends on the overall absorptivity of the soil being reinforced. A study of the effect of different quantities of lime on the rate of development of the structure and the final strength of the cement soil mixtures confirm what has been said.

To avoid any effect of the lime acting as a binder, it was added to the cement soil mixtures in the form of a hydrate. Measures were taken to prevent any carbonation of the lime in the samples during the hardening time.

Adding lime accelerates the hardening process and increases and stabilizes the final strength of the cement soil mixtures in different degrees for different soils (Fig. 6).

The optimum quantities of lime at the early stages of hardening is somewhat less than in the later stages, since in the first week's after laying, the reduction in free lime in the system may still be replaced by the gradually hydrolizing minerals in the cement. Depending on the absorptive capacity of the soils, the optimum quantities of lime to be added after formation of the structure are: for loess 0.25% (calculated "saturation" amount 0.26%), for clay 1.1% (saturation value 1.07%) for initial Krasnodar black earth 3–4%, which is in excess of the saturation value (1.1%). Apparently this occurs because of chemical absorption of $Ca(OH)_2$ with formation of calcium humates and as a result of the increase in absorptive capacity of the soil and in alkaline medium. In a case of Oglanly Bentonite, the optimum addition is close to a theoretical value (3%). The positive effect of adding lime has been established for salty soils as well.

Similar results have been obtained with samples prepared at optimum humidity (Fig. 7, table).

The bending strength of the samples is more sensitive to the amount of lime added than the compressive strength. The optimum amount of lime to add in model systems like clay and loess is close to the calculated "saturation" value. For black earth it is somewhat higher. With bentonite we observe a continuous increase in strength within the limits of the concentration of $Ca(OH)_2$ studied.

Adding small quantities of $Ca(OH)_2$ causes an increase in strength equal to, or even greater than, that produced by adding more cement, which agrees with the data of [14].

From what has been said above the smallest relative effect from adding lime is observed with loess and the greatest with bentonite. Calcium salts, in particular, $CaCl_2$ do not show the same effect (Fig. 8). Adding lime stabilizes the hydrosilicate composition and increases the strength and life of the structure. However, adding $CaCl_2$ may favor coagulational structuration, but the conditions for the development and stable existence of hydrosilicates are not improved thereby.

Increase in Strength of Cement Terrains on Adding "Saturating" Quantities of $Ca(OH)_2$ (Experiment at the Humidity Maintained in the Samples on Drying Without Evaporation)

Soil and absorption capacity, mg-equiv/100 g	Cement concentration, %	Strength, kg/cm²				Strength increase, %	
		in compression		in bending			
		without additive	with $Ca(OH)_2$	without additive	with $Ca(OH)_2$	in compression	in bending
Cheremushki clay, 29	10	50	61	7	23,5	22	236
	14	63	—	29	—	—	—
Krasnodar black earth, 30	10	67	93	9	19,5	39	116
	14	85	—	12	—	—	—
Central asiatic loess, 7	10	140	140	31,5	39	0,0	20
	14	151	—	39	—	—	—
Oglanly bentonite, 80	14	11	22	1	7,5	100	650
	20	16	—	4	—	—	—

SUMMARY

1. In a search for methods of increasing the life of cement reinforced terrains a study has been made of the structuration processes in cement soil and cement mineral mixtures.

2. As a result of adsorptional and chemical absorption of lime by the soils, it becomes possible to reduce the basicity of the hydrosilicates formed below those formed under the ordinary conditions of cement hardening in concretes.

3. Depending on the absorptivity of the soil in the cement concentration, the formation of the less basic hydrosilicates can occur, either in the initial period of formation of the structure, or gradually over the course of time.

3. The recrystallization processes resulting from the change in basicity of the hydrosilicates, can cause retardation and growth or a reduction in strength of these cement soil mixtures with time, which is greater, the higher the absorptivity of the soil being reinforced, and the lower the cement concentration.

4. To increase the life and improve the stability of the engineering properties of the cement soil mixtures, it must be considered useful to add lime along with the cement in reinforcing all useable types of soil. With soils having an absorptional capacity of 20–30 mg-equiv and higher, adding lime is obligatory. The amount of lime that should be added corresponds with the overall absorptive power of the soil.

LITERATURE CITED

1. P. A. Rebinder, Izv, AN, SSSR, Otd, khim, n, 1957, No. 11.
2. N. N. Serb-Serbina, Kolloidn, zh, 20, 563, 1958; L. A. Abduragimova, , P. A. Rebinder, N. N. Serb-Serbina, ibid 17, 184, 1955.
3. P. A. Rebinder, Transactions of the conference on engineering and geological properties of minerals species and methods of investigation, Vol. 1. [in Russian] Academy of Sciences Press, USSR, 1956, p. 31.
4. I. M. Gor'kova, Kolloidn, zh, 18, 26, 1956: Reports of the laboratory for hydro-geologic problems of the Academy of Sciences, USSR, [in Russian] 13, 38, 1956, 14, 222, 1957; Transactions of the conference on engineering and geological properties of mineral species and methods of investigation, Vol. 1, [in Russian] Academy of Sciences Press, USSR, 1956, p. 98, Kolloidn zh, 20, 585, 1958.
5. T. YU. Lyubimova, T. V. Yagodovskaya, Kolloidn, zh, 20, 594, 1958.
6. T. YU. Lyubimova, Ibid, 20, 719, 1958.
7. V. N. Izmailova, E. E. Segalova, P. A. Rebinder, Dokl, AN, SSSR, 107, No. 3, 425, 1956.
8. E. E Segalova, V. I. Izmaillova, Kolloidn, zh, 20, 601, 1958.
9. R. K. Ailer, Colloid Chemistry of Silic and Silicates [in Russian] Government Press for Construction Architecture and Building Materials (Moscow, 1959).
10. F. V. Chukhrov, Colloids in the Earth's Crust [in Russian] Academy of Sciences Press, SSSR, 1956.
11. G. Steinor, Transactions of the Third International Congress on the Chemistry of Cement (1952) [translation from English] Government Press for Construction Architecture and Building Materials, 1958, p. 177.

12. J. Bernal, ibid, p. 137.
13. R. H. Bogue, The chemistry of Portland Cement, The system $CaO-SiO_2-H_2O$, N. Y., 1947.
14. V. M. Bezruk, Theoretical Bases of Reinforcing Terrains with Cements [in Russian] Avtotransizdat (Moscow, 1956).
15. S. S. Morozov, Soil Culture Book III, Problems in the Engineering Improvement of Soils, [in Russian] Moscow State University Press, 1953.
16. V. G. Samoilov, Vestnik, MGU, No. 6, 1950.
17. M. P. Matveev, N. I. Gludina, Transactions of the Mendeleev Moscow Chemical Technological Institute [in Russian] No. 21, 111, 1956.
18. V. F. Abrosenkova, G. I. Logginov, T. A. Rebinder, dokl, AN, SSSR, 115, 509, 1957; G. I. Loggenov, P. A. Rebinder, V. F. Abrosenkova, Kolloidn, Zh, 21, No. 4, 442, 1959.
19. Ya. S. Sominskii, G. G. Kornienko, V. V. Komonova, G. S. Khodakov, The Mechanism of Hardening of a Finely Ground Lime-Sand Binder Without Hydrothermal Treatment [in Russian] Academy of Building and Architecture VNII, TISM, Nauchn soobshch, No. 28, 1957.

All abbreviations of periodicals in the above bibliography are letter-by-letter transliterations of the abbreviations as given in the original Russian journal. *Some or all of this periodical literature may well be available in English translation.* A complete list of the cover-to-cover English translations appears at the back of this issue.

INVESTIGATION OF CHANGES IN THE STRENGTH OF ARGILLACEOUS ROCKS ON ELECTROCHEMICAL TREATMENT

N. I. Maksimova, N. N. Serb-Serbina, N. I. Titkov, and A. S. Korzhueva*

Institute of Mineral-Fuel Geology and Processing, Moscow
Translated from Kolloidnyi Zhurnal, Vol. 23, No. 5
pp. 605-614, September-October, 1961
Original article submitted September 19, 1960

Modern ideas on the nature of the strength of aqueous clay dispersions and other soil systems [1, 2], which have gained wide recognition in soil management and geological-engineering service [3-8], enable one to consider processes of strengthening from the point of view of the presence of two principal types of structures therein: coagulation and crystallization. Coagulation structures, even very strong ones, are devoid of water-stability, and readily become sodden on wetting [2]. These properties are explained by the presence of thin residual films of an aqueous medium in contact with the particles [1, 2]. Crystallization structures, which are formed by strong (primary) chemical bonds between particles, arising on intergrowth of microcrystals under certain conditions of crystallization of a new solid phase, may impart considerable water-stability to the structured system without loss of strength.

The results of laboratory investigations of the strength of wet clays of various single-mineral types on treatment with direct-current electricity, are set forth in the present article. The investigations were conducted with regard for the nature of the clays and with allowance for the effect of various factors operative in electrochemical treatment.

The investigation is both of scientific and practical importance in connection with the development of a technique for electrochemically strengthening unstable rocks composing the walls of oil wells [6, 7].

The subjects of the investigations were Oglanly bentonite, Chasov Yar monothermite, and Prosyanaya Kaolin (enriched)**. The characteristics of the original clays with regard to absorption capacity, exchange-cation composition, and composition of aqueous extracts, are given in Table 1.

TABLE 1. Characteristics of Original Clays

Clay	Aqueous extract (1:7)			Absorption capacity (after Zakharchuk) mg-equiv./100 g of clay	Exchange-cation composition (after Gedroits), mg-equiv./100 g of clay		
	pH	mg-equiv./100 g of clay			$Na^+ + K^+$	$Ca^{2+} + Mg^{2+}$	total cations
		Ca^{2+}	Cl^-				
Bentonite	7,5	0,5	17,5	60,7	45,6	14,5	60,1
Monothermite	7,4	3,9	6,3	12,9	0,47	14,4	14,8
Kaolin	8,8	—	0,8	4,7	0,55	6,0	6,55

*L. E. Kuznetsova (Institute of Physical Chemistry, Academy of Sciences, USSR) and E. G. Getts, S. N. Elovika, A. Ya. Neretina, and S. A. Sytnik (Institute of Mineral-Fuel Geology and Processing, Academy of Sciences, USSR) took part in the experimental work.

**The clay samples were obtained from the Karpinskii Mineral Museum, Academy of Sciences, USSR.

The experiments in electrochemical strengthening were performed in open 20 x 20 x 10 cm Plexiglas baths at a current density of 5-50 ma/cm^2 and a voltage of 30-50 v. Graphite, aluminum, and iron plates, lying horizontally on the surface of the clay sample, 3-4 cm apart, were used as electrodes. Current was passed through the samples for 5-100 hr in separate experiments. Calcium carbonate and calcium chloride were added in some experiments. The calcium carbonate (in the amount of 15% by weight of the solid phase*) was thoroughly mixed into the clay before treatment with current. The calcium chloride was added before and during treatment with current, in the form of a 1% aqueous solution. The experimental conditions precluded electroosmotic drying of the clays under investigation, since distilled water was added to them periodically during the electrical treatment.

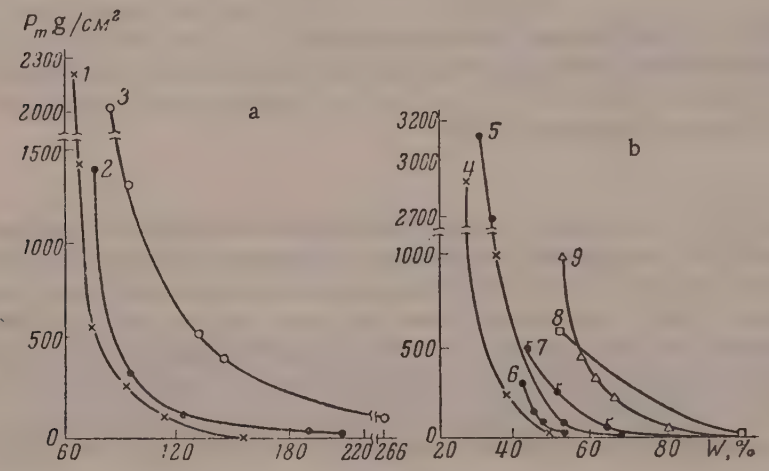


Fig. 1. Plastic strength of aqueous pastes of bentonite (a) and kaolin and monothermite (b), electrically treated for 100 hr, with graphite electrodes and distilled water: 1) original bentonite; 2) bentonite from the anode zone; 3) bentonite from the cathode zone; 4) original kaolin; 5) kaolin from the anode zone; 6) kaolin from the cathode zone; 7) original monothermite; 8) monothermite from the anode zone; 9) monothermite from the cathode zone.

At the end of the experiment the pH in the electrode zones of the sample was measured by means of an LP-5 potentiometer with paired antimony and calomel electrodes, whereas the pH of the aqueous extracts was determined by means of a glass electrode.

After the electrical treatment the clay samples were tested for strength in the undisturbed and disturbed states. Test samples were taken from the electrode zones at a depth of 3-5 cm from the sample surface. Test samples with undisturbed structure were tested for uniaxial compressive strength in the water-saturated state after standing in water for 7 days. Samples with disturbed structure (pastes) were tested in a conical plastometer, which enabled one to determine the limiting shearing stress – plastic strength (P_m, g/cm^2) – characterizing the carrying capacity of the given structured system [1]. The plastic strengths of thixotropically-strengthened pastes (after standing quietly for 15-20 hr in a desiccator over water) are plotted with respect to water content in Figs. 1-6.

Chemical and mineralogical analyses of the electrically-treated clay samples are given in Tables 2-6.

It is evident from Fig. 1 that when a constant electric field is applied, the plastic strength of the clay increases independently of the mineral type of the clay. Strengthening of this type of structure (coagulation) is pronounced in the region of more-concentrated pastes for the anode and cathode zones of the sample. Bentonite clay, taken from the cathode zone, showed coagulation strengthening of thixotropic character at much higher values of water content. Clay samples with undisturbed structure are devoid of strength on keeping in water. This

* This approximately corresponds to the content in natural rock of the Lower Kazanian substage.

may be explained by the fact that the conditions of the electrical treatment do not permit the synthesis of new mineral compounds which might lead to the formation of structures with stronger bonds. The amount of neogenic calcite, whose deposition in the cathode zone was confirmed under the microscope, apparently was insufficient for the appearance of such a structure under the experimental conditions. The curves of Fig. 2a show that application of an electric field to bentonite paste samples containing calcium compounds causes a more noticeable

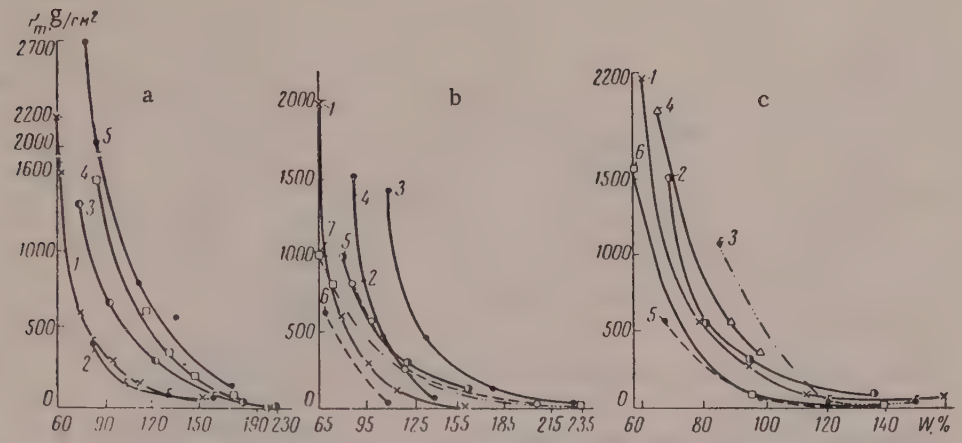


Fig. 2. Plastic strength of aqueous bentonite pastes containing various added compounds, with and without electrical treatment. a) Addition of $CaCl_2$ or $CaCO_3$: 1) original; 2) without electrical treatment, with $CaCl_2$; 3) same, with $CaCO_3$; 4) from the cathode zone, electrically treated, with $CaCl_2$; 5) same, with $CaCO_3$. b) Addition of $Al(OH)_3$ gel: 1) original; 2) without electrical treatment, with 9% $Al(OH)_3$ gel; 3) same, with 17% $Al(OH)_3$ gel; 4) anode zone, treated electrically for 15 hr with aluminum anode and iron cathode, without added $Al(OH)_3$ gel; 5) cathode zone, same; 6) anode zone, electrically treated for 15 hr with aluminum electrodes, without added $Al(OH)_3$ gel; 7) cathode zone, same. c) Addition of $Fe(OH)_3$ gel; 1) original; 2) without electrical treatment, with 9% $Fe(OH)_3$ gel; 3) anode zone, electrically treated with aluminum anode and iron cathode, with added $CaCl_2$ solution, without added $Fe(OH)_3$ gel; 4) cathode zone, same; 5) anode zone, electrically treated with iron electrodes, without added $Fe(OH)_3$ gel; 6) cathode zone, same.

strengthening of test samples from the cathode zone than electrical treatment with distilled water (Fig. 1a). Bentonite samples in the undisturbed and water-saturated states showed uniaxial compressive strengths of 4.8 and 6.0 kg/cm^2. The data obtained permit the conclusion that a crystallization structure is formed in the cathode zone at the expense of neogenic calcite. Data of chemical analysis of aqueous and hydrochloric acid extracts of bentonite electrically treated with and without addition of $CaCO_3$ and $CaCl_2$ (Table 2), showed that large amounts of water-insoluble calcium compounds are deposited in the cathode zone. On electrical treatment with $CaCO_3$ addition, calcite formation was preceded by solution of this salt in the anode zone. Calcium carbonate, added to the clay even in large amounts (15% of the weight of the solid phase) without electrical treatment, has much less effect on the strength (curve 3, Fig. 2a) and does not impart water-stability to the rock (the strength of this sample is zero in the water-saturated state). In this case the calcium carbonate acts as a filler. Addition of 3% $CaCl_2$ to bentonite without electrical treatment showed no strengthening effect (curve 2, Fig. 2a).

On treatment of bentonite pastes with electric current, using only aluminum (curves 6 and 7, Fig. 2b) or iron electrodes (curves 5 and 6, Fig. 2c), no strengthening effect is obtained. Under similar experimental conditions (treatment for 15 hr), but with an aluminum anode and iron cathode, bentonite paste is strengthened, to a greater degree in test samples from the anode zone. This is explained by the fact that when the anode and cathode consist of different materials, a high potential difference is established between the anode and cathode portions of the system, which promotes accelerated corrosion of the metallic electrodes, whereas the corrosion products are additional material for the production of neogenic matter. Thus after electrical treatment of bentonite for 15 hr with an aluminum anode and iron cathode, a test sample in the undisturbed state from the anode zone had a compressive strength of 2.0 kg/cm^2 in the water-saturated state. Microscopic examination of this sample revealed the

presence of colloidal aluminum hydroxide, which apparently caused the strengthening of this sample.

Comparison of the character of strengthening of an electrically-treated bentonite paste and a nonelectrolyzed one containing $Al(OH)_3$ or $Fe(OH)_3$ gel, shows the importance of neogenic colloidal matter in electrochemical clay-treatment processes.

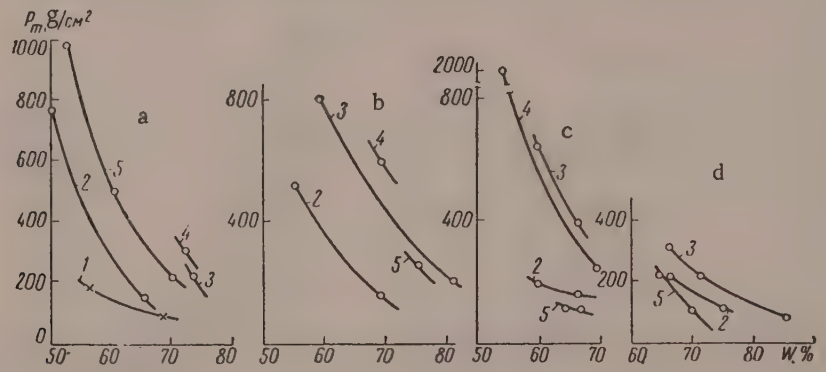


Fig. 3. Plastic strength of aqueous monothermite pastes after electrical treatment for 5 hr (a), 15 hr (b), 30 hr (c), and 100 hr (d) without changing the electrode polarity: 1) original monothermite; monothermite from the zone of an: 2) iron anode; 3) iron cathode; 4) aluminum anode; 5) aluminum cathode.

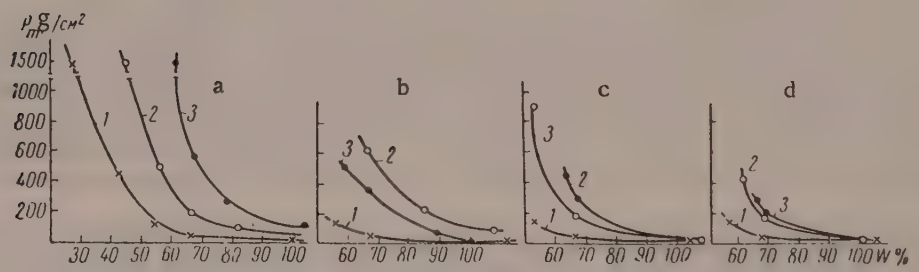


Fig. 4. Plastic strength of aqueous monothermite pastes after electrical treatment for 5 hr (a), 15 hr (b), 30 hr (c), and 100 hr (d) with alternation of electrode polarity: 1) Original monothermite; 2) monothermite from the zone of the iron electrode; 3) same, aluminum electrode.

$Al(OH)_3$ and $Fe(OH)_3$ gels, prepared by precipitation of the chlorides with ammonia, followed by washing of excess precipitant out of the resulting hydrated sesquiozide precipitate, were added to wet clay. The amount of added gel, reckoned on the dry substance Al_2O_3 or Fe_2O_3, approximately corresponded to the amount formed in the clay on electrical treatment with metal electrodes, according to analytical date for hydrochloric acid extracts from bentonite.

The neogenic colloidal substances, originally formed on electrical treatment, can go over to their crystalline modifications. A typical example is the transition of aluminum hydroxide gel to limonite, etc. [6, 7]. The effects of the time of treatment by current and alternation of electrode polarity on the change in composition and strength of clays, have been most fully studied in the case of monothermite. Electrical treatment was carried out with aluminum and iron electrodes for 5, 15, 30, and 100 hr with constant and alternating electrode polarity; the polarity was changed every hour in the latter case. In the course of electrical treatment a 1% $CaCl_2$ solution was added. The results of these experiments (Figs. 3-5) show that the optimum increase in the plastic strength of aqueous monothermite pastes occurs in the interval 5-15 hr of electrical treatment. It is evident from Fig. 5a that

a test sample from the zone of the aluminum electrode has greater optimum strength than one from the zone of the iron electrode when the water content is the same in both (66%); under the conditions of the given experiments a positive charge on the aluminum electrode produced greater plastic strength than a negative charge; this evidently was due to the formation and accumulation of a large amount of aluminum hydroxide gel. It is evident from Fig. 5b that when the electrode polarity is alternated, the optimum increase in the strength of a test sample from the zone of the aluminum electrode, is reached in less than 10 hr, whereas that for a sample from the zone of the iron

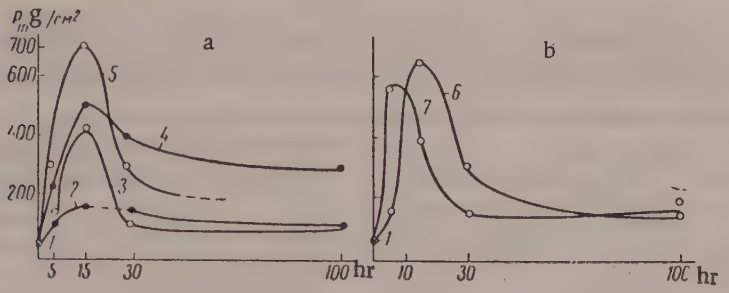


Fig. 5. Plastic strength of aqueous monothermite pastes with respect to kinetics of electrical treatment with constant (a) and alternating (b) electrode polarity; water content in the pastes, 66%. 1) Original monothermite; 2) monothermite from the zone of an iron anode; 3) same for an aluminum cathode; 4) same for an iron cathode; 5) same for an aluminum anode; 6) same for an iron electrode; 7) same for an aluminum electrode.

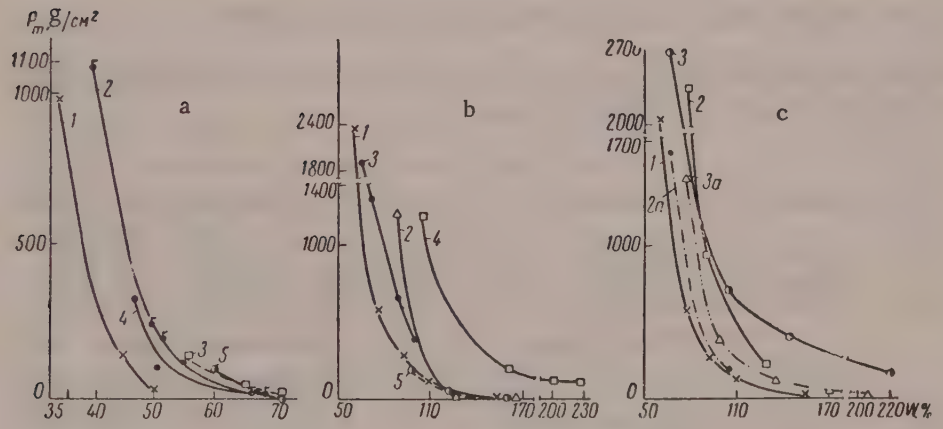


Fig. 6. Plastic strength of aqueous pastes of: a) Kaolin electrically treated for various times with an aluminum anode and iron cathode, $CaCl_2$ solution being added: 1) original; 2) electrical treatment 15 hr, cathode zone; 3) same, anode zone; 4) electrical treatment 100 hr, cathode zone; 5) same, anode zone. b) Bentonite electrically treated with an aluminum anode and iron cathode, $CaCl_2$ solution being added: 1) original; 2) electrical treatment 15 hr, anode zone; 3) same, cathode zone; 4) electrical treatment 100 hr, cathode zone; 5) same, anode zone. c) Bentonite electrically treated for various times with graphite electrodes and distilled water: 1) original; 2) electrical treatment 15 hr, cathode zone; 2a) same, anode zone; 3) electrical treatment 100 hr, cathode zone; 3a) same, anode zone.

electrode is reached within 15 hr. During this period of electrical treatment the strength of a monothermite paste increases from 60 to 600-650 g/cm^2. There is practically no appreciable zonal variation of optimum strength, which is one of the essential advantages of electrical treatment with alternating polarity. When the time of elec-

trical treatment with alternating polarity is increased to 30-100 hr, the strength of the pastes falls to 200-300 g/cm^2 for the same water content. As a result of electrode-corrosion processes taking place, aluminum and iron compounds are deposited in the clay in the form of colloidal or crystalline formations, which changes the character of the clay. This is confirmed by chemical analysis of aqueous and hydrochloric acid extracts, showing the content of the hydrated oxides, Al_2O_3 and Fe_2O_3 (Tables 3-6). After 15 hr of electrical treatment with alternating polarity the content of iron and aluminum compounds is greater than with constant polarity. Thus with alternating polarity the R_2O_3 content in the zone of the iron electrode is 8.7% and that in the zone of the aluminum electrode

TABLE 2. Data of Chemical Analysis of Various Extracts of Electrically-Treated and Nonelectrolyzed Bentonite (Electrical Treatment with Graphite Electrodes for 100 hr)

Additions on electrical treatment	Place of sampling for analysis	pH of aqueous extract S : L = 1 : 7	CaO in aqueous extract, %	Extract in 5% HCl, % relative to dry sample				Extract in 5% Na_2CO_3 (colloidal SiO_2)
				CaO	Al_2O_3	Fe_2O_3	SiO_2*	
Water	Anode	—	—	0,90	2,92	0,43	1,82	0,19
	Cathode	10,2	0,38	1,72	2,48	0,62	1,84	4,14
$CaCO_3$, 15% relative to weight of dry sample	Anode	—	—	0,98	1,89	0,41	2,00	3,28
	Cathode	11,5	0,29	6,84	2,30	0,59	1,47	6,67
$CaCl_2$, 1% solution	Anode	—	—	—	1,61	0,32	1,96	8,70
	Cathode	11,3	0,09	11,9	—	0,54	—	5,90
Bentonite before elect. treatment	—	7,5	0,01	0,47	0,95	0,30	1,02	7,91

*Colloidal hydrous oxide, isolated on precipitation of the sesquioxides.

TABLE 3. Results of Analyses of Aqueous Extracts of Monothermite Electrically Treated With Constant Polarity, and Nonelectrolyzed

Time of treatment, hr	$Ca^{2+}+Mg^{2+}$	Cl^-	Fe_2O_3	Al_2O_3	Extract pH	Dry residue, %	$Ca^{2+}+Mg^{2+}$	Cl^-	Fe_2O_3	Al_2O_3	Extract pH	Dry residue, %
	mg-equiv./100 g of clay		% relative to weight of clay				mg-equiv./100 g of clay		% relative to weight of clay			
	Aluminum anode						Aluminum cathode					
5	29,2	14,9	1,52	—	4,2	2,9	1,2	4,6	None	None	10,0	3,35
15	8,9	17,6	None	0,14	4,03	1,08	4,6	7,6	»	»	10,3	0,58
30	8,1	35,0	Traces	0,48	4,19	1,78	2,7	23,3	»	0,2	11,8	1,82
100	13,0	19,0	None	—	7,18	1,04	2,0	55,8	0,84	—	11,2	0,90
	Iron anode						Iron cathode					
5	10.20	36,3	1,96	Нет	3,3	0,72	2,4	26,70	None	None	8,9	0,03
15	4,8	33,6	—	1,18	2,7	2,32	1,6	0,70	»	»	11,59	0,21
30	21,0	188,9	1,50	0,66	2,9	7,32	3,0	12,90	»	0,19	11,50	0,84
100	11,8	2,4	0,03	0,44	3,9	2,4	—	—	—	—	—	—
Without electrical treatment	1,2	3,8	None	None	7,4	None						

is 10.6%, without alternation of polarity the corresponding figures are 4.6 and 6.3% R_2O_3 in the anode zones, and 0.95 and 3.5% R_2O_3 in the cathode zones. On prolonged electrical treatment with alternating polarity the clay also is enriched by much greater amounts of aluminum and iron compounds than in the case of treatment with constant

polarity. Thus, for instance, after electrical treatment for 100 hr with alternating polarity 35.3% R_2O_3 was found in the zone of the iron electrode, whereas with constant polarity 13.4% R_2O_3 was found in the anode zone and 18.1% in the cathode zone.

Therefore alternation of electrode polarity leads to a large accumulation of neogenic substances as a result of eliminating polarization, and increased electrode corrosion.

The composition of aqueous extracts of the samples (Tables 3, 5) indicates that they contain a considerable amount of chlorides. Presumably the latter strongly affects coagulation processes in these pastes with the formation of compact aggregates, which also has a pronounced influence on the character of structure formation in them. It was found by mineralogical study of the electrically-treated monothermite samples, that with alternating electrode polarity limonite and hydrogoethite are formed in the zone of the iron electrode on treatment for 15 hr, and magnetite is formed there on treatment for 30-100 hr; in the zone of the aluminum electrode after the indicated period of treatment, gibbsite and small amounts of calcite were found. On treatment of monothermite with constant electrode polarity neogenic substances are noted mainly in the cathode zones. When an aluminum cathode is used, gibbsite deposition in the cathode zone is observed even after 5 hr of electrical treatment, and after 15 hr of treatment the test samples contain large amounts of calcite and smaller amounts of gibbsite; after 30 and 100 hr of electrical treatment gibbsite becomes predominant. When an iron cathode is used, calcite formation in the cathode zone of the sample is delayed; under the microscope this mineral was found in cathode test samples of monothermite only after 30 and 100 hr of electrical treatment.

TABLE 4. Results of Analyses of a Hydrochloric Acid Extract of Monothermite Electrically Treated with Constant Polarity

Test sample from zone of	Al_2O_3, % relative to weight of clay				Fe_2O_3, % relative to weight of clay			
	duration of electrical treatment, hr							
	5	15	30	100	5	15	30	100
Aluminum anode	0,13	4,6	4,2	18,0	0,17	0,06	1,1	0,17
Iron cathode	0,09	0,5	5,8	0,0	0,34	0,45	0,6	1,1
Iron anode	3,15	3,5	8,3	6,2	2,69	2,8	2,7	2,6
Aluminum cathode	None	1,0	5,2	4,7	2,2	2,5	9,5	8,7

TABLE 5. Results of Analyses of Aqueous Extracts of Monothermite Treated with Alternating Polarity

Test samples from zone of	Duration of treatment, hr	$Ca^{2+}+Mg^{2+}$	Cl^-	Extract pH	Dry residue, % relative to weight of clay
		mg-equiv./100 g of clay			
Aluminum electrode	5	7,0	8,3	6,5	0,70
	15	2,4	26,3	6,7	1,61
	30	—	25,1	—	—
	100	—	35,7	—	—
Iron electrode	5	10,0	8,7	7,4	—
	15	0,1	11,0	10,5	0,71
	30	5,3	15,7	10,9	1,26
	100	13,8	20,0	9,6	1,48

The effect of the duration of electrical treatment also was studied in other types of clays – bentonite and kaolin – with treatment times of 15 and 100 hr and constant electrode polarity. The law of change of strength with time, which applies to the electrical treatment of monothermite clay, also applies to that of kaolin under the same conditions (Fig. 6a).

Based on data of mineralogical analysis of these samples, one may ascribe the strengthening of kaolin soils to the formation of new minerals in them: allophane and hisingerite in the anode zone, and calcite and hisingerite in the cathode zone. The appearance of allophane in the anode zone is due to corrosion of the aluminum electrode and the presence of colloidal silica in the wet clay.

The results of investigation of bentonite pastes, treated with direct current, metal electrodes and added $CaCl_2$ solutions being used (Fig. 6b), show that strengthening in the zone of the aluminum electrode is observed only in pastes of low water content after 15 hr of electrical treatment. As the water content of these pastes increases, the strength sharply decreases to values corresponding to the strength of the original bentonite.

The coagulation strengthening of clay pastes in the cathode zone after 100 hr of electrical treatment of the sample, is noted for a wide range of water contents in the pastes. Mineralogical analysis of these bentonite samples shows the appearance of allophane and calcite in them. The quantity of these minerals increases with the duration of electrical treatment. Deposition of allophane was observed in the anode zone of the clay sample after 15 hr of treatment, and in both electrode zones after 100 hr.

TABLE 6. Results of Analysis of a Hydrochloric Acid Extract of Monothermite Treated with Alternating Polarity

Test sample from zone of	Al_2O_3, %				Fe_2O_3, %			
	duration of electrical treatment, hr							
	5	15	30	100	5	15	30	100
Aluminum electrode	0,21	10,0	6,62	10,0*	0,15	0,64	0,31	—
Iron electrode	None	2,4	10,0	15,2	0,74	6,36	7,72	20,1

* Total sesquioxides.

The results of electrical treatment for 15 and 100 hr, with graphite electrodes having constant polarity (Fig. 6b), show that the optimum increase in the strength of the coagulation structure of the cathode test sample is noted after 15 hr of treatment with the current and is observed in pastes with low water content, which indicates that the clay sample has a shorter interval of plasticity than test samples from this zone after treatment of bentonite for 100 hr.

This apparently may be explained by the fact that on more prolonged treatment of clay (100 hr), using indifferent electrodes and not adding any electrolyte, the salts present in the clay are carried out to a greater degree, and constitute additional material for the formation of neogenic cementing substances.

After electrical treatment the absorption capacity and the composition of exchange cations in the clay samples, are changed. Thus the absorption capacity (in total cations) of bentonite before electrical treatment is 60.7 mg-equiv./100 g of clay, whereas with addition of 1% $AlCl_3$ solution, after electrical treatment with aluminum electrodes for 100 and 700 hr it is 21.5 and 4.3 mg-equiv./100 g of clay, respectively. The content of $Na^+ + K^+$ ions is decreased from 45.6 to 15.3 mg-equiv./100 g of clay after 100 hr of treatment and to 3.1 mg-equiv./100 g of clay after 700 hr; this indicates a radical change in the character of the soil.

Substantial chemical changes in clays on treatment with direct current are indicated also by analytical data for silicic acid in the soda extracts of the clay samples. As is evident from Table 2, the content of soluble silica decreases after electrical treatment of the clays, which may be explained by its incorporation into various neogenic materials.

SUMMARY

1. The structure strength in aqueous clay dispersions of various mineral types is increased on application of a constant electric field. The mechanism and character of this strengthening are explained by the appearance of new mineral compounds in the form of colloidal or crystalline formations.

2. On electrical treatment of clay with addition of calcium compounds the strength of the clay increases, especially in the cathode zone, owing to the appearance of a new mineral compound – calcite.

In the absence of current calcium carbonate affects the strength of clay pastes as a filler.

3. The optimum increase in the strength of the coagulation structure of clays (monothermite) is attained after 10-15 hr of electrical treatment. The active influence of an aluminum anode on the strengthening of clay, is elucidated.

4. Alternation of the electrode polarity eliminates effects of electrode polarization and increases electrode corrosion, leading to considerable accumulation of neogenic cementing substances.

The authors thank Academician P. A. Rebinder and Prof. V. P. Petrov for a consultation, and manifest interest in the work.

LITERATURE CITED

1. P. A. Rebinder, Transactions of the Conference on the Engineering-Geological Properties of Rocks and Methods for Studying Them [in Russian], Vol. 1 (Moscow, 1956) p. 31.
2. N. N. Serb-Serbina and P. A. Rebinder, Proceedings of the International Conference on Clays at Brussels in 1958 [in Russian] (Moscow, Acad. Sci. USSR Press, 1958), p. 115.
3. I. M. Gor'kova, Transactions of the Academician F. I Savarenskii Laboratory of Hydrogeological Problems [in Russian]; Vol 13 (1956), p. 46.
4. N. Ya. Denisov, On the Nature of Deformation of Argillaceous Rocks [in Russian] (Rechizdat, 1951).
5. G. N. Zhinkin, Kolloidn. zh. 22, 31 (1960).
6. N. I. Titkov, A. S. Korzhuev, V. G. Smolyaninov, V. A. Nikishin, and N. Ya. Neretina, Electrochemical Method of Strengthening Unstable Rocks [in Russian] (Gostoptekhizdat, 1959).
7. A. S. Korzhuev and N. I. Titkov, Electrochemical Method of Strengthening Soils and the Prospects of its Use in Well Drilling [in Russian] (Acad. Sci. USSR Press, 1959).
8. N. I. Maksimova, N. N. Serb-Serbina, N. I. Titkov, and A. S. Korzhuev. Dokl. AN SSSR 132, 413 (1960).

All abbreviations of periodicals in the above bibliography are letter-by-letter transliterations of the abbreviations as given in the original Russian journal. *Some or all of this periodical literature may well be available in English translation.* A complete list of the cover-to-cover English translations appears at the back of this issue.

INFRARED SPECTROSCOPIC INVESTIGATION OF THE STRUCTURATION PROPERTIES OF POLYMERS

G. L. Maslenkova

Agrophysical Scientific Research Institute, Leningrad
Translated from Kolloidnyi Zhurnal, Vol. 23, No. 5,
pp. 615-620, September-October, 1961
Original article submitted July 18, 1960

The use of synthetic structurizers is widespread, Ref. [1].

Many papers have been devoted to the study of the mechanism of the interaction of polymers with soil particles, Refs. [2-6]. Studies have been made with the electron microscope, Ref. [7], by X-ray analysis, Refs. [8 and 9], from infrared spectra, Ref. [10], etc., as a result of which, many different points of view have been expressed as to the mechanism of the interaction.

Some authors regard the macromolecules and soil particles as macro-ions, and electrostatic interaction (Coulomb forces), Ref. [9], plays the principal role. Other authors ascribed the principal role to the active functional groups of the macromolecules (carboxyl, amide, phenyl, hydroxyl). Here, Coulomb forces, Van-der-Waals forces, and hydrogen bonds are invoked, Refs. [8, 13 and 14].

Some authors come to the conclusion that in the interaction between polymers and soil, a large role is played by exchange processes, Ref. [9], while others come to precisely the opposite conclusion, Refs. [11 and 12]. The over-whelming majority of the authors, who try to explain the mechanism of artificial structuration, express the opinion, that hydrogen bonds, Ref. [2], arise in the interaction between the polymer and the soil particle. In a number of papers, these ideas are supported by experimental studies of infrared spectra, Refs. [10 and 15].

It may be regarded as an established fact, Ref. [16], that a hydrogen atom, covalently bound with an atom of a strongly electro-negative element (especially fluorine, nitrogen or oxygen), is able to unite with another atom of the same element by means of the hydrogen bond.

The most common types of hydrogen bond are the following, Ref. [17]:

1. O–H .O, in the hydroxyl group. This is the kind of intermolecular bond which is formed in water, alcohols, and phenol. Polymerization through the hydrogen bond in these compounds can be very large.

2. O–H...O, in the carboxyl group. The carboxyl group $-C\begin{matrix}O\\OH\end{matrix}$ is inclined to form a hydrogen bond: the oxygen atom can unite with hydrogen of other molecules, the hydrogen atom can unite with oxygen of other molecules. A bond of this sort is oberved in carboxylic acids.

3. N–H...N, is formed by compounds of NH_3, NH_2, and RNH when they are dissolved in water.

The hydrogen bond is one of the forms of intermolecular interaction. It occupies an intermediate position between the usual chemical forces and the intermolecular Van-der-Waals forces (the interaction energy of chemical forces is ~ 100 kilo-cal/mol, of Van-der-Waals forces 1-2 kilo-cal/mol, and the energy of hydrogen bonds is 4-8 kilo-cal/mol).

It is known from X-ray structural data, that for the usual molecular crystals the distance between neighboring molecules is equal to 3.2-4.5 A, Ref. [18]; however, for crystals with a hydrogen bond the distances between the various pairs of neighboring molecules are: For O...O, from 2.42 to 2.92 A, for N...O from 2.55 to 3.18 A, for N...N from 2.65 to 3.28 A.

A large number of spectroscopic investigations have made it possible to establish, Ref. [19], that in the gaseous phase or in very dilute solutions, where the molecules are isolated from one another and are unable to form a

hydrogen bond, a sharp line is observed in the spectrum, which corresponds with oscillations of the OH group ($\sim 3600\ cm^{-1}$). In the liquid state, the line becomes quite diffuse, and is converted into a band, whose maximum is considerably displaced relative to the gas line by 200-400 cm^{-1}, which shows that a hydrogen bond has been formed. At high temperatures, where isolated molecules exist along with those that are bound with one another, the band at $\sim 3600\ cm^{-1}$ and the line ~ 3200-$3400\ cm^{-1}$ are observed to exist simultaneously. The intensity of the hydrogen bond band in solutions of substances which contain the OH group depends on the concentration of the dissolved substance.

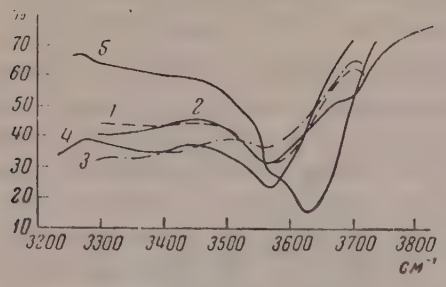


Fig. 1. Infrared transmission curves: 1) Moraine clay 2) cambrian clay; 3) salt soil; 4) montmorillonite; 5) kaolinite.

We have used infrared spectroscopy to study the interaction of structurizing polymers with soil particles. New absorption bands can appear in the infrared absorption spectra from the interaction of the polymers with the soil, which come, for example, from the formation of a hydrogen bond, along with displacement of the already existing bands due to the oscillations caused by free NH and OH groups, while at the same time these absorption bands may also change in intensity. Since all the structurizing polymers (polyacrylamide, hydrolized polyacrylonitrile, and copolymer VIII) form hydrogen bonds themselves, if we are going to study the nature of the bonds arising from the interaction of the polymers with the soil particles, it is impossible to follow the change in the active groups of the polymers, but it is simpler and more reliable to follow the behavior of the active groups in the clay particles.

Of the clay minerals, we investigated: kaolinite, montmorillonite, cambrian clay, moraine clay, and salt soil with a large concentration of clay fractions.

In the infrared spectrum of kaolinite, the absorption band from the hydroxyl group lies at 2.75 μ ($3630\ cm^{-1}$). The same frequency is shown by the absorption band of cambrian, moraine clay and salt soil (Fig. 1), due to the fact, that these samples contain clay minerals of the montmorillonite group. However, the most intense hydroxyl group absorption band occurs in kaolinite, since the ratio of the number of hydroxyl to silicate groups in kaolonite is greater than in montmorillonite, not to mention the soil samples where the clay fraction forms only a constituent part of the sample. Therefore, the study of polymers from the point of view of their structurizing properties, is most easily accomplished by seeing how they react with kaolinite.

In kaolinite, $Al_4[Si_4O_{10}]\ [OH]_8$, (Fig. 2), the tetrahedral silicate groups are bound at three angles into the usual hexagonal network layer, and every fourth apex, occupied by oxygen, takes part in the formation of the lower "hydrargillic layer". At the contact between each layer packet and the following one, there are located on one side hydroxyl groups, and on the other oxygen ions belonging to the following basal tetrahedral layer, Ref. [21]. In the formation of the hydrogen bond between the kaolinite and the polymer, the kaolinite participates through the hydroxyl groups.

The structurizing polymers used were: polyacrylamide, Copolymer VIII (60% metacrylic acid and 40% metacrylimide), and hydrolized polyacrylonitrile. In these polymers there are carboxyl and amide groups, which are able to form hydrogen bonds. Consequently, if the polymers react with kaolinite, they are able to form bonds of the type OH...O and OH...N.

However, if, in observing the reaction of kaolinite with a polymer, we compare the spectrum of pure kaolinite with the spectrum of kaolinite, treated with a polymer (Fig. 3), it turns out, that the intensity of the free hydroxide bands is considerably reduced. This shows, that the number of free hydroxyls is considerably reduced, and this can occur only if the free hydroxyls are bound by a hydrogen bond with the polymer, which is apparently what has occurred. So that this state of affairs may not be subject to any doubt, we took the spectrum of a mechanical mixture of kaolinite and polymer, in which the intensity of the absorption band is comparable with the intensity of the absorption band of pure kaolinite (Fig. 3a). As might be expected, no reaction occurs between the polymers and the mineral in a dry mechanical mixture, and the intensity of the free hydroxide band is not reduced.

When the kaolinite was treated with polymers, a 0.1% solution of polymer was poured into a 100 cc cylinder, and then 100 mg of kaolinite was put in too. The contents of the cylinder were carefully mixed several times over the course of 2-3 days, were then dried and pulverized in a vibration mill, and subjected to study. The spectra

were taken on an IKS-11 infrared spectrometer, and recorded on an EPP-09 electronic potentiometer with an FEOU-18 amplifier. A sodium chloride prism was used in the work.

From the infrared absorption spectra it was also possible to observe a difference in the way the different polymers react with soil.

From Vershinin's data, Ref. [22], the most water stable aggregates are obtained when the soil reacts with polyacrylonitrile, less when it reacts with copolymer VIII, and still less when it reacts with polyacrylamide.

It is clear from the spectra (Fig. 3b), that the free hydroxide band shows the smallest intensity with mixtures of kaolinite and polyacrylonitrile; next in order is copolymer VIII, and finally there is very little change at all in a mixture of kaolinite and polyacrylamide. This means that a large number of kaolinite hydroxyls are bound with a hydrogen bond to polyacrylonitrile molecules, somewhat less to copolymer VIII molecules, and a very small number to polyacrylamide molecules. Consequently, in the structuration process, the appearance of hydrogen bonds between the polymers and the soil particles apparently assumes a leading role. Obviously, the electrostatic interaction also plays an important role in the structuration process. It is perfectly clear that if any kind of a bond is going to be formed between the polymer and the soil particle, they have got to be brought close to one another.

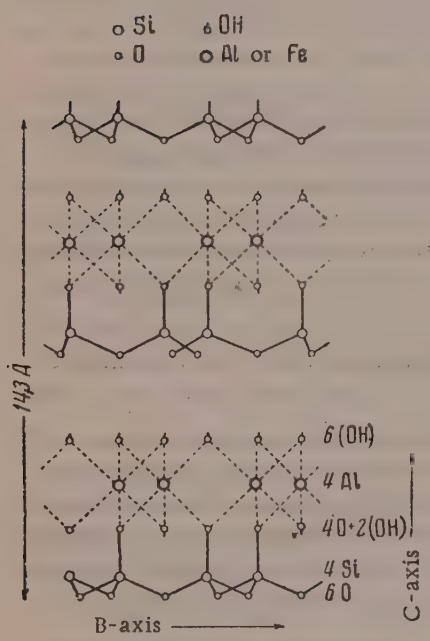


Fig. 2. Kaolinite structure.

It is more correct to consider the structuration processes as consisting of two stages. In the first stage the polymer is brought close to the soil particles by electrostatic attraction forces, which is easily understood, if we are dealing with polycations, but is completely incomprehensible, if we are dealing with polyanions or neutral polymers. It is possible that the interaction between the latter is based on other phenomena. But in ways that are at present not completely clear, the polymer molecule gets close to the soil particles, and then, in the second stage, the hydrogen bonds are formed.

All the structurizing polymers in use are coagulators, and polyacrylamide is the best one of the lot. The more of a coagulator the polymer is, the larger are the particle agglomerations formed in solution (microphotographs). It may be seen from Fig. 4, that the largest particles are formed in polyacrylamide solution. If the structuration process were caused by electrostatic forces, then it would seem that the most water resistant soil aggregates would be formed by treating the soil with polyacrylamide, which is not what actually happens.

If the formation of the soil structure is caused by hydrogen bonds between the polymers in the soil, the question arises of just why polyacrylonitrile forms the most hydrogen bonds with the most water resistant structure, and polyacrylamide forms the least hydrogen bonds and the least water resistant aggregates, while the copolymer VIII occupies an intermediate position.

The explanation of this phenomenon must be sought in the fact that the structurizing effect of polymers is in large measure dependent on the dimensions and form of the macromolecules, the degree of branching, the quantitity and nature of active functional groups, the number of these groups per unit of polymer, and their distribution in the polymer, Ref. [13].

In our case, the difference in structurizing effect is caused by the form of the molecules, which, in turn, is determined by the number of ionized groups. In water solution of polymers the carboxyl groups are weakly dissociated. As they are neutralized with alkali, the strongly dissociated salt $COO^- + Na^+$ is formed, Ref. [23].

If polyacrylamide is not hydrolized Ref. [24], it contains ($-CONH_3^+$) groups, which react with the negatively charged clay particles. But the polyacrylamide molecules wind up into a ball and hydrogen bonds are formed between the molecular chains themselves, which prevents any structurizing effect. At a small degree of hydrolysis the isoelectric point is reached, at which we observe a maximum of winding up and a minimum of structurizing

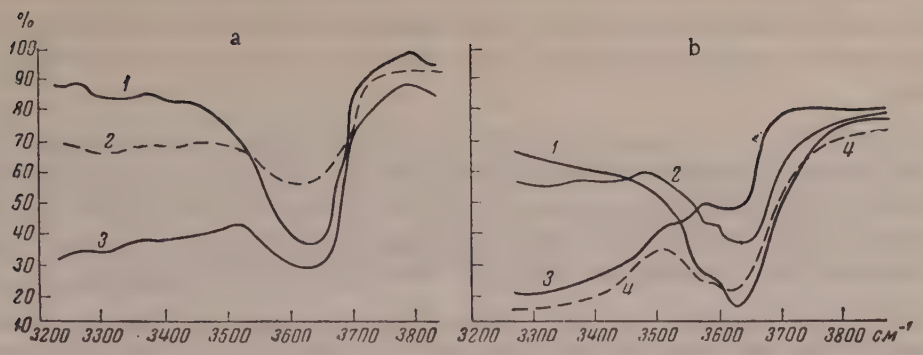


Fig. 3. Infrared transmission curves: a) Kaolinite (1), kaolinite, treated with copolymer VIII (2), mechanical mixture of kaolinite and copolymer (3); b) kaolinite (1), kaolinite and copolymer (2), kaolinite and polyacrylonitrile (3), kaolinite and polyacrylamide (4)

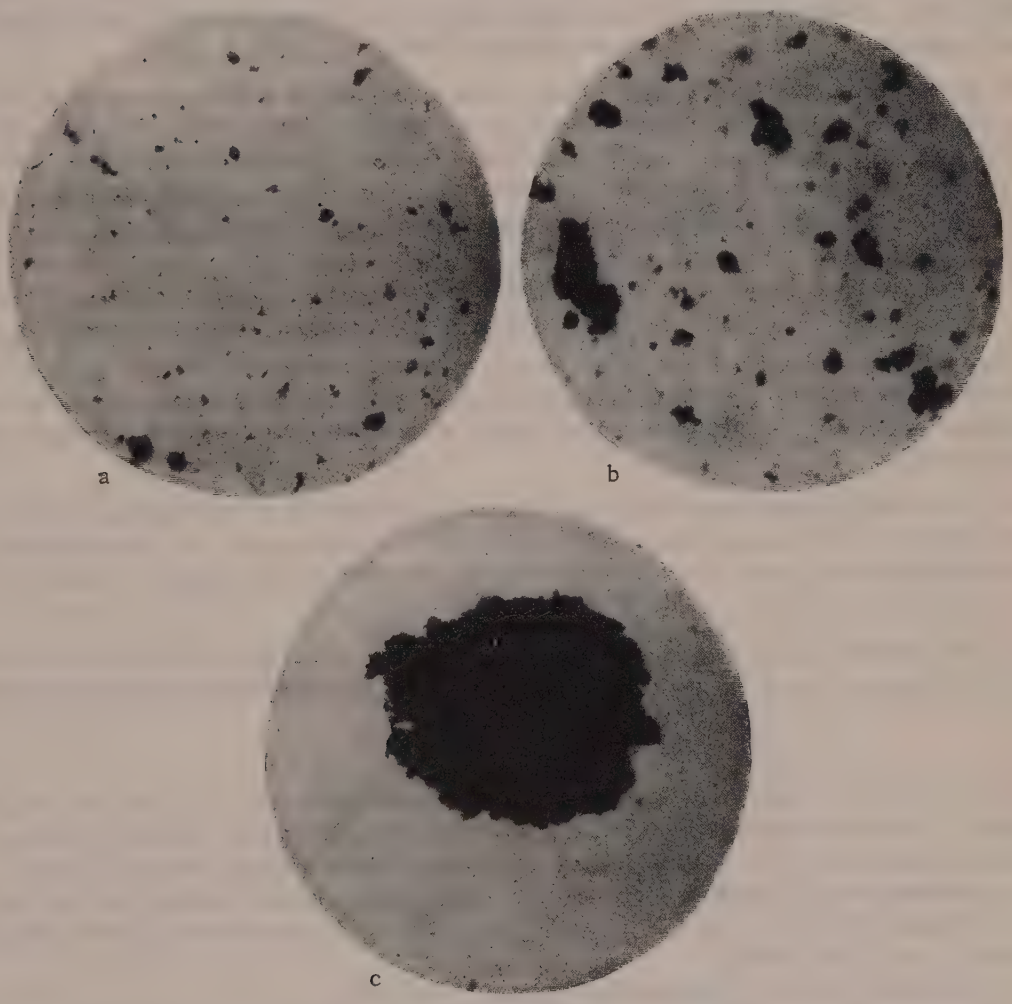


Fig. 4. Microphotographs of kaolinite with polyacrylonitrile (A), copolymer (B), and polyacrylamide (C), (magnified 66 times)

action. The presence of dissociated carboxyl groups keeps the polymers from winding up, and apparently favors the adsorption of the polymer, and the formation of hydrogen bonds between the polymers and the soil particles.

Consequently, there must be enough ionized carboxyl groups present so that the molecule can unwind somewhat and be able to react with the soil. However, if the number of ionized carboxyl groups is large, the charge density of the polymer molecule increases appreciably, which, naturally, will prevent the soil particles from getting close to the polymer.

The copolymer VIII and polyacronitride which we used in our studies must be hydrolized in solution. The copolymer VIII consists of 60% metacrylic acid and 40% metacrylamide acid. This means that before hydrolysis the copolymer already has 60% carboxyl groups and 40% amide groups, but on hydrolysis the number of carboxyl groups is increased. The polyacrylonitrile contains nitrile groups before hydrolysis, and gives amide groups at the start of hydrolysis, while with more thorough going hydrolysis it give carboxyl groups.

Among the hydrolized polymers, a large number of carboxyl groups will come from the copolymer, and there will be so many of them, that because of the charge density the copolymer will have less structurizing properties than polyacrylonitrile.

The polyacrylamide molecules have a positive charge, and they will be readily attracted to the negative clay particles, but since the polyacrylamide molecules are wound up into a ball, and form hydrogen bonds between the chains of the molecule itself, the number of free functional groups is considerably reduced. These are the groups which could form a hydrogen bond with the clay particles, and the reduction is what we observe in the infrared spectrum. And since polyacrylamide gives fewer water resistant aggregates, we may conclude, that the structuration process, in the final count, is accomplished through the hydrogen bonds.

To the first approximation we can say, that the formation of water resistant macroaggregates in the reaction of soil particles with polymers like polyacrylamide, polyacrylonitrile and similar substances proceeds in steps. The formation of coarse aggregates is by no means always identical with the appearance of water resistance, i.e., stability of the aggregates to the dissolving action of water. There is no doubt that this latter property is to some degree due to the formation of hydrogen bonds between the polymer and the soil particle.

SUMMARY

1. The reaction of polymers with clay particles changes the intensity of the free hydroxide band in the infrared spectrum of kaolinite, which occurs, apparently, as a result of the formation of a hydrogen bond between the active groups of the polymers and the hydroxyl groups of the kaolinite. The intensity of the free hydroxide band changes by different amounts when the kaolinite is treated with polyacrylamide copolymer VIII and hydrolized polyacrylonitrile.

2. Since there is a direct relation between the water resistance of the soil aggregates prepared by treating soil with different structurizing polymers, and the reduction in intensity of the free hydroxide band from the formation of the hydrogen bond, there is reason to suppose that the hydrogen bond assumes a leading role in the structuration process.

3. The proposal is made that the difference in structurizing effect shown by the polymers investigated is caused by a change in form of the macromolecule as a result of different degrees of ionization of the polymers.

LITERATURE CITED

1. W. P. Martin, J. B. Page, W. A. Raney, J. D. Ment, Advances in Agron, 7, I, 1955; W. Bergman, H. J. Fiedler, Wiss. Z. Friedrich-Schiller-Univ. Jena, Mathnaturwiss. Reihe 4, No 2-3, 249, 1954-1955; K. Starzynski, Postepy nauki roln. 1, No. 4, 128, 1954; P. V. Vershinin, Pochvovedenie, No 10, 28, 1958.
2. H. J. Fiedler, Wiss, Z. Friedrich-Schiller-Univ. Jena, Math-naturwiss. Reiche 6, No. 5-6, 39, 1956-1957.
3. H. J. Fiedler, ibid 6, No. 3-4, 187, 1956-1957. H. J. Fiedler, Z. landwirtsch. Versuchs und Untersuchungswesen 3, No. 5, 453, 1957.
4. J. L. Mortenson, Soil Sci. America Proc. 21, No. 4, 385, 1957.
5. Bergmann, H. J. Fiedler, Z. Pflanzenernahr. Dung. Bodenkunde 72, No. 2, 114, 1956.
6. W. W. Jones, J. P. Martin, Soil Sci. 83, No. 6, 475, 1957; H. J. Fiedler, Die Deutsche Landwirtschaft 5, 313, 1954; A. Packter, Soil Sci. 83, No. 5, 335, 1957.
7. E. W. Fischer, W. Rentschler, Z. Pilanzenernah. Dung. Bodenkunde 76, No. 3, 232, 1957.
8. W. W. Emerson, Nature 176, 461, 1955.

9. R. A. Ruehrwein, D. W. Ward, Soil Sci. 73, 485, 1952.
10. R. M. Holmes, S. J. Toth. Soil Sci. 84, 479, 1957; D. L. Lynch, L. M. Wright, L. J. Cotnoir, Soil Sci. Amer. Proc. 20, 6, 1956.
11. I. Hagin, G. B. Bodman, Soil Sci. 78, 367, 1954.
12. I. Hagin, Bull. Res. Council Israel 4, 297, 1954.
13. R. S. Montgomery, B. B. Hibbard, Soil Sci. 79, No. 4, 1955.
14. W. W. Emerson, J. Agric. Sci. 47, No. 1, 117, 1956.
15. R. O. French, M. E. Wadsworth, M. A. Cook, I. R. Culter, J. Phys. Chem. 58, 805, 1954.
16. N. L. Glinka, General Chemistry [in Russian] 1956 page 216.
17. M. I. Batuev, Uspekhi Khimii 10, 416, 1941.
18. Uells, Structure of Inorganic Substances [in Russian] 1948.
19. M. V. Vol'kenshtein, M. A. El'yashevich, B. I. Stepnov, Molecular Vibration Volume 2 [in Russian] 1949.
20. Buswell, Dudenbostel, J. Amer. Chem. Soc. 63, 2554, 1941.
21. A. G. Betekhtin, Minerology [in Russian] 849, 1951.
22. P. V. Vershinin, Bulletin of Scientific and Technical Information on Agronomic Physics [in Russian] No. 8-9, 1960.
23. S. E. Bresler, Advances in the Chemistry and Technology of Polymers [in Russian] Goskhimizdat (Moscow, 1957).
24. A. S. Michaels, Industr. and Engng. Chem. 46, 1485, 1954.

All abbreviations of periodicals in the above bibliography are letter-by-letter transliterations of the abbreviations as given in the original Russian journal. *Some or all of this periodical literature may well be available in English translation.* A complete list of the cover-to-cover English translations appears at the back of this issue.

SULFONATED ELASTOMERS AS SORBENTS OF WEAK ELECTROLYTES*

O. R. Skorokhod

V. I. Lenin White Russian University, Minsk

Translated from Kolloidnyi Zhurnal Vol. 23, No. 5,
pp. 621-625, September-October, 1961
Original article submitted June 31, 1960

Some ion exchangers have a considerable absorptive capacity for mineral acids in their salts as well as for organic acids, and thus find application in separating acid mixtures [1].

It was a matter of interest to study the sorptive properties of sulfonated elastomers from the point of view of their selective properties with respect to weak electrolytes vs. aromatic acids from mixed solutions, with the idea of a possible application to chromatography in the separation of substances of closely related nature.

The present paper describes the results of the molecular absorption on ion exchangers shown by three isomers of aminobenzoic acid and phthalic acid from individual water solutions and from a mixture with salicylic acid. The ion exchangers were prepared by sulfonating resins made of butadiene rubbers with the same composition but differing only in sulphur content (SBR-2, SBR-18, SBR-26 [2], a sample of Butadiene styrene rubber (SBS-50) and two samples of butadienenitrile rubber (SKN-26, SKN-40)). Further, the sorptive properties of the SBS-1 ion exchanger were studied, which is obtainable commercially.

The ion exchangers prepared by sulfonation were converted into the H-form with HCl, carefully washed with doubly distilled water, and dried to constant weight at room temperature. The fraction selected for the work had dimension 0.25-1 mm. The technique for studying the sorption of individual acids and mixtures, the analysis of the equilibrium solutions, and the calculations have already been given in [3].

The sorption data was converted to quantity of absorbed acid (in mm/g of ion exchanger) and plotted in the form of a sorption isotherm.

TABLE 1. Sorption, Solubility and Dissociation Constant, K, of Aminobenzoic Acids

Acid	Dissociation constant K	Solubility in water %	Sorption, mm/g (C = 0.002 mole/liter)
p-Aminobenzoic	$1.21 \cdot 10^{-5}$	0.3	0.74
o-Aminobenzoic	$1.32 \cdot 10^{-5}$	0.35	0.70
m-Aminobenzoic	$1.63 \cdot 10^{-5}$	0.6	0.52

In some cases, the limiting sorption on the isotherms was reached at relatively low concentrations, as shown by the horizontal portions of the curves. Figure 1 shows the sorption isotherms of salicylic and aminobenzoic acids on type SBR and SBS ion exchangers.

The sorption of aminobenzoic acids is in the following order: Meta aminobenzoic < orthoaminobenzoic ≤ ≤ para aminobenzoic. This was observed both in the adsorption of each acid individually, and when mixed with salicylic acid with all the ion exchangers which we studied. This variation in sorption by ion exchangers is in good agreement with the other properties of aminobenzoic acids (Table 1).

*G. K. Gaishun and A. F. Kozlova took part in the experimental work.

All the ion exchangers investigated have considerable absorptive capacity for aromatic acids, and may be used for extracting the acids from dilute aqueous solutions.

The SBS exchanger is a better absorber of aromatic acids than the SBR ion exchanger, obviously because of aromatic rings.

The change in sorption of aromatic acids by type SBR ion exchangers in the order SBR-26, SBR-18, SBR-2, must be considered in the light of the mesh structure of the ion exchanger on the one hand, and the structure of the adsorbed acid molecules on the other. The SBR-26 ion exchanger which contains more binding sulfur, shows a more dense structure, less swelling, and a smaller concentration of strongly acid groups. This ion exchanger has even less absorptive capacity for aminobenzoic acids, which contain the NH_2 group (Table 2).

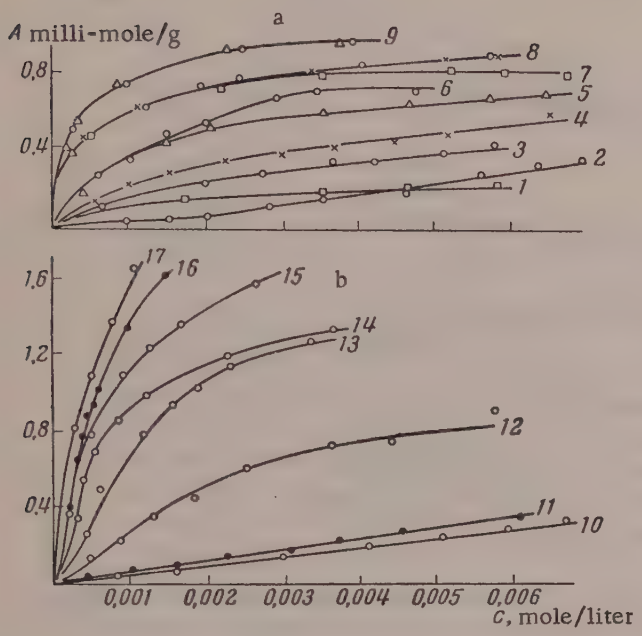


Fig. 1. Acid sorption isotherms on (a) SBR ion exchanger, (b) SBS: 1, 3 and 4—salicylic on SBR-18 and SBR-26: 2—salicylic from a mixture with P-aminobenzoic on SBR-18: 5 and 6—m-aminobenzoic on SBR-26 and SBR-2: 7, 8 and 9—o-and p-aminobenzoic on SBR-26, SBR-18, and SBR-2: 10—salicylic from mixture with anthranilic on SBS-50: 11 and 12—salicylic on SBS-50 and SBS-1: 13—m-aminobenzoic on SBS-1: 14 and 16—anthranilic on SBS-1 and SBS-50: 15—p-aminobenzoic on SBS-1: 17—anthranilic from mixture with salicylic on SBS-50.

TABLE 2. Properties of SBR Ion Exchangers

Ion-Exchanger	Exchange capacity, mg/equiv/g		Degree of swelling, %	Anthranilic Acid Sorption, mm/g
	with NaCl	with NaOH		
SBR-2	1.1	1.9	52	0.75
SBR-18	0.7	1.5	48	0.58
SBR-26	0.5	1.4	46	0.56

One can assume that in the present case an important role is played in the sorption by acid-base interaction. Salicylic acid is sorbed better by the SBR-26 ion exchanger, although the concentration of ionogenic strongly acid groups in it is less than in the SBR-2 ion exchanger. Apparently, the salicylic acid sorption does not occur at the place where the ionogenic strongly acid groups are, but on the skeleton of the ion exchanger. A similar behavior of salicylic acid on other ion exchangers was noted previously [4].

A comparison of the sorptive properties of ion exchangers, prepared by sulfonating butadienenitrile rubbers shows that increasing the nitrile concentration of the acrylic acid causes some increase in the absorption of aromatic acids (Fig. 2). As may be seen from the data of Table 3, the exchange capacity and the swelling of the ion exchangers change in the same order.

The ion exchange sorption of the aromatic acids studied decreases in the series: phthalic < salicylic < o-aminobenzoic. Obviously, this sorption difference has something to do with the presence of different substituent groups: NH_2, in the case of anthranilic, OH, in salicylic COOH, in phthalic. These groups may be arranged in the order of electronegativity as follows: COOH > OH > NH_2.

In almost all cases the salicylic acid is sorbed from a mixture with aminobenzoic acid (at the same equilibrium concentration) to a considerably less degree, than when it is alone, i.e., the salicylic acid gets squeezed out. This is particularly noticeable at small salicylic acid concentrations; if the salicylic acid concentration in the mixture is increased, the difference in the sorption becomes less, and in some cases there is an increase in the adsorption, and the isotherm for sorption from the mixture overshoots the one for the pure substance. A similar behavior is observed with phthalic acid when it is being adsorbed from a mixture with salicylic acid. Thus, the sorption data on ion exchangers confirm the mutual replacement rule, which is in complete agreement with Langmuir's theory for ad-

sorption from a mixture. Thus, it follows that the degree of adsorption of salicylic acid from a mixture with p-aminobenzoic acid is less than from a mixture with m-aminobenzoic acid, the degree of sorption of which, that is the adsorption coefficient, is less than for p-aminobenzoic acid. However, in practice this relation is not quite so simple. When we are studying the sorption of a mixture of organic acids, we must keep in mind that it is possible to form hydrogen bonds and other intermolecular interactions which can bring about either an increase or a decrease in the sorption.

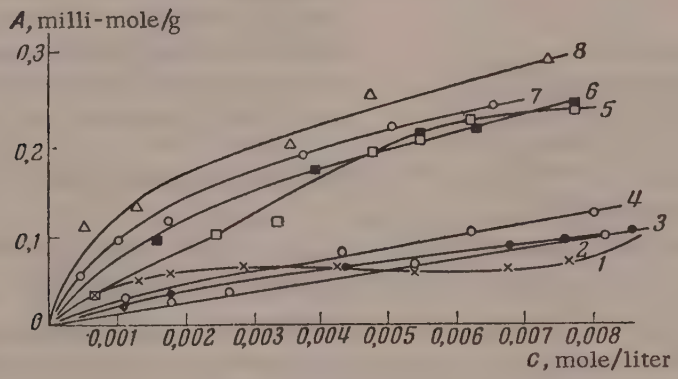


Fig. 2. Sorption isotherms of salicylic and phthalic acids on SKN ion exchangers: 1 and 3 – phthalic from mixture with salicylic on SKN-26 and SKN-40: 2 and 4 – phthalic on SKN-26 and SKN-40: 5 and 6 – salicylic on SKN-26 and SKN-40: 7 and 8 – salicylic from mixture with phthalic on SKN-40 and SKN-26.

An important property of a sorptive process is its selectivity. The data which we have obtained is given in the form of curves showing the distribution of the acids between the solution and the ion exchanger (Fig. 3). In all the systems studied the sorptive process goes selectively, the molar fraction of one of the acids in the mixture is greater in the ion exchanger, than in the equilibrium solution (Ne), i.e., the ion exchanger becomes enriched in one of the acids. In the case of sorption of a mixture of salicylic and aminobenzoic acids, the later is absorbed selectively, and in the case of a mixture of salicylic and phthalic acids, it is the salicylic which is absorbed selectively, i.e., the acid which is sorbed selectively on the ion exchanger is the one which is absorbed more energetically by the given ion exchanger even when it is alone.

TABLE 3. Properties of SKN Ion Exchangers

Ion Exchanger	Exchange capacity with NaCl, mg-equiv/g	Degree of swelling, %	Salicylic acid absorption, mm/g
SKN-26	0.46	50	0.06
SKN-40	0.55	53	0.08

The quantitative composition of the equilibrium solution affects the sorption selectivity. In some cases the distribution curve overshoots the "ideal" curve (diagonal of the square) for uniform distribution of the components between the ion exchanger and the solution, i.e., depending on the ration of components in the mixture, the sorbed phase may be enriched sometimes in one acid and sometimes in the other.

We have set ourselves the task of separating a mixture of two aromatic acids chromatographically using the ion exchangers which we have studied. As a mixture to be separated we have selected salicylic and anthranilic acid. Any ion exchangers which show selective sorption should be suitable for solving the problem. The most effective wasSBS-50, whose distribution curves show greater asymmetry than the other ion exchangers. The separation was made by elutive chromatography in a column 30 cm high and 0.8 cm in diameter. The eluants used were water and dioxane. The rate of solution flow out of the column was 8-10 drops per minute. Yield curves were constructed from the analytical data. As may be seen from Fig. 4a, salicylic acid was washed out quantitatively by the water and anthranilic acid was washed out quantitatively by the dioxane.

We made an experiment on separating a mixture of salicylic and phthalic acids on SKN-40 ion exchanger, in which the sorptive process is less selective than on SBS-50. As shown by the data given in Fig. 4b, it was possible using SKN-40 to get a clear separation of a mixture of salicylic and phthalic acids.

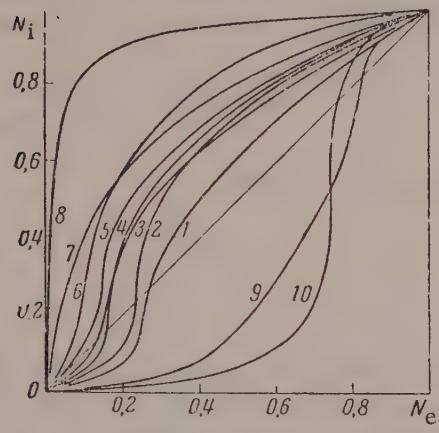


Fig. 3. Distribution curves of aminobenzoic and phthalic acids sorbed from a mixture with salicylic acid: 1 and 3) m-aminobenzoic on SBS-1 and SBR-26: 2 and 5) p-aminobenzoic on SBS-1 and SBR-26; 4, 7 and 8) anthranilic on SBS-1, SRB-26, and SBS-50; 6) m-o-p-aminobenzoic on SBR-2; 9 and 10) phthalic on SKN-40 and SKN-26.

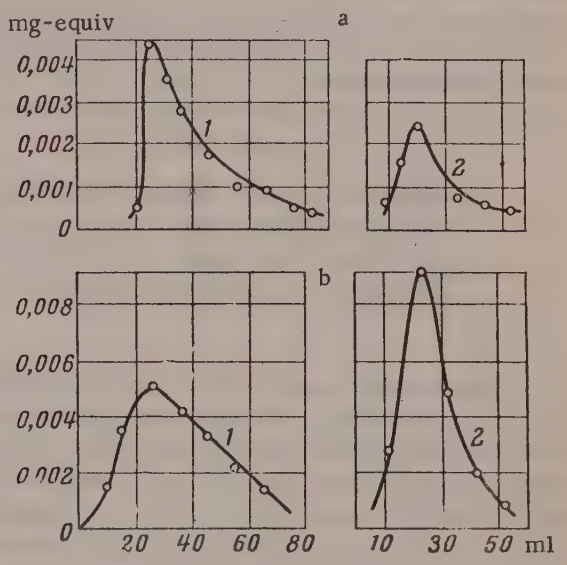


Fig. 4. Yield curves of acid mixture: a) phthalic (1) and salicylic (2); b) salicylic (1) and anthranilic (2).

SUMMARY

1. Ion exchangers prepared by sulfonating elastomers (SKN, SBR, SBS), have considerable absorptive capacity for aromatic acids. The sorptive capacities of the ion exchangers may be arranged in the series: SKN < SBR < SBS.

2. In all the systems studied the sorption is selective in character. The acid which is most absorbed from the mixture by the ion exchanger is the one which is most strongly absorbed when it is alone.

3. A mixture of salicylic and anthranilic acids has been separated by means of the cation exchanger SBS-50, as well as a mixture of salicylic and phthalic acids on the cation exchanger SKN-40 by elutive chromatography. The eluants used were water and dioxane.

LITERATURE CITED

1. K. M. Saldadze, K. M. Ol'shanova, I. I. Ivanova, Studies in the Field of Ion Exchange, Distributive and Precipitative Chromatography [in Russian], Academy of Sciences Press, USSR 1959, p. 138, O. Samuel'son, Use of Ion Exchange in Analytic Chemistry [in Russian] 1955, p. 27, 112, 140; C. W. Dawies, B. Owem, J. Chem. Soc. 1681, 1956; C. W. Davies, G. G. Thomas, J. Chem. Soc. 2624, 1951
2. G. M. Starobinets, L. I. Sevost'yanova, G. N. Bulatskaya, Zh. prikl. khimii, 33, 690, 1960.
3. O. R. Skorokhod, N. F. Ermolenko, N. Lukomskaya, Scientific Papers of the Vilenin White Russian University [in Russian] No. 42, chemical series, 1958, p. 159.
4. O. R. Skorokhod, L. M. Sergeeva, Kolloidn, Zh, 23, 100, 1961.

EFFECT OF N-DECYL ALCOHOL AND POLYISOBUTYLENE ADDITIONS ON ELASTIC RECOIL AND STRUCTURAL STRENGTH IN THE RIPENING AND AGING OF ALUMINUM NAPHTHENATE GEL

A. A. Trapeznikov

Institute of Physical Chemistry of the Academy of Sciences, USSR, Moscow
Translated from Kolloidnyi Zhurnal Vol. 23, No. 5,
pp. 626-631, September-October, 1961
Original article submitted July 19, 1960

The properties of gels of aluminum soaps, principally aluminum laurate, in hydrocarbon liquids have been studied by many investigators [1]. It has been found that additions of polar organic substances lower the viscosity of the solutions and gels. This has been explained by shortening of the aluminum soap chain [2], since the coordination binding of the polar groups of the additives to the aluminum and oxygen atoms in the chain is stronger than the coordination interaction between the oxygen and aluminum atoms in the chain and the monomeric soap molecules. This sort of decomposition is confirmed by infra-red spectroscopy [3].

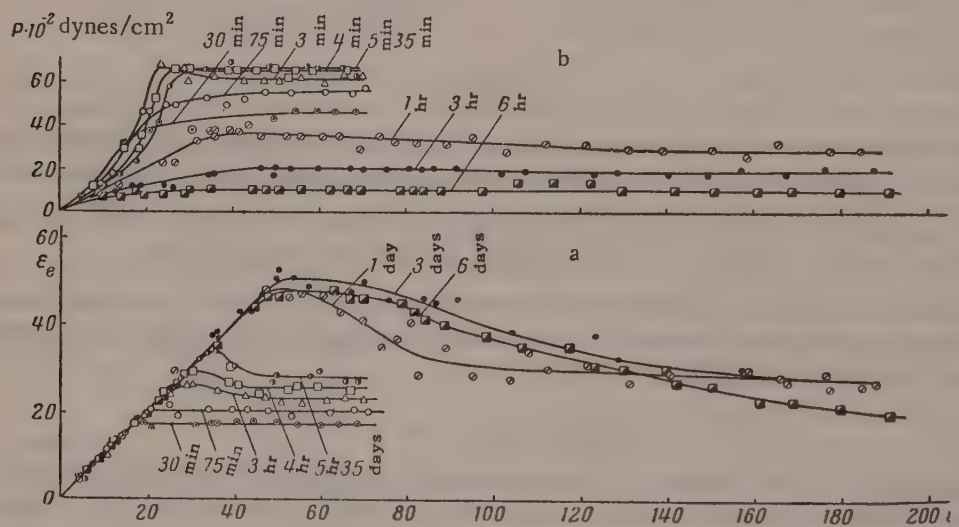


Fig. 1. Curves of $\epsilon_e(\epsilon)$ (a), and $P(\epsilon)$ (b) for a 2% aluminum naphthenate gel with 0.431% n-decyl alcohol added, at various stage of ripening.

Considerable interest is presented by the deformation-strength and thixotropic properties of aluminum soap gels, and the effect shown by additives, in particular, the changes in the magnitude of the largest reversible deformations, and the structural strength during ripening and aging of the gels [4, 5].

It has been shown with an elastorelaxometer (Model 1, [6]) that there are two additives which have a markedly different effect on low concentration naphthenate gel, namely the low molecular polar additive, n-decyl alcohol, and the high molecular nonpolar additive, polyisobutylene.

Figure 1 gives curves elastic recoil $\epsilon_e(\epsilon)$ and displacement stress $P(\epsilon)$ as a function of fixed deformation for 2% aluminum naphthenate gel (portion No. 24) and decaline (not subjected to any special purification) with 0.431% n-decyl alcohol added. The alcohol greatly accelerates the ripening process, and reduces the recovery time of the thixotropic structure. This leads to the condition that the $P(\epsilon)$ curves have no maximum at the very first stages of formation of the gel (under the present visual reading conditions, see [6]), since the ripening in the overall growth in P go faster than the measurement itself. In the later stages of ripening, the structure reestablishes itself so rapidly, that visual measurement of the greatest deflection of the "rabbit" gives, naturally, a constant value of $P = P_r$ for all $\epsilon > \epsilon_r$. The curves of $\epsilon e(\epsilon)$ go very much like the same curves for a gel with no additive at small ripening times. After going through $\epsilon = \epsilon_r$, there is a "flat" stretch, and at large ripening times the maximum, ϵ_e maximum is observed.

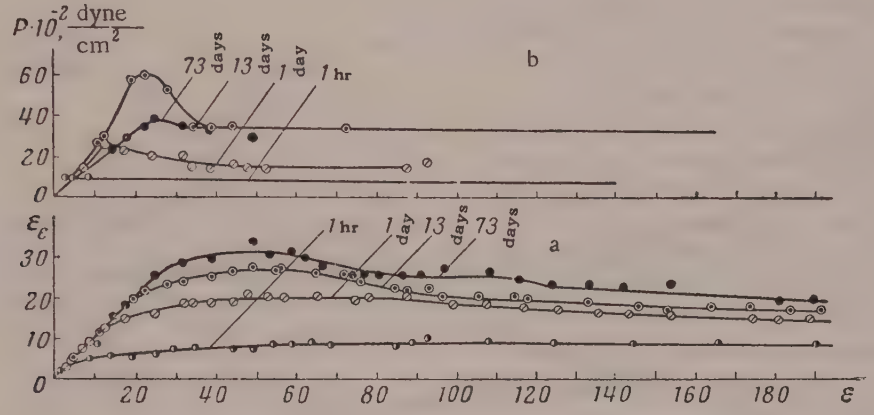


Fig. 2. Curves of $\epsilon_e(\epsilon)$ (a), and $P(\epsilon)$ (b) for 2% aluminum naphthenate gel with 0.5% polyisobutylene added, at various stages of ripening.

The effect of a 0.5% addition of polyisobutylene is different from that of aluminum naphthenate (Fig. 2). In the early stages of maturing the $\epsilon_e(\epsilon)$ curves have almost no initial linear portion, which would indicate that $\epsilon_e = \epsilon$, i.e., over practically the whole curve $\epsilon_c < \epsilon$, the maxima, ϵ_{emax}, being rather weakly pronounced at all aging times. In contradiction to this, the $P(\epsilon)$ curves have pronounced maxima, which are maintained for long aging times. This is explained by the comparatively long thixotropic recovery time of the structure in the range $\epsilon > \epsilon_r$. [7].

If the amount of polyisobutylene is increased to 1%, the $\epsilon_e(\epsilon)$ curves go one below the other over the whole course of prolonged aging, which indicates not only retardation of the aging but a reduction in the elastic recoil of the napthenate under the influence of polyisobutylene.

Under the influence of n-decyl alcohol the ripening is sharply accelerated (Fig. 3). This is shown in the reduction and time required to reach the maxima $(\epsilon_{emax})_{max}$ and P_{rmax}, although the times required to reach the two maxima are just as different from one another as in the case of the gel without additive [5] (Table).

The ripening and aging of the gel with polyisobutylene is very much retarded (Table, Fig. 4). Large quantities of polyisobutylene lower ϵ_{emax} so much, that for 190 24-hour periods it remains practically at the same level: 3000 and 1900% (for 0.5 and 1.0%) instead of 6000% without additive, i.e., the system loses in elasticity by 2-3 times. However, the ϵ_{emax} values are easily reproducible under repeated measurements over an interval of 15-30 seconds, [7], which shows, that they are determined by the long moveable elements in the structure. Obviously, the polyisobutylene molecules prevent the formation of bronze between the naphthenate particles, such as cross linkages, and as a result of this the value of P_r falls off strongly.

It should be noted, that the naphthenate gels with polyisobutylene additive are unstable. At first they are homogeneous but on prolonged standing they break up into layers the more so, the more polyisobutylene they have in them. Obviously, the naphthenate, which contains more polar groups, is incompatible with the nonpolar polyisobutylene. It is possible that the breakup has to do with an entropy factor.

It follows from the path of the $\epsilon_e(\epsilon)$ curves and the initial stage of ripening, that small quantities (0.215%) of a polar additive increases the maximum elastic deformation of the gel, ϵ_{emax}, for example from 30-35 to 40-60 in the course of the first eight days. The structural strength, P_r, and together with it the stress P_s, which sustains stationary flow, is reduced by the effect of the additives, and consequently the viscosity of the system is reduced. However, the usual conception of the chain shortening in the aluminum soap [1,2], used to explain the reduction in viscosity of the gel, cannot explain the properties which have been described. The increase in the ϵ_{emax} value of the system gives a direct indication of elongation of the working elements of the network structure.

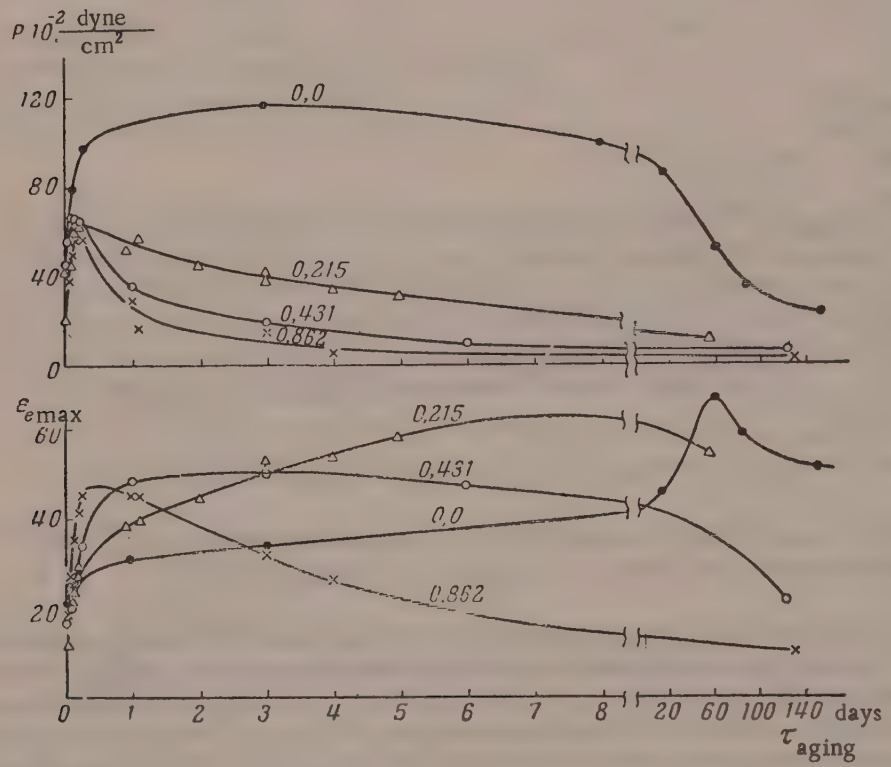


Fig. 3. Curves of ϵ_{emax} (τ_{aging}) (a), and P_r (τ_{aging}) (b) for 2% aluminum naphthenate gel with n-decyl alcohol added in the following amounts: 0, 0.215, 0.431, and 0.862%.

Effect of Additives on the Ripening of an Aluminum Naphthenate Gel

C, % n-decyl alcohol, g/100 g gel	$(\varepsilon_{emax})_{max}$	P_{rmax}, dynes/cm^2	τ_{aging}, hr at $(\varepsilon_{emax})_{max}$	τ_{aging}, hr at P_{rmax}
		n-Decyl alcohol		
0	67	11 700	62	3,0
0,215	63	6300	7,5	0,25
0,431	50,5	6600	3,0	0,166
0,862	47	5700	0,5	0,208
		Polyisobutylene		
0	65,8	11 700	62	3
0,25	57	10 900	190	3
0,5	32,5	6000	190	14
1,0	19,5	2150	74	84

From the point of view of the network structure of the aluminum soap gels, we must keep in mind, that the gel contains both long twisted chains, in which the individual links are bound by bonds strong enough to sustain a stress of approximately $P = P_r$, as well as various kinds of cross linkages or short chains, which join the main chains with one another. The strength of these bonds may be comparable with the bond strength in the chain, however, it is probably less, since they keep on breaking right up to the time the chain gets completely untwisted.

The action of the additives is apparently mainly a matter of blocking the cross linkages and thus forming a looser network, in which it is easier to untwist the long chains [7]. Rupture of the cross linkages greatly weakens the rigidity of the whole structure, and increases the flexibility of the individual elements. Small amounts of additives (0.215%), apparently, sharply accelerate the ripening of two per cent gel, without, however, increasing the maximum value of $(\epsilon_{emax})_{max}$. Additions of n-decyl alcohol in concentrations of 0.431 and 0.862% not only accelerate the ripening, they also reduce $(\epsilon_{emax})_{max}$. This may be explained by the large reduction in the number of nodes between the chains. As a result it becomes harder to extend the chains, since the amount they have to slip over one another is increased, [5]. It is also possible that the chains themselves are shortened. Apparently, both factors play a role, however the first is probably the prevalent one. It follows from the general trend of the curves, that with the amount of additive in question, the overall concentration of gel seems to decrease [5]. Actually, it is quite probable that there is a substantial difference in the distribution of strength and length among the active elements of the structure.

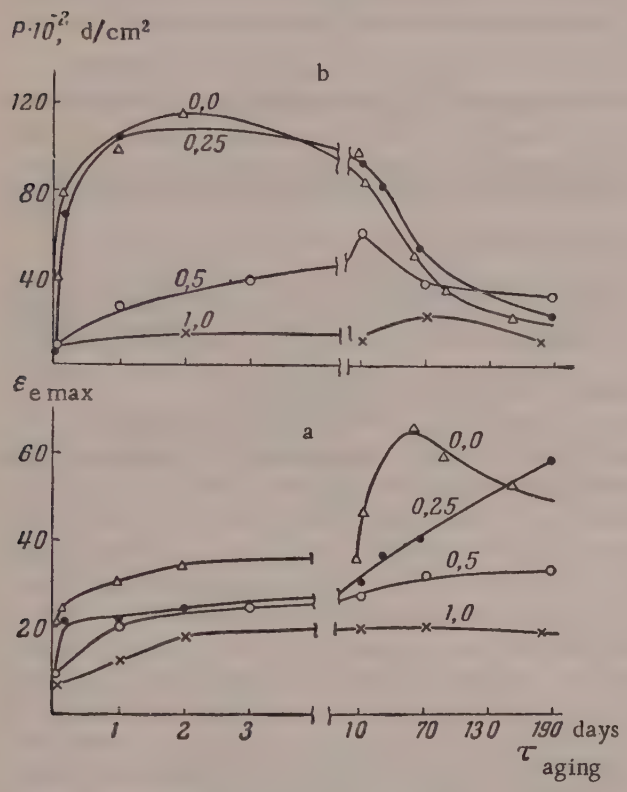


Fig. 4. Curves of a) ε_{max} ($\tau_{e\ aging}$) and b) P_r (τ_{aging}) for 2% aluminum naphthenate gel with additions of 0; 0.25; 0.5 and 1% polyisobutylene.

The viscosity of such structurized gel-like systems is a function not so much of the chain length as of the number of nodes and their relaxation time. Therefore the viscosity cannot be considered as depending only on the chain length, as would be the case in dilute solutions of polymers. The viscosity lowering by additives cannot be related to reduction in chain length, but above all, to a reduction in the number of nodes. The length of the chain acting between nodes is a function of the number of nodes.

In view of the cross linkage blocking idea given above, we can assume, that the stabilization of the system in the sense of reaching properties constant with storage time (viscosity for example) must be in the direction of getting rid of the excess number of cross linkages, which give the system increased viscosity or even rigidity. These bonds, especially some of them, can be ruptured easily during storage under the influence of secondary factors, which causes an undesired reduction in viscosity. A necessary condition for insuring high elasticity of the system and quick recovery of the thixotropic structure is to maintain long chains, bound by a certain number of cross linkages.

Finally, long aging of the aluminum soap gels is accompanied by colloid aging of the aluminum hydro-oxide or aluminum silicate skeleton, which forms a base for the aluminum soap particles.

The acceleration in the ripening of the aluminum soap gel brought about by a polar additive (alcohol) is caused, first, by the alcohol molecules penetrating the micro particles of the soap and thus weakening the bonds which act between the twisted chain-like soap particles, i.e., by facilitating the untangling of the long particles. On the other hand, addition of polyisobutylene slows up the ripening, and, in addition, reduces the maximum elastic deformation $(\epsilon_{emax})_{max}$. This is probably a result of molecular binding of individual segments of the naphthen-

ate chain by polyisobutylene molecules, which interact with the nonpolar radicals of the naphthenic acid molecules, belonging to the different naphthenate chains. Further, the polyisobutylene molecules may "wind up" around one or several naphthenate chains, thus preventing them from rotating in segments.

SUMMARY

1. A study has been made of the effect of additions of n-decyl alcohol and polyisobutylene on the maximum elastic deformation and structural strength of an aluminum naphthenate gel in decaline. It has been shown that adding the alcohol greatly accelerates ripening while polyisobutylene retards it.

2. Small additions of n-decyl alcohol increase the elastic deformation (in the early stages of ripening), larger additions lower the maximum elastic deformation and the chain length which determines it. Along with this there is a reduction in structural strength in viscosity. Adding polyisobutylene lowers the elastic deformation and the structural strength.

3. Aluminum naphthenate gels containing polyisobutylene gradually separate into layers, the more so, the greater the polyisobutylene concentration.

I express deep gratitude to laboratory assistant L. S. Meshcheryakova for carrying out the measurements.

LITERATURE CITED

1. V. R. Gray, Trans. Farad. Soc. 42B, 196, 1946; V. R. Gray, A. E. Alexander, J. Phys. Coll. Chem. 53, 9, 23, 1949; E. K. Rideal, and al., A Discussion Proc. Roy. Soc. 200A, 1950; J. W. McBain, E. B. Working, J. Phys. Chem. 51, 974, 1947.
2. W. O. Ludke, S. E. Wiberley, J. Goldenson, W. H. Bauer, J. Phys. Chem. 59, 222, 1955.
3. W. W. Harple a. al., Analyt. Chem. 24, 635, 1952; W. H. Bauer a. al., J. Phys. Chem. 59, 32, 1955.
4. A. A. Trapeznikov, E. M. Shlosberg, dokl, AN SSSR 62, 791, 1948; A. A. Trapeznikov, V. A. Fedotova, Ibid 81, 1101, 1951; 82, 97, 1952; T. G. Shalopalkina, A. A. Trapeznikov, Ibid 118, 994, 1958.
5. A. A. Trapeznikov, dokl, AN SSSR 129, No. 2, 1959.
6. A. A. Trapeznikov, Kolloidn zh 21, 108, 1959.
7. A. A. Trapeznikov, Kolloidn zh 20, 476, 1958.

All abbreviations of periodicals in the above bibliography are letter-by-letter transliterations of the abbreviations as given in the original Russian journal. *Some or all of this periodical literature may well be available in English translation.* A complete list of the cover-to-cover English translations appears at the back of this issue.

KINETICS OF THE STRUCTURATION OF POLYMER-CEMENTS

Yu. S. Cherkinskii, V. M. Kalashnikova

Scientific Research Institute for New Building Materials, Moscow
Translated from Kolloidnyi Zhurnal, Vol. 23, No. 5,
pp. 632-637. September-October, 1961
Original article submitted May 3, 1960

Polymer-cement materials, prepared by mixing water dispersions of polymers (latexes or polymer emulsions) with cement and a filler, contain two active substances: polymer and cement. The properties of the mineral substance in the polymer in such a material mutually supplement one another, since the cement, reacting with the water, forms cement stone, which unites the filler particles into a single monolithic substance, while the polymer is a high molecular compound, which unites both the individual cement particles and the filler [1 and 2].

The most widely used polymer-cement contain synthetic polymers in the form of latexes, prepared by emulsion polymerization. It is a well known fact that synthetic latexes contain surface active materials (soaps of fatty or sulfur acids, nonionogenic soaps), which are added during emulsion polymerization to make the synthesis grow and to provide a stable enough water dispersion of the polymer [3 and 4]. However, sometimes the emulsifiers and stabilizers, used in emulsion polymerization, are not sufficient to produce an emulsion which will not coagulate when it is mixed with cement.

Therefore, when mixing water dispersions of polymers, such as latexes, with cement, we must take measures to prevent coagulation of the latex. For this purpose hydrophilic colloids are added to the latex (ammonium caseinate, methyl cellulose, sodium alginate, etc.). A colloid such as ammonium caseinate forms a stable film on the surface of the polymer globules, which protects the latex from coagulation when it is mixed with cement. Obviously coagulation occurs only if the cement sets from dehydration of the mixture and gradual hydrophobization of the casein as a result of the formation of calcium caseinate. The latexes may be stabilized by using salts, which in water solutions form insoluble compounds with poly-valent cations. In this case the protection against coagulation is probably provided by raising the ζ-potential on the latex particle-water interface, and especially by the fact that the calcium ions, which can coagulate the latex, are bound in water insoluble complexes. Further, caustic alkalis, formed by alkali metals, also exert a strong stabilizing action. Thus, a synthetic latex, suitable for mixing with cement, may, in addition to the polymer, contain surface active substances, hydrophilic colloids, and electrolytes.

The studies of Refs. [5-7] have made it possible to establish the basic laws governing the effect of surface active agents and electrolytes on the hardening of cement. An effect of certain hydrophilic colloids was also observed on the hardening of fine grain concretes [8]. But the effects of these substances on the hardening of polymer-cements have been insufficiently studied, although some effect of stabilizers on hardening has been noted [9].

In building practice, the question of preparing polymer-concrete mixtures with the required hardening rate is attracting considerable attention. The study of the effect of water dispersions of polymers and stabilizers on the hardening of the polymer-concrete mixture, at the same time determining the effect of stabilizers on the hardening of an ordinary concrete mixture, would make it possible to discover the laws governing the formation of the structure of the cement stone and the polymer cement, and so guide the structuration in the desired direction.

This paper considers the effect of emulsifiers and stabilizers on the hardening of cement and polymer-cement.

An investigation of the hardening process (structuration kinetics) of a cement suspension when stabilized water dispersions of polymers as well as individual stabilizers (colloids surface active agents in electrolytes) were added to it was made by the authors using a lever type chronical plastometer according to a technique developed by the Department of Colloid Chemistry of Moscow University [10].

The water dispersions of polymers and stabilizers which were added to the cement suspension in an effort to

discover their effect on the structuration were divided into four groups:

1. Electrolytes used as latex stabilizers: potash (K_2CO_3), soda (Na_2CO_3), soda mixed with potash, monosodium phosphate (NaH_2PO_4), and potassium silicate (K_2SiO_3).

2. Surface active agents and colloids: polyvinyl alcohol (PVA), necal (NC), necal mixed with potash, ammonium caseinate (AC), sodium alginate (SA), necal mixed with ammonium caseinate (since the stabilized latex contains as stabilizers both the necal emulsifier, and the ammonium caseinate stabilizer).

3. Water dispersions of polymers: a) polyvinylacetate emulsion (PVE-L)*, containing 7% polyvinyl alcohol (with respect to the polymer); b(polyvinylacetate emulsion (PVE-N), synthesized in the presence of 3% necal with respect to the polymer): c(divinylstyrol latex (SKS-65-GP), synthesized in the presence of 3% necal with respect to the polymer.

4. A water dispersion of polymer (PVE-L) with the cement hardening accelerator calcium chloride.

The water dispersions of polymers were added with the value of P/C (ratio of weight of dry polymer to weight of cement) equal to 0.2. The electrolytes, the surface active agents, and the colloids, were taken in quantities corresponding with their concentration in the stabilized polymer-cement suspension, and were calculated relative to cement. The calcium chloride was taken in quantities up to three per cent relative to cement. In all the investigations the ration W/C equal to 0.3 was used. The following portland cement composition was used in the work: C_3S – 34%, C_2S – 34%, C_3A – 11%, C_4AF – 12%. The specific surface of the cement, measured on Tovarov's apparatus, was 3650 cm^2/g.

The effect of electrolytes on the structuration kinetics of the cement suspension may be followed in Fig. 1. As may be seen from Fig. 1 (curve I) the pure cement suspension shows a slow increase in plastic strength (induction period) during the first 3.5 hours, during which the coagulational structure and the initial crystallization structure are formed. Then a sharp rise in the curve begins, the consolidation period, in which the crystallization structure is being intensely developed. If one per cent potash, one per cent soda, or a mixture of 0.4% each of soda and potash is added to the cement suspension, a very rapid increase in plastic strength is observed in the first part of the curves (2, 3, and 4) without any induction period. Adding two per cent of monosodiumphosphate slows down the hardening as shown in curve 5. The curve of plastic strength with 0.4% potasium silicate added (curve 6) almost exactly reproduces the curve for the cement suspension.

It may be concluded on the basis of these data that if electrolytes are added to a portland cement suspension, it is the anions, and not the kations, which in large degree affect the time required to form the structure, i.e., the hardening, since CO_3^{2-} anions strongly accelerate the structuration. The anions may be arranged in the following order of effectiveness: $CO_2^{2-} > SiO_2^{3-} > H_2PO_4^-$. The combined effect of alkaline metals salts and SSB on the structuration kinetics of a cement suspension has been studied in detail by Luk'yanova and Daryusina in Ref. [7]. They found out that with mixed additives, electrolytes, taken in small quantities, increase the induction period, the effectiveness of the anions being arranged in the same order that we noticed ourselves. The shortening rather than lengthening of the induction period for hydration and structuration which we observed using carbonates in our experiments, is probably to be explained by the fact that we used relatively large quantities of soda and potash, under which conditions, as was noted in Ref. [7], the carbonates of alkali metals accelerate hydration of the cement.

If 0.6% necal is added to the cement suspension, it has very little effect on the period in which the structure is being formed (curve 2, Fig. 2), while if the mixture of 0.6% and 1% potash is added, there is first very rapid hardening, which afterwards slows up (curve 3, Fig. 2). It is clear from the graph that curve 3 of Fig. 2 for the combined action of necal in potash may be obtained by geometric addition of the curves for the plastic strength with potash (curve 2, Fig. 1) necal (curve 2, Fig. 2) separately. Thus, if two stabilizers are added to the cement suspension, their combined effect on the hardening of the cement is the sum of the effect of each component.

Addition to the cement suspension of the following hydrophilic colloids: 1% ammonium caseinate (curve 4, Fig. 2) and 1% sodium alginate (curve 6, Fig. 2) causes a sharp retardation in the structuration process. The observed increase in plastic strength from adding sodium alginate is apparently to be explained by the formation of

* The marking of the polyvinylacetate emulsions is given provisionally by us.

a three-dimensional structure of the organic calcium alginate colloid, from a reaction between the carboxyl groups of alginic acid with calcium ions. When the alginate is added a marked thickening of the system is observed. Combined addition of one per cent ammonium caseinate and 0.6% necal (curve 5, Fig. 2) is not materially different in its action of ammonium caseinate alone, but additivity of the effects can also be observed.

The effect of water dispersions of polymers may be seen from Fig. 3. The latex cement suspension (curve 7) gains strength much more slowly with caseinate stabilization than cement suspensions stabilized with potash (curve 2) or with soda (curve 3), and the initial period of formation of its structure becomes longer. If, with potash, a structure of somewhat increased strength is produced in the initial period (curve 2, Fig. 3), which has an effect on the ease of manipulating the mixture, on the other hand, using soda, the plastic strength increases smoothly. However, if 1% soda is added to the cement, deposits are observed on the surface of the samples. Therefore, we tried complex stabilizers (Fig. 3, curves 4 and 5). In the initial period of hardening these stabilizers behave like soda, without, however, changing the period of formation of the structure as in the case of soda and potash. Therefore, for a given cement it is a good idea to use a complex stabilizer which provides temporary stabilization and which contains soda and potash.

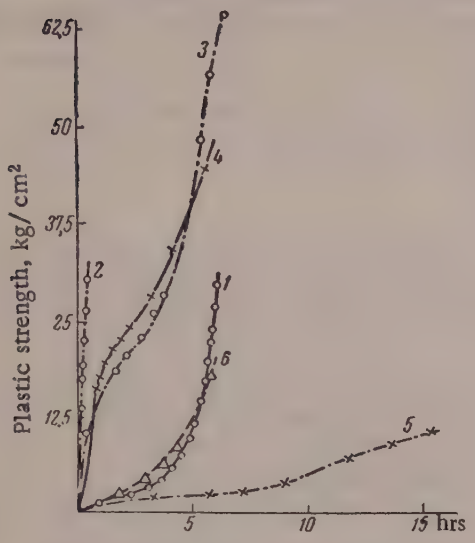


Fig. 1. Plastic strength of a cement suspension as a function of electrolytes added: 1) cement suspension: added electrolytes: 2) 1% K_2CO_3; 3) 1% Na_2CO_3; 4) 0.4% KCO + 0.4% Na_2CO_3; 5) 2% Na_2HPO_4; 6) 0.4% K_2SiO_3

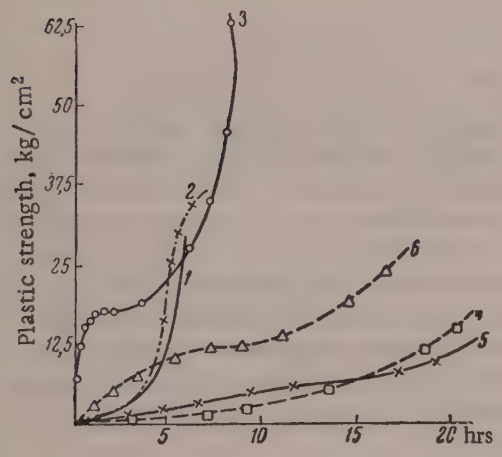


Fig. 2. Plastic strength of a cement suspension as a function of added surface active agents and colloids: 1) cement suspension: added substances: 2) 0.6% NC; 3) 0.6 NC + 1% K_2CO_3; 4) 1% NC; 5) 0.6% NC + 1% AC; 6) 1% AH.

The results of the experiments enable us to conclude that in order to get quick hardening polymer-cement mixture it is a good idea to use ammonium caseinate as the stabilizer. It must not be assumed however that polymer-cement mixtures which are stabilized with ammonium caseinate have high stability, while stabilization with electrolytes only gives temporary stabilization. Taking into consideration the combined action of different stabilizers, it is possible to accelerate the hardening of polymer-cement mixtures, stabilized with caseinate, if, instead of ammonium caseinate we use potassium or sodium caseinate by dissolving casein in an aqueous solution of soda or potash (curve 6, Fig. 3).

The change in plastic strength of a polymer-cement suspension using a polyvinylacetate emulsion, stabilized with polyvinyl alcohol, PVE-L (curve 2), in necal together with ammonium caseinate, PVE-N (curve 3), may be followed in curve 4. In stabilization with necal and ammonium caseinate (curve 3) the induction period for the formation of the structure is increased considerably as compared with the hardening of a purer cement suspension. This curve is similar to the hardening curve of the cement suspension containing only necal and ammonium caseinate (curve 5, Fig. 2). One should note the effect of the strength properties of the polymer on the plastic strength of the polymer-cement suspension. Thus, if SKS-65-GP latex is added, the strength of the system rises extremely slowly (curve 7, Fig. 3), while a polyvinylacetate emulsion, containing the same amount of additive as the latex, gives a considerably more rapid strengthening of the system (curve 3, Fig. 4). These data agree with the results obtained from measuring the rate of growth of the breaking strength under compression and bending of rubber cement concretes with time [11].

Comparing curve 5, Fig. 2, curve 7, Fig. 3, and curve 3, Fig. 4, we can arrive at some conclusion as to the effect of all

the additives on the structuration kinetics of a polymer-cement suspension. The change in plastic strength of such a suspension with time is a characteristic both of the hardening of the cement in the presence of additives, and of the formation of the condensed polymer structure, and its strengthening effect on the crystallization structure of the cement stone being formed.

The use of polyvinylacetate emulsion, stabilized with polyvinyl alcohol, which in itself has a considerable effect on the structuration kinetics, (curve 4, Fig. 4) gives a system which hardens very rapidly (curve 2, Fig. 4).

The hardening rate of a polymer-cement suspension made of polyvinylacetate emulsion is comparatively high (curve 2, Fig. 4), however, it may be increased even more by adding the cement hardening accelerators. As may be seen from Fig. 5, calcium chloride not only accelerates the aging of the plastic strength of the system, but shortens the induction period as well.

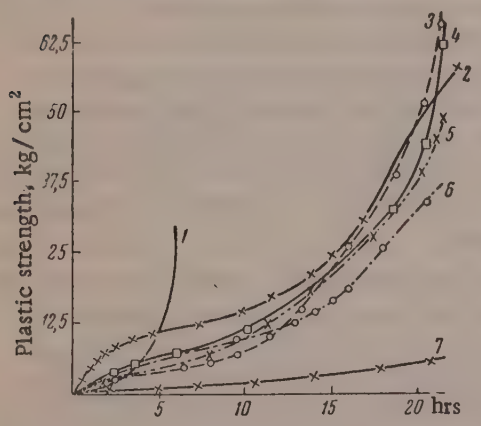


Fig. 3. Plastic strength of a polymer-cement suspension (W/C = 0.3; T/C = 0.2) as a function of SKS-65 stabilizer latex, already containing 0.6% NC: 1) cement suspension, 2) polymer-cement suspension + 1% K_2CO_3; 3) the same + 1% Na_2CO_3; 4) the same + 0.4% Na_2CO_3 and 0.4% K_2CO_3; 5) the same + 0.4% Na_2CO_3 and 0.6% K_2CO_3; 6) the same + 0.6% K_2CO_3 and 0.2% KA; 7) the same + 1% KA.

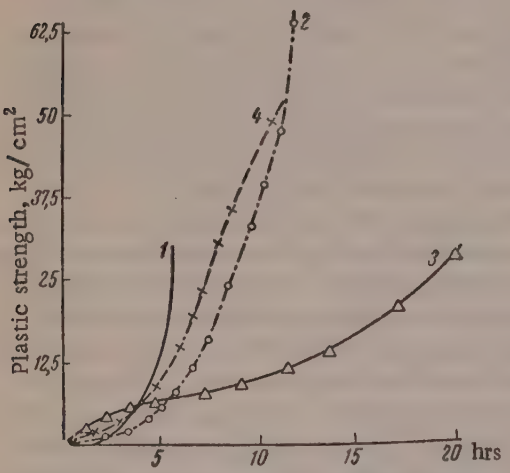


Fig. 4. Plastic strength of a polymer-cement suspension (W/C = 0.3; P/C = 0.2) as a function of polyvinylacetate emulsion stabilizer: 1) cement suspension, 2) polymer-cement suspension + 14% PVA 3) the same + 0.6% NC and 1% AC; 4) cement suspension + 1.4% PVA

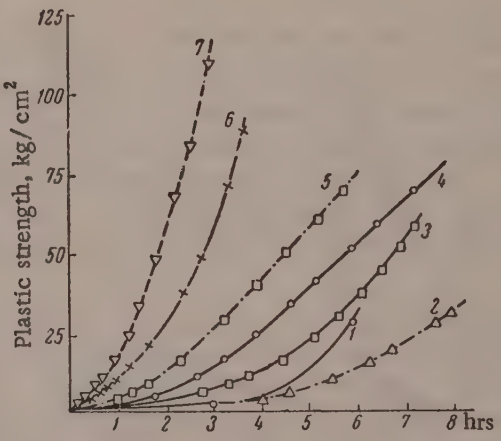


Fig. 5. Plastic strength of a polymer-cement suspension containing PVE-L W/C = 0.3; P/C = 0.2) as a function of amount of calcium chloride added: 1) cement suspension, 2) polymer-cement suspension, 3, 4, 5, 6, 7) the same, and 0.5, 1, 1.5, 2, and 3% $CaCl_2$ respectively.

A consideration of the effect of calcium chloride on the hardening of a polymer-cement suspension (P/C = = 0.2) completely eliminates the assumption that cement of such composition plays merely the role of a filler, or at best of a water absorbing medium. It is well known that the calcium chloride in a polymer-cement suspension can react only with the cement and not with the polymer (polyvinylactate or polyvinyl alcohol). Thus, the acceleration of the hardening can be caused only by an intensification of the process which forms the cement stone structure.

SUMMARY

1. By adding two substances to the cement suspension, namely, potash and soda, potash and necal, or ammonium caseinate and necal, the structuration process is altered, since the effects of each of the added substances, taken separately, add up.

2. The structuration kinetics of a polymer-cement suspension is determined by two parallel running super imposed processes: 1) the formation of the cement stone structure in the presence of additives, which accompany the water dispersion of polymer, 2) the formation of polymer bodies from individual globules under cement hydrated conditions.

3. Latex cement suspension (with SKS-65 GP) stabilized with ammonium caseinate, hardened slowly, and the induction period of such systems is large. Using electrolytes as stabilizer (potash, soda, or a mixture of potash and soda) makes it possible to shorten the induction period and accelerate the hardening. A similar effect may be achieved using a stabilizer, not ammonium caseinate, but the caseinate of sodium or potassium.

4. Emulsifiers and stabilizers of a water dispersion of polymers have a large effect on the structuration of the polymer-cement suspension. To get quick hardening polymer-cement concretes one must use a type PVE-L emulsion, which contains only polyvinyl alcohol in addition to the polymer.

5. The hardening rate of polymer-cement concretes with PVE-L emulsion can be increased even more by adding 1% (relative to the cement) calcium chloride as a hardening accelerator.

LITERATURE CITED

1. Yu. S. Cherkinskii, Polymer-cement concrete [in Russian] Gosstroiizdat, 1960.
2. Yu. S. Cherkinskii, V. M. Kalashnikova, Izv AS and A SSSR, 2, 122, 1959.
3. P. A. Rebinder, A. N. Putilova, Introductory report to Kleiton's book "Emulsions" [Russian translation] IL 1950.
4. P. M. Khomikovskii, Uspekhi, khimii, 28, 547, 1959.
5. P. A. Rebinder, Physical Chemical Mechanics [in Russian] Znanie, 1958.
6. E. E. Segalova, P. A. Rebinder, Structural Material [in Russian] 1, 21, 1960.
7. O. I. Luk'yanova, S. A. Daryusina, Kolloidn, Zh, 20, 628, 1958.
8. K. E. Clare, P. T Sherwood, J. appl. Chem. 4, 625, 1954.
9. W. G. Wren, Frans Inst. Rubler Ind. 13, 89, 1937.
10. P. A. Rebinder, N. A. Semenenko, Dokl, AN SSSR, 64, 385, 1959.
11. Yu. S. Cherkinskii, V. M. Kalashnikova, Structural Material [in Russian] 5, 8, 1960.

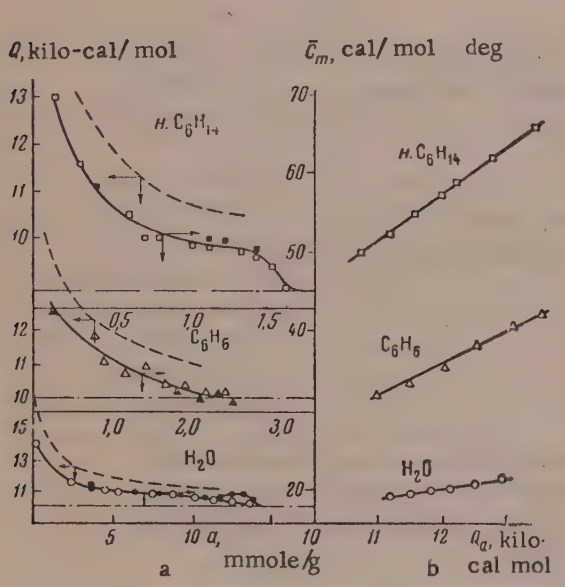
All abbreviations of periodicals in the above bibliography are letter-by-letter transliterations of the abbreviations as given in the original Russian journal. *Some or all of this periodical literature may well be available in English translation.* A complete list of the cover-to-cover English translations appears at the back of this issue.

DEPENDENCE OF THE MEAN MOLAR HEAT CAPACITY OF AN ADSORBATE UPON THE DIFFERENTIAL HEAT OF ADSORPTION

G. I. Berezin, A. V. Kiselev, V. A. Sinitsin

Institute of Physical Chemistry of the Academy of Sciences, USSR
Surface Chemistry Group, Moscow
Translated from Kolloidnyi Zhurnal, Vol. 23, No. 5,
pp. 638-639, September-October, 1961
Original article received April 8, 1961

It has been shown that in ordinary temperatures the mean molar heat capacity of water with a Linde 4A molecular seive [1], or a finely porous silica gel [2], at an adsorption (a), which is less than the limiting value, considerably exceeds the heat capacity of the ordinary liquid. Similar results have been obtained for the systems silica gel-benzene or n-hexane [3]. It is a matter of interest to investigate how the mean molar heat capacity C_m varies with the differential heat of adsorption, Q_a, since for each value of adsorption, C_m is characteristic of the mean state of the adsorbate, and Q_a is an equal potential surface, on which the adsorption occurs for a given value of a. The curves giving C_m as a function of a for the system finely porous silica gel-water, [2], benzene, or N-hexane [3] in the pore volume filling region up to 90% are very similar to the corresponding curves giving Q_a as a function of a, [4]. The figure shows C_m as a function of Q_a for the same values of a. In all three cases there is a linear dependence between C_m and Q_a, their slopes $\partial C_m/\partial Q_a$ are equal to $1.9 \cdot 10^{-3}$, for water, $3.45 \cdot 10^{-3}$ for benzene and $5.57 \cdot 10^{-3}$ deg^{-1} for n-hexane. These values which have the dimension of inverse temperature, are probably related with the nature of the motion and the frequency of vibration of the adsorbed molecules, since the heat capacity is the measure of the degree of free motion of the molecule, while the heat is the bond energy.



a) Mean molar heat capacity of adsorbate, C_m, and differential heat of adsorption, Q_a, as a function of the adsorption a; b) C_m as a function of Q_a.

Setting up such simple relations between C_m and Q_a so far of empirical nature, would be of interest for determining the structure of substances adsorbed on various adsorbents. Therefore, the relation between C_m and Q_a should be investigated in detail for other adsorbed systems.

LITERATURE CITED

1. G. Z. Kington, Co. "The Structure and Properties of Porous Materials", Ed. D. H. Evett, F. Stone, London, 1958, p. 247.
2. G. I. Berezin, A. V. Kiselev, V. A. Sinitsyn, Dokl. AN SSSR, 135, 638, 1960.
3. G. I. Berezin, A. V. Kiselev, V. A. Sinitsyn, Zh. Fiz. Khimii, (in press).
4. A. A. Isirikyan, A. V. Kiselev, Zh, Fiz, Khimii, 31, 2127, 1957; 32, 679, 1958. O. M. Dzhigit, A. V. Kiselev, G. G. Muttik, Kolloidn, Zh, (in press).

THE ROLE OF COLLOID SCIENCE IN THE DEVELOPMENT OF THE MATERIAL AND TECHNOLOGICAL BASIS OF COMMUNISM

Translated from Kolloidnyi Zhurnal Vol. 23, No. 6,
pp. 641-645, November-December, 1961

The XXII Congress of the Communist Party of the Soviet Union adopted the new program of the Communist Party of the Soviet Union – a majestic program for the building of communism in our country. This program envisages an unheard of scale of the measures directed toward the development of a material and technological basis, which, in its turn is designed to insure "in comparison with capitalism, the highest productivity of the labor of society, and an abundance of products delivered for the satisfaction of all the material and cultural needs of society". In the creation of the material and technological basis of communism, and in the growth of the productive forces of society, a decisive role is assigned to science. In his speech on the program of the Communist Party of the Soviet Union, N.S. Khrushchev pointed out that "the creation of the material and technological basis of communism proposes a transition to a new level of the technology and culture of production". "Science is becoming more and more a direct productive force, while production is becoming the technological application of contemporary science".

Among the scientific disciplines, the productional and technological applications of which are designed to insure the new level of the technology and culture of production, an honorable position is occupied by colloid chemistry. Colloid science is engaged in the investigation of surface phenomena in disperse systems. The branches of industry, which carry out the synthesis and treatment of multiphase and multicomponent systems are, to a substantial degree, based on the achievements of the physicochemistry of colloids. Some of these branches are: the polymeric materials treatment industry, the production and application of structural materials, ore refining, wide fields of metallurgy, the food industry, branches of industry which employ synthesis and destruction of emulsions, dispersions, and aerosols, etc. Along with these, the problems of colloid chemistry embrace questions of adsorption and chromatography, which have found the widest practical application. Problems in the geological sciences, agriculture, and agronomy, as well as problems in biology in its widest aspects are, in many cases, solved by the methods of colloid chemistry.

It is perfectly natural that colloid chemistry has developed in the USSR in intimate relation with the solution of the larger problems of the national economy, and in intimate fellowship with neighboring branches of science, such as physical chemistry, molecular physics, and the biological and geological sciences. Particularly intense development has been experienced by the fields of the physicochemistry of dispersed systems, which are based on the theory of surface phenomena at interfaces, as well as problems in the physicochemistry of polymers, their solutions and dispersions.

Researches on the details of the structure of adsorbed layers of surface active molecules and ions have led to the ability to control the lyophilic properties (hydrophobic and hydrophilic properties) of surfaces, through the solution of a number of problems in the theory of flotation or refining, of wetting, for example in the trapping of dust, and in the polygraphic industry, in the processes used in preparing printed forms. Problems have been solved in increasing the stability of highly concentrated dispersed systems, such as films, emulsions, and suspensions, by means of structurized adsorbed layers of a stabilizer, as well as problems in the rapid destruction of such systems, such as film removal and deemulsification processes, particularly in the petroleum industry for the dehydration and desalination of petroleum.

The study of surface forces in the role they play in the kinetics of microheterogeneous systems has been widely developed. Studies made on the molecular attraction and splitting pressure of thin films have given a solid foundation to the theory of the interaction of colloidal particles. This has provided the basis for developing a quantitative theory of the coagulation of dispersed systems by electrolytes, and of the aggregational stability toward coagulation.

Special development has been given to studies on spatial structuration in disperse systems. The mechanical (rheological) properties of such structures have been determined, and it has been shown possible to control these properties over a very wide range. This work has led to the development of a rheology of dispersed systems, and to the

appearance of a new boundary field of science, physicochemical mechanics, which sets itself the task of developing scientifically founded processes of preparing solids and structurized systems, such as disperse structural and building materials with specified mechanical properties.

In the last few years, the physical chemistry of polymers and their solutions, in view of the enormous practical and biological importance of this wide field, has been separated from colloid chemistry into an independent science, but this does not remove the need for colloid chemistry in the treatment of new and important problems on the boundary between colloid chemistry and polymer science, such as the physical chemistry of microheterogeneous disperse systems. Many of these directions of work have already undergone fruitful development in the Soviet Union. Such are the problems of polymerization in emulsions used to produce polymers in a finely dispersed state in the form of latexes. Such also are the probelms of working polymers into materials and products using active highly dispersed fillers, activated adsorptionally or by chemical modification. Here we are also dealing with the recently developed important problem of polymeric protective coatings using lacquer pigment systems, such as highly concentrated suspensions of pigments and in various polymeric binders (including emulsified colors).

In the solution of this problem special attention is given to the study of processes for putting on and forming the coatings, establishing an adhesive bond with the surface being coated, and giving the necessary strength to the coatings.

A large amount of development has been devoted to theoretical and experimental studies in the field of aerodisperse systems, such as fogs and smokes, ways of controlling their properties and stability and the processes by which they arise and are destroyed. Here, as in some other fields of colloid chemistry, a quantitative theory has been developed, based on the study of the mechanism of complicated processes and their elementary acts, and new methods of studying disperse systems have been developed.

The great document of our epoch, the program of the Communist Party of the Soviet Union, supported by the XXII Congress of the Communist Party of the Soviet Union, sets before Soviet science the noble and patriotic tasks of discovering and investigating new possibilities for unheard of technological progress on the road toward a communist society.

Such important problems are set before colloid chemistry as discovering new and better processes in the technology of preparing new high strength and long life materials, and in the technology of frabricating polymers into parts and coverings. To solve these problems we need further development of researchers in the field of the molecular interactions on the surface of bodies, as a basis for the development of a theory of the kinetics of heterogeneous processes: the formation, aging, and destruction of disperse systems, their stabilization and distribution, the appearance and modification of secondary structures, and their rheological and diffusional properties.

It is necessary to develop the theory of flotational and other methods of refining, separating and purifying ores and products of chemical industry in order to raise their efficiency, productivity, and selectivity, as well as to automate the processes. It is necessary to develop the theory of the "boiling layer", of vibrational effects and their various applications in chemical industry, including the use of electrophoresis.

The widest prospects are opened up for the use of the laws discovered from the study of surface phenomena in disperse systems, in the mechanics of terrains, particularly for strengthening terrains in highway and airport construction, and in agronomy (control of the structure of soils), in the peat industry, in hydraulic engineering, in agriculture, and in the ceramic and glass industries.

Concern for the health of the workers gives special importance to the development of new, and the improvement of existing methods of purifying water, trapping harmful aerosol industrial wastes, which blow in the air of cities in the industrial centers, destroy vegetation, and corrode equipment and machinery.

At the same time, there can be an enormous economic advantage to trapping valuable wastes, for example sulfurous gases, as well as improving the utilization of fuel in disperse form. It is a matter of extreme current importance to agriculture to perfect aerosol methods of combating agricultural pests.

Great strides have been made in recent years in the field of adsorption, which promises a change from qualitative to accurate quantitative concepts of adsorptional systems in the form of physicochemical constants.

Widespread practical application has been found for nonporous, highly dispersed substances, such as carbon black, finely dispersed silica, and crystalline pigments.

Methods have been developed for the crystal chemical, geometric, and chemical modification of nonporous, highly disperse bodies, which make it possible to obtain strictly reproducable surface properties. With the accurately reproducable adsorptional properties and physical chemical constants, and the profound study of the geometric and electronic structure of adsorbents and their surface chemistry by new chemical and physical methods (isotope exchange, infrared spectra, nuclear magnetic resonance, etc.), as well as with the study of the electronic structure of the adsorbate molecules, it becomes possible to make an orderly solution of the problem of theoretical calculation of the energy of the adsorptional forces, and of the thermodynamic and kinetic properties of adsorbed systems.

This makes it possible to obtain new and important results in the field of improving the quality of adsorbents for separating mixtures, of improving the properties of fillers, pigments, reinforcing materials, and the corresponding filled polymeric materials and polymer coatings, improving the properties of various kinds of disperse materials, in particular, building materials, in catalysis, in dyeing, and in a number of biological problems, dealing with the interaction of the polyfunctional surfaces of complex organic bodies with gases and solutions etc.

In the field of gas chromatography the apparatus must be perfected and stabilized, in particular, new methods of detection and identification must be introduced employing the diverse properties of the components (mass spectrometry, infrared spectra, ionization, magnetic properties, etc.). It is of fundamental importance to develop solids, both as adsorbents, and as carriers of the immobile phases, as well as materials for capillary columns. All this requires a considerable improvement in the theory of gas chromatography, making its models approach the concrete conditions under which molecular processes occur in real columns, and thus providing scientifically supported design data for the optimum construction of chromatographic columns and their operation.

The program of the Communist Party of the Soviet Union envisages a 2.5 fold increase in agricultural production in the first decade, and 3.5 fold in twenty years. To meet this large scale problem, it is necessary to introduce scientifically based systems of farming, making wide use of rational systems of fertilization and of fighting weeds and plant diseases, to complete a broad program of irrigation construction for watering millions of acres of new lands in arid regions, and to extend the existing use of irrigated land.

For the successful solution of the above mentioned problems, agricultural science, particularly such branches as soil conservation and agrochemistry, are making wide use of the divisions of colloid chemistry involved. All studies of the absorptive properties of soils are based on the advances of colloid science, since the basic properties of the soils are due to that part of the soil which is composed of particles with a colloidal degree of dispersion (of mineral or organic origin). Rational utilization of the many millions of tons of mineral fertilizers, the production of which in the USSR will grow at an accelerated tempo, cannot be successfully achieved without establishing the scientific laws governing the reactions of fertilizing compounds with different soils. These reactions are principally of colloidal and adsorptional nature (cation and anion adsorption). The laws mentioned are also known to be determining factors in the nature of the chemical industry supplying mineral fertilizers. At the present time, wide use is being made of nitrogen compounds, which rapidly nitrify, and, therefore, must be used every year, and not just once at that (refertilization). Meanwhile, the use of polymeric forms of nitrogen compounds (polyamides) could provide extensive mineralization of the nitrogen compounds, on the one hand, and artificial structuration of unstructured soils from these polymers, on the other.

An important problem in colloid chemistry is the study of soil structure, and methods of artificial structuration of soils, particularly in regions using artificial irrigation.

In irrigated farming, a fundamental colloid chemical problem is the struggle with peptization of the soil masses, and formation of dense layers in the soil stratum, when the irrigation water has an unfavorable salt concentration. This calls for rational use of preventive measures involving irreversible coagulation of the soil elements.

A very important problem is the development of colloid chemical methods of sweetening acid soils, especially in the northern parts of the country, by liming, and the improvement of brackish soils by using bivalent and trivalent cations of certain salts.

In agriculture, wide practical use is being made from the achievements of the physical, chemical, and biological sciences. Colloid problems arise in the solution of the problems of general biology, such as the production and transformation of the colloid chemical structures of the biological substrates, which are the carriers of the vital processes. Development of work in the field of molecular biology, accomplished by the cooperative efforts of physical chemists and biologists, is expected to lead to the solution of the fundamental problems of the regulation of vital processes.

The new program of the Communist Party of the Soviet Union contains a great call to action: "all in the name of man, for the good of man". Workers in colloid science will direct all their energy and all their forces toward meeting this magnanimous call to action.

THEORY OF CAPILLARY IMPREGNATION BY WETTING LIQUIDS OF POROUS MATERIALS WITH DEAD-END CAPILLARIES

M.A. Al'tshuler

Scientific Research Institute for the Propagation of Advanced Experimentation in Construction, and for Technical Information, KIEV

Translated from Kolloidnyi Zhurnal Vol. 23, No. 6, pp. 646-651, November-December, 1961
Original article submitted October 20, 1960

The study of the laws of capillary impregnation are a matter of great interest, both from the point of view of using these laws in technological processes, and from the point of view of discovering ways of using the laws to investigate disperse systems. There is a well developed theory of the capillary phenomena in bodies traversed by open-ended capillaries, and the results are usually extended to all porous bodies, and to all the capillary phenomena which occur in them [1]. Subsequently, this theory was substantially enlarged by considering the splitting action of polymolecular liquid films [2]. At the same time, it is possible to point to a number of processes and phenomena, where the important role is played not by open-ended capillaries, but by dead-end capillaries.

Cases are possible, where open-end capillaries behave as if they were dead-ended (for example, when a piece of porous material is completely immersed in a liquid). By dead-end capilaries we mean capillaries which are closed at one end, i.e., capillaries of "test tube" or "crack" type [3]. If wetting liquids penetrate into capillaries of this sort, they will bottle up the air inside, which is compressed as the liquid fills up the capillary, the more so, the larger the value of capillary rise. This phenomenon may have a serious effect on technological impregnation processes, such as the modification of the nature of sorbent surfaces by impregnation methods, etc. The intensification of dispersion in liquids resulting from the splitting action of solvate layers is also limited by the rate of penetration of the liquid into the pores of the materials being dispersed [4]. It is obvious that wetting of the internal surfaces of materials that are being finely divided will be determined by the laws of capillary impregnation of dead end capillaries. Accelerating the wetting process, and consequently the dispersion itself, can be accomplished by resisting pressure of the air compressed in the capillaries, i.e., by previously evacuating the materials that are to be finely divided. However, the effect of dead-end pores on capillary impregnation and other processes has not been studied.

The feeble interest shown in this question can further be accounted for by the lack of methods, which would make it possible to define the dead-end capillaries, distinguish them from open-end capillaries, and find the distribution of their volumes in radius. Actually, the existing methods make it possible to determine either a "mean" hydraulic radius of the open-ended pores from filtration measurements [5-8], or to find the characteristic function of the porous material by methods involving adsorption, forcing in nonwetting liquids, or electron microscopy [3,9-12]. Using these same methods for a selective determination of the characteristic functions of open-ended and dead-end pores is not possible. Only the specific surface of open-ended and dead-end pores can be approximately evaluated separately by methods involving stationary and nonstationary filtration of rarefied air [13].

This paper discusses the peculiarities of the capillary phenomena occurring in dead-end capillaries, and a method of finding the distribution of volumes of dead-end capillaries in radius. A discussion is also given of the general applicability of this method to determining the structure of porous materials with 1–100 μpores. The phenomena occurring in pores of these dimensions are very interesting, but have been insufficiently studied [7,8].

The impregnation rate is determined by the actuating pressure (p_{ac}), which moves the liquid in the capillary.

In an open-ended vertical capillary:

$$p_{ac} = \frac{2\sigma}{r}\cos\theta - \delta gh, \qquad (1)$$

where r is the pore radius, σ is the surface tension, θ is the wetting angle, δ is the specific gravity of the liquid, h is the depth of impregnation, and g is the acceleration of gravity.

In a dead-end capillary of "inverted test tube" type

$$p'_{ac} = \frac{2\sigma}{r}\cos\theta - \delta gh + p_{атм} - p_{атм}\frac{h_0}{h_0 - h}. \tag{2}$$

In a previously pumped-out dead-end capillary

$$p''_{ac} = \frac{2\sigma}{r}\cos\theta - \delta gh + p_{атм} - p_{vac}\frac{h_0}{h_0 - h}. \tag{3}$$

The motion of the liquid in the capillaries is satisfactorily described by Toiseuille's law [14]. The linear rates of capillary rise the liquid for open-end, dead-end, and pumped-out dead-end capillaries are respectively equal to

$$V = \frac{Q}{\pi r^2} = \frac{r^2}{8\eta h}\left(\frac{2\sigma}{r}\cos\theta - \delta gh\right). \tag{4}$$

$$V' = \frac{r^2}{8\eta_1 h}\left(\frac{2\sigma}{r}\cos\theta - \delta gh + p_{атм} - p_{атм}\frac{h_0}{h_0 - h}\right). \tag{5}$$

$$V'' = \frac{r^2}{8\eta_1 h}\left(\frac{2\sigma}{r}\cos\theta - \delta gh + p_{атм} - p_{vac}\frac{h_0}{h_0 - h}\right). \tag{6}$$

In view of the fact that

$$p_{атм} - p_{атм}\frac{h_0}{h_0 - h} = p_{атм}\left(1 - \frac{h_0}{h_0 - h}\right) < 0,$$

то $V \geqslant V'$

from equations (4) and (5) we obtain

$$\frac{V'}{V} = 1 - \frac{P_{атм}\dfrac{h}{h_0 - h}}{\dfrac{2\sigma}{r}\cos\theta - \delta gh}. \tag{7}$$

It is clear from equation (7) that V = V' that h = 0, i.e., at the beginning of capillary rise.

The values of V" at the beginning of the process considerably exceed the value of V, and then rapidly fall to zero. From equations (4) and (6) we obtain

$$\frac{V''}{V} = 1 + \frac{P_{атм} - P_{vac}\dfrac{h_0}{h_0 - h}}{\dfrac{2\sigma}{r}\cos\theta - \delta gh}. \tag{8}$$

At the beginning of the process

$$\frac{V''}{V} = 1 + \frac{P_{атм} - P_{vac}}{\dfrac{2\sigma}{r}\cos\theta},$$

and at

$$\frac{2\sigma}{r}\cos\theta - \delta gh + p_{атм} - p_{vac}\frac{h_0}{h_0 - h} = 0, \tag{9}$$

V"/V becomes equal to zero.

Equation (9), which may be simplified by neglecting as small the product δ gh, gives the maximum height of capillary rise h_∞ in a dead-end capillary:

$$h_\infty = \frac{\left(\frac{2\sigma}{r}\cos\theta - p_{vac} + p_{атм}\right) h_0}{p_{атм} + \frac{2\sigma}{r}\cos\theta}. \tag{9a}$$

The kinetics of capillary suction is described by the equation

$$V = \frac{dh}{dt} = \frac{r^2}{8\eta} \cdot \frac{\Delta p}{h},$$

where Δp is the actuating pressure [14]. For the capillary rise in open-end capillaries

$$\Delta p = \frac{2\sigma}{r}\cos\theta - \delta gh; \text{ and } t = \int \frac{dh}{V} = \frac{8\eta}{r^2 \delta g}\left(h_0 \ln \frac{h_0}{h_0 - h} - h\right).$$

The capillary rise in a dead-end capillary is described by the equations

$$V = \frac{dh}{dt} = \frac{r^2}{8\eta h}\left(\frac{2\sigma}{r}\cos\theta - \delta gh + p_{атм} - p_{атм}\frac{h_0}{h_0 - h}\right); \tag{10}$$

$$t = \int \frac{dh}{V} = \frac{8\eta}{r^2}\int \frac{hdh}{\frac{2\sigma}{r}\cos\theta - \delta gh + p_{атм} - p_{атм}\frac{h_0}{h_0 - h}}. \tag{11}$$

In studying the suction of finely divided materials, equation (11) may be simplified by neglecting the term δ gh, and writing it in the form

$$t \approx \frac{8\eta}{r^2}\int \frac{hdh}{\frac{2\sigma}{r}\cos\theta + p_{атм} - p_{атм}\frac{h_0}{h_0 - h}}. \tag{12}$$

In the case of a capillary that has been previously pumped-out

$$t \approx \frac{8\eta}{r^2}\int \frac{hdh}{\frac{2\sigma}{r}\cos\theta + p_{атм} - p_{vac}\frac{h_0}{h_0 - h}}. \tag{13}$$

To find the solution of these equations we set $h_0 - h = h_1$, $h = h_0 - h_1$, and $dh = dh_1$.

Then equation (12) takes the form

$$t = \frac{8\eta}{r^2}\int \frac{(h_0 - h_1)\, h_1\, dh_1}{h_1\left(\frac{2\sigma}{r}\cos\theta + p_{атм}\right) - p_{атм}\, h_0},$$

and equation (13) takes the form

$$t = \frac{8\eta}{r^2}\int \frac{(h_0 - h_1)\, h_1 dh_1}{h_1\left(\frac{2\sigma}{r}\cos\theta + p_{атм}\right) - p_{vac} h_0}.$$

Set $\frac{2\sigma}{r}\cos\theta + p_{atm} = A$ and $B = -p_{atm}\, h_0$, or, for equation (13), $V = -p_{vac}\, h_0$. Then

$$t = \frac{8\eta}{r^2}\int \frac{(h_0 - h_1)\, h_1 dh_1}{Ah_1 + B}. \qquad (14)$$

This is an approximate equation, the more accurate form should contain the term δ gh. Integrating equation (14), we obtain

$$t = \frac{8\eta}{r^2}\left[-\frac{1}{2A^3}\left(Ah_1 + B\right)^2 + \frac{2B}{A^3}\left(Ah_1 + B\right) + \frac{h_0 h_1}{A} - \left(\frac{h_0 B}{A^2} + \frac{B^2}{A^3}\right)\ln\left(Ah_1 + B\right)\right]. \qquad (15)$$

We shall consider the question of finding the porous structure of materials by determining the equilibrium values of the capillary suction exerted on wetting liquids by previously pumped-out samples.

The condition for cessation of capillary rise is expressed by the equation

$$p_{ext} + \frac{2\sigma}{r}\cos\theta = p_0 \frac{h_0}{h_1} + \delta g\ (h_0 - h_1), \qquad (16)$$

where p_{ext} is the external pressure p_0 is the initial air pressure in the capillary, h_0 is the total length of the capillary, and h_1 is the length of the part of the capillary not filled with water. Neglecting δ g $(h_0 - h_1)$ as in the equation (11), we obtain the expression for the degree of filling of the capillary with water

$$\frac{h_0 - h_1}{h_0} = 1 - \frac{1}{\frac{p_{ext}}{p_0} + \frac{2\sigma}{p_0 r}\cos\theta}. \qquad (17)$$

Capillary Filling Coefficients

Air pressure in porous body, dyne/cm^2	Radius of capillaries, μ		
	100	10	1
Pressure over liquid 1 abs atm			
$0.98 \cdot 10^6$	0.0146	0.129	0.595
$0.5 \cdot 10^6$	0.498	0.555	0.795
$0.25 \cdot 10^6$	0.750	0.780	0.900
$0.1 \cdot 10^6$	0.900	0.915	0.960
$0.1 \cdot 10^6$	0.990	0.990	0.997
Pressure over liquid 2 times 10^6 dyne/cm^2			
$2 \cdot 10^6$	0.007	0.067	0.420
$1 \cdot 10^6$	0.505	0.533	0.710
$0.5 \cdot 10^6$	0.755	0.770	0.855
$0.1 \cdot 10^6$	0.955	0.957	0.972
$0.01 \cdot 10^6$	1.000	1.000	1.000
Pressure over liquid 10^7 dyne/cm^2			
10^7	0.0014	0.0143	0.127
$5 \cdot 10^6$	0.500	0.508	0.568
10^6	0.901	0.910	0.915
$0.1 \cdot 10^6$	1.000	1.000	1.000

It follows from equation (17), that the degree of filling of the capillaries depends on the radius as well as on the values of the pressure over the liquid and the air pressure in the porous body. Using the expression for the degree of filling of the capillaries as a function of the initial air pressure, we can, by experimental means, obtain values for the water absorption of samples previously pumped out to a definite and measured pressure. Having found the values of water absorption at one air pressure in the sample, and different liquid pressures, the sample is dried out, or another sample is taken from the same piece, and a measurement is made of the equilibrium values of the water absorption at another air pressure and different liquid pressures. The difference found in the degrees of filling of dead-end capillaries of different radii make it possible to carry out an analysis of the porous structures of materials having pore diameters from 1 to 100 μ.

The table gives values of the water filling coefficients of capillaries at various pressures.

The experimental data on the equilibrium absorptions of water at different air and liquid pressures are related by a system of first degree equations

$$V_{p_{ext}\, p_0} = \sum K_{p_{ext}\, p_0,\, r_i} V_{r_i},$$
$$V_{p'_{ext}\, p'_0} = \sum K_{p'_{ext}\, p'_0,\, r_i} V_{r_i}, \qquad (18)$$

where $V_{(p_{ext}, p_0)}$ is the equilibrium value of water absorption at the air and liquid pressures in question,

$K_{(p_{ext}, p_0, r_i)}$ is the capillary filling coefficient at a given radius,

V_{r_i} is the total volume of capillaries of a given radius.

Solving this system of equations gives the characteristic function of the porous material.

To find the capillary filling coefficient, the sample is placed in an hermetically sealed vessel, pumped-out to a definite measured pressure, water (or other wetting liquid) is admitted, and a hydrostatic weighing is made at various measured water pressures after reaching equilibrium. Similar measurements can be made at elevated air and water pressures, but in this case the apparatus becomes complicated.

Hydrostatic weighing in a wetting liquid is no different from weighing in a nonwetting liquid, and is described in [12].

The pore volume V, filled under these conditions, is given by the formula

$$V = \frac{Q_r + (V_p - 1)\gamma}{\delta} + 1, \tag{19}$$

where Q_r is the hydrostatic weight of the sample, V_p is the total pore volume, γ and δ are the specific gravities of the test material and the liquid.

To determine the distribution of pores and radius when studying open-end channels, a test sample of regular (for example cubicle) form is covered with paraffin or some other, stronger film on five sides, leaving one side open, and the analysis is carried out as described above.

SUMMARY

1. The equations presented for the kinetics of capillary rise of a liquid in dead-end capillaries take account of the pressure over the liquid being sucked up and the pressure of the air compressed in the pores.

2. Study of the specific features of dead-end capillary impregnation has laid the grounds for a new method of investigating the porous structure of materials in the range 1–100 μ.

The author expresses his deep obligation to corresponding member of the Academy of Sciences, USSR, B.V. Deryagin for directing the present work.

LITERATURE CITED

1. K.S. Washburn, Phys. Rev. 17, 273, 1921.
2. B.V. Deryagin, ZH FIZ KHIMII 14, 137, 1940; Acta phys. chim. URSS 12, No. 2, 181, 1940.
3. B.V. Deryagin, DOKL. AN SSSR 113, No. 4, 1957; Proc. of the II Congress. Surface Activity v. 2, 153, 1957.
4. B.V. Deryagin, E. Obukhov, Kolloidn, ZH 1, No. 5, 385, 1935; P.A. Rebinder, ZH TEKHN FIZ 2, 726, 1932.
5. B.V. Deryagin, N.N. Zakhavaeva, M.V. Talaev and A.M. Lopatima, Tr. In-ta FIZ KHIMII AN SSSR, No. VI, 1957, page 124.
6. M.A. Al'tshuler, Transactions of Conference of Young Scientists [in Russian] ASiA, Ukrainian, SSR, 1958.
7. G.F. Trebin, Filtrations of Liquids and Gases in Porous Media [in Russian] Gostoptekhizdat 1959.
8. M.P. Volarovich, N.V. Churaev and B.Ya. Minkov, Kolloidn ZH 19, 159, 1957.
9. V.M. Luk'yanovich and L.V. Radushkevich, Collection "Methods of Investigating the Structure of Highly Dispersed and Porous Bodies" [in Russian], Academy of Sciences Press, USSR, 1957.
10. N.I. Zalevskii and V.T. Bykov, Collection "Methods of Investigation of Highly Disperse and Porous Bodies", Transactions of second conference [in Russian].
11. S.A. Semenova, Ibid. Mercury Porometry at Low Pressures [in Russian].
12. B.V. Spektor, V.I. Ryazantsev and M.A. Al'tshuler, Patent No. 125689.
13. B.V. Deryagin, N.N. Zakhavaeva, V.V. Filippovskii and M.V. Talaev, ZH FIZ KHIMII 1, No. 8, 1958.
14. V.G. Levich, Physico-Chemical Hydrodynamics [in Russian] Second Edition, 1959.

THE TEMPERATURE OF DROPLETS IN SUPERSATURATED VAPOR

A.G. Amelin, E.V. Yashke and Yu.S. Kurgin

Ya.V. Samoilov Scientific Research Institute of Fertilizers, Insecticides, and Fungicides

Translated from Kolloidnyi Zhurnal Vol. 23, No. 6, pp. 652-657, November-December, 1961
Original article submitted October 26, 1961

Whenever a highly supersaturated vapor comes into contact with droplets of its own liquid phase it will condense on their surface. The heat of condensation will raise the temperature of the droplet above that of the vapor and reduce the condensation rate. Hence in computing how much vapor will condense on a droplet it is necessary to consider its temperature. Maxwell's equation [1] can only be used to calculate the temperature of large drops with a radius r greater than the molecular mean free path l. Yet, spontaneous condensation of vapor gives rise to very small droplets in which $\ll 1$. For the evaporation of droplets Fuks [1] postulated a two-stage process. In the region adjacent to the drop surface (within a sphere of radius the size of the molecular mean free path) the transfer of matter occurs through molecular flow and can be represented by equations of molecular kinetics. Outside this sphere the flow of matter is a diffusion process and can be represented by appropriate mass-transfer equations.

Thus the evaporation of droplets can be represented schematically by the diagram shown in our figure, where Δ is the width of the vapor layer adjacent to the drop surface in which exchange between vapor molecules proceeds unhindered.

As a first approximation we can assume that

$$\Delta = l , \qquad (1)$$

where l is the mean free path of the molecules (cm.)

A more rigorous relationship is [1]

$$\Delta = \beta' l , \quad \beta' > 1. \qquad (2)$$

In cases where the condensation is a stationary process the diffusion current of the vapor can be expressed by the equation [1]

$$I = 4\pi\rho^2 \frac{dc}{d\rho} D, \qquad (3)$$

where I is the vapor current in g/sec; D is the diffusion coefficient in cm^2/sec; c is the vapor concentration in g/cm^3; ρ is the distance from the center of the drop in cm.

If we take $\rho = r + \Delta$ and integrate equation (3) with the appropriate boundary conditions we get

$$I = 4\pi (r + \Delta)(c_\infty - c) D. \qquad (4)$$

The condensation rate on a droplet (in vacuo) is given by

$$I = 4\pi r^2 (c - c_0) \alpha\nu , \qquad (5)$$

where α is the condensation coefficient representing the fraction of vapor molecules which after colliding with the droplet surface remain attached to it;

$$\nu = \frac{\bar{v}}{4} , \qquad (6)$$

where $\bar{v}$ is the average (arithmetic) velocity of the vapor molecules (in cm/sec),

$$\bar{v} = 1{,}457 \cdot 10^4 \sqrt{\frac{T}{M}}, \tag{7}$$

where M is the molecular weight of the vapor.

Assuming that the vapor flows represented by equations (4) and (5) are equal we get

$$I = 4\pi D(r+\Delta)\frac{r^2 \alpha \cdot \nu (c_\infty - c_0)}{D(r+\Delta) + r^2 \alpha \nu}$$

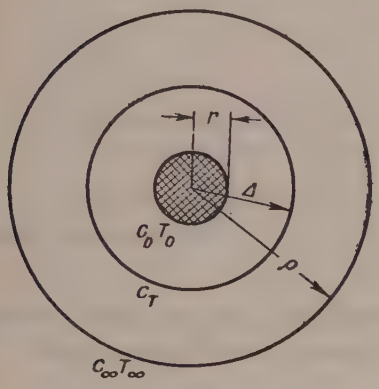
or

$$I = \frac{I_0}{\gamma} = \frac{4\pi Dr(p_\infty - p_0)M}{RT\gamma}, \tag{8}$$

where I_0 is the flow rate of the vapor computed from Maxwell's equation, and

$$\gamma = \frac{D}{r\alpha\nu} + \frac{r}{r+\Delta}, \tag{9}$$

R is the gas constant; M is the molecular weight of the vapor.



A schematic representation of the evaporation of a small droplet (r 1); r is the droplet radius in cm; Δ ≈1, in cm; ρ is the distance from the center of the droplet; c_0, c_T, and c_∞ are the gas concentrations near the boundary between the regions and in the surrounding medium respectively, in g/cm^3; T_0, T, and T_∞ are the droplet surface temperatures at the boundary between the two regions and in the surrounding medium, in °K.

We will use the same approach in deriving expressions for the mass-transfer process.

The rate at which heat is transferred from a droplet to the surrounding vacuum can be represented by

$$Q = 4\pi r^2 (T_0 - T)\beta m, \tag{10}$$

where β is the accomodation coefficient; m is a coefficient characterizing the contact between the droplet and the vapor.

Equation (10) was derived by Langmuir [2] for the heat loss from a hot wire in gases at low pressure where r≪l. The rate of heat transfer given by Equation (10) is equal to the conduction rate into the surrounding medium

$$Q_\lambda = 4\pi\rho^2\lambda\frac{dT}{d\rho}. \tag{11}$$

In this case

$$m = \frac{c_v}{M}\cdot\frac{\bar{v}}{4}c \tag{12}$$

or

$$m = \frac{c_v}{M}\sqrt{\frac{RT}{2\pi M}}\cdot\frac{M}{RT}p,$$

where c_v is the molar heat capacity at a constant volume (cal/mole · deg); M is the molecular weight of the vapor; c is the vapor concentration in g/liter; p is the vapor pressure in dynes/cm^2.

Using Equations (10) and (11) and following the derivation scheme used above we get

$$Q = 4\pi\lambda(T_0 - T_\infty), \tag{13}$$

$$= \frac{Q_0}{\frac{\lambda}{r\beta m} + \frac{r}{r+\Delta}} = \frac{Q_0}{\delta}, \tag{14}$$

$$\delta = \frac{\lambda}{r\beta m} + \frac{r}{r+\Delta}. \tag{15}$$

Under common industrial conditions mist forms only in gaseous mixtures which contain low concentrations of the condensing vapors. So that in examining the loss of heat by the droplet we could assume that the droplet is located in an inert gas. These conditions render the derivation of an expression for the coefficient m relatively easier.

The amount of heat given off when vapor condenses on a droplet is

$$Q = LI, \tag{16}$$

where L is the heat of condensation of the vapor in cal/g; if we now replace Q and I in Equation (16) by the expressions given by Eq. (14) and (8) respectively we will get $\frac{Q_0}{\delta} = \frac{LI_0}{\gamma}$. Using Equation (13) and Maxwell's equation we can replace Q_0 and I_0 by other parameters; taking the gas temperature $T_\infty = T$, the drop surface temperature $T_0 = T_d$, the vapor pressure in the gas phase $p_0 = p$, and the vapor pressure near the surface (the saturated vapor pressure of the droplet at the droplet temperature) $p_0 = p_{sd}(T_d)$ we end up with

$$\frac{4\pi rDML}{RT\gamma}[p - p_{sd}(T_d)] = \frac{4\pi r\lambda(T_d - T)}{\delta};$$

$$T_d - T\frac{DML}{RT\lambda\frac{\gamma}{\delta}}[p - p_{sd}(T_d)] = \frac{DML[p - p_{sd}(T)_d]}{RT\lambda Z}. \tag{17}$$

If the vapor pressure is expressed in mm of Hg Equation (17) will change to

$$T_d - T = \frac{DML[p - p_{sd}(T_d)]}{760 \cdot RT\lambda Z},$$

where

$$Z = \frac{\gamma}{\delta} = \frac{\frac{D}{r\alpha v} + \frac{r}{(r+\Delta)}}{\frac{\lambda}{r\beta m} + \frac{r}{(r+\Delta)}}. \tag{18}$$

The temperature T_d in Equation (17) can be determined by the method of successive approximations; in order to evaulate $p_{sd}(T_d)$ in the numerator of the right hand side of Eq. (17) we have to know the droplet temperature.

To facilitate the calculations Tunitskii [3] assumed that for large drops

$$p_{sd}(T_d) = p_{sd}(T)\left[1 + \frac{E}{T \cdot T_d}(T_d - T)\right], \tag{19}$$

where

$$E = \frac{ML}{1{,}98}. \tag{20}$$

We will show that Equation (19) is also valid for smaller droplets. For very tiny droplets we have to assume that

$$\ln \frac{p_{sd}(T)}{p_{s_\infty}(T)} = \frac{2\sigma M}{RT\rho r} = \frac{n}{T}, \tag{21}$$

where $p_{s_\infty} = (T)$ is the saturated vapor pressure over a plane surface at the given gas temperature (mm Hg); $p_{sd}(T)$ is the saturated vapor pressure over the droplet at the given gas temperature (mm Hg); σ is the surface tension (dynes/cm); ρ is the density of the liquid (g/cm^3);

$$n = \frac{2\sigma M}{R\rho r}, \tag{22}$$

so that

$$p_{sd}(T) = p_{s\infty}(T)\, e^{\frac{2\sigma M}{KT\rho r}} = e^{C-\frac{E}{T}}\, e^{\frac{n}{T}} = e^{C-\frac{E-n}{T}}, \tag{23}$$

and accordingly

$$p_{sd}(T_d) = e^{\frac{C-E-n}{T_d}} \tag{24}$$

Dividing Equation (24) by Equation (23) and rearranging the terms we get

$$p_{sd}(T_d) = p_{sd}(T)\, e^{C-\frac{E-n}{T_d}-C+\frac{E-n}{T}} = p_{sd}(T)\, e^{\frac{(E-n)(T_d-T)}{T_d T}} \tag{25}$$

When the value of $\frac{(E-n)(T_d-T)}{TT_d}$ is small we can assume that

$$e^{\frac{(E-n)(T_d-T)}{TT_d}} \approx 1 + \frac{E-n}{TT_d}(T_d - T). \tag{26}$$

And consequently Equation (25) will assume the form

$$p_{sd}(T_d) \approx p_{sd}(T)\left[1 + \frac{E-n}{TT_d}(T_d - T)\right]. \tag{27}$$

Equation (22) shows that as r decreases n increases and consequently Equation (26) becomes more applicable. So that the smaller the droplet the less the difference between the two sides of the approximate Equation (27).

Replacing $p_{sd}(T_d)$ by the approximation given in Equation (27) and keeping Equation (18) in mind we can convert Equation (17) to

$$T_d - T = \frac{DML}{RT\lambda Z}\left\{p - p_{sd}(T)\left[1 + \frac{E-n}{T \cdot T_d}(T_d - T)\right]\right\},$$

or assuming $TT_d \approx T^2$ we get

$$T_d - T = \frac{p - p_{sd}(T)}{\frac{RT\lambda Z}{DML} + \frac{E-n}{T^2} p_{sd}(T)}. \tag{28}$$

If the vapor pressure is expressed in mm Hg the equation becomes

$$T_d - T = \frac{p - p_{sd}(T)}{\frac{760 \cdot RT\lambda Z}{DML} + \frac{E-n}{T^2} p_{sd}(T)}.$$

Equation (28) showed that n would increase when r is decreased. But for most liquids even when the droplets formed by spontaneous condensation have an $r = 10^{-7}$ the value of n still is much smaller than E (see Eq. (20)). For example for sulfuric acid vapor at 175.3° Equations (20) and (22) yield [4]

$$E = \frac{ML}{1.98} = 6300,$$

$$n = \frac{2\sigma M}{R\rho r} = 630.$$

Hence in practical problems one can frequently neglect $\underline{n}$ in Equation (28) and if Equation (20) is considered we can write

$$T_d - T = \frac{p - p_{sd}(T)}{\frac{pRT\lambda Z}{DML} + \frac{ML p_{sd}(T)}{1{,}98T^2}}. \qquad (29)$$

The data presented above clearly show that under a given set of conditions the temperature of a droplet will depend on its dimensions; in Equation (29) this factor acts through the parameter Z.

In order to get an idea how the coefficients γ, δ, Z, and drop temperature T_d vary with $\underline{r}$ we will evaluate these parameters for sulfuric acid droplets with radii ranging from 10^{-7} to 10^{-3} cm; the droplets were formed by the condensation of catalytically generated sulfuric acid in the wet process [4]. We will take a gas temperature t = 175.3° (T = 448.4°K) and the vapor pressure of sulfuric acid in the vapor phase p = 16.25 mm Hg. Under these conditions D = 0.159 cm^2/sec; $\lambda = 8.4 \times 10^{-5}$ cal/cm · sec · deg; $p_{H_\infty}(T)$ = 3.24 mm Hg; σ = 50.2 dynes/cm; $R = 8.32 \times 10^7$ cal/deg · mole; L = 122 cal/g; ρ = 1.681 g/cm^3; p = 760 mm Hg; $\Delta = l = 10^{-5}$ cm.

Since the vapor pressure of sulfuric acid is relatively low while the gas temperature is high we will assume that the condensation coefficient $\alpha = 1$. We will also take the accomodation coefficient $\beta = 1$.

Using Equations (6) and (7) we get $\nu_n = \bar{v}_n/4 = 7.78 \times 10^3$ for the condensation of sulfuric acid vapor. Hence for a droplet with a radius $r = 10^{-7}$ Equation (9) yields $\gamma = 204.4$. Using the value M = 29 (for air) in Equation (7) we will get from Equation (6)

$$\nu_a = \bar{v}_a/4 = 1.44 \cdot 10^4.$$

Using this value and Equations (12), (15) and (18) we will get m = 1.93, δ = 435.2; Z = 0.47.

The temperature difference between a droplet with a radius of 10^{-7} cm and the surrounding vapor can be determined with the help of Equation (28); however, we first have to determine what the vapor pressure of sulfuric acid would be over the droplet surface if the temperature were the same as that of the vapor phase

$$p_{sd}(T) = p_s(T)\, e^{-2\sigma M/RT\rho r} = 15{,}57 \text{ mm Hg}.$$

Substituting this value in Equation (28) we get T_d-T = 0.64°C.

The Value of Coefficients γ, δ, and Z and of Temperature Difference T_d - T for Droplets of Various Sizes and $\Delta = 10^{-5}$ cm

r, cm	10^{-7}	$1{,}5 \cdot 10^{-7}$	10^{-6}	$5 \cdot 10^{-6}$	10^{-5}	10^{-4}	10^{-3}
$\gamma = \frac{D}{r\nu\alpha} + \frac{r}{r+\Delta}$	204.4	—	20.54	—	2.54	1.11	1.01
$\delta = \frac{\lambda}{rm\beta} + \frac{r}{r+\Delta}$	435.2	—	43.62	—	4.85	1.34	1.03
$Z = \frac{\gamma}{\delta}$	0.4696	—	0.4708	—	0.5242	0.8283	0.9777
$T_d - T$	0.64	9.1	17.9	19.0	17.3	11.6	10.0

The results listed in the table show that Z is not very sensitive to changes in the droplet radius; it changes from 0.47 when $r = 10^{-7}$ cm to 0.98 when $r = 10^{-3}$ cm.

On the other hand the coefficients γ and δ, which represent the processes of mass transfer and heat transfer, are very strongly dependent on droplet dimensions. For droplets with $r = 10^{-7}$ cm these coefficients are 200 and 420 times as large as for a droplet with $r = 10^{-3}$ cm.

The temperature difference between the droplet and the vapor changes very little when the radius is changed; an increase in radius from 10^{-6} to 10^{-3} cm reduces the temperature difference from 17.9 to 10.0°. The reason the

temperature difference decreases is that for very tiny droplets $p_{sd}(T)$ increases while $p-p_{sd}(T)$ decreases, as shown in the table.

SUMMARY

1. A formula was derived from which temperature of droplets in supersaturated vapor can be computed; it turns out that as the droplets increase in size the temperature difference between the droplet and the surrounding vapor at first increases, attains a maximum, then declines.

2. We calculated the temperature difference between droplets of sulfuric acid and the vapor phase. For droplets with a radius $r = 5 \times 10^{-6}$ cm the difference is 19°. For droplets either smaller or greater in size the temperature difference is less.

The authors wish to thank corresponding Member Acad. Sci. USSR B.V. Deryagin and Doctor of Chem. Sci. N.A. Fuks for their valuable advice.

LITERATURE CITED

1. N.A. Fuks, Evaporation and Growth of Droplets in Gaseous Media [in Russian], Izd. AN SSSR, 1958.
2. I. Langmuir, J. Amer. Chem. Soc. 37, 426, 195.
3. N.N. Tunitskii, Zh. Fiz. Khimii 15, 1061 (1941).
4. A.G. Amelin, The Manufacture of Sulfuric Acid from Hydrogen Sulfide by the Wet Process [in Russian], Goskhimizdat, 1960.

All abbreviations of periodicals in the above bibliography are letter-by-letter transliterations of the abbreviations as given in the original Russian journal. *Some or all of this periodical literature may well be available in English translation.* A complete list of the cover-to-cover English translations appears at the back of this issue.

STABILIZATION OF CONCENTRATED SUSPENSIONS BY STRUCTURIZATION OF THE DISPERSION (HYDROCARBON) MEDIUM

G.V. Belugina, S.Kh. Zakieva, V.V. Konstantinova and P.A. Rebinder

Institute of Physical Chemistry, Academy of Sciences, USSR, Moscow
Translated from Kolloidnyi Zhurnal Vol. 23, No. 6,
pp. 658-668, November-December, 1961
Original article submitted July 24, 1961

Concentrated suspensions of dispersed metals, pigments, and fillers in hydrocarbon media are becoming more and more widespread in present day technology.

A study of the aggregational stability of these suspensions is a matter of particular interest, since the fundamental technological requirement made of these suspensions is that they should have a sufficiently high degree of stability. However, the sedimentational stability (in view of the usually considerable difference in densities of the phases) is determined, primarily, by the viscosity of the dispersing medium, and the dimensions of the primary particles of the disperse phase under conditions where they are aggregationally stable, i.e., practically completely stabilized [1,2].

If a sufficiently strong space structure (network) of the gel or jelly is formed in the dispersing medium, the sedimentational stability of the primary particles becomes complete, as, moreover, does the aggregational stability, since the particles in the disperse phase have lost their mobility in the process. For particle fixation of this sort to occur in a structurized dispersing medium, it is necessary for the dimensions of the particles to be large in comparison with the dimensions of the cells of the structure or for the particles to enter into the composition of the structure as nodes of the network, as in the case of active fillers. In addition to this it is of course necessary for the displacement strength of the structure to exceed the tangential stresses which arise on the surface of the particles under the influence of their own weight. This is precisely the way that we regard the problem of the suspensory power of the washed clay solution, which is used in boring, and is a thixotropic coagulationally structurized medium with respect to the bored out rock particles suspended in it, which are 3–5 orders of magnitude larger than the clay particles [3,4].

Thus, aggregational and sedimentational stability of concentrated suspensions may be achieved by structurization of the dispersing medium. One must, however, keep in mind that in almost all cases of technological application, the ability to be pumped through pipes, and the ability to be stirred and homogenized (ease of application in the case of lacquer pigment systems, which are concentrated suspensions of pigments) must be found associated with limiting ease of mobility. This means that the aggregational stability must continue under flow, i.e., under conditions where the structure of the dispersing medium is partially destroyed, and, in addition, that the degree of structurization, i.e., thickening of the medium, must be sufficient to prevent settling and collision of the particles, but not too high to maintain ease of mobility. In the limit of concentrated suspensions, the aggregational stability is usually achieved by adding a stabilizer, which causes structurization only in the adsorbed layers in the immediate vicinity of the surface of the particles. It is conceivable that this factor (adsorptive stabilization) does not provide complete sedimentational stability of dilute suspensions, and, therefore, will not be sufficient to ensure homogeneity of suspensions which do not have the necessary high concentration, especially with large particles and large difference in densities of the phases.

However, the structurizing agents are often surface active substances on the boundary with the solid phase, i.e., which form adsorbed layers on the boundary. This is determined by the same special features of molecular structure as is the development of a special coagulational structure. Such are the various soaps, such as hydrophilic soaps in water, and oleophilic soaps in hydrocarbon liquids. The asymmetric structure of their molecules (or ions) is the general cause both of the formation of micelles, and of the space structure in the colloidal solutions which they form, and in the formation of adsorbed layers. In aqueous medium the structurization is caused by the interaction of hydrocarbon chains, in nonpolar hydrocarbon medium, it is caused by the interaction of polar groups with substituent

metal atoms. Of course there are many intermediate cases here too, and among them some close to the limit. Thus, for example, polymeric hydrocarbons, with no polar groups or unsaturated localities in the macromolecule, can be lacking in surface activity, and, despite this, even at relatively high concentrations, they structurize (thicken) a hydrocarbon medium (polyethylene, polyisobutylene). An entirely different but interesting example is furnished by the well-known water-suspension stabilizer, glucosidesaponin. It is easily adsorbed from aqueous solutions at the various phase boundaries, and, apparently, usually being denatured in the adsorbed layer, it forms structures there (structural and mechanical barriers) with high strength, and high structural viscosity, without at the same time forming space structures, i.e., in contrast with soaps, it does not form gels in the volume of the solution even at very high concentration (50% and higher).

This paper considers the stabilization of rather concentrated suspensions by means of structurization of the dispersing medium.

As structurizing agents we used aluminum soaps of oleic and naphthenic acids, which we prepared especially for this investigation. In addition, we studied polyisobutylene as an example of a surface inactive structurizing agent (molecular weight 200,000).

As the disperse solid phase we took a standard technical surface-oxidized metallic aluminum powder with particles having dimensions from 6 to 13 μ. The dispersing medium was standard T-1 grade fuel (the kerosene fraction of petroleum, going over in the range 150–300°). The concentration of aromatic hydrocarbons was from 20 to 25%, paraffin hydrocarbons 30-60%, naphthenic hydrocarbons 20-45%, and unsaturated hydrocarbons 1-3%. In separate experiments, this fuel was subjected to purification to remove polar contaminants and hydrocarbons of the unsaturated and aromatic series, first down to an aromatic hydrocarbon concentration of about 1.5% (purification 1), and then down to complete removal (purification 2). In some cases cryoscopically pure benzene was used.

The initial concentration of solid phase was 50% by weight (occupying 23% of the volume). We had shown previously [5], that the change in mechanical properties (greatest limiting viscosity) of the suspension with time is determined principally by the nature and aging of the dispersing medium, i.e., of the gel itself. Therefore, in the present paper, we have studied the effect, on the one hand, of concentration, composition (method of preparation), and nature of the structurizing agent, and on the other of the molecular nature of the hydrocarbon solvent, which enters into solvational interaction with the structurizing agent.

Effect of Concentration of Aluminum Naphthenate Additive on Viscosity and Sedimentation Compacting Rate of Oleosuspensions

A study was made of the viscosity and how it changes with time for 50% suspensions of Al powder in T-1 fuel, thickened by additions of aluminum naphthenate in various concentrations (c = 1.2–4.0%).

Using previously developed methods [6], we measured the limiting maximum viscosity (η) of the practically undisturbed structure at sufficiently small flow rates, both for gels, and for Al powder suspensions at various soap concentrations. The viscosity measurements were made as a function of the time the gels and suspensions had been kept, starting from 2-3 days after preparation.

An aluminum soap of naphthenic acids having the general formula Al(OH)n(OOCR)m, where n + m = 3, was prepared by double exchange decomposition (using a method developed by one of the authors [6]) with an excess of NaOH, at 36% precipitation, and a temperature of 93°.

Figure 1 shows curves of the growth of viscosity of the suspensions (η) with increasing concentration of Al soap in the original gel. The curves were taken for suspensions of various ages. In the range of concentrations (c) from 1.2 to 2.0–2.4%, linear curves of the form $\log_{10}\eta = K + a \log_{10} c$ are observed for values of τ from 5 to 120 days. Extrapolating the straight lines to $\log_{10} c = 0$ (c = 1.0%), we obtain the values of $\log_{10} \eta_{c=1} = K$ for various values of τ, given in Figure 4 (curve 1). The large range of viscosity values (3 orders of magnitude) for suspensions with a soap concentration of 1.2–4.0% in the original gels does not permit plotting η against $\underline{c}$ to its natural scale. However, comparing the general course of the curves and the level of the viscosity shows that in the first period of existence of the gel it has clearly pronounced structural viscosity, which increases sharply with the concentration. As the gel ages, the viscosity becomes less, which is a matter of gradual destruction of the space network of the gel. As a result, the viscosity of aged gels increases with increase in concentration along a more gradual curve.

The curve of the viscosity of the suspensions and the gels, from which they are prepared, as a function of soap

concentration is a power law $\eta - \eta_{c=0} = K_1 c^a$, intersecting the y axis at $\eta_{c=0}$ (viscosity of solvent). At c = 1, $\eta_{c=1} - \eta_{c=0} = K_1$, but for $c \gg 1$, $\eta_{c=0}$ may always be neglected in comparison with η for the gel, since η for c>1 is always greater than $\eta_{c=1}$, and $\eta_{c=1} \gg \eta_{c=0}$. In our experiments $\eta_{c=1} \approx 10^3$ poises, and $\eta_{c=0} \approx 10^{-2}$ poises, so that the viscosity of a 1% gel exceeds the viscosity of the solvent by 5 orders of magnitude. Thus, $K_1 \approx \eta_{c=1}$, and $K = \log_{10} K_1$. The equation takes the form $\eta = K_1 c^a$ or in logarithmic coordinates $\log_{10}\eta = K + a \log_{10} c$, where $a = \Delta \log_{10}\eta / \Delta \log_{10} c$ is the slope of the straight line.

Figure 2 shows the typical aging curves, $\log_{10}\eta$ against τ, of these same suspensions. It follows from the curves that the soap concentration in the original gel effects not only the viscosity level of the suspensions, but the rate at which the viscosity falls off with time. The limiting viscosity of this suspension in 4% gel falls off least sharply with time. In suspensions prepared in gels having a soap concentration of 2% and lower, the viscosity falls off sharply with time along (affine) curves, which are all of the same type, and differ only in viscosity level, the suspensions separating into layers on reaching the viscosity level $\log_{10}\eta \approx 1.25$ ($\eta \approx 20$ poises).

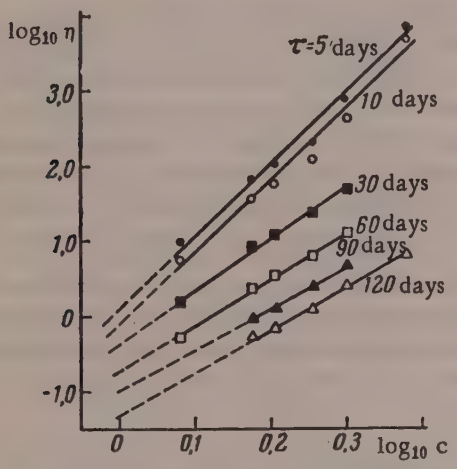


Fig. 1. Viscosity of suspensions as a function of soap concentration in the original gel. τ is time kept.

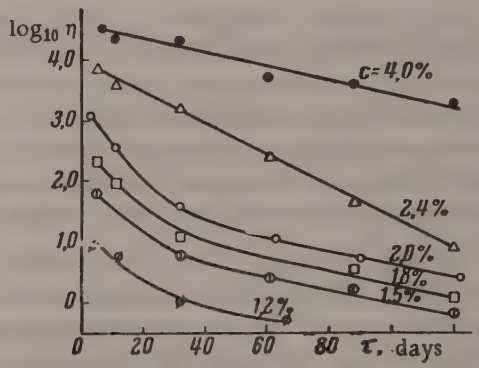


Fig. 2. Curves of aging of suspensions. c is soap concentration in the original gels.

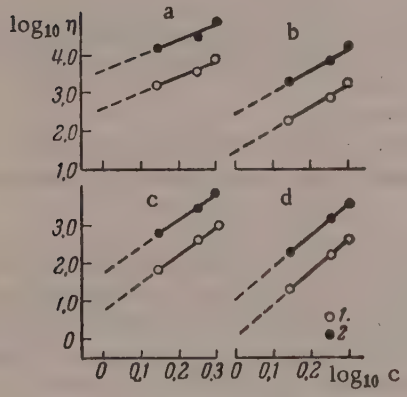


Fig. 3. Viscosity of gels (1) and suspensions (2) as a function of soap concentration in the gel. Time suspension was kept (τ): a) 5; b) 15; c) 20; d) 25 days.

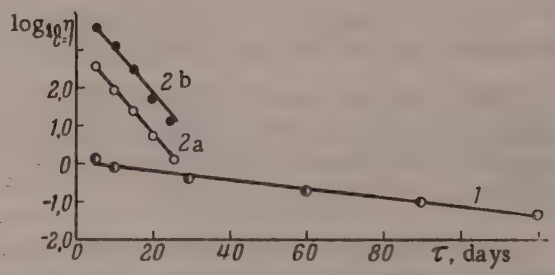


Fig. 4. $\log_{10}\eta_{c=1}$ as a function of τ for suspensions in aluminum naphthenate gels of various composition.

The concentration curve obtained was verified for aluminum naphthenate of another composition*, which had better thickening properties, which made it possible to investigate the region of lower concentrations (2.0—0.8%). The solvent chosen was T-1 fuel (purification 1). Parallel studies were made on original gels with the same soap concentrations, from which the suspensions were prepared. Figure 3 shows the increase in viscosity of the gels in suspensions with increase in Al soap concentration for differ-

* The soap was precipitated with 72% excess NaOH.

ent times kept. The curves for gels and suspensions having the same value of τ are parallel, and are linear in the range of concentrations from 1.4 to 2.0%, as was the case with the suspensions in gels from an Al soap precipitated with 36% excess NaOH (Fig. 1). Extrapolating the straight lines to c = 1.0%, we obtain the values of $\log_{10}\eta_{c=1} = K$ for different lengths of time that the systems were kept.

Plotting the $\eta - c$ curves to logarithimic coordinates for aluminum naphthenate gels and for their suspensions as we did for aluminum oleate gels [7], we obtain for suspensions with $\varphi = 23\%$, the equation $\log_{10}\eta\,\varphi = A - B\tau + \log_{10} k$, which differs from the corresponding equations for the gels, $\log_{10}\eta_0 = A - B\tau$, by the quantity $\log_{10} k$. Figure 4 shows curves of $\log_{10}\eta_{c=1}$ against τ for the gels (curve 2,a) and the corresponding suspensions (curve 2,b), which are linear with the same slope, and have distance between them $\log_{10}\eta_\varphi - \log_{10}\eta_0 = \log_{10} k \approx 1.0$, i.e., $k \approx 10$. Thus, over a wide range of gel viscosity, the viscosity of the suspension is given by an affine transformation, namely, multiplying by the constant quantity $k \approx 10$. For comparison, Fig. 4 used the curve of $\log_{10}\eta_{c=1}$ against τ (curve 1) for suspensions prepared in Al soap gels having another composition. It is also linear, but with a considerably smaller slope, showing that the soap has other structurizing properties*.

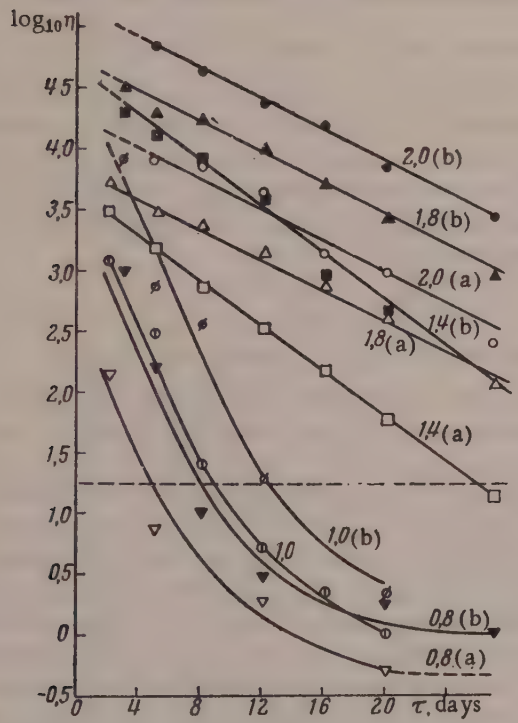


Fig. 5. Aging curves of gels (a) and suspensions (b). The numbers on the curves are subconcentration in the initial gels (%).

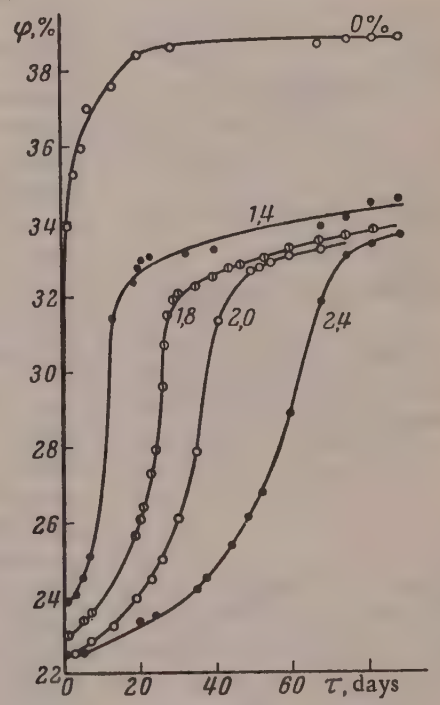


Fig. 6. Sedimentation compacting curves of suspensions in aluminum naphthenate gels of various concentrations (%).

Figure 5 shows the aging curves of these same suspensions in gels. It follows from Fig. 5 that in the range of sufficiently low soap concentrations (2.0–1.4%), the aging curves of the suspensions and gels have the same form as in the case of the higher concentrations (2.0 and 4.0%) considered previously [5]. However, with further reduction in the soap concentration, the form of the aging curves changes, and, beginning at about 1%, the linearity disappears, and the slope increases sharply, showing more rapid aging of the systems.

Parallel with the measurements on the limiting viscosity of the suspensions, a study was made of the spontaneous compacting of the coagulational structure after a drop in the well-defined upper boundary of this structure (settling). The results obtained are given in the form of curves of φ against τ (Fig. 6). The degree of volume filling is $\varphi\% =$

* Soaps with a smaller NaOH concentration during precipitation give gels of smaller viscosity, but with greater stability during storage.

$\frac{100 \cdot V_1}{V_1 + V_2}$ where V_1 is the volume of the solid phase, $V_1 + V_2$ is the volume of the self-compacting structure, namely, the settled suspension. The form of the curves shows that in the initial period, in spite of the very high viscosity, compacting occurs, i.e., there is slow settling of the primary particles. The rate of this "restrained" settling of the suspension particles (in gels of various concentration) is inversely proportional to the viscosity of the medium (gel). Figure 7 gives curves of the reciprocal of the sedimentation compacting rate, $W\varphi = \tau/\Delta\varphi$ (which should be proportional to the viscosity of the gel and consequently of the suspension), as a function of the concentration of Al soap added. For comparison with the curve of $\log_{10} W\varphi$ against c, Fig. 7 shows a curve of $\log_{10}\eta$ against c, the values for the viscosity of the suspensions, η, being taken each time for the mean time $\tau/2$ compared with τ, for which W_φ values were calculated. It follows from Fig. 6 that even for a not very concentrated and comparatively weak structurized gel, if the spontaneous compacting of the sediment reaches $\varphi \approx 34\%$, no more appreciable sedimentation compacting occurs. This shows that in the compacted suspensions the structure has been formed in such a thin region that it prevents any further appreciable compacting.

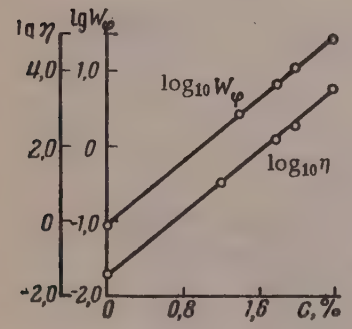


Fig. 7. Curves of $W\varphi$ and η of suspensions as a function of gel concentration.

It is surprising that here φ is still quite small. If, provisionally, we consider the particles to be spherical and having the single dimension $2r \approx 10\,\mu$, this corresponds with the mean layer thickness for the medium $h = \frac{2}{3} r\left(\frac{100}{\varphi} - 1\right)$ between the particles which comes to $h \approx 10\,\mu$ [5]. Thus, when the suspension reaches this limiting value of φ (h), it becomes practically sedimentationally stable. The suspensions are aggregationally stable with the same method of preparation (i.e., at the smallest initial values of $\varphi_0 = 5-23\%$) as we shall show in another communication) at all degrees of structurization of the dispersing medium which we have studied.

Effect of Thickener Composition on the Viscosity and Sedimentation Compacting Rate of Oleo-Suspensions

To elucidate the effect of thickener composition on the properties of suspensions, Al soaps of naphthenic acids were prepared according to various formulas. These soaps were used to prepare 2.0% gels and T-1 fuel, and 50% suspensions of Al powder in the gels. Table 1 gives the formulas according to which the Al soaps were prepared, along with the viscosity values of the suspensions (prepared from the gels of these soaps) after various lengths of time, and Fig. 8 gives the aging curves of the suspensions. The highest level of initial viscosity with subsequent rapid drop-off with time is observed for sample 1, which is characteristic of a soap precipitated at a high concentration of free alkali [6]. The initial viscosity of the suspensions prepared from gels of soaps 2 and 3 (36% excess NaOH) is correspondingly lower, and the stability is also small. The initial viscosity of the suspensions prepared from gels of soap 4 (precipitated with ≈15% excess NaOH) and 5 (soap prepared from another lot of naphthenic acids) is even lower, but they are more stable with time. It must be kept in mind that the 2% aluminum naphthenate gels in which the suspensions were prepared are of low stability, since the stability decreases with increasing soap concentration. Consequently, the composition of the soap to a considerable extent determines the level of viscosity and its stability in time, both for the gels, and for the suspensions prepared from them.

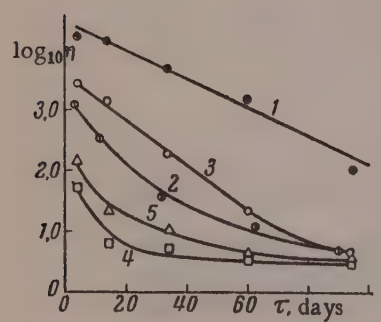


Fig. 8. Effect of method of preparing aluminum naphthenate on viscosity and aging of suspensions. The numbers on the curves are the numbers of the soap sample as given in Table 1.

The sedimentation compacting rate of the suspensions also depends on the soap composition. Fig. 9 shows three typical curves of φ against τ for suspensions in gels from soap samples 1, 4, and 5 (as is shown by the figures on the curves), which are different in form depending on the composition and properties of the structurizing agent.

Effect of the Nature of the Structurizing Agent and the Solvent on the Viscosity of Suspensions and the Time Stability of Viscosity

To investigate the effect of the nature of the structurizing agent, the following were prepared: a 4.0% alumi-

TABLE 1. Effect of Method of Preparation of Al Soap on Viscosity and Aging of Suspensions

Samples	Conditions for aluminum naphthenate preparation			Viscosity of 50% Al powder suspensions and 2% soap gel T-1, poises	
	Method of precipitation	% excess NaOH	t°C	After 3-4 days	After 90-94 days
1	Direct preparation*	72	93	16100	110
2	Same	36	93	1230	5.0
3	Precipitation at pH 5	36	80	2870	4.6
4	The same	14.5	67	56	3.3
5	The same**	50	80	148	3.5

* By gradually adding aluminum sulphate solution to alkaline solution of sodium naphthenate [6].
** From another lot of naphthenic acids.

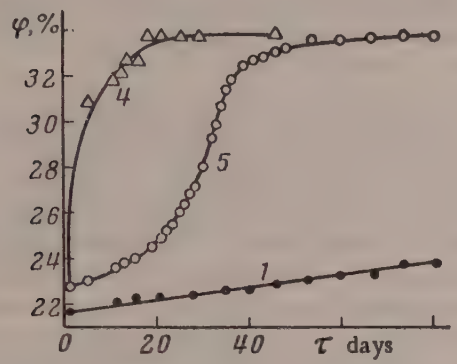


Fig. 9. Sedimentation compacting curves of suspensions in gels of soaps 1, 4, and 5 (Table 1).

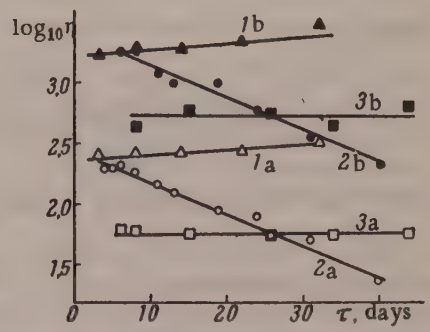


Fig. 10. Effect of nature of structurizing agent on the viscosity and aging of gels (a), and suspensions (b). 1) aluminum naphthenate; 2) aluminum oleate; 3) polyisobutylene.

num naphthenate gel*, and an 8.0% aluminum oleate gel** and benzene, and a 5% solution of polyisobutylene in T-1 fuel. Fig. 10 gives aging curves of these gels and of 50% Al powder suspensions in the same gels. The gels shown in curves 1a and 2a, and the suspensions, 1b and 2b, have the same initial viscosities, but their aging curves are different. The viscosity of the gel 1a and the suspension 1b, in which the structurizing agent is aluminum naphthenate, increases somewhat with time, while the viscosity of the aluminum oleate gel 2a and the suspension in it, 2b, falls off rapidly with time, in spite of the fact that in this case the concentration of the additive is 2 times greater (8.0% instead of 4.0%).

The low stability of aluminum oleate oleogels which causes the drop off in viscosity and the sedimentational instability of suspensions in them is a matter of chemical instability of the aluminum oleates, due to the presence of a double bond in the hydrocarbon radical. We have investigated the properties of aluminum oleate gels previously [7].

If the viscosity of the suspensions drops below a definite level, $\eta \approx 20$ poises, the suspensions begin to separate into layers, and before measuring the viscosity they have to be stirred. However, even in this case the curves of the gel and the suspension maintain the same form (constancy of k), which is a matter of rapid thixotropic re-establishment of the structure in the aluminum naphthenate gels [8]. Here of course the suspension remains homogeneous for a length of time greater than that required for the viscosity measurement.

The viscosity of the 5.0% polyisobutylene solution (curve 3a, Fig. 10) and the corresponding suspension (curve 3b) is small, and does not change appreciably during a time of observation $\tau = 44$ days. It must be noted that, in contrast with the suspensions in Al soap gels, when suspensions are prepared in polyisobutylene solutions the liquid column over the precipitate becomes perfectly transparent (even the finest fractions settle out).

* The soap was precipitated at pH 3.5 in the medium, 36% excess NaOH, and 20°.
** The soap was prepared by "direct" precipitation, with 50% excess NaOH, at 70°.

Figure 11 shows aging curves of 50% Al powder suspensions in 2% aluminum naphthenate gels* in T-1 fuel (curve 1), then T-1, purification 1 (curve 2), and in T-1, purification 2 (curve 3). The highest viscosity level is shown by the suspension in T-1, purification 1, but afterward the viscosity falls off rapidly. The lowest viscosity level is observed in unpurified T-1, caused by its large aromatic hydrocarbon content. All three suspensions have low sedimentational stability, since they were prepared in 2% gels of a soap which has high thickening properties, but which gives gels with a viscosity that drops off rapidly with time. In contrast, the suspensions in 4% gels of aluminum naphthenate**, which has less thickening properties, show larger stability of the viscosity with time (curves: 4) in T-1, purification 1; 5) in T-1 (purification 2; 6) in benzene). The suspension in benzene has smaller viscosity due to the greater dispersing power of benzene as compared with soap.

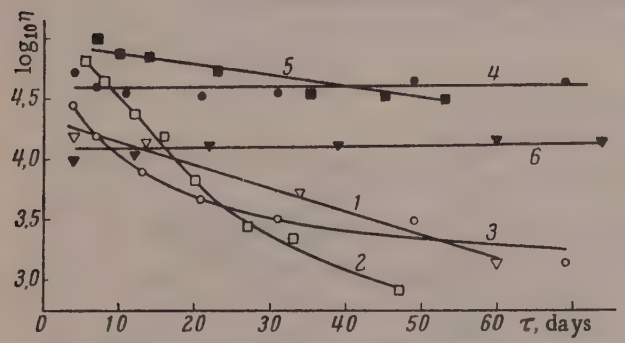


Fig. 11. Effect of the nature of the solvent on the viscosity and aging of suspensions.

TABLE 2. Effect of the Nature of the Dispersing Medium on the Viscosity and Aging of Suspensions. Constancy of values of k_m.

Solvent	Thickening agent; gel concentration, %	η, poises	k_m
After 4–40 days			
Benzene	Aluminum oleate; 8.0	Gel, 194-22 Suspension, 1780-189	9.2
T-1 fuel	Polyisobutylene; 5.0	Solution, 62-58 Suspension, 440-647	9.4
After 4–30 days			
Benzene	Aluminum naphthenate; 4.0	Gel, 256-320 Suspension, 1716-3100	7.9
T-1 fuel, purification 1	The same	Gel, 42-52 Suspension, 410-500	9.7
T-1 fuel, purification 2	The same	Gel, 79-112 Suspension, 818-1155	

Thus, the nature of the solvent also has an effect on the level and on the way of the viscosity changes with time. Thus, for example, the presence of unsaturated hydrocarbons causes a rapid drop off in viscosity, which is, apparently, the result of aggregation (hidden, but sometimes visible). Benzene, which is a good soap disperser, gives gels that are stable with time.

Comparing the aging curves for the gels, $\eta_0 = f_0(\tau)$, with the curves for the suspensions made from them $\eta_\varphi = kf_0(\tau)$ [5] (Fig. 10 and Table 2), shows that the growth coefficient of the limiting viscosity (k) is approximately constant when a solid disperse phase is added, independently of the nature of the structurizing agent and the solvent.

All the same however, somewhat elevated values is $\underline{k}$ are observed for polyisobutylene, which we have also observed in weakly structurized Al soap gels (as high as k = 13 [5]), which shows that there is weak coagulational structurization, i.e., incomplete stabilization of the particles.

Comparisons of the limiting viscosity of gels of aluminum naphthenates of various concentrations, of aluminum oleate, and of polyisobutylene solution, and of the Al powder suspensions formed in them at φ = 23% over a wide range of values of viscosity from 10 to 10^4 poises have shown that adding a solid disperse phase always causes an increase of practically one order of magnitude in the limiting viscosity. Such constancy of $\underline{k}$, independent of the nature of the dispersing medium, over a range of limiting viscosities embracing three orders of magnitude, can be interpreted only by the practically complete aggregational stability of the suspensions, i.e., by the absence of any noticeable coagulational interaction between the particles of the solid disperse phase. Otherwise, the different conditions under which such interaction occurs, and the different strengths of the coagulational structures formed would cause sharp changes in $\underline{k}$. However, the fact that it is constant indicates that there is a uniform distribution of the particles of the disperse phase throughout the volume of the medium (gel), i.e., that the smallest distances between them are everywhere the same, which for not very large values of φ again indicates that

* The soap was precipitated in 72% excess NaOH, at 93°.

** The soap was precipitated at pH 5, 29% excess NaOH, at 67°.

coagulational structure is absent.

In contrast with stabilization by adsorbed layers, the increase in aggregational stability, caused by structurization of the whole volume of the dispersing medium, i.e., by volume gel formation, is characterized by two special features.

1. With strong structurization of the volume of the medium between the particles of the disperse phase, dense packing of the particles, i.e., high degrees of filling cannot be achieved practically, because of the very high viscosity which greatly hinders the gel from flowing out of the comparatively narrow spaces between the particles, under the influence of the weight of the particles themselves, or even under the influence of considerable centrifugal forces. To get the particles of the disperse phase packed, it would be necessary as far as possible to destroy the bonds, but not the ones between the particles, as in the case of loose coagulated structures, since now the particles of the disperse phase are stabilized to the limit. The gel structure must be destroyed (if this structure is then capable of thixotropic re-establishment) during the compacting period, although this may put an end to the stabilization, i.e., it may form separate coagulational aggregates. In any case, under ordinary conditions, suspension stabilized by structurization of the volume of the dispersing medium are not, for the reasons given, able to be densely packed, i.e., they cannot be concentrated to the limit.

2. Stabilization produced by volume gel formation in the dispersing medium may lead not to liquefaction but conversely to densification, i.e., to a diminution in mobility of the system as a whole. It must be kept in mind that the increase in aggregational stability resulting from the formation of adsorbed layers even of particles that are strongly structurized on the surface, causes marked liquefaction of the originally very strong coagulational structures by getting rid of the nonuniform distribution of the particles, i.e., the way they are linked into the chains forming the framework.

Some reduction in strength (liquefaction) of the structurized suspension during stabilization by volume structurization is possible only in the case where the coagulational structure is still considerably stronger than the structure of the stabilizing gel or jelly in the dispersing medium. The optimum stabilization for getting an aggregationally and sedimentationally stable suspension, i.e., one which will not form aggregates or separate into layers, with the maximum concentration of disperse phase, and with the highest mobility under conditions of thixotropic destruction of the structure, may be achieved by making use of both factors, the adsorptional factor and the volume structurization factor in conjunction [9,1]. It is to be expected that in a number of cases stabilization of this sort is realized by making use of surface active structurizing agents of the Al soap type in hydrocarbon media, or, in general, inorganic liquids, since these structurizing agents are, along with their volume thickening properties, distinguished by quite high surface activity [10], i.e., the ability to form adsorbed layers on the surface of the particles in the disperse phase.

SUMMARY

1. A relationship has been found for the limiting (maximum) viscosity (η) as a function of time (τ) and of the concentration of the structurizing agent for aluminum naphthenate gels (serving as the dispersing medium), and 50% suspensions of aluminum powder in the gels (volume filling φ = 23%). For the suspensions, equations were found of the form $\log_{10}\eta_{\varphi} = A - B\tau + \log_{10}k$, which differ from the corresponding equations for gels, $\log_{10}\eta_0 = A - B\tau$, by the quantity $\log_{10}k \approx 1.0$. Thus, over a wide range of gel viscosity, the viscosity of the suspension is given by the affine transformation of multiplying by the constant quantity $k \approx 10$.

2. The composition of the Al soap to a large degree determines the viscosity level and its change with time for the gels, and consequently for suspensions in the gels. Thus, increasing the basicity of the Al soap enhances the structurization properties, while soaps with lower basicity give oleogels which have lower viscosity, but are more stable with time.

3. The compacting rate in suspensions with φ_0 = 23% in aluminum naphthenate gels of various concentrations is inversely proportional to the viscosity, and on reaching $\varphi \approx 34\%$, no further appreciable sedimentation compacting occurs, and the suspension becomes sedimentationally stable. Aggregational stability is, however, always present.

4. The chemical nature of the structurizing agent and the solvent has an effect on the initial viscosity level and on the aging of the suspensions. The maximum viscosity, which changes very little with time, is shown by aluminum naphthenate gels and suspensions made from them (4% gel, 260-320 poises; suspension, 2,000-3,000 poises). The viscosity of aluminum oleate gels and the corresponding suspensions is considerably less, and drops off sharply

with time (8% gel, 200-20 poises; suspension, 1800-200 poises). The viscosity of polyisobutylene solutions and suspensions in them is comparatively small, and does not change appreciably immediately after preparation (5% solution 62-58 poises; suspension 440-650 poises).

5. It has been found that an approximately constant value is shown by the coefficients k for the increase of the limiting viscosity on going from the structurized medium to the corresponding 50% suspensions ($k \approx 10$) in the viscosity range from 10 to 10^4 poises. The fact that k is constant independently of the nature of the dispersing medium, is apparently a matter of the practically complete aggregational stability of the suspensions.

6. The optimum stabilization for getting an aggregationally and sedimentationally stable suspension with the highest possible concentration of disperse phase, and the greatest mobility under conditions of thixotropic destruction of the structure, is to be achieved by combined utilization of both factors, both the absorptional factor and the volume structurizing factor in conjunction.

The Al soaps of various compositions which we have investigated turn out to be precisely those additives, which, along with volume structurization, provide stabilization in the adsorbed layers as a result of their high surface activity.

LITERATURE CITED

1. P.A. Rebinder, Kolloidn ZH 20, 527, 1958.
2. P.A. Rebinder, IZV, OMEN AN SSSR, seriya khim, No. 5, 639, 1936. Investigations on the Physical Chemistry of Technological Suspensions [in Russian] Moscow and Leningrad, 1933; Disc. Faraday Soc. 18, 151, 1954; P.M. Khomikovskii, P.A. Rebinder, Dokl. AN SSSR 18, 575, 1938; Acta phys.-chim. URSS 8, 290, 1938; P.M. Khomikovskii, Kolloidn ZH 8, 439, 1946.
3. P.M. Khomikovskii and D.I. Shilov, Zh Prikl Khimii 19, No. 7, 684, No. 8, 841, 1946.
4. U.Ts. Andres, Dokl AN SSSR 133, 777, 1960.
5. G.V. Belugina, S.Kh. Zakieva, P.A. Rebinder and A.B. Taubman, Dokl. AN SSSR 126, 318, 1959.
6. G.V. Belugina, Dissertation [in Russian] Institute of Physical Chemistry, Academy of Sciences, USSR, 1955; G.V. Belugina and A.A. Trapeznikov, Kolloidn ZH 20, 3, 1958.
7. G.V. Belugina, V.V. Konstantinova, S.Kh. Zakieva and T.A. Rebinder, Dokl. AN SSSR 132, 380, 1960.
8. A.A. Trapeznikov and V.A. Fedotoba, Dokl. AN SSSR 95, 595, 1954.
9. E.M. Natanson, Kolloidn, ZH 20, 556, 1958; "Colloid Metals" [in Russian] Kiev, 1959.
10. L.R. Solov'eva, Kolloidn, ZH 5, 883, 1939.

All abbreviations of periodicals in the above bibliography are letter-by-letter transliterations of the abbreviations as given in the original Russian journal. *Some or all of this periodical literature may well be available in English translation.* A complete list of the cover-to-cover English translations appears at the back of this issue.

THE INFLUENCE OF FREEZING ON THE STABILITY OF GELATINIZED EMULSIONS STABILIZED BY COLLOIDAL MIXED FERROCYANIDES OF COPPER AND IRON

V.I. Borisikhina, L.D. Skrylev, and S.G. Mokrushin

S.M. Kirov Sverdlovsk Urals Polytechnical Institute
Translated from Kolloidnyi Zhurnal, Vol. 23, No. 6,
pp. 669-671, November-December, 1961
Original article submitted July 9, 1960

The problem of the influence of freezing on the stability of emulsions of the oil/water type has not been sufficiently fully studied. It is known that some frozen emulsions break down after thawing, while others emulsify again [1]. Frozen emulsions of benzene and carbon tetrachloride in water, stabilized by a small quantity of sodium oleate, were broken down after thawing, and emulsions were not formed when the shaking was repeated [2,3].

In the present work a study has been made of the influence of freezing on the stability of gelatinized emulsions of carbon tetrachloride, stabilized by colloidal mixed ferrocyanides of copper and trivalent iron.

The emulsions were prepared in the process of isolating these colloids from their hydrosols by the emulsification method; the volume concentration of carbon tetrachloride in the emulsions amounted to 75-80%.

The method for isolating the colloids and the method for preparing the hydrosols have been described earlier [4,5].

The experiments were carried out as follows. 30 ml of the test emulsion was placed in a glass tube with diameter 20 mm and height 200 mm and cooled (frozen) in a thermostat to the required temperature. The duration of freezing of the emulsion was measured from the moment when it reached the required temperature (the freezing temperature) to the start of thawing. The emulsions were thawed in a thermostat at a temperature of +15°.

The table shows that the frozen emulsions break down on thawing, the breakdown being greater, the lower the temperature and the greater the duration of freezing. Complete breakdown of the emulsion takes place at a freezing temperature of −15° and below. In the case where breakdown of the emulsion was complete, 23-24 ml of oil separated. After breakdown of the emulsion, the system in the tube consisted of a lower completely transparent layer of carbon tetrachloride, a central brightly colored layer of coagulum (volume 1-2 ml), and an upper aqueous layer faintly colored with excess potassium ferrocyanide.

Influence of Temperature and Duration of Freezing on the Completeness of Breakdown of Gelatinized Emulsions of Carbon Tetrachloride, Stabilized by Colloidal Mixed Copper Ferrocyanide

Temp. of freezing, °C	Duration of freezing, hr	Volume of CCl_4 separated, ml	Temp. of freezing, °C	Duration of freezing, hr	Volume of CCl_4 separated, ml
— 3	1.0	12.0		0.25	11.0
	2.0	16.0		1.0	21.0
	5.0	16.0		5.0	—
	0.25	6.0	—15	12.0	23.0
	0.5	11.0			
— 7	1.0	18.0		1.0	23.5
	5.0	20.0	—21	5.0	—
	12.0	—		12.0	24.0

No emulsions were formed when these systems were shaken again.

Analogous results were obtained in experiments on the freezing of emulsions of carbon tetrachloride, stabilized by the mixed ferrocyanide of trivalent iron. The mechanism of the breakdown of the emulsions by freezing is apparently influenced by a number of factors.

According to the views of Rebinder and his school [6], the chief factor influencing the stability of emulsions is the structural viscosity and strength of the stabilizing layers on the surface of the films. Freezing of the emulsions leads to breakdown of these layers, due, for example, to the action of low temperatures on the emulsifying power of the gelatin. The emulsifying power of proteins decreases when their solutions are cooled [7], due to the irreversible aggregation of the protein substances; this is accompanied by the evolution of heat, an increase in the viscosity, and a change in the specific rotation of the plane of polarization. An important part in the breakdown of the surface films is played by the mechanical effect exerted by the ice crystals on the drops of the emulsion.

Other important factors influencing the stability of emulsions are the magnitude of the electrical charge of the drops and the thickness of their solvate sheaths. The larger these quantities, the more stable the emulsions. When the emulsions are frozen there is a gradual freezing-out of the water (both free and combined), leading on the one hand to a decrease in the thickness of the protective solvate sheaths separating one drop of oil from another, and on the other to a decrease in the magnitude of their electrical charge, as a result of the increase in the concentration of electrolytes in the aqueous (still unfrozen) phase of the emulsion.

The irreversibility of the process of emulsion breakdown is related to the irreversibility of the process of aggregation of the gelatin micelles and the sharp decrease in its emulsifying power.

SUMMARY

1. By freezing gelatinized emulsions of carbon tetrachloride, stabilized by colloidal mixed ferrocyanides of copper and trivalent iron, it is possible to achieve almost complete breakdown of these emulsions.

2. Suggestions have been put forward regarding the mechanism of the breakdown of the emulsions by freezing.

LITERATURE CITED

1. W. Clayton, Emulsions [Russian translation] (IL, Moscow, 1950), p. 318.
2. Newman, J. Phys. Chem. 18, 45, 1914.
3. T.G. Rochow and C.W. Mason, Industr. and Engng. Chem. 28, 1296, 1936.
4. V.I. Borisikhina and S.G. Mokrushin, Izv. Vysshikh. Uch. Zav. Khimiya i Khimicheskaya Tekhnologiya 2, 711 (1959).
5. L.D. Skrylev and S.G. Mokrushin, Kolloid. Zh. 22, 344 (1960).
6. P.A. Rebinder, Kolloid. Zh. 8, 157 (1946); 20, 527 (1958).
7. V.M. Martynov, Kolloid. Zh. 18, 443 (1946).

All abbreviations of periodicals in the above bibliography are letter-by-letter transliterations of the abbreviations as given in the original Russian journal. *Some or all of this periodical literature may well be available in English translation.* A complete list of the cover-to-cover English translations appears at the back of this issue.

ADHESION OF POLYMERS

9. NEW METHOD OF PREPARING BONDED STRIPS FOR DETERMINING THE MUTUAL ADHESION OF ELASTOMERS

V.L. Vakula and S.S. Voyutskii

M.V. Lomonosov Moscow Institute of Fine Chemical Technology,
Combined Laboratory for Polymers
Translated from Kolloidnyi Zhurnal, Vol. 23, No. 6,
pp. 672-678, November-December, 1961
Original article submitted September 21, 1960

It is a well known fact that in measuring the adhesion of one polymer to another the method of preparing the adhesive joint is a matter of quite fundamental importance. Usually one of the polymers (the adhesive) is applied to the other (the substrate) in the form of a solution (bonding fluid), which is then allowed to dry out until it forms a strong adhesive bond. In our first experiments [1-4], we used one of the modifications of this method. The main advantage of this method of preparing bonded strips, which we may provisionally call the bonding method, is that a layer of adhesive is formed directly on the surface of the substrate, which ensures complete contact between both polymers. However, this technique has a number of fundamental defects.

1. Because of the long period of time required for the solvent to evaporate (several days) it is not possible to make an accurate determination of the length of time during which the substrate and the adhesive are in contact with one another before the bonded strips separate into layers, although this time must be known [1-3].

2. The adhesive layer formed on the substrate surface usually undergoes shrinkage, which causes stresses to appear in the bonded strip, that affect the resistance to separation [5-8].

3. Removing the last traces of solvent from a comparatively thick bonded strip is very difficult.

4. The solvent may cause swelling or even solution of the substrate, which is a complicating factor in the formation of the adhesive bond, and can also effect the results of measuring the adhesive force.

We have tried another method of preparing bonded strips, in which the substrate is brought into direct contact with a film of the adhesives (film method). This method can be used only in case at least one of the polymers is an elastomer, i.e., capable of deformation under pressure so that it can provide complete contact with the other polymer. We have made wide use of this method of preparing bonded strips in measuring the self-adhesion of elastomers [9-11]. A similar method of forming an adhesive joint has been successfully used by Dogadkin [12] in his studies on the adhesion of resin mixtures, as well as by Bright [13] in his work on the adhesion of sticky plasters to various metals.

As adhesives in the film method of preparing bonded strips we used polar SKN-40 butadieneacrylonitrile rubber, and nonpolar P-118 polyisobutylene. These polymers are not too highly adhesive to the substrate used, which ensured that separation of the bonded strips always had an adhesional character. The substrate in both cases was composed of thin films of reclaimed cellulose (cellophane), which had a specularly smooth surface. To see how accurate the measurement of adhesive force was, using bonded strips prepared according to the method that we have developed, we also used other polymers as substrates and adhesives.

In preparing the adhesive film, a strip of percale was stretched out on a hard horizontal surface, and then, one after the other, after definite intervals of time, application was made of several layers of 8-10% SKN-40 copolymer solution in benzene, or a solution of polyisobutylene in benzine, of the sort used in "galoshes", until an adhesive film of the desired thickness was obtained. The adhesive films applied to the fabric were allowed to dry out at room temperature in a location protected from falling dust. Simultaneously, the substrate (cellophane) was freed by extraction with water from the plasticizer (glycerin) contained in it, and stretched out in the moist state on a flat plate. The moist cellophane was then dried in air in the stretched-out state. After drying both components of the bonded strip,

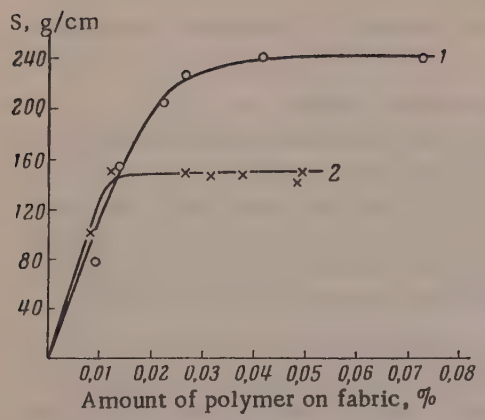


Fig. 1. Effect of amount of elastomer applied to fabric on the adhesive force. 1) Bonded strip of SKN-40 and cellophane; 2) bonded strip of polyisobutylene and cellophane.

the adhesive film was carefully taken up by hand, avoiding bubbles and folds, and laid parallel over the substrate film, after which the strip was rolled on a hard smooth surface with a resin roller. The resulting strip was trimmed down to a strip of the dimensions necessary for determining the adhesive force by separation. Thirty minutes after the sample was put together, it was separated on a TsNIKZ adhesiometer [2,9], with a constant rate of motion of the right hand clamp equal to 0.3 cm/sec.

For each sample tested the automatic recorder drew an adhesiogram, which shows the separating load vs. the length of the separated part of the sample. A visual observation was made of the character of the separation of each bonded strip while it was being tested. Here it was assumed that the resistance to separation was a measure of the adhesion only in those cases where the separated surfaces remained specularly smooth.

In testing various pairs of high polymers, in addition to the adhesional type of separation a mixed type and a cohesional type were also observed. Where the separation was of mixed type, where the failure of the bonded strip showed clearly defined adhesional and cohesional portions, two values of separation resistance were used to describe the samples: a maximum value, giving the cohesional strength of the adhesive, determined from the mean peak loads, and a minimum value, giving the adhesional strength of the bonded strip.

All the values of separation resistance given in this paper represent the arithmetic mean of 8-10 parallel measurements.

To find what effect the thickness of the polymer layer applied to the fabric has on the resistance to separation of the bonded strips, adhesive films were prepared with different amounts of polymer on the fabric. The results on the separation of such bonded strips are given in Fig. 1, from which it follows, that the resistance to separation increases as the thickness of the adhesive film is increased up to a definite limit, after which it remains practically constant.

The curve obtained is to be explained by improvement in the contact conditions as the thickness of the film is increased. With a small amount of adhesive applied to the fabric, the surface of the fabric is covered by a very thin polymer film, which does not overcome the effect of the surface relief of the fabric. Increasing the thickness of the adhesive layer produced greater smoothness of the film, which leads to more complete contact. Finally, at some definite thickness of the adhesive layer, contact between the adhesive and the substrate becomes complete, and further increase in thickness of the adhesive layer ceases to have any effect on the resistance to separation. Therefore, in preparing bonded strips by the bonding method, as soon as complete contact between the two components of the bonded strip has been provided by the conditions under which the adhesive film is formed, the magnitude of the adhesive force becomes practically independent of the thickness of the adhesive layer [1].

It is important that the constant value of resistance to separation is reached with polyisobutylene at much lower amounts of polymer applied to the fabric than for SKN-40. This is because of the greater deformability of polyisobutylene, which facilitates achieving complete contact.

In our subsequent experiments, the amount of adhesive applied to the fabric was not less than 0.025-0.030 g/cm^2.

In order to determine the relationship between the resistance to separation of a bonded strip and the pressure to which it had been subjected after the polymer films were put together, a series of experiments were made in which this pressure was varied. The strip was kept under load for 30 minutes at room temperature.

As the investigation showed, the resistance to separation is practically independent of the pressure when the pressure was raised from 0.02 to 0.15 kg/cm^2.

In this series of experiments the bonded strips were prepared by rolling the fabric with the adhesive film on the substrate with a resin roller, after which they were kept for 30 minutes without pressure or under a pressure of 0.1 kg/cm^2.

The fact that the resistance to separation of bonded strips in which the layer of adhesive on the fabric has its optimum thickness is independent of the magnitude of the compressing pressure is apparently to be explained by the assumption that under these conditions sufficiently complete contact in the adhesive in the substrate is already achieved at the lowest pressures.

As a result of this investigation, it was decided that the best way to put the adhesive film on was with a roller.

Even traces of volatile solvent which have been left in the adhesive can have the most marked effect on the resistance to separation. Since even in the film method the adhesive layer can contain a certain amount of solvent, we made some experiments to find out the length of time required for complete removal of the solvent when drying the adhesive film, and to determine the effect of small quantities of solvent on the resistance to separation of the bonded strip.

We have studied the kinetics of the evaporation of benzene from SKN-40 and of benzine from polyisobutylene after applying the last portion of polymer solution to the adhesive film. Finding the quantity of solvent evaporating from the film was a matter of weighing the film immediately after preparation, and then after definite periods of time, until it reached constant weight. The values found made it possible to calculate the quantity of solvent remaining in the film, during the length of time corresponding to each individual weighing, expressed in percent of the amount of solvent in the film immediately after preparation. As may be seen from Fig. 2, the benzene evaporates initially somewhat more rapidly from the SKN-40 film than the benzene from the P-118 film. If the concentration of solvent is increased, the reverse situation occurs.

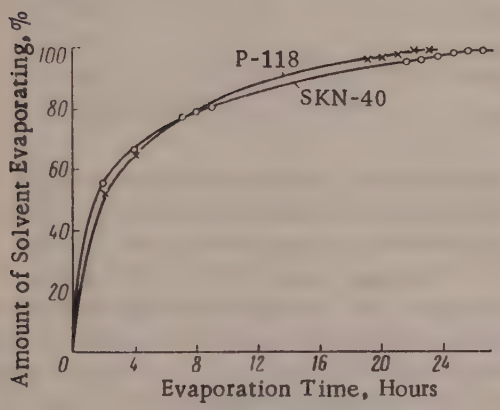


Fig. 2. Kinetic curves of the evaporation of benzene from SKN-40 and P-118 films.

To find the effect which a small amount of solvent in the adhesive has on the resistance to separation of the film, the films of the adhesive in question were joined with a cellulose film after different drying times, starting from the moment the last portion of adhesive solution was applied. The results for the separation of these strips are given in Table 1.

In the case of the polar SKN-40, with relatively large quantities of benzene in the strip, the failure is observed to have cohesional character, and the resistance to separation is comparatively very high. If the amount of solvent is 60% of what it was just after the film was prepared, the failure of the bonded strip takes on a mixed character, in that the parts which show cohesional failure have high resistance to separation, while the parts which show adhesional separation have comparatively small resistance to separation. With further reduction in solvent content and increase in cohesional strength of the adhesive, failure of the strip, as was to be expected, takes on a purely adhesional character, and the resistance to separation gradually increases, approaching a definite limit. Thus, in this case, there is a completely different relationship from the one which was observed by Poretskaya [14], who showed that as the solvent volatilizes on the film of printing inks, the adhesion falls off. The difference between the results of Poretskaya's experiments and ours probably consists in the fact that we put the adhesive film and the substrate together after most of the solvent had volatilized out, i.e., after the shrinkage of the film which could cause considerable weakening of the adhesive joint had for the most part already taken place. The increase in resistance to separation as the solvent content was reduced in our experiments is to be explained by a reduction in the plasticizing effect of the solvent, as a result of which the molecules of the adhesive which have diffused through are more solidly fastened to the substrate. However, after the solvent has completely volatilized, the adhesion of the polar SKN-40 to cellophane is somewhat reduced. This reduction is probably the result of an increase in the number of intermolecular bonds in the polymer, accompanied by a sharp increase in viscosity, which, of course, will hinder diffusion of adhesive into the substrate.

In analyzing the data of Table 1 for bonded strips of SKN-40 and cellophane, it is noteworthy that with comparatively large amounts of solvent in the adhesive, where the adhesive force on the basis of the relationship which we have found should be very small, failure of the strips shows a cohesional character, in spite of the fact that the resistance to separation in this case is considerably higher than the resistance to separation corresponding with the maximum adhesive force. Further study is required to explain a fact of this sort.

TABLE 1. Effect of Solvent Content in the Adhesive Film on the Resistance to Separation of a Bonded Strip

Solvent evaporation time from adhesive films, hours	Solvent remaining		Character of separation	Resistance to separation, g/cm
	% of film weight	% by weight of solvent immediately after preparing film		
		SKN-40–Cellophane		
0.25	12.5	89	Cohesional	345
1	8.5	66	Mixed	65–628
5	4.25	30	Adhesional	134
10	2.41	17	The same	163
15	1.39	9	The same	170
20	0.38	4	The same	175
25	0.15	1	The same	177
27	0	0	The same	169
		Polyisobutylene–Cellophane		
1	10.7	70	Adhesional	0
5	4.6	31	The same	63
10	2.67	17	The same	105
15	0.92	6	The same	129
20	0.3	2	The same	143
25	0	0	The same	147

TABLE 2. Effect of Strip Width on Adhesive Force

Strip width, cm	SKN-40-Cellophane	Polyisobutylene-Cellophane
1	198	150
2	205	144
3	187	133
4	185	146
5	190	139

In the case of nonpolar polyisobutylene, the relationship existing between the character of failure and the resistance to separation of a strip and the quantity of benzene present in the adhesive film is much simpler. With comparatively high amounts of solvent, the resistance to separation is equal to zero, and if the amount of solvent in the polymer is reduced, the resistance to separation gradually increases, approaching a definite limit. Failure of the films is adhesional in all cases.

It may be seen from the results of the experiments that not more than 30 hours in air at 20° is required for complete removal of the usual solvents from the elastomer films. This schedule of drying the adhesive films before putting them onto the substrate was the one which we used in our subsequent work.

To follow the kinetics of the change in adhesive force with gradual evaporation of solvent from the strips, strips made of cellophane, prepared after drying SKN-40 films for 15 minutes, and polyisobutylene films dried for one hour, were tested after 6 and 11 days storage. The resistance to separation exhibited by these strips gradually approaches a limiting value, which, after 6 days is 155 and 99 g/cm, and after 11 days is 175 and 130 g/cm for strips made with cellophane using SKN-40 and polyisobutylene respectively.

The width of the strip has no effect on the magnitude of the resistance to separation (Table 2).

To compare the values of resistance to separation shown by strips prepared by the bonding and film methods, strips were prepared and tested, which separated according to adhesional, cohesional, and mixed types. In the bonding method, the strips were prepared by pouring a solution of adhesive on a film of substrate and special cells, followed by 16 days drying [2]. In the film method, the strips were prepared by the method described above. In all cases the substrate was cellophane washed free of glycerin. The resistance to separation of the strips so prepared is given in Table 3.

As may be seen from Table 3, both the resistance to separation and the character of the separation of the three

TABLE 3. Results of Separating Bonded Strips, Prepared by Various Methods

Adhesive	Character of failure	Resistance to separation, g/cm
	Bonding Method	
SKS-30–1	Cohesional	935
SKS-30	Mixed	190–890
SKS-40	Adhesional	248
	Film Method	
SKN-30–1	Cohesional	940
SKN-30	Mixed	83–701
SKN-40	Adhesional	250

polymer pairs tested are practically independent of what method was used to prepare the strip.

The fact that there is no difference in the adhesive forces found in separating bonded strips prepared by the two different methods is obviously to be explained by noting that the results of tests on the strips made of the adhesives and substrate which we used are comparatively little effected by the factors mentioned at the beginning of the paper (time of contact between polymers, shrinkage of the adhesive, presence of residual solvent in the adhesive, and swelling of the substrate). However, under other conditions, the effect of these factors can of course be rather large, and the two methods of preparation can give bonded strips which have different resistance to separation.

To determine the accuracy of measurement of the resistance to separation of bonded strips prepared by the film method, some other polymers were used as adhesive and substrate besides SKN-40 and polyisobutylene.

When an elastomer was used as substrate, it was applied to the fabric in the same way as the adhesive.

To find the degree of accuracy of the values obtained, statistical calculations were made, the results of which are given in Table 4.

TABLE 4. Accuracy of Measurement of the Mutual Adhesion of High Polymers in the Film Method

Strip	Character of separation	Arithmetic mean* resistance to separation $\bar{X}$	Mean square deviation, σ	Variation factor, v	X_{min}		X_{max}	
					Calculated	Experimental	Calculated	Experimental
SKN-40-Cellophane	Adhesional	170	8.1	4.75	146	150	194	175
Polyisobutylene-Cellophane	The same	171	17.6	10.3	118	150	224	200
Polychloroprene-Polyamide	The same	789	44.4	5.64	656	750	922	880
Polychloroprene-Polyisobutylene	The same	350	26.8	7.66	270	300	430	400
SKB-Cellophane	Cohesional	931	72.9	7.84	712	880	1150	1140
SKJ-Polyamide	The same	1251	51.1	4.1	1098	1170	1404	1330
SKS-30A–SKN-40	Mixed	A. 161	15.1	9.4	116	150	206	190
		K. 1350	42.6	3.2	1221	1280	1479	1410
SKB-Polyethylene	The same	A. 119	17	14.3	68	100	170	160
		K. 699	86	12.3	441	550	957	810

* In all cases the arithmetic mean resistance to separation was calculated from tests on ten samples.

It is clear from Table 4 that the values of the variation factor lie within limits which are admissible in studying the mechanical properties of high polymers. The experimental values of the maximum and minimum resistance to separation for the present series of samples do not, for any one polymer pair, exceed the range of values calculable from the formulas

$$X_{min} = \bar{X} - 3\sigma; \; X_{max} = \bar{X} + 3\sigma,$$

where $\bar{X}$ is the arithmetic mean value of the quantity, and σ is the mean square deviation.

The results of these experiments speak for a sufficient degree of accuracy in determining the adhesion during separation of bonded strips prepared by the film method.

SUMMARY

1. A technique has been developed and tested for preparing bonded strips of two different high polymers so as to determine their mutual adhesion by separation. This technique, which we call the film technique in contrast to the bonding technique, makes it possible to exclude the effect of the following factors on the results of adhesion measurements: time the polymers are in contact during preparation of the strip, shrinkage of the adhesive, presence of traces of solvent in the adhesive and swelling of the substrate. In addition, this technique simplifies preparation of the strips, and considerably shortens the time required for this purpose.

2. A study has been made of the effect of thickness of the adhesive layer, of the magnitude of the compressing pressure, of the solvent content, of the width of the strip, and of the methods of preparing the strips for their resistance to separation.

LITERATURE CITED

1. S.S. Voyutskii, A.I. Shapovalova and A.P. Pisarenko, Dokl AN SSSR 105, 1000, 1955.
2. A.I. Shapovalova, S.S. Voyutskii and A.P. Pisarenko, Kolloidn Zh 18, 485, 1956.
3. S.S. Voyutskii, A.I. Shapovalova and A.P. Pisarenko, Kolloidn Zh 19, 274, 1957.
4. A.P. Pisarenko, A.I. Shapovalova and S.S. Voyutskii, Kolloidn Zh 22, 57, 1960.
5. V.A. Kargin and M.N. Shteding, Zh. fiz. khimii 20, 727, 1946.
6. B.V. Deryagin and N.A. Krotova, Adhesion [in Russian] Academy of Sciences Press, USSR, Moscow and Leningrad, 1949.
7. I. Khekstra and K. Fritsius "Adhesion" Collection edited by N. Debroin and R. Guvink, IL, Moscow, 1954, p. 43.
8. S.A. Shreiner and P.I. Zubov, Dokl. AN SSSR 124, 1102, 1959; Kolloidn Zh 22, 496, 1960.
9. S.S. Voyutskii and V.M. Zamazii, Kolloidn Zh. 15, 407 , 1953.
10. S.S. Voyutskii and B.V. Shtarkh, Kolloidn Zh. 16, 3, 1954.
11. A.I. Shapovalova, N.A. Tsvetkova and S.S. Voyutskii, Scientific Research Papers of the TsNIKZ, Collection 5 [in Russian] Gizlegprom, Moscow, 1953.
12. B.A. Dogadkin, Collection "Bond Strength Between the Elements of Resin-Fabric Parts in Production and Use" [in Russian] Goskhimizdat, Moscow and Leningrad, 1956, p. 16.
13. W.M. Bright, Adhesion and Adhesives. John Wiley and Sons, N.Y., 1954, p. 130.
14. A.P. Poretskaya, Kolloidn Zh 6, 153, 1940.

All abbreviations of periodicals in the above bibliography are letter-by-letter transliterations of the abbreviations as given in the original Russian journal. *Some or all of this periodical literature may well be available in English translation.* A complete list of the cover-to-cover English translations appears at the back of this issue.

EFFECT OF CARBON BLACK ON THE KINETICS OF VULCANIZATION AND THE CHARACTER OF THE SULFUR STRUCTURES OF THE VULCANIZATES

B.A. Dogadkin, M.S. Fel'dshtein and Z.V. Skorodumova

Tire Industry Research Institute, Moscow
Translated from Kolloidnyi Zhurnal, Vol. 23, No. 6,
pp. 679-683, November-December, 1961
Original article submitted July 2, 1961

We have shown previously [1-3] that carbon blacks interact readily with the principal components of a rubber mixture. Data on the sorption of rubber from n-heptane solution and the interaction of rubber with carbon blacks at the vulcanization temperature, as well as data on the chemisorption of sulfur, indicate that the reaction of carbon black with sulfur and rubber is determined by the chemical nature of the carbon black surface. The most active regions of carbon black surfaces are those not occupied by oxygenated functional groups. It has been shown that the chemical nature of the carbon black surface is one of the principal factors affecting vulcanization kinetics. It is well-known that the type of sulfur structure largely determines the kinetic characteristics. It is essential to determine whether the chemical nature of the carbon black surface affects the character of the sulfur structures of vulcanizates.

Investigation of sulfide bonds in vulcanizates containing different carbon blacks. The type of sulfide bonding in vulcanizates determines such important rubber properties as static and dynamic strength, wear and thermal stability [4,5]. Of course it was assumed that carbon blacks possessing an active surface and affecting reactions occurring during vulcanization will affect the character of the sulfide bonds.

The amount of combined, exchangeable (polysulfidic) sulfur and the maximum swelling were determined in vulcanizates without sulfur and in standard mixtures of butadiene-styrene rubber SKS-30A containing 50 parts by weight of channel, stove or lamp blacks or Philblack. The quantity of exchangeable sulfur was determined using radioactive sulfur [6].

The experimental results are given in Figs. 1 and 2.

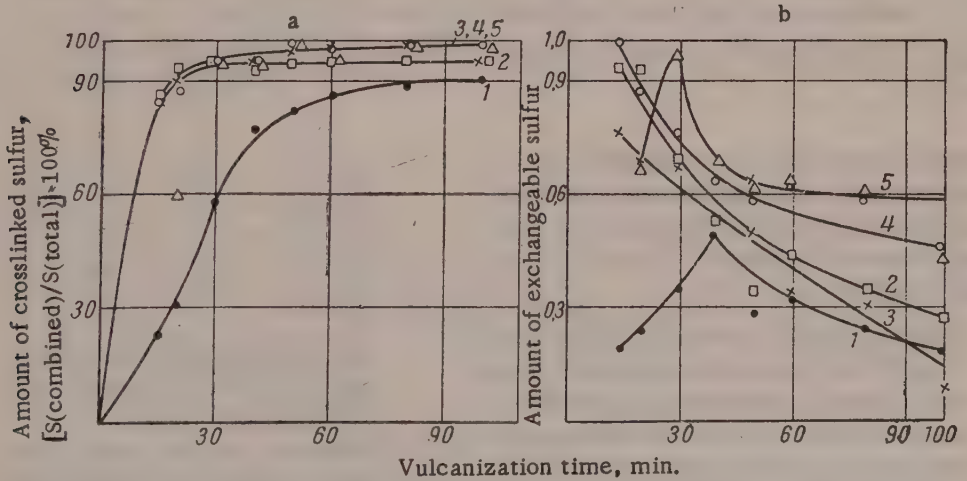


Fig. 1. Kinetics of sulfur crosslinking (a) and the exchangeable (polysulfidic) sulfur content (b) in vulcanizates containing different fillers: 1) channel; 2) stove; 3) Philblack O; 4) lamp; 5) without black.

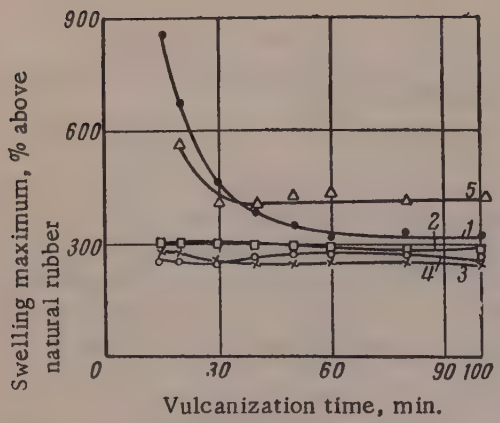


Fig. 2. Swelling maxima of vulcanizates containing different blacks: 1) channel; 2) stove; 3) Philblack O; 4) lamp; 5) without black.

The data in Fig. 1 indicate that the type of carbon black used has a significant effect on the nature of the sulfur bonds formed in the vulcanization process. The amount of polysulfidic sulfur is least in vulcanizates containing channel blacks; it increases in vulcanizates with alkaline blacks and is greatest in vulcanizates without blacks. The greatest contrast in the activities of various blacks is observed in the first minutes of vulcanization. With channel black and in vulcanizates without black the amount of polysulfidic sulfur passes through a maximum, while in vulcanizates with alkaline blacks the maximum is not observed owing to the more rapid combination of sulfur in the initial vulcanization period. After formation of the three-dimensional network, when the free sulfur is almost completely spent, recombination of sulfur bonds occurs at approximately the same rate for all the blacks investigated. In vulcanizates without blacks this recombination occurs more slowly. This is evidence that carbon blacks promote the rupture and redistribution of sulfur bonds.

The data on swelling maxima show the effect of carbon blacks on structuration. The maximum swelling (Fig. 2) is greater in vulcanizates without carbon black than in those containing the same amount of combined sulfur, i.e., containing lamp or stove black or Philblack O; the lattice density of vulcanizates containing carbon black (especially Philblack O) is greater than in vulcanizates without black.

The nature of sulfur bonds in vulcanizates with heat-treated channel black. As shown above, the nature of the sulfur bonds depends significantly on the type of carbon black used. It was important to determine the effect of the chemical nature of the carbon black surface on the sulfur bonds. Two blacks were studied: channel black, and the same black hydrogenated at 225 atm hydrogen pressure and 500°. The characteristics of these blacks are given in the table.

Properties of the Blacks

Black	Specific surface, by adsorption of phenol, m^2/g	pH	Elemental Composition, %		
			C	H	O, by difference
Channel	110	3.47	93.04	1.25	5.71
The same, hydrogenated*	128	7.2	94.65	1.39	3.96

* The hydrogenation was carried out at 500° in a hydrogen atmosphere at 225 atm.

The amounts of combined and exchangeable sulfur and the maximum swelling of the vulcanizates were determined for standard mixtures of SKS-30A butadiene-styrene rubber containing 50 parts by weight of the carbon blacks, using the method described above.

The data obtained are shown in Figs. 3 and 4. As seen from Figs. 3a and 4, the removal of oxygenated groups from the carbon black surface increases the rate of combination of sulfur and the amount of combined sulfur, and decreases the maximum swelling. This confirms results previously obtained by us [1].

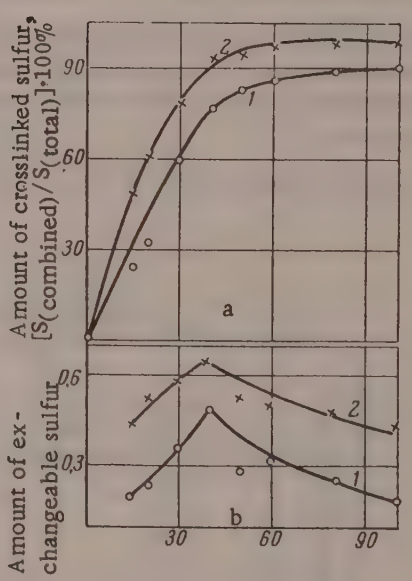


Fig. 3. Kinetics of sulfur crosslinking (a) and the exchangeable (polysulfidic) sulfur content (b) in vulcanizates containing heat-treated channel black: 1) channel black; 2) hydrogenated channel black.

* Studebaker [7] also studied sulfur structures in vulcanizates either without blacks or containing Philblack O.

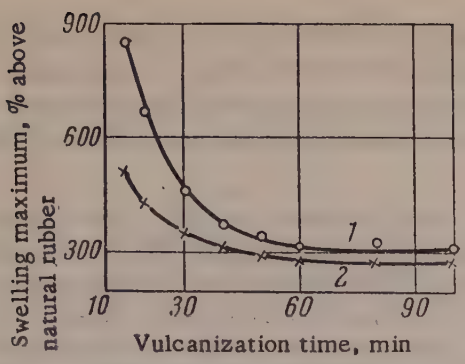


Fig. 4. Swelling maxima of vulcanizates containing heat-treated channel black: 1) channel black; 2) hydrogenated channel black.

The removal of oxygenated groups from the carbon black surface increases the content of polysulfidic (exchangeable) sulfur (Fig. 3b), in agreement with the results shown in Fig. 1b. It is thus established that the chemical nature of the black surface affects the character of the sulfur bonds.

The data presented in the paper is one more piece of evidence that the basic factor influencing the rate and direction of vulcanization reactions in mixtures containing active fillers is the chemical nature of their surfaces.

This situation is confirmed by data on combined sulfur and maximum swelling obtained using standard mixtures of SKS-30AM butadiene-styrene rubber with various blacks and accelerators. The blacks used were: channel, stove, lamp, and Philblack O. The accelerators were: N-cyclohexyl-2-benzthiazolsulfenamide, 2-mercaptobenzthiazole and diphenylguanidine. As seen from the results given in Figs. 5 and 6, Philblack O gave the highest vulcanization rate, largest amount of combined sulfur, and greatest lattice density (from maximum swelling data), independent of the accelerator used. Vulcanizates with channel black were lowest.

As noted previously [3], it appears that the active centers on the carbon black surface, which are more numerous the fewer the oxygenated groups on the surface, assist in the decomposition of the eight-membered sulfur ring and of the accelerators, forming polysulfides which then accelerate the vulcanization process.

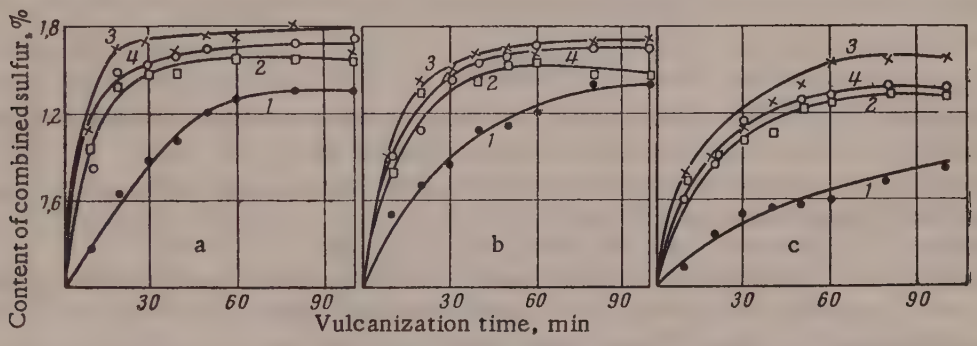


Fig. 5. Kinetics of sulfur crosslinking in vulcanizates containing accelerators: a) N-cyclohexyl-2-benzthiazolsulfenamide (Santocure); b) 2-mercaptobenzthiazole (Captax); c) diphenylguanidine, and the blacks: 1) channel; 2) stove; 3) Philblack O; 4) lamp.

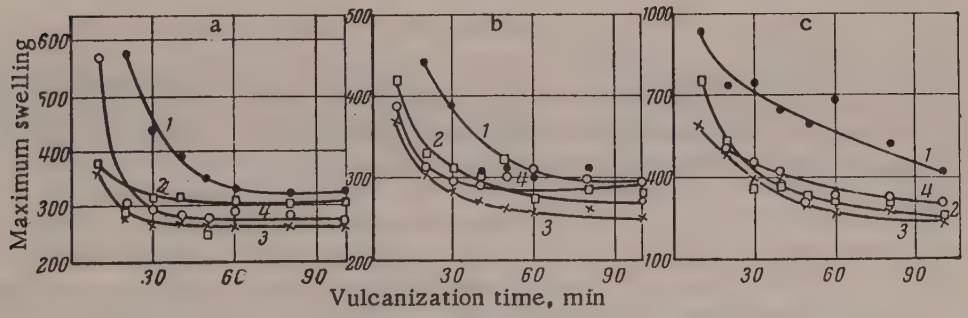


Fig. 6. Maximum swelling of vulcanizates containing accelerators: a) Santocure; b) Captax; c) diphenylguanidine, and the blacks: 1) channel; 2) stove; 3) Philblack O; 4) lamp.

The data in Fig. 1b show that at similar values of bound sulfur, excluding vulcanizates with channel black (Fig. 1a), the amount of polysulfidic sulfur is less in vulcanizates with blacks than in those without them. Consequently, in filled vulcanizates there is less sulfur per crosslink than in unfilled vulcanizates, i.e., a greater number of active sulfur radicals is formed, which is one of the factors leading to increased structuration in the presence of carbon blacks. This is confirmed by the swelling results (Fig. 2).

Vulcanizates with channel black (Fig. 1b) contain fewer polysulfide bonds than those with lamp or stove black or Philblack O. A greater structuration effect might be expected in the presence of channel black. However, as seen from Fig. 2, the number of crosslinks is less in vulcanizates with channel black. This fact may be explained by catalytic action by the black in the dehydrogenation of the rubber by sulfur [8]. As a result of their greater surface activity, alkaline blacks will be better catalysts for the removal of hydrogen atoms from rubber molecules by sulfur and accelerator radicals. The polymeric free radicals formed will react more rapidly with sulfur and, in addition, react with one another to form additional C—C bonds between molecular rubber chains, leading to additional structuration observable by some decrease of the swelling maximum and increase of the modulus.

SUMMARY

1. The nature of the sulfur bonds formed in the vulcanization process depends significantly on the chemical nature of the filler surface. More polysulfide bonds are formed in vulcanizates containing alkaline blacks than in those with channel blacks.

2. The amount of polysulfide sulfur is less in filled vulcanizates than in unfilled.

3. The rate of scission and rearrangement of sulfur bonds is greater in filled vulcanizates than in unfilled.

4. Increase of the structuration effect in black-containing mixes is determined to a considerable extent by the increase in density of the three-dimensional hydrocarbon network in the vulcanizate.

LITERATURE CITED

1. B.A. Dogadkin, B.V. Lukin, E.N. Tarasova, Z.V. Skorodumova and I.A. Tutorskii, Kolloidn. zh. 18, 413, 1956.
2. B.A. Dogadkin, Z.V. Skorodumova and N.V. Kovaleva, Kolloidn. zh. 20, 272, 1958.
3. B.A. Dogadkin, Z.V. Skorodumova and M.S. Fel'dshtein, Kolloidn. zh. 22, 663, 1960.
4. B.A. Dogadkin, Khim. nauka i prom-ct' 4, 55, 1959.
5. Z.N. Tarasova, T.V. Fedorova and B.A. Dogadkin, Kauchuk i rezina, No. 11, 1959.
6. Z.N. Tarasova, M.Ya. Kaplunov, M.A. Vas'kovskaya and B.A. Dogadkin, in the Collection "Vulcanization of Rubber Goods", Yaroslav Council of National Economy, 1960 [in Russian].
7. M.L. Studebaker and L.G. Nabors, Rubber Chem. Techn. 32, 4, 941, 1959.
8. M.L. Studebaker, Rubber Chem. Techn. 30, 5, 1401, 1957.

All abbreviations of periodicals in the above bibliography are letter-by-letter transliterations of the abbreviations as given in the original Russian journal. *Some or all of this periodical literature may well be available in English translation.* A complete list of the cover-to-cover English translations appears at the back of this issue.

RHEOLOGICAL PROPERTIES OF AQUEOUS GLYCEROL SOLUTIONS

I.A. Dumanskii and L.V. Khailenko

Colloid Chemistry Laboratory, Institute of General and Inorganic Chemistry,
Academy of Sciences, Ukrainian SSR, Kiev
Translated from Kolloidnyi Zhurnal, Vol. 23, No. 6,
pp. 684-686, November-December, 1961
Original article submitted December 15, 1960

On deformation in the cylindrical gap of a Shvedov torsion elastometer-viscometer by a constant and sufficiently small shearing stress, aqueous glycerol solutions can give flow curves $\epsilon = \varphi(\tau)\rho$ corresponding to the following rheological systems:

1. An elastic liquid similar to solutions of rubbers in nonpolar solvents, i.e., systems governed by the equation

$$\epsilon_{res} = \tau_1 (\frac{d\epsilon}{d\tau}),$$

where τ_1 is the time during which the liquid remains under stress, and $(d\epsilon/d\tau)$ is the rate of deformation [1,2].

2. An elastic liquid with the yield point P_y, i.e., a liquid whose deformation reaches a certain equilibrium value ϵ_m in time and, after removal of stress, falls to zero, also in time [3].

In this case the equilibrium value ϵ_m and the yield point P_y may be regarded as apparent, whereas irreversible (residual) flow of the system takes place but is so slight that it is practically unnoticed during the experiment, and apparent equilibrium is observed owing to the very high viscosity of the bulk structure of the solution, as occurs in colloidal systems [4].

3. Flow of a liquid with brittle fracture, which is characterized by a sharp deflection of the flow curve $\epsilon = \varphi(\tau)\rho$ upward from the axis of abscissas with a practically instantaneous decrease of viscosity η_1 [5].

In addition to the above-mentioned observations we give two more cases of the deformation properties of aqueous glycerol solutions, noted while obtaining data for the flow curves $\epsilon = \varphi(\tau)\rho$.

Such curves are given in Fig. 1 for a 73% glycerol-water solution. The stress was removed at the point P = 0. As indicated above, for an elastic liquid $\epsilon_{res} = \tau_1 (\frac{d\epsilon}{d\tau})$ corresponds quite well to the value of ϵ_{res} determined experimentally [1]. In our case (curve 1) the observed value of ϵ_{res} is much greater than the calculated; i.e., $\epsilon_{res} = \tau_1 (\frac{d\epsilon}{d\tau})p + \rho$.

A solution of the same concentration but with different values of θ (structuring time) and P (shearing stress) behaves analogously (curve 2). After removal of the stress at the point P = 0 the liquid gives a slight reaction of reverse post-action, although the visible equilibrium value ϵ_m is reached and reverse fall of ϵ_m to zero might be expected. This effect is especially well observed when the system has attained the maximum consolidation due to the structuring time θ, if we use the quantity $\eta_1 = p/(d\epsilon/d\tau)$ as a measure of structuring*. We observed a similar "degeneration" of post-action in gelatin solutions. Moreover, the studied solutions have very high viscosity of flow of the nondisintegrated structure, like all structured colloidal systems [6]. Thus for gelatin solutions of concentrations from 0.35 to 0.55% and structuring times (θ) up to 252 hr, η_1 for the nondisintegrated structure is equal to 1427-4832 poises, whereas N_1 for a structure having the maximum degree of disintegration is 0.3-0.5 poise. For 73.0% aqueous solutions and aging times (θ) from 100 to 135 hr, η_1 for the nondisintegrated structure is 100-700 poises, whereas η_1 for the most completely disintegrated structure is 0.3 poise.

* Kolloidn. zh. 22, 278 (1960) (Fig. 1).

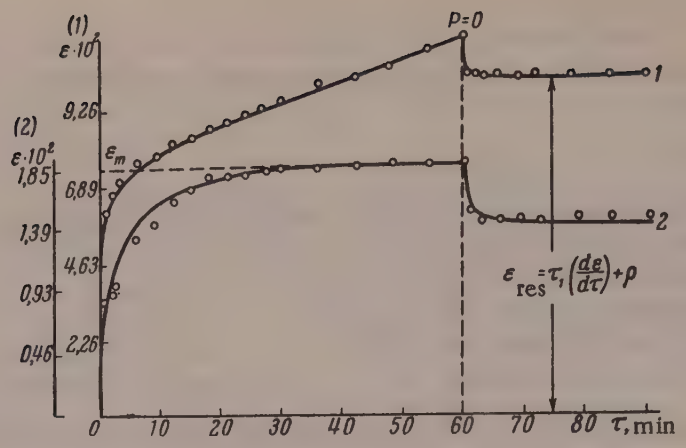


Fig. 1. Increase and decrease of shear deformations in a glycerol-water solution. Glycerol concentration 73.0%; t = 20°. 1) θ = 562 hr, P = 3.21 dyne-cm^{-2}; 2) θ = 461 hr, P = 0.80 dyne-cm^{-2}; ϵ_m is the maximum deformation.

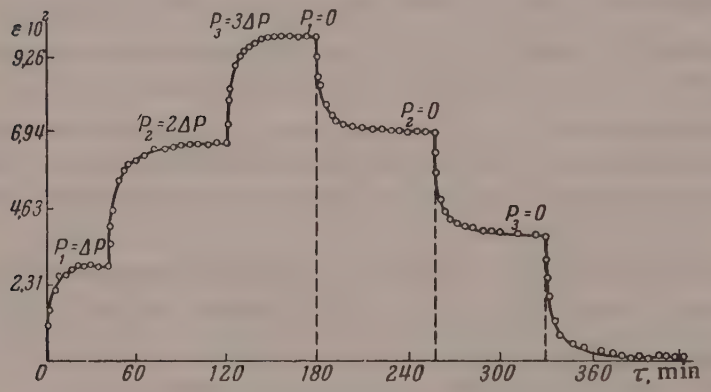


Fig. 2. Rise and fall of stepwise shear deformation in a glycerol-water solution on application of incremental shearing stresses $\Delta P \times 10^4$ = 4.26 dyne-cm^{-2}. Glycerol concentration 61.0%; θ = 70 hr, t = 20°.

In the process of development of shear deformation supermolecular structures, existing in the systems owing to hydrogen bonds [5], obviously are irreversibly reoriented and partially disintegrated.

The method of stepwise application of incremental shearing stresses, proposed by Trapeznikov for study of the mechanical properties of films of saponin, ceryl alcohol and certain heavy lubricating oils [6,7], showed (Fig. 2) that a glycerol-water solution behaves like a liquid with a visible yield point $P_y > 3$ ($\Delta P \times 10^4$ = 13.3 dyne-cm^{-2}). Application of these same incremental stresses ($\Delta P \times 10^4$ = 4.26 dyne-cm^{-2}) shows that the reverse elastic reaction of the liquid to shear qualitatively corresponds fully to the rise of stepwise deformations $\epsilon = \epsilon_1 + \epsilon_2 + \epsilon_3$ on application of the incremental stresses ΔP.

The phenomena of increase and decrease of deformations in glycerol-water solutions described here become plainly observable when the following conditions are met: 1) a sufficiently long time θ must be allowed for the bulk structure to develop in the solution; 2) the solution concentration must be not less than 55-60% of the volumetric content of glycerol in the water; 3) the shearing stress must be not greater than 3 dyne-cm^{-2}; 4) the deformation rates must be as low as possible.

The apparatus parameters providing the proper shearing stresses and deformation rates are given in [2,3].

SUMMARY

1. When shear deformation develops in a glycerol-water solution, part of the elastic deformation goes over into irreversible deformation; this may be explained by steric reorientation of glycerol-water complexes whose existence is due to hydrogen bonds.

A similar phenomenon is noted in dilute gelatin solutions.

2. On application of equal incremental shearing stresses ΔP to the glycerol-water system the stepwise deformation ϵ_m that arises is fully reversible, and the loading branch is qualitatively identical with the unloading branch.

LITERATURE CITED

1. A.S. Kolbanovskaya and P.A. Rebinder, Kolloidn. zh. 21, 194 (1959).
2. I.A. Dumanskii and L.V. Khailenko, Kolloidn. zh. 15, 426 (1953).
3. L.V. Khailenko, Dokl. AN SSSR 115, 1135 (1957).
4. A.A. Trapeznikov, Transactions of the Institute of Physical Chemistry, Academy of Sciences, USSR, No. 1 [in Russian], 1950, p. 32.
5. I.A. Dumanskii and L.V. Khailenko, Kolloidn. zh. 22, 277 (1960).
6. I.A. Dumanskii, Author's Abstract, Master's Thesis, (Kiev, 1953) p. 8.
7. A.A. Trapeznikov, Transactions of the Conference on Colloid Chemistry [in Russian]. Acad. Sce. Ukr. SSR Press, Kiev, 1952, p. 175.
8. A.A. Trapeznikov and S.Kh. Zakieva, Transactions of the Conference on Colloid Chemistry [in Russian]. Kiev, Acad. Sci. Ukr. SSR Press, 1952, p. 362.

All abbreviations of periodicals in the above bibliography are letter-by-letter transliterations of the abbreviations as given in the original Russian journal. ***Some or all of this periodical literature may well be available in English translation.*** **A complete list of the cover-to-cover English translations appears at the back of this issue.**

GRAVITY DEPOSITION OF AEROSOLS FROM LAMINAR FLOW

K.A. Zaitseva, Yu.V. Shukenov and M.A. Al'tshuler

Institute of General and Inorganic Chemistry, Academy of Sciences,
Ukranian SSR, Kiev
Translated from Kolloidnyi Zhurnal, Vol. 23, No. 6,
pp. 687-689, November-December, 1961
Original article submitted August 6, 1960

The problem of the deposition of aerosols from laminar flow is discussed mainly in connection with calculating the efficiency of deposition [1]. In our opinion, the laws governing this process deserve some attention too because of the possibility of using them to study the various properties of the particles and the rates of the condensational and coagulational reactions occurring in aerosols.

In the gravity deposition of particles in laminar flow we can begin by considering the so-called boundary trajectories, above which particles of a certain radius do not exist. For this reason, there must be a limiting dimension of the particles deposited at a given distance from the origin of the stream. For a flow tube of rectangular cross-section inclined at an angle α to the vertical we can obtain the following formula for the boundary diameter of the droplets (D_b) deposited at a distance L from the entrance to the tube, independently of the distribution of velocities

$$D_b = 2\left[\frac{9\eta u_0 h}{2g\gamma (L\sin\alpha - h\cos\alpha)}\right]^{1/2}, \quad (1)$$

where η is the viscosity, g is the acceleration of gravity, γ is the density, h is the height of the tube and u_0 is the mean flow rate.

The value of D_b is of the greatest interest, since experimentally the values may deviate from the calculated value as a result of various effects to which the particle is subjected while it is moving through the tube. These deviations give valuable information on the processes taking place.

In view of the fact that the theory does not take account of the phenomena which are able to distort the limiting trajectories or prevent the boundary diameters from being observed (thermal convection of the gas, coagulation of droplets, etc.), it is of interest to investigate the possibility of making an experimental determination of the boundary diameters which is the problem considered in the present paper.

To verify formula (1) use was made of a flow tube 80 cm long with a rectangular cross-section of 1.6 × 4.1 cm, made from a plexiglass sheet 10 mm thick. The back end of the tube was connected with a suction mechanism and a ragometer. By means of a special attachment, pieces of glass were fastened to the bottom of the tube, which were covered with a layer of a mixture of vaseline and transformer oils or vaseline. In the different experiments this layer was located at distances of 17.5, 21.5, 27, 44 and 77 cm from the entrance to the tube. The construction of the tube-mounting inside the aerosol chamber was such that the tube could be given any desired orientation from horizontal to vertical. The fog used, obtained by pulverization, contained droplets with dimensions from 1 to 70 μ.

The experiment consisted in finding the dimensions and counting the number of droplets deposited on the pieces of glass after a definite period of time with the fog being propelled at a fixed velocity.

The maximum dimensions of the droplets found in the first experiments which were made with water fogs were considerably smaller than those calculated from formula (1), which is to be explained by evaporation of the droplets while they were moving through the tube. In view of this fact, a fog of water-glycerin mixture was used in the subsequent experiments, since here the droplets evaporate very slowly [2].

Table 1 gives the results of measurement of the number of droplets of various diameters for α = 7°30', and α = 90°, and L equal to 17.5, 21.5, 27, 44, and 77 cm.

TABLE 1. Number of Droplets Counted on a Fixed Area at Different Distances from Entrance to Tube (L) for Values of α Equal to 7°30', and 90°

L=17.5 cm		L=21.5 cm		L=27 cm		L=44 cm		L=77 cm	
D, cm	No. of drplts	D, cm	No. of drplts	D, cm	No. of drplts	D, cm	No. of drplts	D, cm	No. of drplts
				α=7°30'					
41—43	18	34—36	28	28,8—30,6	16	18,4—20,1	25	13,1—14,9	36
43—44,5	7	36—37,6	10	30,6—32,4	13	20,1—22	21	14,9—16,6	23
44,5—46,5	6	37,6—39,4	13	32,4—34,7	12	22—23,6	14	16,6—18,4	18
46,5—48	7	39,4—41	1	34,1—36	10	23,6—25,4	12	18,4—20,1	7
48—50	9	41—43	11	36—37,6	8	24,4—27,1	1	20,1—20,9	5
50—51,5	1	43—44,5	1	43—44,5	2	27—29	1	34,1—36	1
51,5—53,5	2	48—50	2	44,5—46,5	1	29—30,6	2	41,1—43	1
53,5—55	1	51,5—53,2	3	51,5—53,5	1	41—43	1	44,5—46,5	2
55—57	1	55—57	1	55—58,5	1	—	—	55,1—47	1
57—58,5	1	58,5—60,5	—	—	—	—	—	—	—
58,5—60,5	2	—	—	—	—	—	—	—	—
				α=90					
4,4—6,1	65	4,4—61	61	4,4—61	53	0—44	54	0—4,4	60
6,1—7,9	55	6,1—7,9	51	6,1—7,9	48	4,4—61	54	4,4—6,1	48
17,9—9,6	46	7,9—9,6	51	7,9—9,6	32	6,1—7,9	44	6,1—7,9	5
9,6—11,4	21	9,6—11,4	35	9,6—11,4	5	7,9—9,6	5	—	—
11,4—13,1	16	11,4—13,1	4	11,4—13,1	1	9,6—11,4	5	—	—
13,1—14,9	3	—	—	—	—	—	1	—	—

TABLE 2. Theoretical and Experimental Values of the Boundary Dimensions of Droplets for α Equal to 7°30' and 90°

L, cm	$D_{theo'}$ μ	$D_{exp'}$ μ	$D_{theo'}$ μ	$D_{exp'}$ μ
	α=7°30'		α=90°	
17,5	52	49±10	11,6	12,2±1,3
21,5	39,5	42±6,3	10,5	10,5±1,0
27	34,6	36,8±4,5	9,4	8,7±0,8
44	23,6	24,5±2	7,3	7,0±0,5
77	16,4	17,5±1,4	5,5	5,2±0,4

Table 2 gives a comparison of the theoretical and calculated values of D_b from formula (1) for these values of α and L.

At small angles of inclination of the tube, the pieces of glass show droplets with a diameter considerably in excess of the theoretical boundary value. However, the surface concentration of these droplets is an order of magnitude lower than the concentration of droplets with dimensions below the boundary. In interpreting these experimental data, it must be kept in mind that fusion of the droplets on the plates caused by falling on top of one another can produce a relatively small number of droplets with a diameter exceeding the calculated value D_b, as we shall show below. But in this case, the calculated values of D_b must be compared with the experimentally determined values of drop diameter which are of such a size that the surface concentration of anything above this is down by about an order of magnitude. The latter are easily discerned from a consideration of the data of Tables 1 and 2, which give values of the maximum possible errors of measurement. As may be seen from Table 2, the experimental and theoretical values of the boundary diameters of the droplets agree within the limits of experimental error.

The number of two-body superpositions of droplets of diameters D_1 and D_2 during deposition on the glass may be evaluated from the formula

$$n = N_1 N_2 \pi (D_1 + D_2)^2 / 4 \sin \alpha, \qquad (2)$$

where N_1 and N_2 are the surface concentrations of droplets with diameters D_1 and D_2. Comparison of the values of n, calculated from the data of Table 1, with the experimental values for the number of droplets having dimensions ex-

ceeding D_b has shown that the latter are produced by two-body superpositions of droplets during deposition on the glass. The largest drops have been produced by three-body superpositions. Since on going from vertical orientation of the glass plates to horizontal the probability of droplet superposition is reduced, with the tube in a horizontal position it was reasonable to expect a sharp drop-off in the number of drops having dimensions exceeding D_b, which was confirmed experimentally (Table 1). With the glass plates in a horizontal position three-body superpositions are practically impossible and accordingly drops with the corresponding dimensions (Table 1) are not observed. The relatively small number of droplets with dimensions slightly exceeding D_b is caused by two-body superpositions of droplets, which is confirmed by the calculations made from formula (2).

We shall point out in conclusion that a similar setup makes it possible to study the kinetics of growth and evaporation of the droplets.

SUMMARY

1. Under definite experimental conditions, thermal convection and fusion of deposited droplets do not prevent measuring the boundary dimensions of the droplets deposited gravitationally from laminar flow.

2. The experimentally determined and the calculated values of the boundary diameters of the droplets agree within the limits of experimental error.

LITERATURE CITED

1. V.A. Fuke, Mechanics of Aerosols [in Russian] Academy of Sciences Press, USSR, Moscow, 1955, p. 110.
2. G.L. Natanson, Zh. fiz. khimii 25, 779, 1951.

All abbreviations of periodicals in the above bibliography are letter-by-letter transliterations of the abbreviations as given in the original Russian journal. *Some or all of this periodical literature may well be available in English translation.* A complete list of the cover-to-cover English translations appears at the back of this issue.

STRENGTH, ELASTIC AND THIXOTROPIC PROPERTIES OF CONCENTRATED ALUMINUM NAPHTHENATE GELS AND THE EFFECT ON THEM OF POLAR ADDITIONS

T.I. Zatsepina and A.A. Trapeznikov

Institute of Physical Chemistry of the Academy of Sciences,
U.S.S.R., Moscow

Translated from Kolloidnyi Zhurnal, Vol. 23, No. 6,
pp. 690-698, November-December, 1961
Original article submitted August 3, 1960

Many papers dealing with the study of the properties of Al soap gels and hydrocarbon liquids [1-3] have considered the effect of the nature of the solvent in the soap on the colloidal nature of the systems, on their phase transformations, and on their rheological properties. Other papers have discussed the effect of polar additives on the viscosity, and on the absorption of infrared radiation [1,4,5]. It has been shown that polar substances lower the viscosity of the gels, due to shortening of the Al soap chains which results from the fact that the coordinational interaction of the polar groups in the additives (OH, NH_2, COOH, etc.) with the Al and O atoms is stronger than the interaction occurring between neighboring soap molecules to the Al...O bond, which is what is responsible for the polymeric linkages.

A 2% aluminum naphthenate gel has been used to show [6] that in a study of the structure and properties of aluminum soap gels along with the effect of additives, considerable interest attaches to the measurement of the high-elastic and thixotropic properties. The same methods of study have been used in the present paper to investigate the properties mentioned with regard to concentrated aluminum naphthenate (AN) gels, as well as to determine the effect of the nature of the additives on these properties, and the aging processes in the gels.

The studies were made on 4-8% gels in decalin, which were stable elastic systems capable of large elastic deformations. The additives used were hexyl alcohol ($C_6H_{13}OH$), ethyl cellosolve ($C_2H_5OC_2H_4OH$) and xylelol ($(CH_3)_2$-C_6H_3OH. The molecular ratio of the additive concentration (c_{add}) to the AN concentration (c_{AN}) varied from 0.25 to 2.0 g-mole to each gram-molecule of AN, assuming it provisionally (for purposes of calculation) to be a monomer with a composition corresponding to aluminum dinaphthenate, as found from an ultimate analysis for Al_2O_3*.

The measurements were made on the second model of the elastorelaxometer [7] with ϵ = const. The magnitude of the elastic deformation ϵ_e and the stress P, developed in the deformation process, were calculated from the formulas

$$\epsilon_e = \frac{2\theta_e \cdot R_2^2}{R_2^2 - R_1^2} \text{ and } P = \frac{c_0 \varphi}{2\pi R_1^2 L}.$$

The spaces between the cylinders were 0.1 cm with radii of the inner and outer cylinders R_1 = 1.4, and R_2 = 1.51 cm respectively, and the height of the internal cylinder L = 7.94 cm.

A study was made of the magnitude of the elastic (reversible) deformation, ϵ_e, of concentrated gels as a function of the applied deformation ϵ, of the effect of additives on this quantity and the form of the ϵ_e (ϵ) curves, of the effect of repeated deformation on the thixotropic properties and the recovery of the systems, and of the effect of polar additives on the aging processes of the gels.

* The aluminum naphthenate sample was obtained from the factory, and differed somewhat in its properties from the one studied previously [6].

Thixotropic properties of concentrated AN gels. Great interest is presented by the data on repeated deformation from the point of view of elucidating the structure of the gels, and the way they fail at various deformations approaching destructive. Repeated deformation leads to a gradual failure of the structure, the extent depending on the magnitude of the deformation applied [8].

In the present paper, a study is made of the effect on 8% gels of repeated deformation at a fixed value of deformation (ϵ = 1900%), which exceeds the disruptive deformation ϵ_r and the deformation ϵ_m corresponding with ϵ_{emax}. Figure 1a shows the curves of elastic deformation ϵ_e as a function of the number of repeated deformations N, with various rest times (τ_{rest}) for ϵ = 36 sec^{-1}. Here, τ_{rest} is the time between repeated deformations of the gel, i.e., τ_{rep} [8]. Figure 1b shows similar curves for the stress. It follows from Fig. 1 that repeated deformation causes a gradual reduction in ϵ_e down to some constant value, which depends on τ_{rest}. Here, the greater the value of τ_{rest}, the smaller the number of deformations required to produce a larger value of constant deformation ϵ_{emax}. For $\tau_{rest} \geq 1$ hour, the magnitude of ϵ_e remains constant and is independent of the number of deformations. Consequently, this length of time is sufficient to reestablish that part of the structure, which determines ϵ_e (curves 1,2).

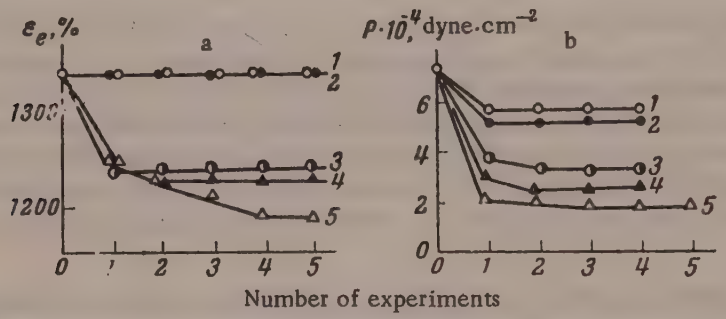


Fig. 1. Curves showing ϵ_e (N experiments), and P (N experiments) for 8% AN gel. The curves correspond with rest times τ_{rest} between experiments equal to: 1) 2 hours; 2) 1 hour; 3) 10 minutes; 4) 5 minutes; 5) 2 minutes.

It follows from Fig. 1b that P is considerably more reduced by repeated deformation than ϵ_e. While ϵ_e is not reduced more than 10%, P is reduced four-fold (for τ_{rest} = 1 minute). Here, even the second deformation gives almost the limiting stress reduction.

From the values of the limiting (constant) values of ϵ_e and P, obtained from repeated deformations at different values of τ_{rest}, the curves ϵ_e (τ_{rest}) and P (τ_{rest}) were constructed (Fig. 2), which refer to various fixed values of ϵ on the ascending wing of the ϵ_e (ϵ) and P (ϵ) curves up to $\epsilon = \epsilon_m$ and $P = P_r$.

It follows from the curves of Fig. 2a and b that in region I (curves 1-5) of the smallest deformations for the gel in question at ϵ < 1330%, both the values of ϵ and the values of P are independent of the rest time, i.e., there is no thixotropic failure in this range. Consequently, there is a region of elastic deformations, in which, for a given ϵ, the stresses and the elastic deformations both show the same thing. In region II of the higher deformations, 1330% < ϵ < 1560% (curve 6), ϵ_e is independent of τ_{rest}, and the curve of P against τ_{rest} maintains complete reversibility of deformation, i.e., $\epsilon_e = \epsilon$. Finally, in region III (curves 7-9), corresponding with even larger deformations, there appears a relationship between ϵ_e and τ_{rest}, which becomes more intense with increasing ϵ, and the dependence of P on τ_{rest} becomes very clearly marked. The deformation ϵ = 1560% corresponds with ϵ_z, above which complete reversibility of deformation is disturbed, i.e., residual deformation appears. In the present case, ϵ_z apparently coincides with ϵ_m, which corresponds with the maximum value ϵ_{emax}. These curves of ϵ_e (τ_{rest}) and P (τ_{rest}), in agreement with previous data [8], indicate the presence in the system of an assembly of structural elements having different critical values ϵ_{ki} and ϑ_i. It is obvious that in region II at 1330% < ϵ < 1560%, some of the structural elements reach the critical deformation, and, undergoing failure, produce a large reduction in P, while other, "longer", elements of the structure (bonds) do not fail, and are responsible for the complete reversibility of ϵ_e. At ϵ > 1560%, even those bonds fail which determine ϵ_e. To reestablish the ruptured bonds requires a time which increases with increase in ϵ and reaches 2 hours for ϵ_e, and 24 hours for P. The dependences ϵ_e (τ_{rest}) and P (τ_{rest}) are so strong

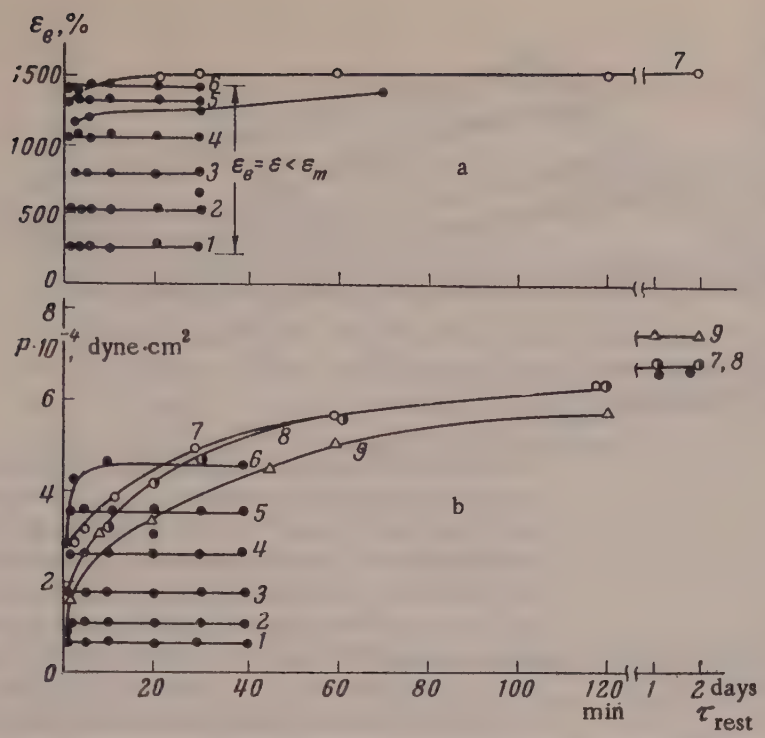


Fig. 2. Curves of ϵ_e (τ_{rest}) and P (τ_{rest}) for 8% AN gel at τ_{age} = 30 days. 1-6) $\epsilon < \epsilon_m$ for ϵ equal to: 1) 60%; 2) 530%; 3) 800%; 4) 1060%; 5) 1330%; 6) 1430%. 7) $\epsilon = \epsilon_m$ = 1560%; 8 and 9) $\epsilon > \epsilon_m$, with ϵ =: 8) 1690%; and 9) 1820%.

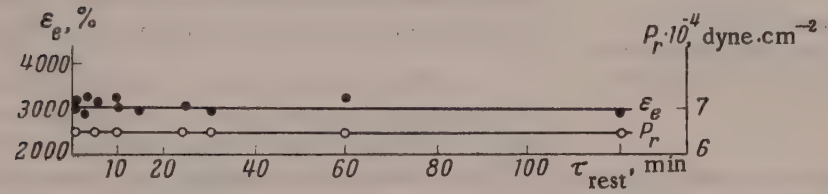


Fig. 3. Curves of ϵ_e (τ_{rest}) and P (τ_{rest}) for an 8% gel of AN + hexyl alcohol (c_{add}:C_{AN} = 2.0:1.0) with $\dot{\epsilon}$ = 570 sec^{-1} and ϵ = 4300%.

that the values of ϵ_e and P at small rest times are much less than the values of ϵ_e and P corresponding with the smaller applied deformations.

The introduction of polar additives sharply reduces the time required to reestablish the thixotropic structure, as well as the extent of failure of the structure altogether. Figure 3 gives the ϵ_e (τ_{rest}) and P (τ_{rest}) curves for an 8% gel with hexyl alcohol added to aluminum naphthenate in the ratio (2:1), for a value of ϵ considerably greater than ϵ_m (ϵ = 4300%). These curves were taken at a considerably higher velocity, $\dot{\epsilon}$ = 570 sec^{-1}, which corresponds, as will be shown later, with inhibiting the relaxation of the rapidly relaxing system, and, consequently, to more extensive failure of the structure. Under these conditions, both ϵ_e and P are completely independent of the time τ_{rest} (for $\tau_{rest} \geq 1$ min). Consequently, the values of ϵ_e and P, described below for solutions with additives, are practically single-valued and have nothing to do with the thixotropic properties.

Effect of additives on the high elastic deformation of AN gels. The addition of polar substances has a large effect on the elastic properties of aluminum naphthenate gels. Hexyl alcohol has been used to show the effect of concentration of the polar substance. Figure 4 gives the ϵ_e (ϵ) curves for a 4% naphthenate gel with different additive to naphthenate ratios, and Fig. 5 gives curves of ϵ_{emax} as a function of the amount of additive. It is clear from these

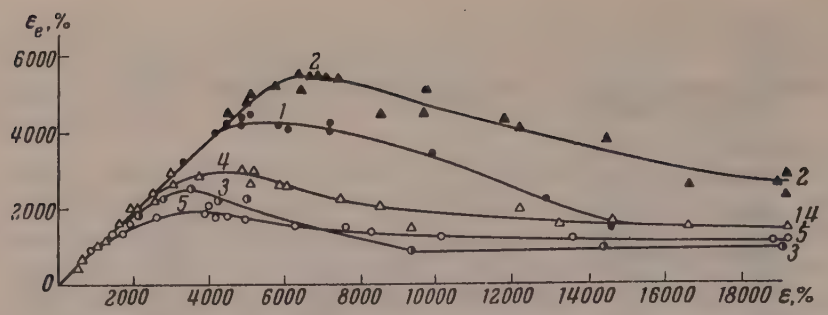


Fig. 4. Curves of ϵ_e (ϵ) at $\dot{\epsilon}$ = 36 sec^{-1} for a 4% AN gel with various hexyl alcohol ratios, c_{add}:c_{AN}, as follows: 1) 0.25 : 1.00; 2) 0.5 : 1.0; 3) 1.0 : 1.0; 4) 1.5 : 1.0; 5) 2.0 : 1.0.

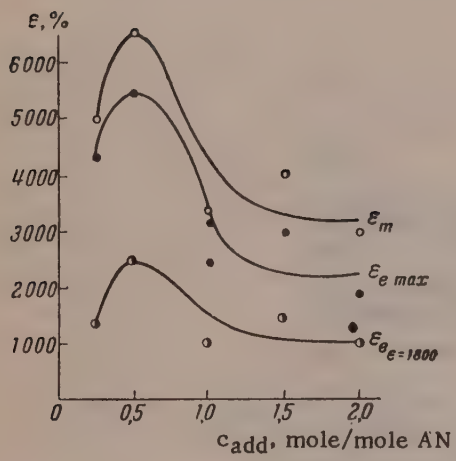


Fig. 5. Curves of ϵ_{emax} (c_{add}), ϵ_m (c_{add}), and $\epsilon_{e,\ \epsilon\ =\ 18000\%}$ (c_{add}) at $\dot{\epsilon}$ = 36 sec^{-1} for a 4% gel of AN + hexyl alcohol.

data that increasing the concentration of the polar substance to 0.5 : 1.0 produces a large increase in ϵ_{emax} (up to 5500%) which is a matter of rupturing "excess" intermolecular bonds. Further increase in the concentration of polar substance to 1 : 1 causes a reduction in ϵ_{emax} (up to 2500%) which must be attributed to an excessive reduction in the number of bonds playing a role in the supporting nodes, from which chain extension occurs, or to shortening of the chains. For $c_{add} : c_{AN} > 1 : 1$, the values of ϵ_{emax} change only slightly. This shows, obviously, that the remaining elastic deformation is not caused by nodes which can be blocked by the additive, but to some other kind. This same kind of variation with additive concentration is observed for both ϵ_m and $\epsilon_{e,\ \epsilon\ =\ 18000\%}$, which approaches the value ϵ_{es} corresponding with stationary flow. As follows from Fig. 4 and Table 1, as the concentration of hexyl alcohol is increased, there is less sharpness in the transition of the ϵ_e (ϵ) curves to the maximum ϵ_{emax}, which means a drop off in failure of the structural elements which basically are what determine the maximum elastic deformation ϵ_{emax}.

Adding polar substances to concentrated gels has a large effect on ripening of the gels. Figure 6 shows ϵ_e (ϵ) curves taken at $\dot{\epsilon}$ = 36 sec^{-1}, for 6% and 8% gels without additive, and for an 8% gel with hexyl alcohol added in the ratios c_{add}:c_{AN} = 2:1 for an early stage of ripening (τ_{age} equal to 5-10 days). In agreement with previous data [9], the curves for gels without additive show a sharp break between two straight lines at the point $\epsilon = \epsilon_z = \epsilon_m$. The left hand part represents a completely reversible deformation, $\epsilon_e = \epsilon$; the right hand part shows that the elastic deformation is practically constant with very large increase in the actual deformation. Curves of this sort are typical of slowly ripening aluminum naphthenate gels consisting, in the initial stage of ripening, of compact, rapidly adhering particles which slowly relax during the period of deformation and cause the solid plastic properties of the system. Adding polar substances sharply accelerates ripening of the gels, as a result of which the ϵ_e (ϵ) curves have a clearly marked maximum, ϵ_{emax} (curve 3, Fig. 6).

TABLE 1. The Quantity $\frac{\epsilon_{e\ max}}{\epsilon_{e,\ \epsilon\ =\ 18000\%}}$ for a 4% AN Gel as a Function of Concentration of Added Hexyl Alcohol (τ_{age} = 40 days)

c_{add}/c_{AN}	0,25:1,00	0,5:1,0	1,0:1,0	1,5:1,0	2,0:1,0
$\frac{\epsilon_{e\ max}}{\epsilon_{e,\ \epsilon=18000\%}}$	2,86	2,11	2,55	2,00	1,82

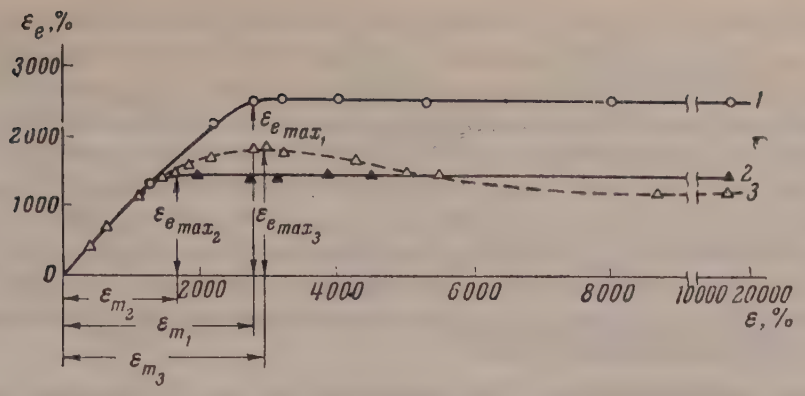


Fig. 6. Curves of ϵ_e (ϵ) for $\dot{\epsilon}$ = 36 sec^{-1} and τ_{age} = 40 days. 1) 6% AN; 2) 8% AN; 3) 8% AN + hexyl alcohol (c_{add}:c_{AN} = 2.0:1.0).

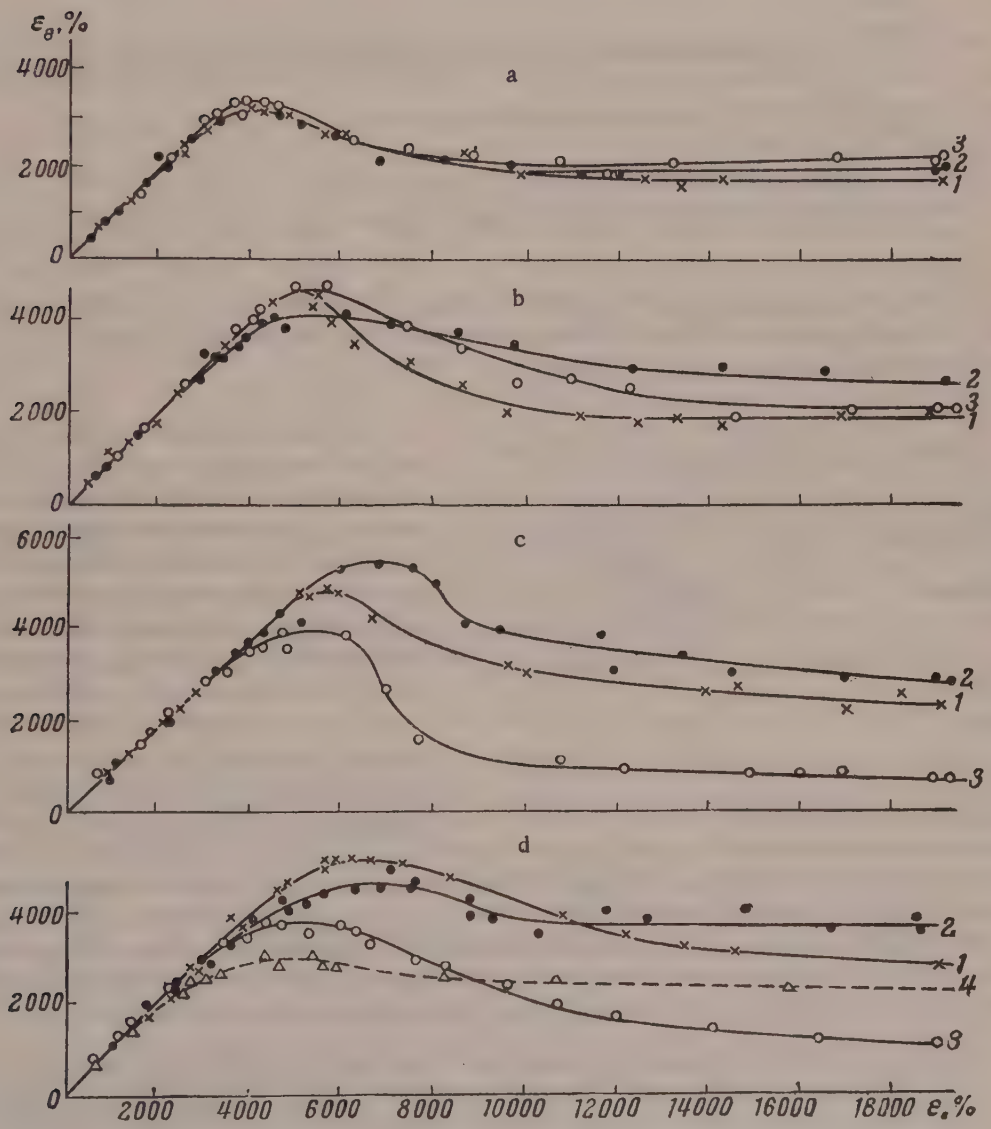


Fig. 7. Curves of ϵ_e (ϵ) for $\dot{\epsilon}$ = 36 sec^{-1}, τ_{age} = 2 hours (a), 1 day (b), 3 days (c), and 40 days (d), for a 4% AN gel + additive (c_{add}:c_{AN} = 0.5:1.0). 1) Hexyl alcohol; 2) ethyl cellosolve; 3) xylelol; 4) for 8% gel + hexyl alcohol (c_{add}:c_{AN} = 2.0:1.0).

The rapid acceleration in the ripening of concentrated gels from the introduction of additives is easily seen from Fig. 7. From the ϵ_{emax} (τ_{age}) curves for these same gels (fig. 8), it is clear that a maximum constant value, ϵ_{emax}, is reached after 3-10 days, which is not observed for gels without additives. In all cases, the ϵ_e (ϵ) curves have definite maxima, however, the form of the curves at different stages of gel ripening, as well as the form of the ϵ_{emax} (τ_{age}) curves is different for different additives, which, obviously, is a matter of specific peculiarities in the nature of each additive. Thus, the ϵ_e (ϵ) curves taken after 2 hours ripening are practically the same for all additives. After 1 and 3 days there is already a marked difference in ϵ_{emax} and $\epsilon_{e,\ \epsilon = 18000\%}$. With further aging, the degree of difference in the values of ϵ_{emax} for different additives remains practically constant. As far as the values of $\epsilon_{e,\ \epsilon = 18000\%}$ are concerned, it increases with gel ripening time most strongly in the gel containing ethyl cellosolve, so that the values of the $\epsilon_{emax}/\epsilon_{e,\epsilon = 18000\%}$ ratios are considerably less than for the gel containing hexyl alcohol and especially the one containing xylenol.

Table 2 gives the values of these ratios on the 10th and 40th day of aging of the gels.

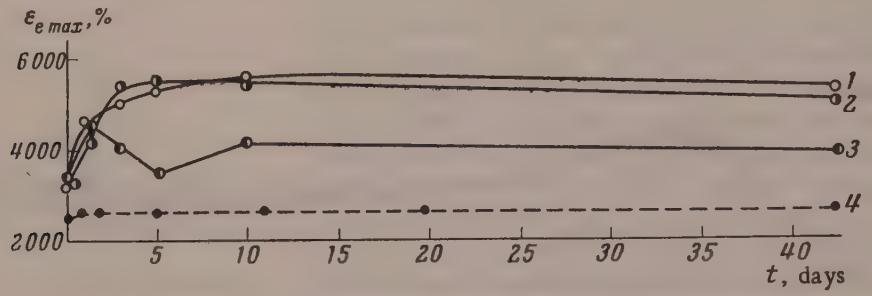


Fig. 8. Curves of ϵ_{emax} (τ_{age}) for $\dot{\epsilon} = 36\ sec^{-1}$ for a 4% gel of AN + additive ($c_{add}:c_{AN} = 0.5:1.0$). 1) Hexyl alcohol; 2) ethyl cellosolve; 3) xylenol; 4) hexyl alcohol ($c_{add}:c_{AN} = 1.0:1.0$).

TABLE 2. Variation of $\frac{\epsilon_{emax}}{\epsilon_{e,\ \epsilon = 18000\%}}$ for 4% AN Gels as a Function of the Nature of the Polar Additives

Additive	τ_{age}, Days	
	10	40
	$\epsilon_{emax}/\epsilon_{e,\ \epsilon = 18000\%}$	
Ethyl Cellosolve	1.22	1.25
Hexyl Alcohol	2.00	1.77
Xylenol	2.56	2.92

If it is once established that ϵ_{emax} is practically constant from three to ten days, it is possible to compare the degree of effect exerted by the various additives on the gels from the point of view of the elastic properties. It follows from the data of Table 3 and Figs. 7 and 8 that the additives considerably increase the value of ϵ_{emax} as compared with gels without additives. The largest increase in ϵ_{emax} is observed on adding hexyl alcohol, the smallest is observed with xylenol. Hence, it follows that hexyl alcohol turns out to be the strongest peptizer for the structure in the sense of blocking bonds in the gel, while xylenol is the weakest peptizer. Ethyl cellosolve occupies a special position. Being bifunctional, it obviously favors "spinning" of two different aluminum naphthenate chains by forming weak nodes which are easily reestablished on deformation. This, on the one hand, causes some reduction in ϵ_{emax} of the gel as compared with what would be expected, but on the other hand, it explains the marked increase in the value of $\epsilon_{e,\ \epsilon = 18000\%}$, which is characteristic of the elastic deformation of the system in flow, and consequently, it explains the reduction in the value of the ratio $\epsilon_{emax}/\epsilon_{e,\ \epsilon = 18000\%}$ (Table 2). Thus, the bifunctional nature of ethyl cellosolve creates favorable conditions for the formation in the gel of very mobile, easily reestablished bonds, which form a structure with the flexible chains.

From the data of Table 3 it must also be noted that as the aluminum naphthenate concentration is increased, the maximum elastic deformation decreases. This is in agreement with the previous data on disruptive deformation [10], and is to be explained by an excessive increase in the number of nodes in the structural network, which prevent the development of elastic deformations.

It is also of interest to consider the effect of the rate of deformation of the gels on the magnitude of elastic deformation without additives and with additives. It follows from the curves of Fig. 9a that for the most elastic and

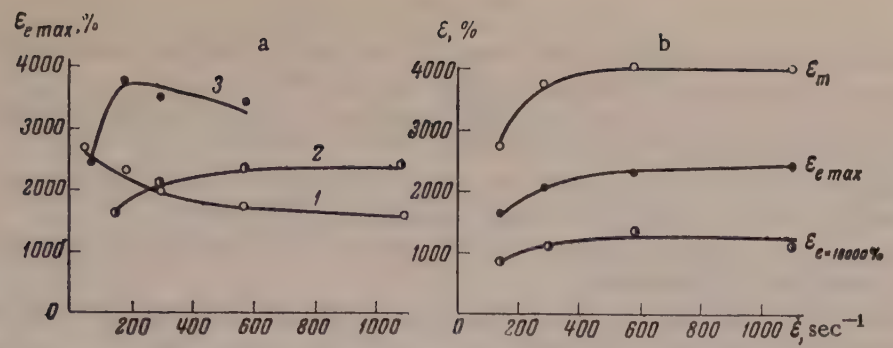


Fig. 9. Curves of ϵ_{emax} (a): 1) 6% AN; 2) 4% AN + hexyl alcohol ($c_{add}:c_{AN}$ = 0.5:1.0); 3) 8% AN + Hexyl alcohol ($c_{add}:c_{AN}$ = 2.0:1.0). Curves of ϵ_{emax} ($\dot{\epsilon}$), ϵ_m ($\dot{\epsilon}$), and ϵ_e, ϵ = 18000% ($\dot{\epsilon}$) (b), for 4% AN gel + Hexyl alcohol ($c_{add}:c_{AN}$ = 0.5:1.0).

TABLE 3. Variation of ϵ_{emax}, and ϑ^{ϵ} as a Function of AN Concentration in the Gel in the Presence of Polar Additives

Additives	c_{HA}, %	$\epsilon_{e,\,max}$, %	ϑ^{ϵ}, sec
Without additive	4	3000	300
Ethyl cellosolve (0.5:1.0)	4	5500	–
Hexyl alcohol (0.5:1.0)	4	5500	–
Xylenol (0.5:1.0)	4	4000	–
Without additive	6	2560	1000
The same	8	1350	1800
Hexyl alcohol (2.0:1.0)	8	3000	10

slowly relaxing gel, the ϵ_{emax} ($\dot{\epsilon}$) curve is falling, i.e., the elasticity of the system decreases with increase in values of $\dot{\epsilon}$. This corresponds with the laws discovered in [11], and is to be ascribed to the fact that in difficultly relaxing systems an increase in $\dot{\epsilon}$ produces failure of the chains which do not succeed in unwinding completely. The large relaxation time of systems of this sort, reaching values of 10^2–10^3 sec, measured from the slope of the ϵ_e ($\tau_{storage}$) according to the method used in [8]. is shown in Table 3. For a system having a small relaxation time, not more than about 10 sec, the ϵ_{emax} ($\dot{\epsilon}$) curve is increasing over the whole range of values of $\dot{\epsilon}$ from 180 to 1100 sec^{-1}, the value of ϵ_{emax} being constant from 580 to 1100 sec^{-1}. This is explained by the fact that increasing ϵ inhibits the relaxation of the rapidly relaxing elements of the structure and makes it possible to reach the greatest ϵ_{emax}, at which relaxation is not able to occur. Finally, for a system having intermediate properties, highly concentrated, and containing polar substances, a curve of ϵ_{emax} ($\dot{\epsilon}$) having a maximum is observed. At the start, the increase in $\dot{\epsilon}$ inhibits relaxation and causes an increase in ϵ_{emax}. Further additional increase in $\dot{\epsilon}$ leads to a small reduction in ϵ_{emax} causing premature rupture of the chains. This most general relationship had been observed previously in 2% aluminum naphthenate gels, containing no additives [11].

SUMMARY

1. With the aid of an elastorelaxometer, using $\dot{\epsilon}$ = const method, a study has been made of the elastic and thixotropic properties of concentrated aluminum naphthenate gels (4-8%) in decaline, with and without polar substances (hexyl alcohol, ethyl cellosolve and xylenol).

2. It has been shown that highly concentrated aluminum naphthenate gels have high limiting elastic deformations (ϵ_{emax}) from 1350 to 5500%. Hence, increasing the naphthenate concentration causes a lowering in ϵ_{emax}, while adding polar substances increases ϵ_{emax}. Of the polar substances studied, hexyl alcohol produces the largest increase in the elastic deformations, while xylenol produces the smallest increase. Increasing the concentration of polar substances causes ϵ_{emax} to go through a maximum at $c_{add}:c_{AN}$ 0.5:1.0, and further makes ϵ_{emax} constant for $c_{add}:c_{AN}$ 1.0:1.0. The relaxation times of the gels are sharply reduced by the effect of the polar substances. The additives greatly accelerate ripening of the gels. Laws have been found governing the peptization mechanism involved in the action of the polar substances.

3. A study has been made of the effect of repeated deformation on the failure and thixotropic reestablishment of the structure of concentrated gels. Three deformation ranges have been found, which differ in thixotropic properties as reflected by ϵ_e and P.

LITERATURE CITED

1. J. W. McBain and E. B. Working, J. Phys. Coll. Chem. 51, 974, 1947; H. Sheffer, Canad. J. Res. 26, 8, 6, 481, 1948; V.R. Gray and A.E. Alexander, J. Phys. Coll. Chem. 53, 1, 9, 1949.
2. J.W. McBain, K.J. Mysels and G.H. Smith, Trans. Faraday Soc. 42B, 197, 1946; S.S. Marsden, K.Y. Mysels and G.H. Smith, J. Coll. Sci. 2, 265, 1947.
3. A.A. Trapeznikov and V.A. Fedotova, Dokl. AN SSSR 81, 1101; 82, 97, 1952; A.A. Trapeznikov and G.V. Belugina, ibid 87, 635, 825, 1952; 94, 97, 1954; Kolloidn Zh. 20, 3, 1958.
4. C.M. Cawley and J.H. Carlile, J. Inst. Petr. 33, 287, 649, 1947; G.H. Smith, L.B. Rogers and K.Y. Mysels, Y. Amer. Oil. Chem. Soc. 26, 136, 1949.
5. A.S. Frederick and S.E. Wiberley, J. Phys. Chem. 58, 1, 61, 1954; W.O. Ludke, S.E. Wiberley, Y. Goldeson and W.H. Bauer, J. Phys. Chem. 59, 3, 222, 1955.
6. A.A. Trapeznikov, Kolloid Zh. 23, 626, 1961.
7. A.A. Trapeznikov, Pribory I Tekhnika Eksperimenta 3, 93, 1958.
8. A.A. Trapeznikov, Kolloid Zh. 20, 476, 1958.
9. A.A. Trapeznikov, Dokl. AN SSSR 129, 387, 1959.
10. V.A. Fedotova and A.A. Trapeznikov, ibid 120, 841, 1958.
11. T.G. Shalopalkina and A.A. Trapeznikov, ibid 118, 994, 1958; kolloidn Zh. 22, 735, 1960.

All abbreviations of periodicals in the above bibliography are letter-by-letter transliterations of the abbreviations as given in the original Russian journal. *Some or all of this periodical literature may well be available in English translation.* A complete list of the cover-to-cover English translations appears at the back of this issue.

A NEW METHOD OF DISPERSION ANALYSIS BY THE CENTRIFUGATION OF HIGHLY OF HIGHLY DISPERSED SYSTEMS AND SYSTEMS SUSPENDED IN A VERY VISCOUS MEDIUM

E. Ya. Zemlitskii

V. A. Malyshev Kharkov Transportation Industry Plant
Translated from Kolloidnyi Zhurnal, Vol. 23, No. 6,
pp. 699-705, November, December, 1961
Original article submitted July 9, 1960

The dispersion analysis of highly dispersed systems andof systems suspended in very viscous media is performed in a centrifugal force field. The first experiment of this type was performed by Dumanskii [1]. Later on Dumanskii's idea was incorporated by Svedberg into his well known apparatus [2]. The original apparatus was designed by Figurovskii [3]. Some interesting work was also done by Sokolova [4].

The author of this paper designed a new apparatus (Fig. 1) for the dispersion analysis by centrifugation [5]; in addition to rendering the measurements more precise, the apparatus has also enabled us to tackle a wider range of problems.

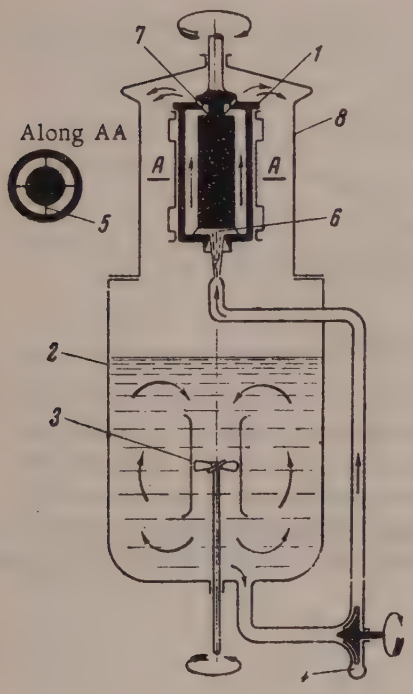


Fig. 1. A schematic representation of the apparatus.

The apparatus consists of a centrifugal separator (rotor) 1 driven by any convenient method, a reservoir 2 with a stirrer 3, a pump 4, and a system of connecting tubes. The enumerated components are linked together to form a closed system for the circulation of the investigated disperse system (solution).

The cylindrical rotor contains an annular channel with radial sections connecting the inlet with the outlet openings. The radial inlet and outlet provide for a flow of solution without any free surface and allow a transfer of motion to layers adjacent to the inner walls of the channel. A number of radial blades 5 produce a drag in the solution when the rotor revolves.

The solution enters the rotor from below through an inlet hole 6 as a jet stream under pressure and comes out at the top through several holes 7 placed in a pattern symmetrical to the axis. The solution then runs freely down the sides of the shell 8 and returns into the reservoir. When the rotor is revolved at very high speeds the outlet should consist of a single small aperture centered along the axis.

While the apparatus is in operation the investigated solution is constantly recirculated; it is vigorously stirred in the reservoir while in the rotor the dispersed phase is screened out. The angular velocity of the rotor and the solution temperature can be maintained constant at any given value.

It should be pointed out that whenever stirring is very vigorous only stable or very dilute solutions can be analyzed.

Let us now examine a circle of radius ρ lying in the plane perpendicular to the axis and concentric with the axis of the rotor and exhibiting the following properties: after a unit volume dV of the cycled solution has passed through the annular channel outside this circle and comes out of the rotor it will not contain any of the particles of the dispersed phase with an equivalent radius r which were present in this volume before the solution entered the

rotor and had been removed by centrifugation. We will now set up expressions in which R is the outer radius of the annular channel in the rotor; $S(\rho) = \alpha\pi(R^2 - \rho^2)$ is the area of circle with a radius ρ in the annular channel; $W(\rho)$ is the average flow velocity inside the area $S(\rho)$; $F(r)$ is a density distribution function of the dispersed phase particles with respect to the equivalent radii $\left(\int_{\infty}^{\infty} F(r)\,dr = 1\right)$; V is the volume of solution in the apparatus; G (t) is the amount of dispersed phase in the solution at time t during the operation of the apparatus; $\rho(t) = G(t)/G(0)$ is the same but with reference to the initial amount: α is a coefficient to allow for the blocking of flow by the blades. Since the solution is vigorously stirred and cycled we can write

$$p(t) = \int_0^{\infty} \left(1 - \frac{dV}{V}\right)^{S(\rho)\,W(\rho)\,t/dV} F(r)\,dr.$$

When $dV \to 0$ the right hand side reduces to the limiting form

$$p(t) = \int_0^{\infty} e^{-S(\rho)\,W(\rho)\,t/V} F(r)\,dr. \qquad (1)$$

$p(t)$ is an experimental curve (Fig. 2) while F (r) has to be determined.

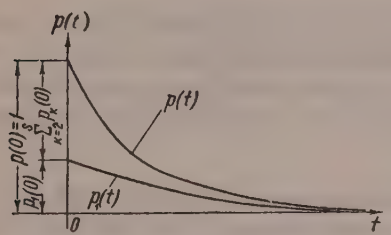


Fig. 2. The ρ (t) plot.

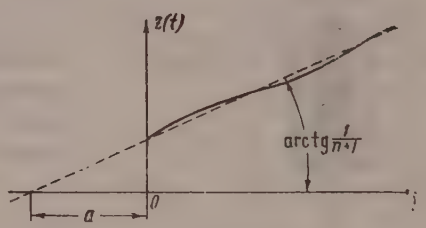


Fig. 3. The z (t) plot.

Analysis of the right hand side of Equation (1). Let us examine the motion of a particle in the annular channel of the rotor. Let L be the length of the annular channel; W is the angular velocity of the rotor; η is the dynamic viscosity of the dispersion medium; δ and δ_1 are the densities of the dispersion medium and of the dispersed phase respectively; x is the distance from the axis of rotation to the point inside the annular channel where the particle finds itself at time τ. We will disregard the inertia of the particles. The particle moves in the axial direction at the same velocity as the stream; the radial movement induced by the centrifugal force is opposed by the Archimedes force and the Stock's frictional force [2],

$$\frac{4}{3}\pi r^3(\delta_1 - \delta)\,\omega^2 x = 6\pi\eta r \frac{dx}{d\tau}.$$

Integrating from $x = \rho$ at $\tau = 0$ to $x = R$ at $\tau = L/W(\rho)$ we get

$$\ln\frac{\rho}{R} = -\frac{2}{9} r^2 \frac{\delta_1 - \delta}{\eta}\,\omega^2 \frac{L}{W(\rho)} \equiv -\lambda.$$

Using this solution we find

$$S(\rho) = \alpha\pi R^2(1 - e^{-2\lambda}) = \alpha\pi R^2\left[2\lambda - \frac{(2\lambda)^2}{2!} + \frac{(2\lambda)^3}{3!} - \ldots\right].$$

In highly dispersed systems and systems suspended in very viscous media λ is small and $S(\rho) \approx \alpha\pi R^2 2\lambda$. In such cases the right hand side of Equation (1) reduces to

$$p(t) = \int_0^\infty e^{-Br^2 t} F(r)\, dr, \tag{2}$$

where B is a parameter determined by the experimental conditions,

$$B = \frac{4}{9} \frac{\delta_1 - \delta}{\eta} \cdot \frac{\alpha\pi R^2 L}{V} \omega^2.$$

Equation (2) leads to a very important result, that the velocity distribution in the stream inside the rotor has very little effect on the screening rate of the dispersed phase. The proposed dispersion analysis hinges on Equation (2).

Analysis of the left hand side of Equation (1). In order to get an experimental curve $p(t)$ at various times t_i samples of the solution are withdrawn from the reservoir and immediately replaced by an equal volume of pure dispersing medium. The first sample ($i = 0$) is taken out before turning the rotor on. Let v_i be the volume of the i-th sample; ΔG_i is the amount of the dispersed phase in the sample; G_i is the amount of the dispersed phase in the total volume V computed from the withdrawn sample $\left(G_i = \Delta G_i \frac{V}{v_i}\right)$; $G_i^{(i-1,\ i-2,\ \ldots,\ i-j)}$ is the same if no samples are taken out the preceding times $t_{i-1}, t_{i-2}, \ldots, t_{i-j}$. It can be shown quite easily that for a normal process

$$G(t_i) = G_i^{(i-1,\ i-2,\ \ldots,\ i-j,\ \ldots,\ 2,\ 1,\ 0)}.$$

All the fractions of the dispersed phase are found in the same proportions in the samples as in the total volume V. Thus one can write

$$\frac{G_i^{(i-1,\ i-2,\ \ldots,\ i-j)}}{G_i^{(i-1,\ i-2,\ \ldots,\ i-(j-1))}} = \frac{G_{i-j}}{G_{i-j} - \Delta G_{i-j}} = \frac{1}{1 - \frac{v_{i-j}}{V}}.$$

Using this relationship we can derive an equation from which points on the $\rho(t)$ curve can be computed,

$$p(t_i) = \frac{G(t_i)}{G(0)} = \frac{\Delta G_i v_0}{\Delta G_0 v_i} : \prod_{j=1}^{i} \left(1 - \frac{v_{i-j}}{V}\right). \tag{3}$$

If all the samples are equal in volume and the volumes are small in comparison with V the Equation can be simplified to

$$p(t_i) = \frac{\Delta G_i}{\Delta G_0} e^{\frac{v}{V} i}.$$

The times t_i at which the samples are withdrawn and the total amount removed yield with the help of preliminary data and simple calculations enough points to enable us to plot $\rho(t)$ by hand. It is advisable to get points at close intervals if $p(t)$ changes rapidly and at wider intervals as the slope decreases. The concentrations of the dispersed phase in the samples (ΔG_i) are determined by the usual methods of quantitative analysis, and since the volume of any one sample may be quite large the analysis of even very dilute solutions can be made quite precise. If the dispersed phase contains heterogeneous components each component is analyzed separately.

Let us find a solution for Equation (2).

The first method. Let us make the substitutions $\xi = Br^2$ and $f(\xi) = F(r)/2Br$ so that the equation is reduced to a Laplace transform integral,

$$p(t) = \int_0^\infty e^{-\xi t} f(\xi)\, d\xi.$$

The experimental curve ρ (t) can be approximated by the analytic function

$$\sum_{k=1}^{S} p_k(t) \equiv \sum_{k=1}^{S} \frac{g_k}{\left(1 + \frac{t}{a_k}\right)^{n_k+1}}, \tag{4}$$

where $\sum_{k=1}^{S} g_k = 1$, $g_k > 0$. One can see immediately that $g_k = \rho_k(0)$. Using Laplace transform tables we can get the desired function for the distribution of particles with respect to their equivalent radii,

$$F(r) = \sum_{k=1}^{S} g_k F_k(r) \equiv \sum_{k=1}^{S} g_k \frac{2(a_k B)^{n_k+1}}{\Gamma(n_k+1)} r^{2n_k+1} e^{-a_k B r^2}.$$

The numbers n_k and a_k can be represented in terms of the distribution moments. Thus, if $n_k > 0$ and we evaluate the integrals

$$\overline{r_k^2} = \int_0^\infty r^2 F_k(r)\, dr \quad \text{and} \quad \overline{r_k^{-2}} = \int_0^\infty r^{-2} F_k(r)\, dr,$$

we will get

$$n_k = \frac{\overline{\left(r_k^{-2}\right)}^{-1}}{\overline{r_k^2} - \overline{\left(r_k^{-2}\right)}^{-1}}; \quad a_k B = \frac{1}{\overline{r_k^2} - \overline{\left(r_k^{-2}\right)}^{-1}}.$$

It is quite obvious that n_k is invariable with respect to the experimental conditions, while a_k is not.

In order to determine the parameters needed to approximate the parabola ρ_k (t) we will construct an auxillary function $z(t) = -p(t) \Big/ \frac{dp(t)}{dt}$. Should the points of this function fall near a certain straight line (the directrix) the summation (4) will contain only one term. The slope of the directrix is 1/n + 1, while the intercept of the directrix with the abcissa falls at a distance a from the origin (Fig. 3). A general solution is obtained by successively subtracting from p (t) partial parabolas p_k (t), the parameters of which are chosen in such a way that the difference

$$p(t) - \sum_{k=1}^{j} p_k(t) = \sum_{k=j+1}^{S} p_k(t) \quad \left[\text{from Fig. 2, } p(t) - p_1(t) = \sum_{k=2}^{S} p_k(t)\right]$$

will be a positive decreasing function convex everywhere.

Second method. Let us replace the true continuous distribution F (r) by an approximate distribution with a discrete spectrum. Then Equation (2) can be rewritten in the form

$$p(t) = \sum_{\nu=1}^{\mu} g_\nu e^{-Br_\nu^2 t} \equiv \sum_{\nu=1}^{\mu} p_\nu(t), \tag{5}$$

where g_ν are the "weights" of fractions with the equivalent radius r_ν. We will define r_ν in such a way as to make it decrease with increasing subscript ν. It is obvious that the terms in summation (5) with small ν decrease faster than do those with large ν. At very large $t \geq t_\mu$ one can assume that only particles with the smallest $r = r_\mu$ still remain in solution, or in other words,

$$p(t) \approx p_\mu(t) = g_\mu e^{-Br_\mu^2 t}. \tag{6}$$

So if we now assume that $t = t_\mu$ we get

$$g_\mu = p(t_\mu) e^{Br_\mu^2 t_\mu}. \tag{7}$$

Differentiating expression (6) and applying equation (7)* we get

$$r_\mu^2 = \frac{1}{Bp(t_\mu)} \cdot \left| \frac{dp(t)}{dt} \right|_{t=t_\mu}.$$

From the last two equations one can compute a lot of data dealing with the relative dimensions of particles and the mass of the μ-th fraction.

After subtracting the curve $\rho_\mu(t)$ from the original curve ρ (t) one gets a new curve representing the sifting of particles from a disperse system which contains all the fractions but the μ-th. Repeating this procedure on the new curve at the time $t_{\mu-1} < t_\mu$ we get $r_{\mu-1}$ and $g_{\mu-1}$, and so on.

To get back a continuous distribution function F(r) one has to relate the mass g_ν to the range of dimensions $r = \frac{r_{\nu-1} + r_\nu}{2}$ to $r = \frac{r_\nu + r_{\nu+1}}{2}$; it is obvious that

$$F(r_\nu) = \frac{2g_\nu}{r_{\nu-1} - r_{\nu+1}}.$$

The F(r) curve is constructed by drawing a smooth curve through the points.

Let us see how various factors will affect the accuracy of the proposed dispersion analysis. We will estimate the error $\Delta\rho$ (t) in Equation (2) relative to Equation (1). Let $\Delta S(\rho)$ be an error in the area $S(\rho)$ which will convert Equation (1) into Eq. (2); then

$$\Delta p(t) = \int_0^\infty \{e^{-S(\rho)W(\rho)t/V} - e^{-[S(\rho)+\Delta S(\rho)]W(\rho)t/V}\} F(r)\, dr.$$

*Similarly Equation (2) yields $\overline{r^2} \equiv \int_0^\infty r^2 F(r)\, dr = \frac{1}{B} \left| \frac{dp(t)}{dt} \right|_{t=0}$. This formula has the advantage that in order to determine $\overline{r^2}$ we do not need the entire curve $\rho(t)$ but only a small segment near t = O.

The function enclosed inside the large brackets is everywhere positive and has a maximum at $t \approx V/S(\rho) W(\rho)$. After evaluating the maximum and introducing the value into the brackets we get the upper limit for $\Delta\rho(t)$.

$$\Delta p(t) < \int_0^\infty \frac{\Delta S(\rho)}{eS(\rho)} F(r)\, dr. \tag{8}$$

As before we will assume that $S(\rho) \approx \alpha\pi R^2 2\lambda$ and $\Delta S(\rho) \approx \alpha\pi R^2 \frac{(2\lambda)^2}{2l}$ (the first term drops when S(p) is expanded in a series); if the channels are not too long $W(\rho)$ can be replaced by W (the average rate of flow through cross section of the annular channel of the rotor); finally considering the desired and probable accuracy with which the ρ (t) curve can be constructed we will fix a safe limit for $\Delta\rho$ (t) (denoting it by $\Delta\rho_1$) and reverse the inequality (8); using a simplified notation $\overline{r^2} = \int_0^\infty r^2 F(r)\, dr$, we get

$$\frac{1}{e} \cdot \frac{2}{9} \overline{r^2} \frac{\delta_1 - \delta}{\eta} \omega^2 \frac{L}{W} < \Delta p_1. \tag{9}$$

This inequality sets the upper limit for ω or the lower limit of W (as well as η). Of course, W has an upper limit too, since we must have laminary flow in the annular channel of the rotor.

Let us see now how precipitation inside the rotor affects the process. Multiplying inequality (9) by eR we get

$$H = \frac{2}{9} \overline{r^2} \frac{\delta_1 - \delta}{\eta} \omega^2 R \frac{L}{W} \leqslant e\Delta p_1 R,$$

The radial velocity of a particle multiplied by the time the particle spends in the annular channel yields H, which is the width of the layer within the limits of which most of the dispersed phase is sifted. Under our limitations H is quite small. Consequently the precipitate deposits fairly evenly on the outside wall of the annular channel.

As the precipitate accumulates R decreases and the process becomes distorted. By assuming that throughout the process the precipitate has the same thickness h as it does at the end we can estimate the upper limit of the error. The analysis is performed as before except that Equation (2) is assumed to hold. The permissible precipitate thickness comes out to be

$$h \leqslant 0{,}5\, e\Delta p_2 R,$$

where $\Delta\rho_2$ is a part of the total error, $\Delta\rho = \Delta\rho_1 + \Delta\rho_2$. The precipitate is removed by periodically stopping the apparatus. The permissible precipitate thickness can be substantially increased if we compensate the decrease in R by increasing W, in such a way, though, as to keep the parameter B constant (WR = const.).

As time goes on other processes accompanying the formation of disperse systems such as coagulation, aggregation and chemical reactions will greatly alter the initial particle distribution. At the same time in numerous cases the knowledge of the initial distribution would be of great scientific and practical value. We will show that the proposed apparatus makes it possible to analyze disperse systems right while they are being formed.

Suppose at the begining we have only the pure dispersion medium, and suppose then that while the apparatus is in operation the disperse phase is introduced evenly from any outside source at the rate I. By introducing another time coordinate θ and using Equation (2) we can find out how much of the disperse phase has accumulated in the solution by the time t:

$$G(t) = \int_0^t I\, d\theta \int_0^\infty e^{-Br^2(t-\theta)} F(r)\, dr = \frac{I}{B} \int_0^\infty r^{-2} F(r)\, dr - \frac{I}{B} \int_0^\infty e^{-Br^{-2}t} r^2 F(r) dr.$$

As $t \to \infty$ the right hand side approaches the limit

$$G(\infty) = \frac{i}{B}\int_0^\infty r^{-2}F(r)\,dr \equiv \frac{I}{B}\overline{r^{-2}}.$$

Let us define $q(t) = \frac{G(\infty) - G(t)}{G(\infty)}$. We can consequently show that

$$q(t) = \int_0^\infty e^{-Br^2t}F(r)\frac{r^{-2}}{\overline{r^{-2}}}dr; \qquad (10)$$

$$\overline{r^{-2}} = B\Big/\left|\frac{dq(t)}{dt}\right|_{t=0}.$$

Comparing Equation (10) with Equation (2) we find out that the former represents a certain nominal process in which particles with an imaginary mass of $G(\infty) - G(t)$ and having a density distribution function with respect to the equivalent radii $F(r)r^{-2}/\overline{r^{-2}}$. are screened out.

Points on the q (t) curve are determined from solution samples withdrawn from the reservoir; in this case the withdrawal of a sample is equivalent to the introduction of an imaginary mass equal in weight to the dispersed phase in the sample ΔG_i (see the derivation of Equation (3)),

$$q(t_i) = \frac{G(\infty) - G_i}{G(\infty)}\prod_{j=1}^{i-1}\left(1 + \frac{\Delta G_{i-j}}{G(\infty) - G_{i-j}}\right).$$

$G(\infty)$ is determined by the method of successive approximations from the asymptote to the curve $G(t) = G_{(\infty)}[1-q(t)]$.

Equation (10) can be solved by making use of the same assumptions as were used to solve Equation (2) making allowance, of course, for the fact that here the real function F (r) is replaced by a nominal function

The described method of dispersion analysis was tried by the author in 1957-1958 at the V. A. Malyshev Kharkov Transportation Industry Plant. The results obtained were in good agreement with other data.

SUMMARY

1. The new method of dispersion analysis of highly dispersed systems and of systems suspended in very viscous media makes it possible to analyze semidispersed systems, systems of many components, very dilute systems, and also provides a means for analyzing various systems as they are being formed. The method is extremely accurate and can be applied to relatively coarse as well as very finely dispersed systems.

2. Due to its relative versatility the new method has considerable advantage over all other currently used methods. The necessary apparatus is relatively simple. The apparatus needed to generate a moderately strong centrifugal field can be assembled in most factory laboratories at little expense.

LITERATURE CITED

1. A. V. Dumanskii Kolloid.-Z. 12, 6, 1913.
2. T. Svedberg, Colloidal Chemistry [Russian translation], IL, M., 1930.
3. N. A. Figurovskii, Sedimentometric Analysis [in Russian], Izd. AN SSSR, M., 1948.
4. V. I. Sokolov, Tubular Ultracentrifuges [in Russian] Gostekhizdat, M., 1949.
5. E. Ya. Zemlitskii, Authors Certificate No. 116881, I.IV. 1958.

EFFECT OF LOWER FATTY ACID SALTS ON THE DISPERSITY OF AN EMULSIFIER SOLUTION AND THE SYNTHETIC LATEXES PREPARED FROM IT

S. S. Ivanchov and A. I. Yurzhenko

I. V. Franko Lwow University, Department of Physical and Colloid Chemistry. Mechnikov Odessa University, Laboratory of High Molecular Compounds.

Translated from Kolloidnyi Zhurnal, Vol. 23, No. 6, pp. 706-711, November-December 1961
Orginial article submitted August 23, 1960

We have shown previously [1-3] that adding salts of lower fatty acids produces a sharp change in the polymerization rate of styrene, and in the molecular weight of the polymers formed. In explaining the data obtained, we proceeded on the assumption that the additives in question change the colloidal properties of the emulsifier, widening or narrowing the zone in which the reaction occurs, and in this way influencing the kinetics of the polymerization process.

The present paper is devoted to a study of the effect of additions of salts of lower fatty acids on the colloidal properties of an emulsifier solution, previously used in polymerization, and on the dimensions of the particles of synthetic latexes.

The emulsifier chosen was a 1% solution of Nekal (sodium salt of dibutylnaphthalenesulfonic acid). Before use the Nekal was twice recrystallized from absolute alcohol to remove electrolytic impurities (Na_2SO_4). The lower fatty acids used and the method of carrying out the polymerization have been described previously [3]. To approximate the sytems under study to polymerized systems, initiator was added to the solution in a concentration of 0.4%, as was done previously in the polymerization experiments. The turbidity of the Nekal solutions was measured on a FM photometer with a nephelometric attachment. The surface tensions of the solutions were evaluated by the maximum bubble pressure method on an improved Kotukov - Lototskii apparatus [4]. The viscosity of the solutions was measured in a closed Ostwald viscosimeter. The solubilizing ability of the Nekel solutions was measured on an MF-1 photo-electrocolorimeter from the intensity of coloration of the solutions by Sudan III, and from the solubilization of ethyl-benzene using a refractometer method [5]. The mean radius of the synthetic latex particles was determined from the optical scattering of dilute solutions [6].

All the measurements were made in a thermostat at 25 ± 0.1.

Adding salts of lower fatty acids increases the turbidity of the Nekal, the more so, the higher the concentration added (Fig. 1). In the low concentration range, the change in turbidity is proportional to the length of the carbon atom chain in the molecule of the salt added. At a concentration of ~ 0.1 N, the salts of lower fatty acids, up to and including the caproate, cause salting-out of the emulsifier, i.e., the Nekal is partially converted into a precipitate at large concentrations of added salt.

We observed a somewhat different sort of change in the turbidity of Nekal solutions on adding sodium laurate, which has emulsifying properties. Adding small amounts of sodium laurate produces a sharp increase in the turbidity of the Nekal, and any further change in turbidity becomes less noticeable. No salting-out effect was observed on adding laurate.

If there is no initiator (potassium persulfate) in the solutions under study, the character of the turbidity change remains the same, but an increase in turbidity is observed at large concentrations of added salts, and salting-out also occurs for large concentrations of added electrolytes.

The surface tension of the Nekal solution decreases with increase in concentration of added electrolytes (Fig. 2). The greater the chain length of the organic radical in the anion of the salt, the more it depresses the surface tension

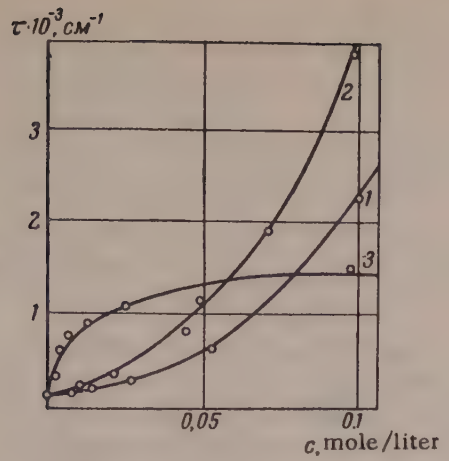


Fig. 1. Turbidity of Nekal solutions as a function of additive concentration. 1) Sodium acetate; 2) sodium caproates; 3) sodium laurate.

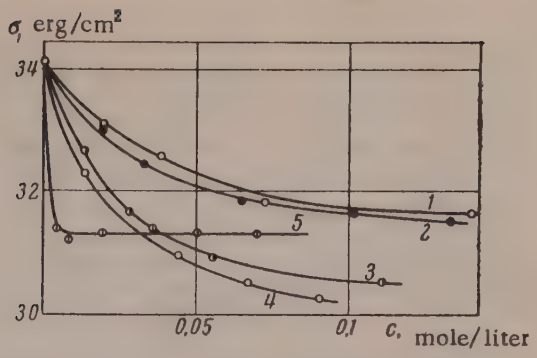


Fig. 2. Surface tension of Nekal solutions as a function of additive concentration. 1) Sodium formate; 2) sodium acetate; 3) sodium butyrate; 4) sodium caproate; 5) sodium laurate.

of the Nekal solution. Here, also, the sodium laurate behaves in a different way. With small amounts of sodium laurate, the surface tension of the Nekal solution drops off sharply and does not change any further over the whole range of additive concentration investigated.

The change in turbidity and surface tension of the Nekal solutions in the presence of added salts as a function of the Nekal concentration was used to find the critical micelle-forming concentration (CMC). The data obtained are given in Fig. 3 and in the table.

It may be seen from the table that the CMC of Nekal is reduced by adding salts of lower fatty acids. Adding sodium butyrate lowers the CMC more than adding sodium acetate.

CMC of Nekal as a Function of Sodium Acetate and Sodium Butyrate Added

Additive	Concentration of Additive mole/liter	CMC, %
Sodium Acetate	-	$11.5 \cdot 10^{-3}$
	0.01	$7.9 \cdot 10^{-3}$
	0.05	$5.7 \cdot 10^{-3}$
	0.10	$4.0 \cdot 10^{-3}$
Sodium Butyrate	0.01	$7.6 \cdot 10^{-3}$
	0.05	$5.0 \cdot 10^{-3}$
	0.10	$3.7 \cdot 10^{-3}$

Similar data are found from measuring the solubilization and surface tension of Nekal solutions of different concentration with constant quantities of additive.

The turbidity of the emulsifier solutions is in some sense an index of the dispersity, and consequently, of the micellar weight. The increase in turbidity of the solutions when salts are added indicated that there is an increase in the micellar weight of the Nekal. This increase is larger, the longer the hydrocarbon radical in the anion of the added fatty acid salt, i.e., it increases in the order acetate–butyrate–caproate–laurate, all of sodium. The micellar weight increases with increase in concentration of lower fatty acid salts added (up to sodium caproate in the series). With sodium laurate, another sort of change in the micellar weight is observed from the turbidity of the solutions. There is a sharp increase when the first portions of sodium laurate are added, but afterwards the increase is small. Here we must also keep in mind that the turbidity of the solution is increased by sodium micellaurate at concentrations above 0.01 N, because of the tendency of sodium laurate to micelle formation. These ideas are supported by the data on the viscosity change of Nekal solutions in the presence of lower fatty acid salts (Fig. 4), since the viscosity increases with increase in concentration of electrolytes added, the more sharply the longer the hydrocarbon radical in the anion of the salt being added. The measurements show that the micellar weight of Nekal increases with increase in concentration of sodium butyrate.

According to the present theory of micelle formation, we can set up the following picture for the effect of adding lower fatty acid salts on the properties of Nekal solutions.

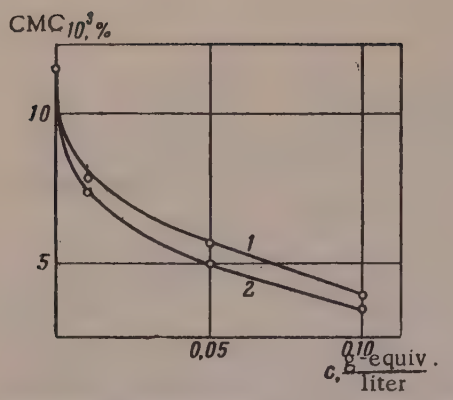


Fig. 3. Effect of adding sodium acetate (1), and sodium butyrate (2) on the CMC of Nekal.

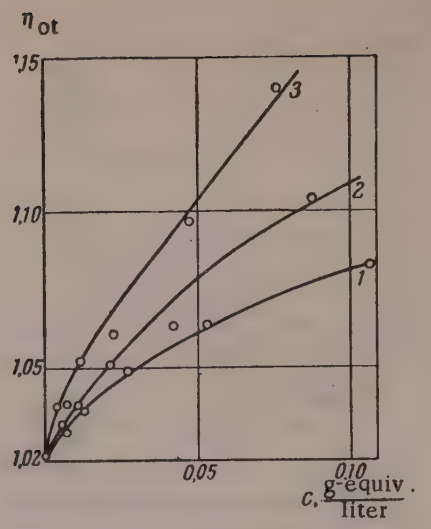


Fig. 4. Viscosity of Nekal solutions as a function of additive concentration. 1) Sodium acetate; 2) sodium caproate; 3) sodium laurate.

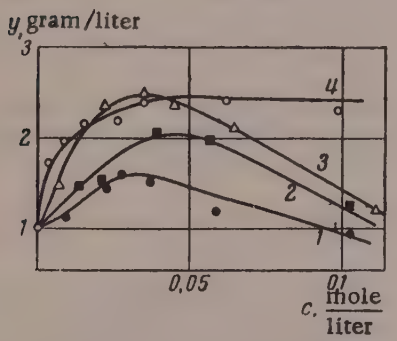


Fig. 5. Variation of solubilizing ability of Nekal solutions with additives. 1) Sodium acetate; 2) sodium butyrate; 3) sodium laurate.

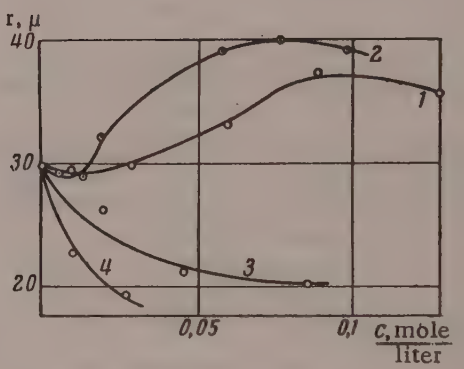


Fig. 6. Mean radius of synthetic latex particles as a function of additive concentration. 1) Sodium formate; 2) sodium butyrate; 3) sodium laurate; 4) sodium palmitate.

The additives introduced, like any electrolytes, decompose into ions as a result of dissociation. The charged ions change the ratio of cohesional to electrical forces in micelle formation; they produce a shielding effect for the electrical repulsive forces of the negative Nekal ions, which enter into the micelle. This in itself enables a large number of particles to be packed into the micelle, i.e., it increases the micellar weight.

As the length of the hydrocarbon radical in the salt anion is changed, a change occurs in the degree of dissociation of the electrolyte and the pH of the solutions, which in its turn also produces an increase in the micellar weight [7]. In addition, the effect of the organic radical in the anion of the added salt may be more specific in micelle formation. Depending on the nature of the emulsifiers, two types of solubilization in aqueous solutions have been described [8]: solubilization of nonpolar substances such as benzene and styrene, and that of polar-nonpolar compounds such as alcohols. Hydrocarbons are solubilized by the hydrocarbon part of the micelle as though they were adding to the particles which constitute it. Polar-nonpolar compounds are solubilized by arranging themselves in the internal phase of the micelle and are oriented parallel to the elements making up the micelle. If the hydrocarbon radical in the fatty acid salt is long enough (sodium butyrate, or sodium caproate), solubilization of these additives by the micelles can occur according to the type of solubilization shown by polar-nonpolar compounds. In this case, the electrolytes or their component parts enter into the micelle itself and change its properties. Here it will be easier

to solubilize anions or molecules of sodium caproate than salts with shorter hydrocarbon radicals. If the concentration of fatty acid salts is increased, the structure of the micelle can apparently change too. The hydrocarbon radicals, located in the micelle come closer together, or there is compression of the hydrocarbon part of the micelle. At a definite concentration of added salts, the hidden coagulation process in the micelle (i.e., enlargement of the micelle) may cause obvious precipitation of the emulsifier accompanied by a reduction of emulsifier concentration in the solution. All these phenomena unquestionably have to do with the properties of the surface layer of the micelles and their solubilizing ability and thus have to do with the kinetics of emulsion polymerization in such systems.

If fatty acid salts are added, which have emulsifying properties, the effect which they exert consists in raising the emulsifier concentration in the solution. In this case, it is possible to form mixed micelles which consist of molecules of Nekal and the corresponding additive, such as, for example, sodium laurate.

The solubilization of the dye Sudan III is increased by adding fatty acid salts, the more so the longer the organic radical in the salt anion (Fig. 5). If the concentration of additive is varied, the curves for the solubilization of salts of acids up to and including caproic show a maximum at a concentration of approximately 0.03-0.05 N. In the light of the ideas expressed previously, this sort of variation of the solubilizing ability of Nekal in the presence of added salts becomes comprehensible.

It is also interesting to note that there is a retardation of the solubilization rate at high concentrations of lower fatty acid salts added. Saturation of the nekal micelles with Sudan III occurs in 8-12 hours without added salts and in 23-25 hours in the presence of 0.12 N sodium acetate. The picture of the change in solubilization of ethylbenzene with these same additives, measured refractometrically, is absolutely the same in character. The solubilizing ability of Nekal is sharply increased as to emulsifying properties when the first portions of fatty acid salts are added and then shows little change. Here the solubilization rate is increased (in the presence of 0.02 mole/liter of sodium laurate saturation is reached in 7-9 hours).

Thus, the data on the effect of fatty acid salt additives on the colloid properties of an emulsifier support the possibility of dividing them into two groups [1, 3], namely, into salts of lower fatty acids (up to and including the caproate), and salts of higher fatty acids. The effect of the lower fatty acid salts is in many ways similar to the effect of inorganic electrolytes.

The change in the colloid properties of the emulsifier should effect not only the kinetics of the polymerization process, but the dispersity of the synthetic latexes prepared as well. Adding fatty acid salts makes it possible to vary the dispersity of the latexes over very wide limits (Fig. 6). For example, sodium butyrate, after a small reduction at low concentrations, causes an increase in the mean radius of the latex particles. The reduction in radius of the latex particles on adding the first portions of sodium butyrate is a matter of increasing the pH of the aqueous phase of the polymerization system, as a result of hydrolysis of the butyrate [6]. The increase in radius of the latex particles with increasing concentration of additives goes up to a definite limit, after which the radius remains practically unchanged. Adding sodium laurate or higher fatty acid salts causes increased dispersity of the resulting latexes, the more so the longer the hydrocarbon radical in the anion of the salt added.

The results obtained are easily explained starting from the general theory of emulsion polymerization. The polymerization, beginning in the micelles, continues in the polymer-monomer particles formed from them. The larger the number of micelles in the original emulsion which are able to start the polymerization process, the more polymer-monomer particles are formed and the higher the dispersity of the synthetic latex being formed. Adding higher fatty acid salts leads mainly to an increase in the number of micelles which means an increase in dispersity of the resulting latex. Salts of the lower fatty acids increase the micelle dimensions, which reduces the total number of micelles and therefore, if they are added, they cause a reduction in dispersity of the synthetic latexes.

The synthetic latexes prepared in the presence of large concentrations of added salts of lower fatty acids partially coagulate on not very long standing and separate out bits of rubber.

Thus, it is possible with fatty acid salts to control not only the polymerization kinetics in the emulsion and the molecular weight of the polymers formed, but the dispersity of the resulting latexes as well.

SUMMARY

1. Adding lower fatty acid salts increases the turbidity and micellar weight while lowering the surface tension and CMC of aqueous Nekal solutions. The effect is dependent on the length of the anion chain of the salt added.

2. Fatty acid salts may be divided into two groups depending on how they effect the colloid properties of Nekal solutions, namely, salts of lower fatty acids (up to and including caproates), and salts of higher fatty acids.

3. The dispersity of the resulting synthetic latexes is completely determined by the dispersity of the emulsifier solution being used. Adding fatty acid salts makes it possible to vary the dispersity of the latexes over wide limits.

LITERATURE CITED

1. A. I. Yurzhenko, S. S. Ivanchov, Dokl AN SSSR, 120, 349, 1958.
2. A. I. Yurzhenko, N. Ya. Ivanova, S. S. Ivanchov, Theses of Papers from the IV All Union Conference on Colloid Chemistry [in Russian] Academy of Sciences Press, USSSR, 1958, p. 247.
3. A. I. Yurzhenko, S. S. Ivanchov, Kolloidn Zh. 22, 120, 1960.
4. A. Z. Kotukov, E. I. Lototskii, Zavodsk Laboratoriya, 9, 1100, 1953.
5. A. I. Yurzhenko, Zh. obshch. khimii 16, 1171, 1946.
6. A. I. Yurzhenko, V. P. Gusyakov, Kolloidn Zh. 16, 72, 1954.
7. R. V. Kucher, Candidates Dissertation [in Russian] Lwow, 1952.
8. H. B. Klevens, Chem. Rev. 47, 1, 1950.

All abbreviations of periodicals in the above bibliography are letter-by-letter transliterations of the abbreviations as given in the original Russian journal. *Some or all of this periodical literature may well be available in English translation.* A complete list of the cover-to-cover English translations appears at the back of this issue.

EFFECT OF STRONG ELECTROLYTES ON THE ADSORPTION OF BENZENE DERIVATIVES FROM AQUEOUS SOLUTIONS BY ACTIVATED CHARCOAL

A. M. Koganovskii and T. M. Rovinskaya

Institute of General and Inorganic Chemistry, Academy of Sciences, Ukrainian SSR, Kiev
Translated from Kolloidnyi Zhurnal, Vol. 23, No. 6, pp. 712-717, November-December, 1961
Original article submitted June 25, 1960

In practice, organic substances often must be adsorbed from solutions in the presence of more or less large amounts of mineral salts, usually salts of alkali or alkaline-earth metals. Notwithstanding this the effect of strong electrolytes on the adsorption of organic nonelectrolytes or weak electrolytes has been investigated very little, and the nature of the phenomena observed under these conditions is still obscure in many respects. Experiments in study of the surface tension of water–salt solutions of phenol [1] led to the conclusion that identical activities of the equilibrium phenol solution correspond to identical values of its specific adsorption at the interface between the phases. Hence salts affect the adsorption of phenol so far as they affect the activity of its aqueous solutions. The observed effect is referred to salt hydration in [2], and the hydration of sodium and potassium salts is calculated on the basis of a determination of the capillary activity of solutions of alcohols and aniline. The hydration of a great number of sodium and potassium salts was determined by this method [3]. Based on experiments on the adsorption of phenol from water–salt solutions, and benzoic acid from water–alcohol solutions of salts [4], one may conclude that the change in the activity of organic substances in the presence of salts amounts to an increase in the true solution concentration, due to a decrease in the solvent volume of water, caused in turn by hydration of the salt ions. When corrections are made for water bound through hydration, the adsorption isotherms of phenol and benzoic acid coincide at all salt concentrations.

However, on investigation of the effect of differently hydrated salts (KNO_3, KCl, NaCl, $CaCl_2$, $MgSO_4$) on the adsorption of phenol, aniline, o-aminobenzoic acid, and o-hydroxybenzoic acid we found that adsorption in the presence of electrolytes does not always increase as would be expected on the basis of the decrease in the solvent volume of water, due to ion hydration. Phenol, aniline and o-hydroxybenzoic salicylic acid are convenient subjects for study of the effect of salts on the adsorption of organic substances from aqueous solutions since the solubility of these substances in water–salt solutions was studied in relatively great detail [5-8].

The adsorption isotherms for phenol, given in Fig. 1a, confirm that phenol is more strongly adsorbed from water–salt solutions than from water.

As was to be expected on the basis of the hydration theory of salt action, the isotherms for aniline adsorption from NaCl solution (Fig. 1b) lie slightly above that for aniline adsorption from water. The isotherms for aniline adsorption from 1 M $CaCl_2$ and $MgSO_4$ solutions lie still higher and practically coincide. The isotherm for aniline adsorption from 1 M KNO_3 solution practically coincides with that for aniline adsorption from water. Therefore adsorption measurements lead to the hypothesis that very little or no hydration of this salt occurs.

When isotherms of phenol or aniline adsorption from water and salt solutions are superposed and corrections made for equilibrium concentration in solutions of various salts, salt hydration numbers are obtained which lie close to literature data and, in particular, to hydration numbers obtained by the solubility and distribution determination methods (Table 1). This fact is understandable, since these methods essentially reflect the decrease in the solvent volume of water. Hydration numbers calculated from different portions of the adsorption isotherms do not coincide. This is due mainly to the equality of the specific adsorption from water to that from salt solutions when the adsorbent surface is saturated. In this case it should be noted that the specific adsorption at saturation depends only on the

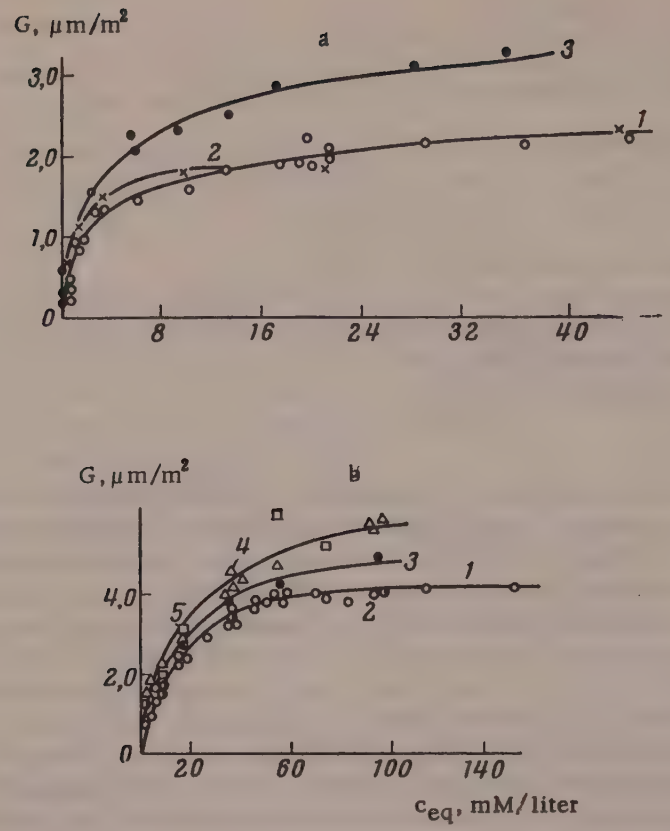


Fig. 1. Adsorption on charcoal at 25°. a) Phenol from water (1); from 1 M KCl (2); from 2 M NaCl (3). b) Aniline from water (1); from 1 M KNO_3 (2); from 1 M NaCl (3); from 1 M $CaCl_2$ (4); from 1 M $MgSO_4$ (5).

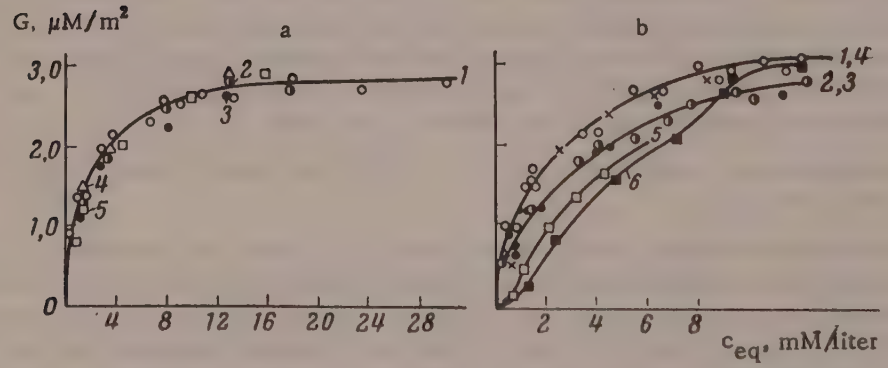


Fig. 2. Adsorption on charcoal at 25°. a) o-Aminobenzoic acid from water (1); from 1 M KNO_3 (2); from 1 M NaCl (3); from 1 M $CaCl_2$ (4); from 1 M $MgSO_4$ (5). b) o-Hydroxybenzoic acid from water (1); from 1 M KNO_3 (2); from 1 M NaCl (3); from 1 M KCl (4); from 0.5 M $MgSO_4$ (5); from 1 M $MgSO_4$ (6).

ratio of the surface covered by an adsorbed molecule to the specific surface of the adsorbent. Salt hydration numbers giving the best agreement with literature data, may be calculated from the initial portions of the isotherms.

TABLE 1. Comparison of Salt Hydration Numbers, Calculated from Isotherms of Phenol and Aniline Adsorption from Water–Salt Solutions, with Those Found from Solubility, Distribution, and the Ratio of Crystallochemical Radii of Ions and Water

Salt	Hydration numbers according to adsorption from water–salt solutions * of		Hydration numbers		
	phenol	aniline	from solubility of aniline * [9]	from the distribution coefficient [10]	from the ratio of crystallochemical radii of ions and water [11]
NaCl	13–18	10.4–17	19.5	16	14
K Cl	15.9–17.7	–	16.65	14	16
KNO_3	–	0	11.45	-	-
$CaCl_2$	–	20.8–27.2	–	-	-
$MgSO_4$	–	20.8–27.2	35.8	-	-

*In calculating the salt hydration number the specific adsorption (G) was taken to be 1-1.4 $\mu M/m^2$ for phenol and 2-3 $\mu M/m^2$ for aniline.

TABLE 2. Apparent "Hydration Numbers" Determined from the Isotherms of o-Aminobenzoic and o-Hydroxybenzoic Acid Adsorption from Water and Water–Salt Solutions *

Salt		Hydration numbers according to adsorption from water–salt solutions of	
		o-aminobenzoic acid	o-hydroxybenzoic acid
NaCl,	1M	0	–18.5; –55.5; –19.9
KCl,	1M	0	0
KNO_3,	1M	0	–18.5; –55.5; –29.9
$CaCl_2$,	0.5M	0	–
$CaCl_2$,	1M	0	–
$MgSO_4$,	0.5M	–	–40.7; –58.5; –111
$MgSO_4$,	1M	0	–33.3; –185; –76.8

*Values of the specific adsorption of o-hydroxybenzoic acid, equal to 0.5, 1, and 1.5 $\mu M/m^2$, respectively, were used in determining the salt hydration numbers.

The adsorption isotherms for o-aminobenzoic acid (Fig. 2a) coincide; therefore the "hydration numbers" of KNO_3, NaCl, $CaCl_2$, and $MgSO_4$ are equal to zero, which contradicts earlier data, the results of independent determinations by various authors [6, 9-11], and is not in accord with modern views on ion hydration.

We obtained results even more incompatible with the hydration theory of the action of strong electrolytes on the adsorption of organic substances from aqueous solutions, in a study of the effect of 1M and 0.5 M $MgSO_4$ solutions on the adsorption of o-hydroxybenzoic acid from aqueous solutions by charcoal (Fig. 2b). In this case all electrolytes (except KCl, which has practically no effect on adsorption), instead of enhancing adsorption, diminish it.

Owing to the diminution of adsorption, the fictitious hydration numbers (Table 2) become negative in this case. The greatest diminution of adsorption occurs in a solution of the strongly hydrated salt $MgSO_4$. This effect is expecially pronounced in the initial portions of the isotherm, since the maximum adsorption, as indicated above, cannot be a function of the substance's concentration in the solution.

It is characteristic that deviations from the results, to be expected in accordance with the concept of solvent binding by salt ions, are observed on adsorption from aqueous solutions of compounds with groupings of substitutents in the nucleus which lead to the appearance of an intramolecular hydrogen bond.

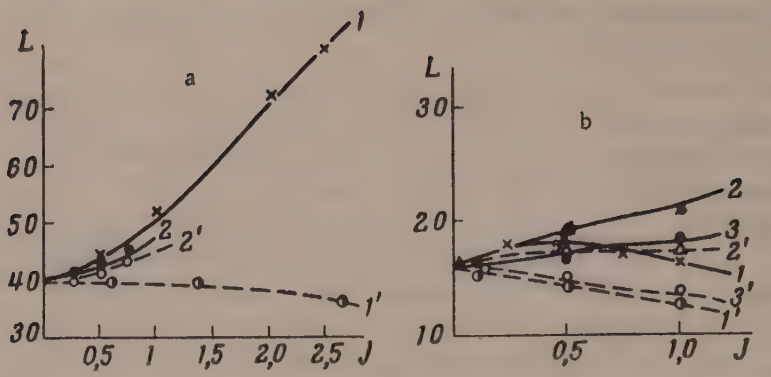


Fig. 3. Dependence of the solubility L_{sv} (in moles per liter of the solvent volume of water) on the ionic strength of solutions: a) o-aminobenzoic acid in KNO_3 (1) and Ba $(NO_3)_2$ (2) b) o-hydroxybenzoic acid in NaCl (1), KNO_3 (2), and KCl (3) solutions. The solubilities of these acids relative to the total volume of water (L) are shown by dashed lines.

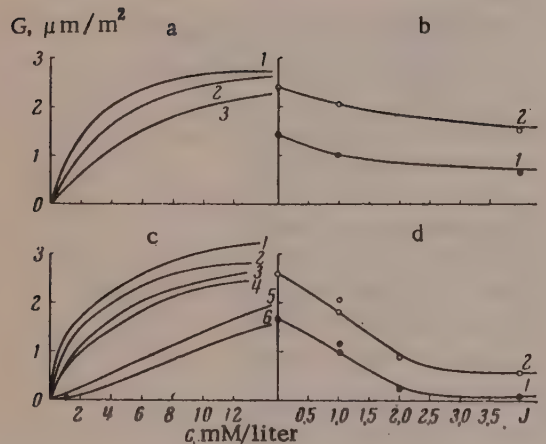


Fig. 4. Isotherms of o-aminobenzoic acid (a) and o-hydroxybenzoic acid (c) adsorption from water (1), 1 M NaCl (2), 1 M $MgSO_4$ (3), 1 M KCl (4), 1 M KNO_3 (5), and 0.5 M $MgSO_4$ (6). Effect of the solution's ionic strength on adsorption: o-aminobenzoic acid (b), o-hydroxybenzoic acid (d). Equilibrium concentrations expressed in terms of the solvent volume of water: c_{eq} = 2(mM/A) (1) and c_{eq} = 6(mM/A) (2)

On the basis of observed differences in the regularities of the effect of salts on adsorption from aqueous solutions, of substances capable of forming intermolecular hydrogen bonds with the solvent, and substances forming intramolecular hydrogen bonds, the following hypothesis may be advanced.

When salts are dissolved, the resulting increase in solvent polarity promotes weakening of intramolecular hydrogen bonds and strengthening of hydrogen bonds between solute and solvent molecules. As a result the standard decrease of free energy on adsorption from solutions (ΔF_{ads}, made up of the change of free energy on adsorption interaction (ΔF_a) and the change of free energy on hydration of molecules (AF_c), falls owing to an increase in the maximum work of hydration: $\Delta F_{ads} = AF_a - (\Delta F_c + \Delta F_c)$. When salts are dissolved in a solution, the increase in its polarity depends on the ionic strength. In accordance with this the solubility of ortho-substituted benzenes capable of forming an intramolecular hydrogen bond must be a function of the solution's ionic strength. Hence the solubility of such substances must increase with the salt concentration more markedly, the more markedly the solution's ionic strength increases, the change in solvent volume due to salt hydration being taken into account in this case, and concentrations being expressed in moles per unit solvent volume of water. The solubility, expressed in such units, will be denoted below by h_{sv}.

In Fig. 3 it is shown that the solubility of o-hydroxybenzoic and o-aminobenzoic acids, expressed in moles per liter of the solvent volume of water (L_{sv}), acutally increases with the ionic strength of the water–salt solutions. In the case of aniline, phenol and other compounds whose adsorption normally increases with the salt hydration, L_{sv} remains a constant quantity which does not depend on the salt concentration or the valence of the salt ions.

According to this the specific adsorption of o-hydroxybenzoic and o-aminobenzoic acids, measured at equal equilibrium concentrations of the substances per unit solvent volume of water, as is evident from Fig. 4, decreases with increase in ionic strength of the solutions, regardless of which salt (KNO_3, NaCl, or $MgSO_4$) caused the increase in ionic strength.

Comparison of the curves illustrating the contrary character of the dependences of adsorption and solubility on the ionic strength of the solutions quite conclusively provides at least qualitative confirmation of the hypothesis on the cause of the anomalous effect of salts on the adsorption of compounds capable of forming intramolecular hydrogen bonds.

SUMMARY

1. The degree of adsorption from aqueous aniline and phenol solutions increases in the presence of strong, neutral electrolytes, adsorption of o-aminobenzoic acid is unchanged and adsorption of o-hydroxybenzoic acid is decreased.

2. The solubility of o-aminobenzoic and o-hydroxybenzoic acids expressed in moles per liter of the solvent volume of water increases with the solution's ionic strength, while the solubility of aniline and phenol, analogously expressed, does not depend on the solution's ionic strength. The specific adsorption of o-aminobenzoic and o-hydroxybenzoic acids at identical equilibrium concentrations, expressed in moles per liter of the solvent volume of water, is a decreasing function of the solution's ionic strength, regardless of which salt caused the increase in ionic strength on dissolving.

3. The hypothesis that the decrease in the degree of adsorption of these substances with increase in the ionic strength of the solutions is due to weakening of intramolecular bonds and strengthening of the hydrogen bonds of o-hydroxybenzoic acid molecules with water i.e., increase in their hydration energies, is advanced, The effect of neutral electrolytes on adsorption from aqueous solutions of organic substances capable of forming intramolecular hydrogen bonds is determined by the relation between two contrary factors – decrease in the solvent volume of water as a result of ion hydration, and strengthening of hydrogen bonds between the dissolved substances and the solvent on increase of the solution's ionic strength.

LITERATURE CITED

1. A. K. Goard, E. K. Rideal, J. Chem. Soc. (London) 1925, 127, 1674.
2. W. Seith, Z. Phys. Chem. 117, 257, 1925.
3. H. Freundlich. A. Schnell, Z. phys. Chem. 133, 151, 1928.
4. P. P. Kozakevich, N. A. Izmailov, Zh. obshch. khimii 1, 105 (1931).
5. W. Herz. F. Hiebenthal, Z. anorgan. Chem. 177, 363, 368, 1928.
6. S. Glasstone, J. Bridgeman. W. R. Hodson, J. Chem. Soc. 1927, 130, 635.
7. I. M. Kolthoff, Proc. Akad. Sci. (Anst) 29, 895, 1927.
8. A. Osol, M. Kilpatrik, J. Amer. Chem. Soc. 55, 4440, 1933.
9. J. C. Phylip, A. Bramley, J. Amer. Chem. Soc. 107, 377, 1831, 1915.
10. N. A. Izmailov, Solution Electrochemistry [in Russian], Khar'kov, 1959, pp 282, 304.
11. T. M. Rovinskaya, A. M. Koganovskii, Kolloidn. zh. 23, 779 (1961).

All abbreviations of periodicals in the above bibliography are letter-by-letter transliterations of the abbreviations as given in the original Russian journal. *Some or all of this periodical literature may well be available in English translation.* A complete list of the cover-to-cover English translations appears at the back of this issue.

INVESTIGATION OF STRUCTURAL–MECHANICAL PROPERTIES OF BITUMENS OF DIFFERENT ORIGIN

1. STUDY OF VISCOUS AND THERMOMECHANICAL PROPERTIES OF ROAD BITUMENS OF DIFFERENT CHEMICAL COMPOSITION*

A. S. Kolbanovskaya and V. V. Mikhailov

The Moscow All Union Road Scientific-Investigational Institute
Translated from Kolloidnyi Zhurnal, Vol. 23, No. 6,
pp. 718-725, November-December, 1961
Original article submitted April 28, 1960

The stability and durability of road linings based on bitumen depend to a considerable extent on the properties of this binder. The difference in the composition of the oils used as stock in the production of bitumens, the different methods and technological processes in their preparation determine the differences in the chemical composition of the bitumens. This also leads to a difference in the technological, constructional and operational properties of the bitumen. The behaviour of the bitumens in road linings in large measure is determined by the following factors: the elastic-plastic and stable (cohesive) properties over a wide range of temperatures and thicknesses of the layers on the surface of the mineral matter; the thermomechanical properties which define the relation between temperature and deformation of the bitumen; the adhesive properties which determine the stability and durability of the bitumen bond with the surface of the minerals under conditions where there is a protracted reaction by water and temperature.

The present work is devoted to the problem of investigating the structural-mechanical properties of bitumens of different composition and origin produced at the present time by oil refineries in the USSR.

In this investigation the chemical properties of a bitumen are obtained from the results of component analysis carried out in a chromatographic column filled with silica-gel. Thus the asphalts are previously deposited by petroleum ether but the different fractions of oils and tars adsorbed by silica gel, are extracted by means of successively washing with selected solvents (petroleum ether, a mixture of petroleum ether and benzene and a mixture of benzene and alcohol). In addition to the component analysis of the bitumen its average molecular weight, ultimate composition (C, H, S, O + N), functional groups (acidity, saponification, ether and iodine values) and paraffin composition were determined. The chemical composition of ten bitumens from different sources are reproduced in Table 1.

The thermal stability of the bitumens over a broad range of temperatures is described by temperature-viscosity curves [1]. Extensive investigations established [2] that the elastic-plastic properties of the bitumens may be well described by their complete rheological curve and are characterized by two limiting values of the viscosity – that of the non-fractured structure η_0 and the totally fractured structure η_m. The authors showed the effect on the elastic-plastic characteristics of the bitumen of the temperature, plasticizer and the active filler.

In order to investigate the bitumens we studied the temperature-viscosity relation of the fractured structure over the range 20-130° with the help of the Volarovich rotating viscometer (RV-8). As the investigational results showed, for all bitumens over the temperature range 20-70° a relation between the values of the viscosity and the shearing stress applied was observed i.e., the bitumen over this range of temperatures behaves like a non-Newtonian fluid. At higher temperatures the bitumen begins to follow the flow laws of genuinely-viscous Newtonian liquids. Over the range investigated, the viscosity of all bitumens lies within the limits from $5 \cdot 10^5$ to 5 poises. The viscosity of the fractured structure of bitumen rapidly falls with a rise in temperature from 20 to 130° (Fig. 1).

The viscosity of bitumen must undoubtedly be a function of its structure and chemical composition. Below 100° there is no relation between the viscosity and the value of the average molecular weight. However, at higher

* The experimental part was done by L. I. Efimova, A. P. Davidova, O. K. Golovkina, and G. N. Bugaeva.

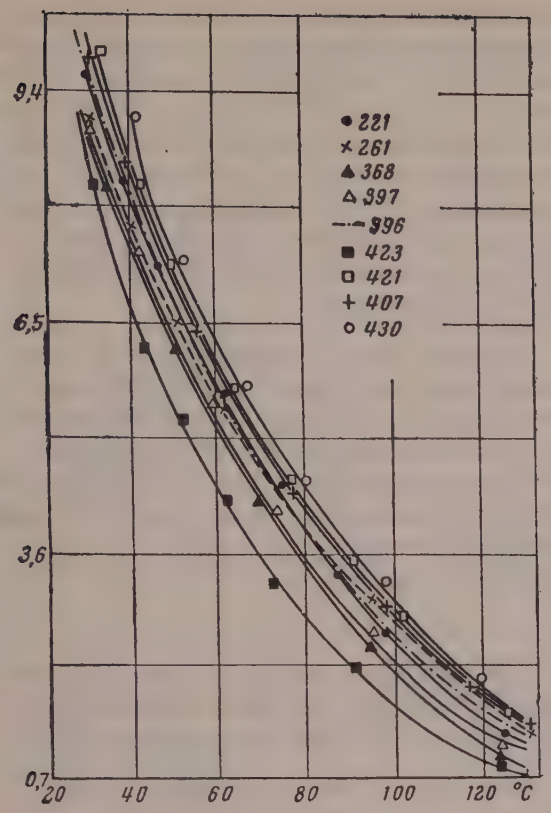


Fig. 1. Relation between visocsity of bitumen and temperature.

temperatures a linear relation is found between them. With an increase in the content of the asphaltenes the viscosity of the bitumen increases. However, the content of the oils and tars do not appear to have any practical effect on the viscosity of the bitumen.

From the molecular structure of the bitumen it is possible to explain the results obtained in the following manner. At comparatively low experimental temperatures the viscosity of the bitumen is largely determined by the interaction between the macromolecules or micelles determining the definite steric structure of the bitumen. The lower the temperature the more the effect of the inter-molecular interaction and the more the viscosity of the bitumen. With an increase of temperature the inter-molecular interaction forces fall due to the increase of the inter-molecular distances and the bitumens begin to behave in a similar manner to Newtonian fluids. Hence the viscosity depends only on the dimensions of the structural units – on the molecular weights of the components, in other words.

In bitumens possessing a high viscosity at relatively low temperatures, the inter-molecular forces of the interaction are very great and an increase of temperature leading to a sudden weakening of these forces strongly reduces the viscosity (bitumens 396, 421, 221, 407, Fig. 1). Bitumens in which the inter-molecular interaction is considerably weaker (368, 39, 423, Fig. 1) give a lower reduction in viscosity with temperature which is proved by their great thermal stability.

Under practical conditions, road-lining bitumens are used in the form of thin layers on stone particles. Hence the structural-mechanical properties, as Gorelyshev [3] showed, to a considerable extent are determined by the properties of this layer of bitumen and are altered depending on the thickness of the layer. Analogous investigations were conducted by a number of investigators abroad [4]. As a consequence of the factors referred to, in order to estimate the properties of a bitumen it is of great interest to investigate the stability and deformation characteristics of thin layers of bitumen on underlayers of mineral matter.

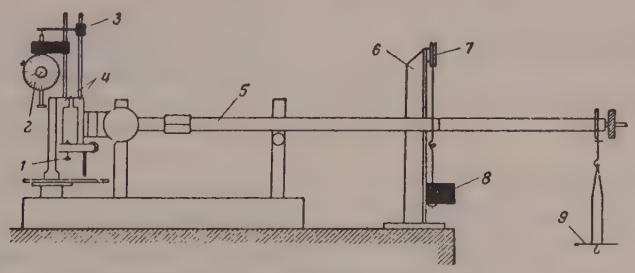


Fig. 2. Cohesiometer (described in the text)

We studied the structural-mechanical properties of thin coatings (5-20μ) with the help of a cohesiometer specially designed for this purpose (Fig. 2) based on the shear of a thin layer of bitumen placed in the gap between two vertical parallel tablets of mineral matter. One of the tablets was fastened immovably but the second was able to move under the action of the load applied. The action of the load is transmitted through a 1:10 lever arm. The parts of the apparatus are as follows: two shoes, 4, (with an adjusting screw, 1) one of which was not free to move and the other which is free, are used to fasten the tablets cemented with the bitumen coating. An indicator, 2, is fastened

TABLE 1. The Chemical Properties of Different Bitumens.

Bitumens and Oils	Average molecular weight	Component comp. %			Functional groups				Ultimate analysis				
		Oils	Tars	Asphaltenes	Acidity mg KOH	Saponif. value mg KOH	Ester value	Iodine number%	C	H	S	O+N	Paraffins
Odessa (Il'skiy) 221	638	57,95	27,8	16,5	3,23	8,72	5,39	34,9	86,56	10,68	0,43	2,33	0,94
Ukhta (Shakhty) 261	981	55,65	20,49	24,15	0,71	9,33	8,62	22,2	86,79	10,82	1,24	1,15	0,62
Odessa cracking (Tuimazy) 368	559	65,31	8,26	26,63	0,87	8,62	7,84	31,1	85,92	10,77	0,61	2,70	2,41
Lyubetsy (Romashki) 396	881	63,83	17,48	20,53	0,87	4,66	3,79	38,5	85,87	10,57	1,32	2,24	4,98
Krasnodar (Anastasii) 397	780	59,31	27,36	14,25	0,64	10,82	10,18	36,2	87,53	10,67	0,58	1,22	2,51
Baku (Buzovinsk) 407	804	53,29	20,1	21,84	0,86	12,98	12,12	32,2	86,16	11,01	0,59	2,24	4,95
Ukhta (Ukhta) 421	749	60,77	18,32	21,17	0,68	16,15	15,47	42,1	87,82	11,45	1,41	—	1,32
Drogobych (Borislav) 423	944	61,37	19,21	19,83	0,77	9,69	8,92	36,8	86,95	10,86	0,33	1,86	7,69
Ufa (Romashki) 429	795	64,88	9,00	25,75	1,14	10,77	9,63	32,8	85,62	10,60	1,47	2,31	4,80
Ufa (Romashki) 430	934	56,67	12,24	31,51	1,14	10,77	9,63	34,5	86,22	10,58	1,68	1,52	4,30

onto the non-movable shoe. By means of the coupling, 3, a metallic strip is fastened onto the adjustable shoe. The indicator shaft is able to move in this strip which moves with the free moving shoe, transmits this motion onto the indicator by which the value of the deformation of the bitumen film is determined. The moving shoe is connected with the lever, 5, at the other end of which there is a hook with a pan for the weights. The lever and pan are balanced by the weight, 8, suspended on a thread running through the block, 7. The block is fastened onto the stand, 6.

The stone tablets of Ignatopolskii granite were purchased for the experiment as follows: tablets of length 50 mm and width 10 mm were ground to attain a flat surface, then polished with a fine abrasive to that the roughness did not exceed 0.5 μ. The batch of bitumen to be examined was coated onto one of the pair of plates. The thickness of the bitumen layer was calculated by the formula

$$h = m/dS$$

where h is the thickness of the film (cm); m is the weighed sample (gram); d is the specific gravity of the bitumen (g/cm^3); S is the area of the table (cm^2).

Before the test, plates containing the bitumen were heated for 15-20 min in a thermostat at 130° after which the bitumen was applied and the cemented plates maintained for 24 hr at 20 ± 2°.

The investigation of the properties of a layer of bitumen between two plates of Ignatopolskii granite was carried out under two sets of experimental conditions: a gradual increase of load and a constant rate of application of the shearing stress. From the results of the experiments using gradual loading the values of the viscosity for the fractured and non-fractured bitumen structure are obtained. The conditions giving a constant rate of application of the shearing stress makes it possible to estimate the stability of the bitumen binder between two granite tablets.

Due to the fact that when the mineral-matter surface is dry the cohesion of the bitumen with this surface is always more than the internal cohesion of the bitumen, the rupture takes place along the bitumen coating. This lays the basis for the assumption that under the given experimental conditions the cohesion values of the bitumen may be obtained. A consistent load rating was applied by water at 3.3 g/sec. The load was continued until the tablet fractured. Hence the value of the maximum shearing stress at which the bitumen binder between the plates fractured was determined. Due to the fact that the results of the measurements alter with variation of the stress the cohesion values obtained are relative for a given rate.

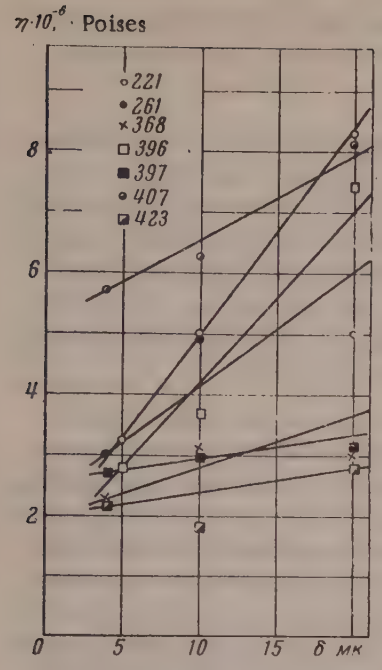


Fig. 3. Relation between the viscosity of bitumen and the thickness of the coating.

In experiments with a gradual increase of load the calculation of viscosity was carried out in the following manner: from the curve of the relation between deformation and time the values of the rate of deformation $d\epsilon/d\tau$ were calculated from the tangent of the slope of the curve at different points. The time curve was constructed in the coordinates $d\epsilon/d\tau$, p and the values of the viscosity of the nonfractured and fractured bitumen calculated. It should be noted that in regions of small shearing stress the values of the maximum viscosity η_0 are invariant for a given thickness of the layer and therefore characterize the viscosity of the unfractured structure of the bitumen.

As can be seen from Fig. 3, for all bitumens with an increase of the coating thickness on a non-reactive granite lining, the viscosity of that not fractured is increased. The viscosity of all bitumens varies linearly with the thickness of the coating. Thus the viscosity of a bitumen film of thickness 20μ is three times more than the viscosity of a bitumen coating of 10μ and 10 times more than the value for a coating of 5μ.

The behaviour of bitumen in thin coatings on the surface of mineral matter is described not only by its viscosity but also by the cohesion determining the stability of the bitumen-mineral mixtures which, in the view of a number of investigators [5] is one of the basic characteristics of highway bitumens. As we have already shown above, the determination of cohesion, as also the determination of viscosity, in large measure depends on the rate at which the load is applied. At very high loading rates the values of cohesion and viscosity obtained are high. During this time relaxation processes are not able to take place and the material behaves like a genuinely elastic body. At very small loading rates the viscosity of the bitumen drops to a minimum value corresponding completely to the fractured structure of bitumen. The cohesive value of the bitumen at very small loading rates becomes equal to zero. Consequently, the determination of cohesion at some particular loading rate is, to a considerable extent, provisional. Moreover, in determining the stability of bitumen it is impossible to entirely eliminate the effect of the viscosity on the results which are obtained.

The cohesion of the bitumen was investigated under the same conditions (5-20μ) with a loading rate of 3.3 g/ sec on a practically unreactive lining of Ignatopol'skii granite. As distinct from the viscosity, the cohesion of all the bitumens for the same range of thicknesses is less dependent on the thickness of the bitumen coating.

It is possible to assume that the main properties of the bitumen are determined by its steric structure consisting of macromolecules i.e., micelles. The motion of structural components relative to one another is conditioned by their interaction and determines the viscosity of the bitumen. The dimensions of the steric structure obviously are commensurate with the thickness of the bitumen films which we investigated and therefore a decrease in the thickness of the coating from 20 to 5μ leads to a partial rupture of this structure and consequently, to a decrease in the viscosity of the bitumen. A further decrease of the thickness of the coating must lead to a still greater rupture of the steric structure and even to separate macromolecules and micelles and, at the limit, the viscosity of the bitumen ceases to depend on the inter-molecular interaction and the viscosity becomes Newtonian in type, similar to the viscosity of bitumen at a high temperature.

From the character of the decrease of the viscosity with a reduced thickness of the coating all bitumens may be divided into two basic groups: 1) bitumens 396, 261, 407, 221 which, in a coating of 20μ, possess the highest viscosity, the value of which, rapidly falls with a reduction in the thickness of the coating; 2) bitumens 397, 423, 368, the viscosity of which alters considerably less than those in the first group as the coating is reduced in thickness. If these results are compared with those obtained from a study of the temperature dependence of viscosity it can be seen that it is precisely those bitumens the viscosities of which rapidly decrease with an increase of temperature which, to a similar degree, alter with a decrease of the thickness of the coating. On the other hand, bitumens, the viscosities of which alter comparatively little with a variation of temperature, also alter slightly with variation in the thickness of the coating.

A decrease of the inter-molecular interaction must, to a very small extent, be reflected by the stability of the structural components themselves, which determine the cohesion of the bitumen. In papers by other investigators it

was shown that the variation of the viscosity of bitumen by 2-3 orders with a decrease of temperature has a very small effect on its cohesion [5]. Therefore, a variation of the coating thickness within the relatively narrow limits of 5-20 μ which alters the viscosity of the bitumen several times (within the limits of one order), in practice must have even less of an effect on the cohesion.

However, all this is only applicable with respect to properties of bitumen in the absence of a vigorous reaction of the surface of the mineral matter. The orientation of the most polar structural components of the bitumen, due to adsorption and chemisorption processes on the surface, must lead to a significant increase of viscosity and stability of the thin coating of bitumen. Hence, the increase of viscosity and cohesion of the bitumen must depend on the active sphere of molecular forces of the mineral surface: the thinner the coating of bitumen the more the viscosity and cohesion of the bitumen must increase. The rupture of the steric structure of the bitumen with decrease of the thickness of the coating, facilitates the orientation of its separate components by the adsorption reaction of the surface of the stone materials, which in turn, leads to an increase of the stability in the thin bitumen coating.

TABLE 2. The Relation Between the Cohesion ($K \cdot 10^{-5}$ dyne/cm^2) and the Character of the Mineral Surface

The character of the mineral surface	Bitumen coating		
	5	10	20
Non-active	18.00	16.88	20.59
Active	30.73	27.52	18.88

It is necessary to note that the surface of the granite which we studied and also the surface of other acidic stone materials cannot possibly be considered as completely nonactive with respect to bitumen. However, the active radius of molecular forces of this surface is considerably less than in the case of active limestone materials and thus is decidedly less than the minimum thickness of our films (5μ). To confirm this assumption the surface of the granite tablets was modified by Ca ions from a saturated solution of $Ca(OH)_2$.

Table 2 reproduces the cohesion values of bitumen 421 in relation to thickness of its coating on granite and on linings activated with $Ca(OH)_2$.

On the lime-activated lining of mineral matter, an increase of the value of the cohesion with bitumen was observed with a decrease of its coating thickness. Consequently, the action of the active surface of the mineral matter is amplified by a layer of bitumen of a definite thickness. A further decrease of the thickness of the coating ($< 5\ \mu$) must probably lead to a still greater rise in the cohesion of the bitumen. At the same time the action of an active lining with a coating of 20μ is hardly increased.

TABLE 3. Thermomechanical Characteristics of Bitumens: The Temperature of Vitrification (T_c), the Temperature of Fluidity (T_t), and the Range of the Elastic State ($T_t - T_c$)

Bitumens	221	261	368	396	397	407	421	423	429	430
T_c, °C	20	12	10	20	15	20	25	20	15	20
$T_т$, °C	39	40	40	50	45	36	50	45	45	50
$(T_т - T_c)$, °C	19	28	30	30	30	16	25	25	30	30

Temperature has a considerable influence on the mechanical properties of bitumen and this is explained by the changes thereby occurring in the structure of the bitumens as also in other amorphous compounds. To investigate the deformation properties of bitumens the study of their thermomechanical properties was carried out over a wide range of temperatures with the help of the dynamometric balance of Kargin [6]. No pronounced breaks were found in the thermomechanical curve for bitumen but the vitreous, high elastic and viscous regions may be separated. Table 3 gives the values of the temperatures of vitrification and the range of the elastic state of different bitumens calculated from the curve.

As can be seen, the temperature of vitrification of the bitumens studied lies within the limits 10-25°. The low temperature of vitrification eliminates the possibility of forming cracks and fractures in the region of temperatures higher than T_c and consequently, in this respect the most favorable properties are possessed by bitumens 368 and 261.

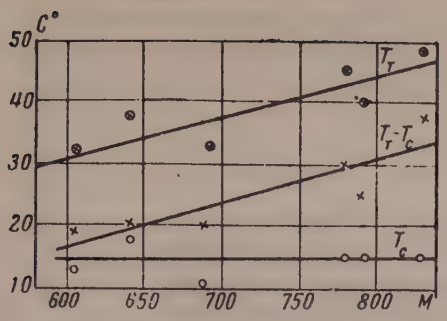


Fig. 4. The relation between the thermo-mechanical characteristics and the average molecular weight.

The fluidity temperature of bitumens lies in the range 36-50.° This temperature describes the boundary of the region of purely viscous flow of bitumen at which irreversible deformation of the bitumen-mineral lining may take place. In this respect bitumen 407 possesses especially unsatisfactory properties since irreversible deformation despite its high viscosity, already begins at 36°.

In the range of temperatures between the vitreous and fluid state the elastic properties appear which, to a certain extent, are accompanied by irreversible flow. But in this region, the deformation occurring in the bitumen under the action of external loads are mainly reversible and disappear with the removal of the load. Therefore the value of the range of elasticity characterizes the temperature range which is the most favorable for operation of the bitumen coatings. The region of temperatures $T_t - T_c$ which describes the range of elasticity of the bitumen was 16-30° in the case of the samples which we studied and the most satisfactory properties were those possessed by bitumen 407. Figure 4 shows that the temperature of vitrification does not depend on the molecular weight of the bitumens whereas the fluidity temperature increases with the increase of temperature. This result agrees well with data obtained for polymers [6]. The more the content of asphaltenes in the bitumen the higher the value of the fluidity temperature and the range of elasticity.

Thus, bitumens from different oils of the same type and described by the same State Standards, with a more thorough investigation, reveal considerable differences in chemical composition and properties. This difference is particularly noticeable in the structural-mechanical properties of bitumens: the behaviour in thin films, the thermo-mechanical properties, the variation of viscosity and of temperature.

SUMMARY

1. Road bitumens of one type differ in chemical, thermomechanical and viscous properties.

2. At a temperature less than 100° the viscosities of bitumens are determined by the difference in their steric structures due to inter-molecular reactions and do not depend on the dimensions of their structural components. At higher temperatures the viscosity increases in proportion to the increase of the average molecular weight of the bitumen. The viscosity of the bitumen increases with increased content of asphaltenes.

3. The character of the variation of the viscosities of different bitumens with decrease of coating thickness is similar to that of the variation of viscosities of these bitumens with an increase of temperature. The presence of vigorous reaction between the mineral surface and the bitumen, causing an orientation of the structural components of the bitumen in the direction of the lining, leads to an increase of viscosity and cohesion of the bitumen as the film is reduced in thickness.

4. By means of thermochemical curves the presence of three temperature regions were revealed for the bitumens: vitrification, elastic and viscous-fluid states. The fluidity temperature and the range of elasticity increases linearly with an increase of the average molecular weight.

LITERATURE CITED

1. N. N. Korotkevich, "The Viscosity of Liquids and Colloidal Solutions" (in Russian). Published by the Academy of Sciences, USSR, p. 7; M. F. Nikishina, Symposium, "The Investigation of Organic Viscous Materials and the Physicochemical Properties of Asphalt Mixtures" (In Russian), Dorizdat, 1949.
2. M. V. Mikhailov and P. A. Rebinder, Kolloidin Zhur., 17, 107, 1955; M. V. Mikhailov, ibid, p. 242; S. Ya. Shalyt, N. V. Mikhailov and P. A. Rebinder, ibid, 19, 244, 1957.
3. N. V. Gorelysheva, Symposium, "Experience in the Construction of Asphalt-Cement Linings" (In Russian), Tr. Moskovovskogo avtodorozhnogo inst. No. 23, 1958.
4. K. Latters, Bitumen, Teere, Asphalte, Peche, No. 3, 83, 1956; Ch. Makk, No. 10, 350, 1957; H. Wood Highway Research Board, Bulletin. No. 6, 10, 1958.
5. N. Ewers, Vortrag uber die Kennizeichen und Prufung bituminoser Bindenmittel, Wien, 12, 1957; K. Zichner, Allg. und Vere 5, 50, 1957.

6. V. A. Kargin and T. I. Sogolova, Zhur fiz. khimii, 23, 530, 1957; V. A. Kargin and Yu. M. Malinskii, Symposium on "The Chemistry and Physical Chemistry of High Molecular Weight Compounds" (in Russian) Published by the Academy of Sciences, USSR, 1952, V. A. Kargin and M. I. Shteding Khimicheskaya prom-st, No.3, 137, 1955.

All abbreviations of periodicals in the above bibliography are letter-by-letter transliterations of the abbreviations as given in the original Russian journal. ***Some or all of this periodical literature may well be available in English translation.*** **A complete list of the cover-to-cover English translations appears at the back of this issue.**

ADSORPTION IN THE SYSTEM $Fe_2O_3 - H_2O - CaCl_2 - NaCl$

P. S. Melshko

I. V. Stalin Crimea Medical Institute, Simferopol' Department of General Chemistry
Translated from Kolloidnyi Zhurnal, Vo. 23, No. 6,
pp. 726-731, November-December, 1961
Original article submitted May 24, 1960

In the present study we tried to find out whether sodium and calcium chloride are adsorbed simultaneously on iron hydroxide gel when submersed in a solution containing both salts or blocking of the surface by molecules (ions) of one of the dissolved substances occurs and whether the character of the observed phenomenon changes when the concentration ratios of these salts in the solution are varied. Our purpose was also to clarify whether one dissolved substance influences the adsorption of the other.

It has been established [1-3] that iron hydroxide gel adsorbs many nonelectrolytes and electrolytes added separately, in particular, calcium and sodium chloride. A freshly precipitated hydroxide gel has the highest adsorption capacity; in the course of time the capacity to adsorb a dissolved substance falls. At the same time this capacity depends on the method of preparation and the temperature at which colloidal iron hydroxide is stored.

In order to obtain comparable data on the adsorption of dissolved substances when added separately or present jointly in the solution, besides the system $Fe_2O_3 - H_2O - CaCl_2 - NaCl$, we have investigated the systems: $Fe_2O_3 - H_2O - NaCl$ and $Fe_2O_3 - H_2O - CaCl_2$. One and the same sample of iron hydroxide gel was used for studying all three systems and the experiments were done simultaneously so that the effect of aging on the adsorption capacity of the hydroxide gel and that of the preparation and storage conditions too were eliminated. Moreover, an analysis of the system $Fe_2O_3 - H_2O - CaCl_2$ or $Fe_2O_3 - H_2O - NaCl$ had to be done in order to find out the composition of the obtained iron oxide hydrate, since without knowing the oxide content in the hydrate one cannot unambiguously determine the amount adsorbed, for, as has been detected previously [2,4,5], the composition of a freshly precipitated hydroxide gel is variable and the gel may contain from two to six moles of chemically bound water per two moles iron oxide.

In order to prepare the iron hydroxide gel a molar solution of ferric chloride was poured slowly under uninterrupted stirring into a 10% ammonia solution taken 100% in excess. After 24 hours the red-brown iron hydroxide gel formed was separated from the mother liquor and pressed out. Then the gel was rinsed and decanted until chlorine ions could no longer be detected in the supernatant water and this required about a month.

The desired amount of rinsed hydroxide gel wrapped in a piece of linen was pressed between sheets of filter paper to free it from the excess water. After the preparate had been pulverized in a mortar and carefully mixed, separate portions of it were weighed in airtight vessels. Each portion was between 1 and 1.5 g. After that a solution of the substance to be adsorbed was poured into each vessel and then the latter was again closed tightly and weighed. Such an amount of the solution was taken that the adsorbent was completely submerged in the solution. Simultaneously in each series of experiments two portions of the hydroxide gel were taken to be heated in order to determine their oxide content (A). The value thus found was taken as the appropriate one for each portion of the given series of experiments. The concentration of the solutions were measured after adsorption equilibrium had been established that is, five days after they had been added to the gel. At that time the content of the vessels was repeatedly mixed by means of stirring wires passed through the stopper. Besides the concentration of the equilibrium solution (c), the concentration of the original solution (C) was determined in each experiment.

The calcium content in the solutions was determined by means of murexide and the chlorine ions were titrated argentometrically (according to Mohr). In the four-component system where both calcium and sodium chloride are present, firstly the total chloride content was determined, then that of calcium and the amount of sodium was found from the difference between the first and the second analysis. The composition of the hydrate was determined by the method of Danil'chenko [6].

TABLE 1. Results for the system $Fe_2O_3 - H_2O - NaCl$

Experiment	Weight, g		Original NaCl concentration % C	Fe_2O_3 content, %		Amount of NaCl in LS % b	Equilibrium NaCl concentration % c	Amount of NaCl adsorbed Y
	gel P_1	solution P		in gel A	in LS a			
1	1.4550	1.9248	5.09	51.50	22.17	2.90	3.44	1.30
2	1.2249	1.9775	10.00	51.50	19.70	6.18	7.54	1.45
3	1.1643	2.3262	14.90	51.50	17.18	9.93	11.97	1.48
4	1.1928	2.2895	19.77	51.50	17.15	13.19	16.01	1.47
5	1.2203	2.7798	25.11	51.50	15.71	17.45	20.91	1.41

Mean 1.45

TABLE 2. Results for the system $Fe_2O_3 - H_2O - CaCl_2$

Experiment	Weight, g		Original $CaCl_2$ concentration % C	Fe_2O_3 content, %		Amount of $CaCl_2$ in LS, % b	Equilibrium $CaCl_2$ concentration % c	Amount adsorbed Y_{CaCl_2}
	gel P_1	solution P		in Gel A	in LS a			
1	1.0642	2.2213	9.81	50.48	16.35	6.63	7.33	3.75
2	1.0273	2.5153	19.20	50.48	14.64	13.63	15.66	3.79
3	1.2388	3.1222	28.90	50.48	14.34	20.69	24.08	3.74
4	1.2922	3.5138	38.19	50.48	13.57	27.92	32 42	3.88

Mean 3.80

The amount of dissolved substance adsorbed on the colloidal gel was calculated by means of the equation

$$Y = \frac{ac - X(cb)}{a(100 - c)} \cdot 100, \qquad (1)$$

where Y is the amount of adsorbed substance in grams per 100 g hydroxide of the composition found; X the oxide content in the iron oxide hydrate; a the iron oxide content in the mixture of liquid and solid phase (mixture LS); b the content of the substance to be adsorbed in the mixture LS. The values of the parameters a and b occurring in equation (1) were calculated beforehand by using the formulas: $a = AP/(P + P_1)$ and $b = CP/(P + P_1)$ where P and P_1 are the weights of solution and hydroxide gel, respectively.

To calculate the amount adsorbed of each dissolved substance in the four-component system we used this same equation (1), but recalculated the parameters c, b, a, applying component "elimination" according to [7].

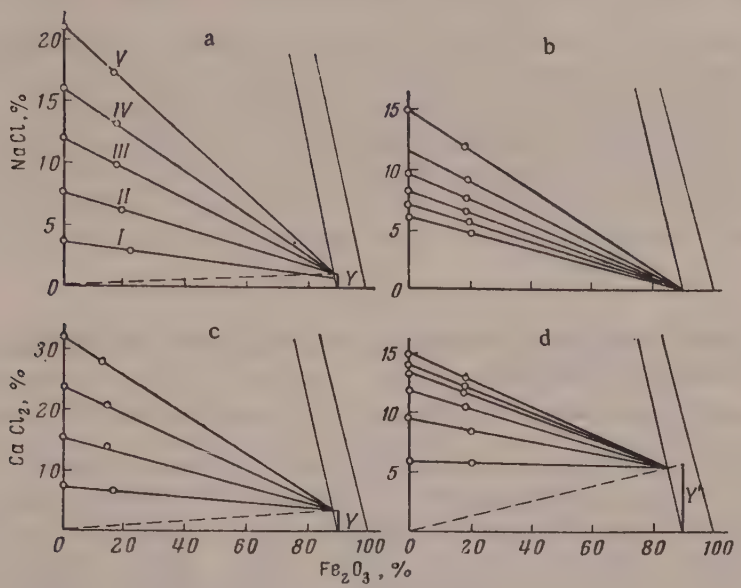
Besides calculating the adsorbed amounts of calcium and sodium chloride which interest us, by means of the formulas given above, we found them also in a graphical way [7].

When studying the system $Fe_2O_3 - H_2O - NaCl$ we carried out five series of experiments with various concentrations (from 5 to 25%) of the original sodium chloride solution. The data obtained are given in Table 1.

When determining the composition of the iron oxide hydrate by means of P.T. Danil'chenko's method in the calculation of the oxide content in the hydrate (X) we used only data from those experiments in which the adsorption limit of sodium chloride was attained. As a plot (Fig., a) shows, in experiment 1 the amount of sodium chloride adsorbed on the iron hydroxide did not attain the limit value since the straight line 1 passes below the point where the other lines intersect.

By combining the data of experiments 2-5 in all possible pairs for a calculation of X we obtained six values, which differ little: $X_{II-III} = 90.37$; $X_{II-IV} = 89.98$; $X_{II-V} = 89.71$; $X_{III-IV} = 89.75$; $X_{III-V} = 89.43$; $X_{IV-V} = 89.27$. The mean of these values $X_{mean} = 89.75$ is very close to the Fe_2O_3 content in the monohydrate of iron oxide. Hence

it follows that the colloidal hydrate which we obtained was the most stable form of iron hydroxide: $Fe_2O_3 \cdot H_2O$. For this reason, we substituted instead of X, the oxide content 89.86% found from the formula $Fe_2O_3 \cdot H_2O$ into equation [1] for all experiments, when we calculated the amount adsorbed (Y).



Graphical determination of the adsorbed amount of sodium and calcium chloride when taken separately (a, b) or present simultaneously in the solution (c, d): a) NaCl adsorption, system $Fe_2O_3 - H_2O - NaCl$; b) $CaCl_2$ adsorption, system $Fe_2O_3 - H_2O - CaCl_2$; c) NaCl adsorption, system $Fe_2O_3 - H_2O - CaCl_2 - NaCl$, $CaCl_2$ eliminated; d) $CaCl_2$ adsorption, system $Fe_2O_3 - H_2O - CaCl_2 - NaCl$, NaCl eliminated.

The values found for the amount adsorbed in the four cases agree with each other within the accuracy of the experiment and this proves that in fact, in the said experiments the adsorption limit amounting to 1.45 g sodium chloride per 100 g iron oxide monohydrate was attained. In the plot (Fig., a) this value is given by the intercept Y. In agreement with the plot, the value of Y_{NaCl} calculated for the first experiment was found to be lower than that for the other ones.

The results found by studying the system $Fe_2O_3 - H_2O - CaCl_2$ are given in Table 2 and plotted in the graph (Fig., b). Single portions of the hydroxide gel were submersed in calcium chloride solutions of various concentrations, while the smallest concentration was high enough to give attainment of the adsorption limit for calcium chloride on iron hydroxide. The concentrations of the original solutions and those at equilibrium were determined both by means of murexide and argentometrically. Both ways gave good agreement, otherwise it would have been impossible to use these methods in the study of the four-component system. As the results of the calculations and the graphical construction show, the magnitude of the adsorption limit for calcium chloride on iron hydroxide is 2.6 times higher than that for sodium chloride. But when expressed in moles these adsorption limits do not differ so much and amount to 0.034 and 0.025 mole, respectively, per 100 g iron hydroxide.

To study adsorption in the system $Fe_2O_3 - H_2O - CaCl_2 - NaCl$ we prepared six mixed solutions of calcium and sodium chloride in which the molar $CaCl_2$:NaCl ratios amounted to 1:4, 1:2, 3:4, 1:1, 5:4, 3:2 and the total salt concentration of ~24.5%. The data found for this system are given in Tables 3 and 4. When determining the adsorbed amounts of both chlorides we carried out an alternative "elimination" of one of them. At first, by "eliminating" $CaCl_2$ for each experiment we found $c_2 = 100c/(100-c')$; $b_2 = 100b/(100-b')$; $a_2 = 100a/(100-b')$. Then "eliminating" NaCl: $c_2' = 100c'/(100-c)$; $b_2' = 100b'(100-b)$; $a_2' = 100a/(100-b)$ (Table 4). By substituting the values of c_2, b_2, a_2 the amount of sodium chloride adsorbed, Y'_{NaCl}, was found.

TABLE 3. Results for the System Fe_2O_3 – H_2O – $CaCl_2$ – NaCl

Experiment	Weight, g		Fe_2O_3 content %		Original concentration %		Equilibrium concentration, %		Content in the mixture LS, %	
	gel P_1	solu. P	in gel A	in LS a	NaCl C	$CaCl_2$ C^1	NaCl c	$CaCl_2$ c'	NaCl b	$CaCl_2$ b'
1	1,1927	2,3530	54,30	18,27	16,92	7,66	14,28	5,10	11,23	5,08
2	1,2158	2,3192	54,30	18,68	12,63	11,75	10,61	8,45	8,29	7,71
3	1,2748	2,6540	54,30	17,62	10,12	14,37	8,62	10,93	6,84	9,71
4	1,3116	2,8289	54,30	17,20	8,53	15,96	7,30	12,37	5,83	10,90
5	1,4868	3,0529	54,30	17,78	7,45	17,06	6,32	13,16	5,01	11,47
6	1,4791	2,9077	54,30	18,31	6,28	18,30	5,30	14,06	4,16	12,13

TABLE 4. Data Obtained upon Recalculating the Results for the System Fe_2O_3–H_2O–$CaCl_2$–NaCl by Using Component Elimination.

Expt.	c_2	a_2	b_2	Y'_{NaCl}	c'_2	a'_2	b'_2	Y'_{CaCl_2}
	$CaCl_2$ eliminated				NaCl eliminated			
1	15,05	19,25	11,83	+0,02	5,95	20,58	5,72	5,25
2	11,59	20,24	8,98	0,00	9,45	20,36	8,41	5,37
3	9,68	19,51	7,58	+0,01	11,96	18,91	10,42	5,27
4	8,33	19,30	6,54	–0,01	13,34	18,26	11,57	5,34
5	7,28	20,08	5,66	+0,03	14,05	18,71	12,07	5,28
6	6,16	20,84	4,73	–0,01	14,85	19,10	12,66	5,34

For all six experiments the calculated values of Y'_{NaCl} were practically zero. When keeping in mind the inevitable experimental errors one should consider that such small deviations from zero as are found for our experiments indicate that no adsorption of sodium chloride takes place in the system discussed.

The calculation of the amount of calcium chloride adsorbed, Y'_{CaCl_2}, led to different results; in all cases the values of Y'_{CaCl_2} found are nearly equal and their mean is 5.3.

The plots (Fig. c and d) graphically confirm the data found in the calculations.

When treating graphically the experimental results we might have plotted in one and the same triangular diagram the data of all six experiments refering to both dissolved substances by using the values of a, b, c and b', c' [7] and thus we would have found both parameters Y'_{NaCl} and Y'_{CaCl_2} which interest us. Since in our experiments the total concentration was always the same, the data of the separate experiments would overlap. To avoid this one would be obliged to construct a separate plot for each experiment. Another possibility is to plot the values of c_2, b_2, a_2 and those of c'_2, b'_2, a'_2 calculated for all experiments in two separate diagrams [7] plotting in one of them the amounts of NaCl adsorbed and those of $CaCl_2$ in the other diagram. We used the latter method.

In the plot (Fig. c) all straight lines for the composition of the mixture LS intersect in a point lying on the horizontal base of the triangle and this indicates that the adsorbed amount of the dissolved substance, in this case NaCl, is zero. The graphically determined value of the adsorbed amount of calcium chloride (Fig. d) being equal to 5.3 is also in good agreement with that calculated.

The data found by studying the system Fe_2O_3 – H_2O – $CaCl_2$ –NaCl show that from the two dissolved substances in this system at various ratios of their concentrations only calcium chloride is adsorbed and the amount of sodium chloride adsorbed is zero. Blocking of the hydroxide gel surface by calcium ions takes place even at the lowest concentration of the said ions in the equilibrium solution (5.1% $CaCl_2$) and the highest sodium ion concentration (14.28% NaCl) at the molar ratio $CaCl_2$:NaCl = 1:5. However, when the solution contains no other salts, sodium chloride is very markedly adsorbed by the iron hydroxide gel (1.45 g NaCl per 100 g $Fe_2O_3 \cdot H_2O$).

Blocking of the iron hydroxide gel by calcium ions was proved by Danil'chenko and Fridman [8], who have studied the system $Fe_2O_3 - H_2O - CaCl_2 - NaCl$ by the method of a "fourth component". By using the same method Boiko [9, 10] came to similar conclusion, but, unlike the first two authors, he stated that in the said system negative adsorption of sodium chloride occurs. Moreover, Boiko's conclusion that one of the two substances present in the solution is adsorbed negatively refers not only to the said system but he even extends it to all cases where another dissolved substance is adsorbed positively. Boiko's statement is not confirmed in our experiments.

The high value of the amount of calcium chloride adsorbed in the four-component system, which markedly surpasses that in the system $Fe_2O_3 - H_2O - CaCl_2$ (5.3 and 3.8, respectively), attracts attention. Such a noticeable rise in the amount of calcium chloride adsorbed on the surface of the colloidal iron hydroxide gel can only be explained by an effect of the sodium chloride present in the system (as has been pointed out, the effect of other factors was eliminated). Moreover, the amount of calcium chloride adsorbed in the system $Fe_2O_3 - H_2O - CaCl_2 - NaCl$ appeared to be almost exactly equal to the sum of the amounts of calcium and sodium chloride adsorbed, when these substances are added singly. Further experiments will show whether this is accidental or expresses a certain regularity.

SUMMARY

1. It has been established that in the system $Fe_2O_3 - H_2O - NaCl - CaCl_2$ the surface of colloidal iron hydroxide gel is blocked by calcium chloride: no NaCl is adsorbed. However, when there are no other dissolved substances, sodium chloride is markedly adsorbed by iron hydroxide (1.45 g NaCl per 100 g $Fe_2O_3 \cdot H_2O$)

2. The amount of calcium chloride adsorbed in the system $Fe_2O_3 - H_2O - CaCl_2$ is considerably greater than that in they system $Fe_2O_3 - H_2O - CaCl_2$. This difference can only be explained by the presence of sodium chloride, since other factors (aging of the hydroxide gel, the conditions of its preparation and storage) were eliminated.

3. The amount of $CaCl_2$ adsorbed in the system $Fe_2O_3 - H_2O - CaCl_2 - NaCl$ was almost exactly equal to the sum of the amounts of $CaCl_2$ and NaCl adsorbed in the ternary systems.

LITERATURE CITED

1. P. T. Danil'chenko and M. I. Bulygina, Izv. Krymskogo ped. inst. 13, 73 (1948).
2. P. S. Meleshko, Amorphous Iron Oxide Hydrates, Dissertation [in Russian] (IONKh, Acad. Sci. USSR Press, 1948).
3. P. S. Meleshko, Izv. Krymskogo ped. inst. Simferopol', 13, 113 (1948).
4. P. T. Danil'chenko and P. S. Meleshko, Tr. Krymskogo filiala AN SSSR, 4, 3 (1953).
5. P. S. Meleshko, Dokl. AN SSSR, 124, 1071 (1959).
6. P. T. Danil'chenko, Zh. analit. khimii, 2, 299 (1947).
7. P. S. Meleshko, Kolloidn. zh. 20, 728 (1958).
8. P. T. Danil'chenko and G. B. Fridman, Kolloidn. zh. 10, 7 (1948).
9. V. F. Boiko, Zh. fiz. khimii, 32, 35 (1958).
10. V. F. Boiko, Zh. obshch. khimii, 29, 1400 (1959).

All abbreviations of periodicals in the above bibliography are letter-by-letter transliterations of the abbreviations as given in the original Russian journal. ***Some or all of this periodical literature may well be available in English translation.*** **A complete list of the cover-to-cover English translations appears at the back of this issue.**

STUDIES ON THE STABILITY AND COAGULATION OF SYNTHETIC LATEXES

1. EFFECT OF ADSORPTIVE SATURATION OF THE GLOBULE SURFACE BY THE EMULSIFIER

R. É. Neiman, O. A. Lyashenko, A. P. Kirdeeva, A. K. Egorov and O. G. Kiseleva

Voronezh University, Chemical Department, Laboratory of High-Molecular Compounds

Translated from Kolloidnyi Zhurnal, Vol. 23, No. 6, pp. 732-738, November-December, 1961
Original article submitted August 27, 1960

There exist various opinions on the reasons why synthetic latexes are stable. Many authors relate it to the effect of electrostatic factors resulting because an electric double layer of ions exists at the surface of the globules. Here usually the ζ-potential of the globules is taken as a measure of the stability [1], although this view meets objection. So, Deryagin [2], in connection with the theory of stability and coagulation which he has developed, finds that the ζ-potential generally is not the main factor and the stability criterion for lyophilic colloids. According to another point of view [3], the stability of synthetic latexes is in an essential way connected with the structural-mechanical properties of the adsorbed emulsifier layer on the surface of the globules. This opinion joins the known ideas of Rebinder and his school [4] on the reason why concentrated emulsions are stable. Glikman and Korchagina [5] came to the conclusion that coagulation of synthetic latexes by electrolytes proceeds in two stages: the first stage is connected with the lowering of the ζ-potential and results in the formation of primary particles, the second stage consists in the coagulation of these particles. We have found [6] that in the slow coagulation of a diluted latex by electrolytes, there is obviously a combined effect of various stabilization factors; consequently the process proceeds in two stages. In order to clarify further the relative roles of the various stabilization factors we have investigated the effect which varying over a broad range the degree of adsorptive saturation of the globule surface by the emulsifier has on some properties of the latex, in particular, on the kinetics of the slow coagulation of a diluted latex by electrolyte.

In the present communication the results obtained are reported.

We studied samples of the divinylstyrene latex SKS-30 - AP (emulsifier:Nekal).* The degree to which the globule surface was saturated with emulsifier was determined by titrating [7] the latexes adsorptively with a solution of Nekal in water using surface tension as indicator. This tension was measured by the method of maximum bubble pressure. The Nekal content in the latexes (which must be known for the calculation of the adsorptive saturation) was determined by colorimetrizing a chloroform extract of the complex compound of sodium dibutylnaphthalenesulfonate (Nekal) with methylene blue. Nekal was extracted from the latex by means of butanol. The degree to which the globule surface was saturated with the emulsifier was measured in two ways.

1. The latex was dialyzed 50 days under repeated periodical renewal of the dialyzate. In this way not only electrolytes but also considerable amounts of emulsifier are removed from the latex. So, in our experiment the saturation of the latex globules with emulsifier was lowered from 70% at the start to 19% after 50 days of dialysis. The dialyzed latex was divided into several portions to which various amounts of Nekal were added. Thus we obtained nine latex samples with various emulsifier content, and, consequently, with various degrees of adsorptive saturation of the globule surface. In Fig. 1 this degree is plotted versus the emulsifier content in the latex. As is evident from Fig. 1, samples 7-9 are characterized by an excess of emulsifier present in the water phase.**

*Dry residue 16%

**If one does not assume that polymolecular adsorption layers can be formed on the globule surface.

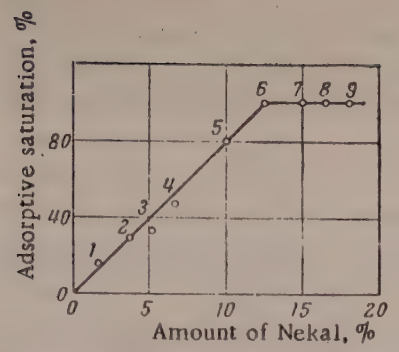


Fig. 1. Adsorptive saturation of the surface of the divinylstyrene latex globules plotted versus the emulsifier content. Here and in the other figures the Nekal content in the latex is expressed as percent rubber.

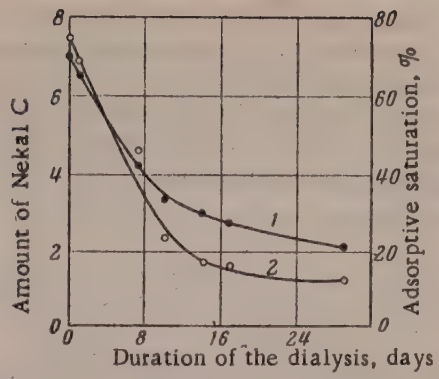


Fig. 2. Change in the amount of emulsifier and adsorptive saturation of the latex in the course of the dialysis: 1) Nekal content in the latex; 2) adsorptive saturation of the globule surface.

2. The latex was exposed to a dialysis during which samples were drawn periodically. The curves of Fig. 2,c characterize the kinetics of emulsifier removal from the latex in the course of the dialysis and, correspondingly, the decrease of adsorptive saturation. In this case we arranged the latex samples in the order of their adsorptive saturations varying from the initial value (~75%) to the minimum one (~11%) at the end of the dialysis. Of course, in this series there were no latex samples having a completely saturated adsorbed layer of emulsifier.

We have studied the effect of the emulsifier content in the latexes (the degree of adsorptive saturation of the globule surface) on the kinetics of the slow coagulation in diluted latexes, the electrophoretic mobility of the globules and surface tension.

The coagulation kinetics of diluted latexes was studied by light scattering. The turbidity was measured in a NFM nephelometer. The latex sample tested was diluted 10^4 times, $CaCl_2$ or NaCl was added and the change in turbidity with time was observed up to complete coagulation. The results of parallel experiments done with and without stirring agreed well. From the turbidity data we determined the mean globule radius. The concentration gradient of the refractive index of the dispersions, which is indespensable in these calculations, was determined by means of an IRF-23 refractometer.

The electrophoretic mobility of the latex globules was determined by macroelectrophoresis in the equipment of Rabinovich and Fodiman [8]. All latex samples tested containing various amounts of emulsifier were diluted to the concentration 2.7% with a phosphate-borate buffer mixture. The buffer mixtures were chosen in such a way that in all latex samples made ready for the electrophoretic test the ionic strength was 0.08 and pH 6.6. As reference liquid we took the same buffer mixtures correspondingly diluted to the same ionic strength. Usually the current during electrophoresis was 2-4 ma. The potential gradient at which electrophoresis was carried out was determined in the usual way from the current, the specific electric conductivity of the dispersion tested and the cross-sectional area of the electrophoretic tube.

The ζ-potential was calculated from the electrophoretic data by Henry's formula [9]. The numberical coefficient in this formula was chosen in accordance with the experimental conditions (composition of the buffer mixture, ionic strength, globule radius) [10].

The electrophoretic measurements were carried out only with the latexes obtained in the first experiment by adding various amounts of Nekal to the latex after it had been dialyzed for fifty days. For the latexes obtained in the second experiment electrophoretic measurements could not be expected to be fully reliable, because it is impossible to maintain a constant ionic strength for samples exposed to dialysis during a variable time.

In Fig. 3 it is shown how the turbidity changes during the coagulation of latexes with various emulsifier contents. Curves 1-5 refer to latexes having an unsaturated layer of emulsifier on the globule surface. Their shape allows us to distinguish two stages in the slow coagulation of these latexes, which sharply differ from each other in kinetics (demarcation point "a"). The globule agglomeration arising in the presence of an electrolyte is sharply

retarded after some time [6]. Since the latexes discussed have no saturated layer of emulsifier, the reason for the observed retardation of the agglomeration started (further on we will call it primary agglomeration) may be connected with the fact that the primary contacts between the globules arise at the surface regions not protected by the emulsifier. The increased degree of saturation with emulsifier hereby caused results in the formation of primary aggregates the surface of which are covered by saturated adsorbed layers. This, obviously, marks completion of the first stage in the slow coagulation.

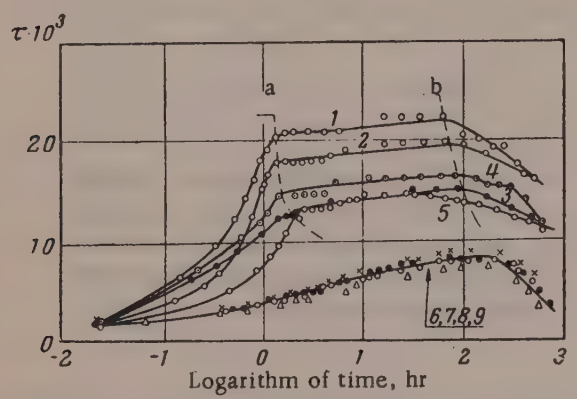


Fig. 3. Kinetics of turbidity change in the coagulation of diluted latexes by $CaCl_2$ (for the numbering of the curves, see Fig. 1). $CaCl_2$ concentration 2.3 m mole/liter.

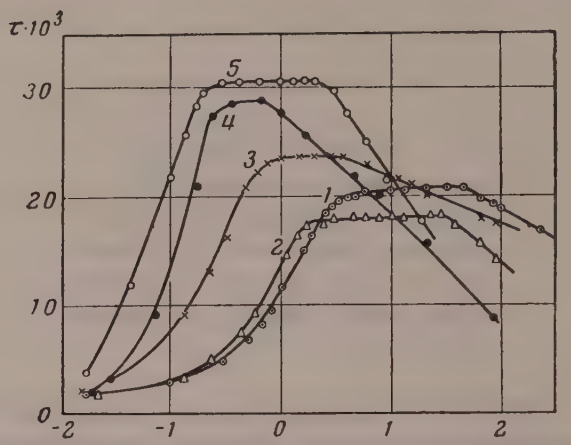


Fig. 4. Kinetics of coagulating diluted latexes by $CaCl_2$ (for the numbering of the curves and the $CaCl_2$ concentration see the table).

The duration of the primary agglomeration period is prolonged when the degree of adsorptive saturation of the globule surface with emulsifier is raised. Under our experimental conditions in the samples with a small emulsifier content the primary agglomeration lasts 80-85 min. The time required for completion of the first stage in the slow coagulation begins to increase markedly at about 35-40% adsorptive saturation. Evidently, at a raised initial saturation of the globule surface with emulsifier the probability that the globules make contact at nonprotected regions of their surfaces decreases. Therefore, at a raised emulsifier content in the latex the primary agglomeration, being completed by the formation of aggregates the surfaces of which are covered with a saturated adsorbed-solvated layer of emulsifier, will slow down. The size of these primary aggregates (calculated from the points a, Fig. 3) increases when the initial saturation of the globule surface with emulsifier is lowered. This should be expected when primary agglomeration takes place at the nonprotected regions of the globule surface. By comparing the radii of the primary aggregates formed with those of the latex globules before coagulation one may determine * the mean coefficient of the primary agglomeration, that is, the ratio of the mean aggregate volume to that of the globules or, which is the same, the mean number of initial globules agglomerating to one aggregate. From the data given it is clear that the coefficient of the primary agglomeration depends on the initial adsorptive saturation of the globule surface with emulsifier and will decrease when the latter is raised. So, for sample 1 (adsorptive saturation less than 20%) the said coefficient is 22 and for sample 5 (80% saturation) it is 12.

The second coagulation stage for all these latexes (beyond point a on the turbidity curves 1-5, Fig. 3) proceeds much more slowly. Obviously, this must be caused by the necessity to surmount an additional potential barrier connected with the structural-mechanical properties of the saturated adsorption-hydration film on the surface created by the emulsifier and with its repulsive force of nonelectrostatic origin. The latter barriers originate from polymolecular hydration shells [2, 11].

When under the conditions of our experiments the primary agglomeration stage lasts 80-150 min (being prolonged at a raised emulsifier content), coagulation is completed after 3-4 days. The ratio of these times characterizes to a certain extent the protective effect of the saturated-hydrated layer of emulsifier, the completion of which, in our opinion, determines the natural frontier between the two stages of the slow coagulation in diluted latexes.

*The mean globule radius of this batch of dialyzed latex before the coagulation experiments was determined from turbidity data. For all samples 1-9 with the varied Nekal content this radius was found to be 20 mμ.

In this respect the second coagulation stage should differ essentially from the first one in its mechanism. The initial coagulation stage is characterized by the fact that at the addition of the coagulating electrolyte to the latex the thickness of the ionic atmospheres decreases and, correspondingly, the action radius of the electrostatic repulsion forces is shortened [2] and the possibility arises of attraction forces coming into the picture and the globules making contact when they approach. But even in latexes in which the initial coverage of the globule surface with emulsifier is small a new potential barrier arises in the course of an initiated agglomeration; the coagulation passes to the second stage the course of which depends essentially on the properties of the saturated adsorbed-hydrated shell formed by the emulsifier on the surface of the primary agglomerates.

This situation is confirmed by the results obtained for the latex samples 6-9 which have a saturated adsorbed emulsifier layer.

When a saturated film of adsorbed emulsifier already exists at the very beginning on the surface of the latex globules, then primary agglomeration in the sense discussed above should not occur.* The samples 6-9 (Fig. 3) give practically coinciding curves for the change in turbidity with time in which the initial region of sharply rising turbidity followed by a pronounced retardation (which is characteristic for the curves 1-5) is absent. It can be easily seen that the curve 6-9 corresponds to the regions of curves 1-5 beyond the points a. In other words, when a saturated layer of adsorbed emulsifier is present, the slow coagulation of a diluted latex skips the stage of primary agglomeration and starts at once with the second stage.

Surmounting the electrostatic repulsion of the ionic atmospheres together with surmounting the nonelectrostatic barrier resulting from the properties of the saturated adsorption-hydrated shell in this case too should be one of the two prerequisites for agglomeration.

The coagulation of all these samples in general is completed after the same time period (under the conditions of our experiments after about seven days). Meanwhile the particles sizes in samples 6-9 before completion of the coagulation are the same. So, the presence of various amounts of emulsifier in excess in these samples, obviously has no substantial effect on the course of coagulation.

It may be supposed that the structure of the products obtained in the coagulation of adsorptively saturated latexes should differ to a certain extent from that obtained from nonsaturated (and, consequently, having passed through the stage of primary agglomeration) latexes.

The slow coagulation of the latexes obtained at various durations of dialysis in the second experiment proceeds quite similarly to that in the samples 1-5 from the first experiment (Fig. 4, Table).

Here too one observes two coagulation stages. When the adsorptive saturation is lowered, the period of primary globule agglomeration is shortened and the sizes of the formed primary aggregates become greater (see Table). Meanwhile, as should be expected, the coefficient of primary agglomeration increases, as the duration of the dialysis is prolonged so that adsorptive saturation is lowered.

It has been found [6] that coagulation of a diluted divinylstyrene latex by $CaCl_2$ or NaCl gives identical kinetic curves**. This was also confirmed in the present study by experiments in which the original latex and the latex after 29 days of dialysis were coagulated by means of NaCl. The parameters characterizing the primary agglomeration depend in a similar way on the degree of adsorptive saturation, only a much higher concentration is required in the case of NaCl.

The radius of the latex globules shows practically no change during dialysis (table), that is, no spontaneous agglomeration of the globules was found. In the present investigation the further behavior of nondialyzed and dialyzed latexes was not observed.

*Upon diluting the latex the degree of adsorptive saturation is lowered because of emulsifier desorption. When the latex becomes adorptively saturated, this has a corresponding effect on the course of coagulation.

**This indicates that in our case coagulation by $CaCl_2$ has no special feature which might be ascribed to the formation of insoluble calcium dibutylnaphthalenesulphonate. Possibly, a specific effect of this kind would occur at higher concentrations, that is, in coagulations of nondiluted latexes, but this question requires a special discussion.

Adsorptive Saturation and Coagulation of Latexes as a Function of the Duration of Dialysis.

Sample	Duration of dialysis, days	Adsorptive saturation	Mean globule radius mμ	Coagulation of the 10^4 times diluted latex by $CaCl_2$ (2.3 mmole/liter)		
				Duration of the primary agglomeration, min	Coefficient of primary agglomeration	Coefficient of primary agglomeration
1	0	75	20*	158	43*	10
2	1	70	20	107	44	11
3	7	47	21	43	54	17
4	10	24	22	18	57	18
5	29	11	21	12	58	21

*A calculation by the method described in the paper [13] gives somewhat higher values.

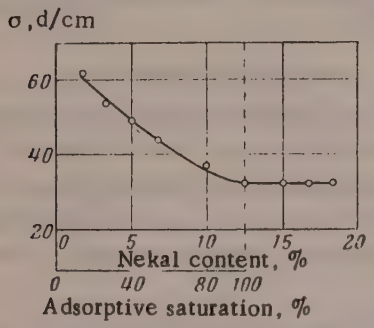


Fig. 5. The surface tension of the latexes plotted versus the emulsifier content. Latex concentration 5.4%

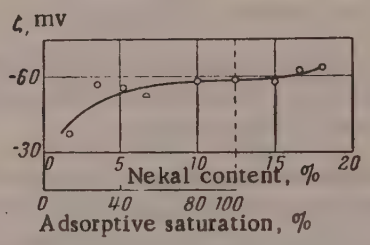


Fig. 6. The ζ-potential of the globules plotted versus the emulsifier content in the latex.

We have also studied the effect which the emulsifier content has on the surface tension and the electrophoretic mobility of the globules in latexes obtained in the first experiment.

The plot of the surface tension versus the amount of emulsifier in the latex, as is shown in Fig. 5, gives a good confirmation of the adsorptive titration data from which the degree of adsorptive saturation of the globule surface was determined. Upon raising the emulsifier content one gets adsorptively saturated latexes, the surface tension of which practically does not depend on the amount of emulsifier in excess.

The plot of the ζ-potential versus the emulsifier content in the latex (Fig. 6) shows that this potential changes little when the degree of adsorptive saturation of the globule surface is varied over a broad range So, from 65 mv for adsorptively saturated latexes containing emulsifier in excess the ζ-potential drops to 55-57 mv for latexes with 25-30% adsorptive saturation. Only at the very smallest degree of saturation a somewhat greater lowering of the ζ-potential is found. In particular, no special changes in the ζ-potential were detected upon passing from nonsaturated to adsorptively saturated latexes. So, in our experiments, in contrast to the paper [12], no lowering of the electrophoretic mobility and the globule ζ-potential was found at a raised emulsifier content in the latex.

SUMMARY

1. It has been studied how the kinetics of coagulating diluted divinylstyrene latexes by an electrolyte depend on the extent to which the globule surface is saturated by adsorbed emulsifier.

2. The coagulation of adsorptively nonsaturated latexes proceeds in two stages: primary and secondary agglomeration. An explanation for this phenomenon has been proposed.

3. In the coagulation of adsorptively saturated latexes the primary agglomeration stage no longer occurs.

4. It has been supposed that the nonelectrostatic barrier connected with the structure and the properties of saturated adsorbed-hydrated shells on the globule surface (or on that of primary aggregates from the latter) as one of the stability factors, is of general importance in the coagulation of divinylstyrene latexes.

5. The ζ-potential of the globules changes little when the degree of adsorptive saturation of the latex is varied over a broad range.

LITERATURE CITED

1. S. S. Voyutskii and R. M. Panich, Uspekhi khimii, 25, 57 (1956); Kolloidn. zh. 19, 113, (1957).
2. B. V. Deryagin, Transactions of the Third All-Union Conference on Colloid Chemistry [in Russian] (Acad. Sci. USSR Press, 1956), p. 225.
3. E. M. Aleksandrova and P. V. Mochalov, Kolloidn. zh. 16, 161 (1954).
4. P. A. Rebinder, Collection: Colloids in the Food Industry Vol. 2 [in Russian] (1949), p. 21.
5. S. A. Glikman and E. P. Korchagina, Kolloidn. zh. 19, 657 (1957).
6. R. E. Neiman and O. A. Lyachenko, Kolloidn. zh. 22, 757 (1960).
7. W. D. Harkins, J. Amer. Chem. Soc. 69, 1428, 1947.
8. A. I. Rabinovich and E. V. Fodiman, Zh. fiz. khimii, 2, 336 (1931).
9. D. C. Henry, Proc. Roy. Soc., London, 133, 106, 1931.
10. J. T. G. Overbeek, Advances in Coll. Science, N. J., 3, 97, 1950.
11. B. V. Deryagin and A. S. Titievskaya, Kolloidn. zh. 15, 416 (1953).
12. S. H. Maron, W. W. Bowler, J. Amer. Chem. Soc. 70, 3893, 1948.
13. I. Ya. Slonim, Optika i spektroskopiya, 8, 98 (1960).

All abbreviations of periodicals in the above bibliography are letter-by-letter transliterations of the abbreviations as given in the original Russian journal. *Some or all of this periodical literature may well be available in English translation.* A complete list of the cover-to-cover English translations appears at the back of this issue.

RELATION BETWEEN SOLUTE STRUCTURE AND ADSORPTION FROM AQUEOUS SOLUTIONS

1. DEPENDENCE OF THE ADSORPTION OF BENZENE DERIVATIVES UPON THE DISSOCIATION OF FUNCTIONAL GROUPS

T. M. Rovinskaya and A. M. Koganovskii

Institute of General and Inorganic Chemistry, Academy of Sciences USSR, Kiev
Translated from Kolloidnyi Zhurnal, Vol. 23, No. 6,
pp. 739-748, November-December, 1961
Original article submitted June 25, 1960

One of the actual problems in the theory of adsorption from solutions is to find out the relation between the structure of dissolved substances and their adsorbability. Owing to thermodynamic studies of the last years, in principle, the adsorption isotherm and the energetic effects, too, connected with adsorption of gases and vapors may be calculated theoretically [1-3].

The solution of the analogous problem for adsorption from solutions is considerably complicated by electrolytic dissociation of ionic groups, solvation of the adsorbate molecule and adsorbent surface.

The first two factors are of great importance in the adsorption of organic substances from aqueous solutions by nonpolar adsorbents. It should also be taken into account that many organic compounds, aromatic ones among them, are weak electrolytes and the activity of their solutions, on which the adsorption equilibrium depends, is determined first of all by the conditions of the electrolytic dissociation of the corresponding functional groups. Only those solutions which have the properties of colloidal electrolytes form an exception; their activity even at great dilutions does not originate from electrolytic dissociation but from association to micelles of various kinds. This fact has not been taken into account in the papers published until now [4].

We undertook to investigate adsorption of organic compounds from aqueous solutions by coal in order to find out how the chief thermodynamic characteristics of the adsorbability depend on the structural parameters of the molecules. In this communication we report results obtained when measuring on the ash-free, activated coal KAD (abbreviation meaning 'granular activated coal') the adsorption of benzene derivatives with one or two ionogenic functional groups in the ring.

The adsorption isotherms of all substances studied are expressed in terms of the specific adsorption (Γ, mmole/m^2) as a function of the activity (a) in the solution. The activity of the studied substances in aqueous solutions coincides with the concentration of undissociated molecules (c_{ud}), since in water there is no association or only so little that it may be neglected [5]. The concentration of the undissociated molecules was calculated from dissociation constants of the functional groups based on the experimentally determined values of pH in the solutions at equilibrium. The adsorbates (aniline, p-toluidine, p-methoxyaniline, p-chloraniline, phenol, p-nitrophenol, p-hydroxybenzoic and o-hydroxybenzoic acid, p-aminobenzoic acid and sulfanilic acid) were purified by repeated distillations and recrystallizations. For the investigation we took fractions the boiling (or melting) points of which did not differ more than 0.5° from the data in the literature.

The KAD coal (the fraction with 0.2-0.5 mm particles) was freed from ash by consecutive treatments with 2 N nitric acid and concentrated hydrofluoric acid during three days, then by washing out it was freed from fluorine ions and dried at 110°. The residual ash in the coal was 0.32%. Upon shaking a portion of the coal with distilled water during three hours the pH did not change. The capacity limit of the coal with respect to chlorine ions was 0.15 mg-eq/g. Cations were not sorbed by the coal.

The specific surface area of the coal was determined by measuring the adsorption of benzene vapor on a spring balance. In this case we thought it most suitable to use benzene for measuring the surface area, since the coal was

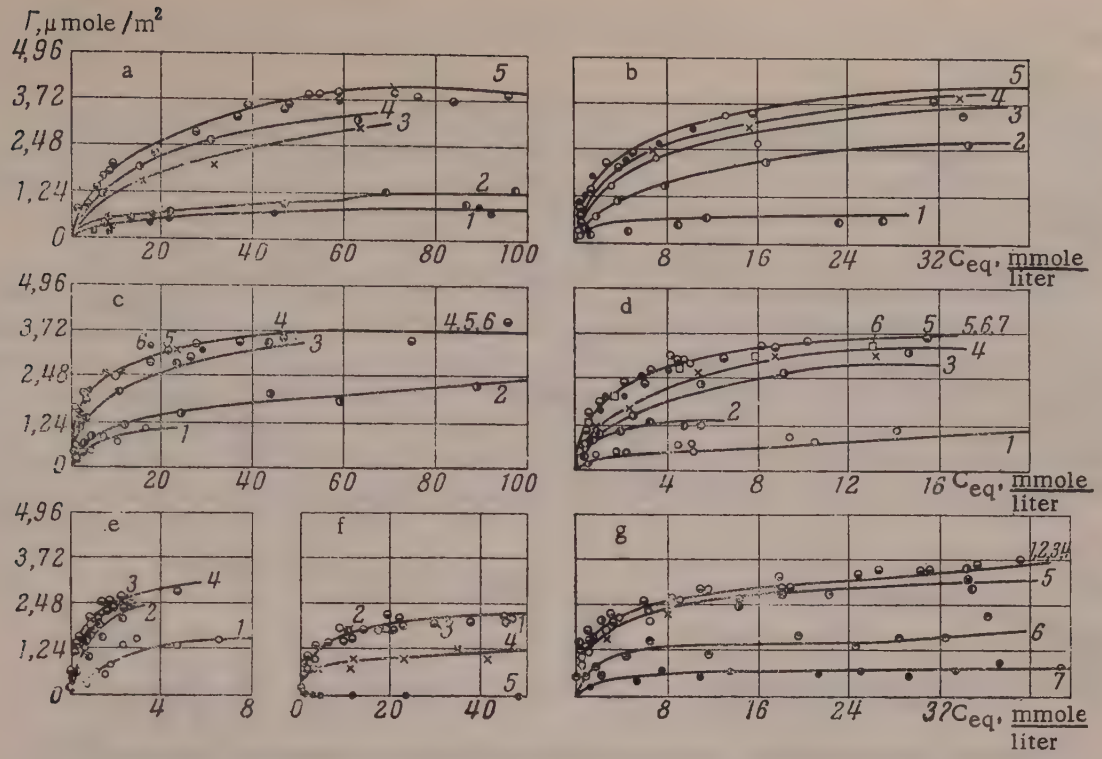


Fig. 1. The specific amount adsorbed plotted versus the total equilibrium concentration at various pH of the solutions: a) aniline: 1) 0; 2) 2.75-2.8; 3) 4.6; 4) 5.75; 5) 8-7.2. b) p-toluidine: 1) 3.85-3.9; 2) 4.4-4.6; 3) 5-5.1; 4) 5.5; 5) 6.9-7.6. c) p-methoxyaniline: 1) 0; 2) 3.3-3.8; 3) 5.1-5.3; 4) 7; 5) 9-12; 6) 14. d) p-chloraniline: 1) 0; 2) 2.5-2.8; 3) 3.7-3.85; 4) 3.95-4.4; 5) 5-7; e) p-nitroaniline: 1) 0; 2) 2.25-2.7; 3) 3; 4) 6.8-7.0. f) phenol; 1) 0; 2) 2.25-3.4; 3) 4.1-4.7; 4) 9.2-9.4; 5) 14. g) p-nitrophenol: 1) 0; 2) 1.8-3; 3) 2.3; 4) 2-4; 5) 6.9-7.35; 6) 7.1-8.9; 7) 14.

destined for adsorption of benzene derivatives, that is, for molecules of the same type with nearly the same sizes. Therefore, it might be expected that in the porous adsorbent practically the entire surface measured will be accessible to the molecules of the substances to be adsorbed. The surface area of the adsorbent was calculated by means of the BET equation. From the diverse values for the area of a benzene molecule, which vary from 30.3 to 46.5 A^2 [2, 6, 7], we chose 40 A^2.

The assumption of a spherical symmetry for the benzene molecule, as is used in the calculation giving the molecular area of 30.3 A^2, does not correspond to reality, since many data [8] indicate that the benzene ring of a molecule adsorbed on coal-air or coal-water boundary surfaces is oriented flatly.

Before we determined the adsorption equilibrium, equal portions of the activated coal were shaken mechanically during three hours at 25 ± 1° in a thermostated apparatus with solutions containing various adsorbate concentrations. By special experiments it had been established that after this time the equilibrium had been attained. After the shaking the solution was filtered from the coal through an ash-free filter and the first 10-15 ml of the filtrate were not used in the analysis. The concentration of aniline and all its derivatives was determined by diazotization using the "dead-stop" method [9]. Moreover, the concentration of p-nitroaniline was also determined by diazotization with iodine-starch paper as an indicator. The concentrations of phenol and nitrophenol were determined by a bromide-bromate countertitration. The concentrations of salicylic and p-benzoic acid were found by a titration with a sodium hydroxide solution in the presence of phenolphthalein, after the previously dissolved carbon dioxide had been removed by boiling with a reflux cooler. The concentrations of p-aminobenzoic, o-aminobenzoic, and sulfanilic acids were determined by dead-stop [9] diazotization. Very low adsorbate concentrations were determined colorimetrically.

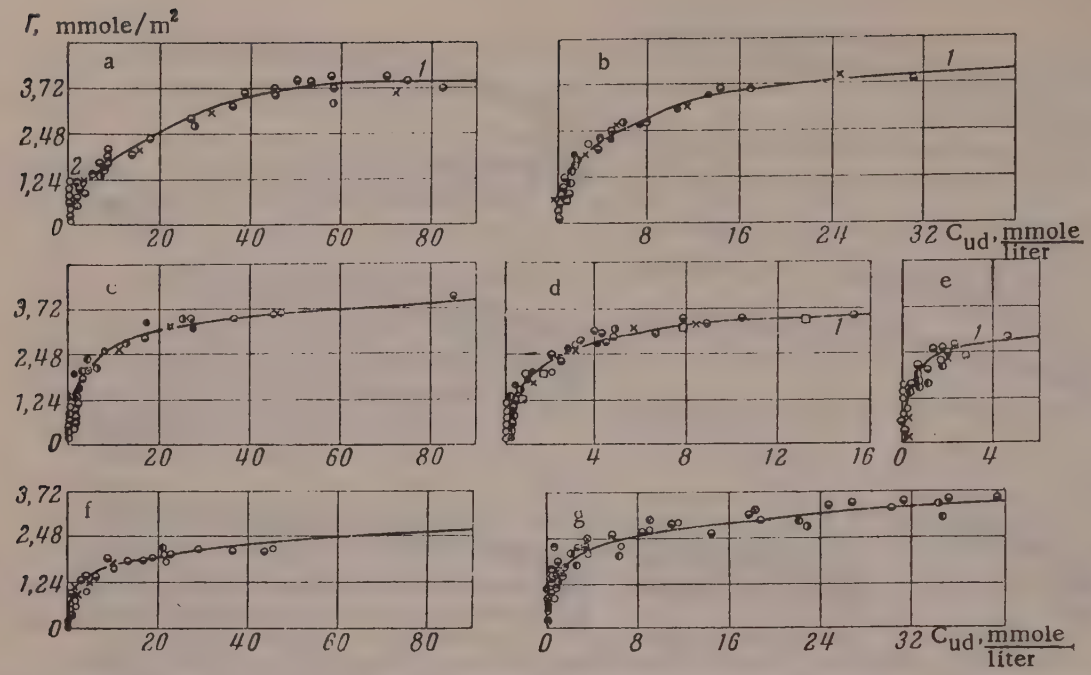


Fig. 2. The specific amount adsorbed plotted versus the equilibrium concentration of undissociated molecules at various pH: aniline (a), p-toluidine (b), p-methoxyaniline (c), p-chloraniline (d), p-nitroaniline (e), phenol (f), and p-nitroaniline (g). (the marking of the points is the same as that in Fig. 1).

In each equilibrium solution the pH was measured by means of an antimony oxide electrode which every day was calibrated in a buffer mixture. The pH of the solutionswere varied by adding hydrochloric acid or sodium hydroxide.

The isotherms for the adsorption from aqueous solutions of aniline and phenol derivatives which are substituted in the ring and have one ionogenic functional group are plotted in Fig. 1 as the specific amount adsorbed (Γ) versus equilibrium concentration C_{eq}.

To calculate the concentrations of undissociated molecules in the equilibrium solutions from the pH measurements we used the values known in the literature for the dissociation constants (K_d).

The value of K_d for an NH_2-group was calculated from the adsorption measurements.

The adsorption isotherms of aniline and phenol derivatives the molecules of which have only one ionogenic functional group are plotted in Fig. 2 in the form of Γ versus C_{ud}.

Upon comparing the adsorption isotherms of these substances as a function of the analytically determined concentration at various pH with those plotted as a function of the concentration of undissociated molecules it is evident that by applying a correction for the degree of dissociation the activity of benzene derivatives in aqueous solutions is quite fully taken into account. This is proved by the fact that for each substance the isotherms measured at various pH coincide, if they are plotted in the coordinates $\Gamma = f(C_{ud})$.

So, it may be said with certainty that in the broad pH range in which the adsorption isotherms coincide only undissociated molecules are adsorbed. When studying the adsorption of aliphatic amines Phelps [10] came to a similar conclusion. But from our data it follows that in those solutions where no undissociated molecules occur the dissociated molecules of aromatic amines and even nitrophenols (but not phenol) are adsorbed quite strongly. This is evident from the fact that adsorption of the amines is also found in a 2 N solution of hydrochloric acid (pH ~0) and adsorption of nitrophenols still occurs even at pH~14 (from 2 N hydroxide solutions), that is, under such conditions that the substance is dissociated completely. When the adsorption isotherm of the completely dissociated substances are plotted in the coordinates $\Gamma = f(C_{ud})$, all values of the specific amount adsorbed (attaining 0.7-1.25 μmole/m²)

lie on the ordinate axis $C_{ud} = 0$, whereas in the coordinates $\Gamma = f(C_{eq})$ these isotherms have the usual convex shape. From this point of view the sharp decrease in the adsorption of p-nitroaniline at raised pH in alkaline solutions is of interest.

As is evident from the isotherms shown in Fig. 3, in the presence of 2N sodium hydroxide there is practically no adsorption of p-nitroaniline. This observation is explained by the fact that in alkaline solutions the shift of electrons from the aromatic ring to the nitro-group of nitroaniline is enhanced and this results in the molecule dissociating as an acid by splitting off one proton and localizing the negative charge on the oxygen of the nitro-group [11] *

The adsorption of dissociated aromatic compounds on the activated coal is no electrochemical adsorption of ions. The following facts support the accuracy of this conclusion. Cations of aromatic amines are adsorbed by the coal, whereas cations of strong electrolytes (Ca^{2+}), as has been noted above, are not adsorbed by the coal used. Phenolate anions are not adsorbed by it, whereas anions of strong electrolytes (Cl^-) are. On one and the same sample of coal both cations of aromatic amines and anions of nitrophenols are adsorbed, whereas adsorption of these and other ions is much higher than the electrochemical adsorption of Cl^-. Consequently, the adsorption of dissociated aromatic amines and nitrophenolates is a molecular process effected by the molecular interaction between the adsorbent surface and the aromatic ring of the dissociated molecule, the interaction being increased owing to polarization resulting from the various substituents in the ring.

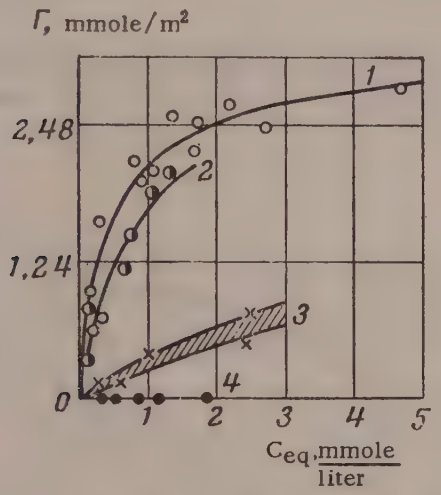


Fig. 3. Adsorption of p-nitroaniline from alkaline solutions: 1) without added alkali; 2 and 3) at molar ratios of p-nitroaniline to alkali 1:1 and 1:2; 4) 2 N NaOH.

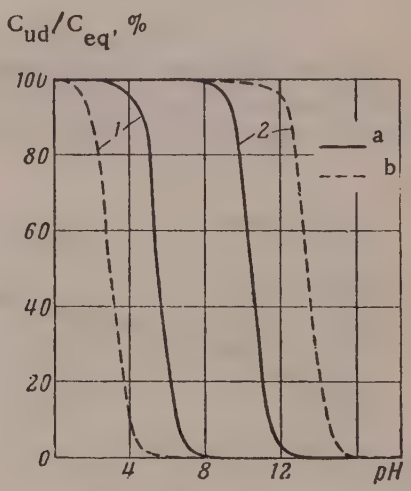


Fig. 4. Curves showing the relative content of undissociated molecules (1) and singly charged ions (2) in p-hydroxybenzoic (a) and salicylic acid (b) as a function of pH.

Nonelectrochemical adsorption of phenolate ions is improbable, because their hydration energy resulting from the localized charge on the oxygen atom is equal to or exceeds the energy of the adsorptive interaction between the π-bonds of the benzene ring and the surface of the activated coal.

The increased polarization of the ring of the phenolate ion by the introduction of a nitro-group results in the adsorption energy surpassing the hydration energy resulting from the presence of the free ionic charge. Due to the fact that the adsorption energy for dissociated molecules in solutions is much lower than that for undissociated molecules, because hydration is enhanced when a charge appears, it may be explained why molecular adsorption of aromatic ions does not occur when undissociated molecules of those same substances are present. Therefore, adsorbed ions will always be driven off from the coal surface by undissociated molecules.

*The scattering of the experimental points for p-nitroaniline adsorption from 2 N hydroxide solutions originated because the amino-group is partially split off (up to 20%) under conversion to nitrophenolate. But, as is evident from Figs. 1 and 2, nitrophenolate is adsorbed more strongly from alkaline solutions than is nitroaniline and, therefore, the occurrence of the side reaction makes it clear that adsorption of nitroaniline no longer occurs at high pH values.

Upon expressing in the coordinates Γ, C_{ud}, the adsorption isotherms of substances the molecules of which contain several functional groups, in principle two cases may be distinguished for the calculation of the equilibrium concentration of undissociated molecules: the functional groups dissociate into ions of the same sign (hydroxybenzoic acids) or of opposite sign (aminobenzoic and aminosulfonic acids). When the molecules dissociate with formation of ions of the same sign, the problem is simplified, because the concentration of undissociated molecules in the solution is determined merely by the greatest dissociation constant. This is clearly seen by comparing the curves for the relative content of undissociated molecules(C_{ud}/C,%) in a solution of p- and o-hydroxybenzoic acid as a function of pH, as are shown in Fig. 4, with the adsorption isotherms of these acids at various pH (Figs 5 and 6).

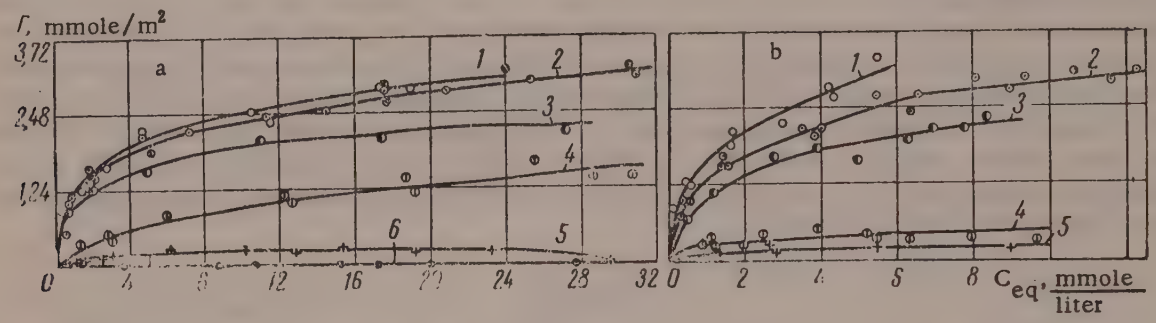


Fig. 5. The specific amount adsorbed plotted versus the total equilibrium concentration at various pH of the solutions: a) p-hydroxybenzoic acid: 1) 0; 2) 3.3-3.75; 3) 7.5-5.0; 4) 7.7.9; 5) 9.0-9.6; 6) 14; b) salicylic acid: 1) 0; 2) 2.55 3.5; 3) 3.5-4.5; 4) 6.6-6.8; 5) 9-11.

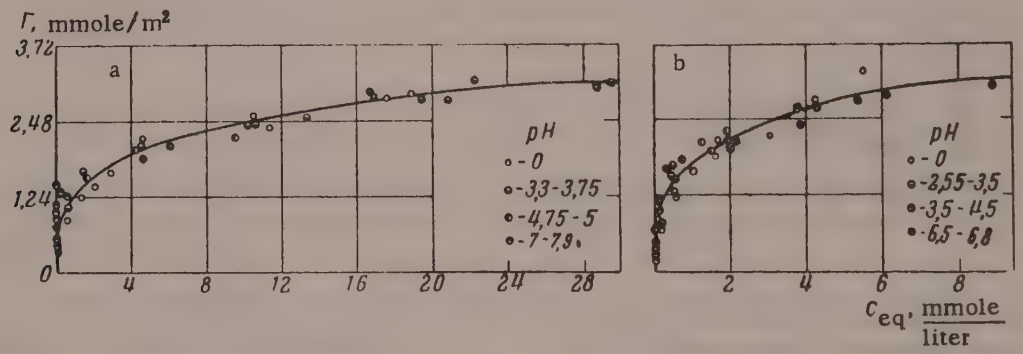


Fig. 6. The specific amount adsorbed plotted versus the equilibrium concentration of undissociated molecules at various pH of p-hydroxybenzoic (a) and salicylic acid (b) solutions.

From the reported data, after correcting for dissociation of the COOH-group, we obtained isotherms of p- and o-hydroxybenzoic acid in the coordinates Γ, C_{ud}, which do not depend on pH in the region below the values at which in aqueous solutions the dissociation of the OH-group in the hydroxybenzoic acids starts.* It is of interest that, after the hydroxybenzoic acids are fully dissociated with respect to the COOH-group, the adsorption is still dependent on the pH although there are no undissociated molecules in the solution. It is found that the adsorption of hydroxybenzoic acids is a function of pH up to their complete dissociation with respect to the second functional group (OH) with formation of doubly charged ions. This effect is particularly clearly manifested in adsorption of p-hydroxybenzoic acid. Whereas we saw above that adsorption of aromatic ions is only possible, when no undissociated molecules are present in the solution, it follows here that the adsorption of the said ions in its turn depends on the number of dissociated functional groups. Certainly, the difference between adsorption of singly and doubly charged aromatic ions is much smaller than that between adsorption of ions and undissociated molecules.

*For p-hydroxybenzoic acid at pH < 7, for o-hydroxybenzoic acid at pH < 9.

The supposition that hydration of aromatic ions is one of the reasons why they are less adsorbed on coal than are undissociated molecules is not in disagreement with the fact that in the case of o-hydroxybenzoic acid the dissociation of the OH-group hardly reduces adsorption of the ion. Apparently, though, this is an exception, since it results because a six-ring is formed between the OH- and COOH-groups in ortho position by means of an intermolecular hydrogen bond [12] and for this reason the hydration of the doubly charged ion is hardly greater than that of the $C_6H_5(OH)COO^-$ ion.

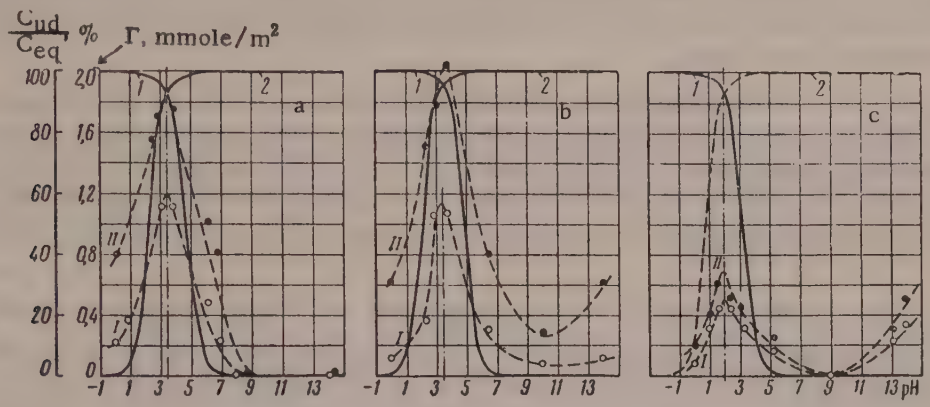


Fig. 7. Adsorption as a function of the relative content of undissociated molecules: p-aminobenzoic (a) and o-aminobenzoic acid (b): 1) dissociation curve of the COOH-group, 2) that of the NH_2 -group; adsorption of sulfanilic acid (c) at C_{eq} equal to 5 (I) and 10 (II) mmole/liter: 1) dissociation curve of the SO_3H-group; 2) that of the NH_2 -group.

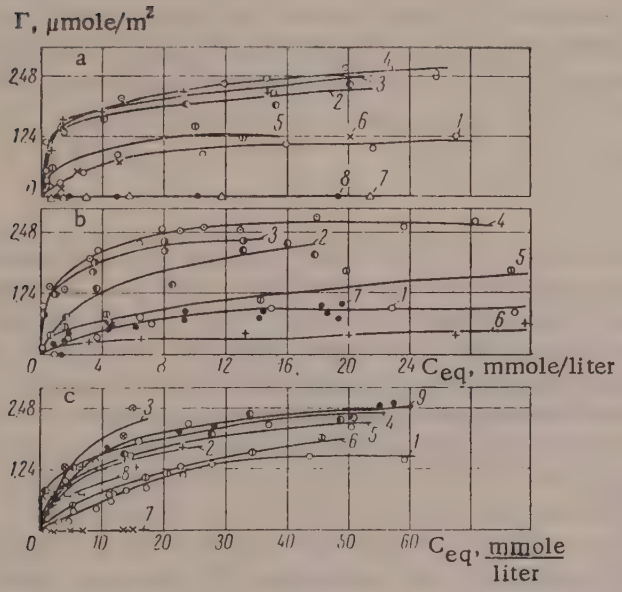


Fig. 8. Specific amount adsorbed as a function of the total equilibrium concentration at various pH: a) p-aminobenzoic acid: 1) 0; 2) 2.5-3; 3) 3-3.2; 4) 3.85; 5) 6; 6) 6.7; 7) 8; 8) 14. b) o-aminobenzoic acid: 1) 0; 2) 2.3; 3) 2.9; 4) 3.7; 5) 6.4; 6) 10; 7) 14. c) sulfanilic acid: 1) 0; 2) 1; 3) 1.65; 4) 2.4; 5) 2.9-3.3; 6) 5.1; 7) 9-9.5; 8) 13; 9) 14.

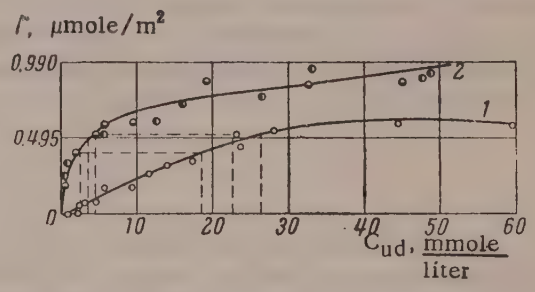


Fig. 9. Specific adsorption of sulfanilic acid plotted versus the concentration of molecules with a nondissociated SO_3H-group; 1) pH 0; 2) pH 2.4-3.9.

Upon studying adsorption of aromatic compounds which on dissociation may give aromatic ions of opposite sign, the concentration of undissociated molecules may be relatively simply calculated at the pH corresponding to the isoelectric point. In first approximation the application of small corrections for the dissociation of the functional groups at this point allows one to estimate the concentration of completely undissociated molecules, since under isoelectric conditions the content of dissociated molecules in the solution is only a small fraction of the total concentration. This is clearly visible from the curve given in Fig.

7 for the relative content of undissociated molecules in p- and o-aminobenzoic and sulfanilic acid (C_{ud}/C) as a function of pH; these curves were calculated from the electrolytic dissociation constants of the corresponding functional groups. Since at the isoelectric point the relative concentration of undissociated molecules attains a maximum, the pH attains its optimum value here for the adsorption of these acid molecules.

In Fig. 8 the adsorption isotherms of p- and o-aminobenzoic acid and sulfanilic acid are plotted as a function of the analytically determined equilibrium concentrations in solutions at various pH. From these data we have constructed the curves for the specific adsorption of the aminobenzoic acids as a function of pH at two values of the total equilibrium concentration in the solution.

As can be seen in Fig. 7, at the isoelectric point the specific adsorption is found to have a maximum in a strongly acidic medium. This appeared to be contradiction with the fact that in the literature for sulfanilic acid only one K_d value, corresponding to dissociation of the SO_3H groups, is given. It might be expected that the K_d value of the NH_2-group in sulfanilic acid actually would be very small, since the K_d of the NH_2-group sharply falls, when the electronegativity of the second substituent in the benzene ring is raised. This may be illustrated by the following sequence:

$$K_{d}C_6H_5 - NH_2\ (3.82 \cdot 10^{-10}) > K_{d}C_6H_4(Cl)NH_2\ (1.49 \cdot 10^{-10}) > K_{d}C_6H_4(NO_2)NH_2\ (1.1 \cdot 10^{-12})\ \text{etc.}$$

In spite of this, the adsorption measurements do not permit neglecting the dissociation of aminogroups in sulfonic acids. When taking into account dissociation of only the SO_3H-group in sulfanilic acid we do not obtain a common adsorption isotherm for all pH (Fig. 9). The adsorption isotherm measured at pH ≃ 0, where the amino-group is completely dissociated, is found to lie considerably below the isotherm connecting the experimental data obtained at higher pH values, where the amino-group is hardly dissociated.

Since at pH close to zero the sulfo-groups are undissociated, the noncoincidence of the isotherms in the coordinates Γ, C_{ud} can only be explained by dissociation of the NH_2-groups and formation of sulfanilic acid cations. It is clear that the factor by which one must multiply the values of C_{eq} for sulfanilic acid adsorption from 2 N HCl solutions to obtain a common isotherm for all pH in the coordinates Γ, C_{ud} will be equal to $(1 - \alpha_{NH_2})$. Here α_{NH_2} represents the extent to which the amino-groups are dissociated. The dissociation constant of the amino-groups can be found from the value of α_{NH_2} by means of the equation

$$K_{dNH_2} = [OH^-]\frac{\alpha_{NH_2}}{1 - \alpha_{NH_2}}.$$

In a 2 N HCl solution the pH is zero. The small shifts in the pH resulting when various amounts of sulfanilic acid (up to 100 mmole/liter) are dissolved in 2 N HCl, were not determined with sufficient accuracy. Therefore, by using the calculated value of $[OH^-] = 10^{-14}$ in all equilibrium solutions, we estimated from the isotherm a value of K_{dNH_2} for sulfanilic acid, which would be correct in order of magnitude. One should keep in mind that, even if in this estimate the pH is in error by 0.5, not only does the order of magnitude of the constant not change but also its absolute value found will not deviate by more than three times from the actual one. Calculations which we carried out for three points on the isotherm of sulfanilic acid adsorption from 2 N HCl with C_{eq} equal to 18.5, 22.5 and 26.2 mmole/liter gave the K_d values $8.25 \cdot 10^{-14}$; $5.45 \cdot 10^{-14}$; $4.81 \cdot 10^{-14}$, respectively (mean $K_{dNH_2} = 6.17\ 10^{-14}$). By means of this mean K_{dNH_2} we calculated the concentrations of sulfanilic acid molecules undissociated with respect to the amino-group at various pH (curve 2 in Fig. 7). The point where this curve intersects the previously calculated curve for the relative content of sulfanilic acid molecules with an undissociated SO_3H-group at various pH (the so-called isoelectric point at pH 1.9) corresponds to maximum specific adsorption at constant equilibrium concentration.

All data reported in this paper indicate that in aqueous solutions the activity of aromatic compounds which have the properties of weak electrolytes is determined by the concentration of undissociated molecules.

SUMMARY

1. Adsorption of benzene derivatives with various substituents in the ring on an activated ash-free coal from aqueous solutions has been studied in a broad pH range.

2. The adsorption isotherms when expressed in terms of specific amount adsorbed as a function of the concentration of undissociated molecules in the solution of aromatic electrolytes do not depend on pH. For this reason it has been concluded that from solutions of aromatic electrolytes only undissociated molecules are adsorbed on ash-free coal.

3. At such pH that the molecules of the aromatic compounds are completely dissociated, aromatic ions are adsorbed and this adsorption does not have an electrochemical character. Both cations and anions of aromatic substances are adsorbed on coal. The activity of aromatic compounds in aqueous solutions is practically equal to the concentration of their undissociated molecules.

LITERATURE CITED

1. A. V. Kiselev, Vestnik AN SSSR, 10, 43 (1957); N. N. Avgul' and A. V. Kiselev, Kokl. AN SSSR, 112, 673 (1957); N. N. Avgul', G. I. Berezin, A. V. Kiselev and I. A. Lygina, Izv. AN SSSR, Otd. khim. n. 1957, No. 9 1021; 1956, No. 11, 1304.
2. A. V. Kiselev, N. N. Avgul', G. I. Berezin, I. A. Lygina and G. G. Muttik, J. chim. phys. et phys. Chim. biol. 55, 197, 1958.
3. B. P. Bering and V. V. Serpinskii, Dokl. AN SSSR, Otd. khim. n. 114, 1254 (1957).
4. H. Freundlich, Z. phys. Chem. 57, 385, 1907; N. A. Shilov and B. V. Nekrasov, Zh. russk. khim. obsh. 60, No. 1,103 (1928); N. F. Ermolenko and O. R. Skorokhod, Uch. zap. Belorus. univ. No. 20, 165 (1954).
5. A. K. Goard, E. K. Rideal, J. Chem. Soc. 127, 1674, 1925; N. M. Baron, E. D. Volova, I. M. Egorov and É. I. Kvyat, Practical Exercises in Physical Chemistry [in Russian] (Goskhimizdat, 1957), p. 108.
6. A. P. Karnaukhov, A. V. Kiselev and E. V. Khrapova, Dokl. AN SSSR, 92, 361 (1953)
7. N. N. Avgul', G. I. Berezin, A. V. Kiselev and A. Ya. Korolev, Kolloidn. zh. 20, 298 (1958); M. M. Dubinin, E. D. Zaverina and L. V. Radushkevich, Zh. Fiz. khimii, 21, 1351 (1947).
8. W. Knop. Z. Vereines dtsch. Zuckerind 83, 125, 1933.
9. H. G. Scholten and K. G. Stone, Analyt. Chem. 24, 671, 1952; 24, 747, 1952; khimiya i khim. tekhnologiya, No. 11, 26 (1952).
10. H. J. Phelps, Proc. Roy Soc. (London) A 133, 155, 1931.
11. W. Hückel, Theoretische Grundlagen der orhanischen Chemie, Leipzig. 2, 1957,
12. N. F. Ermolenko and N. L. Lemets, Zh. obshch. khimii, 23, 1313 (1953); R. Zhonen, Uspekhi khimii, 28, 605 (1959).

All abbreviations of periodicals in the above bibliography are letter-by-letter transliterations of the abbreviations as given in the original Russian journal. *Some or all of this periodical literature may well be available in English translation.* A complete list of the cover-to-cover English translations appears at the back of this issue.

INTERACTION BETWEEN POLYMERS AND PLASTICIZERS

1. PREPARATION AND PROPERTIES OF POLYVINYLCHLORIDE PASTES

E. G. Fedoseeva, R. I. Fel'dman, S. I. Sokolov

Scientific Research Institute of the Cable Industry
N. K. Krupskaya Moscow Regional Pedagogical Institute
Translated from Kolloidnyi Zhurnal, Vol. 26, No. 6,
pp 749-755, November-December, 1961
Original article submitted August 2, 1960

The experimental study of systems, consisting of polymers and plasticizers, the results of which are presented in the present communication *, was carried out for the purpose of obtaining data giving the structure and phase states of some typical polymer systems, and for the practical development of the basis of the technological process, in which these same polymers are used in the form of pastes. The practical process consists in first preparing a paste at room temperature from powder polymer and a practically nonvolatile plasticizer or mixture of plasticizers to give a highly concentrated dispersion of the polymer, and then, depending on what the finished parts are intended for, converting the paste by heating with gelatinization into high elastic films or blocks. The disperse system, owing to the exceedingly small rate of swelling of the polymer in the plasticizer, maintains its relative stability without gelatinizing for a long time and without separating, in some cases, for as long as two years. If the temperature is raised, the interaction between the polymer and the plasticizer becomes more intense, the swelling rate is increased, and they mutually dissolve in one another to form a homogeneous system. Consequently, the essence of gelatinization consists in converting a heterogeneous dispersed system into a homogeneous one, which is a jelly, i.e., a true solution with a three-dimensional structure.

The use of pastes for the production of molded parts is not only simple and convenient, but it eliminates the need for heavy mixing machinery, dissolvers, and recovery installations.

The technological principle just presented is closely bound up with such problems and phenomena as solution and swelling of the polymers [2], the state of aggregation of the complex polymer system [3], phase equilibria, hysteresis phenomena, thixotropy, etc. [4].

Preparation of Pastes. Pastes, used as coatings in film form, consist of two or more basic components, either a polymer and a plasticizer, or a mixture of polymers and a mixture of plasticizers, with the addition of willers, pigments, or stabilizers. Depending on the formula and method of preparation, pastes of various concentrations are prepared: from flowing liquids, to highly viscous masses. The consistency is determined by the field of practice in which the paste is to be used. In all cases where the pastes are used as filling and sealing compounds, they should be easily mobile systems, which completely fill the space, and do not appreciably change in volume after gelatinization. The present paper gives the results of work done on pastes prepared from polyvinylchloride (PVC).

Polyvinylchloride pastes, depending on the nature of the original polymer, are prepared: by mixing the powdered, "paste-forming" polymer with plasticizer, or by rubbing the powdered polymer together with a solution of polymer in plasticizer, previously prepared by heating.

The paste, formed in both cases, is a suspension of polymer particles (globules), swelled to a limited extent in plasticizer, distributed in a solution of the same, but possibly some other, polymer and plasticizer. In storage, the paste must have the relative sedimentational stability established by practice, which is expressed as the time the solid particles (of the disperse phase) remain in the suspended state without visible separation of the system into two layers. In practice, stability is achieved by choosing the proper viscosity of the dispersing medium and the lowest possible density difference between the two phases.

* The eighth communication of a series of papers, devoted to a study of the interaction between polymers and plasticizers [1].

In preparing the pastes, use was made of powdered PVC of various brands: Igelite-R, [gelite-F, PB-1, PB-3, and PB-4, which differ in method of preparation and in particle dimensions. The Igelites, prepared by pulverizing drying of an aqueous PVC latex, contain stabilizing components. The particle dimensions are less than 1μ. PB brand PVC's are prepared by coagulating an aqueous dispersion. The dimensions of the particles are from 10 to 40μ. The principal plasticizers used have been phthalic esters, phosphoric, and sebacic acids. Attention should be given to the fact that polyvinylchloride pastes cannot be prepared by using high viscosity plasticizers alone, such as, for example, chlorinated diphenyl. Igelite-R and Igelite-F brand PVC's are good paste-forming polymers. Pastes which do not separate for 150 days are formed by directly mixing 35-50 parts by weight of Igelite with 65-50 parts by weight of plasticizer. The pastes do not possess fluidity, if the mixture contains more than 50 parts by weight of polymer. Liquid pastes that separate are formed if the mixture contains less than 35% by weight of polymer. It is impossible to prepare nonseparating pastes from PB brand PVC's having particles with a less degree of dispersity than the Igelite particles by mixing them directly with plasticizer. Stable dispersions can be prepared only by distributing the particles in a solution of polymer and plasticizer with a definite concentration which provides the necessary consistency for the dispersing medium.

The solutions which we used as dispersing media were prepared from PVC and plasticizers having the required viscosity. For example, PVC solutions in dibutylphthalate (DBP) met the necessary requirements at the following concentrations: PB-1-2.0%, PB-2-2.5%, PB-4-3.0%, and PB-3-5.75%. The relative viscosity of these solutions varied from PB-1 to PB-3 by unity. The higher the molecular weight of the polymers used in the solutions serving as dispersing media, the lower their concentration needs to be. Polymers having a high degree of polymerization give structurized systems at low concentration, which allow the components of the paste to maintain themselves in the suspended state for a long time.

In order to select the proper concentration and viscosity for the dispersing medium, studies were made of how the viscosity of the solutions varies with concentration. The viscosity of the solution was measured with a Geppler ball viscosimeter. The temperature during the measurements was equal to 20°. Figure 1 gives the results obtained for solutions of various brands of PVC. By extrapolating the curves shown in Fig. 1, calculation were made of the values of characteristic viscosity [η], which are indicative of the mean molecular weight of the paste-forming polymers used in the work. For solutions containing PVC we have: PB-1 [η] = 2.1, for PB-2 or Igelite F [η] = 1.35, for PB-4 or Igelite R [η] = 0.9, and for PB-3 [η] = 0.4. Thus, the properties of the dispersing medium used fit into the laws which are known to hold for polymer solutions prepared in other solvents with smaller viscosity.

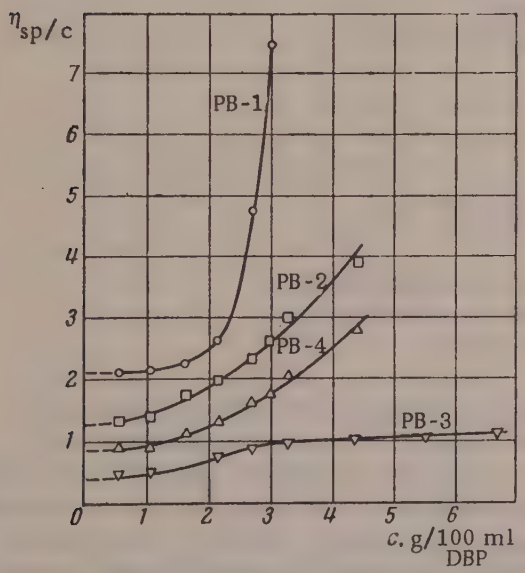


Fig. 1. Normalized viscosity of solutions of various brands of PVC in DBP as a function of concentration.

The pastes of the desired composition were prepared and mixed at room temperature. The polymer solution was mixed for 30-40 minutes with the powdered PVC, the stabilizers and the dyes taken in the quantity prescribed by the formula. The constituent parts were added to the solution in several portions to avoid lumping. After mixing, the pastes were worked up on a dye-rubbing machine (space 0.15 mm) with friction. This treatment increases the sedimentational stability of the pastes, since it reduces the dimensions of the globules (particles) by mechanical action. The approximate composition of one of the pastes (parts by weight) was: PVC (PB-1)-37, lead silicate-6, DBP-15, tricresylphosphate (TCP)-20, and dioctylphthalate (DOP)-22. In all the polyvinylchloride pastes prepared, the presence of charges on the phase boundaries was established by an electrophoretic method. The dispersed phase accumulates at the positive pole, and the plasticizer migrates toward the negative pole. This fits Kohn's rule, since the dielectric permeability of the plasticizers varies from 7 to 10, and PVC ≈3. It is to be assumed that the presence of charge on the interface is an additional factor in stabilizing the dispersed system.

As the dispersing medium it is also possible to use solutions of chlorinated PVC, polychloroprene, polystyrene, polymethylmethacrylate, and nitrile rubber.

The films prepared by gelatinization in the heating of pastes, which contain nitrile rubber, polychloroprene, rosin, or oleic acid, are stable and have higher adhesive strength to metallic surfaces than compositions which do not contain any of the above materials. For example, a nitrile rubber paste was prepared from 45 parts by weight of PVC (PB-1), 8 parts by weight of nitrile rubber (SKN-18), 44 parts by weight of DOP, and 3 parts by weight of lead silicate.

Good adhesive properties are also possessed by films prepared from pastes prepared using methylmethacrylate or styrene. The pastes are prepared in the following order: the monomer in the presence of benzoyl peroxide (~0.13% of the weight of the monomer) is subjected to polymerization until a liquid system of the desired viscosity if formed, to which the other constituent parts of the composition are then added. Mixing is carried out in a closed mixer. A paste of the desired stability is prepared from 48 parts by weight of methylmethacrylate or styrene, 30 parts by weight of PVC (PB-1), 2 parts by weight of lead silicate, and 20 parts by weight of DOP.

Measurement of Paste Properties with Time. During storage, the pastes structurize, which is shown by an increase in viscosity ($\Delta\eta$). Pastes are not suitable for use if they have lost their fluidity during storage, or have separated into layers. In nonequilibrium systems, such as the pastes are, these processes go on concurrently, but if the above described theoretical precautions are observed in practice, they go on at a relatively small rate.

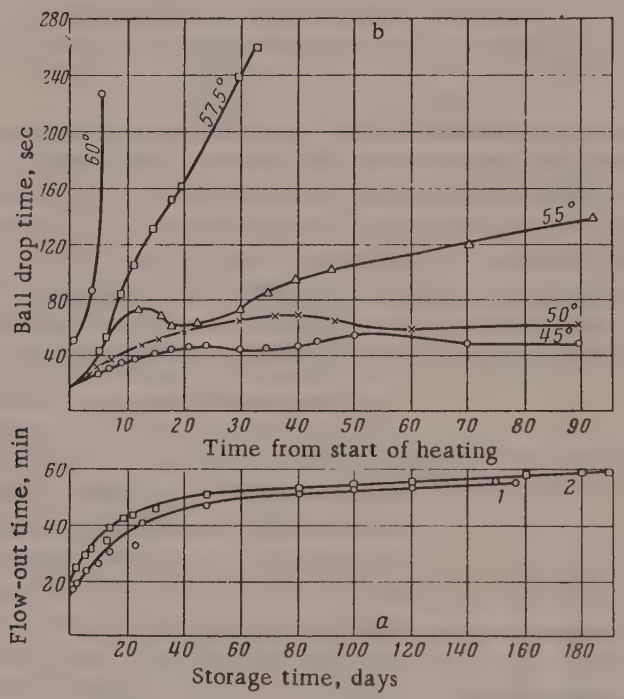


Fig. 2. Change in viscosity characteristics of pastes with time. (a) 1) Paste No. 1; 2) paste No. 2. (b) paste No. 2 at various temperatures. Time from start of heating in minutes.

Figure 2a shows the times required for pastes No. 1 and No. 2 to flow out of a NIILK funnel, as a function of storage time Measurement and storage of the pastes was done at 25°. Paste No. 1 consists of (parts by weight): PVC (PB-1)-37, lead silicate-6, DBP-15, TCP-20, DOP-22. Paste No. 2 consists of (parts by weight): PVC (PB-1)-37, lead silicate-6, DOP-15, TCP-42. Comparing the data on the change in viscosity of the pastes with time at different temperatures explains the nature of the processes going on. For example, Fig. 2b shows the results of experiments made on Paste No. 2 using a Geppler viscosimeter. It is to be assumed that they are the result of increased swelling of the globules, followed by gelatinization with increase in temperature. The gelatinization rate rises sharply starting at 57.5°.

The process of interaction of the dispersed powdered polymer with the plasticizers from the moment of the preparation of the paste to the formation of a uniform film or jelly represents mutual diffusion between the polymer and the plasticizer. At temperatures below 40-50°, what occurs is principally diffusion of the low molecular component, the plasticizer, inside the polymer particles (globules), while from the swollen globules into the dispersing medium there is a low rate of diffusion of only the lowest molecular fractions of the polymer. If the temperature is raised, rate of diffusion of micromolecules from the globules into the dispersing medium is increased, and decomposition of the globules and complete homogenation (gelatinization) of the system occurs. Further increase in temperature favors converting the jelly into a high viscosity liquid. The complicated form of the curves (Fig. 2b) reflects the complexity of the processes occurring in the system. With an over-all increase in visocsity of the system, some of the constituent phenomena are causing a reduction in the viscosity, while others, on the other hand, are causing an increase in viscosity and even loss of fluidity.

Adding highly dispersed fillers and surface active agents to the pastes changes the viscosity as a function of storage time in various ways. Carbon black, lead dioxide, and titanium dioxide reduce the amount of viscosity increase with time. It may be assumed that layers of these substances, formed on the surface of the polymer particles, to some extent prevent formation of the structures which are responsible for the viscosity increase in the system. Talc, kaolin, and particularly chalk and magnesium oxide, added to the pastes, cause an increase in structuration, and an increase in the value of $\Delta\eta$.

The pastes are thixotropic systems. The coagulational structures formed in them may be subjected to mechanical destruction, with subsequent reestablishment. The reversible structuration of the pastes is a positive factor, which protects them from separation and sedimentation.

However, the formation of a stable structure on storage, accompanied by reduction in mobility of the system, is a negative factor from the production point of view. Reestablishing the original properties of the system requires additional engineering operations to destroy the structure in some mechanical way. We have observed that if stored pastes are acted upon mechanically, the initial viscosity value is restored. Subsequent storage again causes structuration, the viscosity of the pastes becomes greater, the longer the storage time alternating in a series of destructions of the structure. From a practical point of view every paste ought to have some optimum degree to which the thixotropic properties occur. The fillers, added to the pastes, affect the thixotropic properties. Thus, for example, carbon black or lead dioxide, added to the paste to the extent of 6%, annihilates the thixotropic phenomena.

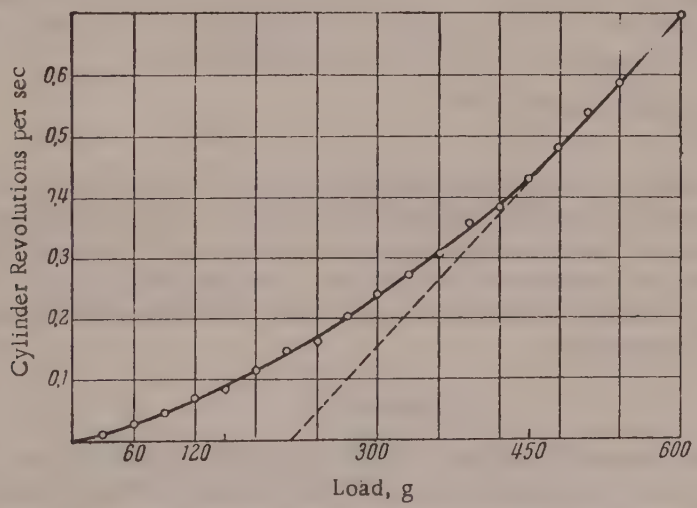


Fig. 3. Flow rate of paste No. 2 as a function of load.

Figure 3 shows one of the curves of paste viscosity as a function of applied load, which shows that there is a movable structure in the system. The viscosity was measured with a RV-8 rotating viscosimeter. As the load is increased, the structure gradually fails, and in their behavior the pastes approximate a normal liquid, in which the viscosity is independent of the load. The pastes resist a force applied to them under static conditions, i.e., they have a limiting displacement stress.

The thixotropic properties and gelatinization observed in storage and reworking of the pastes bear a direct relationship to the problem of jelly formation and behavior of gels. In order to understand the phenomena observed in the preparation and gelatinization of pastes, it must be born in mind that there are two distinct limiting types of gels or jellies*.

First Type - Homogeneous systems (jellies proper), which are true molecular solutions of polymers, only they ave a special structure, which gives them their elastic properties. Systems of this sort are inclined to all sorts of hindered states and hysteresis phenomena, but in prinicpal they may occur in a stable state in thermodynamic equilibrium.

Second Type - Heterogeneous Systems, with solid or liquid particles of colloidal or even larger dimensions. They are able to form coagulational structures with capture (immobilization) of the liquid phase. These systems, which are nonequilibrium from the thermodynamic point of view, have relative stability in the aggregational sense. Usually one type or other of gel is studied in systems widely differing in composition and structure, however, in principal, as we have shown in the present paper, it is possible to form both types of gels in systems having the same composition, by maintaining different conditions. Therefore, the systems of this sort which we have studied are of special interest, not only practically, but theoretically as well.

In considering these systems, we wish to call attention to the fact that the extremely slow rate at which the processes take place makes it difficult to solve theproblem of what state the polymer-plasticizer system is in, when it is at equilibrium at room temperature. Apparently, one of the two following possibilities may occur. The first possibility is that the system under equilibrium conditions will consist of two conjugated solutions (exfoliation). One of the solutions, containing the larger amount of plasticizer, is a viscous liquid, while the other more enriched in polymer, is a jelly swelled to a limited extent. The homogeneous jelly obtained from such a system after gelatin - ization is, on the other hand, in an unstable state, and shows an inclination toward syneresis (division into two phases). This may be written schematically as follows:

I Equilibrium state - two-phase system (paste)

II Nonequilibrium state - jelly (inclined to syneresis)

(The arrow indicates the direction of possible spontaneous transition).

The second possibility is the reverse case, i.e., the paste is a relatively stable system only because of the extremely small rate of solution (homogenation). In fact, the system is far from equilibrium, and a homogeneous equilibrium solution is obtained more rapidly on heating. On cooling, the solution forms a net-like, molecular structure, — a jelly, close to the equlibrium state. Consequently, schematically:

I Nonequilibrium state - two-phase system (paste)
II Equilibrium state - jelly

The jelly obtained in the latter case after heating is in the equilibrium state, and shows no sign revealing any tendency of the system to separate in the form of syneresis. In parts, made of such systems, there should be no so-called "sweating" of plasticizer. The ideas presented may be used to classify individual plasticizers. TCP and some other "sweating" plasticizers may in this respect be considered bad, since with PVC it gives systems which clearly approach the first possibility. Esters of phthalic acid, like DBP, DOP and some other plasticizers, apparently behave with PVC according to the first possibility.

SUMMARY

1. A method has been developed for preparing highly concentrated polyvinylchloride pastes, in which the dispersing medium is a solution of polyvinylchloride, polychloroprene, nitrile rubber, polystyrene, or polymethylmethacrylate in various plasticizers or plasticizer mixtures.

2. Physical factors, as well as highly dispersed fillers such as carbon black, chalk, kaolin, titanium dioxide, lead dioxide, talc, and magnesium oxide react in different ways on the sedimentational stability, the thixotropy, and the aging of dispersed heterogeneous systems, consisting of polymers and plasticizers.

*We attach a wider meaning to the term "gel". A special case is a jelly-a homogeneous system.

3. Reworking the pastes by homogenation (gelatinization) is a transition from a microheterogeneous thixotropic gel to a homogeneous jelly. The stability limits of one or another composition are determined by the nature of the plasticizer.

LITERATURE CITED

1. S. I. Sokolov, R. I. Fel'dman, Investigations in the Field of High Molecular Compounds [in Russian] Academy of Sciences Press, USSR, 1949, p. 329; R. I. Fel'dman, Dokl AN SSSR 97, 1033, 1954; R. I. Fel'dman, A. K. Mironova, Kolloidn Zh. 17, 465, 1955; S. I. Sokolov, S. A. Reitlinger, R. I. Fel'dman, ibid 19, 624, 1957; R. I. Fel'dman, A. K. Mironova, ibid 19, 654, 1957; R. I. Fel'dman, A. K. Mironova, S. I. Sokolov, ibid 20, 106, 1958; R. I. Fel'dman, A. K. Mironova, Uch. zap. MOPI 84, 181, 1959.
2. R. I. Fel'dman, S. I. Sokolov, Theses of Papers at the All-Union Conference on Colloid Chemistry [in Russian] 1950, p. 100.
3. R. I. Fel'dman, Kolloidn Zh. 20, 220, 1958; R. I. Fel'dman, S. I. Sokolov, Chemistry and Physical Chemistry of Polymers [in Russian] Academy of Sciences Press, USSR, 1952, p. 159.
4. N. P. Peskov, Course in Colloid Chemistry [in Russian] Goskhimizdat, 1940; Lecture Notes from Academician P. A. Rebinder's Course on Colloid Chemistry [in Russian] Moscow University Press, 1949; G. R. Kroit, Science of Colloids, I [Russian translation] IL, 1955.

All abbreviations of periodicals in the above bibliography are letter-by-letter transliterations of the abbreviations as given in the original Russian journal. *Some or all of this periodical literature may well be available in English translation.* A complete list of the cover-to-cover English translations appears at the back of this issue.

THE EFFECT OF ACID TREATMENT OF SILICA GEL ON THE PORE STRUCTURE OF THE DRIED GEL

R. Yu. Sheinfain

Physical Chemistry Institute, Academy of Sciences, UkrSSR, Kiev.

Translated from Kolloidnyi Zhurnal, Vol. 23, No. 6
pp. 756-760, November-December 1961
Original article submitted July 16, 1960

One of the possible ways of changing the pore structure of a silica xerogel (dried gel) is treat the hydrogel (hydrated gel) from which it was formed with electrolytes. It has been shown [1,2] that soaking a hydrated silica gel in an ammonia solution gives a larger total pore volume and appreciably increases the average radius of the capillaries [2]. Soaking the gel in hydrochloric acid also increase the pore volume, but this is not accompanied by any great change in the sizes of the pores [2]. The effects are explained in the quoted references by the dehydrating influence of the electrolytes, but the details of the mechanism are not dealt with. Published results in this field have not been concerned with the subject as a whole, and have not provided a satisfactory basis for theoretical evaluations. It therefore seemed of interest to carry out a systematic investigation of the effects on xerogel pore structures of soaking the hydrogel in various electrolytes. In the present work various mineral acids were used.

The silica hydrogel was prepared in an acid medium by adding two volumes of sodium silicate solution to one volume of 6 N sulfuric acid. The specific gravity of the sodium silicate was 1.18, its factor was 3.5, and the Na_2O content was 7%. After syneresis had begun the gel was washed with tap water (pH 6.6) until there was no reaction for SO_4^{2-}, and dried at 250°. In the acid-soaking experiments the washed silica gel was soaked in the appropriate acid for several days and then dried at the same temperature as the original gel*. The xerogel prepared in this way was washed in distilled water for an extended period until there were no ions of the corresponding acid in the wash-water.

The apparent density, static activity towards benzene at $p/p_s = 1$, and adsorption of methylated spirit vapour at 20° in an apparatus with quartz spring weights, were determined for the specimens. From these results the dimensional constants of the specimens were calculated.

Details of the structures of the silica gels prepared are given in the table. The specific surfaces of the adsorption films, S', formed up to the beginning of the capillary condensation, were calculated by Kiselev's method [3]. The diameters of the initial particles, D, were found from the specific surfaces and the density of the silica skeleton (d = 2.2), using the formula $D = 6/2.2S$ [4].

Fig. 1 shows the methylated spirit adsorption isotherms**, and Fig. 2 shows the pore volume distribution plotted against effective pore radius.

As may be seen from the table and Fig. 1, soaking the hydrogel in concentrated hydrochloric or nitric acid increases the specific surface of the xerogel and correspondingly decreases particle sizes in comparison with the original specimen 2. Hydrochloric acid leaves the total pore volume practically unaltered, while nitric acid increases it. The pore sizes in both cases are practically unchanged. Treatment with concentrated sulfuric acid, while leaving the specific surface unchanged, brings about a sharp increase in pore radius and total pore volume (V_Σ). The largest porosity increase on treatment with mineral acid is given by sulfuric acid, then comes nitric, and finally hydrochloric acid.

* The gel which was later soaked in concentrated sulfuric acid was dried at 350°.

** The adsorption isotherm for specimen E was prepared in A. V. Kiselev's laboratory.

Effect of Acid Soaking of Hydrogel on Xerogel Structure

Specimen	Hydrogel treatment	Apparent density δ, g/cc	Total pore volume, cc/g		Effective pore radius, A	Specific surface m^2/g		Particle Diameter D, A
			V_Σ	V_S		Skeleton S	Film S'	
	Water wash with							
1	acidified water, pH 3.5	1.23	0.36	0.36	10	670	-	40
2*	tap water, pH 6.6	0.86	0.71	0.71	21	290	-	94
	Soaking in							
3	Conc. HCl	0.82	0.77	0.77	19	550	-	49
4	Conc. HNO_3	0.66	1.06	1.09	24	625	-	444
5	1.5 N H_2SO_4	0.86	0.71	0.71	21	390	360	70
6	4 N H_2SO_4	0.81	0.78	0.79	33	288	290	94
7	6 N H_2SO_4	0.68	1.02	1.07	52	260	230	105
8	8 N H_2SO_4	0.60	1.21	1.21	59	275	240	99
E	Conc. H_2SO_4	0.47	1.67	1.66	100	315	275	86

*The original hydrogel used in the preparation of the other specimens.

Comparison of the results for the xerogels, the hydrogels of which were treated with sulfuric acid solutions, shows that raising the acid concentration increases both pore radius and total adsorption volume (V_S) for the specimens. All the silica gels in this series, except specimen 5, had similar specific surfaces (and consequently similar size particles), not differing from the original specimen 2.

From Fig. 1 it is seen that for specimens 6, 7, 8 and E there is a marked capillary condensation, so that the corresponding share of the total sorbed methylated spirit falls between 77 and 89%. The curve of pore volume distribution against effective radius (Fig. 2) exhibits sharp maxima. The values of the film specific surface (S') are practically equal to those for the gel skeleton (S), showing that fine pores which are tightly filled in the first part of the adsorption process are not present in these specimens. These results mean that we can put this whole series of silica gels in a single category of coarse-pored adsorbents [5]. One of this series, E [6], appears to be the most coarsely-pored glassy silica gel which has been described in the literature; it has been carefully examined by various independent methods [7-9], has been accepted for inclusion in a standard series of silica gels [10], and because of its single-valued pore distribution has been used as a model adsorbent in the explanation of certain facets of adsorption theory. It has been used to resolve certain problems on the applicability of various methods to the evaluation of pore structures of adsorbents [7-9], as a basis for the corpuscular theory of silica xerogel structure [9, 12], to explain the role of capillary condensation in the adsorption process [11, 13], to throw a certain amount of light on the adsorption activity of the hydroxylated layer of silica gels [14, 15], and so on.

According to the present-day viewpoint, most strongly developed in Kiselev's works, the skeleton of silica gels is made up of spherical particles which are adhering at their areas of contact [4, 12, 16-18]. In such a silica gel structure the pores are considered as the spaces between the globules, which are packed in various ways. A change in the value of specific surface and pore volume is explained [10, 12] by differences in the size and coordination number of the primary particles (globules) making up the xerogel skeleton. A coarsely pored silica gel will correspond to a more open skeleton, and a finely-pored one to a more tightly constructed skeleton.

The results derived in the present work have been examined from the point of view of the effect of acid treatment of the gel on size and packing density of its particles. On the basis of these considerations an increase in the specific surface of the silica gel after acid treatment (specimens 3, 4 and 5) can be explained by a decrease in the size of the constituent particles [19]. An increase in pore radius and volume with only minor changes in the dimensions of the globules is evidently due to a less close packing of the latter. The most open packing is shown in specimen E where the sizes of the capillary-condensed voids are much greater than those of the original particles, which are aggregated in clusters and chains [10].

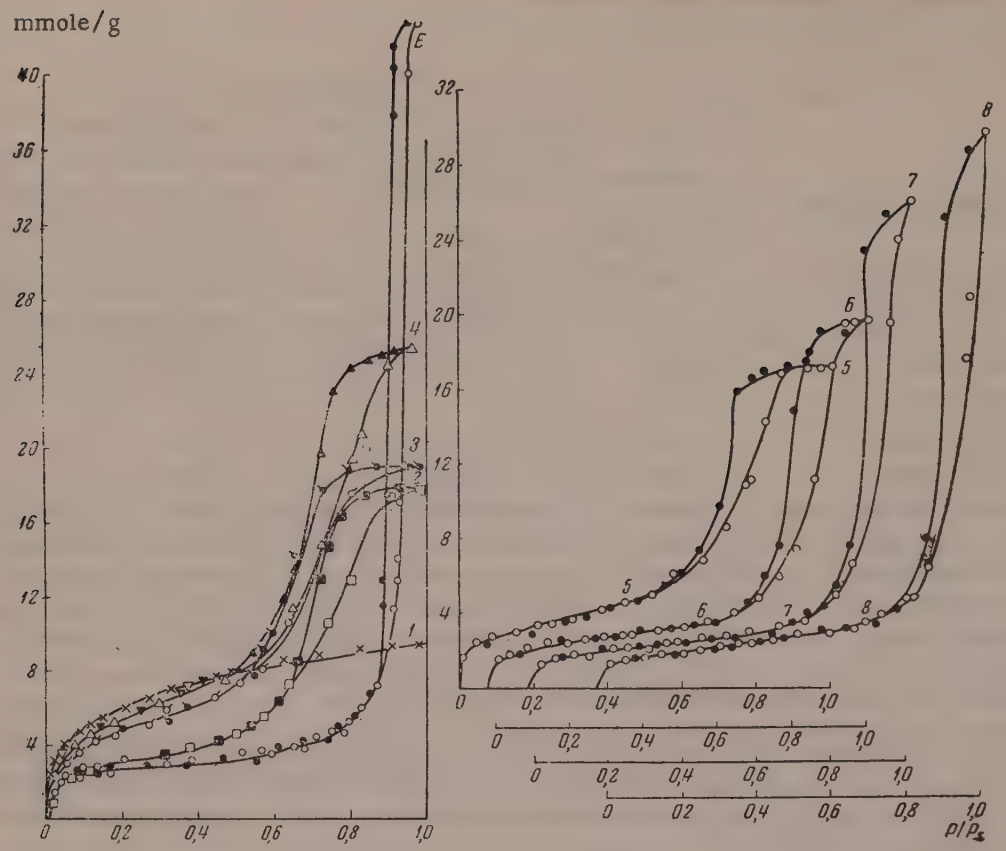


Fig. 1. Adsorption isotherms for methylated spirit vapor on silica gels: the numbers on the curves relate to the specimen numbers in the table; black dots signify desorption.

The following mechanism is suggested for the action of acids on the pore structures of gels. When the hydrogels are soaked in acid, two competing effects come into play, hydrophilization and dehydration of the particles. Increasing the degree of hydrophilic character leads to a decrease in the size of the micellar aggregates, causing closer packing on dehydration, with a consequent decrease in pore radius and increase in specific surface. Speeding-up the dehydration process by the acid treatment, on the other hand, hinders the approach of the gel particles and gives a more open packing. In this case an increase in pore radius and total adsorption volume would be expected.

The structural features of the specimens obtained by soaking the gels in hydrochloric and nitric acids and in 1.5 N sulfuric acid are evidently the result of the superimposition of both these effects. The hydrophlization is due to the fact that in the acid medium the bonds between the particles are strengthened [19-21] because of the lowered dissociation of the silicic acid. The hydrophilizing action of these acids can be estimated by comparing the structures of specimens 3, 4 and 5 with the original. This standpoint is supported by the observed decrease in particle size with a corresponding increase in specific surface. The dehydrating action is apparent on comparing the adsorption characteristics with those of the fine-pored silica gel 1, and was first noted in [2] for hydrochloric acid treatment of a hydrogel. In actual fact, if soaking in concentrated hydrochloric or nitric acid or in 1.5 N sulphuric acid led only to hydrophilization of the particles, formation of fine-pored structures might be expected in these cases. The adsorbents prepared differ from the fine-pored silica gel 1 in having appreciably more pore volume and larger size pores. This is a consequence of the dehydrating effect of these acids, reflected in a decrease in the hydrogel particle packing density. In the series of acids studied the effect becomes more intense from hydrochloric through sulfuric acid.

In the treatment with sulfuric acid, its dehydrating ability is of most importance, increasing with increasing concentration. The consequent rapid aggregation of the original particles without appreciable change in their dimensions leads to the formation of a uniformly coarse-pored silica gel. This appears to tie up with the conclusion that the speeding-up of dehydration in the presence of acid hinders the compact packing of the hydrogel particles [17].

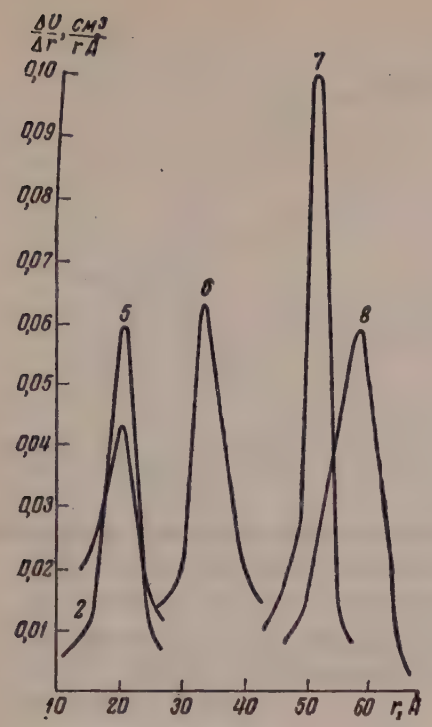


Fig. 2. Curves of pore volume distribution plotted against effective pore radius, calculated from isotherms 5, 6, 7 and 8 in Fig. 1.

SUMMARY

1. Treatment of gels with concentrated hydrochloric, nitric or sulfuric acid leads to an increase in the volume and radius of the silica gel pores. The character of the change depends on the dehydrating ability of the acid.

2. A set of uniformly coarse-pored silica gels has been prepared, with pore radii varying between 33 and 100 A.

3. The results obtained explain the effects of acid treatment of hydrogels on size and packing density o the component particles.

I wish to thank Prof. I. E. Neimark for this continuing interest in this work and for valuable advice, and also N. S. Kruglikova and E. V. Karyakina for help in the experiment.

REFERENCES

1. A. P. Okatov, Zh. Prikl. khimii 2, 21, 1929.
2. G. K. Boreskov, M. S. Borisova, B. A. Dzis'ko, O. M. Dzhigit, V. P. Dreving, A. V. Kiselev, O. A. Likhacheva, Zh. fiz. khimii 22, 603, 1948.
3. A. V. Kiselev, Uspekhi khimii 23, 252, 1949.
4. C. I. Plank, L. C. Drake, J. Colloid. Sci. 2, 399, 1947.
5. A. V. Kiselev, Zh. fiz. khimii 23, 252, 1949.
6. I. E. Neimark, R. Yu. Sheinfain, Avtor. svidetel'stvo No. 88095 ot 20. III. 1950.
7. N. N. Avgul', O. M. Dzhigit, N. M. Kamakin, A. V. Kiselev, M. V. Luk'yanovich, I. E. Neimark, R. Yu. Sheinfain, Dokl. AN SSSR 76, 855,1951.
8. E. A. Porai-koshits, A. M. Kalinina, V. N. Filippovich, Dokl. AN SSSR 86, 985, 1952.
9. E. A. Leont'ev, M. V. Luk'yanovich, Collection: Methods of Investigating the Structures of Highly-Dispersed and Porous Bodies, Izd. AN SSSR, 1958, p. 19.
10. O. M. Dzhigit, A. V. Kiselev, I. E. Neimark, Zh. fiz. khimii 28, 1805, 1954.
11. N. N. Avgul', O. M. Dzhigit, A. V. Kiselev, Zh. fiz. khimii 29, 316, 1955.
12. A. V. Kiselev, Dokl. AN SSSR 98, 431, 1954.
13. I. E. Neimark, E. I. Khatset, Zh. fiz. khimii 27, 50, 1953.
14. A. V. Kiselev, K. O. Krasil'nikov, L. N. Soboleva, Dokl. AN SSSR 94, 85, 1954.
15. A. V. Kiselev, V. V. Kulichenko, Dokl. AN SSSR 93. 101, 1953.
16. E. A. Leont'ev, V. M. Luk'yanovich, Dokl. AN SSSR 103, 1039, 1955.
17. K. D. Ashley, W. D. McInnes, Industr. and Engng. Chem. 44, 2857, 1952.
18. Manegold, Kolloid. Z. 96, 186, 1941.
19. I. E. Neimark, R. Yu. Sheinfain, Kolloidn. zh. 15, 45, 1953.
20. V. N. Krestinskaya, Kolloidn. zh. 8, 401, 1946.
21. Yu. M. Glazman, Tr. Vses. konfer. po kolloidn. khimii, Kiev, 1952, p. 349.

All abbreviations of periodicals in the above bibliography are letter-by-letter transliterations of the abbreviations as given in the original Russian journal. *Some or all of this periodical literature may well be available in English translation.* A complete list of the cover-to-cover English translations appears at the back of this issue.

KINETICS OF SWELLING OF ORGANIC FILMS BY THE FLEXIBLE STRIP BENDING METHOD

M. Ya. Popereka

Absentee Engineering and Building Institute (Branch), Alma-Ata

Translated from Kolloidnyi Zhurnal, Vol. 23, No. 6
pp. 761-762, November-December, 1961
Original article submitted September 12, 1960

The volume and weight methods usually employed to study the kinetics of swelling are laborious. The simpler method which we are proposing is as follows.

The material under test is applied in a thin layer (from solution or in the fused state) to one carefully degreased side of a thin metal strip. After drying, the strip is fastened in a clamp, placed on the bottom of a cell and filled with the solution to be tested.

By swelling in the solution, the film of material under test forces the strip to bend. The amount of bending is measured with the micrometer eye piece (5 μ divisions) of a microscope at magnification ×30 (Fig. 1).

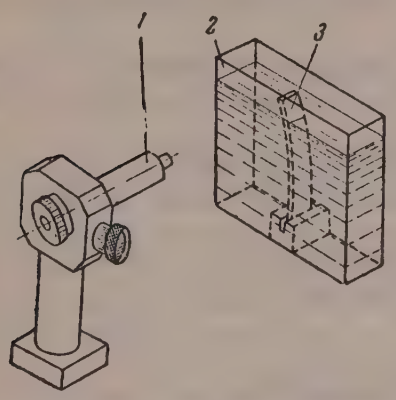


Fig. 1. Diagram of proposed method. 1) Microscope; 2) cell; 3) flexible strip with applied test material.

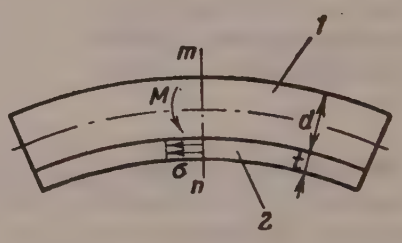


Fig. 2. Diagram for calculating mechanical swelling stress. 1) strip; 2) film under test.

The amount of bending of the strip depends on the thickness of the applied film (t), the thickness of the strip (d), the length of the strip(l), as well as the elastic properties of the metal in the strip (the modulus of elasticity E).

For the results of different experiments to be comparable, it is necessary to introduce a criterion for the degree of swelling, which is independent of the quantities mentioned. As a suitable criterion we can take the quantity σ, which we shall call the "mechanical swelling stress", which is the mechanical stress existing in the cross section of the film that balances the elastic forces arising in the strip from bending.

To calculate this stress, we mentally cut the strip in the film layer at the cross section mn (Fig. 2). The stress σ creates a force in the film given by $P = \sigma tb$, where b is the width of the strip, as a result of which a bending moment arises in the cross-section of the strip of magnitude:

$$M = \sigma tb \frac{d + t}{2} .$$

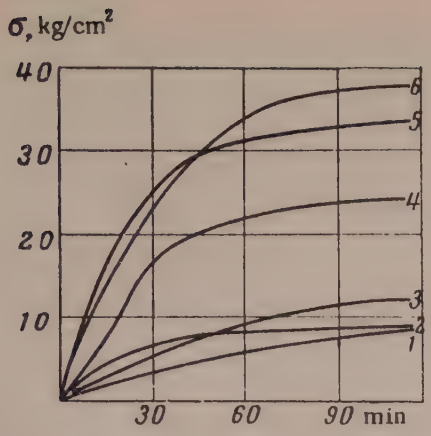


Fig. 3. Kinetics of swelling of organic films as found by the flexible strip bending method. Composition of solution: $ZnSO_3$ $7H_2O$–200 g/liter, $Na_2SO_4 \cdot 10H_2O$–100 g/liter; H_3BO_3–30 g/liter; temperature of solution–20°. 1) Polymethylmethacrylate; 2) celluloid; 3) BF-2; 4) rubber; 5) bakelite; 6) shellac.

Then bending of the end of a strip, loaded along its length by the constant bending moment is:*

$$y = \frac{Ml^2}{2EJ} = \frac{3\sigma t (d+t) l^2}{Ed^3},$$

where E is the modulus of elasticity of the material in the strip, $J = bd^3/12$ is the moment of inertia of the cross-sectional area of the strip. Hence, we obtain a formula for the proposed criterion of the degree of swelling, the mechanical swelling stress:

$$\sigma = Ed^3 y / 3t (d+t) l^2.$$

We have used steel strips ($E = 2 \cdot 10^6$ kg/cm^2), of length $l = 10$ cm, width $b = 1$ cm, and thickness $d = 0.018$ cm. The strips were degreased electrochemically, washed with hot and cold water, dried and weighed, and then the test material was applied to them. After drying the applied film, the strips were then weighed, and the thickness of the film was calculated from the increase in weight. The cell containing the test solution was kept in a thermostat.

Figure 3 shows the results of some experiments which were made to test the proposed method.

SUMMARY

1. A simple method has been proposed for measuring the swelling kinetics of organic films. The substance is applied in a thin layer to one side of a thin metallic strip, which is then immersed in the solution under investigation. On swelling, the film bends the strip. The deflection is measured with a microscope having a micrometer eye piece.

2. The degree of swelling of the film is found from the swelling stress, calculated from the formula derived in the text.

All abbreviations of periodicals in the above bibliography are letter-by-letter transliterations of the abbreviations as given in the original Russian journal. *Some or all of this periodical literature may well be available in English translation.* A complete list of the cover-to-cover English translations appears at the back of this issue.

---

* N. M. Belyaev, Resistance of Materials [in Russian] GITTL, Moscow, 1956.

INDEX

COLLOID JOURNAL
Volume 23, 1961

COLLOID JOURNAL
Volume 23, 1961

A translation of Kolloidnyi Zhurnal

A

Aleksandrova, E. M. -158
Al'tshuler, M. A. -543
Al'tshuler, M. A. -578
Amelin, A. G. -548
Andreva, E. P. -109
Arvan, A. S. -278
Avgul', N. N. -311
Avgul', N. N. -429

B

Bakanov, S. P. -222
Bakanov, S. P. -421
Barboi, V. M. -317
Barboi, V. M. -321
Belugina, G. V. -554
Berezin, G. I. -534
Berman, B. Z. -385
Bezus, A. G. -205
Bezus, A. G. -328
Borisikhina, V. I. -436
Borisikhina, V. I. -563
Borodina, L. A. -243
Bushin, V. V. -369

C

Cherkinskii, Yu, S. -533
Chiang-Lung -177
Chiang-Lung -272
Churaev, N. V. -335
Churaev, N. V. -439
Churakov, V. V. -197

D

Davydov, A. T. -122
Deinega, Yu. F. - 21
Deinega, Yu. F. -218
Demchenko, P. A. - 26
Demchenko, P. A. - 30
Demchenko, P. A. -442
Demchenko, P. A. -444
Deryagin, B. B. -222
Deryagin, B. V. - 33
Deryagin, B. V. - 44
Deryagin, B. V. - 99
Deryagin, B. V. -197
Deryagin, B. V. -304
Deryagin, B. V. -421
Deryagin, B. V. -447
Deryagin, B. V. -454
Divnich, L. F. -211
Dmitrenko, O. I. - 50
Dogadkin, B. A. -126
Dogadkin, B. A. -288
Dogadkin, B. A. -385
Dogadkin, B. A. -571
Dontsov, A. A. -288
Dreving, V. P. -205
Dreving, V. P. -328
Dukhin, S. S. - 44
Dukhin, S. S. -342
Dumanskii, A. V. - 21
Dumanskii, I. A. -575
Dykman, I. M. -317
Dykman, I. M. -321
Dzhigit, O. M. -461
Dzhuvarly, Ch. M. -230

E

Edel'man, L. I. -192
Egorov, A. K. -618
Ermolenko, I. N. -118

F

Fedoseeva, E. G. -632
Fel'dman, R. I. -263
Fel'dman, R. I. -397
Fel'dman, R. I. -632
Fel'dshtein, M. S. -571
Fillipova, N. P. -281

G

Gal'perin, D. I. - 5
Gil'man, T. P. -469
Glazman, Yu. M. -317
Glazman, Yu. M. -321
Glukhova, R. P. -153
Gor'kova, I. M. - 9
Gorodetskaya, A. V. -447
Gorshkov, V. I. -287
Gul', V. E. -307
Gusev, S. S. -118
Gutkin, A. M. - 16
Gutkin, A. M. -292
Gutkin, A. M. -294

I

Il'in, N. I. -439
Isirikyan, A. A. - 56
Isirikyan, A. A. -237
Ivanchov, S. S. -596

K

Kaganova, E. M. -473
Kalashnikova, V. M. -533
Kalyavina, L. F. -410
Katibnikov, M. A. -118
Khailenko, L. V. -575
Khodakov, G. S. -402
Khodzhaeva, I. V. -268
Khrapova, E. V. -137
Kirdeeva, A. P. -618
Kiselev, A. V. - 56
Kiselev, A. V. -132
Kiselev, A. V. -137
Kiselev, A. V. -237
Kiselev, A. V. -250
Kiselev, A. V. -311
Kiselev, A. V. -328
Kiselev, A. V. -420
Kiselev, A. V. -429
Kiselev, A. V. -461
Kiselev, A. V. -478
Kiselev, A. V. -485
Kiselev, A. V. -534
Kiseleva, O. G. -618
Kissin, Yu. V. -268
Klassen, V. I. -426
Klyachko-Gurvich, A. L. -205
Koganovskii, A. M. -601
Koganovskii, A. M. -624
Kolbanovskaya, A. S. -606
Kolganov, V. A. - 71
Kolosova, M. F. -143
Konstantinova, V. V. -554
Kopchikova, N. V. -192
Korolev, A. Ya. -485

Korotkova, A. A. - 44
Korotkova, A. A. - 78
Korzhuev, A. S. -505
Kovaleva, N. V. -485
Kozachek, N. N. -369
Kremnev, L. Ya. -243
Ksenzenko, V. -308
Kul'chitskii, L. I. - 63
Kurgin, Yu. S. -548
Kuznetsova, L. E. -177

L

Lapatukhin, V. S. -494
Lavrov, I. S. -247
Lavrov, I. S. -355
Leites, A. Z. -469
Leonov, L. F. -388
Lepilkina, L. A. -351
Lepilkina, L. A. -469
Levintovich, É. V. -413
Lishtvan, I. I. -335
Lisovina, G. M. -122
Lukash, A. E. -379
Lukomskaya, A. I. -359
Lunina, M. A. -143
Lyashenko, O. A. -618
Lygin, V. I. -132
Lygin, V. I. -250
Lygin, V. I. -478
Lygina, I. A. -311
Lygina, I. A. -429
Lyubimova, T. Yu. -497

M

Maksimova, N. I. -505
Mandel'eil', A. M. -161
Maslenkova, G. L. -514
Meleshko, P. S. -613
Mikhailov, V. V. -606
Milekhina, M. M. -146
Mokrousov, V. A. -426
Mokrushin, S. G. -254
Mokrushin, S. G. -366
Mokrushin, S. G. -436
Mokrushin, S. G. -563
Moshev, V. V. - 5
Mukharskaya, L. A. -230
Muttik, G. G. -420
Muttik, G. G. -461

N

Narinskaya, A. R. -150
Natanson, E. M. -369
Neduzhii, S. A. -374
Neiman, R. É. -618
Neimark, I. E. -379
Nikitina, S. A. -290
Nikolaev, B. A. -153

O

Ovchinnikov, Yu. M. -494
Ostrikov, M. S. -103

P

Panchenkov, G. M. -287
Panitkova, A. E. -473
Pasynskii, A. G. -425
Pechkovskaya, K. A. -385
Pionkovskaya, M. A. -379
Pisarenko, A. P. -150
Polyakov, M. V. -211
Polyakov, M. V. -216
Popereka, M. Ya. -642
Pozin, S. S. -416
Prokhorov, P. S. -388

R

Radushkevich, L. V. - 71
Razumikhina, N. S. -158
Rebinder, P. A. -165
Rebinder, P. A. -272
Rebinder, P. A. -301
Rebinder, P. A. -402
Rebinder, P. A. -554
Rovinskaya, T. M. -601
Rovinskaya, T. M. -624
Rudi, V. P. -161
Ryabinina, A. A. - 50
Ryazantsev, P. P. -281
Rykov, V. I. -186

S

Sandomirskii, D. M. - 78
Segalova, E. E. -109
Segalova, E. E. -165
Segalova, E. E. -170
Segalova, E. E. -256
Senatorskaya, L. G. -385
Serb-Serbina, N. N. -177
Serb-Serbina, N. N. -272
Serb-Serbina, N. N. -505
Sergeeva, L. M. - 83
Shakhkel'dyan, B. N. -410
Shakhova, T. E. -473
Shakhtin, D. M. -413
Shcherbakov, L. M. - 3
Shcherbakov, L. M. -181
Shcherbakov, L. M. -186
Shcherbakov, L. M. -281
Sheinfain, R. Yu. -638
Sheludko, A. -423
Shifrin, K. S. -306
Shokhin, I. A. -126
Shreiner, S. A. -278
Shtarkh, B. V. -150
Shukenov, Yu. V. -578
Sinegub-Lavrenko, A. A. -410
Sinitsin, V. A. -534
Skorodumova, Z. V. -571
Skorokhod, O. D. - 83
Skorokhod, O. R. -520
Skripov, V. P. - 88
Skrylev, L. D. -254
Skrylev, L. D. -436
Skrylev, L. D. -563
Slovetskii, V. I. -287
Sokolov, S. I. -632
Solov'eva, E. S. -165
Solov'eva, E. S. -170
Solov'eva, E. S. -256
Sominskii, D. S. -192
Starobinets, G. L. - 93
Stepanova, V. G. - 5
Svirskaya, O. D. -103

T

Taubman, A. B. -290
Taubman, A. B. -301
Tikavyi, V. F. - 93
Tipikin, S. A. -339
Titievskaya, A. S. -447
Titkov, N. I. -505
Tkachev, Yu. D. -366
Toporov, Yu. P. - 99
Trapeznikov, A. A. -105
Trapeznikov, A. A. -524
Trapeznikov, A. A. -581
Tyutynik, R. S. -379

U

Uskov, I. A. -392
Uskova, E. T. -173
Uskova, E. T. -392

V

Vakula, V. L. -565
Vinogradov, G. V. - 21
Vinogradov, G. V. -218
Vitkevich, N. D. -103
Vlasenko, G. Ya. -197
Volarovich, M. P. -335
Volarovich, M. P. -439
Vol'khin, V. V. -113
Vol'khin, V. V. -233
Vol'khin, V. V. -339
Voskresenskii, A. A. - 1
Vovnenko, A. M. -218
Voyutskii, S. S. -295
Voyutskii, S. S. -565

Vysotskii, Z. Z. -211
Vysotskii, Z. Z. -216

Y

Yagodovskaya, T. V. -497
Yashin, V. N. -447
Yashke, E. V. -548
Yur'ev, V.I. -416
Yurzhenko, A. I. -596

Z

Zachesova, G. N. -126
Zaitseva, K. A. -578
Zakieva, S. Kh. -554
Zatsepina, T. I. -581
Zemlitskii, E. Ya. -589
Zhurina, V. S. -177
Zimon, A. D. -454
Zolotavin, V. L. -113
Zolotavin, V. L. -233
Zolotavin, V. L. -339
Zubov, P. I. -278
Zubov, P. I. -351
Zubov, P. I. -469

COLLOID JOURNAL

Volume 23, Number 1 January-February, 1961

CONTENTS

	PAGE	RUSS. PAGE
Adsorption of Ammonia Vapor on Carbon Black. A. A. Voskresenskii	1	3
Thermomechanical Properties of Plasticized Ethylcellulose. D. I. Gal'perin, V. V. Moshev, and V. G. Stepanova	5	8
Quick and Thixotropic Properties of Disperse Sedimentary Rocks. I. M. Gor'kova	9	12
Extrusion of a Viscoplastic Dispersed Phase Between Sliding Plane-Parallel Walls. A. M. Gutkin	16	20
Electrification and Rheological Properties of Nonaqueous Plastic Dispersed Systems. Yu. F. Deinega, A. V. Dumanskii, and G. V. Vinogradov	21	25
Volumetric Determination of Colloidal Solubility (Solubilization). P. A. Demchenko	26	31
Solubilization of Aromatic Hydrocarbons in Hydrosols of Saturated Fatty Acid Soaps. P. A. Demchenko	30	36
Effect of Surface Forces on Phase Equilibria of Polymolecular Layers and on Contact Angle. B. V. Deryagin and L. M. Shcherbakov	33	40
Diffusiophoresis in Electrolyte Solutions and Its Role in the Mechanism of Film Formation from Rubber Latexes by the Method of Ionic Deposition. B. V. Deryagin, S. S. Dukhin, and A. A. Korotkova	44	53
The Reversion of Electrolyte Adsorption by Ferri- and Aluminosilicate Mixed Gels. O. I. Dmitrenko and A. A. Ryabinina	50	59
Effect of Compression of Carbon Black on the Adsorption Isotherm of n-Hexane. A. A. Isirikyan and A. V. Kiselev	56	67
A Spectrophotometric Study of the Adsorption of Methylene Blue by Highly Dispersed Aluminosilicates. L. I. Kul'chitskii	63	76
Capillary-Retained Liquid in Disperse Systems of Contacting Particles. L. V. Radushkevich and V. A. Kolganov	71	86
Study of Latex Foams. D. M. Sandomirskii and A. A. Korotkova	78	95
Molecular Adsorption of Certain Aromatic Acids on Ion-Exchange Resins. O. R. Skorokhod and L. M. Sergeeva	83	100
Relation Between Dynamic Stability of Droplets and Critical Vapor Supersaturation during Condensation. V. P. Skripov	88	106
The Sorption of Binary Solutions by Butadiene-Nitrile Copolymers. G. L. Starobinets and V. F. Tikavyi	93	112
Methods of Investigating the Frictional Properties of Polymers under Strong Unidirectional Compression. B. V. Deryagin and Yu. P. Toporov	99	118
LETTERS TO THE EDITOR		
Kinetics of the Growth of Contraction Stresses in Systems Undergoing Drying. M. S. Ostrikov, N. D. Vitkevich, and O. D. Svirskaya	103	122
Normal Stresses in Polyisobutylene Solution as Derived from Elastic Deformation and Tangential Force Data. A. A. Trapeznikov	105	125

COLLOID JOURNAL

Volume 23, Number 2 March-April, 1961

CONTENTS

	PAGE	RUSS. PAGE
Contribution to the Investigation of Processes of Crystallization Structure Formation in Aqueous Suspensions of Tricalcium Aluminate in the Presence of Electrolytes. E. P. Andreeva and E. E. Segalova	109	129
The Effect of Freezing on the Properties of Metal Hydroxide Coagulates. Part 2-Effect of Electrolytes on Changes of the Volume of Ferric Hydroxide Coagulate as a Result of Freezing. V. V. Vol'khin and V. L. Zolotavin	113	134
Spectral Investigation of Cation Exchange on Carboxymethylcellulose. S. S. Gusev, M. A. Katibnikov and I. N. Ermolenko	118	140
The Ageing of Anion Exchangers. A. T. Davydov and G. M. Lisovina	122	145
The Preparation and Properties of Aqueous Dispersions of Vulcanized Synthetic and Natural Rubbers. B. A. Dogadkin, G. N. Zachesova, and I. A. Shokhin.	126	150
Infrared Spectra and Thermodynamic Properties of Water Adsorbed on a Hydrated Silica Surface. A. V. Kiselev and V. I. Lygin	132	157
Approximate Expression for the Wave-Like Adsorption Isotherms of Nitrogen on Graphitized Carbon Black, Taking into Account Adsorbate- Adsorbate Interactions in the First and the Second Layer. A. V. Kiselev and E. V. Khrapova	137	163
Stabilization of Aluminum Sols in Benzene by Surface-Active Substances. M. A. Lunina and M. F. Kolosova	143	170
On the Theory of Capillary Osmosis. M. M. Milekhina	146	173
Electron Microscope Investigation of Colloid Particle Formation of White Fillers in Latexes. A. R. Narinskaya, A. P. Pisarenko, and B. V. Shtarkh	150	177
The Adhesion of Dough to the Surface of a Solid. B. A. Nikolaev and R. P. Glukhova	153	180
Adsorption Isotherms of Ionogenic Semicolloidal Surface Active Substances. N. S. Razumikhina and E. M. Aleksandrova	158	186
The Influence of Polyphosphates on Clay Suspensions. V. P. Rudi and A. M. Mandel'eil'	161	190
The Influence of Temperature on the Processes of Crystallization Structure-Formation in Tricalcium Aluminate Suspensions. E. E. Segalova, E. S. Solov'eva, and P. A. Rebinder	165	194
The Relationship between the Strength of a Crystallization Structure and the Degree of Dispersion of the Original Binding Agent in Tricalcium Aluminate Suspensions. E. S. Solov'eva and E. E. Segalova	170	200
An Electrochemical Study of Bentonite Suspensions. 5. The Electrokinetic Potentials of Electrodialyzed Ascangel as a Function of the Degree of Neutralization by Hydroxides of the Alkali Metals. E. T. Uskova	173	204
Investigation of Structure Formation in Aqueous Solutions of Humic Substances. Chiang-lung, N. N. Serb-Serbina, L. E. Kuznetsova, and V. S. Zhurina	177	209

CONTENTS (continued)

	PAGE	RUSS. PAGE
The Surface Tension of a Solid at the Interface with Its Own Melt. L. M. Shcherbakov	181	215
The Heat of Vaporization of Small Drops. L. M. Shcherbakov and V. I. Rykov	186	221
Pore Size Distribution in Cement Rocks. L. I. Edel'man, D. S. Sominskii, and N. V. Kopchikova	192	228
A Flow Ultramicroscope with Automatic Aerosol Particle Counting. B. V. Deryagin, V. V. Churakov, and G. Ya. Vlasenko	197	234
In Memory of Sergei Mikhailovich Lipatov	201	238

COLLOID JOURNAL

Volume 23, Number 3 May-June, 1961

CONTENTS

	PAGE	RUSS. PAGE
Adsorption Isotherms and Heats of Adsorption of Propylene on Silica Gel. A. G. Bezus V. P. Dreving, and A. L. Klyachko-Gurvich	205	241
Effect of Vapor-Phase Forming Agents on Porous Structure and Sorptive Properties of the Surface of Silica Gels. Z. Z. Vysotskii, L. F. Divnich, and M. V. Polyakov	211	248
The Possibility of Preparing Ultraporous Silica Gels with Intraparticle Porosity. Z. Z. Vysotskii and M. V. Polyakov	216	255
Electrokinetic Phenomena in Hydrocarbon Systems with a Hydrophilic Disperse Phase. Yu. F. Deinega, G. V. Vinogradov, and A. M. Vovnenko	218	257
Kinetics of Evaporation of Liquid Drops Covered by an Insoluble Film of a Foreign Substance B. B. Deryagin, S. P. Bakanov, and Yu. S. Kurgin	222	262
Influence of Resins, Naphthenic Acids, and Water on the Electrical Properties of Transformer Oil Containing Sodium Soaps. Ch. M. Dzhuvarly and L. A. Mukharskaya.	230	272
The Effect of Freezing on the Properties of Metal Hydroxide Coagulates. 3. The Effect of Electrolytes on the Change in Particle size of Iron Hydroxide and on the Rate of Filtration. V. L. Zolotavin and V. V. Vol'khin	233	276
Effect of Graphitization and Intergranular Capillary Condensation in Carbon Black on the Isotherm and Differential Heat of n-Hexane Adsorption. A. A. Isirikyan and A. V. Kiselev	237	281
Specific Features in the Stabilization of Bituminous and Tar Emulsions for Use on Roads. L. Ya. Kremnev and L. A. Borodina	243	290
The Porous Structure of Electrophoretic Deposits. I. S. Lavrov	247	295
An Infrared Spectroscopic Study of Isotopic Exchange with the Surface Hydroxyl Groups of Chemically Modified Silicas. V. I. Lygin and A. V. Kiselev	250	299
The Effect of Temperature on the Kinetics of Extraction of Mixed Colloidal Heavy-Metal Ferrocyanides with a Gelatin Foam. L. D. Skrylev and S. G. Mokrushin	254	304
A Study of the Kinetics of Supersaturation in Aqueous Suspensions of Tricalcium Aluminate and the Determination of Its Metastable Solubility. E. S. Solov'eva and E. E. Segalova	256	306
The Aggregation States of High-Molecular Compounds. VIII. Effect of Temperature on Ramie Cellulose Fiber and Hydrocellulose Film. R. I. Fel'dman	263	315
Radiochromatographic Separation of Mixtures of Sulfur and Vulcanization Accelerators. I. V. Khodzhaeva and Yu. V. Kissin	268	322
Investigation of the Structuration and Rheological Properties of Aqueous Dispersions of Bentonite Clays During Their Reaction with Humates. Chiang Lung, N. N. Serb-Serbina and P. A. Rebinder	272	327
Investigation of the Internal Stresses Arising when Nitro- and Acetylcellulose Films are Deposited on Glass. S. A. Shreiner, P. I. Zubov and A. S. Arvan	278	334
The Homogeneous Formation of Nuclei During Vapor Condensation and the Absolute (Limiting) Critical Supersaturation. L. M. Shcherbakov, P. P. Ryazantsev and N. P. Fillipova	281	338

	PAGE	RUSS. PAGE
Apparatus for Determining the Swelling of Granulated Materials at Various Temperatures. V. I. Gorshkov, V. I. Slovetskii and G. M. Panchenkov	287	345
Apparatus for Measuring Swelling at Elevated Temperatures. B. A. Dogadkin and A. A. Dontsov	288	346
Surface Tension Measurement with an Automatic Drop Counting Apparatus. S. A. Nikitina and A. B. Taubman	290	347
LETTERS TO THE EDITOR		
On the Law of Filtration of a Viscoplastic Substance through a Porous Medium. A. M. Gutkin	292	350
Slow Flow of a Viscoplastic Dispersed Medium in Conical and Plane Diffusors with Small Angles of Divergence. A. M. Gutkin	294	352
DISCUSSION		
The Problem of the Stability of Colloidal Systems and its Presentation in the Course of Collodial Chemistry. S. S. Voyutskii	295	353
Remarks on the Problem of the Stability of Dispersed Systems. P. A. Rebinder and A. B. Taubman	301	359
The Problem of the Presentation of Collidal Stability in the Course of Colloidal Chemistry. B. V. Deryagin	304	361
REVIEWS		
Angular Scattering Functions for Spherical Particles. William J. Pangonis and Wilfried Heller Reviewed by K. S. Shifrin	306	363
The Autoadhesion and Adhesion of High Polymers. S. S. Voyutskii. Reviewed by V. E. Gul'	307	364
Chemische Technologie. K. Winnacker and L. Kuchler. Reviewed by V. Ksenzenko	308	365

COLLOID JOURNAL

Volume 23, Number 4 July-August, 1961

CONTENTS

	PAGE	RUSS. PAGE
Isotherms and Heats of Adsorption of Alcohols on Carbon Blacks of Various Degrees of Graphitization. N. N. Avgul', A. V. Kiselev and I. A. Lygina	311	369
Coagulation of Lyophobic Sols by Electrolyte Mixtures. 3. Effect of Counter Ion Adsorption. V. M. Barboi, Yu. M. Glazman, and I. M. Dykman	317	376
Coagulation of Lyophobic Sols by Electrolyte Mixtures. 4. Effect of Counter Ion Adsorption. V. M. Barboi, Yu. M. Glazman, and I. M. Dykman	321	381
Isotherms and Heat of Adsorption of Propane and Propylene on Graphitized Carbon Black. The Energy of the Adsorption Forces. A. G. Bezus, V. P. Dreving, and A. V. Kiselev	328	389
Comparative Study of Mechanical and Chemical Methods of Varying the Dispersity of Peat. M. P. Volarovich, I. I. Lishtvan, and N. V. Churaev	335	399
The Effect of Freezing on the Properties of Metal Hydroxide Coagulates. 4. Manganese Dioxide Coagulate. V. V. Vol'khin, V. L. Zolotavin, and S. A. Tipikin	339	404
Diffusion-Electrokinetic Thinning of Liquid Films. S. S. Dukhin	342	408
Determination of Internal Stresses during Formation of Gelatin Films. P. I. Zubov and L. A. Lepilkina	351	418
Flocculation in the Electrophoretic Deposition of Carbonate Suspensions. I. S. Lavrov	355	423
Mechanism of Rubber Reinforcement. A. I. Lukomskaya	359	428
Experimental Studies of Laminar Systems. 26. The Formation of Ultrathin Films of Cadmium Sulfide at a Solid-Solution Interface. S. G. Mokrushin and Yu. D. Tkachev	366	438
Conditions for the Formation of Colloidal Particles of Intermetallic Compounds. E. M. Natanson, V. V. Bushin, and N. N. Kozachek	369	442
Some Features of Emulsion Formation by Ultrasonics. S. A. Neduzhii	374	448
Synthesis of Artificial Zeolites and Investigation of Their Adsorption Properties. I. E. Neimark, M. A. Pionkovskaya, A. E. Lukash, R. S. Tyutynik	379	454
Reinforcing of Rubber in Latex. 3. Electron Microscope Study of Filled Latex Mixes. K. A. Pechkovskaya, L. G. Senatorskaya, B. Z. Berman, and B. A. Dogadkin	385	462
Investigation of Long-Range Diffusion Forces between Water Droplets and Nonvolatile Particles. P. S. Prokhorov and L. F. Leonov	388	464
Electrochemical Study of Bentonite Suspensions. 6. Potentiometric Titration of Aminobentonite Complexes. I. A. Uskov and E. T. Uskova	392	469
States of Aggregation of High-Molecular Compounds. 9. Thermodilatometric Investigations of Polychloroprene and Natural Rubber. R. I. Fel'dman	397	475

CONTENTS (continued)

	PAGE	RUSS. PAGE
Mechanism of Disintegration of Quartz in Surface Active Media. G. S. Khodakov and P. A. Rebinder	402	482
Changes in the Mechanical Properties of Printing Inks during Ageing. B. N. Shakhkel'dyan, L. F. Kalyavina, A. A. Sinegub-Lavrenko.	410	491
Determination of the Specific Surface of Clays and Kaolins by Means of Radioactive Tungsten. D. M. Shakhtin and E. V. Levintovich	413	495
Electrokinetic Properties of Monocarboxycellulose and some Cellulose Acid Esters. V. I. Yur'ev and S. S. Pozin	416	499
LETTERS TO THE EDITOR		
Heats of Adsorption of Diethyl Ether Vapors on Silica Gel. O. M. Dzhigit, A. V. Kiselev, and G. G. Muttik	420	504
The Question of Priority in the Development of the Theory of the Diffusiophoresis and Thermophoresis of Small Aerosol Particles. B. V. Deryagin and S. P. Bakanov	421	505
BOOK REVIEWS		
Colloid Chemistry. A. Sheludko	423	508
Colloid Chemistry, Higher School Edition. A. G. Pasynskii	425	509
Introduction to Flotation Theory. V. I. Klassen and V. A. Mokrousov	426	509

COLLOID JOURNAL

Volume 23, Number 5 September-October, 1961

CONTENTS

	PAGE	RUSS. PAGE
Adsorption and Heat of Adsorption of Isomeric Butanols on Graphitized Carbon Blacks N. N. Avgul', A. V. Kiselev, and I. A. Lygina	429	513
Emulsion Method of Extracting Colloidal Mixed Uranyl Ferrocyanide from its Hydrosols. V. I. Borisikhina, L. D. Skrylev, and S. G. Mokrushin	436	521
Determination of the Discharge and Rate of Movement of Water in Porous Media by Means of Radioactive Tracers. M. P. Volarovich, N. I. Il'in, and N. V. Churaev	439	524
Effect of Electrolytes on Critical Micelle Concentration and Solubilizing Capacity of Sodium Laurate Solutions. P. A. Demchenko	442	528
Effect of Molecular Weight of Sodium Naphthenates and Salts of Synthetic Fatty Acids on the Solubilization of Hydrocarbons. P. A. Demchenko	444	531
Disjoining Pressure of Electrolyte Solutions on Polarized Mercury. B. V. Deryagin, A. V. Gorodetskaya, A. S. Titievskaya, and V. N. Yashin	447	535
Adhesion of Powder Particles to Plane Surfaces. B. V. Deryagin and A. D. Zimon	454	544
The Heat of Adsorption of Water Vapor on Hydrated and Dehydrated Silica Gels. O. M. Dzhigit, A. V. Kiselev, and G. G. Muttik	461	553
Investigation of Internal Stresses on Hardening of Polyester Resin. P. I. Zubov, L. A. Lepilkina, T. P. Gil'man, and A. Z. Leites	469	563
Formation of Porous Structures in Alumina-Silica Gels. 1. The Role of Syneresis in the Formation of Porous Aluminosilicates. E. M. Kaganova, T. E. Shakhova, and A. E. Panitkova	473	568
Infrared Study of the Adsorption of Benzene and Hexane on Silica. A. V. Kiselev and V. I. Lygin	478	574
Adsorptive Properties of Oxidized Carbon Blacks. 1. Oxidation of Channel Black in Water. A. V. Kiselev, N. V. Kovaleva, and A. Ya. Korolev.	485	582
Radiotracer Method of Determining the Adsorptive Capacity and Specific Surface Area of Phosphate Coatings. V. S. Lapatukhin and Yu. M. Ovchinnikov	494	592
Structuration Processes in Cement – Reinforced Terrains. T. Yu. Lyubimova and T. V. Yagodovskaya	497	596
Investigation of Changes in the Strength of Argillaceous Rocks on Electrochemical Treatment. N. I. Maksimova, N. N. Serb-Serbina, N. I. Titkov, and A. S. Korzhuev	505	605
Infrared Spectroscopic Investigation of the Structuration Properties of Polymers. G. L. Maslenkova	514	615
Sulfonated Elastomers as Sorbents of Weak Electrolytes. O. R. Skorokhod	520	621

CONTENTS (continued)

	PAGE	RUSS. PAGE
Effect of n-Decyl Alcohol and Polyisobutylene Additions on Elastic Recoil and Structural Strength in the Ripening and Aging of Aluminum Naphthenate Gel. A. A. Trapeznikov	524	626
Kinetics of the Structuration of Polymer-Cements. Yu. S. Cherkinskii and V. M. Kalashnikova	533	632
LETTER TO THE EDITORS		
Dependence of the Mean Molar Heat Capacity of an Adsorbate Upon the Differential Heat of Adsorption. G. I. Berezin, A. V. Kiselev, V. A. Sinitsin	534	638

COLLOID JOURNAL

Volume 23, Number 6 November-December, 1961

CONTENTS

	PAGE	RUSS. PAGE
The Role of Colloid Science in the Development of the Material and Technological Basis of Communism	539	641
Theory of Capillary Impregnation by Wetting Liquids of Porous Materials with Dead-End Capillaries. M. A. Al'tshuler	543	646
The Temperature of Droplets in Supersaturated Vapor. A. G. Amelin, E. V. Yashke, and Yu. S. Kurgin	548	652
Stabilization of Concentrated Suspensions by Structurization of the Dispersion (Hydrocarbon)Medium. G. V. Belugina, S. Kh. Zakieva, V. V. Konstantinova, and P. A. Rebinder	554	658
The Influence of Freezing on the Stability of Gelatinized Emulsions Stabilized by Colloidal Mixed Ferrocyanides of Copper and Iron. V. I. Borisikhina, L. D. Skrylev, and S. G. Mokrushin	563	669
Adhesion of Polymers. 9. New Method of Preparing Bonded Strips for Determining the Mutual Adhesion of Elastomers. V. L. Vakula and S. S. Voyutskii	565	672
Effect of Carbon Black on the Kinetics of Vulcanization and the Character of the Sulfur Structures of the Vulcanizates. B. A. Dogadkin, M. S. Fel'dshtein, and Z. V. Skorodumova	571	679
Rheological Properties of Aqueous Glycerol Solutions. I. A. Dumanskii and L. V. Khailenko	575	684
Gravity Deposition of Aerosols from Laminar Flow. K. A. Zaitseva, Yu. V. Shukenov, and M. A. Al'tshuler	578	687
Strength, Elastic, and Thixotropic Properties of Concentrated Aluminum Naphthenate Gels and the Effect on Them of Polar Additions. T. I. Zatsepina and A. A. Trapeznikov	581	690
A New Method of Dispersion Analysis by the Centrifugation of Highly Disperse Systems and Systems Suspended in a Very Viscous Medium. E. Ya. Zemlitskii	589	699
Effect of Lower Fatty Acid Salts on the Dispersity of an Emulsifier Solution and the Synthetic Latexes Prepared from It. S. S. Ivanchov and A. I. Yurzhenko	596	706
Effect of Strong Electrolytes on the Adsorption of Benzene Derivatives from Aqueous Solutions by Activated Charcoal. A. M. Koganovskii and T. M. Rovinskaya	601	712
Investigation of Structural-Mechanical Properties of Bitumens of Different Origin. 1. Study of Viscous and Thermomechanical Properties of Road Bitumens of Different Chemical Composition. A. S. Kolbanovskaya and V. V. Mikhailov	606	718
Adsorption in the System $Fe_2O_3-H_2O-CaCl_2-NaCl$. P. S. Meleshko	613	726
Studies on the Stability and Coagulation of Synthetic Latexes. 1. Effect of Adsorptive Saturation of the Globule Surface by the Emulsifier. R. É. Neiman, O. A. Lyashenko, A. P. Kirdeeva, A. K. Egorov, and O. G. Kiseleva	618	732

CONTENTS (continued)

	PAGE	RUSS. PAGE
Relation Between Solute Structure and Adsorption from Aqueous Solutions. 1. Dependence of Functional Groups. T. M. Rovinskaya and A. M. Koganovskii	624	739
Interaction Between Polymers and Plasticizers. 1. Preparation and Properties of Polyvinylchloride Pastes. E. G. Fedoseeva, R. I. Fel'dman, S. I. Sokolov	632	749
The Effect of Acid Treatment of Silica Gel on the Pore Structure of the Dried Gel. R. Yu. Sheinfain	638	756
Kinetics of Swelling of Organic Films by the Flexible Strip Bending Method. M. Ya. Popereka	642	761
Author Index, Volume 23, 1961	647	
Tables of Contents, Volume 23, 1961	650	